



NCRDSET '16

PROCEEDINGS OF THE 2nd NATIONAL CONFERENCE
ON

RESEARCH AND DEVELOPMENT IN SCIENCE,
ENGINEERING AND TECHNOLOGY

26th February 2016

Organised by

ST. ANNE'S

COLLEGE OF ENGINEERING AND TECHNOLOGY

Anguchettypalayam, Panruti, Cuddalore Dt- 607 110.

Proceedings of the
2nd NATIONAL CONFERENCE
On
**RESEARCH AND DEVELOPMENT IN
SCIENCE, ENGINEERING AND TECHNOLOGY**

(NCRDSET'16)

February 26, 2016



Organized by

**ST. ANNE'S COLLEGE OF
ENGINEERING AND TECHNOLOGY**

(Approved by AICTE, New Delhi and Affiliated to Anna University, Chennai)

Anguchettypalayam, Panruti Taluk, 607 110

Tamilnadu, India

www.stannescet.ac.in

The Second National Conference on Research and Development in Science, Engineering and Technology

(NCRDSET '16)

Editor in Chief: Sr. S. ANITA, M.E, (Ph.D.,)

Editor: A. JOHN PETER, M.Sc., (Ph.D.,)

Copyright © 2016 by the publisher & Editor.

All rights reserved. No part of the contents of this publication may be reproduced or transmitted in any form or by any means without the written permission of the publisher. The authors take responsibility for the material that has been submitted.

ISBN: 978-93-5254-811-8

**Published by: NCRDSET '16
St. Anne's College of Engineering and Technology
Tamilnadu, India**

ABOUT THE SISTERS OF ST. ANNE, THIRUCHIRAPALLI



The Congregation of the Sisters of St. Anne of Tiruchirapalli had its origin in the 19th century. Rev. Mother Annamma was the foundress of the congregation, she was the marvelous beginner of this reformation record in the history of Indian womanhood. She experienced the presence of God among the poor and the suffering people. The members of this Congregation always strive to live up to the charism of the foundress "Simplicity in Life and Service to the Poor" for the past 160 years. Being concerned with the upliftment of the poor and the socially outcast, their ministry has taken different dimensions in the involvement of our multifarious activities namely Evangelical, Educational, Social and Medical with an explicit involvement in working for the differently abled. As a part of their educational ministry specially to work for the youth they have started this esteemed institute.

ABOUT INSTITUTION



St. Anne's College of Engineering and Technology is approved by AICTE, New Delhi and affiliated to Anna University, Chennai. It is located at Panruti. The college bloomed in the year 2009 with an aim of uplifting the life style and providing opportunity for higher professional education to the rural youth in the surrounding districts. The college provides opportunities for our students both for placement training and employment and they can reap the benefits from this Institute with proper coordination. Our college is steadfast to promote its students, the pursuit of individual excellence and participation in the full range of academic, spiritual, cultural, social and physical activities.

St. Anne's College of Engineering and Technology fulfils all these goals by creating a pleasant atmosphere for the students. The campus life helps the students to endeavor and achieve the highest apex. The campus is a place of hope and encouragement that has been nurtured by holy divine and celestial vision. St. Anne's College of Engineering and Technology commenced with four departments Mechanical Engineering, Electrical and Electronics Engineering, Electronics and communication Engineering, Computer Science and Engineering. Learning is an exuberant experience here, with veteran faculty, revitalizing library, vivacious discussion rooms, well equipped labs, Hostels with copious facilities and spacious playground.

ABOUT NCRDSET'16



In the recent days technology has witnessed enormous developments in many fields. To import these developments, the Second National Conference on Research and Development in Science, Engineering and Technology '16 (NCRDSET '16) is organized at St. Anne's College of Engineering and Technology, Anguchettyalayam, Panruti on 26th February 2016. NCRDSET '16 addresses the rapid strides and technological advancements in the fields of Science, Engineering and Technology. This conference offers a platform to track quality R&D updates from Researchers, Engineers, Students and representatives from the Academics and Industry. It also provides them to disport their expertise, talents & innovative ideas that will contribute to all fields of Engineering in the upcoming years.



Secretary Message

"Vision looks inward and becomes duty. Vision looks outward and becomes aspiration. Vision looks upward and becomes faith."

Now, when this vision of duty, aspiration and faith has become a reality, it is an ecstatic moment for me on the occasion of the Second National Conference on Research and Development in Science, Engineering and Technology '16 (NCRDSET '16) is convened by our esteemed institution St. Anne's College of Engineering and Technology.

It is clearly evident that we are experiencing modern changes and invention everyday by innovative research works that are being undertaken by many researches. Now it is high time that everybody from us will have to think and commit for the contribution. The Principal and faculty members of St. Anne's have rightly sensed this need and provided a good platform for all around the nation to bring forward their thoughts and help society at large. The national conference will play a humble role in bringing together researchers, younger scientists, and students in an informal environment for discussing the latest advances.

Hearty congratulations to the Principal, Convener and the organizing committee members for organizing an event of national stature. St. Anne's has always been a front runner to organize such events and this time also I am more than happy to be a part in organizing second National Conference on Research and Development in Science, Engineering and Technology '16 (NCRDSET '16)

Once again I convey my blessings and good wishes to all members of St. Anne's family involved dedicatedly for this event.

REV. MOTHER VICTORIA, SAT



Principal Message

“Research is to see what everybody else has seen and think what nobody else has Thought”

Considering the rate at which the knowledge is advancing, it is education that will determine the level of prosperity, welfare and security of our nation. The progress of our nation depends on the quality of research activities which is being undertaken by the young academician.

In this age of highly competitive globalization, the higher education, particularly the technical education, has assumed newer dimensions. When global interdependence and competition are upon us, we must trigger off our researchers to think logically and analytically with high degree of discipline to keep up and keep pace with the best and the brightest in the world.

This National conference has been designed to provide ample opportunities to researchers to network and to share new inventions and new technologies in the advanced Science and Engineering sectors.

My heartfelt wishes and congratulations to all the participants and the members of organizing committee of NCRDSET'16.

I wish the conference a fabulous success.

Dr. R. AROKIADASS, M.E, Ph.D.,



Vice Principal Message

“Brothers and sisters, rejoice! Encourage one another, be of one mind, and live in peace. And the God of love and peace will be with you.” (2 Corinthians 13:11)

My heartiest greetings and the best wishes for the success of this event NCRDSET ‘16.

Over the past few years technology has taken over society. Everyone uses technology, from children, teenagers, adults and elders. Technology is vital in today’s world and makes everything easier. This is mainly because of the students and the research scholars in the Engineering field who are contributing more for the new inventions. To explore and encourage such kind of new ideas and inventions, the Second National Conference on Research and Development in Science, Engineering and Technology is organized in our St.Anne’s CET campus. I hope all the participants of the National Conference will have fruitful sessions to strengthen their own ideas.

I congratulate the convener and all the coordinators of Second National Conference and thank all the participants for presenting their specialized papers in NCRDSET ‘16.

Sr. G. GNANA JENCY, M.E.,



Convener Message

The technology is developing at a rapid pace. In this era of globalization, the exchange of knowledge and skills has given a further development in the field of technology. Such phenomenal advancements have revolutionized almost every sphere of human life today. We experience new developments every day and every moment. Technology is changing and new areas of research are being taken up by academicians. Now it is high time to bring all academics, researchers, industry representatives and students together from various organizations from all over India to share and enhance knowledge on latest advancements in Science, engineering and technology. This interdisciplinary conference provides finest opportunities to showcase their work and share their expertise.

On behalf of the management, staff of St. Anne's and on my personal behalf I would like to extend my good wishes to all participants to participate with full vigor in this celebrated event which can give immense exposure and global opportunities to them.

I hope this conference will surely prove conducive to all in equal length.

Sr. S. ANITA, M.E., (Ph.D.)
Head /ECE

ADVISORY COMMITTEE



Dr. M. Muralidhara Rao
Principal
Gandhi Institute of Engg & Tech., Odisha



Dr. R. Senthil
Dean
UCE, Villupuram



Dr. S. Sumathy
Associate Professor
VIT University, Vellore



Dr. R. Nakkeeran
Professor & Head
PEC, Puducherry



Dr. S. P. Singh
Professor & HOD/ECE
Mahatma Gandhi Institute of Tech.
Hyderabad



Dr. R. Nakkeeran
Principal
CIT, Puducherry



Dr. P. Yogesh
Associate Professor/DIST
Anna University, Chennai



Dr. G. Florence Sudha
Professor
PEC, Puducherry



Dr. P. Parthiban
Assistant Professor
NIT, Surathkal



Dr. R. Srinivasan Alavandar
Professor & Dean
Agni College of Tech., Chennai



Dr. A. Suhasini
Associate Professor
Annamalai University, Chidambaram



Dr. Thangaraj Chelliah
Assistant Professor
IIT, Roorkee



Dr. R. Rajappan
Professor
MEC, Mailam



Dr. Sheila Royappa
Professor
SACW, Pallathur



Dr. M. Manikandan
Associate Professor
MIT Campus, Chennai

Preface

The Second National Conference on “**Research and Development in Science, Engineering and Technology**” (NCRDSET’16) has become a well established Annual conference. It was held on the campus of St. Anne’s College of Engineering and Technology, Anguchettypalayam at Panruti Taluk in Cuddalore District on 26th February 2016. This conference was jointly organized by the Departments of Mechanical Engineering, Electrical and Electronics Engineering, Electronics and Communication Engineering, Computer Science and Engineering and Science & Humanities in association with Middle-East Journal of Scientific Research (MEJSR), and it aims to exchange and stimulate research in the various areas of Science, Engineering and Technology. It also provides a platform for researchers in Academic institutions to discuss and publish their current research works.

As we all know, research knowledge must be applied, if it is to have an impact on the education industry. This program was designed to maximize the exchange of information and perspectives among the participants. The papers were presented in panel sessions and each was followed by a panel discussion.

After peer review, the editorial board selected 91 papers from 189 paper submissions. The selected papers covered a wide range of topics: Power Systems, Power Electronics, Wireless Communication, Digital Image Processing, Cloud Computing, Security and Machine Learning, Machine design and Analysis, Thermal Engineering and Manufacturing Technology. All the presentations were very impressive with high level of professionalism, and in many cases original ideas and activities have been accomplished or proposed. We would like to thank all the authors for their interests and efforts. All the research papers have been reviewed by experts. Special thanks go to all speakers as well as to the session chairpersons, who drove all the conference sessions on the right track, keeping them in time while permitting enriching discussions.

The credit for the success of the conference is to be shared with the Advisory Committee and the Technical Committee whose members gave precious inputs with vested interest and painstaking efforts and they were always side by side with the Organizers.

Editor in chief,

Sr. S. ANITA, M.E., (Ph.D.,)
Convenor - NCRDSET’16

CONTENTS

Sl.No	PAPER TITLE	PAGE No
1	A Review On Pediatric Foreign Body Aspiration – An Analysis With Image Processing Techniques <i>Vasumathy M , Mythili Thirugnanam</i>	1
2	A Knowledge Discovery Framework for Healthcare Using BDCAM <i>Arunakumari.S ,A.Akilan, M.Senthamarai Selvi</i>	6
3	Real time hand gesture controlled autonomous system using arduino duemilanove <i>K.Latha, D.Mahalakshmi, P.Manjamadevi</i>	16
4	Network Based Application For Students Community On Top Of Android <i>Nivetha.A, Subesha.R, Sivasathiya Vetriselvam</i>	23
5	Co-Extracting Opinion Targets and Opinion Words from Online Reviews Based on the Word Alignment Model <i>R.Sasikumar,N.Neelavannan,P.Murugan,Dr.G.Sankaranarayanan</i>	28
6	Qos aware Web Service Recommendation using Collaborative Filtering with Service Usage Factor <i>Kiruthiga.V,Seethalakshmi.R</i>	32
7	Computer Aided Detection and Classification of Breast Masses in Digital Mammograms <i>K.Vaidehi, T.S.Subashini</i>	41
8	A Study on Different Techniques of Web Mining On Cloud Computing Technologies <i>Lourducaroethan.A, P.Jayanthi, V.Sakthivel.</i>	48
9	Big Data in Cloud Computing <i>P.Manivannan, S.Sri Kurinji, U.Prema</i>	55
10	Secure Data Transmission Technique for iphone using Quick Response (QR)Code <i>D.Rani,M.Kayalvizhi,Ramya</i>	60
11	Cryptography And Efficient Data Transmission For Cluster-Based Wireless Sensor Networks <i>Sr. S. Jothi, Sr. A. Avila Therese, Bhuvana</i>	65
12	Black Hole Attack in MANET Prevented Using Trusted Route <i>K.Maheswari,S.Manavalan,D.Varadharajan</i>	75
13	Data Storage Security And Privacy In Cloud <i>S.Jerald Nirmal kumar</i>	79
14	Dynamic collaboration in multicloud computing environments: framework and security issues <i>S.Rajarajan, S.Jonajenifer, R.Rathika,</i>	83
15	Trusted CBCR Scheme to Enhance the Performance and Security in MANETS <i>D. Pauline Freeda ,D.Sivaranjani, Ms.P.Shanmugapriya</i>	88
16	Home Automation Using Internet of Things <i>E.Veeramani, R.Parthap miras</i>	94
17	Internet of Things for Smart Cities <i>Sindhuja A , Deiveegan A, Martin Lourdu Raj X</i>	99

18	Privacy Enhancement of Social Network Security by Third Party Application <i>N.Umamaheshwari,K.Poornambigai,P.Meena</i>	108
19	Rain Streaks Detection And Removal From Color - Image Video Using Sparse Representation <i>S.K .Adithya kasi swamynathan,A.Thiruvengadam,P.Meena</i>	117
20	GSM Based Automatic Emergency Detection and Alerting System using Sensors <i>G. Jona Nicy Parvatham, M. Vaidehi</i>	123
21	Image Processing Techniques Examination of MRI Images of Rheumatoid Arthritis Through Morphological Image Processing Techniques <i>S.Chandiralekha, K.Dhivya, F.Destonious Dhiraviuam</i>	131
22	Parallel Prefix Speculative Han Carlson Adder <i>Gayathri.G, Raju S.S, Suresh.S</i>	138
23	Modeling and analysis on GABA concentration level for Diagnosis of Parkinson's disease <i>S. Anita, Dr. P. Aruna Priya, Dr. R. Arokiadass</i>	146
24	CMOS-Electromechanical Systems Microsensor Resonator with High Q-Factor at Low Voltage <i>S.Thenappan, N.Porutchelvam</i>	153
25	Different Observation –Modes in Fiber Optic- Cable <i>C. Sivasathyanarayanan, G.Mohankumar</i>	159
26	An Enhanced Speech Based Vmail for Visually Impaired People <i>P.Dhivya, S.Hemalatha, M.Keerthana</i>	166
27	Design of Modified Architecture for Adaptive Viterbi Decoder <i>Venkatesan, G.Mahendiran, R.Radhakrishnan</i>	175
28	Adaptive Hardware Design for Computing Efficient Singular Value Decomposition in MIMO-OFDM System <i>Vaidehi. M,Umamaheswari. D</i>	180
29	Fault Detection using AES-Cipher Block Chaining Mode for secured Wireless Communication Networks <i>B. Mary Amala Jenni, S. Devika</i>	189
30	Reinforcement Learning with Particle Filter (RLPF) <i>J. Joseph Ignatious, V.Lawanya, N.Kirubashankari</i>	196
31	Internet of Things Based Smart Vehicle Management System <i>S.Balabasker, G.Sivasathiya, R.Annamalai</i>	202
32	Design of Context Aware Smart Home Energy Management System Using RFID <i>B.kayalvizhi, S. Boomadevi</i>	209
33	Performance Analysis of OFDM System with QPSK for Wireless Communication <i>Kalaivani.P, Puviyarasi.T, Raju S.S Suresh.S</i>	214
34	Voice Recognition Based Personal Assistant Robot Using Wireless Sensor Networks <i>Poonguzhali.S, Raju S.S Suresh.S</i>	221
35	Arm Based Smart Device For Detecting And Controlling Air Pollution In Vehicles <i>S.Naveenkumar, P.Raghupathi, E.Rubha , P.Umadevi</i>	232

36	License Automation Using Sensors <i>V.Naina Malai Raja, J.Joushuarathina Raj, A.Bharathi Lakshmi, P.Gokila</i>	237
37	A Novel Cyclostationary Feature Detector Model for Spectrum Sensing in Cognitive Radio <i>Nitish Das, P. Aruna Priya</i>	246
38	Color Image Enhancement Based On Dwt Using Linear and Non-Linear Filtering Techniques <i>G. Saravanan, Dr. G. Yamuna, J.Sasikala</i>	251
39	Performance Analysis of Asymmetric Cascaded Nine Level Impedance Source Multilevel Inverter <i>V. Narmadha, G. Irusapparajan</i>	261
40	A Hybrid Grid Connected Wind Driven Pv System With Single Dc-Dc Converter <i>J.Antonysagayanancy, E.Catherinamalapriya, R.Sivasankari</i>	267
41	A Novel approach for Power Factor Correction using Microcontroller in Domestic Loads <i>Eugin Martin Raj. V. C, S.Lese</i>	274
42	Energy Storage Capacitor Reduction For Single Phase Pwm Rectifier <i>A.Annai Theresa, K.Sriram</i>	279
43	Harmonic Reduction Of Single Phase Pwm Rectifier In Ripple Energy Storage System <i>V.balaji, R. Siva Sankari</i>	287
44	Reactive Power Generation Minimization In Power System Using Group Leader Optimization Technique <i>K.Sriram, A. Sundarapandiyan</i>	294
45	Battery Energy Storage System for A Stand Alone Windmill - Based On State-Of-Charge (SOC) Balancing Control <i>A. Sundarapandiyan, R. Arulselvi</i>	299
46	Review on Gate Bias Control Method for RF Power Amplifiers Using ARM Processor <i>J. Ramesh, J. Balaji</i>	306
47	Bat Algorithm for Economic Dispatch problem with Prohibited zones, Ramp rate limits & Multi-fuel options <i>Dr.A.Subramanian, Dr.R.K.Santhi, S.Vijayaraj</i>	312
48	Study of Multi-Area Economic Dispatch on Soft Computing Techniques <i>S.Vijayaraj, Dr.R.K.Santhi</i>	320
49	Student's Perceptions of Plagiarism <i>A. Richard Pravin, A. Kalaivani</i>	332
50	The Indian Education System <i>P. Suruthi, K. Sivaranjani</i>	339
51	Generation of Electricity from Algae <i>M.Elumalai</i>	348
52	Gso Based Load Frequency Controller For Single Area Power System <i>K.Sriram, G. Gnana Sundari, B. Dhivya Bharathi</i>	353
53	Geopolymer Concrete - Concrete Without Cement <i>Annie John, Rahul John Roy</i>	357
54	Design Optimization Of Catalytic Converter <i>Naveenkumar.U, Punitha Raj.A, Prakash.M</i>	362

55	Study Analysis Of Prosopis Juliflora In Split Irrigation Systems <i>R.Sasikumar, K.Shanmuga elango, Neelavannan, Sarthkumar</i>	371
56	Experimental Investigation Of Modified Jatropha Oil Fuel Direct Injection Diesel Engine <i>R.Sasikumar, N.Neelavannan , P.Murugan, V.Murugadass</i>	377
57	Performance Analysis of Compression Ignition Engine by using Hydrogen with Cashew Nut Shell Oil and Feasibility as Bio Fuel <i>V.Thanigaivelan, M.Loganathan, E. James Gunasekaran</i>	382
58	Fabrication and analysis of various Biomass using slow Pyrolysis Reactor <i>M.Balamurugan, K.Saravanan, D.Ommurugadhasan V.Vasantharaj</i>	387
59	Study The Influence Of Machining Parameters In Dry Turning <i>A.Anne Evanglin, A.Anisha Christy, Dr.R.Arokiadass, K.Saravanan</i>	394
60	Design And Analysis Of Lead Crowned Spur Gear Teeth <i>Sr.Josephine Mary Sr.Layoni Margaret, Sr.Jaya Praislin</i>	397
61	Biological Immune System Applications On Mobile Robot For Disabled People <i>L.Vijay, V.Sabarathinam, S.Subash, P.Prithivirajan</i>	404
62	Design And Fabrication Of Three Mode Operation For Automobile Steering <i>K.Shanmuga Elang, k.Saravanan, N.Neelavanan</i>	412
63	Design and Finite Element Analysis of Nose Landing Gear of a Civil Transport aircraft <i>Elavarasan S, Naveenkumar. U</i>	422
64	Experimental Investigation Of Piston Bowl Geometry On Diesel Engine <i>K.Sakthivel, P.Murugan, U.NaveenKumar, Tamilselvan. M</i>	430
65	Communication Skills for Engineering Students <i>L.M.Sowmiya</i>	444
66	Light-Fidelity (Li-Fi) Technology: A Review <i>M. Bala Murali, K.Nithiyanandham, A. John Peter</i>	449
67	Enrich Your English <i>S.Bharathi, D.Datchayani</i>	455
68	Room Temperature Synthesis of NaY(MoO ₄) ₂ :Pr ³⁺ Nanophosphor With Blue Excitation For WLED Applications <i>Ezekiel.A, Padmanathan, A. John Peter</i>	459
69	Transient Analysis of an M/M/1 Queue with Single Working Vacation and Variant Impatient Behavior <i>R.Sudhesh, A.Azhagappan</i>	463
70	Various Display Technologies <i>V.Bala Murugan, A. John Peter</i>	471
71	Photocatalytic disinfection of bacteria by nanocomposite ZnO-TiO ₂ and detoxification of cyanide under visible light. <i>G. Abiramasundari, S.Ramya, T.Natramiz raja venthan</i>	475
72	Transient Analysis of M/M/1 Queue with Server Vacation, Impatient Customers and a Waiting Server Timer <i>R.Sudhesh, A.Azhagappan</i>	482
73	Power Your Entire Home Without Wires <i>T. Alan Arputha Raj, A. John Peter</i>	490
74	Design and Implementation of Ultra Low Power, Ultra Wide Band Low Noise Amplifier <i>Chenna Reddy Peddasomappagari, Dr. P. Aruna Priya</i>	495

75	Chunking and Indexing mechanisms for Data Deduplication in Cloud Storage <i>Z.Asmathunnisa, Dr. P.Yogesh</i>	507
76	Secure Role Based Access Control On Encrypted Data In Cloud Storage <i>Sarah S , Kalaimagal N , Abila G</i>	513
77	Junction less TFET for Performance Driven Mobile System <i>KondaVenkata Ashok, Dr. P. Aruna Priya</i>	518
78	Security for Privacy Preserving Cloud Storage Using Key Based Method <i>R.Gnanakumari</i>	528
79	Reducing the Energy Consumption in DVFS by using Performance Optimizing Scheme <i>K.G. Harishkumar, K.Pushpa Kumar, S.Kishore</i>	534
80	PI Controller Based Bidirectional Soft Switched Converter for Motor Drive Applications <i>V. C Eugin Martin Raj, R. Giritha, V. Rekha, A. Sowmiya, S. Chandraleka</i>	544
81	Android Based Children Tracking System Using Voice Recognition <i>Manju</i>	552
82	E-Voting System Using Android Smartphone <i>Y.Jenifer, B.Prithivi Bala</i>	557
83	Nanoscale Stiffness Distribution In Bone Metastasis <i>B.Prithivi bala, Y.Jenifer</i>	561
84	Integration disease diagnosis using machine learning & evidence medicine drug identification <i>N.Gobinathan M. Kosalai devi M.Abinaya ,K. Kalaiyarasi</i>	569
85	A Review on Air Powered Vehicles <i>S.Pradeep Devaneyan, C.Subramanian, Thamizh Arasan.R, Ravi Prasath.R</i>	573
86	A Study On Aero Hybrid Concept <i>S.Pradeep Devaneyan, R.Saravanan, D.Mugilan, K.Gokul Raj</i>	576
87	Combined Air Conditioner Water Heater <i>A.Sivakumar, P.Chandru Deva Kannan ,D.Balamurali, Anto Sam</i>	581
88	Compressed-Air Powered Vehicle <i>S.Pradeep Devaneyan, C.Subramanian, D.Balamurali, Anto Sam</i>	585
89	A Study On Green Engine (Piston Less Engine) <i>S.Pradeep Devaneyan, C.Subramanian, Selvamuthukumaran.K, Balaji.R</i>	591
90	Magnetic Piston Under Maglev System <i>S.Pradeep Devaneya, S.Madhanraj, M.Mugilan,R. Calvin</i>	594
91	Tidal Power Plant Using Oscillating Motion <i>A.Sivakumar,P.Chandru Deva Kannan, M.Srinivasa, D.Dhinesh Kumar</i>	599
92	Increasing Efficiency of Two Stroke Petrol Engine By Using Pre-Heating Method <i>A.Sivakumar, P.Chandru Deva Kannan, A.Gokulnath, A.Nithin</i>	602

A review on pediatric foreign body aspiration – An analysis with image processing techniques

Vasumathy M¹, Mythili Thirugnanam²
CSE, VIT College, vasumsse@gmail.com

Abstract— Foreign body aspiration(FBA) is the most common cause of accidental death at home in children. In general foreign body can be describing as the component which is not belonging to the human body. Diagnosis of a foreign body as size, shape and location without history of aspiration has always been a challenge to pediatricians. The evidence has to interpret in a timely and accurate manner to benefit health care of children. Image processing plays major role to resolve this issue. The image processing techniques such as image enhancement& segmentation techniques of are helps to improve the accuracy in the early diagnosis and treatment management process of foreign body aspiration. This paper presents a review of identification FBA with it is location. To bring more efficient way of treatment procedure in FBA, a new methodology is proposed. Some of the recent incidents proved the significance of early identification of location, size and shape of the aspired foreign body. With help a proposed methodology, the complication of treatment procedure of FBA and also percentage of fatal ratio will be reduced.

Keywords- Foreign body aspiration; Medical image processing;

I.INTRODUCTION

Foreign body (FB) aspiration is a common problem in children, requiring on time recognition and early treatment to minimize the serious and fatal consequences. The role of radiology is more important to study the anatomical structures and other regions of the human body, especially in case of pediatric foreign body aspiration the localization of interested region extraction is more important for early diagnosis. X-ray is an electromagnetic radiation, which differentially penetrates structures within the body and creates images of these structures on photographic film or a fluorescent screen. Improper way of image acquisition process leads to image with noise, and some time irrelevant information, intensity problems in images and partial volume effect, data saturation which makes the task of locating and analyzing suspicious area difficult by the doctor. When we adopt image processing methodology, we can bring good quality of image in which diagnosis process of foreign body aspiration more accurate.

II.RELATED WORKS

Vijay G Yaliwal et al. (2014) presented a case study of a 21-year-old female accidental swallowing of double coin. X-ray radiographic before and after oesophagoscopy were made repeatedly to find the missing coin. Tariq O et al. (2013) discussed the clinical findings, sites and types of FBs and outcomes in children who undergone endoscopic management of ingested FBs. H. Rizk et al. (2011) presented a review to assess the incidence of foreign body aspiration in pediatric population to improve prevention, early diagnosis of location and shape and suggested that the physician and especially parental education are more important to reduce this pathology. Mohammed H et al. (2010) presented an analytical study of 62 patient's records with different age group. The age of the patients plays major role for initial radiography image diagnosis. Eti V Upadhyaya et al. (2009) discussed the rare case of multiple coins swallowing with its diagnosis and removal technique. The X-ray radiographic

technique was used for the diagnosis and the treatment was given by esophagoscopy. M M Shaariyah et al. (2009) were presented a review of surgical management of foreign body ingestion and conclude that the plain radiograph is helpful to determine surgical removal. A. M. Shivakumar et al. (2006) reviewed 152 patients (104 children and 48 adults) history with ingested foreign body. X-ray radiological examination was helped for all the patients to find the location of foreign body and removed using the endoscopic for all cases. From the literature, it is clear that the radiography plays major role and proved the significance of early diagnosis process of location size and shape of the aspired foreign body.

III.SAMPLE STATISTICAL DATA ANALYSIS ABOUT FBA

The National Electronic Injury Surveillance System - All Injury Program (NEISS-AIP) of India reported that of an estimated 17537 children aged 14 years or younger who were treated for nonfatal choking, more than half (59.5%) were treated for food-related choking, one third (31.4%) were treated for choking on nonfood items, 13% were associated with coins, and 19% were caused by candy or gum. [1] Accidents occurring commonly in children among one to six years include, poisoning (90%), falls (80.7%) burns and scalds (62.5%), and foreign body aspiration and drowning (42%). [2] Data from the National Security Council reported that approximately 80 percent of cases occur in patients younger than 15 years of age, 20 percent presenting over the age of 15 years. Overall, death from FBA is the fourth leading cause of accidental home and community deaths in the United States with over 4600 fatal episodes of FBA reported during 2014. [3]

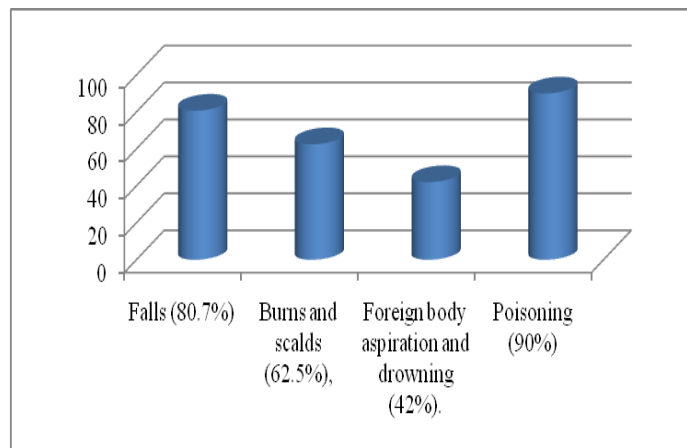


Figure 1. Ratio of pediatric home accidents occurrence

I. SAMPLE CASE STUDY

Foreign body aspiration (FBA) is frequently encountered and is a life-threatening condition in children. The diagnosis of foreign body has always been a challenge for the pediatricians, as the aspiration incident do not have any initial witness and delayed symptoms notification. Some of the recent incidents proved the significance of early identification of location, size and shape of the aspired foreign body.

3.1. Case 1: The failure story

November 13 2015, A 5-year-old girl named Dhamini from ratnagiri dies thinking that eating unexploded crackers as chocolate During deepavali festival that ends up with tragedy of death. The doctor's reports that the fatal is because of delayed diagnosis of symptoms and lack of identifying foreign body location. [5]. Figure 3 shows the paper news reports this incident.



Figure 2. Paper news of case 1 [Courtesy: Dinamalar]

3.2. Case 2: The success story

September 30, 2015 M. Nitish Kumar 11 year-old boy from vellanampatti village near veerakkal ingested a five rupee coin and four-year-old girl T. Keerthika of Karayampatti aspired one rupee coin. A team of doctors, including ENT specialists, at dindigul government headquarter hospital saved the children using laryngoscopy treatment procedure. Finally the doctors reports that the successful removal of foreign bodies are depended on several factors, including location, shape and the type of material. [6]. Figure 3 shows the paper news reports the above incident.



Figure 3. Paper news of case 2 [Courtesy: The Hindu]

IV. CHALLENGES IN DIAGNOSING OF FBA

Most of cases, the symptoms of severe FB aspiration are very noticeable but the localization of aspirated foreign body needs radiography assessment. Radio-opaque foreign body like metal, coin, batteries, bones etc., can be seen on X-ray. The challenge is to identify the radiolucent foreign body objects for example carrot, rubber, pencil, eraser because such objects may not be visualized. It is essential to identify the presence of a foreign body before the surgical extraction, with it is anatomic location, for example larynx, trachea, main lobar or segmented bronchus by identifying the shape, composition, position, and depth of the granulation tissue to reduce the risk level treatment complication. To reduce the noise rate in X-ray images, it is important to determine whether the aspirated foreign body is radio-opaque or not. So this process requires better visualization of interested object region. Shape determination becomes more important for surgical operation that reduces the treatment time. Feature extraction of the intrude object in aspirated pediatric FB images Classification of objects reduces the repeated radiation exposure on children and reduces the misinterpretation of early diagnosis process.

V. DIAGNOSING FBA USING IMAGE PROCESSING TECHNIQUES

Medical Imaging refers to a number of techniques that creates visual representations of the interior of a body for clinical analysis. It can be used to assist diagnosis or treatment of different medical conditions. Image processing plays vital role in medical field. Especially, Image processing techniques developed for analyzing the outputs of medical imaging systems to get best advantage to analyze symptoms of the patients with ease. The radiographic techniques such as X-ray, Computer Topography (CT), Magnetic Resonance Imaging (MRI), are commonly used techniques to analyze the interested regions of the human body. Treatment management of foreign body aspiration is depends on the evidence such as size, shape and location of the aspired foreign body. The evidence has to interpret in a timely and accurate manner to benefit health care of children.

VI. PROPOSED METHODOLOGY

A new methodology is proposed to enhance the quality of image and bring more accurate in diagnosis process of foreign body aspiration. The proposed methodology is shown in figure 4. The steps involved in proposed methodology are enhancement methods, segmentation methods and quantification methods are used to identifying location size and shape of the aspired foreign body in pediatric X-ray images. Enhancement methods such as median filtering and iterative thresholding methods are used to reduce noise and increase the contrast of structure of interest. Segmentation methods are operate based on pixel intensity and texture variations of the images which include Sobel boundary detection and pattern recognition method such as K-Means clustering. Quantification methods are applied to segmented structure to extract the essential diagnostic information such as shape, size, texture and angle. Further using these parameters the procedure of treatment will be predicted.

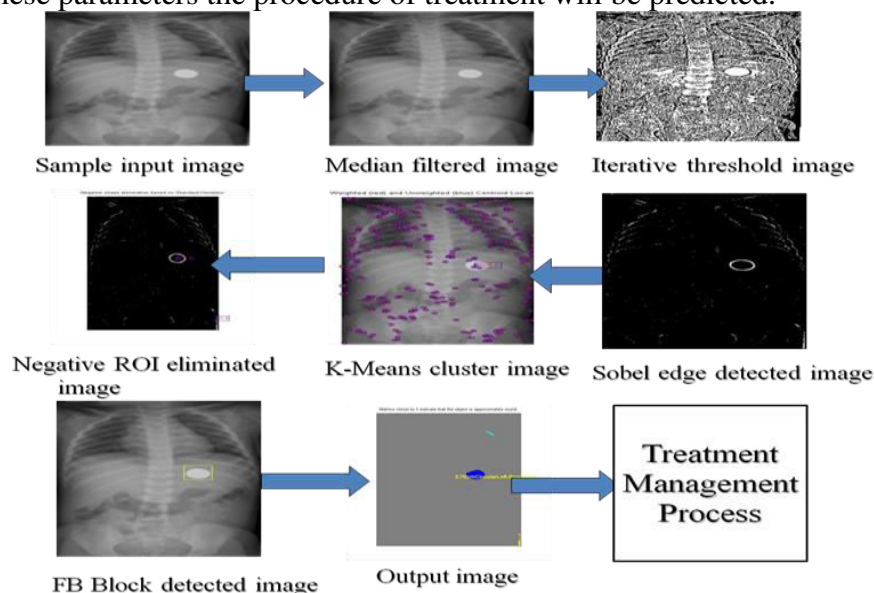


Figure 4. Sample Implementation steps of the proposed work

Table 1. Sample Experimental Results with Suggested Treatment

Img id	Size	Shape	Location	Remarks
coin	2.70 cm	Circle Shape	Left Bronchus	Based on size , shape and location it is Suggested to remove the coin by endoscopy[4] Farzaneh Kaviani et al., (2014),

VIII.CONCLUSION

Foreign body aspiration is a life-threatening event in children that requires early diagnosis and prompt successful management. As it is said ‘prevention is better than cure,’ prevention is the most critical or key in reducing morbidity due to foreign body aspiration. Therefore more effort on caregivers’ education is essential. The case study shows the significance of identifying the foreign body location, size, shape and type of material. At present most of the researchers have contributed their works towards identifying the quality of the X-ray image, but no work carried out especially identifying the location and determining the shape of the intrude object in pediatric foreign body aspirated X-ray images. Hence, there is need for an effective methodology to identify the intrude object automatically with less processing time to assist the medical practitioners to make right decision on right time.

REFERENCES

- [1] Jackson C, Jackson CL. Diseases of the air and food passages of foreign body origin. Philadelphia, PA: Saunders; 1936
- [2] Jayalakshmi LS. Mothers’ awareness about accidents among toddlers. The Nursing Journal of India , Dec;25(12):276-8, 2004.
- [3] National Safety Council. Report on injuries. Injury Facts. 2011 information online: <http://www.nsc.org/learn/safety-knowledge/Pages/safety-at-home.aspx> (Accessed on December 24, 2015).
- [4] Farzaneh Kaviani, Reza Javad Rashid, Zahra Shahmoradi and Masoud Gholamian, ‘Detection of Foreign Bodies by Spiral Computed Tomography and Cone Beam Computed Tomography in Maxillofacial Regions’, *J Dent Res Dent Clin Dent Prospects*, Vol.8, No.3, pp.166–171, 2014.
- [5] [Online] <http://www.indianpediatrics.net/mar2005/mar-288-290.htm>
- [6] [Online] <http://www.thehindu.com/news/national/tamil-nadu/doctors-at-dindigul-gh-take-out-coins-ingested-by-two-children/article7704366.ece>
- [7] Vijay G Yaliwa, Harihar V Hegde, JS Arunkumar, Santosh S Garag, P Raghavendra Rao, Foreign body oesophagus: The case of a missing second coin, *Indian Journal of Anaesthesia* , 58 ,3,364-365, 2014.
- [8] Tariq O. Abbas.; Noora Al Shahwani.; Mansour Ali, ‘Endoscopic management of ingested foreign bodies in children: A retrospective review of cases, and review of the literature’, *Open Journal of Pediatrics*, 3(2), 428-435, 2013.
- [9] Mohammed H. Nemat.; Abdulameer M.Hussein.; Uday H.Juma, ‘Management of Esophageal Foreign Bodies, retrospective study’, *Fac Med, Baghdad*, 53(1), 6-11, 2011.
- [10] Eti V Upadhyaya.; Punit Srivastava.; Vijay D Upadhyaya.; AN Gangopadhyay.; SP Sharma.; DK Gupta.; and Zaheer Hassan, ‘Double coin in esophagus at same location and same alignment — a rare occurrence: a case report’, *Cases Journal*, Retrieved April 24, 2015, from <http://www.casesjournal.com/content/2/1/7758>, 2009.
- [11] M M Shaariyah, MD.; B S Goh, ‘Retrospective Review of Surgical Management of Foreign Body Ingestion’, *Med J Malaysia*, 64(4), 1085-1091, 2009.
- [12] A. M. Shivakumar.; Ashok S. Naik.; K. B. Prashanth.; Girish F. Hongal.; Gaurav Chaturvedy, ‘Foreign bodies in upper digestive tract’, *Indian Journal of Otolaryngology and Head and Neck Surgery*, 58 (1), 63-68, 2006.

A Knowledge Discovery Framework for Healthcare Using BDCAM

Mrs. Arunakumari.S¹, Mr.A.Akilan², Mrs.M.Senthamarai Selvi,M.E.,
CSE, MRK college,akilancs@gmail.com
CSE,stannescet,senthamaha@gmail.com

Abstract-In this paper Context-aware monitoring is a rising technology in which the real-time personalized health-care services and a loaded area of big data application. In this paper, we recommend a new concept which is knowledge discovery-based approach that allows the context-aware system to adapt its behavior in runtime by assessing large amounts of data generated in ambient assisted living (AAL) systems and stored in cloud repositories. The proposed BDCaM model facilitates analysis of big data inside a cloud environment. It first mines the trends and patterns in the data of an individual patient with associated probabilities and utilizes that knowledge to learn proper abnormal conditions. The outcomes of this learning method are then applied in context-aware decision-making processes for the patient. A use case is implemented to illustrate the applicability of the framework that discovers the knowledge of classification to identify the true abnormal conditions of patients having variations such as in blood pressure (BP) and heart rate (HR) ,etc..., . The evaluation shows a much better estimate of detecting proper anomalous situations for different types of patients. The accuracy and efficiency obtained for the implemented case study demonstrate the effectiveness of the proposed model.

Index Terms Context awareness, Assisted Healthcare, Cloud Computing, BigData, Knowledge Discovery, Data Mining

1 INTRODUCTION

AN ambient assisted living (AAL) system consists of heterogeneous sensors and devices which generate huge amounts of patient-specific unstructured raw data everyday [1], [2]. Due to diversity of sensors and devices, the captured data also have wide variations. A data element can be from a few bytes of numerical value (e.g. HR = 72 bpm) to several gigabytes of video stream [3]. For example, if we assume a single AAL system generates 100 kilobytes data every second on average then it will become 2.93 terabytes in one year. If any system targets to support say, 5 million patients, then the data amount will be 14 exabytes per year 1. Even if a healthcare system targets to analyze only continuous ECG of cardiac patients in real-time inside the cloud environment [4], [5], then it will produce around 7 PetaBytes data everyday from 3.5 million patients [6] 2. Including these dynamically generated continuous monitoring data, there are also huge amounts of persistent data such as patient profile, medical records, disease histories and social contacts. If we want to store all these data and patient histories to predict any future abnormality accurately, then the representation of data will be in zeta bytes in a few years. Such concerns necessitate the development of cloud-based assisted healthcare infrastructure [7]. According to IBM data scientists, big data can be characterized in four dimensions: volume, variety,velocity, and veracity (“the 4 V’s”) [9]. Our model also satisfies these four V’s because the context-aware data we are referring to have massive variations (e.g. health data, activity data), is large in volume (several petabytes), continuous in terms of velocity and accurate to satisfy veracity.

Such data also have great value and high impact on future healthcare infrastructure. Furthermore, the growing ageing population and chronic diseases, particularly in Australia and other western nations, increase the demand for a common platform that is capable of handling many patients simultaneously and maintaining the personalized knowledge of every user. This necessitates the initialization of such big data-centric context-aware applications on cloud environments [7].

In a home healthcare system, a typical architecture involves body sensors, ambient and smart sensors, devices, actuators and software services that collect data from a target user who lives alone and has some kind of disability [1]. The data is collected continuously at different times of the day and also, in some cases, on a demand basis. The identification of a patient's abnormal condition can warn the patient by activating a local device (e.g. medication reminder), or send an emergency message to the monitoring centre. Overall, our innovative learning technique on a massive volume of context data enables reliable classification of a patient's situation for qualitative remote monitoring support, using the advantage of cloud computing.

1.1 Motivation

. The main motivations are the following.

- The need for an abstract context-aware framework that improves the confidence of abnormality detection in the home healthcare environment by correlating physiological statistics with various physical activities and environmental factors.
- The use of cloud computing enables faster learning with greater knowledge from continuously generated big data gathered from heterogeneous contexts of various assisted living systems. This also improves the discovery of user-specific rules with stronger support.
- The improved knowledge of understanding the patient's situation through iterative learning of present contexts and substantial historical data can reduce the transmission of repeated false alerts to the remote monitoring systems.

1.2 CONTRIBUTION

The primary contributions of our work are as follows.

- We build an innovative architectural model for context-aware monitoring ,BDCaM that uses cloud computing platforms . Every generated context of AAL systems are sent to the cloud. A number of distributed servers in the cloud store and process those contexts to extract required information for decision-making using this novel technique.
- We develop a 2-step learning methodology. In the first step, the system identifies the correlations between context attributes and the threshold values of vital signs. Using Map Reduce Apriori algorithm over a long term context data of a particular patient, the system generates a set of association rules that are specific to that patient. In the second step, the system uses supervised learning over a new large set of context data generated using the rules discovered in the first step. In this way, the system becomes more robust to accurately predict any patient situation.

1.3 Rest of the paper

The rest of this paper is organized as follows. Section 2 contains the background. The architecture of the BDCaM model is presented in Section 3. Section 4 describes the definitions and concepts used for the model. Section 5 introduces the detailed methodology and algorithms used for the model. Case studies along with experimental evaluations of the proposed methodology are illustrated in Section 6.

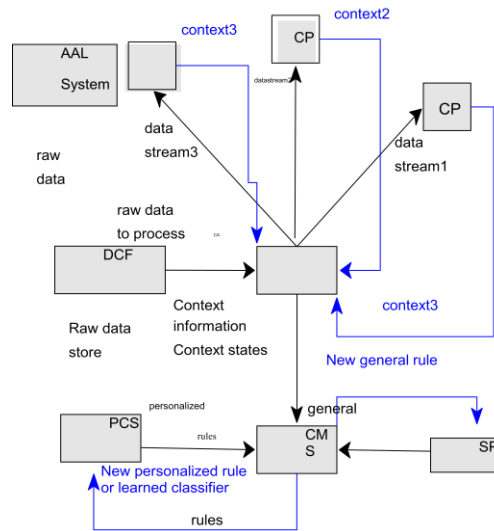
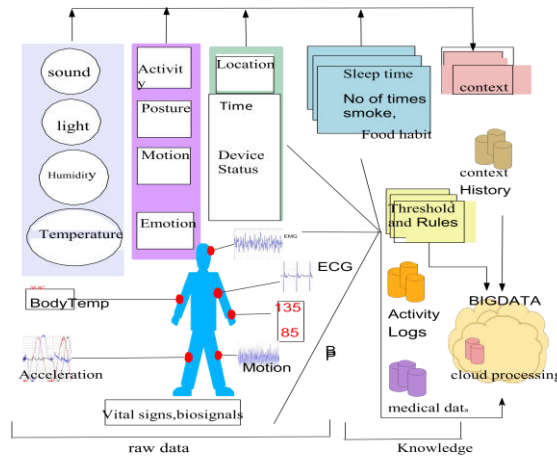


Fig 1 The complete architecture of BDCaM model showing
 Fig. 2. Data flow between cloud all the cloud-based components of the system.

II.BACKGROUND

In the research literature, many examples introduce an integrated system using big data for context awareness in assisted healthcare. However, most systems are described from an architectural point of view and there has been no practical implementation of any of those systems [20], [21]. In our previous paper, we described the CoCaMAAL [7] model and here we have extended that model to illustrate the learning process from big context-aware data to find abnormalities in an individual patient. In our system, we have used the MapReduce-Apriori algorithms proposed in [19] which is an effective process to measure correlations between context attributes. MapReduce is also an efficient programming model to process big data using distributed clusters. In an AAL system, most of the generated contexts are numerical or categorical.

Therefore, together with MapReduce-Apriori, we used the techniques described in [22] to generate rules using numerical attributes of our model. As we do not intend to explore the generation, pre-processing and transmission of real sensor data in the present work, we have assumed that subsystems are responsible for doing this from existing knowledge.

III.ARCHITECTURE

The general architecture of the proposed knowledge discovery-based context-aware framework for assisted healthcare designed over big data model is visualized in Figure 1. The

flow of raw data, context, rules and services between different distributed components are also shown in Figure 1 and as a workflow diagram in Figure 2. The overall architecture can be split into five cloud components. The following subsections discuss different components of the framework in brief.

3.1 Ambient Assisted Living (AAL)

The big data producers of BDCaM model are a large number of AAL systems. The low level setup of each system varies according to the requirements of the patient. The sensors, devices and software services

of each AAL system produce raw data that contain low level information of a patient's health status, location, activities, surrounding ambient conditions, device status, etc. To learn the daily activity patterns of the patient and the effects of other contexts on his/her medical conditions, all data need to be stored and processed. The high level contexts are obtained from these low level data.

3.2 Personal Cloud Servers (PCS)

Each AAL System is connected to a personal cloud server (as in Figure 1). This is a virtual server in the cloud that is highly scalable and managed by trusted entities. It has secure storage facilities to store patient-specific information (e.g. Amazon S3, Microsoft HealthVault) such as the profile (e.g. age, sex, BMI), recognized patterns of his/her daily activities (e.g. smoking habits), identified threshold values of different vital signs [23], medication times, disease treatment plans, prescriptions, preferences, emergency contacts and personal medical records. The local processing device in the AAL system (data collector) can easily exchange information with the PCS. In some cases, the PCS can contain the latest pathological and laboratory test reports, biomedical images (e.g. X-rays) or even raw sensor data (e.g. the latest ECG) that is produced in the AAL system.

3.3 Data Collector and Forwarder (DCF)

Traditional context-aware systems process the low level data and perform the computation in a local server or mobile device and then forward the high level context data to the cloud . But the lack of storage and power in wearable sensors and mobile devices limit them to process large volume of sensor data using decent computational methods. In our proposed model, the job of a local server (which can be a mobile device) is only to collect the low level data (e.g. accelerometer data, ECG data, BP Monitor data, GPS coordinates, RFID status, captured images) from the AAL system and forward them directly to the CA (when processing is required) or to the PCS (Figure 1 and 2) . From current knowledge we are assuming that the DCF has the mechanisms (e.g. blue-tooth) to communicate with all sensors and devices that produce raw data. The computations for the conversion from low level data to a high level context are performed inside cloud servers.

3.4 Context Aggregator (CA)

The job of the context aggregator (CA) is to integrate all the primitive contexts in a single context state using a context model [7]. Sometimes a single context attribute value as an individual has no meaning if it is not interrelated with other contexts. For example, an increment in HR seems an abnormal condition as a single context, but if the user doing exercise, this can be a normal situation. So, using past and present contexts, it can be determined whether the current user situation is normal or not. Therefore, all the contexts need to be aggregated to classify a situation [25] accurately. The CA does this work and forwards the information to the context management system for the individual user.

3.5 Context Providers (CP)

The context providers (CPs) cloud is the main source for generating contexts. The CA distributes the low level data collected from different AAL systems to multiple CPs. Each CP applies well-known techniques to obtain primitive context from the low level data. For example, in applying data mining on accelerometer data it can identify the current activity of the user [26], [27]; using GPS it can identify the location context of the user; it can extract HR value from ECG data and, so on. CP then delivers the converted context with possible high level values to the CA (Figure 2).

3.6 Context Management System (CMS)

A Context Management System (CMS) is the core component of the framework. The CMS consists of a number of distributed cloud servers that hold the big data. It stores the context histories of millions of patients. Different machine learning techniques run inside the CMS that infer different personalized and generic rules for various user events. When the CMS discovers any personalized rules, they are sent to the corresponding PCS. Any newly identified generic rules are forwarded to the service provider's (SP) cloud. This is how the CMS keeps every component of the model up to date with new knowledge. Sometimes, existing rules are required to reason new high level knowledge.

3.7 Service Providers (SP)

In the BDCaM model, the service providers are the cloud servers that sustain the generic medical rules to identify various types of diseases and symptoms. The rules of symptoms and anomalous behaviours are continuously updated by medical experts, doctors and other medical service providers. When any new rule is discovered in the CMS it also triggers the change in the SP cloud. The CMS uses rules of SP for data filtering and classification.

3.8 Remote Monitoring Systems (RMS)

When the CMS discovers any anomalous pattern in the context for a specific user it sends appropriate notification to the RMS. For example, when the BP level of a patient goes relatively high for a given situation, the CMS alerts the doctor to investigate it, but if it goes abnormally high then the CMS sends alerts to the emergency centre. Thus, the selection of RMS depends on situation classification. A major goal of our system is to classify a situation correctly to send proper alerts to the right RMS.

V. SYSTEM FUNCTIONALITIES

5.1 Context Conversion

The data collector module runs in the local server (e.g. mobile device), collects the raw data from an AAL system and forwards them to the CA cloud. As described, the CPs convert low level data to high level context and send them back to the CA cloud (Figure 1 and 2). From existing research literature we assumed that such capabilities of context conversions already exist. To make the computation simpler, each context attribute value set A_i is converted to a numerical value. Some context attributes already have numeric values (e.g. HR, BP, room temperature). Numerical annotations are used for contexts having nominal value (e.g. activity). The static or historical context that have Boolean values (e.g. symptoms) are combined in a single binary string which results a decimal value (e.g. 001100 converted to 12). So, after such numerical conversion every A_i has the value set described in Definition 1.

5.2 Context Aggregation

For a single AAL system, after converting all the context attributes to numerical values described above, the context information (as in Definition 2) for each of the domain are generated. Then they are converted to a context state. This is the aggregated information of all context domains at a specific time of the AAL system. Before converting to context information, some processing such as the elimination of clinically insignificant values, is required. Some attributes have discrete time intervals (e.g. BP measured in time interval t) and some have time duration (e.g. activity x starts at t_s and end at t_e). To represent everything in a single time(t) slot, a standard time interval is chosen. That is, a context state is sampled in interval

5.3 Trend Analysis

All generated context states and context information are sent to the CMS cloud. The CMS stores those inside its cloud repository. One of the roles of the CMS is to detect the trend in the dataset. Some of the patterns are detected using statistical analysis. For example, by summing up the duration of sleeping activity it is possible to summarize how many hours the user usually sleeps in one night. Using this statistic, the daily mean of sleep hours can be measured say, from the observation of 1 month's data. So, for any new data if there is a large deviation of sleep hours from the mean, then it is considered as less sleep symptom. When any symptom is detected from the trend, the CMS acts as a CP and notifies CA. CA then includes this in the IDs of next context state. In this way, other symptoms (e.g. smoking, weight gain, less exercise) can also be detected.

5.4 Correlations Learning and Association Rule Mining

This is the knowledge acquisition phase as shown in Figure 4 and the major part of the learning process of our model. Once m number of context states are gathered in the cloud storage of the CMS for an AAL system j (Definition 4), it starts this learning process. In this phase, the associations between context attributes are measured. Let after aggregation, a context state $C_j t$ contains q different context attributes which is represented by, $C_j t = \{a_{tj} | j=1,2,\dots,q \text{ and } a_{tj} \in A_{ij}\}$. The situation space for context state $C_j t$ can be described as, $S_j = \{a_{tj} | j=1,2,\dots,q \text{ and } a_{tj} \in A_{ij} \text{ and } L_{A_{ij}}\}$ and $L_{A_{ij}}$ is length of value set A_{ij} . That is, set S_j has every possible combination of all a_{tj} . When most of A_{ij} have numerical value ranges, S_j become an infinitely large set. For this reason, S_j is reduced to S_{mj} by attribute value minimization process which is described in Algorithm 2 can run in parallel in multiple clusters inside the CMS. This algorithm significantly reduces the situation space that is used for rule generation. It generates the minimized value set of vital signs using statistical features.

5.5 Learning using the Association Rules

After discovering the knowledge of every AAL system j , the next step is to verify the validity of this learning process using a new set of big data. When a new context state $C_j t$ arrives in the CMS cloud, it classifies the state according to the rules and thresholds found in decision vector U_j . In case of conflict, the CMS uses the rule that has the highest confidence value in P_j .

Let, the classification result of context state $C_j t$ is $r_j t$ where r_j Result. The set, Result contains nominal value such as normal, warning, alert, emergency. After classifying $C_j t$ using U_j the data instance $C_j t$; $r_j t$ is stored in the CMS cloud. When a large number of such instances is available, the CMS uses that big dataset for building a classifier model. The classifier is used for future classification.

5.6 Data Mining

The dataset generated in the previous phase is used to build classifiers for AAL system j and so any new context state can be classified accurately and immediately. The dataset is subdivided into training and test set. Different data mining [33] algorithms (e.g. Multi Layer Perceptron, Decision Table, J48 Decision Tree, Radial Basis function, Bayes Network) are applied over training data and the accuracy of classification is obtained using test data. Comparing the accuracies of different classifiers, the CMS picks the best classifier for decision support. The training and classification process run in distributed clusters inside the CMS.

5.7 Context-aware Decision Support

The CMS uses the classifier generated in the data mining step to classify forthcoming context states and make context-aware decisions. Based on the classification the CMS performs following actions.

- If a situation is normal then do nothing.
- If a situation is abnormal but not dangerous then sends a warning to the user.
- If any vital context attribute has abnormal value then send alert to doctor.
- If two or more context attributes are abnormal or anyone is extremely abnormal then notify to emergency.

VI. USE CASE IMPLEMENTATION

In accordance with the BDCaM functional components described in the previous sections, a case study is implemented to evaluate our algorithms. The objectives of this implementation are: (i) discover knowledge of BP and HR changes on different situations [34] for different patients; (ii) find association rules for specific patient situations using a distributed cloud model, and (iii) classify an unknown situation based on the learned model.

6.1 Description of use case

The continuous BP level of a patient is determined by examining systolic BP (SBP) and diastolic BP (DBP) values in mmHg using a body worn BP sensor, and HR is measured in bpm using the ECG sensor [1], [35]. Abnormal BP or HR is difficult to diagnose and treat if they are only measured once or twice a day. The variations in BP and HR occur due to changes in ambient temperature, physical activity, noise, sleep, fatigue, stress etc. (e.g. HR is high for exercise, BP is high for eating) [36], [37].

TABLE 1:

Different patient categories considered in the experiment and their average values of vital sign

PATIENT NAME	BP LEVEL	PULSE RATE	PH LEVEL	DIABETC PRE / POST
P1	126	85	0.74	-
P2	140	78	0.76	PRE
P3	170	96	0.8	POST

6.2 Synthetic data generation

To validate a learning model that uses a large amount of data, it is important to have data which are very similar to real data. To the best of our knowledge, no real-life dataset that contains daily monitoring data of a patient for a relatively long period is publicly available. Therefore, the first step is to generate data based on continuous BP and HR monitoring that is well established in medical practice. So artificial data are generated using some real medical

observations. The dataset of continuous BP and HR monitoring by Faini [40] and Parati [41] are used for this purpose. The dataset from Physionet MIMIC-II database [42] is also used, because this contains a large number of samples of multiple vital signs (including SBP, DBP and HR). Some of the MIMIC-II records contain more than 24 hours ICU patient data. From these referred works the distributions of SBP, DBP and HR in a day for different patient categories (as in Table 1) during different activities are measured.

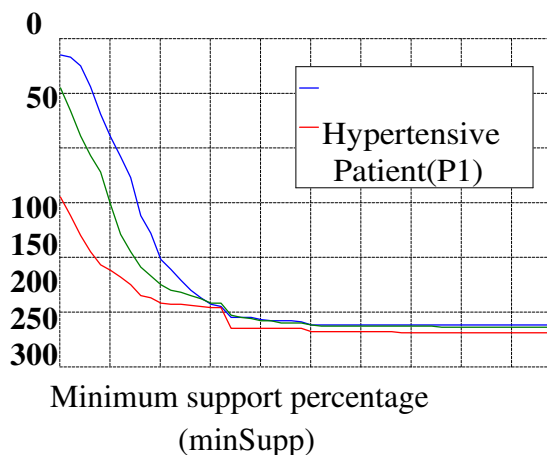
6.3 Cloud evaluation

As described in the previous step, synthetic data taken over 1 year for 3 patients are generated using 15 minutes sampling intervals that results in 35,040 samples per patient. So, the generated data satisfy variety property. The dataset will be very large if millions of patients are considered (instead of 3) and thus it satisfies volume property. A java worker thread is implemented to simulate an AAL system. Multiple threads run in parallel that simulate the scenario of many AAL systems simultaneously send data to the cloud. In our simulated environment, 1 minute is normalized to 1 millisecond (ms). To simulate the velocity of big data, the java worker thread reads one sample of synthetic data from local files every 15 ms and sends it to the Google Cloud Storage (GCS) [16]. The obtained results are compared and discussed in Section 7.

- Standalone mode: Where the algorithms of association rule generation are run as a sequential process on a single core.
- Pseudo-distributed mode: Where the algorithms are run as a parallel process on 2 to 4 cores. Each core has the same processing capability.
- Cloud mode: Where the algorithms are run on a public cloud using Amazon Elastic MapReduce with 1 master and 2 slave clusters.

VII. IMPLEMENTATION

Using the methodology described in Section 5, the correlations of BP and HR with other context attributes (e.g. activity, last activity, symptoms) are measured to predict the accurate state for a context situation. The domains and the context attributes along with their value set considered in the experiment are presented.



The change in number of rules with minSupp values

RESULTS AND DISCUSSION

To evaluate the sensibility, we compared the situation classification of our model with generalized clinical classification based on medical rules [38], [39]. shows the result of such comparison. In general, the rule is that when SBP and DBP values go above/below a certain threshold (e.g. SBP above 135 and DBP below 85 for hypertension) then the situation is

classified as abnormal. An emergency state is not identifiable; it is the doctor's responsibility to manually analyse the values and then make a decision. The term general medical rule is adopted because this is the current manner in which traditional context-aware [24] systems process vital signs data. In contrast, our system learns these patient-specific thresholds and quickly adapts to new changes.

VIII. RELATED WORK

There have been several studies about the context aware approach for assisted healthcare. The works are differentiated by: context-aware platforms for supporting continuous care [24], activity monitoring [50], [30], cloud-based healthcare [21], [51] and personalized care [17]. The context-aware systems that are developed using rule-mining and data mining only proposed systems are restricted to supporting some specific context-aware services and are not capable of detecting a wider range of anomalies. The system that relies on generic rules is not able to predict all the critical situations and suffers from misclassification of normal situations. The studies of big data for healthcare mostly focus on the area of mining electronic health records [53], feature extraction from medical images or pattern recognition based on genome data.

IX. CONCLUSION AND FUTURE WORK

In this work, we have presented BDCaM, a generalized framework for personalized healthcare, which leverages the advantages of context-aware computing, remote-monitoring, cloud computing, machine learning and big data. Our solution provides a systematic approach to support the fast-growing communities of people with chronic illness who live alone and require assisted care. The model also simplifies the tasks of healthcare professionals by not swamping them with false alerts. The system can accurately distinguish emergencies from normal conditions. The data used to validate the model are obtained via artificial data generation based on data derived from real patients, preserving the correlation of a patient's vital signs with different activities and symptoms. The stronger relationship between vital signs and contextual information will make the generated data more consistent and the model will be more accurate for validation.

REFERENCES

- [1] A. Pantelopoulos and N. Bourbakis, "A survey on wearable sensor-based systems for health monitoring and prognosis," *IEEE Transactions on Systems, Man, and Cybernetics, Part C: Applications and Reviews*, vol. 40, no. 1, pp. 1–12, 2010.
- [2] D. N. Monekosso and P. Remagnino, "Behavior analysis for assisted living," *IEEE Transactions on Automation Science and Engineering*, vol. 7, no. 4, pp. 879–886, 2010.
- [3] P. Groves, B. Kayyali, D. Knott, and S. Van Kuiken, "The big data revolution in healthcare," *McKinsey & Company*, 2013.
- [4] S. Pandey, W. Voorsluys, S. Niu, A. Khandoker, and R. Buyya, "An autonomic cloud environment for hosting ecg data analysis services," *Future Generation Computer Systems*, vol. 28, no. 1, pp. 147–154, 2012.
- [5] A. Ibaida, D. Al-Shammary, and I. Khalil, "Cloud enabled fractal based ecg compression in wireless body sensor networks," *Future Generation Computer Systems*, vol. 35, pp. 91–101, 2014.
- [6] Australian bureau of statistics - 4821.0.55.001 – cardiovascular disease in australia: A snapshot, 2004-05. [Online]. Available: <http://www.abs.gov.au/ausstats/abs@.nsf/mf/4821.0.55.001>
- [7] A. Forkan, I. Khalil, and Z. Tari, "Cocamaal: A cloud-oriented context-aware middleware in ambient assisted living," *Future Generation Computer Systems*, vol. 35, pp. 114–127, 2014.
- [8] A. K. Dey, "Providing architectural support for building context-aware applications," Ph.D. dissertation, Georgia Institute of Technology, 2000.
- [9] S. B. Siewert. (2013, July) Big data in the cloud. [Online]. Available: <http://www.ibm.com/developerworks/library/bdbigdatacloud/bd-bigdatacloud-pdf.pdf>
- [10] J. J. Oresko, Z. Jin, J. Cheng, S. Huang, Y. Sun, H. Duschl, and A. C. Cheng, "A wearable smartphone-based platform for realtime cardiovascular disease detection via electrocardiogram processing," *IEEE Transactions on Information Technology in*

Biomedicine, vol. 14, no. 3, pp. 734–740, 2010.

- [11] S. Sridevi, B. Sayantani, K. P. Amutha, C. M. Mohan, and R. Pitchiah, “Context aware health monitoring system,” in *Medical Biometrics*. Springer, 2010, pp. 249–257.
- [12] C. R. Leite, G. Sizilio, A. Neto, R. Valentim, and A. Guerreiro, “A fuzzy model for processing and monitoring vital signs in icu patients,” *BioMedical Engineering Online (Online)*, vol. 10, p. 68, 2011.
- [13] H. Ding, Y. Moodley, Y. Kanagasigam, and M. Karunanithi, “A mobile-health system to manage chronic obstructive pulmonary disease patients at home,” in *Annual International Conference of the IEEE Engineering in Medicine and Biology Society (EMBC)*, 2012. IEEE, 2012, pp. 2178–2181.
- [14] Amazon web service. [Online]. Available: <http://aws.amazon.com/>
- [15] Windows azure. [Online]. Available: <http://azure.microsoft.com>
- [16] Google app engine. [Online]. Available: <https://cloud.google.com/appengine/docs>
- [17] E. Baralis, L. Cagliero, T. Cerquitelli, P. Garza, and M. Marchetti, “Cas-mine: providing personalized services in context-aware applications by means of generalized rules,” *Knowledge and information systems*, vol. 28, no. 2, pp. 283–310, 2011.
- [18] R. Buyya, C. Yeo, S. Venugopal, J. Broberg, and I. Brandic, “Cloud computing and emerging it platforms: Vision, hype, and reality for delivering computing as the 5th utility,” *Future Generation computer systems*, vol. 25, no. 6, pp. 599–616, 2009.
- [19] G. Wu, H. Zhang, M. Qiu, Z. Ming, J. Li, and X. Qin, “A decentralized approach for mining event correlations in distributed system monitoring,” *Journal of Parallel and Distributed Computing*, 2012.
- [20] A. Mukherjee, A. Pal, and P. Misra, “Data analytics in ubiquitous sensor-based health information systems,” in *6th International Conference on Next Generation Mobile Applications, Services and Technologies (NGMAST)*, 2012. IEEE, 2012, pp. 193–198.
- [21] D. Hoang and L. Chen, “Mobile cloud for assistive healthcare (mocash),” in *IEEE Asia-Pacific Services Computing Conference (APSCC)*, 2010. Ieee, 2010, pp. 325–332.
- [22] R. Rastogi and K. Shim, “Mining optimized association rules with categorical and numeric attributes,” *IEEE Transactions on Knowledge and Data Engineering*, vol. 14, no. 1, pp. 29–50, 2002.
- [23] V. S. Tseng, L.-C. Chen, C.-H. Lee, J.-S. Wu, and Y.-C. Hsu, “Development of a vital sign data mining system for chronic patient monitoring,” in *International Conference on Complex, Intelligent and Software Intensive Systems*, 2008. CISIS 2008. IEEE, 2008, pp. 649–654.
- [24] F. Paganelli, E. Spinicci, and D. Giuli, “Ermhan: a contextaware service platform to support continuous care networks for home-based assistance,” *International journal of telemedicine and applications*, vol. 2008, p. 4, 2008.
- [25] J. Ye, S. Dobson, and S. McKeever, “Situation identification techniques in pervasive computing: A review,” *Pervasive and Mobile Computing*, vol. 8, no. 1, pp. 36–66, 2012.
- [26] E. M. Tapia, S. S. Intille, and K. Larson, *Activity recognition in the home using simple and ubiquitous sensors*. Springer, 2004.
- [27] N. Ravi, N. Dandekar, P. Mysore, and M. L. Littman, “Activity recognition from accelerometer data,” in *AAAI*, 2005, pp. 1541–1546.
- [28] Y. Oh, J. Han, and W. Woo, “A context management architecture for large-scale smart environments,” *IEEE Communications Magazine*, vol. 48, no. 3, pp. 118–126, 2010.
- [29] T. Gu, L. Wang, Z. Wu, X. Tao, and J. Lu, “A pattern mining approach to sensor-based human activity recognition,” *IEEE Transactions on Knowledge and Data Engineering*, vol. 23, no. 9, pp. 1359–1372, 2011.
- [30] M. Amoretti, S. Copelli, F. Wientapper, F. Furfari, S. Lenzi, and S. Chessa, “Sensor data fusion for activity monitoring in the persona ambient assisted living project,” *Journal of Ambient Intelligence and Humanized Computing*, vol. 4, no. 1, pp. 67–84, 2013.
- [31] R. Agrawal, R. Srikant et al., “Fast algorithms for mining association rules,” in *Proc. 20th Int. Conf. Very Large Data Bases, VLDB*, vol. 1215, 1994, pp. 487–499.
- [32] J. Dean and S. Ghemawat, “Mapreduce: simplified data processing on large clusters,” *Communications of the ACM*, vol. 51, no. 1, pp. 107–113, 2008.
- [33] P. Haghghi, A. Zaslavsky, S. Krishnaswamy, and M. Gaber, “Mobile data mining for intelligent healthcare support,” in *42nd Hawaii International Conference on System Sciences, HICSS ’09*, 2009.
- [34] T. Tamura, I. Mizukura, M. Sekine, and Y. Kimura, “Monitoring and evaluation of blood pressure changes with a home healthcare system,” *IEEE Transactions on Information Technology in Biomedicine*, vol. 15, no. 4, pp. 602–607, 2011.
- [35] F. Sufi and I. Khalil, “Diagnosis of cardiovascular abnormalities from compressed ecg: A data mining-based approach,” *IEEE Transactions on Information Technology in Biomedicine*, vol. 15, no. 1, pp. 33–39, 2011.

Real time hand gesture controlled autonomous system using arduino duemilanove

K.Latha¹, D.Mahalakshmi², P.Manjamadevi³
CSE,VRS college,manjama1612@gmail.com

Abstract— Now a day's robots are most important in this world. Based on the gesture can control we can control the robots. We give robots and using the Kinect sensor wireless robot to recognize the human gesture movement. Therefore, human interacting with the robotic system .Gesture is a most natural way of communication between human and robotic systems and it is very user friendly interface. The command signals are generated by gesture using image processing. These systems are navigate the wireless robots in specific direction.

Keywords— Gestures; OpenCV; Arduino; WiFly; L293D; Web cam.

I. INTRODUCTION

In today's age, the mechanical business has been creating numerous new patterns to build the effectiveness, openness and exactness of the frameworks. These days, a large portion of the human computer interaction (HCI) depends on equipment gadgets, for example, consoles, mouse, joysticks or gamepads. Fundamental undertakings could be employments that are hurtful to the human, tedious occupations that are exhausting, unpleasant and so forth. Despite the fact that robots can be a substitution to people, regardless they should be controlled by people itself. Robots can be wired or remote, both having a controller gadget. Both have advantages and disadvantages connected with them. Past controlling the automated framework through physical gadgets, late technique for signal control has turned out to be extremely main stream. This mostly includes Image Processing and Machine Learning for the framework or application advancement.

II. EXISTING SYSTEMS

Many systems exist that are used for controlling the robot through gestures. Some gesture recognition systems involve, adaptive color segmentation [1], hand finding and labelling with blocking, morphological filtering, and then gesture actions are found by template matching and skeletonizing. This does not provide dynamicity for the gesture inputs due to template matching. Analog flex sensors are used on the hand glove to measure the finger bending [3], also hand position and orientation are measured by ultrasonic for gesture recognition [4]. And in another approach, gestures are recognized using Microsoft Xbox 360 Kinect(C) [5].

III. PROPOSED SYSTEM

We propose a system, using which the user can navigate the wireless robot in the environment using various gestures commands. In this system, user operates the robot from a control station that can be laptop or a PC with a good quality in-built web cam or external webcam. This webcam is used to capture the Gesture image. Gesture commands are given using hand palm. Robot is moved in all possible directions in the environment using four possible types of commands which are Forward, Backward, Right and Left. Image frame is taken as an input and processed using Image Processing. Processed image is then used to extract the gesture command.

Generated signal is stored in the file at the control station. The Wi-Fi shield transmit the signal to the Arduino micro controller. Arduino takes this signal as input from the Wi-Fi shield and generates some output signals that are passed to the motor driver. Based on the input signal the output signal (command) is generated. The command signal is passed through the robot. Figure 1 shows basic flow of the system.

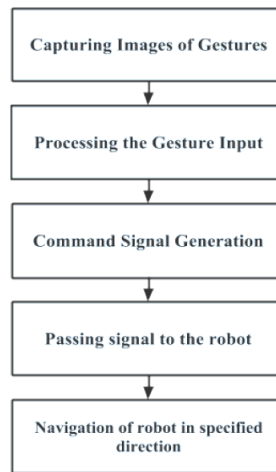


Figure.1.Basic Flow of a system

IV.DESIGN

1. Capturing Gesture Movements

The end result of gesture recognition system is to generate a command and that is given to the robot. There are mainly four possible gesture commands that can be given to the robot (Forward, Backward, Right and Left). It has two ways. First method is the Finger Count and second is on the direction given by the hand palm. Both methods involve recognition of the palm and process.

2. Hand Palm Detection

1. Thresholding of an Image Frame

An image frame is taken as input through webcam. Binary Thresholding is then done on this image frame for the recognition of hand palm. Initially minimum threshold value is set to a certain constant.

2. Drawing Contour and Convex Hull

After thresholding an image frame, contour is determined and drawn on the threshold white blob. Number of contours generated will be many due to noise. So threshold value is incremented and same procedure is applied till one contour is generated. A convex hull is drawn around the generated contour points. Convexity defect is used to generate the list of defects in the convex hull. This is in the form of vectors that provides all the defect parameters which includes defect point in the contour, depth of the defect, start point and end point of the line in the convex hull for which defect has occurred.

3. Command Detection using Specified Method

1. Finger Count based Gesture Control.

The convexity defect's list provides depth parameters for every defect. Defects with the highest depth are easily extracted from the list. These defects are basically gaps between two consecutive fingers. Finger count is determined as one more than the number of defects. For example, for one defect, finger count is two. Thus each count from two to five can be specified as a command for robot to move in the particular direction.

2. Direction of Hand Palm Gesture Control.

In this method instead of giving a finger count, direction of the palm is used to determine the gesture command. Convexity defect specifies the depth point, start point and end point for the line of convex hull where the defect has occurred. Start and end points of the line specify fingertip. By comparing these point coordinate values, command is predicted. For this comparison the midpoint on the defect line is taken into consideration for calculations. This midpoint is then compared with the depth point. For a small difference in x coordinates and large difference in y coordinates, gesture command is predicted as forward and backward respectively.

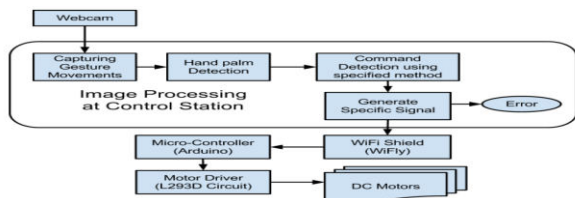


Fig.2. Design of system

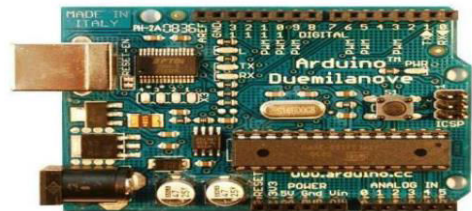


Fig.3. Wi-Fi Shield

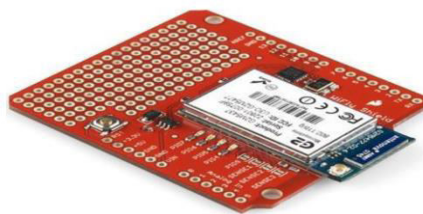


Fig.4. Micro- Controller (Arduino Duemilanove)

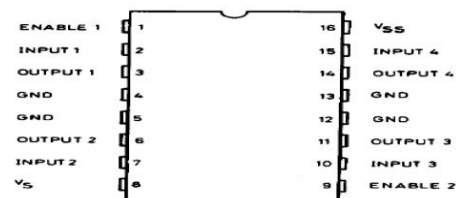


Fig.5. Motor Driver (L293D)



Fig.6. DC Motor

4. Wi-Fi Shield: WiFly

WiFly works on HTTP port 80 for provided library. This library is used for communication of WiFly with the Control station through the Wi-Fi Hotspot. There is a simple web page present on the control station having PHP script. WiFly on the robot connects itself with the Wi-Fi Hotspot. Figure. 3 shows WiFly GSX by Sparkfun.

5. Micro-Controller: Arduino (Duemilanove)

When Arduino gets command signal from the WiFly, it is having HTTP headers sent by web page with a tagged signal. Signal is read character by character and appended in the string. It has four possible methods as forward (), backward (), right (), left (). Each method is defined with a specified command to make each digital pin HIGH or LOW. Figure.4 shows Arduino of Duemilanove.

V.IMPLEMENTATION

1. Capturing Gesture Movements

Image frame is taken as input from the webcam on the control station and further processing is done on each input frame to detect hand palm. Figure.7 is an example of input frame. This involves some background constraints to identify the hand palm correctly with minimum noise in the image.

2. Hand Palm Detection

1. Thresholded Image.

Image frame taken as input from webcam is thresholded starting from minimum thresh value till single contour is formed in an image, same is in the case of intensity based thresholding. In the Figure.7 two fingers are shown by the user as a gesture command having dark background. Thresholded image is shown in Figure 8.

2. Drawing Contour and Convex Hull.

As shown in Figure 9, after obtaining thresholded image two main things are done, drawing the Contour on the thresholded part and fitting this contour in the Convex Hull. Contour is drawn in the thresholded image by using function draw Contour () in the library OpenCV. This is done on the intermediate image, this image is then passed for drawing the convex hull. This covers the whole contour by joining the minimal points to form Convex Hull. These two basic operations are performed on every image frame taken from the webcam, and then depending on the kind of gesture technique chosen by the user, further processing on the images is done. These two techniques are Finger Count based gesture control and Direction of Hand Palm Gesture Control.

3. Command Detection using Specific Method

1. Finger Count based Gesture Control

In this technique of giving gesture commands, first defects in the convex hull are found out using function convexityDefects(). Convex hull is formed using minimal set of points, so it does follow the contour path always, this causes the formation of defects in the convex hull.

2. Direction of Hand Palm.

In the previous technique of Finger Count Gesture Control, image having no large depth fails. For example, for finger count one, there is no such large depth so it is difficult to recognize, as it is count one or there is no such count. So counts from two to five are used as command signals. In this technique of gesture command, orientation of hand palm is taken into the consideration for recognition of the command signal. Thus an orientation of hand palm gives direction in which robot is to be moved. Orientation of these two fingers is towards right side, so the command signal for right is generated and passed to the robot.

4. Wi-Fi Shield: WiFly

This file is read by WiFly after regular interval. As it is a wireless communication, so WiFly communicates with the control station using a hotspot where control station is also in the same network. This hotspot can be a wireless router. Both control station and WiFly is provided with an IP address by using this IP address.

5. Micro-Controller: Arduino- Duemilanove

WiFly is connected to the Arduino through stackable pins shown in Figure 14. When the process of communication starts, WiFly tries to connect itself with the hotspot. For that it requires ssid and passphrase of the hotspot. These are provided in the burned code of the Arduino. After forming a successful connection with the hotspot, WiFly tries to get the access of the control station, with the provided IP address of the control station and port number of HTTP port which is by default 80. For that it requires ssid and passphrase of the hotspot. After forming a successful connection with the hotspot, WiFly tries to get the access of the control station, with the provided IP address of the control station and port number of HTTP port which is by default 80.

6. Motor Driver: L293D

L293D motor driver circuit is shown in the Figure 15. It takes digital signal as an input from the Arduino and gives digital output to the DC motors of the robot. Power supply to the circuit is given by rechargeable batteries. In this system some rechargeable mobile batteries are used as power supply each of 3.7V. To provide more voltage to drive the motors, 2-3 such batteries are connected in series.

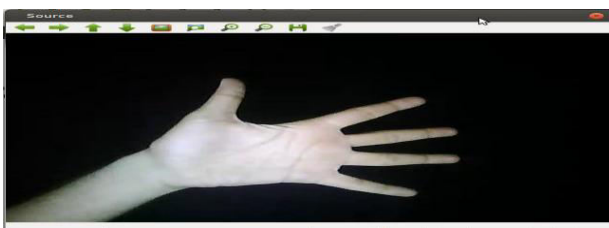


Figure.7. Input image frame

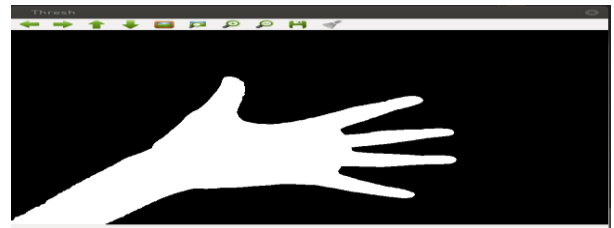


Figure.8. Thresholding Image

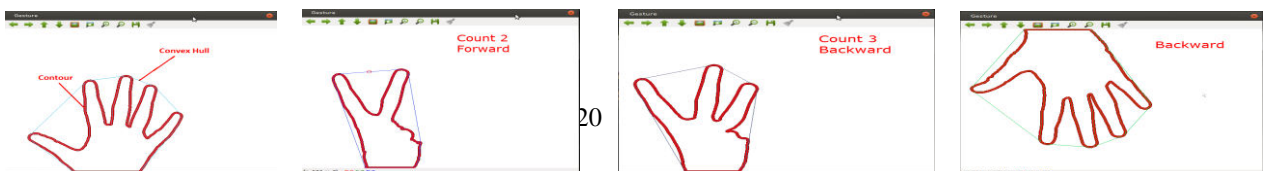


Fig.9. Contour and Convex hull

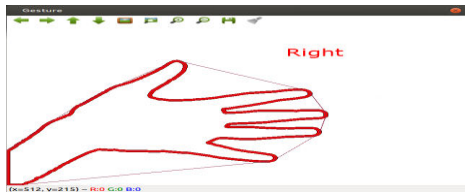


Fig .10. Finger Count base gesture and control I

Fig.11. Finger Count based Gesture control I

Fig.12. Direction of Hand Palm I



Figure.13. Direction of Hand Palm II

Figure.14. WiFly interfaced with Arduino

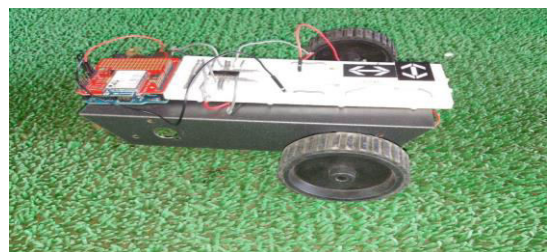
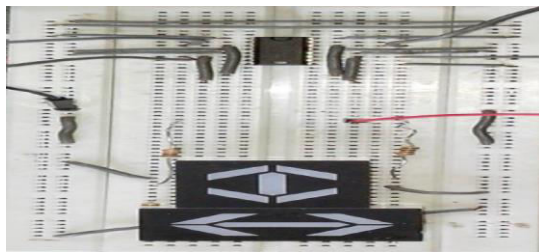


Figure.15. Motor Driver- L293D Circuit

Figure.16. Robot

7. DC Motors in Robot

This is the final end product of robot consisting of all the hardware WiFly, Arduino and L293D motor Driver circuit on the robot chassis having power supply provided by the rechargeable batteries. Four DC motors are connected to this robot chassis as shown in Figure 16. This is controlled through gestures by the user at control station.

VI. COMPARISON WITH EXISTING SYSTEM

The major advantage of our system over other systems is that it provides real time palm gesture recognition. Other Advantages are

- This implemented system is much more cost effective than the existing systems.
- It does not involve any specific hardware for gesture inputs - a normal webcam on laptop or PC can be used for gesture recognition.
- The implemented system takes real-time gesture inputs from the user, processes these gesture inputs to generate command signals.

VI. CONCLUSION

The Gesture Controlled Robot System gives an alternative way of controlling robots.

Gesture control being a more natural way of controlling devices makes control of robots more efficient and easy. We have provided two techniques for giving gesture input, finger count based gesture control and direction of hand palm based gesture control. In which each finger count specifies the command for the robot to navigate in specific direction in the environment and direction based technique directly gives the direction in which robot is to be moved.

At a time any one of the method can be used according to user's reliability, without using any external hardware support for gesture input unlike specified existing system. After gesture recognition command signal is generated and passed to the robot and it moves in specified direction.

VIII.FUTURE SCOPE

Presently in the system a minimum threshold value is set up and using that value input image frame is **THRESHOLDED** to binary. This approach put some constraints on the background, so a dark background is used. To avoid this, color based thresholding can be done. According to user's hand palm color, image can be thresholded within a tight bound limit. So hand palm can be easily detected irrespective of the background. Also the current implementation makes use of periodic polling from WiFly to the web server to access the command signal in real time.

REFERENCES

- [1] Chao Hy Xiang Wang, Mrinal K. Mandal, Max Meng, and Donglin Li, "Efficient Face and Gesture Recognition Techniques for Robot Control", CCECE, 1757-1762, 2003.
- [2] Asanterabi Malima, Erol Ozgur, and Mujdat Cetin, "A Fast Algorithm for Vision-Based Hand Gesture Recognition for Robot Control", IEEE International Conference on Computer Vision, 2006.
- [3] Thomas G. Zimmerman, Jaron Lanier, Chuck Blanchard, Steve Bryson and Young Harvill, "A Hand Gesture Interface Device", 189-192, 1987.
- [4] Jagdish Lal Raheja, Radhey Shyam, Umesh Kumar and P Bhanu Prasad, "Real-Time Robotic Hand Control using Hand Gestures", Second International Conference on Machine Learning and Computing, 2010.
- [5] Gesture Controlled Robot using Kinect <http://www.e-yantra.org/home/projects-wiki/item/180-gesture-controlled-robot-using-firebirdv-and-kinect>
- [6] E. Sanchez-Nielsen, L. Anton-Canalis and M. Hernandez- Tejera. Hand gesture recognition for human-machine interaction. Journal of WSCG, 12(1-3), February 2004.
- [7] M. Klsch and M. Turk. Robust hand detection. Proc. of the 6th IEEE International Conf. on Automatic Face and Gesture Recognition, pages 614619, May 2004.

Network Based Application for Students Community On Top Of Android

Nivetha. A,Subesha. R,Sivasathiya Vetrisevum
CSE,AIHT, nivearul8@gmail

Abstract-The main objective of this paper is to provide an application for the student community where they can share the services easy and locate their friend's position without using their private details like mobile number and e-mail id. For this we are using different technologies and methods for communication. **Google Cloud Messaging (GCM)** is a service that enables developers to send data from servers to both Android applications or Chrome apps and extensions. This is one of the important technology used to send and receive data directly from the server. MySQL database is also one of the important feature used to store data ie. Once the sender sends the message it is stored in database and then send to the receiver. We also use PHP to connect the frontend and backend of the application. JSON is used to connect the phone client with the PHP. This application use all the activities of android and provide an efficient system to the users.

Keywords : GCM, MySQL, PHP, JSON, sharing services.

I. INTRODUCTION

Smart handheld devices are quickly emerging in the market, and almost everyone carries one smart handheld device at any time. Nowadays, as smartphones are becoming more and more powerful, applications providing location based services have been increasingly popular. Every smart phone have the have ability to establish the network connection with the help of GSM, Wi-Fi, and so on. This help the people to communicate with each other through chats and messages and so on. In this application this is highly used for the student community to communicate each other through chats, file sharing and location finder. In general every application needs a medium to communicate each other like phone number and e-mail. But this application need a unique registration ID of the student given by the university. Using this registration Id we can add a friend, block a friend, chat with them, share images, medias, and documents. This also helps people to locate their friends position based on their miles. For every given duration the location gets updated. The localization technologies used today mainly based on Global Positioning System (GPS), other technologies also obtain assistance from WiFi and GSM, each of which can vary widely in energy consumption and localization accuracy. Our main concept is to provide an application where the mobile number is not required. Hence this helps the information more secure and make the user to feel privacy. In this another important feature is that we can find the location of the people only if we are the friend of them. Hence this increase more privacy and accuracy to the people.

II. LITRATURE REVIEW

1] In BASA Building Mobile Ad-hoc Social Networks on top of Android, which enables local communication without utilizing the underlying network infrastructures. Specifically, BASA is designed to fulfill the following functions:

- To create MASN applications
- To customize MASN applications.
- To orchestrate MASN events
- To support value-added community services

2] In NCCU TRACE we consider student's movement's on campus. Each student can have a sporadic schedule on a daily basis. It is natural for a student to move to any place on campus, and to stay for different lengths of time at each place. In order to collect the data of these different movements, we designed an Android app named NCCU Trace Data. The following describes what trace data the app collected.

Position: They collect students' location via their smart handheld devices' GPS.

Wi-Fi access point proximity: Their app records how many Wi-Fi access points are available nearby and their detailed information, such as medium access control (MAC) address, service set identifier (SSID), and received signal strength indication (RSSI) of each access point.

Bluetooth-based device proximity: The number of available nearby Bluetooth devices and their detailed information, such as MAC address and RSSI, are recorded.

Students' behavior using smart handheld devices: Our app records how frequently and how long students use apps (Google Map, WhatsApp, Tweet, etc.) in their smart handheld devices.

III. PREVIOUS WORK

In previous application they used the MASN network to connect the devices for communication between people. They also used routing protocol to trace the student behavior, location and so on. They also used DTN Technology for tracing and to reduce the delay in the system. The main aim of BASA is to create an application using Mobile ad-hoc social networks (MASNs). However, the MASNs cannot be directly derived on demand for various Android systems from existing social networks (SNs) without having access to end-to-end IT network infrastructure. In this article, we propose a detailed solution called BASA which would help in rapidly building local mobile ad-hoc social networks on top of the current Android platform. BASA establishes a four-layer system architecture according to the underlying challenges and requirements in MASNs. In NCCU trace Delay-tolerant networking (DTN) is a network architecture characterized by the lack of continuous connectivity. Messages are delivered by moving nodes in a store-and-forward manner. In such a network, the mobility models of nodes play an important role in DTNs, because messages can only be delivered when two or more nodes contact each other. In this article, we design an Android application to collect the mobility traces of college students in a campus environment, called NCCU Trace Data. We design a mobility model that traces student's movement, and this model can be imported into the ONE simulator to verify routing protocols. More importantly, it can be used to evaluate the performance of a social-based routing method.

III. PROPOSED MODEL

In this model we design an application on top of android for the communication between students in colleges/universities. In this we create a community for the student purpose. In this application all the information's are stored in the backend using the MySQL which provide high security and privacy for the data's. Using this application we can chat with the students who we want. First step is to register the application using the unique registration ID given by the university. After that we can find the friend whom we know and add them to the friends list. If the particular person is not interested to chat then they can block the user for their privacy. They can also send and receive files, media's, and applications in the system. All this messages are first stored in the Database once it is send by the user and then the message is delivered to the receiver.

Another important thing is TRACING. In this application we trace the system friend using the GOOGLE MAP API.

V. SYSTEM ARCHITECTURE

In this we use **Linux Kernel, Hardware, Runtime, Libraries, Application Framework, and Application.**

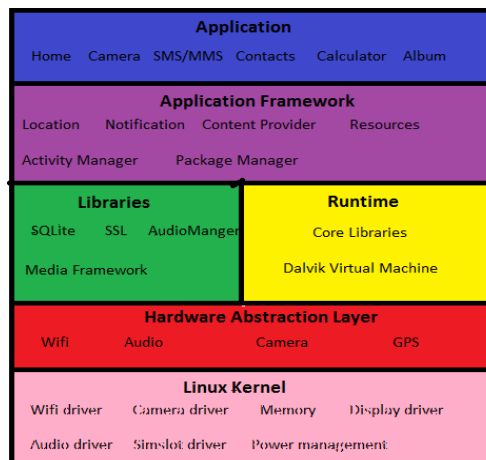


Figure 1: Application architecture

Our application consist of different layers in the architecture where the linux kernel consist of Wifi driver which is used to connect wifi in the mobile devices. GSM is a hardware used to detect the position of the system and also find the connectivity of the network in the system. This also contains the Dalvik Virtual Machine. That is used to run the system. In this we also use the SQLite which is used to store the data in the backend of the system. Also we use location manager for finding the location of the people in the system. All the top of the application run with the help of this hardware's provided in the system.

VI. GENERAL APPROACH

The main aim of the project is to provide secrecy to the user without providing their private details to the registration. For this we use privacy techniques which are in progress. And also we track the person using the GOOGLE MAP API. This consist of certain permissions.

A. Access_Fine_Location

This is used to find whether wifi is available are not. This is done by using fast connection and provide accurate results.

B. Access_Network_State

This is used to find whether the network is present in SIM or not.
Connection_detector cd=new connection detector();

C. Access_Coarse_Location

This is used to find the network like 2G / 3G are available in the devices. This requires less memory. We should use the layout file for the device to show the map in the application

<fragment

Android:id="@+id/map"

Android:name="com.google.android.gms.maps.mapfragment"

Android:layout_width="match_parent"

Android:layout_height="match_parent"/>

JSON (Java Script Object Notation) is a light weight interchange. We use JSON to connect the phone client with the PHP. In this, connection between phone client and PHP is used very efficiently. We use PHP ie. Hypertext Preprocessor which is used to connect the backend and frontend of the application. We use MySQL database on the backend for the storage of the data's. In this application we have used **GCM(GOOGLE CLOUD MESSAGING)** where the datas are stored in the cloud for later purpose. We also use services and receiver concept in the application.

VII. STIMULATED RESULTS

The stimulated results shows the way for easy communication between the systems using the unique registration id. This also provide easy file sharing's and also find the location of the particular person.

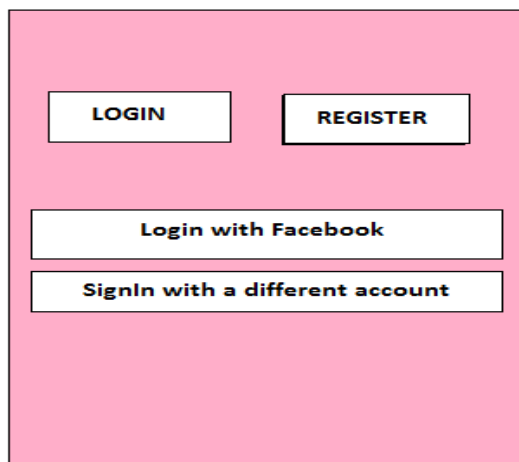


Figure 2: Login page using various account

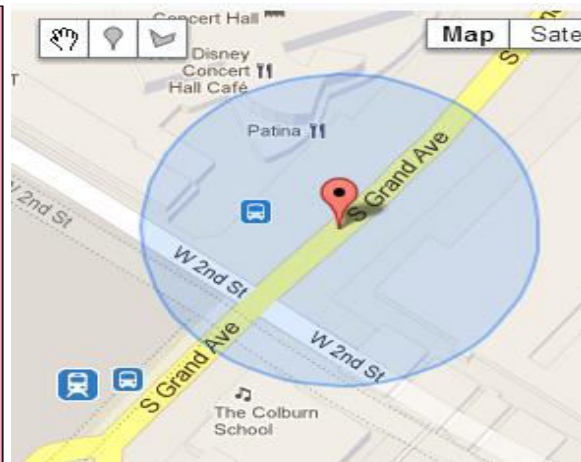


Figure 3: Finding location by giving specific distance

In this we have to register for the first time, the data's are stored in the database for future checks. Then whenever we login the account It checks for validation and then it enter into the application. And then we can add the friend, block the friend, chat with them, share files and documents with them. Another important feature is to trace the location of the person by specifying the miles that we needed.



Figure 4: Pointing the person with their unique registration no Figure 5: Finding the no of friends in particular area

The main specification is that it identifies the person with its registration ID. It also specifies how many friends of you are located in that particular place. By this we can easily find the friend by their location. Thus this provide very efficient and accurate results to the users. It is very helpful for the student's community.

VIII. CONCLUSION AND FUTURE WORK

This application is very efficient and helpful for the students who want to connect with their friend's, and share with them. This also provide location finder which is very helpful in locating their friend's. The main advantage is that no need of their phone numbers and their personal details. This provide a unique facility for the application. The use MySQL and GCM provide a good backups of the data and fast message transfer. In this we are working for the single college but in future we would bring it for the college community and even location of the basic phone user can also be traced by their IMEI number.

REFERENCE

- [1] A. Keränen, J. Ott, and T. Kärkkäinen, "The ONE Simulator for DTN Protocol Evaluation," *Proc. SimuTools*, Mar. 2009.
- [2] A. Mtibaa *et al.*, "PeopleRank: Combining Social and Contact Information for Opportunistic Forwarding," *INFOCOM*, 2010.
- [3] A. Vahdat and D. Becker, "Epidemic Routing for Partially Connected Ad Hoc Networks," Tech. Rep. CS-2000-06, Duke Univ., July 2000.
- [4] A. Lindgren, A. Doria, and O. Schelén, "Probabilistic Routing in Intermittently Connected Networks," LUT, Sweden, *Proc. SIGMOBILE*, vol. 7-3, July 2003.
- [5] E. Bulut and B. K. Szymanski, "Friendship Based Routing in Delay Tolerant Mobile Social Networks," *IEEE GLOBECOM 2010*.
- [6] D. Katsaros, N. Dimokas, and L. Tassiulas, "Social Network Analysis Concepts in the Design of Wireless Ad Hoc Network Protocols," *IEEE Network*, vol. 24.

Co-Extracting Opinion Targets and Opinion Words from Online Reviews Based on the Word Alignment Model

E. Suganthi, T. Premalatha

1Department of CSE, VRS College of Engineering & Tech, premapriya166@gmail.com.

2Department Of CSE, VRS College of Engineering & Tech, santhigowsalyacsc@gmail.com

Abstract—Mining opinion targets and opinion words from online reviews are important tasks for fine-grained opinion mining, the key component of which involves detecting opinion relations among words. To this end, this project proposes a novel approach based on the partially-supervised alignment model, which regards identifying opinion relations as an alignment process. Then, a graph-based co-ranking algorithm is exploited to estimate the confidence of each candidate. Finally, candidates with higher confidence are extracted as opinion targets or opinion words. Compared to previous methods based on the nearest-neighbor rules, our model captures opinion relations more precisely, especially for long-span relations. Compared to syntax-based methods, our word alignment model effectively alleviates the negative effects of parsing errors when dealing with informal online texts. In particular, compared to the traditional unsupervised alignment model, the proposed model obtains better precision because of the usage of partial supervision. In addition, when estimating candidate confidence, we penalize higher-degree vertices in our graph-based co-ranking algorithm to decrease the probability of error generation. Our experimental results on three corpora with different sizes and languages show that our approach effectively outperforms state-of-the-art methods.

Keywords- Opinion mining, opinion targets extraction, opinion words extraction

I. INTRODUCTION

With the rapid development of Web 2.0, a huge number of product reviews are springing up on the Web. From these reviews, customers can obtain first-hand assessments of product information and direct supervision of their purchase actions. Meanwhile, manufacturers can obtain immediate feedback and opportunities to improve the quality of their products in a timely fashion. Thus, mining opinions from online reviews has become an increasingly urgent activity and has attracted a great deal of attention from researchers [1], [2], [3], [4].

To extract and analyze opinions from online reviews, it is unsatisfactory to merely obtain the overall sentiment about a product. In most cases, customers expect to find fine-grained sentiments about an aspect or feature of a product that is reviewed. For example: “This phone has a colorful and big screen, but its LCD resolution is very disappointing.” Readers expect to know that the reviewer expresses a positive opinion of the phone’s screen and a negative opinion of the screen’s resolution, not just the reviewer’s overall sentiment. To fulfill this aim, both opinion targets and opinion words must be detected. First, however, it is necessary to extract and construct an opinion target list and an opinion word lexicon, both of which can provide prior knowledge that is useful for fine-grained opinion mining and both of which are the focus of this project. An opinion target is defined as the object about which users express their opinions, typically as nouns or noun phrases. In the above example, “screen” and “LCD resolution” are two opinion targets. Previous methods have usually generated an opinion target list from online product reviews. As a result, opinion targets usually are product

features or attributes. Accordingly this subtask is also called as product feature extraction [5], [6]. In addition, opinion words are the words that are used to express users' opinions. In the above example, "colorful", "big" and "disappointing" are three opinion words. Constructing an opinion words lexicon is also important because the lexicon is beneficial for identifying opinion expressions.

II. RELATED WORK

Opinion target and opinion word extraction are not new tasks in opinion mining. There is significant effort focused on these tasks [1], [6], [12], [13], [14]. They can be divided into two categories: sentence-level extraction and corpus level extraction according to their extraction aims. In sentence-level extraction, the task of opinion target/ word extraction is to identify the opinion target mentions or opinion expressions in sentences. Thus, these tasks are usually regarded as sequence-labeling problems [13], [14], [15], [16]. Intuitively, contextual words are selected as the features to indicate opinion targets/words in sentences. Additionally, classical sequence labeling models are used to build the extractor, such as CRFs [13] and HMM [17]. Jin and Huang [17] proposed a lexicalized HMM model to perform opinion mining. Both [13] and [15] used CRFs to extract opinion targets from reviews. However, these methods always need the labeled data to train the model. If the labeled training data are insufficient or come from the different domains than the current texts, they would have unsatisfied extraction performance. Although [2] proposed a method based on transfer learning to facilitate cross domain extraction of opinion targets/words, their method still needed the labeled data from out-domains and the extraction performance heavily depended on the relevance between in-domain and out-domain. In addition, much research focused on corpus-level extraction. They did not identify the opinion target/word mentions in sentences, but aimed to extract a list of opinion targets or generate a sentiment word lexicon from texts. Most previous approaches adopted a collective unsupervised extraction framework. As mentioned in our first section, detecting opinion relations and calculating opinion associations among words are the key component of this type of method. Wang and Wang [8] adopted the co-occurrence of opinion targets and opinion words to indicate their opinion associations. Hu and Liu [5] nearest neighbor rules to identify opinion relations among words. Next, frequent and explicit product features were extracted using a bootstrapping process. Only the use of co-occurrence information or nearest-neighbor rules to detect opinion relations among words could not obtain precise results. Thus, [6] exploited syntax information to extract opinion targets, and designed some syntactic patterns to capture the opinion relations among words. The experimental results showed that their method performed better than that of [5]. Moreover, [10] and [7] proposed a method, named as Double Propagation, that exploited syntactic relations among words to expand sentiment words and opinion targets iteratively. Their main limitation is that the patterns based on the dependency parsing tree could not cover all opinion relations. Therefore, Zhang et al. [3] extended the work by [7]. Besides the patterns used in [7], Zhang et al. further designed specific patterns to increase recall. Moreover, they used an HITS [18] algorithm to compute opinion target confidences to improve precision. Liu et al. [4] focused on opinion target extraction based on the WAM. They used a completely unsupervised WAM to capture opinion relations in sentences. Next, opinion targets were extracted in a standard random walk framework. Liu's experimental results showed that the WAM was effective for

extracting opinion targets. Nonetheless, they present no evidence to demonstrate the effectiveness of the WAM on opinion word extraction. Furthermore, a study employed topic modeling to identify implicit topics and sentiment words [19], [20], [21], [22]. The aims of these methods usually were not to extract an opinion target list or opinion word lexicon from reviews.

III. PROPOSED WORK

The key component of which involves detecting opinion relations among words. To this end, this project proposes a novel approach based on the partially-supervised alignment model, which regards identifying opinion relations as an alignment process. Then, a graph-based co-ranking algorithm is exploited to estimate the confidence of each candidate. Finally, candidates with higher confidence are extracted as opinion targets or opinion words. Compared to previous methods based on the nearest-neighbor rules, our model captures opinion relations more precisely, especially for long-span relations. Compared to syntax-based methods, our word alignment model effectively alleviates the negative effects of parsing errors when dealing with informal online texts.

IV. FUNCTIONAL MODULES

WORD ALIGNMENT MODEL

As mentioned in the above section, we formulate opinion relation identification as a word alignment process. We employ the word-based alignment model [23] to perform monolingual word alignment, which has been widely used in many tasks such as collocation extraction [24] and tag suggestion [25]. In practice, every sentence is replicated to generate a parallel corpus. A bilingual word alignment algorithm is applied to the monolingual scenario to align a noun/noun phrase (potential opinion targets) with its modifiers (potential opinion words) in sentences.

Formally, given a sentence with n words

$S = \{w_1; w_2; \dots; w_n\}$, The word alignment $A = \{(i, a_i) | i \in [1; n], a_i \in [1; n]\}$; can be obtained as

$$A^* = \underset{A}{\operatorname{argmax}} P(A/S),$$

where (i, a_i) means that a noun/noun phrase at position i is aligned with its modifier at position a_i .

Partially-Supervised Word Alignment Model

As mentioned in the first section, the standard word alignment model is usually trained in a completely unsupervised manner, which may not obtain precise alignment results. Thus, to improve alignment performance, we perform a partial supervision on the statistic model and employ a partially-supervised alignment model to incorporate partial alignment links into the alignment process. Here, the partial alignment links are regarded as constraints for the trained alignment model.

V. CONCLUSION

This project proposes a novel method for co-extracting opinion targets and opinion words by using a word alignment model. Our main contribution is focused on detecting opinion relations between opinion targets and opinion words. Compared to previous methods

based on nearest neighbor rules and syntactic patterns, in using a word alignment model, our method captures opinion relations more precisely and therefore is more effective for opinion target and opinion word extraction. Next, we construct an Opinion Relation Graph to model all candidates and the detected opinion relations among them, along with a graph co-ranking algorithm to estimate the confidence of each candidate. The items with higher ranks are extracted out. The experimental results for three datasets with different languages and different sizes prove the effectiveness of the proposed method.

VI. REFERENCES

- [1] M.Hu and B. Liu, "Mining and summarizing customer reviews," in Proc. 10th ACM SIGKDD Int.Conf.Knowl. Discovery Data Mining, Seattle, WA, USA, 2004, pp. 168–177.
- [2] F. Li, S. J. Pan, O. Jin, Q. Yang, and X. Zhu, "Cross-domain coextraction of sentiment and topic lexicons," in Proc. 50th Annu. Meeting Assoc.Comput. Linguistics, Jeju, Korea, 2012, pp. 410–419.
- [3] L. Zhang, B. Liu, S. H. Lim, and E. O'Brien-Strain, "Extracting and ranking product features in opinion documents," in Proc. 23th Int. Conf.Comput. Linguistics, Beijing, China, 2010, pp. 1462–1470.
- [4] K.Liu,L.Xu, and J. Zhao, "Opinion target extraction using word based translation model," in Proc. Joint Conf. Empirical Methods Natural Lang.Process. Comput. Natural Lang. Learn., Jeju, Korea, Jul. 2012, pp. 1346–1356.
- [5] M. Hu and B. Liu, "Mining opinion features in customer reviews," in Proc. 19th Nat. Conf. Artif. Intell., San Jose, CA, USA, 2004, pp. 755–760.
- [6] A.-M. Popescu and O. Etzioni, "Extracting product features and opinions from reviews," in Proc. Conf. Human Lang. Technol. Empirical Methods Natural Lang. Process., Vancouver, BC, Canada, 2005, pp. 339–346.
- [7] G. Qiu, L. Bing, J. Bu, and C. Chen, "Opinion word expansion and target extraction through double propagation," *Comput. Linguistics*, vol. 37, no. 1, pp. 9–27, 2011.
- [8] B. Wang and H. Wang, "Bootstrapping both product features and opinion words from chinese customer reviews with crossinducing," in Proc. 3rd Int. Joint Conf. Natural Lang. Process., Hyderabad, India, 2008, pp. 289–295.
- [9] B. Liu, *Web Data Mining: Exploring Hyperlinks, Contents, and Usage Data*, series Data-Centric Systems and Applications. New York, NY, USA: Springer, 2007.
- [10] G. Qiu, B. Liu, J. Bu, and C. Che, "Expanding domain sentiment lexicon through double propagation," in Proc. 21st Int. Jont Conf. Artif. Intell., Pasadena, CA, USA, 2009, pp. 1199–1204.
- [11] R. C. Moore, "A discriminative framework for bilingual word alignment," in Proc. Conf. Human Lang. Technol. Empirical Methods Natural Lang. Process., Vancouver, BC, Canada, 2005, pp. 81–88.
- [12] X. Ding, B. Liu, and P. S. Yu, "A holistic lexicon-based approach to opinion mining," in Proc. Conf. Web Search Web Data Mining, 2008, pp. 231–240.
- [13] F. Li, C. Han, M. Huang, X. Zhu, Y. Xia, S. Zhang, and H. Yu, "Structure-aware review mining and summarization," in Proc. 23th Int. Conf. Comput. Linguistics, Beijing, China, 2010, pp. 653–661.
- [14] Y. Wu, Q. Zhang, X. Huang, and L. Wu, "Phrase dependency parsing for opinion mining," in Proc. Conf. Empirical Methods Natural Lang. Process., Singapore, 2009, pp. 1533–1541.

QoS aware Web Service Recommendation using Collaborative Filtering with Service Usage Factor

Ms.Kiruthiga.V¹, Ms.Seethalakshmi.R²,
CSE, MRK college,senthamaha@gmail.com

Abstract—Over the past 10 years, it has been witnessed that tremendous growth of Web services as a major technology for sharing data, computing resources, and programs on the Web. With the drastic evolution, adoption and presence of Web services, design of novel approaches for effective Web service recommendation to satisfy users' potential requirements has become of paramount importance. Existing Web service recommendation approaches mainly focus on predicting missing QoS values of Web service candidates which are interesting to a user using collaborative filtering approach, content-based approach, or their hybrid. These recommendation approaches assume that recommended Web services are independent to each other, which sometimes may not be true. As a result, many similar or redundant Web services may exist in a recommendation list. In this project, we propose a novel Web Service recommendation approach incorporating a user's potential QoS preferences and diversity feature of user interests on Web services. It can be achieved through the absolute evaluation of service usage factors which is going to act a primary key for traditional collaborative filtering algorithm. User's interests and QoS preferences on Web services are first mined by exploring the Web service usage history. Then we compute scores of Web service candidates by measuring their relevance with historical and potential user interests, and their QoS utility. We also construct a Web service graph based on the functional similarity between Web services. Finally, we present an innovative diversity-aware Web service ranking algorithm to rank the Web service candidates based on their scores, and diversity degrees derived from the Web service graph. Our proposed Web service recommendation approach is found to be effective since it significantly improves the quality of the recommendation results compared with existing methods.

Index Terms—Web service recommendation, diversity, user interest, QoS preference, service usage history

1 INTRODUCTION

Web services are the internet enabled applications for performing business needs considered as the platform-independent and loosely coupled. A web service has three participants: a service provider, a service consumer and a service broker. A service provider sends a WSDL (Web Service Description Language) file to the UDDI (Universal, Description, Discovery, Interface). The service requester contacts UDDI to find the provider for that data it need, and then it contacts the service provider using the SOAP protocol. The service provider validate the service request and sends structured data in an XML file, using the SOAP protocol This XML file would be again validated by the service requester using an XSD file.

The web service are majorly divided into two categories. Functional part and non-functional part. The functional part deals with the operations and behavioral aspects. The non-functional part deals with the QoS(Quality of service) parameters like performance, cost, security, usability etc. The quality of parameter can be measured on both client side and on

server side. So, all these leads to a web service Discovery, Composition, Evaluation, Customization etc of services. The composite web service is the emerging trend. Thus selecting the best fitting web services are much important.

The web service Discovery is a process of finding a suitable web service for a given task. Publishing a web service involves creating a software artifact and making it accessible to potential customers. Web service provider augments a web service endpoint with an interface describing using the Web Services Description Language so that a customer can use the service. Web services may also be discovered using multicast mechanisms like WS-Discovery, thus reducing the need for centralized registries in smaller networks.

The web service Composition is a process of automatically assembling WSs to form compositions that optimize given user preferences.

1.2 OBJECTIVE OF THE STUDY

The proposed work contributes the following key features for the efficient web service quality evaluation approach for finding the best fit best web service. The major contribution is-

- a) To measure the Neighborhood Integrated Matrix Factorization (NIMF) for Web Service QoS values at client side and at server side.
- b) To construct Collaborative filtering of WS-QoS using NIMF which perform factorization for predicting similarities between the users.
- c) To improve the accuracy of prediction for effective recommendation by incorporating a user's potential QoS preferences and diversity feature of user interests on Web services

1.3 PAPER DESCRIPTION

Web services have been rapidly developed in recent years and played an increasingly significant role in e-commerce, enterprise application integration, and other applications. With the growth of the number of Webservices on the Internet, Web service discovery has become a critical issue to be addressed in service computing community [1]. Since there are many Web services with similar functionalities and different non-functional quality, it is important for users to select desirable high-quality Web services which satisfy both users' functional and non-functional requirements. Recently, recommending qualified and preferred Web services to users has attracted much attention in terms of the information overload problem. Web service recommendation is a process of proactively discovering and recommending suitable Web services to end users.

However, there are drawbacks for these approaches. To begin with, they simply recommend users Web services with the best QoS values on a certain QoS criterion without exploiting the user's potential QoS preferences, which may likely be mined from his/her service usage history [7]. A user's QoS preference for services is certainly important for real service recommendation scenarios, since it can be used for measuring the QoS utility of a Web service in a more accurate and personalized way. Moreover, existing service recommendation approaches may have unneeded similar services in the top-k recommendation lists, since there is a default assumption that all the results are independent of each other, which may not be true in many times. red in recommendation.

II. METHODOLOGIES

There methodology that are adopted for performing QoS evaluation . Some of the methodology are discussed below,

2.1 Markov's Chain Model

A Markov model is a stochastic model used for modelling randomly-changing systems in which it is assumed that the future states depends only on the present state and not on the sequence of events that preceded it. Selection of an atomic service during composition process is based on various QoS parameters. Services are ranked based on their QoS values and election is done based on rank. An approach is proposed to model service reputation as a combination of Availability and Reliability. The Markov's Chain Model [1] are used to study the system that could be represented as discrete states. Since service availability can have Boolean discrete states, Markov Chain is used to model availability.

2.2 Weibull Analysis

The Weibull analysis[1] is a continuous probability distribution. Reliability of a service defines the rate of change of failure of a service under test. Various probabilistic distribution mechanisms are used to study reliability. In a realistic scenario services, failure rate can be increasing, decreasing or constant. To accommodate all these cases Weibull analysis has been considered.

2.3 Novel Planning Based Approach

A Novel Planning Based Approach [3] that can automatically converts a QoS-aware composition task to a planning problem with temporal and numerical features. This approach automatically solve the web service composition problem. For a restricted class of Q-WSC (web service composition) problems where there are no global QoS constraints on temporal restriction and average-based constraint, it can be solved by the planning problem using a numeric planner.

2.4 GRASP with Path Re-linking

A GRASP (General Responsibility Assignment Software Pattern) [4] consists of guidelines for assigning responsibility to classes and objects in object-oriented design. Different patterns and principles are used in GRASP. All these patterns answers some software problem, and in almost every software development projects. This approach improves the results of previous of previous proposals up to 40%.This is an hybrid approach that combines GRASP with PR. QoS-Gasp is especially suitable for rebinding problems where short solving times are a must.

III. SURVEY OF THE RELATED WORK

The extract from literature based on the QoS prediction of the web service composition has been discussed in this section with which we can get knowledge of how their works are being used to achieve the desired goal.

[1] This approach helps us to finding out appropriate service selection and higher reputation with lower cost. The methodology used in this paper that models the reputation as a combination of both availability and reliability, giving a precise estimate of reputation. Estimation of QoS can be done with both factors considered together on the simple premise that availability tell about only the probability of that service being up/running, but not tell about its failure trend. The mathematical modeling of these predominant QoS factors was presented using Markov model and Weibull analysis. A scenario has been simulated using Colored Petri Net(CPN) to study the

behavioral aspects. Results in selecting atomic service with robust, high performance and cost effective composite services.

[2] An AI planning based method that automatically converts a QoS-aware composition task to a planning problem with temporal and numerical features. The method first compiles a Q-WSC problem into a CSTE planning problem. Then the method applies SCP planner to handle the CSTE planning problem using temporal planning and numerical optimization and finds a composite service graph. State-of-art planners are used to handle complex temporal planning problems with logical reasoning and numerical optimization. This approach finds a composite service graph with the optimal overall QoS value while satisfying multiple global QoS constraints. The Metric FF is used to transform restricted class of Q-WSC to numerical planning problem. This results in quality and efficient enough for practical deployment.

[3] A Novel algorithm named QoS-GASP for solving the QoS-WSC at runtime has been proposed. The QoS Gasp is an hybrid approach that combines GRASP with Path Relinking. GRASP begins by creating an empty solution. Elements are added iteratively to it until a complete and feasible solution is found. Path Relinking ia an meta heuristic optimization technique that generates new solutions by exploring trajectories connecting promiing solutions. Our proposal GRASP with path Re-linking improves the QOS in terms of cost, increased availability and reductions of execution time.

[4] It deals with personalized web service selection and recommendation. A new similarity measure for web service similarity computation and a novel collaborative filtering approach called normal recovery collaborative filtering is used. This experiment is the largest scale experiment in the field of service computing, improving the previous record by a factor of 100. This results in prediction of better accuracy than other approaches.

[5] A novel collaborative filtering algorithm designed for large-scale web service recommendation. This approach employs the characteristic of QOS and achieves considerable improvement on the recommendation accuracy. To help service users better understand the rationale of the recommendation and remove some of the mystery, it uses a recommendation visualization technique to show how a recommendation is grouped with other choices. This approach was efficient and effective.

IV. FRAMEWORK OF OUR- APPROACH

Now we describe the framework of our service recommendation approach which takes diversity into consideration as shown in Figure 1. In the framework, **Web Service Recommendation with Diversity (WSRD)** is the key component. For simplicity, we suppose that the service usage history and functional description information and QoS information of all services are already provided or acquired. The collected service pool can be updated dynamically by the service search engine. However, we assume that the number of services does not change in the small interval during the process of service recommendation.

WSRD has four subcomponents: functional evaluation, non-functional evaluation, diversity evaluation, and diversified Web service ranking, as shown in Figure 1. The functional evaluation can be further divided into two parts: Functional Evaluation 1 and Functional Evaluation 2. Functional Evaluation 1 evaluates the relevance of the user's historical interest with Web services based on a content-based similarity measure.

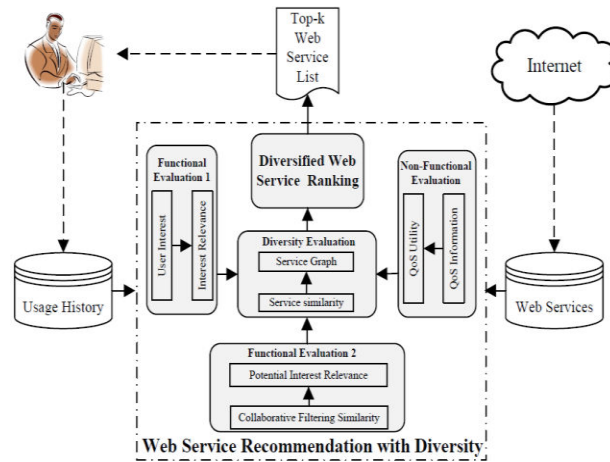


Fig.1 Framework of Our Service Recommendation Approach

Content-based similarity is acquired by text similarity. This work only considers Web services that are described by the Web Service Description Language (WSDL). Nevertheless, it is easy to extend our work to handle other kinds of Web services. The user's historical interest can be mined from his/her own service usage or query history. Functional Evaluation 2 predicts the user's potential interest and evaluates its relevance with Web services by employing collaborative filtering based user similarity. The user similarity is measured based on the service invocation history of all service users. Non-functional Evaluation first infers the user's potential QoS preference on a service candidate through mining the service's usage history, then calculates the QoS utility of the Web service with the obtained QoS information.

V. THE SERVICE RECOMMENDATION APPROACH

Suppose there are M services in the service usage history of an active user, denoted $WS_{u,1}, WS_{u,2}, \dots, WS_{u,M}$, and the QoS preference vector specified by the user on $WS_{u,i}$ is denoted by $P_{u,i}$. If the Web services invoked by the user were recommended by the Web service search engine, their QoS preference vectors may also be empty. Suppose there are N Web service candidates for Web service recommendation, which are WS_1, WS_2, \dots, WS_N . With these notations, next we describe our Web service recommendation approach, which includes functional evaluation, non-functional evaluation, diversity evaluation, and diversified Web service ranking.

5.1 NON-FUNCTIONAL EVALUATION (QoS)

Suppose that m QoS criteria are used for assessing the non-functional quality of WS_i , its QoS vector is denoted by QS_i , i.e., $QS_i = (q_{i,1}, q_{i,2}, \dots, q_{i,m})$, where $q_{i,j}$ represents the value of the j^{th} quality criterion. Generally, there are two types of QoS criteria. A QoS criterion is considered to be negative if the higher the value, the lower the quality, (e.g., Response Time and Cost). On the other hand, if the higher the value, the higher the quality, the QoS criterion is considered to be positive (e.g., Availability and Reliability). Values of different QoS criteria need to be normalized to the same range for uniform measurement purpose. While before normalization, we apply statistical method (i.e., Pauta Criterion method) to preprocess the QoS values in advance to remove the outliers. In this section, we transform each QoS criterion value to a real number between 0 and 1 by comparing it with the maximum and minimum values of the QoS criterion among all available Web service candidates. After such normalization processing, larger value for any quality criterion means better quality. Concretely, for a negative QoS criterion, its value q_i would be normalized as q'_i , according to Formula (7), and for a positive criterion, q_i would be

normalized using Formula (8), which are defined as follows:

$$q'_{i,j} = \begin{cases} \frac{Q_{max}(j)-q_{i,j}}{Q_{max}(j)-Q_{min}(j)}, & \text{if } Q_{max}(j) \neq Q_{min}(j) \\ 1, & \text{if } Q_{max}(j) = Q_{min}(j) \end{cases} \quad (7)$$

$$q'_{i,j} = \begin{cases} \frac{q_{i,j}-Q_{min}(j)}{Q_{max}(j)-Q_{min}(j)}, & \text{if } Q_{max}(j) \neq Q_{min}(j) \\ 1, & \text{if } Q_{max}(j) = Q_{min}(j) \end{cases} \quad (8)$$

where the maximum value $Q_{max}(j)$ and minimum value $Q_{min}(j)$ of the j^{th} QoS criterion are defined as Formula (9) and (10), respectively. We denote QS'_i as the QoS vector of WS_i after normalization processing.

$$Q_{max}(j) = \max\{q_{i,j}\} \quad (9)$$

$$Q_{min}(j) = \min\{q_{i,j}\} \quad (10)$$

Let $P_u=(w_1,w_2,\dots,w_m)$ represents the user's QoS preference on different QoS criteria over the Web service candidate WS_i , where $w_j \geq 0$ and $w_j=1$ $m_j=1$. Then the QoS utility U_u , of WS_i is calculated as follows:

$$U_{u,i} = QS'_i \times P_{u,i}^T = \sum_{j=1}^m w_j \times q'_{i,j} \quad (11)$$

In WSRD, we mine the active user's potential QoS preferences to service candidates from historical QoS preferences of the active user or similar users who used the service candidates. We firstly transform WSDL document of WS_u , into a term vector wu , by using TF/IDF algorithm. Then we compute the similarity S_i , between WS_i and WS_u , i.e., $S_{i,j}^{ws} = wsSim(WS_i, WS_{u,j})$ which is calculated with Formula (5). As for $S_{i,1}^{ws}, S_{i,2}^{ws}, \dots, S_{i,M}^{ws}$, we find the Web services with both the similarity above the threshold ε and valid QoS preferences in service usage history to form the set S_{sim} . It is reasonable to assume that the active user has similar QoS preferences to similar Web service candidates, i.e., Web services with similar functionalities.

Based on this observation, we choose to use the QoS preferences used for the similar Web services in usage history to calculate the potential QoS preference over the current Web service candidate based on their Web service similarities, which is defined as Formula (12).

$$P_{u,i} = \frac{\sum_{WS_{u,j} \in S_{sim}} S_{i,j}^{ws} \times P_{u,j}}{\sum_{WS_{u,j} \in S_{sim}} S_{i,j}^{ws}} \quad (12)$$

In some cases, the number of services in S_{sim} could be very small. In this situation, the resulting QoS preference may not be accurate enough, since limited information can be used. To address this drawback, we use the QoS preferences from similar users who have used the current service before to compensate the problem of lacking in-formation, which is defined as Formula (13), where $P_{u_k,i}$ is the effective QoS preference of WS_i by user u_k , and where ψ_1 and ψ_2 are adjustment parameters, with $\psi_1+\psi_2=1$.

$$P_{u,i} = \psi_1 \frac{\sum_{WS_{u,j} \in S_{sim}} S_{i,j}^{ws} \times P_{u,j}}{\sum_{WS_{u,j} \in S_{sim}} S_{i,j}^{ws}} + \psi_2 \frac{\sum_{u_k \in U_{sim}} S_{u_k,i}^{user} \times P_{u_k,i}}{\sum_{u_k \in U_{sim}} S_{u_k,i}^{user}} \quad (13)$$

For example, when Web services used by a user are from recommendation, there will be no QoS preference information recorded in the usage history. Therefore, they cannot contribute to evaluate the potential QoS preference of the active user to the current Web service in Algorithm 1.

5.2 NEIGHBORHOOD SIMILARITY COMPUTATION

An $m \times n$ user-item matrix R consists of m service users and n web services, each entry in this matrix R_{ij} represents the value of a certain client-side QoS property of web service j observed by service user i . If user i did not invoke the web service j before, then $R_{ij} = \text{null}$. Employing the available web service QoS values in the user item matrix, which are collected from different service users, the similarities between different service users can be computed by PCC. After calculating the similarities between the current user and other users, a set of Top-K similar users can be identified based on the PCC values. In practice, a service user may have limited number of similar users. Traditional Top-K algorithms ignore this problem and still include dissimilar users with negative PCC values, which will greatly influence the prediction accuracy. In our approach, we exclude the dissimilar service users who have negative correlations (negative PCC values). With the neighborhood information, we can now design our CB-NIMF model for the QoS value prediction.

5.3 HISTORICAL USER INTEREST COMPUTATION

Terms in WSDL documents of all the available Web service candidates can be looked upon as a corpus and therefore we employ the well-known TF/IDF (Term Frequency/Inverse Document Frequency) algorithm to weight the importance of terms in the corpus. TF/IDF is a statistical measure to evaluate how important a word is to a document in the corpus. The importance increases proportionally to the number of times a word appearing in the document but is offset by frequency of the word in the corpus. Variations of TF/IDF weighting scheme are often used by search engines as a central tool in scoring and ranking documents' relevance given a user query. It analyzes most common terms appearing in each document and appearing less frequently in other documents.

5.4 SIMILARITY MEASURE COMPUTATION

The relevance of Web services with the user interest computed above is only based on the active user's own Web service usage history, while the service experiences of the other users are neglected. The service experiences of the other users can be used to predict the potential interest of the active user. Thus, we also apply collaborative filtering approach to find the Web services which are probably interesting to the active user. Based on this observation, we use the following formula to calculate the user similarity, between two users.

$$\text{userSim}(u_i, u_j) = \frac{2 \times |CS_{ij}|}{|S_{u_i}| + |S_{u_j}|}$$

Where S_{u_i} and S_{u_j} are the sets of Web services used by user u_i and u_j respectively, CS_{ij} is the set of Web services used by both u_i and u_j , i.e., $CS_{ij} = S_{u_i} \cap S_{u_j}$. If $CS_{ij} = \emptyset$, then we have $\text{userSim}(u_i, u_j) = 0$.

5.5 DIVERSITY EVALUATION

To evaluate the diversity degree of Web services in a recommendation list, we employ a generalized diversified ranking measure modified for Web services. For simplicity, we firstly specify the following definitions and notations for discussing the diversity measurement.

Definition 1. Web Service Graph:

A Web service graph $G = (V, E)$ is an undirected weighted graph consisting of a set of nodes V and a set of edges E , wherein a node denotes a Web service candidate, i.e., v_i , and an edge denotes that the connected nodes are similar. $V = K$ is the number of nodes (i.e., Web services) in the graph.

Here, the intuition behind is that two nodes are dissimilar if they do not share the

common neighbors in the Web service graph. Therefore, the definition of expansion ratio can be considered as a diversity measure. With Def. 2 and 3, we can infer that a set of nodes with larger expansion ratio are more dissimilar to each other.

Algorithm 2 Web Service Graph Construction

Input: $S_1^H, S_2^H, \dots, S_N^H; S_1^P, S_2^P, \dots, S_N^P; U_{u,1}, U_{u,2}, \dots, U_{u,N}; \theta_H, \theta_P, \alpha, \beta, \gamma$

Output: Web Service Graph $G = (V, E)$

- 1: $V = \emptyset, E = \emptyset;$
- 2: **for** $i=1$ to N **do**
- 3: **if** $S_i^H \geq \theta_H$ or $S_i^P \geq \theta_P$ **then**
- 4: add WS_i to $V;$
- 5: **end if**
- 6: **end for**
- 7: **for each** node in V **do**
- 8: $Score_{u,i} = \alpha S_i^H + \beta S_i^P + \gamma U_{u,i};$
- 9: **end for**
- 10: **for each pair of nodes** v_i and v_j **in** V **do**
- 11: **if** $wsSim(WS_{v_i}, WS_{v_j}) \geq \tau$ **then**
- 12: add edge (v_i, v_j) to $E;$
- 13: **end if**
- 14: **end for**
- 15: **return** $G = (V, E);$

Given a Web service graph in Figure (a), let's select three nodes from it. Figure (b) and Figure (c) are two different cases, where white nodes represent the nodes selected. There are six nodes (white nodes and gray nodes) in the expanded set for the case in Figure (b), and nine nodes for the case in Figure (c). We can infer that the expansion ratio of the selected nodes in Figure (b) and Figure (c) are 0.6 and 0.9, respectively. The selected nodes in Figure (b) are well connected, thus they are probably similar to one another. On the contrary, there is no edge between any two selected nodes in Figure (c). Therefore, the selected nodes in Figure (c) are more diverse than those in Figure (b). This example shows that nodes with a larger expansion ratio have better diversity. Our diversified ranking measure is on the above definition.

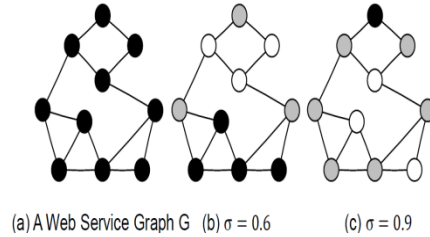


Fig. Illustration of Expansion Ratio v.s. Diversity (white nodes denote the selected nodes and gray nodes are the expanded nodes)

VI. CONCLUSION

Using web service recommendation approach with diversity to find desired Web services for users. We incorporate functional interest, QoS preference, and diversity feature for recommending top-k diversified Web services. A diversified Web service ranking algorithm is proposed to find the top-k diversified Web service ranked list based on their functional relevance including historical user interest relevance and potential user interest relevance, non-functional relevance such as QoS utility, and diversity feature. Experimental results on a real world Web service dataset show that the proposed approach improves the Web service recommendation performance in terms of diversity, the combination of functional relevance and QoS utility, and the diversified ranking evaluation.

VII. FUTURE ENHANCEMENT

In future work, we will study Web service clustering methods to improve the similarity computation and conduct real user survey to evaluate the usefulness of our method further. In addition, our proposed diversified ranking measure mainly focuses on the immediate neighborhood information of S in the Web service graph. More tests will be performed by our diversified ranking measure with k-hop nearest neighbors in the future work.

REFERENCES

- [1] Bruneo.D; Distefano.S; Longo.F; Scarpa.M; Parallel and Distributed Systems“Stochastic Evaluation of QoS in Service based system.” IEEE Transactions 2013.
- [2] GuobingZou, Qiang LU, Yixin Chen, Senior Member, IEEE, Ruoyng Huang, You Xu. ”Qos – Aware Dynamic composition of Web Services using Numerical Temporal Planning.” IEEE Transactions on Services Computing, September 2012.
- [3] Guosheng Kang, Mingdong Tang, Jianxun Liu, Xiaoqing(Frank) Liu ”Diversifying Web Service Recommendation Results Via Exploring Service Usage History.” IEEE Transaction on Service Computing , 2015.
- [4] Hai-hong E, Jun-jie TONG, Mei-na SONG, Jun-de SONG, The journal of China Universities of Posts and Telecommunications, “A location-aware hybrid web service Qos prediction algorithm.” Volume 21, supplement 1, July 2014.
- [5] Huifeng Sun; ZibinZheng, Member IEEE Juliang Chen;Lyu , M.R. Services Computing , “Personalized Web Service Recommendation via Normal Recovery collaborative Filtering.” IEEE transaction On volume 6 , 2013.
- [6] Jianwei Yin, Wei Lo, Shuiguang Deng, Ying Li, Zhaohui Wu, Naixue Xiong, Information and Sciences, “Colbar: A collaborative location-based regularization framework for QoS prediction.” Volume 265, 1 May 2014.
- [7] Jose Antonio Parejo , Sergio Segura , Pablo Fernandez , Antonio Ruiz – Cortes. Experts Systems with Application, ”Qos – Aware Web Service Composition using GRASP with Path Relinking.” Volume 41, July 2014.
- [8] Ming ZHOU, Yan MA, The Journal of China Universities of Posts and Telecommunications, “Qos aware computational method for IoT composite service.” Volume 20, Supplement 1, August 2013.
- [9]M.Rajeswari, G.Sambasivam, N.Balaji, M.S.Saleem Basha, T.Vengattaraman, P.Dhavachelvan, Journal of King Saud University – Computer and Information Sciences, “Appraisal and analysis on various web service composition approaches based on QoS factors.” Volume 26, Issue 1, January 2014.
- [10] Qian Tao, Hui-you Chang, Chun-qin Gu, Yang yi, Expert Systems with Applications, “A novel prediction approach for trustworthy QoS of web services.” Volume 39, Issue 3, February 2012.
- [11] Rajeev Pratap Singh, K.K. Pattanaik, AtalBihari Vajpayee – Indian Institute of Information Technology, Gwalior, India Procedia Computer Science, ”An approach for composite Qos parameter based Web Service selection.” Volume 19, September 2013.
- [12] Ruslan Salakhutdinov &AndriyMnih., Advances in neural information processing systems, “Evaluating probabilistic Matrix Factorization on Data set.” Pp. 1257- 1264, 2007.
- [13] Shengjun Qin, Yan Chen, Xiangwei Mu, Information and Science, “An Optimal Service Selection with Constraints Based on QoS.” Volume 25, August 2013.
- [14] Xi Chen; ZibinZheng; Xudong Liu; Zicheng Huang; Hailong Sun, service computing, “Personalized Qos-Aware Web Service Recommendation and Visualization.” IEEE Transactions 2013.

Computer Aided Detection and Classification of Breast Masses in Digital Mammograms

K.Vaidehi^{1*}, T.S.Subashini²

CSE,annamalaiuniversity,vainakrishna@gmail.com

Abstract- Mammography is the effective imaging modality for early detection and diagnosis of breast cancer. Digital mammogram is a mammography system which takes an electronic image of the breast and stores it directly in to the computer. The aim of the study is to develop an automated system for assisting the radiologist to analyse the digital mammograms. In this study input images are taken from Mammographic Image Analysis Society (MIAS) database. In MIAS database, masses are grouped into either spiculated, well-defined or circumscribed, ill-defined masses with benign and malignant details. Fuzzy C-means technique is used to segment the mass region from the input image. Discrete cosine transform coefficients are extracted from the region of interest. Dimensionality reduction was carried out using Principal Component Analysis (PCA) and the reduced features were classified using Support Vector Machine (SVM) and Sparse Representation Based Classifier (SRC). The experimental results show the effectiveness of the proposed system with the SVM classifier is high with an accuracy of 95.83% and Mathew's correlation coefficient of 91.23%.

Keywords- Benign and malignant mass classification, Fuzzy C-Means clustering, Discrete Cosine Transform, Principal Component Analysis, Performance measures.

I. INTRODUCTION

Worldwide, breast cancer is one of the top two leading cancers in the world. There are an estimated 1,00,000 – 1,25,000 new breast cancer cases in India every year. The number of breast cancer cases in India is estimated to double by 2025 [1]. The breast cancer occurrence rates have increased over the years, and breast cancer mortality has also increased among women. Early detection of breast cancer is essential to reduce mortality and treat adequately. Achieving this will lead to better long term survival as well as a better quality of life.

Mammograms are X-ray images of the breast, which gives information about breast morphology, pathology and anatomy and it is used to detect breast cancer. Digital mammography is the x-ray of the mammogram which stores images directly into the system. It is the most extensively recommended breast screening technique for detecting early breast carcinomas [2]. Digital mammography process, guidelines and advantages are vividly explained in [3].

Masses and micro-calcifications are two important early signs of breast cancer. Masses are often obscured in the surrounding parenchymal tissue, so it is a challenging process to distinguish between the mass region and normal breast region. Mass are found in several shapes namely circumscribed, speculated, ill-defined or lobulated. Masses with more irregular shapes are malignant and masses with regular and smooth boundaries are in benign stage. While malignant are considered as cancerous tumours benign are non-cancerous.

Computer technology has had a tremendous impact on medical imaging which is a keystone for radiologist to interpret the diseases and finding accurate diagnosis in its benign stage. It may assist the radiologist who is not experienced and act as a second reader. This automated system aims to help the radiologist in detecting and classifying breast tumors. In this work, automatic mass classification is done based on the discrete cosine transform coefficients extracted from the mass ROI and SVM, SRC, Adaboost are used as classifiers.

II.LITERATURE REVIEW

Segmentation approaches are classified into region based methods [4], contour based methods [5], clustering and thresholding methods [6] and model based methods [7]. Clustering based segmentation technique is proposed in this work. Breast image characterized into normal/abnormal image and abnormal image into benign/ malignant mass [8] based on feature energy extracted using the shearlet transform and wavelet transform with three wavelets namely bi-orthogonal (bior 3.7), Daubechies-8(db8) and Symlet (sym8) are the mammogram images were characterized using two stage SVM classifier. Shearlet energy features outperformed wavelet energy features using multi-level decomposition. Non subsampled contourlet transform coefficients and SVM classifier is used for benign and malignant classification of mammogram images in [9]. Benign and malignant mass classification from mammogram region of interest is presented in [10] and it is based on Discrete wavelet transform features and Artificial Neural Network classifier.

The authors in [11] classified the benign and malignant masses using the shape based continuous Zernike orthogonal moment and discrete Krawtchouk orthogonal moment descriptors as features. The extracted feature dimensions are reduced using PCA and K-nn classifier. The accuracy obtained was 81% and 90.2% using Zernike moment and Krawtchouk moment respectively. From the four directions of the gray level co-occurrence matrices, texture features such as Contrast, Energy and Homogeneity features were extracted in [12]. These features classified the mass into either spiculated, ill-defined or circumscribed. Decision tree with five criterions was analyzed for classification of masses.

III.MATERIALS AND METHODS

A. Database description

An organization in UK called Mammography Image Analysis Society (MIAS) has created a mammogram database. This database is used in this study. It contains both the right and left breast images of the same patient with a uniform size of 1024 x 1024 pixels. The mammogram in this database is digitized to a resolution of 50m x 50m, 8 bits represents each pixel. The database contains 322 mammograms of 161 patients, in which 209 are normal mammograms and 113 are abnormal mammograms which includes both mass and microcalci-fication. The database has the ground truth details such as tissue types, class of abnormality, severity of abnormality and location of abnormality like xy image-coordinates of centre of abnormality, and approximate radius (in pixels) of a circle enclosing the abnormality [13].

B. Mass region Segmentation

Segmentation is one of the most important step to computer aided detection (CAD) particularly for masses. Breast masses are obscured by the normal breast parenchymal tissue. Fuzzy K-means clustering based segmentation approach is used in this work.

Fuzzy C-Means .

In the medical domain, FCM is one of the most commonly used unsupervised pattern recognition approach for tumor segmentation. In 1981, Bezdek introduced this algorithm as an alternative to earlier hard C-means clustering [14]. FCM employs fuzzy partitioning, this approach partitions the datapoints into K clusters to determine a degree specified by its membership grades between 0 and 1.

Algorithm for Fuzzy C-Means clustering.

The goal of Fuzzy c-means is to minimize the following objective function of weighted distances of the data to the centers.

$$O_m = \sum_{i=1}^C \sum_{j=1}^N v_{ij}^m |x_j - c_i|^2 \quad (1)$$

where m is any real number greater than 1, V_{ij} is the degree of membership of X_j in the cluster C_i , x_j is the i th data point of the n -dimensional data, C_i is the i th cluster of the n -dimensional center.

C. Feature Extraction

The discrete cosine transform (DCT) helps to separate the image into parts (or spectral sub-bands) of differing importance (with respect to the image's visual quality). The DCT transforms a signal from a spatial representation into a frequency representation which maps an n -dimensional vector to set of n coefficients. Properties of DCT are decorrelation, energy compaction, separability, symmetry, orthogonality [15].

One-dimensional DCT is given by:

$$F(u) = C(u) \sum_{x=0}^{N-1} f(x) \cos\left[\frac{\pi(2x+1)u}{2N}\right] \quad (3)$$

where $u=0,1,\dots,N-1$

$$C(u) = \begin{cases} \frac{1}{\sqrt{N}} & \text{when } u = 0 \\ \frac{2}{\sqrt{N}} & \text{when } u \neq 0 \end{cases}$$

Two-dimensional DCT is given by:

$$F(u, v) = C(u)C(v) \sum_{x=0}^{N-1} \sum_{y=0}^{M-1} f(x, y) \cos\left[\frac{\pi(2x+1)u}{2N}\right] \cos\left[\frac{\pi(2y+1)v}{2N}\right] \quad (4)$$

where $u=0,1,\dots,N-1$ $v=0,1,\dots,M-1$

$$C(u), C(v) = \begin{cases} \frac{1}{\sqrt{N}} & \text{when } u,v=0 \\ \frac{2}{\sqrt{N}} & \text{when } u,v \neq 0 \end{cases}$$

E. Classification

Ada Boost.

In 2003, Yoav Freund and Robert Schaphire formulated a machine learning meta-algorithm called Adaptive Boosting (AdaBoost). It is very simple to implement and good for generalization. It improves the classification accuracy and not prone to overfitting. It is an iterative algorithm and during an each iteration of the training phase, a new weak learner is added to create a strong learner that is only slightly correlated to the classifier. The weighting vector is adjusted every time the weak learner is added to the ensemble to focus on examples that were misclassified in the earlier iteration. Hence it is called adaptive and finally results with a classifier with better accuracy.

The Sparse Representation based classifier.

In this work for mass classification sparse representation based classifier (SRC) is used. In SRC, the given test sample can be represented as a linear combination of the training sample and does not require any formal training process [17,18].

Let A be the training sample matrix of p classes.

$$A = \{A_1, A_2, \dots, A_p\} = \{v_{i1}, v_{i12}, \dots, v_i n_i\} \quad (5)$$

A test mammaogram image y could be well approximated by a linear combination of the training sample from A_i which is given by

$$y = \sum_{j=1}^{n_i} a_{ij} v_{ij} \quad (6)$$

where n is the number of sample in class i . Now eqn. (6) can be rewritten as

$$y = Ax_0 \quad (7)$$

Since A is the dictionary which includes all the training samples.

$x_0 = \{0, \dots, 0, \alpha_{i,1}, \alpha_{i,2}, \dots, \alpha_{i,n_i}, 0, \dots, 0\}^T$ is the coefficient vector in which most coefficients are

zero except the ones associated with class i . This motivation us to seek its sparse solution and this is the same as solving the following optimization problem (l_0 minimization)

$$\hat{x}_0 = \arg \min_x \|x\|_0 \quad \text{subject to } Ax=y \quad (8)$$

The noisy model is modified as:

$$y = Ax_0 + \varepsilon \quad (9)$$

where ε is the noise level. Then, the equation (8) is converted into:

$$\hat{x}_0 = \arg \min_x \|x\|_0 \quad \text{subject to } \|Ax - y\|_2 \leq \varepsilon \quad (10)$$

We consider using the residual error to classify y . After estimating \hat{x}_1 , the given test mass image \hat{y} is approximated as:

$$\hat{y}_i = A\delta_i(\hat{x}_i) \quad (11)$$

where $\delta_i(\hat{x}_i)$ is a new vector whose only nonzero entries in \hat{x}_i are associated with the class i .

The residual error $r_i(y)$ is:

$$r_i(y) = y_i - A\delta_i(x_i) \quad (12)$$

The test sample y is classified with the class having the minimal residual error. The SRC algorithm has good generalization ability so it is more suitable for medical applications.

Support Vector Machine (SVM).

In the 1990s, support vector machine learning algorithm was developed by Vapnik [20]. SVM can be used for pattern classification and nonlinear regression. Either linearly or non-linearly, it maps the input vectors into a high dimensional feature space with the help of kernel functions. Some common kernels using SVM are Polynomial (homogeneous), Polynomial (inhomogeneous), Gaussian radial basis function and Sigmoid. A hyperplane is created in the feature space to separate the features into two classes. An optimum hyperplane is a hyperplane which separates the data without error and maximizes the distance between the two classes. The goal of SVM modeling is to find the optimal hyperplane that separates the clusters of vector in such a way that cases with one class of the target variable are on one side of the plane and cases with the other class are on the other side of the plane. The vectors near the hyperplane are the support vectors. Margin is the distance between the two hyperplanes. SVM separates the two classes well if the margin is maximum. Fig. 4 illustrates the maximum margin hyperplane.

G. Performance measures

In this work, the classification accuracies were used to evaluate the performance measure of the mass classification system. Sensitivity measures how reliable a system is making positive (mass) identifications and specificity measures how well a system can make a negative (non-mass) identification. Matthews Correlation Coefficient (MCC) is a powerful accuracy evaluation criterion of machine learning methods. It is more suitable for the number of negative samples and positive samples are obviously unbalanced.

IV. EXPERIMENTAL RESULTS

The MIAS database contains ground truth of the image which includes the center of the mass (i.e) xy image-coordinates of center of abnormality, and approximate radius (in pixels) of a circle enclosing the abnormality. Totally 48 abnormal mammograms containing mass is considered for this study. Out of which 16 are malignant mammograms and 32 are benign mammograms. A square region of area 174x174 pixels is taken as the ROI for further processing. The value 174 is chosen in consultation with the radiologist because it is the radius of the largest mass present in the database and moreover mass will not be more than the size of 174x174.

Discrete cosine transform exploits interpixel redundancies to render excellent decorrelation of the mass ROI. Thus, all transform coefficients can be encoded independently without compromising coding efficiency. In addition, the DCT has the ability to pack the energy (image data) into as few DCT coefficients as possible without any distortion. A zigzag scan is performed on the DCT coefficients obtained to retain the most relevant DCT values. Top 100 DCT coefficients are considered as feature vectors and fed into PCA for dimension reduction. PCA produced 9 projected vectors, which is fed into the classifiers namely Adaboost, SRC and SVM.

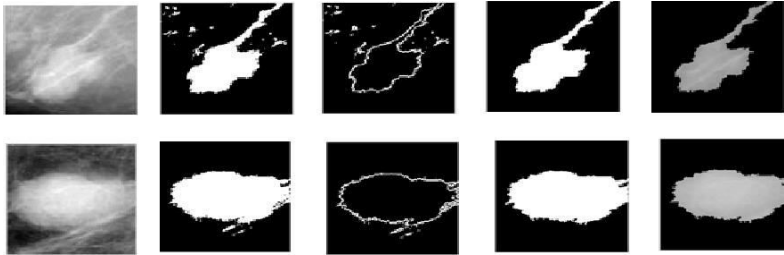


Fig. 3. a) input ROI b) FCM segmented mass image c) contour of mass d) after applying morphological operation e) original pixel values of the segmented mass.

Table 1. Performance evaluation of three classifiers

Type	Accuracy (%)	Sensitivity (%)	Specificity (%)	PPV (%)	NPV (%)	MCC (%)
Adaboost	91.66	90.62	93.75	96.66	83.33	82.15
SRC	87.50	87.5	87.50	93.33	77.77	73.02
SVM	95.83	93.75	99.99	99.99	88.88	91.23

The performance measures used for classification are accuracy, sensitivity, specificity, PPV, NPV and MCC. Leave one out procedure has been adopted in testing the performance of the various classifiers. Table 1 shows the performance of the three classifiers with PCA applied DCT coefficients. It could be seen that the SVM outperformed Adaboost and SRC in classifying benign and malignant masses. The accuracy obtained using SVM was 95.83%. Since the number of samples in the two classes is unbalanced, Mathews Correlation Coefficient (MCC) is calculated which helps to evaluate the system better than the overall accuracy. SVM obtained the highest MCC of 91.23% whereas the other classifiers reported relatively poor MCC.

V.CONCLUSION

In this paper, we proposed an automatic system which detects and categorizes benign mass and malignant mass regions from the breast ROI. Mini-mias database images are used for this study. This automatic detection of masses is beneficial to the radiologist in detecting and classifying the early stage of (benign) mass and cancerous stage (malignant) without

con-fusion. Even though the mass regions are obscured in the dense regions, fuzzy C-means clustering algorithm is efficient in segmenting mass regions from the ROI. The study reveals that the PCA reduced DCT coefficients along with SVM classifier was effective in classification of benign mass and malignant masses in digital mammograms. The SVM classifier obtained the highest accuracy of 95.83%. The proposed work was carried out using MATLAB 2012a.

REFERENCES.

1. Cancer statistics in Indian Women, The Times of India, http://articles.timesofindia.inadiatimes.com/2012-10-21/special-report/34626683_1_breast-cancer-commonest-cancer-cancer-statistics
2. American Cancer Society recommendations for early breast cancer detection in women without breast symptoms, Breast Cancer Early Detection, reviewed: 09/17/2013, re-vised:1/28/2014, [www.cancer.org/cancer/breastcancer/moreinformation/breastcancerearly detection/breast-cancer-early-detection-ac-s-recs](http://www.cancer.org/cancer/breastcancer/moreinformation/breastcancerearly%20detection/breast-cancer-early-detection-ac-s-recs)
3. Bowes, M.P.: Digital Mammography: Process, Guidelines and potential advantages. eRadimaging. (2012). www.eradimaging.com/site/article.cfm?ID=791#.U0t41fkWXDA
4. Wei, J., Chan, H. P., Sahiner, B., Hadjiiski, L. M., Helvie, M. A., Roubidoux, M. A. & Ge, J.: Dual system approach to computer-aided detection of breast masses on mammo-grams. Medical physics. 33(11), pp. 4157-4168 (2006).
5. Sahiner, B., Chan, H. P., Petrick, N., Helvie, M. A., & Hadjiiski, L. M.: Improvement of mammographic mass characterization using spiculation measures and morphological fea-tures. Medical Physics. 28(7), pp. 1455-1465 (2001).
6. Bellotti, R., De Carlo, F., Tangaro, S., Gargano, G., Maggipinto, G., Castellano, M., De Nunzio, G.: A completely automated CAD system for mass detection in a large mammo-graphic database. Medical physics. 33(8), pp. 3066-3075 (2006).
7. Cheng, H. D., & Cui, M.: Mass lesion detection with a fuzzy neural network. Pattern recognition. 37(6), pp. 1189-1200 (2004).
8. Amjath Ali, J., Janet, J.: Mass classification in digital mammograms based on discrete shearlet transform. Journal of Computer Science. 9(6) (2013).
9. Jasmine, J. S., S. Baskaran, and A. Govardhan.: An Automated Mass Classification Sys-tem in Digital Mammograms using Contourlet Transform and Support Vector Ma-chine. International Journal of Computer Applications. 31 (2011).
10. Fraschini, M. Mammographic masses classification: novel and simple signal analysis method. Electronics letters. 47(1), pp. 14-15 (2011).
11. Narváez, F., & Romero, E.: Breast mass classification using orthogonal moments. In Breast Imaging. Springer. pp. 64-71 (2012).
12. Khuzi, A. M., Besar, R., Zaki, W. W., Ahmad, N. N.: Identification of masses in digital mammogram using gray level co-occurrence matrices. Biomedical Imaging and Interven-tion Journal. 5(3), e17 (2009).
13. Suckling, J., Parker, J., Dance D., et al.: The Mammogram Image Analysis Society Digi-tal Mammogram Database. Excerpta Medica, International Congress Series. 1069, pp.375-378 (1994).
14. Bezdek, J. C.: Pattern recognition with fuzzy objective function algorithms. Kluwer Aca-demic Publishers (1981).
15. Vaidehi, K., Subashini, T.S., Ramalingam, V., Palanivel, S., Kalaimani, M.: Transform based approaches for Palmprint Identification. International Journal of Computer Applica-tions. 41(1), pp.1-5 (2012).
16. Principal component analysis, www.fon.hum.uva.nl/praat/manual/principal_component_analysis.html.
17. Zhang, L., Zhou, W. D., Chang, P. C., Liu, J., Yan, Z., Wang, T., & Li, F. Z.: Kernel sparse representation-based classifier. IEEE Transactions on Signal Processing. 60(4), pp.1684-1695 (2012).
18. Sokolova, M., Japkowicz, N., Szpakowicz, S.: Beyond accuracy, F-score and ROC: a family of discriminant measures for performance evaluation. In AI 2006: Advances in Ar-tificial Intelligence . Springer. pp. 1015-1021 (2006).
19. Donoho, D. L.: For most large underdetermined systems of linear equations the minimal 1-norm solution is also the sparsest solution. Communications on pure and applied math-ematics. 59(6), pp.797-829 (2006).
20. V. Vapnik, Statistical Learning Theory, Wiley, New York (1998).

A Study on Different Techniques of Web Mining On Cloud Computing Technologies

Lourducaroethan.A, P.Jayanthi,V.Sakthivel.
CSE,st joseph's college,caroethan@yahoo.co.in

Abstract-Web mining techniques and applications are much needed in cloud computing. This paper surveys web mining techniques to mine information on cloud computing platform. In this paper, the problem is to identify those web data mining techniques that are proved to be appropriate for their usage in cloud computing technologies. To accomplish this task, this paper analyses the problems existing in the traditional data mining system. Aiming at these problems, this paper designs some Web data mining techniques based on cloud computing. This paper also explains about the different types of web mining that are encountered in the data analysis on Web. Each Mining technique is used in different ways to manage the data in cloud i.e. Cloud Mining that can be seen as future of Web Mining. This paper also describes web mining through cloud computing. This paper discusses the current, past and future of web mining and Cloud Computing.

Keywords: Web Mining, Data Mining, Cloud Computing, Cloud Mining.

1. INTRODUCTION

1.1 Web Mining

As in conventional Data Mining, the aim of Web Mining is to discover and retrieve useful and interesting patterns from very large web dataset. Web Mining (WM), is defined as automatic crawling and extraction of relevant information from the artefacts, activities, and hidden patterns found in WWW. WM is used for tracking customers' online behaviour, most importantly cookies tracking and hyperlinks correlations.

WM is extraction of relevant information from the relics and mannerism recorded by the stakeholders on World Wide Web for knowledge management purpose. The online information resource is very large and organizations are utilizing web content mining and access through the web servers. In addition, the Internet has an integral role as network and communications are ubiquitous today, mining is carried over the world through the network of databases.

Web data mining can be classified into three. These are: Web content mining, Web structure mining and Web usage mining.

A. Web Content Mining

This is the process of extracting or quest the specified information or knowledge from Web page contents. It mainly includes summary, classification, clustering, association analysis to the content on the Web page document and query results of search engine.

B. Cloud Computing and Web Content Mining

The web content mining mines large information on the web which is contained in regularly structured data objects. The Web data records often represent the important information on the web. For cloud computing, web content mining is used in applications like comparative shopping, meta-search, query etc.

C. Web Structure Mining

This is the process of discovering useful knowledge from hyperlinks which represent structure of the Web and its content. For example, from the hyperlinks related important Web

pages can be fetched and discovered. This is the one of the key technology used in search engines to search Web content.

D. Cloud Computing and Web Structure Mining

Web Structure Mining helps in predicting the importance of the links available on web. Through this mining technique unused service on the cloud can be removed and the services which are on demand by the users can be increased. This also helps in understanding the structural usage of links on the web, so that the service providers can place the most profit-able service or most used service on the link which is accessed the most.

E. Web Usage Mining

The objective of Web usage mining is to find the mode of users to access the Web pages through mining the Web log files and the related data. It also can identify e-commerce potential customers through analysing and exploring the principles in the Web log records.

F. Cloud Computing and Web Usage Mining

Cloud Mining's Software as Service (SaaS) is used for implementing Web Mining, as it reduces the cost and increases the security. The following are the ways how the usage patterns are identified.

G. Web Mining Algorithms

A link analysis ranking algorithm starts with a set of Web pages; depending on how this set of pages is obtained. There are several algorithms proposed based on link analysis. Five important algorithms PageRank, Weighted PageRank, HITS (Hyper-link Induced Topic Search), TSPR (Topic-Sensitive PageRank) and SALSA (Stochastic Approach for Link-Structure Analysis).

1.2 Cloud Computing

NIST defines cloud computing as: "Cloud computing is a model for enabling convenient, on-demand network access to a shared pool of configurable computing resources (e.g., networks, servers, storage, applications, and services) that can be rapidly provisioned and released with minimal management effort or service provider interaction."

In cloud computing, everything is treated as a service (i.e. XaaS). There are three services delivery models that define a layered system structure for cloud computing. At the Infrastructure layer IaaS (Infrastructure as a Service) fundamental computing resources like processing, storage, networks, and other are defined as standardized services over the network. The clients of Cloud providers' can deploy and run operating systems and software for their underlying infrastructures. PaaS (Platform as a service) provides abstractions and services for developing, testing, deploying, hosting, and maintaining applications in the integrated development environment. The application layer provides a complete application set of SaaS (Software as a Service).

III. Related Works

Many researchers have looked for a way of representing the three types of web mining, different techniques of web data mining and future of web mining on Cloud Computing. Some of these researchers have said that web mining through cloud computing i.e. cloud mining, that can be seen as future of Web Mining. This paper attempts to survey on the different techniques of web data mining that can be used on cloud computing technologies.

Kumar, T. Vijaya, et al. [4] proposed a model which incorporates website knowledge in web usage mining techniques. In this paper, the authors have introduced a new idea of incorporating available website knowledge for better session construction which would eventually lead to better patterns during pattern discovery.

Sharma et al. [9] explains that when applied to Web Usage Mining, association rule mines are used to find associations among web pages that frequently appear together in users' sessions. The authors have proposed different learning web usage patterns and evaluated some interesting measures to evaluate the association rules mined from web usage data.

Munibalaji et al. [7] has given a survey of page ranking algorithms and description about Weighted Page Content Rank (WPCR) based on web content mining and structure mining that shows the relevancy of the pages to a given query is better determined, as compared to the Page Rank and Weighted Page Rank algorithms.

Rao, T. K., et al. [8] has explained how cloud computing can be used effectively for Web mining in e-commerce organizations to reduce costs and increase the profitability of the e-commerce enterprise. Combination of cloud computing and Web data mining can rationally change resources use and improve the efficiency of data processing and analysis.

Manish Kumar Khar [5] says that the objective of their proposal is to build an e-healthcare framework that is discovered by converging the semantic web and web mining techniques. By applying web mining techniques on ontology based structure of web, useful patterns and knowledge can be discovered for making intelligent decisions for the care of individuals. Valuable knowledge can be discovered with the application of web mining techniques that can be used to equip patients with knowledge for managing health for disease specific better care and understanding through E-Healthcare.

Wang et al. [10] combines cloud computing with the existing features of the Web log file and designs a mining platform based on Hadoop cluster framework. Using the Hadoop cluster architecture technology of cloud computing, the author constructs a massive Web log data mining system based on Cloud Computing. Combination of cloud computing and web data mining not only overcomes the bottle-neck of original system but also can rationally use resources and improve the efficiency of data processing and analysis.

Yin, Changqing et al. [11] points out that in Web data mining, processing relational data is very common, especially for the user characteristic extraction and analysis. The authors have introduced an improvised model in Web data mining named Map-Reduce-Merge, to merge the heterogeneous data produced by Reduce end effectively by increasing the Merge stage. In the meantime, it enhances the efficiency of Web data mining through optimizing the scheduling strategy, Map and Reduce tasks.

Kaur et al. [3] have discussed about Web content mining techniques and tools in brief. The Web Content varies in three ways: Firstly, it could be unstructured such as free text or in semi structured form such as HTML documents or in purely structured form such as data in tabular form. Different technique was applied on each type of web content mining.

Mohata et al. [6] has applied Web Data Mining with Information Visualization techniques to the web domain in order to benefit from the power of both human visual perception and computing that can be termed as Visual Web Mining (VWM). In response to the two challenges of such large amount of Big Data, the authors propose a generic framework, where they apply Data Mining techniques to large web data sets and use Information Visualization methods on the results. The goal is to correlate the outcomes of mining Web Usage Logs and the extracted Web Structure, by visually superimposing the results. The authors have introduced web data mining techniques and its implementation for handling the big amount web data

with VWM and Apache Hadoop Map reduce framework to handle big data. They have mainly focused on web data mining techniques, for mining of images, videos and audios, as this large amount of data leads to the big data and points out that it is today's need to mine and handle such a large amount of big data.

Jitendra Singh Tomar [2] have introduced the various cloud mining techniques that are invariably used by various organizations and individuals to extract relevant information from the cloud based service on relics and mannerism recorded by the stakeholders on the cloud. It is a new approach to enhance search interface of the data on the cloud. The technology is framed with new dimensions to support cloud computing and modifications that are brought in web mining to counter the demands of cloud computing. Utilities like SaaS (Software-as-a-Service) are used for reducing the cost of web mining and try to provide information management with cloud mining and computing techniques. The authors have developed powerful frameworks for doing predictive analytics over the cloud as compared to complex distributed information sources.

Al-Azmi et al. [1] have focused on the web mining technologies mainly used through information systems for business applications to gain new levels of business intelligence. Furthermore, the authors have concentrated on at how these techniques can help in achieving both business leadership and risk management by illustrating real enterprises' own experience using web mining techniques.

IV. Existing System

There is a rapid development of World Wide Web in its volume of traffic and the size and complexity of web sites. The main components of Web Mining Technology have been under development for decades, in research area such as internet, artificial intelligence, and machine learning. Today, the maturity of these techniques, coupled with high performance relational database engines and broad data integration efforts, makes these technologies practical for current data warehouse environments.

Cloud computing is a great area to be focused by Webdata mining, as Cloud computing is penetrating more and more in all ranges of business and scientific computing. Web Data mining techniques and applications are very much needed in cloud computing paradigm. Due to low cost of setup and maintenance, cloud computing becomes a great area to be focused by Web data mining. Data mining in cloud computing involves the process of extracting structured information from unstructured or semi structured Web data sources. The future of computing is very strong with cloud computing with economies of scale strongly justifying the concept. The computing resource and applications are generic in nature and if consolidated, could offer tremendous economies of scale and business organizations are certainly taking advantage of cloud computing and its mining features. Cloud computing is the pulse of today's computing environment and is rich in features providing advantages such as on demand self-services, broad network access, resource pooling, rapid elasticity, measure services, and multi tenacity. This adds on the dynamism to computing requirements of today.

Mining too is a great application required in analysis of information and hence knowledge building. The data mining tools are enhanced to support cloud mining with the basic operations of supporting information management through techniques like clustering, classification, association, regression, attribute importance, fault & anomaly detection, and feature extraction to help in personal as well in professional arena. Content mining, structure mining, and usage mining are helping the business organizations to strategize them accordingly.

A. Drawbacks in the existing approaches

1. The explosive growth of the Web has imposed a heavy demand on networking resources and Web servers. Hence, an obvious solution in order to improve the quality of Web services would be the increase of bandwidth, but such a choice involves increasing economic cost.

2. Web caching scheme has three significant drawbacks: If the proxy is not properly updated, a user might receive stale data, and, as the number of users grows, origin servers typically become bottleneck, and, main drawback of systems which have enhanced prefetching policies is that some pre-fetched objects may not be eventually requested by the users.

V. Proposed System

In the Internet era, the problem faced by the users is not the difficulty to obtain information, but to grasp the truly valuable information that is hidden behind huge amounts of data. Since the users want to access only the relevant information required by them, useful knowledge extraction from the web is a breakthrough which is considered to be beyond the human efforts limit. Web Data Mining, which can be used to solve this problem, is on the road to provide the necessary help.

Web mining can be viewed as the use of data mining techniques to automatically retrieve, extract and evaluate information for knowledge discovery from web documents and services. Here, evaluation includes both generalization and analysis. Since, Web mining techniques could be more efficiently used to solve the information overload problem directly or indirectly, in this work, we have noticed that, we can aim to find a more accurate and faster techniques for Web data mining, also based on cloud computing.

On the Internet, huge amounts of data generated is distributed which are heterogeneous, dynamic and more complex. So, the use of the existing centralized data mining methods cannot meet these application requirements. To solve these problems, we propose to identify the different Web data mining techniques based on cloud computing technologies.

The massive data and mining tasks are decomposed on multiple computers to be parallelly processed for which data mining and web mining techniques can be used. This paper proposes a design, thinking that these techniques can be analysed in order to find out, if these data and web mining techniques can be used for cloud computing technologies.

Since, the evolution of cloud computing technologies is taking place rapidly, the technological improvements that are resulted by it have extensive usage in computing which makes it worth to be considered as rich as that of the available traditional data mining methods for managing mass data storage. Massive web data mining techniques based on cloud computing will drive the Internet advanced technological achievements in the public service, by providing the necessary depth to promote information resources sharing and sustainable use of new web data mining methods in innovative ways of computing.

VI. Execution

In order to find out the different techniques of web data mining, that can be used on cloud computing technologies, the following steps can be considered for the implementation procedure. First, the data mining algorithm design and programming which is a need has to be seriously considered. Only select the appropriate algorithm, and take appropriate parallel

strategy, in order to improve efficiency. Parameter setting and adjustment is also very important, and improper disposal will directly affect the final result. Second, in the data mining process, there are many uncertainties, such as: the description of the tasks, data collection, and the methods used and the results arrived by using them also have uncertainties. All these uncertainties that are encountered in the data mining process can be finalized by the analysis of every data mining procedure.

6. Problem Statement

Previous studies, have mainly dealt with the usage of three types of web data mining on Cloud Computing technologies, but no study has yet been made on focusing the different web data mining techniques that are based on cloud computing. So, the basic idea behind this paper can be proposed as “ A Study on Different Techniques of Web Mining on Cloud Computing Technologies”.

The purpose of the paper is to provide past, current evaluation and future direction in each of the three different types of web mining i.e. web content mining, web structure mining and web usage mining. Hence, in this paper we present the technology of cloud computing using different web data mining techniques.

VII. Discussion

In this paper, we have concentrated to conduct a study on the web data mining techniques, which is the application of data mining techniques to extract knowledge from Web data, including Web documents, hyperlinks between documents, usage logs of web sites, etc. As it is very much important to mine particular data from web, we have studied effective techniques to mine this web data.

In this paper we have discussed how cloud computing is changing the computing scenario and how Web data mining can be used in cloud computing by the e-commerce organizations to reduce setup costs and maximize return on investments. This paper introduces web data mining concepts and relevant technology of cloud computing.

In this paper we have briefly described the key computer science contributions made by the field of web mining and cloud computing, the prominent successful applications that are developed in these areas, and outlined some promising areas of future research that can be carried out by focussing mainly on these fields. Our hope is that, this overview provides a starting point for fruitful discussion.

VIII. Conclusion

As the Web has become a major source of information, techniques and methodologies to extract quality information is of paramount importance for many Web applications and users. In this paper, various concepts are outlined to extract the useful information from the web. Web design patterns are useful tools for web data mining. Web pages are analysed to find out which useful information is included in web data.

Web Data mining technologies provided through Cloud computing is an absolutely necessary characteristic for today's businesses to make proactive, knowledge driven decisions, as it helps them have future trends and behaviours predicted. This paper provides an overview of the necessity and utility of web data mining in cloud computing. As the need for data mining tools is growing every day, the ability of integrating them in cloud computing becomes more and more stringent.

The Future work of web mining is to introduce a hierarchy on the information about the website. Now we also work for the process mining and try to combine usage mining with structure mining. We can also go for the mining from cloud. Whenever we work on mining over cloud computing that time we hesitate for the cost but that comes very less by cloud mining. So, we can say that cloud mining can be seen as future of web mining.

IX. Future Works

There are so many data mining algorithm for discovering, sharing and utilising the knowledge existing on the web , but there are also quite a few existing problems that should be taken into consideration, such as the inadequate utilization of network resources and the lack of individualisation of the existed platforms.

As the development of World Wide Web and its usage grows, it will continue to generate ever more content, structure, and usage data and the value of Web mining will keep increasing. Research needs to be done in developing the right set of Web metrics, and their measurement procedures, extracting process models from usage data, understanding how different parts of the process model impact various Web metrics of interest, how the process models change in response to various changes that are made for changing stimuli to the user,

Future extensions using cloud computing will include adding up of more data mining services to be provided by the cloud server.

REFERENCES

- [1] Al-Azmi, Abdul-Aziz Rashid. "Data, text and web mining for business intelligence: a survey." *arXiv preprint arXiv:1304.3563* (2013).
- [2] Jitendra Singh Tomar. "Web Mining Over Cloud – A Prerequisite for Today’s Enterprises." *International Journal of Advanced Research in Computer and Communication Engineering* Volume 4 (2015).
- [3] Kaur, Harmeet, and SonalChawla. "Web Data Mining: Exploring Hidden Patterns, its Types and Web Content Mining Techniques and Tools."
- [4] Kumar, T. Vijaya, et al. "A New Web Usage Mining approach for Website recommendations using Concept hierarchy and Website Graph." *International Journal of Computer and Electrical Engineering* 6.1 (2014): 67.
- [5] Manish Kumar Khar. "Ontology based Machine Learning using Data Mining Techniques."
- [6] Mohata, Pranit B., and SheetalDhande. "Web Data Mining Techniques and Implementation for Handling Big Data." (2015).
- [7] Munibalaji, T., and C. Balamurugan. "Analysis of link algorithms for web mining." *International Journal of engineering and Innovative Technology* 1.2 (2012).
- [8] Rao, T. K., et al. "Mining the E-commerce cloud: A survey on emerging relationship between web mining, E-commerce and cloud computing." *Computational Intelligence and Computing Research (ICCIC), 2013 IEEE International Conference on.* IEEE, 2013.
- [9] Sharma, Ashish, and NiketBhargava. "An Approach to Enhance Web Service Resource Framework using the Improved PLWAP Algorithm for Large Scale Hybrid Data in Distributed Environment." *International Journal of Computer Technology and Electronics Engineering (IJCTEE) Volume 1.*
- [10] Wang, Zhen Qi, and Hai Long Li. "Research of massive Web log data mining based on cloud computing." *Computational and Information Sciences (ICCIS), 2013 Fifth International Conference on.* IEEE, 2013.

Big Data in Cloud Computing

*P.Manivannan¹, S.Sri Kurinji², U.Prema³,
CSE,vrs college, , manivannanp08@gmail.com
CSE,vrs college,srikurinjimalar@gmail.com*

Abstract -In this paper, we discuss security issues for cloud computing, Big data, Map Reduce and Hadoop environment. The main focus is on security issues in cloud computing that are associated with big data. Big data applications are a great benefit to organizations, business, companies and many large scale and small scale industries. We also discuss various possible solutions for the issues in cloud computing security and Hadoop. Cloud computing security is developing at a rapid pace which includes computer security, network security, information security, and data privacy. Cloud computing plays a very vital role in protecting data, applications and the related infrastructure with the help of policies, technologies, controls, and big data tools. Moreover, cloud computing, big data and its applications, advantages are likely to represent the most promising new frontiers in science.

Keywords – Big Data, Cloud Computing, Hadoop, Map Reduce.

1.INTRODUCTION

In order to analyze complex data and to identify patterns it is very important to securely store, manage and share large amounts of complex data. Cloud comes with an explicit security challenge. The reason behind this control issue is that if one wants to get the benefits of cloud computing, he/she must also utilize the allocation of resources and also the scheduling given by the controls. Hence it is required to protect the data in the midst of untrustworthy processes. Since cloud involves extensive complexity, we believe that rather than providing a holistic solution to securing the cloud, it would be ideal to make noteworthy enhancements in securing the cloud that will ultimately provide us with a secure cloud.

1.1 Cloud Computing

Cloud Computing is a technology which depends on sharing of computing resources than having local servers or personal devices to handle the applications. In Cloud Computing, the word “Cloud” means “The Internet”, so Cloud Computing means a type of computing in which services are delivered through the Internet. The goal of Cloud Computing is to make use of increasing computing power to execute millions of instructions per second.

Cloud computing technology is being used to minimize the usage cost of computing resources. The cloud network, consisting of a network of computers, handles the load instead. The cost of software and hardware on the user end decreases. The growth of research articles about Big Data from 2008 to the present can be easily explained as the topic gained much attention over the last few years in the figure. It is, however, interesting to take a closer look at older instances where the term was used. For example, the first appearance of term Big Data appears in a 1970 article on atmospheric and oceanic soundings (according to data available in Scopus; see study limitations).



Figure 1: Overview of Cloud Computing

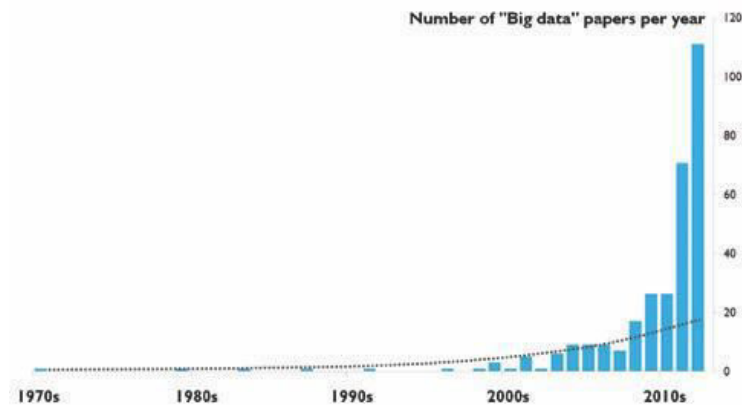


Figure 2: Time Line of Big Data

1.2 Big Data

Big Data is the word used to describe massive volumes of structured and unstructured data. Big data is a broad term for data sets so large or complex that traditional data processing applications are inadequate. Challenges include analysis, capture, data curation, search, sharing, storage, transfer, visualization, querying and information privacy. The three main terms that signify Big Data have the following properties:

- **Volume:** Many factors contribute towards increasing volume - storing transaction data, live streaming data and collect from sensors etc.
- **Variety:** Today data comes in all types of formats – from traditional databases, text documents, emails, video, audio, transactions etc.,
- **Velocity:** This means how fast the data is being produced and how fast the data needs to be processed to meet the demand.
- **Variability:** Along with the Velocity, the data flows can be highly inconsistent with periodic peaks.
- **Complexity:** Complexity of the data also needs to be considered when the data is coming from multiple sources. The data must be linked, matched, cleansed and transformed into required formats before actual processing.

Technologies today not only support the collection of large amounts of data, but also help in utilizing such data effectively.



Figure 3: Big Data Analysis

1.3 Big Data Application

The big data application refers to the large scale distributed applications which usually work with large data sets. Data exploration and analysis turned into a difficult problem in many sectors in the span of big data. With large and complex data, computation becomes difficult to be handled by the traditional data processing applications which triggers the development of big data applications.

II. ISSUES AND CHALLENGES

Cloud computing comes with numerous security issues because it encompasses many technologies including networks, databases, operating systems, virtualization, resource scheduling, transaction management, load balancing, concurrency control and memory management. Hence, security issues of these systems and technologies are applicable to cloud computing.

2.1 Distributed Data

In order to alleviate parallel computation, a large data set can be stored in many pieces across many machines. Also, redundant copies of data are made to ensure data reliability. In case a particular chunk is corrupted, the data can be retrieved from its copies. In the cloud environment, it is extremely difficult to find exactly where pieces of a file are stored. Also, these pieces of data are copied to another node/machines based on availability and maintenance operations.

2.2 Internode Communication

Much Hadoop distributions use RPC over TCP/IP for user data/operational data transfer between nodes. This happens over a network, distributed around globe consisting of wireless and wired networks. Therefore, anyone can tap and modify the inter node communication for breaking into systems.

2.3 Data Protection

Many cloud environments like Hadoop store the data as it is without encryption to improve efficiency. If a hacker can access a set of machines, there is no way to stop him to steal the critical data present in those machines.

III. PROPOSED APPROACHES

We present various security measures which would improve the security of cloud computing environment. Since the cloud environment is a mixture of many different technologies, we propose various solutions which collectively will make the environment secure.

3.1 File Encryption

Since the data is present in the machines in a cluster, a hacker can steal all the critical information. Therefore, all the data stored should be encrypted. Different encryption keys should be used on different machines and the key information should be stored centrally behind strong firewalls.

3.2 Network Encryption

All the network communication should be encrypted as per industry standards. The RPC procedure calls which take place should happen over SSL so that even if a hacker can tap into network communication packets. Whenever a node joins a cluster, it should be authenticated. In case of a malicious node, it should not be allowed to join the cluster.

3.3 Layered Framework for Assuring Cloud

A layered framework for assuring cloud computing consists of the secure virtual machine layer, secure cloud storage layer, secure cloud data layer, and the secure virtual network monitor layer.

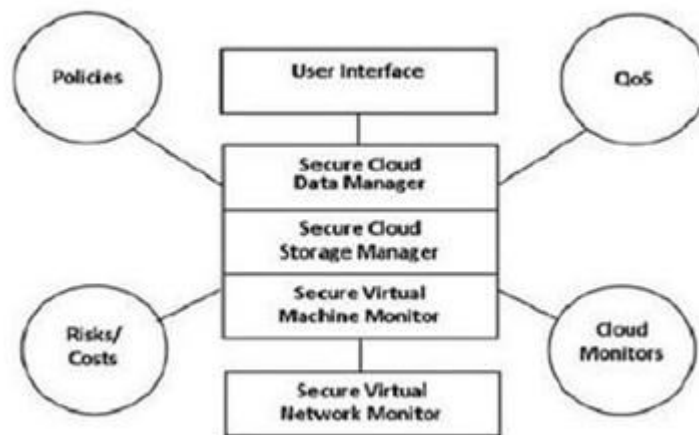


Figure 4: Layered Framework for Assuring Cloud

Third Party Secure Data Publication to cloud computing helps in storing of data at a remote site in order to maximize resource utilization. Therefore, it is very important for this data to be protected and access should be given only to authorized individuals. In the cloud environment, the machine serves the role of a third party publisher, which stores the sensitive data in the cloud. This data needs to be protected, and the above discussed techniques have to be applied to ensure the maintenance of authenticity and completeness.

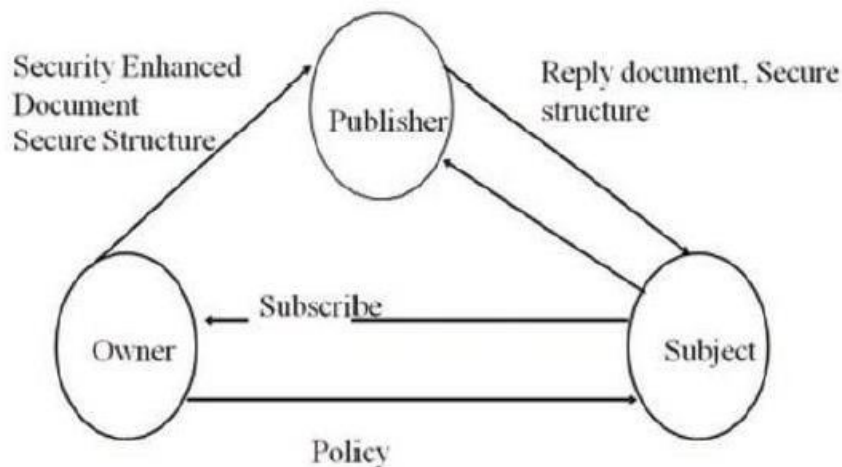


Figure 5: Third Party Secure Data Publication Applied to Cloud

IV. BIG DATA TOOLS

All the softwares listed below are open source softwares which will act as a framework/ platform for bigdata analytics.

- Hadoop (Apache Software Foundation)
- Mahout (Machine Learning Tool / Data Mining Library – Provides Data Mining Algorithms)
- MongoDB
- ZooKeeper (Apache Software Foundation)

V. CONCLUSION

In contrast to more conventional machine learning and feature engineering algorithms, Deep Learning has an advantage of potentially providing a solution to address the data analysis and learning problems found in massive volumes of input data. More specifically, it aids in automatically extracting complex data representations from large volumes of unsupervised data. This makes it a valuable tool for Big Data Analytics, which involves data analysis from very large collections of raw data that is generally unsupervised and un-categorized. The hierarchical learning and extraction of different levels of complex, data abstractions in Deep Learning provides a certain degree of simplification for Big Data Analytics tasks, especially for analyzing massive volumes of data, semantic indexing, data tagging, information retrieval, and discriminative tasks such a classification and prediction.

REFERENCES:

- [1] Ren, Yulong, and Wen Tang. "A Service Integrity Assurance Framework for CLOUD Computing based on Mapreduce." *Proceedings of IEEE CCIS2012*. Hangzhou: 2012, pp 240 – 244, Oct. 30 2012-Nov. 1 2012.
- [2] N, Gonzalez, Miers C, Redigolo F, Carvalho T, Simplicio M, de Sousa G.T, and Pourzandi M. "A Quantitative Analysis of Current Security Concerns and Solutions for Cloud Computing.". Athens: 2011., pp 231 – 238, Nov. 29 2011- Dec. 1 2011.
- [3] Hao, Chen, and Ying Qiao. "Research of Cloud Computing based on the Hadoop platform." Chengdu, China: 2011, pp. 181 – 184, 21-23 Oct 2011.
- [4] Y, Amanatullah, Ipung H.P., Juliandri A, and Lim C. "Toward cloud computing reference architecture: Cloud service management perspective.". Jakarta: 2013, pp. 1-4, 13-14 Jun. 2013.
- [5] A, Katal, Wazid M, and Goudar R.H. "Big data: Issues, challenges, tools and Good practices.". Noida: 2013, pp. 404 – 409, 8-10 Aug. 2013.
- [6] Lu, Huang, Ting-tin Hu, and Hai-shan Chen. "Research on Hadoop Cloud Computing Model and its Applications." Hangzhou, China: 2012, pp. 59 – 63, 21-24 Oct. 2012.
- [7] Wie, Jiang , Ravi V.T, and Agrawal G. "A Map-Reduce System with an Alternate API for Multi-core Environments.". Melbourne, VIC: 2010, pp. 84-93, 17-20 May. 2010.
- [8] K. Chitharanjan, and Kala Karun A. "A review on hadoop — HDFS infrastructure extensions.". JeJu Island: 2013, pp. 132-137, 11-12 Apr. 2013.
- [9] F.C.P, Muhtaroglu, Demir S, Obali M, and Girgin C. "Business model canvas perspective on big data applications." *Big Data, 2013 IEEE International Conference*, Silicon Valley, CA, Oct 6-9, 2013, pp.32 - 37.
- [10] Zhao, Yaxiong , and Jie Wu. "Dache: A data aware caching for big-data applications using the MapReduce framework." *INFOCOM, 2013 Proceedings IEEE*, Turin, Apr 14-19, 2013, pp. 35 - 39.

Secure Data Transmission Technique for iPhone using Quick Response (QR) Code

D.RANI¹, M.KAYALVIZHI¹, RAMYA¹
CSE:stannescet,ranimonise@gmail.com

ABSTRACT-The increasing use of smartphones and tablet computers as personal and business tools poses new levels of complexity to IT management and security. With continued growth of smartphones, and associated increase of mobile security concerns, users of mobile devices must be assured that the services they receive must be secured and trustworthy. A QR code (quick response code) is a type of 2D bar code that is used widely to provide easy access to information through a smartphone. It is envisioned that the technology of QR code could be applied for secured communications using smart phones. This paper provides a design framework for sending encrypted message using QR code, and decrypting the received QR code. An application is developed using Apple's iPhone to demonstrate how mobile devices such as smart phones can communicate securely with another device using QR code. The sending smartphone can encode encrypted data in a QR code, and receiving smart phone can then decrypt the data encoded in QR code and retrieve the information. User can choose different encryption/decryption algorithm such as AES for secured transmission of data. The iOS SDK together with XcodeIDE is used for the design and development of the iPhone application. The design architecture is developed using Apple's iOS mobile operating system, PHP server and MySQL database. The paper successfully demonstrates the feasibility of using QR code to securely transmit message between mobile users. The system works as expected, however rigorous analysis to assess the performance is deferred for future study.

I. INTRODUCTION

With the widespread use of smartphones, digital tablets, and other mobile devices, the deployment of QR codes for encoding information has dramatically increased. QR codes have many advantages over traditional barcodes because of their small size, superior security mechanisms, quantity of information that can be embedded, and low cost of implementation [1]. More and more smartphone applications are developed to meet different user needs, and to make the device more convenient to use. One example is the text messaging service. Other than the traditional SMS provided by the mobile phone company, many messengers such as “WeChat” [2], “LINE” [3], are using internet to send messages. Number of researchers have demonstrated using QR code for authentication purposes. For example, a secure authentication system for on-line banking that uses a two factor authentication by combining a password and a camera equipped mobile phone, where mobile phone is acting as an authentication token is detailed by Sonawane et.al [4]. This paper presents the design and implementation of application named QR Send, a proof-of-concept secure message transmission system for mobile devices that uses well known RC4/AES encryption algorithms to transmit encrypted data which will be received and decrypted by the receiving device.

This paper is organized as follows: First a brief introduction and objective of the study is provided in section 1, which is followed by literature survey in section 2 detailing some related works in this area of interest. Section 3 provides the overview of the proposed design. Section 4 describes in detail how the prototype system works. The Section 5 discusses the results and highlights the overall performance and advantages of application designed. Section 6 discusses the limitations of the study and provides suggestion in detail for future research in this area of research.

A. OBJECTIVE OF THE STUDY

The objective of the study is to design, develop and implement an application that will demonstrate how mobile devices such as smart phones can communicate in a secured fashion with another device using QR code. The sending smartphone can encrypt data using appropriate cryptographic algorithms and encode the data in a QR code. The receiving smart phone can then decrypt the data encoded in QR code and retrieve the information. This software project aims to: 1. Implement a security scheme for information exchange between two parties using QR codes as the exchange medium.

II. LITERATURE REVIEW

QR code has been widely used in many applications [1,5, 6] such as storing URLs, contact addresses and various forms of data on posters, signs and business cards. The security issues related to the use of QR code as attack vectors are discussed in [7]. The paper [7] explains how QR Codes can be used to attack both human interaction and automated systems by utilizing manipulated QR Codes. Various secure authentication systems such as single factor and two factor authentication based on QR code are detailed in [4, 8]. Liao et.al [9] proposes a QR-code based one-time password authentication protocol which eliminates the usage of the password verification table. QR code is employed to design the secret sharing mechanism so that the data privacy during data transmission can be enhanced. The secret data is divided into some shadows by the secret sharing mechanism and the results are embedded into barcode tags. The secret can be recovered only when the number of shadows is greater than or equal to the predefined threshold. In [11], Huang et.al have proposed a data hiding scheme through application of QR codes.

III. OVERVIEW OF DESIGN

The following procedures are followed in the design and implementation of the application

- Identification of the Development environment
- Design of User interface and layout
- Application design

Run and debug mobile applications The design is based on three-tier architecture and consists of the following components:

- iOS client: Any sending or receiving mobile device such as iPhone
- php server: The server authenticates login user credentials and implements services to store and gather encrypted data from My SQL database.

- MySQL database: Data base server stores user’s login credentials and QR encoded encryptedmessage
- The figure 1 shows schematically the architecture used for this application. The figure 2 shows a typical query of QR coded embedded message stored in the database. As seen each sender receiver session is given a unique id which is used as a filename to store the coded message. For example a specific message sent by user andyto yourdon with unique id d60d8d0b267a1ce is encrypted and encoded as QRcode and stored inthe file named d60d8d0b267a1ce.jpg.



Figure 1: Three tier Architecture

Showing rows 0 - 5 (6 total, Query took 0.0005 sec)

SQL query:
 SELECT *
 FROM qrcode
 WHERE 1
 LIMIT 0, 30

Show: 30 row(s) starting from record # 0
 in horizontal mode and repeat headers after 100 cells
 Sort by key: None

	id	sender	receiver
<input type="checkbox"/>	b36ab9862cb3dc8	yourdon	yourdon
<input type="checkbox"/>	d60d8d0b267a1ce	andy	yourdon
<input type="checkbox"/>	c4d5a8c48a1ce8f	andy	yourdon
<input type="checkbox"/>	cc3a7b8c95845af	yourdon	andy
<input type="checkbox"/>	13220382e4a9237	yourdon	yourdon
<input type="checkbox"/>	b64cda81f2cdf5	andy	yourdon

Figure 2: Unique id for each Sender-Receiver session

IV. PROTOTYPE IMPLEMENTATIONS

The prototype application named QR Send enables user to send and receive RC4 or AES encrypted message using QR code as a transport medium. The receiver on receiving QR encoded RC4 or AES encrypted message can decrypt the message. The application consists of three main functionalities:

- Login as different users
- Generation of Encrypted QR Code and Sending the Encrypted QR Code to intended receiver
- Receiving the Encrypted QR Code and Decrypting

V. LOGIN PROCESS

Users will login before they start the application named QR Send. This allows them to use “QR Send” to send encrypted QR message to other QR Senders.

Figure 3: Login Process

Generation and Sending of Secure QR code

A QR Code will be generated with message text, and encryption key given by users. RC4 or AES encryption methods are allowed. After that, users can select “Send” to send an encrypted message to another user. If the sending is completed, a success message will

displayed as shown in Figure 4

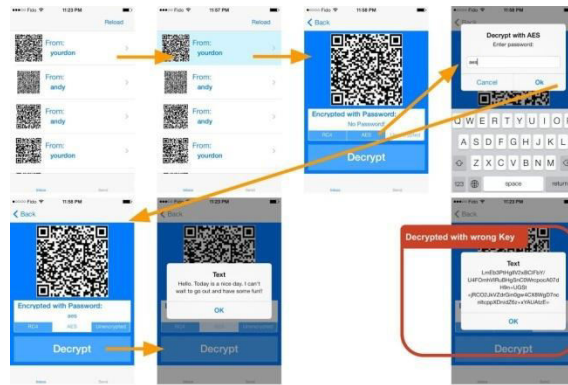


Figure 4: Decryption of received message

As a consequence of these advantages one can envision using QR code to transmit message in a secure manner. The present paper successfully demonstrates that using appropriate encryption algorithms, smart phone users can transmit and receive messages using QRcode.

We have demonstrated one application which is the stated objective of the paper. Some sample examples of useful mobile applications among many that can be developed utilizing the concepts

- Password transmission using QRcode
- Session Key distribution using QRcode
- File and document transfer using QRcode
- Delivery of Academic transcript using QRcode

However we have not conducted any performance analysis using different message sizes. This is left for future analysis.

VI. CONCLUSION

In this paper we have discussed the design and implementation of QR-based secured message transfer application using smartphone. We have proposed design and implementation framework to enable mobile users equipped with devices such as smartphones to transmit data securely to a smart phone receiver who has the capabilities of decrypting the received data. We have successfully demonstrated that mobile users equipped with iPhone can easily communicate in a secured manner. This paper only demonstrates the design and implementation of QR-based secured message transmission between mobile devices. No attempt is made to integrate authentication schemes between sender and receiver in the current implementation. The paper does not address the issue of key distribution between the sender and the receiver. Performance issues related to transmission of large amount of data securely using QR code is also not addressed, neither any attempt is made to study the vulnerability of the proposed system to various types of attacks. Future research in the areas of key distribution, authentication, performance analysis and vulnerability analysis will be carried out in future.

REFERENCES

- [1] Huang, Y.P., Chang, Y.T., Sandnes, F. E. (2010) Ubiquitous information transfer across different platforms by qr codes. *Journal of Mobile Multimedia*, 6(1), pp.3-14.

- [3]LINE, Retrieved from:<http://line.me/en/>
- [4]Sonawane, S., Khandave, M., Nemade, N. (2014)Secure Authentication for Online Banking Using QR Code, *International Journal of Emerging Technology and Advanced Engineering*, Volume (4), Issue (30), pp.778-781.
- [5] Narayanan, A. S. (2012)QR Codes and Security Solutions. *International Journal of Computer Science and Telecommunications*, Volume (3), Issue (7), pp.69-71.
- [6] Lee, Jaesik; Cho, Chang-Hyun; Jun, Moon-Seog. (2011) Secure quick response-payment (QRPay) system using mobile device. *Advanced Communication Technology (ICACT), 13th International Conference, Feb. 2011.*
- [7] Kieseberg, P., Leithner M., Mulazzani, M., Munroe, L., Schrittwieser S., Sinha, M., Weippl,E. (2010)QR Code Security.*MoMM '10 Proceedings of the 8th International Conference on Advances in Mobile Computing and Multimedia*, pp.430-435.
- [8]Pintor, D. M(2012)QRP: An improved secure authentication method using QR codes,*MasterThesisUniversitatOberta de Catalunya, Barcelona, Spain. Retrieved from: https://www.grc.com/sqrl/files/QRP-secure-authentication.pdf*
- [9]Liao, K., Lee, W. (2010)A Novel User Authentication Scheme Based on QR-Code, *Journal of NetworksVolume (5): No (8)*, pp. 937-941, 2010.
- [10]Chuang,J., Hu,Y.,Ko,H. (2010) A NovelSecret Sharing Technique Using QR Code, *International Journal of Image Processing (IJIP)*, Volume (4): Issue (5), pp.468-475, 2010.
- [11] Huang,H., Chang,F., Fang, W. (2011). Reversible data hiding with histogram-based difference expansion for QR code applications, *Consumer Electronics, IEEE Transactions on* , Volume (57), No (2), pp.779,787, May 2011.

Cryptography and Efficient Data Transmission for Cluster-Based Wireless Sensor Networks

Sr. S. Jothi¹, Sr. A. Avila Therese², Bhuvana³

1. Assistant Professor, Department of Computer Science, Jayaraj Annapackiam College for Women, Periyakulam
2. Assistant Professor, Department of Computer Science and Engineering, St. Anne's College of Engineering and Technology, Panruti
3. UG Student, Department of Computer Science, St. Anne's College of Engineering and Technology, Panruti

ABSTRACT - Secure data transmission is a critical issue for wireless sensor networks (WSNs). Clustering is an effective and practical way to enhance the system performance of WSNs. The study in this paper is, a secure data transmission for cluster-based WSNs (CWSNs), where the clusters are formed dynamically and periodically. There are two Secure and Efficient data Transmission (SET) protocols for CWSNs, called SET-IBS and SET-IBOOS, by using the Identity-Based digital Signature (IBS) scheme and the Identity-Based Online/Offline digital Signature (IBOOS) scheme, respectively. In SET-IBS, security relies on the hardness of the Diffie-Hellman problem in the pairing domain. SET-IBOOS further reduces the computational overhead for protocol security, which is crucial for WSNs, while its security relies on the hardness of the discrete logarithm problem. The feasibility of the SET-IBS and SET-IBOOS protocols with respect to the security requirements and security analysis against various attacks. The calculations and simulations are provided to illustrate the efficiency of the proposed protocols. The results show that, the proposed protocols have better performance than the existing secure protocols for CWSNs, in terms of security overhead and energy consumption.

Keywords: Wireless Sensor Networks; Cluster-based WSNs; Identity-based digital signature; Identity-based online/offline digital signature

I. INTRODUCTION

Data security and storage has become very important issue in Sensor networks for future information retrieval. Storage nodes serve as an intermediate tier between sensors and a sink for storing data and processing queries in wireless sensor networks. The importance of storage nodes also makes them attractive to attackers. Data Storage happens via the Forwarding nodes and Storage nodes. Storage nodes are introduced in this paper to store collected data from the sensors in their proximities, it reduce the energy cost and communication cost induced by network query.

Aim of the research is to deploy the storage nodes and secure data transmission for cluster-based WSNs (CWSNs), where the clusters are formed dynamically and periodically. There are two Secure and Efficient data Transmission (SET) protocols for CWSNs, called SET-IBS and SET-IBOOS, by using the Identity-Based digital Signature (IBS) scheme and the Identity-Based Online/Offline digital Signature (IBOOS) scheme, respectively. The cluster routing protocol LEACH (Low-Energy Adaptive Clustering Hierarchy) is considered and improved. A clustering routing protocol named Enhanced LEACH is proposed in this paper, which extend LEACH protocol by balancing the energy consumption in the network. The simulation results show that Enhanced LEACH outperforms LEACH in terms of network lifetime and power consumption minimization.

II. LITERATURE SURVEY

[1] Y. Wang, G. Attebury, and B. Ramamurthy, "A Survey of Security Issues in Wireless Sensor Networks," *IEEE Comm. Surveys & Tutorials*, vol. 8, no. 2, pp. 2-23, Second Quarter 2006; Clustering is a critical task in Wireless Sensor Networks for energy efficiency and network stability. In the existing method, a secure data transmission for cluster-based WSNs is presented in which the clusters are formed in a dynamic and periodic manner. A two secure and efficient data transmission protocols for CWSNs is presented which is called SET-IBS and SET- IBOOS, by using the identity - based digital signature (IBS) scheme and the identity-based online/offline digital signature (IBOOS) scheme, respectively.

[2] L.B. Oliveira et al., "SecLEACH-On the Security of Clustered Sensor Networks", Key management in wireless sensor network is a complex task due to its nature of environment. Wireless sensor network comprise of large number of sensor nodes with different hardware abilities and functions. Due to the limited memory resources and energy constraints, complex security algorithms cannot be used in sensor networks. Therefore, an energy efficient key management scheme is necessary to mitigate the security risks.

[3] W. Diffie and M. Hellman, "New Directions in Cryptography," Two kinds of contemporary developments in Cryptography are examined. Widening applications of teleprocessing have given rise to a need for new types of cryptographic systems, which minimize the need for secure key distribution channels and supply the equivalent of a written signature. This paper suggests ways to solve these currently open problems. It also discusses how the theories of communication and computation are beginning to provide the tools to solve cryptographic problems of long standing.

[4] D.W. Carman, "New Directions in Sensor Network Key Management," Secure data transmission network is a decisive issue for wireless technology networks (WTNs). Clustering is an effective and practical way to enhance the system performance & methods of WTNs.

III. WIRELESS SENSOR NETWORK

Wireless sensor network is ad-hoc network. It consists of small light weighted wireless nodes called sensor nodes, deployed in physical or environmental condition. All sensor nodes in the wireless sensor network are interacting with each other or by intermediate sensor nodes. A sensor nodes that generates data, based on its sensing mechanisms observation and transmit sensed data packet to the base station (sink). This process basically direct transmission since the base station may locate very far away from sensor nodes needs. More energy to transmit data over long distances so that a better technique is to have fewer nodes sends data to the base station. These nodes called aggregator nodes and processes called data aggregation in wireless sensor network.

a) Clustering in WSN

Group of sensor node can be combined or compress data together and transmit only compact data. This can reduce localized traffic in individual group and also reduce global data. This grouping process of sensor nodes in a densely deployed large scale sensor node is Target User Sensor node Sensor field Internet BS known as clustering.

b) Data Aggregation in WSN

The way of combing data and compress data belonging to a single cluster called data fusion (aggregation). The aim of data aggregation is that eliminates redundant data transmission and enhances the lifetime of energy in wireless sensor network.

i. Performance measure of data aggregation

The performance measures of data fusion algorithms are highly dependent on the desired application. In the data-aggregation scheme, every sensor node should have spent the same amount of energy in every data gathering round. Network lifetime, data accuracy, and latency are some of the significant performance measures of data-aggregation algorithms.

ii. Impact of data aggregation in wireless sensor network

In this paper we discuss the two main factors that affect the performance of data aggregation methods in wireless sensor network, such as energy saving and delay. Data aggregation is the process, in which aggregating the data packet coming from the different sources; the number of transmission is reduced. With the help of this process we can save the energy in the network. Delay is the latency connected with aggregation data from closer sources may have to hold back at intermediate nodes in order to combine them with data from source that are farther away.

c) LEACH PROTOCOL

LEACH protocol is difficult to attack as compared to the more conventional multi hop protocols. In the conventional multi-hop protocols, the nodes around the base station are more attractive to compromise. Whereas in LEACH, the CHs are the only node that directly communicate with the base station. The location of these CHs can be anywhere in the network irrespective of the base station. And more over the CHs are periodically randomly changed. So spotting these CHs is very difficult for the adversary. However, because it is a cluster-based protocol, relying fundamentally on the CHs for data aggregation and routing, attacks involving CHs are the most damaging. If any adversary nodes become a CH, then it can facilitate attacks like Sybil attack, HELLO good attack and selective forwarding. The intruder can broadcast a powerful advertisement to all the nodes in the network and hence, every node is likely to choose the adversary as the cluster-head. The adversary can then selectively forward information to the base-station or modify or dump it. Key management is an effective method to improve network security. However, clusters in LEACH are formed dynamically (at random) and periodically, which changes interactions among the nodes and requires that any node needs to be ready to join any CH at any time.

d) SET-IBS and SET-IBOOS PROTOCOLS

In the proposed system, an innovative technique is introduced which is called Enhanced Secure Data Transmission protocol (ESDT) which is used to improve the SET-IBS and SET-IBOOS protocol. The goal of the proposed secure data transmission for CWSNs is to guarantee the secure and efficient data transmissions between leaf nodes and CHs, as well as transmission between CHs and the BS. Also, the computational complexity is an important concern.

i. Initialization of SET-IBS protocol.

Workflow of SET-IBS Protocol and its Operation Secure communication in SET-IBS relies on ID based cryptography in which user public keys are their ID information. Thus, users can obtain their corresponding private keys without auxiliary data transmission, which is efficient in communication and saves energy. Figure 6.1 illustrates the process of encryption and decryption using the keys generated. As shown in figure private key is generated from nodes ID and the mask (msk) function of Base station (BS). Similarly, public key is generated from msk function of CH. Using these keys security can be provided to the data.

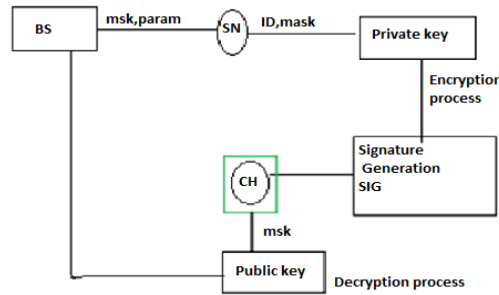


Figure 1: Workflow of SET-IBS protocol Workflow of SET-IBOOS and its Operation

Setup phase: In the protocol initialization the Base Station generates a master key msk and public parameter $param$ for the generation of private key and sends them all to the sensor nodes.

Extraction process: Node j first obtains its private key from msk and where is its ID_j , and is the time stamp of node j 's time interval in the current round that is generated by its CH_j from the TDMA control.

Signature signing: The sensor node j picks a random number and computes. The sensor node further computes $c_j = h(C_j | t_j | \theta_j)$ and $\sigma_j = c_j se_{k_j} + \alpha_j P$. Where $\langle c_j, \sigma_j \rangle$ is the digital signature of node j on the encrypted message C_j . The broadcast message is now concatenated in the form of $\langle ID_j, t_j, C_j, \sigma_j, c_j \rangle$.

Verification: Upon receiving the message, each sensor node verifies the authenticity in the following way. It checks the time stamp of current time interval and determines whether the received message is fresh. Then, if the time stamp is correct, the sensor node further computes $\theta_j = e(\cdot, P) e(H(ID_j | t_j) - P_{pub}) C_j$ using the time stamp of current time interval t_j . For authentication, which is equal to that in the received message, the sensor node considers the received message authentic, and propagates the message to the next hop or user. If the verification above fails, the sensor node considers the message as either bogus or a replaced one, even a mistaken one, and ignores it.

ii. Operation of SET-IBS protocol

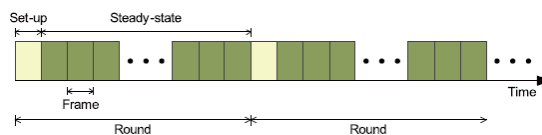


Figure 2 Operations of protocol

After the protocol initialization, SET-IBS operates in rounds during communication. Each round includes a setup phase for constructing clusters from CHs, and a steady-state phase for transmitting data from sensor nodes to the BS. In each round, the timeline is divided into consecutive time slots by the TDMA control. Sensor nodes transmit the sensed data to the CHs in each frame of the steady-state phase. For fair energy consumption, nodes are randomly elected as CHs in each round, and other non-CH sensor nodes join clusters using one-hop transmission, depending on the highest received signal strength of CHs. In the setup phase, the time stamp T_s and node IDs are used for the signature generation. Whereas in the steady state phase, the time stamp t_j is used for the signature generation securing the inner cluster communications, and T_s is used for the signature generation securing the CHs to- BS data transmission.

iii. Initialization of SET-IBOOS protocol

SET-IBOOS is proposed in order to further reduce the computational overhead for security using the IBOOS scheme, in which security relies on the hardness of the discrete logarithmic problem. Private key is generated in similar way as that of IBS, Along with private key online signature is generated for encrypting the data. This online signature is obtained using offline signature. While decrypting the data online signature, sensor node ID and message M parameters.

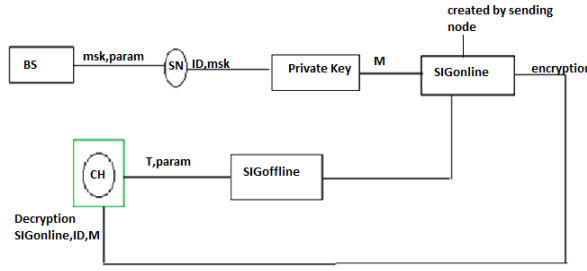


Figure 3 Workflow of IBOOS protocol

Setup phase: In the protocol initialization the Base Station generates a master key msk and public parameter $param$ for the generation of private key and sends them all to the sensor nodes.

Extraction process: Before the signature process, node j first extracts the private key from the $msk\tau$ and its identity ID , as where

$$R_j = g^{r_j} \quad \text{-----(4)}$$

$$s_j = r_j + H(R_j, ID_j)\tau \text{ mod } q.$$

Offline signing: At the offline stage, node j generates the offline value $\langle \hat{\sigma}_j \rangle$ with the time stamp of its time slot t_j for transmission, and store the knowledge for signing online signature when it sends the message. Notice that, this offline signature can be done by the sensor node itself or by the trustful third party, for example, the CH sensor node. Let then

$$g^{s_j} = g^{r_j} g^{H(R_j, ID_j)\tau \text{ mod } q} = R_j X^{H(R_j, ID_j)\text{ mod } q}$$

$$\hat{\sigma}_j = g^{-t_j}$$

Online signing: At this stage, node j computes the online signature based on the encrypted data C_j and the offline signature $\hat{\sigma}_j$.

$$h_j = H(C_j, ID_j) \quad \text{Then, node } j \text{ sends the message to its destination with, and the online}$$

$$z_j = \hat{\sigma}_j + h_j s_j \text{ mod } q \quad \text{signature, in the form of } \langle ID_j, t_j, R, \sigma_j, z_j, C_j \rangle .$$

$$\sigma_j = g^{\hat{\sigma}_j}$$

Verification process: Upon receiving the message, each sensor node verifies the authenticity in the following way. It checks the current time stamp t_j or freshness. Then, if the time stamp is correct, the sensor node further computes the values of g^{z_j} and $\sigma_j R_j^{h_j} X^{h_j H(R_j, ID_j)\text{ mod } q}$. If the values of g^{z_j} and $\sigma_j R_j^{h_j} X^{h_j H(R_j, ID_j)\text{ mod } q}$, are equal from the received message, the node i considers the received message authentic, accepts it, and propagates the message to the next hop or user. If the verification above fails, the sensor node considers the message as either bogus or a replaced one, even a mistaken one, then rejects or ignores it.

iv. Operation of SET-IBS protocol

The proposed SET-IBOOS operates same as that of SET-IBS protocol. SET-IBOOS works in rounds during communication, and the self-elected CHs are decided based on their local decisions, thus it functions without data transmission in the CH rotations. However, the differences is that digital signature are changed from ID-based signature to the online signature of the IBOOS scheme. Once the setup phase is over, the system turns into the steady-state phase, in which

e) IMPROVED SET-IBS PROTOCOL

In the improved SET-IBS protocol, to enhance the security a new secret key is created by using the master secret key for every identity.

Setup phase: The setup algorithm takes as input a security parameter λ and produces the master public key mpk and the master secret key msk . The master public key defines an identity set ID , and an encapsulated-key set K . All other algorithms $KeyGen$, $Encap$, $Decap$, implicitly include mpk as an input.

Key generation: For any identity the $KeyGen$ algorithm uses the master secret key msk to sample an identity secret key.

Valid Encapsulation: The valid encapsulation algorithm creates pairs (C, k) where C is a valid cipher text, and k is the encapsulated-key.

Invalid Encapsulation: The alternative invalid encapsulation algorithm samples an invalid cipher text C for a given id .

Decapsulation: The decapsulation algorithm is deterministic, takes a cipher text C and an identity secret key and outputs the encapsulated key k .

f) IMPROVED SET-IBOOS PROTOCOL

To improve the efficiency in the SET-IBOOS protocol, the improved SET-IBOOS protocol is proposed which the online/offline attribute based encryption method is used.

Setup phase: The setup algorithm takes as input a security parameter λ and a universe description U , which defines the set of allowed attributes in the system. It outputs are the public parameters PK and the master secret key MK .

Extraction process: The extract algorithm takes as input the master secret key MK and an access structure (resp., set of attributes) $Ikey$ and outputs a private key SK associated with the attributes.

Offline. Encrypt (PK): The offline encryption algorithm takes as input the public parameters PK and outputs an intermediate cipher text IT .

Online. Encrypt (PK, IT, Ikey): The online encryption algorithm takes as input the public parameters PK , an intermediate cipher text IT and a set of attributes (resp., access structure) and outputs a session key and a cipher text CT .

Decrypt (SK; CT) \rightarrow key. The decryption algorithm takes as input a private key SK for $Ikey$ and a cipher text CT associated with $Ienc$ and decapsulates cipher text CT to recover a session key.

IV. CRYPTOGRAPHY

Cryptography is the most offered security service in WSN. Applying any encryption scheme requires transmission of extra bits, hence extra processing, memory and battery power are needed. For ensuring robust security for the network, the keys are to be managed, revoked, assigned to a new sensor network or renewed. In different cryptographic schemes and their encountered issues are discussed.

KEY-BASEDALGORITHMS

1. Symmetric And Asymmetric Key – Based Algorithm
2. Symmetric Key Encryption

Diffie-Hellman & Discrete Logarithm for Encryption and Decryption

1. Diffie–Hellman Key Exchange
2. The Discrete Logarithm Problem
3. Security of the Diffie-Hellman Key Exchange
4. The Elgamal Encryption Scheme

The Diffie–Hellman protocol is a widely used method for key exchange. It is based on cyclic groups. The discrete logarithm problem is one of the most important one-way functions in modern asymmetric cryptography. For the Diffie–Hellman protocol in Zp^* , the prime p should be at least 1024 bits long. This provides a security roughly equivalent to an 80-bit symmetric cipher. For a better long-term security, a prime of length 2048 bits should be chosen. The Elgamal scheme is an extension of the DHKE where the derived session key is used as a multiplicative mask to encrypt a message. Elgamal is a probabilistic encryption scheme, i.e., encrypting two identical messages does not yield two identical ciphertexts.

V. RESULT

Comprehending the extra energy consumption by the auxiliary security overhead and prolonging the network lifetime are essential in the proposed SET-IBS and SET-IBOOS. In order to evaluate the energy consumption of the computational overhead for security in communication, we consider three metrics for the performance evaluation of Network lifetime, system energy consumption and the number of alive nodes. For the performance evaluation, we compare the SET-IB and SET-IBOOS with LEACH protocol and SecLEACH protocol.

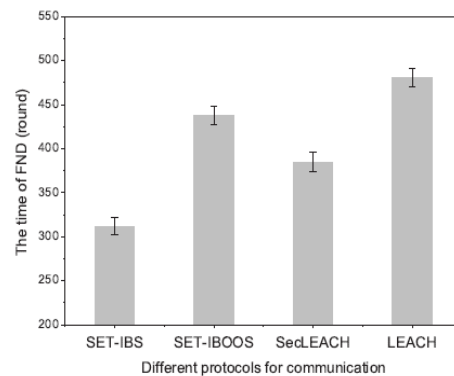


Figure 4 different protocols for communication

We simulate a clustered wireless sensor network in a field with dimensions 100m X100m. The total number of sensors $n = 100$. The nodes, both normal and advanced, are randomly (uniformly) distributed over the field. This means that the horizontal and vertical coordinates of each sensor are randomly selected between 0 and the maximum value of the dimension. The sink is in the center and so, the maximum distance of any node from the sink is approximately 70m (i.e. $2\sqrt{(A/2)}$, where A is the length of the network area).

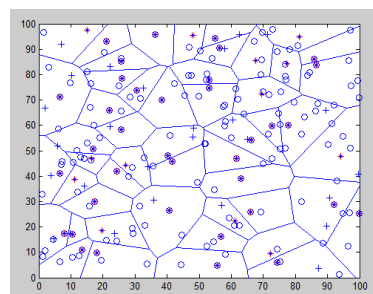


Figure 5. A snapshot of the random deployment of nodes when all the nodes are alive

Network lifetime (the time of FND)

The below figure illustrates the time of FND using different protocols. We apply confidence intervals to the simulation results, and a certain percentage (confidence level) is set to 90%. We mainly consider the LEACH and SET for particularly LEACH to provided better performance for compare to all other protocols. The number of round increases to reduced number of dead node.

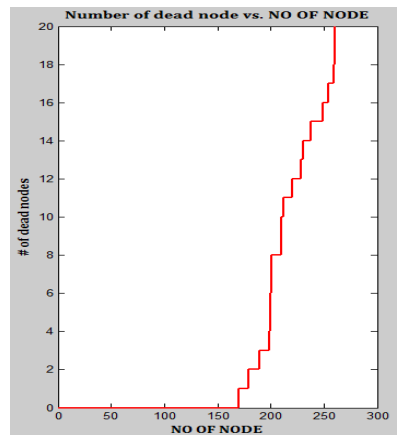


Figure 6 number of dead node vs. no of node

The number of alive nodes

The ability of sensing and collecting information in a WSN depends on the set of alive nodes (nodes that have not failed). Therefore, we evaluate the functionality of the WSN depending on counting the number of alive nodes in the network. Consider the below diagram to increase the number of rounds there is no dead node occur. So using LEACH and SET protocol there is no dead node present for increasing the number of rounds.

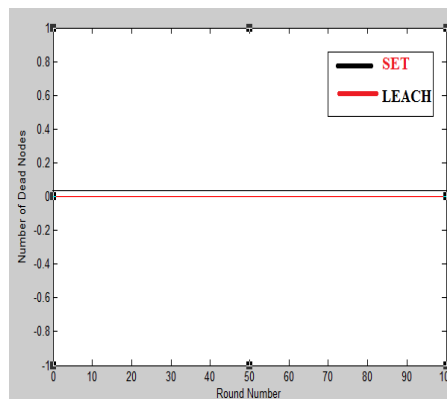


Figure 7 round numbers vs number of nodes

Total system energy consumption

It refers to the amount of energy consumed in a WSN. We evaluate the variation of energy consumption in secure data transmission protocols. The below figure shows to increase the number of nodes as well as increased number of rounds the overall network energy consumption low in LEACH protocol. In a cluster we used two types of node. One is normal node and another one is advanced node. The advanced node reduces the power consumption of the overall cluster.

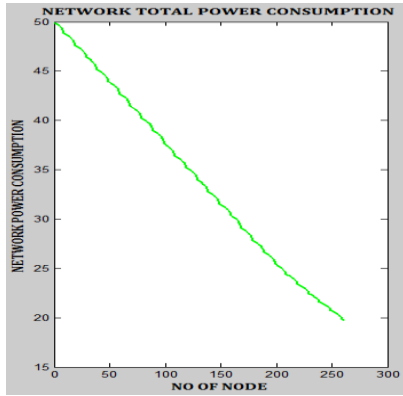


Figure 8 total power consumption

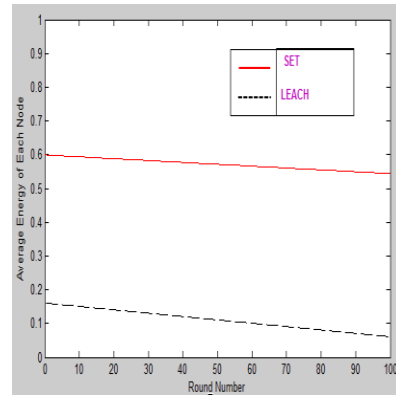


Figure 9 round number vs average energy of each nodes

Security and Throughput

SET protocol mainly used for secure and efficient data transmission in CWSN . We implement two types of algorithm in SET protocol . But compare to LEACH, SET provided low throughput. Only advantage is using security purpose but performance analysis is very low in SET. The above figure shows the comparison of the power consumption in two protocol LEACH only to provide low power compare to SET.

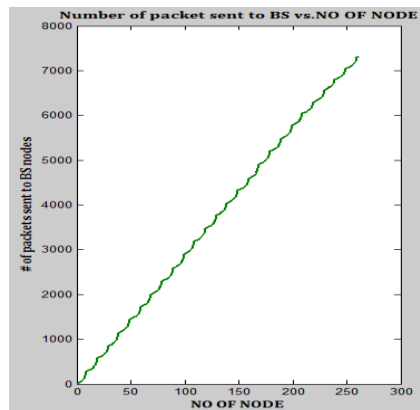


Figure 10. Number of packets sends to BS vs number of nodes

VI. CONCLUSION

In this paper, we presented two secure and efficient data transmission protocols respectively for CWSNs, SET-IBS and SET-IBOOS. In the evaluation section, we provided feasibility of the proposed SET-IBS and SET-IBOOS with respect to the security requirements and analysis against routing attacks. SET-IBS and SET-IBOOS are efficient in communication and applying the ID-based crypto-system, which achieves security requirements in CWSNs, as well as solved the orphan node problem in the secure transmission protocols with the symmetric key management. Finally, the comparison in the calculation and simulation results show that, the proposed protocols have better performance and security than existing secure protocols for CWSNs, with respect to both computation and communication costs.

VII. REFERENCE

1. K. Dasgupta, K. Kalpakis, and P. Namjoshi, "An Efficient Clustering-based Heuristic for Data Gathering and Aggregation in Sensor Networks", IEEE 2003
2. E. Fasolo, M. Rossi, J. Widmer, and M. Zorzi, "In-Network Aggregation Techniques for Wireless Sensor Networks: A Survey", IEEE Wireless communication 2007.
3. Wendi RabinerHeinzelman, AnanthaCh, and HariBalakrishnan. Energy-efficient communication protocol for wireless microsensor networks.2000.
4. H. Lu, J. Li, and G. Wang, "A Novel Energy Efficient Routing Algorithm for Hierarchically Clustered Wireless Sensor Networks," in *Proc. FCST*, 2009.
5. K. Pradeepa, W. R. Anne, and S. Duraisamy, "Design and Implementation Issues of Clustering in Wireless Sensor Networks," *Int. J. Comput. Applications*, vol. 47, no. 11, 2012.
6. D. Boneh and M. Franklin, "Identity-Based Encryption from the Weil Pairing," in *Lect. Notes. Comput. Sc. - CRYPTO*, 2001.
7. A. Shamir, "Identity-Based Cryptosystems and Signature Schemes," in *Lect. Notes. Comput. Sc. - CRYPTO*, 1985.
8. T. Hara, V.I. Zadorozhny, and E. Buchmann, *Wireless Sensor Network Technologies for the Information Explosion Era*, Studies in Computational Intelligence, vol. 278. Springer-Verlag, 2010.
9. S. Xu, Y. Mu, and W. Susilo, "Online/Offline Signatures and Multisignatures for AODV and DSR Routing Security," *Proc. 11th Australasian Conf. Information Security and Privacy*, pp. 99-110, 2006.
10. K. Zhang, C. Wang, and C. Wang, "A Secure Routing Protocol for Cluster-Based Wireless Sensor Networks Using Group Key Management," *Proc. Fourth Int'l Conf. Wireless Comm., Networking and Mobile Computing (WiCOM)*, pp. 1-5, 2008.
11. K. Dasgupta et al., "Maximum Lifetime Data Gathering and Aggregation in Wireless Sensor Networks", In *Proc. of IEEE Networks '02 Conference*, 2002.
12. Y. Wang, G. Attebury, and B. Ramamurthy, "A Survey of Security Issues in Wireless Sensor Networks," *IEEE Commun. Surveys Tuts.*, vol. 8, no. 2, pp. 2–23, 2006.
13. A. A. Abbasi and M. Younis, "A survey on clustering algorithms for wireless sensor networks," *Comput. Commun.*, vol. 30, no. 14-15, pp. 2826–2841, 2007.
14. W. Heinzelman, A. Chandrakasan, and H. Balakrishnan, "An Application-Specific Protocol Architecture for Wireless Microsensor Networks," *IEEE Trans. Wireless Commun.*, vol. 1, no. 4, pp. 660–670, 2002.
15. A. Manjeshwar, Q.-A.Zeng, and D. P. Agrawal, "An Analytical Model for Information Retrieval in Wireless Sensor Networks Using Enhanced APTEEN Protocol," *IEEE Trans. Parallel Distrib. Syst.*, vol. 13, pp. 1290–1302, 2002.

Black Hole Attack in MANET Prevented Using Trusted Route

K.Maheswari¹,S.Manavalan²,D.Varadharajan³

¹*CSE,St.Anne's College of Engg & Tech,kn20maheswari@gmail.com*

²*CSE,St.Anne's College of Engg & Tech,mano5500@gmail.com*

³*CSE,St.Anne's College of Engg & Tech,varadharajan.d@gmail.com*

Abstract-- MANET is a set of mobile nodes connected together in a network with wireless links. There is no infrastructure for forwarding packets from source to destination in mobile nodes. This leads to many malicious attacks on MANET. One type of attack on MANET is the black hole attack. In this attack the malicious node interprets itself as the shortest route to the destination. But after receiving the packets, it instead of forwarding the packets drops it. So to solve this problem, we propose a trusted route by setting trust values between nodes in mobility before forwarding packets. The node which is dropping the packets will have a very less trust value and automatically it will be removed from the trusted route. The nodes which successfully forwards the packets will have a high trust value and again will be considered for forwarding packets.

Keyword--Black Hole Attack, MANET, DSR, Throughput, Packet drop

I. INTRODUCTION

In MANET there is no infrastructure and the topology is highly dynamic. This causes many challenges when routing packets between nodes. The security in MANET is less and is exposed to many malicious attacks. Black hole attack is one type of attack in MANET. A node claims falsely itself to have the shortest path to the destination and receives packets from other nodes[2]. It finally drops the packets rather than forwarding it. This obstructs the packets from reaching its destination node.

Many routing protocols was developed for routing in ad-hoc networks [7]. Dynamic Source Routing (DSR) protocol is a protocol which is used to establish a path between two nodes only on requirement. Route Request packet (RREQ) is broadcasted by the node to all its neighbours before transmitting packets. The nodes receiving RREQ checks if it has previously processed RREQ if so drops it. If not processed, it forwards the RREQ. This is continued till a node has a route to the destination. ROUTE REPLY packet (RREP) is sent in the opposite direction to the source node from destination. The path which is the shortest is selected among all paths and the data is sent along it.

The transfer of packets is done after identifying the optimal path from source to destination. To identify the path which is optimal, all nodes records the trust value of all other nodes in the network. The trust value is the value obtained by noting the number of data and control packets dropped by the receiving node. The node having the highest trust value is selected for transmitting packets. This is continued until the destination is reached. The malicious node which cannot have a highest trust value will not be a part of the path from source to destination which prevents the black hole attack.

II. RELATED WORK

A weighted average of the trust value of nodes in the route is used to determine a secure route to the destination in "Trust Based Multi Path DSR Protocol" [1]. Multiple paths between two nodes are identified and best path among them is selected. RREQ and RREP packets are modified to store the trust value of node from which packet is received.

Parameters k_trust and l_trust store the sum of trust values of nodes transmitting RREQ and RREP respectively. Value $path_trust$ is calculated for every path using the k_trust and l_trust value. The path having maximum $path_trust$ is chosen for forwarding the packets in future. The disadvantage of this method is that the embedding of trust information in the packet and processing done at each node increases the route discovery time.

“Preventing Cooperative Black Hole Attacks in Mobile Ad Hoc Networks” [3] is a slightly modified version of AODV protocol by introducing Data Routing Information (DRI) table and cross checking using Further Request (FREQ) and Further Reply (FREP). If the intermediate node (IN) generates the Route Reply (RREP), it has to provide its next hop node (NHN) and its DRI entry for the next hop node. Upon receiving RREP message from IN, the source node will check its own DRI table to see whether IN is a reliable node or not. If the source node has used IN before to route data, then IN is a reliable node and source will first send a route establishment message to IN node along the path that RREP comes according to the information contains in the RREP message. If IN has not been used before, source sends a message to IN’s NHN to verify its reliability. If IN is not a black hole node and the NHN is a reliable node, then route to destination is secure. Drawback is that it blindly trusts a node that has been used for transmission before.

III. PROPOSED SYSTEM

Let n_1 and n_2 be two nodes that are participating in forwarding the packets to the destination. Let us assume that the n_1 forwards the packets to n_2 . Since the n_1 forwards the packets to n_2 , it is essential for n_1 knowing the trust value of n_2 . The trust value of n_2 is calculated by n_1 based on the number of data/control packets sent by n_1 and forwarded by n_2 . Let T_d be the trust value of n_2 based on the data packets received/forwarded. Let T_c be the trust value of n_2 based on the control packets received/forwarded. Let D_s be the number of data packets sent by n_1 and received by n_2 . D_f is the number of data packets forwarded by n_2 . Let C_s be the number of control packets sent by n_1 and received by n_2 . C_f is the number of control packets forwarded by n_2 . Let D_1 be the number of data packets dropped and C_1 be the number of control packets dropped.

The trust value of the node n_2 based on data/control packets sent/forwarded as observed by the node n_1 is calculated as below

$$T_d = (D_s - D_f) * \cos(D_1) \quad (1)$$

$$T_c = (C_s - C_f) * \cos(C_1) \quad (2)$$

where \cos is a decreasing function. Hence more the number of packets being dropped, then the value of T_d and T_c is less and in turn trust value also becomes less. This ensures that the malicious node has a low value of trust. Similarly every node in the adhoc network calculated the trust value of the neighbor nodes. If the trust value is high, then the node is selected to forward the packets. Therefore a trusted route is determined in which the black hole attack is avoided.

IV. SIMULATION AND PERFORMANCE ANALYSIS

In order to analyze the performance of the proposed method to avoid the black hole attack, we used ns-2 simulator [8]. We used Routing Protocol called Dynamic Source Routing (DSR) [7]. The source node sends the TCP packets to the destination through eight forwarding nodes. The Constant Bit Rate (CBR) traffic at application is used to generate the packets in the simulation. The bandwidth between the nodes is set to 200Mbps. All the ns-2

environmental parameters are shown in Table 1.

Initially the no attacker is introduced in the network and simulation is done for 200sec. The trace information such as number of data packet sent/forwarded/dropped is obtained from the trace file. Each node in the network maintains a table in which the trust values for every neighbor node are calculated using Equation no. and updated. Based on the trust value of neighbor nodes, the packets are forwarded. Since there is no black hole attack, the packets are forwarded by nodes to the destination. Fig.1 shows the throughput of sender before introducing the black hole attacker in the network. Next we introduce a black hole attacker at 60sec into the network and the simulation is performed for 200sec. Since there is black hole attack, the packets are dropped. Therefore the throughput of sender is decreased after 60sec which is shown in Fig. 2. Using the proposed method, the forwarding node identifies the attacker and avoids dropping of packets by not sending the packets to the black hole attacker. The packets are sent by the nodes to new path to the destination. Thus the black hole attacker is excluded from the route. This ensures that the number of packets dropped is reduced thereby the throughput is increased. Fig. 2 shows the throughput of sender after the invoking of proposed method.

Simulation parameter	Simulation Setting
Area	1000m x 1000m
Simulation Time	200 sec.
Number of Nodes	10
Maximum Speed of node	20m/s
Bandwidth	200Mbps
Wireless Propagation Model	Two Ray Ground Model
MAC Protocol	IEEE 802.11
Routing Protocol	DSR
Transport Protocol	TCP
Application Traffic	CBR

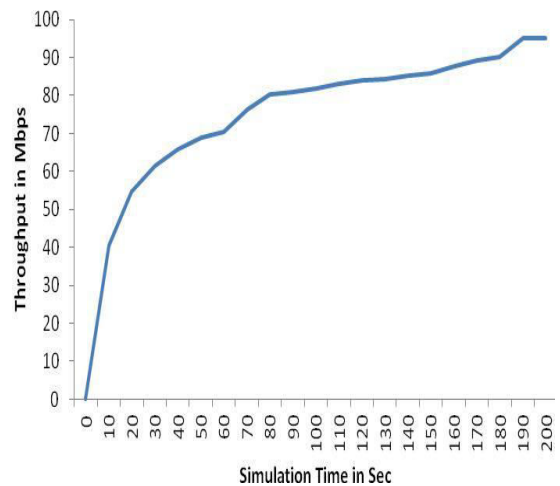


Table 1. Ns-2 Simulation Environmental Parameters

Fig. 1. Throughput of sender before the introduction of black hole attacker

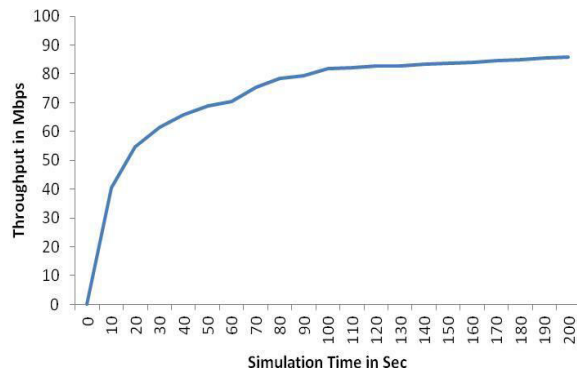
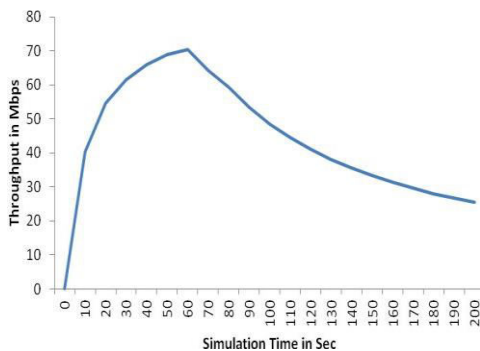


Fig. 2. Throughput of sender after the introduction of black hole attacker

Fig. 3. Throughput of sender after the introduction of black hole attacker and invoking of proposed method

V. CONCLUSION AND FUTURE WORK

After trust value is calculated and a secure route is established, the throughput of sender is increased. Moreover, the nodes dropping packets in the initial simulation are successfully eliminated from the route established between source node and destination node. Thus the proposed method of excluding malicious nodes from the route used for packet transfer is fulfilled thereby enhancing throughput of the sender node. We have implemented our scheme using the Dynamic Source Routing or DSR protocol. This is an on-demand routing protocol that broadcasts RREQ and RREP packets to establish a path from source to destination. In the future one can apply this model to other routing protocols of MANETs like AODV and observe the behavior of nodes in the network. We propose a method to establish a trusted route by calculating trust value of all nodes in the network to combat black hole attack. There are many other malicious attacks like grey hole attack and flooding. Our scheme of calculating trust value and establishing a path can be extended to combat these attacks as well.

REFERENCES

- [1] Poonam, K. Garg, M. Misra, "Trust based multi path DSR protocol", ARES 10th International Conference on Availability, Reliability and Security, 15-18 Feb 2010, Krakow, pp. 204-209
- [2] N. Bhalaji, A. Shanmugam, "Association between nodes to combat black hole attack in DSR based MANET", WOCN IFIP conference on wireless and optical communication networks, 28- 30 Apr 2009, Cairo, pp. 1-5.
- [3] Djamel Djenouril, Othmane Mahmoudil, Mohamed Bouamamal, David Llewellyn-Jones, Madjid Merabti, "On securing MANET routing protocol against control packet dropping", IEEE International Conference on Pervasive Services, 15-20 July 2007, Istanbul, pp. 100-108.
- [4] Hesiri Weerasinghe, Huirong Fu, "Preventing Cooperative black hole attacks in Mobile Adhoc Networks", FGNC-Future Generation Communication and Networking, 6-8 Dec 2007, Jeju, pp. 362-367.
- [5] Changgeng Tan, Songqiao Chen, Wenyan Luo, "An optimal local reputation system in Mobile Ad hoc Networks", ICYCS 9th International conference for young computer scientists, 18-21 Nov 2008, Hunan, pp. 588-593..
- [6] Asad Amir Pirzada, Cris McDonald, "Establishing trust in pure Ad hoc Networks" 27th Australian Computer Science Conference, Vol 26, 2004, pp. 47-54.
- [7] C. Siva Ram Murthy and B.S. Manoj (2004) 'Ad Hoc Wireless Networks: Architectures and Protocols' Prentice Hall
- [8] NS-2 software and its manual downloaded from <http://www.isi.edu/nsnam/ns/doc/index.html>

Data Storage Security and Privacy in Cloud

S.Jerald Nirmal kumar¹,K.Subashini²

¹*CSE, St. Anne's College of Engg & Tech, jeraldcse@gmail.com*

²*CSE, Final Year, St. Anne's College of Engg & Tech, Panruti.*

Abstract-- Cloud computing is often referred as the cloud, It is the delivery of on-demand computing resources—everything from applications to data centre. Cloud computing emerges a guaranteed computation environments for cloud, the previous work on the cloud security focuses on the storage security rather than taking the computation security In this paper, we propose a privacy cheating discouragement and secure computation to improve the efficiency of the computation security in cloud.

Keyword-- Storage Security, Computational Security, Privacy Cheating Discouragement.

I. INTRODUCTION

Cloud computation offers customers to rent the necessary resources than owning . It minimize the cost because user can pay only for the resources they actually use[1] .Security and privacy are the major challenges[2] . One straight forward method to maintain the privacy is to double check the result and it the waste of I/O and resources . further. we classify cloud computing security into two major classes: Cloud Storage Security and Cloud Computation Security, cloud storage ensuring the integrity of outsourced data stored at untrustworthy cloud servers while the cloud computation refers to checking the correctness of the outsourced computation performed by untrustworthy cloud servers. it is quite natural for the servers to initially suspect a problem with the customer's software, and vice versa [3].To ensure the storage and privacy of data in cloud computation, we model the security problems in cloud computing and define the concepts: uncheatable cloud computation and privacy cheating discouragement in our cloud computing, which are our design goals.

II. RELATED WORK

Cloud computing has the potential to transform a large part of the IT industry, Developers with innovative ideas for new Internet services no longer require the large capital outlays in hardware to deploy their service. Moreover, companies with large batch-oriented tasks can get results as quickly as their programs can scale This elasticity of resources, without paying a premium for large scale, is unprecedented in the history of IT. we believe computing, storage, and networking must all focus on horizontal scalability of virtualized resources rather than on single node performance.

1. Applications software needs to both scale down rapidly as well as scale up, which is a new requirement. Such software also needs a pay-for-use licensing model to match needs of cloud computing.
2. Infrastructure software must be aware that it is no longer running moreover, metering and billing need to be built in from the start.

We introduce a model for provable data possession (PDP) that allows a client that has stored data at an untrusted server to verify that the server possesses the original data without retrieving it. The model generates probabilistic proofs of possession by sampling random sets of blocks from the server, which drastically reduces I/O costs . Thus, the PDP model for remote data checking supports large data sets in widely-distributed storage systems .Verifying the authenticity of data has emerged as a critical issue in storing data on untrusted servers . It arises in peer-to-peer storage systems network file systems long-term archives web-service object store and database systems. Such

systems prevent storage servers from misrepresenting or modifying data by providing authenticity checks when accessing data. The server has to store an amount of data at least as large as the client's data, but not necessarily the same exact data. Moreover, all previous techniques require the server to access the entire file, which is not feasible when dealing with large amounts of data. We define a model for provable data possession (PDP) that provides probabilistic proof that a third party stores a file. The model is unique in that it allows the server to access small portions of the file in generating the proof; all other techniques must access the entire file.

Our PDP schemes provide data format independence, which is a relevant feature in practical deployment and put no restriction on the number of times the client can challenge the server to prove data possession. We focused on the problem of verifying if an untrusted server stores a client's data. We introduced a model for provable data possession, in which it is desirable to minimize the file block accesses, the computation on the server, and the client-server communication components of our schemes are the homomorphic verifiable tags. They allow to verify data possession without having access to the actual data file.

The privacy manager for cloud computing, which reduces the risk to the cloud computing user of their private data being stolen or misused, and also assists the cloud computing provider to conform to privacy law[5]. We describe different possible architectures for privacy management in cloud computing; give an algebraic description of obfuscation, one of the features of the privacy manager; and describe how the privacy manager might be used to protect private metadata of online photos. We consider the problem of efficiently proving the integrity of data stored at untrusted servers. In the provable data possession (PDP) model, the client preprocesses the data and then sends it to an untrusted server for storage, while keeping a small amount of meta-data[6]. The client later asks the server to prove that the stored data has not been tampered with or deleted (without downloading the actual data). However, the original PDP scheme applies only to static (or append-only) files.

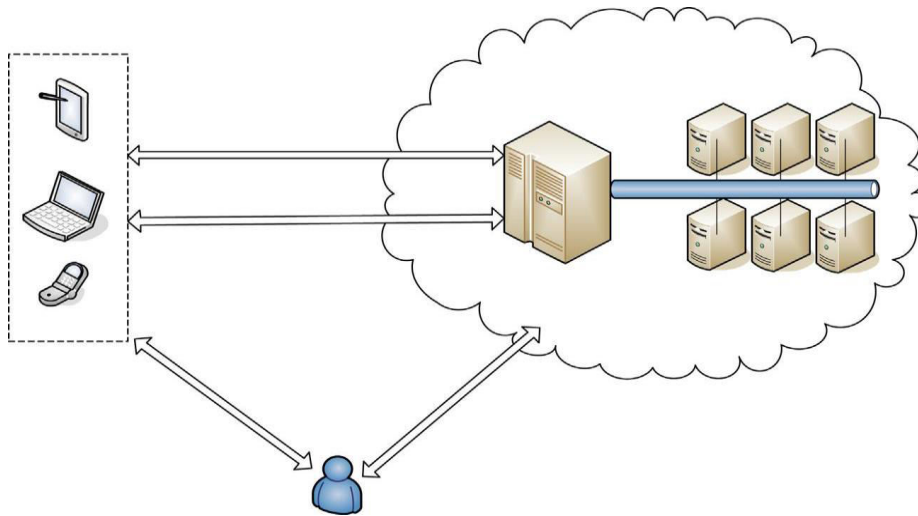
We present a definitional framework and efficient constructions for dynamic provable data possession (DPDP), which extends the PDP model to support provable updates to stored data. We use a new version of authenticated dictionaries based on rank information. The price of dynamic updates is a performance change from $O(1)$ to $O(\log n)$ (or $O(n^\epsilon \log n)$, for a file consisting of n blocks, while maintaining the same (or better, respectively) probability of misbehavior detection. Our experiments show that this slowdown is very low in practice (e.g. 415KB proof size and 30ms computational overhead for a 1GB file). We also show how to apply our DPDP scheme to outsourced file systems and version control systems (e.g. CVS).

Map Reduce is a programming model and an associated implementation for processing and generating large datasets that is amenable to a broad variety of real-world tasks[7]. Users specify the computation in terms of a *map* and a *reduce* function, and the underlying runtime system automatically parallelizes the computation across large-scale clusters of machines, handles machine failures, and schedules inter-machine communication to make efficient use of the network and disks. Programmers find the system easy to use: more than ten thousand distinct MapReduce programs have been implemented internally at Google over the past four years, and an average of one hundred thousand MapReduce jobs are executed on Google's clusters every day, processing a total of more than twenty petabytes of data per day.

III. EXISTING SYSTEM

These cloud servers process plenty of computation resource and storage resource. CSP allocates these resources by means of customized Service Level Agreements [28]. For example, to perform a batch-processing tasks, by employing the existing programming abstraction techniques such as MapReduce [12] and its open-source counterpart Hadoop [5], CSP divides such a large task into

multiple small sub-tasks and allows them parallelly executed across up to hundreds of cloud servers.



We assume the cloud user (CU), such as a mobile phone, a laptop, and an apple ipad, which has lower computation re-source and smaller storage resource than those of the cloud servers. Most of the communication are through wireless, even if an ordinary computer with limited hours (not 24-h) wired-connecting to the cloud servers. CU would submit storage service requests and computation service requests to CSP when it demands. Similar to existing secure storage auditing schemes, we also assume the existence of a number of verification agencies (VAs), which are chosen and trusted by CU and responsible for auditing the cloud services on data storage and computation. VAs are expected to have more powerful computation and storage capability to perform the auditing operations than those of CU.

IV. PROPOSED SYSTEM

Uncheatable cloud computation

To formally define the security model in the cloud computing, we introduce two concepts Secure Computation Confidence (SCC) and Secure Storage Confidence (SSC) to indicate the trust level of computation security and storage security, respectively. SCC is defined as jF^0j/jFj and SSC is formalized as jX^0j/jXj . In both cases, cloud computation or cloud storage is regarded as fully trusted if SCC (SSC) equals 1. Otherwise, it is semi-trusted.

Definition 1 (Uncheatable cloud computation). Let $\text{Pr}[\text{CheatingSuccessfully}]$ be the probability that an adversary with the trust level of SCC and SSC could successfully cheat without being detected by sampling based verifiers. We denote the computation is uncheatable, if for arbitrary sufficiently small positive number ϵ , there exists a sampling size t such that the following conditions always satisfies:

$$\text{Pr}[\text{Cheating Successfully}] \leq \epsilon \text{ for } \text{Pr}[\text{SCC} > 1 - \epsilon; \text{SSC} > 1 - \epsilon; t \leq \frac{1}{\epsilon}]$$

Privacy-cheating discouragement

To discourage the adversary from leaking the cloud users' sensitive data, we introduce a novel privacy-cheating discouragement model where the adversary wants to illegally sells the cloud users'

sensitive data to others. Similar to software sales [21], the software vendor may embed a digital signature in its products to allow the users to authenticate them. Such an authentication could be strictly limited to paying customers rather than the illegitimate users to avoid software piracy. Therefore, it is required that any storage and computation auditing should be authorized by the cloud users. In other words, this could discourage adversaries from leaking users' private data. To achieve this target, we introduce the following definition.

Definition 2 (Privacy cheating discouragement). Let InfoLeak denote the event that valid information is leaked by the adversary. The cloud computing is privacy cheating discouragement, if for a sufficiently small positive number ϵ , the following equation holds in a polynomial time t :

IV. PERFORMANCE ANALYSIS

To analyze uncheatability of our computation, we evaluate the sampling performance of SecCloud in terms of the number of sampling blocks to be retrieved.

Theorem 1. According to Definition 1, our protocol is uncheatable.

Proof. We first define FCS as the event that the adversary could successfully cheat by guessing the results of f or behave normally. For simplicity, let $|f|$ be the result range of f . Thus, the probability that an adversary could randomly guess the correct result of $f(x)$ is $\frac{1}{|f|}$ without any auxiliary information if f is uniform distribution. Besides, we adapt the concept of SCC in our definition to qualify the probability of the adversary's attacks. Therefore, the probability that the adversary could successfully cheat a t -time sampling scheme without being detected is as follows:

CONCLUSION AND FUTURE WORK

In this paper, we have proposed, SecCloud, a privacy-cheating discouragement and secure-computation auditing protocol for data security in the cloud. To the best of our knowledge, it is the first work that jointly considers both of data storage security and computation auditing security in the cloud. We have defined the concepts of uncheatable cloud computation and privacy-cheating discouragement and proposed SecCloud to achieve the security goals. To improve the efficiency, different users' requests can be concurrently handled through the batch verification.

REFERENCES

- [1] M. Armbrust, A. Fox, R. Griffith, A. Joseph, R. Katz, A. Konwinski, G. Lee, D. Patterson, A. Rabkin, I. Stoica, et al, A view of cloud computing, *Communications of the ACM* 53 (4) (2010) 50–58.
- [2] H. Takabi, J. Joshi, G. Ahn, Security and privacy challenges in cloud computing environments, *IEEE Security & Privacy* 8 (6) (2010) 24–31.
- [3] A. Haeberlen, A case for the accountable cloud, in: 3rd ACM SIGOPS International Workshop on Large Scale Distributed Systems and Middleware, Big Sky Resort, Big Sky, MT, October 10–11, 2009.
- [4] G. Ateniese, R. Burns, R. Curtmola, J. Herring, L. Kissner, Z. Peterson, D. Song, Provable data possession at untrusted stores, in: *Proceedings of the 14th ACM Conference on Computer and Communications Security (CCS'07)*, Alexandria, Virginia, USA, October 28–31, 2007.
- [5] S. Pearson, Y. Shen, M. Mowbray, A privacy manager for cloud computing, in: *First International Conference (CloudCom 2009)*, Beijing, China, December 1–4, 2009.
- [6] C. Erway, A. Kupcu, C. Papamanthou, R. Tamassia, Dynamic provable data possession, in: *Proceedings of the 16th*

Dynamic collaboration in multicloud computing environments: framework and security issues

Mr.S.Rajarajan, Asst.Professor (AP), S.Jonajenifer, R.Rathika,
CSE Department, St.Anne's CET, rajansme@gmail.com

Abstract— Cloud environment oriented by requirement of trust management in multiple cloud environments, this paper presents *T-broker*, a trust-aware service brokering scheme for efficient matching cloud services (or resources) to satisfy various user requests. First, a trusted third party-based service brokering architecture is proposed for multiple cloud environments, in which the *T-broker* acts as a middleware for cloud trust management and service matching. Then, *T-broker* uses a hybrid and adaptive trust model to compute the overall trust degree of service resources, in which trust is defined as a fusion evaluation result from adaptively combining the direct monitored evidence with the social feedback of the service resources. More importantly, *T-broker* uses the maximizing deviation method to compute the direct experience based on multiple key trusted attributes of service resources, which can overcome the limitations of traditional trust schemes, in which the trusted attributes are weighted manually or subjectively. Finally, *T-broker* uses a lightweight feedback mechanism, which can effectively reduce networking risk and improve system efficiency. The experimental results show that, compared with the existing approaches, our *T-broker* yields very good results in many typical cases, and the proposed system is robust to deal with various numbers of dynamic service behavior from multiple cloud sites.

Index Terms— Multiple cloud computing, trust-aware service brokering, resource matching, feedback aggregation.

1. INTRODUCTION

MULTIPLE cloud theories and technologies are the hot directions in the cloud computing industry, which a lot of companies and government are putting much concern to make sure that they have benefited from this new innovation [1], [2]. However, compared with traditional networks, multiple cloud computing environment has many unique features such as resources belonging to each cloud provider, and such resources being completely distributed, heterogeneous, and totally virtualized; these features indicate that unmodified traditional trust mechanisms can no longer be used in multiple cloud computing environments. A lack of trust between cloud users and providers has hindered the universal acceptance of clouds as outsourced computing services [3], [4]. Thus, the development of trust awareness technology for cloud computing has become a key and urgent research direction [5]–[8]. Today, the problem of trusted cloud computing has become a paramount concern for most users. It's not that the users don't trust cloud computing's capabilities; rather, they mainly question the cloud computing's trustworthiness [9]–[11].

A. Motivation

The future of cloud computing will be the emergence of cloud brokers acting as an intermediary between cloud providers and users to negotiate and allocate resources among multiple sites. Unfortunately, apart from OPTIMIS [12], most of these brokers do not provide trust management capabilities for multiple cloud collaborative computing, such as how to select the optimal cloud resources to deploy a service, how to optimally distribute the different components of a service among different clouds, or even when to move a given service component from a cloud to another to satisfy some optimization criteria.

B. Our Contributions

Based on previous work on trust management [10], [11], [30], [31], [36], this paper presents *T-broker* for efficient matching computing resources to satisfy various user requests in the multi-cloud environment. The main innovations of our scheme go beyond those of existing approaches in terms of distributed soft-sensors, this brokering architecture can real-time monitor both dynamic service behavior of resource providers and feedbacks from users.

- *T-broker* uses a hybrid and adaptive trust model to compute the overall trust degree of service resources, in which trust is defined as a fusion evaluation result from adaptively combining dynamic service behavior with the social feedback of the service resources.
- *T-broker* uses a maximizing deviation method to compute the direct trust of service resource, which can overcome the limitations of traditional trust models, in which the trusted attributes are weighted manually or subjectively. At the same time, this method has a faster convergence than other existing approaches.

II. RELATED WORK

The main contributions of our trust scheme are based on many existing representative work. In this section, we first review the typical work of cloud brokers. We then analyze the developments of trust management in cloud computing.

A. Development of Cloud Brokers

In recent years, there are many cloud service brokers or monitoring systems emerged as a promising concept to offer enhanced service delivery over large-scale cloud environments. Some private companies offer brokering solutions for the current cloud market, e.g., Right Scale [20] or Spot Cloud [21].

In [18], the authors use the Lattice monitoring framework as a real-time feed for the management of a service cloud. Monitoring is a fundamental aspect of Future Internet elements, and in particular for service clouds, where it is used for both the infrastructure and service management. The authors present the issues relating to the management of service clouds, discussing the key design requirements and how these are addressed in the RESERVOIR project

B. Trust in Cloud Computing

Several research groups both in academia and industry are working in the area of trust management in cloud computing environment. This section will take an in-depth look at the recent developments in this area.

Khan et al. have reviewed the trust needs in the cloud system [5]. They analyze the issues of trust from what a cloud user would expect with respect to their data in terms of security and privacy. They further discuss that what kind of strategy the service providers may undertake to enhance the trust of the user in cloud services and providers. They have identified control, ownership, prevention and security as the key aspects that decide users' level of trust on services. Diminishing control and lack of transparency have identified as the issues that diminishes the user's trust on cloud systems. The authors have predicted that remote access control facilities for resources of the users, transparency with respect to cloud providers actions in the form of automatic traceability facilities, certification of cloud security properties and capabilities through an independent certification authority and providing security enclave for users could be used to enhance the trust of users in the services.

Noor and Sheng propose the "Trust as a Service" (TaaS) framework to improve ways on trust management in cloud environments [17]. In particular, the authors introduce an adaptive credibility model that distinguishes between credible trust feedbacks and malicious feedbacks by considering cloud service consumers' capability and majority consensus of their feedbacks. However, this framework does not allow to assess trustworthiness based on monitoring information as well as users' feedback.

In the author's previous research [10], based on technology of distributed agents, trusted cloud service architecture is suggested for efficient scheduling cloud resources satisfying

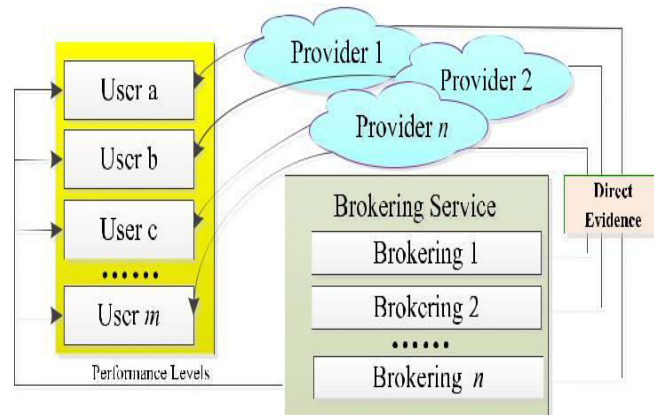


Fig. 1. Some existing brokering scenario without user feedback.

various user requests. The cloud service architecture aims to monitor servers dynamically and allocate high quality computing resources to users. The trusted data acquisition mechanism in this paper uses the monitored information of nodes in the cloud environment. This information consists of each node's spec information, resources usage, and response time. Then the model analyzes this information and prepares suitable resources on each occasion, and then allocates them immediately when user requests.

III. T-Broker's ARCHITECTURE

As mentioned in Part A of Section I, most current cloud brokering systems do not provide trust management capabilities to make trust decisions, which will greatly hinder the development of cloud computing. Fig.1 depicts the brokering scenario in existing brokers (e.g., RESERVOIR [18], PCMONS [19], RightScale [20], SpotCloud [21], and Aeolus [22]). We can see that this existing brokering architecture for cloud computing do not consider user feedback only relying on some direct monitoring information.

As depicted in Fig. 2, *T-broker* architecture, a service brokering system is proposed based on direct monitoring information and indirect feedbacks for the multiple cloud environment, in which *T-broker* is designed as the TTP for cloud trust management and resource matching. Before introducing the principles for assessing, representing and computing trust, we first present the basic architecture of *T-broker* and a brief description of its internal components.

A. Sensor-Based Service Monitoring (SSM)

SLA (Service Level Agreement) with the users. In the inter-active process, this module dynamically monitors the service parameters and is responsible for getting run-time service data. The monitored data is stored in the evidence base, which is maintained by the broker. To calculating QoS-based trustworthiness of a resource [7], [10], we mainly focus on five

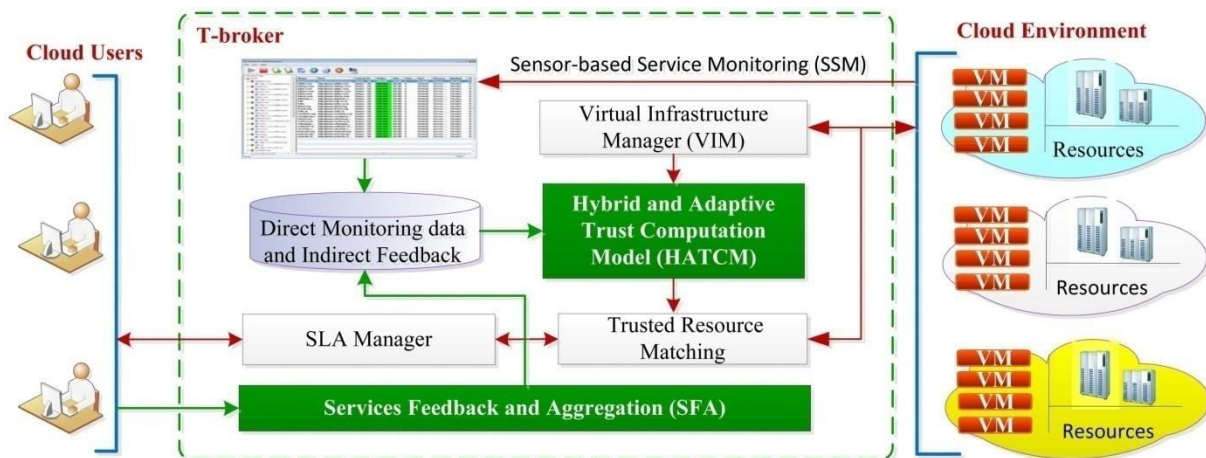


Fig. 2. *T-broker's Architecture and main function modules.*

kinds of trusted attributes of cloud services, which consists of node spec profile, average resource usage information, average response time, average task success ratio, and the number of malicious access. The node spec profile includes four trusted evidences: CPU frequency, memory size, hard disk capacity and network bandwidth. The average resource usage information consists of the current CPU utilization rate, current memory utilization rate, current hard disk utilization rate and current bandwidth utilization rate. The number of malicious access includes the number of illegal connections and the times of scanning sensitive ports.

B. Virtual Infrastructure Manager (VIM)

Each cloud provider offers several VM configurations, often referred to as instance types. An instance type is defined in terms of hardware metrics such as CPU frequency, memory size, hard disk capacity, etc. In this work, the VIM component is based on the OpenNebula virtual infrastructure manager [42], [43], this module is used to collect and index all these resources information from multiple cloud providers.

VI. CONCLUSION AND FUTURE WORK

In this paper, we present *T-broker*, a trust-aware service brokering system for efficient matching multiple cloud services to satisfy various user requests. Experimental results show that *T-broker* yields very good results in many typical cases, and the proposed mechanism is robust to deal with various number of service resources. In the future, we will continue our research from two aspects. First is how to accurately calculate the trust value of resources with only few monitored evidences reports and how to motivate more users to submit their feedback to the trust measurement engine. Implementing and evaluating the proposed mechanism in a large-scale multiple cloud system, such as distributed data sharing and remote computing, is another important direction for future research.

V. REFERENCES

- [1] M. Singhal et al., "Collaboration in multicloud computing environments: Framework and security issues," *Computer*, vol. 46, no. 2, pp. 76–84, Feb. 2013.
- [2] H. M. Fard, R. Prodan, and T. Fahringer, "A truthful dynamic workflow scheduling mechanism for commercial multicloud environments," *IEEE Trans. Parallel Distrib. Syst.*, vol. 24, no. 6, pp. 1203–1212, Jun. 2013.
- [3] F. Paraiso, N. Haderer, P. Merle, R. Rouvoy, and L. Seinturier, "A federated multi-cloud PaaS infrastructure," in *Proc. 5th IEEE Int. Conf. Cloud Comput. (CLOUD)*, Jun. 2012, pp. 392–399.
- [4] P. Jain, D. Rane, and S. Patidar, "A novel cloud bursting brokerage and aggregation (CBBA) algorithm for multi cloud environment," in *Proc. 2nd Int. Conf. Adv. Comput. Commun. Technol. (ACCT)*, Jan. 2012, pp. 383–387.
- [5] K. M. Khan and Q. Malluhi, "Establishing trust in cloud computing," *IT Prof.*, vol. 12, no. 5, pp. 20–27, Sep./Oct. 2010.
- [6] K. Hwang and D. Li, "Trusted cloud computing with secure resources and data coloring," *IEEE Internet Comput.*, vol. 14, no. 5, pp. 14–22, Sep./Oct. 2010.
- [7] H. Kim, H. Lee, W. Kim, and Y. Kim, "A trust evaluation model for QoS guarantee in cloud systems," *Int. J. Grid Distrib. Comput.*, vol. 3, no. 1, pp. 1–10, Mar. 2010.
- [8] P. D. Manuel, S. Thamarai Selvi, and M. I. A.-E. Barr, "Trust management system for grid and cloud resources," in *Proc. 1st Int. Conf. Adv. Comput. (ICAC)*, Dec. 2009, pp. 176–181.
- [9] L.-Q. Tian, C. Lin, and Y. Ni, "Evaluation of user behavior trust in cloud computing," in *Proc. Int. Conf. Comput. Appl. Syst. Modeling (ICCASM)*, Oct. 2010, pp. V7-576–V7-572.
- [10] X. Li and Y. Yang, "Trusted data acquisition mechanism for cloud resource scheduling based on distributed agents," *Chin. Commun.*, vol. 8, no. 6, pp. 108–116, 2011.

Trusted CBCR Scheme to Enhance the Performance and Security in MANETS

Mrs.D. Pauline Freeda¹, Ms.D.Sivaranjani², Ms.P.Shanmugapriya³

¹*Asst.Professor,Dept.of CSE,St.Anne's CET ,p_freeda@yahoo.com*

²*UG Scholar,Dept.of CSE,St.Anne's CET ,ranjinisiva43@gmail.com*

³*UG Scholar,Dept.of CSE,St.Anne's CET, shanmugapriyap960@gmail.com*

Abstract - The Mobile Ad hoc networks (MANETs) is a self organized infrastructure less networks than wired networks. The main challenge is to provide secure network services. Certificate revocation process provides secure network communications. The Certificate Authority (CA) issue certificates to all nodes. The certificates can be revoked from attackers and cut off from further network activities. The proposed cluster based certificate revocation with vindication capability (CCRVC) scheme can be used for quick and accurate certificate revocation. The falsely accused nodes are revoked to improve the reliability of the scheme. The threshold based mechanism is proposed to enhance the accuracy. This certificate revocation scheme is more effective and efficient to provide secure communications.

Keywords: Mobile Ad Hoc Networks , Cluster, Certificate Revocation, Warning list, Black list.

I. INTRODUCTION

Mobile Ad Hoc Networks (MANET) is dynamic in nature consisting of cell phones, laptops, this can freely move in the network. MANET is used in various applications such as military, emergency communications and other real time applications by forward packets in limited transmission range.

Security is an important requirement for network services. Implementing security [1], [2] is to protect networks against malicious nodes, the attacker can network so nodes can move freely it may join and leave the network. Therefore, the MANET's having more security attacks than wired networks. The certificate management can be used for secure application which gives trusted public key infrastructure [3], [4]. It encompasses three components they are prevention, detection and revocation. Certificate Revocation [11], [12], [13], [14], [15], [16], [17] plays an important role in MANET's. The misbehaved nodes certificates should be removed and stop to access the network immediately.

II. RELATED WORK

MANET's is difficult to secure ad hoc networks because of limited protection, vulnerable attacks and dynamically changing networks. A different type of techniques has been proposed to improve network security. This section introduces existing approaches of certificate revocation they are voting-based mechanism and non-voting based mechanism.

2.1. Voting-Based Mechanism

Voting-based mechanism means revoking certificates from malicious nodes with the help of neighboring nodes. The new nodes are getting certificates from neighbors. The attacker node certificates can be revoked basis on the neighbor's nodes votes. In URSA [14], every node performs one hop monitoring and exchanges that information with other neighbor nodes. When the number of negative of negative votes exceeds, the certificates can be revoked from accused node and it cannot participate in network activities. The main thing is the node cannot

communicate with others without having valid certificates. If the degree, it cannot be revoked that attack nodes and it freely communicate with others. Another drawback is it does not address false accusation from attacker nodes.

III. CLUSTER-BASED SCHEME

In this section introduce the proposed cluster-based revocation scheme, which can quickly revoking attacker nodes from neighboring node. This scheme maintains warning list and black list, in order to protect legitimate nodes from malicious nodes. Using cluster head, falsely accused nodes are revoked. This scheme address only the issue of certificate revocation not certificate distribution [5], [6].

3.1. Cluster Construction

To construct the topology, the cluster based [20] architecture is implemented. Here the nodes are combined to form a cluster. Each cluster consist cluster head (CH) with cluster members (CM). They are located in certain transmission range of CH. The certificate authority issues certificates to all nodes. After getting the certificate the nodes can join the network. The certificate authority is responsible for both distributing and managing certificates so the nodes can communicate with each other. The neighboring nodes often check the availability of the nodes using neighbor sensing protocols. It broadcast the hello message then it assumes new link is added to the network. If it is not received hello message in certain period of time, it assumes that node is disconnected from the network.

3.2. Certification Authority

A trusted third party is said to be certification authority, which can be used to provide the certificates for new node and revoking the certificates from attacker node. The CA is responsible for maintaining WL and BL, which are hold accusing and accused node respectively. The BL hold the accused nodes as an attacker and WL hold the corresponding accused node. The CA updates the two lists and it broadcast that list to the whole network. After that malicious nodes can be identified easily and isolate them from further network activities.

IV. THRESHOLD – BASED MECHANISM

Conventional voting mechanisms set the threshold value K as a constant. This mechanism is mainly proposed to find the warned nodes are legitimate nodes or not. We have to set the constant value K . if the threshold value is set too big, it will take a long time to find that the warned node as a legitimate node because the method has to wait for more accusations to reach the verdict. If the threshold value is set too small, revoked malicious nodes can be released by other malicious nodes from the WL. To overcome these problems, we propose to determine the optimum threshold value K based on the neighboring nodes.

V. NODE CLASSIFICATION

Based on their behavior, the nodes can be classified as legitimate node, malicious node and attacker node. A node having valid certificates and it does not launch any attacks that is said to be legitimate node and it have secure communications. A node which can launch attack and disrupt network communications then it is attacker node. Further, the nodes can be categorized as normal node, warned node and revoked node. The normal node does not launch any attacks and it has high reliability, also it has the ability to accuse other nodes. The low reliability nodes are warned nodes that are placed in the warning list. The warning list contains a mixture of legitimate nodes and malicious nodes. The warned nodes cannot accuse any neighbor node. The accused nodes are placed in the BL that is said to be revoked nodes.

5.1. Certificate Revocation

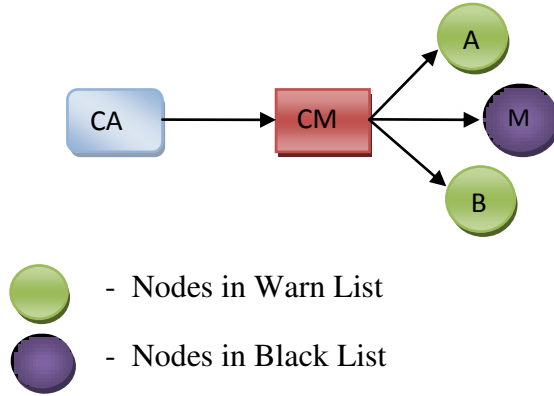


Fig 1: Certificate Revocation

In certificate revocation process, three stages are implemented they are accusing, verifying and notifying to revoke a malicious attacker’s certificate. The nodes can be identified by neighboring nodes. The CA is responsible for maintaining the BL and WL and broadcast that list to all cluster members. The CM updates that two lists and check malicious nodes availability. It checks the local BL to match with any node. If it detects any detect any attacker node, its send an Accusation Packet (AP) to CA. The CA verifies the certificate validation of the accusing node. If it confirms then it put that node in to BL and revoked that node successfully. In between time, that malicious node is put in to WL. The CA updates the WL and BL and propagates that list to whole network.

5.2. Recovering false accusation

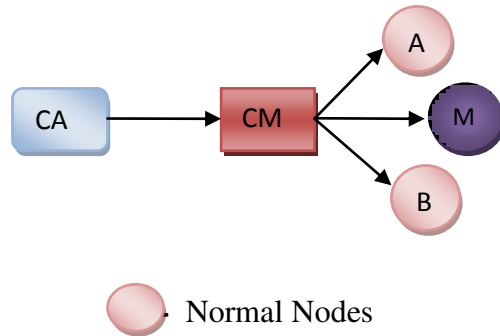


Fig 2: Certificate Recovery

Sometimes the legitimate node may address as malicious node and the CA put that node in to BL and disseminates to all CH and CM. The CH is responsible for detecting false accusation node against legitimate node and restores that node within its cluster. CH can detect attacks from CM then and revoked it. If the legitimate node is identified as malicious node that will be added to the BL and propagates to all nodes. The CH updates and detects any node as falsely accused, it send a Recovery Packet (RP) to the CA. The CA validates that recovery packet and restores that node in to cluster and updates the BL.

VI. PERFORMANCE EVALUATION

In this section, we discuss the simulation results using Qualnet4.0 network simulator. The purpose of our simulations is to improve the performance of the scheme in terms of efficiency. In particular, we simulate our proposed scheme to verify its efficiency in revoking attacker nodes.

6.1. Simulation Setup

We can use many devices (mobile phones, laptops, PDA) to construct a MANET in particular area. These devices are randomly moved and communicate with neighboring nodes.

TABLE 1

Simulation Parameters

Parameter	Value
Number of nodes	50-100
Node Placement	Random
Node transmission range	250m
Mobility model	Random-Waypoint
Node speed	1-10m/s
Simulation time	500s
Routing protocol	AODV

We simulate a MANET with 50-100 normal nodes in Qualnet 4.0 simulator and use ad hoc on-demand distance vector (AODV) as an IP routing protocol. The node movements followed by random way-point mobility pattern [23], [24], in which each node moves to a randomly selected location at different velocities from 1 to 10m/s. The simulation parameters are shown in Table 1. The transmission range is set to be 250m. An attacker node periodically launches attacks every 5 seconds that can be detected by other nodes.

6.2. Simulation Results

6.2.1. The detection performance

Here, we analyze the detection performance to verify the efficiency of our method. Fig. 3 shows comparative results of previous method versus our method. For simulation, we consider 60 normal nodes and malicious nodes are changes as 15,30,45,60. As numbers of malicious nodes are increases detection time varies between previous method and our method. The detection time is reduced fast compared with previous method. Also falsely accused nodes are released from WL after certificate revocation.

6.2.2. Impact of mobility

To evaluate the detection performance of the scheme, we study the impact of mobility on the detection. Fig. 4 shows the detection time as the node mobility changes. Here the threshold value is equal to 2 and mobility is set to be 1m/s, 2m/s, 5m/s, 10m/s. The results show that the detection time decreases as the node mobility increases.

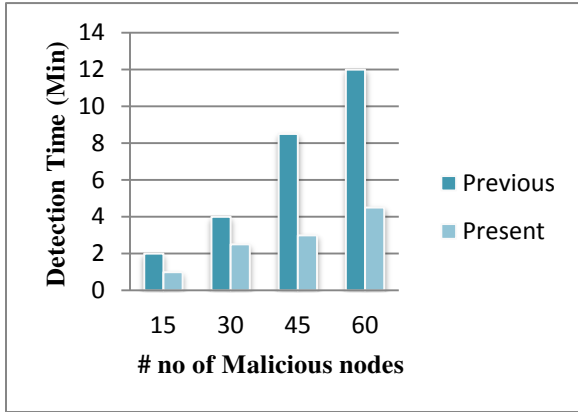


Fig. 3. Previous method versus our method

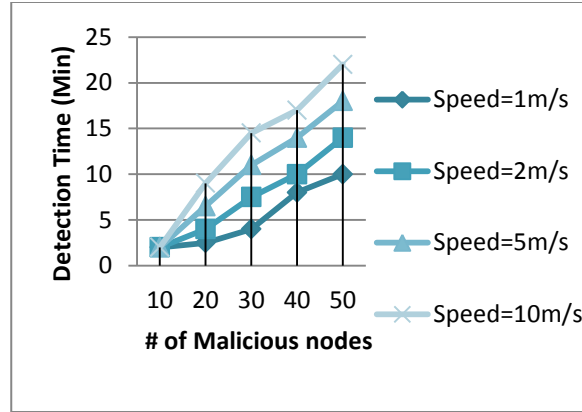


Fig. 4. Impact of mobility

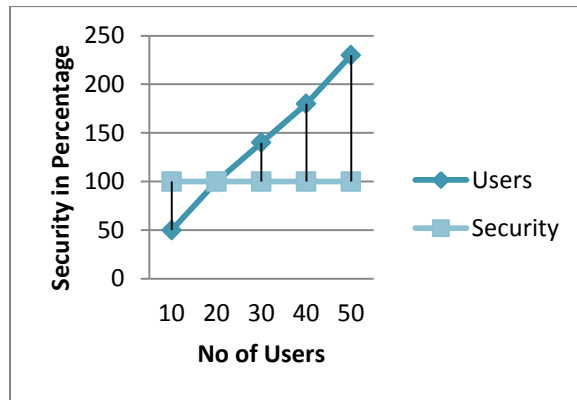


Fig. 5. Impact of security

6.2.3. Security Analysis

In the proposed scheme, a CH can recover the falsely accused node certificate from BL and revoking the malicious node certificate by certificate revocation process so the mobile network allowing only authenticated nodes and get secured. To enhance the security, threshold-based mechanism is used. Here the threshold value is considered as 5, 10, and 15 having constant movement in mobile network. When threshold becomes large, the detection time increases. Fig. 5 shows that all users having full security in mobile network.

VII. CONCLUSION

This paper focused on the secure network communication in MANETs. Certificate revocation process makes ensure the secure communication. The proposed CCRVC scheme can be used to revoke the malicious certificate and restore false accusation node. The revocation time is reduced by single node accusation and improving the accuracy by restores the falsely accused node using CH. Therefore this scheme increases the normal node in MANET. To enhance the accuracy, threshold-based mechanism is used.

REFERENCES

- [1] T. R. Panke and B. M. Patil “ Improved Certificate Revocation method in Mobile ad hoc Network ”
International Journal of Computer applications (0975 – 8887) Volume 80 – No. 12, October 2013.
- [2] H. Yang, H. Luo, F. Ye, S. Lu, and L. Zhang, “Security in Mobile Ad Hoc Networks: Challenges and Solutions,” *IEEE Wireless Comm.*, vol. 11, no. 1, pp. 38-47, Feb. 2004.
- [3] P. Sakarindr and N. Ansari, “Security Services in Group Communications Over Wireless Infrastructure, Mobile Ad Hoc and Wireless Sensor Networks,” *IEEE Wireless Comm.*, vol 14, no. 5, pp. 8-20, Oct. 2007.
- [4] A. M. Hegland, E. Winjum, C. Rong, and P. Spilling, “A Survey of Key Management in Ad Hoc Networks,” *IEEE Comm. Surveys and Tutorials*, vol. 8, no. 3, pp. 48-66, Third Quarter 2006.
- [5] L. Zhou and Z. J. Haas, “Securing Ad Hoc Networks,” *IEEE Network Magazine*, vol. 13, no. 6, pp. 24-30, Nov./Dec. 1999.
- [6] L. Zhou, B. Cchneider, and R. Van Renesse, “COCA: A Secure Distributed Online Certification Authority,” *ACM Trans. Computer Systems*, vol. 20, no. 4, pp. 329-368, Nov. 2002.
- [7] H. Chan, V. Gligor, A. Perrig, and G. Muralidharan, “On the Distribution and Revocation of Cryptographic Keys in Sensor Networks,” *IEEE Trans. Dependable and Secure Computing*, vol. 2, no. 3, pp. 233-247,
- [8] P. Yi, Z. Dai, Y. Zhong, and S. Zhang, “Resisting Flooding Attacks in Ad Hoc Networks,” *Proc. Int’l Conf. Information Technology: Coding and Computing*, vol. 2, pp. 657-662, Apr. 2005.
- [9] B. Kannhavong, H. Nakayama, A. Jamalipour, Y. Nemoto, and N. Kato, “A Survey of Routing Attacks in MANET,” *IEEE Wireless Comm. Magazine*, vol. 14, no. 5, pp. 85-91, Oct. 2007.
- [10] H. Nakayama, S. Kurosawa, A. Jamalipour, Y. Nemoto, and N. Kato, “A Dynamic Anomaly Detection Scheme for Aodv-Based Mobile Ad Hoc Networks,” *IEEE Trans. Vehicular Technology*, vol. 58, no. 5, pp. 2471-2481, June 2009.
- [11] J. Newsome, E. Shi, D. Song, and A. Perrig, “The Sybil Attack in Sensor Network: Analysis & Defenses,” *Proc. Third Int’l Symp. Information Processing in Sensor Networks*, pp. 259- 268, 2004.
- [12] S. Micali, “Efficient Certificate Revocation,” *Massachusetts Inst. Of Technology, Cambridge, MA*, 1996.
- [13] C. Gentry, “Certificate-Based Encryption and the Certificate Revocation Problem,” *EUROCRYPT: Proc. 22nd Int’l Conf. Theory and Applications of Cryptographic Techniques*, pp. 272- 293, 2003.
- [14] H. Yang, J. Shu, X. Meng, and S. Lu, “SCAN: Self-Organized Network-Layer Security in Mobile Ad Hoc Networks,” *IEEE J. Selected Areas in Comm.*, vol. 24, no. 2, pp. 261-273, Feb. 2006.

Home Automation Using Internet of Things

E. Veeramani – cse/sacet eveeramani306@gmail.com

S. Salman - salmannac1996@hotmail.com

R. Parthap miras-cse/sacet pvathapmiras@hotmail.com

Abstract- with advancement of Automation technology, life is getting simpler and easier in all aspects. In today's world Automatic systems are being preferred over manual system. With the rapid increase in the number of users of internet over the past decade has made Internet a part and parcel of life, and IoT is the latest and emerging internet technology. Internet of things is a growing network of everyday object-from industrial machine to consumer goods that can share information and complete tasks while you are busy with other activities. Wireless Home Automation system(WHAS) using IoT is a system that uses computers or mobile devices to control basic home functions and features automatically through internet from anywhere around the world, an automated home is sometimes called a smart home. It is meant to save the electric power and human energy. The home automation system differs from other system by allowing the user to operate the system from anywhere around the world through internet connection. In this paper we present a Home Automation system(HAS) using Intel Galileo that employs the integration of cloud networking, wireless communication, to provide the user with remote control of various lights, fans, and appliances within their home and storing the data in the cloud. The system will automatically change on the basis of sensors' data. This system is designed to be low cost and expandable allowing a variety of devices to be controlled.

Key Words: Home automation System (HAS), Internet of Things (IoT), Cloud networking, Wi-Fi network, Intel Galileo Microcontroller

I. INTRODUCTION

A. Overview

Homes of the 21st century will become more and more self-controlled and automated due to the comfort it provides, especially when employed in a private home. A home automation system is a means that allow users to control electric appliances of varying kind. Many existing, well-established home automation systems are based on wired communication. This does not pose a problem until the system is planned well in advance and installed during the physical construction of the building. But for already existing buildings the implementation cost goes very high. In contrast, Wireless systems can be of great help for automation systems. With the advancement of wireless technologies such as Wi-Fi, cloud networks in the recent past, wireless systems are used every day and everywhere.

B. Advantages of Home automation systems

In recent years, wireless systems like Wi-Fi have become more and more common in home networking. Also in home and building automation systems, the use of wireless technologies gives several advantages that could not be achieved using a wired network only. 1) Reduced installation costs: First and foremost, installation costs are significantly reduced since no cabling is necessary. Wired solutions require cabling, where material as well as the professional laying of cables (e.g. into walls) is expensive. 2) System scalability and easy extension: Deploying a wireless network is especially advantageous when, due to new or changed requirements, extension of the network is necessary. In contrast to wired installations, in which cabling

extension is tedious. This makes wireless installations a seminal investment. 3) Aesthetical benefits: Apart from covering a larger area, this attribute helps to full aesthetical requirements as well. Examples include representative buildings with all-glass architecture and historical buildings where design or conservatory reasons do not allow laying of cables. 4) Integration of mobile devices: With wireless networks, associating mobile devices such as PDAs and Smartphones with the automation system becomes possible everywhere and at any time, as a device's exact physical location is no longer crucial for a connection (as long as the device is in reach of the network). For all these reasons, wireless technology is not only an attractive choice in renovation and refurbishment, but also for new installations.

II. RELATED WORK

[1] Sirsath N. S, Dhole P. S, Mohire N. P, Naik S. C & Ratnaparkhi N.S This paper proposes a Home Automation system that employs the integration of multi-touch mobile devices, cloud networking, wireless communication, and power-line communication to provide the user with remote control of various lights and appliances within their home. This system uses a consolidation of a mobile phone application, handheld wireless remote, and PC based program to provide a means of user interface to the consumer.

[2] Basil Hamed The main objective of this Paper is to design and implement a control and monitor system for smart house. Smart house system consists of many systems that controlled by LabVIEW software as the main controlling system in this paper. Also, the smart house system was supported by remote control system as a sub controlling system. The system also is connected to the internet to monitor and control the house equipment's from anywhere in the world using LabVIEW. [3] Deepali Javale, Mohd. Mohsin, Shreerang Nandanwar The prime objective of this paper is to assist handicapped/old aged people. It gives basic idea of how to control various home appliances and provide a security using Android phone/tab. The design consists of Android phone with home automation application, Arduino Mega ADK. User can interact with the android phone and send control signal to the Arduino ADK which in turn will control other embedded devices/sensors.

III. SYSTEM ANALYSIS

A. Problem Definition

Home automation systems face four main challenges, these are high cost of ownership, inflexibility, poor manageability, and difficulty in achieving security. The main objectives of this research is to design and implement a home automation system using IoT that is capable of controlling and automating most of the house appliances through an easy manageable web interface. The proposed system has a great flexibility by using Wi-Fi technology to interconnect its distributed sensors to home automation server. This will decrease the deployment cost and will increase the ability of upgrading, and system reconfiguration.

B. Proposed System Feature

The proposed system is a distributed home automation system, consists of server, sensors. Server controls and monitors the various sensors, and can be easily configured to handle more hardware interface module (sensors). The Intel Galileo development board, with built in WiFi card port to which the card is inserted, acts as web server. Automation System can be

accessed from the web browser of any local PC in the same LAN using server IP, or remotely from any PC or mobile handheld device connected to the internet with appropriate web browser through server real IP (internet IP). WiFi technology is selected to be the network infrastructure that connects server and the sensors. WiFi is chosen to improve system security (by using secure WiFi connection), and to increase system mobility and scalability.

IV. SYSTEM DESIGN AND IMPLEMENTATION

A. Proposed Home Automation System

Figure 1: Proposed model of Home automation system

The proposed model of the home automation system is as shown in the figure1. The model consist of different sensors like temperature, gas, motion and LDR. Initially the Intel Galileo connects to the internet through WiFi. When the connection is established it will start reading the parameters of sensors like p1, p2, p3 etc. The threshold levels for the required sensors are set as t1, t2, t3 etc. The sensor data are sent to the web server and stored in the cloud. The data can be analyzed anywhere any time. If the sensor parameters are greater than the threshold level then the respective alarm a1, a2, a3 etc. will be raised and the required actuation is done for the controlling of the parameters. In the proposed model the temperature, gas leakage, motion in the house is monitored. The temperature and the motion detection is stored in cloud for analysis. If the temperature exceeds the threshold level then the cooler will turn on automatically and it will off when the temperature comes to control. Similarly when there is a leakage of gas in the house alarm is raised giving the alert sound. The required lights are turned on/off automatically by detecting the light outside the house. The user can also monitor the electric appliances through the internet via web server. If the lights or any electrical appliances are left on in hurry can be seen and turned off remotely through simply typing the IP address of the web server.

B. Proposed Home Automation System Functions

The proposed home automation system has the capabilities to control the following components in users home and monitor the following alarms:

- Temperature and humidity
- Motion detection
- Fire and smoke detection
- Light level
- The proposed home automation system can control the following appliance:
- Lights on/off/dim
- Fan on/off
- On/off different appliance

C. Software design

Front End Design: HTML is a format that tells a computer how to display a web page. The documents themselves are plain text files with special "tags" or codes that a web browser uses to interpret and display information on your computer screen. HTML stands for Hyper Text Markup Language; an HTML file is a text file containing small markup tags. The markup tags tell the Web browser how to display the page. An HTML files must have an htm or html file extension.

Cloud Storage: Cloud computing is the practice of using remote servers on the internet to manage, store and process data instead of using a personal computer. Cloud computing is a general term that is better divided into three categories: Infrastructure-as-a-Service, Platform-as-a-Service, and Software-as-a-Service. IaaS (or utility computing) follows a traditional utilities model, providing servers and storage on demand with the consumer paying accordingly. PaaS allows for the construction of applications within a provider's framework, like Google's App Engine. SaaS enables customers to use an application on demand via a browser. A common example of cloud computing is **Gmail**, where you can access your stored data from any computer with internet access. Here we are using Gmail for the storage of the data.

VI. CONCLUSION AND FUTURE WORK

A. Conclusion

The home automation using Internet of Things has been experimentally proven to work satisfactorily by connecting simple appliances to it and the appliances were successfully controlled remotely through internet. The designed system not only monitors the sensor data, like temperature, gas, light, motion sensors, but also actuates a process according to the requirement, for example switching on the light when it gets dark. It also stores the sensor parameters in the cloud (Gmail) in a timely manner. This will help the user to analyze the condition of various parameters in the home anytime anywhere.

B. Future work

Using this system as framework, the system can be expanded to include various other options which could include home security feature like capturing the photo of a person moving around the house and storing it onto the cloud. This will reduce the data storage than using the CCTV camera which will record all the time and stores it. The system can be expanded for energy monitoring, or weather stations. This kind of a system with respective changes can be implemented in the hospitals for disable people or in industries where human invasion is impossible or dangerous, and it can also be implemented for environmental monitoring.

REFERENCES

- [1] Sirsath N. S, Dhole P. S, Mohire N. P, Naik S. C & Ratnaparkhi N.S Department of Computer Engineering, 44, Vidyanagari, Parvati, Pune-411009, India University of Pune, "Home Automation using Cloud Network and Mobile Devices"
- [2] Deepali Javale, Mohd. Mohsin, Shreerang Nandanwar "Home Automation and Security System Using Android ADK" in International Journal of Electronics Communication and Computer Technology (IJECCCT) Volume 3 Issue 2 (March 2013)
- [3] Charith Perera, Student Member, IEEE, Arkady Zaslavsky, Member, IEEE, Peter Christen, and Dimitrios Georgakopoulos, Member, IEEE "Context Aware Computing for The Internet of Things: A Survey". IEEE COMMUNICATIONS SURVEYS & TUTORIAL
- [4] Charith Perera_y, Arkady Zaslavskyy, Peter Christen_ and Dimitrios Georgakopoulosy Research School of Computer Science, The Australian National University, Canberra, ACT 0200, Australia yCSIRO ICT Center, Canberra, ACT 2601, Australia " CA4IOT: Context Awareness for Internet of Things"
- [5] Bill N. Schilit, Norman Adams, and Roy Want, "Context-Aware Computing Applications"
- [6] Jayavardhana Gubbi, Rajkumar Buyya, Slaven Marusic, a Marimuthu Palaniswamia, "Internet of Things (IoT): A Vision, Architectural Elements, and Future Directions"
- [7] S.P.Pande, Prof.Pravin Sen, "Review On: Home Automation System For Disabled People Using BCI" in IOSR Journal of Computer Science (IOSR-JCE) e-ISSN: 2278-0661, p-ISSN: 2278-8727 PP 76-80

- [8] Basil Hamed, "Design & Implementation of Smart House Control Using LabVIEW" at International Journal of Soft Computing and Engineering (IJSCE) ISSN: 2231-2307, Volume-1, Issue-6, January 2012
- [9] Basma M. Mohammad El-Basioni¹, Sherine M. Abd El-kader² and Mahmoud Abdelmonim Fakhreldin³, "Smart Home Design using Wireless Sensor Network and Biometric Technologies" at Volume 2, Issue 3, March 2013
- [10] Inderpreet Kaur, "Microcontroller Based Home Automation System With Security" at IJACSA) International Journal of Advanced Computer Science and Applications, Vol. 1, No. 6, December 2010
- [11] Roslin John Robles and Tai-hoon Kim, "Review: Context Aware Tools for Smart Home Development", International Journal of Smart Home, Vol.4, No.1, January, 2010
- [12] Hitendra Rawat, Ashish Kushwah, Khyati Asthana, Akanksha Shivhare, "LPG Gas Leakage Detection & Control System", National Conference on Synergetic Trends in engineering and Technology (STET-2014) International Journal of Engineering and Technical Research ISSN: 2321-0869, Special Issue
- [13] Nicholas D., Darrell B., Somsak S., "Home Automation using Cloud Network and Mobile Devices", IEEE Southeastcon 2012, Proceedings of IEEE.
- [14] Chan, M., Campo, E., Esteve, D., Fourniols, J.Y., "Smart homes-current features and future perspectives," Maturitas, vol. 64, issue 2, pp. 90-97, 2009
- [15] Das, S.R., Chita, S., Peterson, N., Shirazi, B.A., Bhadkamkar, M., "Home automation and security for mobile devices," IEEE PERCOM Workshops, pp. 141-146, 2011
- [16] S.D.T. Kelly, N.K. Suryadevara, S.C. Mukhopadhyay, "Towards the Implementation of IoT for Environmental Condition Monitoring in Homes", IEEE, Vol. 13, pp. 3846-3853, 2013
- [17] Rajeev Piyare "Internet of Things: Ubiquitous Home Control and Monitoring System using Android based Smart Phone" International Journal of Internet of Things 2013, 2(1): 5-11 DOI: 10.5923/j.ijit.20130201.02
- [18] G. Kortuem, F. Kawsar, D. Fitton, and V.Sundramoorthy, "Smart objects as building blocks for the internet of things," Internet Computing, IEEE, vol. 14, pp. 44-51, 2010.
- [19] S. Hilton. (2012, 14 January). Progression from M2M to the Internet of Things: an introductory blog. Available: <http://blog.bosch-si.com/progression-from-m2m-to-internet-of-things-an-introductory-blog/>
- [20] C.-H. Chen, C.-C. Gao, and J.-J. Chen, "Intelligent Home Energy Conservation System Based On WSN," presented at the International Conference on Electrical, Electronics and Civil Engineering, Pattaya, 2011.
- [21] R. Piyare and M. Tazil, "Bluetooth based home automation system using cell phone," in Consumer Electronics (ISCE), 2011 IEEE 15th International Symposium on, 2011, pp. 192-195.
- [22] Wikipedia. (2012, 12th December). Home automation. Available: http://en.wikipedia.org/wiki/Home_automation
- [23] <http://www.smartcomputing.com/editorial/article.asp?article=articles%2F1995%2Fmar95%2Fpcn0323%2Fpcn0323.asp> retrieved 2010 09 02
- [24] "U.S. Patent 613809: Method of and apparatus for controlling mechanism of moving vessels and vehicles". United States Patent and Trademark Office. 1898-11-08. Retrieved 2010-06-16.
- [25] William C. Mann (ed.) Smart technology for aging, disability and independence : the state of the science, John Wiley and Sons, 2005 0- 471-69694-3, pp. 34-66
- [26] N. Sriskanthan and Tan Karand. "Bluetooth Based Home Automation System". Journal of Microprocessors and Microsystems, Vol. 26, pp.281-289, 2002.
- [27] Muhammad Izhar Ramli, Mohd Helmy Abd Wahab, Nabihah, "TOWARDS SMART HOME: CONTROL ELECTRICAL DEVICES ONLINE" ,Nornabihah Ahmad International Conference on Science and Technology: Application in Industry and Education (2006)
- [28] Al-Ali, Member, IEEE & M. AL-Rousan, "Java-Based Home Automation System R." IEEE Transactions on Consumer Electronics, Vol. 50, No. 2, MAY 2004
- [29] BCC Research, "Sensors: Technologies and global markets,"
- [30] BCC Research, Market Forecasting, March 2011, <http://www.bccresearch.com/report/sensors-technologies-markets-ias006d.html> [Accessed on: 2012-01-05].
- [31] European Commission, "Internet of things in 2020 road map for the future," Working Group RFID of the ETP EPOSS, Tech. Rep., May 2008, <http://ec.europa.eu/information society/policy/rfid/documents/iotprague2009.pdf> [Accessed on: 2011-06-12].
- [32] T. Lu and W. Neng, "Future internet: The internet of things," in 3rd International Conference on Advanced Computer Theory and Engineering (ICACTE), vol. 5, August 2010, pp. V5-376-V5-380. Available: <http://dx.doi.org/10.1109/ICACTE.2010.5579543>.

Internet of Things for Smart Cities

Sindhuja A¹, Deiveegan A², Martin Lourdu Raj X³

¹ BE Final Year, *sindhuja*, ^{2,3} Assistant Professor,
Department of CSE, St. Anne's College Of Engineering and Technology

Abstract—The Internet of Things (IoT) shall be able to incorporate transparently and seamlessly a large number of different and heterogeneous end systems, while providing open access to selected subsets of data for the development of a plethora of digital services. Building a general architecture for the IoT is hence a very complex task, mainly because of the extremely large variety of devices, link layer technologies, and services that may be involved in such a system. In this paper we focus specifically to an urban IoT systems that, while still being quite a broad category, are characterized by their specific application domain. Urban IoTs, in fact, are designed to support the Smart City vision, which aims at exploiting the most advanced communication technologies to support added-value services for the administration of the city and for the citizens. This paper hence provides a comprehensive survey of the enabling technologies, protocols and architecture for an urban IoT. Furthermore, the paper will present and discuss the technical solutions and best-practice guidelines adopted in the Padova Smart City project, a proof of concept deployment of an IoT island in the city of Padova, Italy, performed in collaboration with the city municipality.

I. INTRODUCTION

The IoT is a recent communication paradigm that envisions a near future in which the objects of everyday life will be equipped with microcontrollers, transceivers for digital communication, and suitable protocol stacks that will make them able to communicate with one another and with the users, becoming an integral part of the Internet [1]. The IoT concept, hence, aims at making the Internet even more immersive and pervasive. Furthermore, by enabling easy access and interaction with a wide variety of devices such as, for instance, home appliances, surveillance cameras, monitoring sensors, actuators, displays, vehicles, and so on, the IoT will foster the development of a number of applications that make use of the potentially enormous amount and variety of data generated by such objects to provide new services to citizens, companies, and public administrations. This paradigm indeed finds application in many different domains, such as home automation, industrial automation, medical aids, mobile health care, elderly assistance, intelligent energy management and smart grids, automotive, traffic management and many others [2].

However, such a heterogeneous field of application makes the identification of solutions capable of satisfying the requirements of all possible application scenarios a formidable challenge. This difficulty has led to the proliferation of different and, sometimes, incompatible proposals for the practical realization of IoT systems. Therefore, from a system perspective, the realization of an IoT network, together with the required backend network services and devices, still lacks an established best practice because of its novelty and complexity.

The objective of this paper is to discuss a general reference framework for the design of an urban IoT. We describe the specific characteristics of an urban IoT, and the services that may drive the adoption of urban IoT by local governments. We then overview the web-based approach for the

design of IoT services, and the related protocols and technologies, discussing their suitability for the Smart City environment. Finally, we substantiate the discussion by reporting our experience in the “Padova Smart City” project, which is a proof of concept IoT island deployed in the city of Padova (Italy) and interconnected with the data network of the city municipality. In this regard, we describe the technical solutions adopted for the realization of the IoT island and we report some of the measurements that have been collected by the system in its first operational days.

The rest of the paper is organized as follows. Sec. II overviews the services that are commonly associated to the Smart City vision and that can be enabled by the deployment of an urban IoT. Sec. III provides a general overview of the system architecture for an urban IoT. More in detail, the section describes the web service approach for the realization of IoT services, with the related data formats and communication protocols, and the link layer technologies. Finally, Sec. IV presents the “Padova Smart City” project, which exemplifies a possible implementation of an urban IoT, and provides examples of the type of data that can be collected with such a structure.

II. SMART CITY CONCEPT AND SERVICES

According to [7], the Smart City market is estimated at hundreds of billion dollars by 2020, with an annual spending reaching nearly 16 billion. This market springs from the synergic interconnection of key industry and service sectors, such as Smart Governance, Smart Mobility, Smart Utilities, Smart Buildings, and Smart Environment. These sectors have also been considered in the European Smart Cities project (<http://www.smart-cities.eu>) to define a ranking criterion that can be used to assess the level of “smartness” of European cities. Nonetheless, the Smart City market has not really taken off yet, for a number of political, technical, and financial barriers [8]. Under the political dimension, the primary obstacle is the attribution of decision-making power to the different stakeholders. A possible way to remove this roadblock is to institutionalize the entire decision and execution process, concentrating the strategic planning and management of the smart city aspects into a single, dedicated department in the city [9].

In the rest of this section we overview some of the services that might be enabled by an urban IoT paradigm and that are of potential interest in the Smart City context because they can realize the win-win situation of increasing the quality and enhancing the services offered to the citizens while bringing an economical advantage for the city administration in terms of reduction of the operational costs [8]. To better appreciate the level of maturity of the enabling technologies for these services, we report in Tab. I a synoptic view of the services in terms of suggested type(s) of network to be deployed; expected traffic generated by the service; maximum tolerable delay; device powering; and an estimate of the feasibility of each service with currently available technologies. From the table it clearly emerges that, in general, the practical realization of most of such services is not hindered by technical issues, but rather by the lack of a widely accepted communication and service architecture that can abstract from the specific features of the single technologies and provide harmonized access to the services.

Structural health of buildings. Proper maintenance of the historical buildings of a city requires the continuous monitoring of the actual conditions of each building and the identification of the areas that are most subject to the impact of external agents. The urban IoT may provide a distributed database of building structural integrity measurements, collected by suitable sensors located in the buildings, such as vibration and deformation sensors to monitor the building stress, atmospheric agent sensors in the surrounding areas to monitor pollution levels, and temperature and humidity sensors to have a complete characterization of the environmental conditions [13].

Waste management. Waste management is a primary issue in many modern cities, due to both the cost of the service and the problem of the storage of garbage in landfills. A deeper penetration of

ICT solutions in this domain, however, may result in significant savings and economical and ecological advantages. For instance, the use of intelligent waste containers that detect the level of load and allow for an optimization of the collector trucks route, can reduce the cost of waste collection and improve the quality of recycling [14], [15]. To realize such a smart waste management service, the IoT shall connect the end devices, i.e., intelligent waste containers, to a control center where an optimization software processes the data and determines the optimal management of the collector truck fleet.

TABLE I
SERVICES SPECIFICATION FOR THE PADOVA SMART CITY PROJECT

Service	Network type(s)	Traffic rate	Tolerable delay	Energy source	Feasibility
Structural health	802.15.4; WiFi; Ethernet	1 pkt every 10 min per device	30 min for data; 10 seconds for alarms.	Mostly battery powered.	1: easy to realize, but seismograph may be difficult to integrate
Waste Management	WiFi; 3G; 4G	1 pkt every hour per device	30 min for data	Battery powered or energy harvesters.	2: possible to realize, but requires smart garbage containers
Air quality monitoring	802.15.4; Bluetooth; WiFi	1 pkt every 30 min per device	5 min for data	Photovoltaic panels for each device	1: easy to realize, but greenhouse gas sensors may not be cost effective
Noise monitoring	802.15.4; Ethernet	1 pkt every 10 min per device	5 min for data; 10 seconds for alarms	Battery powered or energy harvesters.	2: the sound pattern detection scheme may be difficult to implement on constrained devices
Traffic congestion	802.15.4; Bluetooth; WiFi; Ethernet	1 pkt every 10 min per device	5 min for data	Battery powered or energy harvesters.	3: requires the realization of both Air Quality and Noise Monitoring
City energy consumption	PLC; Ethernet	1 pkt every 10 min per device	5 min for data; tighter requirements for control	Mains powered	2: simple to realize, but requires authorization from energy operators
Smart parking	802.15.4; Ethernet	On demand	1 minute	Energy harvester	1: Smart parking systems are already available on the market and their integration should be simple.
Smart lighting	802.15.4; WiFi; Ethernet	On demand	1 minute	Mains powered	2: does not present major difficulties, but requires intervention on existing infrastructures.
Automation and salubrity of public buildings	802.15.4; WiFi; Ethernet	1 pkt every 10 minutes for remote monitoring; 1 pck every 30" for in-loco control	5 minutes for remote monitoring, few seconds for in-loco control	Mains powered and battery powered	2: does not present major difficulties, but requires intervention on existing infrastructures.

Air quality. The European Union officially adopted a 20-20-20 Renewable Energy Directive setting climate change reduction goals for the next decade [16]. The targets call for a 20 percent reduction in greenhouse gas emissions by 2020 compared with 1990 levels, a 20 percent cut in energy consumption through improved energy efficiency by 2020 and a 20 percent increase in the use of renewable energy by 2020.

Noise monitoring. Noise can be seen as a form of acoustic pollution as much as carbon oxide (CO) is for air. In that sense, the city authorities have already issued specific laws to reduce the amount of noise in the city centre at specific hours. An urban IoT can offer a noise monitoring service to measure the amount of noise produced at any given hour in the places that adopt the service [18]. Besides building a space-time map of the noise pollution in the area, such a service can also be used to enforce public security, by means of sound detection algorithms that can recognize, for instance, the noise of glass crashes or brawls.

Traffic congestion. On the same line of air quality and noise monitoring, a possible Smart City service that can be enabled by urban IoT consists in monitoring the traffic congestion in the city. Even though camera-based traffic monitoring systems are already available and deployed in many cities, low-power widespread communication can provide a denser source of information. Traffic monitoring may be realized by using the sensing capabilities and GPS installed on modern vehicles [19], but also adopting a combination of air quality and acoustic sensors along a given road. This information is of great importance for city authorities and citizens: for the former to discipline traffic and to send officers where needed, for the latter to plan in advance the route to reach the office or to better schedule a shopping trip to the city centre.

City energy consumption. Together with the air quality monitoring service, an urban IoT may provide a service to monitor the energy consumption of the whole city, thus enabling authorities and citizens to get a clear and detailed view of the amount of energy required by the different services (public lighting, transportation, traffic lights, control cameras, heating/cooling of public

buildings, and so on). In turn, this will make it possible to identify the main energy consumption sources and to set priorities in order to optimize their behavior.

Smart parking. The smart parking service is based on road sensors and intelligent displays that direct motorists along the best path for parking in the city [20]. The benefits deriving from this service are manifold: faster time to locate a parking slot means fewer CO emission from the car, less traffic congestion, and happier citizens.

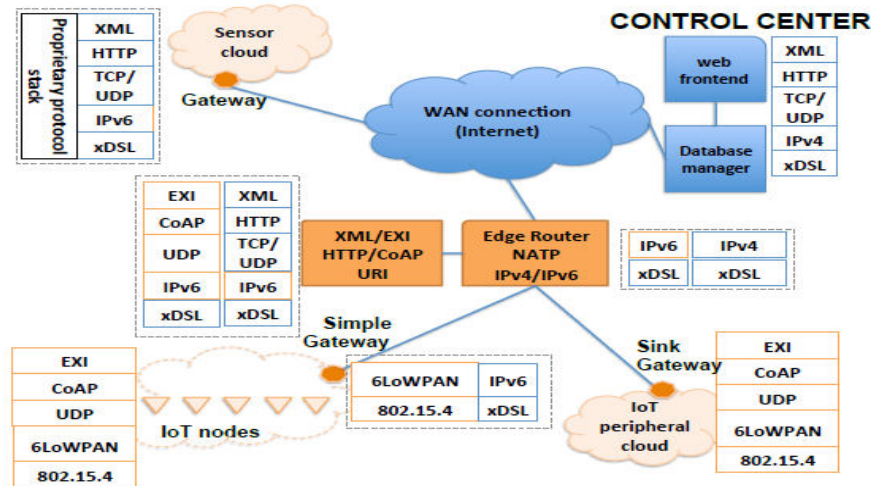


Fig. 1. Conceptual representation of an urban IoT network based on the web service approach.

The smart parking service can be directly integrated in the urban IoT infrastructure, because many companies in Europe are providing market products for this application. Furthermore, by using short-range communication technologies, such as Radio Frequency Identifiers (RFID) or Near Field Communication (NFC), it is possible to realize an electronic verification system of parking permits in slots reserved for residents or disabled, thus offering a better service to citizens that can legitimately use those slots and an efficient tool for quickly spot violations.

Smart lighting. In order to support the 2020 directive, the optimization of the street lighting efficiency is an important feature. In particular, this service can optimize the street lamp intensity according to the time of the day, the weather conditions and the presence of people. In order to properly work, such a service needs to include the street lights into the Smart City infrastructure. It is also possible to exploit the increased number of connected spots to provide WiFi connection to citizens. In addition, a fault detection system will be easily realized on top of the street light controllers.

Automation and salubrity of public buildings. Another important application of IoT technologies is the monitoring of the energy consumption and the salubrity of the environment in public buildings (schools, administration offices, museums) by means of different types of sensors and actuators that control lights, temperature, and humidity. By controlling these parameters, indeed, it is possible to enhance the level of comfort of the persons that live in these environments, which may also have a positive return in terms of productivity, while reducing the costs for heating/cooling [21]

I. URBAN IOT ARCHITECTURE

From the analysis of the services described in Sec. II, it clearly emerges that most Smart City services are based on a centralized architecture, where a dense and heterogeneous set of peripheral

devices deployed over the urban area generate describing the web service approach for the design of IoT services, which requires the deployment of suitable protocol layers in the different elements of the network, as shown in the protocol stacks depicted in Fig. 1 besides the key elements of the architecture. Then, we briefly overview the link layer technologies that can be used to interconnect the different parts of the IoT. Finally, we describe the heterogeneous set of devices that concur to the realization of an urban IoT.

A. Web service approach for IoT service architecture

Although in the IoT many different standards are still struggling to be the reference one and the most adopted, in this section we focus specifically on IETF standards because they are open and royalty-free, are based on Internet best practices, and can count on a wide community.

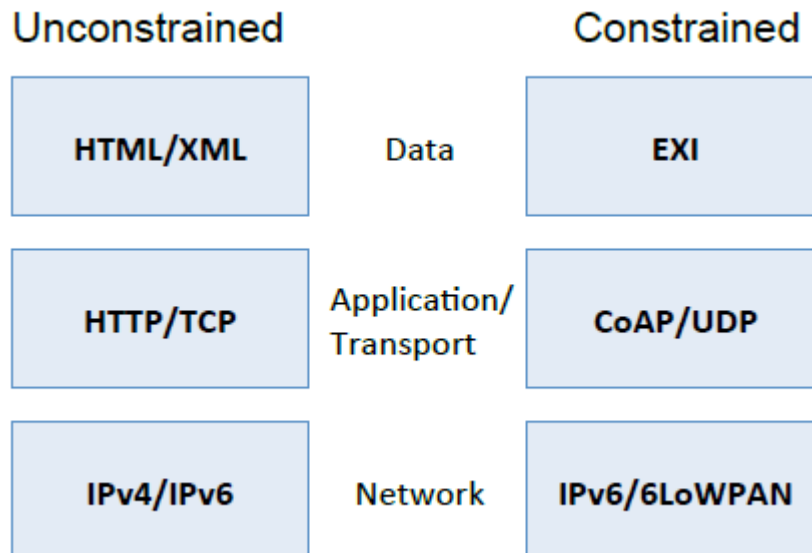
The IETF standards for IoT embrace a web service architecture for IoT services, which has been widely documented in the literature as a very promising and flexible approach. In fact, web services permit to realize a flexible and interoperable system that can be extended to IoT nodes, through the adoption of the web-based paradigm known as Representational State Transfer (ReST) [22]. IoT services designed in accordance with the ReST paradigm exhibit very strong similarity with traditional web services, thus greatly facilitating the adoption and use of IoT by both end users and service developers, which will be able to easily reuse much of the knowledge gained from traditional web technologies in the development of services for networks containing smart objects. The web service approach is also promoted by international standardization bodies such as IETF, ETSI and W3C, among others, as well as European research projects on the Internet of Things such as SENSEI [23], IoT-A [24] and SmartSantander [5].

1) Data format: As mentioned, the urban IoT paradigm sets specific requirements in terms of data accessibility. In architectures based on web services, data exchange is typically accompanied by a description of the transferred content by means of semantic representation languages, of which the eXtensible Markup Language (XML) is probably the most common. Nevertheless, the size of XML messages is often too large for the limited capacity of typical devices for the IoT. Furthermore, the text nature of XML representation makes the parsing of messages by CPU-limited devices more complex compared to the binary formats. For these reasons, the working group of the World Wide Web Consortium (W3C) [25] has proposed the EXI format [26], which makes it possible even for very constrained devices to natively support and generate messages using an open data format compatible with XML.

2) Application and transport layers: Most of the traffic that crosses the Internet today is carried at the application layer by HTTP over TCP. However, the verbosity and complexity of native HTTP make it unsuitable for a straight **Fig. Fig 2. Protocol stacks for unconstrained (left) and constrained (right) IoT nodes.**

deployment on constrained IoT devices. For such an environment, in fact, the human-readable format of HTTP, which has been one of the reasons of its success in traditional networks, turns out to be a limiting factor due to the large amount of heavily correlated (and, hence, redundant) data. Moreover, HTTP typically relies upon the TCP transport protocol that, however, does not scale well on constrained devices, yielding poor performance for small data flows in lossy environments.

The CoAP protocol [29] overcomes these difficulties by proposing a binary format transported over UDP, handling only the retransmissions strictly required to provide a reliable service. Moreover, CoAP can easily interoperate with HTTP because: (i) it supports the ReST methods of HTTP (GET, PUT, POST, and DELETE), (ii) there is a one-to-one correspondence between the response codes of the two protocols, and (iii) the CoAP options can support a wide range of HTTP usage scenarios. Even though regular Internet hosts can natively support CoAP to directly talk to IoT



devices, the most general and easily interoperable solution requires the deployment of an HTTP-CoAP intermediary, also known as cross proxy that can straightforwardly translate requests/responses between the two protocols, thus enabling transparent interoperation with native HTTP devices and applications [30].

3) Network layer: IPv4 is the leading addressing technology supported by Internet hosts. However, IANA, the international organization that assigns IP addresses at a global level, has recently announced the exhaustion of IPv4 address blocks. IoT networks, in turn, are expected to include billions of nodes, each of which shall be (in principle) uniquely addressable. A solution to this problem is offered by the IPv6 standard [31], which provides a 128-bit address field, thus making it possible to assign a unique IPv6 address to any possible node in the IoT network.

While the deployment of a 6LoWPAN border router enables transparent interaction between IoT nodes and any IPv6 host in the Internet, the interaction with IPv4-only hosts remains an issue. More specifically, the problem consists in finding a way to address a specific IPv6 host using an IPv4 address and other meta-data available in the packet.

B. Link Layer Technologies

An urban IoT system, due to its inherently large deployment area, requires a set of link layer technologies that can easily cover a wide geographical area and, at the same time, support a possibly large amount of traffic resulting from the aggregation of an extremely high number of smaller data flows. For these reasons, link layer technologies enabling the realization of an urban IoT system are classified into unconstrained and constrained technologies. The first group includes all the traditional LAN, MAN and WAN communication technologies, such as Ethernet, Wi-Fi, fiber optic, broadband Power Line Communication (PLC), and cellular technologies as such as UMTS and LTE. They are generally characterized by high reliability, low latency, and high transfer rates (order of Mbit/s or higher), and due to their inherent complexity and energy consumption are generally not suitable for peripheral IoT nodes. The constrained physical and link layer technologies are, instead, generally characterized by low energy consumption and relatively low transfer rates, typically smaller than

C. Devices

We finally describe the devices that are essential to realize an urban IoT, classified based on the position they occupy in the communication

1) Backend servers: At the root of the system, we find the backend servers, located in the control center, where data are collected, stored, and processed to produce added-value services. In principle, backend servers are not mandatory for an IoT system to properly operate, though they become a fundamental component of an urban IoT where they can facilitate the access to the smart city services and open data through the legacy network infrastructure. Backend systems commonly considered for interfacing with the IoT data feeders include the following. These systems are in charge of storing the large amount of information produced by IoT peripheral nodes, such as sensors. Depending on the particular usage scenario, the load on these systems can be quite large, so that proper dimensioning of the backend system is required.

Web Sites. The widespread acquaintance of people with web interfaces makes them the first option to enable interoperation between the IoT system and the “data consumers,” e.g., public authorities, service operators, utility providers, and common citizens.

Enterprise Resource Planning systems (ERP). ERP components support a variety of business functions and are precious tools to manage the flow of information across a complex organization, such as a city administration. Interfacing ERP components with database management systems that collect the data generated by the IoT allows for a simpler management of the potentially massive amount of data gathered by the IoT, making it possible to separate the information flows based on their nature and relevance and easing the creation of new services.

2) Gateways: Moving toward the “edge” of the IoT, we find the gateways, whose role is to interconnect the end devices to the main communication infrastructure of the system. With reference to the conceptual protocol architecture depicted in Fig. 2, the gateway is hence required to provide protocol translation and functional mapping between the unconstrained protocols and their constrained counterparts, that is to say XML-EXI, HTTP-CoAP, IPv4/v6-6LoWPAN.

Note that, while all these translations may be required in order to enable interoperability with IoT peripheral devices and control stations, it is not necessary to concentrate all of them in a single gateway. Rather, it is possible, and sometimes convenient, to distribute the translation tasks over different devices in the network. For example, a single HTTP-CoAP proxy can be deployed to support multiple 6LoWPAN border routers. Gateway devices shall also provide the interconnection between unconstrained link layer technologies, mainly used in the core of the IoT network, and constrained technologies that, instead, provide connectivity among the IoT peripheral nodes.

3) IoT peripheral nodes: Finally, at the periphery of the IoT system we find the devices in charge of producing the data to be delivered to the control center, which are usually called IoT peripheral nodes or, more simply, IoT nodes. Generally speaking, the cost of these devices is very low, starting from 10 USD or even less, depending on the kind and number of sensors/actuators mounted on the board. IoT nodes may be classified based on a wide number of characteristics, such as powering mode, networking role (relay or leaf), sensor/actuator equipment, supported link layer technologies. The most constrained IoT nodes are likely the Radio Frequency tags (RFtags) that, despite their very limited capabilities, can still play an important role in IoT systems, mainly because of the extremely low cost and the passive nature of their communication hardware, which does not require any internal energy source. The typical application of RFtags is object identification by proximity reading, which can be used for logistics, maintenance, monitoring, and other services.

IV. AN EXPERIMENTAL STUDY: PADOVA SMART CITY

The framework discussed in this paper has already been successfully applied to a number of different use cases in the context of IoT systems. For instance, the experimental wireless sensor network testbed, with more than 300 nodes, deployed at the University of Padova [39], [40] has been designed according to these guidelines, and successfully used to realize proof-of-concept demonstrations of smart grid [41], and health care [42] services.

In this section we describe a practical implementation of an urban IoT, named “Padova Smart City,” that has been realized in the city of Padova thanks to the collaboration between public and private parties, such as the municipality of Padova, which has sponsored the project, the Department of Information Engineering of the University of Padova, which has provided the theoretical background and the feasibility analysis of the project, and Patavina Technologies s.r.l.,¹ a spin-off of the University of Padova specialized in the development of innovative IoT solutions, which has developed the IoT nodes and the control software.

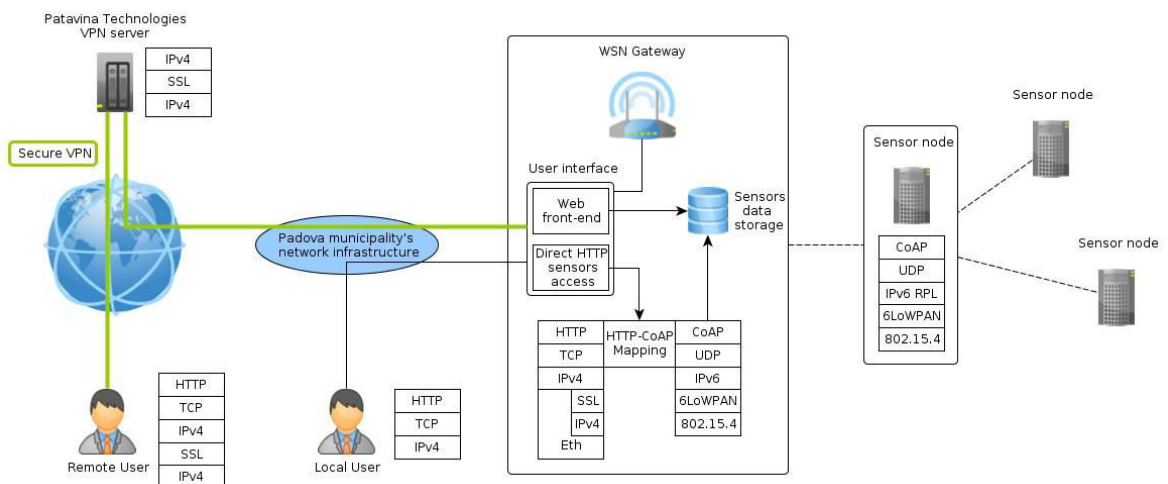


Fig. 3. System architecture of “Padova Smart City.”

Padova Smart City components. A conceptual sketch of the Padova Smart City system architecture is given in Fig. 3. In the following, we describe in more details the different hardware and software components of the system.

Street light. It is the leaf part of the system where IoT nodes are placed. Each streetlight is geographically localized on the city map and uniquely associated to the IoT node attached to it, so that IoT data can be enhanced with context information. The monitoring of the correct operation of the bulbs is performed through photometer sensors that directly measure the intensity of the light emitted by the lamps (or, actually, by any source whose light reaches the sensor) at regular time intervals or upon request. The wireless IoT nodes are also equipped with temperature and humidity sensors, which provide data concerning weather conditions, and one node is also equipped with a benzene (C_6H_6) sensor, which monitors air quality.

WSN Gateway. The gateway has the role of interfacing the constrained link layer technology used in the sensors cloud with traditional WAN technologies used to provide connectivity to the central backend servers. The gateway hence plays the role of 6LoWPAN border router and RPL root node. Furthermore, since sensor nodes do not support CoAP services, the gateway also operates as the sink node for the sensor cloud, collecting all the data that need to be exported to the backend services. The connection to the backend services is provided by common unconstrained communication technologies, optical fiber in this specific example.

HTTP-CoAP Proxy. The HTTP-CoAP proxy enables transparent communication with CoAP devices. The proxy logic can be extended to better support monitoring applications and limit the amount of traffic injected into the IoT peripheral network. For instance, it is possible to specify a list of resources that need to be monitored, so that the server can autonomously update the entries in a cache related to those devices. This mechanism can be supported by two different approaches: (i) by polling the selected resource proactively, thus enabling the implementation of traffic shaping techniques at the proxy or at the gateway, and (ii) by subscribing to the selected resource using the “observe” functionality of CoAP, thus enabling the server on the node to send the updates only when the value measured by the sensor falls outside a certain

V. CONCLUSIONS

In this paper we analyzed the solutions currently available for the implementation of urban IoTs. The discussed technologies are close to being standardized, and industry players are already active in the production of devices that take advantage of these technologies to enable the applications of interest, such as those described in Sec. II. In fact, while the range of design options for IoT systems is rather wide, the set of open and standardized protocols is significantly smaller. The enabling technologies, furthermore, have reached a level of maturity that allows for the practical realization of IoT solutions and services, starting from field trials that will hopefully help clear the uncertainty that still prevents a massive adoption of the IoT paradigm. A concrete proof of concept implementation, deployed in collaboration with the city of Padova, Italy, has also been described as a relevant example of application of the IoT paradigm to smart cities

VI. REFERENCES

- [1] L. Atzori, A. Iera, and G. Morabito, “The internet of things: A survey,” *Computer Networks*, vol. 54, no. 15, pp. 2787-2805, 2010.
- [2] P. Bellavista, G. Cardone, A. Corradi, and L. Foschini, “Convergence of MANET and WSN in IoT Urban Scenarios,” *IEEE Sensors Journal*, vol.13, no.10, pp. 3558-3567, Jun. 2013.
- [3] A. Laya, V. I. Bratu, and J. Markendahl, “Who is investing in machine- to-machine communications?”, 24th European Regional ITS Conference, Florence, Italy, 20-23 Oct. 2013.
- [4] H. Schaffers, N. Komninos, M. Pallot, B. Trousse, M. Nilsson, and A.Oliveira, “Smart Cities and the Future Internet: Towards Cooperation Frameworks for Open Innovation”, *The Future Internet, Lecture Notes in Computer Science Volume 6656*, pp. 431-446, 2011.
- [5] SmartSantander. [Online]. Available: <http://www.smartsantander.eu/>.
- [6] D. Cuff, M. Hansen, and J. Kang, “Urban sensing: out of the woods.” *Communications of the ACM* vol. 51, no. 3, pp. 24-33, Mar. 2008.
- [7] Pike Research on Smart Cities. [Online]. Available: <http://www.pikeresearch.com/research/smart-cities>.
- [8] M. Dohler, I. Vilajosana, X. Vilajosana, and J. Llosa, “Smart Cities: An Action Plan,” *Barcelona Smart Cities Congress 2011, Barcelona, Spain*, Dec. 2011.
- [9] I. Vilajosana, J. Llosa, B. Martinez, M. Domingo-Prieto, A. Angles, and X. Vilajosana, “Bootstrapping smart cities through a self-sustainable model based on big data flows,” *IEEE Communications Magazine*, vol. 51, no. 6, pp. 128-134, Jun. 2013.
- [10] J. M. Hernández-Muñoz, J. B. Vercher, L. Muñoz, J. A. Galache, M. Presser, L. A. Hernández Gómez, and J. Pettersson, “Smart Cities at the Forefront of the Future Internet,” *The Future Internet, Lecture Notes in Computer Science*, vol. 6656, pp. 447-462, 2011.
- [11] C. E. A. Mulligan, M. Olsson, “Architectural implications of smart city business models: an evolutionary perspective” *IEEE Communications Magazine*, vol. 51, no. 6, pp. 80-85, Jun. 2013.
- [12] N. Walravens, P. Ballon, “Platform business models for smart cities: from control and value to governance and public value” *IEEE Communications Magazine*, vol. 51, no. 6, pp. 72-79, Jun. 2013.
- [13] J. P. Lynch, and J. L. Kenneth, “A summary review of wireless sensors and sensor networks for structural health monitoring.” *Shock and Vibration Digest* vol. 38 no. 2, pp. 91-130, 2006.
- [14] T. Nuortio, J. Kytöjoki, H. Niska, and O. Bräysy, “Improved route planning and scheduling of waste collection and transport,” *Expert Systems with Applications*, vol. 30, no. 2, pp. 223-232, Feb. 2006.
- [15] FP7-ENVIRONMENT program, “EcoWeb a dynamic e-dissemination platform for EU eco-innovation research results” [Online]. Available: <http://ecoweb-project.info/>

Privacy Enhancement of Social Network Security by Third Party Application

N.Umamaheshwari¹,K.Poornambigai²,P.Meena³

¹*CSE Dept .Student,St.Anne'sCollege of Engg&Tech, umamaheswarimani1986@gmail.com*

²*AP/CSE, St.Anne'sCollege of Engg&Tech,k.poornilashmi15@gmail.com*

³*AP/CSE St.Anne'sCollege of Engg&Tech,meenasarathy.08@gmail.com*

Abstract-Social networking sites such as Facebook ,Google,twitter provide third party applications such as games and productivity applications by providing a social application platform. These interfaces enable popular site enhancements but poses privacy risks by exposing user data to third party developers. The current security mechanisms, such as privacy policies and access control mechanisms fall short on protecting the privacy of the users. In this paper, we are representing a framework for a privacy enhanced social network security application that technically enforces the protection of the personal data of a user, when interacting with social applications.Let us propose a multicriteria recommendation model that uses application based, category based, user based, and collaborative filtering mechanisms which are based on previous user decisions, and application requests to increase the privacy of the overall site's user population. Our project on the collected information indicate that the proposed framework enhanced the user security and privacy related to third-party application authorizations.

Keywords— OAuth, Random number generation ,collaborative filtering, social networks, Prediction model

I. INTRODUCTION

Online social networks (OSNs) are now the condition in modern society. The number and the size of OSNs grows, there is increasing concern about the security of the terabytes of personal information entrusted to OSNs and how the privacy of this data is managed. Third party applications, generally within social networking platforms have become very popular and penetrative. For example, with over eight million third party applications on Facebook and its users install applications more than 21 million times a day . Before using applications, users are required to authorize them and grant them access to certain permissions they request, e.g., access to a user's data such as e-mail, location, etc. With the pervasiveness of such applications, preventing the user's online personal data becomes a necessity. Open standards and third party software development have long formed a partnership that affords users the tools to better manage their own privacy, identity, and confidentiality. Seeing a need of users to better know the privacy policies in force for various websites led the World Wide Web Consortium to construct the Platform for Privacy Preferences specification and the corresponding Preference Exchange Language (APPEL) that is in use today by various internet websites to stipulate in machine readable format, the particular file specifying that site's particular privacy policies . The OAuth open standard protocol (OAuth) is another example of an available standard created to provide users with the ability to share data and resources with third party application components of other and more primary web applications. The OAuth framework might allow for the sharing of images from a primary webbased photo sharing site [4] .So, a third party photo printing service might access the permitted images. Popular social network , Facebook today represents the largest single OAuth 2.0 permitting a mechanism for third party web-based applications to access Facebook user identity and privacy and resources.

Third party application software developers have led charges to enhance user privacy and protection using extensible frameworks available in the web browsers such as Chrome, Firefox, and Safari. These browser extensions protect users from unwanted advertisements, spiteful software installations, and compromise of user credential information. Indeed, Joshi et al. showcase a browser plug-in which attempts to solve man-in-the-middle attacks prevalent in modern Phishing attacks. While the relationship between standards and browser-based extensions is rich in history and likely to continue, there may exist one gap that requires fulfilling. Appreciating that individual privacy preferences may be just individual, how can a single extension reflect the privacy preferences for a unique set of individuals? In this paper, we represent a novel browser extension (FBSecure) that implements a proposed recommender model which enables users to make important privacy decisions at the time of third party application installation and integrates in the existing OAuth 2.0. Recommendations give users confidence in making their decisions, especially many privacy requests would not clearly convey the accesses granted [7]. The decisions which users make are their own of course, but the algorithm and model provides a mechanism to inform them and provide recommendations based on the collaborative decisions (grant / deny) on same privacy requests in the user's larger social network.

A browser extension that intercepts the default OAuth 2.0 request flow, interprets and provides the user with a simple interface to make decisions that provide for the protection of personal identity attributes before installation of an application. A multicriteria recommender-model approaches to provide users with recommendations on requested privacy attributes based on the collaborative effort of users who have historically made decisions for similarly requested privacy attributes. A recommendation to extend the OAuth 2.0 specification to provide an attainment through which webbrowsers might assist users in making informed decisions regarding their full privacy attributes before the installation of an application [10]. A user study that shows the results and effectiveness of using our proposed browser extension.



Figure 1. Social network 3rd party application permission request.

II. PROBLEM DEFINITION

The OAuth framework provides a mechanism for third party service providers to access end user resources without releasing the user's access credentials to the service provider. Sometimes, specific implementations neither provide the user with the necessary fine-grain access control, nor provide any recommendations in which access control decisions may be the most appropriate. As an example we use entire this paper is one of the

free Facebook online video and voice calling applications available through website(friendcameo.com).The friendcameo Facebook application requests the following extended permissions when users first install the application: access to the user's e-mail , ability to publish status and post messages in the user's wall and the ability to access the Facebook chat application, and the ability to count the online presence status of other users.It becomes quickly clear that some of the extended once granted, permissions, cannot genuine be revoked. As a example, once users to provide the friendcameo access to their e-mail addresses, they cannot remove that genuine e-mail address from FriendCameo's servers and databases by preventing further access to the information through Facebook's application by privacy settings [16]. We find there are different user character that are practically irrevocable once granted, since the attributes are generally constant (i.e., birthday) or generally change with very little frequency (i.e., hometown locations, religious and political views). (See Fig. 1) We view the permanent loss of personal attributes as only one part of the problem; should a method be devised to permit users a "last line of defense" against such information loss, how may they know best what decisions can take users benefit from a knowledge of people to better inform their own decision making? Our proposed approach provides both the aforementioned "last line of defense" mechanism and a recommender model based on the decisions of other users within the area of people, and the previous decisions of an indivisible user.

III. EXISTING SYSTEM

Major online platforms such as Google,Facebook and Twitter allow third-party applications such as productivity applications, Games are access to user online private data. Such accesses must be certified by users at installation time.The Open Authorization protocol (OAuth) was introduced as a secure and efficient method for authorizing third - party applications without releasing a user's access credentials.

IV.PROPOSED SYSTEM

Proposed model was introduced as a secure and efficient mechanism for authorizing third-party applications. This requires users to present their credentials to third-party applications, hence allowed them large access to all their online resources with no restrictions. In OAuth, these new credentials are represented via an Access Token. It is a string which denotes a certain scope of permissions granted to an application is called Access Token & it also signify to other attributes such as the duration the Access Token is considered valid. We are mainly interested in the scope of character within an Access Token. And it was issued by an authorized server after the approval of the resource owner. We propose an abstract access paradigm, which can be applied to the design of the filtering systems, and the formalizes the access to the filtering results via multi-corridors (based on content-based categories) at the same time.). We use these measures to evaluate the use of various kinds of multi-corridors for our prototype user-adapting Website in the: Active of Web Museum [15]. It can be used to create user-adapting Web sites through Information filtering techniques. User-adapting Web sites adapt their presentation to the user's preferences. It is hard to relate the classic measurements to actual user satisfaction because of the way the user interacts with the recommendations, influences the benefits for the user and determined by their representation,. The systems consider every user as an expert for his taste, so that personalized recommendations can be provided based on the expertise of taste-related users. Collaborative filtering has been applied to several domains of information: News articles. Collaborative filtering systems then use this rating matrix in order to derive predictions [9]. Several algorithms have been proposed on how to use the rating matrix to predict ratings. The dynamic topology is achieved by dynamic corridors virtual corridors which contain paintings of a chosen category sorted according to personalized predictions

produced by collaborative filtering. When this paradigm is applied to user-adapting Web sites or other types of recommender systems, more choice for the users can be provided via various multi-corridors and therefore increase performance from the perspective of the user.

V. PRELIMINARIES

Most of the major online platforms such as Google, Twitter and Facebook is provide an open API which allows third - party applications to directly interact with their own platform. An APIs provide a mechanism to write, read,or modify the user data on such platforms through other third party applications on behalf of the users themselves and an API comes with a set of the methods,to each representing a secure user interaction executed through a third-party application.

For example, the FriendCameo application is able to post content (e.g., messages, photos) to a user's Facebook feed/wall using profile_id/Facebook's/feed of an API method, where the profile_id is the targeted on Facebook user ID and it is important to indicate that third-party applications can potentially execute any API call on behalf of a relying on the type,user and scope of permissions granted to these applications.In this previous example, the application of FriendCameo should only perform the profile_id/feed API call given it the publish_stream permission to user has granted [8]. The set of the permissions available to the thirdparty applications are defined by the third-party applications and it is up to the online platforms whose to request the proper subset of permissions to be need. We believe on the users should have the final decision on which permissions to grant or deny.

A. OAuth Standard :

With an increasing trend toward offering online services that provide third-party applications the ability to interact through access user resources and open APIs, OAuth was introduced as an efficient and secure mechanism for authorizing third-party applications. Traditional authentication models such as the client-server model require third-party applications to authenticate with online services using the resource owner's typically a username,password and private credentials. This requires users to present their authorization to third-party applications, hence its allow them to broad access to all their online resources with no restrictions. A user may be revoke access from a third-party application by changed her credential, but doing so subsequently revokes access from all third-party applications that continue to use her previous accreditation. These issues are effect given the high number of the third-party applications that may be get access to a user's online resources. OAuth uses a component where the roles of resource owners and third-party applications are separated [6].

It doesn't require users to share that private credentials with the third-party applications, instead it issues a new set of the credentials for each application.These are new set of reflect an unique set of permissions to a user's online resources and credential as per application. In OAuth, these new authorization are represented via an Access Token and It is a string which denotes a certain scope of permissions granted to an application, it also denotes other features such as the duration of the Access Token is considered authentic string. We are mainly interested in the scope attribute within an Access Token and These Access Token are issued by an authorization server after the approval of the resource owner. In this paper, we have spread upon this authorization stage of the OAuth 2.0 protocol. When a third-party application needs to it presents its Access Token to the service provider hosting the resource which in turn verifies the requested access against the scope of permissions denoted by the Token and access a user's protected resources, . For example, Alice (resource owner) on Facebook (service provider and resource server) can grant the FriendCameo

application (client) access to her e-mail address on her Facebook profile without ever sharing her username and password with FriendCameo. Instead, she authorize the FriendCameo application with Facebook which in turn provides FriendCameo with a proper Access Token that denotes permission to access Alice's e-mail address. OAuth provides multiple authorization flows depending on the client (third-party application) type (e.g., webserver, native applications). In this paper, shown in Fig. 2 and detailed in the OAuth 2.0 specification [28] and we focus on the Authorization Code flow. The authorization code flow is used by third-party applications that and are able to receive incoming requests via redirection,are able to interact with a user's web browser. The authorization flow process consists of three parties: 1)Client (third-party application) , 2)End-user (resource owner) at browser , and 3) Authorization server (e.g., Facebook). Our main focus is on the steps "(A)" and "(B)" within the approval of code flow. Step "(A)" is where third-party applications initiate the flow by redirecting a user's browser to the authorization server and pass along the requested scope of permissions [10].

In step "(B)," it establishes her decision on whether to grant or deny the third-party application's access request and the authorization server authenticates the end user.

B. OAuth and User Privacy:

One of the main reasons behind OAuth was to increase user privacy by separating the role of users from that of third party applications. OAuth uses the concept of Access Tokens, where a token denotes a set of credentials granted to third-party applications by the resource owners. This avoids the need for users to share their private credentials such as their username and password. It also allows users to revoke access to a specific third-party application by revoking its Access Token. OAuth 2.0 allows third-party applications to request a set of permissions via the scope attribute, and for users to grant/deny such requests. If a user grants a third-party application's request, then an Access Token (denoting the scope) is issued for that application, hence granting it the scope of permissions requested. The scope attribute represents the set of permissions requested by third-party applications, and is our main focus in this paper. In the authorization code,OAuth flow, the scope parameter is part of the request URI that is generated by third-party applications (Step "(A)") . The scope is a list of space-delimited strings, each string mapped to a certain permission or access level. For example, the FriendCameo application requests permission to post to a user's Facebook feed/wall, to log in to Facebook chat, to access her e-mail address, and to check her friend's online/ offline presence. FriendCameo requests these permissions with a scope attribute value of "publish_stream, xmpp_login, e-mail, friends_online_presence." The scope value becomes part of the OAuth request URI sent to the authorization server (Facebook's OAuth implementation uses commas rather than spaces to separate each requested permission) [13]. Step "(B)" is where users grant/deny the requested scope value.

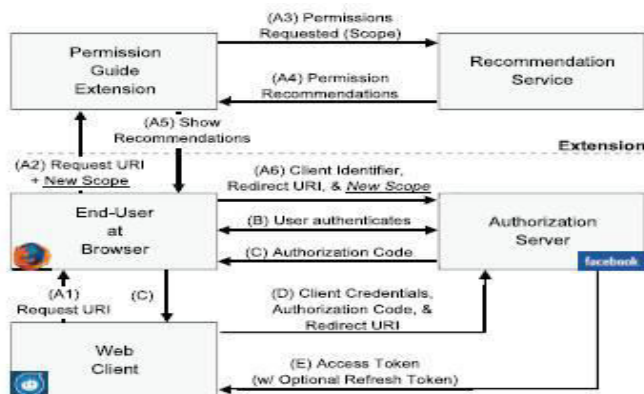


Fig. 2 : System Architecture of OAuth & User Privacy.

C. Collaborative Filtering

Recommendation systems are systems that try to assist users in evaluating and making decisions on items by providing them opinions and prediction values as a set of recommendations. These set of recommendations are usually based on other people's opinions and the potential relevance of items to a target user. The first recommender system Tapestry, followed the approach of "Collaborative Filtering," in which users collaborate toward filtering documents via their individual reactions after reading certain documents. Since then, collaborative filtering has been widely adopted and is accepted as a highly successful technique in recommender systems. In a context of access control and user privacy, items in a collaborative filtering model can be mapped to individual privacy attributes or permissions. Users make decisions on privacy attributes, i.e., grant/deny them to third-party applications in Fig 2. This is similar to other recommendation systems in which users make decisions on items, e.g., to rent a movie or not. Users have their own privacy preferences, but may benefit from the community's collaborative privacy decisions to make their own, especially if they lack the knowledge to make good privacy decisions. The effect of community data on user privacy has been investigated by Besmer et al., who explored the effect of community data on user behavior when configuring access control policies. Their work indicated that community data impacts user behavior, when substantial visual cues were provided [18]. Goecks et al. explored the effects of community data in the domain of firewall policy configuration and web browser cookie management. Their results also indicated that users did utilize community data in making their own decisions. In this paper, we propose a collaborative filtering model that utilizes community decisions in providing recommendations to users who install third-party applications requesting access to their privacy attributes.

VI. PROPOSED OAUTH FLOW

We proposed an extension to the OAuth 2.0 code flow, by introducing two new modules into the flow: 1) A Recommendation Service that retrieves a set of recommendations for the requested permissions following a collaborative filtering model as seen in Section V (B), shows them a set of recommendations on each of the requested permissions and 2) A Permission Guide that guides users through their requested permissions. Our OAuth continuing focuses on step "(A)" of the authorization code flow in OAuth 2.0. We revise step "(A)" to become a six stage process and its explained in the following steps: A1. The Permission Guide extension captures the scope value from the request URI and parses the requested permissions. At this step, the extension allows the users to choose a subset of the permissions requested. A2. The client redirects the browser to the end-user authorization endpoint by initiating a request URI that includes a scope parameter. A3. The Permission Guide extension requests a set of recommendations on the parsed permissions. This is achieved by passing the set of permissions to our Recommendation Service. A4. The Recommendation Service returns a set of recommendations for the permissions requested by the client. A5. Using the set of returned recommendations, the extension presents the permissions with their respective recommendations in a user-friendly manner. A6. The Permission Guide extension redirects the enduser's browser to a new request URI with a new scope (scope'), assuming the user chooses to modify the requested permissions.

A. Permission Guide

The Permission Guide is represented by a browser extension that integrates into the authorization process by capturing the scope parameter value within the request URI generated by a third-party application. Once the scope is captured, the extension parses the requested permissions and presents them in a user-friendly manner. A readable label of each requested permission is shown to the end-user, e.g., it shows "Facebook Chat" rather than

xmpp_login. The extension also shows users a set of recommendations for the requested permissions. For each permission, there is a thumbs-up and thumbs-down recommendation value. These recommendations represent prediction values that we calculate following our model in Section V (B). These prediction values represent the likeliness of a user to grant or deny a certain permission based on her previous decisions and on the collaborative decisions of other users. Users who have not made any decisions yet are shown recommendations based on other user decisions [25]. The extension also allows users to customize the requested permissions by checking or unchecking individual permissions, where a checked permission is one the user wishes to grant to the third-party application and an unchecked permission is one she wishes to deny access to. Once a user decides on the permissions she wishes to grant and deny, she simply needs to click a Set Permissions button on the extension. This will trigger the extension to generate a new request URI with a new scope `scope'`, and forward the user's browser to this new request URI. `scope'` will always be a subset of the original requested scope.

An example `scope'` for the FriendCameo application could be as follows: `scope'=publish_stream` reflecting the user's desire to allow FriendCameo to post to her feed/wall, but deny it access to her e-mail, Facebook chat and friend's online/offline presence. Note that using a subset of the permissions requested could potentially hinder the functionality of a third-party application once installed. Investigating such consequence is out of the scope of this paper, but we include it as part of our future work. Our Permission Guide extension also collects the user's decisions on the requested permissions, hence allows us to generate a data set of decisions to be used in our recommendation model explained in Section V (B). That is, our Recommendation Service as seen in Fig. 3 will utilize these decisions in making its recommendation predictions. These decisions are uploaded to our servers once a user sets her desired permissions within the extension, i.e., clicks the Set Permissions button. The data uploaded to our servers includes: `app_id`, `requested_perms`, `decisions`, `recommendations`, where the `app_id` is the application's unique id which is assigned by the service provider (e.g., Facebook), the `requested_perms` is the scope of permissions requested by the third-party application, the `decisions` are the individual user decisions (grant or deny) on each of the requested permissions, and the `recommendations` are the recommendation values at the time the user made her decisions. Our goal is to provide a simple user interface for interacting with permission requests, hence increasing user awareness and providing an easy mechanism for guiding users in making their decisions.

B. Recommendation Model for Permission Guide

We propose a Recommendation Service component that extends upon our Permission Guide extension. Let A , U , and P represent the set of users, applications and permissions, respectively. A user $u_i \in U$ can make a decision $d_i \in \{\text{grant}; \text{deny}\}$ on a permission $p_j \in P$ for an application $a_k \in A$. An application a_k which requests permissions $p_1; \dots; p_m$ is mapped to a set of decisions $d_1; \dots; d_m$ made by the user installing a_k .

C. Collaborative Filtering

Our model follows the multicriteria recommendation model where user recommendations are calculated per criterion. The model utilizes the set of permissions P as a set of criteria, i.e., each permission $p_j \in P$ represents an individual criterion within the model. The multicriteria recommendation approach fits our model as decisions are made per permission (criteria) rather than an application as a whole. We model a user's advantage for a given application with the user's decisions $d_1; \dots; d_m$ on each individual permission $p_1; \dots; p_m$ using Function 1 $D : \text{Users} \times \text{Applications} \rightarrow \mathcal{D}^P$. Function 1 represents a user's overall decision on a certain application via the set of decisions made on each individually requested permission. That is, a user u_i makes a decision d_i on an application a_k with respect

to an individual permission. For each permission p_j , there exists a matrix C_{pj} representing user decisions on p_j for each application a_k . A matrix entry d_{ik} with a value of 1 denotes a user has granted a_k the permission p_j , whereas a 0 denotes a deny. Entries with "what" values denote the user is still to make a decision on permission p_j for application a_k . Our model provides recommendations to users that guide them in making these future decisions. Applications that are handled properly in our implementation and do not request a permission p_j have an empty entry in C_{pj} . For example, let $p_1 = \text{birthday}$, $p_2 = \text{e-mail}$, and $p_3 = \text{location}$, where each represents a single criterion within a three-criteria model. Let $u_1 = \text{Alice}$ who installed application a_1 that requests access to the permissions e-mail, birthday, and location. Alice has granted a_1 the permissions birthday and location ($d_{11} = \text{grant}$; $d_{31} = \text{grant}$), whereas denied e-mail ($d_{21} = \text{deny}$). Alice has yet to make a decision on a_2 , i.e., a single decision on each requested permission p_j : birthday; e-mail; location. Our proposed model utilizes the set of decisions for each C_{pj} , hence providing a recommendation that fits each criterion [29]

. Our overall collaborative model. The model utilizes them in building the multicriteria matrices C for each permission and relies on decisions made by the community users. By utilizing the C matrices, we generate two probability matrices, GA and GU . GA is app based, whereas GU is user based. GA captures the probability of a certain application being granted a certain permission, whereas GU captures the probability of a certain user granting a certain permission. An example GA matrix, with a set of applications (a_1, a_2, a_3, a_4, a_5), permissions (birthday, e-mail, location, sms, photos) and their corresponding GA_{ij} values. For example, $GA_{\text{location}; a_2} = 0.15$, denotes a low probability of the permission location being granted to application a_2 by users who installed a_2 . Our proposed collaborative model adopts an user-based and item-based collaborative filtering process. In our model, we refer to application-based filtering as item-based filtering (here items are applications). Application-based filtering utilizes the app-based probabilities of GA . whereas User-based filtering utilizes the user-based probability values of GU .

VII. MODULES

A. User Registration

To access the third party applications and access the account, the user needs to register with the server. For this reason, we've implemented this module. First the user have to create an account with the server by providing the username, password, mobile number, date of birth, access privileges to view their account and other details. All the information provided by the user will be stored in the server's database for future purpose.

B. Server

The Server is the module in which the entire user's information will be stored and the all the access information and what are the application they are accessing by the user and update will stored. Also the it will allow the third party application in their site. The server will prevent unauthorized users entering into the site.

C. Permission Guide

Once the user successfully register with the server, the will send a request email regarding the third party applications. If the user willing to install and access those applications, the user will send the response to the server with the access privileges [32]. The third party applications are not allowed access beyond their access privileges.

D. Authentication Server

If the user provides the permission to access the third party application, the authentication server will generate an SMS alert send to third party application. This helps to

identify the exact third party application. So that the concerned administrator of the third party application will enter the one time password that was send to their mobile.

E. Access The Application

Once the third party application's administrator enter the authentication key, the user can access the application. So that in overall, we can provide the security while accessing the account and the application. This provides the user more trust worthiness and reliability.

VIII.CONCLUSION AND FUTURE WORK

Usable privacy configuration tools are essential in providing the protecting their data from third-party applications and user privacy in social networks. We proposed an implemented a browser extension that integrates into the existing OAuth flow, an extension to the authorization code flow of OAuth 2.0 and, and allows users to easily configure their privacy settings for applications at installation time. We also proposed in a different multicriteria recommendation model which adopts three collaborative filtering techniques: user-based, app-based, and category-based, each incorporating the previous decisions of an individual user and decisions of the community. Our browser extension provides users with recommendations on permissions requested by applications was based on this model, . We successfully demonstrate that our extension, linked with our multicriteria recommendation model leads to the preservation of immutable private identity attributes, irrevocable and the preventing of their uninformed disclosure during application installation. Individually, when given the choice are more likely to deny the requested permission, among popularly requested permissions. We found them to be more willing to grant permissions to third-party applications than those who were provided with recommendations and we demonstrate the effectiveness of the recommendations through a causal group of users who were not shown any recommendations. In the future, we will investigate an address possible application misconfigurations due to insufficient permissions and application permission evolution over time. We also plan on investigating hybrid and probabilistic collaborative filtering systems for providing better predictions in cases of sparse user decision data [33]. we would like to investigate the merits of our approach on other platforms, e.g., mobile platforms. Additionally, We'd also like to investigate the benefits of providing additional information (e.g., population age distribution) to users when making their privacy decisions.

REFERENCES

- [1] A. Acquisti and R. Gross, "*Imagined Communities: Awareness, Information Sharing, and Privacy on the Facebook,*" Proc. Int Workshop Privacy Enhancing Technologies, pp. 36-58, 2006.
- [2] G. Adomavicius and Y. Kwon, "*Multi-Criteria Recommender Systems,*" Recommender Systems Handbook: A Complete Guide for Research Scientists and Practitioners, Springer, 2010.
- [3] G.-J. Ahn, M. Ko, and M. Shehab, "*Privacy-Enhanced User-Centric Identity Management,*" Proc. IEEE Intl Conf. Comm. (ICC), pp. 1-5, 2009.
- [4] A. Besmer, J. Watson, and H.R. Lipford, "*The Impact of Social Navigation on Privacy Policy Configuration,*" Proc. Sixth Symp. Usable Privacy and Security (SOUPS '10), July 2010.
- [5] W. Bin, H.H. Yuan, L.X. Xi, and X.J. Min, "*Open Identity Management Framework for Saas Ecosystem,*" Proc. IEEE Intl Conf. e-Business Eng. (ICEBE '09), pp. 512- 517, 2009.
- [6] D. Carrie and E. Gates, "*Access Control Requirements for Web 2.0 Security and Privacy,*" Proc. Workshop Web 2.0 Security & Privacy (W2SP '07), 2007.
- [7] S. Chen and M.-A. Williams, "*Towards a Comprehensive Requirements Architecture for Privacy-Aware Social Recommender Systems,*" APCCM '10: Proc. Seventh Asia-Pacific Conf. Conceptual Modelling, pp. 33-42, 2010.
- [8] Facebook, Facebook Press Room, <http://www.facebook.com/press/info.php?statistics>, 2011.
- [9] L. Fang and K. LeFevre, "*Privacy Wizards for Social Networking Sites,*" Proc. Int'l Conf. World Wide Web (WWW), M. Rappa, P. Jones, J. Freire, and S. Chakrabarti, ed., pp. 351-360, 2010.

RAIN STREAKS DETECTION AND REMOVAL FROM COLOR - IMAGE VIDEO USING SPARSE REPRESENTATION

S.K .Adithya kasi swamynathan,A.Thiruvengadam,P.Meena³

¹ IV YR /CSE,St.Anne's College of Engineering and Technology, aadihotsun@gmail.com

² IV YR /CSE,St.Anne's College of Engineering and Technology, aadihotsun@gmail.com

³ AP/CSE,St.Anne's College of Engineering and Technology,meenasarathy.08@gmail.com

Abstract-Rain streaks detection and removal from color image -video is a challenging problem. The rain streak removal is considered as image denoising task. In color image –video based rain streaks removal, where the dictionary learning process can be only applied once for the first frame in a video clip of the same scene. The dictionary learning can be also used for removal of rain streaks for the succeeding frames in the clip, which is useful to both reduce the computational complexity and maintain the temporal consistency of the video. The proposed Color image - video based rain streaks removal framework based on the sparse representation. Then the high frequency part was decomposed into rain and non-rain component by using the learning sparse representation based dictionaries. To separate a rain streaks from high frequency part using the multi set feature. The multi set feature, including HOG (Histogram Oriented Gradients), DOF (Depth of Field), and eigen color. The high frequency part and multi set features is applied to remove the most rain streaks. The DOF feature is used to help to identify the main subjects to preserve in a rain image. The rain streaks are usually neutral color, where the eigen color feature is used to analyse the key features of the rain streaks. The both DOF and Eigen color features are used to identify and separate the non rain component from the misidentified rain component of an image. Our Proposed framework may be also integrated with any sparse representation–based super-resolution framework to achieve super-resolution of a low quality video and noisy image video. Rain removal is a very useful and important technique in applications such as security surveillance, audio/video editing and investigations.

keywords-Color image rain removal, depth of field (DoF), dictionary learning, Eigen color, histogram of oriented gradients (HoG), image decomposition, rain removal, sparse representation.

1. INTRODUCTION

Different weather conditions such as rain, snow, haze, or fog will cause complex visual effects of spatial or temporal domains in images or videos [1]–[16]. Removal of rain streaks from videos has recently received much attention [1]–[8]. A pioneering work on detecting and removing rain streaks in a video was proposed in [4], developed a correlation model capturing the dynamics of rain and a physics-based motion blur model characterizing the photometry of rain. It was subsequently shown in [5] that some camera parameters, such as exposure time and depth of field (DoF) can be selected to mitigate the effects of rain without altering the appearance of the scene. Moreover, an improved video rain streak removal algorithm incorporating both temporal and chromatic properties was proposed in [7]. In addition, some research works [9], [10] focus on raindrop detection in images or videos (usually on car windshields), which are different from the detection of rain streaks.

II. SINGLE-IMAGE-BASED RAIN STREAKS REMOVAL

Recently, a few research works have focused on the more challenging task, that is, color-video-based rain streaks removal [12]–[14] based on the real requirement that only a single image is available, such as an image captured from a digital camera/camera-phone or downloaded from the Internet. In [12], a pioneering work on color-video-based rain removal was proposed, which approaches the rain removal task as the image decomposition problem based on sparse representation. In [12], a rain image was first separated into low- and high-frequency parts via bilateral filtering [17]. The high-frequency part was then decomposed into the rain component and nonrain component by learning the two associated sparse representation- in an image, some portions of the nonrain component with similar gradient directions to the rain component might be also simultaneously removed. Moreover, in [13], a rain image was also first separated into low- and high-frequency parts. The low-frequency part is then modified as a guidance image and the high-frequency part is treated as an input image of the guided filter, so that a nonrain component of the high-frequency part can be obtained. In addition, as the rain streaks usually reveal similar and repeated patterns on an imaging scene [14], a low-rank appearance model for removing rain streaks was proposed to capture the spatio-temporally correlated rain streaks. With the appearance model, rain streaks can be removed from a single image or video in a unified way. based dictionaries for representing rain and nonrain components, respectively. Since rain streaks usually have similar edge directions or gradients in an image, the rain dictionary is thus identified by calculating the variance of gradient direction for each dictionary atom. Nevertheless, based on this assumption, the main weakness of [12] is that in an image, some portions of the nonrain component with similar gradient directions to the rain component might be also simultaneously removed.

III. PROPOSED METHOD

In this paper, we propose a color-video-based rain removal framework by formulating rain removal as an image decomposition problem based on sparse representation [20]–[22]. In our framework, an input color image is first decomposed into low- and high-frequency parts by using the guided image filter [19] so that the rain streaks would be in the high-frequency part with nonrain textures/edges, and the high-frequency part is then decomposed into a rain component and a nonrain component by performing dictionary learning and sparse coding. To separate rain streaks from the high-frequency part, a hybrid feature set, including histogram of oriented gradients (HoGs) [23], depth of field (DoF), and Eigen color, is employed to further decompose the high-frequency part. With the hybrid feature set applied, most rain streaks can be removed, while the nonrain component can be enhanced. The main novelties and contributions of this paper include the following: 1) To the best of our knowledge, we are among the first to exploit the property of photography to facilitate the single-color-image-based rain removal task, where the DoF, is calculated as a feature for a rain image. Because the rain streaks in an image are usually more blurred than the focused subject(s), their visual effect is relatively weak and likely appears as fog. Therefore, properly employing the DoF feature is helpful for identifying the main subjects to be preserved in a rain image. 2) Based on our observation, in a rain image, the rain streaks usually reveal neutral color in analyzing the atoms of rain in our method. Hence, in our paper, color information is also a key feature to be employed for rain removal, where the Eigen color feature is used. 3) Similar to [12], our method is also fully automatic and self-contained, where no extra training samples are required in the dictionary learning stage. In addition, the

usage of the DoF feature mainly contributes to the rain removal task in threefold: 1) it facilitates to enhance the low-frequency part of an image; 2) it facilitates to enhance the qualities of the learned dictionary atoms for the highfrequency part of an image; and 3) it facilitates to recover some nonrain information with similar orientations to the rain streaks, from the roughly reconstructed rain component.

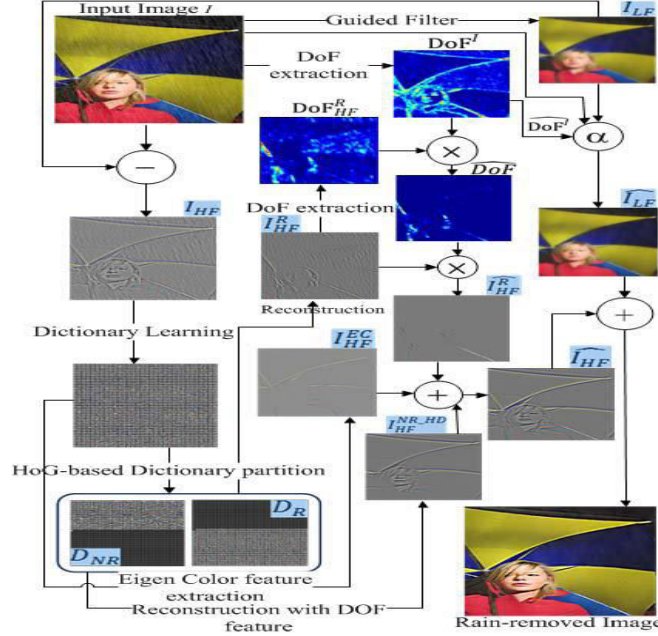


Fig 1. Block Diagram

IV. EXTRACTION OF DOF

A professional photographer usually makes the subject(s) of a photo clear and the background or the other unfocused scenes/objects in the photo blurred, such as rain streaks. Therefore, the visual effect of rain streaks in an image would be relatively weak and the rain streaks may even appear as fog. As a result, we propose to employ the feature, named DoF for extracting the region of interest (ROI) in a rain image to improve the performance of rain removal, and simultaneously enhancing the perceived visual quality of rain-removed images. DoF is defined as the distance between the nearest and farthest objects in a scene that appears acceptably sharp in an image. A shallow DoF is often used to emphasize the ROI in an image. In our method, DoF is used to measure local correlative information in an image. With the DoF of an image can be calculated as follows. Let I an input image and f_{κ} the uniform blurring kernel of size $\kappa \times \kappa$ ($\kappa = \{3, 5, 7\}$ in our experiments). The blurring kernels are first applied on the luminance component of I and the vertical and horizontal derivatives are then calculated, respectively, by

$$\rho_{x\kappa} \propto \text{hist}(I * f_{\kappa} * dx) \quad (1)$$

$$\rho_{y\kappa} \propto \text{hist}(I * f_{\kappa} * dy) \quad (2)$$

$$D(i, j) = \sum_{(n,m) \in W_{i,j}} \text{KL}(\rho_{x\kappa} | \rho_{x1})(n,m) + \text{KL}(\rho_{y\kappa} | \rho_{y1})(n,m) \quad (3)$$

V. RAIN STREAKS REMOVAL USING MULTI SET FEATURES

Fig. 1 shows the proposed framework of visual depth guided rain streak removal, in which rain streak removal is formulated as an image decomposition problem via sparse representation. In our method, an input rain image I is first roughly decomposed into the low-frequency (LF) part I_{LF} and the high-frequency (HF) part I_{HF} using the guidedfilter [19]. The HF part (I_{HF}) can then be further roughly decomposed into the rain component I_{RHF} and the nonrain (geometric) component I_{NR_HDHF} via image decomposition. In the decomposition of the HF part, the learned dictionary D_{HF} for the HF part is separated into the two subdictionaries, D_{NR} and D_R , respectively, where $D_{HF} = [D_{NR} | D_R]$, via the HoG feature-based dictionary atom clustering [12]. Then to refine I_{RHF} by extracting misclassified nonrain region from I_{RHF} , DoF_{RHF} (the DoF saliency map of I_{RHF}) is first multiplied by DoF_I (the DoF saliency map of the input image I) to obtain $_DoF$ (the DoF saliency map of the nonrain region extracted from I_{RHF}). I_{RHF} is then refined by being multiplied by $_DoF$ to obtain $_I_{RHF}$ (the nonrain region extracted from I_{RHF}).

VI. RAIN REMOVAL AND RESTORATION OF NONRAIN COMPONENT

In this section, we describe the details about how to identify which subdictionary (cluster) consists of rain atoms and which one consists of nonrain atoms. Then, we present the procedures about rain removal and restoration of nonrain component, respectively, based on the rain dictionary D_R using the DoF feature and the dictionary D_{HF} using the Eigen color feature.

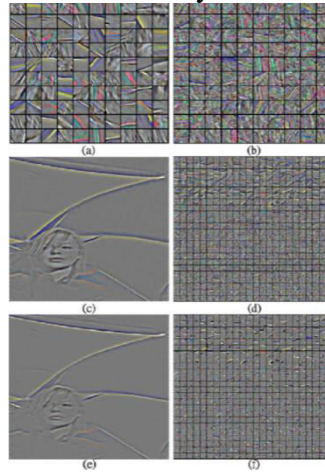


Figure 2. Further restoration of the nonrain component.

(a) Original rain component I_{RHF} . (b) Nonrain information out of focus remained in I_{RHF} with similar orientations to rain streaks obtained by $I_{RHF} = I_{RHF} \times _DoD$. (c) Original nonrain component I_{NR_HDHF} . (d) Further enhanced nonrain component obtained by $I_{RHF} + I_{NR_HDHF}$.

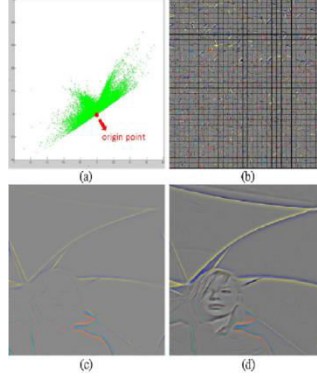


Figure 3. Further restoration of the nonrain component based on the Eigen color feature.

(a) Eigen color in 2-D space for DHF . (b) Dictionary DHF with rain atoms masked out by the Eigen color feature. (c) Nonrain component IEC_{HF} reconstructed with respect to (b). (d) Enhanced nonrain component obtained by $IHF = INR_{HDHF} + IEC_{HF} + IRHF$.

VII. EXPERIMENTAL RESULTS

To evaluate the performance of the proposed Color video-based rain removal framework, the proposed method is implemented in MATLAB on a personal computer equipped with Intel Core E5200 2.5G processor and 2 GB memory. The parameter settings of the proposed method are described as follows. The implementation of the Guided image filter is provided by [19].

VIII. CONCLUSION

In this paper, we have proposed a color video based rain streaks removal framework by properly formulating rain removal as an image decomposition problem based on sparse representation. where the dictionary learning process may be only applied once for the first frame in a video clip of the same scene. The learned dictionary can be also used for removal of rain streaks for the succeeding frames in the clip, which is useful to both reduce the computational complexity and maintain the temporal consistency of the video. In addition, the proposed framework may be also extended to remove other structural patterns in an image/video. In our method, an input color rain image is first decomposed into LF part and HF part by using the guided image filter. The HF part is then decomposed into a rain component and a nonrain component by performing dictionary learning and sparse coding. To separate rain streaks from the HF part, a hybrid feature set, including HoG, DoF, and Eigen color, is employed to further decompose the HF part. With the hybrid feature set applied, most rain streaks can be removed, while nonrain component can be enhanced. Our experimental results have shown that the proposed method achieves better or comparable performance with the state-of-the-art color video based rain removal and denoising algorithms.

REFERENCES

- [1] P. C. Barnum, S. Narasimhan, and T. Kanade, "Analysis of rain and snow in frequency space," *Int. J. Comput. Vis.*, vol. 86, nos. 2–3, pp. 256–274, 2010.
- [2] J. Bossu, N. Hautière, and J. P. Tarel, "Rain or snow detection in image sequences through use of a histogram of orientation of streaks," *Int. J. Comput. Vis.*, vol. 93, no. 3, pp. 348–367, Jul. 2011. [3] K. Garg and S. K. Nayar, "Vision and rain," *Int. J. Comput. Vis.*, vol. 75, no. 1, pp. 3–27, 2007.
- [4] K. Garg and S. K. Nayar, "Detection and removal of rain from videos," in *Proc. IEEE Conf. Comput. Vis. Pattern Recognit.*, vol. 1. Jun. 2004, pp. 528–535.
- [5] K. Garg and S. K. Nayar, "When does a camera see rain?" in *Proc. IEEE Int. Conf. Comput. Vis.*, vol. 2. Oct. 2005, pp. 1067–1074.
- [6] K. Garg and S. K. Nayar, "Photorealistic rendering of rain streaks," *ACM Trans. Graph.*, vol. 25, no. 3, pp. 996–1002, Jul. 2006.
- [7] X. Zhang, H. Li, Y. Qi, W. K. Leow, and T. K. Ng, "Rain removal in video by combining temporal and chromatic properties," in *Proc. IEEE Int. Conf. Multimedia Expo*, Toronto, ON, Canada, Jul. 2006, pp. 461–464.
- [8] N. Brewer and N. Liu, "Using the shape characteristics of rain to identify and remove rain from video," in *Proc. Struct., Syntactic, Statist. Pattern Recognit.*, vol. 5342. 2008, pp. 451–458.
- [9] M. Roser and A. Geiger, "Video-based raindrop detection for improved image registration," in *Proc. IEEE Int. Conf. Comput. Vis. Workshops*, Kyoto, Japan, Sep. 2009, pp. 570–577.
- [10] J. C. Halimeh and M. Roser, "Raindrop detection on car windshields using geometric-photometric environment construction and intensitybased correlation," in *Proc. IEEE Intell. Veh. Symp.*, Xi'an, China, Jun. 2009, pp. 610–615.
- [11] M. S. Shehata et al., "Video-based automatic incident detection for smart roads: The outdoor environmental challenges regarding false alarms," *IEEE Trans. Intell. Transp. Syst.*, vol. 9, no. 2, pp. 349–360, Jun. 2008.
- [12] L.-W. Kang, C.-W. Lin, and Y.-H. Fu, "Automatic single-image-based rain streaks removal via image decomposition," *IEEE Trans. Image Process.*, vol. 21, no. 4, pp. 1742–1755, Apr. 2012.
- [13] X. Zheng, Y. Liao, W. Guo, X. Fu, and X. Ding, "Single-image-based rain and snow removal using multi-guided filter," in *Proc. Neural Inf. Process.*, vol. 8228. Nov. 2013, pp. 25–265.
- [14] Y.-L. Chen and C.-T. Hsu, "A generalized low-rank appearance model for spatio-temporally correlated rain streaks," in *Proc. IEEE Int. Conf. Comput. Vis.*, Sydney, Australia, Dec. 2013, pp. 1968–1975.
- [15] K. He, J. Sun, and X. Tang, "Single image haze removal using dark channel prior," *IEEE Trans. Pattern Anal. Mach. Intell.*, vol. 33, no. 12, pp. 2341–2353, Dec. 2011.
- [16] C.-H. Yeh, L.-W. Kang, M.-S. Lee, and C.-Y. Lin, "Haze effect removal from image via haze density estimation in optical model," *Opt. Exp.*, vol. 21, no. 22, pp. 27127–27141, Nov. 2013.
- [17] C. Tomasi and R. Manduchi, "Bilateral filtering for gray and color images," in *Proc. IEEE Int. Conf. Comput. Vis.*, Bombay, India, Jan. 1998, pp. 839–846.
- [18] D.-A. Huang, L.-W. Kang, Y.-C. F. Wang, and C.-W. Lin, "Self-learning based image decomposition with applications to single image denoising," *IEEE Trans. Multimedia*, vol. 16, no. 1, pp. 83–93, Jan. 2014.
- [19] K. He, J. Sun, and X. Tang, "Guided image filtering," *IEEE Trans. Pattern Anal. Mach. Intell.*, vol. 35, no. 6, pp. 1397–1409, Jun. 2013.
- [20] J. M. Fadili, J. L. Starck, J. Bobin, and Y. Moudden, "Image decomposition and separation using sparse representations: An overview," *Proc. IEEE*, vol. 98, no. 6, pp. 983–994, Jun. 2010.
- [21] J. M. Fadili, J. L. Starck, M. Elad, and D. L. Donoho, "MCALab: Reproducible research in signal and image decomposition and inpainting," *IEEE Comput. Sci. Eng.*, vol. 12, no. 1, pp. 44–63, Feb. 2010.
- [22] J. L. Starck, M. Elad, and D. L. Donoho, "Image decomposition via the combination of sparse representations and a variational approach," *IEEE Trans. Image Process.*, vol. 14, no. 10, pp. 1570–1582, Oct. 2005.
- [23] N. Dalal and B. Triggs, "Histograms of oriented gradients for human detection," in *Proc. IEEE Conf. Comput. Vis. Pattern Recognit.*, vol. 1. San Diego, CA, USA, Jun. 2005, pp. 886–893.

GSM Based Automatic Emergency Detection and Alerting System using Sensors

G. Jona Nicy Parvatham¹, M. Vaidehi²

¹ Student, Department of ECE, St. Anne's CET, cindrellaamul@gmail.com

² Faculty, Department of ECE, St. Anne's CET, vaidehi.divakaran@gmail.com

Abstract: Safety plays a major role in today's world and it is necessary that good safety systems are to be implemented in places of education and work. This work modifies the existing safety model installed in industries and this system also be used in homes and offices. The main objective of the work is designing microcontroller based toxic gas detecting and alerting system. The hazardous gases like LPG and propane were sensed and displayed each and every second in the LCD display. If these gases exceed the normal level then an alarm is generated immediately and also an alert message (SMS) is sent to the authorized person through the GSM. Also the authorized person Can automatically turn off the gas cylinder using mobile phones. Additionally with this paper we also detecting the theft inside home and giving information to the police station automatically. The advantage of this automated detection and alerting system over the manual method is that it offers quick response time and accurate detection of an emergency and in turn leading faster diffusion of the critical situation.

Keywords- Air pollution Monitoring, gas sensors, GSM module, wireless networks.

I INTRODUCTION

The increase in the development of technology and the human race, we failed to take care about the surroundings in which we live in. Thus we polluted the environment and thereby reducing the quality of the place we live. Even though there are several aspects of pollution such as soil, air and water pollution, out of these air pollution acts as the serious aspect as the other can detected visually and by taste, but the polluted air cannot be detected as it can be odorless, tasteless and colorless. Hence there is a growing demand for the environmental pollution monitoring and control systems.

In the view of the ever-increasing pollution sources with toxic chemicals, these systems should have the facilities to detect and quantify the sources rapidly. Toxic gases are one that causes serious health impacts, but are also used in industries in large quantities. These gases have to be monitored; such that increase in the normal level of them could be known and proper precaution measures can be taken. But the current systems available are not so portable and are costly and difficult to implement. So an embedded system is designed using PIC 16F877 Microcontroller, for the purpose of detection of hazardous gas leakage, which in turn avoids the endangering of human lives.

The hazardous gases like LPG and propane were considered here. If these hazardous gases level exceeds normal level that is LPG>1000ppm or Propane>10000ppm then an alarm is generated immediately, and a SMS is sent to the authorized user as an alert message, which leads to faster diffusion of emergency situation. The system is affordable and can be easily implement

in the chemical industries and in residential area which is surrounded by the chemical industries or plants, to avoid endangering of human lives. The system also supports to provide real-time monitoring of concentration of the gases which presents in the air. As this method is automatic the information can be given in time such that the endangering of human lives can be avoided.

II RELATED WORK

In the year of 2008, LIU zhen-ya, WANG Zhen-dong and CHEN Rong, “Intelligent Residential Security Alarm and Remote Control System Based On Single Chip Computer”, the paper focuses on, Intelligent residential burglar alarm, emergency alarm, fire alarm, toxic gas leakageremote automatic sound alarm and remote control system, which is based on 89c51 single chipcomputer. The system can perform an automatic alarm, which calls the police hotline numberautomatically. It can also be a voice alarm and shows alarm occurred address. This intelligentsecurity system can be used control the electrical power remotely through telephone [8].In the year of 2008, Chen Peijiang and Jiang Xuehua, “Design and implementation of RemoteMonitoring System Based on GSM”, this paper focuses on the wireless monitoring system,because the wireless remote monitoring system has more and more application, a remotemonitoring system based on SMS through GSM. Based on the overall architecture of thesystem, the hardware and software architecture of the system is designed. In this system, theremote signal is transmitted through GSM network. The system includes two parts which are the monitoring centre and the remote monitoring station. The monitoring centre consists of a computer and a TC35 communication module for GSM. The computer and the TC35 are connected by RS232. The remote monitoring station consist of a TC35 communication modulefor GSM, a MSP430F149 MCU, a display unit, sensors and a data gathering and processingunit. The software for the monitoring center and the remote monitoring station were designedusing VB [7].In the year of 2006, IoanLita, Ion BogdanCioc and Daniel AlexandruVisan, “A New Approach of Automatic Localization System Using GPS and GSM/GPRS Transmission”, thispaper focuses on, a low cost automotive localization system using GPS and GSM-SMSServices, which provides the position of the vehicle on the driver’s or owner’s mobile phone asa short message (SMS) on his request. The system can be interconnected with the car alarmsystem which alerts the owner, on his mobile phone, about the events that occurs with his carwhen it is parked. The system is composed by a GPS receiver, a microcontroller and a GSMphone. In additional the system can be settled for acquiring and transmitting the information,whenever requested about automobile status and alerts the user about the vehicle started engine.The system can be used as a low cost solution for automobile position localizing as well as incar tracking system application [16].In the year of 2002, K. Galatsis, W. Wlodarsla, K. Kalantar-Zadeh and A. Trinchi,“Investigation of gas sensors for vehicle cabin air quality monitoring”, this paper focuses on,car cabin air quality monitoring can be effectively analyzed using metal oxide semiconducting(MOS) gas sensors. In this paper, commercially available gas sensors are compared withfabricated Moo3 based sensors possessed comparable gas sensing properties. The sensor hasresponse 74% higher relative to the hest commercial sensor tested [21]. In the year 2000, K.Galatsis, W. Woldarsla, Y.X. Li and K. Kalantar-zadeh, “A Vehicle air quality monitor usinggas sensors for improved safety”, this paper focuses on A vehicle cabin air quality monitor using carbon monoxide (CO) and oxygen (O₂) gas sensors has been designed, developed andon-road tested. The continuous monitoring of oxygen and carbon monoxide provides addedvehicle safety as alarms could be set off when dangerous

gas concentrations are reached, preventing driver fatigue, drowsiness, and exhaust gas suicides. CO concentrations of 30ppm and oxygen levels lower than 19.5% were experienced whilst driving [22].

III EMBEDDED AND REAL TIME SYSTEMS

Embedded system is a field in which the terminology is inconsistent. A real time system is one in which the correctness of the computations not only depends on the accuracy of the result, but also on the time when the result is produced. This implies that a late is a wrong answer. A hard real time system should always respond to an event within the deadline or else the system fails and endangers human lives but in soft real time system, failing to meet the deadline produces false output and does not endanger the human lives. All embedded systems or not real time systems and vice versa. And our designed embedded system is a soft real time system.

3.1 Features of Embedded Systems

- Multiple operations can be performed using single chip
- Fully automatic.
- Compact and Faster

3.2 Components of Embedded System

- Hardware specifically built for that application
- An embedded operating system
- User interface like push buttons, LCD, numeric displays
- Stepper motor

The major part of this project is the hardware model consisting of sufficient sensor with embedded system. Embedded systems are computer in the widest sense. Based on functionality and performance requirements, embedded systems can be categorized as, Stand-alone system, Real time system, Networked information appliances and Mobile devices. Every embedded system consists of custom-built hardware built around a central processing unit (CPU). This hardware also contains memory chips onto which the software is loaded. The software residing on the memory chip is also called as the firmware.

3.3 Air Quality (AQ):

Air quality is defined as a measure of the condition of air relative to the requirements of one or more biotic species and/or to any human need or purpose.[1] Air quality indices (AQI) are numbers used by government agencies to characterize the quality of the air at a given location. As the AQI increases, an increasingly large percentage of the population is likely to experience increasingly severe adverse health effects. To compute the AQI requires an air pollutant concentration from a monitor or model. The function used to convert from air pollutant concentration to AQI varies by pollutant, and is different in different countries. Air quality index values are divided into ranges, and each range is assigned a descriptor and color code. Standardized public health advisories are associated with each AQI range. An agency

might also encourage members of the public to take public transportation or work from home when AQI levels are high.

3.4 Limitations of the AQI:

Most air contaminants do not have an associated AQI. Many countries monitor ground-level ozone, particulates, sulfur dioxide, carbon monoxide and nitrogen dioxide and calculate air quality indices for these pollutants. The AQI can worsen (go up) due to lack of dilution of air emissions by fresh air. Stagnant air, often caused by an anticyclone or temperature inversion or lack of wind lets air pollution remain in a local area.



Figure: 2 Thick haze and smoke over Ganga basin

3.5 Environmental Issues in India:

The rapid growing population and economic development is leading to a number of environmental issues in India because of the uncontrolled growth of urbanization and industrialization, expansion and massive intensification of agriculture, and the destruction of forests. Major environmental issues are forest and agricultural degradation of land, resource depletion (water, mineral, forest, sand, rocks etc.), environmental degradation, public health, loss of biodiversity, loss of resilience in ecosystems, livelihood security for the poor. Road dust due to vehicles also contributes up to 33% of air pollution. In cities like Bangalore, around 50% of children suffers from asthma and also it causes a significant risk factor for multiple health conditions including respiratory infections, heart disease, and lung cancer, according to the WHO. One of the biggest causes of air pollution in India is from the transport system. Hundreds of millions of old diesel engines are continuously burning away diesel which has the range between 150 to 190 times the amounts of sulphur than the European diesel has.

3.6 Necessity of AQ measurement:

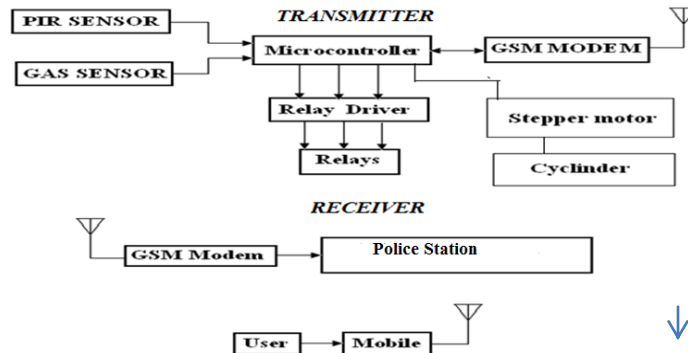
Air pollution levels has been monitored for over 100 years, however, it has really only been in the last 25 years that the technology has been available to measure air pollution on a real-time basis. There are several important reasons to measure air pollution are,

- Ensuring the long-term goals and targets to reduce levels of air pollution.
- Providing information to the general public about the air quality of their locality.

There are many ways of calculating the levels of air quality in an area - this can be done by estimating the rates of emissions from sources such as cars, housing estates and factories etc. However, in order to verify these calculations and get up-to-the-minute information on air quality, it is essential to measure air quality with sophisticated instrumentation and such a system is designed here.

IV HARDWARE SYSTEM DESIGN

4.1 Block Diagram of the Proposed System



The gas levels are sensed through the respective gas sensors (here MQ-2 and MQ-7 are used for sensing LPG and propane respectively for demonstration purpose) and sent to the PIC micro controller. The sensed analog signals are converted to digital through ADC (inbuilt in case of PIC). The sensed gas levels are displayed in the LCD; if any one gas level exceeds the set point then an alarm is generated immediately. At the same time an alert message is sent as SMS to the authorized user through the GSM modem. The block diagram of the proposed system is shown in figure 3.

4.2 Gas Sensor:

Normally a gas sensor is the one which is made up of transducer that senses the gas molecules. It sends electrical signals as the output which is proportional to the gas concentration. The gas sensors do not sense a particular gas, thus they must tend to employ analytical techniques to adopt to identify a particular gas. However these analytical methods suffer from many disadvantages of skilled operator, specially designed PC's and slow response time etc., and the proposed system does not suffer such disadvantages. The proposed system is an automated one, but it requires resetting after every critical situation.

4.3 LPG Sensor:

It is an ideal sensor to detect the presence of a dangerous LPG leak in our home or in a service station, storage tank environment and even in vehicle which uses LPG gas as its fuel. This unit can be easily incorporated into an alarm circuit/unit, to sound an alarm or provide a visual indication of the LPG concentration. The sensor has excellent sensitivity combined with a quick response time. When the target combustible gas exists, the sensor's conductivity is higher along with the gas concentration rising.



Figure: 4 LPG gas sensors

A simple electronic circuit is used to convert change of conductivity to its corresponding output signal of gas concentration. MQ-6 gas sensor shown in figure 4 is used to sense the poisonous gas and has high sensitivity to LPG, and also response to Natural gas. It is a portable gas detector which has long life with low cost. The specification of the LPG gas sensor is shown in the table 1

4.4 Combustible Gas sensor:

Sensitive material of MQ-2 gas sensor is SnO₂, with lower conductivity in clean air. When the target combustible gases exist, the sensor's conductivity is higher along the gas concentration increasing. A simple electronic circuit is used to convert the change of conductivity to its corresponding output signal of gas concentration. MQ-2 gas sensor is shown in figure 5, which has sensitivity to propane, butane and also to natural gas especially Methane.

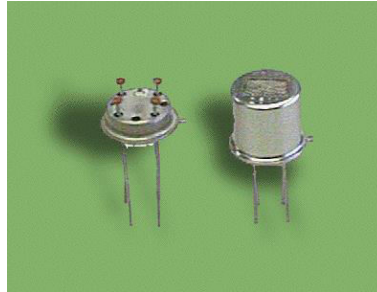


Figure: 5 Combustible gas sensors

V SOFTWARE DESCRIPTION

5.1 Software Development

Application development on desktop computers is called native development as development and executions are done on the same hardware platform. Embedded software cannot be developed directly on the embedded system. Embedded software development is done in two stages. Initially, the software is developed on a desktop computer or a workstation. This is called the host system. Subsequently, the software is transferred to the actual embedded hardware called the target system. The host and the target system can be connected through a serial interface such as RS232 or through Ethernet. The processors of the host and the target system are generally different. Hence, this development is known as cross-platform development. The embedded software can be transferred to the target system by programming an EEPROM or Flash memory using a programmer, or downloading through a communication interface or JTAG port. There are several different ways of writing code for embedded systems depending on the complexity of the system and the amount of time and the money that can be spent. Many ready built designs provide libraries and additional software

support which dramatically cut the development time. Fig 8 shows the software cross-platform development.

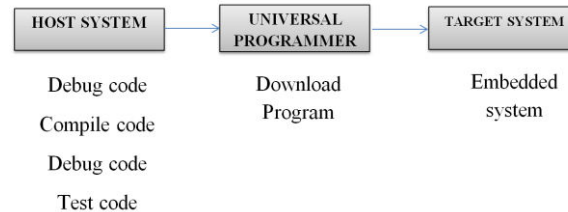


Figure: 8 Software Developments

5.2 Programming the PIC:

- Step 1: Click the Start Menu and select the MPLAB IDE from the program Menu and a window will be opened.
- Step 2: Click Project_ new project (a window will be opened)
- Step 3: Enter the PROJECT NAME, PROJECT DIRECTORY where the program to be stored in the corresponding fields and clicks ok.
- Step 4: Click Configure_ Select device (a window will be opened)
- Step 5: Select the device name as PIC16f877 and click ok
- Step 6: Click project_ set language tool locations
- Step 7: Expand CCS C compiler for PIC12/14/16/18 in line displayed window. Further expand the executable and select the CCS C compiler (CCSC.exe) and click ok.
- Step 8: Click Project_ set language suits
- Step 9: Select CCS C compiler for PIC12/14/16/18 in the active tool suite and click ok
- Step 10: Click file_ new file. Now type the corresponding program and save it as <filename.c> in the corresponding location where the project name is denoted.
- Step 11: Click project_ add file to the project
(Select the saved file and click open)
- Step 12: Click project_ build option_ project (a window will be opened)
- Step 13: Select CCS C compiler in the window, click none in the debug option, tick the use alternate settings and enter +p in the space provided and click ok.
- Step 14: Click Project_ build all the CCS compiler will denote the result if any errors indicated, go to step 10 else continue.
- Step 15: Click Start menu and select the PIC ISP from the program menu and a window will be opened.

5.3 Cross Compilation:

A compiler is mainly to translate program written in some human readable language into an equivalent set of opcodes for a particular processor. Each processor has its own unique machine language, and then we need to choose a compiler that is capable of producing programs for the specific target processor. In the embedded system, this compiler almost always runs on the host computer. It simply does not make sense to execute the compiler on the embedded system itself. A compiler that runs on one computer platform and produces code for another is called a cross compiler. The use of a cross compiler is one of the defining features of

embedded software development, and these tools support an impressive set of host-target combinations. Toll chain for building the embedded software is shown in fig 9.

VI IMPLEMENTATION:

The hazardous gases like LPG and combustible gas were sensed by the MQ-2 and MQ-6 sensors respectively and are monitored by the PIC microcontroller and displayed in the LCD. In critical situation that is when the LPG exceeds from normal level above 1000ppm and in the same way when the Propane exceeds the normal level of 10000ppm then an alarm is generated and a SMS is sent to the authorized user as an alerting system, which helps in faster diffusion of the critical situation. The prototype of the proposed is shown in the Fig 10.

VII CONCLUSION:

An embedded system for hazardous gas detection has been implemented; here only two gases (LPG and Propane) have been detected for demo purpose. The gas sensors and the critical level of the respective gas should be known, and then this system can be implemented for detecting various gases either in domestic area such as places of educational institutions, residential and industrial areas which avoids endangering of human lives. This system provides quick response rate and the diffusion of the critical situation can be made faster than the manual methods.



Figure: 10 Prototype of the proposed system

REFERENCES

- [1]. R. Al-Ali, Member, IEEE, Imran Zuolkernan, and Fadi Aloul, Senior Member, IEEE, "A Mobile GPRS-sensors array for Air Pollution Monitoring" vol.6, pp.410-422, Oct.2010.
- [2]. Nihal Kularatna, Senior Member, IEEE, and B. H. Sudantha, Member, IEEE "An Environment Air Pollution Monitoring System Based on the IEEE1451 Standard for Low Cost Requirements" IEEE Sensors J., Vol. 8, pp.415-422, Apr. 2008.
- [3]. M. Abu Jayyab, S. Al Ahdab, M. Taji, Z. Al Hamdani, F. Aloul, "Pollumap: Air Pollution mapper for cities", in Proc. IEEE Innovations in Information Technology Conf., Dubai, UAE, Nov.2006, pp.1-5.
- [4]. Y. J. Jung, Y. K. Lee, D. G. Lee, K. H. Ryu, and S. Nittel, "Air pollution monitoring system based on geosensor network", in Proc. IEEE Int. Geoscience Remote Sensing Symp., 2008, vol. 3, pp. 1370-1373.

Image Processing Techniques Examination of MRI Images of Rheumatoid Arthritis Through Morphological Image Processing Techniques

S.Chandiralekha¹, K.Dhivya²

¹*Computer science and Engineering, V.R.S college of Engineering and technology,
chandiralekha@gmail.com*

²*Computer science and Engineering, V.R.S college of Engineering and
technology,diyakanna4015@gmail.com*

Mr.F.Destonious Dhiraviuam, M.E.,

*Assistant Professor, Computer science and Engineering, V.R.S college of Engineering and
technology,premauit@gmail.com.*

Abstract—This paper is use of picture preparing procedures for recognizable proof of most regular infection i.e. Rheumatoid Arthritis (RA). Till date there is no demonstrated cure for the infection, consequently close observing of the sickness is vital in the medicinal treatment of this malady. In this paper Fingers and Knee pictures of the patient having RA have been broke down through Morphological Image preparing methods. This incorporates disintegration, widening, Perimeter determination and Skeletonization. The handled pictures discover their application in the field of Medical Science and can be valuable for specialists in distinguishing proof of illness stages from observing perspective.

Watchwords: Rheumatoid Arthritis (RA), Morphological Image preparing, disintegration, widening, Perimeter determination and Skeletonization.

I. PRESENTATION

Rheumatoid Arthritis (RA) is an infection, which is a typical, endless, systemic, auto invulnerable in flammatory sickness in nature that for the most part influences the joints of the body; fundamentally fingers, hands, knees and cause inability, untimely profound quality and perpetual sick wellbeing [1]. It targets synovial joints, in which there is an enormous collection of blood-borne cells, for example, T cells and macrophages. Veins are framed to backing this new tissue and the entire mass is known as a pannus dynamic disintegration to ligament and bone prompts inability in patients. RA influences around 0.5% – 1% of the populace (proportion of female to male patients is around 3:1).Mainly after the third year begin of the 75% of all patients get debilitated [2]. The future of a patient is diminished by 4 – 10 years. Till today there is no demonstrated cure for the sickness, henceforth close checking of the ailment is vital in therapeutic treatment of the illness. There are different strategies accessible for treatment of the +disease, among which Joint harm evaluation close by radiographs is the most as often as possible utilized strategy [2]. Furthermore, the delicate biomarkers of the sickness movement are being created, so that the execution of the applicant malady by the adjusting medications can be measured in a brief timeframe.

1.1 Signs and Symptoms Of Rheumatoid Arthritis (RA):

The early determination, and to assess the adequacy of the frequently and the costly harmful treatments MR is taken. In any case, on clinical foundation MR remains not entirely acknowledged [5] [6]. The real constraints experienced in right on time work were its extensive size of sensors, low determination, and the restricted force of PCs for the picture post handling [7]. The utilization and advancement of imaging biomarkers are currently turning out to be more basic and essential in the medication disclosure. The Drug organization (FDA) and US Food report "Advancement/Stagnation: Challenge and Opportunity on the Critical Path to New Medical Products" addresses the late lull in imaginative restorative treatments submitted to the FDA for endorsement, portrays the most dire requirements for modernizing the medicinal item improvement process – the Critical Path - to make item advancement more unsurprising and proficient [8]. In this paper, completely computerized, another, content-based framework is being proposed for the knee bone division from attractive reverberation pictures (MRI). The motivation behind the bone division is to bolster the disclosure and portrayal of imaging biomarkers for the frequency and movement of osteoarthritis, a weakening joint infection [9] [10]. Picture Compression is fundamentally a method in which superfluous commotion/information is diminished and is by and large alluded as Digital Compression. There are two sorts of picture pressure procedures: "Lossless" or reversible pressure and "Lossy" or "irreversible pressure" A Lossless Compression system is a strategy in which there is no loss of data and picture information while in Lossy Compression method there is picture change, measurement, a encoding [11]. Every one of these strategies work with a typical goal, i.e., to give an answer for effective programmed medicinal picture division. Presently the utilization of wavelet change and morphological change are increasing more consideration for dividing restorative pictures Morphological change consolidates geometrical elements and edge components to fragment the picture. With the utilization of morphological-based division the issue of over and under division can be kept away from [12].

II. TECHNIQUE

For adjustment of pixels in a picture the method known as Morphological picture handling is utilized. For grayscale picture, the pixels are distinguished by their parallel qualities i.e. 0 and 1, and for this procedure are directed by utilizing either advanced picture preparing calculations or by less numerically entangled operations, which incorporates disintegration and expansion and additionally opening and shutting of pictures. Essentially the fundamental reason for the Morphological Picture Handling is to uproot undesirable ancient rarities in a picture or to enhance picture's clarity. In the displayed paper for the distinguishing proof of infection, I am utilizing the procedures of disintegration and expansion alongside the mix of Skeletonization and edge determination. For picture representation of objects of a picture, particular arrangement of pixels called object pixels is utilized. Foundation pixels are white and are spoken to independently. By disintegration operation, the transformation of the pixels connected with the item's limit to pixels out of sight is conceivable, while with the assistance of enlargement operation, the circumscribing foundation pixels can be changed to the ones that are connected with the article. Essentially disintegration procedure is utilized for making the items littler and widening procedure is utilized for developing or notwithstanding to merge the article.

2.1 Enlarging A Picture

For enlarging a picture, the imdilate capacity is utilized. The imdilate capacity is a capacity that for the most part acknowledges two essential contentions i.e. the info picture, which is to be handled (twofold, stuffed double picture or a dark scale image). For giving back an organizing component an item, either the strel capacity is utilized, or a parallel network characterizing the area of an organizing component can be utilized. The base worth managed by the information sort is appointed to the Pixels past the picture fringe. These pixels are thought to be set to 0, for double pictures and if there should arise an occurrence of grayscale pictures, for the uint8 pictures; the base quality is set to 0. With the assistance of organizing component b the Morphological expansion of f picture is given as:

$$\delta(f, b)(s, t) = \max\{f(s-x, t-y) + b(x, y) \mid (s-x, t-y) \in D_f; (x, y) \in D_b\}$$

Where D_b and D_f primarily are the spaces of the b and f capacities.

2.2 Dissolving a Picture

For dissolving a picture, the imerode capacity is utilized. The imerode work fundamentally acknowledges two essential contentions i.e. The information picture, which is to be prepared (paired, pressed double picture or a dark scale image). For giving back An organizing component object, either strel capacity, or a parallel grid that characterizes the area of an organizing component is utilized and for the pixels that past the picture fringe are fundamentally doled out the greatest quality managed by the information sort. These pixel values for parallel pictures, are thought to be set to 1 and for the grayscale pictures, the most extreme quality for the uint8 pictures is set to 255. Essentially the Morphological disintegration of a f picture by the organizing component is given by:

$$\varepsilon(f, b)(s, t) = \min\{f(s+x, t+y) - b(x, y) \mid (s+x, t+y) \in D_f; (x, y) \in D_b\}$$

Where D_b and D_f are chiefly the areas of b and f capacities.

2.3. Organizing Component

The widening and disintegration capacities acknowledge organizing component objects, called STRELS. The strel capacity is use to make STRELS of any self-assertive size and shape. The strel capacity can be of numerous basic shapes, for the most part as intermittent lines, plates, precious stones, balls and lines. Here in this paper I commonly picked an organizing component which is of precious stone, rectangular and self-assertive formed. It ought to be observable that the organizing component must be of the same shape and size as that of the item's information picture.

2.4. Joining Enlargement and Disintegration

For usage of picture preparing operations blend of widening and disintegration are for the most part utilized, for instance, the meaning of a morphological opening of a picture says that it is disintegration which is trailed by expansion, with the assistance of the comparative organizing component for both operations. The related operation, for morphological shutting of a picture, is only the opposite, which comprises of enlargement took after by disintegration with the comparable organizing component.

Skeletonization and Edge determination which are mostly the two basic picture preparing operations in view of the methods of the enlargement and disintegration. For diminishing all articles in a picture to lines Skeletonization is utilized, in which the crucial structure of the picture is not changed, then again the Border pixels of the items in a paired

picture is the operation called Edge Determination. For a pixel that is to be considered as an edge pixel in the event that it fulfills both of these criteria i.e. the pixel ought to be on and one (or more) of the pixels in its neighborhood ought to be off.

III. RESULTS AND DISCOURSE

To start with read the pictures of Fingers and Knee having Rheumatoid Joint inflammation into the MATLAB workspace than make an organizing component. For dissolving a picture, the organizing component ought to be is of jewel and rectangular fit as a fiddle sort and the organizing component taken ought to be sufficiently expansive to be to be to evacuate the lines, yet it ought not be sufficiently extensive to uproot the rectangles. It ought to be contains each of the 1's, thus on extensive bordering patches of closer view pixels it ought to uproot everything. At long last to restore the rectangles to their unique sizes, the dissolved picture utilizing the same organizing component is widened, SE, will evacuates every one of the lines, additionally recoils the rectangles. The jewel shape organizing component makes 9x9 lattice, having all 1's fit as a fiddle alongside 41 neighbors. Essentially discretionary molded organizing component makes a corner to corner organizing component object having 5x5 grid having all askew component 1, a Level STREL object containing 5 neighbors. For upgrading the execution of Organizing Component Disintegration, the strel capacity might separate the organizing components to littler pieces, a method is Called as organizing component decay.

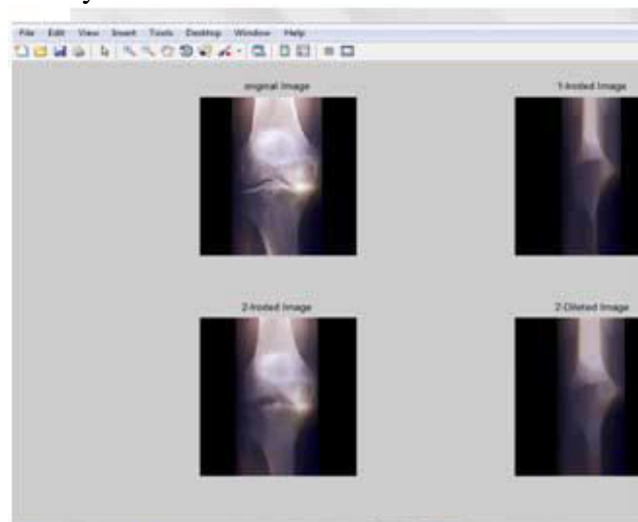


Figure 1: Eroded and Expanded Pictures of Knee Picture 1 Eroded/Widened pictures are created because of Rectangular organizing capacity and 2 Eroded/Enlarged pictures are produced because of jewel shape organizing capacity. Picture arrangement (2, 3, and 6) is the skeletonized hand picture.

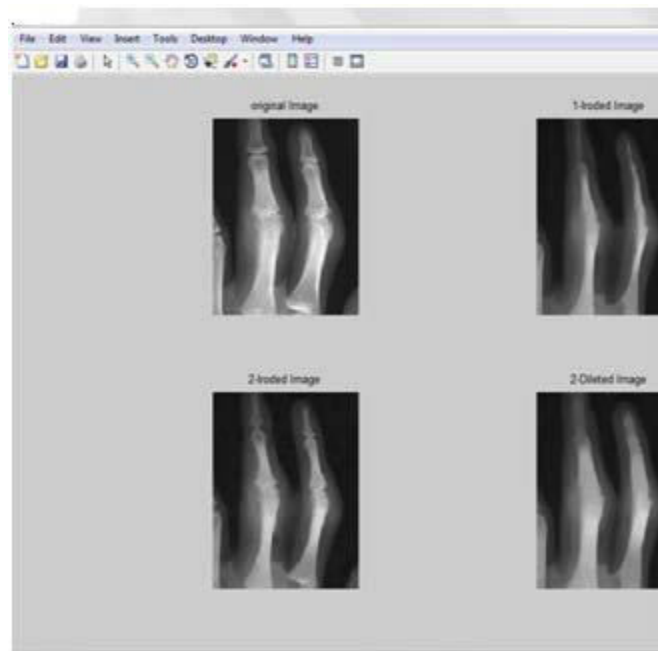


Figure 2: Iroded and Widened Pictures of Fingers Picture 1 Iroded/Enlarged pictures are created because of Rectangular organizing capacity and 2 Iroded/Expanded pictures are produced because of jewel shape organizing capacity. Picture arrangement (2, 3, and 6) is the skeletonized Fingers picture

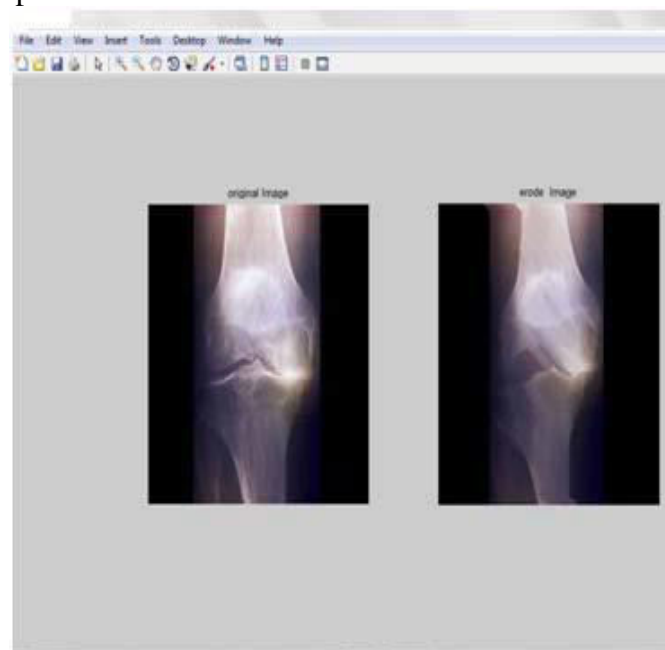


Figure 3: Iroded and Widened Pictures of Fingers Picture, created because of subjective formed organizing capacity. Figure

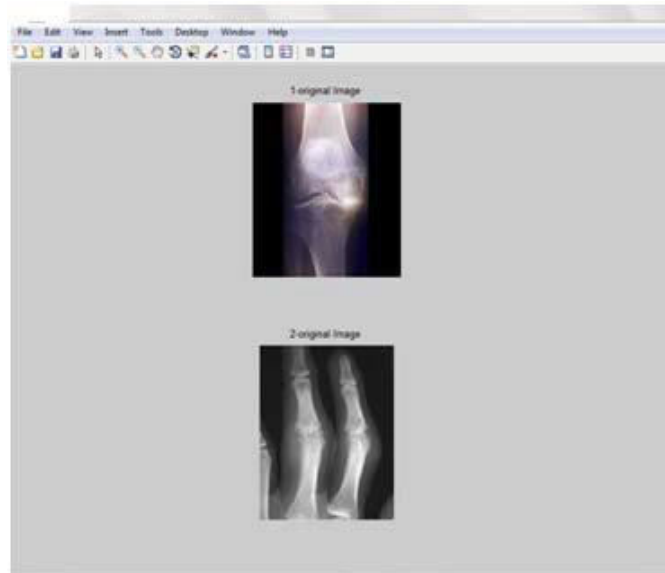


Figure 4: Parameterized Pictures of Knee and Fingers.

IV. CONCLUSION AND FUTURE EXTENSION

For building up a picture strategy that will get to be productive for restorative imaging bones. For those Specialists won't have the capacity to analyze the ailments in the prior stages, if Rheumatoid Joint inflammation won't be happening in the prior stages, specialists will request Ultra Sounds and X-beams, over and over. By the work exhibited in this paper they will have the capacity to analyze the sickness in the principal X-Beam, X-ray and Ultrasound. In this paper a radiographic Picture handling based procedure is introduced to precisely and dependably determination of the vicinity of illness rheumatoid joint pain. The outcomes displayed here are preparatory and concentrated just the reproducibility parts of the method. This system is being connected towards observing early stage rheumatoid joint pain patients in a progressing clinical trial. Results that are gotten from the clinical trial information ought to be giving a superior comprehension. The displayed venture gives considered better comprehension towards the malady comparatively.

V. REFERENCES

- [1]. M. Akil and r. S. Amos. Abc of Rheumatology rheumatoid Arthritis–i: clinical elements and analysis. *Bmj*, 310(6979):587, 1995.
- [2]. Kelvin Ka-fai Leung, Longitudinal examination of X-ray pictures in rheumatoid joint inflammation, November 16, 2007.
- [3]. Monique Frize, Cynthia Adéaa, Pierre Payeurb, Gina Di Primioc, Jacob Karshd, Abiola Ogungbemilea, *Proc. of SPIE*, Vol. 7962, 79620M-1, Therapeutic Imaging 2011, CCC code: 1605-7422/11/\$18.
- [4]. Anne-Christine Rodent and Marie-Christophe Boissier. Rheumatoid joint pain: immediate And Aberrant expenses. *Joint Bone Spine*, 71(6):518–524, November 2004.
- [5]. P.P. Cheung, M. Dougados, L. Gossec. "Unwavering quality of ultrasonography to distinguish synovitis in rheumatoid joint inflammation: a deliberate writing survey of 35 studies (1,415 patients)" *Ligament Care Res (Hoboken)*. 2010 Blemish; 62(3):323-34.
- [6]. J.E. Freeston, P. Flying creature, P.G. Conaghan. "The part of X-ray in rheumatoid joint pain research and clinical issues." *Cur Rheumatol*. 2009 Mar; 21(2):95-101. Review.
- [7]. M.A. Cimmino, M. Parodi, E. Silvestri et al. "Correlation between radiographic, echographic and MRI changes and rheumatoid arthritis progression." *Reumatismo*, 2004 Jan-Mar; 56(1 Suppl 1): 28-40 Italian.
- [8]. D. Symmons, G. Turner, R. Webb, P. Asten, E. Barrett, M. Lunt, D. Scott, and A. Silman. The prevalence of rheumatoid arthritis in the United Kingdom: new estimates for a new century. *Rheumatology*. 41(7):793, 2002.
- [9]. Automatic graph-cut based segmentation of bones from knee magnetic resonance images for osteoarthritis research by Sufyan Y. Ababneh, Jeff W. Prescott, and Metin N. Gurcan *Med Image Anal*. 2011 August; 15(4): 438–448.
- [10]. Bourgeat P, Fripp J, Stanwell P, Ramadan S, Ourselin S. MR image segmentation of the knee bone using phase information *Med Image Anal*. 2007; 11(4):325–335.
- [11]. Euclid Seeram RTR, BSc, MSc, FCAMRT
Associate Consultant INSITE Consultancy Inc Ottawa – Canada, Irreversible Compression in Digital Radiology-A Literature Review, INSITE Consultancy Inc., 2004.
- [12]. Najman, L. and Schmitt, M. (1996) Geodesic saliency of watershed contours and Hierarchical segmentation, *Pattern Analysis and Machine Intelligence*, IEEE Transactions on Pattern Analysis and Machine Intelligence, Vol.18, No. 12, Pp.1163-1173.

Parallel Prefix Speculative Han Carlson Adder

Gayathri.G¹, Raju S.S², Suresh.S³

¹Master of engineering student, ²Assitant Professor, ³Associate Professor,
^{1,2,3} Department of E.C.E, A.K.T Memorial college of Engineering and Technology, Kallakurichi,
 Tamilnadu, India
 Email ID: gaya3_1027@yahoo.com

Abstract- Binary addition is one of the most important arithmetic function in modern digital VLSI systems. Adders are extensively used as DSP lattice filter where the ripple carry adders are replaced by the parallel prefix adder to decrease the delay. The requirement of the adder is fast and secondly efficient in terms of power consumption and chip area. Speculative variable latency adders have attracted strong interest thanks to their capability to reduce average delay compared to traditional architectures. This paper proposes a novel variable latency speculative adder based on Han-Carlson parallel-prefix topology that resulted more effective than variable latency Kogge-Stone topology. The paper describes the stages in which variable latency speculative prefix adders can be subdivided and presents a novel error detection network that reduces error probability compared to variable latency adder.

Keywords- Parallel Prefix Adder, Kogge Stone Adder, Han-Carlson Adder.

I. INTRODUCTION

VLSI binary adders are critically important elements in processor chips, they are used in floating-point arithmetic units, ALUs, and memory addresses program counter update and magnitude comparator. Adders are extensively used as a part of the filter such as DSP lattice filter. Ripple carry adder is the fundamental adder that is capable of performing binary number addition. Since its latency is proportional to the length of its input operands, it is not very useful. To speed up the addition, carry look ahead adder is introduced. Parallel prefix adders provide good results as compared to the conventional adder [1].

Parallel Prefix Adder includes Brent-Kung [2], Kogge-Stone [3]. The architecture operates at fixed latency. It proposes a novel variable latency speculative adder based on Han-Carlson parallel-prefix topology. The Han-Carlson topology uses one more stage than Kogge-Stone adder, while requiring a reduced number of cells and simplified wiring. Thus, it can achieve similar speed performance compared to Kogge-Stone adder, at lower power consumption and area. We show that a speculative carry tree can be obtained by pruning some intermediate levels of the classical Han-Carlson topology. It provides rigorous derivation of the error detection network and shows that the error detection network required in speculative Han-Carlson adders is significantly faster than the one used by speculative Kogge-Stone architecture.

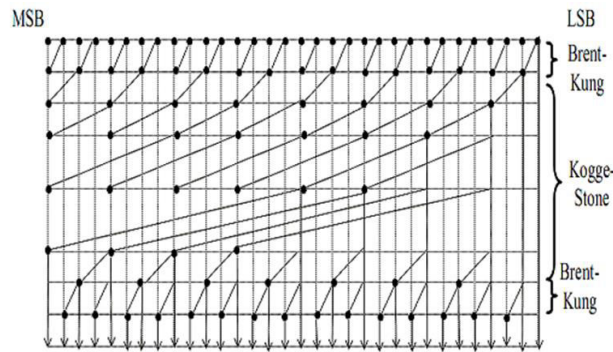
The main aim in ALU design is to reduce the adder critical path, which decides execution time in terms of delay (6.133ns) and power(35%). These two factors are most essential in adder design [4]. Parallel prefix adder design is most preferable for their higher speed of operation. There are different algorithms are used in process of addition. They main aim on improvising the performance of Parallel Prefix Adder (PPAs) by optimizing performance parameters such as Speed, Power, Area and number of gate counts. There are various topologies of prefix adders are there, they give the comparisons among the various parallel tree adders.

By using variable latency speculative adder, kogge stone speculative adder produces 45% of area is reduced and 35% of power is saved compared to kogge stone non- speculative adder. The kogge stone adder uses the minimum number of logic levels and has fan-out of 2[5, 7].

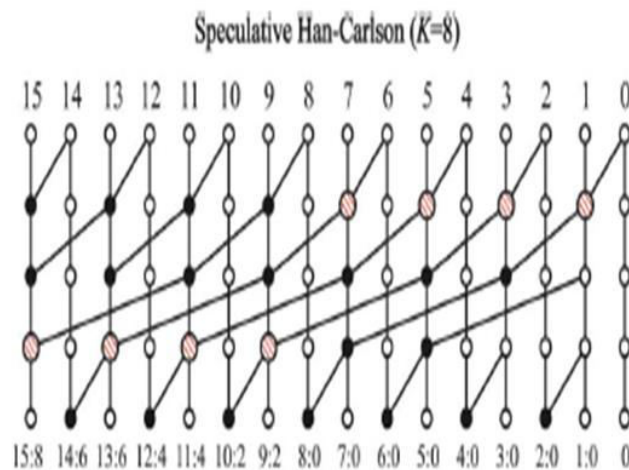
These tree structures validate the benefits of each one of them with the other by making use of the performance parameters [8]. The various tree structures are mentioned in the literature based on area (45%), fan-out-2 and complexity in circuit design. [9]In case of the Kogge-Stone, it uses recursive doubling property which leads to the fan-out limited to unity at the each stage of carry merge [10].

II.HAN-CARLSON ADDER

The Han-Carlson adder is a blend of the Brent-Kung and Kogge-Stone adders. It uses one Brent-Kung stage at the beginning followed by Kogge-Stone stages, terminating with another Brent-Kung stage to compute the odd numbered prefixes. It provides better performance compared to Kogge-Stone for smaller adders.



GRAPICAL REPRESENTATION OF HAN CARLSON ADDER



HAN CARLSON ADDER CARRY LENGTH (K=16)

The Han-Carlson is the family of networks between Kogge-Stone and Brent-Kung. Han-Carlson adder can be viewed of Kogge-Stone adder. This adder is different from Kogge-Stone adder in the sense that these performs carry-merge operations on even bits and generate/propagate operation on odd bits. At the end, these odd bits recombine with even bits carry signals to produce the true carry bits.

This adder has five stages in which the middle three stages resembles with the Kogge-Stone structure. The advantage of the adder is that it uses much less cells and its shorter. Thus there is a reduction in complexity at the cost of an additional stage for carry-merge path.

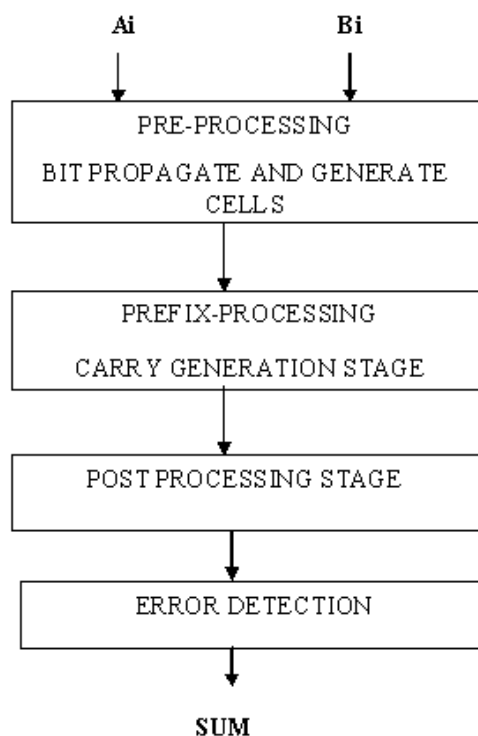
We have generated a Han- Carlson Speculative Prefix Processing stage by deleting the last rows of the kogge stone adder. This yields a speculative stage with $k=8=n/2^p$, where p is the number of pruned levels.

III.PARALLEL PREFIX ADDER

Parallel prefix adders are suitable for VLSI implementation since it differs from other adders, it can be used for large word sizes. The proposed design reduces the number of prefix operation by using more number of Brent-Kung stages and lesser number of Kogge-Stone Stages. This also reduces the complexity, silicon area and power consumption. Parallel Prefix Adder can be subdivided in the following stages: Pre-Processing, Post-Processing, Error Detection and Error Correction. The Error Correction Stage is Off the critical path, as it has two clock cycles to obtain the exact sum when speculation fails.

The Pre-Processing and Post-Processing Stages of a Prefix adder involve only simple operations on signals to each bit location. Hence, adder performs mainly on Prefix operation. Therefore black dots represent the prefix operator, while white dots represent simple place holders.

IV BLOCK DIAGRAM

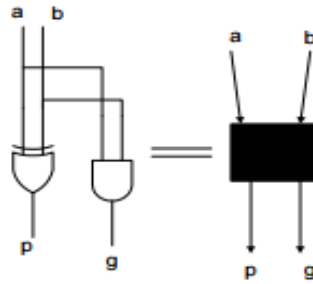


4.1. PRE PROCESSING

In the pre processing stage generate (G_i) and propagate (P_i) signals are calculated.

$$G_i = a \text{ and } b \ \&$$

$$P_i = a \text{ xor } b$$

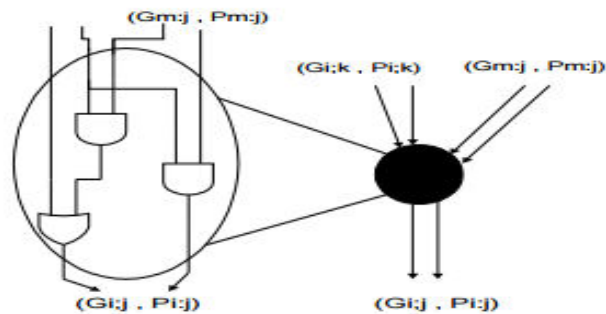


Square cell structure

4.2. SPECULATIVE PREFIX-PROCESSING

Instead of computing all the $g(i:0)$ and $p(i:0)$ required to obtain the exact carry values, only a subset of block generate and propagate signals is calculated; block generate and propagate signals is calculated;

Han-Carlson adder constitutes a good trade-off between fan out, number of logic levels and number of black cells. Because of this, Han-Carlson adder can Achieve equal speed performance respect to Kogge-Stone adder, at lower power consumption and area. Therefore it is interesting to implement a speculative Han-Carlson adder.



4.3. SPECULATIVE PREFIX PROCESSING

Circular cells: for computation of prefix operation

Calculations of all carry signals:

$$G_{i:j} = G_{i:k} + P_{i:k} \cdot G_{k-1:j}$$

$$P_{i:j} = P_{i:k} \cdot P_{k-1:j}$$

1. Bit propagate and generate

This block implements the following logic:

$$G_i = A_i \text{ AND } B_i$$

$$P_i = A_i \text{ XOR } B_i$$

2. Group propagates and generate

This block implements the following logic:

$$G_2 = G_1 \text{ OR } (G_0 \text{ AND } P_1)$$

$$P_2 = P_1 \text{ AND } P_0$$

4.4. POST PROCESSING

In the post processing stage approximate carry values are obtained from this subset and then use them to obtain the approximate sum bits S_i as follows: The approximate carries are already available at the output of the prefix-processing stage. The post-processing is equal to the one of a non-speculative adder and consists of xor gates.

Calculation of Final Sum:

$$S_i = P_i \oplus G_{i-1:0}$$

4.5. ERROR DETECTION

The error detection circuit that flags an error if the sum computed by the almost Carry Adder is incorrect. This only occurs when there is a chain of more than k propagates in the addenda. To check for the presence of an error, we must consider all chains of length $k + 1$, and check if any of them contain solely propagates. The expression for error signal is stated as follows:

$$ER = \sum_{i=0}^{n-k-1} p_i p_{i+1} \dots p_{i+k}$$

The conditions in which at least one of the approximate carries is wrong (misprediction) are signaled by the error detection stage. In case of misprediction, an error signal is asserted by error detection stage and the output of the post-processing stage is discarded.

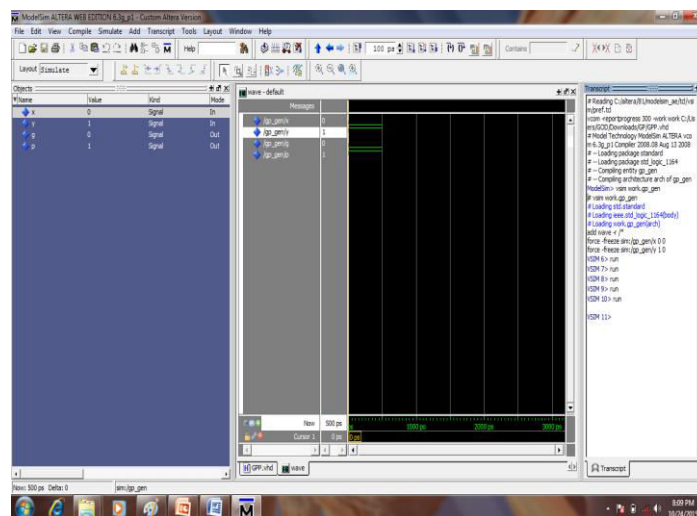
4.6. ERROR CORRECTION

This stage computes the exact carry signals to be used, in case of misprediction. It is composed by the levels of the prefix, processing stage pruned to obtain the speculative adder.

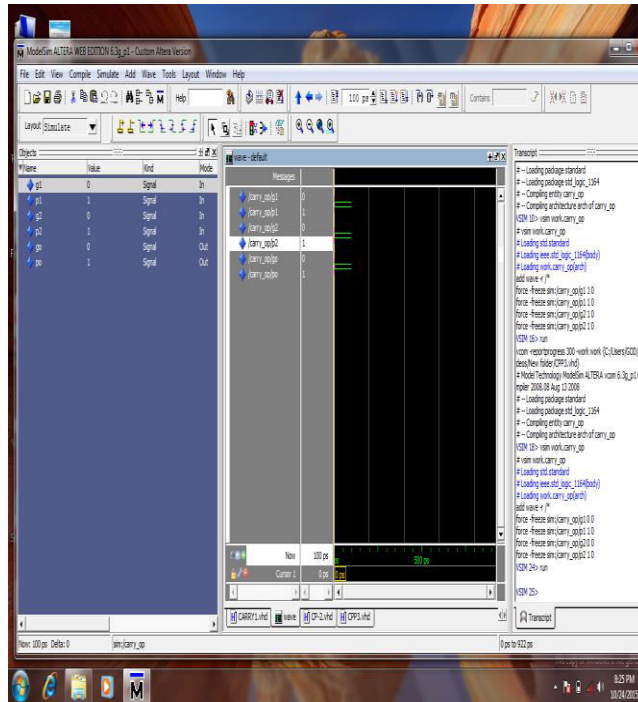
V RESULTS AND DISCUSSION

The proposed Parallel Prefix Adder can be analyzed using Xilinx. It reduces the minimum achievable delay. The analysis of Area and Power shows that speculative adders are not effective for large average delay. At timing constraint imposed during synthesis is made tighter speculative adders become advantageous.

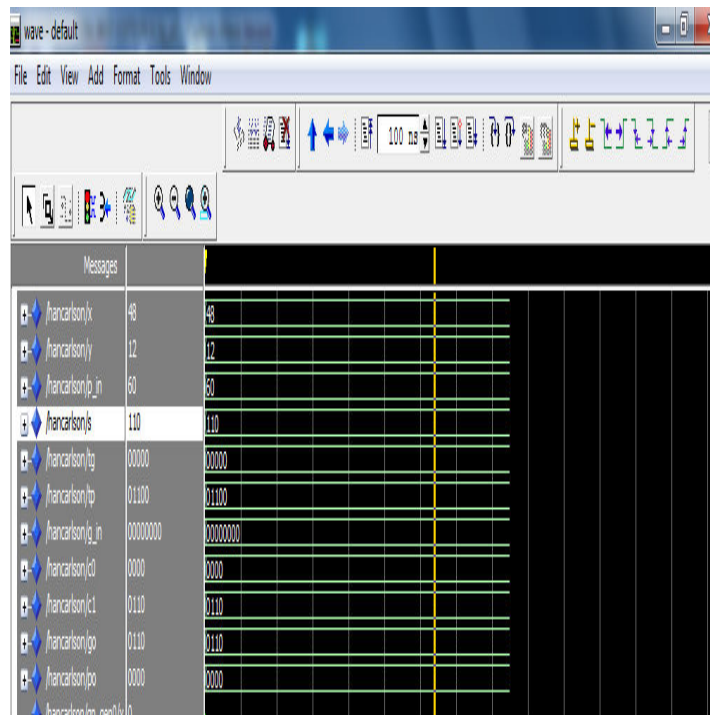
5.1 PRE-PROCESSING



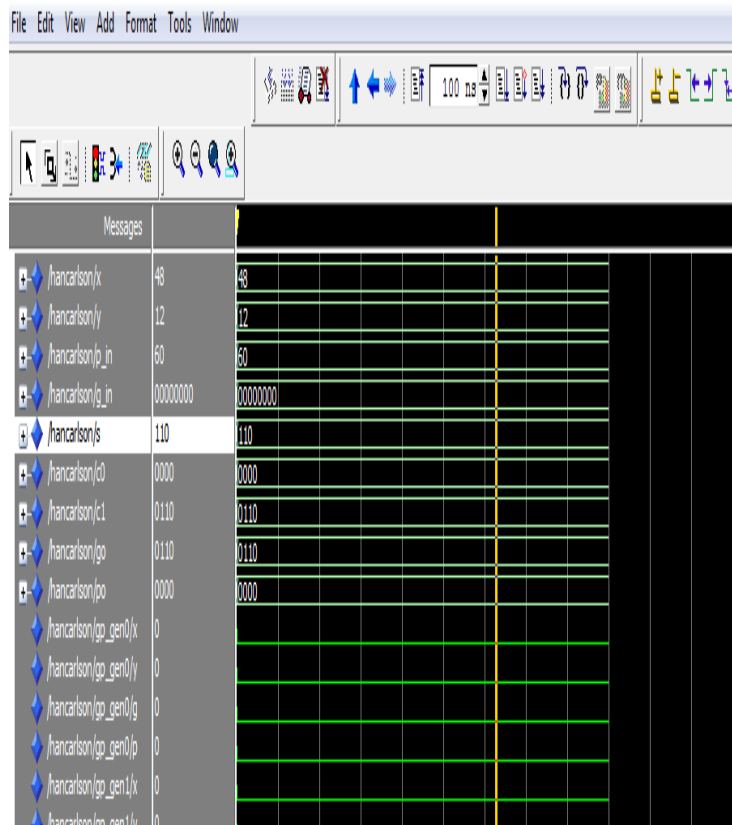
5.2 SPECULATIVE PREFIX PROCESSING



5.3 POST-PROCESSING



5.4 ERROR CORRECTION



VI CONCLUSION

In this paper Han-Carlson adder presented reduction in the complexity and hence provides a tradeoffs for the construction of large adders. These wide adders are useful in applications like cryptography for security purpose, global unique identifiers used as a identifier in computer software and this wide adder also provides good speed. It is used to reduce error by using error correction and detection techniques. It is used to reduce number of prefix operation and reduces complexity.

REFERENCES

1. Darjn Esposito, Davide De Caro, Senior Member,IEEE, Ettore Napoli, Nicola Petra, Member, IEEE and Antonio Giuseppe Maria Strollo, Senior Member, IEEE, “ Variable Latency Speculative Han-Carlson Adder”, May 2015.
2. R.P.Brent and H.T.Kung, “A regular layout of parallel adders”,IEEE Trans.Comput., Vol C-31, Mar 1982
3. P.M.Kogge and H.S.Stone, “A Parallel Algorithm for the efficient solution of a general class of recurrence equations”, IEEE Trans.comput, vol C-22, Aug 1973.

4. Cong Liu, Jie Han and Fabrizio Lombardi, "A Low Power, High Performance Approximate Multiplier with Configurable Partial Error Recovery,(DATE'14) Apr 2014.
5. K.Du, P.Varman, and K.Mohanram,"High Performance reliable Variable Latency Carry select addition ", in Proc. Design, Autom, Test Eur.Conf. Exhib (DATE'12), Mar 2012.
6. A.Cilardo, "A new Speculative addition architecture suitable for two's complement operations", in Proc. Design, Autom, Test Eur, Conf. Exhib.(DATE'09), Apr 2009.
7. A.K.Verma, P.Brisk, and P.Jenne, "Variable Latency Speculative Addition, A New Paradigm for Arithmetic circuit Design, Autom, Test Eur. (DATE'08), Mar 2008.
8. S-L.Lu,"Speeding up processing with Approximation Circuits", Computer, Mar 2004.
9. I.Koren, "Computer Arithmetic Algorithms", Natick, MA, USA AK Peters, June 2002.
10. S.Knowles, "A Family of Adders", in Proc, 14th IEEE symp. Comput.Arith, Vail, CO, USA, June 2001.
11. S.K.Mathew, R.K.Krishnamoorthy, M.A.Anders, R.Rios, K.R.Mistry, and K.Soumyanath, "'Sub-500-ps 64-b ALUs, Design and scaling trends, "IEEE J.Solid-State Circuits, Nov 2001.
12. Tong Liu and Shih-Lien Lu, Intel Corporation," Performance Improvement with Circuit-Level Speculation", May 2000.

Modeling and analysis on GABA concentration level for Diagnosis of Parkinson's disease

S. Anita¹, Dr. P. Aruna Priya¹, Dr. R. Arokiadass²

¹Department of Electronics and Commn. Engg., SRM University, Chennai, Tamilnadu, India.

³Department of Mechanical Engineering, St. Anne's college of Engg. & Tech, Panruti, Tamilnadu, India.

Abstract— Early and accurate diagnosis of Parkinson's disease is essential for effective neuroprotection. Modern and advanced neuroimaging technique such as Single Photon Emission Computed Tomography imaging using [123I] FP-CIT from Parkinson's Progression Markers Initiative database is used even in the early stage of detection. In the present work, Striatal Binding Ratio (SBR) values are calculated from SPECT images obtained from the Parkinson's Progression Markers Initiative (PPMI) database. We measure Gamma-amino butyric acid (GABA) concentration level from SBR values in Parkinson's diseased. Thus the three parameters such as Caudate, Putamen, and Age have been selected to measure the GABA concentration level. Central Composite Design (CCD) using Response Surface Methodology (RSM) is used to develop a mathematical model for GABA concentration level. Graphs were obtained to study the effect of these parameters. An ANOVA analysis was also performed to obtain significant parameters influencing GABA concentration level.

Keywords- Parkinson's disease; Striatal Binding Ratio; GABA; Response Surface Methodology; Central Composite Design; ANOVA.

I. INTRODUCTION

PD is a slowly progressive and complex disorder of the central nervous system, involving primarily a loss of dopamine nerve terminal (neurochemical messengers) in the midbrain called substantia nigra, and the results are impairment of movement with tremor, Gait problem, slowness, stiffness, or balance problems and impairment of posture. The rate of progression will vary from person to person [1]. The advanced stage of the disease is trouble-free to diagnosis. However, in its early symptoms are mild, an accurate diagnosis becomes very difficult [2].

PPMI is a longitudinal observational study that aims to identify one or more markers of progression for Parkinson's disease, points out that the early diagnosis of PD subjects, like those being recruited for PPMI, is difficult as characteristic signs and symptoms have not yet fully emerged and patients may present atypical signs and symptoms [3].

[123I] FP-CIT using SPECT Imaging is the most widely used nuclear medicine technique for continuous assessment of dopamine transporters in suspected Parkinson's disease patients to discriminate PD patients from healthy controls. The confirmation of reduction of the [123I] FP-CIT specific uptake on the putamen and caudate results PD [4, 5, 6].

Early and accurate diagnosis of PD is critical for the reasons of early management, avoidance of unnecessary medical examinations and therapies and their economic status, side effects and safety risks [7]. Recently, early detection of PD plays a vital role, but it is critical too. SBR values of caudate and putamen is the main features of diagnosis of early PD. It plays a major role in early management of PD. This reduces the complexity of the feature extraction method. The extraction of regional count densities in the caudate and putamen are calculated using occipital lobe region as the reference [8].

Gamma-aminobutyric acid was first known only as a plant and microbe metabolic product. Later, it is discovered that GABA is primary part of the central nervous system [9]. It is an inhibitory transmitter in the matured human brain; its actions are primarily excitatory in the developing brain [10, 11]. Alzheimer's disease, late cortical cerebellar atrophy, Neuro Behcet's syndrome, olivopontocerebellar atrophy, Huntington's chorea, Parkinson's disease and cerebral haemorrhage patients have quite low Gamma-amino butyric acid (GABA) concentration levels. GABA concentration levels were measured using a radio receptor assay technique [12, 13]. Hence the Parkinson's disease is detected by measuring the level of GABA concentration.

The purposes of the current work are 1. To investigate the level GABA concentration of Parkinson's disease using SBR values. 2. To develop a mathematical model for GABA concentration using Caudate, Putamen and Age of PD patients by CCD design. 3. Analyse the influence of the parameters like Caudate, Putamen and Age with GABA concentration level to diagnose the Parkinson's disease. 4. Analysis of variance is employed to carry out the effects of various parameters on the GABA concentration.

II. DESIGN OF EXPERIMENT BASED ON RESPONSE SURFACE METHODOLOGY

The response surface methodology was applied for modeling and analyzing the input parameters such as Caudate (X_1), Putamen (X_2) and Age (X_3) so as to obtain the concentration level of GABA in early Parkinson's disease. The quantitative form of relationship between the desired output (Y) and independent input variables (X_1 , X_2 , and X_3) is represented in RSM as follows:

$$Y = F(X_1, X_2, X_3) \quad (1)$$

Where Y is the desired output and F is the function of response. In the procedure of analysis, the approximation of Y was proposed using the fitted second-order polynomial regression model, which is called the quadratic model. The quadratic model of Y can be written as follows:

$$Y = a_0 + \sum a_i X_i + \sum a_{ii} X_i^2 + \sum a_{ij} X_i X_j \quad (2)$$

Where a_0 is constant, a_i , a_{ii} , and a_{ij} represent the coefficients of linear, quadratic, and cross product terms, respectively. X_i reveals the coded variables that correspond to the studied input parameters.

The necessary data for building the response models are generally collected by the experimental design. In this study, the collections of experimental data were adopted using Central Composite Design (CCD). The factorial portion of CCD is a full factorial design with all combinations of the factors at two levels (high, +1 and low, -1) and composed of the eight cube points, six axial points and six central points (coded level 0) which is the midpoint between the high and low levels. The star points are at the face of the cubic portion on the design which corresponds to a value of 1 and this type of design is commonly called the face-centered CCD. Table 1 shows the levels of three PD parameters and their levels. The experimental plans were carried out using the stipulated conditions based on the face-centered CCD involving 20 runs in the coded form as shown in Table 2. The design was generated and analyzed using MINITAB statistical package [16].

Table 1. Input parameters and their levels

Parameters	Levels		
	-1	0	+2
CAUDATE_L (X_1)	0.75	1.45	2.15
PUTAMEN_L (X_2)	0.25	0.60	0.95
AGE (X_3)	35	55	75

Table 2. Uncoded Designs (Randomized)

Sl. No.	CAUDATE_L (X_1)	PUTAMEN_L (X_2)	AGE (X_3)	GABA Concentration level
1	0.75	0.25	35	0.213
2	2.15	0.25	35	0.231
3	0.75	0.95	35	0.103
4	2.15	0.95	35	0.175
5	0.75	0.25	75	0.207
6	2.15	0.25	75	0.209
7	0.75	0.95	75	0.095
8	2.15	0.95	75	0.119
9	0.75	0.60	55	0.132
10	2.15	0.60	55	0.173
11	1.45	0.25	55	0.219
12	1.45	0.95	55	0.123
13	1.45	0.60	35	0.142
14	1.45	0.60	75	0.117
15	1.45	0.60	55	0.146
16	1.45	0.60	55	0.146
17	1.45	0.60	55	0.145
18	1.45	0.60	55	0.144
19	1.45	0.60	55	0.145
20	1.45	0.60	55	0.146

III. RESULTS AND DISCUSSION

3.1 Development of mathematical model

The mathematical relations between responses (i.e., GABA) and PD input parameters were established using the investigation results shown in Table 2. The coefficients of regression analysis for GABA concentration level are shown in Tables 3 along with the P value of the input parameters, higher order, and interactions. The P value of regression analysis of GABA concentration level indicates that linear, square, and interactions of putamen and age are significant, whereas linear of caudate is not so significant.

Equations 3 represent the regression equation for GABA concentration level. Regression equation for GABA concentration level:

$$\begin{aligned} \text{GABA} = & 0.207267 - 0.023481 X_1 - 0.424162 X_2 + 0.004442 X_3 + 0.018646 X_1^2 + \\ & 0.225603 X_2^2 \\ & - 0.000035 X_3^2 + 0.038776 X_1 X_2 - 0.000571 X_1 X_3 - 0.000643 X_2 X_3 \end{aligned} \quad (3)$$

Table 3. Regression analysis of GABA concentration level

Term	Coefficient	P value
Constant	0.207267	<0.000
X ₁	-0.023481	0.301
X ₂	-0.424162	<0.000
X ₃	0.004442	<0.001
X ₁ ²	0.018646	<0.019
X ₂ ²	0.225603	<0.000
X ₃ ²	-0.000035	<0.002
X ₁ X ₂	0.038776	<0.001
X ₁ X ₃	-0.000571	<0.002
X ₂ X ₃	-0.000643	<0.042

Where GABA is the response (Gamma-amino butyric acid) and X₁, X₂ and X₃ represent the decoded values of Caudate (X₁), Putamen (X₂) and Age (X₃) respectively. Single variable terms have the main effect on the response and interaction, square effect also considered. The developed mathematical model can be used to analyze the effects of input parameters on GABA concentration level for diagnosing the PD.

Where S is the estimated standard deviation about the regression line, R² also called the coefficient of determination which is calculated as $R^2 = (SS \text{ Regression}) - (SS \text{ Total})$, where SS stands for sums of squares. R² (Adj) is an approximately unbiased estimate of the population R². The S value being measurement of error it is smaller the better. So, from Table 4 it is clear that the mathematical model for GABA concentration level is less deviated from the regression line.

Table 4. Summary of Regression analysis

Response	S Value	R ² (%)	Adjusted R ² (%)
GABA	0.00545194	99.03	98.16

The higher value of R² is better to determine the coefficients of regression equation. So the coefficient in the regression equation for GABA concentration level has been determined more effectively. The closeness of the adjusted R² with R² determines the fitness of model [14, 15]. In both cases, the adjusted R² value is closer to the R² value.

3.2 Analysis of the developed mathematical models

The ANOVA and F ratio test have been performed to validate the goodness of fit of the developed mathematical models. The F ratios are calculated for lack-of-fit have been compared to standard values of F ratios corresponding to their degrees of freedom to find the

adequacy of the developed mathematical models. The F ratio calculated from ratio of Mean Sum of Square of source to Mean Sum of experimental error [16].

The ANOVA tables are shown in Table 5 for GABA. The standard percentage point of F distribution for 95% confidence limit is 4.06. As shown in Tables 5, the F value is 3.95 for lack-of-fit is smaller than the standard value of 95% confidence limit. Thus, the model is adequate in 95% confidence limit. It is also seen that from the P values, GABA model linear, square, and interaction effects of caudate, putamen and age are significant.

Table 5. Analysis of variance for GABA

Source of variation	Degree of freedom	Sum of squares	Mean sum of squares	F- value	P- value
Regression	9	0.030413	0.003379	113.69	0.000
Linear	3	0.025363	0.001399	47.06	0.000
Square	3	0.003653	0.001218	40.97	0.000
Interaction	3	0.001396	0.000465	15.66	0.000
Residual Error	10	0.000297	0.000030		
Lack of fit	5	0.000237	0.000047	3.95	
Pure Error	5	0.000060	0.000012		
Total	19	0.030710			

The normal probability plot is presented in Fig.1. It is observed that the residuals fall on a straight line, which indicates that the errors are distributed normally and the regression model is well fitted with the observed values. Figure 2 shows the residual values with fitted values for GABA concentration level. Figure 2 indicates that the maximum variation of -0.005 to 0.010, which confirms the high correlation presented between fitted values and observed values.

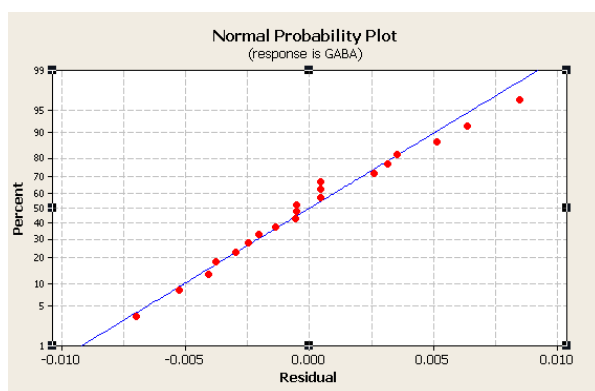


Figure 1. Normal probability plot for GABA

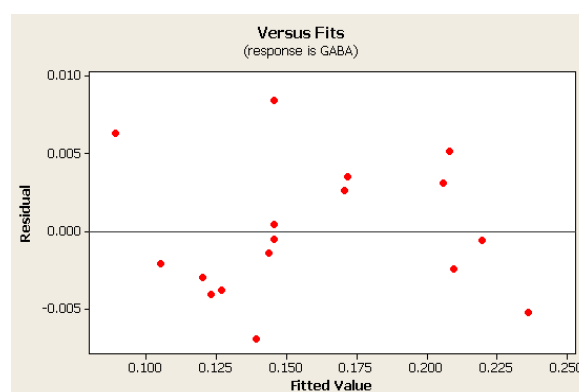


Figure 2. Residual Vs fitted values for GABA

Figs. 3, 4 and 5 shows the relationship of GABA concentration level at different SBR values that are calculated from SPECT images obtained from the Parkinson's Progression Markers Initiative (PPMI) database and age.

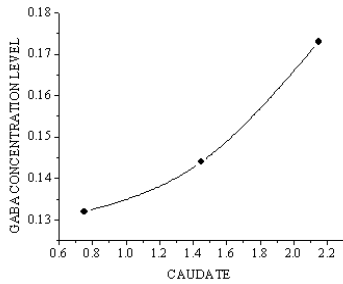


Figure 3. Effect of Caudate with GABA

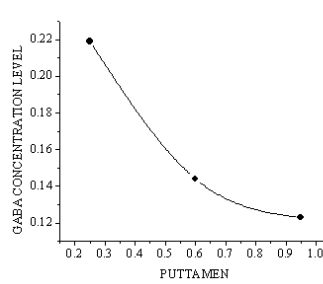


Figure 4. Effect of Puttamen with GABA

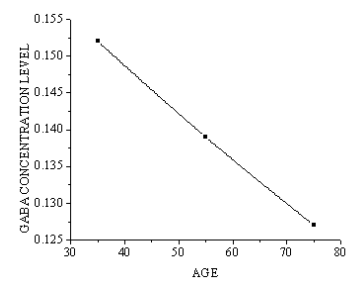


Figure 5. Effect of Age with GABA

In Fig. 3, GABA concentration level is examined at caudate of 0.75, 1.45 and 2.15. GABA concentration level increases by 4.1% with the increase of caudate from 0.75 to 2.15 at putamen of 0.60 and age of 55. In Fig. 4, GABA concentration level is examined at putamen of 0.25, 0.60 and 0.95. GABA concentration level decreases by 9.6% with the increase of putamen from 0.25 to 0.95 at caudate of 1.45 and age of 55. In Fig. 5, GABA concentration level is examined at age of 35, 55 and 75. GABA concentration level decreases by 2.5% with the increase of age from 35 to 75 at caudate of 1.45 and putamen of 0.60.

IV. CONCLUSIONS

The main results that can be deduced from the present study concerning the GABA concentration level for Diagnosis of Parkinson's disease are summarized here:

1. The developed RSM based mathematical modeling has the possible to evaluate GABA concentration level under various Input parameter settings.
2. The developed model is also employed to analyze the influence of these process parameters on GABA concentration level for diagnosing of Parkinson's disease.
3. GABA concentration level increases with increasing the Caudate. But it decreases with increasing the Putamen and Age. From the analysis it is clearly evident that Putamen has more influence on GABA concentration followed by Caudate and Age.

REFERENCES

- [1] Lawrence I. Golbe., Margery H. Mark., Jacob I. Sage.,(2010), PARKINSON'S DISEASE HANDBOOK, The American Parkinson Disease Association, Inc.
- [2] Booij, J., & Knol, R. J. (2007). SPECT imaging of the dopaminergic system in (premotor) Parkinson's disease. *Parkinsonism Related Disorder*, 13(Suppl. 3), S425–S428.
- [3] <http://www.ppmi-info.org/study-design/research-documents-and-sops/>
- [4] Varrone A and Halldin C 2012 New developments of dopaminergic imaging in Parkinson's disease Q. J. Nucl. Med. Mol. Imaging 56 68–82
- [5] O'Brien J T et al 2004 Dopamine transporter loss visualized with FP-CIT SPECT in the differential diagnosis of dementia with Lewy bodies *Arch. Neurol.* 61 919–25
- [6] Francisco P M Oliveira¹ and Miguel Castelo-Branco² *Journal of Neural Engineering* Computer-aided diagnosis of Parkinson's disease based on [123I]FP-CIT SPECT binding potential images, using the voxels-as-features approach and support vector machines 12 026008 (10pp) ;2015
- [7] Cummings, J. L., Henchcliffe, C., Schaier, S., Simuni, T., Waxman, A., & Kemp, P. (2011). The role of dopaminergic imaging in patients with symptoms of dopaminergic system neurodegeneration. *Brain*, 134, 3146–3166.
- [8] Automatic classification and prediction models for early Parkinson's disease diagnosis from SPECT imaging R. Prashanth, Sumantra Dutta Roy a Pravat K. Mandal , Shantanu Ghosh, *Expert Systems with Applications* 41; 3333–3342 ; 2014
- [9] Roth RJ, Cooper JR, Bloom FE (2003). *The Biochemical Basis of Neuropharmacology*. Oxford [Oxfordshire]: Oxford University Press. p. 106. ISBN 0-19-514008-7.

- [10] Li K, Xu E (June 2008). "The role and the mechanism of γ -aminobutyric acid during central nervous system development". *Neurosci Bull* 24 (3): 195–200. doi:10.1007/s12264-008-0109-3. PMID 18500393.
- [11] Ben-Ari Y, Gaiarsa JL, Tyzio R, Khazipov R (October 2007). "GABA: a pioneer transmitter that excites immature neurons and generates primitive oscillations". *Physiol. Rev.* 87 (4): 1215–1284. doi:10.1152/physrev.00017.2006. PMID 17928584.
- [12] *Acta Med Okayama*. 1983 Jun;37(3):167-77. Gamma-aminobutyric acid (GABA) in cerebrospinal fluid. Kuroda H.
- [13] CSF and plasma GABA levels in Parkinson's disease RJ ABBOTT, IF PYE, SR NAHORSKI* *Journal of Neurology, Neurosurgery, and Psychiatry*, 45 :253-256;1982
- [14] R.Arokiadass*, K. Palaniradja, N. Alagumoorthi, Prediction and optimization of end milling process parameters of cast Aluminium based MMC , *Transaction of non ferrous metals society of china*, Vol. 22, pp. 1568–1574,2012
- [15] Palanikumar K (2007) Modeling and analysis for surface roughness in machining glass fibre reinforced plastics using response surface methodology. *Mater Des* 28:2611–2618.
- [16] M.Seeman," Study on tool wear and surface roughness in machining of particulate aluminum metal matrix composite-response surface methodology approach",*Journal of Advanced Manufacturing Technology*, 09/22/2009

CMOS-Electromechanical Systems Micro sensor Resonator with High Q-Factor at Low Voltage

S.Thenappan¹, N.Porutchelvam²

¹ Department of ECE, Gnanamani College of Technology, India
Email:thenappan@gct.org.in

² Department of ECE, Gnanamani College of Technology, India
Email:porutchelvam@gct.org.in

Abstract: The paper presents a novel resonant-micro sensor platform for chemical and biological sensing applications in gaseous and liquid environment. We report a thermally driven and piezo resistively sensed CMOS-micro electromechanical systems (MEMS) resonator with quality factor $Q > 15\ 000$ and stop band rejection of 15 dB under CMOS-compatible bias voltage which is the basic requirement of CMOS under the influence of this bias voltage. In addition, the combination of the bulk-mode resonator design and high- Q SiO₂/polysilicon structural material leads to resonator $Q > 15\ 000$, a key index for low-phase-noise oscillators and low-insertion-loss filters. The resonator with a center frequency at 7.1 MHz was fabricated using a standard 0.85 μm 3-poly-7-metal CMOS process, featuring low cost, batch production, fast turnaround time, easy prototyping, and MEMS/IC integration. To resolve the feed through issue often seen in conventional thermal-piezo resistive resonators: 1) separation of the heater and piezo resistor is first adopted because of the routing flexibility of the structural configuration offered by CMOS back-end-of-line materials and 5) fully differential measurement scheme is then applied to the proposed device, both of which enable a low-feed through level with 85-dB improvement as compared with its single-ended counterpart.

Index Terms: CMOS-MEMS, micro-resonators, piezo resistive device thermal stability, Q factor, thermo-elasticity, micro electro-mechanical system.

I. INTRODUCTION

THERMAL-PIEZORESISTIVE MEMS resonators recently attracted significant attention due to their simple design, easy fabrication, high Q , operation in air and liquid environment, and low actuation voltage [1]–[3]. The combination of thermal actuation and piezo resistive detection not only prevents the need for deep submicron gap spacing in capacitive transducers but also resolves exotic material issue caused by piezoelectric transducers, which becomes a simple and effective transduction mechanism using mere resistors. The main structural materials of these resonators are silicon carbide or single crystal silicon to attain high Q while the heater for driving and piezo resistor for sensing are formed using either the same structural materials via doping [2], [3] or deposited metal layers [1]. However, none of the prior literature addresses the practical integration with circuits

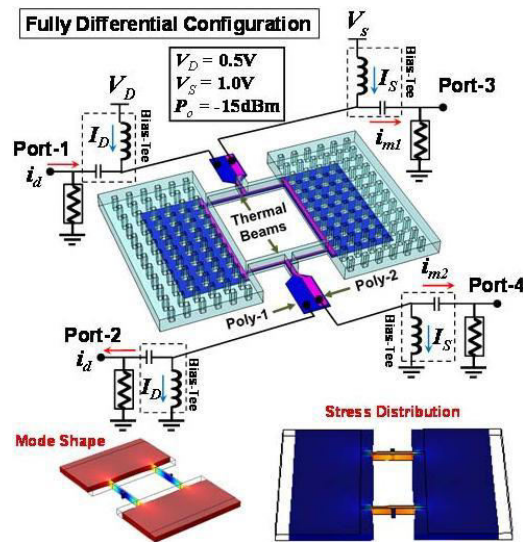


Fig. 1. Perspective-view schematic of a CMOS-MEMS bulk mode resonator driven by a resistive heater and sensed through a piezo resistor. The heater and piezo resistor are embedded inside a high- Q SiO_2 resonant structure. The inset shows its finite-element simulated mode shape and stress distribution.

to deploy their implementations on sensing and frequency control applications. Thanks to the recent advance on CMOS-MEMS technology through which MEMS resonators can be monolithically integrated with amplifier circuits to realize single-chip configuration [4], the thermal-piezo resistive resonators could also be realized through CMOS BEOL materials, demonstrated in our previous work [5].

To perform differential testing for feed through cancellation, the design of our first prototype [5] is rather involved (i.e., array design) and the characterization still necessitates de-embedding and post-data processing to extract the motional signal, which is not practical for real application. In addition, Q (lower than 1,000) and signal intensity of the resonator is limited due to the improper choice of the CMOS BEOL materials.

In this letter, we explore the material properties of the polysilicon layers offered by a $0.35\ \mu\text{m}$ 2P4M CMOS technology node for the heater and sensor, both of which are embedded inside a high- Q SiO_2 (i.e., CMOS dielectrics) vibrating dog-bone resonator as shown in Fig. 1. With (i) decoupling scheme of the heater and sensor and (ii) proper selection of their materials, the resonator can be operated in with decent resonance performance and low feed through floor (~ 40 -dB improvement). To go one step further, a fully differential testing configuration can be carried out through a simple dog-bone structure thanks to the routing flexibility of the CMOS-MEMS resonators, hence leading to additional feed through rejection of more than 30 dB as compared to its single-ended counterpart.

II. DEVICE DESIGN AND OPERATION

To overcome the high feed through level often seen in thermal-piezo resistive resonators where the resistor serves as both heater and sensor, a decoupling scheme of heating and sensing elements is adopted as shown in Fig. 1 to prevent the resistive feed through. A low-loss structural material from the dielectric (i.e., SiO_2) layers of CMOS BEOL yields (i) high Q for mechanical vibration, (ii) electrical insulator for embedded heater and sensor routing. Based on the material properties of the two polysilicon layers from the foundry, poly-1 layer, originally acting as gate polysilicon for transistors, possesses low resistance and high current density capability. It is suitable for heater operation. In contrast, poly-2 layer, serving as resistors in IC, features high gauge factor, which is well suited for the use as piezo resistors. To operate the resonator in Fig. 1, one dc current (I_D) flows through poly-1 heater to generate biasing for thermal drive while another dc current (I_S) is applied into poly-2 sensor to provide resistive readout. Such a design enables single-ended, single-to-differential, differential-to-signal, and fully differential test configurations, thus allowing us to explore the optimized operation of the device. A fully-differential scheme is illustrated here to explain the working principle of the proposed device. The combination of an ac input i_d (induced by v_{in+} of port-1 and v_{in-} of port-2 from a network analyzer) and dc biasing I_D generates a time-varying thermo-elastic force to excite the resonator into resonance with a mode shape shown in the inset of Fig. 1. Then the stress/strain modulated by the mechanical vibration of the thermal beams and further enhanced by the end proof-masses induces resistance change of the embedded piezo resistors, which can be sensed by v_{out+} of port-3 and v_{out-} of port-4 in the network analyzer. The common-mode noise would be either circulated in the input loop from v_{in+} to v_{in-} or cancelled by the differential readout of v_{out+} and v_{out-} , therefore significantly reducing the feed through floor. The differential readout also doubles the signal intensity of the resonance as compared to its single-ended detection.

III. EXPERIMENT RESULTS

The resonator was fabricated by a TSMC 0.35 μm 2P4M process, followed by a mask less metal wet etching process [5] with SEM's shown in Fig. 2. Fig. 2(a) presents a MEMS/IC integration feature offered by the CMOS-MEMS platform while Fig. 2(c) shows a Focus-Ion-Beam (FIB) cut cross-sectional view on the longitudinal drive/sense beam where the poly-1 heater and poly-2 piezo resistor are clearly seen. The width of the beam is around 3 μm and the thickness of the whole structure ideally is about 6 μm .

To characterize the resonator, the device was placed in a vacuum chamber with an electrical setup shown in Fig. 1 where different configurations can be performed, including (i) conventional single-ended scheme (i.e., one-port) with the heater and sensor using the same polysilicon layer,

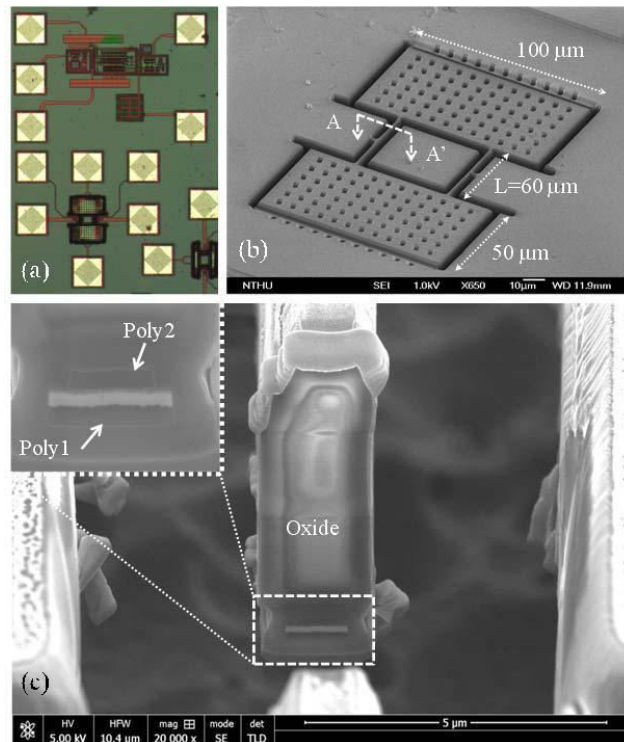


Fig. 2. Photos of a fabricated CMOS-MEMS thermal-piezo resistive resonator, including (a) global MEMS/IC optical view, (b) standalone device SEM view, and (c) FIB cut cross-sectional view of the beam.

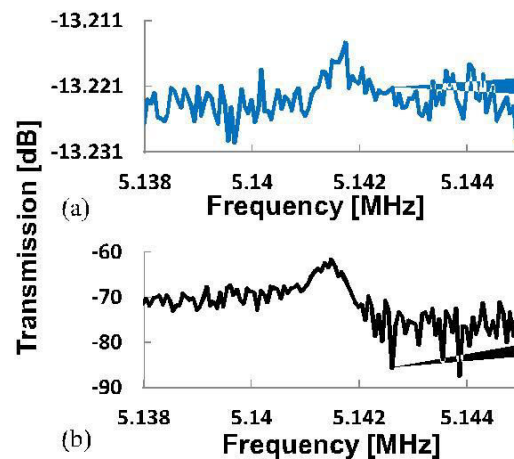


Fig. 3. Measured transmission spectra of the thermally driven and piezo resistively sensed CMOS-MEMS resonator by using (a) one-port configuration and (b) decoupled heater and sensor scheme.

(ii) two-port scheme with decoupled heater and sensor using different polysilicon layers, (iii) common-mode driving and differential sensing, and (iv) fully differential scheme. Fig. 3(a) presents the measured transmission characteristic of a conventional one-port configuration using port-1 as the driving input and port-2 as the sensing output, all under the poly-1 layer. The measured result shows a very high floor at -13.21 dB caused by the resistive feedthrough, indicating the motional signal of the resonance is significantly masked.

Therefore, the one-port configuration of the thermal- piezoresistive resonator often necessitates a post-data processing to extract the motional signal [3]. To overcome the feedthrough issue, in contrast to the previous single crystal silicon resonators [3], the material flexibility of the CMOS-MEMS technology offers decoupling of thermal actuator and piezoresistive sensor, thus removing the resistive feedthrough to improve the floor. As shown in Fig. 3(b), the decoupled configuration utilizing port-1 and port-3 for the thermal drive and piezoresistive sense, respectively, leads to a feedthrough reduction of 30 dB.

Fig. 4 provides the measured transmission spectrum by using differentially thermal drive (port-1 and port-2) and differentially piezoresistive sense (port-3 and port-4). Thanks to the excellent thermal isolation properties of the oxide structure (also a great electrical insulator), the heating performance is well sufficient to drive the resonator into vibration. The dc-bias V_D on the heater and V_S on the piezoresistor are only 0.5 V and 1 V, respectively, thus leading to the total dc power consumption of about 1.25 mW. The measured signal feedthrough floor in this case improves 33 dB as compared To the two-port decoupled scheme of Fig. 3(b), exhibiting a clean resonance with Q of 11,916. Table I provides a comparison of state-of-the-art CMOS-MEMS resonators with various transductions.

Finally, the thermal stability measurement of the devices was performed with results shown in Fig. 5. Since the operation scheme requires the dc-bias currents I_D and I_S through the heater and piezoresistor for driving and sensing, the heating power varies due to the temperature coefficient of resistance (TC_R) of the polysilicon heater. Constant voltage/ current schemes were applied on the polysilicon layer, showing that the constant voltage approach provides better thermal stability due to its positive TC_R . To further improve the thermal stability, the constant resistance technique [5] was also employed with TC_f of only -8.46 ppm/K.

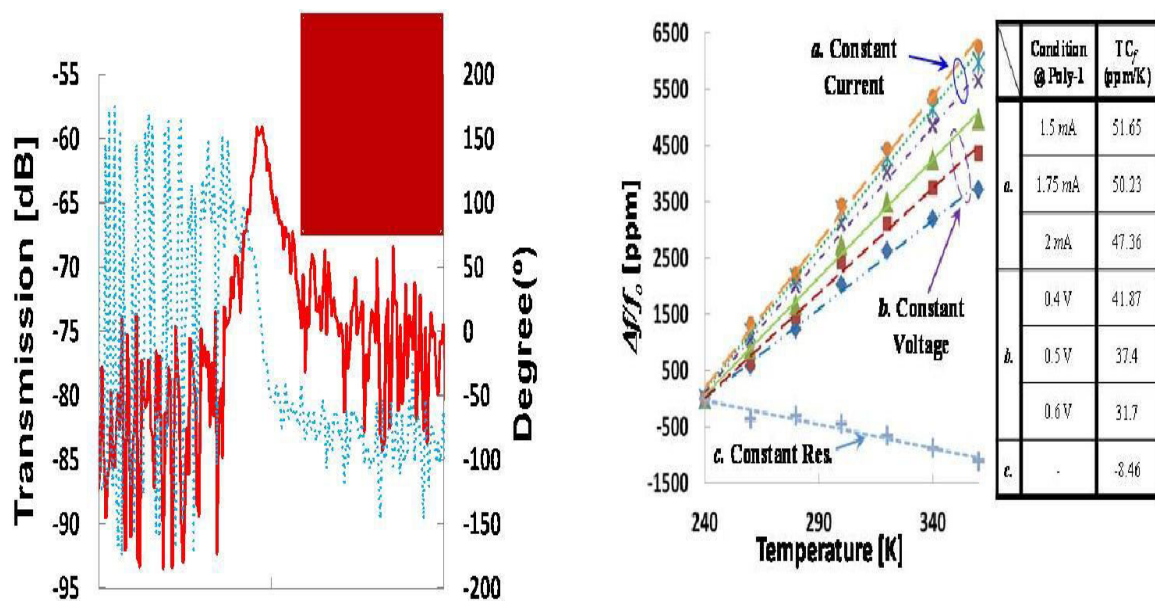


Fig. 4. Measured transmission spectrum under a fully differential measurement configuration depicted in Fig. 1. The insertion loss, 58.5 dB, is referenced to the 50Ω network analyzer port impedance.

Fig.5 Thermal stability measurement under various operations

TABLE I COMPARISON OF CMOS-MEMS RESONATORS

	Parameters	J. T. M. Van Beek [6]	Marigo [7]	Chen [5]	This work
Platform	<i>Driving /Sensing</i>	Cap. /Piezo-R.	Cap. /Cap.	Thermal /Piezo-R.	Thermal /Piezo-R.
	<i>Process</i>	SOI	CMOS	SOI	CMOS
	<i>d_e (μm)</i>	1.3	0.04	No Need	No Need
	<i>Used Materials</i>	Silicon	Poly-Si	Silicon	SiO ₂ / Poly-Si
Measured Characteristics	<i>Mode</i>	Dog-Bone	In-plane FF-Beam	Dog-Bone	Dog-Bone
	<i>f_o (MHz)</i>	10	25	15.48	5.14
	<i>Q</i>	125,000	334	49,539	11,916
	<i>V_p or Bias (V)</i>	80 V _p 0.75(ωsilicon)	7 V _p	1.92	0.5(@p1 / 1(@p2 (368Ω/2.64kΩ)
	<i>1/g_m or R_m (Ω)</i>	11.11k	5M	14.1k	*116.7 k
	<i>Static Power_s (mW)</i>	3.22 (4.3mA)	-	96 (50mA)	1.25 (1.36mA@p1) (0.57mA@p2)
	<i>f_o × Q</i>	1.25 × 10 ¹²	8.35 × 10 ⁹	7.67 × 10 ¹¹	6.17 × 10¹⁰

IV. CONCLUSION

This letter demonstrates a thermally actuated and piezo resistively sensed CMOS-MEMS resonator under very low dc voltage operation. With a fully differential measurement scheme, the resonance peak is clearly resolved in the transmission measurement without the need for de-embedding of the feed through signal. As compared to the capacitive type CMOS-MEMS resonators, this letter offers a CMOS-compatible bias configuration (no need for charge pump), which paves the way for the future integrated thermal-piezo resistive oscillators particularly in sensor applications.

REFERENCES

- [1] I.Bargatin, I.Kozinsky, and M.L.Roukes, "Efficient electrothermal actuation of multiple modes of high-frequency nano electromechanical resonators," *Appl.Phys.Lett*, Vol.90, no.9,p.093116, 2007
- [2] J.H.Seo and O.Brand, "High Q-factor in plane moderesonant microsensor platform for gaseous/liquid environment," *J. Microelectromech. Syst.*, vol. 17, no. 2, pp. 483–493, Apr. 2008.
- [3] A. Rahafruz and S. Pourkamali, "High-frequency thermally actuated electromechanical resonators with piezoresistive readout," *IEEE Trans. Electron Devices*, vol. 58, no. 4, pp. 1205–1214, Apr. 2011.
- [4] A. Rahafruz and S. Pourkamali, "High-frequency thermally actuated electromechanical resonators with piezoresistive readout," *IEEE Trans. Electron Devices*, vol. 58, no. 4, pp. 1205–1214, Apr. 2011.
- [5] C.-C. Chen et al., "Enhancement of temperature stability via constant-structural-resistance control for MEMS resonators," in *Proc. IEEE 26th Int. Micro Electro Mech. Syst. Conf.*, Taipei, Taiwan, Jan. 2013, pp. 765–768.
- [6] J. T. M. van Beek, P. G. Steeneken, and B. Giesbers, "A 10 MHz piezoresistive MEMS resonator with high Q," in *Proc. IEEE IFCS, Miami, FL, USA, Jun. 2006*, pp. 475–480.
- [7] E. Marigo et al., "Zero-level packaging of MEMS in standard CMOS technology," *J. Micromech. Microeng.*

Different Observation –Modes in Fiber Optic- Cable

Mr. C. Sivasathyanarayanan, M.Tech.,(Dept. of Emb.Sys. 1st year) PRIST University,Puducherry .
Mr.G.Mohankumar (HOD), Dept. of ECE, PRIST University, Puducherry.

Abstract: In this project you learn to couple laser light into single mode glass fiber cable and observe different modes in the fiber. The ray picture of light propagating is adequate for describing large-core diameter fibers with many propagating modes, but it fails with only a single mode. For fibers of this type, it is necessary to describe the allowed modes of propagation of light in the fibers.

I. DETAILED DESCRIPTION

A detailed description of the propagation characteristics of an optical fiber can be obtained by solving Maxwell's equations for the cylindrical fiber waveguide. This leads to knowledge of the allowed modes which may propagate in the fiber. This is represented by the equation $V = K_i * a * NA$, where $K_i = 2\pi/\lambda_0$ is the free-space wave number (λ_0 is the wavelength of the light in free space), a is the radius of the core and NA is the numerical aperture of the fiber. The V number is used to characterize which guided modes are allowed to propagate in a particular waveguide structure.

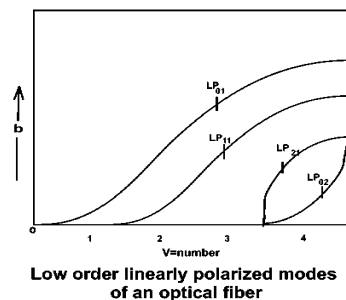
When $V < 2.405$, only a single mode, the HE_{11} mode, may propagate in the waveguide. This is the single-mode regime. The wavelength at which V is equal to 2.405 is called the "cut-off wavelength", because that is the wavelength at which the next higher-order mode is cut off and no longer propagates.

When $V > 2.405$, other modes may propagate in the fiber waveguide. The first such linearly-polarized mode, which comes in at $V = 2.405$, is the LP_{11} mode, the next-lowest order mode in the weakly-guiding approximation.

When V is just slightly greater than 2.405, only the LP_{01} and the LP_{11} modes may propagate. However, when $V = 3.832$, two more linearly-polarized modes are allowed to propagate. These are the LP_{21} mode and the LP_{02} mode.

II. LOW ORDER LINEARLY POLARIZED MODES OF GRAPH

If we have a fiber with the proper V -number, modes higher than one can be selectively launched by varying the position and angle at which a tightly focused beam of proper wavelength is projected onto the fiber core.



When this is done, the near-field of the fiber output can be inspected and the field distribution of the individual modes can be identified.

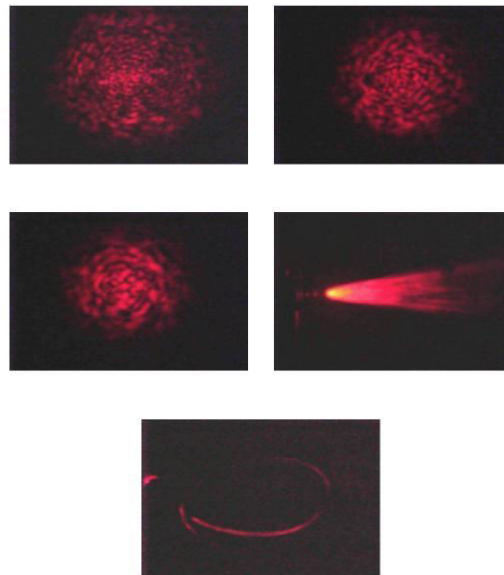
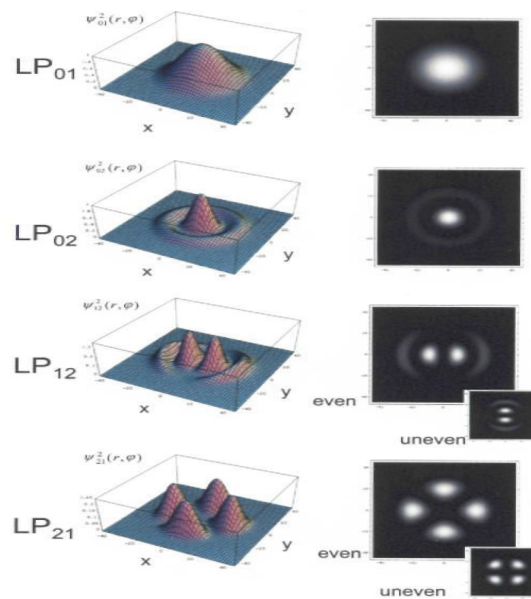


Fig 1 Light Is Divergent

2.1. Multimedia Fiber (output)

The output from a multimode fiber will not emit a uniform, Gaussian output. Instead, it will exhibit speckle pattern. These speckles are caused by interference between many different modes traveling within the fiber. The larger the fiber core size, more are the modes appearing in the fiber output. This pattern of speckles will change with changes in temperature, movement, vibration, and other external factors. If the fiber is only being used as a means of delivering the light energy, then the speckle patterns should not be important.



Transverse structure of several modes in a step index single-mode fiber

The output from a single mode fiber is an almost ideal Gaussian output. Single mode fibers have much smaller core sizes, so they only propagate one mode. The output beam

quality is excellent, with as low as M 5 distortion. However they will not preserve information about the polarization from a fiber. As the fiber is bent, the output polarization changes.

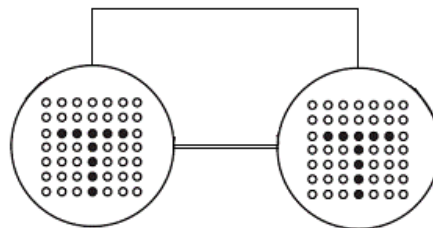
III. COHERENT IMAGE BUNDLE

A large number of fibers put together form what is known as a bundle. If the fibers are not aligned, they are all jumbled up, the bundle is said to be an *incoherent bundle*. However, if the fibers are aligned properly, if the relative positions of the fibers in the input and output ends are the same, the bundle is said to be a coherent bundle. If a particular fiber in this coherent bundle is illuminated at one of its ends, there will be a bright spot at the other end of the same fiber.

Thus a coherent bundle will transmit the image from one end to another (see Figure-A). On the other hand, in an incoherent bundle the output image will be scrambled. Because of this property, an incoherent bundle can be used as a coder; the transmitted image can be decoded by using a similar bundle at the output end. In a bundle, since there can be hundreds of thousands of fibers, decoding without the original bundle configuration would be extremely difficult.

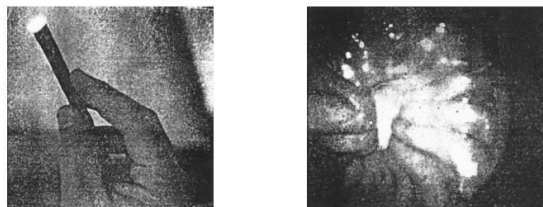
Incoherent bundles are also used in illumination such as in traffic lights or road signs even for lighting applications in buildings wherein the light source is removed from relatively inaccessible areas and fibers are used to guide light from a lamp. They can also be used as cold light sources (light sources giving only light and no heat) by cutting off the heat radiation with a filter at the input to the fiber bundle. The light emerging from the bundle is also free from UV radiation and is suitable for illumination of paintings in museums.

Figure-A



(A) A bundle of aligned fibers. A bright (or dark) spot at the input end of the coherent fiber bundle produces a bright (or dark) spot at the output end. Thus, an image will be transmitted (in the form of bright and dark spots) through a bundle of aligned fibers, forming, for example, the letter T shown above.

Figure-B



(B) An optical fiber medical probe called an endoscope enables doctors to examine the inner parts of the human body. (b) A stomach ulcer as seen through an endoscope

Perhaps the most important application of a coherent bundle is in a fiber optic endoscope where it can be inserted inside a human body and the interior of the body can be viewed from outside. For illuminating the portion that is to be seen, the bundle is enclosed in a sheath of fibers that carry light from outside to the interior of the body (see Figure-B). A

state-of-the-art fiberscope can have about 10,000 fibers, which would form a coherent bundle of about 1 mm in diameter, capable of resolving objects 70 μm across. Fiber optic bundles can also be used for viewing internal machine parts that are otherwise inaccessible.

Coupling light into a multimode fiber is relatively easy; however maximizing the coupling to a single-mode fiber is much more difficult. In addition to very precise alignment of the fiber to the incoming beam, it is necessary to match the incident electromagnetic field distribution to that of the mode which will be propagated by the fiber.

Single mode source couplers use high quality, AR coated, diffraction limited lenses, and precision tolerance receptacles. Focusing lenses are selected for optimum coupling efficiency for particular beam characteristics. The laser cavity is sensitive to back reflection. Reflections from either the input or output fiber end cause feedback within the laser cavity, causing the laser output to change in both intensity and frequency.

Back reflection problems can be reduced in one of three ways. First, an isolator can be added between the laser and the coupler. Unfortunately this method is often very expensive. Hence AR coated lenses that have no flat surfaces are used. Couplers are designed to operate over a temperature range of -35 X to +65 X. They have also been used in heavy vibration environments, such as helicopters. To achieve optimum coupling and stability, it is very important that the tilt alignment be securely locked using the locking screws on the coupler.

IV LIGHT GUIDANCE THROUGH OPTICAL FIBERS EXPERIMENTAL VIEW – TRANSMITTING LIGHT BEAM.

Take a 2-meter length or so of optical fiber—preferably a large-diameter plastic optical fiber—and make perpendicular cuts at both the ends. Couple light from a laser pointer into one of the ends and see for you how the light is guided through the fiber. If the room is dark, you should be able to observe the entire fiber glowing all along its length due to scattering (Rayleigh scattering). Observe the light emerging from the other end of the fiber. Try tying the fibers in a knot and you will notice that light still is guided, in spite of the severe bend of the fiber. If you use a long reel of the optical fiber, you should still see the emerging light at the other end and the glow along the entire reel. Figure C & D shows.

Fig 2 Typical Setup

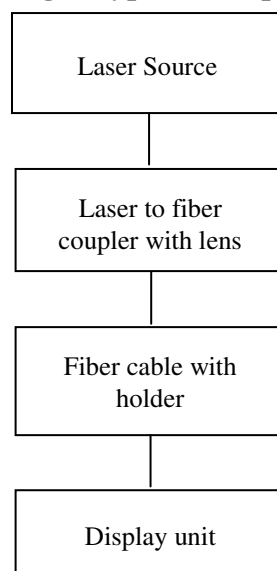


Fig 3 Experimentation categories of fiber cable visual imaging method

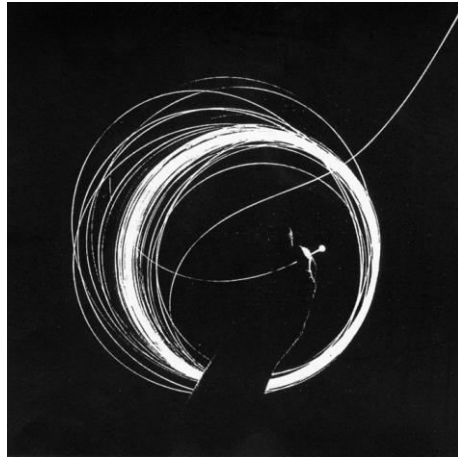
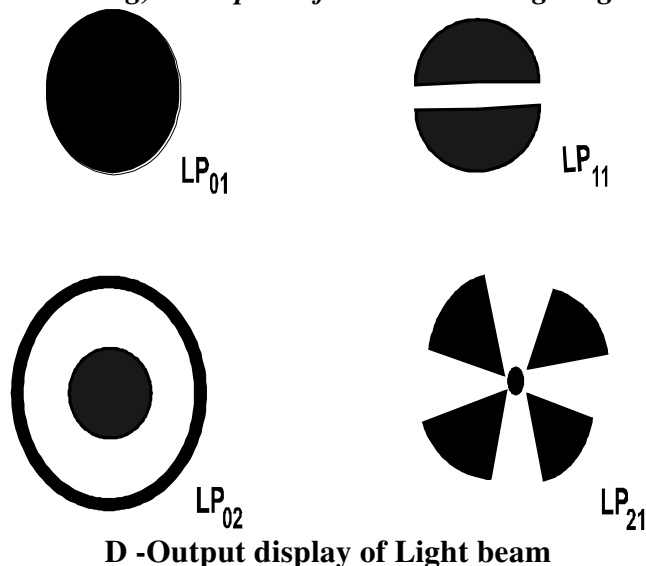


Fig 4 C -A long, thin optical fiber transmitting a light beam



V DIFFERENT (SINGLE MODE & MULTI MODE) BETWEEN TWO KINDS OF FIBERS

Take short pieces (~ 2 m) of a multimode optical fiber and a single-mode optical fiber. Focus the light from a HeNe laser onto the input end of the fiber using a lens such as a microscope objective, and observe the output by projecting it onto a white screen. The output from the multimode fiber will show a speckle pattern while that from a single-mode fiber will show a very uniform beam much like the output from a good laser. In the former case, the light propagates via a large number of modes, and the interference between the various modes causes the speckle pattern.

VI IMAGE SENSING PROPERTY OF OPTICAL FIBERS.

Perform the previous demonstration using a multimode fiber reel by fixing the entire setup on a table and observing the output speckle pattern as you bring your hand close to the optical fiber reel. The warmth of the hand is enough to change the phase difference between the interfering modes, which in turn changes the interference pattern. The speckle pattern will

keep changing as you move your hand closer to and farther from the reel. If you try to press or twist the fiber, you will immediately notice the change in the speckle pattern. Such changes in the pattern due to external influence demonstrate in a very simple fashion the possibility of using optical fibers for sensing.

VII RAYLEIGH SCATTERING IN AN OPTICAL FIBER.



Rayleigh scattering is responsible for the blue color of the sky and the red color of the setting sun. It is very interesting to demonstrate the wavelength dependence of Rayleigh scattering using a long optical fiber. Couple white light from a lamp, such as a tungsten halogen lamp emitting white light, into a 1-km length or so of multimode optical fiber and look into the output. Notice the color of the light. Cut the fiber, leaving about 1 m from the input end of the fiber, and repeat the experiment with this 1 m of fiber. You will see that, in the former case, the emerging light looks reddish while in the latter case it looks white.

This difference is due to the *decrease of loss with increase in wavelength* due to Rayleigh scattering. Thus, shorter wavelengths toward the blue region have suffered greater scattering out of the fiber than longer wavelengths near the red region. Even though all wavelengths at the input end are coupled, there is more power in the red part at the output end, thereby giving the light a reddish color.

VII CONCLUSION

A preform is Mode image view used to draw an optical fiber Cable. The preform may consist of several pieces of a glass Cable and plastic cable with different refractive indices, to provide the core and cladding of the fiber cable image. The shape of the preform may be circular, although for some applications such as double-clad fibers another form is preferred. Wavelengths of light are transmitted through the doped fiber cable & Different mode will be displayed in the Unit.

REFERENCE

1. D. Gloge, "Optical power flow in multimode fiber," Bell Sys. Tech. J., vol. 51, no. 8, pp. 1767–1780, 1972.
2. R. Olshansky, "Mode-coupling effects in graded-index optical fibers," Appl. Opt., vol. 14, no. 4, pp. 935–945, 1975.
3. H. R. Stuart, "Dispersive multiplexing in multimode optical fiber," Science, vol. 289, pp. 281–283, 2000.
4. H. R. Stuart, "Dispersive multiplexing in multimode optical fiber," Science, vol. 289, pp. 281–283, 2000.
5. Y. Koike and S. Takahashi, "Plastic optical fibers: Technologies and communication links," in Optical Fiber Telecommunications VB: Systems and Networks, I. P. Kaminow, T. Li, and A. E. Willner, Eds. San Diego, CA: Academic, 2008.
6. J. P. Gordon and H. Kogelnik, "PMD fundamentals: Polarization mode dispersion in optical fibers," Proc. Natl. Acad. Sci., vol. 97, no. 9, pp. 4541–4550, 2000.
7. Ajoy Ghalak & K. Thyagarajan "Optical Wave guides and Fibers" Fundamental of Photonics, © 2000 University of Connecticut, Viva Book Pvt. Ltd.,
8. P. P. Mitra and J. B. Stark, "Nonlinear limits to the information capacity of optical fibre communications," Nature, vol.

411, pp. 1027–1030, 2001.

9. M. Salsi, C. Koebele, D. Sperti, P. Tran, P. Brindel, H. Margoyan, S. Bigo, A. Boutin, F. Verluise, P. Sillard, M. Bigot-

Astruc, L. Provost, F. Cerou, and G. Charlet, “Transmission at 2 100 Gb/s, over two modes of 40 km-long prototype

few-mode fiber, using LCOS based mode multiplexer and demultiplexer,” presented at the Opt. Fiber Commun., Los

Angeles, CA, 2011, Paper PDPB9.

10. M. Salsi, C. Koebele, D. Sperti, P. Tran, P. Brindel, H. Margoyan, S. Bigo, A. Boutin, F. Verluise, P. Sillard, M.

Bigot-Astruc, L. Provost, F. Cerou, and G. Charlet, “Transmission at 2 100 Gb/s, over two modes of 40 km-long

prototype few-mode fiber, using LCOS based mode multiplexer and demultiplexer,” presented at the Opt. Fiber

Commun., Los Angeles, CA, 2011, Paper PDPB9.

An Enhanced Speech Based Vmail for Visually Impaired People

P.Dhivya¹, S.Hemalatha², M.Keerthana³

^{1,2,3} U.G. Scholar, Department of Computer Science & Engineering

V.R.S.College of Engineering & Technology

¹ rajuranjith1@gmail.com, ² hemalatha2710@gmail.com, ³ manikamkeerthana@gmail.com

Abstract— In today's reality correspondence has turned out to be so natural because of coordination of correspondence innovations with web. However the outwardly tested individuals discover it extremely hard to use this innovation in view of the way that utilizing them requires visual observation. Voice message building design blinds individuals to get to email and other interactive media elements of working framework (tunes, text). Also in versatile application SMS can be perused by framework itself. Presently a days the headway made in PC innovation opened stages for outwardly weakened individuals over the world. This paper goes for adding to an email framework that wills even an innocent outwardly impeded individual to utilize the administrations for correspondence without past preparing. This building design will likewise diminish subjective burden taken by heedless to recall and sort characters utilizing console. This framework can be utilized by any ordinary individual likewise for instance the person who is not ready to peruse. The framework is totally taking into account intelligent voice reaction which will make it easy to understand and proficient to utilize.

Keywords - IVR, Mouse click event, Screen reader, Voice Mail.

I. INTRODUCTION

Web is considered as a noteworthy storage facility of data in today's reality. No single work should be possible without the assistance of it. It has even ended up one of the defacto systems utilized as a part of correspondence [1]. With a specific end goal to get to the web you would need to comprehend what is composed on the screen. In the event that that is not noticeable it is of no utilization. This makes web a totally futile innovation for the outwardly impeded and uneducated individuals. They can't get to their mail and can't send a mail. Indeed, even the frameworks that are accessible right now like the screen per users TTS and ASR don't give full proficiency to the visually impaired individuals in order to utilize the web. As almost 285 million individuals overall are assessed outwardly disabled it get to be important to make web offices for correspondence usable for them too.

Hence we have thought of this undertaking in which we will be adding to a voice based email framework which will help the outwardly impeded individuals who are guileless to PC frameworks to utilize email offices in a bother free way [16]. The clients of this framework would not need any fundamental data with respect to console alternate routes or where the keys are found. All capacities depend on basic mouse click operations making it simple for a client to utilize this framework [9], [11]. Additionally the client need not stress over recollecting which mouse click operation he/she needs to perform keeping in mind the end goal to profit a given administration as the framework itself will be provoking them as to which snap will give them what operations. A novel Voice based Search Engine and Web page Reader which allows the users to command and control the web browser through their voice, is introduced [4], [12].

When issuing commands or correcting dictated text, it is vital to be confident that what you say is correctly recognized. If you manage to correct every mistake the recognition rate will

improve, otherwise it may actually get worse [14]. The most well-known mail benefits that we use in our everyday life can't be utilized by outwardly tested individuals. This is on the grounds that they don't give any office so that the individual in front can hear out the substance of the screen [3]. As they can't imagine what is as of now present on screen they can't make out where to click so as to perform the required operations. For an outwardly tested individual utilizing a PC for the first time is not that advantageous as it is for a typical client despite the fact that it is easy to use. Several English words for particular Bangla word in the grammar file of SAPI is found to overcome tone variation of persons as well as pronunciation variation in language communities and shown to improve overall performance of the system [5]. Despite the fact that there are numerous screen per users accessible then likewise these individuals confront some minor troubles. Screen per users read out whatever substance arrives on the screen and to perform those activities the individual will need to utilize console easy routes as mouse area can't be followed by the screen per users. Several approaches are presented to reduce the distortions due to diphone concatenation [15]. They are based on appropriate manipulations of the phase spectrum, either by phase equalization across all the diphones, or by phase smoothing between successive diphones [6], [10]. This implies two things; one that the client can't make utilization of mouse pointer as it is totally badly arranged if the pointer area can't be followed and second that client should be knowledgeable with the console as to where each furthermore, every key is found.

A client is new to PC can along these lines not utilize this administration as they don't know about the key areas. Email

Clients desktop or web -based interfaces for accessing and working with email [2]. Another downside that sets in is that screen per users read out the substance in consecutive way and in this manner client can make out the substance of the screen just on the off chance that they are in fundamental HTML design [7], [8]. Accordingly the new propelled site pages which don't take after this worldview keeping in mind the end goal to make the site easier to understand just make additional bothers for these individuals. This system can be used as an aid for the people who suffer with visual impairment. It helps us to convert written Telugu text to audio files and play them. The user can receive, compose and send a mail to another VMAIL user [13]. All these are a few disadvantages of the present framework which we will overcome in the framework we are creating.

II. PROPOSED SYSTEM

The most vital perspective that has been remembered while adding to the proposed framework is availability. A web framework is said to be impeccably available just on the off chance that it can be utilized proficiently by a wide range of individuals whether capable or cripple. The present frameworks don't give this availability. Consequently the framework we are creating is totally unique in relation to the present framework. Our framework concentrates more on ease of use of a wide range of individuals including ordinary individuals outwardly weakened individuals and additionally unskilled individuals. The complete framework depends on IVR-intuitive voice reaction. One of the significant focal points of this framework is that client won't require to utilize the console. All operations will be in view of mouse snap occasions. Presently the inquiry that emerges is that in what manner the visually impaired clients will discover area of the mouse pointer. As specific area can't be followed by the visually impaired client the framework, which kind of snap will perform which capacity will be indicated by the IVR. This framework will be superbly open to a wide range of clients as it is simply in view of straightforward mouse clicks and discourse inputs and there is no compelling reason to recollect console easy routes.

2.1. Client Interface Design

The client interface is planned utilizing Adobe Dream weaver CS3. The complete site concentrates more on effectiveness in understanding the IVR instead of the look and feel of the framework as the framework is fundamentally created for the visually impaired individuals to whom the look and feel won't be of that essential significance as the effectiveness of comprehension the provoking would be.

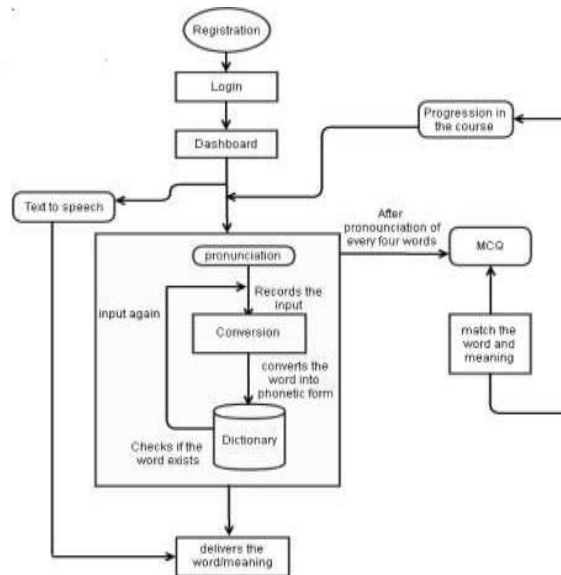


Fig.1 User interface design

2.2. Database Design

Our framework keeps up a database for client acceptance and putting away sends of the client. There is a sum of five tables. The relationship between them is doled out after much thought. The Inbox, Sent-Mail and Trash mappings will store all sends of the particular administration that has a place with that specific client.

2.3. Framework Design

Fig.2 delineates the complete framework plan. It is the level-2 information stream graph which gives complete itemized stream of occasions in the framework. As should be obvious all operations are performed by mouse click occasions just. Additionally at some places voice information is required.

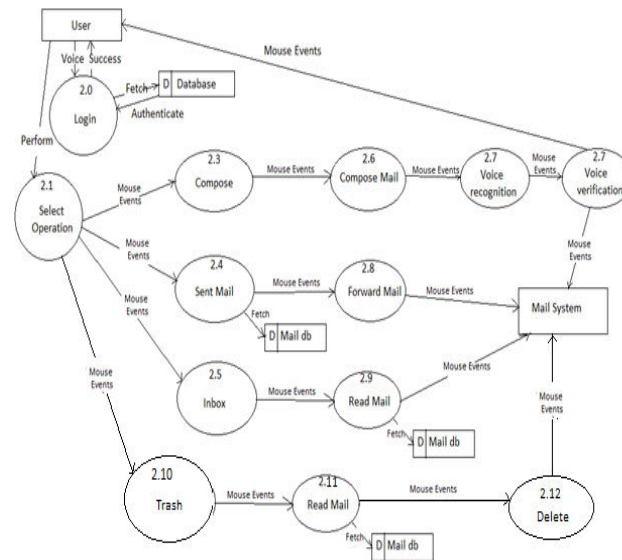


Fig .2 Framework design for our system

2.3.1. Registration

This is the first module of the framework. Any client who wishes to utilize the framework ought to first enlist to acquire username and secret word. This module will gather complete data of the client by provoking the client as whatever subtle elements should be entered. The client should talk up the points of interest to which the framework will once more affirm by provoking sequentially. In the event that the data is not remedy client can re-enter else the brief will determine the operation to be performed to affirm.

2.3.2. Enlistment Page

Once the enrollment is done the client can login to the framework. This module will request that the client give the username and secret key. This will be acknowledged in discourse. Discourse transformation will be done to content and client will be advised to approve whether the subtle elements are entered accurately or not. Once the passage is done effectively database will be checked for passage. In the event that the client is approved it will be coordinated to landing page.

2.3.3. Login

Once the registration is done the user can login to the system. This module will ask the user to provide the username and password. This will be accepted in speech. Speech conversion will be done to text and user will be told to validate whether the details are entered correctly or not. Once the entry is done correctly database will be checked for entry. If the user is authorized it will be directed to homepage.

Fig.3 Enlistmentpage diagram

Fig.4 Login diagram

2.3.4. Overlooked Password

On the off chance that where an approved client overlooks the secret word and consequently is not ready to login he/she can choose overlooked secret word module. In this module the client will be first advised to enter username. As indicated by username the security question will be sought in database. This is the issue gave at time of enlistment. The inquiry will be stood up by the PC. The client ought to thus indicate the answer that was given by him/her amid enlistment. On the off chance that both get coordinated, client is offered alternative to change watchword.

III. HOME PAGE

The client is diverted to this page once sign in done effectively. From this page now the client can perform operations that the client wishes to perform. The choices accessible are:

1. Inbox
2. Create
3. Sent mail
4. Garbage

3.1. Client Authentication System

In client confirmation module client needs to give login data, for example, his/her username, secret word through voice order. For Blind clients, all operation performed will get a voice based criticism. There are choices to spare a specific clients profile so that the client does not need to enter the same points of interest once more.

3.2. GUI Accessing By Using Voice Command and Mouse Keypress

The GUI operation access by utilizing voice order and mouse operation performed by the client as opposed to looking the alternate way key from the console. The client can apply the same console charge by performing distinctive mouse operation and voice operation in our framework every voice operation mapping to certain console operation furthermore voice operation map with certain console operation. This mouse operation can be change effectively. Some illustration of mapping guidelines is appeared in table I as underneath.

3.3 Inbox

This choice offers the client some assistance with viewing every one of the sends that has been gotten to his/her record. The client can listen to sends he/she needs to by performing the snap operation determined by the brief. With a specific end goal to explore through distinctive sends brief will determine which operations to perform. Every time the mail is chosen the client will be provoked as whom the sender is and what the subject of that specific mail is. Appropriately client can choose whether the mail should be perused or not or it ought to be erased. Erased sends will be spared in waste area. By performing the snap operation determined by the brief. With a specific end goal to explore through distinctive sends brief will determine which operations to perform. Every time the mail is chosen the client will be provoked as whom the sender is and what the subject of that specific mail is. Appropriately client can choose whether the mail should be perused or not or it ought to be erased. Erased sends will be spared in waste area.

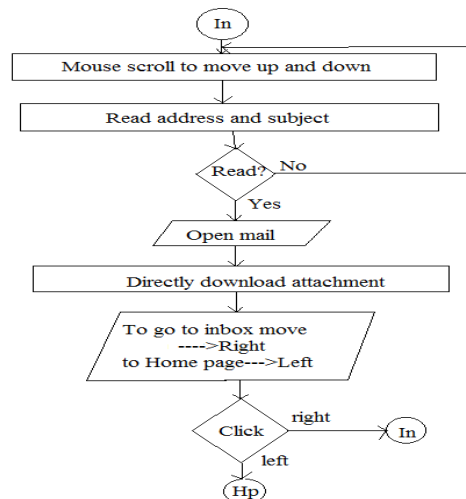


Fig. 5 Flow chart for inbox

3.4. Create Mail

This is a standout amongst the most imperative alternatives gave by the mail administrations. The usefulness of create mail choice would not coordinate the effectively existing mail framework. Since the framework is for outwardly tested individuals and console

operations are totally abstained from creating mail would just be done on voice include and mouse operations. No written information will be required. Client can straightforwardly record message that should be proliferated and can send it. This voice back rub will go in type of connection. The beneficiary can hear the recording and get the message client needed to send. Client would not require appending the record. Record alternative will be given in the form window itself. Once recorded it will affirm whether the recording is consummate or not by letting the client hear it and if the client affirms it will be naturally joined to the mail.

3.5. *Sending mail*

In send letters module the form window will open; the client has choice of either to record a voice message or to sort content. So as to record a voice message a client can either tap on the —Initialize Recording catch or can press the mouse right catch anyplace on the screen. The GUI of the framework has been planned in a manner that gruffly of the position of the mouse pointer, the mouse click operation will be enrolled and the framework will work in like manner. With a specific end goal to stop the recording, again the client can either tap on the End Recording catch or discharge the mouse right catch anyplace on the screen i.e. the pressing so as to record has been introduced the mouse right snap catch. Once the recording is done, the framework will request that the client select the beneficiaries street number. This is finished by perusing out all the mail ids of the sender one after another in order. Once the beneficiary mail id is entered, the framework will provoke the client to send the mail or to drop the operation. Keeping in mind the end goal to send the mail the client can either press the send mail catch or Left tap on the mouse to send the mail. We will characterize all the mouse click operations in subtle elements in the accompanying areas.

TABLE I
MOUSE CLICK OPTIONS

Mouse Click And Voice Command Operation Mouse Click	Operation Performed	Voice Command
Right single	Compose Mail	Compose
Right double	Cancel Mail	Cancel
Right triple	NOP	NOP
Left single	Check Inbox	Open Inbox
Left double	Send Mail	Send
Left triple	NOP	NOP
Mouse Scroll Up	Select Next Mail	Next mail
Mouse Scroll Down	Previous Mail	Previous mail
Middle single	Attach Document	Attach
Middle single	Discard	Discard

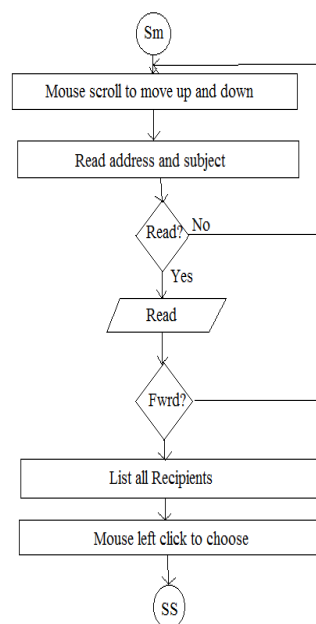


Fig.6 Flow chart for send mail

3.6. Waste

This alternative will keep a track of the considerable number of sends erased by the client. Erased sends could be the ones from inbox or sent mail. In the event that whenever the client needs to recover a mail which was erased it should possible from this option.

IV.CONCLUSION

The main reason for developing this system described in the paper is to create ease for visually impaired people to use the most pervasive form of communication in today's world email. This mail system will help overcoming all the minor difficulties which are faced by visually impaired people as the system works on vocal abilities. This will reduce the software load of using screen readers and automatic speech recognizer and also the user's cognitive load of remembering keyboard shortcuts. The system will be guiding the user as to what operation needs to be performed for obtaining desired results through IVR thus making the system much user friendly.

REFERENCES

- [1] The WHO website. [Online]. Available :<http://www.who.int/media/centre/factsheets/fs282/en/>.
- [2] The Radicati website. [Online]. Available: [http://www.Radicati.com/wp/wpcontent/uploads/2014/01/Email Statistics -Report-2014-2018-Executive-Summary.pdf](http://www.Radicati.com/wp/wpcontent/uploads/2014/01/Email%20Statistics%20Report%202014-2018-Executive-Summary.pdf).
- [3] JagtapNilesh, Pawan Alai, Chavhan Swapnil and Bendre M.R. . "Voice Based System in Desktop and Mobile Devices for Blind People". In International Journal of Emerging Technology and Advanced Engineering (IJETA), 2014 on Pages 404-407 (Volume 4, issue 2).
- [4] Ummuhanyifa U.NizarBanu P K, "Voice Based Search Engine and Web page Reader". In International Journal of Computational Engineering Research (IJCER).Pages 1-5.
- [5] Sultana, S.; Akhand, M. A H; Das, P.K.; Hafizur Rahman, M.M., "Bangla Speech-to-Text conversionusing SAPI," Computer and Communication Engineering (ICCCE),2012 International Conference on ,vol., no., pp.385,390, 3- 5 July 2012.
- [6] F.; Moulines, E., "Text-to-speech algorithms based on FFT synthesis," Acoustics, Speech, and Signal Processing,1988. ICASSP-88., 1988 International Conference on , vol., no., pp.667,670 vol.1, 11-14
- [7] T. Lauwers, D. Dewey, N. Kalra, T. Stepleton, and M.B.Dias. Iterative design of a braille writing tutor to combat illiteracy. In Information and Communication Technologies and Development, 2007. ICTD 2007.

- International Conference on, pages 1–8. IEEE, 2007.
- [8] A.King, G. Evans, and P. Blenkhorn. Webbie: a web browser for visually impaired people. In Proceedings of the 2nd Cambridge Workshop on Universal Access and Assistive Technology, Springer-Verlag, London, UK, pages 35–44. Citeseer, 2004.
 - [9] P. Verma, R. Singh, A.K. Singh, V. Yadav, and A. Pandey. An enhanced speech-based internet browsing system for visually challenged. In Computer and Communication Technology (ICCT), 2010 International Conference on, pages 724–730. IEEE, 2010.
 - [10] Chung -Hsien Wu and Jau- Hung Chen. Speech activated telephony email reader (sater) based on speaker verification and text – to –speech conversion, IEEE Transactions on Consumer Electronics, Vol. 43, No. 3, AUGUST 1997.
 - [11] Nuno Baptista, Rui Prior, Manuel E. Correia. Telephone Interface for the Email Service, Computation World: Future Computing, Service Computation, Cognitive, Adaptive, Content, Patterns, 2009
 - [12] Gaurav Anand, Geethamsi S, Mr. R V R Chary, CH.Madhu Babu. Email Access By Visually Impaired, International Conference on Communication Systems and Network Technologies, 2013
 - [13] K.V.N.Sunitha, N.Kalyani. VMAIL - Voice Enabled Mail Reader, International Conference on Recent Trends in Information, Telecommunication and Computing, 2010.
 - [14] Halimah B.Z. , Azlina A. , Behrang P., Choo W.O. Voice Recognition System for the Visually Impaired: Virtual Cognitive Approach, 2008.
 - [15] Brian G., Taylor H. (2001). "Cataract Blindness – Challenges for the 21st Century". Bulletin Of the World Health Organization 79 (3): 249–56.
 - [16] Global Data On Visual Impairments 2010 (PDF). WHO. 2012. p. 6.

Design of Modified Architecture for Adaptive Viterbi Decoder

VENKATESAN¹, G.MAHENDIRAN², R.RADHAKRISHNAN³

¹ Faculty ECE, St. Anne's College of Engineering and Technology, vv2620@gmail.com

² Faculty ECE, St. Anne's College of Engineering and Technology, mahe15.indiran@gmail.com

³ Faculty ECE, St. Anne's College of Engineering and Technology, rocky.radha@gmail.com

Abstract: The demand for high speed, low power and low cost for Viterbi decoding especially in wireless communication are always required. Thus the paper presents the design of an adaptive Viterbi decoder that uses survivor path with parameters for wireless communication in an attempt to reduce the power and cost and at the same time increase the speed. The decoder was simulated using MULTISIM. The adopted design was coded in VHDL. The results show that speed has been increased since the processing execution time has been reduced. The survivor path decoder is capable of supporting frequency up to 790MHz. Finally, the cost has been reduced and the processing time of computing the correct path.

1. INTRODUCTION

Most digital communication systems nowadays convolutionally encoded the transmitted data to compensate for Additive White Gaussian Noise, fading of the channel. For its efficiency the Viterbi algorithm has proven to be a very practical algorithm for forward error correction of convolutionally encoded messages. Most of the researches work to reduce cost, the power consumption, or work with high frequency for using the decoder in the modern applications such as 3GPP, DVB.

First Method for back trace unit is to find the correct path, and the other trying to work with high frequency by using parallel operations of decoder units. Thus the paper attempts to Design an adaptive Viterbi decoder that uses survivor path storage with parameters for wireless communication. Analyze and simulate the decoders by comparing the different models performances using MULTISIM. Design and implement the decoder using Xilinx system generator modeling tool. Evaluate the decoder for timing accuracy and resource utilization.

2. ADAPTIVE VITERBI DECODER (AVD)

The aim of the adaptive Viterbi algorithm is to reduce the average computation and path storage required by the Viterbi algorithm. A threshold T indicates that a path is retained if its path cost is less than $d_m + T$, where d_m is the minimum cost among all surviving paths in the previous trellis stage. The total number of survivor paths per trellis stage is limited to a fixed number, N_{max} , which is preset prior to the start of communication. The first criterion allows a high cost paths, likely do not represent the transmitted data to be eliminated from consideration early in the decoding process. In the case of many paths with similar cost, the second criterion restricts the number of paths to N_{max} . At each stage, the minimum cost of the previous stage d_m , threshold T , and maximum survivors N_{max} are used to prune the number of surviving paths. If the threshold T is set to a small value, the average number of

paths retained at each trellis stage will be reduced. This can result in an increased BER, since the decision on the most likely path has to be taken from a reduced number of possible paths. As a result, there are increased decoded acronyms at the expense of additional computation and a large path storage memory.

A high level view of the implemented adaptive Viterbi decoder architecture is shown in Fig. 1. The decoder contains a data path and an associated control path. Like most Viterbi decoder, the data path is split into four parts: the Branch Metric Generator, Add Compare Select units, the survivor memory unit, and path metric storage and control. A BMG unit determines path costs and identifies slowest cost paths. The survivor memory stores lowest cost bit sequence paths on decisions made by the ACS units, and the path metric array holds per state path metrics. The flow of data in the data path and the storage of results are determined by control path.

2.1 Input / Output Data

The input data of the decoder are three parallel bits represents the information data and the control signal of the Viterbi decoder processing with the CLK which is a standard input signal to the input port of the decoder. Furthermore, the OE_In is a control signal that enables the input of the decoder and the last input is the OE_out control signal that enables the output of the decoder.

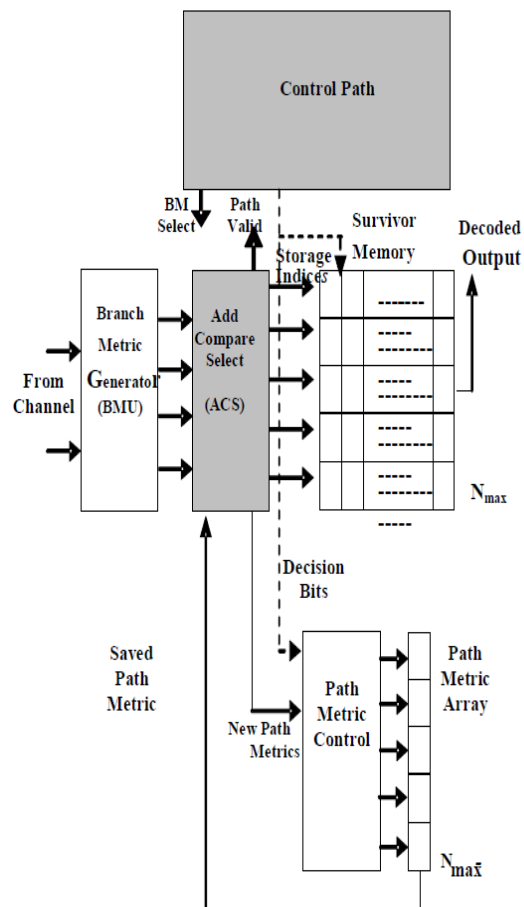


Fig-1 Adaptive viterbi Decoder

2.2 Branch Metric Unit (BMU)

The responsibility of this unit is to compute the Hamming code between the expected code and the receiving code as a frame. Each frame contains four symbols. At each processing, the BMU finds the Hamming code for these four symbols. This will be compared with the expected code represented by the address value that replaced by a counter started with '0000' to '1111'. At each step, the Hamming code is computed and the total value is stored in the Hamming code buffer, ST in the ST buffer, and counter value in the address buffer.

Therefore more execution time will be required to find the suitable path and to select the output code. The parallel operation of these steps becomes more efficient to reduce the execution processing time. The parallel execution can be divided into two types. The first type involves parallelism to compute the Hamming code in the 8th probability paths, and this type needs four BMUs. Each BMU is responsible for the computation of the Hamming code of a suitable received symbol with the expected code. The four symbols, given a probability path starting from path '0000' to '1111', need an even path for computing the Hamming codes of all nodes. This model for parallel computing needs a memory bank RAM to store the Hamming code of each node. It is clear that this design will be more complicated and need more elements to represent this model. Therefore, it has not been considered in the proposed design.

2.3 The Add Compare Select Unit

This Add Compare select unit is the main unit of the survivor path decoder. The function of this unit is to find the addition of the four Hamming codes received from BMUs and to compare the total Hamming code stored in the HC_buffer for the even and odd paths. This unit also compares the values and stores the minimum Hamming code and the counter value. At the end of the 8th even state, the minimum Hamming code and the counter value are stored in HC_buffer and AD_buffer. The AD_buffer represents the opposite output code. The other value stored in ST_buffer represents the address of the next state number. For each four symbols selected, the initial value of HC_buffer is set to '1100' and compared to find the minimum value. The 3 bits counter is used in the ACSU and SMU. The same counter will be used in the SMU to lead the address ROM to find the correct state number and expected code for the next state.

2.4 Adding process

The adder block computes the total sum of the three Hamming codes with the output value of multiplexer. The three 2 bits Hamming codes with 1 bit output of the multiplexer are added and the output of the adder is formed by 4 bits and sent to the comparator unit. At the beginning of each four symbols, the HC_buffer is set to '1100' which represents the maximum value of the Hamming codes for 4 symbols, because the maximum Hamming code of each symbol is '11'.

2.5 Comparing Process

The comparator receives two codes, the first came from the adder which represents the additive of the Hamming code, and the second came from the HC_buffer. The value stored in this buffer is initiated to '1100' and updated through the processing. The

updated is executed while the value entered to the comparator from the adder is less than the value stored in the buffer. Generate an enable signal which will be able to replace the old value store in the HC_buffer with the new small value came from adder. Store the state number in the ST_buffer which perform the ADDRESS value of the Viterbi ROM. Store the value of the counter in the output code buffer. Give a clock signal to the counter to generate the next counters value. The new value of the counter will allow the ACSU to start with the next values of the Hamming codes and repeated all the above processing. The last processing of ACSU started at the last counter value '111'.

2.6 Output process

The output process is started at the counter value equal to '111'. At this value all of the above processing steps are finished and the paths starting from path '0000' and end at path '1111' were computed. The ST_buffer contains the ADDRESS ROM of the next state, and the output code represents the opposite code of the counter that contains the minimum Hamming code of four encoded symbols. The output code represents the decoded bits of these symbols. The enable signal of the ST_buffer and output code come from the output of AND gate become '1' at the three input bits '111' the end value of the counter. The enable signal can to be able to move the ST_buffer and output code to the execution state of the decoder.

3 ST PROCESS

Initially, the ST value came from the ACSU. This value is the same at each code of the counter for the same four symbols and will be changed after the ending of 16th paths. Another value of ST is reached from the ST0 ROM. The multiplexer selects which one is available at a time. At any value of counter, the ST is still the same but through the execution steps of each counter code the ST value is arrived from the ST0 ROM and changed 4 times in each counter code.

3.1 Expected code process

The expected code is received from EC0 ROM with the suitable ADDRESS. In this process the expected code read from the ROM will be transferred to the 3 bits shift register. The serial bits moved from 3 bits shift register to the 12 bits shift registers, at the end process of the expected code computation with four steps. The 12 bits shift register contains the all expected code of four steps. The first 3 bits represent the expected code for the first step, the second 3 bits is the expected code for the second steps, and so on. The 12 bits are moved to the BMU to be compared with the suitable codes.

4 SYSTEM SIMULATIONS

The simulation results of the survivor path algorithm are obtained. The path lengths are varied from 3 to 6, for these simulations, the length may be more than 6. Therefore, the size of the survivor memory, and the computing time will be increased. The increasing of the survivor path lengths didn't affect the coding gain compared with that of increasing the, complexity, RAM size, and computing time. The coding gain of the proposed Viterbi decoder for 1bit/symbol is about 3.5 dB, 4.5 dB and 5 dB for survivor path lengths of 3, 4, and 6, respectively. On the other hand, for 2 bit symbol the coding gain is approximately varying from 7.5dB at survivor path length 3 to 8 dB at survivor path length of 6.

5 THE POWER REPORTS

The following reports give the information of the power consumption of Viterbi core.

Total estimated power usage: 0.213W

Estimated junction temperature: 27 C

6 CONCLUSIONS

New Viterbi decoder architecture has been proposed. The architecture is simple and suitable for very high data rate decoding, reconfigurable the Viterbi decoders units adding a unit called Viterbi ROM. The structure is used to store all the possible paths and expecting code for all states. The model used the survivor path storage to store the probability paths and select the correct path. Reconfigure the Viterbi decoder, and adaptive Viterbi decoder units will give simple elements in each unit and new algorithms.

REFERENCES

1. Y. Gang, A. T. Erdogan, and T. Arslan, "An efficient pre-traceback architecture for the Viterbi decoder targeting wireless communication applications," IEEE Trans. Circuits Syst. I, Reg. Papers, vol. 52, no. 6 pp.1148–1156, Jun, 2005.
2. Jan.M.Rabaey, "Wireless beyond the third generation facing the energy challenge," in ISLPED Proceedings of the International Symposium on Low Power Electronics and Design, August 2001.
3. Obeid A. M., Ortiz A. G., Ludewig R., and Glenser M., "Prototype of a high performance generic Viterbi decoder", Proceedings. 13th IEEE International Workshop on Rapid System Prototyping I 2002.
4. S.W.Shaker, S.H.Alamely and K.A.Shehata, "Design and implementation of low-power Viterbi decoder for software-defined WiMAX receiver", 17th Telecommunication Forum TELFOR, Serbia, Belgrade, 2009.

Adaptive Hardware Design for Computing Efficient Singular Value Decomposition in MIMO-OFDM System

Vaidehi. M¹, Umamaheswari. D²

¹Faculty, ECE Department, St.Anne's CET, vaidehi.divakaran@gmail.com

²Faculty, ECE Department, St.Anne's CET, amarkavibalu@gmail.com

Abstract: This paper presents an adaptive hardware design for computing Singular Value Decomposition (SVD) of the radio communication channel characteristic matrix and is suitable for computing the SVD of a maximum of 4×4 real-value matrices used in (multiple input Multiple output) MIMO-OFDM(orthogonal frequency division multiplexing) standards, such as the IEEE 802.11n applications. Hence the data is transmitted without any interference from the transmitting antenna. Also the data obtained is more reliable. The proposed method is able to deal with any matrix size implementation and is able to deal with several channel matrices. The information of the right singular-vector matrix can be fed back to the transmitter for beam forming to improve the error performance when facing the channel matrix. The algorithms to decompose the channel matrix were implemented using the Spartan6 FPGA from Xilinx as the target device. The implementation concentrates on utilizing the features of the FPGA to speed up operations and reduce the area required by reducing the device utilization, thus reducing the effective cost.

Keywords: Hardware Decomposition; MIMO; OFDM; SVD; Throughput.

1. INTRODUCTION

Wireless access of high data rate is demanded by many applications. For higher data-rate transmission more bandwidth is required. Hence in wireless communication SISO (single input and single output) is found to be insufficient for use. Multiple transmit antennas can be used to form a MIMO system. Earlier SISO [1] [2] system were used for transmission of data streams. But it offered less reliability and capacity. But G. J. Foschini, proved in his studies that, compared with a SISO system, a MIMO system can improve the capacity by a factor of the minimum number of transmit and receive antennas[3].Hence MIMO system became more important in the wireless communication system. But in a MIMO system it became hard for the receiving section to obtain the correct data. Thus compared with a single-input single-output (SISO) system, capacities of a MIMO system can be improved by minimum number of transmit and receive antennas. But one of the disadvantages of the MIMO system is that, since there are more than single transmitters and receiver, the receiving section may suffer from interference due to other transmitter antennas. Hence the above all disadvantages of the paper was eliminated and the throughput and coverage of a MIMO system can be greatly enhanced which was studied by I. E. Telatar From an information theoretical viewpoint, the use of SVD can be claimed as an optimal solution. It is also shown that the application of the SVD technique has the highest throughput compared with other MIMO signal processing techniques in the IEEE 802.11n systems. In many wireless [9] communication standards, a MIMO system is usually combined with orthogonal frequency division multiplexing (OFDM) technology. OFDM is becoming a very popular multi-carrier modulation technique

for transmission of signals over wireless channels. As mentioned above SVD is found to be applicable in MIMO-OFDM [3] [4] system in order to obtain high throughput and enhance system performance. Its application is found to be mainly in the wireless communication systems. One of the advantages of the MIMO-OFDM system is that it is able to obtain a reliable data. Many traditional methods of SVD[2] were found to be less advantageous due to its low throughput and with higher hardware utilization and more over earlier methods of SVD supported only 4×4 matrices. Hence the proposed method of SVD[6] is such that it able to deal with hundred of channel matrices as possible which reduces the decomposing latency and also a reconfigurable architecture for all antenna configuration.

2. SVD TECHNIQUE

Consider a MIMO system with N_T transmitter and N_R receiver antennas. The baseband, discrete-time equivalent model is written by $y = Hx + z$, where value of H is the complex channel matrix, z is the Gaussian noise vector, x is the transmitted data vector, and y is the received data vector. If decomposition [7] [8] is done in the channel matrix H by the SVD technique, i.e., $H = U \Sigma V^H$ where U and V are left singular matrix and right singular matrix, respectively. Both U and V are unitary matrices and Σ is diagonal matrix with only real and nonnegative main diagonal entries. The entry (i, i) of Σ denotes the i th largest value σ_i , which is the singular value with $1 \leq i \leq \min(N_R, N_T)$. The channel between x' and y' can be written as:

$$y' = U^H y = U^H (Hx + z) = U^H (H V x' + z) = \Sigma x' + z' \quad (1)$$

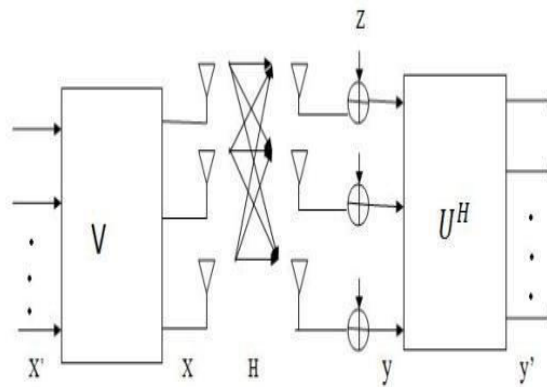


Figure 1: MIMO modeling

Here x' is the symbol vector such that $x = Vx'$ and the received signal y is multiplied by U^H as shown in the above Fig 1. Singular Value Decomposition (SVD) of the channel characteristic matrix is used in pre-coding, equalization and beam forming for MIMO and OFDM communication systems (e.g IEEE 802.11n) to efficiently arrange the setup of the data streams. The SVD problems of MIMO and OFDM systems such as the IEEE 802.11n standard are computationally intensive and complex. Singular value decomposition is an optimal way to extract spatial multiplexing gains in MIMO channels. SVD can be

represented as a product of and are unitary, and is a diagonal matrix.SVD can be also viewed as a composition of three operations: a rotation, a scaling operation, and another rotation. When the channel matrix is partially known to the transmitter, the optimal strategy is to transmit independent streams in the directions of the eigenvectors.

Projection of modulated symbols onto matrix essentially directs the transmit symbols along Eigen modes of the fading channel. If the receive signal is post-processed by rotated orthogonally. Data streams can be send independently through the spatial sub-channels with gains corresponding to the entries in the matrix. At the receiver, data streams arrive orthogonally without interference between the streams.

3. PROPOSED SYSTEM

The SVD design block consists of various blocks to obtain the values of u_i, v_i, σ_i . Various block included here are zero padding, deflation unit, update unit, partial update unit, singular calculation unit. In zero padding block it is extended to the original channel matrix of size 4×4 . From the zero padding block semi definite matrix value $R1$ is calculated. And from the deflation unit values of Ri is obtained. And each value of update unit is fed back to the deflation unit. This is used to calculate (w_i, λ_i) . The deflation process cancels the information of the pair (w_i, λ_i) for the estimation of next pair (w_{i+1}, λ_{i+1}) . The blind-tracking and deflation process continues until all pairs are estimated. The above mentioned process is established via the adaptive blind tracking algorithm. After finding different values sequentially, these values are fed to the partial update unit, sigma unit to find the values u, v, σ . But these values are for the square matrix. For a non-square matrix, the remaining values are obtained by using gram Schmidt unit.

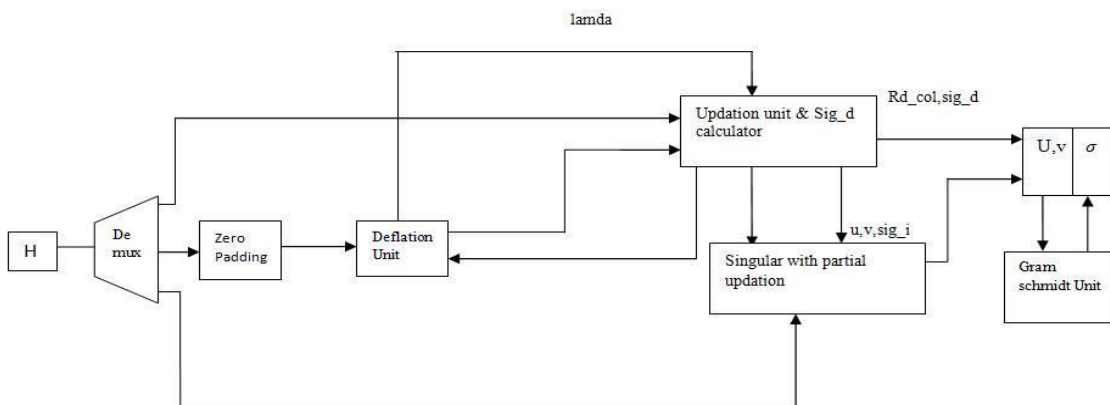


Figure 2: Architectural unit of the proposed system

But these values are for the square matrix. The MIMO channel can be treated as singular valued = $\min(N_R, N_T)$ independent parallel Gaussian sub channels. The i^{th} sub channel has the gain being σ_i . Hence, the transmitter can send independent data streams across these parallel sub channels without any interference from an antenna. Values $\sigma_1, \sigma_2, \dots, \sigma_d$ are called the singular values. The column vectors of V (i.e., v_1, v_2, \dots, v_{N_T}) are the right singular vectors of H , and the column vectors of U (i.e., u_1, u_2, \dots, u_{N_R}) are the left singular vectors of H .

3.1 Zero Padding

In a MIMO system, assume that the maximum number transmitter and receiver antenna in the system is M_R and M_T respectively. This means that, there is possibly $M_R \cdot M_T$ different sizes of channel matrices. Therefore, a scheme which is reconfigurable is proposed to support all antenna configurations [6]. Hence an SVD engine is designed to support the maximum channel size. If the size of a given matrix is $N_R \times N_T$ the extended channel matrix is $M_R \times M_T$. After extending the original channel matrix by $M_R \times M_T$ inserting zeros, channel matrix extended to by inserting zeros, and the multiplexer is used to construct the positive semi-definite matrix R_1 . The positive semi definite matrix R_1 is estimated by a moving average of the recent received signal vectors. In many MIMO OFDM-based standards, the channel matrix H is already known by channel estimation.

$$\begin{aligned} R_1 &= \{H^H H, N_R \geq N_T\} & \text{or} \\ R_1 &= \{H H^H, N_R < N_T\} \end{aligned} \quad (2)$$

With this definition of R_1 , still the same update and deflation process is used to find the pairs (w_i, λ_i) sequentially.

3.2 Deflation Unit

The deflation process is used to estimate the pair (w_i, λ_i) . The deflation process cancels the information of the pair (w_i, λ_i) for the estimation of next pair (w_{i+1}, λ_{i+1}) . In the deflation process, where $d = \min(N_R, N_T)$ and the i^{th} deflation process is given by:

$$R_{i+1} = R_i - (n+1) W_i W_i^H \quad i=1, 2, \dots, (d-1) \quad (3)$$

Only the semi definite matrix is calculated from this block. Remaining value, i.e, R_i is found sequentially in the deflation unit post adaptive blind tracking algorithm. Deflation process continues until all pairs are estimated. ie all the pairs are determined up to $d-1$. Value of d depends on the size of the original channel matrix.

3.3 Updation and Sigma Calculator

This unit finds the different values of (w_i, λ_i) In the update process, equation is:

$$W_{i(n+1)} = W_{i(n)} + \mu_i (R_i - \lambda_i(n)) W_{i(n)} \quad (4)$$

$$\lambda_{i(n+1)} = W_{i(n+1)}^H W_{i(n+1)} \quad i=1, 2, \dots, (d-1) \quad (5)$$

As in the Partial update unit, W_d and λ_d are derived by applying the update operation. From the observation, after the $(d-1)$ time deflation, the positive semi-definite matrix R_d can be expressed as:

$$R_d = W_d W_d^H \quad (6)$$

Here the d^{th} singular value of the singular value is obtained as soon as the values are obtained. Here in this block; sum of diagonal entries is calculated from the column of the

matrix. And the value of σ is obtained by taking the square root. Hence, the update operation for W_d and λd is unnecessary, where singular value is found directly and the corresponding singular vectors by some simple operations.

$$\sigma_d = \sqrt{\text{tr}(R_d)} \tag{7}$$

Thus the d^{th} singular value σ is obtained.

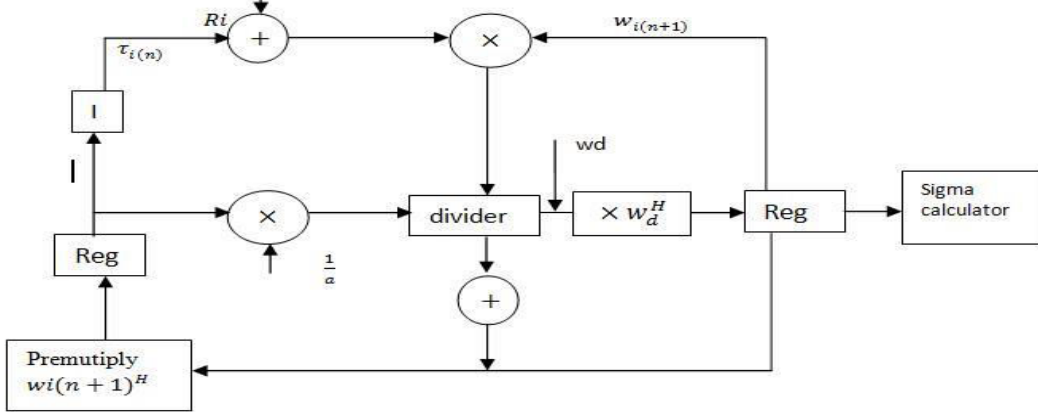


Figure 4: Updation and sigma calculator

3.4 Singular with Partial Update Unit

Compared to the paper [6], algorithm of SVD takes much iteration to calculate the different values in the update unit, singular calculation and the partial update unit. So here the algorithm is modified in such a way that number of iterations was less for calculating the different units as explained above. One of greatest advantage was that with the modification in this algorithm the number of hardware units was also reduced. In singular calculation unit, it is used to find the value of u_i, v_i, σ_i values as mentioned in the paper[6]. Hence the singular values, N_R left singular vectors, and N_T right singular vectors need to be found. And it depend on whether $d = \min(N_R, N_T)$. But in this case singular vectors are found up to $(d-1)$ values are found for and have found that in the sigma calculator, as a result of reducing the hardware. If the channel matrix is square, it means that $d = N_R = N_T$.

$$V_d = R_d(:, 1) / \|R_d(:, 1)\| \tag{8}$$

$$U_d = H V_d / \sigma_d \tag{9}$$

On the other hand, when $N_R < N_T$, V_d with U_d is interchange and H is changed to H^H .

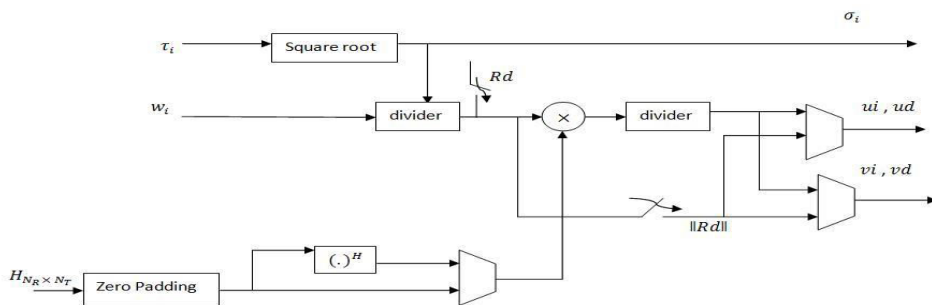


Figure 3: Singular with partial update unit

3.5 Gram Schmidt Unit

For the case of non square channel matrix, assume that $N_R > N_T$, $d = N_T$ there are still $N_R - N_T$ unsolved left singular vectors. The unresolved left singular values is, V (i.e., v_1, v_2, \dots, v_{N_T}) are the right singular vectors of H , On the other hand, when $N_R < N_T$ there are still $N_T - N_R$ unsolved right singular vectors U (i.e., u_1, u_2, \dots, u_{N_R}) are the left singular vectors of H .

$$W_{d+k} = e_k - \sum (e_k, u_i) \cdot u_i \quad i=1, 2, \dots, d+k-1 \quad (10)$$

$$U_{d+k} = W_{d+k} / \|W_{d+k}\| \quad (11)$$

For the case of $N_R < N_T$ replace u_i with v_i

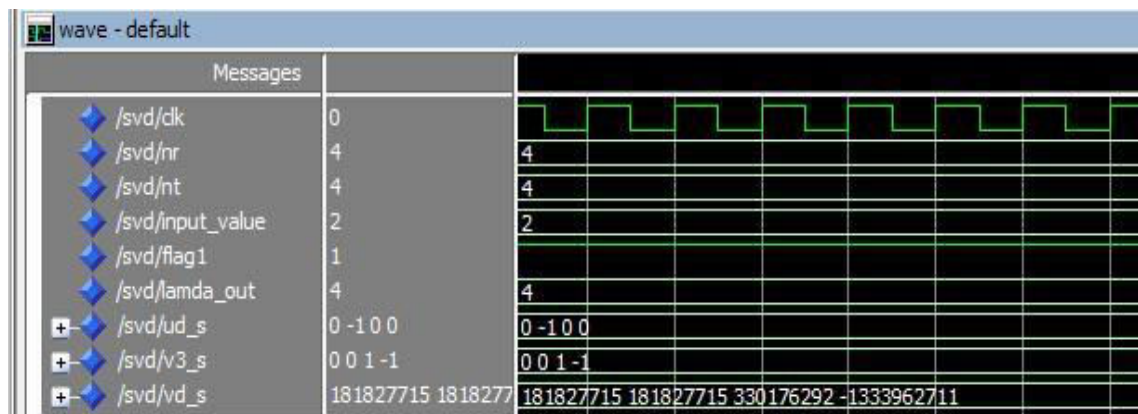


Figure 5: Singular with partial update unit

4. REQUIREMENTS

4.1 Software and Hardware Requirements

The hardware implementation is done in Xilinx ISE 14.1 and the project is implemented in Spartan 6 with the help of VHDL (verilog hardware description language). Required files are synthesized in the Xilinx device. Spartan 6 Family device XC6SLX45 with the package CSG324 is used for its hardware implementation

5. RESULT ANALYSIS AND DISCUSSION

The waveforms of the various parts of the blocks are simulated and its various waveforms are also observed. The comparison is studied in accordance with the design summary generated in the Xilinx device.

5.1 Design Summary

Design summary allows you to quickly access design overview information, reports. By default, the design summary displays information specific to the targeted device and software tool. Here from the design summary generated both from base [6] and the modified block. These two blocks are compared and studied. Below shows the estimated value and design summary of both modified block and the base block. The design gives an overall view of different units used for the implementation of SVD device.

5.2 Comparison

In comparison of the two blocks it is seen that the number of LUT'S used, memory slice registers, logic blocks used and everything is reduced. Here the design summary is generated for the algorithm which is implemented and also for the already implemented SVD [6].

svd Project Status (08/04/2014 - 11:23:30)			
Project File:	svd_mod_x.xise	Parser Errors:	No Errors
Module Name:	svd	Implementation State:	Synthesized
Target Device:	xc6slx16-3csg324	• Errors:	No Errors
Product Version:	ISE 14.1	• Warnings:	102 Warnings (62 new)
Design Goal:	Balanced	• Routing Results:	
Design Strategy:	Xilinx Default (unlocked)	• Timing Constraints:	
Environment:	System Settings	• Final Timing Score:	

Device Utilization Summary (estimated values)			
Logic Utilization	Used	Available	Utilization
Number of Slice Registers	71	18224	0%
Number of Slice LUTs	367	9112	4%
Number of fully used LUT-FF pairs	70	368	19%
Number of bonded IOBs	98	232	42%
Number of BUFG/BUFGCTRLs	1	16	6%

Figure 6: Design summary of the proposed block

In comparison with both the blocks it is found that the device utilization is reduced for the proposed method mentioned in this paper; hence the overall hardware is also reduced. When many number of channel matrices are taken into account, device utilization will be lesser than this due to reduction in the number of iterations.

TABLE 1: Device Utilization

Parameters	Device utilization		
	USED	AVAILABLE	<i>USED MODIFIED</i>
	BASE	BASE	
Slice register	106	18,224	71
Slice LUT's	416	9112	300
Logic block's	412	9112	310
Muxes	208	4556	140

5.3 Simulation Results

Here three inputs and an internal clock is given. There N_R and N_T to give the number of transmitters and receivers. Here the maximum size given to the number of transmitter and receivers i.e., are of size N_R and N_T respectively. And also the maximum input value which is given to 4×4 matrix of 16 values. Different blocks of SVD are simulated and their outputs are obtained. Fig. 5 and Fig.7 shows simulation block.

6. CONCLUSION AND FUTURE WORK

The intended modification is done and the output is obtained and implemented in Spartan 6 FPGA. It is also found that the proposed method when in comparison with the base paper was extremely advantageous. Thus the overall cost was also reduced by decreasing the total hardware utilization.

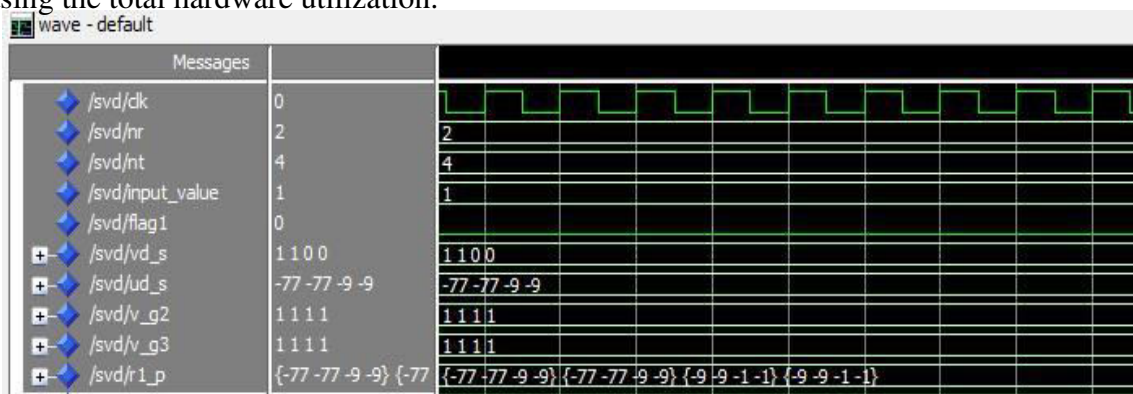


Figure 7: Simulation of SVD engine of singular value of gram Schmidt technique

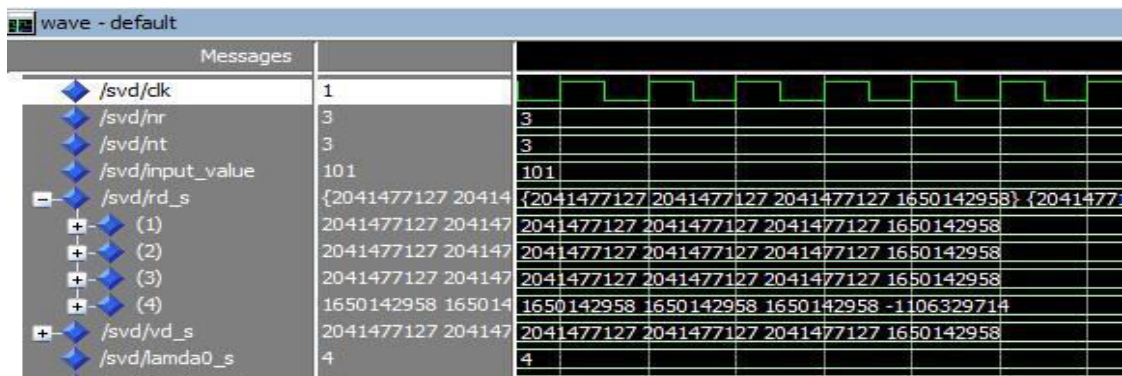


Figure 8: Simulation of SVD engine of Partial update unit

These design strategies enable the use of SVD to be effectively applied to high throughput wireless communication system and also with effectively reducing the hardware units, the chip area required is reduced, thus leading to the overall reduction in hardware cost.

Future works for this paper can be done for different transmit and receive antennae sets such as 8×8 , 16×16 matrices. And also further work can be done so that high throughput is achieved. Also more refined work can be done to reduce the decomposing period require to calculate the different values of the SVD further hardware reduction is also another arena where hardware utilization is reduced.

REFERENCES

- [1] S.M Alamouti, "A simple transmit diversity technique for wireless communications," *IEEE j.Sel Areas Communication*, vol. 16, no. 8, pp. 1451-1458, oct 1998.
- [2] A.Goldsmith,S.A. Jafar,N. Jindal ans S. Viswanath,"Capacity limits of MIMO channels," *IEEE j.Sel Areas Communication*, vol. 21,no. 5,pp. 684-702, Jun 2003.
- [3] H. Sampath,S. Talwar,J. Talwar,V. Erceg and A. Paulraj,"A fourth generation MIMO OFDM: Broadband wireless system: Design, performance, and field trial results," *IEEE Commun Mag.*, vol. 40,no. 9,pp. 143-149, sep 2002.
- [4] Minn and N. Al-Dhahir, "Optimal training signals for MIMO OFDM channel estimation," *IEEE wireless Communication*, vol. 5,no. 5,pp. 1158-1168, may 2006.
- [5] G. Foschini, "Layered space-time architecture for wireless communication in a fading environment when using multi-element antennas," *BellLabs Tech.J.*, pp. 41–59, 1996.
- [6] Yen-LiangChen, Cheng-Zhou Zhan, Reconfigurable Adaptive Singular Value Decomposition Engine Design for High Throughput MIMO-OFDM Systems *IEEE transactions on very large scale integration systems* 2013, Vol. 21, NO. 4, April 2013.
- [7] D. Markovic, B. Nikolic and R. W. Brodersen, "Power and area minimization for multidimensional signal processing," *IEEE J. Solid state circuits syst msg.*, Vol. 42, NO. 4, April 2007.
- [8] A. Poon, D. Tse, and R. W. Brodersen, "An adaptive multi antenna transceiver for slowly flat fading channels," *IEEE Trans. Commun.*, vol. 51, no. 11, pp. 1820–1827, Nov. 2003.
- [9] T. K. Paul and T.Ogunfunmi, "Wireless LAN comes of age: Understanding the IEEE 802.11n amendment," *IEEE Circuits Syst. Mag.*, vol. 8, no. 1, pp. 28–54, Jan. 2008.
- [10] N.D. Hemkumar and J.R. Cavallaro. A systolic VLSI architecture for complex SVD. In *Circuits and Systems*, 1992. ISCAS '92. Proceedings, 1992 IEEE International Symposium.

Fault Detection using AES-Cipher Block Chaining Mode for secured Wireless Communication Networks

B. Mary Amala Jenni¹, S. Devika²

¹*ECE Department, St. Anne's College of Engineering and Technology, amalajenni@gmail.com*

²*ECE Department, St. Anne's College of Engineering and Technology, devikaifetece@gmail.com*

Abstract— The challenge in securizing communications networks is to obtain flexible means able to deal with the intensive computation needed by the cryptography algorithms. A representative example of this algorithm is the Rijndael. The 128-bit AES block cipher combines a 128-bit key and a 128-bit plaintext data block to get a 128-bit block of cipher text data. The Electronic Code Book (ECB) mode is the simplest encryption mode. In this mode, the message is split into blocks and each one is separately encrypted. So, therefore identical plaintext blocks are encrypted to identical cipher text blocks. This drawback generates vulnerabilities like modification of ciphered messages. In order to solve this problem, more complex modes of operation combine the data of the previous ciphered blocks and use Initialization Vectors (IV) to make each ciphered message unique. The AES Cipher-Block Chaining (CBC) mode includes these features. Before encrypting a block, it is XORed with the cipher text of the previous cipher text block. In this paper, the design and analysis of AES-CBC mode is presented to find the fault during the encryption process. Simulation is performed to analyze the chip size reduction.

Keywords - AES, CBC mode, Initialization Vectors, Electronic Code Block

1. INTRODUCTION

Earth observation (EO) satellites take images of the Earth with smart and sophisticated imaging sensors. Multispectral images of the Earth captured by optical on-board cameras can be used in monitoring of the environment and disasters, vegetation control, map marking, urban planning, etc. The latest trend now is towards small EO satellites, as they require smaller budgets to build and launch and also involve less maintenance costs [1]. A typical EO small satellite weighs approximately 100 kg and the orbit average power generated by solar panels is 30 to 60 W. The imaging payload units of such satellites comprise imagers, mass memory, and high-rate data transceivers and consume up to 70% of the average orbit power. At present, more and more EO satellites are equipped with on-board encryption to protect the data transmitted to the ground station. However due to confidentiality and security reasons the coverage of this topic in the open literature is very limited [3].

Encryption, by far the most widely adopted security service in terrestrial networks, is used to protect data from unauthorized users. Although there are many encryption products and algorithms, the use of these products and algorithms on-board satellites has been overlooked until recently. But now satellite manufacturers are realizing the importance of on-board encryption to protect valuable data, especially after cases, which have proved that intrusion into

satellite data is not an impossible task. At present, more and more EO satellites are equipped with on-board encryption to protect the data transmitted to the ground station.

Ever since DES was phased out in 2001 and its successor, the Advanced Encryption Standard (also known as Rijndael) took its place, various AES implementations have been proposed both in software and hardware [2].

The Rijndael algorithm approved as the Advanced Encryption Standard (AES) by the US National Institute of Standards and Technology (NIST) is a block cipher, which encrypts one block of data at a time. To encrypt multiple blocks, modes of operation have been defined by NIST. AES is being adopted by many organizations across the world. Because of its simplicity, flexibility, easiness of implementation, and high throughput AES is used in many different applications ranging from smart cards to big servers. In fact, hardware implementations of AES are well suited to resource-constrained embedded applications like satellites [5].

There are various hardware implementations of the AES algorithm on platforms like application specific integrated circuits (ASICs) and field programmable gate arrays (FPGAs) that achieve a significant throughput ranging from a few Mbit/s to Gbit/s. Thus the requirements of small EO satellites for high-rate data transmission are met by existing AES implementations. However, in addition to high throughput, immunity of the encryption process against faults is very important in satellites. Satellites operate in a harsh radiation environment and consequently any electronic system used on board, including the encryption processor, is susceptible to radiation-induced faults. Most of the faults that occur in satellite on-board electronic devices are radiation-induced bit flips called single event upsets (SEUs). If faulty data is transmitted to the ground station, the user's request for data retransmission has to wait until the next satellite revisit period, with revisit time varying from a couple of hours to weeks. In order to prevent faulty data transmissions, there is a need for an error-free encryption scheme on board.

Satellite data can further get corrupted during transmission to ground due to noise in the transmission channel. The impact of radiation on semiconductor devices on board depends on orbit altitude, orientation, and time. Reliability is the most important issue in avionics design. SEUs must be detected and corrected on board before sending the data to ground. The triple modular redundancy (TMR) technique is one of the most widely used redundancy-based SEU mitigation techniques in satellites. A TMR design consists of three identical modules, which are connected by a majority voting circuit to determine the output. However, with the TMR technique the area and power overheads triplicate in comparison with the original module. This paper addresses reliability issues of the AES algorithm. A detailed analysis of the impact of faults during on-board encryption and during transmission for the AES-CBC mode is presented [4].

II. ADVANCED ENCRYPTION STANDARD–ALGORITHM AND MODES OPERATION

The AES is a symmetric key algorithm, in which both the sender and the receiver use a single key for encryption and decryption. AES defines the data block length to 128 bits, and the key lengths to 128,192, or 256 bits. It is an iterative algorithm and each iteration is called a round. The total number of rounds, N_r , is 10, 12, or 14 when the key length is 128, 192, or 256 bits, respectively [9]. Each round in AES, except the final round, consists of four transformations: Sub Bytes, Shift Rows, Mix Columns, and Add Round Key [3]. The final round does not have the Mix Columns transformation the decryption flow is simply the reverse of the encryption flow and each operation is the inverse of the corresponding one in the encryption process. The round transformation of AES and its steps operate on some intermediate results, called state. State can be visualized as a rectangular matrix with four rows. The number of columns in the state is denoted by N_b and is equal to the block length in bits divided by 32. For a 128 bit data block (16bytes) the value of N_b is 4, hence the state is treated as a 4×4 matrix and each element in the matrix represents a byte. For the sake of simplicity, in the rest of the paper, both the data block and the key lengths are considered.

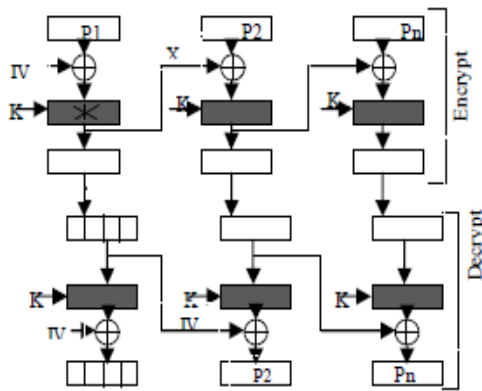


Figure 1. Fault Propagation during encryption in AES-CBC mode.

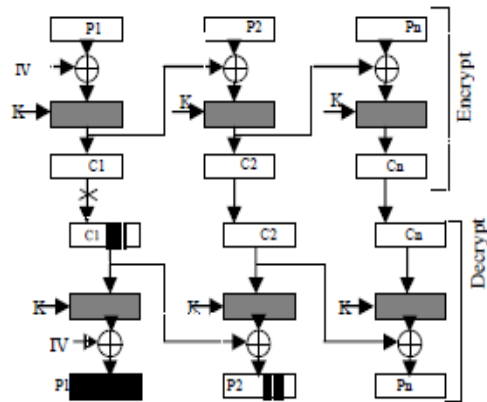


Figure 2. Transmission Fault Propagation in CBC mode

as 128 bit long. However all the discussions and the results hold true for 192 bit and 256 bit keys as well [8].

III. FAULT PROPAGATION ANALYSIS

Due to fault propagation even a single bit error during encryption of one block of AES can result in corruption of 50% of the bits in the final encrypted data on average. In addition, when using the AES feedback modes faults occurring in one block can propagate to other blocks because of the feedback. In this section propagation to subsequent blocks of single bit faults occurring both during encryption and during transmission is investigated.

A. Fault Propagation in AES-CBC Mode

Cipher Block Chaining Mode: The CBC mode, illustrated in Fig. 3, is the mode in which the plain data block is XOR-ed with the cipher data of the previous block before it is encrypted. The

first block is XOR-ed with an initial vector (IV), which is a random number. In Fig.2, P1,P2.... Pn represent the plain data, C1, C2....Cn represent the cipher data and K is the key used in both encryption and decryption. The plain data blocks, the cipher data blocks, and the key are of 128 bit length each. The “E” and “D” blocks in Fig.2 denote an encryption and decryption function using the AES algorithm, respectively [9].

The effect of an SEU during encryption in the CBC mode is illustrated in Fig.2, where the SEU occurrence is marked by the star symbol * and the corrupted data blocks are represented by black boxes. If an SEU occurs while encrypting the plain block P1, the cipher

block C1 will be corrupted and hence the decrypted block P1 will also be corrupted. However, this corrupted data is not propagated to the subsequent blocks despite the feedback. The reason for this is that the corrupted cipher block C1 is XOR-ed twice (with the plain block P2 before encryption and with the cipher block C2 after decryption) as shown in Fig.2. Performing the XOR operation two times with this corrupted cipher block C1 neutralizes the fault and prevents propagation of faults to subsequent blocks as shown below:

In contrast, a fault occurring in an encrypted block during transmission propagates to the next block, as shown in Fig.3, where the transmission fault is shown by the star symbol during the transmission of the cipher block C1. The decrypted block P1 is completely garbled and the subsequent decrypted block P2 will have bit errors at the same positions as the original erroneous block C1. The decrypted blocks following the second block will not be affected by the fault. Hence the CBC mode is self synchronizing [6].

IV. FAULT-TOLERANT MODEL OF THE AES ALGORITHM

This section presents a novel fault-tolerant model for the AES algorithm, which is immune to radiation-induced SEUs occurring during encryption and can be used in hardware implementations on-board small OE satellites. The model is based on a self-repairing EDAC scheme, which is built in the AES algorithmic flow and utilizes the Hamming error correcting code. The proposed Hamming code based fault-tolerant model of AES can be adapted to all the five modes of AES to correct SEUs on board. Even though the calculation of the Hamming code is carried out within the AES it does not alter any of the transformations of the algorithm and does not affect in any way the operation of AES. The disadvantage of this method is that the implementation of the codes based EDAC will require an additional encoding stage to encode the plain data blocks to code-word symbols which will inevitably add an overhead to on-board resources and processing.

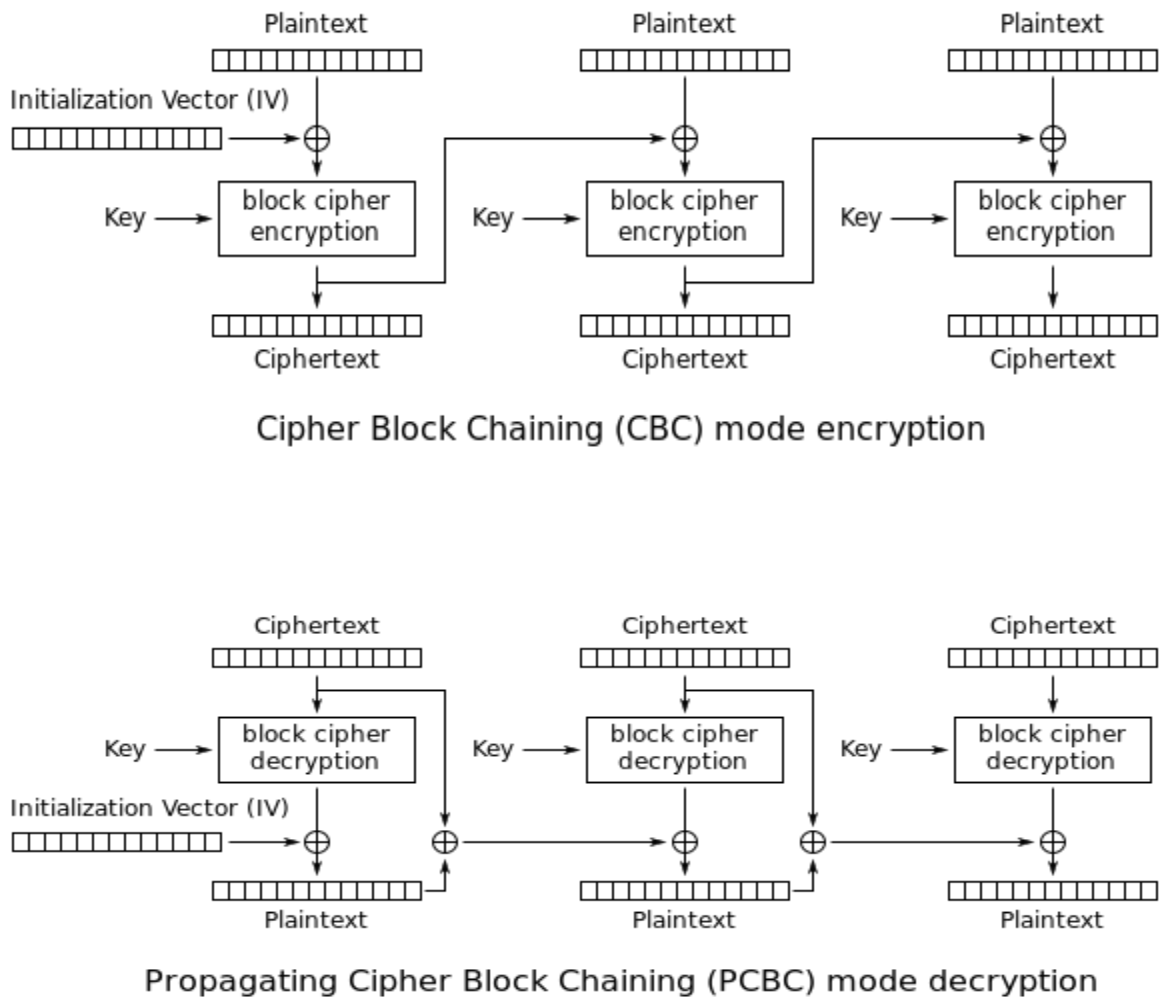


Figure3. Cipher Block Chaining mode encryption and decryption

A. Software Simulation

In EO satellites high throughput encryption processing is required to comply with high-rate data transmission bandwidth of up to a few hundred Mbit/s. In order to meet the requirement for high throughput processing, hardware implementation is considered to be the preferred choice on board satellites. The Verilog hardware description language (HDL) is used for the coding, and ModelSim is used for the functional, pre synthesis, and post synthesis simulations of the design. The HDL designs are tested extensively using the KAT and MCT vectors by NIST. Synthesis and implementation are carried out using Xilinx ISE.

Figure 4. AES encryption using ModelSim.

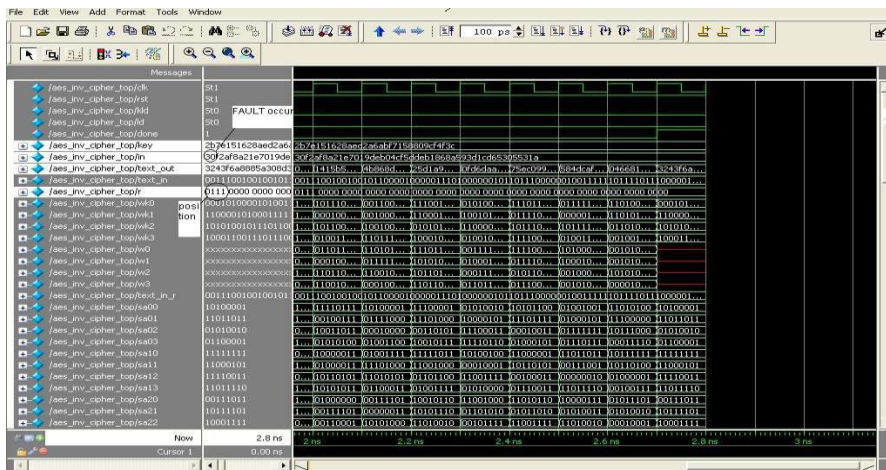
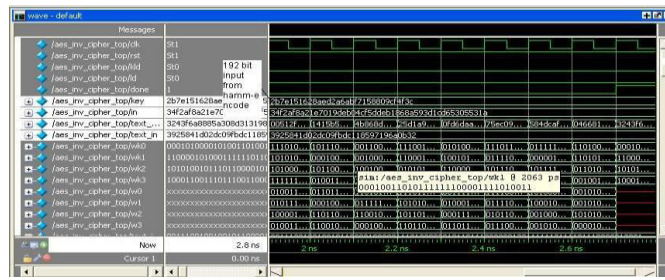


Figure 5. AES fault detection and correction using Hamming Code.

V. CONCLUSION AND FUTURE WORK

This paper examines the trustworthiness of the AES algorithm for employ on board EO small satellites. The AES mode CBC, was converted in specify the impact of the propagation of SEU errors happening during on-board encryption is examined. In adding together, an examination of the Propagation of errors that occur during transmission due to noise is carried out. So as to keep away from data corruption because of SEUs, a fault detection and correction model of AES is presented based on the Hamming code (12, 8). The model offers an SEU self-recovering capability, which is built in the AES data path. Also it consumes a less amount of the power accessible to the payload unit. The predictable hardware overhead of the best fault-tolerant AES is in terms of area.

The model can be enlarged for detection and correction of multiple bit faults by using other new complicated error-correcting codes such as modified Hamming code, etc. The proposed fault detection and correction AES model aims the satellite application domain,

though it can also be used in other applications aimed at hostile environments like, interplanetary exploration, nuclear reactors unmanned aerial vehicles, etc. Terrestrial applications, which need sophisticated of reliability, such as bank servers, telecommunication servers, etc. can advantage from the use of AES fault-tolerant techniques also.

REFERENCES

- [1] Sun, W., Stephens, P., and Sweeting, M. N. Micro-minisatellites for affordable EO Constellations–Rapid Eye and DMC. In Proceedings of the IAA Symposium on Small Satellites for Earth Observation, Berlin, Germany, Apr. 2001, IAA-B3-0603.
- [2] Surrey Satellite Technology Ltd. www.sstl.co.uk (last accessed on 18th June 2007).
- [3] Directory of Earth Observation Resources. http://directory.eoportal.org/pres_TopSat.html (last Accessed 18th June 2007).
- [4] Sweet, K. The increasing threat to satellite communications. *Online Journal of Space Communication*, 6 (Nov. 2003).
- [5] Mariani, R., and Boschi, G. Scrubbing and partitioning for protection of memory systems. In Proceedings of the 11th IEEE International Symposium on On-Line Testing, July 6—8, 2005, 195—196.
- [6] S. Kim, Ingrid Verbauwhede, "AES implementation on 8-bit microcontroller," Department of Electrical Engineering, University of California, Los Angeles, USA, September, 2002.
- [7] Guido Bertoni, Luca Breveglieri, Israel Kor "Error Analysis and Detection Procedures for a Hardware Implementation of the Advanced Encryption Standard", *IEEE transactions on computers*, vol. 52, no. 4, april 2003
- [8] Ramesh Karri, Kaijie Wu, Piyush Mishra, and Yongkook Kim, "Concurrent Error Detection Schemes for Fault-Based Side-Channel Cryptanalysis of Symmetric Block Ciphers", *IEEE transactions on computer-aided design of integrated circuits and systems*, vol. 21, no. 12, December 2002
- [9] HyeopgeonLee, KyoungghwaLee, YongtaeShin, "Implementation and performance Analysis of AES-128CBC algorithmic WSNs", Feb.7-10, 2010 ICACT 2010.

Reinforcement Learning with Particle Filter (RLPF)

Mr. J. Joseph Ignatious¹, Ms. V. Lawanya², Ms. N. Kirubashankari³

¹*ECE Department, V.R.S College of Engineering and Technology, jjignatious@gmail.com*

²*ECE Department, V.R.S College of Engineering and Technology, lawanya9590@gmail.com*

³*ECE Department, V.R.S College of Engineering and Technology, kiruban2810@gmail.com*

Abstract: Reinforcement Learning with Particle Filter (RLPF) is a reproduction based procedure helpful in unraveling Markov choice procedures if their move probabilities are not effortlessly possible or if the issues have an extensive number of states. An exact investigation of the impact of step-sizes (learning rules) in the joining of RLPF calculations, stochastic briefest ways in taking care of normal prize issues by means of RLPF, furthermore, the idea of survival probabilities (drawback hazard) in RLPF have illustrated. The effect of step sizes when capacity estimation is joined with RLPF. Our trials yield some fascinating bits of knowledge that will be helpful when RLPF calculations are executed inside of test systems were examined.

Keyword: Reinforcement learning with particle filters (RLPF), Q-learning, Machine learning, Markov decision process (MDP), Bellman equation

I. INTRODUCTION

Reinforcement Learning with Particle Filter (RLPF) is a reproduction based procedure that is valuable on expansive scale and complex Markov decision procedures (MDPs) [1]. In this paper, they address the part of step sizes (learning rules) in reduced prize issues and that of the establishing component of the most brief stochastic way (SSP) in normal prize issues and the idea of presenting survival likelihood (drawback hazard) inside RL. The effect of these elements on the qualities of repeats and inspect by the amount of qualities can wander from the qualities acquired from element programming were examined. In the setting of step sizes, they performed a study utilizing some standard tenets to decide how they perform. The survival likelihood is characterized with appreciation to a known target income. The survival likelihood of a framework is the likelihood that the income in unit time will surpass the objective. It is straightforwardly identified with the drawback hazard in operations research and the exceedance likelihood in the protection business [2]. Bellman mathematical statement demonstrate RLPF calculation merge to an ideal arrangement. Section II shows an examination with marked down prize. Section III presents our outcomes with the SSP-establishing system on average reward issues, and Section IV examines our calculation with the survival likelihood contemplations and section V Conclude this paper.

II. DISCOUNTED REWARD

The impact of the rate of convergence of linear and polynomial step sizes on the values to which Q-values in RLPF converge has been studied. [3]. they have established theoretically that linear rules (e., g, $1/k$, where k denotes the iteration number) can take an exponential time to converge while polynomial rules (e.g., $1/k^\Psi$ where Ψ is some integer) can converge in polynomial time. In this paper they to conduct experiments with simple step sizes to test how they perform empirically and how far they stray from the optimal values in

an empirical are setting. A disadvantage of $a/(b+k)$ is that one has to conduct numerous trials to determine suitable values of a and b , where as the other rules do not have such parameters. We will limit our thoughtfulness regarding the offbeat Q Learning [4] for which union has been built up under offbeat conditions in various works [4]. On the whole the writing, the stride sizes are required to fulfill some essential conditions, for example, $\sum_{k=1}^{\infty} \alpha^k = \infty$

and $\sum_{k=1}^{\infty} (\alpha^k)^2 < \infty$ where α^k indicates the stride size in the k^{th} emphasis. For some different

less understood conditions,; all the three standards we consider fulfill these conditions. Our tests will analyze the execution of a Q-Learning calculation with that of quality cycle [5] which of processing the quality capacity registers Q-values. They exhibit some documentation, such as Let $r(i, a, j)$ indicate the prize earned in going from state i to state j under activity a . Let $p(i, a, j)$ indicate the likelihood related with the same move. We will utilize μ to signify a strategy for which $\mu(i)$ will signify the (deterministic) activity to be picked in state i ; e.g., (2,1) will signify a strategy with activity 2 in state 1 and activity 1 in state 2. Let λ signify the rebate component. Likewise, P_{μ} and R_{μ} will mean the move likelihood what's more, move prize lattices, separately, connected with arrangement μ . At long last, $Q(i,a)$ will mean the Q-esteem for state i and action a .

Parameters for mdp1

The first test instance, which we call mdp1, is a 2-state MDP with the following parameters: $\lambda = 0.8$, and

$$P(1,1) = \begin{bmatrix} 0.7 & 0.3 \\ 0.4 & 0.6 \end{bmatrix}; P(2,2) = \begin{bmatrix} 0.9 & 0.1 \\ 0.2 & 0.8 \end{bmatrix}; R(1,1) = \begin{bmatrix} 6.0 & -5 \\ 7.0 & 12 \end{bmatrix}; R(2,2) = \begin{bmatrix} 10.0 & 17 \\ -14 & 13 \end{bmatrix}.$$

The three other test occasions, are characterized as takes after. Every one of the parameters for the remaining test occasions are indistinguishable to those of mdp1 with the accompanying special cases: mdp2 — $r(1,1,2)=5$ and $r(2,2,1)=14$; mdp3— $r(1,2,1)=12$; mdp4 — $r(1,1,1)=16$.

Q-Learning with the three distinctive step-size standards, Q-learning with a neuron that uses the log-standard for the neuron's learning govern, and esteem emphasis performed with Q-values; see Table 1. The estimation of $a = 150$ and $b = 300$ in our tests. Additionally, $\epsilon = 0.01$ in the worth emphasis calculation [5]; the primary change in that calculation is: For all (i,a) do until ϵ -union: $Q(i,a) \leftarrow \sum_j p(i, a, j) [r(I, a, j) + \lambda \max_b Q(j, b)]$. The Q Learning calculations were keep running for 10,000 emphases, with an investigation likelihood set at 0.5 all through were composed in MATLAB.

Table 1

	<i>Method</i>	<i>Q(1,1)</i>	<i>Q(1,2)</i>	<i>Q(2,1)</i>	<i>Q(2,2)</i>
<i>mdp1</i>	<i>Q-VI</i>	43.84	53.02	52.87	49.28
<i>mdp1</i>	<i>Q-L-ab</i>	44.40	56.97	50.84	42.63
<i>mdp1</i>	<i>Q-L-k</i>	17.46	19.74	14.62	12.52
<i>mdp1</i>	<i>Q-L-log</i>	32.24	48.79	47.26	41.24
<i>mdp1</i>	<i>N-QL</i>	41.90	51.90	56.54	40.26
<i>mdp2</i>	<i>Q-VI</i>	50.67	55.76	57.34	62.45
<i>mdp2</i>	<i>Q-L-ab</i>	51.55	54.53	52.11	61.94
<i>mdp2</i>	<i>Q-L-k</i>	12.12	21.38	22.08	24.53
<i>mdp2</i>	<i>Q-L-log</i>	44.61	51.16	52.07	54.78

<i>mdp2</i>	<i>N-QL</i>	<i>39.99</i>	<i>53.70</i>	<i>55.27</i>	<i>63.01</i>
<i>mdp3</i>	<i>Q-VI</i>	<i>51.36</i>	<i>61.83</i>	<i>56.66</i>	<i>58.59</i>
<i>mdp3</i>	<i>Q-L-ab</i>	<i>49.89</i>	<i>60.82</i>	<i>55.66</i>	<i>57.18</i>
<i>mdp3</i>	<i>Q-L-k</i>	<i>13.54</i>	<i>23.72</i>	<i>20.17</i>	<i>15.89</i>
<i>mdp3</i>	<i>Q-L-log</i>	<i>44.96</i>	<i>53.83</i>	<i>48.09</i>	<i>45.60</i>
<i>mdp3</i>	<i>N-QL</i>	<i>48.20</i>	<i>55.43</i>	<i>56.19</i>	<i>54.38</i>
<i>mdp4</i>	<i>Q-VI</i>	<i>48.97</i>	<i>40.91</i>	<i>49.36</i>	<i>47.02</i>
<i>mdp4</i>	<i>Q-L-ab</i>	<i>47.72</i>	<i>40.29</i>	<i>48.93</i>	<i>43.93</i>
<i>mdp4</i>	<i>Q-L-k</i>	<i>16.16</i>	<i>9.16</i>	<i>18.96</i>	<i>16.04</i>
<i>mdp4</i>	<i>Q-L-log</i>	<i>42.73</i>	<i>34.97</i>	<i>42.38</i>	<i>39.72</i>
<i>mdp4</i>	<i>N-QL</i>	<i>48.64</i>	<i>40.72</i>	<i>49.71</i>	<i>47.76</i>

Table 1 analyzes the Q-values acquired by means of Q Learning (Q-L) under the different step-size guidelines, by means of a neuron combined with Q-Learning (N-QL), and by means of worth cycle utilizing Q-values (Q-VI). Q-L-abdominal muscle will mean Q-Learning with guideline a/(b+k), Q-L-k will mean Q-Learning with principle 1/k furthermore, Q-Learning with the log guideline will be meant by Q-L-log. The outcomes demonstrate that all the RLPF calculations meet to the ideal approach, the 1/k-guideline produces values that stay far from the ideal Q-values created by the worth emphasis calculations can be enhanced by decreasing investigation, yet that will present extra parameters for tuning. The best execution created by the/ (b+k) principle; that the log-guideline which does not have any tuning parameter performs much superior to the 1/k-principle as far as approximating the quality capacity. The poor execution of 1/k can be clarified by the way that it rots rapidly. Additionally, promising is the execution of a neuron-coupled Q-Learning calculation that uses a log-standard for the neuron's inward learning and a/ (b+k) - standard for the calculation.

III AVERAGE REWARD

MDPs perform computational studies with a Q-Learning calculation that uses two time scales for upgrading and henceforth needs two diverse step sizes at the same time. Other calculations with demonstrated joining properties incorporate a variant of Q-Learning in light of relative worth cycle [7]. Let ρ^μ mean the normal prize of the strategy μ and ρ^* mean the ideal normal prize. At that point if ρ^* is known, one can add to a quality cycle calculation for normal prize issues. A quality cycle calculation is being concentrated on here just for the sole purpose of testing how far the Q-Learning calculation strays from the idea values (plainly, by ρ^* is obscure, and one must utilize different calculations [8]. The quality emphasis calculation will have the accompanying fundamental change: For all (i, a) do until ε -meeting: $Q(i,a) \leftarrow \sum_j p(i,a,j) [r(i,a,j) - \rho^* + \max_b Q(j,b)]$. The Q-learning calculation with its SSP-establishing system is depicted in the Appendix. It has two stage sizes: $\alpha(k)$ for the Q-esteem and $\beta(k)$ for the estimation of ρ , where $\lim_{k \rightarrow \infty} \beta(k)/\alpha(k) = 0$. The cases utilized as a part of the last area with the understanding that there is currently no rebate component. The outcomes are arranged in Table 2, the Q-learning calculation taken for 10,000 cycles and utilized $\varepsilon = 0.01$; likewise mdp1 — $\rho^* = 10.56$, mdp2 — $\rho^* = 11.53$, mdp3 — $\rho^* = 12.00$ and mdp4 — $\rho^* = 9.83$. These qualities for ρ^* were controlled by a thorough assessment of the normal prize of each deterministic arrangement. The investigation likelihood was settled at 0.5 for both activities. The outcomes demonstrate that the quality capacity, which is characterized as $v(i) = \max_a Q(i,a)$, is sensibly approximated by the Q-Learning calculation, albeit some Q-qualities are not really all around. Table 2 shows the Q-values got through Q-Learning (Q-L) for normal prize (see Appendix) and through quality

cycle utilizing Q-values (Q-VI). For mdp2 $\alpha(k) = 500/(1000+k)$ and $\beta(k) = 150/(300+k)$, while for the remaining occurrences we utilized $\alpha(k) = 150/(300+k)$ and $\beta(k) = 50/(49+k)$.

Table 2

	<i>Method</i>	<i>Q(1,1)</i>	<i>Q(1,2)</i>	<i>Q(2,1)</i>	<i>Q(2,2)</i>
<i>mdp1</i>	<i>Q-L</i>	-2.46	1.1710	-2.89	-3.12
<i>mdp1</i>	<i>Q-VI</i>	-6.99	2.2789	-1.12	-3.80
<i>mdp2</i>	<i>Q-L</i>	-3.85	2.57	3.48	5.10
<i>mdp2</i>	<i>Q-VI</i>	-2.85	0.37	6.18	7.31
<i>mdp3</i>	<i>Q-L</i>	-5.99	1.1061	-3.81	-6.19
<i>mdp3</i>	<i>Q-VI</i>	-8.80	1.99	-4.996	-7.39
<i>mdp4</i>	<i>Q-L</i>	-2.14	-5.19	-0.58	-3.94
<i>mdp4</i>	<i>Q-VI</i>	-1.1904	-8.28	0.24	-2.08

IV SURVIVAL PROBABILITY

The idea of danger has been concentrated on in the setting of RLPF through utility capacities [7], difference punishments [8], and likelihood of entering prohibited states [9] [10] for a prior work. Different punishments in the setting of MDPs were examined in Filar, Kallenberg, and Lee (1989). MDPs consider the punishments connected with drawback hazard which is characterized as for an objective and characterize the drawback hazard (DR) to be the likelihood of the prize falling beneath the focus on; this danger ought to be minimized. Thus 1-DR we indicate the likelihood of survival, which is amplified. In the event that one considers costs rather than prizes, the likelihood of surpassing the objective will be the related drawback hazard; this is likewise called the exceedance likelihood in fiasco displaying [2].

Let τ signify the objective one-stage reward. At that point for a given deterministic, stationary approach μ , the drawback danger is characterized as:

$$DR^\mu = \sum_{i \in \zeta} \pi^\mu(i) \sum_{j \in \zeta} p(i, \mu(i), j) I(r(i, \mu(i), j) < \tau) \text{ -----(1)}$$

Where $I(\cdot)$ signifies the marker capacity (which breaks even with 1 in the event that the condition inside the sections is genuine and 0 generally) also, $\pi^\mu(i)$ indicates the restricting likelihood (invariant likelihood) for state i under approach μ . Our target capacity in the drawback hazard punished issue will be: $\phi = \rho - \theta DR$ where ρ signifies the normal prize and θ is a positive scalar picked by the danger administrator. For semi-fluctuation, the pointer capacity would be supplanted by $(\tau - r(i, \mu(i), j))^2_+$ in the Poisson comparison and by $(\tau - r(i, a, j))^2_+$ in the Bellman comparison [8], and for difference, we would supplant the marker capacity in the Bellman comparison by $(r(i, a, j) - \rho^*)^2$, where ρ^* the normal prize of the ideal approach of the difference is punished MDP [8]. While difference and semi-fluctuation are worthy measures of danger, drawback danger is considerably additionally engaging on the grounds that it is a likelihood measure. RLPF calculation for hazard penalties and drawbacks are listed.

A Q-esteem rendition of the Bellman mathematical statement can be created from Equation above. From that, it is not hard to determine a Q-Learning calculation. Since the Bellman comparison models the ideal estimation of the goal capacity ϕ^* , (this is

undifferentiated from ρ^* in the danger unbiased Bellman mathematical statement for normal prize),

Four test occurrences are named mdp5 through mdp8. For all the test occasions, $\tau = 8$ and $\theta = 2$.

mdp5: Identical to mdp1 with the exception of: $r(1,1,1) = 3$; $r(1,1,2) = 11$; $r(1,2,1) = 6$; $r(2,2,2) = 7$.

mdp6: Identical to mdp1 with the exception of: $r(1,1,1) = 3$; $r(1,1,2) = 11$; $r(2,1,2) = 9$; $r(1,2,1) = 6$; $r(2,2,2) = 7$.

mdp7: Identical to mdp1 as far as the move probabilities, be that as it may, with the accompanying prize structures:

$$R_{(1,1)} = \begin{bmatrix} 9.0 & -1 \\ 12.0 & 8 \end{bmatrix}; \quad R_{(2,2)} = \begin{bmatrix} 6.0 & 20 \\ -14 & 7 \end{bmatrix}$$

mdp8: Identical to mdp1 as far as the move probabilities, be that as it may, with the accompanying prize structures:

$$R_{(1,1)} = \begin{bmatrix} 3.0 & 7 \\ 9.0 & 1 \end{bmatrix}; \quad R_{(2,2)} = \begin{bmatrix} 6.0 & 9 \\ 14 & 7 \end{bmatrix}$$

A. Simulation tests

Through the normal comprehensive assessment reward and the drawback hazard for every strategy in the four test examples were examined. The normal prize is $\rho^\mu = \sum_{i \in \zeta} \pi(i) \sum_{j \in \zeta} p(i, \mu(i), j) r(i, \mu(i), j)$. The drawback danger is characterized in Equation

(1). The constraining probabilities of every state can be dictated by unraveling the established invariant mathematical statements: $\sum_{j \in \zeta} \pi^\mu(j) p(j, \mu(i), i) = \pi^\mu(i)$ for all $i \in \zeta$ and

$$\sum_{i \in \zeta} \pi^\mu(i) = 1.$$

A characteristic and vital augmentation of MDP hypothesis is to Semi- Markov choice procedures (SMDPs) [7], where the time spent in every move is displayed as an irregular variable. Let $t(i, a, j)$ signify the time spent in going from i to j under activity. Drawback danger will be characterized as:

$$DR^\mu = \sum_{i \in \zeta} \pi^\mu(i) p(i, \mu(i), j) I \left(\frac{r(i, \mu(i), j)}{t(i, \mu(i), j)} < \tau \right).$$

Semi-change in the SMDP can be characterized as:

$\sum_{i \in \zeta} \pi^\mu(i) \sum_{j \in \zeta} p(i, \mu(i), j) (\pi(i, \mu(i), j) - r(i, \mu(i), j))^2_+$. The SMDP Bellman mathematical statement for semi-difference can be acquired from that of drawback danger through substitution of the pointer capacity by $(\pi(i, a, j) - r(i, a, j))^2_+$.

$E[R] = \sum_{i \in \zeta} \pi(i) \sum_{j \in \zeta} p(i, a, j) r(i, a, j)$ and $E[T] = \sum_{i \in \zeta} \pi(i) \sum_{j \in \zeta} p(i, a, j) t(i, a, j)$. The characteristic definition for the asymptotic difference is characterized in (4) beneath. From the RRT, (w.p.1), $\lim_{t \rightarrow \infty} \frac{N(t)}{t} = \frac{1}{E[T]}$ using which The Bellman mathematical statement for the fluctuation punished SMDP can be acquired by supplanting the pointer capacity in the relating mathematical statement for drawback hazard by $(r(i, a, j) - \rho^* t(i, a, j))^2$.

V CONCLUSIONS

An exact investigation of (i) the utilization of distinctive step-sizes in marked down RLPF, (ii) the utilization of most brief stochastic ways in normal prize RLPF, and (iii) the idea of survival likelihood or drawback hazard in RLPF were examined. The experimental study demonstrates that the $1/k$ -principle does not give off an impression of being a dependable or powerful decision even on exceptionally little issues, and that the $(a/b + k)$ - standard performs extremely well on little issues, however the estimations of a and b need to be resolved. The log-guideline performs sensibly well, that it doesn't have any tuning parameters. The observational study shows that utilizing SSP establishing, one acquires sensible approximations of the genuine quality capacity. Our observational results point out the requirement for concentrate the amount of deviation can be endured from Bellman optimality.

REFERENCES

- [1] Morgan Kauffman. Sutton. R., and A. G. Bartow. "Reinforcement learning: An introduction. Cambridge", MA, USA: The MIT Press. 1998.
- [2] Grossi, P., and H. Kunreuther. "Catastrophe modeling: A new approach to managing risk. Springer". 2005.
- [3] Even-Dar, E., and Y. Mansour. "Learning rates for Q learning. Journal of Machine Learning Research" 5:1–25. 2003.
- [4] Watkins, C., May. "Learning from delayed rewards". Ph. D. thesis, Kings College, Cambridge, England. 1989
- [5] Borkar, V. S., and S. Meyn. "The ODE method for convergence of stochastic approximation and reinforcement learning. SIAM Journal of Control and Optimization" 38(2):447–469. 2000.
- [6] Borkar, "V. S. Asynchronous stochastic approximation, SIAM Journal of Control and Optimization" 36No3:840–851. 1998.
- [7] Puterman, M. L. Markov "decision processes. New York: Wiley Interscience. 1994.
- [8] Gosavi, A. "A reinforcement learning algorithm based on policy iteration for average reward: Empirical results with yield management and convergence analysis. Machine Learning" 55(1):5–29. 2004a.
- [9] Borkar, V. "Q-learning for risk-sensitive control. Mathematics of Operations Research" 27(2):294–311. 2002.
- [10] Sato, M., and S. Kobayashi. "Average-reward reinforcement learning for variance-penalized Markov decision problems. In Proceedings of the 18th International Conference on Machine Learning", 473–480. 2001.
- [11] Geibel, P., and F. Wyszotzki. "Risk-sensitive reinforcement learning applied to control under constraints. Journal of Artificial Intelligence Research" 24:81–108. 2005.
- [12] Heger, M. "Consideration of risk in reinforcement learning. Proceedings of the 11th International Conference on Machine Learning": 105–111. 1994.
- [13] Filar, J., L. Kallenberg, and H. Lee. "Variance-penalized Markov decision processes. Mathematics of Operations Research" 14(1):147–161. 1989.

Internet of Things Based Smart Vehicle Management System

S.BALABASKER¹, G.SIVASATHIYA², R.ANNAMALAI³

¹ Faculty ECE, St. Anne's College of Engineering and Technology, balabasker.s@gmail.com

² Faculty IT, Anand Institute of Higher Technology, chattosathya29@gmail.com

³ Faculty ECE, St. Anne's College of Engineering and Technology, vino.anna@gmail.com

Abstract— Due to the increase in the population the usages of vehicles have been increased in the recent years, and monitoring, managing it is one of the challenging work. With the rise of the Internet of Things (IoT), my system is also aimed at improving the existing system by incorporating better management and monitoring schemes as well as providing road users with real time information. The proposed system uses Raspberry Pi which acts as a cloud server to collect, manage and monitor vehicle insurance, tax and crime through smart devices like phone, laptop, tablet, etc. A handheld device is given to police officers to find the insurance, tax expired and crime involved vehicles remotely. The handheld device which has ARM Controller (LPC2148), RFID reader and GPS antenna, it also consist of a LED light and Buzzer, if a crime involved or Insurance expired vehicle passes the device then the ARM controller makes the LED light to glow and also make Buzzer to sound which makes the nearby police officer alert. Subsequently, the vehicles Unique ID and GPS latitude and longitude data are transmitted from ARM controller to the cloud server and updated into the database using IoT.

Keywords- IoT , LED, Raspberry Pi, ARM controller, Buzzer.

I. INTRODUCTION

Vehicle management in many places like India still relies heavily on physical operations of police officers. Police officers sometimes have to interfere traffic for some routine operations. For example, they have to block the road at irregular intervals to detect vehicles that violate traffic regulations i.e. motor tax expired or vehicle complicated in crimes that causes serious congestion in traffic flow.

So my proposed system which likes to remove this hurdle by making the vehicle management smart by implementing it with the new technology IoT. The IoT is the interconnection of uniquely known embedded computing devices within the existing Internet infrastructure. So IoT basically connects many Embedded System, sensors to internet. The proposed solution is targeted at add the technologies i.e. RFID and IoT to fit them into the current traffic operations instead of entirely changing the way the system operates. The proposed system which clears the following problems in the existing systems they are

- ❖ The police officers stops the traffic flow to check the status of vehicle (e.g. checking expiry of motor tax or insurance or crime involved vehicles)
- ❖ The system also uses GPS to track vehicles that involved in crimes or that belongs to stolen vehicle.
- ❖ The system should also allow a police officer to receive information about adjacent junction's data for decision making.

II. WORKING PRINCIPLE

Radio Frequency Identification (RFID) is a competitive technology for identifying, tracing, and counting real-life objects plays an important role in a research standard of IoT. The RFID technology has been used in many domains, and traffic management is one of those. However, the focus of my project is to put the concern on applying an Internet of Things standard to solve more practical operation requirements for human-oriented traffic control. IoT is a kind of system that enables objects to communicate with other objects for certain purposes.

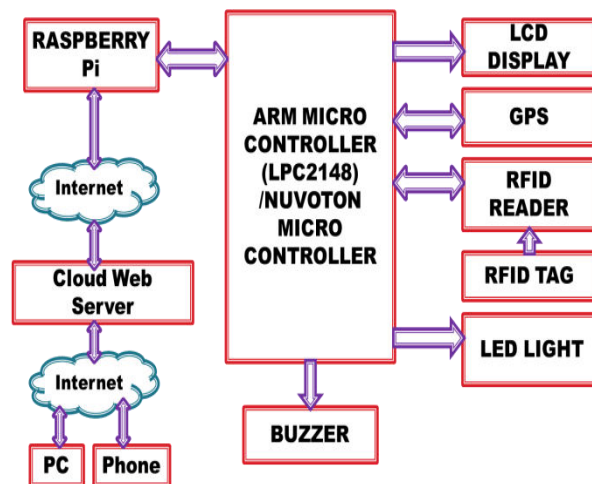


Fig.1. Proposed System

The RFID Reader reads the Vehicle ID and it is transferred to the ARM controller, which intends send the ID value through one of the UART port to the cloud server. Then the Vehicle ID is checked with the already available data in the cloud server using raspberry pi and the result is transferred back to the ARM controller. If the vehicle involved in crime or insurance expired one then the LED will glow and also makes the Buzzer to sound which is already connected with the ARM controller.

III. HARDWARE REQUIRIEMENTS

Raspberry Pi: Raspberry Pi is a small compact sized computer developed for computer science education and Raspberry Pi Foundation developed this device. Raspberry PI has a 32-bit ARM processor and uses a Fedora distribution of Linux. It can be programmed with php, phyton or any other language that will compile for ARM v6. The Raspberry Pi computer is a system-on-a-chip(SoC) with connection ports. It can be operated by hooking up a USB keyboard and plugging the computer into a television. It is a capable little device that enables people of all ages to explore computing. It also useful for beginners to learn how to program in languages like Scratch and Python. It can do everything that a desktop computer to do, from browsing the internet and playing high-definition video, to making spreadsheets, word-processing, and playing games. It also has the ability to interact with the outside world, and has been used in a wide array of projects, from music machines and parent detectors to weather stations and tweeting birdhouses with infra-red cameras.

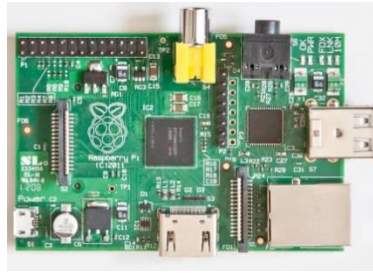


Fig.2. Raspberry Pi version 2.0(B Model)

ARM Microcontroller: The ARM microcontroller LPC2148 is based on a 32 bit ARM7TDMI-S CPU with real-time emulation and embedded trace support. It also has an embedded high speed flash memory ranging from 32 kB to 512 kB.

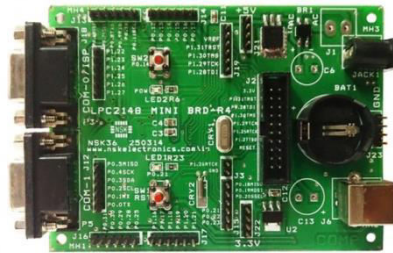


Fig.3. ARM Microcontroller LPC2148

RFID Reader: RFID Proximity OEM Reader Module has a built-in This Low Frequency reader module with an internal or an external antenna which facilitates communication with Read-Only transponders like TK5530 via the air interface. The tag data is sent to the host systems through the wired communication interface with a protocol selected from both the module RS232 and Wiegand Protocol.

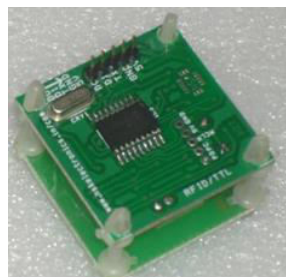


Fig.4. RFID Reader

The Low Frequency module is best suited for applications in Asset Management, Access Control, Time and Attendance, Handheld Readers, Immobiliser, and other RFID enabled applications. It is designed to work on the industry standard carrier frequency of 125 kHz.

RFID TAG: RFID tagging uses small radio frequency identification devices for identification and tracking purposes. An RFID tagging system has a tag by itself, a read/write device, a host system application for data collection, a processing unit, and transmission unit. An RFID tag (sometimes called an RFID transponder) consists of a chip, some memory and an antenna. RFID tags are known as active tags if it has its own power source. Those without a power source are known as passive tags which are activated by the radio frequency scan of the

reader. The electrical current generated is small generally enough for transmission of an ID number. Active tags have more memory and can be read at greater ranges.



Fig.5. RFID TAG

LED Lights: A light-emitting diode(LED) is a two leads PN-junction diode, which emits light when activated. When a suitable voltage is applied across the leads, electrons are able to recombine with electron holes within the device and releases energy in the form of photons and this result is called electroluminescence. The color of the light is determined by the energy band gap of the semiconductor.



Fig.6. LED light (3mm)

BUZZER: The generation of pressure variation or force by the application of electric potential across a piezoelectric material results the piezo buzzer to sound based on reverse of the piezoelectric effect. These buzzers can be used alert a user of an event corresponding to a switching action, sensor input or counter signal. They are also used in alarm circuits.



Fig.7. Piezo Electric Buzzer

Global Positioning System (GPS): GPS is a new branded technology used for determining a location using signals from a network of satellites that orbit Earth. It works well anywhere around the planet that includes remote locations also. To locate the position we need a GPS receiver and a clear view of the sky to receive signals from at least three or four GPS satellites. Common uses of GPS include finding restaurants, navigation, vehicle tracking, location of business assets, mapping for outdoor recreation

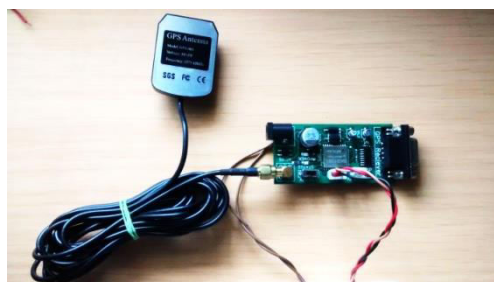


Fig.8. GPS Receiver

IV. SOFTWARE DESIGN

OPERATING SYSTEM: The software for the development of this project uses python scripting and it uses NOOBS which is raspberry pi's preferred operating system. New Out of Box Software (NOOBS) is an easy operating system installer with contains Raspbian. It also contains various operating systems as follows Raspbian, Pidora, OpenELEC, RaspBMC, RISC OS, Arch Linux. The NOOBS v1.3.10 released on September 2014 is the only Raspbian is installed by default in NOOBS. The others can be installed with a network connection.

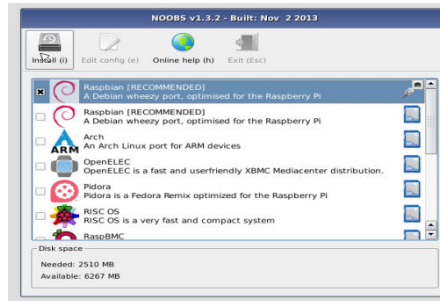


Fig.9. NOOBS Operating System Installation

PHPMYADMIN: PhpMyAdmin is an open source software tool written in PHP, intended to handle the administration of MySQL over the Web. It also supports a wide range of operations on MySQL, MariaDB and Drizzle. Frequently used operations are managing databases, columns, indexes, user's data, permissions for files, etc which can be performed via the user interface to directly execute any SQL statement. PHP is a programming language evaluates form data sent from a browser and build custom data from web. The database is bring into effective action in MySQL where the Tag ID is associated with other vehicular details to make traceable for its owner information, expiration of tax, criminal case, tracking information and reader information etc. Only some data is accessible by every type of users. And some data can be viewed only after the user is authorized like tag registration and vehicle registration require administrator level while any police officer who is given rights can view crime and vehicle information.

V. RESULT

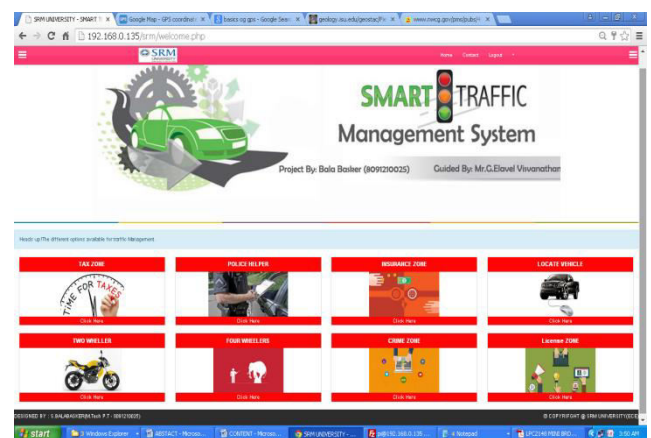
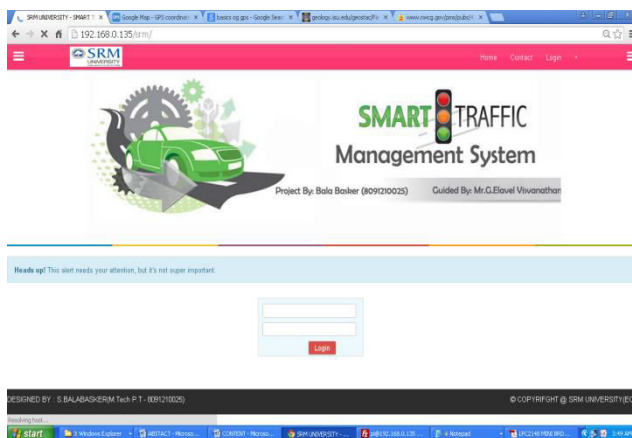


Fig.10. Simulation Result for Login Screen

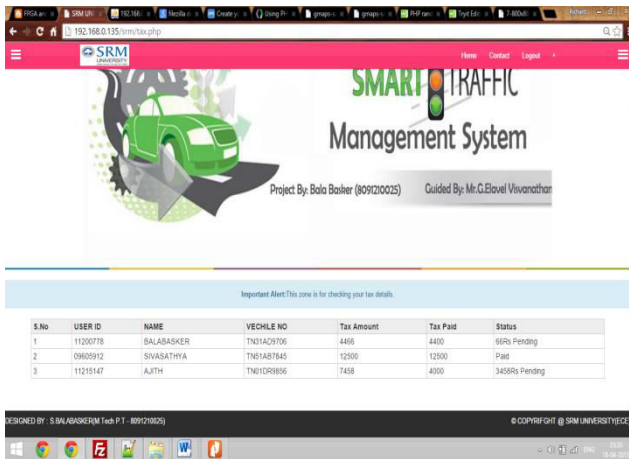


Fig.12.Simulation Result for Tax Zone



Fig.14. Simulation Result for Insurance

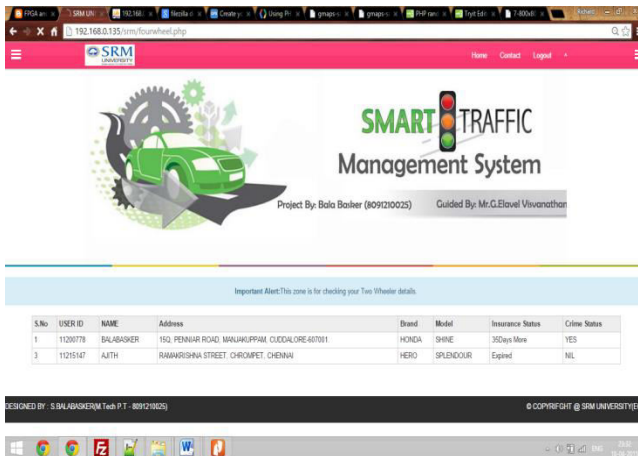


Fig.16 Simulation Result for Four Wheeler Check

Fig.11.Simulation Result Welcome Screen

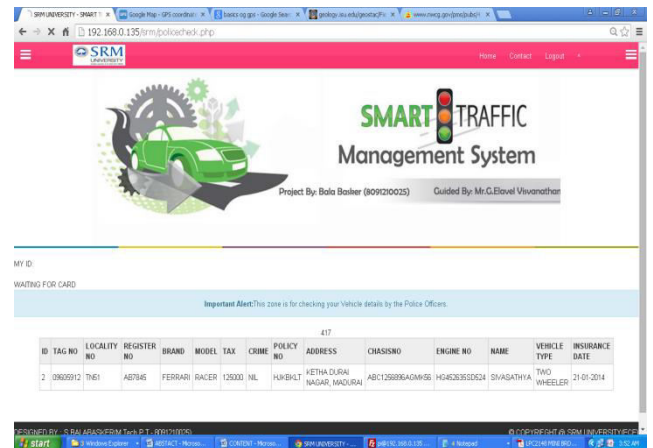


Fig.13.Simulation Result for Police Check

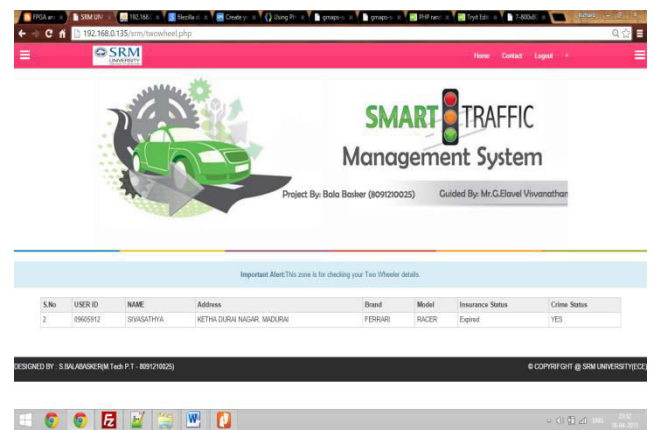


Fig.15.Simulation Result for Two Wheeler Check

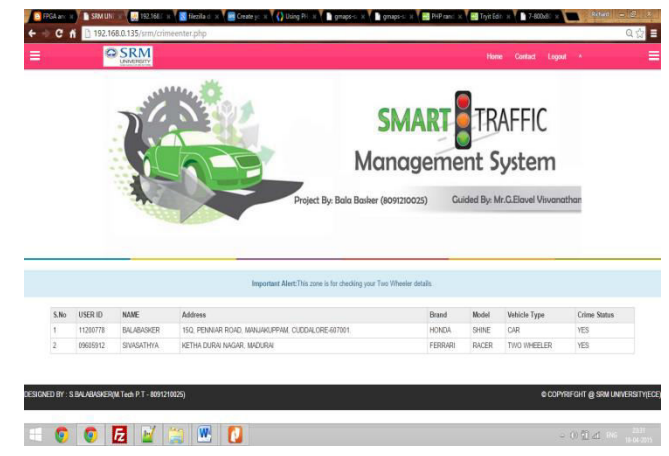


Fig.17 Simulation Result to Check Crime

S.No	USER ID	NAME	REGISTER NO	LOCATION	ANTENNA ID	TIME	CHECK LOCATION
68	1121547	AJITH	1121547	CUDDALORE BEACH ROAD	1	2015-03-14 16:15:52	Check Location
69	0968942	SWASATHYA	0968942	CUDDALORE BEACH ROAD	1	2015-03-14 16:16:56	Check Location
70	1120078	BALABAKSER	1120078	CUDDALORE BEACH ROAD	1	2015-03-14 16:16:56	Check Location
71	1121547	AJITH	1121547	CUDDALORE BEACH ROAD	1	2015-03-14 16:16:56	Check Location
72	0968942	SWASATHYA	TWO WHEELER	CUDDALORE BEACH ROAD	1	2015-03-14 16:20:26	Check Location
73	1121547	AJITH	BUS	CUDDALORE BEACH ROAD	1	2015-03-14 16:20:24	Check Location
74	1120078	BALABAKSER	CAR	CUDDALORE BEACH ROAD	1	2015-03-14 16:20:26	Check Location
75	0968942	SWASATHYA	TWO WHEELER	CUDDALORE BEACH ROAD	1	2015-03-14 16:50:53	Check Location
76	1121547	AJITH	BUS	CUDDALORE BEACH ROAD	1	2015-03-14 18:51:03	Check Location

Fig.18 Simulation Result to Track Vehicle Online

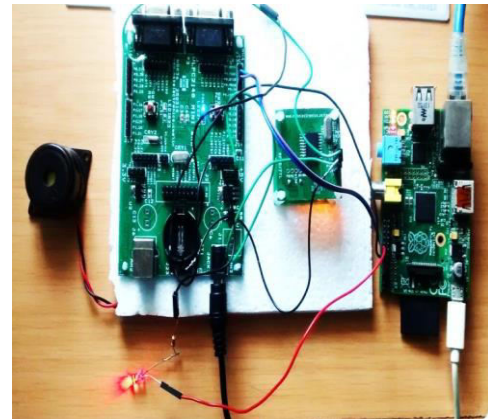


Fig.19 Hardware Result for Crime Detected Vehicle

V. CONCLUSION

Implementation of Vehicle Management System using Internet of Things had been proposed and suitable for real time management. The system also provides more flexibility that it can be controlled remotely from anywhere using any smart devices. In future the same project can be made available to be added as an external interface in Smart device likes Tablet and mobiles so that it can be easily used anywhere. So my project is more useful for the police officers to check the vehicle status.

REFERENCES

- [1] "Dynamic traffic light sequence algorithm using RFID," by K. A. Al-Khateeb, J. A. Johari, and W. F. Al-Khateeb, Journal of Computer Science, vol. 4, no. 7, 2008.
- [2] "An intelligent traffic management expert system with RFID technology," by W. Wen, Expert Systems with Applications, vol. 37, no. 4, pp. 3024-3035, 2010.
- [3] "Controlling of traffic lights using rfid technology and neural network," by S. Mohammadi, A. Rajabi, and M. Tavassoli, Advanced Materials Research, vol. 433, pp. 740-745, 2012.
- [4] "RFID based vehicular networks for smart cities," by J. Paul et presented at 2013 IEEE 29th International Conference on Data Engineering Workshops (ICDEW), 2013.
- [5] Raspberry Pi, <http://www.raspberrypi.org/about/>
- [6] Early prototype of Raspberry Pi, <http://www.raspberrypi.org/raspberrypi-2006-edition/>
- [7] Raspberry Pi Hardware information, http://elinux.org/RPi_Hardware
- [8] How SoC works, <http://www.androidauthority.com/how-it-works-systems-on-a-chip-soc-93587/>
- [9] Boot process, <http://thekandyancode.wordpress.com/>
- [10] NOOBS, <http://www.raspberrypi.org/introducing-noobs/>

Design of Context Aware Smart Home Energy Management System Using RFID

B.kayalvizhi¹, S. Boomadevi²

¹Department of ECE, V.R.S College of Engineering and Technology, kayalvizhi5237@gmail.com

² Department of ECE, V.R.S College of Engineering and Technology, boomadevisundar@gmail.com

Abstract— Energy wastage in buildings is to be minimized to reduce the carbon footprint of electricity. Wireless Sensor and actor networks (WSAN) have been providing solutions for effective energy management within buildings. The sensors collect the physical information required to identify the context and these information are send to Arduino board. The Arduino controls the load through Relay according to the commands received from the sensors. In our project, we are using sensors like RFID, PIR, LM35 and LDR.

Keywords- WSAN, Sensors, RFID, Arduino, Relay.

I. INTRODUCTION

Energy management is very crucial role in our society. To save the energy, we have to choose the suitable resources. It should be done in real time and at the same time power and cost to be saved. The ever growing energy demand needs has to be thoroughly reviewed to reduce the greenhouse gas effects and climatic changes. U.S. Department of energy reports 39percent of total energy consumption by buildings. The energy consumption of the buildings is contributing to 8percent of total emissions. Information and communication Technologies (ICT) play a key tool to support smart energy management within buildings thereby reducing the carbon footprint by at least 15 percent according to smart2020 report. We have designed this paper to reduce the energy usage and for security purpose. We have designed this paper to reduce the energy usage and for security purpose.

In this paper, we have used RFID for identification purpose after that it will Switch ON the PIR sensor it will detect the human motion, after motion is detected it will switch on the LM 35 and LDR. LM35 sense the temperature and compare the temperature with surrounding temperature and the information is send to the Arduino board. The Arduino controls the load (fan) that is switch ON/OFF through relay according to the commands received from the LM 35.LDR sense the light intensity and the information is send to the arduino and it controls the load (light) that is switch ON/OFF through relay according to the information received from the LDR.

II. SYSTEM ARCHITECTURE

The System architecture consists of four layer, where each layer perform special function.

They are,

1. Sensor Layer
2. Mote Layer
3. Control Layer

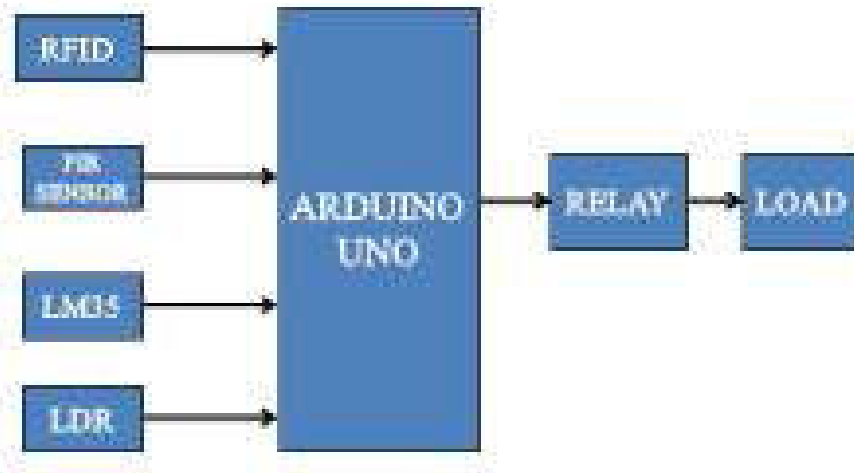


Fig. No.1 Block Diagram

The design and implementation of these layers are discussed in detail below,

2.1 Sensor Layer:

The Sensor Layer consists of Sensors like RFID, PIR, LDR (light dependent resistor) and LM 35 (Temperature sensor).Sensors collect the physical information required to identify context. Functionality and implementation of each sensor is explained below,

2.2 RFID

It consists of RFID Tag and RFID Reader.

2.3 RFID Tag

RFID tag is a small device which stores and sends data to RFID reader. They are categorized in two types – active tag and passive tag. Active tags are which has an internal battery and do not require power from the reader. Usually active tags have a longer distance range than passive tags. Passive tags are small in size and light weight than the active tags. They do not have an internal battery and thus depend on RFID reader for operating power and certainly have a low range limited up to few meters.

RFID Reader: An RFID reader sends an encoded radio signal to grill with the tag. The RFID tag get the message and then responds with its identification and other information. This may have a exclusive tag serial number, such as a stock number, lot or batch number, or other specific information. Since tags have its own serial numbers, the RFID system design can differentiate among several tags that might be within the range of the RFID reader and read them simultaneously.

RFID systems can be classified by the type of tag and reader. A Passive Reader Active Tag (PRAT) system has a passive reader which only receives radio signals from active tags .The reception range of a PRAT system reader can be adjusted from 1–2,000 feet (0–600 m), allowing flexibility in applications such as asset protection and supervision.

An Active Reader Passive Tag (ARPT) system has an active reader, which transmits interrogator signals and also receives authentication replies from passive tags.

An Active Reader Active Tag (ARAT) system uses active tags awoken with an interrogator signal from the active reader. A change in the system could also use a Battery-Assisted Passive (BAP) tag which acts like a passive tag but has a small battery to power the tag's return reporting signal.

2.4 PIR Sensor

PIR Sensor is a motion sensor. It sense the human being by the body heat and the motion of people like(walking, moving)within the sensor's range It allow you to sense motion, and also used to detect human has moved in or out of the sensors range. They are small, low cost, low-power, easy to handle and don't wear out. Due to this reason they are commonly found in appliances and gadgets used in homes or businesses. PIRs are usually made from a pyroelectric sensor, which can notice the levels of infrared radiation. Each and Everything emits certain low level radiation, and the hotter, so the more radiation is emitted.

2.5 LM35 (Temperature Sensor)

LM35 is a temperature sensor and widely used in electronics. The output voltage of LM35 is directly proportional to the Celsius (Centigrade) temperature. The output of LM35 is of 10mV/°C scale factor, that means for each 1°C increase in temperature there will be a corresponding increase in 10mV and temperature value can be easily predicted.

2.6 LDR (Light Dependent Resistor)

A light dependent resistor works on the principle of photo conductivity. Photo conductivity is based on optical phenomenon in which the materials conductivity (Hence resistivity) reduces when light is absorbed by the material. If light falls then the photons will fall on the device, the electrons are in the valence band of the semiconductor material is excited to the conduction band. All these photons in the incident light should have energy greater than the band gap of the semiconductor material to make the electrons jump from the valence band to the conduction band. Therefore while light having enough energy is incident on the device more & more electrons are excited to the conduction band which results in large number of charge carriers. The outcome of this process is more and more current starts flowing and hence it is said that the resistance of the device has decreased.

2.7 Arduino

Arduino is an open-source platform used for building electronics projects. It contains both a physical programmable circuit board and a piece of software, or IDE (Integrated Development Environment) that runs on the computer, which is used to write and upload computer code to the physical board. The Arduino platform has become most popular because it is easy to handle. Unlike most previous programmable circuit boards, the Arduino does not require a separate piece of hardware. In Arduino to load a new code onto the board use a USB cable. Moreover, the Arduino IDE uses a simplified version of C++, so it is easy to learn the program. At last, Arduino provides a standard form factor that breaks out the functions of the micro-controller into a more accessible package.

2.8 Relay

Relays are simple switches which are operated both electrically and mechanically. The main operation of a relay comes in places where only a low-power signal can be used to control a circuit. It is also used where only one signal can be used to control a lot of circuits. It is a device which is used for controlling purpose.

III. WORKING

In our project, the purpose of RFID is to identify the secret code in the RFID Tag (Human being) for this we have dumped the code in the Arduino Uno board. While entering the room, the object want to show the RFID card to the RFID reader .If it is a valid code, then switch ON the PIR Sensor. After that, PIR sensor is ON & it will switches ON/OFF the Fan and Light through Relay depending on the commands received from the LM35 & LDR.

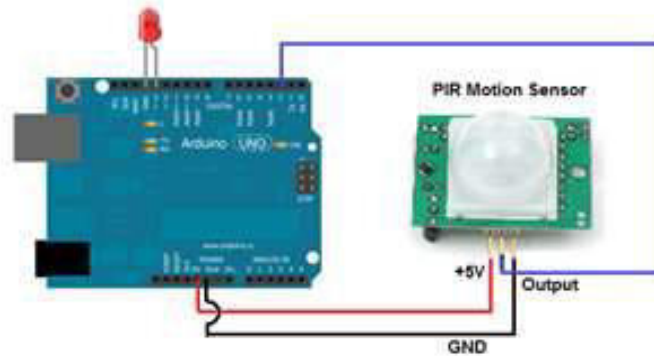


Fig No. 2 Connection for PIR Sensor with Arduino Uno

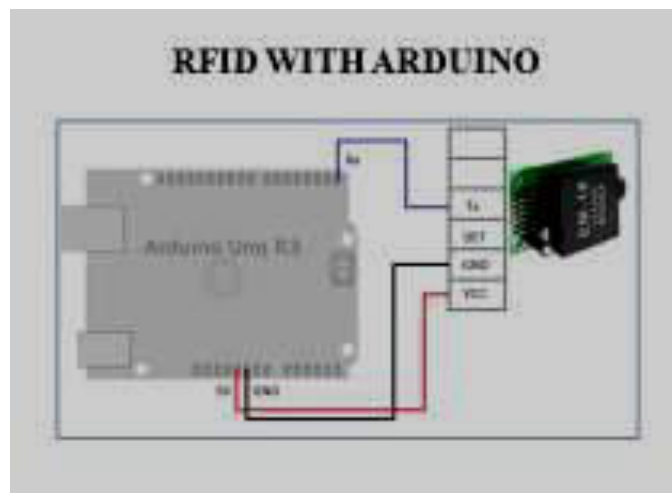


Fig.No. 3 Connection for RFID Reader with Arduino Uno

IV. CONCLUSION

Optimal energy usage in buildings is achieved with the help of RFID and Sensors. In this paper, we have used sensors like PIR, LM35 & LDR. Depending up on the physical parameters sensed from these sensors, relay control the loads. The future scope of the work is to develop the Smart Phone and Tablet Pcs to the remote people for access/remote control. Web based GUI developed is really useful for monitoring energy usage of the building/home for both local and remote operation of electrical loads.

V. FUTURE ENHANCEMENT

In future, we can improve this project by adding Security system like (fingerprint, face recognition, retina scanning) and GSM (sending day energy consumption). We can use this system for Industry purpose also.

REFERENCES

- [1] Alan Marchiori “Enabling distributed building control with wireless Sensor networks”2011 IEEE.
- [2] Dae-Man Han and Jae-Hyun Lim “Design and Implementation of Smart Home Energy Management Systems based on Zigbee” 0098 3063/10/2010 IEEE
- [3] Hiroshi Mineno, Yuichiro Kato, Kenji Obata, Hiroshi Kuriyama, Keiichi Abe, Norihiro Ishikawa and Tadanori Mizuno “Adaptive Home/ Building Energy Management System Using Heterogenous Sensor/ Actuator Networks” IEEE CCNC 2010 proceedings, IEEE Communication Society
- [4] J.J.Jamiana M.W.Mustafa a.H.Mokhlis b,M.A.Baharudina “Conceptual Data Management and Communication for Smart IEEE Sponsored 2nd International Conference on Innovations in Information Embedded and Communication Systems ICIIECS’15 1627
- [5] Distribution System” 2011 IEEE First Conference on Clean Energy and Technology CET.
- [6] Raja Vara Prasad Y,Rajalakshmi P “Context Aware Building Energy Management System with Heterogenous Wireless Network Architecture” IFIP WMNC’2013.

Performance Analysis of OFDM System with QPSK for Wireless Communication

Kalaivani.P¹, Puviyarasi.T², Raju S.S³, Suresh.S⁴

¹ Department of Electronics and Communication Engineering, A.K.T Memorial college of Engineering and Technology, Kallakurichi, E-mail Id- vanikala2322@gmail.com

² Department of Electronics and Communication Engineering, A.K.T Memorial college of Engineering and Technology, Kallakurichi, E-mail Id- kavinila9023@gmail.com

³ Department of Electronics and Communication Engineering, A.K.T Memorial college of Engineering and Technology, Kallakurichi, E-mail Id- ssrajvmd@gmail.com

⁴ Department of Electronics and Communication Engineering, A.K.T Memorial college of Engineering and Technology, Kallakurichi, E-mail Id- write2suresh@gmail.com

Abstract — Communication is one of the important aspects in life. Modulation and Demodulation plays an important role in transmission of data from transmitter to receiver in all communication system. Working with wireless system using various multiplexing techniques like FDMA, CDMA and TDMA which encountered various problems such as multi-path fading, time dispersion, ISI and low bit rate. The use of OFDM technique provides better solution for above mentioned problems. The OFDM based wireless communication system includes OFDM transmitter and OFDM receiver with different modulation technique. In this work, an OFDM based QPSK wireless system is demonstrated which incorporates diverse channel encoding techniques over Rayleigh fading channel. The performance of the simulated result is investigated via BER assessment as a function of SNR.

Keywords- OFDM, QPSK, BER, ISI, SNR.

I. INTRODUCTION

In a typical terrestrial broadcasting, the transmitted signal arrives at the receiver using various paths of different lengths. Since multiple versions of the signal interfere with each other, it becomes difficult to extract the original information. In wireless communications system allow the subscriber to send the receiving information to the base station while receiving information from the base station. It is called duplexing and the performed device called duplexer. Multiple access schemes are used to allow many mobile users to share simultaneously a finite amount of radio spectrum. The use of orthogonal frequency division multiplexing (OFDM) technique provides better solution [1].

Orthogonal Frequency Division Multiplexing or OFDM is a modulation format that is being used for many of the latest wireless and telecommunications standards. Orthogonal frequency division multiplexing has also been adopted for a number of broadcast standards from DAB, Digital Radio to the Digital Video Broadcast standards, DVB [2]. IFFT is used instead of after serial to parallel conversion of modulated data. It is converted to parallel form and fed to FFT block [3]. Then, the signal is demodulated and undergoes different channel decoding algorithms. Subsequently, the information data is recovered back after decoding.

The cyclic prefixes (CP) are added before transmitting the signal. The purpose of adding cyclic prefix is to reduce inter-symbol interference (ISI). The drawback of CP is reducing the spectral containment of the channels. OFDM requires a cyclic prefix to remove ISI, this causes overhead and this overhead may be sometimes much large for the system to be

effective. BCH codes form a class of cyclic error-correcting codes that are constructed using finite fields. One of the key features of BCH codes is that during code design, there is a precise control over the number of symbol errors correctable by the code. In particular, it is possible to design binary BCH codes that can correct multiple bit errors. Bit error rate, BER is a key parameter that is used in assessing systems that transmit digital data from one location to another [3]. Systems for which bit error rate, BER is applicable include radio data links as well as fiber optic data systems, Ethernet, or any system that transmits data over a network of some form where noise, interference, and phase jitter may cause degradation of the digital signal. When data is transmitted over a data link, there is a possibility of errors being introduced into the system. If errors are introduced into the data, then the integrity of the system may be compromised. As a result, it is necessary to assess the performance of the system, and bit error rate, BER, provides an ideal way in which this can be achieved.

II. PEAK TO AVERAGE POWER RATIO (PAPR)

Large number of independently modulated sub-carriers in an OFDM system the peak value of the system can be very high as compared to the average of the whole system. This ratio of the peak to average power value is termed as Peak-to-Average Power Ratio (PAPR). Coherent addition of N signals of same phase produces a peak which is N times the average signal [4]. The PAPR increased complexity in the analog to digital and digital to analog converter and also reduce efficiency of RF amplifiers.

The peak to average power ratio for a signal $x(t)$ is defined as

$$\text{Papr} = \max [x(t)x^*(t)]/E[x(t)x^*(t)]$$

PAPR was represented by decibels

$$\text{Papr}_{\text{db}} = 10 \log_{10}(\text{papr})$$

III. MODULATION TECHNIQUE

There are different types of modulation like MPSK, BPSK, QPSK, 16-PSK, 32-PSK, QAM etc. Each modulation technique has its own error function, so the performance of modulation technique is different at the time when noise is present. But high data rate transmission in limited bandwidth increase the BER. Some time it destroys the original data. QPSK is a form of four possible carrier the carrier phase shifts $(0, \pi/2, \pi$ and $3\pi/2)$ [4,5].

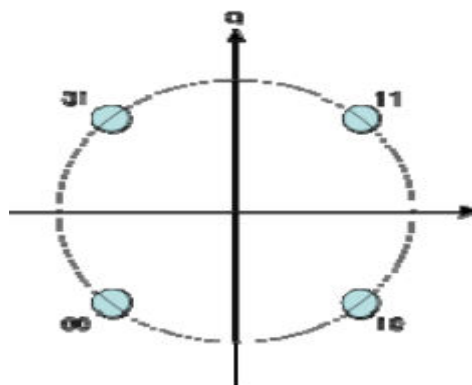


Figure 3.1 Constellation diagram of QPSK

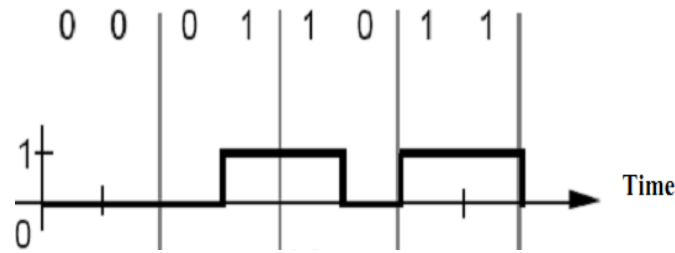


Figure 3.2 Binary Sequence

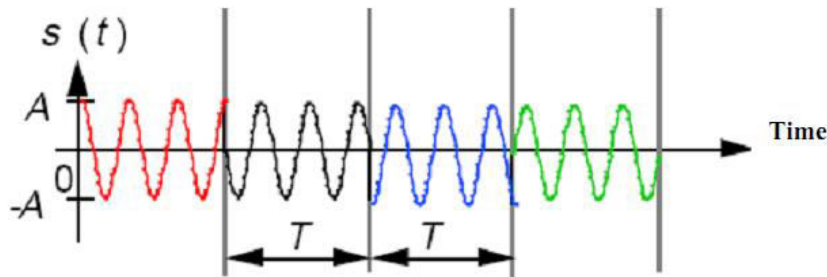


Figure 3.3 QPSK Signal

The techniques which are generally used in wireless communication are QAM (Quadrature Amplitude Modulation) and QPSK (Quadrature phase shift keying). Higher order modulation technique transmits high data rate but higher order modulation techniques required high SNR. Larger area the QPSK technique is more efficient than the QAM.

IV.OFDM SYSTEM

The source data is being encoded by using different channel encoding schemes viz. CC-, RS- and BCH-encoding independently [6]. After this encoded data is given to modulation block which is configured to implement modulation. Then, IFFT is used instead of after serial to parallel conversion of modulated data. After this, data is again being converted to serial form for the purpose of CP addition and transmitted through the channel. At the receiver, first of all CP is removed from the signal then it is converted to parallel form and fed to FFT block. Then, the signal is demodulated and undergoes different channel decoding algorithms. Subsequently, the information data is recovered back after decoding.

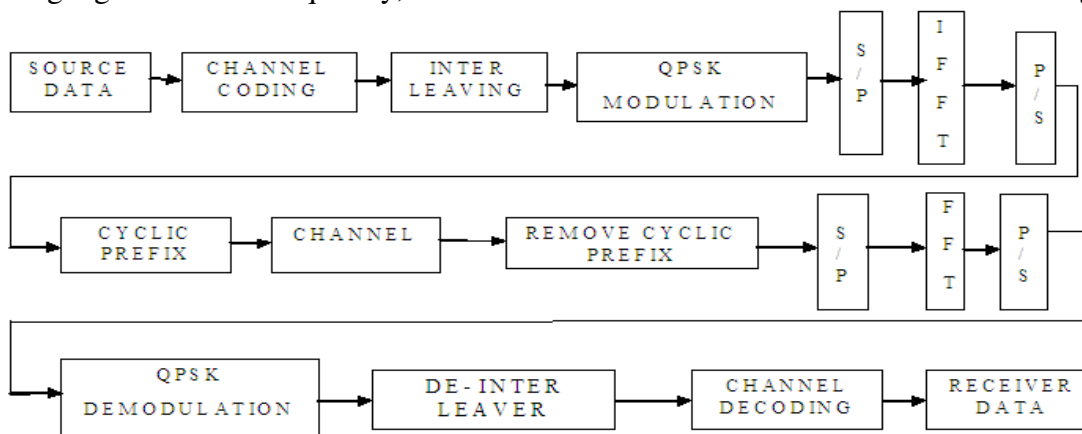


Figure 4.1 Block diagram of OFDM

4.1 BCH CODES

BCH codes form a class of cyclic error-correcting codes that are constructed using finite fields. One of the key features of BCH codes is that during code design, there is a precise control over the number of symbol errors correctable by the code. In particular, it is possible to design binary BCH codes that can correct multiple bit errors. Another advantage of BCH codes is the ease with which they can be decoded, namely, via an algebraic method known as syndrome decoding. This simplifies the design of the decoder for these codes, using small low-power electronic hardware.

The Encoder design by Random number is used in this project is most commonly used in the modern digital communication system. This Encoder design is almost common to all the BCH code architecture, which uses the random number generator for polynomial division. BCH encoder is usually implemented.

4.2 INTERLEAVING

Interleaving is a process or methodology to make a system more efficient, fast and reliable by arranging data in a noncontiguous manner. There are many uses for interleaving at the system level, including:

Storage: As hard disks and other storage devices are used to store user and system data, there is always a need to arrange the stored data in an appropriate way.

Error Correction: Errors in data communication and memory can be corrected through interleaving. Multi-Dimensional Data Structures. Interleavers and Deinterleavers are designed and used in the context of characteristics of the errors that might occur when the message bits are transmitted through a noisy channel. To understand the functions of an Interleaver/Deinterleaver, understanding of errors characteristics is essential. Two types are errors concern communication system design engineer. They are burst error and random error. One of the most popular ways to correct burst errors is to take a code that works well on random errors and interleave the bursts to “spread out” the errors so that they appear random to the decoder.

4.3 CYCLIC PREFIX

Use of cyclic prefix is a key element of enabling the OFDM signal to operate reliably. The cyclic prefix acts as a buffer region or guard interval to protect the OFDM signals from intersymbol ISI. This can be an issue in some circumstances even with the much lower data rates that are transmitted in the multicarrier OFDM signal.

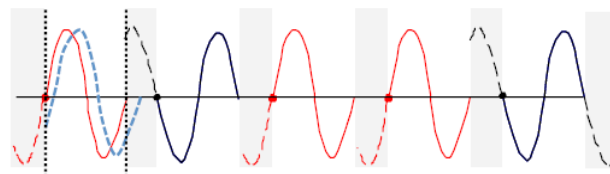


Figure 4.2 Cyclic Prefix

FFT based OFDM. In the conventional OFDM system Fast Fourier transform (FFT) and inverse fast Fourier Transform (IFFT) are used to multiplex all the signals together in

transmitter and decode the signal at the receiver. The cyclic prefixes (CP) are added before transmitting the signal. The purpose of adding cyclic prefix is to reduce inter-symbol interference (ISI).

The drawback of CP is reducing the spectral containment of the channels. In the transmitter side, the input digital data is processed by M- ary QAM or PSK modulator to map the data with N subcarriers.

IFFT block is then used to modulate this low data rate stream and also converts the domain of the input signal. Then the output of IFFT is the sum of the information signals in the discrete time domain. After applying IFFT on the symbols in all the channels, cyclic prefix is added. The addition of a cyclic prefix to each symbol solves for both the Inter Symbol Interference and Inter Carrier Interference. If the channel impulse response has a known length L, then the prefix consists simply of copying the last L-1 values from each symbol and appending them in the same order to the front of the symbol. Digital data is then converted to serial form and transmitted over the channel. At the receiver side, the process is reversed and decoded the data. The output of FFT is the sum of the received signal in discrete frequency domain. After FFT, the signal is converted back to parallel form and demodulated to yield the transmitted signal back. In wireless applications particularly, calculating the channel impulse response length is a tiresome task. So other techniques have to be introduced. One can attempt to go for other compensating methods, making the overall system more and more complex. Another solution is to replace the Fourier Transform by a transform that is less subject to all these channel effects, and that can thus more easily compensate for the resultant effect.

V . RESULTS AND DISCUSSION

The OFDM based QPSK wireless system was simulated using MATLAB environment. The simulation result was obtained for the OFDM system. The performance analysis for BER vs SNR curve was obtained. In that BER ranges from 10^{-1} to 10^{-2} was obtained.

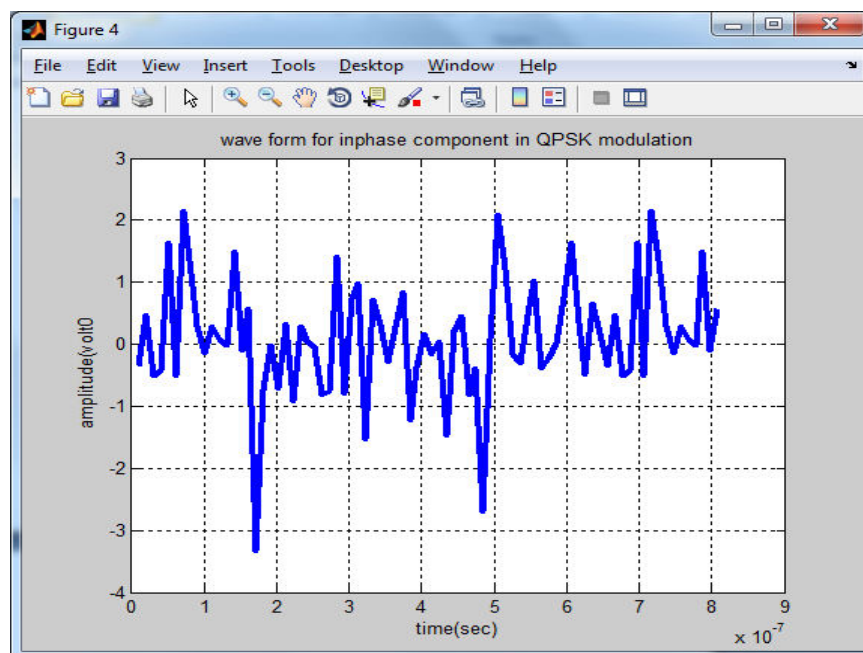


Figure 5.1 QPSK modulated output signal

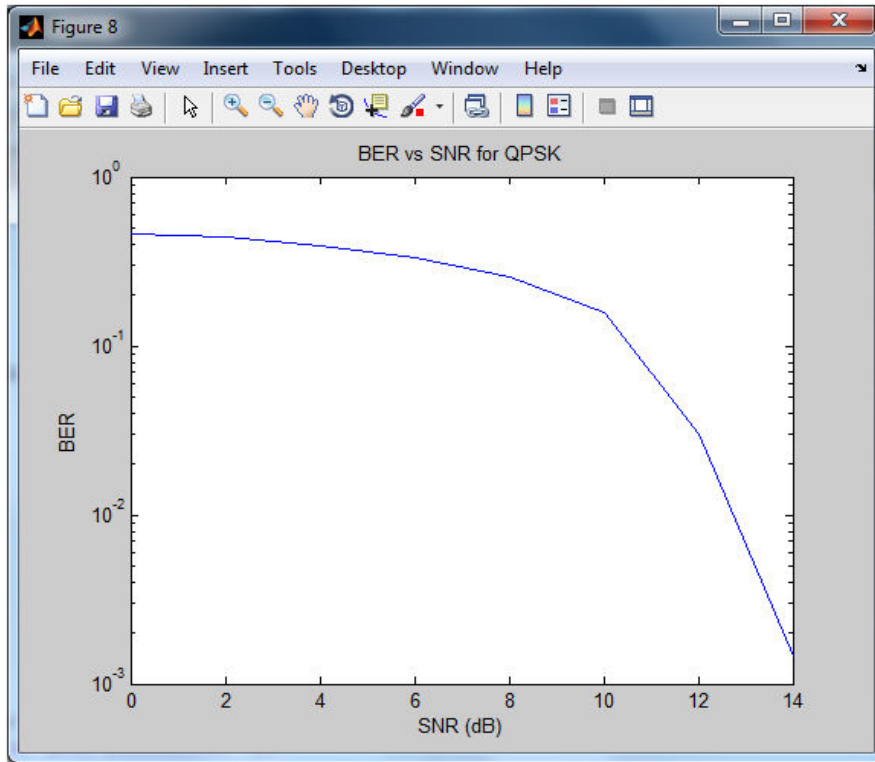


Figure 5.2 BER vs SNR performance of input signal

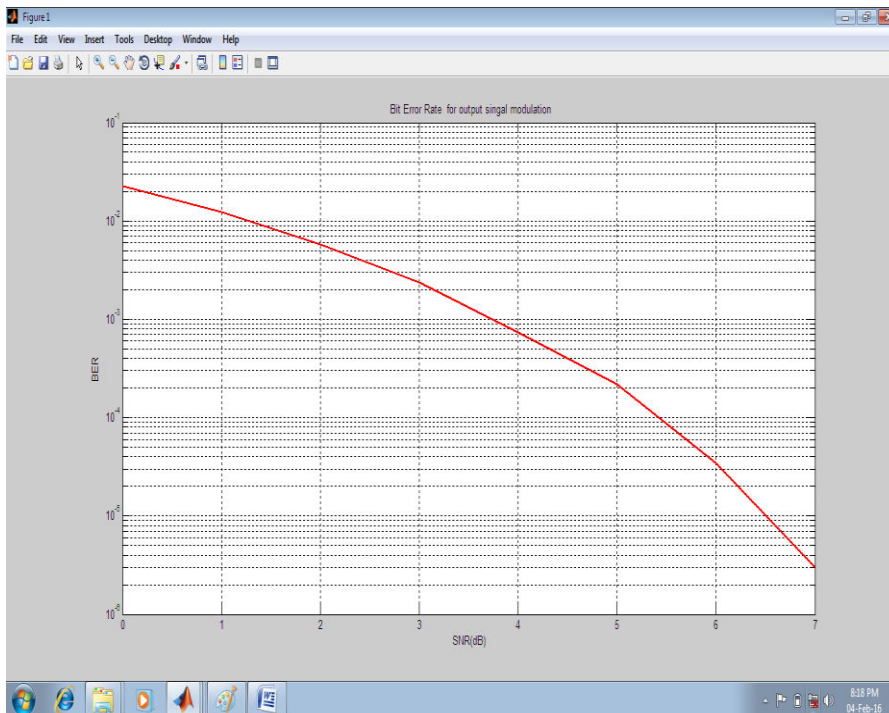


Figure 5.3 BER vs SNR performance of output signal

VI.CONCLUSION

The OFDM system characteristic depends upon the modulation technique. The performance of OFDM was increasing by improving the BER value. It uses higher order modulation of QPSK modulation and it was using various coding technique. In this paper BCH coding was used to encoding the source data. The simulation result was obtained with low BER value for OFDM based QPSK wireless system.

REFERENCES

- [1]. Lavish Kansal, Vishal Sharma, Jagjit Singh, "BER Assessment of FEC incorporated OFDM-MPSK Wireless System", IEEE Transaction on Adv.com & comm.tech, 2015.
- [2]. Sandeep Kaur, Gurpreet Bharti, "Orthogonal Frequency Division Multiplexing in Wireless Communication Systems: A Review", Int.Jour. Adv.Res.Com.Eng.& Tech.,2012.
- [3]. Lavish Kansal, Ankush Kansal and Kulbir Singh, "Performance Analysis of MIMO-OFDM System Using QOSTBC Code Structure for M-QA", Can.Jour.Sig.Proc.,2011.
- [4]. AthinarayananVallavaraj,Stewart,G.B,David,K.Harrison,Francis ,G.McIntosh., "The Effects of Convolutional Coding On BER Performance of Companded OFDM Signals",Int.Conf.,Comm.Com & Pow, 2005.
- [5]. Arpita Mishra, Stuti Rastogi, Ritu Saxena, Pankaj Sharma, Sachin Kumar, "Performance Analysis Of MB-OFDM System With QPSK and QAM For Wireless Communication", Int.Jour.Adv.Res.Com.Comm.Eng, 2013.
- [6]. Hamood Shehab,Widad Ismail,"The Development & Implementation of Reed Solomon Codes for OFDM Using Software"-Defined Radio Platform, Int. Jour.Com.Sci.& Comm.,2010.
- [7]. Geert Van Meerbergen, Member, IEEE, Marc Moonen, Fellow, IEEE, and Hugo De Man, Fellow, IEEE., "Reed-Solomon codes implementing a coded Single-Carrier with Cyclic Prefix scheme", 2006.
- [8]. Hindumathi,V. RamaLinga,K. Reddy and Prabhakara Rao,K, " Performance Analysis of OFDM by using different Modulation Techniques", Int.Jour. Eng.Res. & Dev., 2012.
- [9]. Riaz Ahamed,S.S., " Performance Analysis of OFDM", Jour.Theor.&App. Infor.,tech, 2008.

Voice Recognition Based Personal Assistant Robot Using Wireless Sensor Networks

Poonguzhali.S¹, Raju S.S², Suresh.S³

¹Department of Electronics and Communication Engineering, A.K.T Memorial college of Engineering and Technology, Kallakurichi, E-mail Id- lirasri28@gmail.com

²Department of Electronics and Communication Engineering, A.K.T Memorial college of Engineering and Technology, Kallakurichi, E-mail Id- ssrajuvmd@gmail.com

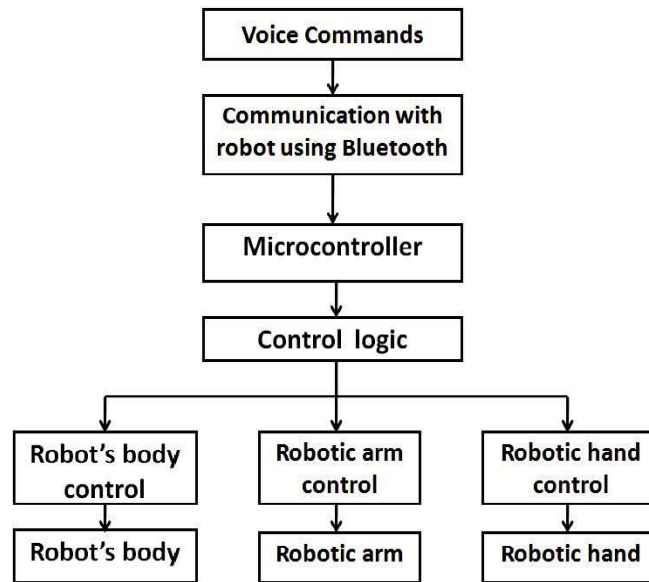
³Department of Electronics and Communication Engineering, A.K.T Memorial college of Engineering and Technology, Kallakurichi, E-mail Id- write2suresh@gmail.com

Abstract: Personal robotic assistants help reducing the manual efforts being put by humans in their day-to-day tasks. In this paper, we develop a voice-controlled personal assistant robot. The human voice commands are given to the robotic assistant remotely, by using a smart mobile phone. The robot can perform different movements, turns, start/stop operations and relocate an object from one place to another. The voice commands are processed in real-time, using an online cloud server. The speech signal commands converted to text form are communicated to the robot over a Bluetooth network. The personal assistant robot is developed on a micro-controller based platform and can be aware of its current location. The effectiveness of the voice control communicated over a distance is measured through several experiments. Performance evaluation is carried out with encouraging results of the initial experiments. Possible improvements are also discussed towards potential applications in home, hospitals and industries.

Key words: smart assistant robot, control over voice, Blue-tooth, Android based smart devices.

I. INTRODUCTION

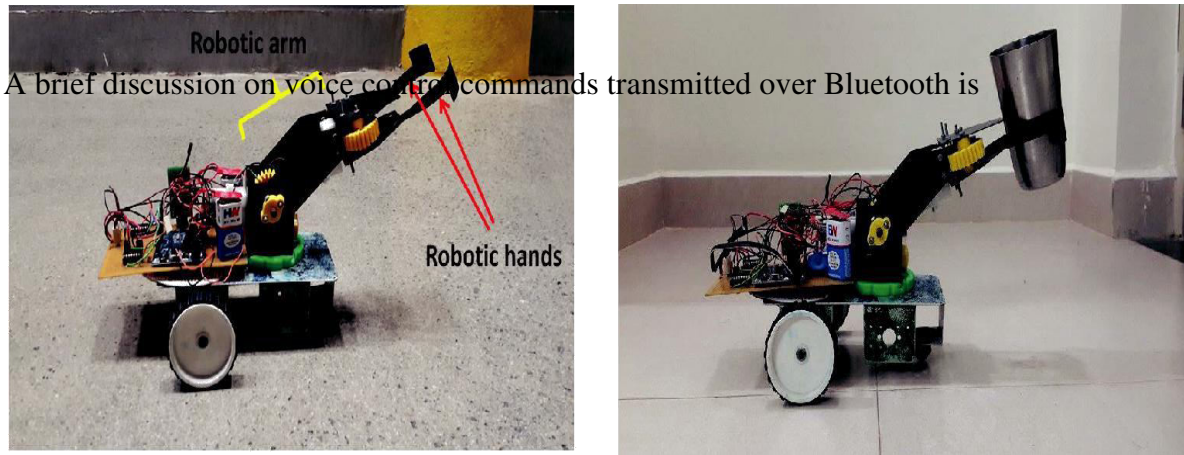
Over the years, humans have evolved in inventing new technologies for reducing human efforts and saving human life. In chemical and explosives manufacturing industries, people often get injured while handling hazardous chemicals due to lack of due care or precaution taken. Physically challenged and elderly people face difficulties while handling objects and hence they need assistance for the same. Thus, if a robotic assistant is developed that can be operated using speech commands would be of immense use. Assistant robots can be used for range of purposes such as in chemical industries or in homes for the purpose of handling hazardous chemicals and objects respectively. These robotic assistants can be used for shaping, manufacturing and tooling purposes in various sectors such as manufacturing, defence etc. In hospitals, these robotic assistant can be used for the purpose of performing surgeries and operations with high precision. In this paper, we develop an assistant robot that can be operated using speech commands.



Robotic arm, developed using 6 degrees of freedom, could follow a predefined trajectory with much better accuracy and precision value. A PC-interfaced low cost robotic arm was developed that could be integrated with a robotic arm, used for light weight lifting applications. Another robotic arm was developed which had special applications for the physically challenged people. A robotic arm was designed in such a way that it could be controlled using human brain. A robotic arm was designed which could drill boreholes and in congested urban areas with effectiveness. An intelligent robotic arm was also used to perform various tasks such as weight-lifting, color classification using image processing and could also function by speech recognition. A robotic arm was developed which replicate the gestures of the humans and replicate the movements. A robotic arm was developed which could recognize human voice and convert the same to a text, thus functioning as a speech-to-write converter. Various applications of the robotic arm were discussed extensively. The design and construction issues in laboratories of educational institutes were also addressed using a laboratory robotic arm.

A robotic assistant that can be controlled using speech commands is developed in this paper and it can be used in hospitals, homes, industries and Educational institute. Various experiments are conducted on the prototype to study about the robot's acceleration, power consumed by the robot for it's functioning, angular velocity of the robotic arm, the range in which the speech commands can be executed and various limitations of the assistant robot. Use of renewable source of energy, effect of background noise towards performance of the robot, role of distance to be kept between mouth and smart phone are some of the areas that can be explored further.

This paper is organized as follows. In Section II, the construction details of the robot i.e. hardware information, block diagram and functioning are discussed.



<p>Fig. 2(a): Side view of the robot with 'robotic hands' open</p>	<p>Fig. 2(b): Side View of the robot holding an object ('robotic hands' closed)</p>
--	---

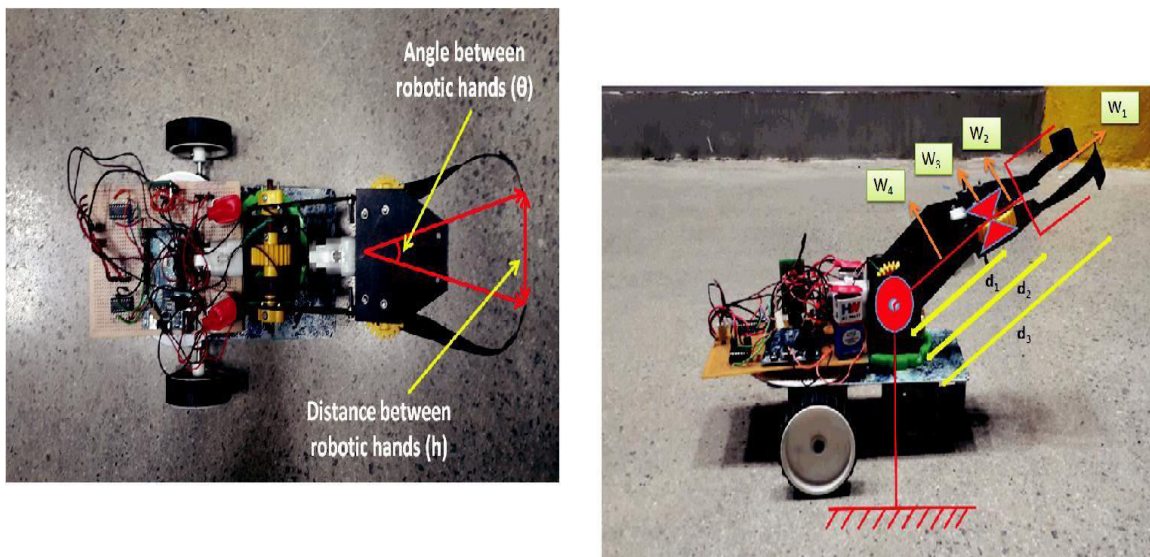


Fig. 2(c): Top View of the robot with 'robotic hands' open

made in the Section III. Section IV discusses operation of the robotic assistant on commands communicated using Bluetooth network. In Section V, the experiments conducted and the observations made are discussed. The results and inferences made are discussed in Section VI. The possible applications of the robotic assistant are discussed in Section VII. A brief summary of the paper is given in Section VIII, along with scope of further work on this topic.

II. CONSTRUCTION DETAILS OF THE ROBOTIC ASSISTANT

The movement of the robot is controlled using speech commands i.e. the movement of the (i) *robot's body*, (ii) *hands* and (iii) *the arm* depend upon the voice command which are given. The voice commands are given to the robot using a smart mobile phone which is based on an Android OS based platform. The voice signal is then converted to the text from using an online cloud server, in real time. This text command is sent via Bluetooth network of the smart-phone to the Bluetooth module on the robot. The Bluetooth module on-board the robot receives the text signals and forwards it to the microcontroller.

The hardware platform consists of a *robotic arm* built on the robot's body that can move. The robotic arm consists of an arm and two hands. Arm is used to position the hands position and the hands are used to hold and drop any object. It is just like human's hands where the robotic arm acts same like our arm and the *robotic hands* act like our hands. Two DC motors are used to control the movement of the robot's body. Another two DC motors are used to control the movement of the robotic arm and the robotic hands. Motor driver IC is used to control the movement of DC motor. A single motor driver (L293D) IC can control two DC motors.

Android based smart phone is used for connecting to the robotic arm and the robot's body using speech signals which are transferred by the Bluetooth. Depending upon the voice commands given, the robot performs the actions accordingly. Arduino based micro-controller platform is used which acts as an interface between the Bluetooth module and the robotic assistant. Movement of the robot's body, hands and arm are independent of each other's movements. Side view of the robot with the robotic hands open is shown in Fig. 2(a), side view of the robot holding an object is shown in Fig. 2(b), and in Fig. 2(c) the top view of the robot with its hands open is shown along with the angle θ and the distance (h) between the two hands.

Voice command	Movement
Forward	robot's body moves forward
Backward	robot's body moves backward
Left	robot's body moves left
Right	robot's body moves right
Up	robotic arm moves up
Down	robotic arm moves down
Open	robotic hands open
Close	robotic hands close

III. VOICE CONTROL OVER BLUETOOTH

The Android application converts the input voice command given on the smart phone to the text form. Then this signal which is in the text form is transmitted to the Bluetooth module present on the robot which intern sends the signal to the micro-controller. The micro-controller then would process the signal and moves the robot accordingly. The block diagram of the operation of the assistant robot is shown in Fig. 1.

Communication is done to the robot using the smart phone. The movements of the robot's body, the robotic hands and the robot's arm can be controlled simultaneously as different

motors are used for the different parts of the robot. Table 1 shows the commands used by for the movement of the robot.

IV. OPERATION USING BLUETOOTH

Table 2: The angle and distance between the 'robotic hands': (a) time interval 'robotic hands open' (t sec), and (b) the distance and (c) the angle between the 'robotic hands'

(a)	(b)	(c)
t(s)	l(cm)	θ(degree)
1	4.1	16.84
2	9.4	39.23
3	15.0	64.78
4	19.1	86.02
5	22.6	107.63
6	27	149.28

Table 3: Distance between the 'robotic hands': A fixed time interval of 3 sec is taken. (a) the separation h between robotic after opened for 3 sec, (b) the zero error observed in h as after the hands closed for 3 sec, (c) the angle between robotic hands and (d) the % error observed in θ . θ is θ h mean h and θ_c is mean θ_c .

(a)	(b)	(c)	(d)
h(cm)	h _c (cm)	θ(degree)	θ _c (%)
13.0	0.24	55.32	1.85
13.4	0.12	57.18	0.89
13.1	0.14	55.79	1.07
13.0	0.24	55.32	1.85
12.9	0.34	54.86	2.63
13.2	0.04	56.25	0.30
13.5	0.22	57.65	1.63
14.0	0.72	60.00	5.14
13.3	0.02	56.72	0.15
$\bar{h} = 13.28$ cm			$\bar{\theta}_c = 1.72\%$

The assistant robot's movements on the voice commands are discussed in this section. Speech commands used to control the movement of the robot make it easier and comfortable for the humans to control the assistant. Accuracy and precision of voice signal conversion to text form depends on the distance that is kept between the smart phone, signal strength and other factors as well.

Degree of Freedom (DoF) of a robot is a joint about which the robot can bend, rotate or perform transnational movement. Degree of freedom of a robot is defined according to the number of motors that have been used in the same. Perspective diagram of the robotic

assistant is given in Fig. 3. The figure shows different distances (d_i) of weights (w_i) which are applying torque on the robotic arm. The pivot point of the robotic arm is at its base. The assistant robot can execute two kinds of motions: *Rotation* and *Translation* (which adds up 2 more DoFs to the robot). *Translation motion* of the robotic assistant gives 2 Degree of Freedom to the robot. *Robotic arm* and *robotic hands* consists of one motor each and they give total of 2 degree of freedom to the robot. Thus a robot with a total of 4 Degree of freedom is developed in this work.

V. EXPERIMENTS AND RESULTS

In this section, the outcomes of the experiments done on the robotic assistant are encapsulated in.

A. Experiment 1: A study on kinematics of the 'robotic hands'

- (i) Observing the variation of angle and distance between the 'robotic hands' with time.
- (ii) The approximation of the observed values.

B. Experiment 2: Calculating the on-board power consumption.

C. Experiment 3: Estimating angular velocity of the 'robotic arm'

D. Experiment 4: Performance parameters of the robot

- (i) Analysis of the speed of the robot
- (ii) Estimation of acceleration of the robot
- (iii) Analysis of distance of chord from the center.
- (iv) Variation of distance the chord from center.

A. Experiment 1: Study of the kinematics of robotic hands

Table 2 shows the angle and the distance between robotic hands after they are opened for time intervals t where $t(=1, 2, 3, 4, 5 \text{ sec})$ and, corresponding to it is the distance and the angle subtended between robotic hands.

The time t , the distance h and the (θ) between angle the robotic hands are represented by (a), (b) and (c) respectively. The robotic hands are opened for different intervals of time t ($=1, 2, 3, 4, 5$ etc). The variation of the distance h between the robotic hands with the angle θ follows:

$$h = 2l \sin \frac{\theta}{2} \quad (5)$$

Where, θ is the angle between the robotic hands and l is the length of each hand.

In table 3, the irregular behavior of the robotic *hands open* and *hands close* functions is discussed. The robotic hands are opened and closed for 3 sec. In ideal situation, when robotic hands are opened and then closed for the same interval of time, they should return to their mean position. Since the robotic hands do not return to their mean position, the error is

observed. Here h (cm) is the distance between the robotic hands after 3 sec and θ is the angle subtended between the | – | robotic hands after 3 sec. The error in distance h (cm) is the distance measured between the claws when closed (as they don't return to mean position). The distance between robotic hands in open position is tabulated in column (a). Angle subtended between the robotic hands and the error in distance between the robotic hands in closed position (as it does not return to the mean position always) are represented columns (c) and (d) respectively.

B. Experiment 2: Estimating the power consumption

In Table 4, the drop in the battery supplying power to micro-controller is measured for a fixed time interval of 120 sec (in standby mode). Based on the above data the battery life is predicted. The initial and final voltage values across the battery are given in columns (a) and (b), respectively, with change in the voltage and its rate of change (Volts/sec) in columns (c) and (d), respectively. Since, the observation period is 120 sec, the voltage drop per second is calculated as follows:

$$\text{Voltage drop} = \frac{V}{120} \quad (\text{Volts/sec}) \quad (6)$$

$$\text{Mean voltage drop rate} = -3.48\text{mV/s} \quad (7)$$

Thus, a 9V battery can live up till: 2586.20 sec = 43 min approx.

C. Experiment 3: Estimation of angular velocity of the robotic arm.

In Table 5, the time t , the angle subtended by the robotic arm with respect to ground, the angle swept in time $i - j$, the angular velocity during time t and the percentage error in ω_t are given in columns (a), (b), (c), (d), and (e), respectively. In column (c), i and j are initial and final time, respectively. Thus, δ_{ij} is the angle covered within a time interval $i - j$. This analysis is carried out to observe the overall performance of the robotic arm which provided better and more accurate results. The values in column (c) are used to calculate ω_t in column (d). The upward and downward movements of the robotic arm were found to be identical as the error ($_t$) in the angle subtended (θ_t) is of the order 10^{-3} degrees.

E. Experiment 4: Performance parameters of the robot.

Fig. 4 and Fig. 5 represent the distance-time and velocity-time plots, respectively for studying the performance parameters of the robot. The slopes of the distance-time graph and velocity-time graph give the speed and acceleration, respectively. The deviation from the ideal curves is conspicuous from the two plots. The three segments (I, II & III) of the velocity-time curve (Fig. 5) are directly related to the deviation from ideal behavior of the distance-time curve. From $t = 0$ to $t = 1$ sec, the robot gains the full of its speed. At $t = 1$ sec the velocity takes a gradual rise till $t = 2$ sec. The corresponding change from $t = 1$ sec to $t = 2$ sec is seen in the distance-time curve as the slope rises at $t = 1$ sec and remains constant till $t = 2$ sec. From here, the robot experiences retardation throughout the segment-II because of the subtle change in the slope as observed in Fig. 4. A small amount of speed is again gained in segment-III of Fig. 5 which is evident from the change of the slope of distance-time curve in Fig. 4.

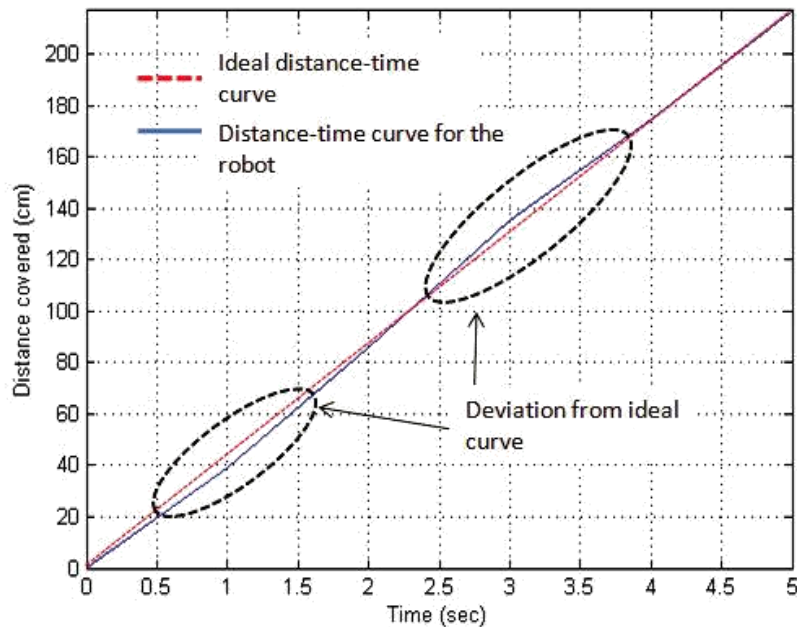


Fig. 4: Distance-time plot of the robot. Figure illustrates the speed of the robot with distance on y-axis and time on x-axis. The deviation from ideal behavior is highlighted by dashed ovals resulting from sudden change in voltage drop across motor driver IC.

The figure shows the variation of distance between the robotic hands as the robotic hands are opened for a certain period of time. Here, distance between robotic hands is represented on the x-axis along with various time intervals for which robotic hands are opened on y-axis. Theoretically, the coordinates of any point on the curve satisfy equation (5). The abnormal curve in the graph is due to non-linear behavior of the robotic hands as they follow a circular trajectory while opening.

VI. DISCUSSION ON RESULTS

As per the observations, the maximum range for the Blue-tooth operation is in the range of 90 m-100 m. This range is relatively more dependent on the transmitter power of the smart mobile phone.

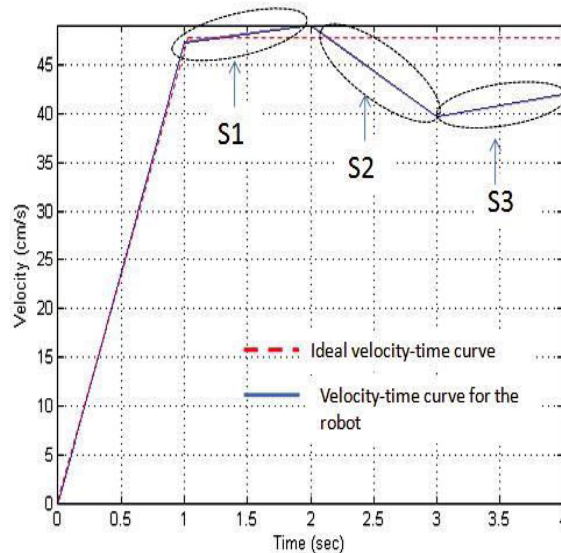


Fig. 5: Speed-time plot of the robot. Figure depicts the velocity of the robot on y-axis against time on x-axis. The unusual behavior of the curve is shown in sections S1, S2 & S3 respectively resulting from the unusual drop in voltage across motor driver IC.

From Table 2, it can be observed that the movement of the hands of the robot is not linear with time *maximum angle* that can be subtended between the robotic hands is *174 degrees*.

Table 3, the observed error is that the hands of the robotic assistant once closed and then opened in a certain duration of time, the robotic hands do not always return to the mean position. This error might take place due to the *effect of friction on robotic hands*. The motor can bear a torque of *2.04 kg (Theoretical payload)* and the maximum weight that the robotic hands can bear without getting De-shaped is *325 grams (Practical payload)*.

The difference observed between the actual and practical value indicates that the maximum weight the robotic hands can lift is directly dependent on the strength of the robotic hands.

VII. APPLICATIONS OF THE ASSISTANT ROBOT

The assistant robot can be used for various purposes as listed below:

(i) *In chemical industries*: In chemical industry, people cannot handle the chemicals which might be having high temperature. Thus, industrial robot is a vital development towards improving the safety standards in industries. In such hazardous situations, the assistant robot's can be used to hold the chemicals and carry them from one place to another without human interference. Also, there might be places in the industries where humans cannot go and work, in all such cases this robot can be controlled by the voice commands and can be directed to go and work in that place. It can also be used to carry small objects in the industry within a certain distance to reduce the time and the manual labour. Robotic assistant can also be used in manufacturing sector for different re-positioning operations.

(ii) *In homes and for daily needs*: People may need assistance to reduce their manual effort, which may be mostly needed in the case of physically handicapped people or the old-aged people. Robotic assistant can be used by physically challenged people or the old-aged people as it helps them to place an object from one place to another which would be difficult for them in general. These assistant robot's can move around quickly and also can be controlled easily by voice commands and can be used to obtain the desired result in a quicker span of time and much easily.

(iii) *In hospitals*: This assistant can be used extensively in the hospitals where it can be used in surgical operations. Robotic arm has been used in various surgeries across hospitals.

Furthermore, if it can be guided by the voice commands and carry out the specified task, efficiency can be increased thus also causing the human labour to reduce.

VIII. SUMMARY AND CONCLUSION

Voice control for a home assistant robot is developed in this paper. Voice commands, given at the user end, are converted to text from using an on-line server in using real-time speech signal processing. Speech commands converted to text commands are then transmitted to the robotic assistant the Bluetooth network of an Android based smart phone. The text commands transmitted by the smart phone are received by a Bluetooth module on-board the robot which in turn sends the signal to the micro-controller board. The assistant robot then performs the various actions as per the speech commands received.

Various performance parameters of the robotic assistant are studied. Analysis of rate of separation between the robotic hands, angular velocity of the robotic arm and power consumption by the robot is done through experiments conducted on the prototype. Computed and practical values are compared. Also reasons for deviation of the robot from ideal behavior are also discussed.

The effects of the distance between the mouth and the smart-phone on the performance of the robot, effect of noise on the speech to text conversion are some of the areas that can be further explored. The accent of the speaker does not affect the operation of the robot as the voice commands are processed using a cloud server which functions irrespective of the accent of the speaker. Using renewable source of energy for the functioning of the robot would not only improve upon the cost of the robot but would also prove to be eco-friendly. Solar cells can be a possible source of energy that can be used.

The prototype designed has an operating range of 90-100 m, which can be increased using Wi-Fi modules. The weight carrying capacity of the robot can be increased by using a stronger metal of the arms and the motors with high torque.

The robotic assistant developed has potential applications ranging from chemical industries to comfortable scenario inside homes. This paper should be helpful in showcasing a signal processing application in developing a voice-controlled robotic assistant.

REFERENCES

- [1] Wong Guan Hao, Y. Y. Leck and Lim Chot Hun, "6-DOF PC-Based Robotic Arm PC-ROBOARM with efficient trajectory planning and speed control", 4th International Conference Mechatronics (ICOM), Kuala Lumpur, pp. 1-7, April 2011, ISBN:978-1-61284-435-0
- [2] H. Uehara, H. Higa and T. Soken, "A Mobile Robotic Arm for people with severe disabilities", International Conference on Biomedical Robotics and Biomechanics (BioRob), 3rd IEEE RAS and EMBS , Tokyo, pp. 126-129, September 2010, ISSN:2155-1774
- [3] David Orenstein, "People with paralysis control robotic arms using brain", <https://news.brown.edu/articles/2012/05/braingate2> (Last viewed on October 23, 2014)
- [4] Lin. H. C, Lee. S. T, Wu. C. T, Lee. W. Y and Lin. C. C, "Robotic Arm drilling surgical navigation system", International conference on Advanced Robotics and Intelligent Systems (ARIS), Taipei, pp. 144-147, June 2014
- [5] Rong-Jyue Wang, Jun-Wei Zhang, Jia-Ming Xu and Hsin-Yu Liu, "The Multiple-function Intelligent Robotic Arms", IEEE International Confer-ence on Fuzzy Systems, FUZZ-IEEE, Jeju Island, pp. 1995 - 2000, August 2009, ISSN:1098-7584
- [6] S. Karamchandani, S. Sinari, A. Aurora and D. Ruparel, "The Gesture Replicating Robotic Arm", International Symposium Computational and Business Intelligence (ISCBI), New Delhi, pp. 15-19, August 2013
- [7] M. Balaganesh, E. Logashanmugam, C. S. Aadhyta and R. Manikandan, "Robotic Arm showing writing skills by speech recognition", Interna-tional Conference on Emerging Trends in Robotics and Communication Technologies (INTERACT), Chennai, pp. 12 - 15, December 2010
- [8] M. Wongphati, Y. Matsuda, H. Osawa and M. Imai, "Where do you want to use a robotic arm? And what do you want from the robot?", IEEE RO-MAN, Paris, pp. 322-327, September 2012, ISSN:1944-9445
- [9] P. Krasnansky, F. Toth, V. V. Huertas, Rohal' -Ilkiv, "Basic laboratory experiments with an educational robotic arm", Process Control (PC), Strbske Pleso , pp. 510 - 515, June 2013

Arm Based Smart Device for Detecting and Controlling Air Pollution in Vehicles

S.NAVEENKUMAR¹, P.RAGHUPATHI², E.RUBHA³, P.UMADEVI⁴

¹Professor, Dept. of Electronics and communication Engineering, Nandha College of Technology, Erode, Anna University, Sharmila.rajamanickam@nandhatech.org

²U.G Student, Dept. of Electronics and communication Engineering, Nandha College of Technology, Erode. Anna University, uma30devi@gmail.com

Abstract: Every one's life vehicles are very importing integral part. In this fast paced urban life vehicles usage for situation and circumstances demand. Problem occurs because, every vehicle will have emission so standardized values are beyond .Incomplete combustion of fuel supplied to engine. It is a primary reason for breach and affects the vehicles. It is definitely can be controlled for emission from vehicles but cannot be completely avoided. The various gases are detecting by using semi-conductor sensors. In semi-conductor sensors at the emission outlets of vehicles which detects the level of pollutants and also indicates this level with a meter that is a main aim of this paper. The already set threshold level, there will be a buzz in the vehicle to indicate that the limit has been breached and after certain period vehicle will stop, a cushion time given for the driver to park his/her vehicles. Travelling the time period identify the nearest services stations by using GPS. After the timer runs out, supplied for the fuel in engine will be cutoff and the mechanic or to the nearest services station by using of vehicles towed.ARM 7 is used for entire process of synchronization and execution. In our project will benefit the society and controlling the air pollution

Keywords: Air Pollution, Sensors, threshold level, GPS, Micro Controller.

I. INTRODUCTION

The beginning of the 21st century was the time when importance for Environmental awareness was instigated. One of the major concerns regarding the environment is air pollution. Air pollution contributes to the green houses gases, which causes the green house effect, whose side effects are now well known to all of us after the findings about the hole in the ozone layer. Air pollution is not only harmful to the environment but, also to all other living beings on earth. Air pollutants that are inhaled have serious impact on human health affecting the lungs and the respiratory system; they are also taken up by the blood and pumped all round the body. These pollutants are also deposited on soil, plants, and in the water, further contributing to human exposure and also affecting the sea life. Vehicles are one of the major contributors to air pollution apart from industries. The main vehicles are the oxides of carbon and nitrogen, which can be easily detected these days with the help of semi conductor gas sensors. Therefore, in this paper an idea is suggested, which would be very helpful in reducing the amount of pollution from vehicles. The rest of the paper is organized as follows. Section II gives the background information and a brief note about the various research activities, on gas sensors and monitoring systems. Section III discusses about the various blocks of the proposed system. Section IV concludes the paper with an idea to implement the same as a real time project.

II. LITERATURE SURVEY

Over the years, there have been several regulations made by the Government to control the emission from vehicles; most of them being unsuccessful at the same. The standards and the timeline for implementation are set by the Central Pollution Control Board under the Ministry of Environment & Forests. Bharat stage emission standards are emission standards instituted by the Government of India to regulate the output of air pollutants from internal combustion engine equipment, including motor vehicles.

The first emission norms were introduced in India in 1991 for petrol and 1992 for diesel vehicles. These were followed by making the Catalytic converter mandatory for petrol vehicles and the introduction of unleaded petrol in the market.

On April 29, 1999 the Supreme Court of India ruled that all vehicles in India have to meet Euro I or India 2000 norms by June 1, 1999 and Euro II will be mandatory in the NCR by April 2000. Car makers were not prepared for this transition and in a subsequent judgment the implementation date for Euro II was not enforced.

The standards, based on European regulations were first introduced in 2000.

III PROPOSED SYSTEM

The overall block diagram of the proposed system is given in figure

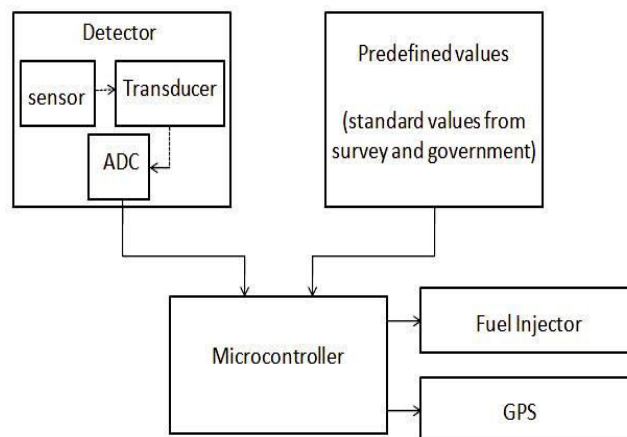


Fig.1. Block diagram

3.1 Detector

The detector consists of three sub-blocks namely smoke sensor, transducer and ADC. The smoke sensor is the main component of the detector block which is embedded onto the exhaust of the vehicle. The sensor senses the amount of emission from the vehicle and feeds the data to the microcontroller through the transducer and the analog to digital converter at regular intervals of time. The transducer is used to convert the output of the sensor into an electrical signal. The analog electrical signal is then converted into a digital signal using an ADC, so that, it can be compared with the predefined values, in the microcontroller.

In this paper, carbon monoxide sensor (MQ-7) which can measure CO concentrations ranging from 10 to 10,000 ppm is considered. This sensor basically finds usage in sensing carbon monoxide concentrations (ppm), in the exhaust of cars as shown in figure.3.3 and gives an analog output. The MQ-7 gas sensor is mainly made up of SnO₂; whose

conductivity varies with the cleanliness of air i.e. it has a lower conductivity in clean air and vice-versa. A simple circuit as shown in figure is used to map the changes in conductivity to the corresponding output signal of the gas concentration. The main advantage of the MQ-7 gas sensor is that it has high sensitivity to Carbon Monoxide. Additionally, it has a very long life time and is available at a low cost. Also it can be used for a wide range of applications.

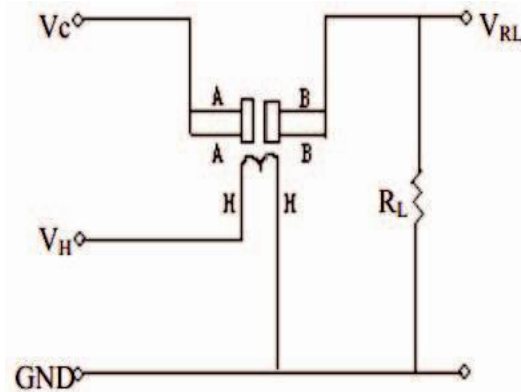


Fig.2. Equivalent Circuit of MQ-7

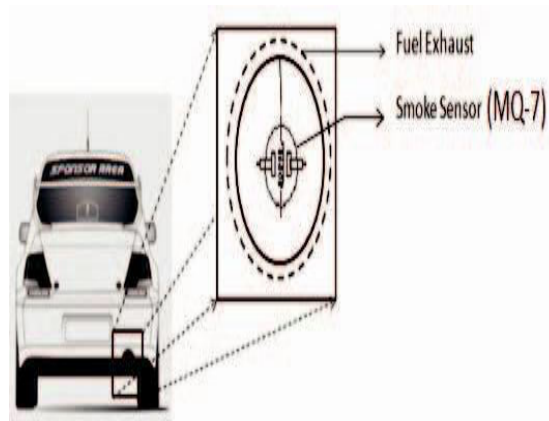


Fig.3. Smoke sensor

3.2 Microcontroller

In this paper, ATMEL 89S52 is used, which is an 8bit micro controller. It consists of three inbuilt timer/counter which will be used for the timer configuration. The microcontroller is programmed to do three functions namely comparison, timer and triggering circuit. The microcontroller takes in two inputs; one from the smoke sensor's output and another being the pre-defined threshold value specified by the government. When the smoke Sensor output is more than the threshold value, the microcontroller triggers the timer circuit and an alarm [5] is set off to inform the driver of the vehicle, about the same and also indicate that the vehicle will come to a halt as soon as the timer runs out. Apart from the timer being triggered, a trigger is also given to the GPS, which helps in locating the nearest service station. Once the timer runs out, a trigger pulse is generated by the microcontroller which is fed to the fuel injector, which in turn stops the flow of fuel to the engine, as a result of which, the vehicle comes to a halt.

3.3 Fuel Injector

The main function of the fuel injector is to cut the supply of fuel to the engine, when the pollution limit is breached. The relay circuit shown in the figure.3.4 is used to control the on and off position of the fuel pump[4]. In this paper, the engine control unit is programmed in such a way that, when the microcontroller sends a trigger pulse after the timer runs out, relay should get back to its original position, that is the fuel cut off switch, is on. Then the fuel supply from the pump will be stopped

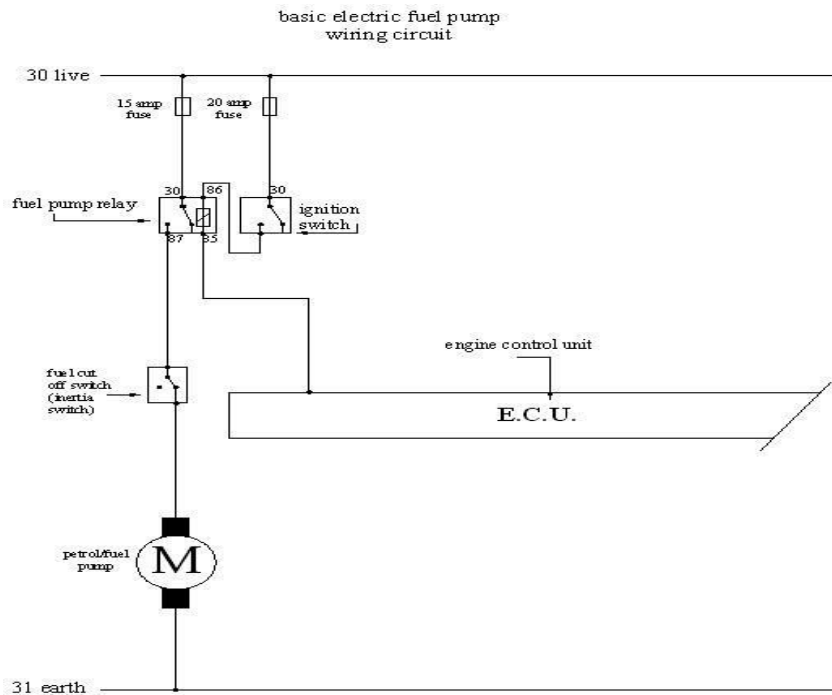


Fig.4. Fuel pump wiring circuit

IV CONCLUSION

Two things are mainly focused in this paper. First thing detecting the level of pollution and indicating to the driver. Several Environmental problems are affected reason for increase the level of pollution over the last couple of decades. Mentioned by the Government, Second reason is greatest improvements in technology to keep the Environment free from emission of vehicular and pollution level is more than the standards. Add-on the fact of this system, as it does not change the configuration of the engine. It's mean the existing vehicles will make it easier to employ this system. This concept can also be implemented to industries.

REFERENCES

- [1] Siva Shankar Chandrasekharan, Sudharshan Muthukumar & Sabeshkumar Rajendran “ Automated Control System For Air Pollution Detection In Vehicles” 2013 4th International Conference On Intelligent Systems, Modeling And Simulation, 2013 Ieee 2166-0662/13.
- [2] Usb Complete: Everything You Need To Develop Custom Usb Peripherals By Jan Axelson, 1999 Check Pricing And Availability: In Usb Complete, The Author Reveals The Programming Secrets For The Universal Serial Bus (Usb), Which Was Designed From The Ground Up To Provide A Single, Easy-To-Use Interface For Multiple Peripherals
- [3] George F. Fine, Leon M. Cavanagh, Ayo Afonja And Russell Binions
“Metal Oxide Semi-Conductor Gas Sensors In Environmental Monitoring”, Sensors 2010, 10, 5469-5502; Doi:10.3390/S100605469
- [4] K. Galatsis, W. Wlodarsla, K. Kalantar-Zadeh And A. Trinchi, " Investigation Of Gas Sensors For Vehicle Cabin Air Quality Monitoring,” Vol. 42, Pp. 167-175, 2002.
- [5] “Trade Of Motor Mechanic”; Module 5; Unit 2 Electronic Fuel Injection; Phase 2 By Fás Learning Innovation Unit With Martin Mcmahon & Cdx Global; Curriculum Revision 2.2 16-01-07.
- [6] Liu Zhen-Ya, Wang Zhen-Dong, Chen Rong, “Intelligent Residential Security Alarm And Remote Control System Based On Single
- [7] Chip Computer,” Vol. 42, Pp. 143-166, 2008. Digi International Inc, “Xbee/Xbee-Pro Rf Modules”, Available [Http: //Ftp1. Digi. Com / Support /Documentation/90000982_B.Pdf](http://Ftp1.Digi.Com/Support/Documentation/90000982_B.Pdf)
- [8] Atmel Corporation, “Atmega16 Datasheet”, Available [Http://Www.Atmel.Com/Dyn/Resources/Prod_Documents/Doc2466](http://Www.Atmel.Com/Dyn/Resources/Prod_Documents/Doc2466)
- [9] An Embedded Software Primer By David Simon, 2000 Check Pricing And Availability: This Book Is Written For Newcomers To Embedded Systems Programmers And Gives A Good Overview On The Different Microcontroller Architectures Available. Other Topics Include When And How To Use A Real-Time Os And Commonly Made Mistakes.
- [10] Arm System-On-Chip Architecture By Steve Furber, 2000 Check Pricing And Availability: The Arm (Advanced Risc Machine) Is Probably The Most Popular 32-Bit Architecture For Embedded Systems. This Book Gives An Introduction To The Arm Architecture And Compares Derivatives Such As Arm7, Arm9 And Arm10.
- [11] The 8051 Microcontroller: Hardware, Software And Interfacing By James Stewart, Kai Mia. 1998 Check Pricing And Availability: One Of Many Books On The 8051. This Is One Is High-Rated For Providing Fast Access To Hands-On Experience. All Examples And An 8051 Assembler Are Included On Floppy Disks.
- [12] Industrial Motor Control By Stephen Herman And Walter Alerich, 1998 Check Pricing And Availability: This Book Provides Easy-To-Follow Instructions And The Essential Information For Controlling Industrial Motors. Most Commonly-Used Devices In Contemporary Industrial Settings Are Covered. Many Circuits Are Explained With Clear And Concise Step-By-Step Sequences That Help Students Learn The Concepts And Applications Of Control Logic.

License Automation Using Sensors

V.Naina Malai Raja, J.Joushuarathina Raj, A.Bharathi Lakshmi, P.Gokila

Bachelor of Engineering(ECE), Nandha college Of Technology

Vaikkalmedu, Erode, India.

Vnmraja2@gmail.com

Abstract: This project is about the automation of driving license test system. Normally, in license tests a candidate applied for license have to drive over a closed loop path like the number (8) in front of the authorities. The candidate has to drive over the path without any support over the land surface and if he fails to do he will be disqualified. For that, the authorities have to watch him/her manually.

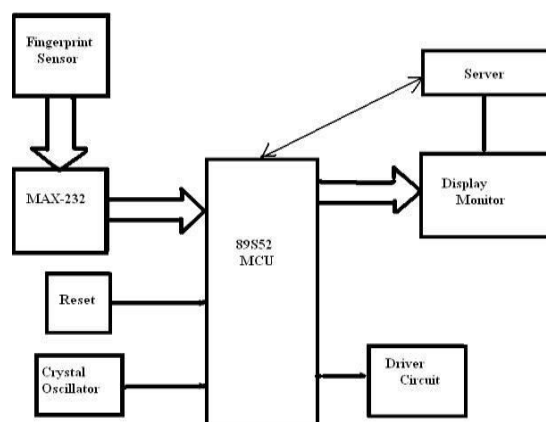
Index Terms: ATmega8A microcontroller, Load cell, Proximity Sensors, Fingerprint Sensor, LCD, Power Supply Unit, Buzzer, PC with VB

1. INTRODUCTION

2.

In our project, we have developed a system for watching the candidate whether he/she is eligible for getting license by using a load cell. The load cell changes its output when there is any pressure change over the surface. Thus, we can detect the candidate who fails to keep his/her foot in the vehicle by differential output from the load cell. Then, it was processed by the micro-controller and the output can be obtained and we placed ultrasonic sensor for hand signal detection and no of count detection. While a person entering for license test he was authenticated by finger.

II BLOCK DIAGRAM



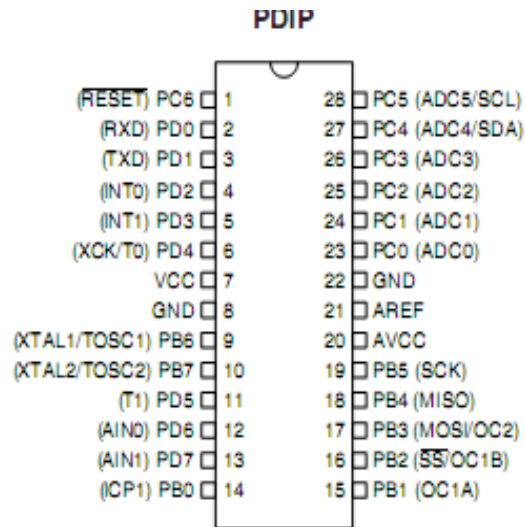
2.1. Power supply:

- ❖ **Transformer:** A transformer is an electro-magnetic static device, which transfers electrical energy from one circuit to another, either at the same voltage or at different voltage but at the same frequency.
- ❖ **Rectifier:** The function of the rectifier is to convert AC to DC current or voltage. Usually in the rectifier circuit full wave bridge rectifier is used.
- ❖ **Filter:** The Filter is used to remove the pulsated AC. A filter circuit uses capacitor and inductor. The function of the capacitor is to block the DC voltage and bypass the AC voltage. The function of the inductor is to block the AC voltage and bypass the DC voltage.
- ❖ **Voltage Regulator:** Voltage regulator constitutes an indispensable part of the power supply section of any electronic systems. The main advantage of the regulator ICs is that it regulates or maintains the output constant, in spite of the variation in the input supply.

2.2. Microcontroller – ATMEGA8:

- ❖ High-performance, Low-power AVR® 8-bit Microcontroller
- ❖ Advanced RISC Architecture
- ❖ High Endurance Non-volatile Memory segments
- ❖ Peripheral Features
- ❖ Special Microcontroller Features
- ❖ I/O and Packages
- ❖ Operating Voltages
- ❖ – 2.7 - 5.5V (ATmega8L)
- ❖ Speed Grades
- ❖ – 0 - 8 MHz (ATmega8L)
- ❖ – 0 - 16 MHz (ATmega8)
- ❖ Power Consumption at 4 MHz, 3V, 25°C

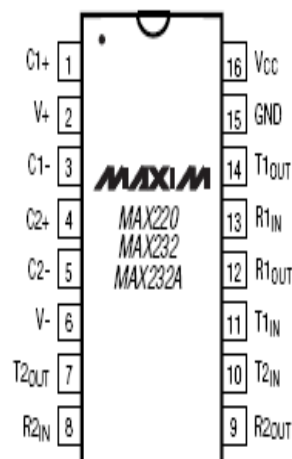
2.3. Pin configuration:



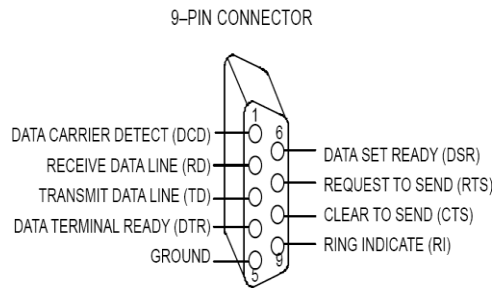
2.4. MAX 232:

- ❖ The MAX220–MAX249 family of line drivers/receivers is intended for all EIA/TIA-232E and V.28/V.24 communications interfaces, particularly applications where $\pm 12V$ is not available.
- ❖ These parts are especially useful in battery-powered systems, since their low-power shutdown mode reduces power dissipation to less than $5\mu W$.

2.5. Pin diagram of MAX232:



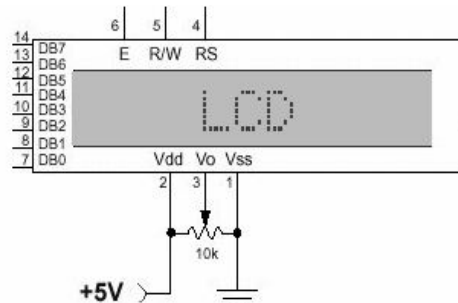
2.6. DB-9 Connector:



2.7. LCD Display:

- ❖ A liquid crystal display (LCD) is a thin, flat display device made up of any number of color or monochrome pixels arrayed in front of a light source or reflector.
- ❖ Each pixel consists of a column of liquid crystal molecules suspended between two transparent electrodes, and two polarizing filters, the axes of polarity of which are perpendicular to each other.
- ❖ Without the liquid crystals between them, light passing through one would be blocked by the other. The liquid crystal twists the polarization of light entering one filter to allow it to pass through the other.

2.8. Pin Diagram of LCD:



2.9. Load cell:

It is a transducer that is used to convert a force into electrical signal. This conversion is indirect and happens in two stages. Through a mechanical arrangement, the force being sensed deforms a strain gauge. The strain gauge measures the deformation (strain) as an electrical signal, because the strain changes the effective electrical resistance of the wire. A load cell usually consists of four strain gauges in a Wheatstone bridge configuration. Load cells of one strain gauge (quarter bridge) or two strain gauges (half bridge) are also available.^[citation needed] The electrical signal output is typically in the order of a few millivolts and requires amplification by an instrumentation amplifier before it can be used. The output of the transducer is plugged into an algorithm to calculate the force applied to the transducer.



Load Cell

2.10. Specification:

- capacity g 500g
- Output sensitivity mv/v 0.5 ± 0.1
- Nonlinearity %F.S 0.05
- Hysteresis %F.S 0.05
- Repeatability %F.S 0.05
- Creep(30min) %F.S 0.05
- Temperature effect on sensitivity %F.S/10°C 0.05
- Temperature effect on zero %F.S/10°C 0.05
- Zero Balance %F.S ± 0.5
- Input resistance Ω (ohms) 1120 ± 10
- Output resistance Ω (ohms) 1000 ± 10
- Insulation resistance $M\Omega$ (ohms) ≥ 2000
- Recommended excitation voltage v 5v

III SENSOR

In this we are using “U 4000B” sensor for getting the Fingerprint image and to store that in the database. It is an excellent fingerprint input device can be widely applied in social security, public security, attendance, fingerprint encryption, embedded, and many other applications. U 4000B miniature fingerprint scanner to automatically read the fingerprint image, and through USB interface to transfer digital fingerprint images to the computer-controlled technology to support the Biokey SDK development tools. Require authentication for laptop computers, desktop computer or other personal computing devices, it is the ideal accessory.



U 4000B

3.1. Sensing:

Fingerprints can be sensed using numerous technologies. The traditional “ink and paper” method, still used by many law enforcement agencies, involves applying ink to the finger surface, rolling the finger from one side of the nail to the other on a card, and finally scanning the card to generate a digital image.

In the more popular *live-scan* method, a digital image is directly obtained by placing the finger on the surface of a fingerprint reader as shown in Figure 2. Optical sensors based on the frustrated total internal reflection (FTIR) technique are commonly used to capture live-scan fingerprints in forensic and government applications, while solid-state touch and sweep sensors—silicon-based devices that measure the differences in physical properties such as capacitance or conductance of the friction ridges and valleys—dominate in commercial applications.

Latent fingerprint impressions left at crime scenes require manual “lifting” techniques like dusting.³

The most significant characteristics of fingerprint readers are their resolution and capture area. The standard fingerprint image resolution in law enforcement applications is 500 pixels per inch (ppi), but some readers now have dual-resolution capability (500 and 1,000 ppi). The sensing surface of readers used by law enforcement tends to be large so that they can capture palm prints and all four fingers simultaneously—such sensors are referred to as 10-print scanners.

Low-resolution and small-area readers are preferred in commercial applications so that they can be easily embedded in consumer devices. Sweep sensors are popular in mobile phones, PDAs, and laptops because of their small size (for example, 14 mm × 5 mm) and low cost (under \$5). However, such sensors require users to sweep their finger across the sensing surface; the reader fuses overlapping image slices obtained during sweeping to form a full fingerprint. Fingerprint sensors embedded in mobile phones or PDAs are also used to support navigation and hot-key functions, with each finger assigned to a specific functionality.

3.2. Feature extraction:

Features extracted from a fingerprint image are generally categorized into three levels, as shown in Figure 3a. Level 1 features capture macro details such as friction ridge flow, pattern type, and singular points. Level 2 features refer to minutiae such as ridge bifurcations and endings. Level 3 features include all dimensional attributes of the ridge such as ridge path deviation, width, shappores, edge contour, and other details, including incipient ridges, creases, and scars.

Level 1 features can be used to categorize fingerprints into major pattern types such as arch, loop, or whorl; level 2 and level 3 features can be used to establish a fingerprints individuality or uniqueness. Higher-level features can usually be extracted only if the fingerprint image resolution is high. For example, level 3 feature extraction requires images with more than 500-ppi resolution.

Figure 3b shows the flow chart of a typical minutiae feature extraction algorithm. First, the algorithm estimates the friction ridge orientation and frequency from the image.

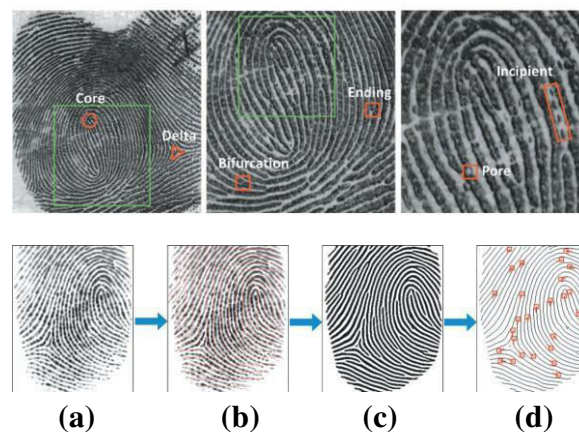
IV HOW THE FINGERPRINT IS RECOGNIZED AND STORED IN THE DATABASE

During the *enrollment phase*, the sensor scans the user's fingerprint and converts it into a digital image. The minutiae extractor processes the fingerprint image to identify specific details known as *minutiapoints* that are used to distinguish different users.

Minutia points represent locations where friction ridges end abruptly or where a ridge branches into two or more ridges. A typical good-quality fingerprint image contains about 20-70 minutiae points; the actual number depends on the size of the sensor surface and how the user places his or her finger on the sensor. The system stores the minutiae information—location and direction—along with the user's demographic information as a template in the enrollment database.

During the *identification phase*, the user touches the same sensor, generating a new fingerprint image called a *query print*. Minutia points are extracted from the query print, and the matcher module compares the query minutia set with the stored minutia templates in the enrollment database to find the number of common minutia points. Due to variations in finger placement and pressure applied on the sensor, the minutia points extracted from the template and query fingerprints must be aligned, or registered, before matching. After aligning the fingerprints, the matcher determines the number of pairs of matching minutiae—two minutia points that have similar location and directions. The system determines the user's identity by comparing the match score to a threshold set by the administrator.

V HOW THE DATABASE ACCEPTS THE FINGERPRINT IMAGE:



At first the Fingerprint image i.e., the Grayscale image **(a)** is converted into Orientation Field **(b)** and then into binary image **(c)** and at last the minutiae **(d)** is matched and stored in the database.

VI MATCHING

A fingerprint matching module computes a match score between two fingerprints, which should be high for fingerprints from the same finger and low for those from different fingers. Fingerprint matching is a difficult **pattern-recognition** problem due to large intraclass variations (variations in fingerprint images of the same finger) and large interclass similarity (similarity between fingerprint images from different fingers). Intraclass variations are caused by finger pressure and placement—rotation, translation, and contact area—with

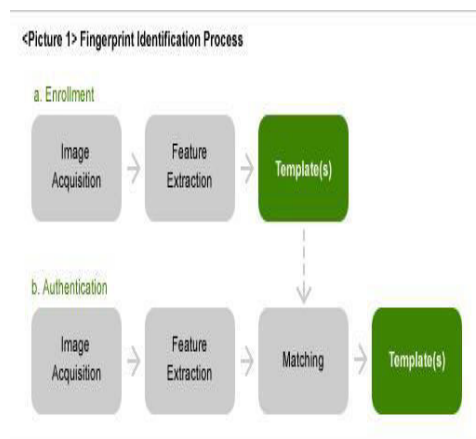
respect to the sensor and condition of the finger such as skin dryness and cuts. Meanwhile, interclass similarity can be large because there are only three types of major fingerprint patterns (arch, loop, and whorl).

Most fingerprint-matching algorithms adopt one of four approaches: image correlation, phase matching, skeleton matching, and minutiae matching. Minutiae-based representation is commonly used, primarily because

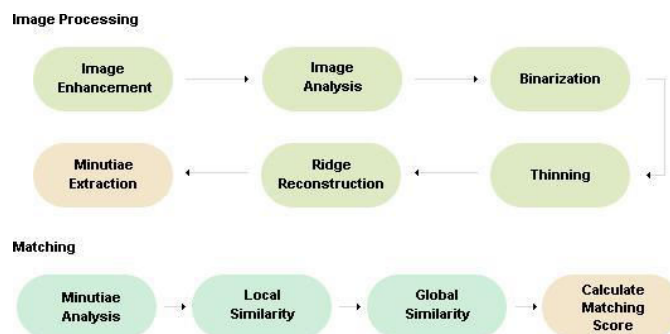
- Forensic examiners have successfully relied on minutiae to match fingerprints for more than a century,
- Minutiae-based representation is storage efficient, and
- expert testimony about suspect identity based on mated minutiae is admissible in courts of law.

The current trend in minutiae matching is to use local minutiae structures to quickly find a coarse alignment between two fingerprints and then consolidate the local matching results at a global level. This kind of matching algorithm typically consists of four steps, as Figure 4 shows. First, the algorithm computes pair wise similarity between minutiae of two fingerprints by comparing minutiae *descriptors* that are invariant to rotation and translation. Next, it aligns two fingerprints according to the most similar minutiae pair. The algorithm then establishes minutiae correspondence—minutiae that are close enough both in location and direction are deemed to be corresponding (mated) minutiae. Finally, the algorithm computes a similarity score to reflect the degree of match between two fingerprints based on factors such as the number of matching minutiae, the percentage of matching minutiae in the overlapping area of two fingerprints, and the consistency of ridge count between matching minutiae.

6.1. How it matches with the stored image 6.1.1. Sensor’s identification process:



6.1.2. Recognition Algorithm:



6.1.3. Image Processing:

This part consists of six stages. At the image enhancement stage, noise on the input fingerprint image is eliminated and contrast is fortified for the sake of successive stages. At the image analysis stage, area where fingerprint is severely corrupted is cut out to prevent adverse effects on recognition. The binarization stage is designed to binarize a gray-level fingerprint image. The thinning stage thins the binarized image. The ridge reconstruction stage reconstructs the ridges by removing pseudo minutiae. At the last stage, minutiae are extracted from the reconstructed ridge image.

VII CONCLUSION

Automated license system is very much need now a days. Because in this system they can find only suitable candidates. These process applications will continue to rely on fingerprint recognition because of its proven performance, the existence of large legacy databases, and the availability of compact and cheap fingerprint readers. Further, fingerprint evidence is acceptable in courts of law to convict criminals. In this paper we have proposed method based on “Minutiae-based” algorithm for efficient and more secured because of these features **Universality, Uniqueness, Permanence, Collectability, Acceptability, Circumvention and Performance** when compared to the existing system. The security can be further increased using some modern technologies like advanced sensors, e.g. Retina Sensors, but these increases the cost of the project.

REFERENCES

1. National Science and Technology Government Post-9/11: Advancing Science, Enhancing Operations, Aug 2008.
2. A.K. Jain, P. Flynn, and A.A.Ross, eds., Handbook of Biometrics, Springer, 2007.
3. H.C.Lee and R.E.Gaensslen. eds., advances in Finger printing Technology, 2nd, CRC press 2001.
4. J. Feng, “Combining Minutiae Descriptors for Fingerprint Matching,” Pattern Recognition, Jan. 2008, pp. 342-352
5. A.A. Ross, K. Nandakumar, and A.K. Jain, Handbook of Multibiometrics, Springer, 2006.
6. S. Pankanti, S. Prabhakar, and A.K. Jain, “On the Individuality of Fingerprints,” IEEE

A Novel Cyclostationary Feature Detector Model for Spectrum Sensing in Cognitive Radio

Nitish Das¹, P. Aruna Priya²

¹Dept. of ECE, SRM University, nitishdas99@gmail.com

²Dept. of ECE, SRM University, p.arunapriya@gmail.com

Abstract: Spectrum sensing is a crucial facilitator for cognitive radios (CRs). Cyclostationary feature detection has the capability to distinguish between the primary user signal and unwanted noise signal. This paper explores the cyclostationary feature detection method under different modulation schemes that are BPSK and QPSK. The output is plotted on the graph and various modulation schemes are studied in cyclostationary feature detection method. The spectral correlation function (SCF) is used in this paper, which shows a peak in the center of the graph if primary user is present.

Keywords: Cognitive Radio; Spectrum Sensing; Cyclostationary feature detection.

I. INTRODUCTION

The fleeting extension in wireless communications has come up to a huge desire on the deployment of advanced wireless services in both the licensed and unlicensed frequency spectrum. The basic idea behind cyclostationary transmission rests on the observation that, in a wireless environment, the signal transmitted or broadcast by a source to a destination node, each employing a single antenna, is also received by other terminals, which are often referred to as relays or partners [1]. In this paper, we propose durable cyclostationary spectrum sensing technique to address these challenging affair. With speedy and agile sensing ability, CR can opportunistically fill in spectrum holes to improve the spectrum occupancy utilization [1]. However, once the PU returns to access the licensed band, the CR should immediately stop operating in the PU licensed band. This rapid switching off of the CR can guarantee least interference to the primary system. However, from the point of perspective of the cognitive system, the interruptive transmissions will lead to a discontinuous data service and intolerable delay [2]. To manage with this complication, we propose a cognitive relay network in which distributed cognitive users participate each other so that they can divide their distinct spectrum bands. In this proposed method, centralized sensing is used to collect sensing information from cognitive devices, distinguishes the accessible spectrum, and report this information to other cognitive radios or directly controls the cognitive radio traffic [3].

II. CHARACTERISTICS OF SPECTRUM SENSING

Spectrum sensing is based on a well-known technique called signal detection. Signal detection can be described as a method for identifying the presence of a signal in a noisy environment. Analytically, signal detection can be reduced to a simple identification problem, which is formalized as a hypothesis test:

$$H1 : x(n) = s(n)h + w(n)$$

$$H0 : x(n) = w(n)$$

Where, $x(n)$ is the received signal by the secondary user, $s(n)$ is the transmitted signal of the primary user, h is the channel coefficient and $w(n)$ is additive white gaussian noise. $H0$ and $H1$ are the sensing parameters for absence and presence of signal respectively.

Here, H0 is the null hypothesis which indicates that primary user does not communicate and H1 is the other hypothesis that indicates the existence of the primary user. We can define three possible cases for the detected signals:

Case (1): H1 under H1 hypothesis which leads to Probability of detection (Pd)

Case (2): H0 under H1 hypothesis which leads to Probability of missed detection (Pmd)

Case (3): H1 under H0 hypothesis which leads to Probability of false alarm (Pf)

III. THE PRINCIPLE OF CYCLOSTATIONARY DETECTION

Detection method that can be applied for spectrum sensing is the cyclostationary feature detector. Cyclostationary feature detectors can distinguish between modulated signals and noise [5]. Cyclostationary processes are random processes for which statistical properties such as mean and autocorrelation change periodically as a function of time. Wireless communication signals typically exhibit cyclostationary at multiple cyclic frequencies that may be related to the carrier frequency, symbol as well as their harmonics, sums and differences. These periodicities can be exploited to design powerful sensing algorithms for cognitive radios.

Cyclostationary processes are random process, which is the second order statistics such as mean and autocorrelation change periodically with time [4]. A zero-mean continuous signal x(t) is called second order cyclostationary, if its time varying autocorrelation function defined as:

$$R_x(t, \tau) = E\{x(t)x^*(t, \tau)\} \dots\dots\dots(1)$$

$$= R_x(t + T_o, \tau + T_o)$$

Where $T_0 = 1/f_0$. Eq. (3) shows that autocorrelation function is periodic with time t for each time lag τ . By using the fourier series, autocorrelation function can be expressed as:

$$R_x(t, \tau) = \sum_{\alpha} R_x(\tau) e^{j2\pi\alpha t} \dots\dots\dots(2)$$

Where, α is the fundamental cyclic frequency and $\alpha = mf_0$, and m is a integer. The fourier coefficient can be obtained by:

$$R_x^{\alpha}(\tau) = \lim_{T \rightarrow \infty} \frac{1}{T} \int_{T/2}^{T/2} R_x(t, \tau) e^{-j2\pi\alpha t} dt \dots\dots\dots(3)$$

Here, T is the interval time. By applying the fourier transform of the cyclic autocorrelation in Eq. (3), the cyclic spectrum correlation function can be obtained as:

$$S_x^{\alpha}(f) = \int_{-\infty}^{\infty} R_x^{\alpha}(\tau) e^{-j2\pi f \tau} d\tau \dots\dots\dots(4)$$

The spectral correlation needs a finite set of samples. Consider the time interval is T i.e. from (t-T/2) to (t+ T/2). Hence the time variant complex spectrum is then defined by:

$$X_T(t, f) = \int_{-T/2}^{+T/2} x(u) e^{-j2\pi fu} du \dots\dots\dots(5)$$

The cyclic spectrum is expressed as

$$S_{x_T}^{\alpha}(t, f) = \frac{1}{T} X_T(t, f + \alpha/2) X_T^*(t, f - \alpha/2) \dots\dots\dots(6)$$

The cyclic spectrum by time average (using $T = 1/\Delta f$)

$$S_{x_T/\Delta f}^{\alpha}(u, f)_T = \frac{1}{T} \int_{t-T/2}^{t+T/2} S_{x_T/\Delta f}^{\alpha}(u, f) du \dots\dots\dots(7)$$

Or by frequency smoothing:

$$S_{x_T}^\alpha(t, f)_{\Delta f} = \frac{1}{\Delta f} \int_{f-\Delta f/2}^{f+\Delta f/2} S_{x_T}^\alpha(t, \nu) d\nu \quad \dots\dots\dots(8)$$

As in [6], cyclostationary spectrum density or the spectral correlation function is:

$$S_x^\alpha(f) = \lim_{\Delta f \rightarrow 0} \lim_{T \rightarrow \infty} S_{x_T}^\alpha(t, f)_{\Delta f} \quad \dots\dots\dots(9)$$

Contrary to power spectral density which is a real-valued one dimensional transform, spectral correlation function is a two dimensional transform, in general complex valued and the parameter α is called cyclic frequency. It obviously can be said that the power spectral density is a special form of spectral correlation function for $\alpha = 0$. Implementation of cyclostationary feature detection is performed by using fast Fourier transform (FFT) and spectral correlation function.

IV. SYSTEM MODEL

Some random signal is taken which is transmitted via primary transmitter. These signals are then modulated by either BPSK or QPSK modulation scheme. These signals are passed through the AWGN channel model because it mimics the effect of many random processes that occur in nature.

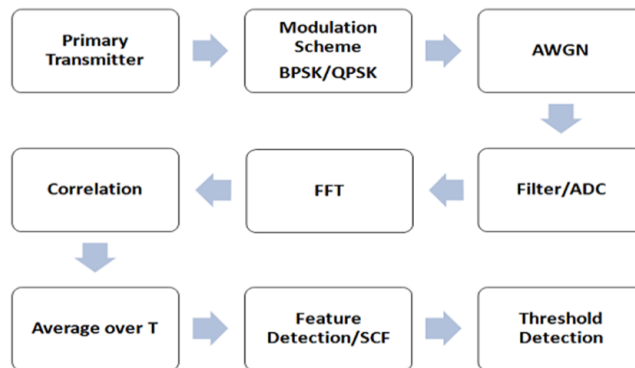


Figure 1. System model of Cyclostationary feature detector

4.1. Threshold Determination

Spectrum sensing is to calculate the presence or absence of primary user’s signal so we need to distinguish between these two hypotheses [4]:

$$\begin{aligned} x(t) &= s(t) + n(t) && H(1) \text{ signal present} \\ x(t) &= w(t) && H(0) \text{ signal absent} \end{aligned}$$

Firstly determine the threshold C_{TH} for signal detection. When there is no presence of signal i.e. $x(t) = n(t)$, C_{TH} can be calculated by using the following relationship:

$$C_{TH} = \max [I(\alpha)] / \sqrt{(\sum_{\alpha=0}^N I^2(\alpha)) / N} \quad \dots\dots\dots(10)$$

Where, N is the length of the observation data and I is given by:

$$I(\alpha) = \max_f |C_x^\alpha(f)| \quad \dots\dots\dots(11)$$

Where,

$$C_x^\alpha(f) = \frac{S_x^\alpha(\alpha)}{[S(f + \alpha/2)S(f - \alpha/2)]^{1/2}} \quad \dots\dots\dots(12)$$

Detection decision will be as follows:

$$I(\alpha) < C_{TH} \quad \text{no signal}$$

$$I(\alpha) > C_{TH} \quad \text{signal present}$$

V. IMPLEMENTATION MODEL

Step (1): First compute the FFT of the signal R.

Step (2): Multiply these signals with its complex exponential and find signal XT.

Step (3): Then compute the correlation between R and XT using $XY = X\text{corr}(R, XT)$.

Step (4): Averaging and compute the spectrum correlation function $YT = \text{fft}(XY) \cdot \text{conj}(\text{fft}(XY))$

Step (5): Determine the Threshold value and estimate the cyclic spectrum correlation function (SCF).

Step (6): Channel is considered to be busy if there is a peak at the double of frequency and at non-zero value in cyclic frequency. Otherwise channel is vacant.

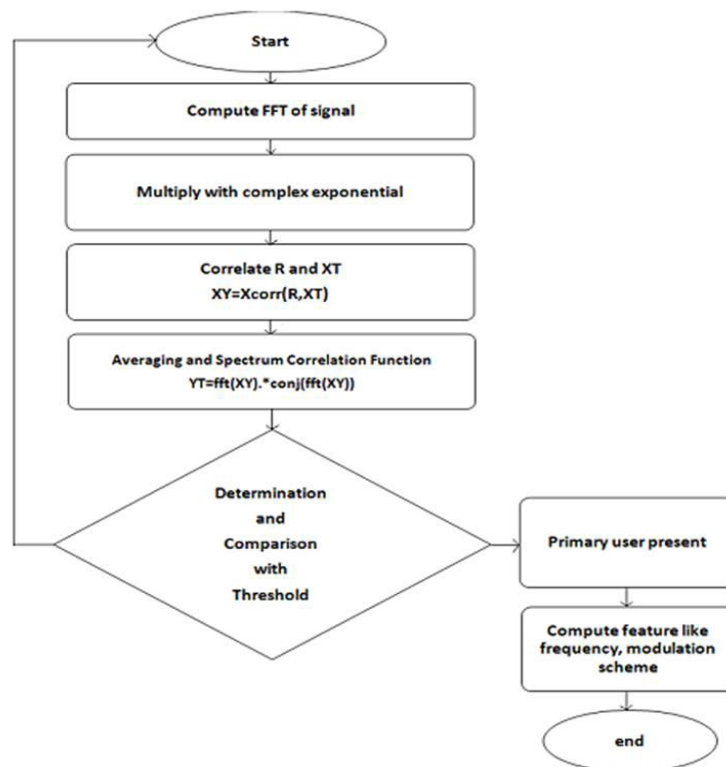


Figure 2. Flowchart of Cyclostationary feature detector

VI. SIMULATION RESULTS

A random input is taken and modulated by either BPSK or QPSK scheme. The operating frequency is chosen to be 2 MHz and sampling frequency at 40 MHz. After adding noise, it is passed through the AWGN channel. The received signal is demodulated and fed to the cyclostationary feature detector (CFD) block.

The output plot thus obtained is the cyclic SCF. The cyclic SCF contains a peak at the center, if there is a primary user in the spectrum.

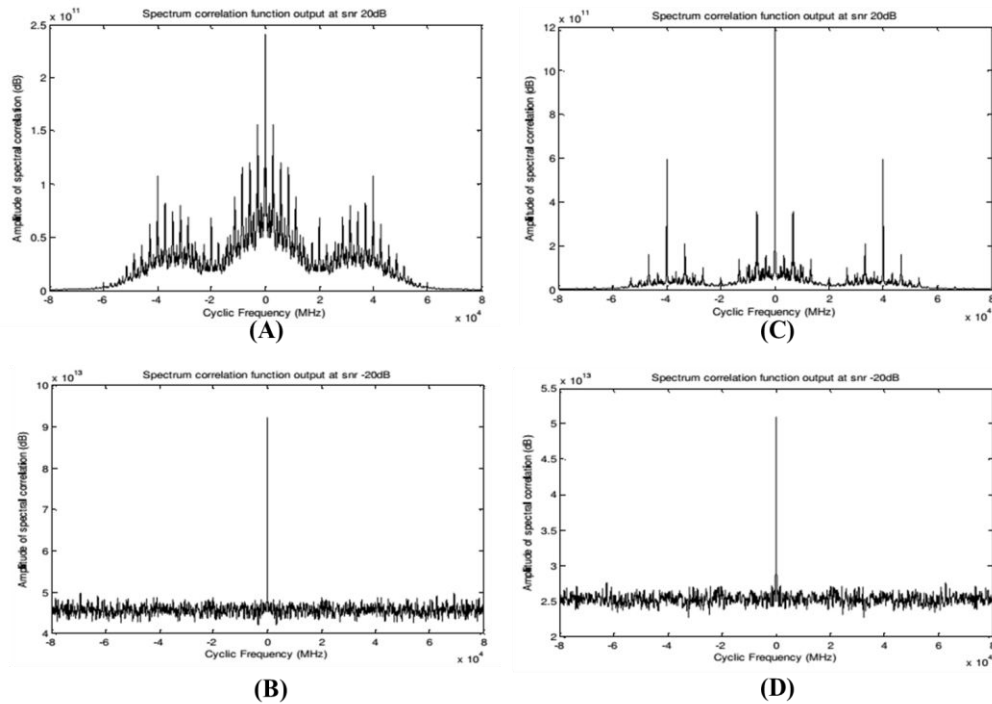


Figure 3. (A) & (B) Spectrum correlation function for BPSK, (C) & (D) Spectrum correlation function for QPSK,

VII. Conclusion

In this paper spectrum sensing technique has been successfully performed by using cyclostationary feature detector with BPSK and QPSK modulation schemes. By the help of spectrum correlation function, it is also possible to distinguish between BPSK and QPSK in the given scenario. Receiver operating characteristics curve validates that this detection method is useful in low SNR value.

REFERENCES

- [1] Mikio Hasegawa and Hiroshi Harada, "Optimization for Centralized and Decentralized Cognitive Radio Networks", IEEE Transactions on Communications, Vol. 102, No.4, pp.no. 1188-1200, 2014.
- [2] Ning Zhang, Nan Cheng, Haibo Zhou, Jon W. Mark and Xuemin (Sherman) Shen, "Risk-Aware Cooperative Spectrum Access for Multi-Channel Cognitive Radio Networks", IEEE Journal on selected areas in Communications, Vol. 32, No.3, pp.no.516-527, 2014.
- [3] Wonsuk Chung, Sungsoo Park, Sungmook Lim and Daesik Hong, "Spectrum Sensing Optimization for EnergyHarvesting Cognitive Radio Systems", IEEE Transactions on Wireless Communications, Vol.13, No.5, pp. no. 1345-1355, 2014.
- [4] Wonsuk Chung, Sungsoo Park, Sungmook Lim and Daesik Hong, "Spectrum Sensing Optimization for EnergyHarvesting Cognitive Radio Systems," IEEE Transactions on Wireless Communications, Vol. 13, No 5, pp.no.2601-2612, 2014.
- [5] S. Park, H. Kim, and D. Hong, "Cognitive radio networks with energy harvesting," IEEE Trans. Wireless Communication., Vol. 12, No. 3, pp.no. 1386– 1397, 2013.
- [6] O. Ozel, K. Tutuncuoglu, J. Yang, S. Ulukus, and A. Yener, "Transmission with energy harvesting nodes in fading wireless channels: optimal policies," IEEE J. Sel. Areas Communication., Vol. 29, No. 8, pp.no 1732–1743, 2014.

Color Image Enhancement Based On Dwt Using Linear and Non-Linear Filtering Techniques

G. Saravanan¹, Dr. G. Yamuna², J.Sasikala³

¹ *Asst. Professor, Dept. of Electrical Engineering, Annamalai University, gsaravananau@gmail.com*

² *Professor, Dept. of Electrical Engineering, Annamalai University, yamuna.sky@gmail.com*

³ *P.G Student, Dept. of Electrical Engineering, Annamalai University, sasi12692@gmail.com*

Abstract: Image enhancement is the practice of adjusting digital images as a result that the outcome is more suitable further image analysis. The main objective is to enhance the color image by converting the RGB value of each pixel of the original image to HSV then 2D-DWT applied to the luminance value of V element. It decomposes the V element into four sub bands. The low frequency sub band is smoothed by using various linear filters and Non-linear filters. Then the IDWT applied with new low frequency sub band. The Saturation is globally equalized by histogram equalization. The enhanced V and S are combined with H then converted back into RGB. H is unaltered due to color distortion. The experimental results vividly displays the proposed algorithm is efficient and enough to remove the noise resulting good enhancement and the quality of the image is measured by using quality measures and the values are tabulated. Finally the geometric mean filter from linear and the median filter from nonlinear filters gives less MSE and good PSNR values.

Keywords - Color Space Conversion, DWT, Linear filters, Non linear filters, Quality Measures.

I. INTRODUCTION

Image enhancement [1] refers to emphasis, sharpening of image features such as edges, boundaries, or contrast to formulate a graphic present more useful for analysis. Nowadays color image enhancement [2] is becoming a progressively more significant research area. Color image enhancement may require improvement of color balance or color contrast in a color image. The RGB color representation is the most widely used color space. The HSV color space [3] is based on cylindrical coordinate. The HSV representation defines a color space in terms of three constituent components. Gang Song et al. [4] proposed an adaptive color image enhancement based on human visual properties in HSV space. The color images enhanced by this algorithm have better visual effect. However, the image enhancement is based on arithmetic mean and difference calculation. While an arithmetic mean filter smoothes neighboring variation in an image and noise is reduced to some level, it really results in blurring of the image. Many algorithms have been described to enhance gray level images. Newly, an image resolution improvement technique using Discrete Wavelet Transform (DWT) for Satellite images was reported by Demirel and Anbarjafari [5]. Later, these techniques were used for enhancing color images as well. Wu and Su projected an image resolution improvement technique based on wavelet transform [6]. Since a part of the high-pass filtered image is added to the unique data, the ensuing effect produces edge enrichment and noise magnification as fine. In order to deal with this problem, more effective approaches resort to nonlinear filtering that can recognize a enhanced compromise among image sharpening and noise reduction [7]. Meanwhile homomorphic filtering, Low pass, and high pass filtering are the additional technique to work in spatial domain [8]. The contrast of

the color image is improved with saturation feedback from saturation components and incorporating spatial information into luminance components. Hue is sealed in order to evade color deformation. The adaptive luminance enhancement is achieved by using a geometric mean filter in position of arithmetic mean filter because arithmetic mean filter tends to lose image detail such as boundaries and sharpness while compared to geometric mean filter. The traditional algorithm uses the arithmetic mean filter which smooth's neighboring variations of luminance and saturation [9]. An improved median filter algorithm is implemented for the denoising of greatly degraded images and edge conservation. Mean, Median and improved mean filter is used for the noise detection. The pictures are corrupted with different noise density and reconstructed. The noise is Gaussian and impulse (salt-and pepper) noise [10]. Fabrizio Russo proposed enhancement system adopts a simple piecewise linear function, the algorithm only one piecewise linear function to merge the smoothing and sharpening effects [11]. F. Russo and G. Ramponi projected fuzzy systems are well apt to model the uncertainty that occurs when conflicting operations must be performed, that is feature sharpening and noise cancellation [12, 13]. S.Gopinath et.al was developed a piece wise linear algorithm for a non linear filtering scheme of gray level images by using discrete wavelet Transforms [14]. Kaganami, et.al presented a color conversion scheme of color image improvement based on Hue Invariability with individuality of human visual color realization in HSV color pattern [15].

The rest of the paper is structured as follows. Section II discusses about the proposed color image enhancement scheme. Section III deals with colour spaces conversion. The 2D-DWT for Image is given in section IV. Section V discusses the various types of linear and non-linear filters for image enhancement applications. Section VI discusses the results obtained and Section VII concludes the paper.

II PROPOSED COLOR IMAGE ENHANCEMENT SCHEME

In this work, HSV color space is chosen since it offers good image enhancement. The projected new algorithm for color image improvement is as follows and shown in Fig. 1.

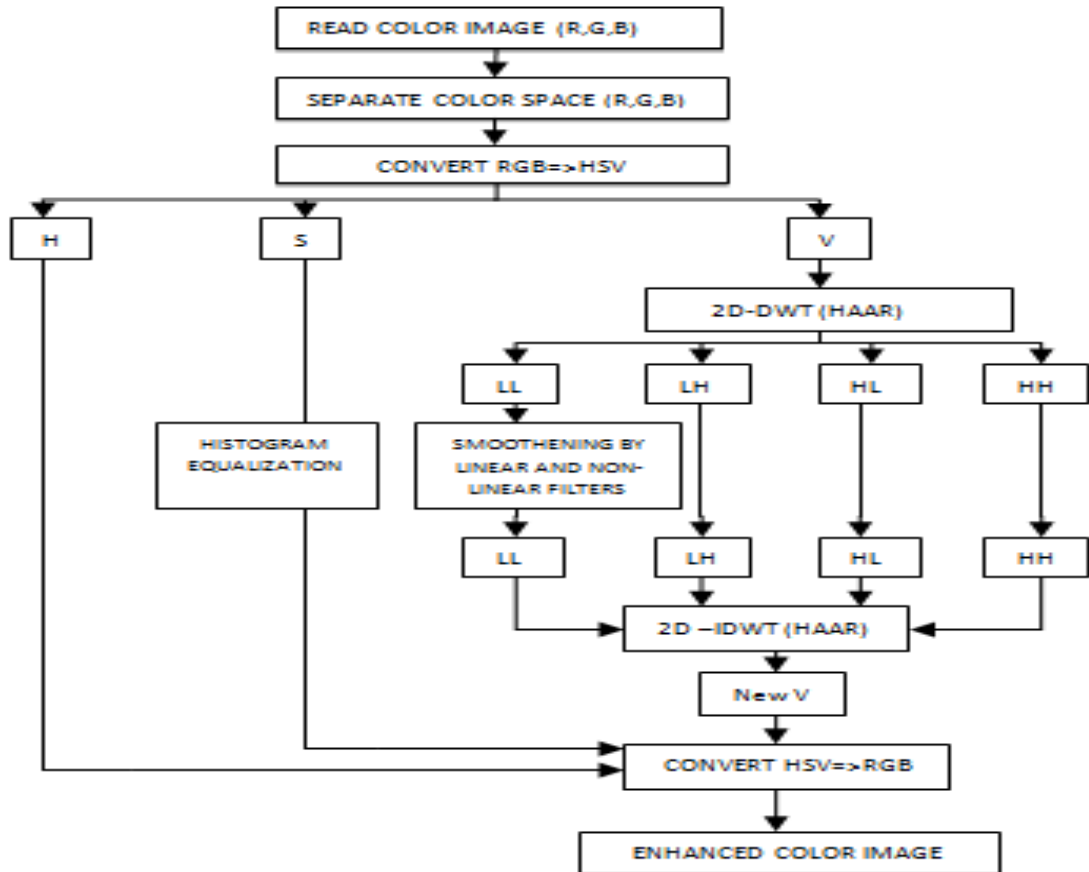
1. Read the Color Image.
2. Convert Color Image from RGB color space to HSV space.
3. Separate collective HSV into individual components H, S and V.
4. Using linear and non-linear filtering techniques, the luminance (V) component is enhanced, saturation is globally enhanced by histogram equalization and hue remains unchanged in order to avoid color distortion.
5. Combine separated parts of H, S and V into combined HSV.
6. Transform back HSV space to RGB color space.
7. Display the enhanced color image.

III COLOR SPACE CONVERSION

3.1. RGB \leftrightarrow HSV Color Space Conversion

These primary colors can be combined to produce enormous amount of secondary colors. Even though it is feasible to improve a digital real color image by applying existing grey-level image improvement algorithms to every red, green and blue channel, the resulting image may not be enhanced optimally. RGB color space has limitation in representing shading property or rapid illumination changing. In order to solve this problem, converting an image from RGB space to HSV space is done. . The HSV model defines a color space in terms of three constituent components. Hue represents category of color such as red, blue, or

yellow that ranges from 0 to 360 degrees. Saturation is the vitality of color that ranges from 0 to 100%. The lower the saturation of a color, the more gray the image looks and extra dull the color appears. Value is the brightness of the color that ranges from 0 to 100%. HSV space is as well recognized as hex cone color model. The HSV color space is widely used to generate high quality computer graphics.



The RGB to HSV conversion formula is shown by the equation (1).

$$\begin{aligned}
 R' &= R/255; \quad G' = G/255; \quad B' = B/255 \\
 C_{\max} &= \text{MAX}(R', G', B') \\
 C_{\min} &= \text{MIN}(R', G', B') \\
 \Delta &= C_{\max} - C_{\min} \\
 H &= \begin{cases} 60^\circ \times \left(\frac{G' - B'}{\Delta} \text{ mod } 6 \right), & C_{\max} = R' \\ 60^\circ \times \left(\frac{B' - R'}{\Delta} + 2 \right), & C_{\max} = G' \\ 60^\circ \times \left(\frac{R' - G'}{\Delta} + 4 \right), & C_{\max} = B' \end{cases} \quad (1)
 \end{aligned}$$

$$S = \begin{cases} 0 & , \Delta = 0 \\ \frac{\Delta}{C_{\max}} & , \Delta > 0 \end{cases}$$

$$V = C_{\max}$$

3.1.1. Reverse Transformation: HSV to RGB Color Space Conversion

$$C = V \times S_{\text{HSV}}$$

$$X = C \times \left(1 - \left| (H / 60^\circ) \bmod 2 - 1 \right| \right)$$

$$(R_1 \ G_1 \ B_1) = \begin{cases} (0,0,0) & \text{If } H \text{ is Undefined} \\ (C,X,0) & \text{If } 0^\circ \leq H < 60^\circ \\ (X,C,0) & \text{If } 60^\circ \leq H < 120^\circ \\ (0,C,X) & \text{If } 120^\circ \leq H < 180^\circ \\ (0,X,C) & \text{If } 180^\circ \leq H < 240^\circ \\ (X,0,C) & \text{If } 240^\circ \leq H < 300^\circ \\ (C,0,X) & \text{If } 300^\circ \leq H < 360^\circ \end{cases} \quad (2)$$

$$m = V - C$$

$$(R, G, B) = (R_1 + m, G_1 + m, B_1 + m)$$

IV 2-D DISCRETE WAVELET TRANSFORMS

4.1. 2D-Discrete Wavelet Transform

In this mechanism uses 2-D Discrete Wavelet Transformation (DWT) to change the image from the spatial domain to frequency domain. According to the Fig.2, the image can be separated with four parts those are LL, LH, HL and HH. In additional, those four parts are represented four frequency areas in the image. For the low-frequency domain LL is sensitively with human eyes.

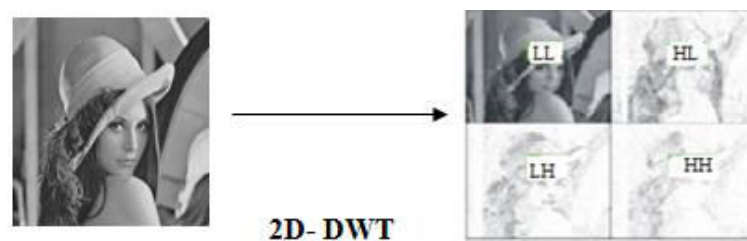


Fig.1. Frequency distribution of DWT.

V. IMAGE ENHANCEMENT

5. 1. Linear Filter

Linear filters are well implicit and speedy to calculate, but are helpless of smoothing without simultaneously blurring edges. Linear filter output values are linear combinations of the pixels in the original image. Linear methods are far more agreeable to mathematical examination than are nonlinear ones, and they are consequently far better understood.

5.1.1 Arithmetic Mean Filter

This is the simplest of the mean filter. Let S_{xy} represent the setoff coordinate in a rectangular sub image mask of size $m \times n$, centered at point (x,y) . The arithmetic filtering process computer the average value of the corrupted image $g(x,y)$ in the region defined by S_{xy} . The significance of the restored image at every point (x,y) is basically the Arithmetic Mean computed by the pixels in the section defined by S as shown in equation (3).

$$\hat{f}(x,y) = \frac{1}{mn} \sum_{(s,t) \in S_{xy}} g(s,t) \quad (3)$$

This operation can be implemented using a convolution template in which all coefficient has value $1 / m \times n$. Mean filter simply smoothes local variation in an image. Noise is reduced as an effect of blurring.

5.1.2. Geometric Mean Filter

An image reconstructed using a geometric mean filter in given by the expressions shown in equation (4).

$$\hat{f}(x,y) = \left[\prod_{(s,t) \in S_{xy}} g(s,t) \right]^{\frac{1}{mn}} \quad (4)$$

Here, each restored pixel is given by the product of the pixels in the sub image mask, raised to the power $1/ m \times n$. A geometric mean filter achieves smoothing comparable to the arithmetic mean filter, but it tends to lose less image details in the process.

5.1.3. Harmonic Mean Filter

Applies a harmonic mean filter to an image in the harmonic mean scheme, The color value of each pixel in replaced through the harmonics mean of color values of the in a neighboring region shown in equation (5).

$$\hat{f}(x,y) = \frac{mn}{\sum_{(s,t) \in S_{xy}} \frac{1}{g(s,t)}} \quad (5)$$

The harmonic mean filter works well for salt noise, but fails for pepper noise. It does fine as well with other type of noise like Gaussian noise.

5.1.4. Contra Harmonic Mean Filter

The contra harmonic filtering action yields a restored image based on the term (6).Where Q is called the order of the filter. The filter is well apt for dropping or practically eliminating the effect of salt and pepper noise. For positive values of Q , the filter eliminates pepper noise. For negative values of Q it eliminates salt noise. It cannot do both simultaneously. The contra harmonic filter reduces to the arithmetic mean filter if $Q = 0$, and to the harmonic mean filter if $Q = -1$ is given by the equation (6).

$$\hat{f}(x, y) = \frac{\sum_{(s,t) \in S_{xy}} g(s, t)^{Q+1}}{\sum_{(s,t) \in S_{xy}} g(s, t)^Q} \quad (6)$$

5.2. Non Linear Filter

Nonlinear filters can smooth without blurring edges and can sense edges at the entire orientations concurrently but have less secure theoretical foundations and can be slow to compute. Nonlinear methods effectively preserve edges and details of images while methods using linear operators lean to blur and alter them. In addition, nonlinear image improvement tools are less susceptible to noise. Noise is always present due to the substantial chance of image acquisition systems. For example, underexposure and low-light conditions in analog shooting conditions guide to images with film-grain noise which, together with the image signal itself are captured during the digitization process.

5.2.1. Median Filter

The best known order-statistics filter is the median filter, which replaces the significance of a pixel by the median of the gray levels in the neighborhood of that pixel is given by the equation (7).

$$\hat{f}(x, y) = \text{median}_{(s,t) \in S_{xy}} \{g(s, t)\} \quad (7)$$

The original value of the pixel is included in the computation of the median. Median filters are somewhat accepted because, for definite types of random noise they provide excellent noise reduction capabilities, through considerably lesser blurring than linear smooth filters of related size.

5.2.2. Max and Min Filter

Although the median filters by far the order-statistics filter most used in image processing. It is by no means the only one. The median represent the 50th percentile of a ranked set of information's, but the reader will recall from basic statistics that ranking lends itself to several other possibilities. Using the 100th percentile result in the so-called max filter given by equation (8).

$$\hat{f}(x, y) = \max_{(s,t) \in S_{xy}} \{g(s, t)\} \quad (8)$$

This filter is useful for finding the brightest points in an image. Also, because pepper noise has extremely small values, it is reduced by this filter as a effect of the max selection process in the sub image area S. The 0th percentile filter is the min filter given by equation (9).

$$\hat{f}(x, y) = \min_{(s, t) \in S_{xy}} \{g(s, t)\} \quad (9)$$

5.2.3. Mid-Point Filter

The midpoint filter is normally used to filter images containing small tailed noise such as Gaussian and uniform type noises. The midpoint filter is defined as equation (10).

$$\text{MidPoint}(A) = \frac{\min[A(x+i, y+j)] + \max[A(x+i, y+j)]}{2} \quad (10)$$

where the coordinate $(x+i, y+j)$ is defined over the image A and the coordinate (i, j) is distinct above the $n \times n$ size square mask.

VI. EXPERIMENTAL RESULTS

Table. 1 Quality Measures for Lena Color Image

Quality Measure	Input Image lena (512x512)							
	Linear Filter				Non- Linear Filter			
	Arithmetic mean	Contra harmonic mean	Geometric mean	Harmonic Mean	Max	Median	Mid-point	Minimum
MSE	681.063	665.088	346.520	651.448	954.629	644.313	678.060	947.994
PSNR	28.677	28.985	29.371	28.568	31.355	28.778	28.667	26.618
NCC	0.974	1.000	0.977	0.972	1.000	0.981	0.974	0.871
AD	0.2484	-1.4511	0.5966	1.1069	-13.980	-0.141	0.344	15.045
NAE	0.167	0.165	0.119	0.163	0.196	0.163	0.166	0.194
SC	1.000	0.987	1.000	1.000	0.834	1.000	1.000	1.000
MD	121	112	102	136	127	124	177	184

Fig. 2 Output Enhanced by Geometric Mean Filter.

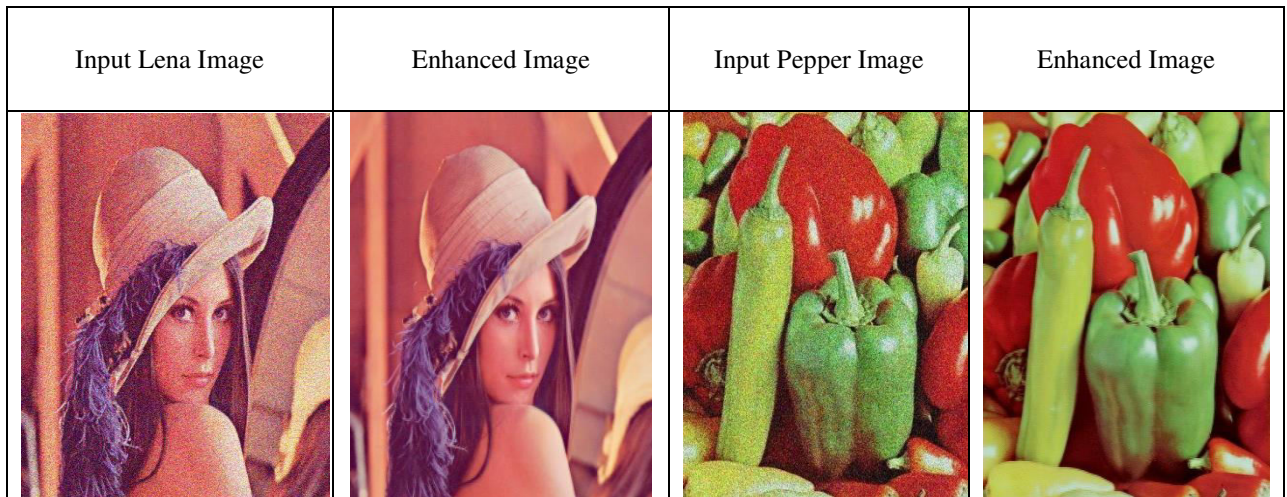


Table. 2 Quality Measures for Pepper Color Image

S.No:	TYPE	
1	MSE (Mean Square Error)	$MSE = \frac{1}{MN} \sum_{i=1}^M \sum_{j=1}^N (x(i, j) - y(i, j))^2$
2	PSNR (Peak Signal to Noise Ratio)	$PSNR = 10 \cdot \log_{10} \frac{(2^n - 1)^2}{\sqrt{MSE}}$
3	AD (Average Difference)	$AD = \frac{1}{MN} \sum_{i=1}^M \sum_{j=1}^N (x(i, j) - y(i, j))$
4	MD (Maximum Difference)	$MD = MAX x(i, j) - y(i, j) $
5	NK (Normalized Cross-Correlation)	$NK = \frac{\sum_{i=1}^M \sum_{j=1}^N (x(i, j) - y(i, j))}{\sum_{i=1}^M \sum_{j=1}^N (x(i, j))^2}$
6	SC (Structural Content)	$SC = \frac{\sum_{i=1}^M \sum_{j=1}^N (y(i, j))^2}{\sum_{i=1}^M \sum_{j=1}^N (x(i, j))^2}$
7	NAE (Normalized Absolute Error)	$NAE = \frac{\sum_{i=1}^M \sum_{j=1}^N x(i, j) - y(i, j) }{\sum_{i=1}^M \sum_{j=1}^N x(i, j) }$
8	SSIM (Structural Similarity Index Metrics)	$SSIM(X, Y) = \frac{2(\mu_x \mu_y + C_1) \quad 2(\sigma_{xy} + C_2)}{(\mu_x^2 + \mu_y^2 + C_1) \quad (\sigma_x^2 + \sigma_y^2 + C_2)}$

Using the Tables Compute the Quality measures, then tabulated results are shown in Table 1 and Table 2 for Lena color image and Pepper color image respectively. From the result, the geometric mean filter in linear and median filter in non-linear filtering gives the less MSE and MD value when compared with other filtering and regarding PSNR geometric mean filter in linear and Max filter in non-linear filtering gives good results and compare with other filtering techniques. Even though the Max filter gives good PSNR but comparing with other quality measures Median filter has good outputs. The result of geometric mean filter shown in Figure 3.

VII CONCLUSION

Different filters have been analyzed and evaluate for their performance in image enhancement application, such as Linear and Non-linear Filtering techniques. On the above reported theory and results the geometric mean filter in linear and median filter in non-linear filter are suggested for image enhancement applications. This paper can be extending by converting these files into VHSIC Hardware Description Language (VHDL) and implementing through Field- programmable Gate Array (FPGA) Processor; so that these filtering techniques can be compared with conversion time and other quality performances.

REFERENCES

- [1] R. C. Gonzalez and R. E. Woods, Digital Image Processing Reading, MA: Addison-Wesley, 1992.
- [2] Anil. K. Jain, Fundamentals of Digital Image Processing. Englewood Cliffs, NJ: Prentice-Hall, 1989.
- [3] Dong Yu, Li-Hong Ma and Han-Qing Lu, "Normalized SI Correction for Hue-Preserving Color Image Enhancement", Proceedings of the *6th International Conference on Machine Learning and Cybernetics (ICMLC 2007)*, Vol. 3, pp. 1498-1503, 2007.
- [4] Gang Song and Xiang-Lei Qiao, "Adaptive Color Image Enhancement based on Human Visual Properties", Proceedings of *International Conference on Image and Signal Processing*, 2008.
- [5] Demirel and G.Anbarjafari, "Discrete Wavelet Transform-Based Satellite Image Resolution Enhancement", *IEEE Trans. on Geoscience and Remote Sensing*, Vol.49, No. 6, 1997-2000, Jun-2011.
- [6] X. Wu, and B. Su, "A Wavelet-based Image Resolution Enhancement Technique", *Int. Conf on Electronics and Optoelectronics (ICEOE 2011)*, 2011, pp 62- 65.
- [7] S. C. Matz and R. J. P. de Figueiredo, "A nonlinear technique for image contrast enhancement and sharpening," in Proc. *IEEE Int. Symp. Circuits and Systems (ISCAS '99)*, vol. 4 pp. 175–178, Orlando, Fla, USA, May–June 1999.
- [8] J. S. Lim, "Two-Dimensional Signal and Image Processing", Englewood Cliffs, NJ: Prentice-Hall, 1990.
- [9] M.C Hanumantharaju, M. Ravishankar, D.R. Rameshbabu "Adaptive Color Image Enhancement based Geometric Mean Filter", pp.403-408
- [10] Gajanand Gupta "Algorithm for image processing using Improved Median Filter and Comparison of Mean, Median and Improved Median Filter", Proceeding of *International Journal of Soft-Computing and Engineering (IJSCE)*, ISSN:2231-2307, Vol. 1, pp. 304-311, Issue.5, November , 2011.

- [11] Fabrizio Russo “Piecewise Linear Model-Based Image Enhancement,” *EURASIP, Journal on Applied Signal Processing*, vol.12, pp. 1861–1869, 2004.
- [12] F. Russo and G. Ramponi, “Fuzzy operator for sharpening of noisy images,” *Electronics Letters*, vol. 28, no. 18, pp. 1715–1717, 1992.
- [13] F. Russo and G. Ramponi, “Nonlinear fuzzy operators for image processing,” *Signal Processing*, vol. 38, no. 3, pp. 429–440, 1994.
- [14] S.Gopinathan and P.Thnagavel, “A Non Linear Technique for image enhancement based on Discrete wavelet Transform”, *European journal of Scientific Research*, Vol.79, No.3, pp.328–336, 2012.
- [15] H. G. Kaganami, Z. Beiji and M. S. Soliman, “Optimal Color Image Enhancement Using Wavelet and K-means Clustering”, in *IJDCT and Its Applications*, Vol.5, No.1, pp 112-121, January, 2011.

Performance Analysis of Asymmetric Cascaded Nine Level Impedance Source Multilevel Inverter

V. Narmadha¹, G. Irusapparajan²

¹PG Scholar, Department of EEE, Mailam Engineering College

²Professor, Department of EEE, Mailam Engineering College, mailam

Abstract – In this research, a single phase Z-source cascading Multilevel Inverter, Nine-level inverter topologies with a trinary DC sources are offered. The recommended topologies are expanded by cascading a full bridge inverter with dissimilar DC sources. This paper recommends advanced pulse with modulation technique as a switching scheme. In this PWM technology, sinusoidal modulation technique is used as variable amplitude pulse width modulation. These topologies compromise reduced harmonics present in the output voltage and superior root mean square (RMS) values of the output voltages linked with the traditional sinusoidal pulse width modulation. The simulation of proposed circuit is carried out by using MATLAB/SIMULINK.

Keywords--- *Z-Source Multilevel Inverter, Total Harmonic distortion, Variable amplitude Pulse Width Modulation, Cascaded multilevel inverter.*

1. INTRODUCTION

Multilevel DC-AC converter have drained incredible interest in recent years and have been planned for several high-voltage and high-power applications. Switching losses in these high-power high-voltage DC-AC converters characterize an issue and any switching conversions that can be rejected with Z-source cascaded multilevel inverter. The term multilevel starts with the outline of the nine-level DC-AC converter. All probable steady states of a Z-source inverter are recognized and analyzed with the objective of developing design plans for the symmetrical impedance network [1]. Three level Z-source inverters are latest single stage topological explanations proposed for buck boost energy conversion with all encouraging advantages of three level switching recollected [2]. A multi loop controller for a Z-source inverter was established for distributed generation applications. En route for that end, the Z-source inverter was demonstrated with a state space an average of technique, and essential transfer functions are derivative [3]. To overcome the restricted operating range, these inverters necessity to be connected with a discrete DC-DC converter step in the front end. This permits them to operate in both buck and boost operation. This topology is frequently known as a two stage inverter. Lesser scale two stage inverters have been developed for domestic distributed generation applications with fuel cells [4]–[6]. A five level cascaded multilevel inverter built Z-source inverter has been offered. In the suggested topology output voltage amplitude can be enhanced with Z network shoot through state controller [7]. The improvement of two three level cascaded Z-source inverters, whose the output voltage can be paced down or up dissimilar a outdated buck three level inverter. The anticipated inverters are premeditated using two three phase voltage source inverter bridges, provided by two exclusively designed Z-source impedance systems [8]. The Z-source neutral point clamped inverter has been projected with different three levels up - down

power conversion resolution with upgraded output voltage waveform superiority. In principle, the design of Z-source inverter gatherings by selectively shooting through its input power sources, joined to the inverter using two inimitable Z-source impedance systems, to boost up the inverter three level output voltage waveform [9]. A seven level Z-source cascaded multilevel inverter premeditated with three midway Z-source networks system associated between the input dc source and multilevel inverter circuit [10].

2. IMPEDANCE NETWORK

The arrangement of impedance network is shown in the Fig. 1. It comprises of a pair of inductors and capacitors respectively. The rate of inductors and capacitor can be preferred based on the output voltage requirement of inverter. A diode is coupled in the impedance network as shown Fig. 1 to block the reverse flow of current. A voltage nature impedance source inverter can assume all active and null switching states of voltage source inverter. Unlike predictable voltage source inverter, an impedance source (Z-source) fed inverter has a unique feature of permitting both power semiconductor switches of a phase leg to be turned ON instantaneously (shoot through state) without injuring the inverter. The impedance network (Z-source) changes the circuit arrangement from that of a voltage source to an impedance source (i.e. Z-source). It permits the voltage source inverter to be operated in a new state called the shoot through state in which the two power semiconductor switching devices in the same leg are instantaneously turned on to effect short circuit of the dc link [16]. During this state, energy is transmitted from the capacitors to inductors, thereby giving rise to the voltage boost ability of the impedance source (Z-source) fed inverter. The effect of the phase leg shoot through on the inverter presentation can be investigated by allowing for the circuit.

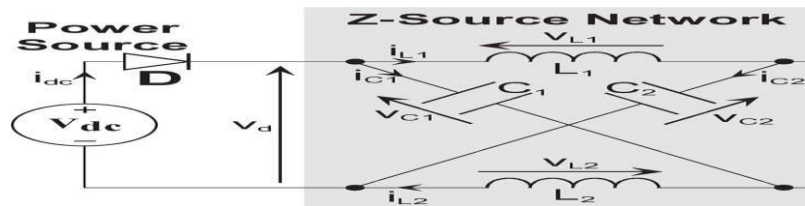


Fig.1 Impedance Network Circuit

3. PROPOSED IMPEDANCE SOURCE CASCADED MULTILEVEL INVERTER

The Simulated circuit structure of an impedance source (Z source) nine level cascaded multilevel inverter is shown in Fig.2. It comprises of series single phase half bridge inverter units, (Z) impedances and input DC source voltages. Input DC voltage sources can be found from battery bank, solar cells and fuel cells. It contains of eight IGBT/Diode power semiconductor switches. Each Half bridge contains of four power semiconductor switches respectively. Input source for each half bridge is fed from impedance network (Z-source). This voltage will be lesser or larger than input DC source voltage. Nature of the load is resistive and inductive. Based on the rate of capacitor pairs and inductor pairs in the impedance network (Z-source) magnitude of V_{dc} is preferred. Since each and every half bridge in an inverter circuit can offer three output voltage levels ($0V_{dc}$, $+V_{dc}$ and $-V_{dc}$). The output voltage of the inverter values for $-4V_{dc}$, $-3V_{dc}$, $-2V_{dc}$, $-1V_{dc}$, 0 , $4V_{dc}$, $3V_{dc}$, $2V_{dc}$, $1V_{dc}$, can be planned, as represented in Fig. 1. The output voltage of the first bridge is indicated by V_{dc} and the second full bridge is indicated by $3V_{dc}$. Then the output voltage of the load is $V=V_{dc}+3V_{dc}$.

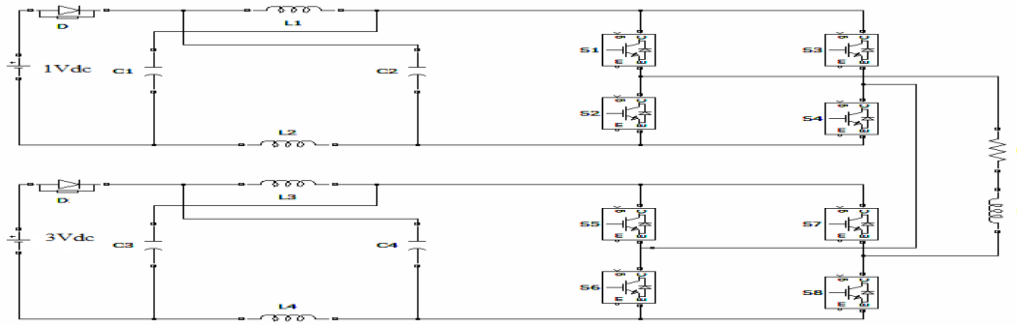


Fig.2 Proposed impedance source cascaded multilevel inverter.

4. SIMULATION RESULT

A single phase impedance source (Z- source) cascaded multilevel inverter with unequal voltage sources to yield nine level inverter output is modeled in SIMULINK using power systems block set. Simulations are implemented for different values of m_a ranges from 0.8 to 1 and the equivalent %THD is measured using the FFT block and their values are shown in Table 1. Table 5 shows the fundamental V_{rms} of inverter output for the same values of modulation indices. Table 3 and Table 4 show the corresponding values of crest and form factor. Table 2 demonstrate percentage distortion factor of the inverters output voltage. Fig 3 -11 display the simulation output voltage and FFT plot of three phase multilevel inverters and their respective harmonic order of a spectrum with various modulation techniques but for only one sample of modulation indices($m_a=0.85$).

For modulation indices ($m_a=0.85$) it is observed from the figures (4, 6, and 8) the harmonic energy level is governing in: Fig.4 represent the harmonic energy level in POD PWM techniques shows 40th order of harmonic. Fig. 6 represents the harmonic energy level in POD PWM techniques shows 35th 39th order of harmonic. Fig. 8 represent the harmonic energy level in APOD PWM techniques shows 29th, 31st, 35th, 37th, 39th order of harmonic

Simulations are performed for various values of m_a ranges from 0.8 to 1 and the results are obtained by using following parameter such as $V_{dc} = 25V$, $3V_{dc} = 75V$, load resistance is 200Ω , and load inductance 20mH, carrier frequency f_c is 2000Hz and modulation frequency f_m is 50Hz.

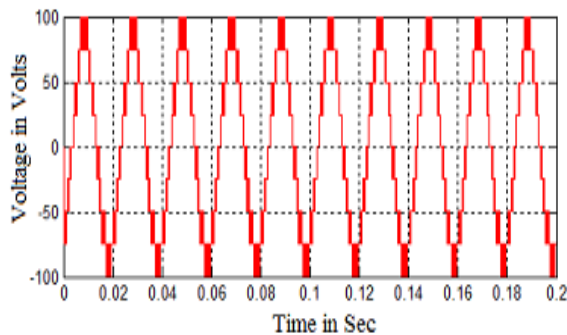


Fig.3. Output voltages generated by in phase

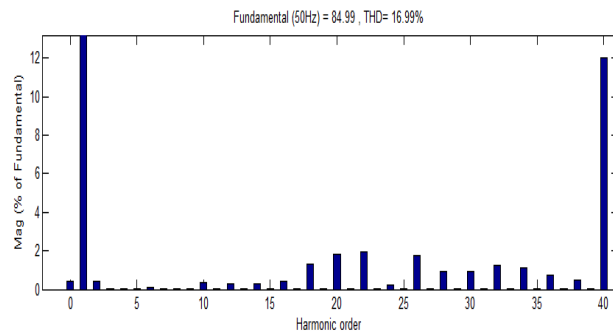


Fig.4. FFT plot for output voltage of in phase

disposition PWM control

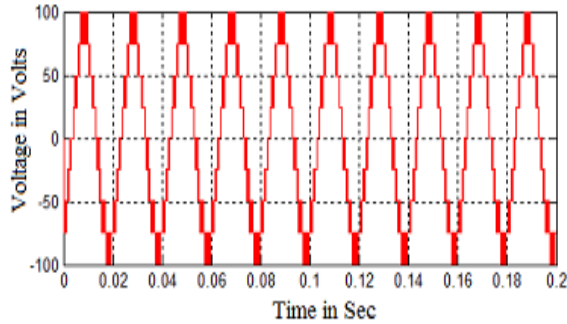


Fig.5 Output voltage generated by phase opposition disposition PWM control

disposition PWM control

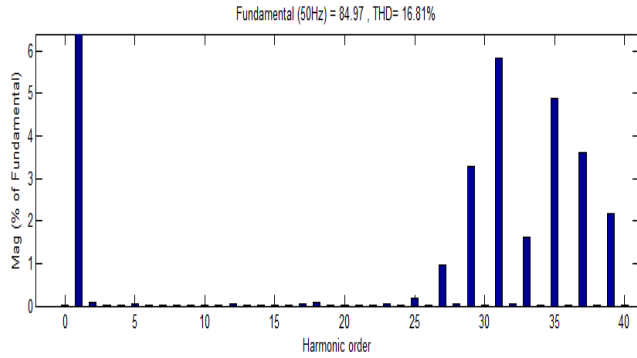


Fig.6 FFT plot for output voltage of phase opposition disposition PWM control

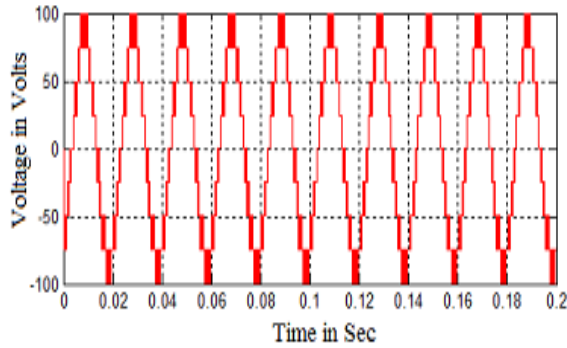


Fig.7. Output voltages generated by alternate phase opposition disposition PWM control

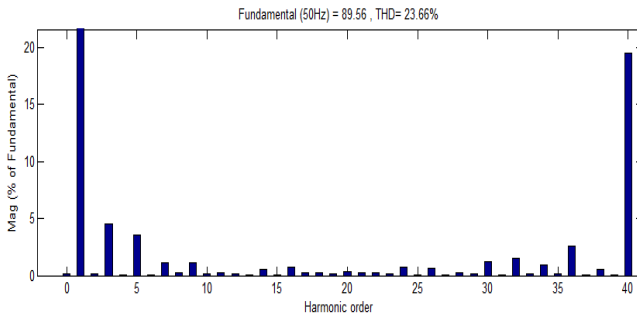


Fig.8. FFT plot for output voltage of alternate phase opposition disposition PWM control

Table1: %THD for different modulation indices

Ma	PD	POD	APOD
1	0.00072	0.00034	7.66E-05
0.95	0.00012	0.00039	8.06E-05
0.9	0.00018	0.00011	9.13E-05
0.85	0.0071	0.00057	0.00021
0.8	0.0056	0.00039	0.00011

Table2:Distortion Factor for Different Modulation indices

Ma	PD	POD	APOD
1	13.57	13.10	13.15

0.95	15.67	15.51	15.63
0.9	16.71	16.60	16.64
0.85	16.99	16.81	23.66
0.8	17.17	16.90	17.43

Table3:Crest factor for different modulation indices

Ma	PD	POD	APOD
1	1.41422	1.41345	1.41345
0.95	1.41413	1.41417	1.41432
0.9	1.41429	1.41430	1.41420
0.85	1.41437	1.41425	1.41404
0.8	1.41420	1.41425	1.41414

Table4:Fundamental RMS voltage for different modulation

Ma	PD	POD	APOD
1	91.71	90.89	90.69
0.95	90.16	89.29	87.17
0.9	89.65	88.62	89.60
0.85	84.99	84.97	89.56
0.8	82.59	80.54	81.55

6. CONCLUSION

In this work the simulation results of single phase impedance source (Z source) cascaded multilevel inverter with R load with different modulation Techniques are obtained with help of MATLAB/SIMULINK, Various performance parameter measures such as THD, Fundamental V_{RMS} , form factor and Crest factor was obtained and tabulated. Single phase impedance source (z source) cascaded multilevel inverter produce the nine level output voltage. It is showed that phase opposition disposition techniques provides the low harmonics distortion and in phase disposition techniques provides larger value of Fundamental RMS voltage compared to all other pulse width modulation techniques.

REFERENCES

- [1] S.Rajakaruna and L.Jayawickrama, "Steady-State Analysis and Designing Impedance Network of Z-Source Inverters," *IEEE Transactions on Industrial Electronics*, Vol. 57, No. 7, pp. 2483-249, July-2010.
- [2] Poh Chiang Loh, Sok Wei Lim, Feng Gao, and Frede Blaabjerg, "Three-Level Z-Source Inverters Using A Single L_c Impedance Network," *IEEE Transactions on Power Electronics*, Vol. 22, No. 2, pp.706-711, March -2007.
- [3] Chandana Jayampathi Gajanayake, D. Mahinda Vilathgamuwa, and Poh Chiang Loh, "Development of a Comprehensive Model and a Multiloop Controller for Z-Source Inverter DG Systems," *IEEE Transactions on Industrial Electronics*, vol. 54, No. 4, pp.2352-2359, August-2007.
- [4] A. M. Tuckey and J. N. Kruse, "A low-cost inverter for domestic fuel cell applications," in *Proc. 33rd Annu. IEEE PESC*, 2002, pp. 339–346.
- [5] J.-M. Kwon, K.-H. Nam, and B.-H. Kwon, "Photovoltaic power conditioning system with line connection," *IEEE Trans. Ind. Electron.*, vol. 53, no. 4, pp. 1048–1054, Jun. 2006.
- [6] J. Wang, F. Z. Peng, J. Anderson, A. Joseph, and R. Buffenbarger, "Low cost fuel cell converter system for residential power generation," *IEEE Trans. Power Electron.*, vol. 19, no. 5, pp. 1315–1322, Sep. 2004.
- [7] A. Shanmuga priyaa, Dr. R. Seyezhai, and Dr. B. L. Mathur, "Performance Analysis of Cascaded Z-Source Multilevel Inverter using Third Harmonic Injection PWM," *International Journal of Computer Technology and Electronics Engineering (IJCTEE)* Vol 2, no 1, pp.143-149.
- [8] Poh Chiang Loh, Feng Gao, and Frede Blaabjerg, "Topological and Modulation Design of Three-Level Z-Source Inverters," *IEEE Transactions on Power Electronics*, vol. 23, no. 5, pp.2268-2277, September 2008.
- [9] Poh Chiang Loh, Frede Blaabjerg and Chow Pang Wong, "Comparative Evaluation of Pulsewidth Modulation Strategies for Z-Source Neutral-Point-Clamped Inverter," *IEEE Transactions on Power Electronics*, Vol. 22, no. 3, pp.1005-1013, May 2007.
- [10] S. Kanimozhi and R. Senthil Kumar, "Z-Source Multilevel Inverter for Uninterruptible Power Supply Application," *Bonfring International Journal of Power Systems and Integrated Circuits*, Vol. 2, Special Issue 1, Part 1, pp. 20-24, February 2012.

A Hybrid Grid Connected Wind Driven Pv System With Single Dc-Dc Converter

J.Antonysagayanancy¹, E.Catherinamalapriya² R.Sivasankari³

^{1,3} PG Student Department of EEE, jeppiaar engineering college, chennai-119

² Assistant Professor, Department of EEE, jeppiaar engineering college, chennai-119

Abstract— A new topology of a grid connected hybrid wind driven PMSG-PV system is proposed. In this system, the two sources are connected together to the grid with the help of only a single DC-DC converter and then followed by an inverter. Hence, compared to earlier system, the proposed system has fewer power converters. The proposed system is developed by a model of $d-q$ axes reference frame. For tracking maximum power from both the sources converter and inverter uses two low cost controllers. Through simulation and experimentation the proposed module controllers demonstration is performed. comparison of the experimental and simulation results are given to validate the simulation module. steady state performance and transients response of both the controllers are explained successfully.

I. INTRODUCTION

Zero net energy buildings which have its cumulative energy consumption being met by renewable energy sources installed within its area have become increasingly popular. These distributed generators (DGs) require new power electronic interfaces and control strategies to improve the efficiency and quality. DG systems consisting of two or more renewable sources have a higher reliability, due to the complementary nature of the resources. In such hybrid schemes, permanent magnet synchronous generators (PMSG) are generally employed, as they do not require any reactive power support. Further, PMSG can be driven directly by wind turbine, thereby avoiding a gear box arrangement which requires regular maintenance. Various possible combinations of hybrid PMSG-PV systems are illustrated in the literature. Earlier, a six-arm converter topology was attempted, in which the outputs of a PV array and wind generator were subjected to a boost operation through individual switches to match the DC bus voltage. In , a hybrid wind-PV system along with battery was explained, in which both the sources were connected to a common DC bus through individual power converters, then the DC bus was connected to the utility grid through an inverter. Grid connected PMSG-PV hybrid system with battery backup was described in , where the DC link voltage was fixed to battery voltage, but the maximum power extraction from wind-driven PMSG was not performed. A PMSG – PV hybrid system with multi-input DC- DC converter and multi- input inverter was also brought out in . In all the above hybrid DG systems with PMSG-PV attempted so far, the system either had individual power converters for each of the sources or a battery backup. Further, each converter was controlled using complex algorithms for peak power tracking. In order to minimize the conduction and switching losses of the devices, it is necessary to have the minimum number of power converters (power conversion stages) and this has been attempted in this paper. It should be noted that losses in conversion stages have to be compensated by increasing the sizes of the generators. This in turn increases the cost of hybrid generator. Generally, efficiency of DC-DC converter is maximum around 95 % when it is operated in full load condition. Since source powers are varying, it is not always possible to operate the DC-DC converter at its maximum efficiency. In the above context, the proposed new topology avoids 5% loss in efficiency by eliminating an additional conversion stage. The

DC link voltage is varied by a DC-DC converter interposed between the rectifier fed by PMSG and the grid connected inverter. The output voltage of the DC-DC converter forms the load line for the PV array. The inverter current is varied to extract maximum current from both the sources using current control strategy. The proposed topology could thus dispense with a DC-DC converter, which in earlier schemes were connected after the PV array for maximum power extraction. A $d-q$ axes model of the scheme has been developed and validated. The successful operation of this scheme in extracting maximum power from both the sources or from each of the sources has been established through simulation and experimental investigations. Further, the proposed scheme is also for employment by domestic consumers in a smart grid scenario, and hence maintenance free simple operation is envisaged. The proposed scheme is for a grid connected operation and hence battery storage is not necessary.

II. DESCRIPTION OF THE SCHEME

The block diagram of proposed DG scheme is given in Fig.1, where a direct driven PMSG and a PV array are the sources. The PMSG output is rectified and fed into a DC-DC boost converter. The rectifier output voltage varies

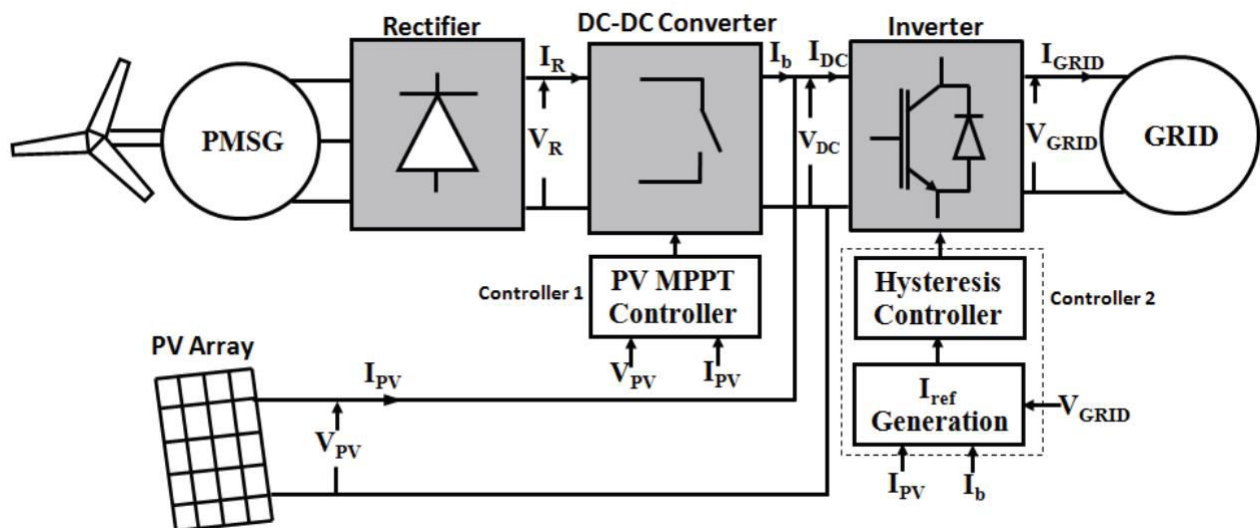


Fig. No.1 Proposed DG system based on PMSG-PV sources

with the wind-speed. The PV array terminals are connected to the output of the DC-DC converter to form a common DC link for the proposed system. The inverter input terminals are tied to this common DC link. The PV array voltage (V_{PV}) is fixed to the output voltage of the DC-DC converter (V_{DC}) since the output terminals of both the PV array and the DC – DC converter are tied together. The output voltage of the DC-DC converter is automatically varied by a PV MPPT controller (Controller 1) to PV array's maximum power point voltage. Under this condition, the maximum current for the given irradiation is drawn from the PV array by the action of current controller (controller 2) of the inverter. The basic Fuzzy logic control algorithm is employed with an inverted duty-cycle adjustment in controller 1. The output voltage of the current controlled inverter is tied to the grid voltage and the frequency and the phase requirement for synchronization are automatically met. The current fed to the grid by the inverter (I_{GRID}) follows the reference current signal (I_{ref}), which is automatically varied by controller 2 for drawing the maximum current from both PMSG & PV array

III. MODEL OF THE PROPOSED SYSTEM

A model of the proposed DG system is developed to investigate the system performance. The rectifier DC output voltage (V_R) and current (I_R) in terms of stator phase voltage V_S (rms) and stator current I_S (rms) are given as [16, 17];

$$V_R = 3 \sqrt{6} / \pi V_S, \quad (1)$$

$$I_R = \pi / \sqrt{6} I_S \quad (2)$$

The output voltage of the DC-DC converter is given as

$$V_b = V_{DC} = V_R / (1 - \delta) \quad (3)$$

The DC link current is

$$I_{DC} = I_b + I_{pv}, \quad (4)$$

the PV array current (I_{PV}) is given by [5]

$$I_{PV} = I_{SC} - I_d \quad (5)$$

The d -axis and q -axis voltage of the inverter are related with the DC link voltage as [18,19],

$$v_d = V_{DC} g_d \quad (6)$$

$$v_q = V_{DC} g_q \quad (7) \text{ Considering zero power loss in the inverter,}$$

$$I_{DC} = 1/2 (i_d g_d + i_q g_q) \quad (8) \text{ Assuming zero power loss in DC-DC converter,}$$

$$V_R I_R = V_b I_b \quad (9)$$

The d axis and q axis circuits of the system are shown in Fig. 3 and Fig. 4 respectively. In the proposed scheme, δ and I_{ref} are varied to extract the maximum IDC at any instant of time. MATLAB has been employed to simulate the proposed scheme in this paper.

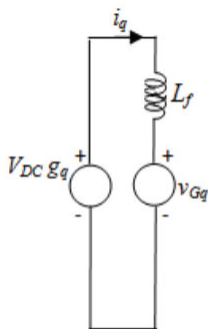


Fig. 2. q-axis equivalent of the system

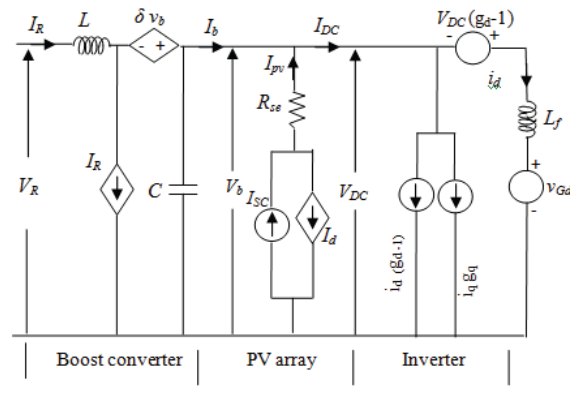


Fig3.d-axis equivalent

A. Case 1 (PV and PMSG generating power) The wind and solar sources are generating power together in this case and the variation of duty-cycle of the DC-DC converter will eventually disturb the PV array's terminal voltage (since $V_{DC} = V_{PV}$). The rectifier voltage varies with the wind-speed and the duty-cycle of the boost converter needs to be automatically adjusted such that V_{DC} is equal to the peak power point voltage (V_m) of the PV array. At this point the PV array delivers the maximum current (I_m) which is concurrently drawn by the current controlled inverter.

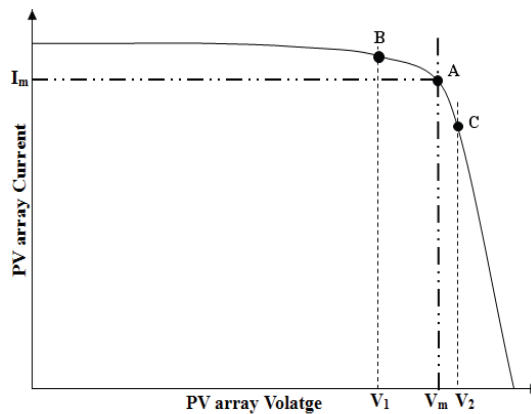


Fig. 4. IV curve of the PV array

To operate the PV array at its maximum power point (A), the DC-DC converter output (DC link voltage) is adjusted to V_m by varying the duty-cycle of the DC-DC converter by controller 1 is given by

$$\delta_{new} = \delta_{old} + \text{sgn}(\Delta P) \text{sgn}(\Delta V_{PV}) \Delta \delta, \quad (10)$$

where $\Delta \delta$ is the perturbation in duty-cycle, sgn is Signum function. ΔP is the difference in PV array power and ΔV_{PV} is difference in PV array voltage before and after perturbation. The duty-cycle variation in this scheme is hence exactly opposite to the duty-cycle variation of a P&O controller used in existing schemes, where a PV array precedes a boost converter. The main objective of controller 2 (Fig. 1) is to vary the inverter output current fed to the grid. The reference current (I_{ref}) for this hysteresis current controller is derived based on the available maximum power from the both the sources for a particular condition (i.e. irradiation and PMSG shaft torque). At steady-state, the reference current value for a particular condition of irradiation and wind speed is

$$I_{ref} = 2(V_{PV} I_{PV} + V_R I_R) / V_{GRID}. \quad (11)$$

B. Case 2 (PMSG alone generating power) During night time the current transducer which is connected with the PV system will not produce any output current. At that time the controller 1 will not operate the MPPT algorithm of the PV system and it starts working in a voltage control mode. Now the output voltage from the voltage transducer acts as a feedback signal, the ratio of the duty cycle is varied by the controller 1 of the boost converter to get the corresponding DC output voltage in a rated RMS voltage value of the grid through the DC link voltage. As the current transducer value is said to be zero, the controller 2 will start adjusting the $i(\text{ref})$ value.

$$I_{\text{ref}}(\text{new}) = I_{\text{ref}}(\text{old}) + \text{sgn}[\Delta(I_b)]K \quad (12)$$

C. Case 3 (PV alone generating power) When PV array alone working, no power is generated through PMSG and hence there is no input fed to the DC-DC boost converter and there is no triggering pulse generated.

Since current in the boost converter I_b is zero, the controller 2 varies the $I(\text{ref})$ values.

$$I_{\text{ref}}(\text{new}) = I_{\text{ref}}(\text{old}) + \text{sgn}[\Delta(I_{PV})]K, \quad (13)$$

D. Composite operation of controllers

It is clearly seen from the above cases, when the PV system alone generates power, the controller 1 is idle and by adjusting I_{ref} value, controller 2 always gets maximum power from either from both the sources or any one of the sources to the grid. Functions of controllers under different conditions are shown below in the table.

Source	Controller 1	Controller 2
Both PV and PMSG operate	Generates duty-cycle for PV array MPPT voltage.	Generate maximum current from both the sources
PV array is operate alone	Triggering pulse not generated (duty-cycle is zero)	Generate maximum power from the PV system
PMSG is operate alone	Duty-cycle is generated and maintain constant DC link.	Generate maximum power from PMSG alone

V. IMPLEMENTATION OF THE CONTROLLERS

A. Controller for DC-DC Converter (Controller 1)

DC-DC converter is formed by a very low cost 16-bit microcontroller along with inbuilt pulse width modulation module to produce signals. This controller gets the feedback signal from both the current and voltage transducers. These signals are further processed by a signal conditioning circuit and fed to an analog-to-digital conversion module. The 16-bit microcontroller is programmed with a fuzzy logic algorithm for PV array.

B. Hysteresis Current Controller (Controller 2)

The schematic diagram of hysteresis current controller is shown above in the fig. The base current I_b and PV current I_{pv} are flow through the ADC module from current transducer. Based on I_{ref} from ADC is converted into analog form by DAC. This DAC will produce a DC value corresponding to I_{ref} . To get current to the controller 2 the DC value is multiplied with I_{ref} and current from grid. Hence the hysteresis controller works with grid current as input. Thus the output from the controller 2 is fed to the inverter for the working of PV array alone or PMSG alone. When both the sources working together DC link will get

maximum value of power. The sine wave reference is taken from the grid so the output of the inverter will also have the phase frequency value.

VI. SIMULATION AND EXPERIMENTAL VALIDATION

For the proposed hybrid generator a single phase inverter was concoct with available IGBT. The input pulses are given from the hysteresis controller. A DC-DC boost converter was also concoct with IGBT and also has a hyper fast diode. Both the experimental and simulation was done by a 6 panel series PV and PMSG. The base values for the above mentioned is given by: base power=1Kva; base voltage=100V; base current=10A; base speed=500rpm.

A. Steady-state investigations

DC motor was used as PMSG to simulate the wind turbine. The grid voltage is greater than the PV and PMSG voltage hence a step-up transformer is connected between the inverter and grid. The steady-state DC link voltage and current simulated waveform is shown in the fig.

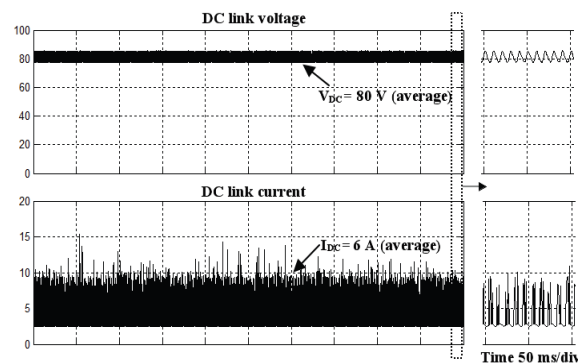


Fig. 6. DC link steady state waveforms (voltage-20V/div,current 5A/div,time500ms/div)

The grid side simulated voltage and current waveform is shown in the fig it is clear that unity power factor is delivered to the grid by inverter.

B. Investigations on MPPT operation

In order to get successful operation of the hybrid generator for different irradiation and PMSG speed the following performance was carried out. Irradiation is maintained constant without major variation. The open circuit voltage is $v_{oc}=1.1p.u$ and short circuit current is $i_{sc}=0.2p.u$ for short time-period. By varying the motor speed (0.4 to 0.95 p.u) the corresponding PMSG power, boost converter duty-cycle and i_{ref} are noted. The fig shows that PMSG shaft speed increases and the output power of it also increases and proportional to the i_{ref} of the controller² increases to extract maximum power when DC motor speed increases input voltage of DC-DC converter increases and duty-cycle of the boost converter decreases to maintain maximum power point. This changes in the PV duty-cycle ratio and reference current variations

The fig shows that PMSG shaft speed increases and the output power of it also increases and proportional to the i_{ref} of the controller² increases to extract maximum power when DC motor speed increases input voltage of DC-DC converter increases and duty-cycle of the boost converter decreases to maintain maximum power point. This changes in the PV duty-cycle ratio and reference current variations is shown in the fig,

C. Total harmonic distortion

To improve the power quality total harmonic distortion(THD) is applied in this paper. The THD value of current and voltage is measured in the by a power quality analyzer and the it shown in the fig .The current and voltag THD value4.6% and 1.8% are below the allowable reference value.

III. CONCLUSION

The new topology of hybrid dg system based on wind-driven and PV system with a boost converter followed by a inverter has been successfully implemented. The mathematical model for this system is used to sudy the system performance in MATLAB. It has been established through experimental and sumulation with the help of two controllers digital MPPT controller and hysteresis controller which tracks the maximum power from both sources. This proposed system has a advantages of maintance free operation ,realiability and lowcost circuits.Also the expermental and simulated output matches closely. The steady state wavefrom of the grid system shows thatdg system fed to the grid at unity power factor.The power quality improvement of the THD voltage and THD current is found to be the value below the norms.The proposed system can be applied for the appliction of erection and smard grid in domestic consumers sites.

REFERENCES

- C. Liu, K.T. Chau, X. Zhang, "An Efficient Wind-Photovoltaic Hybrid Generation System Using Doubly Excited Permanent-Magnet Brushless Machine", *IEEE Trans.Ind.Electron*,vol.57, no.3, pp.831-839,Mar.2010.
- C. N. Bhende, S. Mishra, Siva Ganesh Malla, "Permanent Magnet Synchronous Generator-Based Standalone Wind Energy Supply System" *IEEE ans. Sustain. Energy*, vol. 2, no. 4, pp. 361-373, Oct2011.
- B. Subudhi, R. Pradhan, "A Comparative Study on Maximum Power Point Tracking Techniques for Photovoltaic Power Systems," *IEEE Trans. Sustain. Energy*. vol. 4, no. 1, pp.89-98, Jan 2013.
- A. Timbus , M. Liserre , R. Teodorescu , P. Rodriguez and F. Blaabjerg "Evaluation of current controllers for distributed power generation systems", *IEEE Trans. Power Electron.*, vol. 24,no. 3, pp.654 -664 2009
- P. Mattavelli "A closed-loop selective harmonic compensation for active filters", *IEEE Trans. Ind. Appl.*, vol. 37, no. 1, pp.81 -89 2001
- T. F. Chan and L. L. Lai "Permanent-magnet machines for distributed generation: A review", *Proc. 2007 IEEE Power Engineering Annual Meeting*, pp.1 -6
- D.C. Aliprantis, S.A. Papathanassiou, M.P. Papadopoulos, A.G. Kladas, "Modelling and control of variable-speed wind turbine equipped with permanent synchronous generator", *ICEM 2000* 28-30 August 2000 Espoo, Finland
- L. Malesani and P. Tenti,"A novel hysteresis control method for current controlled VSI PWM inverters with constant modulation frequency", *IEEE Trans. Ind. Applicat.*,vol. 26,pp.88 -92 1990

A Novel approach for Power Factor Correction using Microcontroller in Domestic Loads

Eugin Martin Raj. V. C¹, S.Lese²

¹*Department of EEE, St. Anne's College of Engineering and Technology, martinbe24@gmail.com*

²*Department of EEE, St. Anne's College of Engineering and Technology, leselouis@gmail.com*

Abstract - The need for power factor correction is for compensating the lagging reactive power due to the highly varying inductive loads and is done by either switching on the capacitor banks or by synchronous condenser. Presently, capacitors switching is done manually. The disadvantages are definite time lag, reduction in operating efficiency and lower reliability of the entire system. In the present modern trends of computerization, the use of computers and microcontrollers can also be applied to solve this problem. In this paper, we have utilized the most common microcontroller for the purpose of switching on or off the capacitor banks. In today's trend there is ever growing demand for power and more stress is being laid on optimum utilization of available power. This is where power factor plays a vital role. For efficient utilization of electrical power, power factor of the system should be high.

Keywords – power factor; microcontroller; capacitors; power utilization; reactive power.

I. INTRODUCTION

In the today's trend there is ever growing demand for power and more stress is being laid on optimum utilisation of available power. This is where power factor plays a vital role. For efficient utilisation of electrical power, power factor of the system should be high. To obtain the best possible economic advantage from electric power, both generating and consumer plants should be operated at high efficiency, to achieve this it is essential to have a high power factor throughout the system.

Most of the machines operated in industries have a inherent low power factor which means that supply authorities have to generate much more current than theoretical requirements. In addition, transformers and cables have to carry this extra current, when the overall power factor of generating system is insufficient and the loss of power goes high, to avoid this power factor improvement is a must.

The methods employed to activate the improvements involves injecting KVAR into the system in phase opposition to wattless current and effectively cancel its effect in the system. The power factor can be improved by connecting devices like static capacitors or synchronous condensers which takes a leading power in parallel with load. They are compact, reliable, highly efficient and they can be used easily for automatic power factor control.

Power factor correction brings the power factor of an AC power circuit closer to 1 by supplying reactive power of opposite sign, adding capacitors or inductors which act to cancel the inductive or capacitive effects of the load, respectively. For example, the inductive effect of motor loads may be offset by locally connected capacitors. If a load had a capacitive value, inductors (also known as *reactors* in this context) are connected to correct the power factor. In the electricity industry, inductors are said to consume reactive power and capacitors are said to supply it, even though the reactive power is actually just moving back and forth on each AC cycle.

The low power factor is mainly due to the fact that most of the power loads are inductive and therefore take lagging current. In order to improve the power factor, some devices taking leading power should be connected parallel with the load. One such device can

be a capacitor. The capacitor draws a leading current and partly or completely neutralizes the lagging reactive component of load current. This raises the power factor of the load.

II. AUTOMATIC POWER FACTOR CORRECTION

Basically in a large power system, an automatic power factor correction unit is used to improve power factor. A power factor correction unit usually consists of a number of capacitors that are switched by means of contactors. These contactors are controlled by a regulator that measures power factor in an electrical network. To be able to measure 'power factor', the regulator uses a CT (Current transformer) to measure the current in one phase.

Depending on the load and power factor of the network, the power factor controller will switch the necessary blocks of capacitors in steps to make sure the power factor stays above 0.9 or other selected values (usually demanded by the energy supplier).

Instead of using a set of switched capacitors, an unloaded synchronous motor can supply reactive power. The reactive power drawn by the synchronous motor is a function of its field excitation. This is referred to as a synchronous condenser. It is started and connected to the electrical network. It operates at full leading power factor and puts VARs onto the network as required to support a system's voltage or to maintain the system power factor at a specified level. The condenser's installation and operation are identical to large electric motors. Its principal advantage is the ease with which the amount of correction can be adjusted; it behaves like an electrically variable capacitor. Unlike capacitors, the amount of reactive power supplied is proportional to voltage, not the square of voltage; this improves voltage stability on large networks. Synchronous condensers are often used in connection with high voltage direct current transmission projects or in large industrial plants such as steel mills.

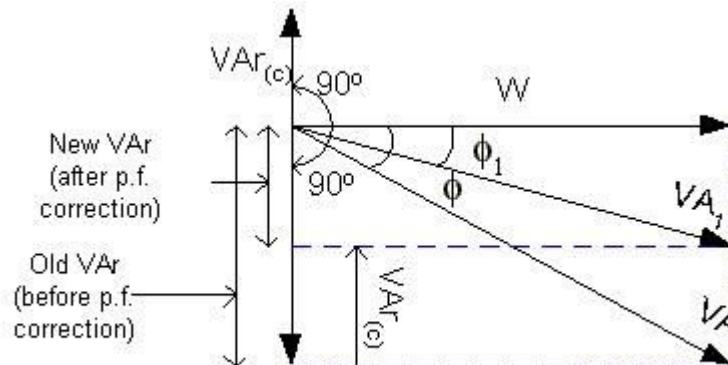


Figure 1. Phasor Diagram for power factor correction

III. PROPOSED METHODOLOGY

In this methodology, we propose the hardware for the automatic power correction for domestic loads, which in turn can be connected with input supply of the secondary consumers. So that the power factor can be maintained at a rate of 0.8 to 0.9 which in turn reduce the power loss due to minimized power factor. A standard 5V dc supply is given from the supply unit. First of all a 230V supply is stepped down to 9V. The voltage at the secondary is then passed to the bridge rectifier. The 9V ac is converted to dc. From there it is passed to the voltage regulator circuit. The output of the voltage regulator is a standard 5V dc supply. This 5V supply is given to the zero crossing detectors, microcontroller, LCD display, inverter circuit etc.

The line voltage is given to the potential transformer. Similarly current is passed to the current transformer from the line. The voltage and current are stepped down in the potential and current transformer respectively. Then the voltage and current from the instrumentation transformer are passed to the zero crossing detectors. Here the sine wave inputs are converted to square wave outputs of either two states, high or low.

Then the output voltage and current waveform are given to microcontroller to port 1.0 and 1.1 respectively. In the microcontroller difference in the instant of crossing zero is calculated by using timer in the program. After skipping a high and low pulse of voltage waveform timer starts counting (T1). This is continued for a full cycle of the voltage waveform. The above process is repeated for the current waveform with reference to the reference point of the voltage waveform (T2).

Φ is calculated by using the conversion,

$$\Phi = (T2 * 360) / T1$$

From the look up table corresponding $\cos \Phi$ is calculated. This calculated power factor is then compared with the reference power factor. If the calculated power factor is less than the reference power factor then a low pulse is given to 7404IC which sends a high pulse to the relay circuit which in turn close the capacitor bank. If the calculated power factor is more than the reference power factor then a high pulse is given to 7404IC, which will send a low pulse to the relay circuit. Thus the closed capacitor bank gets disconnected from the circuit. All the above mentioned processes are repeated for infinite loop.

The actual value, preset value and corrected value is displayed through the LCD display. When the supply is turned on, the first screen of the LCD display is “power factor controller”. To see the preset value and the actual value, the menu key is pressed. In other words, to view the next screen, the menu key is pressed. The preset value can be incremented or decremented by using the increment key or the decrement key. This updated value is made reference by pressing the enter key

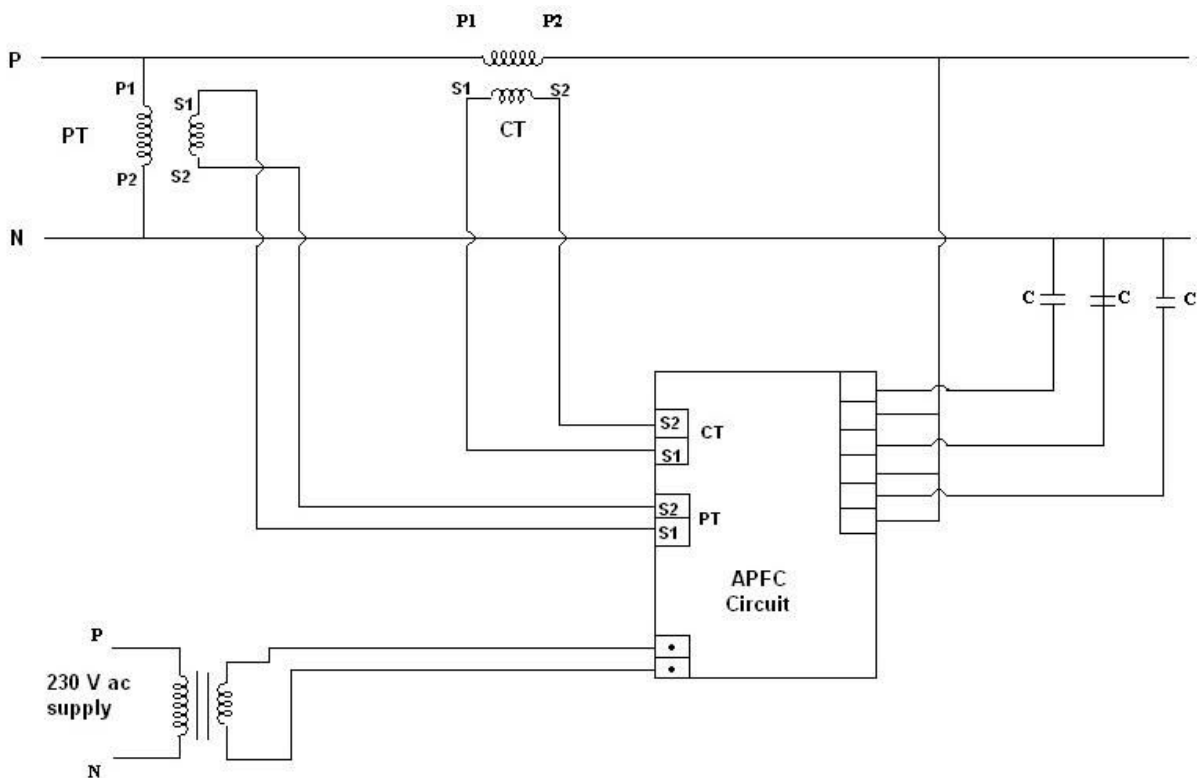


Figure2. Power circuit for proposed system

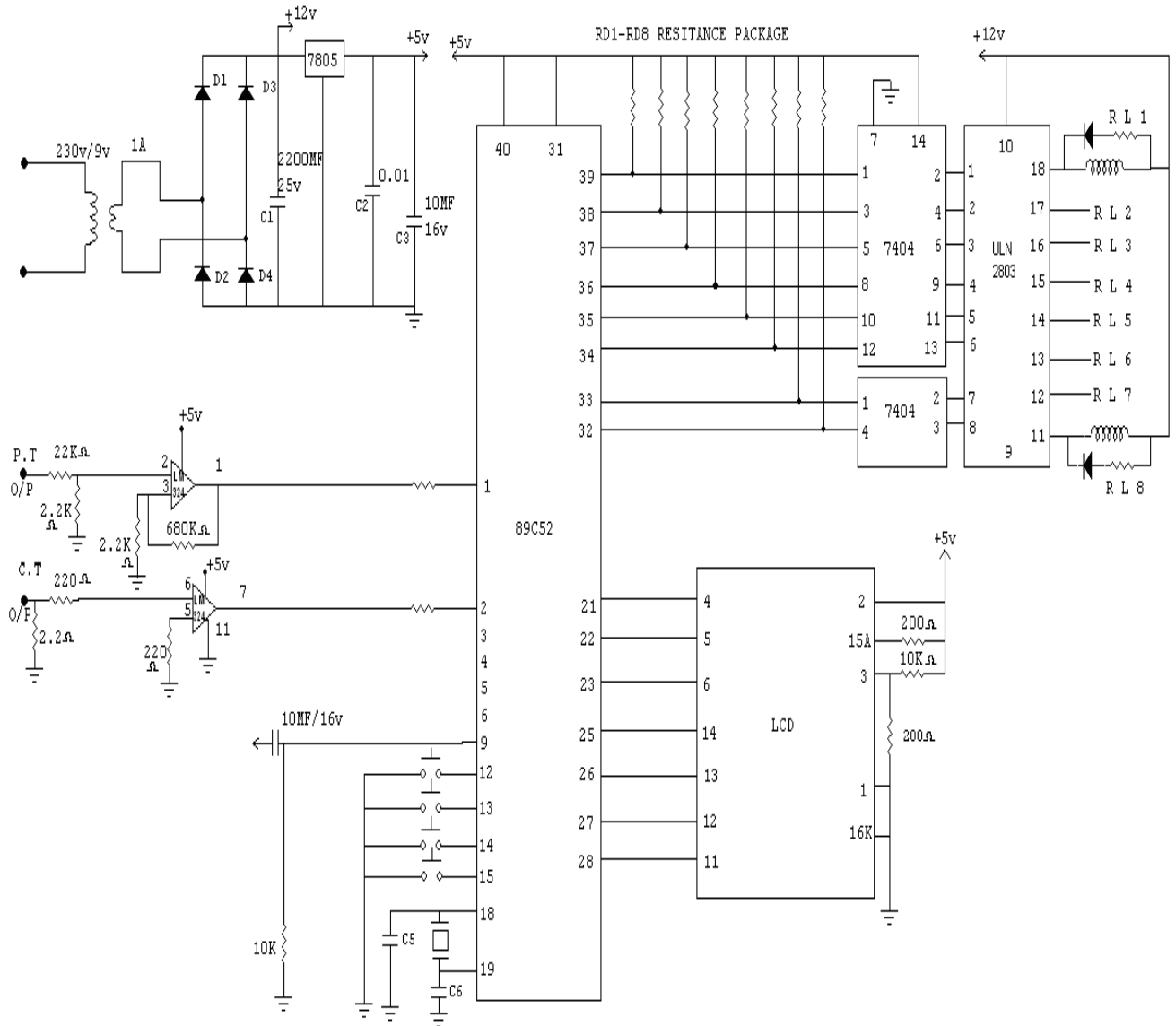


Figure3. APFC Circuit Diagram for proposed system

At the beginning high signal is given to alarm circuit to avoid the working of relays under normal conditions. For this purpose alarm the program initializes circuit. As per the program low signal will be given as an alarm to the switching circuit, which in turn activates the relay. If measured power factor is less than the reference power factor, then the alarm is given to relays.

To calculate the time period of voltage waveform for a complete 360 degree a reference point is fixed by skipping a high and low pulse. Then the timer starts counting as per the software (T1). From the same reference point, time period for current waveform is calculated (T2).

$$\Phi = (T2 * 360) / T1$$

The controller using timers measures power factor. This is explained through waveforms as follows,

Actual $\cos\phi$ is calculated from the look-up table. Using DPTR register does this. At the beginning of the program, a reference power factor is set and stored in the internal data memory. This reference power factor is compared with the calculated or actual power factor. If the carry flag is set, then controller will send a low signal to relay circuit. Carry flag is set means reference power factor is higher than the calculated power factor.

LCD display displays the calculated and reference power factor and has the provision to increment or to decrement the reference power factor. Using the inc/dec keys does this.

IV. DISCUSSIONS

So, the proposed hardware for the automatic power correction for domestic loads, which in turn can be connected with input supply of the secondary consumers. So that the power factor can be maintained at a rate of 0.8 to 0.9 which in turn reduce the power loss due to minimized power factor. A novel approach has been proposed here for implementing this in the state of Tamilnadu for all the secondary consumers. Which would help us to save a loads in our consumption and losses due to power factor. The various salient features of the system developed by us are mentioned below

- Fully automated control will be available to control power factor.
- This system consumes less power and hence there is not much of effect in regulation as a result of this power.
- Easy control and switching is possible in our system. This is because we use static capacitors banks for power factor improvement and also, they are added or removed in steps.
- The proposed system is highly accurate, precise and also has a quick response. Hence it is very efficient and economic.

So, the system proposed will work to a great extend in the power factor correction in domestic loads which would move the power consumption to further level of energy saving.

V. REFERENCES

- [1]. Okoboi, Geoffrey, and Joseph Mawejje. "The impact of adoption of power factor correction technology on electricity peak demand in Uganda." *Journal of Economic Structures* 5.1 (2016): 1-14.
- [2]. García, Oscar, et al. "Single phase power factor correction: a survey." *Power Electronics, IEEE Transactions on* 18.3 (2003): 749-755.
- [3]. Menke, M. F., et al. "Comparative Analysis of Self-Oscillating Electronic Ballast Dimming Methods With Power Factor Correction for Fluorescent Lamps." *Industry Applications, IEEE Transactions on* 51.1 (2015): 770-782.
- [4]. Devkar, Priya S. "Microcontroller Based Power Factor Correction Using IC L6561."
- [5]. Xu, Jiangtao, Meng Zhu, and Suying Yao. "Distortion Elimination for Buck PFC Converter with Power Factor Improvement." *Journal of Power Electronics* 15.1 (2015): 10-17.
- [6]. Bouafassa, Amar, Lazhar Rahmani, and Saad Mekhilef. "Design and real time implementation of single phase boost power factor correction converter." *ISA transactions* 55 (2015): 267-274.
- [7]. Ghosh, Arindam, and Avinash Joshi. "A new approach to load balancing and power factor correction in power distribution system." *Power Delivery, IEEE Transactions on* 15.1 (2000): 417-422.
- [8]. Hejab, Abdallah S., and Ahmad H. Sakhrieh. "Energy Savings Potential Associated with Reactive Power in Water Pumping Systems." *Int. J. of Thermal & Environmental Engineering* 11.1 (2016): 61-65.
- [9]. Genannt Berghegger, Ralf Schroeder. "Controller for providing a corrected signal to a sensed peak current through a circuit element of a power converter." U.S. Patent No. 9,246,391. 26 Jan. 2016.
- [10]. Zhang, Michael T., et al. "Single-phase three-level boost power factor correction converter." *Applied Power Electronics Conference and Exposition, 1995. APEC'95. Conference Proceedings 1995., Tenth Annual. IEEE, 1995.*
- [11]. Lamar, Diego G., et al. "A unity power factor correction preregulator with fast dynamic response based on a low-cost microcontroller." *Power Electronics, IEEE Transactions on* 23.2 (2008): 635-642.
- [12]. Lev, Arie, et al. "Power factor correction method and apparatus." U.S. Patent No. 6,043,633. 28 Mar. 2000.

ENERGY STORAGE CAPACITOR REDUCTION FOR SINGLE PHASE PWM RECTIFIER

A. Annai Theresa¹, K. Sriram²

^{1,2}Department of Electrical and Electronics Engineering, St. Anne's College of Engineering and Technology, Panruti, Tamilnadu.

Abstract — The demand for energy will carry on to rise as long as world population rises and people continue to demand an advanced standard of living. The challenge lies in providing this energy from dependable and sustainable sources while preserving respect for the environment. Renewable energy presently faces a number of problems on its way to become the sole source of electric power generation. One major drawback is its dependency on environmental location. It is clear that an energy storage system is desirable in order to solve the problems associated with both peak demand loading and the intermittent nature of renewable energy. This paper presents a proposed topology follows an active ripple energy storage method that can effectively reduce the energy storage capacitance. A novel feed forward control scheme is also developed so that both the rectifier and inverter mode can be operated in a good manner. The features of the proposed scheme will be verified by the simulation using MATLAB.

Keywords — renewable energy, active ripple energy, feed forward control, energy storage capacitance.

I. INTRODUCTION

The single-phase ac/dc pulse PWM converter is extensively used in many applications such as adjustable-speed drives, switch-mode power supplies, and uninterrupted power supplies. The single-phase ac/dc PWM converters [1], [2], [3] are customarily employed as the utility interface in a grid-tied renewable resource system, as shown in Fig. 1. To consume the distributed energy resources (DERs) resourcefully and preserve power system stability, the bidirectional ac/dc converter plays a significant role in the renewable energy system. When DERs have plentiful power, the energy from the dc bus can be easily shifted into the ac grid through the bidirectional ac/dc converter. In contrast, when the DER power does not have plentiful energy to deliver electricity to the load in the dc bus, the bidirectional ac/dc converters can instantaneously and quickly change the power flow direction (PFD) from ac grid to dc grid and give adequate power to the dc load and energy storage system.

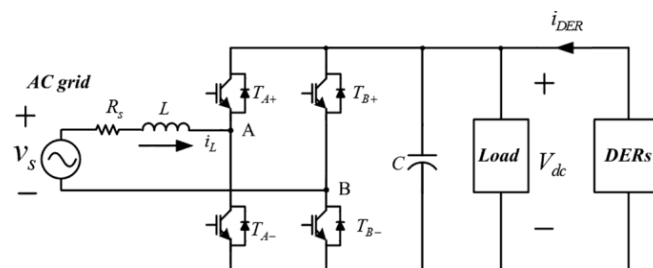


Fig. 1. Distribution Energy System.

One of the essential characteristics of the single-phase rectifier is the low frequency ripple power on the dc link when the ac input voltage and current are sinusoidal. The converter power has both a dc and a ripple component with the ripple frequency to be twofold

that of the ac input frequency, and can therefore cause a second-order frequency ripple in dc link voltage. To limit this low frequency ripple, a bulk dc link capacitor is generally required, which results in large converter volume and low power density. The electrolytic capacitors frequently used in this case for their cost and energy density benefits can also pose complications due to their poorer life-time and reliability. To progress the power density of a single-phase rectifier, it is essential to lessen the dc-link capacitor required for filtering the low-frequency ripple energy. In this paper, an active ripple energy storage system with feed forward control scheme is presented.

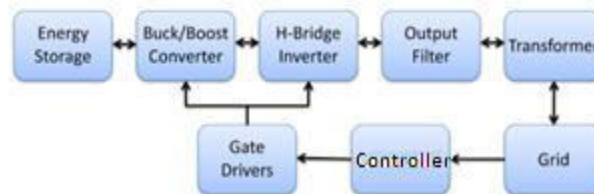


Fig.2. Distribution Energy System.

Numerous active methods have been discovered to deal with this second-order ripple power from the ac side in single-phase applications, namely, a dc ripple reduction circuit [4]–[5], two-stage cascaded power factor correction (PFC) [6], parallel PFC [7],[8], dc bus conditioners [9], and ac side active filter [10]. Any of these can be used to shrink the dc ripple current, rise the regulation of the output voltage, and expand the transient dynamic response of the system while also serving to maintain the dc bus stability. All these methods have the common use of an auxiliary circuit and auxiliary ripple energy storage devices. In terms of storage elements, the methods are classified into inductive and capacitive energy storage, whereas from a topology stand point they are classified into single and multistage active circuits. For the second case, the auxiliary circuit can be connected either in series or in parallel with the main power circuit, and its control strategy can be realized dependent or independent of the control of the single-phase PWM rectifier. The ripple cancellation methods discussed previously have not considered quantitatively the low-frequency ripple energy storage requirements for single-phase rectifiers; in the meantime, they have not concentrated on the lessening of the converter volume. This paper proposes a bidirectional buck–boost converter as an auxiliary ripple energy storage circuit, which can effectively reduce the converter energy storage capacitance and thus lead to a 50% volume reduction of the system size.

The choice of the capacitor with a particular voltage rating is based on two characteristics: capacitance and current rating. Thus the capacitive energy storage analysis should be conducted based on these two aspects. When charging a capacitor, its voltage rises from the capacitor's minimum value to the maximum value. When discharging a capacitor, its voltage drops from the maximum value to the minimum value. As a result, the voltage ripple fluctuation of a capacitor makes it proficient of absorbing ripple power. For a conventional single-phase PWM rectifier design, a ripple energy storage capacitor is typically put in the dc bus when there is a tight voltage ripple requirement.

II. PROPOSED TOPOLOGY OF THE RIPPLE ENERGY STORAGE SYSTEM

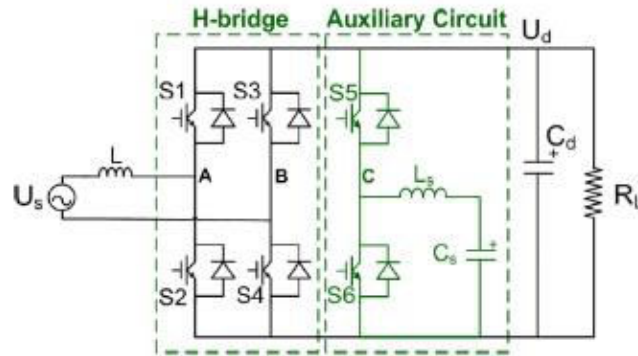


Fig. 3 High power density single phase rectifier.

At the output of the typical single phase PWM rectifier a bidirectional buck-boost converter is connected. An auxiliary capacitor with capacitance C_s is used as an energy storage element. We switch the bidirectional converter as a buck mode when ripple energy needs to be put in storage in the C_s . It is controlled as a boost mode when ripple energy needs to be released back to the dc link. A dc link capacitor with capacitance C_d is still desired at the output of the PWM rectifier. C_d can be noticeably smaller than the capacitance required in the conservative method, since it essentials only to filter the switching ripple energy and the residual second-order harmonic ripple energy not completely absorbed by the auxiliary capacitor C_s . The switching ripple energy, consequences from both the PWM rectifier and the bidirectional buck boost converter.

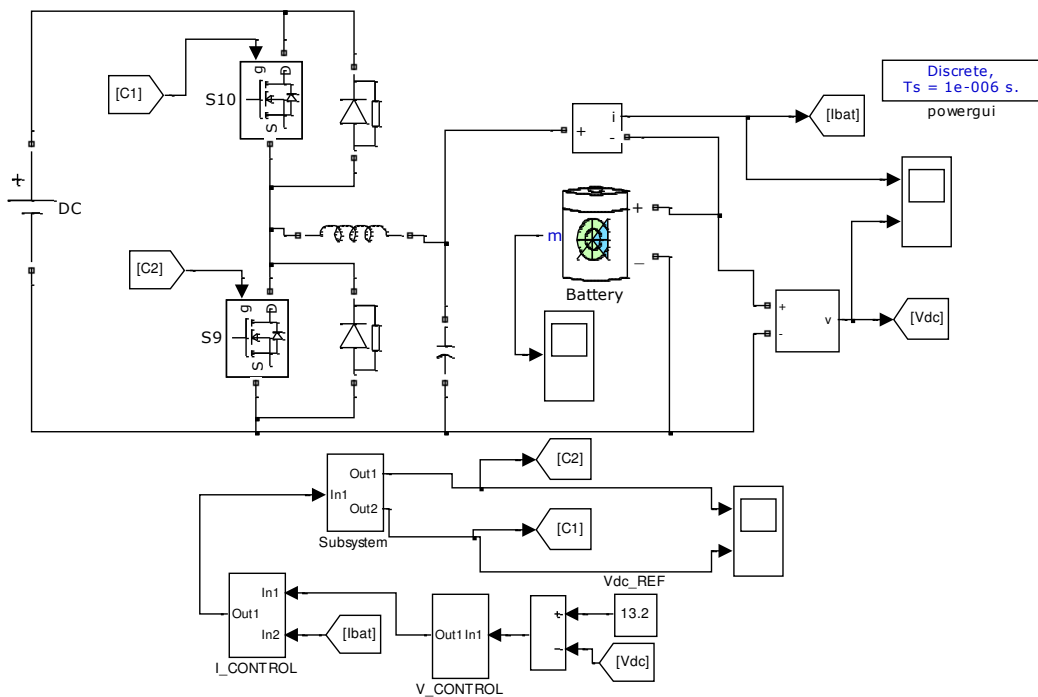


Fig. 4 SIMULINK model for proposed System

Another bidirectional buck–boost converter connected in addition to the typical H-bridge rectifier on the dc bus works as an auxiliary circuit. The auxiliary circuit is composed of one phase leg, an auxiliary inductor, and an auxiliary capacitor. The dc bus voltage is still controlled by the H-bridge rectifier, while the ripple power that comes from the ac side is controlled by the auxiliary circuit. The auxiliary capacitor C_s is used as the energy storage component, and the auxiliary inductor L_s works as the energy transfer component that transfers the ripple energy between the auxiliary capacitor and the dc bus. When the ripple energy necessities to be transferred from the dc bus to the auxiliary capacitor, switch S_5 is used to control the auxiliary circuit functioning in buck phase. During the trigger interval of switch S_5 , the dc bus charges both the auxiliary inductor and the capacitor. The auxiliary inductor will further discharge its energy to the auxiliary capacitor during the S_5 turn-off interval. If the ripple energy desires to be released from the auxiliary capacitor back to the dc bus, switch S_6 is used to control the auxiliary circuit functioning in boost phase. During the turn-on interval of switch S_6 , the auxiliary inductor is charged by the auxiliary capacitor. During the turn-off interval of S_6 , both the auxiliary capacitor C_s and auxiliary inductor L_s will discharge energy back to the dc bus. Because the auxiliary capacitor is not put in the dc bus, and there is no necessity for the auxiliary capacitor voltage ripple, using the auxiliary capacitor C_s to store the ripple power is much more effective than using the dc bus capacitor, as stated earlier.

Note that a dc bus capacitor C_d is still required at the output of the PWM rectifier for filtering the high-frequency ripple power and very minor low-frequency ripple power that is not fully absorbed by the auxiliary circuit. However, in this case, C_d is significantly smaller than what it would be in the conservative method without the auxiliary ripple energy storage circuit. The expected active ripple energy storage method has several advantages. As shown in Fig. the active components in the auxiliary circuit form a typical phase leg (S_5 and S_6), which could be easily combined together with the main circuit as another phase leg. For the meantime, because the auxiliary circuit belongs to the voltage step-down circuit, there is no voltage greater than the dc bus in this system. As mentioned earlier, the inductor is found not to be as good as a capacitor in terms of energy density for applications of a few hundred hertz. Therefore, the auxiliary circuit is controlled in discontinuous current mode (DCM) to store all the ripple energy stored in the auxiliary capacitor but not in the auxiliary inductor, which shows that the auxiliary inductor works only as an energy transfer component. During each switching period, the auxiliary inductor liberates all its energy to the dc bus or to the auxiliary capacitor. Therefore, once the ripple energy storage requirement is defined, the minimum required capacitance is also set. The capacitance can decrease to 12.5 times less than the capacitance with the traditional method by using the active method. Thus, the theoretical minimum capacitance is 125 μF . The total charge and discharge of the capacitor leads to a high capacitor current rating. To leave some margin, the auxiliary capacitance C_s in our system is selected as 200 μF . The DC bus capacitor C_d put in the system to filter the high-frequency ripple is a selection of as 140 μF . The auxiliary inductance is a selection of as 45 μH .

Since second-order harmonic current is generated from the single phase H-bridge rectifier, the auxiliary circuit is used as a parallel current filter. The proposed system is conceived to operate where the single-phase utility grid is the unique option available. Compared to the conventional topology, the proposed system permits: to reduce the rectifier switch currents; the total harmonic distortion (THD) of the grid current with same switching frequency or the switching frequency with same THD of the grid current; and to increase the fault tolerance characteristics. In addition, the losses of the proposed system may be lower than that of the conventional counterpart.

III ENERGY STORAGE SYSTEM TOPOLOGY

Fig 5 shows a general grid-connected ESS in single-phase system. The ESS consists of a battery, bi-directional DC/DC converter, bi-directional DC/AC inverter and filter. An interleaved topology composed of two converters connected in parallel is used to moderate the switching ripple in the battery-side current. Because the ESS requirements the bi-directional power transfer, a bi-directional DC/DC converter and the bi-directional DC/AC inverter are essential. The DC/AC inverter controls the DC-link voltage and power factor. On the other hand, the DC/DC converter normalizes the output current.

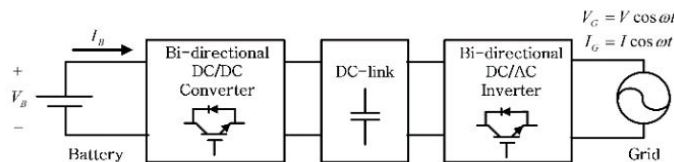


Fig 5. Grid Connected DC/AC Inverter

The full-bridge topology is implemented to set the DC/AC inverter for the proposed ESS as shown in Figure 6. The single-phase full-bridge inverter converts from the AC to DC constant voltage. Figure 7 displays a block diagram of the control scheme for the grid connected inverter in the single-phase system.

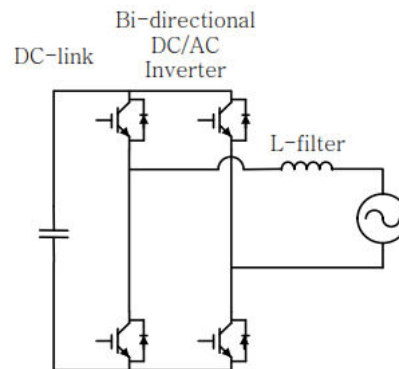


Fig.6 DC/DC Converter

This inverter controls the DC-link voltage using a typical PI controller. To use the PI controller, a synchronous reference frame is mandatory. In the single system, there is a necessity to create an imaginary axis because only one axis be existent. An all pass filter (APF) has characteristic which permits all frequencies correspondingly and shifts the phase by 90 degrees. The APF is used to make an imaginary axis because of the characteristics stated above. The phase angle which is assessed by the phase locked loop (PLL) is used in the synchronous reference frame. The grid voltage and current are transformed to active and reactive components by using the synchronous reference frame and APF. The output of the DC-link controller is the active component which is the reference grid current. The inverter controls the power factor at 1 because the current controller controls the reactive component at zero and the active component to the reference grid current.

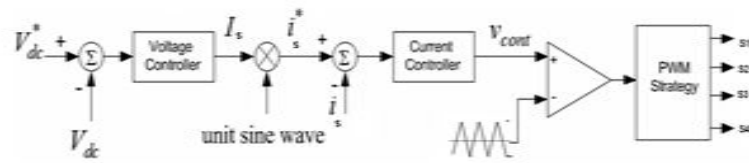


Fig.7 Block diagram of the control scheme

Figure 8 shows the interleaved bi-directional converter used in the proposed ESS. The bi-directional converter is composed of a power semi-conductor switch, capacitor, and inductor. The bi-directional converter can function in buck and boost mode according to the power flow of the ESS. The converter works with the buck mode in the charging mode and with the boost mode in the discharging mode.

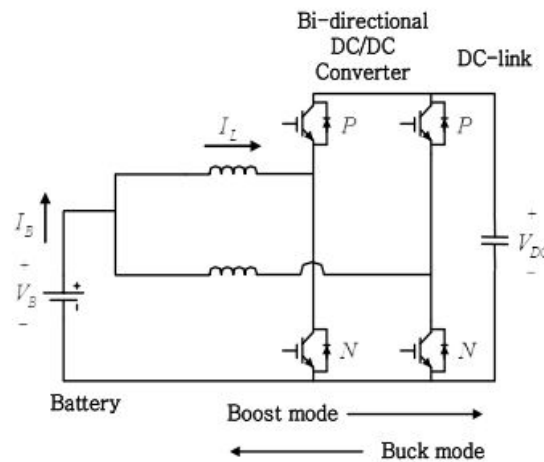


Fig.8 Construction of the bi-directional DC/DC converter

IV. PI CONTROLLERS FOR DC-BUS VOLTAGE CONTROL

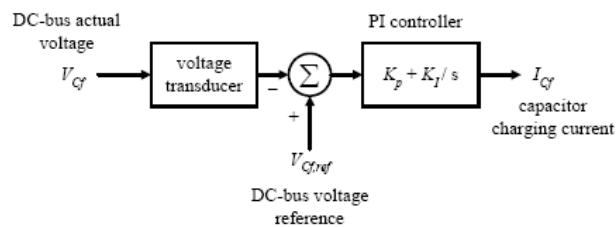


Fig.9 Construction of the bi-directional DC/DC converter

A PI controller used to control the DC-bus voltage is exposed in Figure. Its transfer function can be represented as $K_p + K_i/s$. where K_p is the proportional constant that decides the dynamic response of the DC-bus voltage control, and K_i is the integration constant that decides its settling time. It can be well-known that if K_p and K_i are large, the DC-bus voltage regulation is leading, and the steady-state DC-bus voltage error is small. On the hand, if K_p and K_i are small, the real power unbalance provides little effect to the transient performance.

In the design of single-phase PWM rectifier control system, the common use is dual-loop control, namely, voltage and current loops. The outer voltage loop controls the voltage in DC side, while the current loop as the inner loop, it forces the input current tracking current instruction (gained from the output of the outer voltage loop), in order to attain sinusoidal current control unity power factor. The current instruction and grid- side voltage have same frequency and opposite phase.

V. SIMULATION RESULTS

To verify the validity of the proposed active ripple energy storage and the current control scheme, the well-known software MATLAB was adopted to carry out the simulation process. The High power density single phase PWM rectifier is simulated using Mat lab and the results are presented.

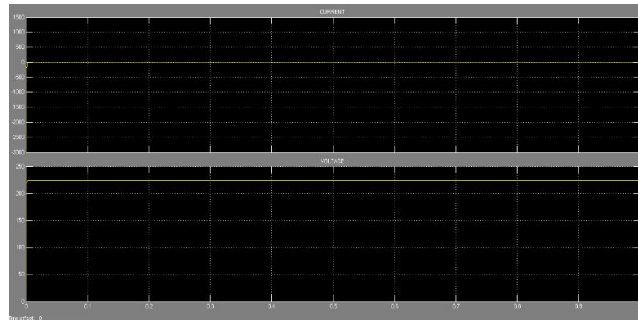


Fig.10 Capacitor output voltage and current

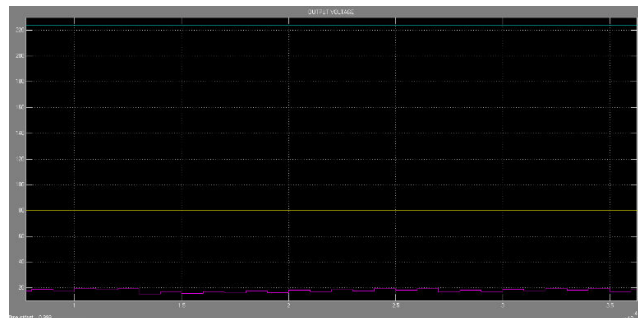


Fig.11 Battery discharge characteristics

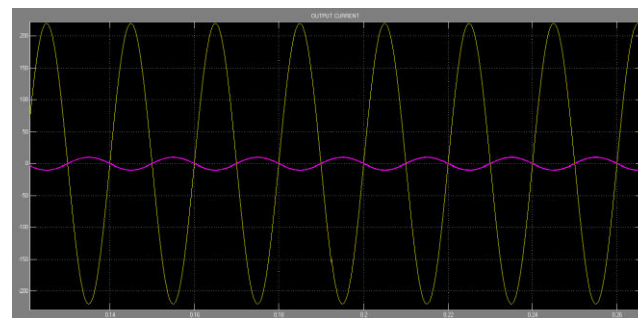


Fig.12 Inversion mode –voltage and current out of phase

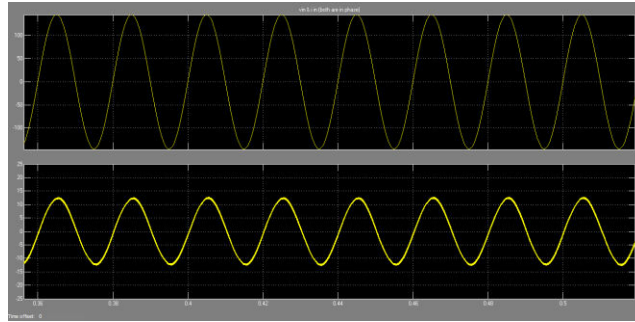


Fig.13 Sinusoidal input voltage and current in-phase

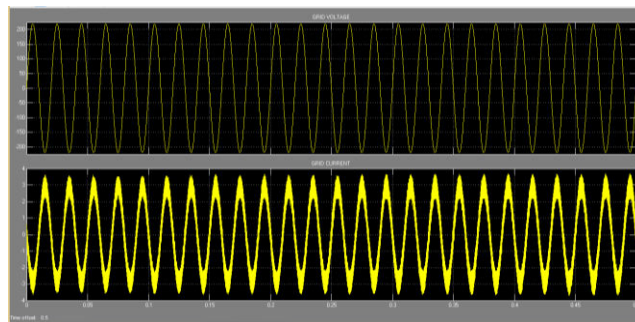


Fig.14 Grid Injection in the Absence of PV-Only With Battery

It can be seen that a single-phase ac/dc converter can be operated obtaining sinusoidal input voltage and current in both rectifier and inverter modes. The auxiliary capacitor voltage ripple and the auxiliary capacitor current i_c and the discharging characteristics of the battery is shown in Fig. 10 .

VI. CONCLUSION

This paper presented a proposed active ripple energy storage method that can effectively reduce the energy storage capacitance. A novel feed forward control scheme is also developed so that both the rectifier and inverter mode can be operated in a good manner. The features of the proposed scheme are verified by the simulation using MATLAB.

VI. REFERENCES

- [1]. R. Wang, F. Wang, D. Boroyevich, R. Burgos, R. Lai, P. Ning, and K. Rajashekar, "A high power density single-phase PWM rectifier with active ripple energy storage," *IEEE Trans. Power Electron.*, vol. 26, no.5, pp. 1430–1443, May 2011.
- [2]. S.-H. Hwang, L. Liu, H. Li, and J.-M. Kim, "DC offset error compensation for synchronous reference frame PLL in single-phase grid-connected converters," *IEEE Trans. Power Electron.*, vol. 27, no. 8, pp.3467–3471, Aug. 2012.
- [3]. R. I. Bojoi, L. R. Limongi, D. Ruiu, and A. Tenconi, "Enhanced power quality control strategy for single-phase inverters in distributed generation systems," *IEEE Trans. Power Electron.*, vol. 26, no. 3, pp. 798–806, Mar.2011.
- [4]. T. Shimizu, Y. Jin, and G. Kimura, "DC ripple current reduction on a single-phase PWM voltage-source rectifier," *Industry Appl. IEEE Trans.*, vol. 36, no. 5, pp. 1419–1428, Sep. 2000.
- [5]. T. Shimizu, T. Fujita, G. Kimura, and J. Hirose, "A unity power factor PWM rectifier with DC ripple compensation," *Industrial Electron., IEEE Trans.*, vol. 44, no. 4, pp. 447–455, Aug. 1997.
- [6]. L. H. Dixon, "High power factor pre-regulators for off-line power supplies," *Unitrode Power Supply Design Seminar Manual*, Paper 12, SEM- 700, 1990.
- [7]. Y. M. Jiang and F. C. Lee, "Single-stage single-phase parallel power factor correction scheme," in *Proc. 25th Annual IEEE Power Electron. Specialists Conf. 1994 Record*, pp. 1145–1151.
- [8]. Y. M. Jiang, "Development of advanced power factor correction techniques," Ph.D. dissertation, Virginia Polytech. Inst. State Univ., Blacksburg, 1994.

Harmonic Reduction Of Single Phase Pwm Rectifier In Ripple Energy Storage System

V.balaji¹, R. Siva Sankari²

^{1,2}*Department of Electrical and Electronics Engineering
St. Anne's College of Engineering and Technology Panruti, Tamilnadu*

Abstract – The low frequency harmonic current normally present in the converter side. This is filtered using a bulk capacitor which results in low power density. The proposed topology permits to reduce the harmonic distortion at the input converter side with decrease in the capacitor volume. The single phase pwm rectifier has the property of low distortion input current with PI controller. Then the buck boost converter is used to filter the harmonic current and the ripple energy storage. With a suitable control strategy, including the pulse width modulation technique (PWM) and PI controller is developed and simulation results are presented using MATLAB.

Keywords – pulse with modulation (pwm), discontinuous Pulse Width Modulation, PI Controller.

I. INTRODUCTION

The single-phase PWM rectifier is now becoming more and more popular due to its low distortion input current, unity power factor operation and bi- directional power flow ability. In general, the selection of an appropriate controller of a PWM rectifier in consideration of stability and dynamic performances requires good knowledge about the characteristics of the system to be controlled. The proposed rectifier based on the small signal model is reasonable and feasible. Normally this type of rectifier used in small scale application only, does not involve with large scale application, to improve the efficiency of rectifier to drives the motor, a new two single phase pwm rectifier are connected anti parallel. This proposed topology permits to reduce the rectifier switch currents, the harmonic distortion at the input converter side, and presents improvements on the fault tolerance characteristics. Even with the increase in the number of switches, the total energy loss of the proposed system may be lower than that of a conventional one. The system may be extended to the application by replacing combination of two parallel rectifiers without the use of transformers for three phase drive system. The system model and the control strategy, including the PWM technique, have been developed. Both of single phase pwm rectifier and anti-parallel single phase pwm rectifier to limit the low frequency ripple a bulk electrolytic dc-link capacitor is usually required, this results in large converter volume, low power density and poor life-time due to the electrolytic capacitors needed. To avoid this above conditions the system is implemented with Energy Storage Capacitor Reduction for Single Phase PWM Rectifier.

This paper focuses on the important characteristics of the single-phase rectifier is the low-frequency ripple power on the dc link when the ac input voltage and current are sinusoidal. The converter power has both a DC and AC component namely ripple energy with the ripple frequency to be twice that of the ac input frequency, and can therefore cause a second-order frequency ripple in dc link voltage. To limit this low frequency ripple, a bulk dc link capacitor is usually required, which results in large converter volume and low power density. The electrolytic capacitors often used in this case for their cost and energy density advantages can also pose problems due to their inferior life-time and reliability. To improve the power density of a single-phase rectifier, it is essential to reduce the dc-link

capacitor required for filtering the low-frequency ripple energy. A bidirectional buck-boost converter is connected at the output of the typical single phase PWM rectifier. An auxiliary capacitor with dc capacitance is used as an energy storage element. We control the bidirectional converter as a buck mode when ripple energy needs to be stored in the Capacitor. It is controlled as a boost mode when ripple energy needs to be released back to the dc link. The auxiliary capacitor reduces the harmonic current developed and the dc link capacitor with capacitance is still needed at the output of the PWM rectifier to filter the residual harmonic. The DC capacitance can be considerably smaller than the capacitance required in the conventional method, since it needs only to filter the switching ripple energy and the residual second-order harmonic ripple energy not fully absorbed by the auxiliary capacitor. The switching ripple energy, results from both the PWM rectifier and the bidirectional buck boost converter.

II. BASIC CONCEPTS OF HARMONIC DISTORTION

Harmonic contamination has become a major concern for power system specialists due to its effects on sensitive loads and on the power distribution system. Therefore the compensation for harmonic and reactive current is important owing to the wide use of power electronic equipments. A classical solution is suitable power conditioning methodology such as passive filtering and active power filtering to suppress harmonics in power systems. Passive LC filters have been employed to eliminate line current harmonics and to improve the power factor. However, the harmonic problems still persists because of its inability to compensate random frequency variations in currents, tuning problems and parallel resonance. Hence a very interesting solution is active power filter, which is connected either in series or parallel with the non-linear loads. The active power filter concept uses power electronics to produce harmonic components, which cancel the harmonic components from the non-linear loads.

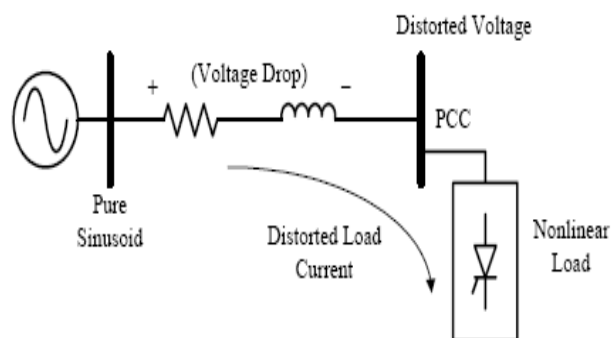


Fig 1 Harmonic currents flowing through the system impedance

As the number of harmonic producing loads has increased over the years, it has become increasingly necessary to address their influence when making any additions or changes to an installation. To fully appreciate the impact of this phenomenon, there are two important concepts to bear in mind with regard to power system harmonics. The first is the nature of harmonic current producing loads (non-linear loads) and the second is the way in which harmonic currents flow and how the resulting harmonic voltages develop.

III. PROPOSED CONTROL IMPLEMENTATION

The proposed topology of the ripple energy storage method is depicted in Fig.4.1. A bidirectional buck-boost converter is connected as auxiliary circuit at the output of a typical single-phase bidirectional PWM rectifier. Since second-order harmonic current is generated from the single phase H-bridge rectifier, the auxiliary circuit is used as a parallel current filter. An auxiliary capacitor, with capacitance C_s , is used as an energy storage element; while the inductor L_s is used as an energy transfer component. A dc-link capacitor, with capacitance C_d , is still needed at the output of the PWM rectifier to filter the switching ripple energy and the residual second-order harmonic ripple energy not fully absorbed by the auxiliary capacitor C_s . S_5 is controlled as a buck switch for charging and S_6 is controlled as a boost switch for discharging. The current of switch S_5 is discontinuous, so this auxiliary circuit can only be used as low frequency current filter which is typical for single phase. Meanwhile, there is no voltage higher than the dc bus existing in this system and the auxiliary circuit can be integrated together with the main circuit easily as one additional phase leg.

IV. CONTROL ANALYSIS

4.1. DESIGN CONSIDERATIONS

For single phase H-bridge rectifier, the modulation method is specified to achieve both the minimum loss and balanced temperature distribution. For the auxiliary circuit, the auxiliary capacitor is selected according to the ripple energy requirements and the auxiliary inductor is designed as below.

Modulation method

This method shows the single phase discontinuous PWM modulation method. One phase leg will not switch within half of the supply frequency. It can lead to the minimum switching loss with a fixed frequency.

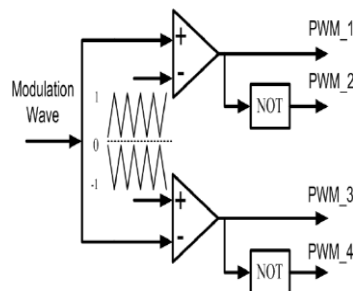


Fig:2. Harmonic currents flowing through the system impedance

S_1 and S_2 are clamped when S_3 and S_4 switching during half frequency. during clamp period S_1 is always turned on and S_2 is always turned off. Then the loss distribution is not equal for top and bottom switches

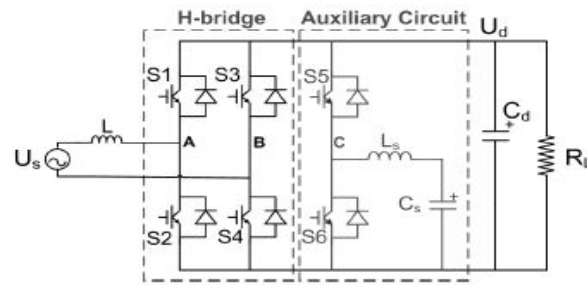


Fig:3 Typical diagram of rectifier circuit

4.2 DESIGN OF PI REGULATOR

In the design of single-phase rectifier control system, the general use is dual-loop control, namely, voltage and current loops. The outer voltage loop controls the voltage in DC side, while the current loop as the inner loop, it forces the input current tracking current instruction (gained from the output of the outer voltage loop), in order to achieve sinusoidal current control unity power factor. The current instruction and grid-side voltage have same frequency and opposite phase.

A. The design of inner current loop

The control performance of input current is the key of rectifier control, because the essence of the rectifier is an energy conversion system between the AC and DC power, the grid voltage is essentially certain, so the rapid and effective control of the input current is important. The block diagram of PI regulator in current loop is shown in Figure

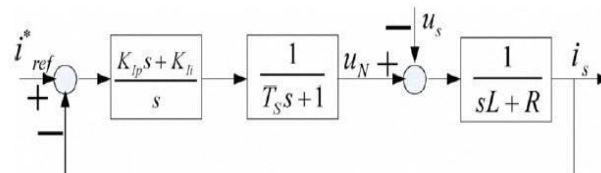


Fig:4. The block diagram of transfer function in current loop

The open loop transfer function is shown as follow

$$G_{op}(s) = \frac{(K_{Ip}s + K_{Ii})}{s(T_s s + 1)(sL + R)}$$

When the switching frequency is high (e.g., 10k Hz), the first-order inertia loop $1/(T_s s + 1)$ is approximately 1, could be ignored, the type can be simplified to

$$G_{op}(s) = \frac{(K_{Ip}s + K_{Ii})}{s(sL + R)}$$

B. The design of outer voltage loop

If the filter capacitor of DC side is large enough, the DC voltage ripple can be ignored. The block diagram of PI regulator in voltage loop is shown in Figure.

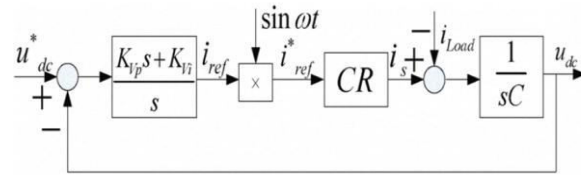


Fig:5 The block diagram of transfer function working in voltage loop

The open-loop transfer function is shown as follow

$$G_{opV}(s) = \frac{K_{vp}s + K_{vi}}{s} \frac{1}{sC} G_{cl}(s) = \frac{K_{vi}}{C} \frac{(K_{vp}s + 1)}{s^2} G_{cl}(s)$$

The open-loop transfer function is shown as follow

In the above function, $G_{cl}(s)$ is equivalent to the current closed-loop transfer function

$$G_{opV}(s) = \frac{K_{vp}s + K_{vi}}{s} \frac{1}{sC} G_{cl}(s) = \frac{K_{vi}}{C} \frac{(K_{vp}s + 1)}{s^2} G_{cl}(s)$$

V. SIMULATION DIAGRAM

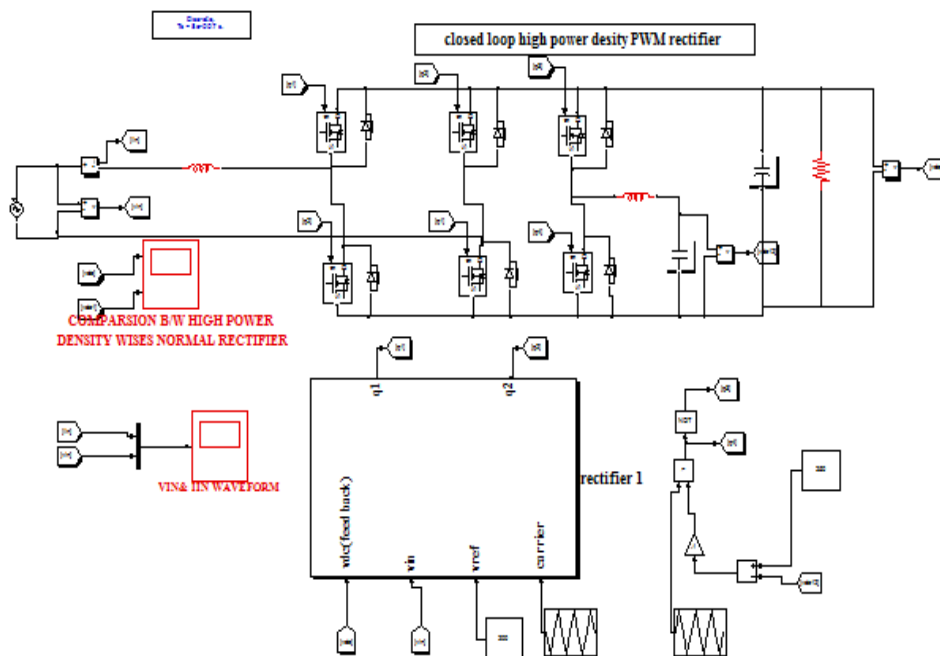


Fig:6 SIMULINK diagram for the proposed system

VI. SIMULATION RESULT

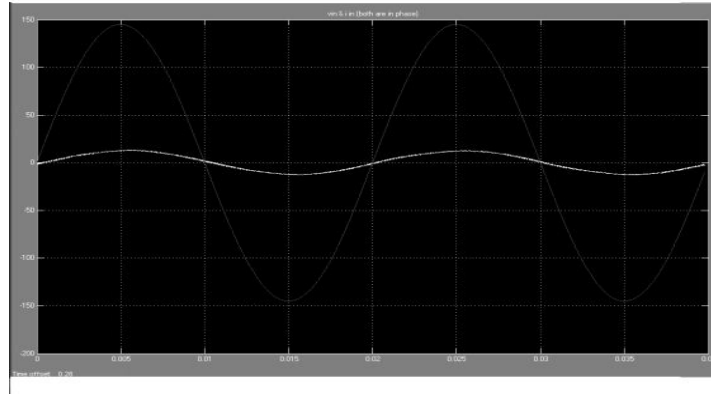


Fig:7 Supply voltage and current are in phase

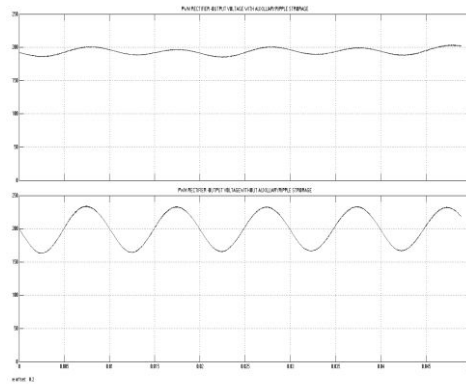


Fig:8 Output voltage without ripple energy

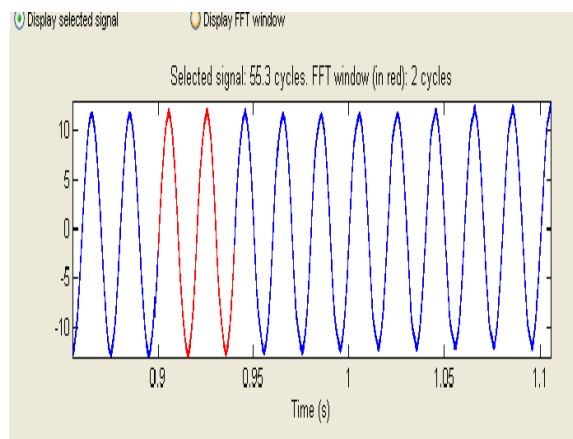


Fig 9 Harmonic analysis

VII. CONCLUSION

In this work, an active ripple energy storage method is proposed to increase the single phase PWM rectifier's power density. Based on analysis, simulation and experiment, the following conclusions are the proposed auxiliary circuits will bring no voltage higher than the dc bus in the system and it can be easily integrated together with the H-bridge rectifier as an additional phase leg. Different from the traditional parallel active power filter, the auxiliary circuit compensation current is in discontinuous current mode so that it can only filter out the low frequency ripple current that dominates in single phase rectifier system. The proposed feed-forward control method can generate the compensation current reference as fast as one switching period and can effectively filter out the low frequency ripple current from the H- bridge rectifier. Although the total capacitance will decrease dramatically compared with traditional method, the total ripple current in capacitors will increase by using the active method. Finally, simulation results were provided for verification purposes.

VIII. REFERENCES

- [1] Cursino Brenda Jacobina, Single-Phase to Three-Phase Drive System Using Two Parallel Single-Phase Rectifiers *Senior Member, IEEE*, Euzeli Cipriano dos Santos Jr., *Member, IEEE*, Nady Rocha and Edgard Luiz Lopes Fabrício VOL. 25, NO. 5, MAY 2010.
- [2] Ricardo Quadros Machado, Simone Buso, A Line-Interactive Single-Phase to Three-Phase Converter System, *Member, IEEE*, and José Antenor Pomilio, *Senior Member, IEEE* VOL. 21, NO. 6, NOVEMBER 2006.
- [3] Dong-Choon Lee, Control of Single- Phase-to-Three-Phase AC/DC/AC PWM Converters for Induction Motor Drives *Member, IEEE*, and Young-Sin Kim VOL. 54, NO. 2, APRIL 2007.
- [4] P. Enjeti and A. Rahman, a new single phase to three phase converter with active input current shaping for low cost ac motor drives Power Electronics Laboratory Department Of Electrical Engineering Texas A&M University College Station.
- [5] Li Taofeng, Ouyang Hui, Kang Yong, Xiong Jian, Fan Shengfang, Zhang Kai, "The Research of Single-phase PWM Rectifier Based on Direct Current Control" IEEE2009.
- [6] M. P. Kazmierkowski and L. Malesani, "Current control techniques for Three- phase voltage-source PWM converters: A survey," *IEEE Trans. Ind. Electron*, vol.45, no. 5, pp. 691–703, Oct. 1998.
- [7] M. Liserre, "Innovative control techniques of power converters for industrial Automation," Ph.D. dissertation, Politecnico di Bari, Bari, Italy, 2001.
- [8] P. N. Enjeti and S. A. Choudhury, "A new control strategy to improve the performance of a PWM ac to dc converter under unbalanced operating Conditions," *IEEE Trans. Power Electron.*, vol. 8, no.4, pp.493–500

Reactive Power Generation Minimization In Power System Using Group Leader Optimization Technique

K.Sriram^{1 A}, Sundarapandiyan²

^{1,2}*Department of Electrical and Electronics Engineering St. Anne's College of Engineering and Technology Panruti, Tamilnadu*

Abstract - Everyday a bulk amount of power is generated, transmitted and distributed via transmission network. The active power or the real power generated from the generator needs the reactive power for supporting its own transmission. This reactive power generation has some minimum limit which if generator fails to produce it has to take support from system operator for smooth real power flow in worth of paying money. While the generator produces excess reactive power it can expect remuneration from the system operator. In this paper IEEE 14-bus test system is considered for solving the problem. As a solving tool a well known population based metaheuristics technique: particle swarm optimisation is chosen which tries to optimize the problem by controlling the generator bus voltage. The choice of the objective function and the mentioned optimisation technique is considered by through literature survey.

Key words-- Balanced voltage profile, minimal of reactive power generation, particle swarm optimisation, real power output.

I. INTRODUCTION

Around the world, the power system structure is undergoing through restructuring process during the last decades. Before deregulation a traditional monopoly structure in the power sector was ruling the market. In the deregulation process the buyers and sellers starts to interact among them regarding power transaction and maintain system security through system operator. That means a competitive market environment develops via several Gencos (Generating Companies), Transco's (Transmission Companies) and Discos (Distribution Companies) along with the system operators.

Under the competitive market each and every essential terms like active power output, balanced voltage profile, reactive power generation etc related to system operation and control are accounted as a commercial product. The shipment of generator active power needs the support of reactive power generated from the same generator. Therefore generated reactive power from any generators is utilized to compensate required reactive power loss developed in the system along with the supporting of real power flow. In connection with deregulatory power environment the target is to minimize reactive power generation required for supporting real power flow. If the reactive power generation remains within the minimum value no penalty charge will be paid. From the viewpoint of profit, the power producers should try to sell as much as active power with minimum generated reactive power keeping the system security uninterrupted. Therefore overall cost minimization of active and reactive power generation depends on minimum reactive power generation.

II. GROUP LEADER OPTIMIZATION

Global optimization is one of the most important computational problems in science and engineering. Because of the complexity of optimization problems and the high dimension of the search space, in most cases, using linear or deterministic methods to solve them may not be a feasible way. Wille and Vennik argued that global optimization of a cluster of identical atoms interacting under two-body central forces, belong to the class of NP-hard problems. This means that as yet no polynomial time algorithm solving this problem is known. Recently,

Adib reexamined the computational complexity of the cluster optimization problem and suggested that the original NP level of complexity does not apply to pair wise potentials of physical interest, such as those that depend on the geometric distance between the particles. A geometric analogue of the original problem is formulated and new sub problems that bear more direct consequences to the numerical study of cluster optimization were suggested. However, the intractability of this sub problem remains unknown, suggesting the need for good heuristics. Many optimization methods have been developed and these can be largely classified into two groups, deterministic and stochastic. Deterministic methods include variations on Newton's method such as discrete Newton, quasi Newton and truncated Newton, tunneling method and renormalization group methods . Stochastic methods include simulated annealing, quantum annealing, J-walking, tabu search, genetic algorithms (GA) and basin-hopping approach. More recent work on probabilistic techniques have been proposed to solve these optimization problems by observing nature and modeling social behaviors and characteristics, including GA, evolutionary algorithms (EA), such as the particle swarm optimization algorithm (PSO), and the Pivot methods. Implementation of many of these algorithms on complex problems requires exhausting computational time and a growing need for more computer resources depending upon: the dimension, the solution space and the type of problem. The key to speed up the optimization process is reducing the number of computations in the algorithms while keeping the amount of iterations low and the success rate of the algorithms high. This paper introduces a new global optimization algorithm which reduces the optimization time, and is both simple and easy to implement. In the following sections, the inspiration and the implementation of the algorithm will be explained and test results will be given for some of the most famous optimization test problems; for the global optimization of the minimum energy structures of complex Lennard-Jones clusters; and for the quantum circuit design of the Grover search algorithm.

i. Algorithm steps

In this section, algorithm steps are described with their reasons in sequence and are shown in Figures 1.

Step 1: Generate p number of population for each group randomly

The total population for each group is p, hence, the whole population is $n * p$ where n is the number of groups. Creation of the groups and the members are totally random.

Step 2: Calculate fitness values for all members in all groups

All solution candidates, group members, are evaluated in the optimization problem and their fitness values are assigned.

Step 3: Determine the leaders for each group:

Each group has one leader and the leaders are ones whose fitness values are the best within their respective groups. The algorithm steps 1–3 are shown in Figure 1.

Step 4: Mutation and recombination:

Create new member by using the old one, its group leader, and a random element. If the new member has better fitness value than the old one, then replace the old one with the new one. Otherwise, keep the old member. For numerical problems, the expression simply reads;

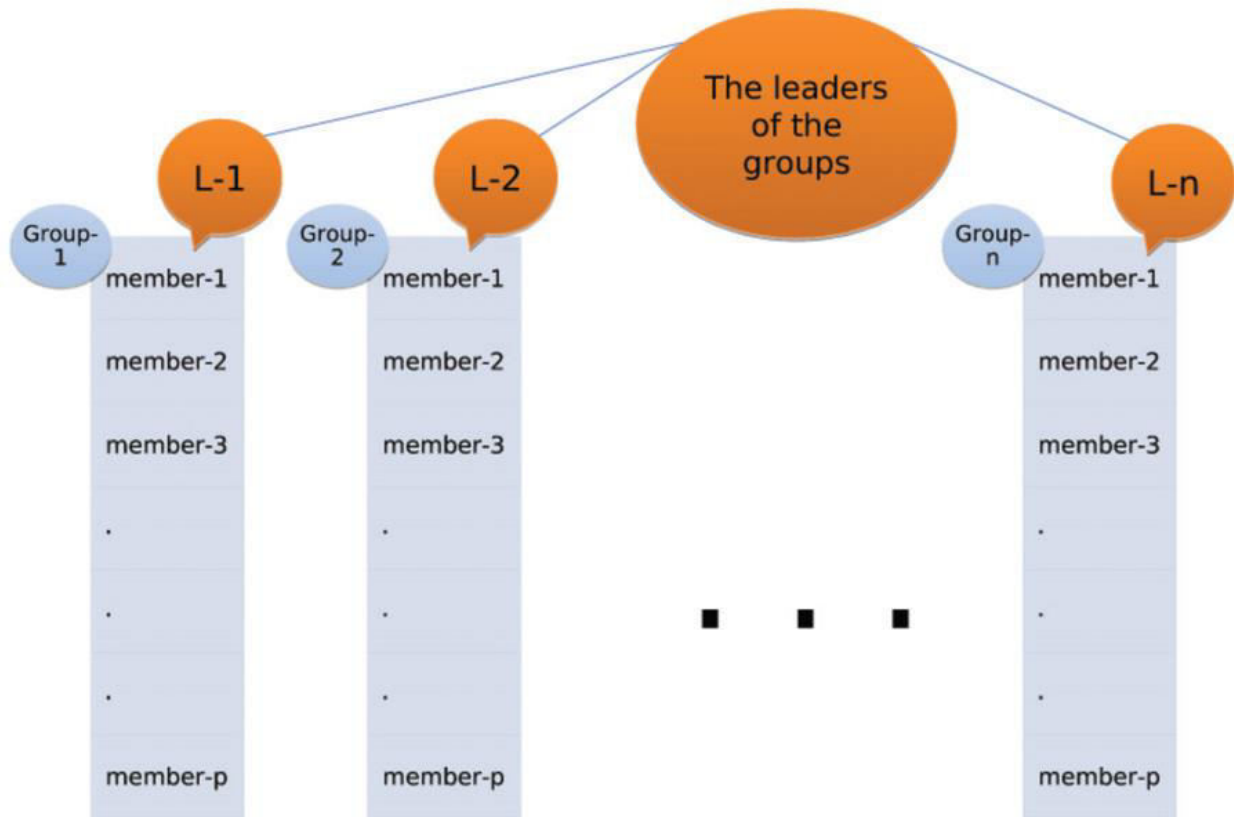


Figure 1. Steps 1–3 of the algorithm; groups consisting of p number of members are created, and their leaders are chosen based on the fitness values.

Step 5: Parameter transfer from other groups (One way crossover)

Choose random members starting from the first group, and then transfer some parameters by choosing another random member from another group. If this transfer makes a member have a better fitness value, then change the member, otherwise keep the original form. This process is shown in Figure 2 via pseudo code.

Step 6: Repeat step 3–step 5 number of given iteration times

if a group has found some parameters correctly or very close to correct, then transferring parameters between groups allows other groups to get these parameters and find their solutions faster. Since only parameters are transferred which make the member have better fitness value, the spreading of a member who has a bad fitness value is avoided.

III. OPTIMIZATION RESULTS

The parameters for the algorithm have effects on the quality of results. As stated in the previous section, choosing r_3 , r_2 less than and r_1 greater than 0.5 makes the algorithm more stable and minimizes the effects of these parameters. The number of groups and the population of the groups should be chosen to be large enough depending on the complexity of the problem. Therefore, while generating new elements, the rate of crossover between groups and the portions of elements, leaders, and random elements should be carefully adjusted for the type and the complexity of the optimization problem. For instance, if one takes crossover rate or the portion of the leaders too high in relation to the chosen group and population number, this may cause the whole population to become uniform very quickly. Hence, the algorithm may get stuck in a local solution, and not search the whole solution space. The algorithm was

tested on different types of optimization problems, one-dimensional and multidimensional optimization test functions, and it was also used to find the minimum energy structures of Lennard-Jones clusters.

IV. RESULTS AND DISCUSSIONS

The proposed algorithm is developed using MATLAB-7.10 software. In this paper GLO algorithm is applied to solve minimal reactive power generation by controlling VG keeping all the equality and inequality constraints under deregulated power system operating range. Optimization process stops whenever preset convergence criteria matches.

Table. 1 Line flow & losses after optimization by using GLO

From Bus	To Bus	P	Q	From Bus	To Bus	P	Q	Line Loss	
		MW	MVar			MW	Mvar	MW	MVar
1	2	-0.064	0.021	2	1	0.064	-0.021	0.000	0.000
1	5	10.609	7.219	5	1	-10.520	-6.852	0.089	0.367
2	3	7.233	-1.659	3	2	-7.207	1.768	0.026	0.109
2	4	19.524	6.911	4	2	-19.275	-6.155	0.249	0.756
2	5	14.000	7.972	5	2	-13.853	-7.521	0.148	0.451
3	4	12.543	8.641	4	3	-12.387	-8.244	0.155	0.397
4	5	-23.37	4.241	5	4	23.449	-3.992	0.079	0.249
4	7	1.722	-2.479	7	4	-1.722	2.499	0.000	0.020
4	9	5.510	2.608	9	4	-5.510	-2.398	0.000	0.210
5	6	-6.676	-8.958	6	5	6.676	9.264	-0.00	0.306
6	11	16.603	4.573	11	6	-16.321	-3.983	0.282	0.590
6	12	9.040	2.489	12	6	-8.932	-2.265	0.108	0.225
6	13	22.587	7.938	13	6	-22.208	-7.192	0.379	0.747
7	8	-22.26	-9.514	8	7	22.263	10.584	0.000	1.070
7	9	23.985	17.391	9	7	-23.985	-16.39	-0.00	1.001
9	10	-3.666	3.985	10	9	3.676	-3.958	0.010	0.027
9	14	3.661	3.538	14	9	-3.625	-3.462	0.036	0.076
10	11	-12.67	-1.842	11	10	12.821	2.183	0.146	0.341
12	13	2.832	0.665	13	12	-2.813	-0.647	0.019	0.018
13	14	11.521	2.039	14	13	-11.275	-1.538	0.246	0.501
Total Loss								1.972	7.461

In this paper, as test case IEEE 14-bus system is considered where four generator buses are there for which minimal reactive power generation is tried to be implemented.

V. CONCLUSION

In this paper the MRPG problem is solved to make smooth real power flow in supporting to generators requirement with the help of GLO technique for IEEE 14-bus system. Initially parameter estimation is processed by tuning the variables and thereafter the result is obtained by increasing the population size. According to the problem criteria, minimization of reactive power generation brings a new corner in the field of deregulated power environment. MRPG problem is a very important aspect for the power generating companies as reward in terms of money is related to this. GLO is a very well known soft-

computing technique which is applied previously to solve similar problem like optimal power flow, reactive power dispatch etc. The application of GLO technique to solve MRPG problem raising a value of 3.5000MVAR from the base value of 5.89MVAR shows credibility.

Due to sake of simplicity some parameters are neglected during the network analysis like voltage index and sensitivity analysis which may be included in future study. Furthermore, MRPG problem is considered as single objective problem which can be improved as multi-objective problem by incorporating cost or real power loss minimization in the future study. On account of novelty of the proposed issue, GLO based MRPG problem solved in this paper shows satisfactory performance.

VI. REFERNCES

1. L. L. Lai. **“Power system restructuring and deregulation”**, Fourteenth reprint, John Wiely and Sons Limited, april, 2002.
2. H. Yang, H. Chao and C. Kun-wei, “Optimal power flow in deregulated electricity markets”.
3. V.L. Paucar and M.J. Rider, “Reactive power pricing in deregulated electrical market using a methodology based on the theory of marginal costs”, IEEE Proc, 2001
4. Saini and A. K. Saxena, “Optimal power flow based congestion management methods for competitive electricity markets”, IJCEE, vol. 2(1), pp. 1793-81633, 2010.
5. H. Wu, C. W. Yu, N. Xu and X. J. Lin, “An OPF based approach for assessing the minimal reactive power support for generators in deregulated power systems”, Electric Power & Energy Systems, vol. 30, pp. 23-30, 2008.
6. H. Sadat. “Power system analysis”, Fourteenth reprint, Tata McGraw-Hill Publishing Company limited, 2008.
7. Saini and A. K. Saxena, “Optimal power flow based congestion management methods for competitive electricity markets”, IJCEE, vol. 2(1), pp. 1793-81633, 2010
8. V.L. Paucar and M.J. Rider, “Reactive power pricing in deregulated Electrical market using a methodology based on the theory of marginal Costs”, IEEE Proc, 2001.
9. Dommel H.W. and Tinney W.F “Optimal power flow solutions“IEEE Transactions on Power Apparatus and Systems, PAS- 87, pp. 1866– 1876, October 1968.
10. Barbosa HJC and Lemonge ACC. “A new adaptive penalty scheme for genetic algorithms” Information Sciences 2003; 156(3–4):215–251.

Battery Energy Storage System for A Stand Alone Windmill - Based On State-Of-Charge (SOC) Balancing Control

A. Sundarapandiyani¹, R. Arulselvi²

1,2Department of Electrical and Electronics Engineering St. Anne's College of Engineering and Technology Panruti, Tamilnadu

Abstract-- Renewable energy sources such as wind turbine generators produce fluctuating electric power. The fluctuating power can be compensated by installing an energy storage system in the vicinity of these sources. This paper proposes the integration of a Battery energy storage system with a typical stand-alone wind energy system during wind speed variation as well as transient performance under variable load. The investigated system consists of a 200 W variable speed wind turbine with permanent magnet DC generator, buck-boost converter, charge controller, loads and battery unit with focus on a control method for state-of-charge (SOC) balancing of the battery units. The State of Charge (SOC) method control is used for controlling the battery units in order to ensure the difference of energy, if the wind turbine can't supply the total energy for the loads. Laboratory system combining a State of Charge (SOC) balancing control with four sealed lead acid battery units is designed, constructed, and tested to verify the validity and effectiveness of the proposed balancing control. Simulation of the system using Matlab/Simulink software was performed in order to validate the SOC balancing control.

Index: Terms--wind energy, SOC, energy storage, stand-alone system.

I. INTRODUCTION

Environmental concern and continuous depletion of fossil fuel reserves have spurred significant interest in renewable energy sources [1]. However, renewable energy sources such as wind turbine generators are intermittent in nature, and produce fluctuating active power. Interconnecting these intermittent sources to the utility load at a large scale may affect the voltage/frequency control of the load, and may lead to severe power quality issues [2]. An energy storage system is indispensable for compensation of the active-power fluctuation, which is often referred to as "power levelling." If a wind turbine generator produces a larger power than an average power over a period of time, say several seconds to 30 min, the energy storage system stores the excess power available to the load. On the other hand, if the generator produces a smaller power, it releases the shortage of power back to the load. The energy storage system brings a significant enhancement in power quality, stability, and reliability to the load [3].

There is a growing interest in using storage devices for power smoothing and power quality in stand-alone wind energy systems. The small wind turbines in conjunction with battery storage, is best suit for the electrical energy produced for stand-alone applications. For wind applications, the following characteristics are desirable in a storage system: long term storage, operation over a wide range of power outputs, high efficiency, low maintenance, long life and fast response to rapid changes.

Wind energy systems have a fluctuating power output due to the variability of the wind speed with power output varying by the cube of the speed. Integrating an appropriate energy storage system in conjunction with a wind generator removes the fluctuations and can maximize the reliability of power to the loads. It is therefore necessary to have methods capable of accurately estimating battery SOC to avoid overcharge for battery protection. In [4], [5], [6]

are presented different methods for estimating SOC such as, electrolyte specific gravity, stabilized float current, coulomb metric measurement, open circuit battery voltage, and loaded battery voltage. The battery SOC balanced control is achieved by permanent update from one time step to the next, with a discrete integrator.

The paper is organized as follows: in Section II the system configuration Section III presents the SOC control method; Section IV describes the developed model and simulation results while experiments are in section V and conclusions are provided in Section VI.

II. SYSTEM CONFIGURATION

A. Stand-alone wind energy conversion system

The proposed wind stand-alone system for a residential location is a 200W wind turbine system with a permanent magnet DC generator, buck-boost converter, charge controller, sealed lead acid battery storage device, inverter, load splitter and loads. It supplies 24 V DC load and single-phase consumers, at 230V and 50Hz.

A block representation of the stand-alone wind energy system with battery energy storage is provided in Fig. 1.

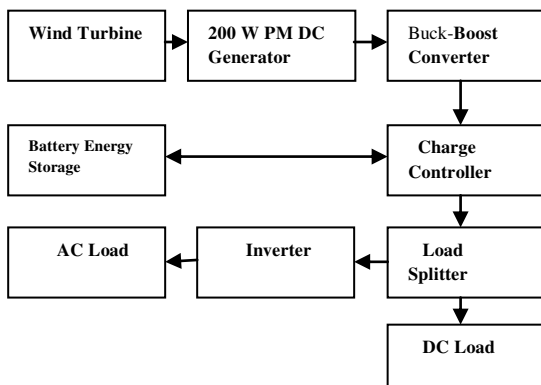


Fig. 1. Stand-alone wind energy system with battery energy storage

The wind turbine (Parameters are listed in Table I and Table II) generates a variable dc. While the input voltage to the buck-boost converter varies with the wind speed, the output voltage is kept constant to the battery storage by the charge controller. The Battery Bank is connected to a load splitter through the charge controller, connected to a dc-ac inverter and DC load. The Battery energy storage is able to supplement the power provided to the load by the wind turbine when the wind speed is below a threshold value. Current flow into and out of the Battery energy storage system is controlled by the bidirectional charge controller [7].

**TABLE I
WIND MILL PARAMETERS**

Generator type	PM DC
Voltage (V)	110 V DC
Watts @ Rated wind speed	200 watts
Type of hub	Fixed pitch
Rotor diameter	1.85 m
Swept area	2.4m ²
Number of blades	3
Rotor speed @	500 RPM

rated wind speed	
Rotor tip speed	45 m/s
Tower height	4 m

TABLE II
WIND MILL PERFORMANCE PARAMETERS

Rated electrical power	200 w @8m/s
Rated wind speed	8 m/s
Cut - in	3.5 m/s
Shut - down (high wind)	23 m/s
Peak (survival)	60 m/s
Calculated annual output	1100 kwh @ 4.5 m/s Annual Average

B. Energy Storage Systems

Energy storage systems based on different storage devices have been investigated [8]. Recently, batteries have emerged as promising storage devices for power system applications. Batteries have the highest energy density. Batteries have the potential of being used for power levelling of renewable energy sources.

A typical Sealed Lead-Acid battery bank (Parameters listed in Table III) consists of four cells in series, this combination gives both the voltage and power necessary for load. While common, these configurations are not as efficient as they could be, because any capacity mismatch between series-connected batteries reduces the overall battery bank capacity. Battery balancing techniques increase the capacity, and system operating time.

TABLE II
BATTERY BANK PARAMETERS

Type	Sealed Lead-Acid
Voltage (V)	12 DC
Capacity	26 AH
Standby use	13.6 V – 13.8 V
Cycle use	14.1 V – 14.4 V
Max initial current	5.2 A
Temperature	27° C
No. of Battery	4 Nos.

Loss of bank capacity in a series connected pack results from two main factors. First, battery must maintain a voltage within strict limits. If the voltage on any battery goes too high, charging must stop. If the voltage on any battery goes too low, discharge must stop. Second, series-connected batteries in a battery bank usually have capacity mismatches.

Lead-Acid battery experience two primary kinds of mismatch. State-of-charge (SoC) mismatch occurs when initially-equal-capacity batteries gradually diverge to contain different amounts of charge. Capacity/energy (C/E) mismatch occurs when cells with different initial capacities are used together. Because batteries are typically matched fairly well in the assembly, SoC mismatch is the more common.

The combination of cell voltage limits and SoC mismatch ties the battery bank capacity (Ah) to the capacity of the weakest battery. In a battery pack where the batteries all have roughly the same capacity, the open-circuit voltage (OCV) of the bank is a good measure of the SoC. So, charging an unbalanced battery bank results in one or more battery reaching the maximum charge level before the rest of the cells in the series string. During discharge the batteries that are not fully charged will be depleted before the other cells in the string, causing an early under-voltage shutdown of the bank. These early charge and discharge limits reduce the usable charge in the battery.

Manufactured battery capacities are usually matched within 3% self-discharge, or if cells with differing self-discharge characteristics are allowed to remain on the shelf for long periods prior to pack manufacture, battery voltage differences of 150 mV at full charge are possible. These differences could result in an initial 13 - 18% reduction in battery capacity. Even if they are matched by capacity in the assembly, the varying battery-to-battery self discharge rates could reduce the capacity of a battery bank over time, simply by sitting on the shelf.

A battery management system (BMS) plays an important part in estimating the SOC, which is often called the “fuel gauge” function. The SOC estimation may be based on measuring some convenient parameters such as voltage, current, and internal impedance, which vary with the SOC [9]. For stable operation of the battery bank, state-of-charge (SOC)-balancing control would be indispensable.

This paper focuses on SOC-balancing control for a battery energy storage system based on a cascade PWM converter. The experimental system includes no voltage-balancing control because it uses four lead acid battery units that have an almost flat charge/discharge voltage profile. Voltage-balancing control may, however, be required to a practical battery energy storage system for the purpose of mitigating the undesired harmonic currents injected into the load [10]. The SOC-balancing control presented in this paper.

III. STATE OF CHARGE (SOC) CONTROL METHOD

The system state of charge can be defined as (1):

$$SOC = \frac{\text{Current Energy in Battery}}{\text{Total Energy Capacity}} \quad (1)$$

If the battery is fully charged, $SOC = 1$ and if the battery is discharged at the maximum value, $SOC = SOC_{min}$. For instance the maximum recommended discharge for battery is 80%, thus $SOC_{min}=0.2$.

The control method used to keep track of the state of charge is to update the SOC variable from one time step to the next, based on the power that goes through the battery bank. The change in SOC is implemented as follows:

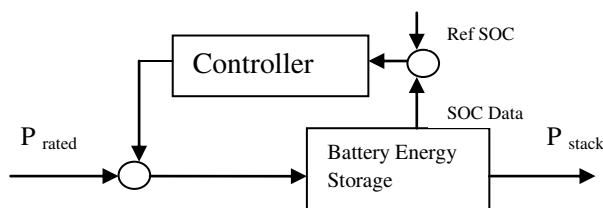


Fig. 2. Control method for battery energy storage

$$SOC_{t+1} = SOC_t + \Delta SOC \quad (2)$$

In this method, the data of the Energy Storage SoC is fed back to the battery bank itself via micro controller. This is a conventional method to control SoC. The Energy Storage system

has the fastest response in the Standalone wind mill, this bias caused by the SoC control would not be compensated. This would result in deterioration of the tie line's power quality.

$$\Delta\text{SOC} = \frac{\Delta E}{E_{\text{capacity}}} = \frac{P_{\text{stack}} * \text{TimeStep}}{E_{\text{capacity}}} \quad (3)$$

$$\Delta\text{SOC} = \frac{I_{\text{stack}} * V_{\text{stack}} * \text{TimeStep}}{P_{\text{rating}} * \text{TimeRating}} \quad (4)$$

This control algorithm uses two variable parameters (I_{stack} , V_{stack}). With a discrete time-integrator block by accumulation the SOC is thus computed each cycle based on the previous SOC, depending on the input values. The simplified control methods block is shown in Fig. 3.

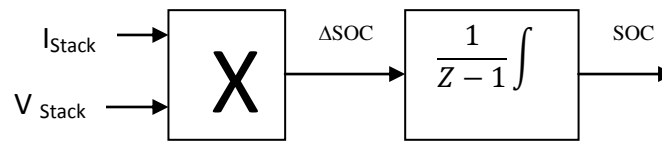


Fig. 3. Control method for battery energy storage

The calculations Battery parameters are based on estimating losses of 21% (15 % internal losses + 6% parasitic losses) in the worse case operating point, for a maximum voltage of 12V, and a current of 26 A, therefore the value of the power rating is greater than 300W. The discharging process of a charged battery (SOC = 80%) at a constant output power of 300W.

IV. SIMULATION

Using the control system proposed in section III, a control simulation by use of the model Standalone wind mill has been carried out (Fig 4). Load data acquired from previous experiments was used in the simulation.

A. Conditions of the Simulation

In the simulation, the controller is represented by first-order delay elements whose delays are decided by the output response characteristics. Samplers in the system hold signals averaged over a second for a second. The control system sends its signals every second and the autonomous control system for the battery bank sends its signals every millisecond. The reference value of the tie line power flow was set at 200W and nominal value of the battery bank DC voltage was set at 24V.

The simulation was done in two following cases.

1. without any SoC control
2. with SoC control

B. Results

The results of the simulation are shown in Fig.4. In the simulation, The value of K has been set at K=0.1875. The parameters of the PI controller in autonomous SoC control have been set at KP=0, KI=0.003 respectively.

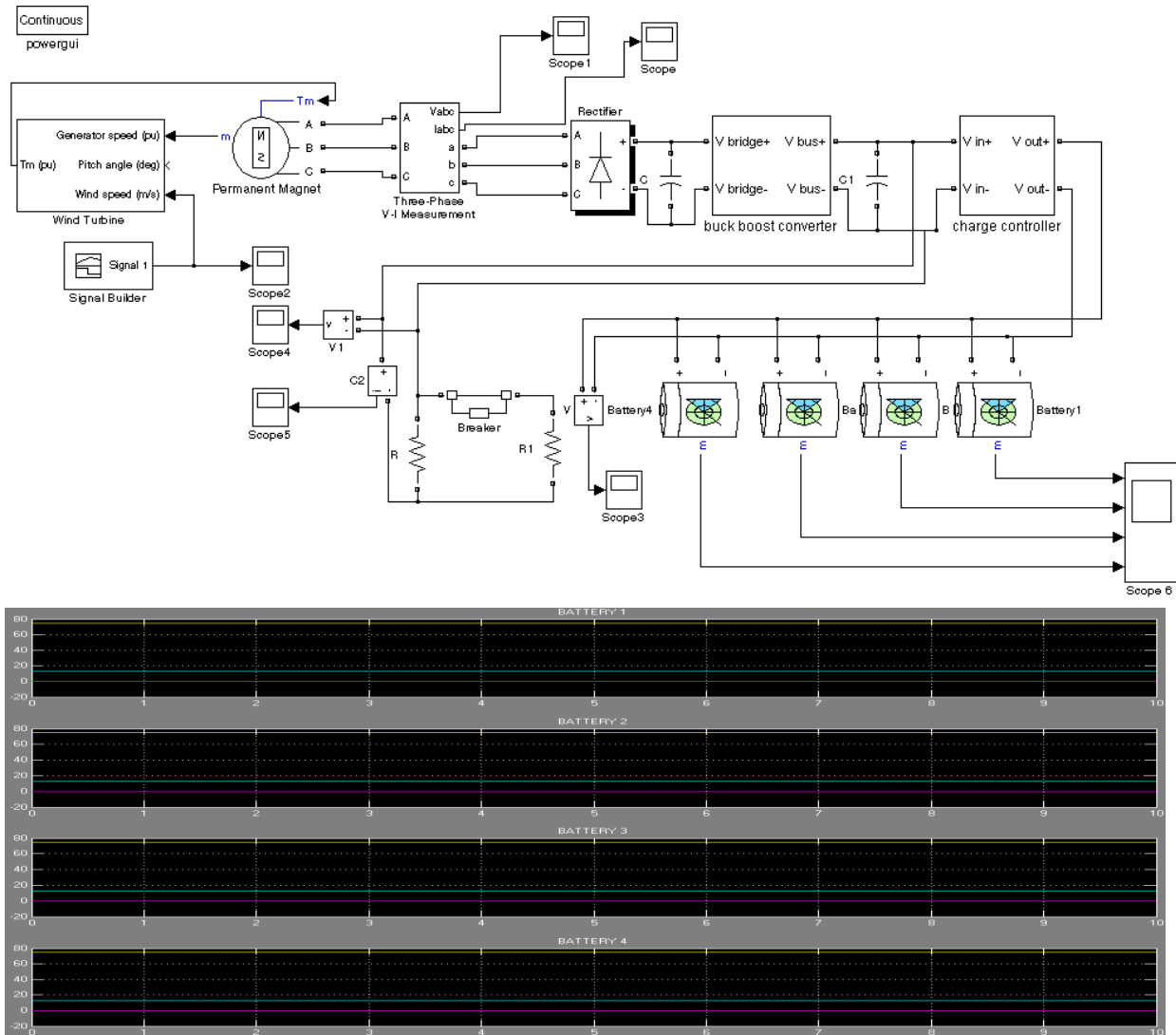


Fig. 4. SIMULINK model and output for standalone windmill with battery energy storage

V. EXPERIMENT

Since the effectiveness of proposed SoC balancing control system has been confirmed by the simulation, a verification test using real machines has been carried out using the Standalone wind mill.

A. Experiment Conditions

The control system of the Standalone wind mill is same as the system used in the simulation (Shown in Fig.2). The experiment has been carried out for the following two cases.

1. Without SoC control
2. With SoC balancing control

In case, the DC voltage constantly decreased for the first 100 seconds of the experiment. Since the parameter of the PI controller in autonomous SoC balance control is set at a very low level, this period is the time when autonomous SoC control is relatively ineffective. It can be assumed that the DC voltage would continue to drop in the case autonomous control was cancelled completely. In the actual measurement, the DC voltage swings in the range of 0-110V DC.

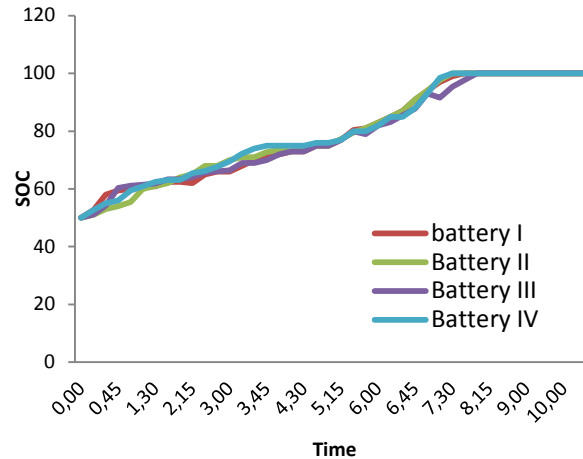


Fig. 7. Experimental output for standalone windmill with battery energy storage with SOC balanced.

The effect of SoC balance control to the power quality can be increased by setting its parameter at lower level, but this will cause larger swing in DC voltage (fig 7) and require larger energy capacity.

VI. CONCLUSION

In this paper, a SoC balancing control system has been proposed and its effectiveness has been verified by simulation and experiment using real machine (standalone 200W Windmill). The proposed SoC balancing control system enables to control battery bank's SoC with little effect to the power quality of the tie line with less energy capacity.

REFERENCES

- [1] S. R. Bull, "Renewable energy today and tomorrow," *Proc. IEEE*, vol. 89, no. 8, pp. 1216–1226, Aug. 2001.
- [2] R. D. Richardson and G. M. McNerney, "Wind energy systems," *Proc. IEEE*, vol. 81, no. 3, pp. 378–389, Mar. 1993.
- [3] P. F. Ribeiro, B. K. Johnson, M. L. Crow, A. Arsoy, and Y. Liu, "Energy storage systems for advanced power applications," *Proc. IEEE*, vol. 89, no. 12, pp. 1744–1756, Dec. 2001.
- [4] Shuo Pang, Jay Farrell, Jie Du, and Matthew Barth: *Battery State-of-Charge Estimation*, Proceedings of the American Control Conference Arlington, VA June 25-27, 2001, pp. 1644 – 1649.
- [5] Martin Coleman, Chi Kwan Lee, Chunbo Zhu, and William Gerard Hurley: *State-of-Charge Determination From EMF Voltage Estimation: Using Impedance, Terminal Voltage, and Current for Lead-Acid and Lithium-Ion Batteries*, IEEE Transactions on Industrial Electronics, Vol. 54, no. 5, October 2007, pp. 2550 – 2557.
- [6] Katsuhisa Yoshimoto; Toshiya Nanahara; Gentaro Koshimizu; Yoshihsa Uchida: *New Control Method for Regulating State-of-Charge of a Battery in Hybrid Wind Power/Battery Energy Storage System*, PSCE 2006, IEEE, pp. 1244 – 1251.
- [7] Barote L.; Weissbach R.; Teodorescu R.; Marinescu C.; Cirstea M.: *Stand-Alone Wind System with Vanadium Redox Battery Energy Storage*, IEEE, International Conference on Optimization of Electrical and Electronic Equipments, OPTIM'08, 22-24 May, Brasov, Romania, 2008, ISBN: 978-973-131-030-5, pp. 407-412.
- [8] P. F. Ribeiro, B. K. Johnson, M. L. Crow, A. Arsoy, and Y. Liu, "Energy storage systems for advanced power applications," *Proc. IEEE*, vol. 89, no. 12, pp. 1744–1756, Dec. 2001.
- [9] S. Piller, M. Perrin, and A. Jossen, "Methods for state-of-charge determination and their applications," *J. Power Sources*, vol. 96, no. 1, pp. 113–120, Jun. 2001.
- [10] Q. Song, W. Liu, Z. Yuan, W. Wei, and Y. Chen, "DC voltage balancing technique using multi-pulse optimal PWM for cascade H-bridge inverters based STATCOM," in *Proc. IEEE PESC*, 2004, vol. 6, pp. 4768–4772.

Review on Gate Bias Control Method for RF Power Amplifiers Using ARM Processor

J. Ramesh¹, J. Balaji²

¹*Department of Electrical and Electronics Engineering St. Anne's College of Engineering and Technology Panruti, Tamilnadu*

²*Department of Electrical and Electronics Engineering Annai Velankanni polytechnic college, Panruti, Tamilnadu*

ABSTRACT: The present paper is a review of the past work done in the field of analysis on various control techniques used in wireless communication to control power amplifier's important parameters. In wireless applications, the power amplifier (PA) dominates signal-chain performance in terms of power dissipation, linearity, efficiency and cost. Hence on the basis of performance concern of a base station's power amplifier makes it possible to maximize the output power while achieving optimum linearity and efficiency. This paper discusses the elements of a monitoring-and- controlling solution for the Power amplifiers and for various systems. Failures were observed with the traditional ways of gate voltage control techniques and the failures are because of changes of load with respect to current and temperature being taken in to account and the voltage surges at the load line. With traditional gate control method power dissipation is high. The effects of temperature making the trade-offs between the above mentioned Power amplifier parameters which determine the optimum bias condition for the Power amplifier transistor. The drain current should be maintained at an optimum value over temperature and time that can significantly improve the overall performance of the PA gate bias control system. The use of ARM microcontroller makes the system more efficient, cost effective way and a more efficient control system with the use of real time operations using real time operating system uC/OSII.

KEYWORDS: PA power amplifier, gate voltage, ARM 7, uC/OS-II.

I.INTRODUCTION

In wireless systems, the power amplifiers (PA) are the important elements which are responsible for more than half of their total power consumption. Hence to lower the power consumption and dissipation a control system need to be designed so as to compensate for the losses and for maintaining the device as well. To improve efficiency Power amplifier's monitoring and controlling in necessary and the system operating cost is reduced and can increase output power and reaches to the highest possible linearity to obtain less distortion and allow the operator to discover and solve problems, thus helps in improving operating reliability and life of power amplifier.[1]

For this the performance parameters of RF PA need to be studied. In order to ensure the performance of RF power amplifier it is important to maintain a constant static operating point to keep its work status stable . A base station's power efficiency is a key environmental consideration for base stations and its optimization dependency. Necessary efforts are being made to improve the overall energy consumption of base stations to

reduce their effect on the environment. Operating system costs in a PA is responsible for more than half of the power dissipation. Thus, PA's power efficiency can improve the operational performance, and provide environmental and financial benefits. In this paper, a new reference design with respect to changes of temperature and drain current through the real time operating system uC/OS-II system to the main-controller ARM7 to real-time compensate for the differences of the linear MOS Power amplifier at different points of temperature.

II. LITERATURE SURVEY

RF POWER AMPLIFIERS FACTORS

To provide a stable gate voltage for power amplifier is of great importance amplifier, since the gate voltage will affect the quiescent current of MOS. However, the quiescent current of device is very susceptible to the influence of temperature, leading to its quiescent point drift which would influence the best matching load, IP3 (Third-order Intercept Point), efficiency and other parameters of power amplifier. In order to ensure the performance of RF power amplifier it is important to maintain a constant static operating point to keep its work status stable. The effect of the temperature on the different DC parameters, g_m , I_{dss} , $r_{ds(on)}$ and capacitances, and the correlation with the figures of merit of a PA (power capability, efficiency and linearity). [2]

RF power amplifiers (PAs) require more powerful Transistors. Therefore, thermal management then becomes a real challenge. Here are the following characteristics for RF MOS PA which are taken into considerations while changing of parameters.

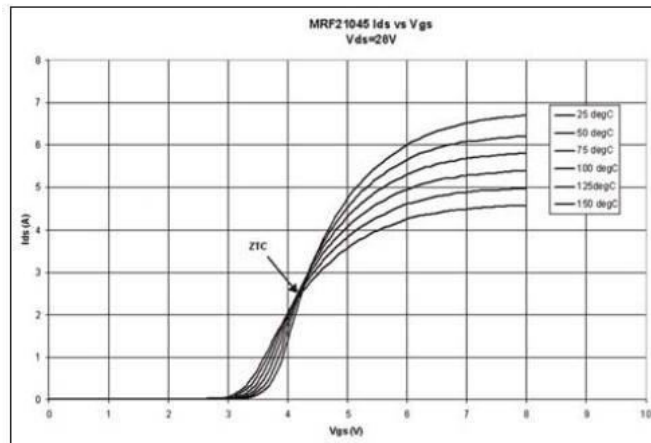


Fig. 1 I_{ds} versus V_{gs} for different die temperature

Characteristics curve shows the effects of temperature on the gate voltage.

The above characteristics shows the temperature variations and its effects on transconductance.

Another efficient method is laterally diffused metal-oxide semiconductor (LDMOS) transistors. Nowadays these are the effective components for the RF power amplifiers in industries. PAs are more likely to suffer from high temperature stress due to large power dissipation of the circuit. A temperature-accelerated channel hot electron effects on class-AB PA performances. Again a model parameters obtained from stress measurement are used in Cadence RF simulations to examine class-AB PA performances such as output power P_{out} , power-added efficiency η_{add} , third-order intercept point (IP3), and adjacent channel power ratio (ACPR) after electrical and temperature stresses.[3] And there are various technologies used for the power control which can b obtained by various diffusions materials to be used for the construction which ultimately leads to the changes in the composition and the various effects like improvement in transconductance, the break down voltage, reduction in on-resistance and in switching delays as well.[4] The effect of the temperature on the different DC parameters, gm, Idss, rds(on) and capacitances, and the correlation with the figures of merit of a PA (power capability, efficiency and linearity).The drain-to-source current of the LDMOS transistor, I_{DS} , is a function of the gate-to-source voltage, V_{gs} , has two temperature-dependent terms:

- The effective electron mobility, μ .
- The threshold voltage, V_{th} .

Drain to source current is by the expression:[5]

$$I_{DS} = \frac{\mu(T)CoxW}{2L} (V_{gs} - V_{th}(T))^2$$

..... 1

V_{th} and μ decrease with increasing temperature. Hence due to the changes in these terms will cause variations in output power. The main factors impacting the drain current bias point are due to variations of the high-voltage supply line and the die temperature. [6]

A better approach is dynamic control of the PA gate voltage which makes use of a control algorithm to be applicable digitally tin order to measure the drain current then digitizing it with an analog to digital convertor, and setting the required bias via a high-resolution digital to analog convertor or a lower-resolution digital pot. Here the system allows the PA to maintain the required bias condition for optimized performance set by a user-programmable set point despite of the changes in parameters.

III. TRADITIONAL GATE VOLTAGE CONTROL TECHNIQUES

In practical applications, LDMOS power amplifiers operate in Class A or AB, with the positive temperature characteristics near quiescent point. This bias scheme creates a linearization due to the cancellation of intermodular distortion generated by the carrier and peaking amplifiers.[7] That is, under a certain gate voltage, when working temperature rises, the static current I_{dq} increases, when work temperature decreases, I_{dq} reduces. This determines the need for automatic control of gate voltage for LDMOS amplifier to ensure high efficiency and linear work of RF power amplifier. Earlier at the biasing terminal the load pull transistors were also used which acquires the large space as well as the large power dissipation and the maintainability required for the individual transistors, external transformer for the supply also increases its cost and power consumption is more.[8]

There are traditionally two kinds of gate voltage control technology in practical applications:

- The first one is to use temperature compensated components, such as diodes, transistors, voltage regulator ICs, thermistors in the bias circuit, to achieve the gate voltage compensation based on the temperature properties.
- The other one is the utilizing of SCM and EEPROM storage of table for gate voltage value compensation related with temperature. Finding the suitable quiescent point through experiment and determining a gate voltage value accordingly at first. When the outside temperature changes, in accordance with the temperature coefficient of gate voltage for RF MOS approximately 3mV/degree relationship, or a look-up table is utilized to get gate voltage compensation through the corresponding relations between environment temperature and gate voltage values.

IV. EMBEDDED GATE BIAS CONTROL SYSTEM DESIGN

ARM7 (Advanced RISC Machines) processor is a kind of 32 bit microprocessor having small volume, light weight, low cost and high speed and dependability are its merits compared with industrial control computer and higher speed, multi-functions, low power consumption and well extensibility are its strengths compared with 16 bit single chip. The ARM 7 based CPU LPC2119 was used in the power system, which supports the real-time simulation and embedded-track, and includes many periphery components, such as zero waited 256K in-chip Flash ,16K SRAM(no need extensible memory), UART, hardware I2C,SPI bus, PWM, timer, ADC, CAN field bus controller, all which make it powerful.[9]

There can be three options for implementing a PA control:

- A discrete solution
- An integrated solution.
- Integrated solution based on ARM7 microcontroller

The discrete implementation requires many parts such as a complicated PCB layout and a more circuit design area, all of which lead to higher cost. The integrated solution design has a higher level of compactness, lower cost, and higher reliability, but it needs another device outside the integrated chip a microcontroller (MCU) to control the functions.

Fig3. Shows a complete structure with the help of discrete components can be mounted on a single chip. But here again an external controlling unit is needed. And with the use of these discrete components the task becomes more tedious, since the interfacing and matching should be among each and every device shown in the connection properly and hence the reliability cannot be maintained and if one of the component is damaged the whole system would come to an adverse effect of shutdown. Hence a system should be made with the ARM processor which has inbuilt ADCs and DACs in chip and flash memory also for the storage of tables and it shares many of the benefits of integrated design, but it includes the MCU.

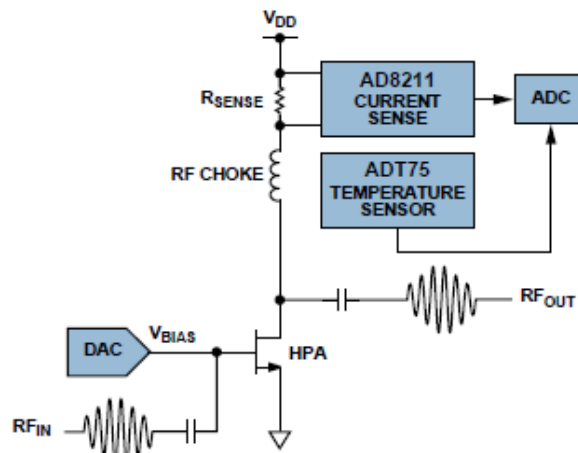


Fig.3 Simplified control system

The temperature and high-voltage supply affects the drain current and this high supply voltage also matters the drain voltage. The RF MOS drain current can be measured with a high voltage current amplifier. If the current at the gate terminal is monitored in a continuous fashion, an operator can make adjustments in voltage at the gate point when a voltage surge occurs on the high-voltage supply to keep the RF MOS working at the best operating point.

A better approach is dynamic control of the PA gate voltage using a digital control algorithm to measure the drain current, digitizing it with the help of ADC, and setting the required bias via a DAC or a lower-resolution digital variable switch. An control system that allows the PA to maintain the required bias condition for optimized performance which can be set by user though the changes in voltage, temperature, and other environmental parameters.[10]

The control and management of the V_{gs} based on ARM7 is designed by the support of uC/OS-II having better quality of high real-time and adopts real-time multitask kernel

which is based on fixed-priority scheduling mode, it could be easily solidified and clipped, getting the high stability and reliability. In addition, the source code of uC/OSII could be shared to make it convenient to transplant and maintain. A lot of system services such as real time tasks are performed as, queues, semaphores, fixed-sized memory partitions, time related functions and etc are offered.[11]

V. CONCLUSION

In this paper different ways of gate voltage control system design and various affecting measures such as temperature and current are found to be the sensitive parameters which are responsible for the hampering effect for an RF PA so among the available method the LUT design using flash memory in ARM processor a feasible one. Still there is an essential need for an efficient monitor and a control system which can be useful for wide range of RF amplification in terms of power, current and with due effects of temperature on this technique with other multiuser software so that accuracy of result could be maintained for better performances. In order to accurately analyse and optimize the, control system there is a need to experiment with temperature and current factors responsible for efficient performance and the maintainability of the device and controlling this with the ARM7. Hence, from a variety of aspects, such as references, features, hardware and software designs and technologies is being discussed a new reference design can be made using an ARM processor which can be operated at real time measurement using uC/OSII real time operating system and correction of the parameters responsible for affecting the gate bias automatically.

REFERENCES

- [1] Liang Li, Taijun Liu, Yan Ye, Ying Zhang, Jun Li., "Embedded ARM-Based Automatic Gate Bias Control System for LDMOS RF Power Amplifiers", IEEE 2011.
- [2] Olivier Lembeye and Jean-Christophe Nanan. "The Effects of Temperature on High-Power RF LDMOS Transistor". Motorola SPS. Technical feature, August 2002.
- [3] Chuanzhao Yu, J. S. Yuan, "Electrical and temperature stress effects of Class-AB Power Amplifier Performances", IEEE transactions on electron devices, vol. 54, no. 6, June 2007
- [4] Radhakrishnan Sithanandam et.al. "A new HSG SOI LDMOS for RF power Amplifier applications". VLSI design conference. 2010 [5] WANG et al. IEEE journal of solid-state circuits, vol. 29, July 1994. "MOSFET thermal noise modeling for analog integrated circuits"
- [6] Liam Riordan, "Analogue dialogue. 2008. Discrete- and Integrated Control of Power Amplifiers", April 2008
- [7] Jeonghyeon Cha et.al. "Bias, Controlled Power Amplifier with a Load-Modulated Scheme for High Efficiency and Linearity", IEEE. 2003
- [8] Cheng-Yung Chiang and Huey-Ru Chuang, "Effective Load-Pull System for transistor Large-Signal Measurements for wireless systems", IEEE transactions on instrumentation and measurement, vol 46, October 1997.
- [9] Hao Jianmin, Guo Kai, Cheng Hong, Ren Na. 2007, "Design of Microoxidation power control system based on LPC2119", Conference Electronic Measurement and Instruments, 2007

Bat Algorithm for Economic Dispatch problem with Prohibited zones, Ramp rate limits & Multi-fuel options

Dr.A.Subramanian¹, Dr.R.K.Santhi², S.Vijayaraj³

¹EEE Department , IFET Engineering College,annamalaiasmani@gmail.com

²EEE Department , Annamalai university, rkscdm@gmail.com

³EEE Department, Annamalai university, veejay_raj@yahoo.co.in

Abstract:-This paper presents application of Bat algorithm for solving Economic Load Dispatch problem considering Transmission loss, multiple fuel options, Valve point loading effect and Prohibited operating zones. Bat algorithm is an optimization algorithm motivated by the echo location behavior of natural bats in finding their prey. Potency of the algorithm is tested on two different test cases consist of varying degree of complexity .The promising results show the quick convergence and effectiveness of the Bat algorithm and the improvement in the performance parameters of the system.

Keywords:-Economic Load Dispatch, Prohibited operating zones, Valve point loading effect, Bat algorithm, Transmission loss, Multi-fuel.

I.INTRODUCTION

Nowadays, planning and operation of power system is a challenging task for power engineers because of its complexity and to satisfy the demand for electric energy of the area served by the system continuously with reliability. An elite objective here is to perform the service at the lowest possible cost. The role of soft computing techniques has influenced a lot in the field of power system especially in solving optimization problems because of their reliability, speed of convergence and robustness [1]. The Economic Load Dispatch (ELD) problem, one of the different non-linear programming commitments in power system, is about minimizing the fuel cost of generating units for a specific period of operation so as to accomplish optimal generation dispatch among operating units and to satisfy the system load demand and generator operation constraints with ramp rate limits and prohibited operating zones [2]. S.K.Dash [3] was presented a new method to solve the problem of optimal generation and dispatch with multiple fuel options using a Radial basis function neural network along with a heuristic rule based search algorithm and a Hopfield neural network. Dr .G. Srinivasan, et al. [4] solved economic load dispatch problem with Valve point effects and multi Fuels using particle swarm algorithm with chaotic sequences and the crossover operation to improve the global searching capability by preventing premature convergence through increased diversity of the population. Radhakrishnan Anandhakumar, et al. [5] was proposed a non-iterative direct composite cost Function method, to solve economic dispatch of the online units with less computation time. Umamaheswari Krishnasamy,et al. [6] presented a Refined Teaching-Learning Based Optimization Algorithm for Dynamic Economic Dispatch of Integrated Multiple Fuel integrated with Wind Power Plants.R.Balamurugan, et al. [7] proposed a self-adaptive mechanism is used to change these control parameters during the evolution process. These control parameters are applied at the individual levels in the population to solve economic dispatch with valve point and multi fuel options. Xin-She Yang. [8] proposed the Bat algorithm and its characteristic with implementation of various functions for global optimization.

In this paper, Economic load Dispatch problem with two different cases with inclusion of operating zones, transmission loss, valve point effect and multiple fuel sources has been solved by using the flower pollination algorithm. The Bat algorithm approach has been verified by applying it to two different test systems. The performance of the proposed Bat algorithm is analysed with different values of its parameters. Because this parameter plays a major role in controlling the searching process of algorithm.

II. FORMULATION OF ECONOMIC LOAD DISPATCH PROBLEM

2.1. Total Cost Function:-

The main objective of Economic Load Dispatch in electrical power system is to reduce the overall production cost of supplying loads while satisfying constraints. The total cost function can be formulated as the following equation.

$$F_t = \sum_{i=1}^N F_i(P_i) = \sum_{i=1}^N a_i + b_i P_i + c_i P_i^2 \quad (1)$$

where $F_i(P_i)$ is the cost function of i_{th} generator and is usually expressed as a quadratic polynomial; a_i , b_i and c_i are the fuel cost coefficients of i_{th} generator; N is the number of generators, P_i is the real power output of i_{th} generator. The Economic Load Dispatch problem minimizes F_t subject to the following constraints and effects.

2.2. Equality constraints:-

The power balance equation is given by

$$\sum_{i=1}^N P_i = P_D + P_L \quad (2)$$

The transmission loss P_L of system may be expressed by using B-coefficients.

$$P_{Li} = \sum_{i=1}^N \sum_{j=1}^N P_i B_{ij} P_j + \sum_{j=1}^{M_i} B_{0i} P_i + B_{00} \quad (3)$$

where, P_D is the power demand of the system. B_{ij} , B_{0i} , and B_{00} are transmission loss coefficients.

2.3. Inequality constraints:

The upper and the lower operating region of the generator is given by the equation

$$P_i^{\min} \leq P_i \leq P_i^{\max} \quad i \in N \quad (4)$$

Where P_i^{\min} and P_i^{\max} are the minimum and maximum power outputs of generator i , respectively. The maximum output power of generator is limited by thermal consideration and minimum power generation is limited by the flame instability of a boiler.

2.4. prohibited operating

The prohibited operating zones are the range of power output of a generator where the operation causes undue vibration

of the turbine shaft bearing caused by opening or closing of the steam valve. This undue vibration might cause damage to the shaft and bearings. Normally operation is avoided in such regions. The feasible operating zones of unit can be described and represented as.

$$\begin{aligned} P_i^{\min} &\leq P_i \leq P_{i,1}^l \\ P_{i,m-1}^u &\leq P_i \leq P_{i,m}^l; \quad m = 2, 3, \dots, n_i \\ P_{i,n_i}^u &\leq P_i \leq P_i^{\max} \end{aligned} \quad (5)$$

Where m represents the number of prohibited operating zones of j_{th} generator in area i . $P_{i,m-1}^u$ is the upper limit of $(m-1)_{th}$ prohibited operating zone of i_{th} generator. $P_{i,m}^l$ is the

lower of m_{th} prohibited operating zone of i_{th} generator. Total number of prohibited operating zone of i_{th} the generator is n_i .

2.5. Ramp Rate Limit Constraint

The generator constraints due to ramp rate limits of generating units are given as:

2.5.1.As generation increases

$$P_{i(t)} - P_{i(t-1)} \leq UR_i \quad (6)$$

2.5.2.As generation decreases

$$P_{i(t-1)} - P_{i(t)} \leq DR_i \quad (7)$$

Therefore the generator power limit constraints can be modified as:

$$\max(P_i^{\min}, P_{i(t-1)} - DR_i) \leq P_{i(t)} \leq \min(P_i^{\max}, P_{i(t-1)} + UR_i) \quad (8)$$

from equation (7), the limit of minimum and maximum output powers of generating units are modified as

$$P_i^{\min, \text{ramp}} = \max(P_i^{\min}, P_{i(t-1)} - DR_i) \quad (9)$$

$$P_i^{\max, \text{ramp}} = \min(P_i^{\max}, P_{i(t-1)} + UR_i) \quad (10)$$

Where $P_{i(t)}$ is the output power of generating unit i in the time interval (t) , $P_{i(t-1)}$ is the output power of generating unit i (MW) in the previous time interval $(t-1)$, UR_i is the up ramp limit of generating unit i (MW/time-period) and DR_i is the down ramp limit of generating unit i (MW/time-period). The generating units will operate in three modes of operation such as steady state operation, increasing the level of the power generation and decreasing the power output.

2.5.3 Valve-point Effects

The generator cost function is obtained from a data point taken during “heat run” tests when input and output data are measured as the unit slowly varies through its operating region. Wire drawing effects, which occur as each steam admission valve in a turbine starts to open, produce a rippling effect on the unit curve. To consider the accurate cost curve of each generating unit, the valve point results in as each steam valve starts to open, the ripples like the cost function addressing valve-point loadings of generating units is accurately represented as

$$\begin{aligned} F_t &= \sum_{i=1}^N F_i(P_i) \\ &= \sum_{i=1}^N a_i + b_i P_i + c_i P_i^2 \\ &\quad + |d_i \times \sin\{e_i \times (p_i^{\min} - P_i)\}| \end{aligned} \quad (11)$$

2.5.4. Valve-point Effects and Multi Fuels effect

To obtain an accurate and practical economic dispatch solution, the realistic operation of the ELD problem should be considered both valve-point effects and multiple fuels. This project proposed an incorporated cost model, which combines the valve-point loadings and the fuel changes into one frame. as explained .

$$F_i(P_i) = \begin{cases} a_{i1} + b_{i1}P_{i1} + c_{i1}P_{i1}^2 + |d_{i1} \times \sin\{e_{i1} \times (p_{i1}^{\min} - P_{i1})\}|, & \text{for fuel 1, } p_{i1}^{\min} \leq P_i \leq P_{i1} \\ a_{i2} + b_{i2}P_{i2} + c_{i2}P_{i2}^2 + |d_{i2} \times \sin\{e_{i2} \times (p_{i2}^{\min} - P_{i2})\}|, & \text{for fuel 2, } p_{i2}^{\min} \leq P_i \leq P_{i2} \\ \vdots \\ a_{ik} + b_{ik}P_{ik} + c_{ik}P_{ik}^2 + |d_{ik} \times \sin\{e_{ik} \times (p_{ik}^{\min} - P_{ik})\}|, & \text{for fuel k, } p_{ik-1}^{\min} \leq P_i \leq p_i^{\max} \end{cases} \quad (12)$$

III. Bat Algorithm

Bat algorithm is an optimization algorithm motivated by the echolocation behaviour of natural bats in finding their foods. It is introduced by Yang and is used for solving many real world optimization problems. Each virtual bat in the initial population employs a homologous manner by doing echolocation for updating its position. Bat echolocation is a perceptual system in which a series of loud ultrasound waves are released to produce echoes. These waves are returned with delays and various sound levels which make bats to discover a specific prey as shown in Fig-1. Some guidelines are studied to enhance the structure of BAT algorithm and use the echolocation nature of bats.

- Each bat identify the distance between the prey and background barriers using echolocation.
- Bats fly randomly with velocity v_i at position x_i with a fixed frequency f_{min} (or Wavelength λ), varying wavelength λ (or frequency f) and loudness A_0 to search for prey. They can naturally adopt the wavelength (or frequency) of their emitted pulses and adjust the rate of pulse emission $r \in [0, 1]$, depending on the closeness of their prey;
- Although the loudness of the bats can be modified in many ways, we consider that the loudness varies from a large (positive) A_0 to a minimum value A_{min} according to the problem taken.

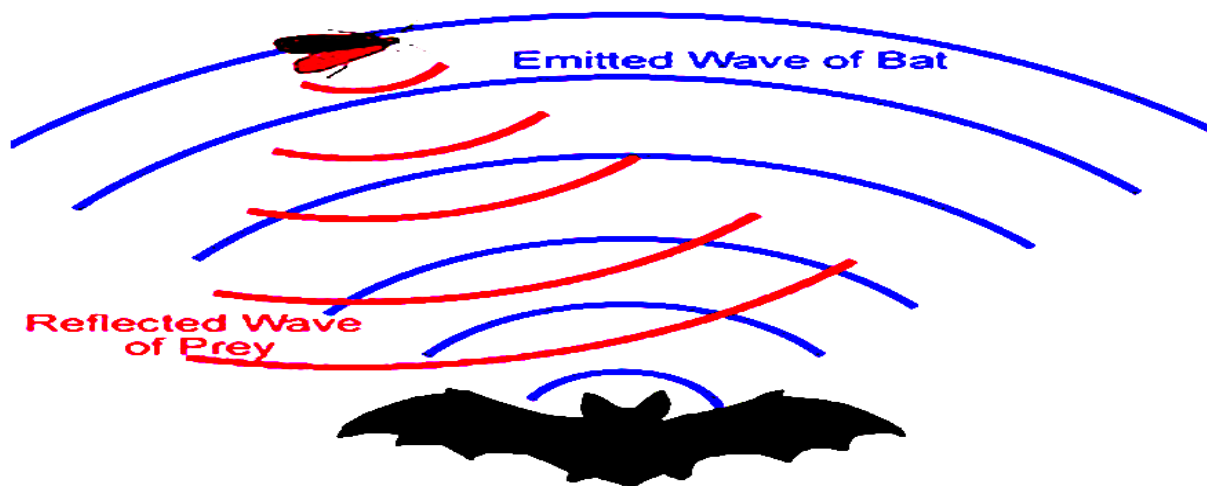


Fig.1. Echolocation behaviour of bats

3.1. Initialization of Bat Population

Population initialization of bats randomly in between the lower and the upper boundary can be achieved by the equation.

$$x_{ij} = x_{minj} + \text{rand}(0,1)(x_{maxj} - x_{minj}) \quad (13)$$

where $i=1, 2, \dots, n$, $j=1, 2, \dots, d$, x_{minj} and x_{maxj} are lower and upper boundaries for dimension j respectively.

3.2. Update Process of Frequency, Velocity and Solution

The step size of the solution is controlled with the frequency factor in BA. This frequency factor is generated randomly in between the minimum and maximum frequency $[f_{min}, f_{max}]$.

Velocity of a solution is proportional to frequency and new solution depends on its new velocity and it is represented as.

$$f_i = f_{\min} + (f_{\max} - f_{\min})\beta \quad (14)$$

$$v_i^t = v_i^{t-1} + (x_i^t - x^*)f_i \quad (15)$$

$$x_i^t = x_i^{t-1} + v_i^t \quad (16)$$

Where $\beta \in [0, 1]$ indicates randomly generated number, x^* represents current global best solutions. For local search part of algorithm (exploitation) one solution is selected among the selected best solutions and random walk is applied.

$$x_{new} = x_{old} + \varepsilon A^t \quad (17)$$

Where A^t , is average loudness of all bats, $\varepsilon \in [0, 1]$ is random number and represents direction and intensity of random-walk.

3.3. Update Process of Loudness and Pulse Emission Rate

As iteration increases, the loudness and pulse emission must be updated because when the bat gets closer to its prey then their loudness usually decreases and pulse emission rate also increases, the updating equation for loudness and pulse emission is given by

$$A_i^{t+1} = \alpha A_i^t \quad (18)$$

$$r_i^{t+1} = r_i^0 [1 - e^{(-\gamma t)}] \quad (19)$$

where α and γ are constants. r_i^0 and A_i are factors which consist of random values and A_i^0 can typically be $[1, 2]$, while r_i^0 can typically be $[0, 1]$.

3.4. Pseudo Code of Bat algorithm

- 1). Objective function: $f(x)$, $x = (x_1 \dots x_d)^t$
- 2). Initialize bat population x_i and velocity v_i $i = 1, 2, \dots, n$
- 3). Define pulse frequency f_i at x_i
- 4). Initialize pulse rate r_i and loudness A_i
- 5). While ($t < \text{maximum number of iterations}$)
- 6). Generate new solutions by adjusting frequency, and updating velocities and location/solutions.
- 7). If ($\text{rand} > r_i$)
- 8). Select a solution among the best solutions
- 9). Generate a local solution around the selected best solution
- 10). End if
- 11). If ($\text{rand} < A_i$ and $f(x_i) < f(x^*)$)
- 12). Accept new solutions
- 13). Increase r_i , reduce A_i
- 14). End if
- 15). Rank the bats and find current best x^*
- 16). End while
- 17). Display results.

IV. RESULT AND DISCUSSION

In this work the Bat algorithm is applied to solve the economic dispatch for two different cases having various complexities and the effectiveness of the algorithm is compared with change of parameter in algorithm.

4.1. Six unit system

The Bat algorithm is employed to solve the economic dispatch of six system with demand 1263MW consist of a smooth quadratic cost function with generator constraints, power loss

and ramp rate limits and prohibited operating zones .the simulation results are for $f_{max}= 1$ and for $f_{max}= 2$ as shown in Table-1 and the converge of the cost function is shown in Fig-2 for 500 iterations. the frequency value change over the iteration for the case-1 which controls the searching process is shown in Fig-3 and the circle highlighted in green is the iteration converged area.

Table 1.Simulation results for Six unit system with $f_{max}=1$ and $f_{max} = 2$.

f_{max}	PG1	PG2	PG3	PG4	PG5	PG6	PL	FUEL COST (\$/H)
1	474.4188	179.0558	262.6278	134.4938	152.1148	74.210	12.55	15457.117
2	445.3884	170.4760	261.3294	138.2719	170.4926	90.103	12.53	15443.456

In the Fig-2.Convergence characteristics of six unit system is better at $f_{max} = 2$ when compared with the convergence characteristics of six unit system with at $f_{max}=1$,the reason for this is in Bat algorithm when the frequency factor increases then the probability of getting the quality solution also increase because the frequency goes higher means the Bat will cover more area in search space. So if the searching for the solution in the search area increases means the probability of getting the nearer to global solution also increases. Thus $f_{max} = 2$ is the better option for the optimization programs for the test case considered in this paper.

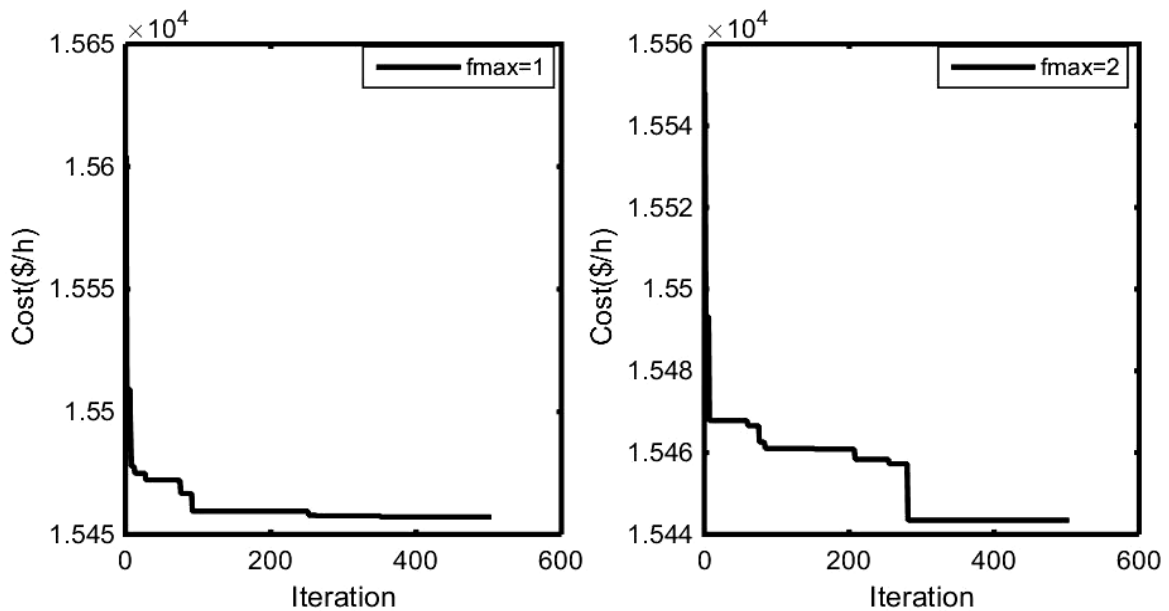


Figure-2.Iteration vs cost for six unit system.

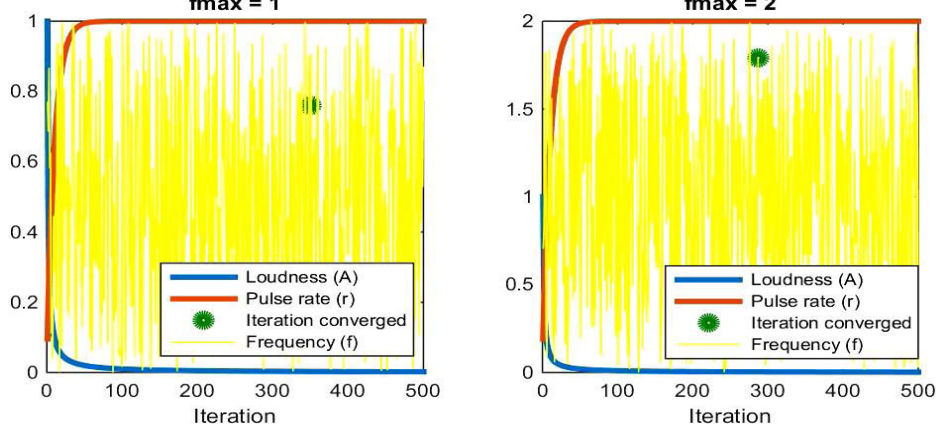


Figure3.Iteration to parameters variation.

4.2. Ten unit multi-fuel system

In this case Bat algorithm is employed to solve the economic dispatch of ten unit system with demand 2700MW consist of valve-point effect and multi-fuel options. the simulation results are for both $f_{\max} = 2$ and for $f_{\max} = 1$ as shown in Table-2 and the converge of the cost function is shown in Fig-4 for 500 iterations. The random value of frequency change for the case-2 is shown in Fig-5.

Table 2.Simulation results for ten unit multi-fuel system with $f_{\max} = 1$ and $f_{\max} = 2$

$f_{\max} = 1$			$f_{\max} = 2$		
PG		Fuel	PG		Fuel
PG1	222.2660	2	PG1	218.6965	2
PG2	211.2552	1	PG2	213.7533	1
PG3	284.2007	1	PG3	281.1293	1
PG4	237.0964	3	PG4	237.2393	3
PG5	280.5554	1	PG5	278.7999	1
PG6	236.1074	3	PG6	239.2963	3
PG7	292.1573	1	PG7	288.0833	1
PG8	241.4200	3	PG8	239.2903	3
PG9	424.6211	3	PG9	428.8663	3
PG10	270.3205	1	PG10	274.8365	1
COST(\$/H)	623.6617		COST(\$/H)	623.4232	

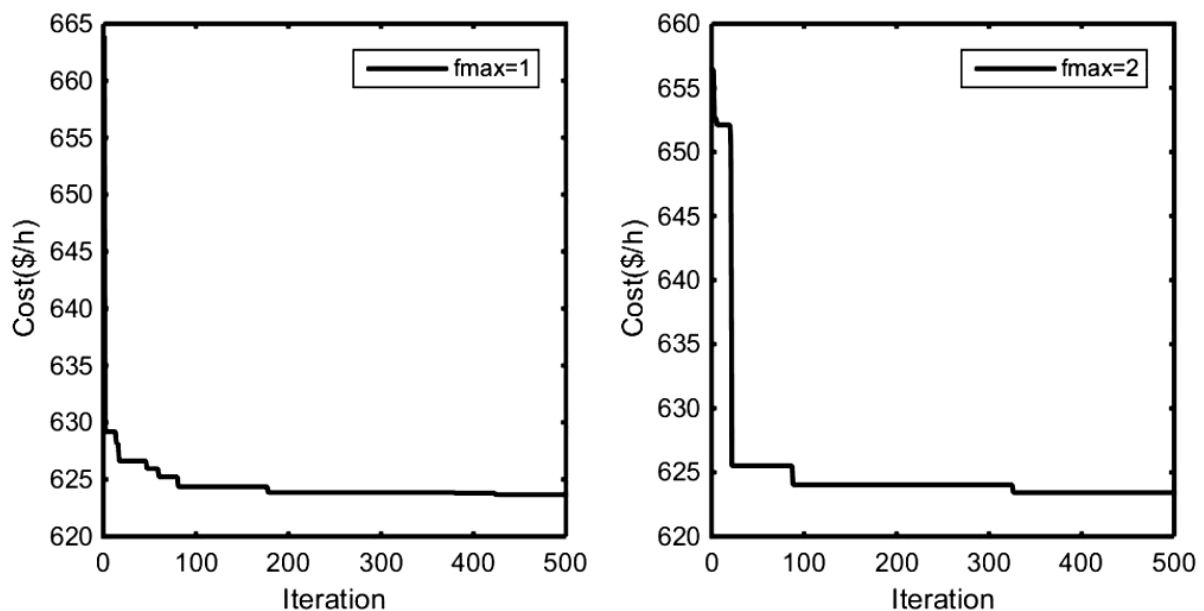


Figure4.Iteration to cost for ten unit system.

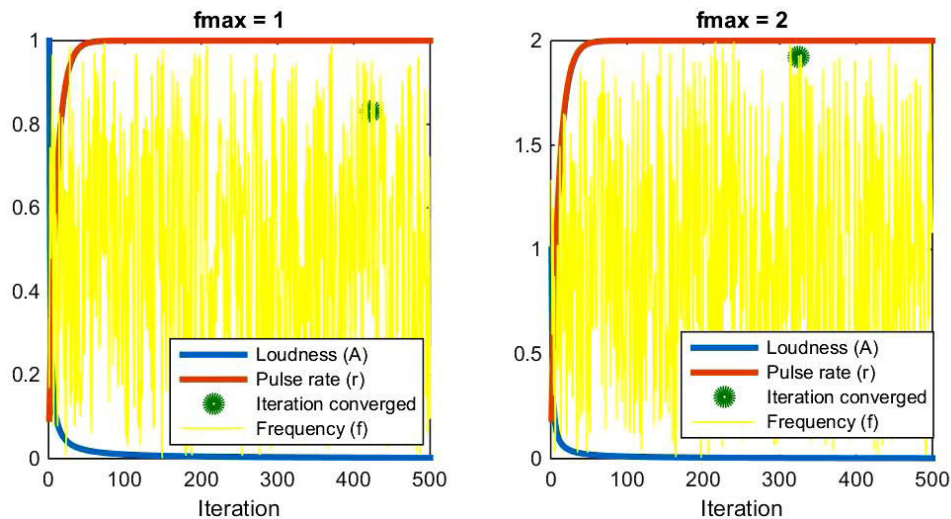


Figure 5. Iteration to parameters variation.

Conclusion

In this paper, Bat algorithm is applied to economic load dispatch problems with two different cases. The results obtained by this method are compared with two different f_{\max} values. The comparison shows that Bat algorithm performs better when $f_{\max} = 2$ and shows good convergence characteristics. The Bat algorithm has superior features, including quality of solution, stable convergence characteristics and good computational efficiency. Therefore, this results shows that Bat algorithm is a promising technique for solving complicated problems in power system.

References

- [1]. B. H. Chowdhury and S. Rahman, "A Review of Recent Advances in Economic Dispatch", IEEE Trans. Power Syst 5(4), 1990, pp. 1248-1259.
- [2]. F. N. Lee and A. M. Breipohl, "Reserve Constrained Economic Dispatch with Prohibited Operating Zones", IEEE Trans Power Syst 8(1), 1993, pp. 246-254.
- [3]. S.K. Dash, "An Artificial Neural Network Method For Optimal Generation Dispatch With Multiple Fuel Options", International Journal of Advanced Electrical and Electronics Engineering, ISSN (Print) : 2278-8948, Volume-2, Issue- 1, 2013.
- [4]. Dr G. Sreenivasan, B. Dheeraj Merin Babu, K. Srikanth, and B. Rajesh Kiran, "solution of eld problem with valve point effects and multi-fuels using IPSO algorithm", International Journal of Advanced Research in Electrical, Electronics and Instrumentation Engineering, ISSN (Print) : 2320 – 3765, Vol. 2, Issue 11, November 2013.
- [5]. Radhakrishnan Anandhakumar, and Srikrishna Subramanian, "Economic Dispatch with Multiple Fuel Options Using CCF", Scientific Research Journal, doi:10.4236/epe.2011.32015 Published Online May 2011.
- [6]. Umamaheswari Krishnasamy and Devarajan Nanjundappan, "A Refined Teaching-Learning Based Optimization Algorithm for Dynamic Economic Dispatch of Integrated Multiple Fuel and Wind Power Plants", Hindawi Publishing Corporation, Volume 2014, Article ID 956405, <http://dx.doi.org/10.1155/2014/956405>.
- [7]. R. Balamurugan and S. Subramanian, "Self-Adaptive Differential Evolution Based Power Economic Dispatch of Generators with Valve-Point Effects and Multiple Fuel Options", World Academy of Science, Engineering and Technology, International Journal of Electrical, Computer, Energetic, Electronic and Communication Engineering Vol: 1, No: 3, 2007.
- [8]. Xin-She Yang, Bat algorithm: literature review and applications, Int. J. Bio-Inspired Computation, Vol. 5, No. 3, pp. 141–149 (2013). DOI: 10.1504/IJBIC.2013.055093

Study of Multi-Area Economic Dispatch on Soft Computing Techniques

S.Vijayaraj¹, Dr.R.K.Santhi²

¹EEE Department, College,veejay_raj@yahoo.co.in.

²EEE Department name, College,rkscdm@gmail.com.

Abstract - This paper analyses the performance of soft computing techniques to solve single and multi area economic dispatch problems. The paper also includes of inter-area flow constraints on power system network, which are normally ignored in most economic load dispatch problems. Economic load dispatch results for these two area, three area and four area systems are presented in the paper and they determine the importance of multiple area representation of a system in economic load dispatch. Such representation affects the cost and assures the determination of optimum dispatch.

Keywords:-Multi-area economic dispatch, Flower pollination algorithm Bat algorithm, Particle swarm optimization, Transmission loss, Prohibited zones, Multi-fuel.

I. INTRODUCTION

Economic load dispatch [1] issue is one of the fundamental optimization problems in the industrial operation of power systems. The essential goal of the monetary dispatch issue is to determine the excellent schedule of online generating units so as to meet the power demand at least possible operating cost under various systems and operating constraints. Generally, in power system the generators are separated into many generation areas and they interconnected by utilizing tie-lines. Multi-area economic dispatch (MAED) is an development of economic dispatch. MAED decides the generation level and exchange of power between areas such that total fuel cost in all areas is curtailed while satisfying power balance constraints, generating limits constraints and tie-line capacity constraints. Romano et al. [2] Solved constrained economic dispatch of multi-area systems using the Danzig-Wolfe decomposition principle diminishes the unpredictability of the issue by isolating it into a few sub-issues. Ouyang and Shahidehpour [3] proposed heuristic multi-area unit commitment with economic dispatch with an incorporation of basic and successful tie-line imperative checking. Shoultz et al [4] included power exchange limits between areas for solving the economic dispatch problem. This study gives a complete formulation of multi-area generation scheduling, and an idea for multi-area studies. Jayabarathi et al. [5] tackled multi-area economic dispatch problems with tie line constraints using evolutionary programming technique. Prasanna et al. [6] solved the Security Constrained Economic Dispatch in interconnected power system by using Fuzzy logic strategy incorporated with Evolutionary Programming and with Tabu-Search algorithms Desell et al. [7] Applied a linear programming to transmission constrained generation production cost analysis in power system planning for a large electrical network. Wang et al. [8] Proposed a decomposition approach for the multi-area generation scheduling with tie-line constraints having non-linear characteristics using expert systems. M. Zarei et al. [9] proposed a Direct search method (DSM) is used to solve the two-area economic dispatch of the generating units with some equality and inequality constraints with different kind of complex fuel cost function. Dan Streiffert et al. [10] proposed an Incremental Network Flow Programming algorithm for solving the multi-area economic dispatch problem with transmission constraints. P. S. Manoharan et al. [11] proposed an Evolutionary Programming with Levenberg-Marquardt Optimization technique to solve multi-area economic dispatch problems with multiple fuel

options. Manoharan et al. [12] investigated the proficiency and adequacy of the various evolutionary algorithms such as the Real-coded Genetic Algorithm, Particle Swarm Optimization, Differential Evolution and Covariance Matrix Adapted Evolution Strategy on multi-area economic dispatch problems. Manisha Sharma et al.[13] compared the search ability and convergence behavior of algorithms such as Classical differential evolution (DE) and its various strategies, Classical particle swarm optimization (PSO), An improved PSO with a parameter automation strategy having time varying acceleration coefficients for solving MAED problems. Flower pollination algorithm (FPA) [14] is an optimization algorithm inspired by the pollination process of flowers. The exploration and exploitation mechanism of FPA was well suitable for the real world optimization problems. Bat algorithm (BA) [15] is an optimization algorithm based on echolocation characteristics of bats and developed by mimics of ‘bats’ foraging behaviour. The exploration and exploitation mechanism of BA was well suitable for the real world optimization problems. In this paper, single area and two area economic dispatch problem with inclusion of operating zones, transmission loss has been solved by using the flower pollination algorithm(FPA),Bat algorithm(BA),and particle swarm optimization(PSO).The result obtained by the techniques are compared with each other.

II. Particle Swarm Optimization

Particle swarm optimization (PSO) is a population-based optimization method first proposed by Kennedy and Eberhart in 1995, inspired by social behaviour of bird flocking or fish schooling. The PSO as an optimization tool provides a population-based search procedure in which individuals called particles change their position (state) with time. In a PSO system, particles fly around in a multidimensional search space. During flight, each particle adjusts its position according to its own experience (This value is called pbest), and according to the experience of a neighbouring particle (This value is called gbest), made use of the best position encountered by itself and its neighbour.

This modification can be represented by the concept of velocity. Velocity of each agent can be modified by the following equation:

$$V_{id}^{k+1} = \omega_i V_i^k + c_1 \text{rand} * (pbest_i - S_i^k) + c_2 \text{rand} * (gbest - S_i^k) \quad (1)$$

Using the above equation, a certain velocity, which gradually gets close to pbest and gbest can be calculated. The current position (searching point in the solution space) can be modified by the following equation:

$$s_i^{k+1} = s_i^k + V_i^{k+1} \quad (2)$$

where s_k is current searching point, s_{k+1} is modified searching point, v_k is current velocity, v_{k+1} is modified velocity of agent i , v_{pbest} is velocity based on pbest, v_{gbest} is velocity based on gbest, n is number of particles in a group, $pbest_i$ is pbest of agent i , $gbest_i$ is gbest of the group, ω_i is weight function for velocity of agent i , C_i is weight coefficients for each term. Appropriate value ranges for $C1$ and $C2$ are 1 to 2, ω_i is taken as 1.

1.1.Pseudo code for PSO

- 1) Initialize the group (swarm size, initial velocity, particle position).
- 2) Set the value for iteration count
- 3) Check for fitness value of each particle
- 4) If step 3 is satisfactory then update *pbest and gbest*
- 5) Update position and velocity
- 6) Go to step 3 until satisfying stopping criteria otherwise go to

- 7) when stopping criteria is satisfied.
- 8) Print the final results.

II. Bat Algorithm

- Each bats identify the distance between the prey and background barriers using echolocation.
- Bats fly randomly with velocity v_i at position x_i with a fixed frequency f_{\min} (or Wavelength λ), varying wavelength λ (or frequency f) and loudness A_0 to search for prey. They can naturally adopt the wavelength (or frequency) of their emitted pulses and adjust the rate of pulse emission $r \in [0, 1]$, depending on the closeness of their prey;
- Although the loudness of the bats can be modified in many ways, we consider that the loudness varies from a large (positive) A_0 to a minimum value A_{\min} according to the problem taken.

2.1. Initialization of Bat Population

Population initialization of bats randomly in between the lower and the upper boundary can be achieved by the equation.

$$x_{ij} = x_{\min j} + \text{rand}(0,1)(x_{\max j} - x_{\min j}) \quad (3)$$

where $i=1, 2, \dots, n$, $j=1, 2, \dots, d$, $x_{\min j}$ and $x_{\max j}$ are lower and upper boundaries for dimension j respectively.

2.2. Update Process of Frequency, Velocity and Solution

The step size of the solution is controlled with the frequency factor in BA. This frequency factor is generated randomly in between the minimum and maximum frequency [f_{\min} , f_{\max}]. Velocity of a solution is proportional to frequency and new solution depends on its new velocity and it is represented as.

$$f_i = f_{\min} + (f_{\max} - f_{\min})\beta \quad (4)$$

$$v_i^t = v_i^{t-1} + (x_i^t - x^*)f_i \quad (5)$$

$$x_i^t = x_i^{t-1} + v_i^t \quad (6)$$

Where $\beta \in [0, 1]$ indicates randomly generated number, x^* represents current global best solutions. For local search part of algorithm (exploitation) one solution is selected among the selected best solutions and random walk is applied.

$$x_{\text{new}} = x_{\text{old}} + \epsilon A^t \quad (7)$$

Where A^t , is average loudness of all bats, $\epsilon \in [0, 1]$ is random number and represents direction and intensity of random-walk.

2.3. Update Process of Loudness and Pulse Emission Rate

As iteration increases, the loudness and pulse emission must be updated because when the bat gets closer to its prey then their loudness usually decreases and pulse emission rate also increases, the updating equation for loudness and pulse emission is given by

$$A_i^{t+1} = \alpha A_i^t \quad (8)$$

$$r_i^{t+1} = r_i^0 [1 - e^{(-\gamma t)}] \quad (9)$$

where α and γ are constants. r_i^0 and A_i are factors which consist of random values and A_i^0 can typically be $[1, 2]$, while r_i^0 can typically be $[0, 1]$.

2.4. Pseudo Code of Bat algorithm

1). Objective function: $f(x)$, $x = (x_1, \dots, x_d)^t$

- 2). Initialize bat population x_i and velocity v_i $i=1, 2, \dots, n$
- 3). Define pulse frequency f_i at x_i
- 4). Initialize pulse rate r_i and loudness A_i
- 5). While ($t < \text{maximum number of iterations}$)
- 6). Generate new solutions by adjusting frequency, and updating velocities and location/solutions.
- 7). If ($\text{rand} > r_i$)
- 8). Select a solution among the best solutions
- 9) Generate a local solution around the selected best solution
- 10) End if
- 11) If ($\text{rand} < A_i$ and $f(x_i) < f(x^*)$)
- 12) Accept new solutions
- 13) Increase r_i , reduce A_i
- 14) End if
- 15) Ranks the bats and find current best x^*
- 16) End while
- 17) Display results.

III. NATURE-INSPIRED FLOWER POLLINATION ALGORITHM

3.1. Rules For Flower Pollination Algorithm.

- Biotic and cross-pollination is considered as global pollination process with pollen-carrying pollinators performing Levy flights.
- Abiotic and self-pollination are considered as local pollination.
- Flower constancy can be considered as the reproduction probability is proportional to the similarity of two flowers involved.
- Local pollination and global pollination is controlled by a switch probability $P_a \in [0, 1]$. Due to the physical proximity and other factors such as wind, local pollination can have a significant fraction p_a in the overall pollination activities.

3.2. Mathematical representation of Flower Pollination Algorithm.

The first rule plus flower constancy can be represented mathematically as

$$x_i^{t+1} = X_i^t + L(X_i^t - g_*) \quad (10)$$

where X_i^t is the pollen i or solution vector X_i at iteration t , and g_* is the current best solution found among all solutions at the current generation/iteration.

Levy distribution is given by

$$L \sim \frac{\lambda \Gamma \sin\left(\frac{\pi \lambda}{2}\right)}{\pi} \frac{1}{S^{1+\lambda}}, (S \gg S_0 > 0) \quad (11)$$

where L is the strength of the pollination should be greater than zero, $\Gamma(\lambda)$ is the gamma function and this distribution is valid for large steps $s > 0$.

The local pollination can be represented as

$$x_i^{t+1} = X_i^t + \varepsilon(X_j^t - X_k^t) \quad (12)$$

where, X_j^t and X_k^t are pollens from the different flowers of the same plant species. This essentially mimic the flower constancy in a limited neighbourhood. Mathematically, if X_j^t and X_k^t comes from the same species or selected from the same population, this become a local random walk if we draw from a uniform distribution in $[0, 1]$.

3.3. Switch probability or proximity probability(p_a).

Most flower pollination activities can occur at both local and global scale. In practice, adjacent flower patches or flowers in the not-so-far-away neighbourhood are more likely to be pollinated by local flower pollens that those far away. For this, we use a switch probability

(Rule 4) or proximity probability p_a to switch between common global pollination to intensive local pollination.

3.4. Pseudo code of Flower Pollination Algorithm .

- 1)Objective min or max $f(x)$, $x = (x_1, x_2, \dots, x_d)$
- 2)Initialize a population of n flowers/pollen gametes with random solutions
- 4)Find the best solution g_* in the initial population
- 5)Define a switch probability $P_a \in [0, 1]$.
- 6)while ($t < \text{MaxGeneration}$)
- 7)for $i = 1 : n$ (all n flowers in the population)
- 8)if $\text{rand} < p_a$,
- 9)Draw a (d -dimensional) step vector L which obeys a Levy distribution
- 10)Global pollination via $x_i^{t+1} = X_i^t + L(X_i^t - g_*)$
- 11)else
- 12)Draw ε from a uniform distribution in $[0,1]$
- 13)Randomly choose j and k among all the solutions
- 14)Do local pollination via $x_i^{t+1} = X_i^t + \varepsilon(X_j^t - X_k^t)$
- 15)end if
- 16)Evaluate new solutions
- 17)If new solutions are better, update them in the population
- 18)end for
- 19)Find the current best solution g_*
- 20)end while.

IV. PROBLEM FORMULATION

4.1. Total Cost Function:-

The main objective of Economic Load Dispatch in electrical power system is to reduce the overall production cost of supplying loads while satisfying constraints. The total cost function can be formulated as the following equation.

$$F_t = \sum_{i=1}^N F_i(P_i) = \sum_{i=1}^N a_i + b_i P_i + c_i P_i^2 \quad (13)$$

where $F_i(P_i)$ is the cost function of i_{th} generator and is usually expressed as a quadratic polynomial; a_i , b_i and c_i are the fuel cost coefficients of i_{th} generator; N is the number of generators, P_i is the real power output of i_{th} generator. The Economic Load Dispatch problem minimizes F_t subject to the following constraints and effects.

4.1.2. Equality constraints:-

The power balance equation is given by

$$\sum_{i=1}^N P_i = P_D + P_L \quad (14)$$

The transmission loss P_L of system may be expressed by using B-coefficients.

$$P_{Li} = \sum_{i=1}^N \sum_{j=1}^N P_i B_{ij} P_j + \sum_{j=1}^{M_i} B_{0i} P_i + B_{00} \quad (15)$$

where, P_D is the power demand of the system. B_{ij} , B_{0i} , and B_{00} are transmission loss coefficients.

4.1.3. Inequality constraints:

The upper and the lower operating region of the generator is given by the equation

$$P_i^{\min} \leq P_i \leq P_i^{\max} \quad i \in N \quad (16)$$

Where P_i^{\min} and P_i^{\max} are the minimum and maximum power outputs of generator i , respectively. The maximum output power of generator is limited by thermal consideration and minimum power generation is limited by the flame instability of a boiler.

4.1.4. prohibited operating

The prohibited operating zones are the range of power output of a generator where the operation causes undue vibration

of the turbine shaft bearing caused by opening or closing of the steam valve. This undue vibration might cause damage to the shaft and bearings. Normally operation is avoided in such regions. The feasible operating zones of unit can be described and represented as.

$$\begin{aligned}
 P_i^{\min} &\leq P_i \leq P_{i,1}^l \\
 P_{i,m-1}^u &\leq P_i \leq P_{i,m}^l; \quad m = 2,3, \dots n_i \\
 P_{i,n_i}^u &\leq P_i \leq P_i^{\max}
 \end{aligned}
 \tag{17}$$

Where m represents the number of prohibited operating zones of j th generator in area i . $P_{i,m-1}^u$ is the upper limit of $(m - 1)$ th prohibited operating zone of i th generator. $P_{i,m}^l$ is the lower of m th prohibited operating zone of i th generator. Total number of prohibited operating zone of i th generator is n_i .

4.1.5. Valve-point Effects

The generator cost function is obtained from a data point taken during “heat run” tests when input and output data are measured as the unit slowly varies through its operating region. Wire drawing effects, which occur as each steam admission valve in a turbine starts to open, produce a rippling effect on the unit curve. To consider the accurate cost curve of each generating unit, the valve point results in as each steam valve starts to open, the ripples like the cost function addressing valve-point loadings of generating units is accurately represented as

$$\begin{aligned}
 F_t &= \sum_{i=1}^N F_i(P_i) \\
 &= \sum_{i=1}^N a_i + b_i P_i + c_i P_i^2 \\
 &\quad + |d_i \times \sin\{e_i \times (p_i^{\min} - P_i)\}|
 \end{aligned}
 \tag{18}$$

4.1.6. Valve-point Effects and Multi Fuels effect

To obtain an accurate and practical economic dispatch solution, the realistic operation of the ELD problem should be considered both valve-point effects and multiple fuels. This project proposed an incorporated cost model, which combines the valve-point loadings and the fuel changes into one frame. as explained .

$$\begin{aligned}
 &F_i(P_i) \\
 &= \begin{cases} a_{i1} + b_{i1}P_{i1} + c_{i1}P_{i1}^2 + |d_{i1} \times \sin\{e_{i1} \times (p_{i1}^{\min} - P_{i1})\}|, & \text{for fuel 1, } p_{i1}^{\min} \leq P_i \leq P_{i1} \\ a_{i2} + b_{i2}P_{i1} + c_{i2}P_{i2}^2 + |d_{i2} \times \sin\{e_{i2} \times (p_{i2}^{\min} - P_{i2})\}|, & \text{for fuel 2, } p_i^{\min} \leq P_i \leq P_{i2} \\ \vdots \\ a_{ik} + b_{ik}P_{ik} + c_{ik}P_{ik}^2 + |d_{ik} \times \sin\{e_{ik} \times (p_{ik}^{\min} - P_{ik})\}|, & \text{for fuel k, } p_{ik-1}^{\min} \leq P_i \leq p_i^{\max} \end{cases}
 \end{aligned}
 \tag{19}$$

4.2. Multi- area economic dispatch with transmission loss and prohibited zones

The objective of the MAED problem is:-

$$F_t = \sum_{i=1}^N \sum_{j=1}^{M_i} F_{ij}(P_{ij}) = \sum_{i=1}^N \sum_{j=1}^{M_i} a_{ij} + b_{ij}P_{ij} + c_{ij}P_{ij}^2
 \tag{20}$$

where $F_{ij}(P_{ij})$ is the cost function of j th generator in area i and is usually expressed as a quadratic polynomial; a_{ij} , b_{ij} and c_{ij} are the fuel cost coefficients of j th generator in area i ; N is the number of areas, M_i is the number of committed generators in area i ; P_{ij} is the real power output of j th generator in area i . The MAED problem minimizes F_t subject to the following constraints

4.2.1. Active power balance constraint

$$\sum_{j=1}^{M_i-1} P_{ij} = P_{Di} + P_{Li} + \sum_{k,k \neq i} T_{ik} \quad i \in N \quad (21)$$

The transmission loss P_{Li} of area i may be expressed by using B-coefficients as

$$\sum_i P_{Li} = \sum_i \left(\sum_{l=1}^{M_i} \sum_{j=1}^{M_i} P_{ij} B_{ilj} P_{il} + \sum_{j=1}^{M_i} B_{oij} P_{ij} + B_{ooi} \right) \quad (22)$$

where P_{Di} real power demand of area i ; T_{ik} is the tie line real power transfer from area i to area k . T_{ik} is positive when power flows from area i to area k and T_{ik} is negative when power flows from area k to area i .

4.2.2. Tie line capacity constraints

The tie line real power transfer T_{ik} from area i to area k should not exceed the tie line transfer capacity for security consideration.

$$-T_{ik}^{\max} \leq T_{ik} \leq T_{ik}^{\max} \quad (4)$$

Where T_{ik}^{\max} the power flow is limit from area i to area k and $-T_{ik}^{\max}$ is the power flow limit from area k to area i .

4.2.3. Real power generation capacity constraints

The real power generated by each generator should be within its lower limit P_{ij}^{\min} and upper limit P_{ij}^{\max} , so that

$$P_{ij}^{\min} \leq P_{ij} \leq P_{ij}^{\max} \quad i \in N \quad j \in M_j \quad (23)$$

4.2.4. Prohibited operating zone

The feasible operating zones of unit can be described as follows:-

$$\begin{aligned} P_{ij}^{\min} &\leq P_{ij} \leq P_{ij,1}^l \\ P_{ij,m-1}^u &\leq P_{ij} \leq P_{ij,m}^l; \quad m = 2,3, \dots, n_{ij} \quad (6) \\ P_{ij,n_{ij}}^u &\leq P_{ij} \leq P_{ij}^{\max} \end{aligned}$$

Where m represents the number of prohibited operating zones of j the generator in area i . $P_{ij,m-1}^u$ is the upper limit of $(m - 1)$ th prohibited operating zone of j th generator in area i . $P_{ij,m}^l$ is the lower of m th prohibited operating zone of j the generator in area i . Total number of prohibited operating zone of j th generator in area i is n_{ij} .

V. TEST SYSTEM

5.1.Single area six unit system

This system consists of six generating units, The total power demand is 1263 MW. Prohibited operating zones of each generator have been considered here with transmission loss. The entire generator data and B coefficients are taken from[16].The problem is solved by PSO,BA and FPA .The results obtained by the three algorithms is compared with each other and the convergence characteristics of algorithms is shown in fig-1.

Table-1.Simulation Result For single area six unit system

FPA	BA	PSO
-----	----	-----

P ₁ (MW)	438.5482	447.5761	474.9573
P ₂ (MW)	167.3454	173.4012	178.7870
P ₃ (MW)	274.7946	263.5536	262.3596
P ₄ (MW)	136.0322	139.0129	133.8642
P ₅ (MW)	159.8192	165.5552	152.0546
P ₆ (MW)	99.1532	87.2071	74.3319
P _L (MW)	12.3000	12.8328	12.4526
Cost (\$/h)	15,442	15,447	15,452
CPU time (s)	4.256	5.112	6.489

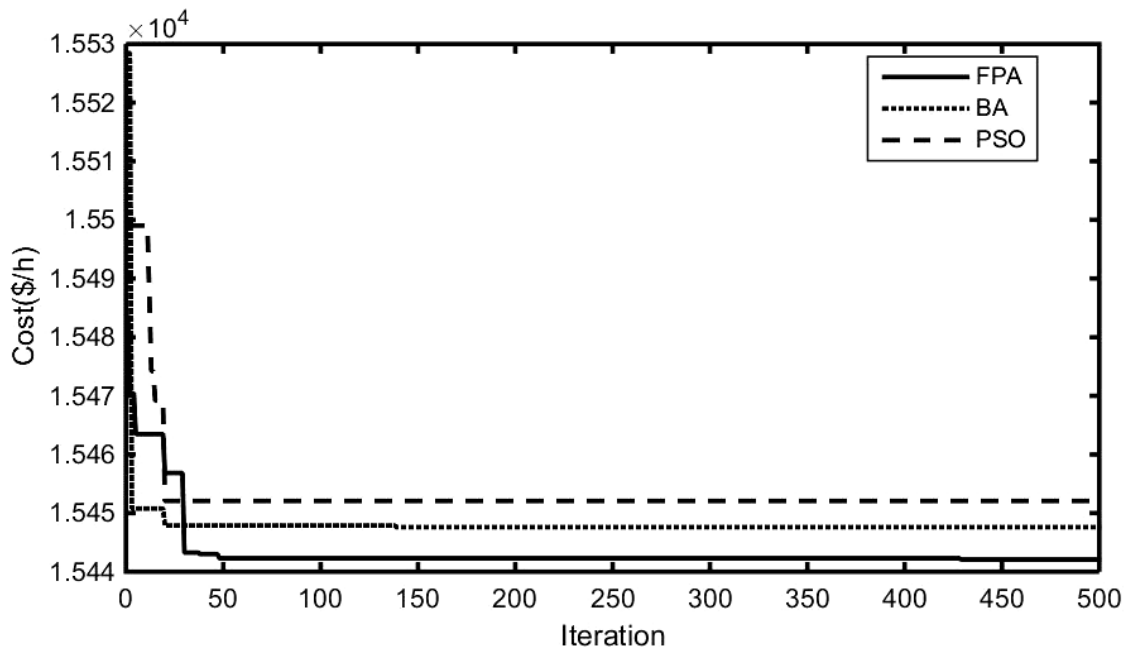


Figure-1. Iteration Vs Cost Curve for Single area six unit system

5.1.2. Two area six unit system

In this system six generator single area system is decomposed into two area with three generators on each with consideration of prohibited operation zones and transmission loss. the total demand for two area system is 1263MW and it is shared by two areas, area1 demand is 757.8MW (60%), area2 demand is 505.2MW (40%). and Tie-line power flow limit of the system is 100 MW. The problem is solved by PSO, BA and FPA. The results obtained by the three algorithms is compared with each other and the convergence characteristics of algorithms is shown in fig-2.

Table- 2. Simulation Result For Two area six unit system

	FPA	BA	PSO
P _{1,1} (MW)	500.0000	500.0000	500.0000
P _{1,2} (MW)	200.0000	200.0000	200.0000
P _{1,3} (MW)	149.6134	149.6093	149.4261
P _{2,1} (MW)	204.1206	206.4481	205.7301
P _{2,2} (MW)	154.6103	154.6758	155.7290
P _{2,3} (MW)	67.5768	65.1840	65.2231
T ₁₂ (MW)	82.3866	82.3826	82.2067
P _{L1} (MW)	9.2135	9.2134	9.2097
P _{L2} (MW)	4.0945	4.0877	4.2064

Cost (\$/h)	12252.35	12254.38	12255.41
CPU time (s)	7.8641	9.9612	11.0089

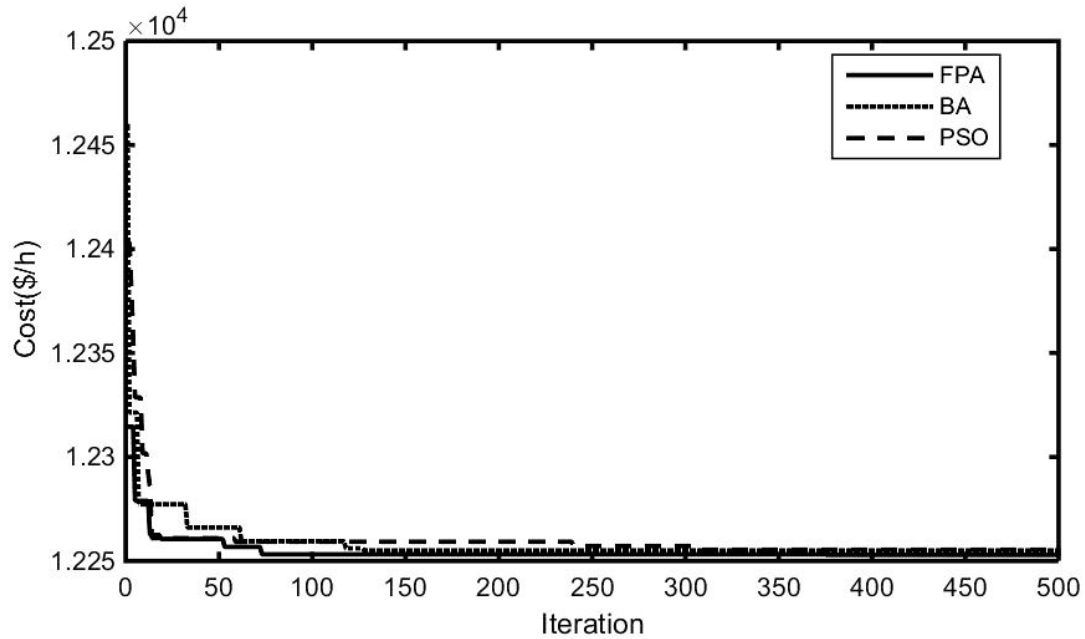


Figure-2. Iteration Vs Cost Curve for Two area six unit system

5.2 Single area with ten unit system

This system consists of ten generating units, The total power demand is 2700 MW. Multi-fuel option of each generator have been considered here without transmission loss. The entire generator data are taken from [16]. The problem is solved by PSO, BA and FPA. The results obtained by the three algorithms is compared with each other and the convergence characteristics of algorithms is shown in fig-3.

	FPA		BA		PSO	
		Fuel		Fuel		Fuel
P ₁ (MW)	225.0893	2	225.0943	2	225.5446	2
P ₂ (MW)	211.2476	1	211.2537	1	210.2665	1
P ₃ (MW)	490.8353	2	490.0159	2	491.3842	2
P ₄ (MW)	240.7118	3	240.7175	3	240.9954	3
P ₅ (MW)	254.2451	1	254.1340	1	251.1047	1
P ₆ (MW)	235.5809	3	235.5870	3	238.9601	3
P ₇ (MW)	263.0884	1	263.9780	1	264.1904	1
P ₈ (MW)	237.1411	3	237.0949	3	236.0998	3
P ₉ (MW)	328.8254	1	328.8316	1	326.6392	1
P ₁₀ (MW)	248.9499	1	248.9550	1	250.4337	1
Cost (\$/h)	624.39		624.5139		625.8136	
Time (s)	6.5319		7.4963		12.0381	

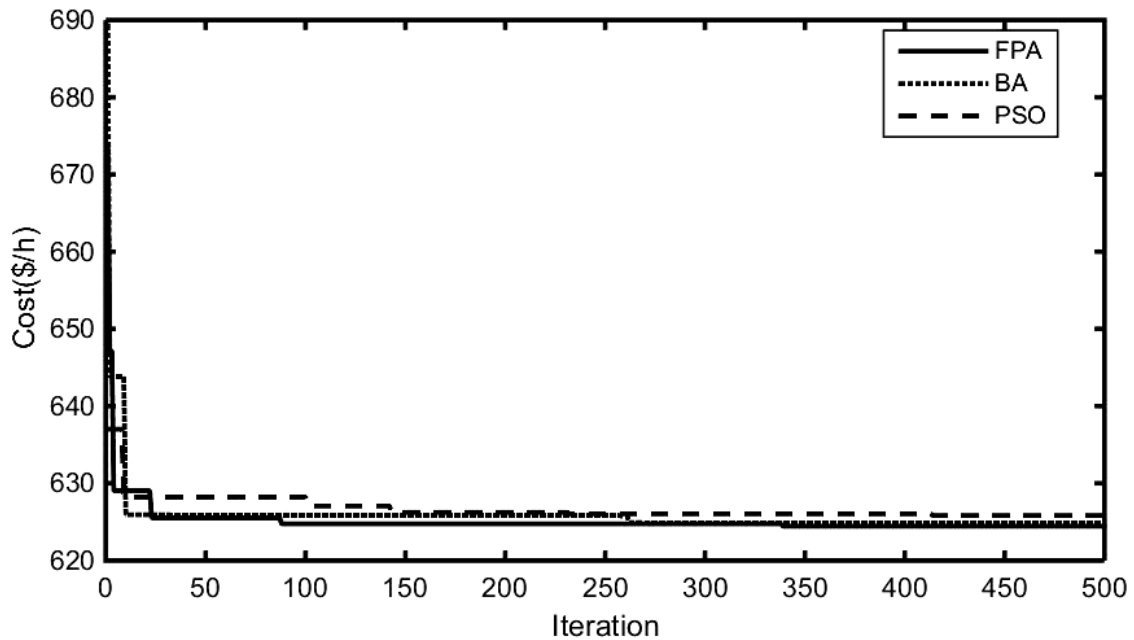


Figure-3. Iteration Vs Cost Curve for single area ten unit system.

5.2.1 Three area with ten unit system

This test system has ten generating units with valve point loading, multi fuel options and transmission losses are also considered. The total demand for three areas is 2700MW and it is shared by three areas, area1 demand is 1350MW (50%), area2 demand is 675MW (25%), area3 demand is 675MW (25%) and the tie-line power flow limit between area 1 and area 2 or from area 2 and area 1 is 100MW. the tie-line power flow limit between area 1 and area 3 or from area 3 and area 1 is 100MW. the tie-line power flow limit between area 3 and area 2 or from area 2 and area 3 is 100MW. so all the three tie line in area three having the same limit as 100MW, the loss coefficients for the two area generators are given in [16]. The problem is solved by PSO, BA and FPA. The results obtained by the three algorithms is compared with each other and the convergence characteristics of algorithms is shown in fig-4.

Table-4. Simulation Result for Three area ten unit system

	FPA		BA		PSO	
	Fuel		Fuel		Fuel	
P _{1,1} (MW)	225.0632	2	225.9431	2	225.4448	2
P _{1,2} (MW)	211.2215	1	211.1594	1	210.1667	1
P _{1,3} (MW)	490.8092	2	489.9216	2	491.2844	2
P _{1,4} (MW)	240.0623	3	240.6232	3	240.8956	3
P _{2,1} (MW)	254.2190	1	254.0397	1	251.0049	1
P _{2,2} (MW)	235.5548	3	235.4927	3	238.8603	3
P _{2,3} (MW)	263.9462	1	263.8837	1	264.0906	1
P _{3,1} (MW)	237.1150	3	237.0006	3	236.9982	3
P _{3,2} (MW)	328.7993	1	328.7373	1	326.5394	1
P _{3,3} (MW)	248.9238	1	248.8607	1	250.3339	1
T ₂₁ (MW)	99.3310		99.8288		99.468	
T ₃₁ (MW)	100.0647		99.7334		100	
T ₃₂ (MW)	31.6448		31.2615		30.281	
P _{L1} (MW)	17.5418		17.2095		17.268	
P _{L2} (MW)	9.2846		9.8488		9.7688	
P _{L3} (MW)	8.8884		8.6037		8.5905	
Cost (\$/h)	653.5641		653.8115		654.4134	
Time (s)	60.9746		72.4683		80.0961	

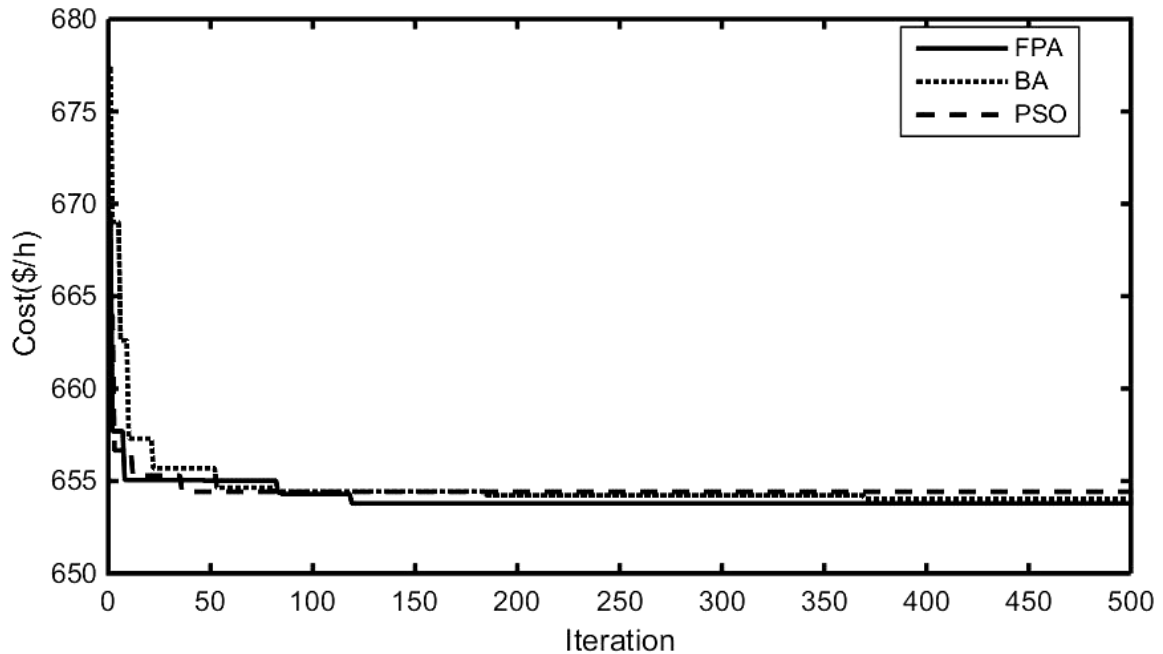


Figure-4. Iteration Vs Cost Curve for Three area ten unit system.

5.3 Single area with forty unit system

This system consists of forty generating units, The total power demand is 10500 MW. valve point effect of each generator have been considered here without transmission loss. The entire generator data are taken from [16]. The problem is solved by PSO, BA and FPA. The results obtained by the three algorithms is compared with each other and the convergence characteristics of algorithms is shown in fig-5.

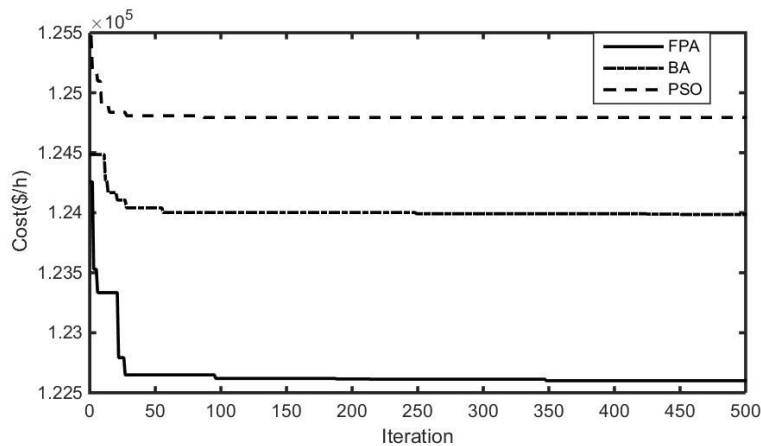


Figure-5. Iteration Vs Cost Curve for Single area forty unit system.

5.3.1 Four area with forty unit system

This test system has forty generating units with valve point loading effect without transmission loss. The total demand for three areas is 10500 MW and it is shared by four areas, area1 demand is 1575 MW (15%), area2 demand is 4200 MW (40%), area3 demand is 3150 MW (30%), area4 demand is 1575 MW (15%) and the tie-line power flow limit between area 1 and area 2 or from area 2 and area 1 is 200 MW. the tie-line power flow limit between area 1 and area 3 or from area 3 and area 1 is 200 MW. the tie-line power flow limit between area 3 and area 2 or from area 2 and area 3 is 200 MW. the tie-line power flow limit between area 4 and area 1 or from area 1 and area 4 is 100 MW. the tie-line power flow limit between area 4 and area 2 or from area 2 and area 4 is 100 MW. the tie-line power flow limit between

The problem is solved by PSO, BA and FPA. The results obtained by the three algorithms is compared with each other and the convergence characteristics of algorithms is shown in fig-6.

VI. Conclusion:-

The results of the study show the importance of the multi area economic dispatch and The comparison of results for the test cases shows that the FPA method is capable of obtaining higher quality solution efficiently for higher degree ELD problems. The convergence tends to be improving as the system complexity increases. Thus solution for higher order systems can be obtained in much less computation time duration than the BA and PSO.

REFERENCES

- [1] Chowdhury BH, Rahman S. A review of recent advances in economic dispatch. *IEEE Trans Power System* 1990;5(4):1248–59.
- [2] Romano R, Quintana VH, Lopez R, Valadez V. Constrained economic dispatch of multi-area systems using the Dantzig–Wolfe decomposition principle. *IEEE Trans Power Apparatus Syst* 1981;100(4):2127–37.
- [3] Ouyang Z, Shahidehpour SM. Heuristic multi-area unit commitment with economic dispatch. *IEE Proc-C* 1991;138(3):242–52.
- [4] Shoults RR, Chang SK, Helmick S, Grady WM. A practical approach to unit commitment, economic dispatch and savings allocation for multiple-area pool operation with import/export constraints. *IEEE Trans Power Apparatus System* 1980;99(2):625–35.
- [5] Jayabarathi T, Sadasivam G, Ramachandran V. Evolutionary programming based multi-area economic dispatch with tie line constraints. *Electr Mach Power Syst* 2000;28:1165–76.
- [6] Prasanna. T.S, and Somasundaram.P. multi-area security constrained economic dispatch by fuzzy- stochastic algorithms. *journal of theoretical and applied information technology*. 2005 – 2009.
- [7] Desell AL, McClelland EC, Tammar K, Van Horne PR. Transmission constrained production cost analysis in power system planning. *IEEE Trans Power Apparatus Syst* 1984;103(8):2192–8.
- [8] Wang C, Shahidehpour SM. A decomposition approach to non-linear multi area generation scheduling with tie-line constraints using expert systems. *IEEE Trans Power Syst* 1992;7(4):1409–18.
- [9] Zarei. M, Roozegar.A, Kazemzadeh.R., and Kauffmann J.M. Two Area Power Systems Economic Dispatch Problem Solving Considering Transmission Capacity Constraints. *World Academy of Science, Engineering and Technology International Journal of Electrical, Computer, Energetic, Electronic and Communication Engineering* Vol:1, No:9, 2007.
- [10] Streiffert D. Multi-area economic dispatch with tie line constraints. *IEEE Trans Power Syst* 1995;10(4):1946–51.
- [11] Manoharan .P. S., Kannan p. S., Ramanathan. V. A Novel EP Approach for Multi-area Economic Dispatch with Multiple Fuel Options *Turk J Elec Eng & Comp Sci*, Vol.17, No.1, 2009, doi:10.3906/elk-0705-10.
- [12] Manoharan PS, Kannan PS, Baskar S, Willjuice Iruthayarajan M. Evolutionary algorithm solution and KKT based optimality verification to multi-area economic dispatch. *Int J Electr Power Energy Syst* 2009;31(7–8):365–73.
- [13] Sharma Manisha, Pandit Manjaree, Srivastava Laxmi. Reserve constrained multi-area economic dispatch employing differential evolution with timevarying mutation. *Int J Electr Power Energy Syst* 2011;33(3):753–66.
- [14] Xin-She Yang, Bat algorithm: literature review and applications, *Int. J. Bio-Inspired Computation*, Vol. 5, No. 3, pp. 141–149 (2013). DOI: 10.1504/IJBIC.2013.055093.
- [15] Xin-She Yang, "Flower Pollination Algorithm for Global Optimization", *Unconventional Computation and Natural Computation* 2012, Lecture Notes in Computer Science, Vol. 7445, pp. 240-249 (2012).
- [16] Basu.M .Artificial bee colony optimization for multi-area economic dispatch .*Electricla power and energy systems* 49(2013)181-187.
- [17].S.Vijayaraj and Dr.R.K.Santhi, " Multi-area economic dispatch using Improved Bat Algorithm", *International Journal of Applied Engineering Research*. ISSN 0973-4562 Volume 10, Number 19 (2015) pp 40139-40146.

STUDENT'S PERCEPTIONS OF PLAGIARISM

A. Richard Pravin¹, A. Kalaivani²

^{1,2}Assistant Professor, St. Anne's college of Engineering & Technology.

²Student, St. Anne's college of Engineering & Technology.

Abstract: While plagiarism by college students is a serious problem that must be addressed, students generally overestimate the frequency of plagiarism at their schools and blame students they do not know for the majority of incidents. This study looked at students' estimations of the frequency of plagiarism at a large urban college and explored how that varied over the full range of types of plagiarism, from using another author's ideas to submitting an entire document copied verbatim from another author's work. Analysis of student responses to survey items revealed they believe other students are far more likely than them to commit each type of plagiarism and they recognize that some types of plagiarism are more serious than others. The opportunity to reduce incidents of plagiarism by providing students with accurate information about plagiarism at their schools is discussed in the context of social norms theory.

Keywords: plagiarism, college, higher education, social norms theory

I. INTRODUCTION

While plagiarism is a widespread problem, college instructors tend to overestimate its frequency (Hard, Conway, & Moran, 2006). Students also believe plagiarism occurs more often than it does, to an even greater extent than faculty, and they generally attribute the high rate of incidents to strangers rather than people they know or themselves (Engler, Landau, & Epstein, 2008).

It is important to understand students' beliefs about the frequency and nature of incidents of plagiarism at their schools. Even though students expect faculty to impose consequences for academic misconduct (Kuther, 2003; Brown, 2012), they also look to other students' behavior to determine how far they can push the boundaries of a professor's course policies (Feldman, 2001; McCabe, Trevino, & Butterfield, 2001; Hard et al., 2006; Rettinger & Kramer, 2009). Their opinion that some unidentified group of students at their school regularly submits work they did not do themselves can distort students' understandings of acceptable strategies they should use to complete assignments. Students who see some forms of plagiarism as less serious than others and who believe other students plagiarize frequently may become more likely to plagiarize themselves.

This study looked at students' estimations of the frequency of plagiarism at a large urban college and explored how that varied over the full range of types of plagiarism, from using another author's ideas to submitting an entire document copied verbatim from another author's work. It also looked at whether students believe some types of plagiarism are more serious than others. The consequences of students' beliefs that plagiarism is a common practice and how institutions should address that are discussed.

A. Research Perspectives.

Plagiarism is a complex issue which has been studied using a variety of frameworks. Some research has focused on student characteristics that predict a greater likelihood of committing plagiarism, including levels of moral reasoning and self-esteem as well as achievement and motivation orientations (Angell, 2006; Rettinger & Kramer, 2009; Williams,

Nathanson, & Paulhus, 2010). This perspective attributes the decision to plagiarize to characteristics of the students, discounting outside factors that might contribute to the choice to plagiarize.

Other research has regarded incidents of plagiarism as being the result of teaching style (Barnas, 2000) or classroom culture (Brown, 2012; Feldman, 2001) indicating the cause of plagiarism originates outside the student. From these perspectives, instructors are seen as contributing to students' beliefs that they can submit another author's work as their own by not providing an adequate level of rigor in their classrooms or by not checking student work for plagiarism.

Engler et al. (2008), Hard et al. (2006), and the present study looked at plagiarism from the perspective of social/peer norms. According to social norms theory, individuals learn which behaviors are appropriate by observing the generally accepted behavior of others. For example, young adults have been found to overestimate the frequency of negative behaviors such as substance abuse by their peers, resulting in an inaccurate understanding of what is considered socially acceptable and an increase in those negative behaviors on their part (Berkowitz, 2004; Perkins, 2003; Perkins & Berkowitz, 1986). Based on this theory, if students have the misperception that acts of plagiarism are common among their classmates, and that consequences, if any, are minor, they are more likely to commit plagiarism themselves.

B. What is Plagiarism?

Many studies of plagiarism do not provide an operational definition of it, seeming to assume there is a one common understanding that does not need explication. Powers (2009) points out that this can affect research findings because students' self-reports of plagiarism are affected by an individual understanding of the practices that could be considered plagiarism. Further, faculty and students often disagree about exactly what constitutes plagiarism (Kwong et al., 2010). Definitions of plagiarism from several of the studies that provided one are listed below.

Definitions of plagiarism.

Belter & DuPre (2009): "One or more passages that was word-for-word the same as another source without appropriate citation and quotation marks." p. 259

Colnerud & Rosander (2009): "Using parts, or the whole, of a text written by another person without acknowledgement; submitting the same paper or parts of it, for credit in more than one course, falsification of information." p. 506

Hard, Conway, & Moran (2006): "Presenting, as one's own, the ideas or words of another person or persons for academic evaluation without proper acknowledgement." p. 1059

Park (2003): "Plagiarism involves literary theft, stealing (by copying) the words or ideas of someone else and passing them off as one's own without crediting the source." p. 472

Wang (2008): "Using somebody else's work (words and thoughts) without attribution." p. 743

Williams, Nathanson, & Paulhus (2010): "Any nonzero percentage detected by Turn-It-In (after screening)." p. 294

A common element across definitions is that plagiarism is the act of using another author's work without citation, thus portraying it as one's own work. Other common elements of definitions include descriptions of the length of the copied text, whether taking solely ideas from other authors is plagiarism, and the extent that the copied words were taken verbatim. For the present study a definition of plagiarism was developed that addressed these elements:

Plagiarism is representing another author's ideas or words as your own in course documents or electronic postings. This would include submitting an entire document by another author as well as using a portion of text or ideas from another author's work and not citing the source. This would include information obtained from the internet, from other students, and

from published and unpublished documents. This definition was provided to the students on the survey they completed.

C. Plagiarism along a Continuum.

Incidents of plagiarism are viewed along a continuum, with some incidents regarded as more serious than others (Blum, 2009; Hudd et al., 2009; Jones, 2011; Kwong et al., 2010, Salmons, 2007). Studies of faculty and student understandings of plagiarism have found that faculty view most types of plagiarism as more serious than students view them (Kwong et al., 2010). Jones (2011) found that while all students recognized submitting an entire document written by another author as plagiarism, students saw copying a limited amount of text as less serious. Seventy-five percent of students saw purchasing a paper online as plagiarism, 67% thought copying text verbatim without quotation marks was plagiarism, 50% saw paraphrasing text without citation as plagiarism, and 17% stated that students should not self-plagiarize by submitting the same work for assignments in different classes.

D. Student and Faculty Perceptions of Plagiarism Frequency.

Faculty and students tend to overestimate the frequency of student plagiarism (Engler et al., 2008; Hard et al., 2006; Wang, 2008). Students, in particular, see plagiarism as a common practice even though they report they have never plagiarized themselves (Wang, 2008). Students believe their friends are more likely to plagiarize than they are, but their friends are less likely to plagiarize than students they do not know (Engler et al., 2008; Kwong et al., 2010).

It is important to consider student overestimates of plagiarism by others because students' perceptions of peer behavior have a powerful effect on their own behavior (Hard et al., 2006; McCabe et al., 2001; Rettinger & Kramer, 2009). Both McCabe et al. (2001) and Rettinger and Kramer (2009) found that while there are a number of factors that predict cheating, knowing that other students have cheated has the greatest influence on a student's decision to cheat.

Even faculty, whose role it is to discover and address incidents of plagiarism, overestimate its occurrence, although to a lesser degree than students (Hard et al., 2006). An advantage to faculty overestimations of plagiarism is that it may make them more vigilant, benefitting students who do not plagiarize and who want it addressed (Kuther, 2003). Students generally appreciate instructors who can effectively monitor classroom learning and provide an appropriate level of rigor (Barnas, 2000). They want faculty to show respect for all students' efforts by not tolerating any form of cheating, including plagiarism – the most common form of cheating in higher education (Trost, 2009). Faculty can specifically mention in the course syllabus that submitting another author's work will not be tolerated, and the consequences if this happens, so students do not mistakenly believe that cheating will be ignored (Brown, 2012; Feldman, 2001). When incidents of plagiarism are uncovered, if faculty discuss the circumstances with the class, without disclosing the name of the student who plagiarized, they can show their vigilance when reviewing assignments and prevent additional incidents of plagiarism by students who thought it would be ignored (Feldman, 2001).

The research reported here is a part of a larger study that explored the scope and nature of plagiarism by students at a large urban college in order to determine the current extent of plagiarism there and how past institutional efforts to curb plagiarism were faring. These included implementation of an academic misconduct policy and use of plagiarism detection software.

The questions addressed in this report of the study are:

1. What is the frequency and nature of plagiarism admitted to by students?
2. What do students believe is the frequency and nature of plagiarism committed by

other students?

3. Do students view some types of plagiarism as more serious than others?
4. Do students believe that the types of plagiarism they view as more serious are more likely to be committed by other students?

II. Method.

A. Participants.

A survey was conducted at a large urban public comprehensive college with over ten thousand students, undergraduate and graduate, enrolled each year. An email was sent to all students, inviting them to complete the anonymous electronic survey and providing them with an internet link to it. The number of emails sent varied by department, but all students received at least one email. Information about the survey was also posted on the home page of the campus library website and on the webpage students use to access email, check grades, register for courses, and so forth. The data collection process was reviewed and approved by the college's institutional review board.

Of the 626 students who responded to the survey, 334 students reported that they had been enrolled in classes which had assignments that could have been plagiarized and completed the survey items analyzed in the present study. Assignments which could be plagiarized were described in the survey as writing assignments that included information that could have been obtained from another source and misrepresented as the student's own work. The 334 students included 194 undergraduates and 131 graduate students. Nine students did not report their student level. Respondents ages ranged from 18 years to 62 years, and almost 52% of the students had a self-reported grade point average over 3.5, on a scale of 0.0 to 4.0. Table 2 provides full demographic information about the sample.

B. Instrument.

The student survey asked respondents about their views and experiences regarding plagiarism and was developed by reviewing published studies on plagiarism, examining efforts to address plagiarism at institutions across the country, and discussing current concerns with administrators and faculty at the institution where the study was conducted. This report of the research will focus on three questions from the survey.

In the first of these questions, the students were asked to rate four types of plagiarism as *not at all serious*, *somewhat serious*, or *very serious*. The four types of plagiarism they rated were:

- Using ideas from another author's work and not citing the source
- Using phrases from another author's work and not citing the source
- Using sentences/paragraphs from another author's work and not citing the source
- Submitting an entire document by another author as your own work

In the second question, students were asked to indicate how often they thought students committed each of the four types of plagiarism in writing assignments. The response choices were *Never*, *Once*, *Rarely (Few of them)*, *Occasionally (Up to one-half of them)*, *Regularly (More than half of them)*, *Always (All of them)*.

The third question was the same as the second question, but asked each student to indicate how often they had committed each of the four types of plagiarism. The response choices were the same as those in the second question.

Student Characteristic	Percent (n)
Gender	
Male	32.6 (109)
Female	66.8 (223)
Gender not provided	0.6 (2)

Level	
Freshman	6.6 (22)
Sophomore	5.1 (17)
Junior	16.5 (55)
Senior	29.9 (100)
Graduate	39.2 (131)
Level not provided	2.7 (9)
Grade Point Average	
< 2.00	0.9 (3)
2.00 to 2.50	3.9 (13)
2.51 to 3.00	9.3 (31)
3.01 to 3.50	20.0 (67)
3.51 to 4.00	51.5 (172)
Grade point average not provided	14.4 (48)
Age	
< 20	75. (25)
20 to 25	51.2 (171)
26 to 30	13.1 (44)
> 30	18.9 (63)
Age not provided	9.3 (31)

Data analysis was carried out in two stages. In the first stage, descriptive statistics of the categorical and Likert-type scale survey responses were used to answer the first two research questions. In the second stage, the third and fourth research questions were answered using inferential z tests to determine if there were statistically significant differences in proportions of the sample who selected survey item responses. In each analysis the requirement of at least five cases for each of the two responses compared, to approximate a normal distribution, was met. A type-1 error rate of $\alpha = .05$ was used for all tests of significance. Odds ratios (OR) were used to determine the strength-of-effect for all significant results, with OR 1.50, 3.00, and 5.00 used to indicate small, medium, and large effect sizes, respectively (Chen, Cohen, & Chen, 2010). For ease of interpretation, all odds ratios were calculated so that a value greater than 1.00 would result (McHugh, 2009)

III Results

Table 3 shows the results for question 1: What is the frequency and nature of plagiarism admitted to by students? A majority of the respondents said they had *never* used another author's phrases (62.6%), sentences/paragraphs (82.3%), or entire piece of writing (96.4%). A majority of the students also reported that had either *never* or *once* used another author's idea and portrayed it as their own work (40.7% and 10.5%, respectively). As evident from the values in the table, there was a systematic decline in the admissions of plagiarism as the amount of text that was copied and the rate of occurrence increased. None of the students reported *always* committing plagiarism of any type and few to none reported plagiarizing *regularly* (0.0% to 3.9%).

Question: How often have you done the following, without citing the source?

Table 3. Survey question about how often respondent plagiarizes.

	Never Percent(n)	Once Percent(n)	Rarely Percent(n)	Occasionally Percent(n)	Regularly Percent(n)	Always Percent(n)
Used another author's ideas	40.7	10.5	32.6	12.3	3.9	0.0
	(136)	(35)	(109)	(41)	(13)	(0)
Used another author's phrases	62.6	10.8	18.6	6.6	1.5	0.0
	(209)	(36)	(62)	(22)	(5)	(0)
Used another author's sentences/paragraphs	82.3	6.6	7.2	3.0	0.9	0.0
	(275)	(22)	(24)	(10)	(3)	(0)
Used entire document by another author	96.4	0.0	2.7	0.9	0.0	0.0
	(322)	(0)	(9)	(3)	(0)	(0)

Table 4 provides information about question 2: What do students believe is the frequency and nature of plagiarism committed by other students? The majority of respondents believe that other students are either *occasionally* or *regularly* plagiarizing ideas and phrases (39.8% and 40.1%, 48.5% and 22.8%, respectively), and that other students are *rarely* or *occasionally* plagiarizing sentences/paragraphs or entire documents by other authors (40.7% and 34.7%, 49.1% and 9.6%, respectively). A small proportion of respondents reported they believe other students *always* commit each of the four types of plagiarism (1.2% to 3.6%). Overall, respondent's reports of their beliefs about other students' plagiarism do not show the systematic decline seen in the students' reports of their own plagiarism as the amount of work that was copied and the frequency increased.

Table 4. Survey question about how often other students plagiarize.

Question: How often do you think most students do the following, without citing the source?

	Never Percent(n)	Once Percent(n)	Rarely Percent(n)	Occasionally Percent(n)	Regularly Percent(n)	Always Percent(n)
Used another author's ideas	1.5	1.5	13.5	39.3	40.1	3.6
	(5)	(5)	(45)	(133)	(134)	(12)
Used another author's phrases	2.7	2.4	22.2	48.5	22.8	1.5
	(9)	(8)	(74)	(162)	(76)	(5)
Used another author's sentences/paragraphs	5.7	7.8	40.7	34.7	9.9	1.2
	(19)	(26)	(136)	(116)	(33)	(4)
Used entire document by another author	19.2	18.0	49.1	9.6	3.0	1.2
	(64)	(60)	(164)	(32)	(10)	(4)

IV. Discussion.

This study surveyed students at a large urban college to explore their beliefs about

plagiarism. Students were asked how often they commit plagiarism and how often they think other students commit plagiarism. They were also asked about how serious an incident they considered each of four types of plagiarism – using another author’s ideas, phrases, sentences/paragraphs, and submitting an entire document written by another author. Most of the students in the sample reported never committing plagiarism of any type and there was a systematic decline in the admissions of plagiarism as the amount of text that was copied and the frequency of occurrence increased. The participants indicated they believe that some types of plagiarism are more serious than others, with taking larger sections of text from another author seen as the more serious incidents of plagiarism. Still, even using another author’s ideas was believed to be at least somewhat serious by most students.

Informing students that instructors look for plagiarism in assignments and that there are consequences if it is discovered can help to deter students from plagiarizing and create an environment where it is clear that ethical behavior is valued. Reducing plagiarism provides benefits beyond an ethical education environment; it can also improve student learning. When students do their own work, instead of copying it from another author, they learn research and writing skills, and they learn the topic content of the papers they write. The long-term benefits of an academic environment where integrity and learning are cultivated cannot be overestimated.

It should be noted that the finding that students believe taking any amount of text is more serious than taking another author’s idea may be due to the order that the types of plagiarism were listed in the survey -- with taking ideas listed first, followed by taking increasing amounts of text. While it is clear that an increased amount of copied text – from phrases/sentences to paragraphs to an entire document – indicates a more serious incident of plagiarism, it is not as clear whether copying another author’s ideas is less or more serious than copying text. Course instructors, especially those who are published authors in their field, may believe that plagiarism of an original idea is more egregious. Students, who typically have no experience in professional writing, may not understand the value of developing a unique idea in a field of study and, therefore, see taking another author’s idea as less important than copying text.

References

- [1] Angell, L. R. (2006). The relationship of impulsiveness, personal efficacy, and academic motivation to college cheating. *College Student Journal*, 40(1), 118-131.
- [2] Barnas, M. (2000). “Parenting” students: Applying developmental psychology to the college classroom. *Teaching of Psychology*, 27, 276-277.
- [3] Belter, R. W., & DuPre A. (2009). A strategy to reduce plagiarism in an undergraduate course. *Teaching of Psychology*, 36(4), 257-261
- [4] Berkowitz, A. D. (2004). An overview of the social norms approach. In L. Lederman, L. Stewart, F. Goodhart and L. Laitman (Eds). *Changing the Culture of College Drinking: A Socially Situated Prevention Campaign* (187-208). New York, NY: Hampton Press.
- [5] Blum, S. D. (2009). *My word! Plagiarism and college culture*. Ithaca NY: Cornell University Press.
- [6] Brown, G. (2012). Student disruption in a global college classroom: Multicultural issues as predisposing factors. *Association of Black Nursing Faculty Journal*, 23(3), 63-69.
- [7] Chen, H., Cohen, P., & Chen S. (2010). How big is a big odds ratio? Interpreting the magnitudes of odds ratios in epidemiological studies. *Communications in Statistics – Simulation and Computation*, 39(4), 860-864.
- [8] Colnerud, G., & Rosander, M. (2009). Academic dishonesty, ethical norms, and learning. *Assessment and Evaluation in Higher Education*, 34(5), 505-517.

THE INDIAN EDUCATION SYSTEM

P. Suruthi¹, K. Sivaranjani²

¹ Student, IFET College of Engineering, Villupuram

² Assistant Professor of English, IFET College of Engineering- Villupuram

Abstract The best thing in everyone's life is the education. The blooming youngsters without any knowledge of education will really feel hard to invent newfangled technologies. The creativity of the students can disentangle technical issues, communicate and envisage without basic knowledge. Even operating lovely mobile phones then it would be a great task. "India being an emergent country and having an optimum rank in education among other countries can accomplish great heights in science and technology. A slight renovation in education method can create a mind-boggling revolution in education.

Key words: blooming youngsters, newfangled technologies, renovation, mind-boggling revolution

INTRODUCTION

This article proposed the alterations needed in an Education structure of India – its contribution, functions, challenges and the makeover needed. Our education system is not a weak one. The Education system in India is competitive and trains students austerely to withstand fierce competition on an international extent. We must admit that our scholars are on a par with most of the students abroad. Indians are a power to reckon with due to their absolute talent and efficiency, and this can be attributed to their rigorous training at school and college degree. The problem is always a problem; if we are not going to confer about it we don't discover the solution. Tackling and solving the minor problem in our education system may put our India first across the globe! Indians are basically "Hardworking" and that is the main reason why there are many famous Indians in Different Field. To start with positive notes there are many merits of Indian education which are not guessed before like learning a great deal of subjects, having tests, etc. Imagine the power of the Indian education long back which attracted students from Egypt, Greece, China, Ceylon and Indonesia. There is a demand in revising the syllabus periodically to make it interesting for scholars, which is really a great thing. In Modern day education is aided with a variety of technology, computers, projectors, internet, and many more. Diverse knowledge is being spread among the people. Everything that can be simplified has been made simpler. Science has explored every aspect of life. There is much to learn and more to assimilate. There is no end to it. One can learn everything he wishes to. Every topic has developed into a subject.

The most awful part is that, our education system is too much information and leaves only a little scope of creativity, inventions and self-learning. Even an infant would say "we lag in practical knowledge." This is the most frequent answer anybody would give. If we stress more on education, there will arise a criticism, stating that we give preference only to books and not to sports and extra-curricular activities. Gosh! I feel the education department must be pitied. It is also miserable that the political causes does harm the education system to a great extent. The Education of an individual forms a nation and thus dramatic changes in the system also lead to

social issues. Since nothing is impossible we should really work hard to develop our education system, “better late than never.”

EDUCATION

Education is the imparting and acquiring of knowledge through teaching and learning, especially at a school or similar institution. Before the invention of reading and writing, people lived in an environment in which they struggled to survive against natural forces, animals, and other humans. To survive, preliterate people developed skills that grew into cultural and educational patterns. Education developed from the human struggle for survival and enlightenment.

ORIGIN OF INDIAN EDUCATION SYSTEM

It’s so mean to talk about origin nowadays. But for everything that is happening now had a cause in the past. Hence brushing up with the origin, it really takes back to the teaching of traditional elements such as Indian religions, Indian mathematics, Indian logic at early Hindu and Buddhist Centre’s of learning such as Taxila (in modern-day Pakistan) and Nalanda (in India) before the common era. Islamic education became ingrained with the establishment of the Islamic empires in the Indian subcontinent in the middle ages while the coming of the Europeans later brought western education in colonial India.

A series of measures continuing throughout the early half of the 20th century ultimately laid the foundation of education in the Republic of India, education in Pakistan and much of South Asia. The past cannot be changed, but the future can be made for the better, so focused on the colonial era- present, let’s discuss its functions, contributions, challenges and makeover needed for a fabulous Indian Education system. The British established English education in the colonial era to improve modernization and to reduce administrative charges.

TYPES OF EDUCATION SYSTEM

1. Informal education
2. Formal education

Informal education refers to the general social process by which human beings acquire the knowledge and skills needed to function in their culture.

Formal education refers to the process by which teachers instruct students in courses of study within institutions.

The informal education doesn’t cause any imbalance, but the formal education does. Due to the imbalance in the formal education there arises the need to improve the existing education system. I guess this is also due to the improper implementation of the formal education. Let us discuss in detail about the “formal education”.

TYPES OF FORMAL EDUCATION

1) **Pre-primary education in India:** Pre-primary school education in India is not a fundamental right and, is divided into two levels – Lower KG (for children between 3 – 4 years) and Upper KG (for children between 4 – 5 years).

2) **Primary Education in India:** This serves as the link between primary school and elementary education. However, not much emphasis is laid on this level by the prevailing education system and policies in this regard continue to exist solely on paper.

3) **Elementary Education:** The Government has made elementary education compulsory for children between the age group of years 6 and 14.

4) **Secondary Education in India:** Serves as a link between elementary and higher education in the Indian education setup, which draws a blank again as far as policy is concerned.

5) **Higher Education in India:** Undergraduate and postgraduate level: After completion of secondary education, students can choose fields of their interest and pursue undergraduate and then post graduate courses.

At this point there also arises a partition stating public schools and private schools. The functioning of these schools largely depends on the following factors:

1. The medium of language
2. Fees
3. Syllabus structure
4. Availability of tutors
5. "STATUS OF THE STUDENTS"

The gloomiest part is education is considered as a business and the poor students and their parents are the victims. The improvement of the colonial education had developed IIT's and IIM's. That was the maximum improvement it could attain.

FUNCTIONING OF THE EXISTING EDUCATION SYSTEM

The children enter their PRE-KG at the age of 3 or even at 2.5 years where they are just allowed to play. The invention in technology nowadays has peeped in, where the basics of alphabets and numbers are taught. Poor child! Why does it need this at this early stage??? The parents are entirely responsible for such an awful act. The only have the motive of making their child first in their primary education. This "URGE TO MAKE THEIR CHILDREN FIRST", is actually the main problem which is degrading the Indian education system.

The child grows with fewer amounts of opportunities to prove his/her talent in the primary education. But not the worse they have fewer classes which improves their creativity. We should really acknowledge the schools that are practicing this even today. Yet problem arises when the balance between creativity and studies is lost.

The secondary education in 90% of the schools has the motive to make the children bookworm. This is because the results of the board exams decide the future of the students. In many schools as of now they really concentrate on the +2 exams or 2nd year HSC and skip the 1st year HSC portions which are actually the basics for the succeeding year. I really wonder where the system is up to. The higher secondary education in turn helps the student to choose their desired degree in higher education. The higher education in turn does not relate solely with the job they do in future. They require only 5% of the basic knowledge imparted in their higher education. Last but not the least, the different forms of syllabus systems also plays a vital role in this function.

TECHNOLOGY USED IN THE EXISTING SYSTEM

An extreme use of smart class technology is used in imparting education to students in primary and mid-secondary level. The students of higher secondary levels use only “books”.

DEFECTS OF THE EXISTING SYSTEM

The fundamental drawbacks of the current education system are as follows:

1. Education System Promotes Rat Race

Our education system basically promotes rat race among our children. They have to read and mug-up entire text book without any understanding of it. So a student who scores 90 out of 100 and comes first actually remains a rat. He or she does not have any analytical skills that a child must have except in a few cases where the student gains knowledge as well.

2. Education Does Not Builds Persona of a Child

Unfortunately, our education system is not helping to develop persona of a child. Remember, it is a personality that is more important than academic qualifications. Our system demands good numbers of a child in an exam not to show his personality. Hence a child is not well exposed to the outer world and he or she might not be able to develop a personality. So this is another flaw in our education system.

3. No Critical Analysis, only Following the Establishment

The children are not able to do critical analysis of anything, for example, our history, culture and religion. They take the line of establishment or the views of predominant majority. They are simply not able to look things from their own perspective. If you want a society should become a lot better, then we must develop a culture of looking at things critically. We are simply failing at this because of our education system. Children must learn to criticize our own culture and other established narratives.

4. Too Much Parochialism Rather Global Outlook

Our education teaches too much of nationalism and it could create a negative mindset in our younger generation. Loving your country is a good thing, but just blind love is dangerous. Our school children are not able to get a global outlook. It means how to see yourself that you are actually a global citizen rather confined to a place or a country.

5. Enhancement of Teachers is needed

To make things worse, our teachers themselves are not sufficiently trained in some areas to teach the kids. The government must identify the training needed area and train the staff members to enhance the level. Hence, to improve our education system teachers should be better trained and more importantly better paid.

6. Medium of Language of our Education System

This is also a big problem that needs to be addressed. We are not able to decide on the medium of language of our education system. The medium should be set standard throughout the country since it will help the students to a large extent.

7. Education Given is Irrelevant to Job-Market

This is perhaps the most apparent failure of our education system that after completing graduation in any discipline students are not able to get jobs. It is simply because the skills that are required in a job market are simply not present in a fresh graduate. All that a student is taught in his entire school and college life is almost redundant for job markets. Skill that is required by them is not taught in schools and colleges. Hence our education system is needed to be revamped and must be designed according to our economic policies.

8. Missing Innovation & Creation because Only Aping West

Though the privileged children in India are not even able to innovate and create new things. Although they have everything that a child need, but still they lack something in them. What they are doing is only aping western culture and not being able to do something new. On the one hand, children are not able to go to school and on the other hand, if they are going then are not able to innovate or solve the problems that the country is facing. Hence, this is yet another fundamental problem with our education system.

9. Students Happy in Getting a Highly Paid Salary Job but Lacks Ambition to Become Entrepreneur

Now, in college campuses it has become a common thing that every young student is interested in a getting a job that pays them well. However, they would never like to become an entrepreneur. This lack of ambition does not allow our country to excel in any field. This attitude of our children making them slaves of a few multinational companies. Therefore, our education system should be designed to make our children a successful entrepreneur rather going for a salaried job. They must believe in “INVENT IN INDIA RATHER THAN MADE IN INDIA”.

10. Gross Failure of Our Education System to End Social Disparity

The failure of our education system is after so many years, it has not been able to reduce social disparity in our country. In fact, social disparity has gone up. It is such a shame that education itself has become a tool for creating divisions. A child of a rich parent would get a good education and a child of poor parent cannot afford even a basic education. Government should intervene and make education its prime responsibility.

11. Variety in education streams

Why do we always see students being envious of their counterparts in the USA?

It's because there are just three options that students have after Class 10 – they're stuck with Science, Arts or Commerce. If they're not good enough for either of these, they jet set straight into diplomas and certificate courses. Don't you think the Indian education system needs to introduce combination courses in which students can opt for a major and a minor subject? If students in America can pursue Physiotherapy with Art History and Biological Science with Photography, **why not in India?**

12. The system of tuition classes

The system of tuition classes

Commenting on this subject is like plunging one's hand into a vicious cycle which seems to have no beginning or end. Reasons for tuition classes mushrooming are because students say that the teaching in schools is lax and not good enough for them to clear exams. Whereas teachers say that students jump ahead many chapters in the tuition classes before they are even taught in the school, this makes them lose all motivation and steam to attend school in the first place. Forget all of this, what about the poor parent whose hard earned salary is spent at school and tuition fees alone?

13. Same old concepts

The same old concepts must be changed in the trending society. Learning the detailed description of the same old concept during the early 60's and 70's when the technology is at its peak is an utter waste.

14. Too easy question papers and evaluation plan

To specify the question papers of the present 10th standard syllabus are too easy to crack the exam. The result is too many state ranks. Example: The numbers of state rankers in 2014-2015 exams in Tamil Nadu were 41 got 499/500 and got state first rank, 192 students got 498/500 and got state second rank and 540 students got state third by scoring 497/500. The criticism for such results in social media states that the worth of state ranks have gone down.

MAKEOVER NEEDED

a. Focus on, skill based education

Our education system is geared towards teaching and testing knowledge at every level as opposed to teaching skills. "Give a man a fish and you feed him one day, teach him how to catch fishes and you feed him for a lifetime." I believe that if you teach a man a skill, you enable him for a lifetime. Knowledge is largely forgotten after the semester exam is over. Still, year after year Indian students focus on cramming information. So they must be made to understand whatever they learn and utilize it in their activity.

b. Reward creativity, original thinking, research and innovation

Our education system rarely rewards what deserve highest academic accolades. Deviance is discouraged. Risk taking is mocked. Our testing and marking systems need to be built to recognize original contributions, in the form of creativity, problem solving, valuable original research and innovation. If we could do this successfully Indian education system would have changed overnight. Memorizing is no learning; this biggest flaw in our education system must be rectified.

c. Get smarter people to teach

For way too long teaching became the sanctuary of the incompetent. Teaching jobs are until today widely regarded as safe, well-paying, risk-free and low-pressure jobs. Thousands of terrible teachers all over India are wasting valuable time of young children every day all over India. It is high time to encourage a breed of superstar teachers. The internet has created this possibility – the performance of a teacher now need not be restricted to a small classroom. Now the performance of a teacher can be opened up for the world to see. The virtuous teacher will be more popular, and acquire more students. That's the way of the future. Read here about why I

think that we are closing on to the age of rock-star teachers. We need leaders, entrepreneurs in teaching positions, not salaried people trying to hold on to their mantle.

d. Implement massive technology infrastructure for education

India needs to embrace the internet and technology if it has to teach all of its huge population, the majority of which is located in remote villages. Now that we have computers and internet, it makes sense to invest in technological infrastructure that will make access to knowledge easier than ever. Instead of focusing on outdated models of brick and mortar colleges and universities, we need to create educational delivery mechanisms that can actually take the wealth of human knowledge to the masses. The tools for this dissemination will be cheap smartphones, tablets and computers with high speed internet connection. While all these are becoming more possible than ever before, there is a lot of innovation yet to take place in this space.

e. Re-define the purpose of the education system

Our education system is still a colonial education system geared towards generating pen-pushers under the newly acquired skin of modernity. We may have the most number of engineering graduates in the world, but that certainly has not translated into much technological innovation here. Rather, we are busy running the call Centre's of the rest of the world – that is where our engineering skills end. The goal of our new education system should be to create entrepreneurs, innovators, artists, scientists, thinkers and writers who can establish the foundation of a knowledge based economy rather than the low-quality service provider nation that we are turning into.

f. Effective deregulation

Until today, an institute of higher education in India must be operated on a not-for profit basis. This is discouraging for entrepreneurs and innovators who could have worked in these spaces. On the other hand, many people are using education institutions to hide their black money, and often earning a hefty income from the education business through clever structuring and therefore bypassing the rule with respect to not earning a profit from recognized educational institutions. As a matter of fact, private equity companies have been investing in some education service provider companies which in turn provide services to not-for-profit educational institutions and earn enviable profits. Sometimes these institutes are so costly that they are outside the reach of most Indian students. There is an urgent need for effective de-regulation of the Indian education sector so that there is infusion of sufficient capital and those who provide or create extraordinary educational products or services are adequately rewarded.

g. Take mediocrity out of the system

Our education system today encourages mediocrity – in students, in teachers, throughout the system. It is easy to survive as a mediocre student, or a mediocre teacher in an educational institution. No one shuts down a mediocre college or mediocre school. Hard work is always tough; the path to excellence is fraught with difficulties. Mediocrity is comfortable. Our education system will remain sub-par or mediocre until we make it clear that it is not ok to be mediocre. If we want excellence, mediocrity cannot be tolerated. Mediocrity has to be discarded as an option. The life of those who are mediocre must be made difficult, so that excellence will prevail.

h. Personalize education – one size does not fit all

Assembly line education prepares assembly line workers. However, the drift of the economic world is away from the assembly line production. The Indian education system is built on the presumption that if something is good for one kid, it is good for all kids. Some kids learn faster, some are comparatively slow. Some people are visual learners, others are auditory learners, and still some others learn faster from experience. If one massive monolithic education system has to provide education to everyone, then there is no option but to assume that one size fits all.

If, however, we can effectively decentralize education, and if the government did not obsessively control what would be the “syllabus” and what will be the method of instruction, there could be an explosion of new and innovative courses geared towards serving various niches of learners, take for example, the market for learning dancing. There are very different dance forms that attract students with different tastes.

More importantly, different teachers and institutes have developed different ways of teaching dancing. This could never happen if there was a central board of dancing education which enforced strict standards of what will be taught and how such things are to be taught. Central regulation kills choice, and stifles innovation too. As far as education is concerned, availability of choices, de-regulation, profitability, entrepreneurship and emergence of niche courses are all interconnected.

i. Allow private capital in education

The government cannot afford to provide higher education to all the people in the country. It is too costly for the government to do so. The central government spends about 4% of budget expenditure on education, compared to 40% on defense. Historically, the government just did not have enough money to spend on even opening new schools and universities, forget overhauling the entire system and investing in technology and innovation related to the education system. Still, until today, at least on paper only non-profit organizations are allowed to run educational institutions apart from government institutions.

Naturally, the good money, coming from honest investors who want to earn from honest, but high impact businesses do not get into the education sector. Rather, there are crooks, money launderers and politicians opening “private” educational institutions which extract money from the educational institution through creative structuring. The focus is on marketing rather than innovation or providing great educational service – one of the major examples of this being IIPM. Allowing profit making will encourage serious entrepreneurs, innovators and investors to take interest in the education sector. The government does not have enough money to provide higher education of reasonable quality to all of us, and it has no excuse to prevent private capital from coming into the educational sector.

j. Make reservation irrelevant

We have a reservation in education today because education is not available universally. Education has to be rationed. This is not a long –term solution. If we want to emerge as a country build on a knowledge economy, driven by highly educated people, we need to make good education so universally available that reservation will lose its meaning.

k. Education reservation India

There is no reservation in online education – because it scales. Today top universities worldwide is taking various courses online, and today you can easily attend a live class taught by a top professor of Harvard University online if you want, no matter which country is belongs to. This is the future, this is the easy way to beat reservation and make it inconsequential.

CONCLUSION

Thus, I hope, of overcoming the flaws of the existing system will really result in stronger and developed India. Solving a problem at its peak is really hard. So let's start developing India into a developed country from the basic step of imparting quality education with more practical analysis to people of all walks of life.

Reference

- [1] https://www.britishcouncil.in/sites/default/files/indian_school_education_system_-_an_overview_1.pdf
- [2] History of Indian education system by Y.K. Singh
- [3] Issues in Indian education by M.L. Dhawan
- [4] *The Times of India*.
- [5] "Indian Education: creating Zombies focussed on passing exam".
- [6] "Rote system of learning still rules the roost". ExpressIndia. 2008.[dead link]
- [7] "Reality Check for Parents: Preschools in India – Reviews, Top, Compare, List, Good". Preschool for Child Rights. Retrieved 23 January 2014.[dead link]
- [8] "44 institutions to lose deemed university status – Economy and Politics". livemint.com. 18 January 2010. Retrieved 1 September 2010.
- [9] "22 universities across India fake: UGC". Express India.
- [10] "Country Strategy for India (CAS) 2009–2012" (PDF). World Bank.
- [11] Education in India – Problems and their solutions, www.careerride.com › Topics › Civil Services
- [12] ""Higher Education", National Informatics Centre, Government of India". Education.nic.in. Retrieved 2010-09-01.
- [13] "Latest Statistics on Indian Higher Education". DrEducation.com. 2012-07-17. Retrieved 2012-08-28.
- [14] "Central Universities". ugc.ac.in. Retrieved 6 June 2011.
- [15] "List of State Universities" (PDF). 27 May 2011. Retrieved 2011-06-06.
- [16] "Deemed University - University Grants Commission :::". ugc.ac.in. 23 June 2008. Retrieved 6 June 2011.
- [17] "Global Education". University Analytics. Retrieved 10 December 2015.
- [18] "Indian schools dwarfed in global ratings programme". Indian Express. Retrieved 15 August 2014. August 2014.
- [19] "Indian education: Sector outlook" (PDF). Retrieved 23 January 2014.
- [20] Enrolment in schools rises 14% to 23 crore The Times of India (22 January 2013)
- [21] Sharath Jeevan & James Townsend, Teachers: A Solution to Education Reform in India Stanford Social Innovation Review (17 July 2013)
- [22] B.P. Khandelwal, Examinations and test systems at school level in India UNESCO, pages 100-114
- [23] Indian Education System: What needs to change?
- [24] "National Policy on Education (with modifications undertaken in 1992)" (PDF). National Council of Educational Research and Training. Retrieved 10 December 2012.
- [25] Secondary Education. Education.nic.in. Retrieved on 21 March 2011. Archived 22 July 2009 at the Wayback Machine.

GENERATION OF ELECTRICITY FROM ALGAE

M.Elumalai

Final Year – Eee, Aktmcet, Elumalai2394@Gmail.Com

Abstract— The algae is biological material that consist of biotic characteristics and put in glass cylinders or cylindrical cistern where water, carbon dioxide, and sun light can trigger photosynthesis. The subsequent biomass will be treated further to produce a fuel to turn turbines. The carbon dioxide produced in the process will be fed back to the algae, resulting in zero emissions from the plant.

Keyword- water, carbon dioxide, light energy, photosynthesis reaction, biomass, energy.

I. INTRODUCTION

This technologies which are getting more and more heed is bio-energy from algae material. global warming, high oil prices and emphasis in renewable technology are draw towards oneself new interest in a potentially rich source of biofuels that is algae. Currently no alternative technology seems to be able to entirely replace our enormous energy demands. Yet, we need new technologies to provide us the energy we need. Algae can contain up to 40% oil, they can grow in wastewater and in live places where no agriculture is possible. They are able to grow very fast and they even capture large amounts carbon dioxide while doing so. These facts look very pledging for use of algae in bio energy.

II. PHYSIOGNOMIES OF ALGAE

The algae are an antique group of aquatic plants. There are supposed to be about 23,000 class of algae. The algae have three features which differentiate from other plants, namely their body plant and reproductive system. There is no specialization of the algae body into root, system, leaves with vascular flesh. The photosynthetic portion of the alga is a thallus while the attachment portion comprises hair. For most algae, sperm and eggs fuse in the open water and the zygote develops into a new plant without any protection. For other plant groups the zygote develops into an beginning within the protection of the parent plant. The gametes are produced within a single cell. There is no cover of antiseptic cells protecting the gametes.

APPROACHES OF ALGAE GROWTH

There are some important factors that determine the growth rate of algae

- Type of algae: different types of algae have different growth rates
- Nutrients/Medium: composition of the water
- pH: algae need a pH between 7 and 9 to have an optimum growth rate
- Light energy: Sun light is needed for the photosynthesis process
- Aeration: the algae need to have contact with (CO₂)
- Mixing: mixing prevents sedimentation of algae and makes sure all cells are equally exposed to light
- Temperature: there is an ideal temperature for algae to grow.

III. RACEWAY POND

The 'raceway pond' is a large open water raceway track where algae and nutrients are pumped around by a motorized paddle. Carbon dioxide also has to be added to the pond. The algae culture will grow continuously and part of the algae will be removed during the growing process. The biggest advantage of these open ponds is their simplicity, yielding low production costs and low operating costs. However, not all algae species can be grown in these ponds, due to contamination of other algae and bacteria. Also the process conditions, like temperature and the amount of light, are hard or impossible to control.



Figure 1. Raceway pond.

IV. PHOTO BIOREACTOR

The photo bioreactor is a closed tube method. The number of tube connected as parallel in inside of the room and we are making hole on the wall. The light energy passes through the hole, on the tube setup so the photosynthetic reaction developed. From this method we can generate low energy as comparatively and this method require less space.

Here, the number of tubes arranged in parallel manner and that connected with other tube by the external electrical circuit. The example can shown in *Figure 2. photo bioreactor.*



Figure 2. photo bioreactor

V. METHANE FROM ANAEROBIC DIGESTORS

Methane is a gas that contains molecules of methane with one atom of carbon and four atoms of hydrogen (CH₄). It is the major component of the "natural" gas used in many homes for cooking and heating. It is odorless, colorless, and yields about 1,000 British Thermal Units (Btu) [252 kilocalories (kcal)] of heat energy per cubic foot (0.028 cubic meters) when burned. Natural gas is a fossil fuel that was created eons ago by the anaerobic decomposition of organic materials. It is often found in association with oil and coal. The same types of anaerobic bacteria that produced natural gas also produce methane today. Anaerobic bacteria are some of the oldest forms of life on earth. They evolved before the photosynthesis of green plants released large quantities of oxygen into the atmosphere. Anaerobic bacteria break down or "digest" organic material in the absence of oxygen and produce "biogas" as a waste product. (Aerobic decomposition, or composting, requires large amounts of oxygen and produces heat.) Anaerobic decomposition occurs naturally in swamps, water-logged soils and rice fields, deep bodies of water, and in the digestive systems of termites and large animals. Anaerobic processes can be managed in a "digester" (an airtight tank) or a covered lagoon (a pond used to store manure) for waste treatment. The primary benefits of anaerobic digestion are nutrient recycling, waste treatment, and odor control. Except in very large systems, biogas production is a highly useful but secondary benefit. Biogas produced in anaerobic digesters consists of methane (50%-80%), carbon dioxide (20%-50%), and trace levels of other gases such as hydrogen, carbon monoxide, nitrogen, oxygen, and hydrogen sulfide. The relative percentage of these gases in biogas depends on the feed material and management of the process. When burned, a cubic foot (0.028 cubic meters) of biogas yields about 10 Btu (2.52 kcal) of heat energy per percentage of methane composition. For example, biogas composed of 65% methane yields 650 Btu per cubic foot (5,857 kcal/cubic meters).

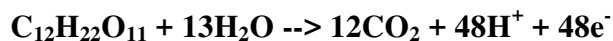
VI. DIGESTION PROCESS

Anaerobic decomposition is a complex process. It occurs in three basic stages as the result of the activity of a variety of microorganisms. Initially, a group of microorganisms converts organic material to a form that a second group of organisms utilizes to form organic acids. Methane-producing (methanogenic) anaerobic bacteria utilize these acids and complete the decomposition process. In the thermophilic range, decomposition and biogas production occur more rapidly than in the mesophytic range. However, the process is highly sensitive to disturbances such as changes in feed materials or temperature. While all anaerobic digesters reduce the viability of weed seeds and disease-producing (pathogenic) organisms, the higher temperatures of thermophilic digestion result in more complete destruction. Although digesters operated in the mesophilic range must be larger (to accommodate a longer period of decomposition within the tank [residence time]), the process is less sensitive to upset or change in operating regimen.

To optimize the digestion process, the digester must be kept at a consistent temperature, as rapid changes will upset bacterial activity. In most areas of the United States, digestion vessels require some level of insulation and/or heating. Some installations circulate the coolant from their biogas-powered engines in or around the digester to keep it warm, while others burn part of the biogas to heat the digester. In a properly designed system, heating generally results in an increase in biogas production during colder periods. The trade-offs in maintaining optimum digester temperatures to maximize gas production while minimizing expenses are somewhat complex. Studies on digesters in the north-central areas of the country indicate that maximum net biogas production can occur in digesters maintained at temperatures as low as 72°F (22.2°C).

VII. GENERATING ELECTRICITY

When micro-organisms consume a substrate such as sugar in aerobic conditions they produce carbon dioxide and water. However when oxygen is not present they produce carbon dioxide, protons and electrons as described below



Microbial fuel cells use inorganic mediators to tap into the electron transport chain of cells and steal the electrons that are produced. The mediator crosses the outer cell lipid membranes and plasma wall; it then begins to liberate electrons from the electron transport chain that would normally be taken up by oxygen or other intermediates. The now-reduced mediator exits the cell laden with electrons that it shuttles to an electrode where it deposits them; this electrode becomes the electro-generative anode (negatively charged electrode). The release of the electrons means that the mediator returns to its original oxidized state ready

to repeat the process. It is important to note that this can only happen under anaerobic conditions, if oxygen is present then it will collect all the electrons as it has a greater electronegativity than the mediator.

Table 1. The voltage & current of single MFC

This is the principle behind generating a flow of electrons from most micro-organisms. The organisms capable of producing an electric current are termed Exoelectrogens. In order to turn this into a usable supply of electricity this process has to be accommodated in a fuel cell so that it creates a complete circuit, not just shuttles electrons to a single point. In the second chamber of the MFC is another solution and electrode. This electrode, called the cathode is positively charged and is the equivalent of the oxygen sink at

Anode	Cathode	Voltage (vot)	Current (mA)
Carbon fabric	Carbon fabric	0.1	0.3
Carbon fabric	Carbon fabric	0.2	0.5
Carbon fabric	Aluminium	0.4	0.6
Carbon fabric	Aluminium	1.1	2.0
Carbon fabric	Aluminium	0.6	1.5
Aluminium	Aluminium	1.0	1.6

the end of the electron transport chain, only now it is external to the biological cell. The solution is an oxidizing agent that picks up the electrons at the cathode. As with the electron chain in the yeast cell, this could be a number of molecules such as oxygen. However, this is not particularly practical as it would require large volumes of circulating gas. A more convenient option is to use a solution of a solid oxidizing agent.

Connecting the two electrodes is a wire (or other electrically conductive path which may include some electrically powered device such as a light bulb) and completing the circuit and

connecting the two chambers is a salt bridge or ion-exchange membrane. This last feature allows the protons produced, to pass from the anode chamber to the cathode chamber.

The reduced mediator carries electrons from the cell to the electrode. Here the mediator is oxidized as it deposits the electrons. These then flow across the wire to the second electrode, which acts as an electron sink. From here they pass to an oxidizing material.

VIII. ADVANTAGES

One of the biggest advantages of using algae as a source for methane is the fact that the total process is neutral with regard to carbon dioxide. With an increasing focus on environmental friendliness this could point out to be the most important advantage. Also the fact that algae can use carbon dioxide and other flue gasses to grow makes them a very interesting subject of research. Furthermore, algae are a sustainable source of energy. Furthermore all conditions for algae to grow fast are present in abundance: feedstock in the form of carbon dioxide and water and energy source in the form of sunlight. A second advantage is the fact that algae are highly efficient converters of solar energy to biomass, compared to crops or trees. It is possible for algae to use almost 10% of the incoming sunlight for the photosynthesis process. This makes it possible to get a high biomass output per square meter per day. A third advantage is that some algae grow in water and not on land. If grown in traditional lakes, or even salty waters, they don't compete with other sources for biomass.

IX. CONCLUSION

At this moment it is commercially not viable to produce methane from algae. Cheap algae can be produced by open pool systems, but they need a too large surface to replace fossil fuels. Bioreactors need about ten times less surface to produce the algae, but the costs for these systems are far higher. A lot of technological progression has to be made in order to make power generation from algae feasible. Initial focus of research should be on growing mass cultures of algae efficiently. By genetic engineering more productive species and species that are more suitable for open pond systems should be created.

REFERENCES

- [1] Yang Fei Qiu Yejing Wu Wei, Rong fei Lin Wang Keshu, "Energy From Microbial Fuel Cell constructed of Algae From lake Taihu", "Third International Conference on measuring Technology and Mechatronics Automation", DOI 10.1109/.2011.298, pp 45-47, Jul 2011
- [2] Salman Habib, Arif haque, Jubeyar Rahman, "Production of MHD Power from Municipal Waste & Ajgal Biodiesel", "Third International Conference on measuring Technology and Mechatronics Automation", 978-1-4673-2729, 9/12/2012
- [3] L. H. Meyer *et al.*, "A study of algae energy generation progression", "International journal of Research and development", Oct. 2011 pp.398-402,
- [4] I. Ramirez, R. Hernandez, and G. Montoya, "Alternative energy generation using algae", "International journal of Research and development for Measurement and instrumentation", vol.28, no.4, pp.29-34 Jul/Aug 2012.

Gso Based Load Frequency Controller For Single Area Power System

K.Sriram¹ G. Gnana Sundari² B. Dhivya Bharathi³

^{1,2}*Department of Electrical and Electronics Engineering St. Anne's College of Engineering and Technology Panruti, Tamilnadu*

Abstract - The Load Frequency Control (LFC) in power systems is required for supplying good quality reliable electric power. The purpose of the LFC is to maintain the frequency constant. Conventional Proportional Integral (PI) and Proportional Integral and Derivative (PID) controllers are used in the LFC. The controller parameters K_c , K_i and K_d are tuned to accomplish LFC to have minimum error and minimum overshoot according to the system dynamics with respect to the load. In this paper, the control of the load frequency in a single area power system with different controllers is discussed. Comparison of the conventional PI, PID controllers and the proposed GSO-PID was made for a step change in load. Simulation results demonstrate that the proposed controller (GSO-PID) adapts itself appropriately to varying loads and hence provides better performance with respect to settling time, overshoot and undershoot. The effectiveness of the proposed scheme is confirmed by using MATLAB-Simulink.

Key words- Load Frequency Control, Proportional Integral, Proportional Integral Derivative, Particle Swarm Optimization.

I. INTRODUCTION

The main objective of a power system is to maintain continuous quality supply to the consumers in the system. These qualities of the power system are denoted by three parameters such as the frequency, the voltage and the reliability. For better performance and reliability two or more systems are interconnected through a tie-line. The main objective of a power system is to maintain continuous quality supply to the consumers in the system.

These qualities of the power system are denoted by three parameters such as the frequency, the voltage and the reliability. For better performance and reliability two or more systems are interconnected through a tie-line. The power system will be in equilibrium until there is a change in the power demand or the power generated. The load change in one system can affect the performance of the remaining systems. If the power demand is more than the generated power, system frequency will decrease and vice-versa, i.e. the real power of the system varies. Whereas changes in the voltage due to load variation, affects the reactive power.

In order to maintain the power balance in the system, both the real power and the reactive power balance is to be balanced. The real power can be achieved by the LFC (frequency) while the reactive power balance can be achieved by the Automatic Voltage Regulator (voltage).

The growing needs of the complex and the huge modern power systems require an optimal and flexible operation. The dynamic and static properties of the system must be well known to design an efficient controller. As the dynamic behavior, even for a reduced mathematical model of a power system is usually nonlinear, time variant and governed by strong cross-couplings of the input variables, special care has to be taken in the design of the controllers.

For this reason, recently, a lot of artificial intelligence based robust controllers such as the genetic algorithm, the tabu search algorithm; the fuzzy logic and the neural networks are used for tuning the parameters of the PID parameters in the LFC by authors [5, 6, 7]. The Group Search Optimization (GSO) algorithm is an optimization method that finds the best parameters for the controller in the uncertainty area of controller parameters.

In this study, the GSO is used to determine the parameters of a PID controller according to the changes of the system dynamics with the load. A comparative study is made between the conventional PI, the PID and the GSO tuned PID controller for a single area power system and by adjusting the maximum and minimum values of proportional (K_c) and integral (K_i) gain, the response of the system can be improved. In this simulation study, the K_c is made equal to a regulation constant "R" to obtain robustness, and it is shown that the overshoots and settling times with the proposed GSO-PID controller are lesser than the outputs of the other controllers.

II. LOAD FREQUENCY CONTROLLER

The objectives of the LFC are to maintain reasonably uniform frequency, to divide the load between the generators, and to control the tie-line interchange schedules. The single area power system consists of a governor, a turbine and a generator with the feedback of the constant regulation. A step load change in demand is fed to the generator.

The dynamic model of a single area power system is carried out in this section. Each area of power system consists of a speed governor, a turbine and a generator. For simplicity, the final derived transfer function is represented for each block of the system and shown in figure 1.

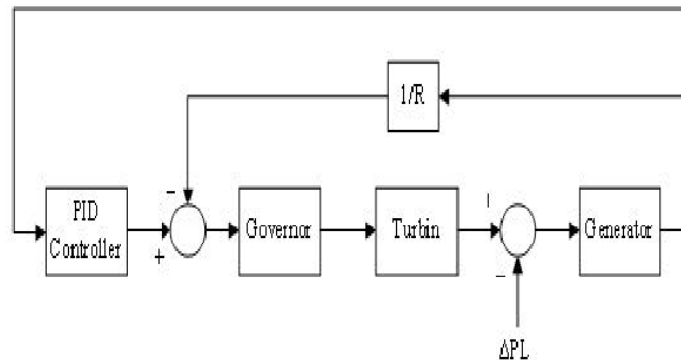
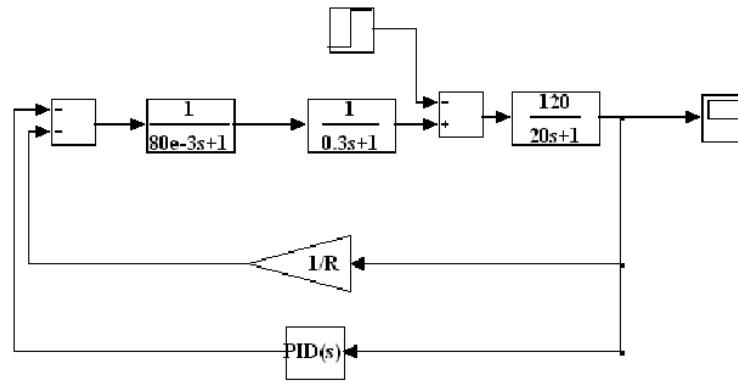


Figure 1. Block diagram of single area power system

III. PID CONTROLLER

The PID controller improves the transient response so as to reduce the error amplitude with each oscillation and then output eventually settles to a final desired value. Better margin of stability is ensured with the PID controllers. The conventional PI and PID controllers are slow and lack efficiency in handling system non-linearity. Generally, these gains are tuned with help of different optimizing methods such as the Ziegler Nicholas method, the Genetic algorithm, etc., The optimum gain values once obtained is fixed for the controller. But in the case deregulated environment, large uncertainties in load and change in system parameters often occur. The optimum controller gains calculated previously may not be suitable for new conditions, which results in improper working of the controller. To avoid such situations, the gains of the controller must be tuned continuously. Fig 2 shows the simulation block diagram of the single area power system using the PID controller.



. Figure 2. Simulation diagram of single area power system using PID controller.

III. GSO FOR SINGLE AREA SYSTEM

In this simulation, the objective is to minimize the error and minimize the maximum overshoot. For this reason the objective function is chosen as the Integral Square Error (ISE). The ISE squares the error to remove negative error components.

During the simulation study, error signal which is required for the controller is transferred to GSO software with error.mat component. The simulation block diagram of the PSO –PID is shown in the figure 3.

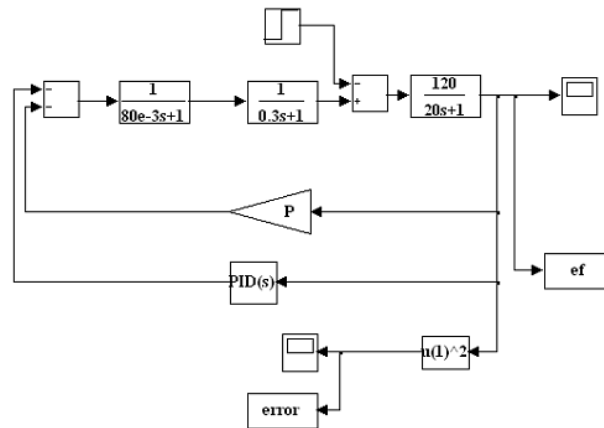


Figure 3. Block Diagram of GSO tuned LFC.

IV. SIMULATION RESULTS

The simulated output and the comparison of the controllers are shown as tables and figures. Table 1 shows the settling time, overshoot and undershoot of the above said three controllers. From the table we observe that the GSO –PID has lesser settling time, lesser overshoots and lesser undershoots.

Regulator	Settling Time	Max Overshoot	Max Undershoot
PI	26	$16 \cdot 10^{-3}$	$-26 \cdot 10^{-3}$
PID	13	$0.4 \cdot 10^{-3}$	$-3.8 \cdot 10^{-3}$
GSO -PID	4.5	$0.5 \cdot 10^{-3}$	$-0.25 \cdot 10^{-3}$

Table 1. Comparison of settling time of different regulators

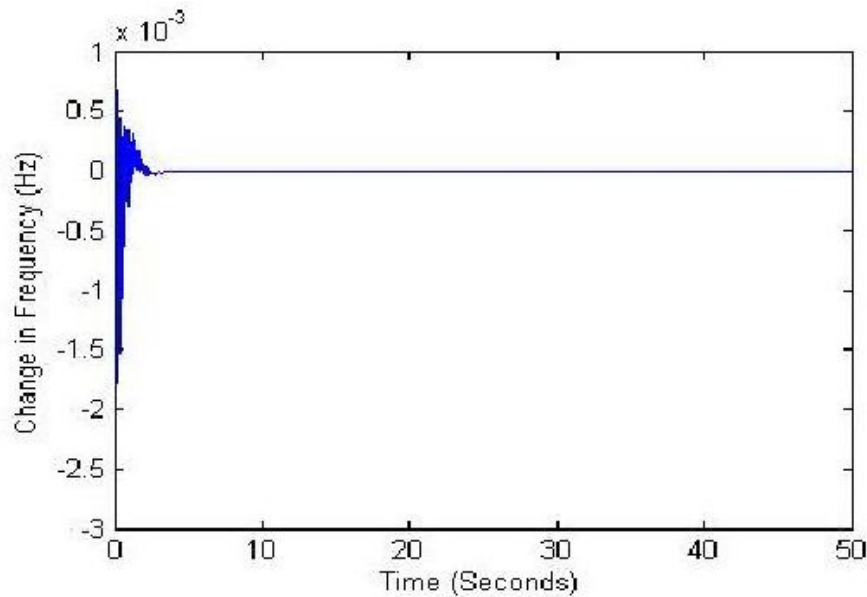


Figure 4. Dynamic response of frequency deviation GSO controller

It is observed that PSO-PID controller has the least settling time of 4.5 s which is three times lower than PID controller and 5 times lower than PI controller. Similarly, the overshoots and the undershoots are the lowest for the proposed PSO-PID controller when compared to the PID and PI controllers

V. CONCLUSION

The performance of load frequency control using MATLAB/SIMULINK is analyzed. The tuning of the PID controller using the PSO for load frequency control of a single area power system for a step load change of 10% has been presented. It is shown analytically and graphically that there is a substantial improvement in the time domain specification in terms of lesser rise time, lesser peak time, lower settling time as well as a lower overshoot. The proposed controller using the PSO algorithm proves to be better than the conventional PI and PID controller. Therefore, the proposed PSO-PID controller is recommended to generate good quality and reliable electric energy. In addition, the proposed controller is very simple and easy to implement since it does not require much information about system parameters.

VI. REFERENCES

- [1] Elgerd. O. I., —Electric Energy Systems Theory: an introduction, New York: McGraw-Hill, 1982.
- [2] P. Kundur, Power System Stability and Control. New York: McGrawHill, 1994.
- [3] A.J.Wood, B.F Woolen berg, Power Generation Operation and Control, John Wiley and sons, 1984.
- [4] O.I. Elgerd and C.E Fosha, “Optimum megawatt- frequency control of multi area electric power systems”, IEEE Trans on Power Apparatus and System, Vol PAS89, No.4, April 1970 pp556-563
- [5] Unbehauen, H., Keuchel, U., Kocaarslan, I., Real- Time Adaptive Control of Electrical Power and Enthalpy for a 750 MW Once-Through Boiler, Proceedings of IEE International Control Conference91, Edinburg, Scotland, Vol.1, pp. 42-47, 25-28 March 1991.
- [6] Shayeghi, H., Jalili, A., Shayanfar, H.A., Robust Modified GA Based MultiStage Fuzzy LFC,Elsevier Energy Conversion and Management48, 1656–1670, 2007.

Geopolymer Concrete - Concrete Without Cement

Annie John¹ Rahul John Roy²

1 Assistant Professor, St Anne's College of Engineering and Technology, Panruti.

2 Student, Civil Engineering Department, NIT Trichy.

Abstract - Continuous increase in production of cement causes large amount of carbon dioxide emission which results in green house effect. In order to overcome this problem many researchers have put in their efforts to achieve optimum strength of concrete by replacing cement with flyash, when it combine with alkaline solution to produce Geopolymers concrete(GPC). GPC is an improved way of concreting execution made by complete elimination of ordinary Portland cement. GPC were synthesized from low calcium fly ash, activated by combination of Sodium Hydroxide and Sodium Silicate solution. This report is an attempt to find out suitable utilization of fly ash by studying the compressive strength of GPC and to observe durability characteristics of GPC. In this experimental study different concentrations of alkaline liquid are being used. Mix samples of different molarities were prepared to study the influence of alkaline solution on compressive strength of GPC. Increased alkaline solution concentration proved to have positive effect on Geopolymerization process and this is revealed by the improved compressive strength.

I INTRODUCTION

The global demand of cement for construction of infrastructures is continuously increasing in order to maintain the ongoing growth and accommodate the needs of the increasing population. OPC has been traditionally used as the binder in concrete. About 1 tonne of carbon dioxide is emitted into the atmosphere in the production process of 1 tonne of cement. This makes a significant contribution to the global greenhouse gas emission. Therefore, development of alternative binders utilising industrial by-products is necessary to reduce the carbon footprint of the construction industry. Geo polymer is an emerging alternative binder for concrete that uses by-product materials. A base material that is rich in Silicon (Si) and Aluminium (Al) is reacted by an alkaline solution to produce the geopolymer binder. Source materials such as fly ash, metakaolin and blast furnace slag can be used to make geopolymer. Fly ash blended with blast furnace slag and rice husk ash has also been used as the base material for geopolymer. The product of the reaction is an inorganic polymer which binds the aggregates together to make geopolymer concrete. The coal-fired power stations worldwide generate substantial amount of fly ash as a by-product that can be efficiently used in geopolymer concrete to help reduce the carbon footprint of concrete production.

The results of recent studies have shown the potential use of heat-cured fly ash based geopolymer concrete as a construction material. As a relatively new material, it is necessary to study the various properties of GPC as compared to the traditional OPC concrete in order to determine its suitability for structural applications. The ongoing research on fly ash-based geopolymer concrete studied several short-term and long-term properties. It was shown that heat-cured geopolymer concrete possesses the properties of high compressive strength, low drying shrinkage and creep, and good resistance to sulphate and acid. Geopolymer concrete was found to have higher bond strength with reinforcing steel and relatively higher splitting tensile strength than OPC concrete. Geopolymer concrete beams and columns were tested to failure and they showed similar or better performance as compared to OPC concrete members. Heat-cured geopolymer concrete showed higher residual strength than OPC

concrete cylinders after exposure to high temperature heat of up to 800⁰ C. Therefore heat-cured geopolymer concrete is considered as an ideal material for precast concrete structural members.

Development of the constitutive model for a material requires its fracture parameters. The fracture characteristics of a material are used to describe the formation and propagation of cracks in the material. The crack path through a composite material such as concrete is dependent on the mechanical interaction between the aggregates and the binder matrix. Fracture energy of a composite material depends on the deviation of the crack path from an idealized crack plane. Since the binder in geopolymer concrete is different from that in OPC concrete, the effect of the interaction between the aggregates and the geopolymer binder needs to be investigated. Thus, it is necessary to study the fracture parameters of geopolymer concrete to understand its failure behaviour. In this study, the fracture properties of heat cured fly ash based geopolymer concrete specimens were determined from three-point bending test of notched beams. Fracture energy and the critical stress intensity factor were also determined for OPC concrete specimens to compare with those of geopolymer concrete specimens of similar compressive strengths and containing the same aggregates. The fracture behaviours of both types of concrete were compared using the test results.

II EXPERIMENTAL DETAILS

2.1 Materials

Lignite fly ash was obtained from Neyveli Lignite Power Station, Neyveli, Tamil Nadu. The particle shape of fly ash was mainly spherical with the main chemical composition of 37% SiO₂, 2% Fe₂O₃, 21% Al₂O₃, 14% CaO. A median particle size of fly ash was 50µm. Sodium Silicate solution (Na₂SiO₃) and Sodium Hydroxide (NaOH) were used as Alkali activators. Coarse aggregate with a maximum size of 20mm diameter with a specific gravity of 2.85 was used for making Geopolymer concrete. Sand used for the experiment was passed through the 4.75mm IS Sieve with a fineness modulus of 2.46.

2.2 Mix proportion, mixing and casting.

Mix chosen in this study is 1:1.5:3 with 100% replacement of cement with fly ash. Alkaline liquid was a combination of Sodium hydroxide and Sodium Silicate solution. Sodium hydroxide and Sodium Silicate obtained as pellets were dissolved in distilled water to form the alkaline liquid. In order to study the effects of alkaline solution on the geopolymer concrete properties, three concentrations of alkaline solutions 8, 10, 12 molar were used. Mix proportions are shown in Table 1.

The coarse aggregate and sand is saturated surface dry condition was first mixed in laboratory pan mixer with the fly ash for about three minutes. At the end of this mixing, the alkaline solutions and extra water were added to the dry materials and the mixing continued for another four minutes. Immediately after mixing, the fresh concrete was cast into moulds. All cubes were cast in two layers. Each layer was compacted into limited capacity of the laboratory mixer. The slump of every batch of fresh concrete was measured in order to observe the consistency of the mixtures. Casted cubes were kept in oven for 48 hours at the temperature of 70⁰C for curing. After curing, the cubes were removed from the chamber and left air-dry at room temperature for another 24 hours before demoulding. The test specimens were then left in the laboratory ambient conditions until the day of testing. The laboratory temperature varied between 25⁰C and 35⁰C during that period.

2.3 Testing Detail.

2.3.1 Void Content.

The void content of Geopolymer concrete was tested using the casted cubes. The void content was determined in accordance with ASTM and calculated using Eq (1).The reported void contents were the average of three samples.

Table 2 Total void ratio

Mix	Void content%
S1	15.5
S2	16.6
S3	17.1
S4	17.7
S5	18.6
S6	10.5
S7	11.1
S8	12.3

$$V_T = (T-D)*100/ T-----(1)$$

$$T = M_s /V_s$$

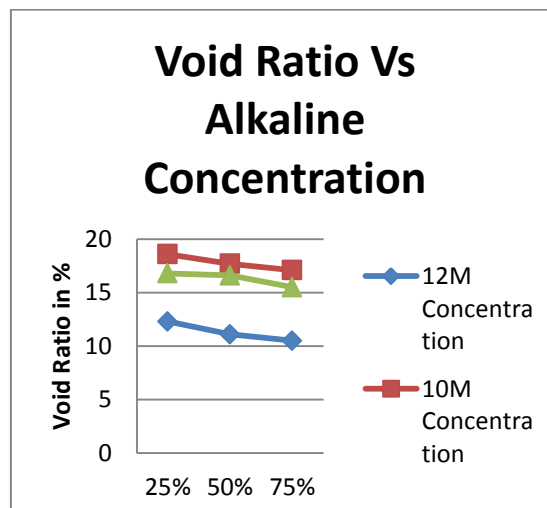
Where V_T is the void content (%),

T is the theoretical density of Geopolymer concrete computed on an air free basis (kg/m^3).

M_s is the total mass of all the materials batched (kg), V_s is the sum of absolute volumes of component ingredients in the batch (m^3).

2.3.2 Compressive strength.

The compressive strength was tested at the age of 3rd day. The crushing strength of concrete cube is determined by applying a compressive load at the rate of $2.88N/mm^2$, till the specimen fails.



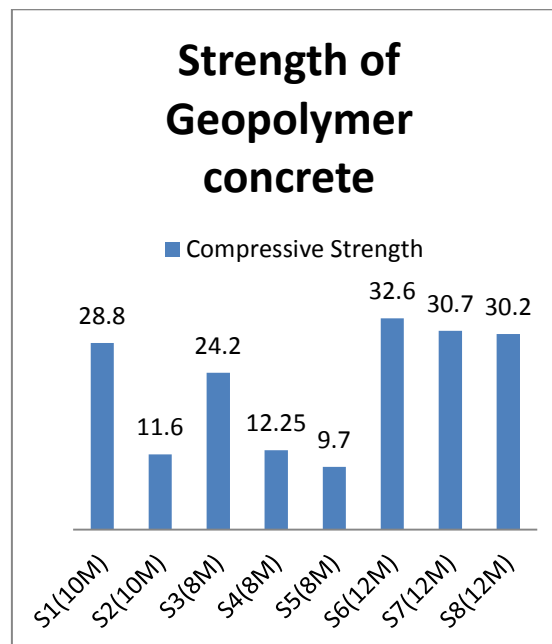
III RESULTS AND DISCUSSION

3.1 Void Content.

The results of void content are summarized in Table 2. The void content of geopolymer concrete were relatively low between 10.5% and 18.6%. Generally the void content of Portland cement concrete depends on the gradation of aggregate and the method of compaction. However in this test, the gradation of aggregate and the method of compaction were not varied. The results however indicated that voids content in this study slightly decreased with the increase in the alkaline concentration. For instance the void content of S₆, S₇, S₈ were 10.5%, 10.8% and 11.2% respectively. The adding of alkali liquid in the mixture increased the paste content and the excess paste fill the voids resulting in a dense concrete with low void content.

Compressive Strength.

Compressive strength tests of all specimens were conducted using a compressive testing machine. A minimum of three specimens (150mm*150mm) cubes for each type were tested for 3-day compressive strengths after casting, which is equivalent to a typical OPC strength development after 28 days. It has been found that age does not have a significant effect on strength of Geopolymers after completion of heating curing cycle.



The strength of the fly ash based geopolymer concrete is significantly increased the geopolymer paste undergoes high early strength development at an accelerated rate. This behaviour is the characteristics' of the quick geopolymerization process, which contrasts with the hydration process of OPC that gains strength over longer time periods. In geopolymers, alumino-silicate gel is the major binding phase that provides interparticle bonding, which in turn enhances the macroscopic strength.

Compressive strength of Geopolymer concrete increases marginally with an increase in alkaline content. For example compressive strength of 9.70 – 24.2, 11.6 – 28.8, 30.2 – 32.6 MPa were obtained for GPC with 8 M, 10M and 12M respectively. With regard to Sodium Hydroxide concentration, the optimum concentration to produce GPC is 12M. Increasing the concentration to 12M increases the compressive strength.

3.2 Relationship of void content and compressive strength.

The relationship between void content and compressive strength can be shown using the exponential curve as in figure. It can be seen that compressive strength increases as void content decreases.

IV CONCLUSION

In order to expand the use of fly ash Geopolymer concrete which can be prepared easily from alkali activated fly ash and coarse aggregate. The void content and compressive strength were determined. Compressive strength between 9.7 and 32.6 were obtained according to the molarity of the alkaline content. These values show that optimum alkaline content can be chosen between 10M and 12M according to the requirement. In addition the relationship of void content – alkaline content, compressive strength – alkaline content of GPC was shown in graph. It has therefore been demonstrated that fly ash geo polymer concrete could be used as replacement for ordinary Portland cement concrete with acceptable strength.

REFERNECES

- [1] N P Raja mane Head, Concrete Composites Lab, and N Lakshmana, former Director and Project Advisor, Structural Engineering Research Centre,,Chennai,Nataraja M C, S J College of Engineering, Mysore; Geo polymer Concrete-A New Eco friendly Material of Construction, 2009.
- [2] Davidovits, J, “Soft Mineralogy and Geo polymers.” In proceeding of Geo polymer 88 International Conference, the University de Technologies, Compiegne, France, 1988.
- [3] Davidovits, J, “Chemistry of geo polymer systems, terminology.” In Proceedings of Geo polymer ‘99 International Conferences, France.1992.
- [4] Malhotra, V. M, “Making concrete ‘greener’ with fly ash.” ACI Concrete International, 21, pp. 61-66, 1999.
- [5] M D J Sumajouw & B V Rangan, Low Calcium fly ash based Geo-polymer concrete, Faculty of Engineering, Curtin University of Technology, Perth, Australia, 2006.
- [6] Davidovts.J, Soft Mineral usage and Geo polymers,” In proceeds of Geo polymer 88 International Conference, The University de Technologies’, Compiegne, France, 1988.
- [7] V.M. Malhotra, “Introduction: Sustainable Development & Concrete Technology”, ACI Concrete International, 24(7), pp. 22, 2002.
- [8] J. Davidovits, “Geo polymers: inorganic polymeric new materials” Journal of Thermal Analysis, 37(8), pp. 1633–1656, 1991.

Design Optimization Of Catalytic Converter

Naveenkumar.U¹, Punitha Raj.A², Prakash.M³

¹ Assistant professor, Dept of Mechanical Engineering, ST.Anne's College of Engg and Tech Panruti,

^{2,3} Sstudents Dept of Mechanical Engineering, ST.Anne's College of Engg and Tech Panruti,

Abstract- The source of pollution and global warming is air pollution. It is to be noted that air pollution is mainly caused by the toxic gases from the exhaust of the automobiles. Only 30 percentage of the fuel is converted into energy source to run the engine remaining 70 percentage of fuel is of un burnt hydrocarbon, carbon monoxide and nitrogen oxides. This toxic content is reduced by the invention of catalytic converter. Here the performance of the catalytic converter is studied and analysis of fluid flow is done. This project deals with the different inlet cone angle of catalytic converter to study the amount of conversion taking place inside the converter after maintaining uniform flow. The uniform flow inside the converter is achieved by increasing the cone angle of the converter. By utilizing the maximum amount of substrate life span of the converter will be increased. It helps to design a better converter model so that it may beneficial for the customer in performance.

Key words – carbon monoxide, Inlet cone Angle, Nitrogen oxides, pressure, Uniform flow.

I. INTRODUCTION

This paper deals with the study of flow inside the catalytic converter; flow inside the converter is non uniform due to the geometry of the catalytic converter. Analysis of real time catalytic converter is more expensive and if there is any error we have to change the whole model. By using CFD (Computational Fluid Dynamics) Analysis it is easy to spot the errors and rectifying it in an easy way. Catalytic converters are made of substrate at the centre through which the conversion of pollutant will take place [2-4]. When the burnt gases enter into the catalytic converter of certain velocity it will directly hit the substrate at the centre and chemical reactions will take place. The distance between the substrate and the exit of the inlet cone is less so the gas hit the centre portion of the substrate. By this only the centre portion of the substrate is reacted to the inlet gases, so the flow separation at the inlet is not sufficient to expand the flow in all the surfaces of the substrate so that there will be uniform flow inside the converter. Back pressure is the factor which affects the conversion rate of the redox reaction if back pressure increases it leads to failure of the engine.

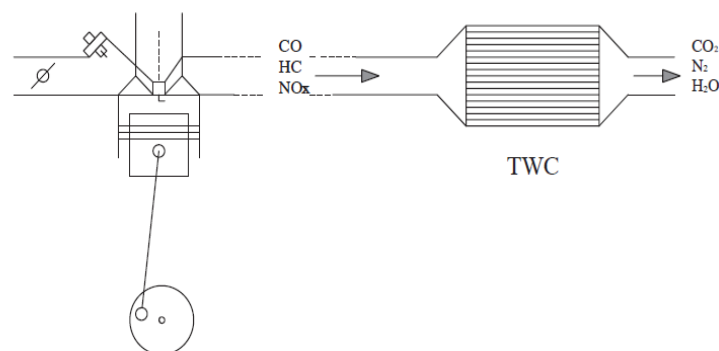


Fig 1. Catalytic converter

1.1 Catalytic Converter

A catalytic converter is an emissions control device which is used in vehicles that converts toxic pollutants in exhaust gas to less toxic pollutants by catalytic reaction (oxidation or reduction) [1]. Catalytic converters are used in IC engines fuel by either petrol (gasoline) or diesel including lean burn engines. The catalytic converter was invented by Eugene Houdry, a French mechanical engineer in 1950. Houdry concerned about the smoke stack exhaust and automobile exhaust in air pollution and founded a company, Oxy-Catalyst. Houdry first developed catalytic converters for smoke stacks called cats. Then he developed catalytic converters for warehouse forklifts that used low grade non-leaded gasoline.

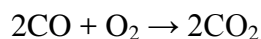
1.2. Catalytic Reaction

There are two types of catalytic converter used in automobiles. This is classified on basis of type of catalytic reaction taking place in the catalytic converter. They are 2 way catalytic converter and 3 way catalytic converter.

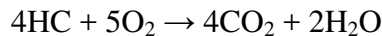
1.3 Two Way Catalytic Converter

In two way catalytic converter, it will control the emission of two different toxic sources. The carbon monoxide and hydrocarbons will be converted into carbon dioxide and water [2].

- Oxidation of carbon monoxide to carbon dioxide:



- Oxidation of hydrocarbons to carbon dioxide and water:

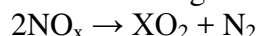


The two way catalytic converter is superseded by three-way converters because of their inability to control oxides of nitrogen.

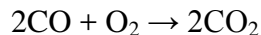
1.4 Three Way Catalytic Converter

The oxides of nitrogen are more toxic than carbon monoxide and hydrocarbons, to control the toxic content of nitrogen oxides effectively with the carbon monoxide and hydrocarbons, three way converters are designed and used in the automobile industries [2].

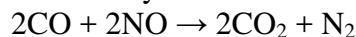
- Reduction of nitrogen oxides to nitrogen and oxygen:



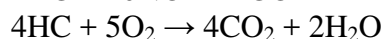
- Oxidation of carbon monoxide to carbon dioxide:



- Oxidation of hydrocarbons to carbon dioxide and water:



- Reduction of nitrogen oxides by reactions involving HC and CO:



II. PROBLEM DESCRIPTION

2.1 Non Uniform Flow

The harmful emissions from engines (such as oxides of nitrogen, hydrocarbons, and carbon monoxide) are because of incomplete combustion. Recent catalytic converters are substrate coated with platinum, rhodium, or palladium. Which are Nobel metals and expensive [5-6]. Due to non uniform flow inside the catalytic converter the outer most region of substrate are less reactant to the emission by utilizing these regions we may able to increase the efficiency

and life span of the converter. The fig 2.1 shows that due to the non uniform flow the outer most regions are less reactant to the emissions. Pressure at the inlet section increase due to presence of substrate, because of this the flow at the inlet section will reverse in the direction of engine. If this back pressure exceeds then there will be stall in the performance of engine. So reducing back pressure i.e. reverse flow should be less.

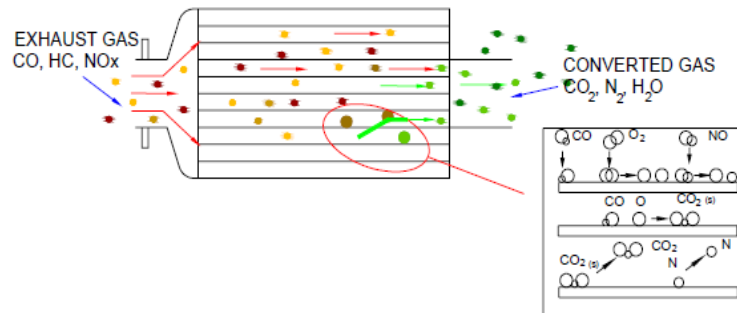


Fig 2. Non uniform flow of Exhaust gases at inlet

2.2. Reverse Flow

When the fluid flows inside the converter it flows through the inlet section to enter the substrate. The inlet section is an divergence section, the flow passes through the diverging section posses flow separation and as soon the flow comes the end of the divergence section it will start to form vertices near the substrate area which create a reverse flow in the inlet section [3].

Due to the reverse flow the fluid entering into the converter is also affected because of disturbance. This disturbance creates turbulence inside the converter and pressure at the inlet section increases.

III. MODELING THROUGH POROUS MEDIUM

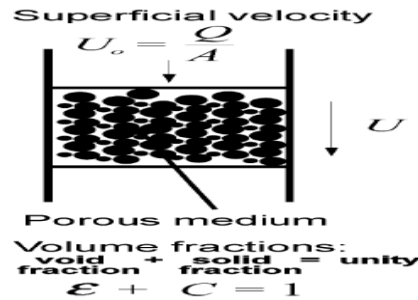
The fluid flows into the converter are designed to be Carbon monoxide. Since the Reynolds number is high, k- ϵ turbulence model is taken [7]

$$Re = \frac{\text{inertial forces}}{\text{viscous forces}} = \frac{\rho VL}{\mu} = \frac{VL}{\nu}$$

Where V is the mean velocity of the object relative to the fluid, L is a characteristic linear dimension, μ is the dynamic viscosity, ν is the kinematic viscosity, ρ is the density of the fluid. SIMPLE algorithm is used to get velocity and pressure in the fluid domain by solving the equation of Mass and momentum [7]. The substrate of catalytic converter which is catalyst is taken as porous medium and porosity is given as 1.

3.1. Consideration of Volume Fraction in Porous Medium

The superficial flow inside the porous bed is defined as total flow rate inside the bed divided by the cross section area.



Where U_0 is superficial velocity, Q is fluid flow rate, A is area of the porous bed, and U is interstitial velocity. To preserve fluid continuity with the entering superficial flow the fluid will have to pass through a smaller area; hence the velocity within the bed will be greater than the superficial. In particle technology calculations it is the volume fraction is most important than the mass fraction

3.2. Governing Equation

Governing equations solved by the software for this study in tensor Cartesian form are Continuity and Momentum equations.

Continuity equation:

$$\rho \left(\frac{\partial u_j}{\partial x_j} \right) = 0$$

Momentum equation:

Momentum x:

$$\rho \frac{\partial u}{\partial t} = \rho g_x - \frac{\partial p}{\partial x} + \mu \left(\frac{\partial^2 u}{\partial x^2} + \frac{\partial^2 u}{\partial y^2} + \frac{\partial^2 u}{\partial z^2} \right)$$

Momentum y:

$$\rho \frac{\partial v}{\partial t} = \rho g_y - \frac{\partial p}{\partial x} + \mu \left(\frac{\partial^2 v}{\partial x^2} + \frac{\partial^2 v}{\partial y^2} + \frac{\partial^2 v}{\partial z^2} \right)$$

Momentum z:

$$\rho \frac{\partial w}{\partial t} = \rho g_z - \frac{\partial p}{\partial x} + \mu \left(\frac{\partial^2 w}{\partial x^2} + \frac{\partial^2 w}{\partial y^2} + \frac{\partial^2 w}{\partial z^2} \right)$$

Where,

ρ = density, g = gravitational force

IV. METHODOLOGY

In this paper CFD study for five different geometry of catalytic converter is studied. The inlet geometry of the converter is changed with respect to right angle triangle theorem. From the converter the portion of substrate to the inlet angle is said to be in form of right angled triangle.

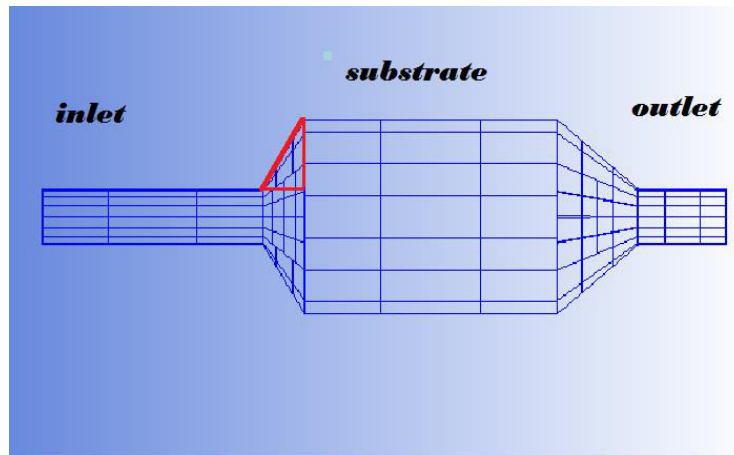


Fig4.1. Inlet Geometry of Converter

4.1. Inlet Geometry

The inlet geometry of the converter is calculated from the known values of height and required angle.

Table 4.1. Inlet Geometry

ANGLE (degree)	DISTANCE BETWEEN SUBSTRATE AND DIVERGENCE SECTION (mm)
90	50 (OFFSET)
60	47.5
50	70
30	142
15	300
10	466
5	940

The above table contains the calculated inlet geometry for new converter with respect to various divergence angles at inlet. By analysis we can able to predict the pressure at inlet for all the above converters. The performance of the converter is high when the pressure at inlet is less. Flow uniformity index at the porous section is also predicted from the analysis to justify there is less flow separation at the inlet section.

4.2. Boundary Condition

For incompressible flow through a channel, any perturbation of the flow at one point is instantly felt everywhere in the fluid. The state of flow is everywhere consistent. In such case Inlet and outlet boundary can be set as velocity and pressure respectively.

Table 4.2. Boundary Condition

Inlet	velocity
Outlet	pressure
Porosity	1
Fluid	Carbon Monoxide
Velocity	25ms^{-1}
Pressure	1 atm

V. RESULTS AND DISCUSSIONS

The fluid flow inside the catalytic converter is discussed here; the non uniform flow inside the converter is due to the flow separation at the inlet divergence section. The Pressure at inlet increases because of the substrate, which is placed at the path of flow. The following contour of total pressure and mass flow rate plot will explain the efficiency of catalytic converter after changing the inlet geometry.

5.1. Total Pressure

Model I

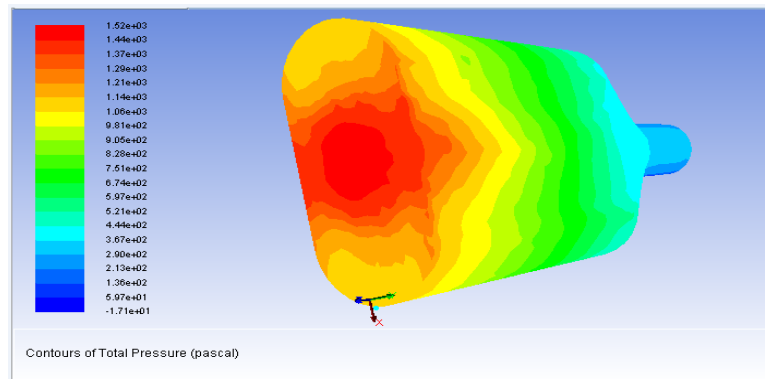


Fig 3. Total Pressure Contour of Inlet Angle 90^0

Model II

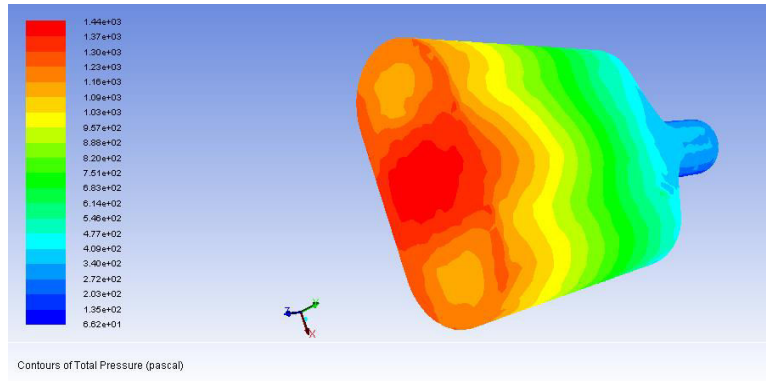


Fig 4. Total Pressure Contour of Inlet Angle 60°

Model III

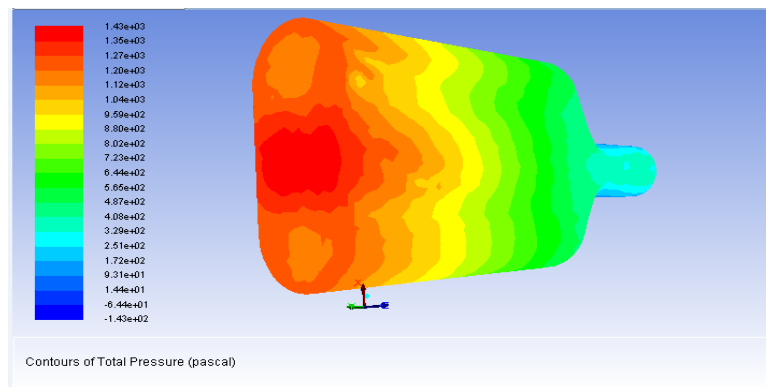


Fig 5. Total Pressure Contour of Inlet Angle 50°

Model IV

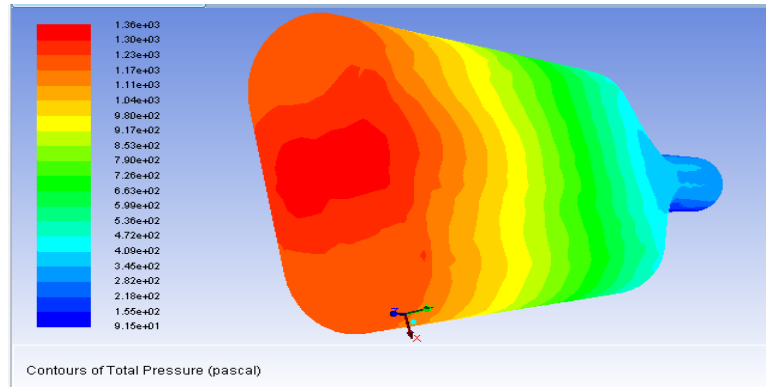


Fig 6. Total Pressure Contour of Inlet Angle 30°

Model V

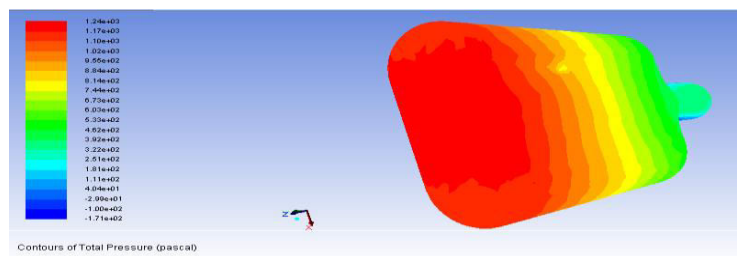


Fig 7. Total Pressure Contour of Inlet Angle 15°

Models of 10° and 5° are not taken for analysis because of space constrain. It is not possible to design a converter with huge inlet dimension. The pressure at inlet of all the Models is tabulated for study.

Table 3. Pressure at Inlet

Angle	Pressure (Pa)
90	1520
60	1440
50	1430
30	1360
15	1240

The above tabulation showed that the pressure for each inlet angle of converter.

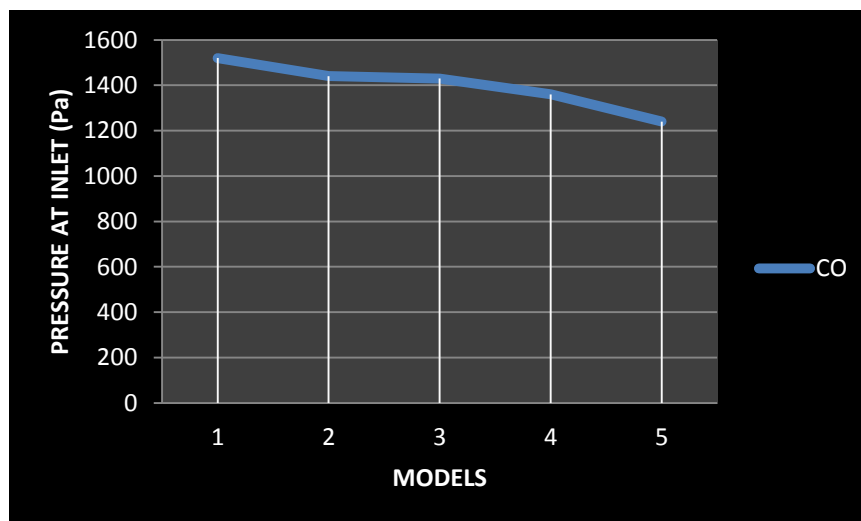


Fig 8. Angle and Pressure Chart

The total pressure and angle of the converter shows that pressure at inlet is directly proportional to divergence angle. When inlet angle decreases, then the pressure at inlet decrease. Flow separation is less at low divergence angle is justified.

5.2. Flow Uniformity Index

Uniformity index is the normalized RMS of the difference between the local velocity and the spatial mean of the velocity integrated over the area of cross section

$$\gamma = 1 - \int_A \frac{\sqrt{(U' - U)^2}}{2AU'}$$

Where, γ is the Uniformity index, A is Area of cross section U' is Average Velocity and U local velocity. Uniform flow inside the converter may help in improving the performance, lack of uniformity is due to the flow separation at divergence section. Flow uniformity increases the amount of substrate utilized by the toxic fluids with is the sign of good converter. Here flow uniformity index at the porous section is plotted below.

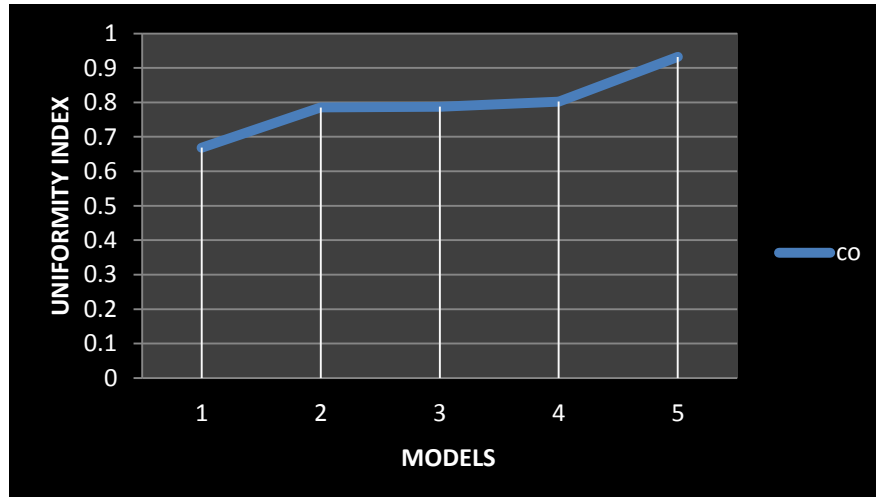


Fig 9. Uniformity index

VI. CONCLUSION

In this paper it is clearly stated the performance of the catalytic converter can be increased by decreasing the divergence angle [1]. The pressure at inlet increases with respect to inlet divergence angle. By decreasing the inlet divergence angle of the catalytic converter we may able to increase the flow uniformity is shown in the graph. Pressure at inlet is directly proportional to inlet angle. Analysis is done in FLUENT package and substrate is considered as porous medium with proper resistance.

The flow inside the converter is non uniform due to the vortices formed at the inlet section and pressure reduction is achieved by this modification is shown clearly in result and discussion topic. The results of the analysis show that the lower pressure can be achieved by changing the inlet angel to 15^0 for better performance.

REFERENCES

- [1] Hermann Schlichting, "Boundary Layer Theory" 1970, Page 697-700.
- [2] Mohiuddin.A.K.M and muhammad nurhafez,"Experimental analysis and comparison of performance Characteristics of catalytic converters including simulation", International journal of mechanical and materials engineering (IJMME), vol. 2 (2007), no. 1, 1-7.
- [3] E.M. Sparrow, J.P. Abraham, W.J. Minkowycz," Flow separation in a diverging conical duct: Effect of Reynolds number and divergence angle", International Journal of Heat and Mass Transfer 52 (2009) 3079–3083.
- [4] Balakrishna.B, Srinivasarao Mamidala, "Design Optimization of Catalytic Converter to reduce Particulate Matter and Achieve Limited Back Pressure in Diesel Engine by CFD", International Journal of Current Engineering and Technology Special Issue-2, (February 2014).

Study Analysis Of Prosopis Juliflora In Split Irrigation Systems

Mr.R.Sasikumar¹, Mr.K.Shanmuga elango², Mr.Neelavannan³,
Mr.Sarthkumar⁴

^{1, 2, 3} Assistant Professor, Mechanical Engineering, st.Anne's College of Engg and Tech, Panruti.

⁴ Student Mechanical Engineering, st.Anne's College of Engg and Tech, Panruti

Abstract- Biodiesel is produced by mechanically extracting natural vegetable oils from seeds, such as rape, and reacting the oil with methanol in the presence of a sodium or potassium hydroxide catalyst. Valuable by-products are produced during the production including straw (which can be used as a fuel), oilseed cake (a protein rich animal feed) and glycerol used in the production of soap and as a pharmaceutical medium. The production of biodiesel, such as rape methyl ester, is still done on a small scale and does not presently enjoy the economies of scale available to the production and distribution of diesel. So analysis of Prosopis juliflora seed is converted into biodiesel production in split irrigation systems

I. INTRODUCTION

This practical note describes one of the most invasive shrubs in split irrigation systems prosopis juliflora also known as mesquite. The note focuses on how it disturbs the management of split irrigation systems and crop cultivation in Eritrea, Ethiopia, Pakistan, Sudan and Yemen. It gives country overviews of when and for what purpose prosopis juliflora was introduced and the programs that have taken place to eradicate or manage the plant (chapter 2). Further the different mechanical, chemical and biological eradication methods are mentioned (chapter 3) and how prosopis juliflora can be used as a valuable resource for purposes such as charcoal or timber (chapter 4). From this, it aims to take stock of the problems and draws some tentative lessons on how to control or use the shrub. Prosopis juliflora invades land and even worse encroaches on river beds and canal beds – blocking them and causing drainage patterns to uncontrollably shift. Yet prosopis juliflora is a blessing as well, albeit mixed. It is a source of biomass in some of the most marginal lands and provides fuel wood, charcoal and fodder. This practical note takes stock of how to manage this ‘mixed blessing’ in split irrigation systems, based on first-hand experience and grey literature. In the last thirty years the hardy well rooted shrub made its way from Latin America to all parts of the world, covering millions of hectares in for instance India, Pakistan, Yemen, Sudan, Somalia or Ethiopia. In many places it was first introduced in sand dune stabilization projects. However prosopis juliflora has the habit to ‘overstay its welcome’ and expand rapidly and not go away. The area estimated conquered by the invasive species in the last ten years in India, Pakistan, Yemen, Kenya, Sudan and Ethiopia is way above 10 million hectares. Particularly in areas where there is livestock grazing prosopis juliflora spreads rapidly: the seedpods cling to the animal skins and are distributed widely. Prosopis juliflora germinates easily and once it has settled in an area it is difficult to get rid of it. It takes over the natural vegetation, does not allow undergrowth and hence greatly reduces the grazing value of land. It also tends to creep into waterways – including dry riverbeds – choking them in the process and causing flood rivers to run wild. The prosopis juliflora thorns are poisonous and can even cause blindness. Livestock, particularly cattle, can become ill when they are almost exclusively fed with pods of prosopis juliflora. Symptoms can be facial contortions and constipation, sometimes resulting in death.

Geographical range:

Native range: Native to Colombia, Ecuador, Mexico, Peru, Venezuela. Known introduced range: An exotic invasive weed in



Source: F.M. Blanco (1845) Flora de Filipinas.

Sudan, Eritrea, Ethiopia, Kenya, Iraq, Pakistan, India, Australia, South Africa, Caribbean, Atlantic Islands, Bolivia, Brazil, Dominican Republic, El Salvador, Nicaragua, United States (USA) and Uruguay. *Prosopis juliflora* is a woody stemmed, thorned, evergreen shrub or small tree usually up to about five metres tall. High level of seed dormancy. Seed coat usually requires damage to germinate. Roots develop rapidly after germination and can reach a depth of 40cm in eight weeks (Pasicznik, 2002). It grows in dense and impenetrable thickets and is a colonising species. Often invading land that has never before supported vegetation cover of any description. Its foliage is unpalatable to most animals, although the seed pods are palatable which facilitates spread in animals' dung.

Power invader because:

- production of many, small and hard seeds capable of surviving passage through the digestive system of animals
- attractive pods for animals
- accumulation of dormant seed reserves
- production of a mixture of seeds, with a few capable of germinating immediately after dispersal, while the majority remain dormant for spreading germination
- great ability of re-sprouting and fast coppice growth from damaged trees

Prosopis juliflora is not only a scourge. It also has benefits to its credit. It is important for people in providing fuel and timber. The sweet nutritious pods are eaten by all livestock and can be made into different foods and drinks. Honey is made from the flowers and the gum is similar to gum arabic. The bark and roots are rich in tannin and the leaves can be used as mulch or to help in reducing pests and weeds. Also as a nitrogen fixing tree it improves the land and can reclaim saline soils. Furthermore in India charcoal generated from biomass of *Prosopis juliflora* improved the fertility of alkaline soils (Sai Bhaskar N. Reddy 2009). On balance however if unmanaged it is a scourge that is steadily undermining the livelihoods of large populations in some of the most vulnerable dry agricultural and pastoralist areas.

II. Control or management

Many efforts have been done to eradicate and control *Prosopis juliflora* from its areas of invasion. Geesing et al. (2004) categorized the eradication methods into three broad types: • Mechanical; plants are removed by machine or people mechanically by hand pulling, cutting, hand digging or mechanical uprooting. This is severely done in Gash, Sudan and Afar, Ethiopia but it didn't give the expected result, due to lack of maintenance. In Australia several mechanical methods have been used. This is **stick racking** (best results are achieved when soil moisture is sufficient to allow machinery to work with minimum strain, but soil is dry enough so the root system desiccates), **chain pulling** (may kill up to 90% of trees in a mesquite infestation. However, the effectiveness of control may be reduced when either very dense infestations or a high proportion of young trees and seedlings are present) **bulldozer pushing** and **blade ploughing**. • Chemical; Larger trees and shrubs are killed by cutting the stem at ground level and spraying or painting the freshly cut stumps with suitable herbicide. Herbicides like Round up, 2-4, D, Glenside Kerosene and diesel oil are used. • Biological; predators or pathogens are used to control the *Prosopis juliflora* reproduction. Sudanese researchers found some predator insects that attack the leaves that lead to deterioration of the tree canopy. In Australia four species of insects have been introduced as biological control agents against mesquite: The **Algarobius bottimeri** and **Algarobius prosopis** (The larvae of these beetles destroy mesquite seeds in mature pods both in the trees and on the ground), the **Prosopidopsylla flava** (a sap-sucking psyllid that causes dieback) and **Evippe spp.** (a leaf-tying moth that causes defoliation). Nevertheless, this is a very slow operation to eradicate the tree. (DAFF Queensland 2013). Another method that has been used in several countries is burning the stump after it has been cut. In Yemen for example the application of kerosene over the stump followed by burning has shown to be a way of eradicating the plant. However this only works when the plant is dry (not in stage of flowering) and the root system is not too deep to survive. Otherwise regrowth will occur. In general, experiences from America, Asia and Australia have shown that eradication of *Prosopis juliflora*, by the different methods, especially the mechanical and chemical ones are highly expensive and mostly ineffective (HDRA, 2005). The magnitude of resilience and distribution of the plant makes *Prosopis juliflora* virtually impossible to eradicate once established.



Figure 1: Prosopis eradication; cutting.



Figure 2 : Prosopis eradication; burning.

Eradication is also difficult, because a significant number of local people are depending on *Prosopis juliflora* for different purposes. Furthermore because of its invasive nature, it asks a lot of maintenance keeping the land clean from *Prosopis* sprouts. Without any clear policies, organisation and regulations maintenance it will not happen. In Ethiopia for instance, although the stumps were cleared and seedlings uprooted to rehabilitate the land, due to lack of land use right, people were not allowed to manage and use the land and *Prosopis juliflora*

re-invaded (Tegegn 2008). Because most of the conventional control methods are expensive, it could be argued that the utilization of *prosopis juliflora* is the best option to control the invasion for many invaded areas (Tessema 2012). Many farmers and artisans, as well as researchers, argue that the tree is a valuable resource (HDRA 2005). Exploring beneficial uses of the tree will help to turn it into a more useful tree and perhaps even, to some extent, curb its expansive growth. Thus more ecosystem services can be derived from *prosopis juliflora*, though its disservice to biodiversity remains a reason for caution.

An overview of the positive aspects of *prosopis juliflora*

1. Can play a role in sustaining the livelihood of poor rural households
2. Source of fuel and dry season animal feed
3. Wood does not spit, spark or smoke excessively
4. Often in the commonly owned areas where they are freely available to the whole community
5. High quality and hard timber
6. Good animal feed especially for dairy cows
7. Wood can be processed into furniture or construction material
8. Can act as vegetative fencing to delimit and protect properties
9. Produces good charcoal

An overview of the negative aspects of *prosopis juliflora*

1. Lack of traditional knowledge on how to manage and control the Plants
2. Obstructs paths and roads
3. Hard and costly to remove
4. Expands quickly even in the harshest conditions
5. Thorns can injure animals and people
6. Depletes the water moisture and limits availability to local plants
7. Few plants are able to grow under its crown shade
8. Can favour the breeding of malaria spreading mosquitoes
9. Causes pastoralist communal lands to shrink

III. Making use of *prosopis juliflora*

Converting *prosopis juliflora* into a valuable resource presents an opportunity to the communities living in marginal areas. (Pasicznik 2007). However to manage, control and utilize *prosopis juliflora* full participation of local communities is necessary. Also appropriate control measures and follow up management activities need to be done. Furthermore strategic development and encouragement of the private sector to establish a market for *prosopis juliflora* products is important. Marketing policies and interventions from government could help in this. Finally research have to be done about constraints in the harvest, processing and marketing of *prosopis juliflora* products and success stories have to be documented.

IV. Fuel and charcoal production

Prosopis juliflora wood is hard, burns slowly and has excellent heating properties. Also, the charcoal it can produce has good properties and can be easily traded on urban markets. In Ethiopia farmers were trained in labour efficient charcoal production techniques using metal kilns instead of traditional kilns. (Admasu 2008).

V. Timber

Prosopis juliflora wood is extremely hard and durable. It also has an appealing coloration that makes it ideal to make furniture with. The wood matures quickly and stems become dark inside when the plant is trained as a tree. The mature timber is resistant to pest attack and weathering and thus can be used for furniture making and other useful purposes especially housing. It is also used as parquet flooring wood. However particularly in stressful conditions

of dry areas, prosopis juliflora trees remain craggy, crooked and small, which makes using them to make furniture or charcoal less attractive.

VI. Wood chips

Wooden residues from prosopis juliflora can be chipped off and used as mulch in gardens and little vegetable gardens. The mulch is effective in reducing evapotranspiration. Consequently, it also reduces the plant water consumption. The chips have also been successfully processed into wooden pulp, which is the primary raw material for paper production

VII. Fodder

Free ranging animals can eat prosopis juliflora pods directly from the tree. Alternatively, the pods can be collected and ground to produce coarse flour which can be included in the animals' diet. The percentage of the flour in the mix should be kept below 50% in order to avoid digestion disorders among the livestock

VIII. Land reclamation

By spreading charcoal and using it as bio-char, acidic degraded land can be rehabilitated and yields can be increased. Charcoal improves the physical, biological and chemical properties of the soil by releasing and storing nutrients, increasing the bulk density, improving the overall porosity and creating favourable conditions for micro-biological activity. It can be applied in conjunction with farmyard manure and/or soil microbes

IX. Bio-fuel

Prosopis juliflora is an underestimated source of sugars that can be converted into ethanol. Trials in the USA have shown that up to 80% of the pods carbohydrates can be converted in the process.



Figure 3: Wood collection, India an experimental stage.

Making charcoal

Approximately three to six kg of wood of prosopis juliflora is required to produce one kg of charcoal depending on the method used. Charcoal is manufactured in traditional or improved earth

X. Biomass to generate power

The biomass of prosopis juliflora can be used to generate power. In Kenya, the private electricity producer Tower Power is planning to develop two biomass power plants in Baringo and Kwale districts. The new plant will be fed by the prosopis juliflora tree. The project is set to transform the tree from a noxious weed to a cash crop when about 2,000 households begin supplying the company with the tree stems. Baringo has a Prosopis forest cover of about 30,000 hectares, the highest density of the invasive plant in Kenya. Tower Power estimates that the forest can serve its power plant for 10 years (Business daily 2014).

10.1 Honey and gum

Prosopis juliflora blossoms abundantly. It is known to produce high amount of pollen that can be transformed into high-quality honey. The only constraint in dry-lands is the lack of water sources for the bees. The gum that exudates from prosopis juliflora is comparable to gum Arabica and can be used in the food-cosmetic industry. Its use is constrained by the absence of toxicological tests necessary for it to enter the industrial market.

XI. CONCLUSION

11.1 How to address the proposed juliflora challenge

Based on the diverse experience documented so far, the most viable strategy appears to be either to remove *Prosopis juliflora* altogether and keep the land 'clean' by intensive usage - and especially ensure it does not encroach river beds and in areas where this is not possible, to make use of proposed *Prosopis juliflora* products. Efforts to completely and permanently eradicate *Prosopis juliflora* often fail to reach the objective. Pragmatic utilization of the shrub's outputs, such as wood, bark, flower and pods in a complementary kilns, or less commonly in metal kilns. Before processing, wood is first sorted into similar diameters and lengths. Earth kilns can be made up on flat ground, but charcoal manufacturers use large pits, on sloping ground. Wood is stacked and moistened before firing. The stack is covered with soil and burns very slowly for several days depending on the size and condition of the stack and site. The moisture content of the wood is reduced from approximately 45% to close to zero. After two to eight days, the stack is opened and the coals are removed, allowed to cool, graded and bagged up for use or for sale. (Pasicznik 2001). approach. This can help to generate income (and improve livelihood) of the affected communities. The main element in a controlled use strategy:

- Focus on removal of *Prosopis juliflora* from water ways, highly productive land or land important for local food security. Keep close vigilance and intense use of these lands
- Land using communities should be encouraged to uproot *Prosopis juliflora* seedlings when they are still easy to remove.

REFERENCES

1. Abebe (1994) Growth-performance of some multi-purpose trees and shrubs in the semiarid areas of southern Ethiopia. *Agroforestry Systems* 26:237-248.
2. Admasu, D. (2008). Invasive plants and food security: the case of *Prosopis Juliflora* in the Afar region of Ethiopia. FARM-Africa, IUCN.
3. Ali, A., & Labrada, R. (2006). Problems posed by *Prosopis Juliflora* in Yemen. Problems posed by the introduction of *Prosopis Juliflora* spp. in selected countries. Food and Agricultural Organization of the United Nations (FAO) Plant Production and Protection Division, Rome, Italy
4. Ahmad, R., Ismail, S., Moinuddin, M., & Shaheen, T. A. R. A. N. A. (1994). Screening of mesquite (*Prosopis Juliflora* spp) for biomass production at barren sandy areas using highly saline water for irrigation. *Pakistan Journal of Botany*, 26(2), 265-282.
5. Bokrezi, H. (2008). The ecological and socio-economic role of *Prosopis Juliflora* in Eritrea. Academic Dissertation, Johannes Gutenberg-Universität Mainz, Germany. (PhD report)
6. Broun A.F., Massey R.E. (1929): *Flora of the Sudan*: Thomas Murby and CO. pp 376.
7. Business daily (2014) [online] available at < <http://www.businessdailyafrica.com/Corporate-News/Nema-permits-Tower-Power-to-build-Sh1-8bn-electricity-plant-/-/539550/1306264/-/nuuybwz/-/index.html>> [Accessed on January 24th 2014]
8. Chaturvedi A. & H.M. Behl (1996) Biomass production trials on sodic site. *Indian Forester* 122:439-455.
9. DAFF Queensland (2013) [online] available at: < http://www.daff.qld.gov.au/__data/assets/pdf_file/0004/73489/IPA-Mesquite-PP37.pdf> [Accessed on January 22th 2014]
10. FAO (miscellaneous) [online] [available at: <<http://www.fao.org/ag/agp/agpc/doc/publicat/field2/tcp0169.htm>> [Accessed on November 21th 2013]
11. Geesing D., Al-Khawlani M. & Abba M.L. 2004. Management of introduced *Prosopis Juliflora* species: can economic exploitation control an invasive species? *Unasylva*, 55:36-44.
12. Hamza, N. B. (2010). Genetic variation within and among three invasive *Prosopis Juliflora* (Leguminosae) populations in the River Nile State, Sudan. *International Journal of Genetics and Molecular Biology*, 2(5), 92-100.
13. IFAD (2011) COSOP Guidelines and Source Book, (from Volume 1)
14. IFAD (2009) Country Programme Evaluation Republic of Sudan, Report No. 2060-SD
15. IFAD (2004); Republic of the Sudan Gash Sustainable Livelihoods Regeneration Project, Target Group and Project Description (From volume 1 of Appraisal Report 1462-SD).
16. Kaarakka, V. & S. Johansson (1992) Yield and water use efficiency of 32 two-year-old *Prosopis* provenances under irrigation in Bura, eastern Kenya. *Nitrogen Fixing Tree Research Reports* 10:182- 185.

Experimental Investigation Of Modified Jatropha Oil Fuel Direct Injection Diesel Engine

Mr.R.Sasikumar¹, Mr.N.Neelavannan², Mr.P.Murugan³, V.Murugadass⁴
Assistant Professor, Dept of Mechanical Engineering, St. Anne's college of Engg and Tech^{1,2,3}
Student, Dept of Mechanical Engineering, St. Anne's college of Engg and Tech⁴

Abstract The performance of kirloskar, AV1 model, Single cylinder, Water cooled, Vertical, Direct injection diesel engine is evaluated using modified jatropha oil as fuel. This performance is compared for the same engine using mineral diesel as fuel. The exhaust emission parameters are also compared for these two fuels. The various fuel properties of jatropha oil and biodiesel like calorific value, flash point, fire point, viscosity, cetane index, ash residue, etc., were determined. Some of the properties were found out in AdhiParaksakthi Engineering College thermal lab and some of them were tested in Ita lab, Chennai. The engine is loaded using alternator and rheostat. Biodiesel is tested in engine with various combinations. It was found out that the brake thermal efficiency for biodiesel was slightly higher than the brake thermal efficiency diesel. Additional observation is less emission.

Keywords: *Jatropha oil, Transesterification, I.C.engines, Brake thermal efficiency, Specific fuel consumption.*

I. INTRODUCTION

1.1 General

Increasing industrialization and modernization of world lead to steep rise in petroleum cost. Also with the present consumption rate, deplete all petroleum resources within a decade or two. In addition, combustion of fossil fuel accumulates greenhouse gas emissions and leads to rapid rate of global warming. By spending more amount of money we import not only petroleum fuel but also much emission. Considering these disaster effect many alternative fuels were identified and tested successfully in IC engines. However, due to availability and lack of compatibility with the existing engine of such fuels they are not having ability to replace the existing fuel completely. Bio fuels are one, which has an ability to reduce the greenhouse gas emission as they were derived from bio-resources. Considering this, the bio fuel, Modified Jatropha oil is considered for this investigation. The detailed investigation report is given in these following chapters.

1.2 Present work

The vegetable oils are found to be promising alternative fuels because of their renewable, eco-friendly and can be produced easily in rural areas. The cost of edible oil is some what more. So that the use of non-edible oil is more significant. The Jatropha curcas grows in all over India irrespective of any climate conditions and areas. The neat vegetable oil (Jatropha) is not suitable to use as the fuel directly in IC engines. So due to esterification and / or transesterification process the fuel is modified into more suitable one. Then it is mixed with diesel and thereby bio-diesel is prepared. The bio-diesel can be conveniently used in conventional diesel engine. The engine is tested under various load conditions. At each and every load the performance and emission parameters are measured and compared with standard diesel operations.

1.3 Objective

The objective of the investigation is to study the performance and emission characteristics of a diesel engine run by modified Jatropha oil based bio-diesel.

II. PREPARATION OF BIO-DIESEL

Biodiesel is prepared from any of the following methods. i) Blending ii) Transesterification iii) Emulsification and iv) Cracking. Among these, Transesterification is the popular & widely applied. In Transesterification process neat Jatropha oil is converted into modified oil using methyl alcohol (carbonyl) and small amount of sodium hydroxide which is used as a catalyst.

Neat Jatropha oil + Methanol \rightarrow Modified Jatropha oil + Glycerol. This process requires jatropha oil, methanol and NaOH in the proportion of 1litre, 500ml & 6gram respectively. The process is carried out at a temperature of about 65^o C. At the end of reaction ester is obtained. Glycerol is also obtained as a bi-product. This ester is washed by removing catalyst, alcohol & other impurities. In our investigation we prepared a bio-diesel by mixing 20% Jatropha oil and 80% diesel. This is used in our test rig and the performance of the engine is evaluated.

III. PROPERTIES OF DIESEL AND NEAT JATROPHA OIL

The various fuel properties of conventional diesel & jatropha oil is given in table 1.

Table 3.1 Fuel Properties

Fuel property	Diesel	Neat jatropha oil
Density	837 kg/m ³	921 kg/m ³
Flash point	68 °C	258°C
Kinematic viscosity at 38 °C	2.51 cst	36.46 cst
Cetane index	47-53	40-43
Calorific value	42927 kJ/kg	39200 kJ/kg

IV. EXPERIMENTAL SET-UP

A single cylinder, 4- stroke, water-cooled, diesel engine coupled with electrical dynamometer as shown in figure 1 was used as experimental set-up. The specifications of engine & dynamometer are given in table 2 & 3. The measuring instruments used in this project is listed in table 4. The suction side of the test engine is attached with anti-pulsating drum to measure air inflow quantity. The inlet temperature of air is measured with inlet air thermometer. The exhaust side of the engine consisting of series of devices such as Exhaust Gas Thermometer (EGT), gas analyser probe and smoke meter probe. A combustion analyser is also attached with the test rig to study the combustion behavior of engine. The set-up also consists of fuel flow measuring device to measure the fuel consumption of the engine. The output side of the engine consisting of an electrical dynamometer and followed by a loading rheostat. The output is measured in terms of watts using digital wattmeter mounted in the panel. An 8 bit Data Acquisition System (DAS) is also connected with the test rig to acquire the combustion pressure and crank angle data for a stipulated number of cycles.

EXPERIMENTAL SET-UP

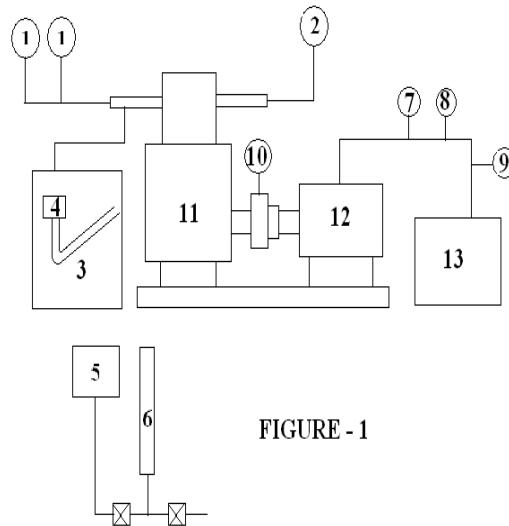


FIGURE - 1

1. Inlet Temperature
2. Exhaust Gas Temperature
3. Anti Pulsating Air drum
4. Inclined Manometer
5. Fuel Tank
6. Burette
7. Voltmeter
8. Ammeter
9. Wattmeter
10. Tachometer
11. Engine
12. Alternator
13. Loading Rheostat

Table 4.2 Engine Specification

Make	Kirloskar AV 1 model
Number of Cylinder	One
Type of cooling	Water cooled
Ignition	Compression ignition
Bore	80 mm
Stroke	110mm
Speed	1500 rpm
Brake power	5 Hp
Fuel	Diesel
Lubrication	Full pressure lubrication

Table 4.3 Alternator Specification

Make	Kirloskar
Power	5 KVA
Speed	1500 rpm
Voltage	230 v
Ampere	21.7 amps
Frequency	50 Hz
Power factor	0.8

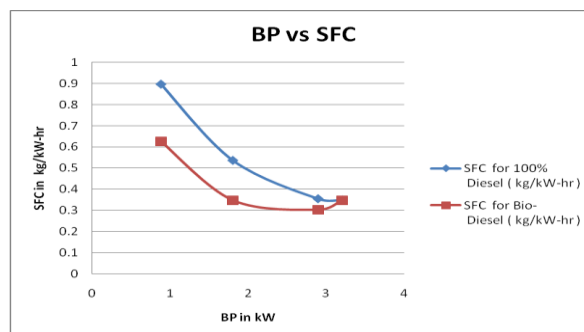
Table 4.4 Measuring Instruments Used

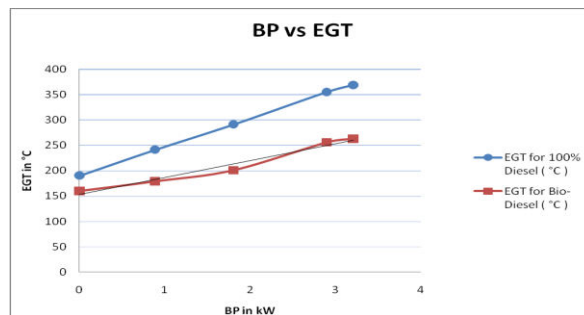
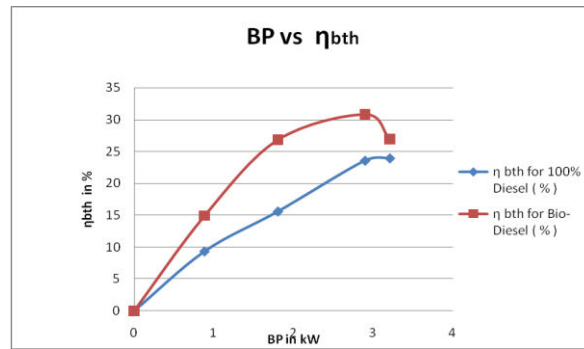
S.No.	Measuring Parameters	Instruments Used
1	HC,CO,NO _x	Exhaust gas Analyser
2	Smoke	Smoke meter
3	Cylinder pr, and Crank Angle	Data aquisition system
4	Exhaust gas temperature	Digital Thermometer
5	Air flow rate	Orifice & manometer

V. EXPERIMENTAL PROCEDURE

Experimental investigations is carried out in the same engine test rig using (i) Bio-diesel and (ii) Mineral diesel. The various steps involved in carrying out this project work is listed below.

- Preparation of bio-diesel
- Performance test on engine using mineral diesel at constant speed of 1500 rpm under natural aspirated condition.
- Performance test on the same engine using Jatropha bio-diesel at the same specified condition.
- Comparison of these two performances using graphs.





VI CONCLUSION

A kirloskar 5 hp engine was tested successfully using mineral diesel and biodiesel (Jatropha based) separately. From the results the following conclusions were arrived while using biodiesel as fuel.

- Higher thermal efficiency
- Smooth running of engine
- Lesser emission
- Low exhaust gas temperature.

REFERENCES

1. Amba Prasad Rao G, Rama Mohan P (2004) Performance Evaluation of DI and IDI Engines with Jatropha Oil based Bio-diesel. IE(I) Journal-MC, p72-76.
2. Channapattana S V, Dr. Kulkarni R R(2009) Bio-diesel as a fuel in IC engines- A review. International Journal of computer science and applications, vol 2 no:1, p 22-26.
3. Chauhan R D, Sharma M P, Saini R P and Singal S K(2007) Bio-diesel from Jatropha as transport fuel- A case study of UP state, India. Journal of scientific and industrial research, vol 66, May 2007, pp 394-398.
4. Chincholkar S P, Saurabh Srivastava, Rehman A, Savita Dixit & Atul Lanjewar(2005) Bio-diesel as an alternative fuel for pollution control in Diesel Engine. Asian J.Exp. Sci, vol 19, no:2, 2005, p 13-22.
5. Hanumentha Rao Y.V, Ram Sudheer Voleti, Sitarama Raju A.V and Nageswara Reddy P (2009) Experimental investigations on jatropha Bio-diesel and additive in diesel engine. Indian Journal of Science and Technology, Vol.2, no:4, Page 25-31.
6. Jindal S (2010) Effect of engine parameters on NO_x emissions with Jatropha biodiesel as fuel. Energy and Environment, volume 1, Issue 2, PP 343-350.
7. Singh R K and Saroj K Padli (2009) Characterization of Jatropha oil for the preparation of bio-diesel. Natural product Radiance, vol. 8(2), 2009, pp 127-132.
8. Tint Tint Kywe, Mya Mya OO (2009) Production of Bio-diesel from Jatropha oil (Jatropha curcas) in pilot plant. World Academy of Science, Engineering and Technology, PP477-483.

Performance Analysis of Compression Ignition Engine by using Hydrogen with Cashew Nut Shell Oil and Feasibility as Bio Fuel

V.Thanigaivelan¹, M.Loganathan², E. James Gunasekaran³

¹Faculty Mechanical Department, SRM University, thanigailav@gmail.com

² Faculty Mechanical Dept, Annamalai University, logu692002@rediffmail.com

³ Faculty Mechanical Dept, Annamalai University, jamesgunasekaran@gmail.com @gmail.com

Abstract — Petroleum is non renewable source of energy and the petroleum reserves are scarce nowadays, there is a need to search for alternative fuels for automobiles. The intensive search for alternative fuels for compression ignition engines has been focused attention on fuels which can be derived from bio mass in this regard cashew nut oil and cottonseed oil is found to be a potential fuel for C.I Engines. The properties of cashew nut oil are determined by using standard methods. The objective of the present work is to reveal the effects of crude cashew nut shell oil blends performance on a direct injection diesel engine. This actually aims to find out suitability of cashew nut oil, and its blends with diesel. In this paper cashew nut oil with diesel blends are taken up for study on 10HP, Multi cylinder, four stroke, water cooled Operations of the test engine with cashew nut shell oil blends for a wide range of engine load conditions were performed. During the experiments, the performance characteristics of the test engine was analyzed and compared with the neat diesel fuel performance. The results were shown to be successful even without any engine modifications.

Keywords- Diesel engine; alternate fuel; cashew nut shell oil; performance; Hydrogen; Bio fuel

I. INTRODUCTION

Biodiesel is considered an attractive fuel, which is renewable and offers, from a life-cycle perspective, an important decreased atmospheric carbon emission compared with conventional diesel fuels. Its reported advantages include generally lower emissions of CO, hydrocarbons HC and particulate matter PM, but with eventually increased NO_x emissions compared to fossil diesel fuels. Increased environmental awareness and depletion of fossil fuel resources are driving the researchers, engineers and the fuel industry to develop alternative fuels that are environmentally more acceptable and renewable in nature [1]. The idea of using vegetable oils as fuel for diesel engine is not new. Vegetable oils can be used in diesel engines either in raw form, or can be converted into biodiesel. Some properties are to be considered as important for the selection of biofuel and are namely, viscosity, flash point, fire point, density, calorific value, corrosive nature, miscibility, sulphur content, molecular weight, cetane number, etc. It was very interesting that most of the properties were very closer to the conventional diesel fuel. The viscosity, though on the higher side at room temperature, reduces drastically at higher temperature. Observed viscosity at 30°C for cardanol was 31.97 cSt, and at 60°C it was 15.96 cSt. The flash point and fire point of the cardanol was registered at 208°C and 220°C respectively. The density value was 0.92 gm/cc. The calorific value shows that 9845 Kcal/kg. Corrosive nature of cardanol is very mild on copper and stainless steel. Cardanol is completely miscible in alcohol and diesel and they are insoluble in water. There is no sulphur present in it. The molecular weight of cardanol is 298.5 g/mol. CNSL oil is amber-colored, poisonous, viscous oil and it is often considered as the better and cheaper source of unsaturated phenols. CNSL oil has many biological and industrial applications due to the fact that it can easily react forming various derivatives,

including polymers and resins (Patel R N 2006). It can replace phenol in any applications with equivalent or better result.

III. EXPERIMENTAL SETUP AND ANALYSIS

Cashew nut shell oil was purchased from the local market in Panruti, Cuddalore district. Diesel was purchased from the local bunk. The properties of diesel and cashew nut shell oil are given in table 1.

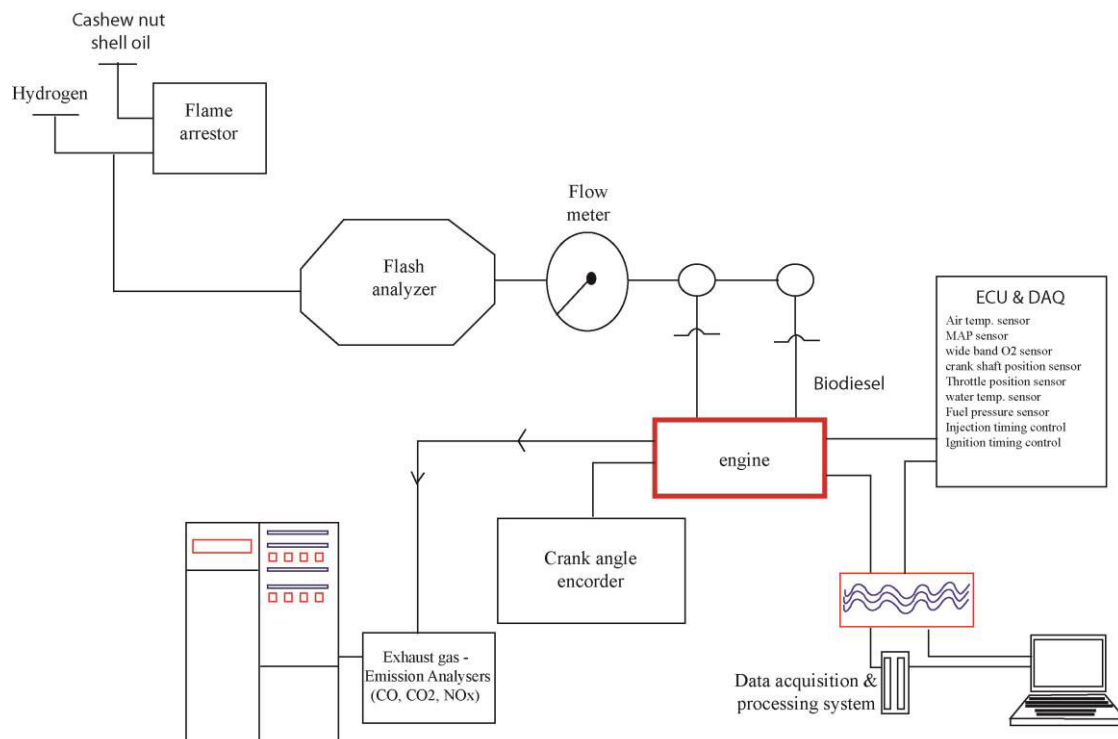
Table 1. Properties of diesel and CNSO

Property	Diesel	CNSO
Calorific value (MJ/kg)	42.8	40.69
Viscosity (cSt)	840	952
Density (kg/m ³)	3.6	9.4
Fire Point (°C)	61	256
Flash point (°C)	70	264

Experiments were carried out in a vertical, single cylinder, naturally aspirated, four stroke, constant speed, water cooled, direct injection diesel engine. The layout of experimental setup is shown in the figure 1.

3.1. Extraction of CNSL oil

Extraction of CNSL oil from cashew nut shell includes open pan roasting, drum roasting, hot oil roasting, cold extraction, solvent extraction, super critical fluid extraction



(Rajesh N. Patel 2006), pyrolysis process (Das 2004, Tsamba 2004), Soxhlet extraction method (Castro 1998, Tyman 1989) and research have been carried out to improve the percentage of yield from raw cashew nut by using new extraction methods like Sub Critical Water extraction and two-step extraction methods (Maria Yuliana 2011). The percentage yield of oil varies with the type of extraction process. As the extraction method varies, the quantity and quality of oil varies with the composition percentage of Anacardic acid, Cardanol and cardol. There are two types of CNSL oils and are known as natural or immature oil (iCNSL)

and technical oil (tCNSL). The compositions of iCNSL are anacardic acid 70%, cardol 18%, Cardanol 5%, and remaining are the other phenols and less polar substances.

3.2. Effect of hydrogen on biodiesel blends

The depletion of fossil diesel fuels, global warming concerns and the stricter limits on regulated pollutant emissions encourage the use of renewable fuels. Biodiesel is the most used renewable fuel in compression ignition (CI) engines. The majority of the literature agrees that particulate matter (PM), and carbon monoxide (CO) emissions from biodiesel are lower than from conventional diesel fuel [1-3]. One of the most important reasons for this is the oxygen content of biodiesel [4, 5], this induces a more complete and cleaner combustion process. When compared to standard diesel, the use of biodiesel can lead to more effective CO and particulate matter oxidation [6] and increased NO_x emissions [7-9], depending on the engine technology employed, combustion characteristics and other physical and chemical properties of the biodiesel. The absence of aromatic compounds in biodiesel is another factor which justifies the particulate matter reduction with respect to diesel [3, 10].

3.3. Experimental investigation

The experiments were conducted by considering various parameters. The tests were conducted for cashew nut oil and its blends at different proportions (15%, 25%, 35% and 45%) for conventional engine. The tests were conducted from no load to maximum load conditions. The readings such as time taken to consume 20cc of fuel consumption, speed of the engine, temperatures, etc, were noted. The observations were recorded in tabular column and calculations are made using appropriate equations. The experiments were conducted on a compression ignition diesel engine. The general specifications of the engine are given in table 2. By taking the engine performance and plot the graphs.

Table 2. Engine specifications

Item	Specifications
Engine power	10 H.P
Cylinder bore	84 mm
Stroke length	110 mm
Arrangement of cylinder	Vertical
Engine speed	1500 rpm
Compression ratio	15:1

IV. RESULTS AND DISCUSSIONS

Figure 2 shows the variation of brake thermal efficiency with respect to load. The brake thermal efficiency of the cashew nut shell oil blends are lower than the diesel in all the loads starting from no load to full load. This is due to poor mixture formation as a result of low volatility, higher viscosity and higher density of biodiesel compared with diesel. At maximum load, the brake power efficiency of 20, 40 and 60% CSNO blends are 9.41, 15.25, and 20.4% lower than diesel respectively. In the above graph Brake power is taken in x-axis and is taken BSFC in y-axis. The BSFC of the blends has been compared with diesel fuel at various loads. It is observed that the BSFC is less for the B20 Over the entire range of load.

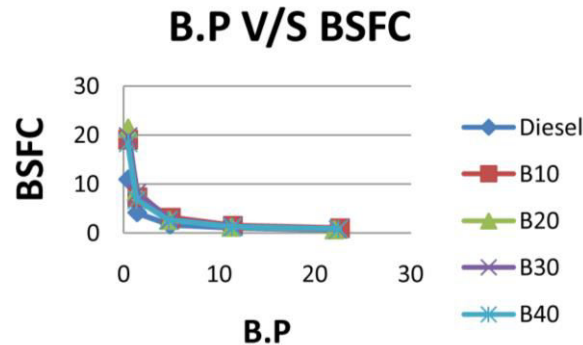


Figure 2. Brake power Vs Specific fuel consumption

The specific fuel consumption of cashew nut shell oil blends is higher than that of diesel in all loads. The specific fuel consumption varies depends upon the mass flow rate of hydrogen. The mass flow rate of hydrogen is low for cashew nut shell oil whereas for diesel, it is slightly high. So it leads to increase in specific fuel consumption.

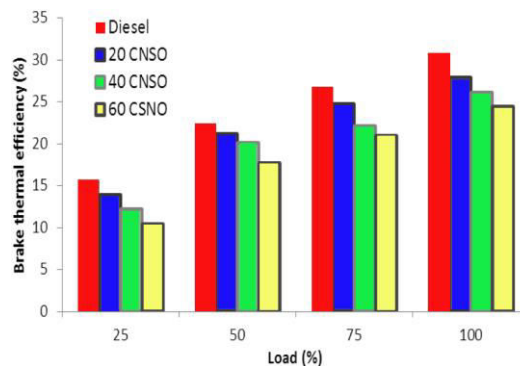


Figure 3. Brake thermal efficiency vs. Load

In Figure 3 Brake power is taken in x-axis and Brake Thermal Efficiency should be taken in y-axis. The Brake Thermal efficiency of the blends has been compared with diesel fuel at various loads and it is shown in figure. It is observed that the Brake Thermal Efficiency for B40 blend was considering higher for first three loads remaining B20 is higher over the other blends operation over entire load range.

IV. CONCLUSION

A Multi cylinder, water cooled direct injection compression ignition diesel engine was operated successfully using the mixing of cashew nut oil and diesel blends as fuel. The following conclusions are made based on the experimental results. The Specific fuel Consumption for Blend 20 is less when compared to diesel and all other blends over the entire load range. The efficiencies such as Brake Thermal Efficiency, Indicated Thermal Efficiency and Mechanical Efficiency values for blend 20% is more than diesel and other blends over the entire load range. Thus it was shown that cashew nut shell oil blends as alternative diesel engine fuels i.e. biodiesel can be used successfully to operate the engine without modifications to the engine.

REFERENCES

- [1] Carraretto, C.; Macor, A.; Mirandola, A.; Stoppato, A.; and Tonon, S. (2004). Biodiesel as alternative fuel: Experimental analysis and energetic evaluations. *Energy*, 29(12-15), 2195-2211.
- [2] Sridhar G, Paul PJ, Mukunda HS. "Biomass derived producer gas as a reciprocating engine fuel -an experimental analysis." *Biomass and Bioenergy*. 21, pp 61-67, 2001.
- [3] Krawczyk, T. Biodiesel – alternative fuel makes inroads but hurdle remains. *Int. News Fats, Oils Related Mater.* (INFORM), 1996, 7, 801–815.
- [4] S Sinha and A K Agarwal, Experimental investigation of the combustion characteristics of a biodiesel (rice-bran oil methyl ester)-fuelled direct-injection transportation diesel engine, *Proceedings of the Institution of Mechanical Engineers, Part D: Journal of Automobile Engineering* 2007 221: 921.
- [5] Piyali Das, Sreelatha T, Anuradda Ganesh, Bio-oil from pyrolysis of cashew nut shell-characterization and related properties, *Biomass and Bioenergy*, 27, 2004, 265–275.
- [6] Ganeshan.V "Internal Combustion Engines", 7 Tata Mc.Graw Hill Publishing, New Delhi, 2002.
- [7] Michel SG and Robert LM (1998) Combustion of fat and vegetables oil derived fuels in diesel engines. *Prog. Energy. Combustion Sci.* 24,125-64.
- [8] Ertan Alptekin and Mustafa Canakci(2006) Determination of the density and the viscosities of biodiesel–diesel fuel blends. *Renewable Energy* (33), 2623– 2630.
- [9] Deepak Agarwal, Lokesh Kumar, Avinash Kumar Agarwal, "Performance evaluation of a vegetable oil fuelled compression ignition engine", *Renewable Energy*, Vol.33, 2008, pp.1147–1156.
- [10] P. Lawrence, P. Koshy Mathews and B. Deepanraj, Effect of Prickly Poppy Methyl Ester Blends on CI Engine Performance and Emission Characteristics, *American Journal of Environmental Sciences*, Vol.7, 2011, pp.145-149.
- [11] Saravanan N, Nagarajan G. An experimental investigation of hydrogen-enriched air induction in a diesel engine. *Int J Hydrogen Energy* 2008;33:1769-75.
- [12] Senthil Kumar M, Ramesh A, Nagalingam B. Use of hydrogen to enhance the performance of a vegetable oil fuelled compression ignition engine. *Int J Hydrogen Energy* 2003;28: 1143-54.
- [13] Miyamoto T, Hasegawa H, Mikami M, Kojima N, Kabashima H, Urata Y. Effect of hydrogen addition to intake gas on combustion and exhaust emission characteristics of a diesel engine. *Int J Hydrogen Energy* 2011;36:13138-49.
- [14] M. Young, *The Technical Writer's Handbook*. Mill Valley, CA: University Science, 1989.
- [15] Furuhashi S. State of the art and future trends in hydrogen fueled engine. *Int J Veh Des* 1983;4:359-85.
- [16] Das LM. Hydrogen engines: a review of the past and a look into future. *Int J Hydrogen Energy* 1990;5:425-43.
- [17] White CM, Steeper RR, Lutz AE. The hydrogen-fueled internal combustion engine: a technical review. *Int J Hydrogen Energy* 2006;31:1292-350.
- [18] Karim GA. Combustion in gas fueled compression ignition engines of the dual fuel type. *Trans ASME, J Eng Gas Turbines Power* 2003;125:827-36.
- [19] Sahoo BB, Sahoo N, Saha UK. Effect of engine parameters and type of gaseous fuel on the performance of dual-fuel gas diesel engines: a critical review. *Renew Sust Energ Rev* 2009; 13:1151-84.
- [20] Gopal G, Rao PS, Gopalakrishnan KV, Murthy BS. Use of hydrogen in dual fuel engine. *Int J Hydrogen Energy* 1982;7: 267-72.
- [21] Varde KS, Frame GA. Hydrogen aspiration in direct injection type diesel engine-it's effect on smoke and other engine performance parameters. *Int J Hydrogen Energy* 1983;8:549-55.
- [22] McWilliam L, Megaritis T, Zhao H. Experimental investigation of the effects of combined hydrogen and diesel combustion on the emissions of a HSDI diesel engine. Paper 2008-01-1787. SAE; 2008.
- [23] Turns SR. *An introduction to combustion: concepts and applications*. 2nd ed. New York, NY: McGraw-Hill Higher Education; 1999.
- [24] J. Clerk Maxwell, *A Treatise on Electricity and Magnetism*, 3rd ed., vol. 2. Oxford: Clarendon, 1892, pp.68-73.

Fabrication and analysis of various Biomass using slow Pyrolysis Reactor

M.Balamurugan¹, K.Saravanan², D.Ommurugadhasan³ V.Vasantharaj⁴.

¹ P.G Scholar, Mechanical Department, Pondicherry Engineering College.

² Assistant Professor, Mechanical Department, St. Anne's College of Engg and Tech Panruti

³ Associate Professor, Mechanical Department, St. Anne's College of Engg and Tech. Panruti

⁴ Assistant Professor, Mechanical Department, CIT college of Engineering. Puducherry

Abstract— Disposal of commonly used Biomass particals into land fill was becoming more undesirable due to environmental concerns. Therefore, recycling through mechanical and thermo chemical process the various bio mass are converted into useful products. Pyrolysis is a thermal decomposition process that takes place in the absence of oxygen. Slow pyrolysis of BioMass is one of the most emerging technology. A slow pyrolysis reactor was designed and fabricated. It consists of a reactor, heating element and water cooled condenser. . Slow pyrolysis of various biomass was carried out in the pyrolysis reactor to determine the effect of temperature and raw material size on the yield of pyrolysis products. These project concentrates on production and yields of thermo-chemical conversion of biomass into bio-fuels (bio-oil, bio-char and bio-gas).

Keywords— Biochar, Bio-oil, Biogas.

I. INTRODUCTION

Renewable energy is of growing importance in satisfying environmental concerns over fossil fuel usage. Wood and other forms of biomass are one of the main renewable energy resources available. Utilizing this energy does not add cabondioxide, which is a greenhouse gas to the atmospheric environment in contrast to fossil. Like other biomass wastes, agricultural wastes contain high amount organic constituents (i.e. cellulose, hemicellulose and lignin) and posse's high energy content. Therefore it can be recognized as a potential source of renewable energy. Due to the lower contents of sulphur and nitrogen in biomass waste, it creates less environmental pollution and health risk than fossil combustion. Some biomass produced in our country is listed.

II. PYROLYSIS

Pyrolysis is the thermal decomposition of organic matter under vacuum of inert atmospheric conditions. And it is thermo-chemical process that converts biomass into liquid, charcoal and non-condensable gases and chemical by heating the biomass to about 500°C in the absence of oxygen. Conventional pyrolysis is defined as the pyrolysis, which occurs under a slow heating rate. This condition permits the production of solid, liquid, and gases pyrolysis products in significant portions.

2.1. Slow pyrolysis

Slow pyrolysis of biomass is associated with high charcoal continent, but the fast pyrolysis is associated with tar, at low temperature (675-775K), and/or gas, at high temperature. at present, the preferred technology is fast pyrolysis at high temperatures with very short residence time.

2.2. Fast pyrolysis

Fast pyrolysis (more accurately defined as thermolysis) is a process in which a material, such as biomass, is rapidly heated to high temperature in the absence of oxygen.

2.3. Flash pyrolysis

The flash pyrolysis of biomass is the thermo-chemical process that converts small dried biomass particles into a liquid fuel (bio-oil or bio-crude) for almost 75%, and char and non-condensable gases by heating the biomass to 775K in the absence of oxygen. Char in the vapour phase catalyzes secondary cracking.

III. PRODUCTS OF PYROLYSIS

1. Gas 2. Char 3. Oil

2. ADVANTAGES OF PYROLYSIS

1. Combustion performance: The combustion processes for solid and the gases fuels can be more effectively separated and this allows the combustion condition for each to be closer to its ideal. 2. Low dust carry over: The flue gas volume and the dust carry-over levels can be significantly reduced which results in a simplification of the downstream gas cleaning equipment. 3. Thermal efficiency: The thermal balance is improved as a result of reduction in excess air required for incineration. Feed calorific value: Feed materials with high calorific contents, does not cause any problem since the furnace temperature are readily controllable.

4. Low NO_x: As the Multiple Hearth Furnace is considered more or less as a fixed bed system (versus fluidized bed), this alone ensures that NO_x emissions are lower than in any other system.

IV. LITERATURE REVIEW

Peter Mckendry [1] reviewed the main conversion process with specific regard to the production of a fuel suitable for spark ignition gas engines. Graham et.al [2] made the studies on applications of rapid thermal processing of biomass. They found that the rapid thermal processing is a generic technology to convert carbonaceous feedstock to high yields of chemical and liquid fuels products. They also find that this method is suitable for short term application include the production of specialty chemicals, fuel oil substitutes and engine fuels for both the diesel and turbine engine applications. Samolada et.al.[3] Made the pyrolysis of biomass sample in the fluid bed reactor. They studied the effect of the experimental conditions on their yield, composition of the phenolic fraction of the liquids and pyrolysis gas. They found that the bed temperature acts as main factor, for control the yields of products and the bed temperature of approximately 700°C is recommended for max.yields.

Bridwater[4] reviewed the design consideration faced by the developers of the batch type pyrolysis, upgrading and utilization process in order to successfully implement the technologies. Here the aspect of batch type reactor is studied. Boukis et.al. [5] Made the experiments on circulating fluid bed reactor operators in relatively high velocity studied the hydrodynamic behavior of the designed reactor. They observed that circulating fluid bed hydrodynamic and stability Wagenaar et.al [6] made experiments on rotating cone reactor and absorbed that the particles large than 400µm seem to be unaffected by the viscous forces because their mass inertia and the resistance time of such particles is hardly dependent on the particle diameter. If the particle diameter is smaller than 200µm the viscous become important compared to the mass inertia and the particle residence time is strongly dependant on the particle diameter. westerhout et.al [7] made the experiments on the techno economic evaluation of high temperature pyrolysis process for mixed plastics waste. From experiments it is observed that the rotating cone reactor is competitive with other types of gas-solid reactor such as bubbling fluid bed and riser system

V. DESIGN OF PYROLYSIS SETUP

5.1. REACTOR SETUP

Reactor is the place where the pyrolysis reactor takes place. The reactor is made up of stainless steel in order to avoid the corrosion resistance compare to mild steel.

Types of Reactors

1. Ablative type reactor
2. Circulating fluid bed type reactor.
3. Fluid bed type reactor.
4. Entrained flow type reactor

5.2.DESIRABLE PARAMETERS FOR THE DESIGN:

- a) Melting point of the substance: If mp is high, substance easily vaporizes & more oil is obtained.
- b) Density: If density is lower, substance easily vaporizes & more oil is obtained.
- c) Moisture content: More is moisture, less is the oil yield.
- d) Reactor Temp: More is the reactor temp, more is the yield
- e) Heating rate: More is the heating rate, more is the yield
- f) Reactor size: There is an optimum for the reactor size to get maximum oil yield.
- g) Feed rate: Feed rate is given according to the demand for the oil.

Calculation

$$\begin{aligned}\text{Volume of the reactor} &= 3.14 \times r^2 \times h \\ &= 3.14 \times 9 \times 9 \times 31 \\ &= 7.884 \times 10^{-3} \text{ m}^3\end{aligned}$$

Based on the density and volume of the biomass, the volume of the reactor is calculated as follows.

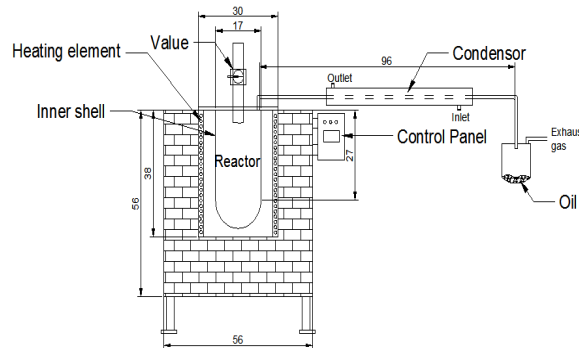


Fig5.1 Front view

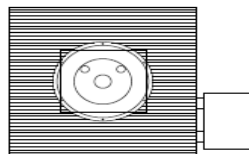


Fig5.2 Top view

VI. CHARACTERIZATION OF BIOMASS

The raw material is characterized as follows

1. Thermogravimetric Analysis
2. FTIR Analysis

6.1.THERMO-GRAVIMETRIC ANALYSIS

Thermo-gravimetric analysis was performed on a Q600 SDT TGA instrument for the stem, flower and leaf. Combustion runs were carried out in the inert atmosphere heating from 25 to 900 °C at a rate of 10°C/min. A sample of about 12.093 mg is taken for T.G.A. The temperature maintained for the sample is 25°C to 700°C at the heating rate of 10°C/min. in the TGA model of Q600SDT.

4.1.1 TGA of water hycanith stem

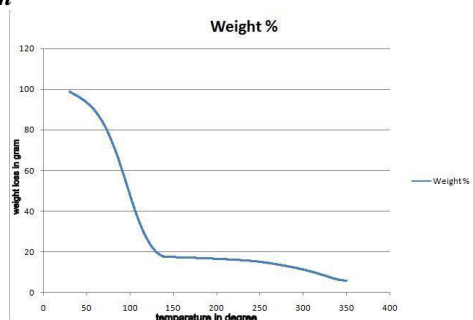


Fig 6.1 TGA of water hycanith stem

From the graph, it is seen that the sample has started decomposing from 300°C and the maximum decomposition occurs between 300°C – 450°C. Finally decomposition ends at 550°C.

TGA of banana stem:

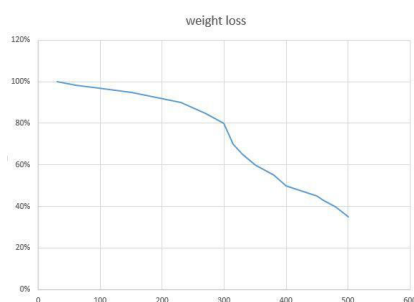


Fig 6.2 TGA of banana stem

From the graph, it is seen that the decomposition of the flower starts at 220°C and the maximum decomposition occurs between 220°C - 430°C.

TGA of pseudo stem :

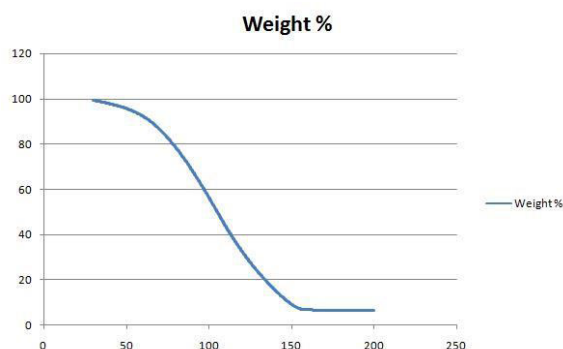


Fig 6.3 TGA of pseudo stem leaf

From the graph, the decomposition of the leaf starts at 200°C onwards and the maximum decomposition occurs between 200°C - 400°C.

6.2. Fourier Transform Infrared Analysis

FTIR For water hycanith

FTIR analysis result of water hycanith Bio-oil sample. The result are tabulated in Table 6.2

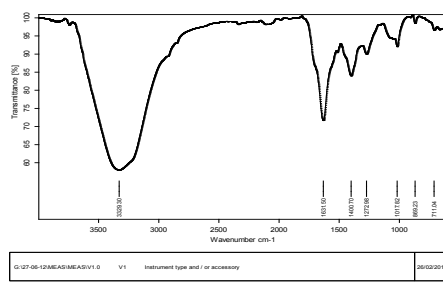


Fig 6.4 FTIR of pyrolytic oil

Table 4.1 Components Present in the pyrolytic oil(Water Hycanith)

Peak value	Group name	Functions
3329.30	Alcohols	O-H stretch
1631.50	Ketones	C-O Bend
1400.70	Secondary Amines	N-H Bend
1272.98	Esters	C-O stretch
1017.62	Ethers	C-o stretch

Fourier Transform for Banana Stem

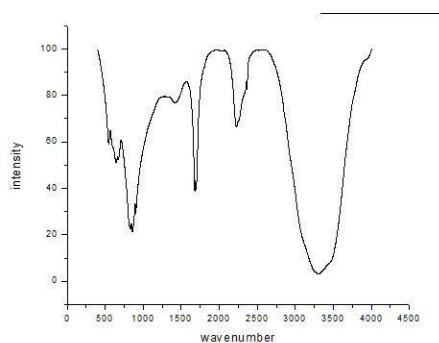


Fig 6.5 Pyrolytic oil of Banana stem

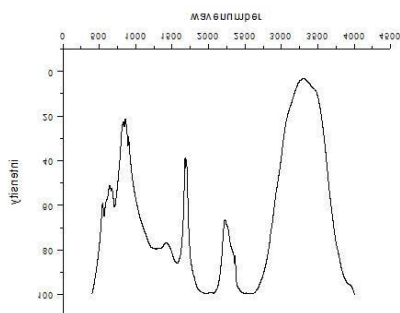


Fig 6.6 Pyrolytic oil of Banana Pseudo Stem

VII. SLOW PYROLYSIS OF VARIOUS BIOMASS

7.1.EXPERIMENTAL PROCEDURE

The stem of various biomass was cut into pieces and it is dried in the sunlight for 2-3 days. A sample weighing 250g was kept in the reactor. The biomass was heated to a maximum temperature from room temperature. When the maximum temperature was reached the reactor turns off automatically. When the reactor was completely cooled to room temperature, the char was removed from the The slow pyrolysis experiments were conducted at the following conditions.

- Reactor temperatures of 250°C, 350°C, 450°C, 550°C, and 650°C with stem length of 3cm.
- Different stem lengths of 0.02cm, 2cm, 3cm, and 20cm, keeping the reactor temperature at 550°C.
- By providing ice bath in the collecting tank in order to find the effect on the amount of oil collected.

VIII. RESULT AND DISCUSSION

8.1.PYROLYSIS AT TEMPERATURE

The stem was subjected to the slow pyrolysis under different temperatures of 150°C, 200°C, 250°C, and 300°C. The results of the process was given in terms of oil, char and

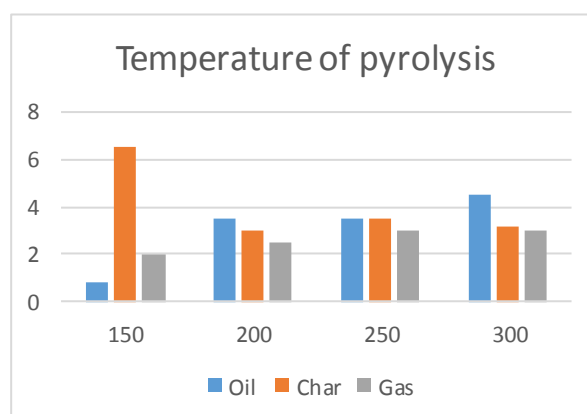


Fig 8.1Yield of the pyrolysis products at different temperature

From the graph, it is seen that the maximum oil yield take place at 550°C, whereas char and gas yield is high at 150°C and 300°C respectively.

PYROLYSIS EXPERIMENTS BY USING ICE-BATH IN COLLECTING TANK

The pyrolysis experiments were conducted by surrounding the collecting tank with ice bath and at reactor temperature of 550°C. A comparison of yields of different products with and without ice bath is shown in the Table 6.1. It is seen that the oil yield is increased by 20 percentages.

Table 8.1 Variation in experiment by using ice bath

S.No	Without ice bath	With ice bath
Oil (%)	42.4	51.2
Gas (%)	25.6	16.8
Char (%)	32	32

IX. CONCLUSION

In our project, pyrolysis of various biomass is carried out in circular slow pyrolysis reactor and using TGA curve the various decomposing temperature of Water hyacinth, Banana stem, banana pseudo stem was found and the yields like char,oil,gas are obtained by varying with the temperature and particle size which describes lowering the temperature the char yield high, and for increasing temperature the gas yield is high ,in and the oil is at between . our setup consists of electric controller which reduces the power loss.

REFERENCES

- [1] Peter Mckendry., “Energy production from biomass”, 83, pp. 47-54. (2002)
- [2] Graham, R.G., Freel, B.A., Huffman, D.R. and Bergounou, M.A., “Applications of rapid thermal processing of biomass”. In Advances in Thermochemical Biomass Conversion, vol.2. pp.1275-1288, Blackie, London, (1993)
- [3] Samolada, M.C., and Vasalos, I.A.,” Effect of experimental conditions on the composition of gases and liquids from biomass pyrolysis”. In Advances in Thermo chemical Biomass Conversion. Vol.2., pp. 859-873, Blackie Academic and Professional, (1994)
- [4] Bridgwater, A.V., “Principles and practice of biomass fast pyrolysis processes for liquids”. Journals of Analytical and Applied Pyrolysis. Vol 51. pp.3-22.(1999)
- [5] Boukis, I.,Maniatis, K., Bridgwater, A.V., Kyritsis Flitris, S.Y. and Vassilatos, V. Flash “pyrolysis of bio-mass in an air blown circulating fluidized bed reactor”. In Advances in Thermochemical Biomass Conversion. Vol 2, pp. 1151-1164, Blackie (1994)
- [6] Brigwater, A.V. and Peacocke, G.V.C., “Fast pyrolysis processes for biomass”. Renewable and Sustainable Energy Reviews. Vol 4. Pp. 1-73.(2000)
- [7] Wagenaar, B.M., Kuipers, J.A.M., Prins, W. and Swaaij van, W.P.M., “The rotating cone flash pyrolysis reactor”, In: Advances in Thermochemical Biomass Conversion, Vol 2, pp. 1122-1133, Blackie Academic and Professional (1994)

Study the Influence of Machining Parameters in Dry Turning

A.Anne Evanglin¹, A.Anisha Christy², Dr.R.Arokiadass³, K.Saravanan⁴

^{1, 2} Students, Department of Mechanical Engineering, St.Anne's College of Engineering and Technology,

³ Professor, Department of Mechanical Engineering, St.Anne's College of Engineering and Technology,
E-Mail: raja_arokiadass@yahoo.com

⁴ Asst.Prof, Department of Mechanical Engineering, St.Anne's College of Engineering and Technology,

Abstract- Dry machining is a machining process without coolant, and it has become more popular as a finishing process. Thus, it is especially crucial to select the machining parameters to obtain the desired surface finish of machined component. In the present investigation, the influence of process parameters like speed, feed and depth of cut in dry-machining, are studied as surface roughness as the output response variable. The concept of Design of Experiments (DOE) was used for necessary experimentation. Mild steel material was considered in the present study. The experimental results were analyzed statistically to study the influence of process parameters on surface roughness.

Keywords: Turning, Mild steel, HSS tool, surface roughness.

1. INTRODUCTION

Machining hardened steels has become an important manufacturing process, particularly in the automotive and bearing industries. Abrasive processes such as grinding have typically been required to machine hardened steels, but advances in machine tools and cutting materials have allowed hard turning on modern lathes to become a realistic replacement for many grinding applications. There are many advantages of dry machining, such as increased flexibility, decreased cycle times, reductions in machine tool costs, and elimination of environmentally hazardous cutting fluids. Despite these advantages, implementation of hard turning remains relatively low, primarily due to concerns about the quality of hard turned surfaces and a lack of understanding about the surface behavior of HSS tool.

Dimensional accuracy and high quality surfaces are also required if hard turning is to replace any grinding process. A primary concern in hard turning is the generation of undesirable changes to the surface microstructure and the formation of tensile residual stresses. Additionally, surface roughness must be comparable to grinding if hard turned Surfaces are to be accepted. The results of this work indicate that proper selection of machining conditions yields acceptable dimensional accuracy and surface quality, and allows adequate tool life for most applications. This paper focuses on dry-machining of the mild steel which is widely used in engineering applications.

2. SELECTION OF PROCESS PARAMETERS

Performance of HSS cutting tools is highly dependent on the cutting conditions i.e. cutting speed, feed-rate, and depth of cut. Especially cutting speed and depth of cut significantly influence tool life. Increased cutting speed and depth of cut result in increased temperatures at the cutting zone. In addition, when feed rate is increased, residual stresses change from compressive to tensile. Based on the extensive literature review, process parameters considered for the present study are: speed, feed and depth of cut, Table-1 shows the details of the process variables and their levels considered.

Table1. Process parameters.

Parameters	Levels		
	-1	0	1
Cutting speed, rpm	300	500	700
Feed rate, mm/min	50	60	70
Depth of cut, mm	0.5	0.75	1

3. EXPERIMENTAL INVESTIGATION

Design of experiments concept was used for planning the necessary experimentation, L9 OA was used for experimental layout. The details of experimental layout are shown in Table-3. All the work pieces were machined and the surface roughness values for all the nine samples were measured, the corresponding surface roughness values are shown in the Table-2.

Table3. Experimental layout and output response

Exp. No.	Speed, RPM	Feed rate, mm/min	Depth of cut, mm	Surface roughness, μm
1	355	50	0.5	2.67
2	355	63	0.75	4.05
3	355	80	1	4.76
4	500	50	0.75	3.04
5	500	63	1	4.56
6	500	80	0.5	4.73
7	710	50	1	2.08
8	710	63	0.5	3.02
9	710	80	0.75	2.79

4. ANALYSIS OF RESULTS

The results were analyzed and the response table for data means was shown in Table 3. From the table it is clear that feed rate is the most influencing factor on surface roughness, then speed and depth of cut. The data was further analyzed to study the interaction among process parameters and the main effects plot and interaction plots were generated and shown in Figures 1 and 2, respectively. From fig. 1 and 2, it is clear that surface roughness decreases with increase

in speed. But when feed rate is increased surface roughness increases. Compare to feed and speed, depth of cut has less influence on surface roughness.

Table 3. Response Table for Means

Level	Speed, RPM	Feed rate, mm/min	Depth of cut, mm
1	3.827	2.597	3.473
2	4.110	3.877	3.293
3	2.630	4.093	3.800
Delta	1.480	1.497	0.507
Rank	2	1	3

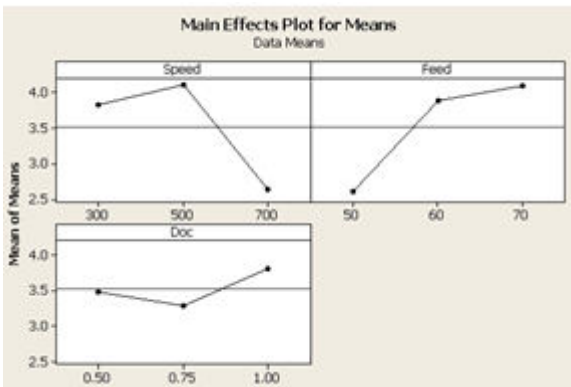


Fig.1 Main effects plot for surface roughness.

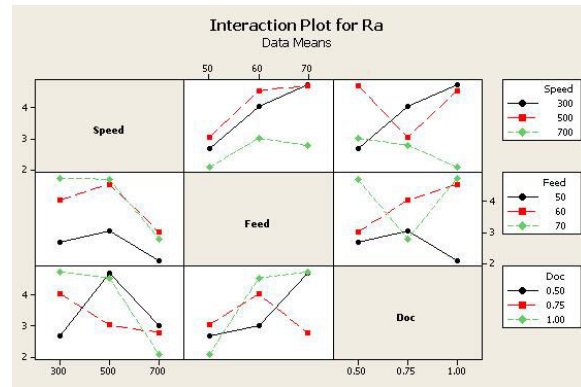


Fig2. Interaction plot for surface roughness.

5. CONCLUSIONS

The following are the conclusions drawn from the present work: Concepts of dry machining and its importance in hard turning and the influence of environmental impact were studied.

1. Surface roughness (Ra) values are decreasing with increasing the speed; but surface roughness increases with increase of feed rate. Depth of cut is not influencing much on surface roughness.
2. Strong interaction among all input process parameters was observed. Contour plots developed from analysis of results can be used for selecting the process parameters for desired surface roughness values.
3. From this experimental study and also from table 3, feed rate is the most influencing factor on surface roughness, followed by cutting speed

REFERENCES

- [1] A Parameter Design study in a turning operation using the Taguchi Method-E. Daniel Kirby.
- [2] Surface Roughness prediction models for fine turning-International journal of production research.
- [3] Design of experiments for engineers and scientists by Jiju Antony.
- [4] Taguchi methods explained by Tapan P. Bagehi.

Design And Analysis Of Lead Crowned Spur Gear Teeth

Sr. Josephine Mary¹, Sr. Layoni Margaret², Sr. Jaya Praislin³

¹*Sr. Lecturer, Mechanical Department, Annai Velankanni Polytechnic College, Panruti.*

^{2,3}*Students, Mechanical Department, St. Annes College of Engineering and Technology, Panruti.*

Abstract- In this study, the geometry of the tooth and the gear is obtained using mathematical formulations. The profile of the tooth is an involute one for the entire analysis. Geometrical modeling of spur gear tooth for performance and contact analysis is developed by using Diametral Pitch method in Pro/ENGINEER Wildfire [5]. Radius of curvature at the point of contact is found out for the selected crowning magnitude of 0.21mm. The major performance characteristics for uncrowned spur gear teeth and the lead circular crowned spur gears including root bending strength, surface compressive strength and gear tooth deflection are considered for static analysis. Effect of these parameters are studied and compared by applying load at the pitch point. The results of three dimensional FEM analysis from ANSYS are presented.

Keywords- Spur gear, Profile modifications, Crowning, Tooth contact analysis, FEM.

I. INTRODUCTION

Gears have long been widely used in machines of all kinds, with increasing requirement in recent times for smaller and lighter designs. So the gears are essential and used in all applications where power transfer is required, such as automobiles, industrial equipment, airplanes, and marine vessels. In the present study analysis of performance, contact and dynamic characteristics involute spur gears teeth with and without tooth modifications using FEM. Optimized gear model for minimum weight and size is directly taken for the study. Basic fatigue performance characteristics like surface contact stress, root bending stress and gear tooth deflection of standard and circular crowned gears are carried out. The geometry of the tooth and the gear is obtained using mathematical formulations for real cases of manufacturing. The study of influence of performance parameters of standard and crowned modifications restricted to contact ratio less than two. The material is assumed to be isotropic and homogeneous. Geometrical modeling of spur gear tooth for performance and contact analysis is developed using Pro/Engineer Wildfire [5]. Radius of curvature at the point of contact is found for the selected crowning magnitude. Effect of these parameters are studied by applying load at the pitch point and compared for uncrowned spur gear teeth and for the lead crowned spur gears. The results of three dimensional FEM analyses from ANSYS are presented. Tooth contact analysis is studied to investigate the crowning effects. Gear tooth failure is a major concern in all gear applications. Two spur gear teeth in action are generally subjected to two types of stresses. One is bending stress and the other is contact stress. These two types of stresses may not get their maximum values at the same point of contact. The above mentioned types of failures can be minimized by careful analysis of the problem during the design stage and creating proper tooth surface profile with proper manufacturing methods. Lead Crowning is considered to provide a solution for the problem so as to reduce the uneven stress distribution in the gear.

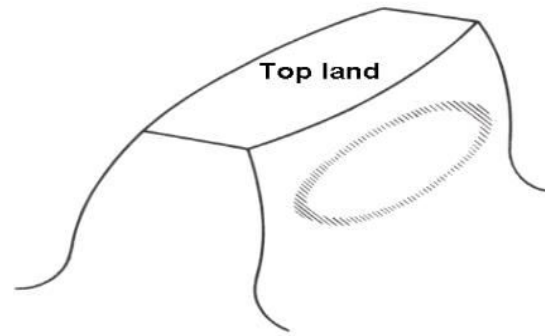


Figure.1 Crowning of Tooth to Overcome Edge Loading.

Crowning is generally done for minimization of misalignment problems, Noise reduction, Overcoming edge loading, Reduction of backlash requirements due to improper contact, Uneven wear. Ali Raad Hassan et al. [1] carried out contact stress analysis between two spur gear teeth in different contact position during rotation. The point of contact was moving from the tip to the root of tooth according to angular motion. Ellen Bergseth and Stefan Bjorklund* et al. [2] compared with traditional lead profile modifications for gears. The Logarithmical profile resulted in lower maximum contact pressure for small misalignment. Ramalingam Gurumani*, Subramaniam Shanmugam* et al. [3] did a study on the effect of major performance characteristics of uncrowned spur gear teeth at the pitch point and compared with longitudinally modified spur gear teeth by FEM analysis. The result reveals that the area of contact of involute crowned gears is slightly lower than the circular crowned gears which show the existence of more point contact compared to circular crowned gears.

III. METHODOLOGY

3.1: Modeling the spur gear by Diametral pitch method is done by using Pro/ENGINEER Wildfire[5].

Table-3.1

The input parameters to design the non-modified spur gear teeth are as follows.

Material	40Ni2Cr1Mo28 (En24) High strength alloy steel
Ultimate tensile strength , MPa	1500
Yield strength , MPa	1300
Modulus of elasticity , MPa	2.07×10^5
Density , kg/m ³	7840
Poisson's ratio	0.25
Pressure angle	20

Radius of curvature of circular crowning (ρ_{sym}) for crowning magnitude $C_C = 0.21$ mm is found out from the following relation. Radius of curvature of symmetrical circular

$$\text{crowning } (\rho_{\text{sym}}) = (4C_C^2 + b^2) / (8C_C) = 535.82 \text{ mm}$$

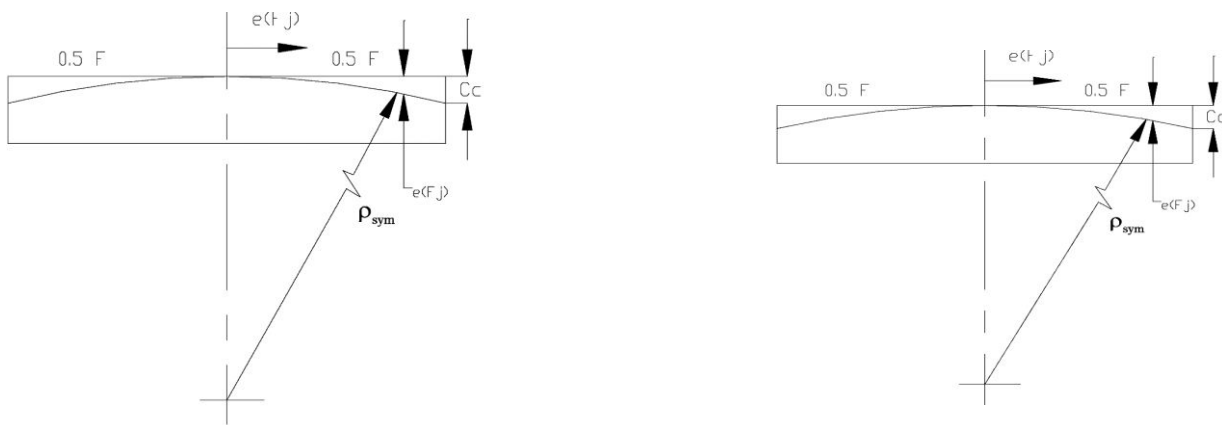


Figure 3.1 Radius of Curvature-Circular Crowning

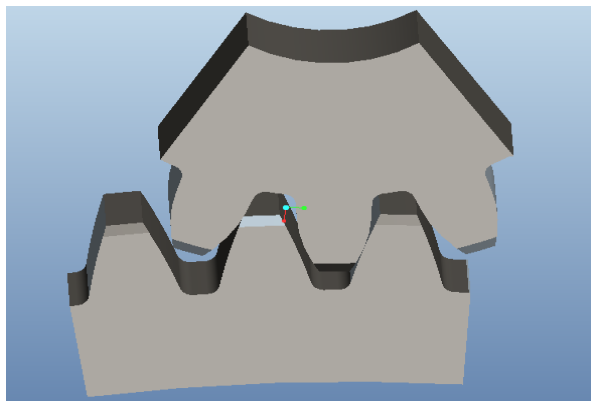


Figure 3.2 Assembled view of Non-modified Spur gear

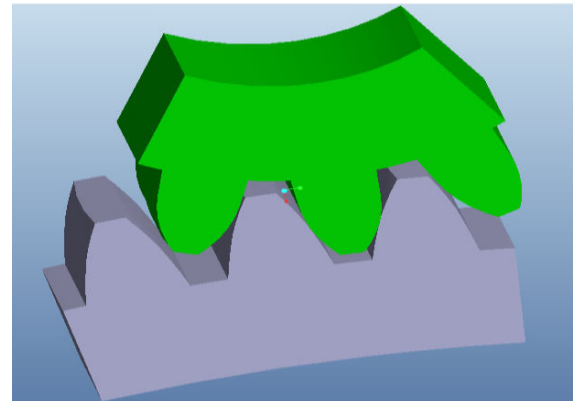


Figure 3.3 Assembled view of Modified Spur gear..

3.2: Finite Element Analysis

Finite element method is the easy and the most powerful technique as compared to the theoretical methods to find out the stress developed in a pair of gears. Therefore FEM is widely used for the stress analysis of mating gears. Element types involved are SOLID185, TARGE170, CONTA174. The contact compressive stress, root bending stress is calculated with load application at the pitch point. In the case of crowned gear, entire load is assumed to take place at the point of contact. Initially it is assumed that at anytime only one pair of teeth is in contact and takes the total load. Nodes at the side portions and the bottom portion of rim of the gear are fixed during crowned gear analysis to localize the load distribution.

IV. RESULTS AND DISCUSSION

The Stress and deflection values are obtained for the different tooth modifications of Non-modified and Circular Crowned Spur gear tooth. The Contact stress at the point of contact is found out. The maximum principal stress at the root on the tensile side of tooth is used for evaluating the tooth bending strength of a gear. The Von Mises stress at the critical contact points was found out. Also the deflection of the gear tooth is given out. The analyzed results obtained from ANSYS are given in the solid form of tabular column for different tooth modifications of non-modified and circular crowned spur gear teeth.

Table 4.1: Tooth modifications of non-modified and circular crowned spur gear teeth.

Tooth modification	Contact stress MPa	Tooth bending stress MPa	Gear tooth deflection mm
Non – modified	646.443	378.454	0.016321
Circular Crowned	1273.2	717.014	0.0161

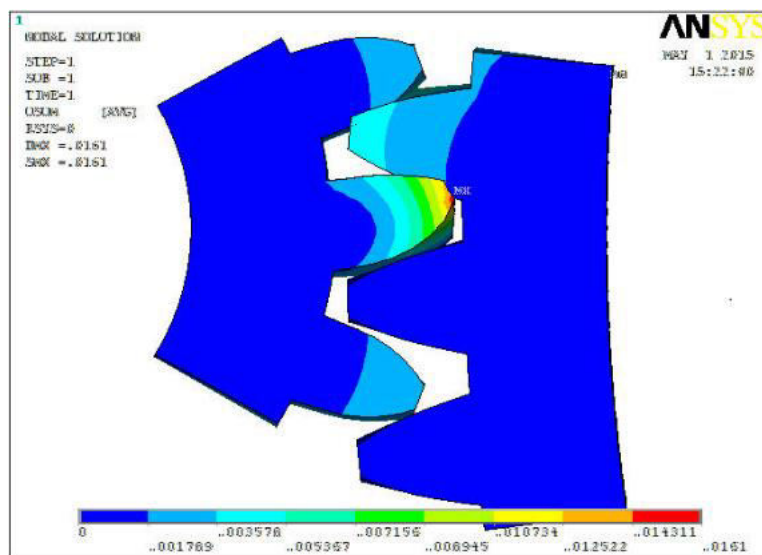


Figure4.1 Deflection of Circular Crowned Spur gear teeth

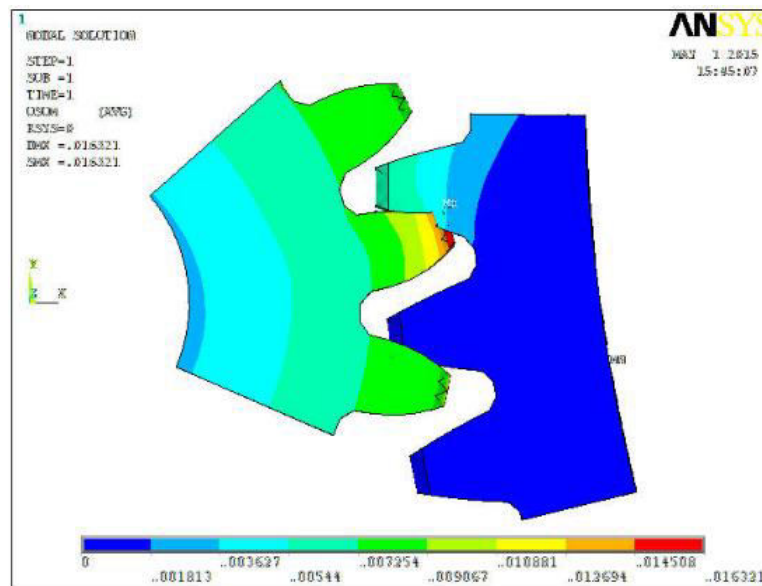


Figure.4.2 Deflection of Non-modified gear.

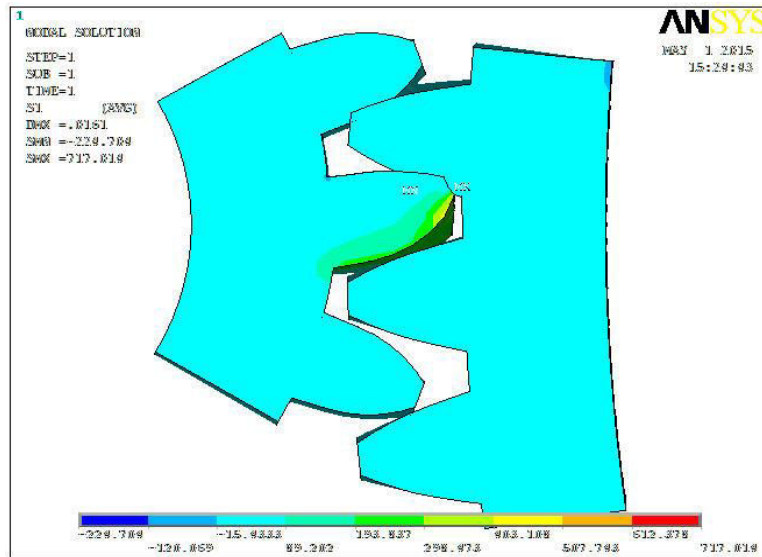


Figure 4.3 Bending Stress of Circular Crowned Spur gear teeth

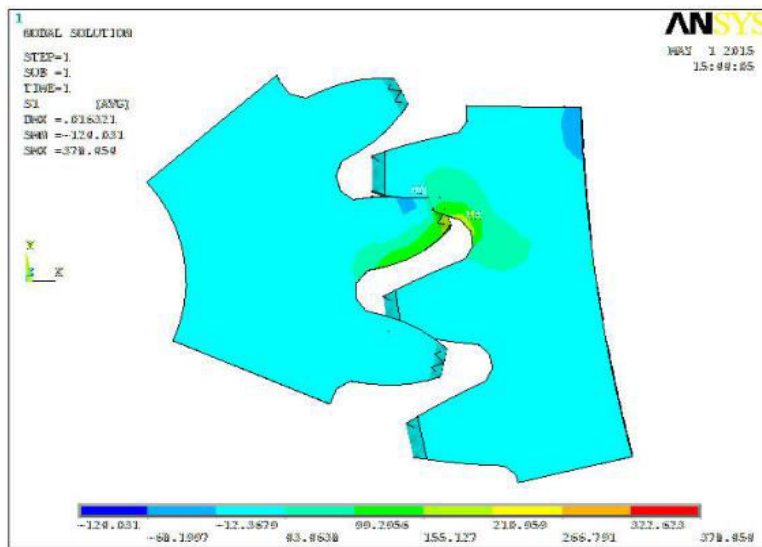


Figure 4.4 Bending Stress of Non-modified gear.

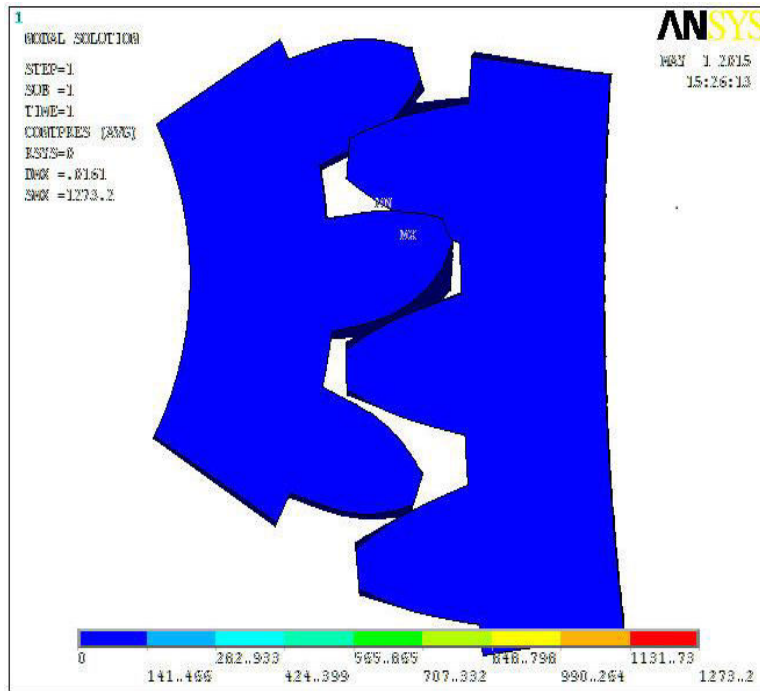


Figure 4.5 Contact Stress of Circular Crowned Spur gear teeth.

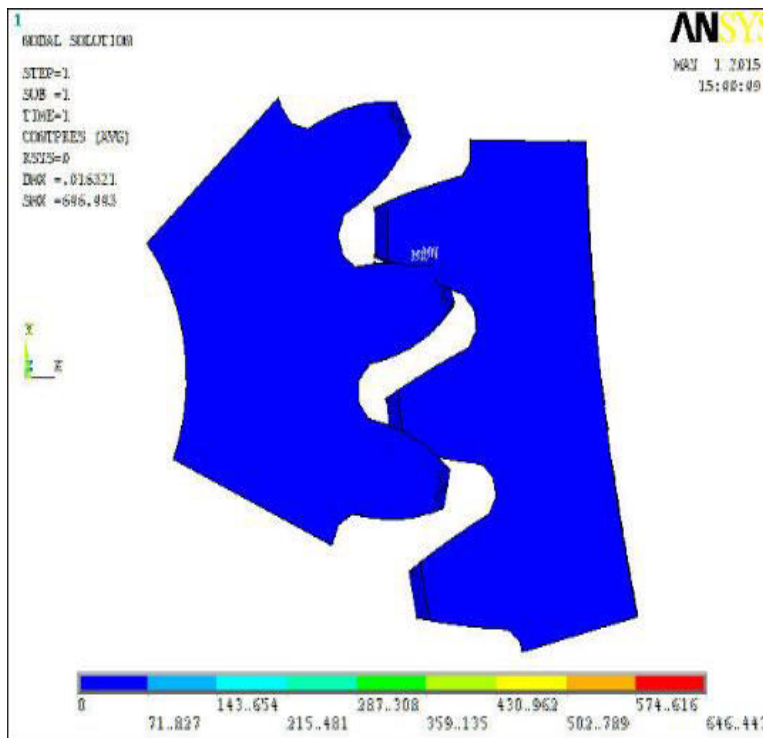


Figure 4.6 Contact stress of Non-modified gear

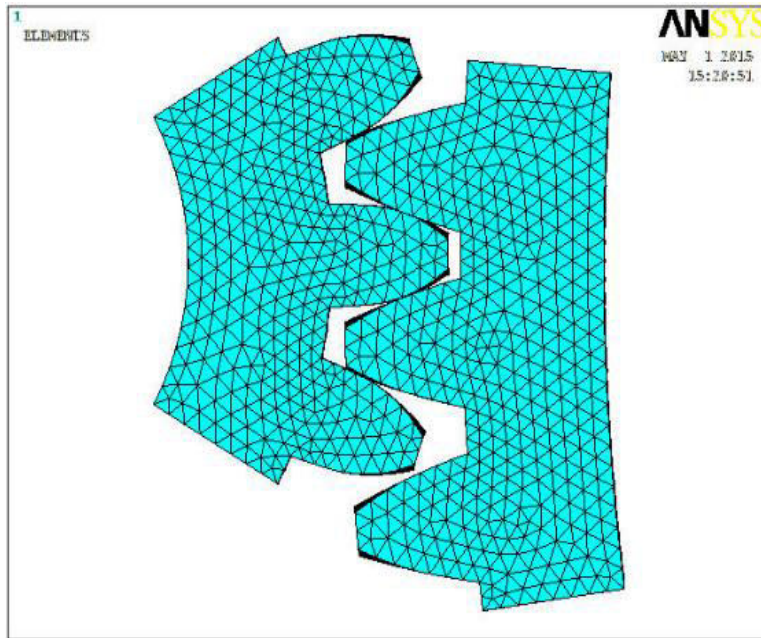


Figure 4.7 Meshed Components of Circular Crowned Spur gear teeth.

V.CONCLUSION

Uncrowned gear has line contact which causes an uneven stress distribution pattern resulting in short service life of gear. Crowned gear has point contact which in turn increases the contact stresses but within material limits. It is noted that contact period at center is minimal and stress distribution is even along the face width which in turn leads to increase in service life of the gear. It is also observed that deflection for circular crowned is lesser than that of non-modified spur gear teeth which ultimately improves the strength of the teeth.

REFERENCES

- [1] Ali Raad Hassan 2009: "Contact Stress Analysis of Spur Gear Teeth Pair".
- [2] Ellen Bergseth& Stefan Bjork Lund*: "Logarithmical Crowning for spur gears".
- [3] Ramalingam Gurumani*, Subramanian Shanmugam*: "Modeling and Contact Analysis of Crowned Spur Gear Teeth".
- [4] SB Koganti: "Finding the Stressess and Deflection of a Snag Crane".
- [5] Vivek Karaveer, Ashish Mogrekar and T.Preman Reynold Joseph: "Modeling and Finite Element Analysis of Spur gear".

Biological Immune System Applications On

Mobile Robot For Disabled People

L.Vijay¹ V.Sabarathinam² S.Subash³ P.Prithivirajan⁴

^{1,2}*Students, Dept of Mechanical St.Anne's college of Engg and Tech .Panruti*

Abstract -To improve the service quality of service robots for the disabled, immune system is applied on robot for its advantages such as diversity, dynamic, parallel management, self-organization, and self-adaptation. According to the immune system theory, local environment condition sensed by robot is considered an antigen while robot is regarded as B cell and possible node as antibody, respectively. Antibody-antigen affinity is employed to choose the optimal possible node to ensure the service robot can pass through the optimal path. The paper details the immune system applications on service robot and gives experimental results.

1. INTRODUCTION

For recent years, the robots have already massively been applied in many fields. Service robots especially have developed rapidly to complete tasks for the humanity's beneficial services. Recently, with the aging problem of the global community being increasingly serious, the service robots mainly for the elderly and the disabled have been a hot research focus. Li et al. [1] developed seven degrees of freedom movable nursing robot taking high paraplegia as the nursing object to help the patients fetch medicine, water, and books in nobody situations. Zhihua et al. [2] had presented a movable service robot with double working arms to serve the elderly and the disabled. For these service robots, path planning is an important issue. In large-scale environment with obstacles, path planning is to make the robot move along the optimal path and evade obstacles from a start position to the target location. The research of robot path planning was started at the middle of the 1960s. The interests in this area grew rapidly after the publication of Wesley [3] in 1979. From then on, many methods have been developed. There are many traditional methods, such as grid theory [4], potential field method [5], the genetic algorithm [6], and neural network [7]. Nowadays, immune system is receiving more attention and is realized as a new research hotspot of biologically inspired computational intelligence approach after the genetic algorithms, neural networks, and evolutionary computation in the research of intelligent systems [8]. It is now widely used in the fields such as data mining, network security, pattern recognition, learning, and optimization for the immune system has lots of appealing features such as diversity, dynamic, parallel management, self-organization, and self-adaptation. In this paper, biological system is applied on mobile robot to serve the disabled with better path. To ensure the service robot can pass through the optimal path, the robot needs to move along an optimal path. Firstly, admissible space tree is generated to obtain possible nodes. Then immune system is applied for its appealing features. Referring to the immune system theory, local environment information is counted as antigen and the possible node is regarded as antibody. On this basis, the affinity is calculated to choose the optimal possible node. Finally, with the node update rules, the optimal path is planned. The remainder of this paper is

organized as follows. In Section 2, the overall design is addressed. Section 3 presents biological immune system in detail. Section 4 describes the application of immune

system on mobile robot followed by experiment results given in Section 5. Conclusions and future work are discussed in Section 6.

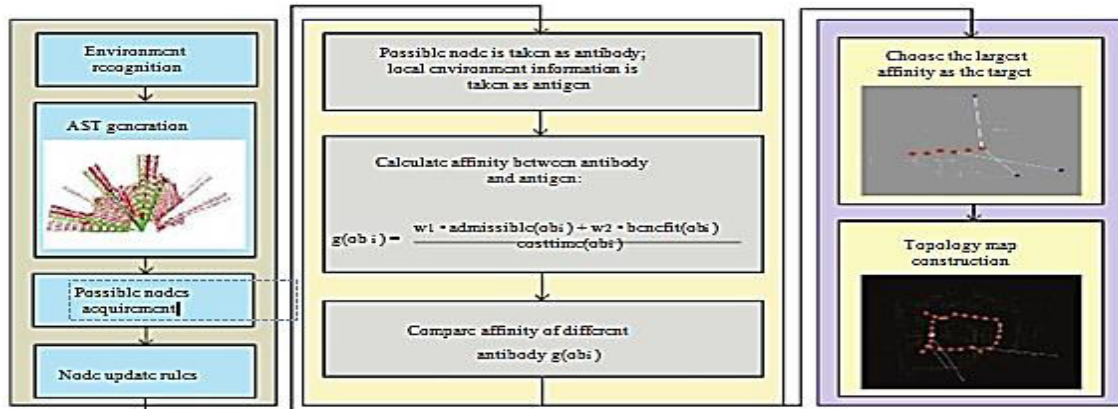


Figure 1: Details of immune system application on mobile robot.

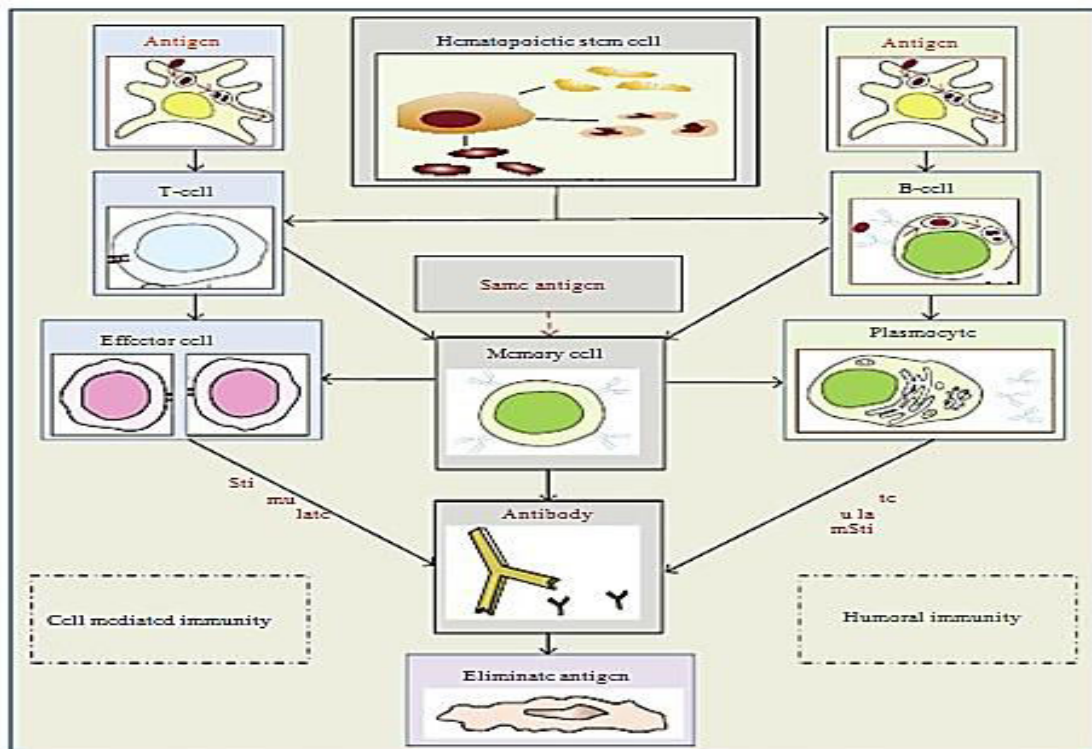


Figure 2: Abstract model of immune system.

II. OVERALL DESIGN FOR IMMUNE SYSTEM

Application on Mobile Robot To serve the disabled well, immune system is applied on mobile robot for its advantages such as self-organization, parallel management, self-adaptation, diversity, and dynamic. The detail of application is shown in Figure 1. Broadly speaking, to accomplish the serving task, this proposed method can be divided into three parts. One is admissible space tree generation. The purpose of this part is to find possible nodes for robot. Another one is immune system application. This part aims to optimize possible nodes; thus the robot path can be optimal during serving process. Last one is topology map construction. For this part, topology map is constructed to demonstrate the path which the robot has passed.

III .THE BIOLOGICAL IMMUNE SYSTEM THEORY:

The biological immune system, which protects living bodies from the invading of foreign substances such as viruses, bacteria, and other parasites (called antigens), has two types of immunity in the human body. One is the humoral immunity and the other one is the cell mediated immunity. Two main types of lymphocyte, namely, B-cell and T-cell, play a remarkable role in both immunities [9]. B-cell participates in the humoral immunity with secreting antibodies by the clonal proliferation and T-cell takes part in cell mediated immunity. For T-cells, there are two classes. One class is called killer T-cells, which destroy the infected cell when the infection is recognized. The other class is called helper T-cells, which trigger clonal expansion and stimulate or suppress antibody formation. Lymphocytes float freely in the blood and lymph nodes to patrol for foreign antigens. When an infectious foreign pathogen attacks the human body, the lymphocytes will be sensitive to these antigens and become activated. Then the helper T-cell releases the cytokines, which are the proliferate signals acting on the producing B-cell or the other remote cells. On the other hand, B-cell becomes stimulated and creates antibodies when a B-cell recognizes an antigen. The secreted antibodies are the soluble receptors of B-cell and these antibodies can be distributed throughout the body. An antibody's paratope can bind with an antigen's epitope according to their affinity. Moreover, an antibody cannot only distinguish an antigen, but also be distinguished by other antibodies [10]. The biological immune system abstract model is illustrated in Figure 2.

IV IMMUNE SYSTEM APPLICATION ON ROBOT

With the aging problem of the global community being increasingly serious, the service robots mainly for the elderly and the disabled have been paid more attention to. Therefore, path planning, as a key issue for serving task, has been a hot research topic. Meanwhile, biological immune system is receiving more attention and is widely applied in many fields for advantages of diversity, dynamic, parallel management, self-organization, and self-adaptation.

To meet the elderly and the disabled demands and serve delivery tasks well, immune system is applied on robot with its specific advantages. According to the biological immune system, possible nodes are regarded as antibodies and local environment information is considered an antigen. Affinity between antibody and antigen is the chosen reference of target node to ensure the robot path is optimal throughout the delivery task service.

4.1. POSSIBLE NODES

Admissible space tree, a set of nodes and graphs, is presented to demonstrate that the robot can move from current position to the nodes directly in the environment. The gathered reading data from laser scanning is separated into several layers according to the Euclidean distance far from the robot. Some of layers are usually partitioned into different sections since the existence of obstacles. At current stage, there are two approaches that can be used to obtain the admissible space tree of the robot. One requires the area covered with obstacle to be dilated, and whether a section is wide enough to pass the robot will be accordingly discriminated. The other one uses the width of the robot as measurement criterion in selection of admissible space tree [11]. When the current AST is available, the furthest node is selected as current possible node, which describes the admissible direction. A set of possible nodes P_c is established for the current node. It is defined as follows:

$$P_c = \{P_{jc}\} \quad (1)$$

While the robot is exploring in the unknown environment autonomously, possible nodes are generated continuously. Sometimes, some of those nodes closed to the established topology or possible nodes may not belong to a former topology's admissible space tree. Therefore, in order to avoid revisiting and guarantee the global convergence of instant goal node, node updating rules are used to append, rebind, or get rid of those nodes. The details of the possible nodes chosen process and node updating rules are illustrated in Figure 3.

4.2. IMMUNE SYSTEM APPLICATION:

In the biological immune system, the antibody can recognize antigen based on affinity. Immune response will produce when the affinity between antibody and antigen is large. Through combining with each other, binding is formed and the antigen is promoted to be apoptotic gradually. To apply immune system on service robot, the service robot is counted as B-cell, possible node is considered an antibody, and local environment information is regarded as an antigen. For biological immune system, the larger the affinity is, the more benefits the body has. So following the immune system theory, affinity of service robot system, which is defined as $g()$, is calculated as follows:

$$g(ob_i) = \frac{w_1 \cdot \text{obstacle}() + w_2 \cdot \text{benefit}()}{\text{costtime}(ob_i)} \quad (2)$$

where w_1 , w_2 mean harmonic parameters. $\text{benefit}(obi)$ is defined as forecast ability of environmental information acquisition. It represents unknown grid unit number in the circle area with the antibody as center and laser scan range as radius. During the delivery task, the more environmental information the exploration environment includes, the larger the exploration worth is. $\text{obstacle}(obi)$ is defined as exploration attractor when the robot moves to the obstacle; it is usually valued from one to ten. The higher the value is, the more the occupied grid number is. This is one fixed thought based on autonomous exploration, which means the area nearby the obstacle has much more environmental information. Meanwhile, $\text{costtime}(obi)$ stands for the time cost in the robot moving from current position to the corresponding possible node. In conclusion, the larger the parameter (obi) is, the better the robot can serve. So, the possible node with a larger affinity will be chosen as target node where the robot will move.

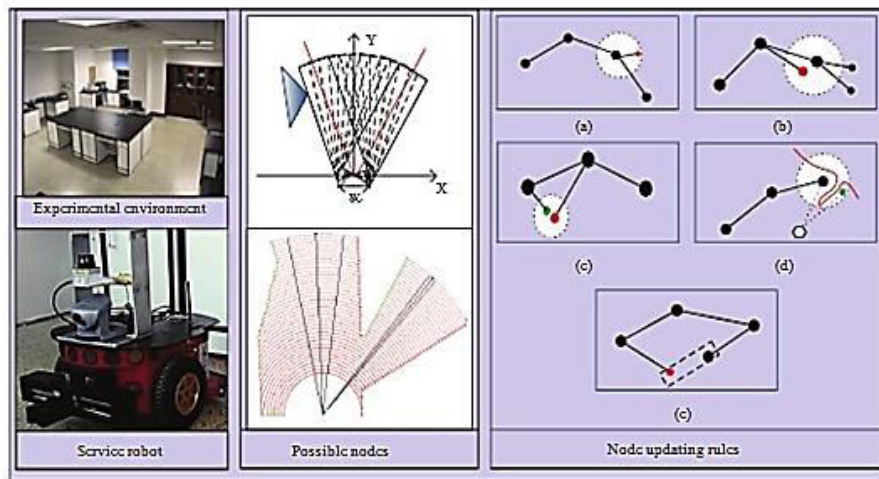


Figure 3: Possible nodes abstraction process

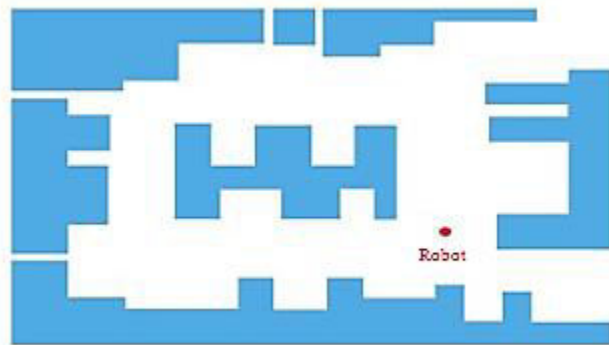
V EXPERIMENTAL RESULTS

To verify the good performance of path planning brought by immune system application, some experiments are conducted.

5.1. EXPERIMENTS ON ROBOT

The experiment on robot is carried out in the experimental environment. The experiment results are demonstrated in Figure 4. Figure 4(a) illustrates the experimental environment and Figure 4(b) shows robot positions at four moments. Moreover, Figure 4(c) describes the possible nodes abstraction process and Figure 4(d) illustrates the topological map. The red nodes donate topology nodes, which mean the position the robot passed during delivery service. Blue nodes are possible nodes. To illustrate advantages brought by introducing immune system, comparative experiment without immune system introduced is described in Figure 5(a), and the exploration result with immune system is illustrated in Figure 5(b). As shown in Figure 5(a), the robot explored areas repeatedly in the rectangles

surrounded by blue lines, while the exploration performance of robot with immune system in Figure 5(b) is obviously better.



(a) *Experimental environment*



(1)



(2)

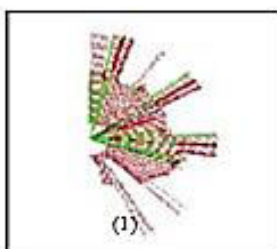


(3)

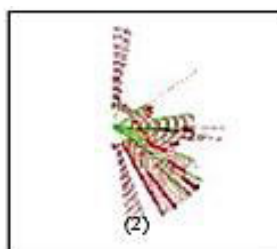


(4)

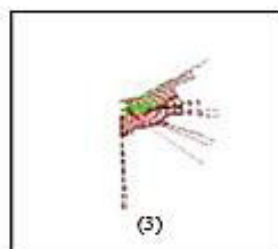
(b) *Robot positions at four moment*



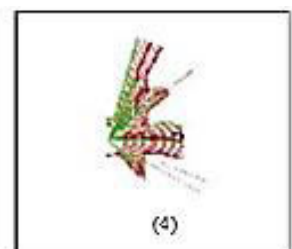
(1)



(2)

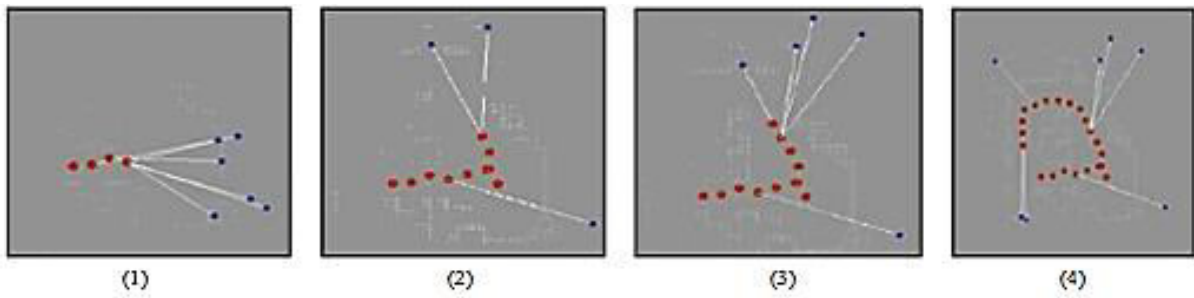


(3)



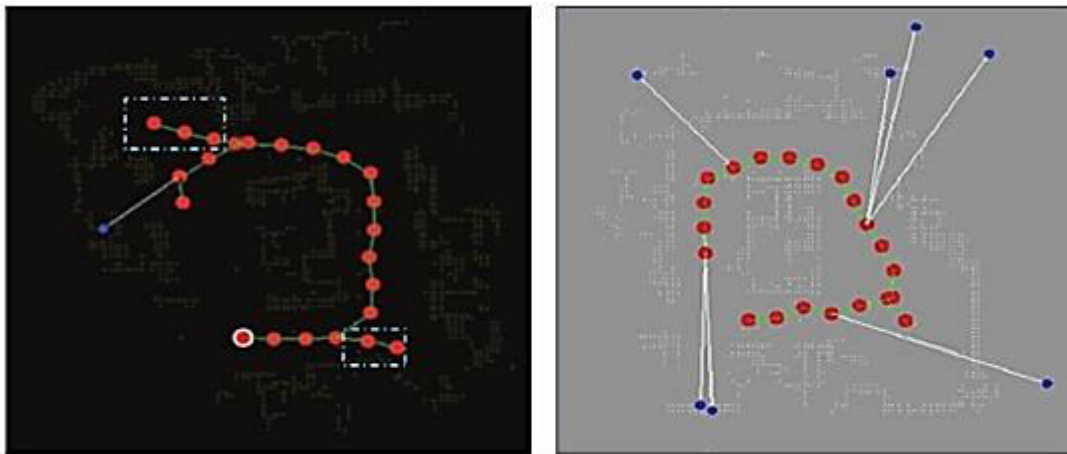
(4)

(C) Possible nodes abstraction



(d) Topology map construction

Figure 4: Experiment on robot.

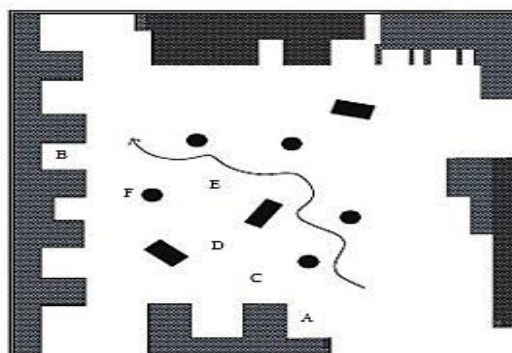


(a)

(b)

(a) Environment exploration without immune system (b) Environment exploration with immune system

Figure 5: Comparative experiments.



(a) Environment and path*(b) Wheelchair movement*

VI CONCLUSION

To serve the elderly and the disabled better, the service robot must move through an optimal path. So immune system is applied on service robot for its advantages. Firstly, the robot abstracts admissible space tree to find possible nodes. Then, compared with immune system, possible node is regarded as antibody and local environmental information is considered an antigen. Finally, experiments on robot and wheelchair are conducted to verify practicality of our path planning strategy. Further endeavor will be made to investigate the improvement of current algorithm and will focus on multi-robotic system in the future.

REFERENCES

- [1] J. Li, J. Zhang, and D. Jin, "Development of a mobile health care robot," *Chinese Journal of Rehabilitation Medicine*, vol. 10, no. 3, pp. 126–128, 1995 (Chinese).
- [2] Z. Zhihua, Z. Jianyong, L. Yang, and L. Gang, "Development of a movable service robot with double working arms for the elderly and the disabled," in *Proceedings of the International Conference on Electronic Computer Technology (ICECT '09)*, pp. 636–640, February 2009.
- [3] M. A. Wesley, "An algorithm for planning collision-free path among polyedral obstacles," *Communications of ACM*, vol. 2, pp. 959–962, 1979.
- [4] Y.-S. Liu, N. Wei, and Y.-M. Sun, "Path planning algorithm based on grid method for virtual human," *Computer Engineering and Design*, vol. 29, no. 5, pp. 1229–1230, 2008.

Design and fabrication of three mode operation for automobile steering

K.Shanmuga Elango¹k.Saravanan,²N.Neelavanan,³

^{1,2,3} Assistant professor, Dept of Mechanical Engineering, ST.Anne's College of Engg and Tech Panruti

Abstract-The title of the project is design and fabrication of three mode operation for automobile steering. In transportation industry, light commercial vehicles are required to transit, human and heavy loads through longer distance under varying road conditions. In certain conditions, the vehicle is required to pass through loose soil, narrow roads. In addition, parking four wheeler in narrow roads/area where normal turning radius is not possible. Since the vehicle steering is generally with single mode operations, smooth and comfortable steering under these conditions is always a challenge. A new Automobile Steering with Three Mode Operations is designed to facilitate smooth steering under different road conditions. A steering system is designed and fabricated for four wheels with three mode operation. The main aim of this project is to steer the vehicle in narrow and desert roads according to the requirement. In this project it is propose to implement three steering modes in a single vehicle and the modes can be changed as needed. Design of Three Mode Operations for Automobile Steering and its components would be carried out. By introducing Three Mode Operations for Automobile Steering, the vehicle would able to steer smoothly and comfortably according to the requirement in narrow and desert roads.

Key Words: Steering; Wheels, bevel gears, three mode operation, Universal joint.

I.INTRODUCTION

The steering system is a group of parts that transmit the movement of the steering wheel to the front, and sometimes the rear, wheels. The primary purpose of the steering system is to allow the driver to guide the vehicle. When a vehicle is being driven straight ahead, the steering system must keep it from wandering without requiring the driver to make constant corrections. The steering system must also allow the driver to have some *road feel* (feedback through the steering wheel about road surface conditions). The steering system must help maintain proper tire-to-road contact. For maximum tire life, the steering system should maintain the proper angle between the tires both during turns and straight-ahead driving. The driver should be able to turn the vehicle with little effort, but not so easily that it is hard to control.

II. FOUR WHEEL AUTOMOBILE STEERING

2.1 Functions of steering system

The functions of steering system are control of front wheel (sometimes rear wheel) direction, maintain correct amount of effort needed to turn the wheels. transmit road feel (slight steering wheel pull caused by the road surface) to the driver's hand., absorb most of the shock going to the steering wheel as the tyre hits holes and bumps in the road, allow for suspension action, control the angular motion of the wheels and thus the direction of motion of the vehicle, provide directional stability of the vehicle while going straight ahead, facilitate straight ahead condition of the vehicle after completing a turn and minimize tyre wear and increase the life of the tyres.

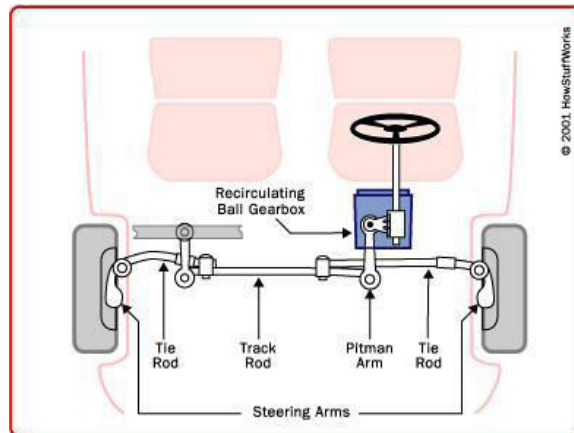


Fig 2.1 Functions of steering system

2.2 Common Steering System Parts

All steering systems contain several common parts. Every steering system, no matter what type, will have a steering wheel, a steering shaft and column, a flexible coupler, universal joints, steering arms, and ball sockets.

- 1) **Steering Wheel** Used by the driver to rotate a steering shaft that passes through the steering column. **Steering Shaft** – transfers turning motion from the steering wheel to the steering gearbox.
- 2) **Steering Column**
The steering shaft is installed in the steering column. Bearings are generally used to hold the shaft in position. The shaft and column assembly is usually removed and replaced as a unit. however, individual parts are often replaced without removing the shaft or column.
- 3) **Steering Gearbox**
Changes turning motion into a straight-line motion to the left or right. Steering gear box ratios range from 15:1 to 24:1 (with 15:1, the worm gear turns 15 times to turn the selector shaft once).
- 4) **Steering linkage** – connects the steering gearbox to the steering knuckles and wheels.

III. STEERING GEOMETRY

The term “steering geometry “refers to the angular Relationship between suspension and steering parts, front wheels, and the road surface. Because alignment deals with angles and affects steering, the method of describing alignment measurements is called steering geometry. There are five steering geometry angles: Camber, Caster, Toe, Steering axis inclination, and Toe-out on turns .There are two more steering geometry angles that are not specific to each wheel but measure the spatial relationship among all four wheels .These are Setback and Thrust angle.

3.1 Ackerman steering mechanism.

With perfect Ackermann, at any angle of steering, the centre point of all of the circles traced by all wheels will lie at a common point. But this may be difficult to arrange in practice with simple linkages. Hence, modern cars do not use pure Ackermann steering, partly because it ignores important dynamic and compliant effects, but the principle is sound for low speed maneuvers.

3.2 Turning the Car.

When turning, front wheels don't point the same direction. Inside wheel turns at a smaller radius, hence the inside wheel turns at a steeper angle than the outside wheel.

3.3 Turning Radius and Turning Circles.

The turning radius of a vehicle is the radius of the smallest circular turn (i.e. U-turn) that the vehicle is capable of making. It refers to the tightest turn a vehicle can make and is dependent on several factors. The turning circle of a car is the diameter of the circle described by the outside wheels when turning on full lock. There is no hard and fast formula to calculate the turning circle but you can get close by using this, Turning circle radius = $(\text{track}/2) + (\text{wheelbase}/\sin(\text{average steer angle}))$. A typical passenger car turning circle is normally between 11m and 13m with SUV turning circles going out as much as 15m to 17m.

3.4 Camber Angle

The camber angle is the inward or outward lean of the wheel relative to the vertical reference. Originally, the camber angle was used in a similar way to the steering axis inclination. Shown are the three possible options for camber. The downside to positive camber is the tyre thrust generated at the contact with the road. In order for the tyre to sit on the road surface some deformation of the tyre must occur. A reaction thrust is generated by the tyre tending to force the tyre to move outwards. For example, when a vehicle is travelling around a left hand bend the positive camber will tend to force the tyre to the right and reduce the cornering ability of the vehicle. If you also consider that the body roll experienced during cornering will increase the positive camber on the outside wheel this effect is not very desirable. To reduce this effect, high performance vehicles will use a negative camber arrangement. Again, this will generate a camber thrust but this time in the same direction as the corner. Both negative and positive camber will increase the tyre wear due to the deformation that occurs with this set-up. As a result, most modern vehicles will tend to be set close to zero camber. This reduces wear and rolling resistance generated by the tyre deformation.

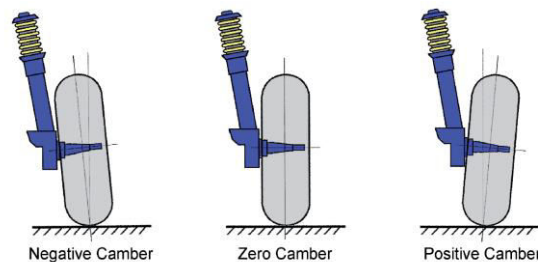


Fig 3.1 Camber Angle

5. Toe-In&Toe-Out.

The front wheels are usually turned in slightly in front so that the distance between the front ends (a) is slightly less than the distance between the back ends (b), when viewed from the top. The difference between these distances is called toe in.

Toe-out is the difference in angles between the two front wheels and the car frame during turns. The toe-out is secured by providing the proper relationship between the steering knuckle arms, tie rods and pitman arm.

3.6 Steering Axis Inclination

The steering axis inclination is the angle formed by a line drawn through the upper and lower swivel joint or steering axis. The inclination of the steering axis is necessary to allow the steering axis line and the contact point of the tyre to intersect close to the road surface.

The advantage of this arrangement is to reduce the offset between the steering axis line and the contact point of the tyre. The size of the offset, also known as the scrub radius, affects the effort required to turn the steering. A larger offset increases the steering effort. Reducing the offset will reduce the loading on the stub axle.

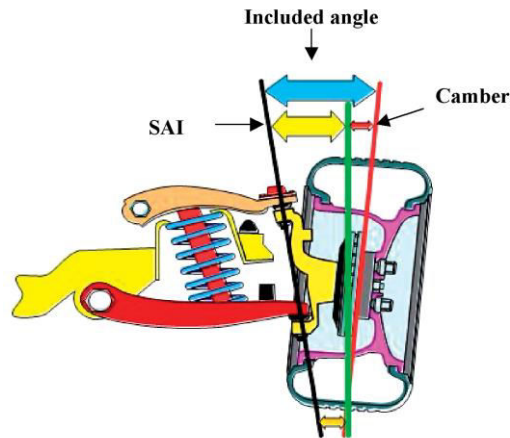


Fig 3.2 Steering Axis Inclination

3.6 .Castor Angle

The castor angle is the rearward lean of the steering axis relative to the vertical reference. The main purpose of the castor angle is to create a self-centring effect in the steering. Tilting the steering axis in this way means that the driving force acts at the point where the castor angle intersects the road. The resistance between the tyre and the road creates an opposite force that acts along the axis of the tyre. The effect is to generate side force, pushing the tyre back in line with the driving force. The further away from the straight ahead position the greater the side force.

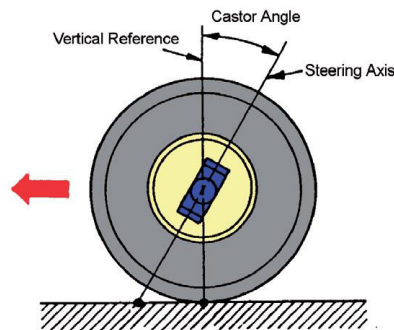


Fig. 3.3 .Castor Angle

IV. STEERING SYSTEMS TYPES

4.1 Basic Rack-and-Pinion Steering

Rack-and-pinion steering is a simple system that directly converts the rotation of the steering wheel to Straight line movement at the wheels. Figure illustrates the principle of the rack-and-pinion steering gear. The steering gear consists of the rack, pinion, and related housings and support bearings. Turning the steering wheel causes the pinion to rotate. Since the pinion teeth are in mesh with the rack teeth, turning the pinion causes the rack to move to one side. The rack is attached to the steering knuckles through linkage, so moving the rack causes the wheels to turn.

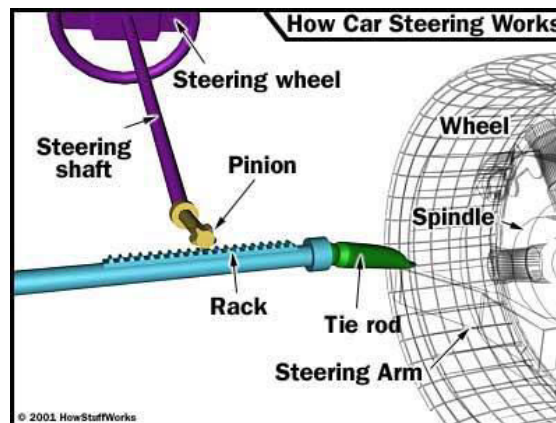


Fig 4.1 Basic Rack-and-Pinion Steering

4.2 Recirculating-Ball Steering Gear

The recirculating-ball steering gear is commonly used on modern vehicles. This steering gear is known by many names, depending on the manufacturer. Common names for this type of steering gear include worm and nut, worm and ball, and recirculating nut and worm. No matter what the name, the basic design is the same. The basic principle of this type of steering gear is shown in Figure 9-27. The worm gear is the screw, and the ball nut rides up and down as the screw turns. Teeth on one side of the ball nut contact matching teeth on the sector gear. When the steering shaft turns the worm gear, the ball nut moves on the worm gear shaft. Teeth on the ball nut cause the sector gear to turn

4.3 Worm-and-Roller Steering Gear

The worm-and-roller steering gear is found on Asian vehicles, as well as some older Jeep vehicles and European cars. Figure is an illustration of a typical worm-and-roller steering gear. Unlike the recirculating-ball steering gear, the worm-and-roller steering gear does not use a ball nut. Instead, the worm gear turns against a roller installed in the sector gear. Turning the worm gear causes the sector gear to move. The rolling action between the worm gear and the sector roller reduces friction. Note that the worm gear is tapered, with the end sections being larger than the center. This worm gear design results in constant full contact between the worm and roller, no matter what the sector position. The worm-and-roller steering gear may have a provision for adjustment.

4.4 Power Steering system

Power steering is a steering system feature that reduces driver effort by providing extra force to steer the vehicle. The use of power steering has increased to the point that all but the smallest cars are equipped with power steering as standard equipment. Power steering systems are used on both rack-and-pinion and conventional steering systems. Principles of power steering are discussed in the following sections. The basic operating principle of power steering is that normally uses an engine driven pump and a hydraulic system to assist steering action. Three major types of power steering systems are Integral-piston linkage system, External power steering system and Rack-and-pinion system

V. STEERING TYPES

The steering arrangement is classified based on wheels steered as Front wheel steering, Rear wheel steering and four wheel steering.

5.1 Rear Wheel Steering System

The Rear Wheel Steering System, in combination with the front steering System, offers several benefits over typical non-rear steering systems:
 Reduced turning radius-The turning radius of a vehicle is significantly enhanced with Rear Wheel Steering.

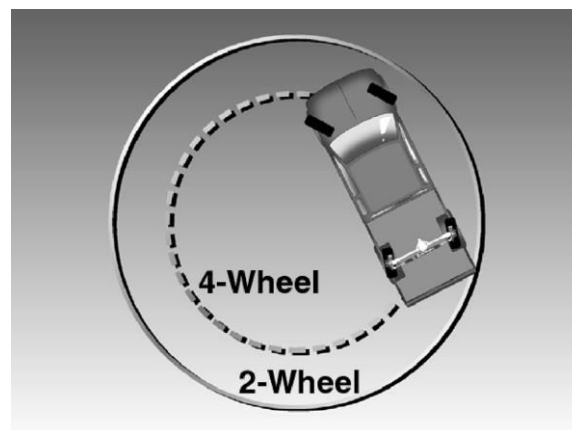


Fig 5.1 Rear Wheel Steering System

Increased stability during high-speed maneuvers such as passing and lane changes
 Increased maneuverability when towing a trailer
 Better maneuverability during low-speed maneuvers such as parking

5.2 Four wheel steering.

Four wheel steering is a method developed in automobile industry for the effective turning of the vehicle and to increase the maneuverability. In a typical front wheel steering system the rear wheels do not turn in the direction of the curve and thus curb on the efficiency of the steering. In four wheel steering the rear wheels turn with the front wheels thus increasing the efficiency of the vehicle. The direction of steering the rear wheels relative to the front wheels depends on the operating conditions. At low speed wheel movement is pronounced, so that rear wheels are steered in the opposite direction to that of front wheels. At high speed, when steering

adjustments are subtle, the front wheels and the rear wheels turn in the same direction. Modes in four wheel steering system.

Two modes are generally used in these 4WS model. a. Slow Speeds - Rear Steer Mode and b. High speeds – Crab Mode Four-wheel steering (or all wheel steering) is a system employed by some vehicles to improve steering response, increase vehicle stability while maneuvering at high speed, or to decrease turning radius at low speed. A 4- wheel steering system is superior to a 2- wheel steering system. It reduces the turning radius as well as the space required for turning. It also enables to change road lane while driving even at high speed. • At lower speeds, turning the rear wheels in the opposite direction to the front wheels results in a smaller turning radius and faster cornering responses. At high speeds, turning all four wheels in concert improves high-speed stability. The Four Wheel steering system offers a 21% reduction in turning radius. So if a vehicle is capable of making a U-turn in a 25-foot space. It allows the driver to do it in about 20 feet. . A front wheel active steering function was added to Rear Active Steer adopted on the Fuga. By controlling the steering angle of all four wheels, this active steering system helps improve stability and response at high speed and helps reduce driver’s steering workload at low speed. To achieve precise vehicle • Vehicles move smoothly and are easy to drive both in the city and on winding roads. • Added stability means vehicles can be driven safely on expressways and when changing lanes. • Quick and responsive control system will allow gentle steering operation.

VI. DIFFERENT MODES OF FOUR WHEEL STEERING

Four-wheel steering (or all-wheel steering) is a system employed by some vehicles to improve steering response, increase vehicle stability while maneuvering at high speed, or to decrease turning radius at low speed. In an *active* four-wheel steering system, all four wheels turn at the same time when the driver steers. In most active four-wheel steering systems, the rear wheels are steered by a computer and actuators. The rear wheels generally cannot turn as far as the front wheels. During parking, difficulties experienced to have good maneuverability in small areas, to change position with less turning radius and yawing. in existing four wheel automobile steering, three modes of operation through mechanical elements are designed , developed by fabrication. The three modes of steering operations are First mode operation, Second mode operation and Third mode operation.

6.1. Working principle

In the existing steering system, the three modes of operations are introduced .a steering setup, spur gears, bevel gears and lock nut. The new system designed and developed consists of a set of rack and pinion for rear and front wheels ,spiral gear train to effect rear wheel and front wheel steer in same direction and bevel gear train for rear and front wheel steer in opposite direction. The spur gear trains, bevel gear trains and rack and pinions are hinged and linked to ensure positive transfer of desired effort. The three modes of operations and the respective steer. First mode operation -Front wheel steer Second mode operation-Both front and rear wheel steer in same direction Third mode operation-Both rear wheels in opposite direction

When the lock nut is removed, the steering operation is carried out in normal condition. That is only front wheels steer. But when the lock nut is inserted, the other two modes can be used. When the gear arrangement is pushed to one position, the spur gears get engaged and the steering of rear wheel is ensured and is in same direction as that of the front wheels. When the gear arrangement is moved to other side, the spur gear disengages and the bevel gear gets engaged. Due to bevel gear arrangement, the rear wheel steers in opposite direction to the front wheel. This results in third mode steering. The advantages are easy maintenance and easy mode change.

6.2. First mode operation

When the lock nut is removed, the steering operation is carried out in normal condition. That is only front wheels steer.

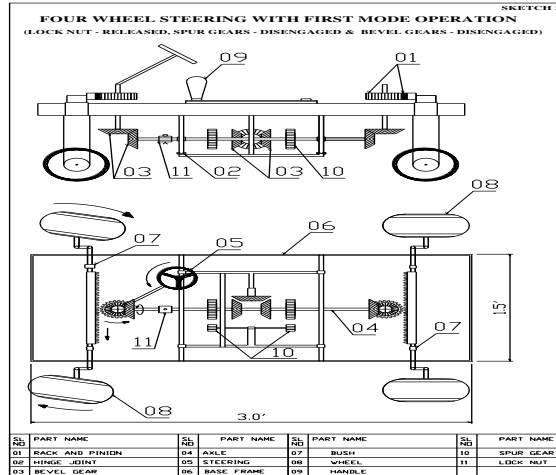


Fig 6.1. First mode operation

6.3 Second mode operation

But when the lock nut is inserted, the other two modes can be used. When the gear arrangement is pushed to one position, the spur gears get engaged and the steering of rear wheel is ensured and is in same direction as that of the front wheels.

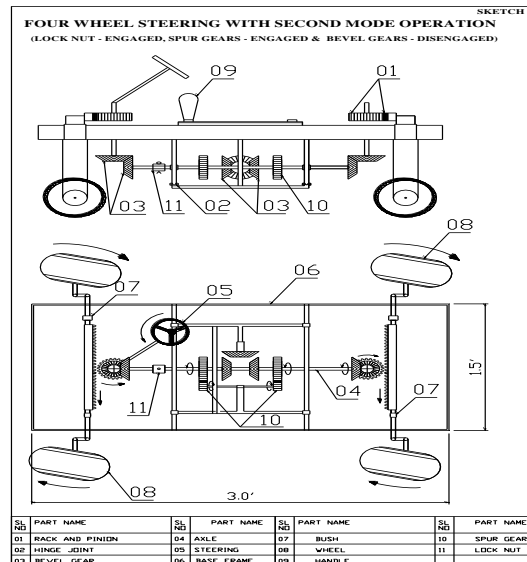


Fig 6.2 Second mode operation

6.4 Third mode operation

When the gear arrangement is moved to other side, the spur gear disengages and the bevel gear gets engaged. Due to bevel gear arrangement, the rear wheel steers in opposite direction to the front wheel. This results in third mode steering. The advantages are easy maintenance and easy mode change.

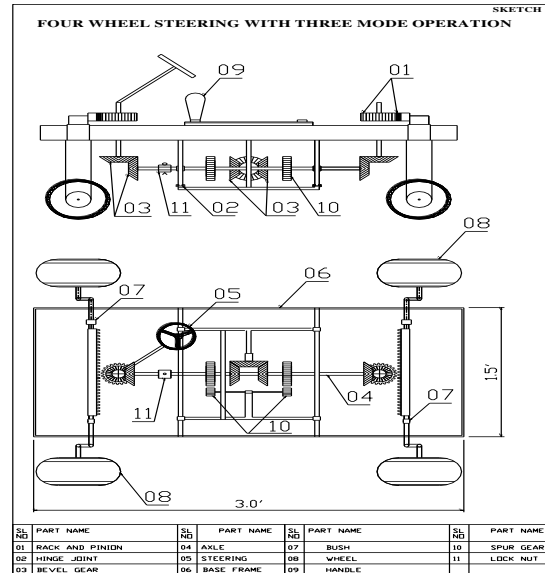


Fig 6.3 Third mode operation

VII DESIGN AND FABRICATION

The various components used in the system are Spur gear, Bevel gear, Rack and pinion, Joints and linkages the components designed to effect proper steering ration with less effort.

7.1. Spur gears

A gear is a rotating machine part having cut teeth, or cogs, which mesh with another toothed part in order to transmit torque. Two or more gears working in tandem are called a transmission and can produce a mechanical advantage through a gear ratio and thus may be considered a simple machine. Geared devices can change the speed, torque, and direction of a power source. The most common situation is for a gear to mesh with another gear; however a gear can also mesh a non-rotating toothed part, called a rack, thereby producing translation instead of rotation.

7.2 Bevel gears

Bevel gears are gears where the axes of the two shafts intersect and the tooth-bearing faces of the gears themselves are conically shaped. Bevel gears are most often mounted on shafts that are 90 degrees apart, but can be designed to work at other angles as well. The pitch surface of bevel gears is a cone.three types of bevel gears viz. 1) Straight Bevel Gears,2) Spiral Bevel Gears 3) Hypoidal Bevel Gears are chosen based on requirement and merit of each.

7.3 Rack And Pinion

A rack is a toothed bar or rod that can be thought of as a sector gear with an infinitely large radius of curvature. Torque can be converted to linear force by meshing a rack with a pinion: the pinion turns; the rack moves in a straight line. Such a mechanism is used in automobiles to convert the rotation of the steering wheel into the left-to-right motion of the tie rod(s). Racks also feature in the theory of gear geometry, where, for instance, the tooth shape of an interchangeable set of gears may be specified for the rack (infinite radius), and the tooth shapes for gears of

particular actual radii then derived from that. A rack and pinion is a pair of gears which convert rotational motion into linear motion. The circular pinion engages teeth on a flat bar - the rack. Rotational motion applied to the pinion will cause the rack to move to the side, up to the limit of its travel. The pinion is in mesh with a rack. The circular motion of the pinion is transferred into the linear rack movement.

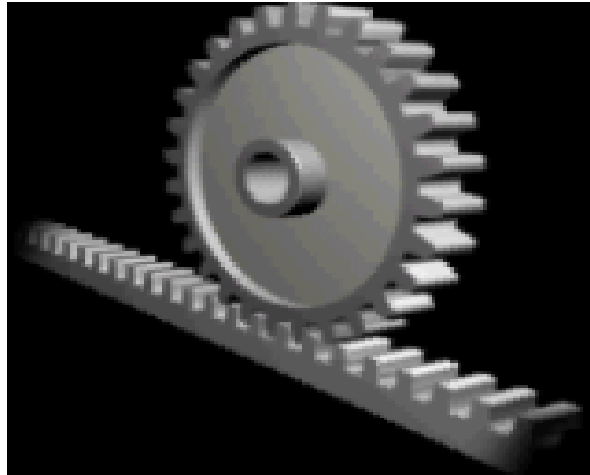


Fig 7.1 Rack And Pinion

VIII.OBJECTIVE OF THE SYSTEM.

A new Design & fabrication of Three Mode Operations for Automobile Steering is designed taking into consideration of different critical/narrow and desert roads. The Three Mode Operations for Automobile Steering would facilitate smooth and comfortable steering improves vehicle's versatile capability for different/narrow roads and reduces driving fatigue.

IX. CONCLUSION.

An innovative feature of this three mode operation for automobile steering linkage design and its ability to drive all four wheels using mechanical elements and links. Its successful implementation will allow for the development of a four-wheel steering power base with maximum maneuverability, static stability, front- and rear-wheel tracking. As per the focus of the project, an innovative 4 wheel steering mechanism designed and prototype developed which is feasible to manufacture, easy to install and highly efficient in achieving in-phase and counter-phase rear steering with respect to the front wheels. This system assists in better cornering and combats the problems faced in sharp turning. It reduces the turning circle radius of the car and gives better maneuverability and control while driving at low speeds. Moreover components used in this system are easy to manufacture, material used is feasible, reliable and easily available in market.

REFERENCE

- [1] Dr. Kirpal Singh "Automobile Engineering" Standard Publishers Distributors, vol. 1, 12th Edition, 2011.
- [2] V. B. Bhandari "Design of Machine Elements" McGraw Hill Education India Pvt. Ltd., vol. 3, 11th Edition, 2013.
- [3] PSG College of Technology "Design Data Book" Kalaikathir Achchagam, 2013.
- [4]. "Honda Prelude Si 4WS: It Will Never Steer You Wrong," Car and Driver, Vol. 33, No. 2, pps. 40-45, August 1987.
- [5]. Lee, A.Y., "Vehicle Stability Augmentation Systems Designs for Four Wheel Steering Vehicles," ASME Journal of Dynamical Systems, Measurements and Control, Vol. 112, No. 3, pps.489-495, September 1990.

Design and Finite Element Analysis of Nose Landing Gear of a Civil Transport aircraft

Elavarasan S¹, Naveenkumar.U²

¹ME-Industrial Engineering, Anna University Regional Campus, Coimbatore

¹ Assistant professor, Dept of Mechanical Engineering, ST. Anne's College of Engg and Tech Panruti,

Abstract: In conceptual design phase of aircraft landing gear system is very important than other systems and it is difficult to design. Most of the commercial aircrafts, nose wheel tricycle type landing gear is used. The objective of this project is to increase the landing gear strength and minimize the weight of the system. The process includes preliminary design of landing gear and sizing. The analysis of landing gear is made of AISI 4340 done through MSC.Nastran/Patran. CATIA-V5 is used to design the landing gear components. Civil aircraft load conditions are Side, Drag and Vertical load is applied in axle, the maximum stresses and displacement are obtained. The landing gear withstands and failure range is determined.

I. INTRODUCTION

The Landing gear is the structure that supports an aircraft on the ground and allows it to taxi, take-off and land. The most common type of landing gear consists of wheels, but airplanes can also be equipped with floats for water operations, or skis for landing on snow. Landing gear is essentially one dimension structure under heavy compressive loads. Drag load and side load do act on landing gear however. Landing gears enable the aircraft to land and takeoff from the ground. A number of loads curve are specified in FAR rules books for which landing gear for a given type of aircraft is to be designed.

The type of landing gear configuration is based up on aircraft. Tricycle Nose landing gear type is mostly used in commercial transport aircrafts. Nose and main landing gear attachment in more important.

Nose wheel carries only 15 to 20% of total load, main wheel carries 75 to 80% load. Height of the landing gear and distance from C.G is must give stable condition to aircraft during ground operations. Retractable landing gear creates less drag during flight.

II. MODELING PROCESS

CATIA-V5 software is used to design the nose landing gear. First landing gear components are separately designed. Landing gear components are main strut, drag strut, axle, retract rod etc. Finally all components are assembled in the Assembly workbench and assembled. Assembled landing gear is saved in .iges file format. There are two types of landing gear design, one is normal and another one is redesigned model (thickness added more in torque link and retract connecting point). These landing gears are shown in fig: 1 to fig: 6.

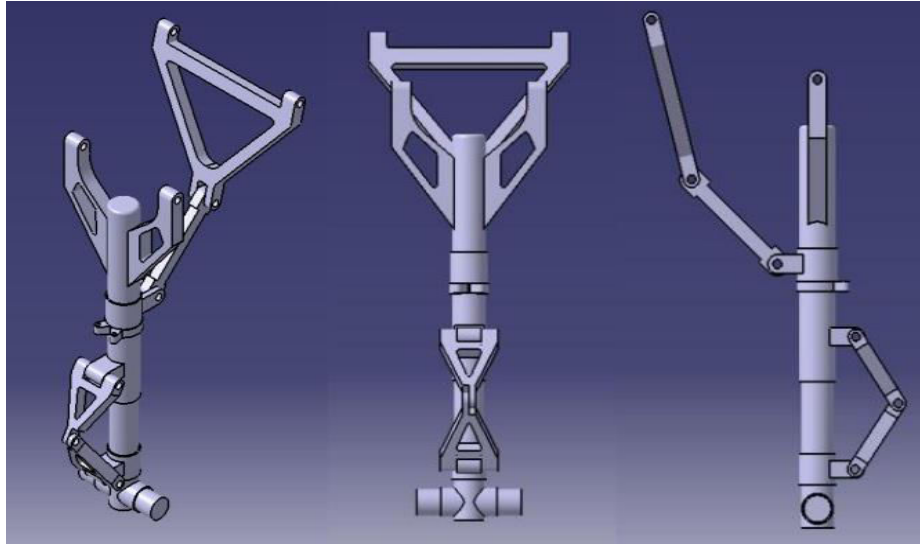


Fig : 1

Fig : 2

Fig : 3

Fig 2.1 Normal model

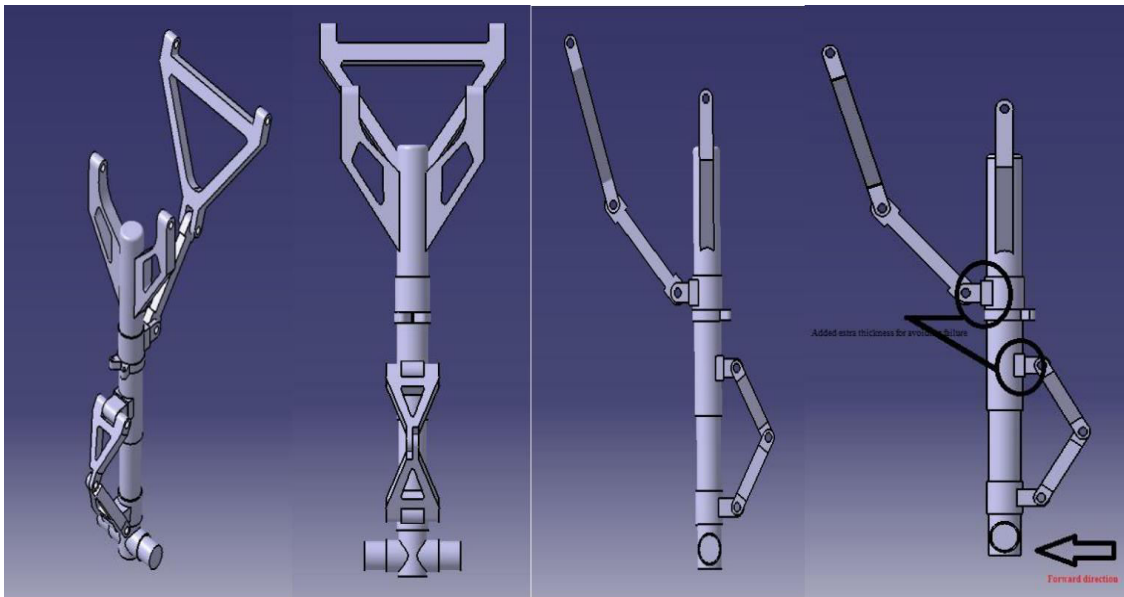


Fig : 4

Fig : 5

Fig : 6

Fig 2.2 Re-designed Model

III. FINITE ELEMENT MODEL

CATIA designed model is imported in MSC-Patran software. Patran is a Pre-processor software. The imported model is shown in Fig: 7&8. The finite element model of landing gear is meshed by using 3D solid tetrahedron 10 element, meshed model as shown in Fig: 9&10. RBE2 elements are used to transfer the load in one component to another component act as a bolt.

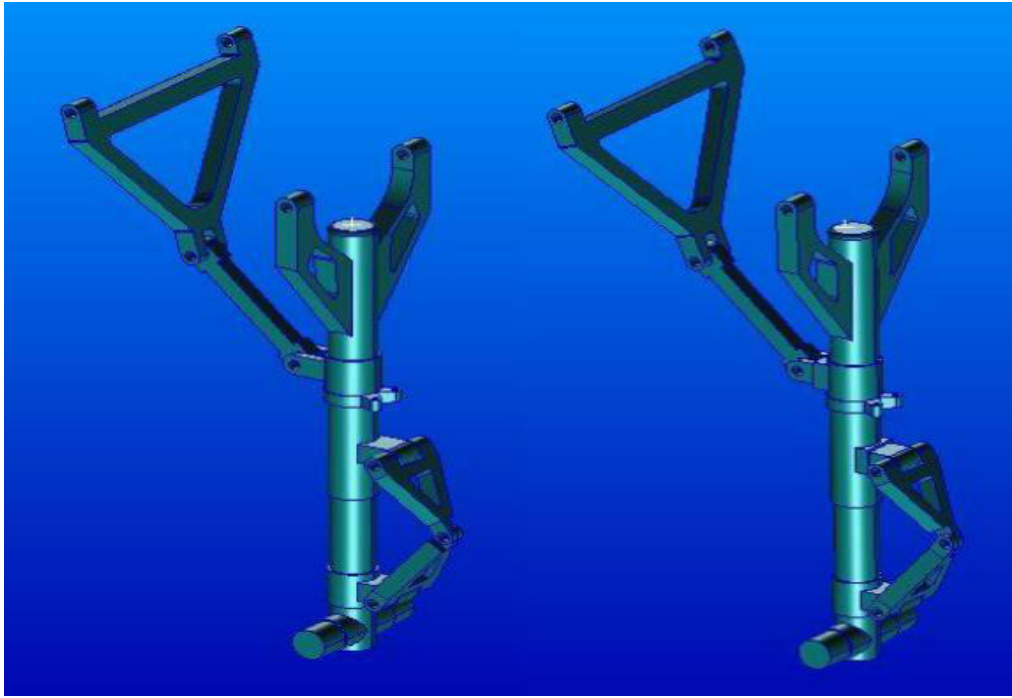


Fig: 3.1 Normal model.

Fig: 3.2 Re-designed model.

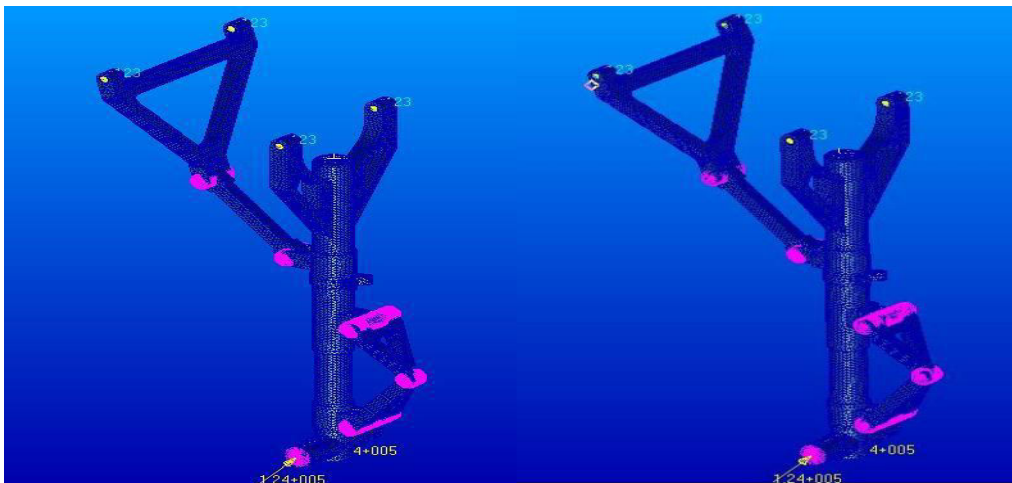


Fig: 3.3 Normal model

Fig: 3.4 Re-designed model

IV. LOADS, BOUNDARY CONDITIONS AND MATERIAL

At the time of landing Nose landing gear carries only 15 to 20% of total load because Main landing gear first touches the ground. Main strut and drag strut lug points are fixed. At fixed point 1d BAR elements are used. Total impact Load is applied through RBE3 element. Design and ultimate loads. Design load is the limit load; ultimate load is maximum load carrying capacity of the component without failure. For safety purpose ultimate load is considered. Various types of load case are tabulated below.

Design Loads	Vertical load	drag load	side load
Max design load	64931.95225	25972.7809	16232.98806
spin up design load	53445.48989	24794.26596	0
spring back design load	62659.33392	53967.38046	0
Ultimate load	Vertical load Z	drag load X	side load Y(-)
Max ultimate load	97397.92837	38959.17135	24349.48209
spin up ultimate load	80168.23484	37191.39895	0
spring back ultimate load	93989.00088	80951.07069	0

Table: 4.1 Amount of load acting in landing gear

Several different types of material is used in aircrafts. Main strut is made up of steel and piston cylinder is made up of titanium. AISI 4340 alloy steel material is used. Steel is having high strength compare to other materials. AISI 4340 properties are tabulated bellow.

AISI 4340 steel	
Ultimate stress	1110mpa
Yield stress	710mpa
Modulus elasticity	205gpa
poissons ratio	0.29

Table: 4.2 stress analysis result

V. ANALYSIS RESULT

Post processing is carried by MSC-Nastran. Patran output .bdf file is selected as an input file to Nastean solver. Both case is analyzed and maximum principal stress, von mises stress, displacement is determined. Material is safe for given all load conditions. Graph is plotted for various loads. Result figures are given in below.

Maximum design vertical load:

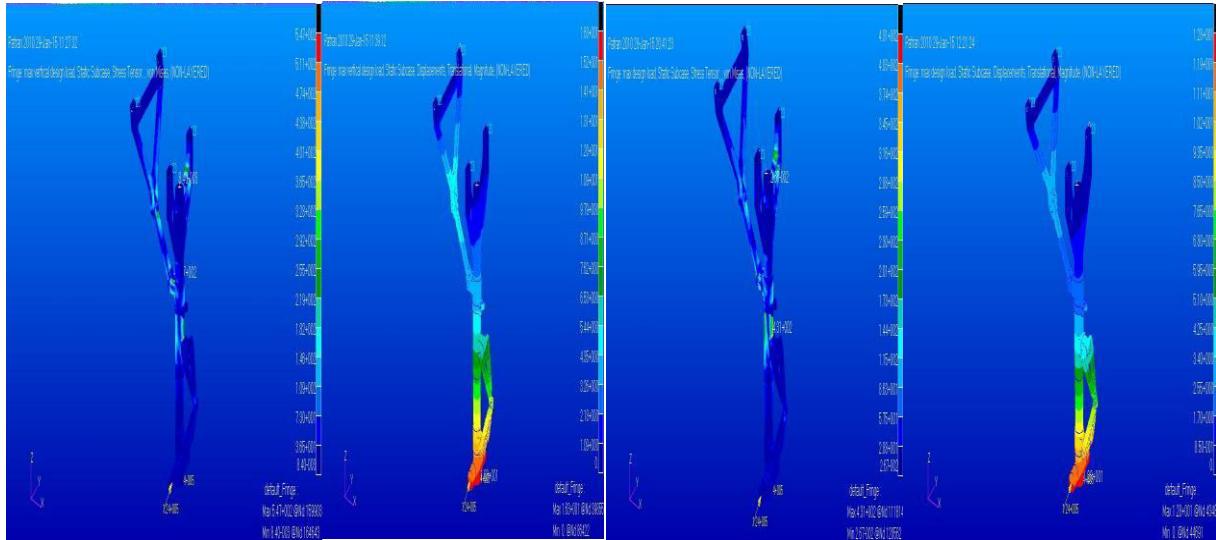


Fig 5.1 Case: 1 normal model

Fig 5.2 Case: 2 Re-Designed model

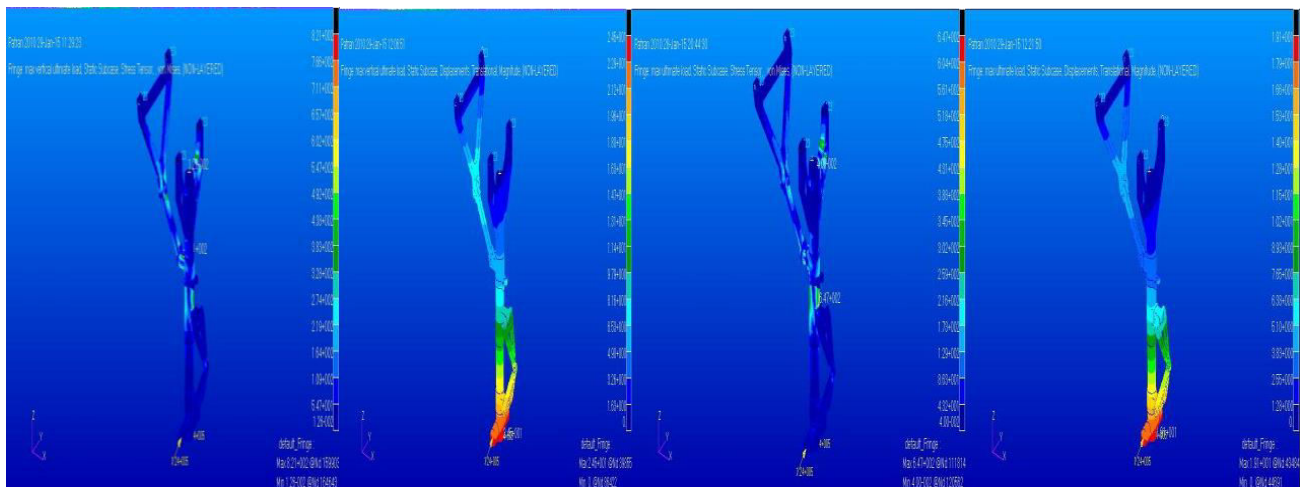


Fig 5.3 Max vertical ultimate load

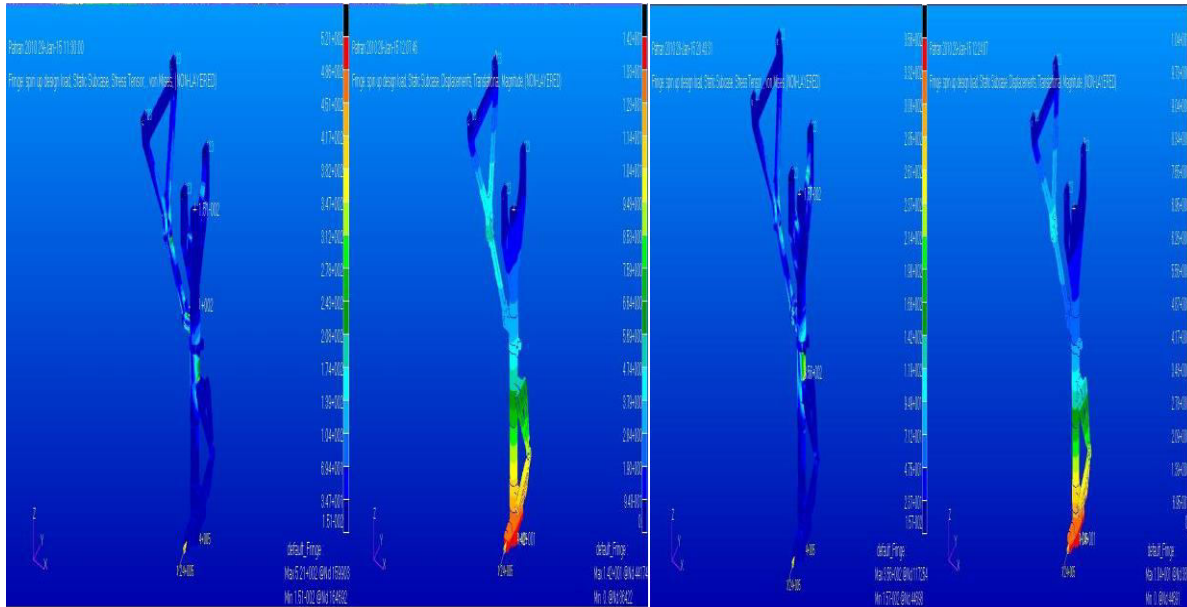


Fig 5.4 Spin up design load

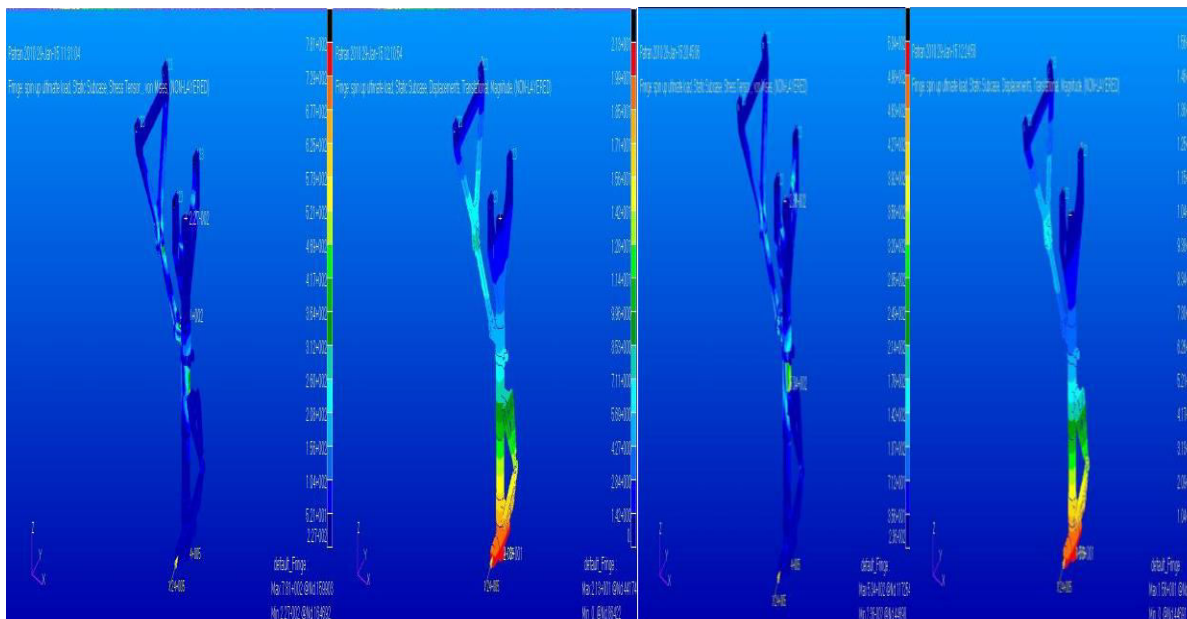


Fig 5.5 Spin up ultimate load

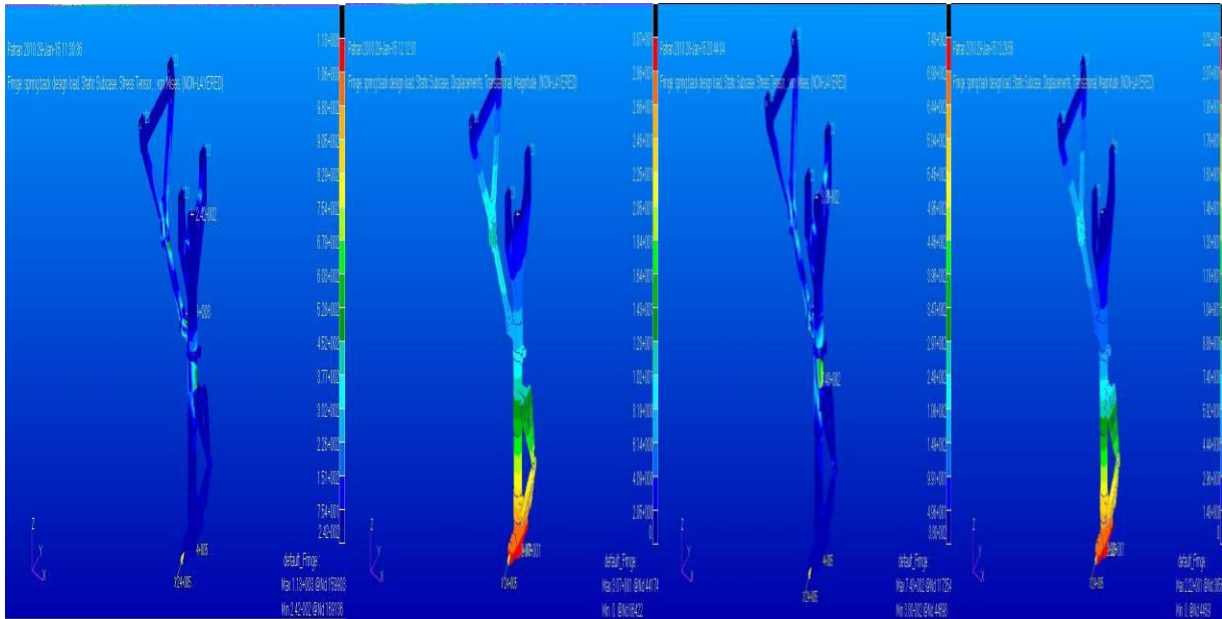


Fig 5.6 Spring back design load

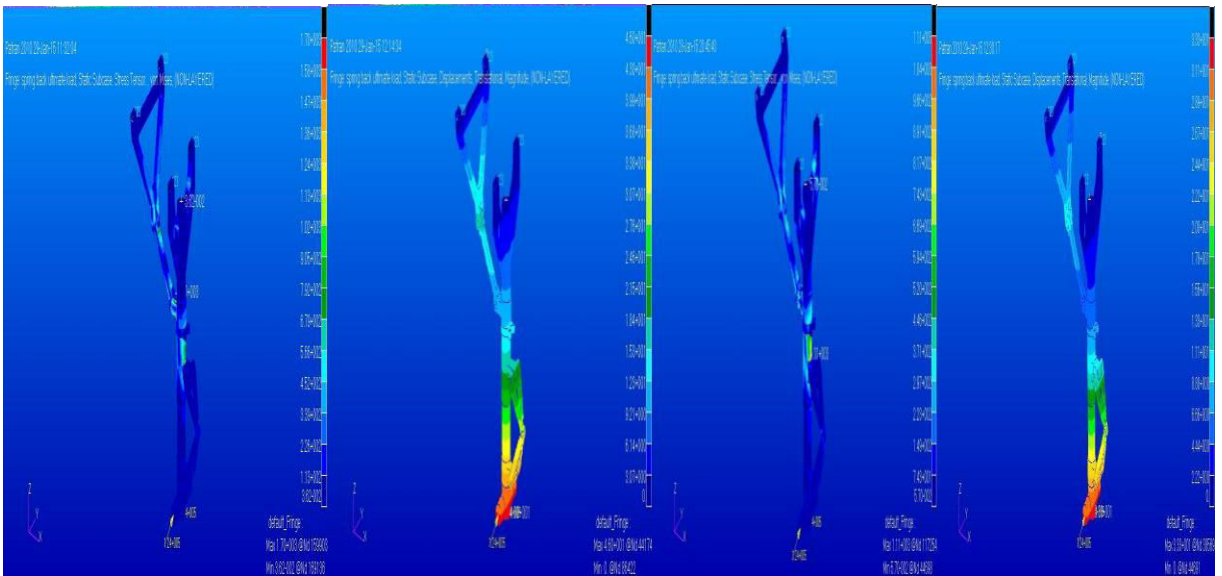


Fig 5.7 Spring back ultimate load

Case: 1 Normal model	Ultimate stress	Displacement	Max Principal stress	Von Mises	Max shear	Reserve Factor
----------------------	-----------------	--------------	----------------------	-----------	-----------	----------------

Max design load	1110	16.3	523	547	282	2.02
spin up design load	1110	10.6	508	521	268	2.13
spring back design	1110	30.7	1110	1130	582	0.98
Max ultimate load	1110	24.5	785	821	423	1.35
spin up ultimate load	1110	21.3	761	781	402	1.42
spring back ultimate	1110	46	1660	1700	873	0.65

Table: 5.1 shows displacement, principal stress, shear and Reserve factor. In this normal model maximum displacement is 46mm. The lowest Reserve factor is 0.652.

Case: 2 Re-edited model	Ultimate stress	Displacement	Max Principal stress	Von Mises	Max shear	Reserve Factor
Max design load	1110	12.8	391	431	244	2.57
spin up design load	1110	10.4	335	356	202	3.11
spring back design load	1110	22.2	749	743	422	1.49
Max ultimate load	1110	19.1	586	647	365	1.71
spin up ultimate load	1110	15.6	503	534	303	2.07
spring back ultimate	1110	33.3	1120	1110	633	1

Table: 5.2 shows Re-designed model displacement and stress details. The maximum displacement is 33.3mm. Smallest Reserve factor is one. This is more safe compare to normal design model.

VI. CONCLUSION

Finite element analysis of landing gear is carried out using finite element software. In that first case the maximum principal stress 1660Mpa, that is greater than material allowable stress 1110Mpa. Displacement also high 46mm. There is possible of component failure. In that Second case the maximum stress 1110Mpa is equal to material allowable stress. Displacement 33.3mm also less compare to first case. So material is safe and withstands all loads.

REFERENCE

- [1] R.ravi kumar, p. K dash, s r basavaraddi [1] worked on a topic of "Design and analysis of main landing gear structure Of a transport aircraft and fatigue life estimation For the critical lug".
- [2] Amit Goyal, Dr. H.V lakshminarayan [2] worked on a topic of "Design, analysis and simulation of a composite main landing gear for a light aircraft".
- [3] Prasad Kabade, Ravi Lingannavar, [3] worked on a topic of "Design and Analysis of Landing Gear Lug attachment in an Airframe".
- [4] Flugge W., "Landing Gear Impact", NACA, TN2743,9016,1952.
- [5] Jocelyn I. Pritchard, "An Overview of Landing Gear Dynamics", NASA/TM-1999-209143 ARL- TR-1976.
- [6] Dobrzynski W., and Buchholz H., "Full-Scale Noise Testing on Airbus Landing Gears in the German Dutch Wind Tunnel," 3rd AIAA/CEAS Aero acoustics Conference, Atlanta, GA, May 1997. AIAA 97-1597-CP.

EXPERIMENTAL INVESTIGATION OF PISTON BOWL GEOMETRY ON DIESEL ENGINE

K.Sakthivel¹, P.Murugan², U.NaveenKumar³, Tamilselvan.M⁴

¹Assistant Professor, Department of Mechanical Engineering, A.R College of Engineering, Villupuram.

^{2,3} Assistant Professor, Department of Mechanical Engineering, ST.Anne's College of engineering and Technology, Panruti.

⁴Student, Department of Mechanical Engineering, ST.Anne's College of engineering and Technology, Panruti

Abstract-Continuous use of petroleum sourced fuels is now widely recognized as unsustainable because of depleting supplies and the contribution of these fuels to the accumulation of carbon di-oxide and carbon monoxide in the environment. Renewable, carbon neutral, transport fuels are necessary for environmental and economic sustainability. In this work, vegetable oil (papaya oil) as a fuel for engine and to convert into bio-diesel by transesterification process. To study the performance and emission characteristics of diesel engine.

There are number of techniques to enhance the engine performance and to reduce emission characteristics all the three pistons diesel engine. One of the methods to change the piston bowl geometry the piston bowl geometry is varied. In this work three (ϕ 2mm, ϕ 2.5mm, ϕ 3mm) different piston bowl geometry is designed and experimental investigation of the engine is studied with standard piston and modified pistons. The modified piston bowl geometry characteristic is investigated by using conventional fuel.

The investigation was carried out in the single cylinder water cooled diesel engine with the sole fuel blended and the engine performance, emission, characteristics will be analyzed for various piston bowl geometry to analyze the performance of the engine. From the experimental investigation it is observed that the brake thermal efficiency increased for piston-2 (modified piston- ϕ 2mm, 6 holes) by 5.71% when compared to that of standard piston. The CO, HC, NOx are found to modified piston bowl geometry with increase in smoke emission.

I. INTRODUCTION

Environmental pollution is very serious problem for our human beings and flora-fauna. The environment is polluted day by day from industrial emissions and road vehicle emissions. Petrol engine and diesel engine produced different types of harmful gases during combustion like NOx, CO, CO₂, HC and some quality SOx due to incomplete combustion. These gases are produced by different engine factor such as piston bowl geometry, injection timing, compression ratio etc., These entire factors also affect the combustion efficiency, fuel consumption and engine brake power. To reduce the emissions engine manufacturers try

to best design, the combustion chamber and other level. At combustion chamber geometry design to reduce the NO_x many researchers studied the different piston bowl geometry .

Flow phenomena in internal combustion (IC) engines are extremely complex, and the flow field is further complicated by the presence of swirl squish tumble and the chemical reaction. A complete understand standing our physical processes of fluid motion in combustion chambers is essential in developing efficient engine design and control diagnostics.

Diesel engines have been greatly improved in terms of efficiency and reduced emission level . however , the combustion process also depends highly on an efficient fuel-air mixture ,particularly in high-speed direct-injection diesel engines. Among these processes, the flow conditions inside the cylinder at the end of compression stroke and near the top dead center for fuel air mixing ,wall heat transfer and engine performance improvement. The mixing process is affected by the intake swirls ,fuel injection system and combustion chamber configuration . Thus good engine operation requires fuel spray matching air movement and combustion chamber configuration

II. METHODOLOGY

1. In this project work, three shapes of swirl enhancing piston bowl is designed and implemented in Di Diesel engine using conventional diesel fuel.
2. In order to improve the efficiency of the engine, swirl enhancing piston bowl is designed and implemented in DI Diesel engine.
3. The experiment has been carried out in Kirloskar TV 1, single cylinder, 4 stroke, water cooled diesel engine with all necessary equipment to study the engine performance and emission characteristics.
4. To study the experimental investigation of the engine with three piston geometry with sole fuel and compared with the standard piston geometry.

III. EXPERIMENTAL SETUP

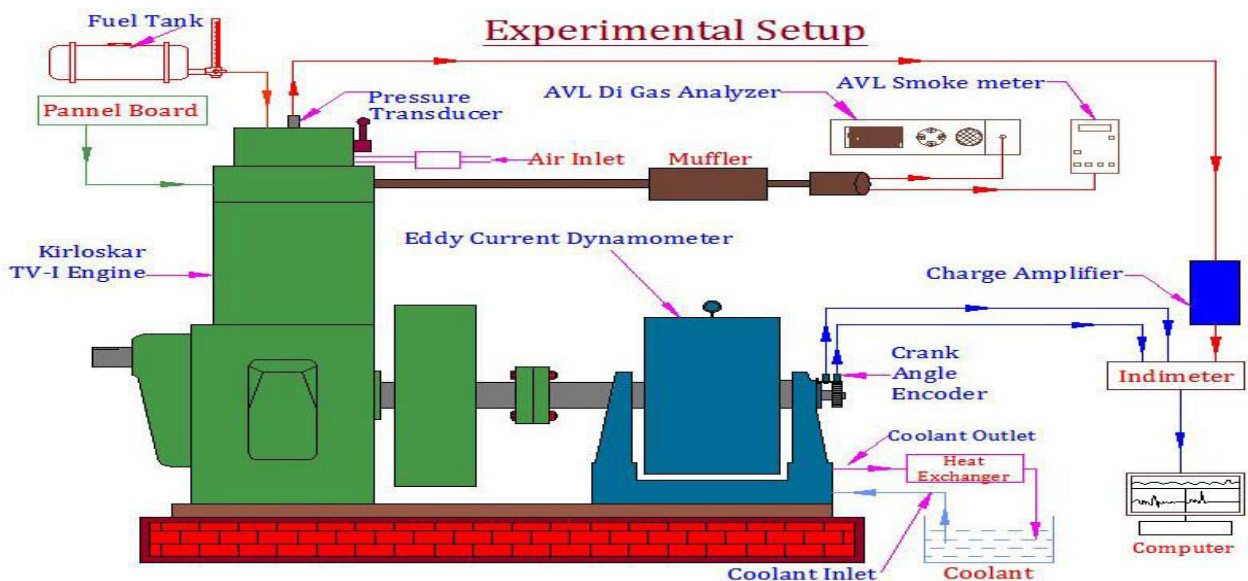


Fig 3.1 Experimental Setup

Type	Vertical, water cooled, Four stroke
Number of cylinder	1
Bore Diameter	87.5 mm
Compression ratio	17.5:1
Maximum power	5.2 kW
Speed	1500 rpm
Dynamometer	Eddy current
Injecting timing	23° before TDC
Injection pressure	220 kgf/cm ²

Table 3.1 Engine Specification

This project work has been carried out using different blends of furnace oil as fuel on a single cylinder, water cooled, 4 stroke, diesel engine.

Fuel flow rate is obtained on the gravimetric basis and the air flow rate is obtained on the volumetric basis. The engine was coupled to an eddy current dynamometer for load measurement and the smoke density was measured using an AVL smoke meter. NO_x emission is measured with the help of an exhaust gas analyser. AVL Di gas analyser is used to measure the rest of the pollutant. The AVL combustion analyser is used to measure the combustion characteristic of the engine. A burette is used to measure the fuel combustion for a specified time interval. During this interval of time how much fuel the engine consumes is measured, with the help of the stop watch.

3.1 Test Engine Specifications

Make	AVL
Type	AVL Di gas 444
Power supply	11...22 voltage ≈25 W
Warm up time	≈7 min
Connector gas in	≈180 I/h, max. over pressure 450 hPa
Response time	T ₉₅ ≤ ! 5s
Operating temperature	5...45 °c
Storage temperature	0...50 °c
Relative humidity	≤95%, non-condensing
Inclination	0...90°
Dimension(w × d × h)	270×320×85 mm ³
Weight	4.5 kg net weight without accessories
Interfaces	RS 232 C, pick ip, oil temperature probe

Table 3.2 Specifications of ALV Di Gas Analyzer

Make	AVL 437 Smoke meter
Type	IP 52
Accuracy and reproducibility	$\pm 1\%$ full scale reading
Measuring range	0 to 100 opacity in % 0 to 99.99 absorption m^{-1}
Measuring chamber	Effective length $0.430\text{ m} \pm 0.005\text{ m}$
Heating time	220 V approximately 20 min
Light source	Halogen bulb 12 V/5W
Maximum smoke temperature	250°C
Power supply	190-240 V AC, 50 Hz, 2.5 A
Dimension	570mm×500mm×1250mm

Table 3.3 Specifications of ALV smoke

3.2 Experimental procedure

The engine was allowed to run with neat diesel at various loads for nearly 10 minutes to attain the steady state constant speed conditions. Then the following observations were made,

1. The water flow is started and maintain constant throughout the experiment.
2. The load, speed and temperature indicators were switched ON.
3. The engine was started by cranking after ensuring that there is no load.
4. The engine is allowed to run at the rated speed of 1500 rpm for a period of 20 minutes to reach the steady state.
5. The fuel consumption is measured by a stop watch.
6. Smoke readings were measured by using the AVL smoke meter at exhaust outlet.
7. The amount of NO_x was measured using AVL Di gas analyser exhaust outlet.
8. The exhaust temperature was measured at the indicator by using the sensor.
9. Then the load is applied by adjusting the knob, which is connected to the eddy current dynamometer.
10. The experiment were conducted with standard piston and standard fuel.
11. The modified pistons is replaced and the same procedure is repeated.
12. Compare the results.

3.3 Piston modification

Swirl is usually defined as organized rotation of the charge about the crystal axis. Swirl is created by bringing the intake flow into the cylinder with an intial angular momentum. While some decay in swirl due to the friction occurs during the engine cycle, intake generated swirl usually persists through the compression, combustion and expansion process. In engine design with blow_in_piston combustion chambers, the rotational motion set up during intake is substainly modified during compression. Swirl is used in diesels and some stratified – change engine concept to promote more rapid mixing between the inducted air charge

IV. RESULTS AND DISCUSSION

4.1 Swirl modification within the cylinder

The angular momentum of the air which enters the cylinder at each crank angle during induction decays throughout the rest of the intake process and during the compression process due to the friction at the walls and turbulent dissipation within the fluid. Typically one-quarter to one-third of the initial moment of momentum about the cylinder axis will be lost by top center at the end of compression. However, swirl velocities in the charge can be substantially increased during compression by suitable design of the combustion chamber.

4.2 Squish

Squish is the name given to the radically inward or transverse gas motion that occurs towards the end of the compression stroke when a portion of piston face and cylinder head approach each other closely. The amount of squish is often defined by the percentage squish area i.e., the percentage of the piston area, $\pi B^2/4$ which closely approaches the cylinder head. Squish generated gas motion results from using a compact combustion chamber geometry.

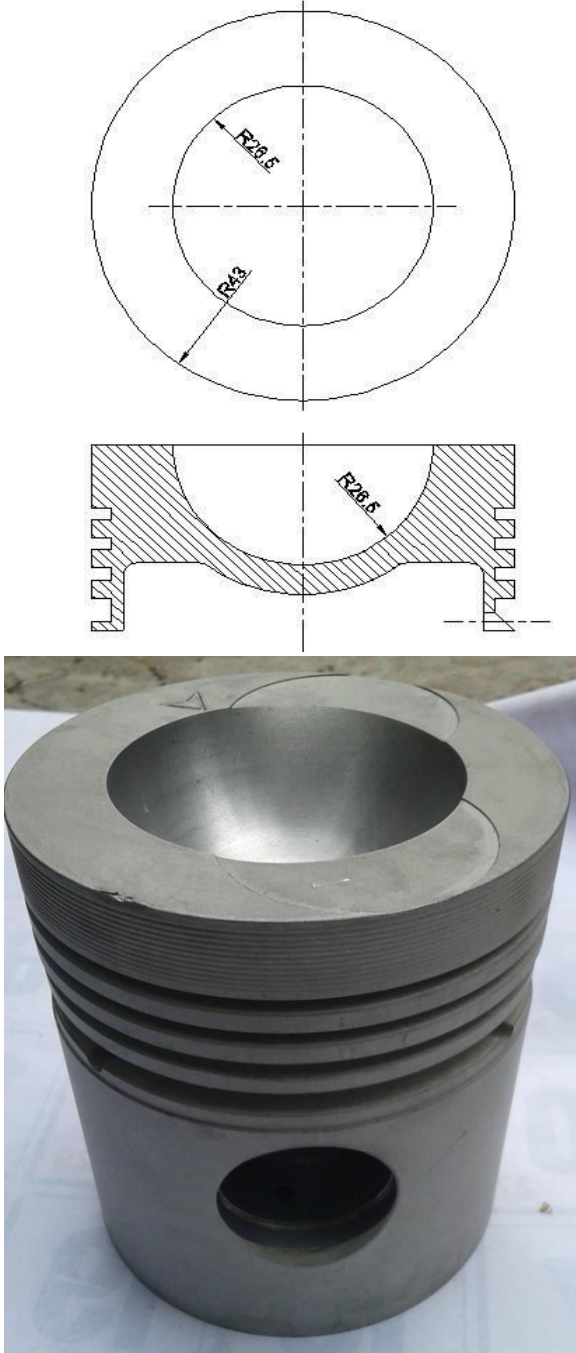


Fig 4.1 Piston 1 – Standard Piston

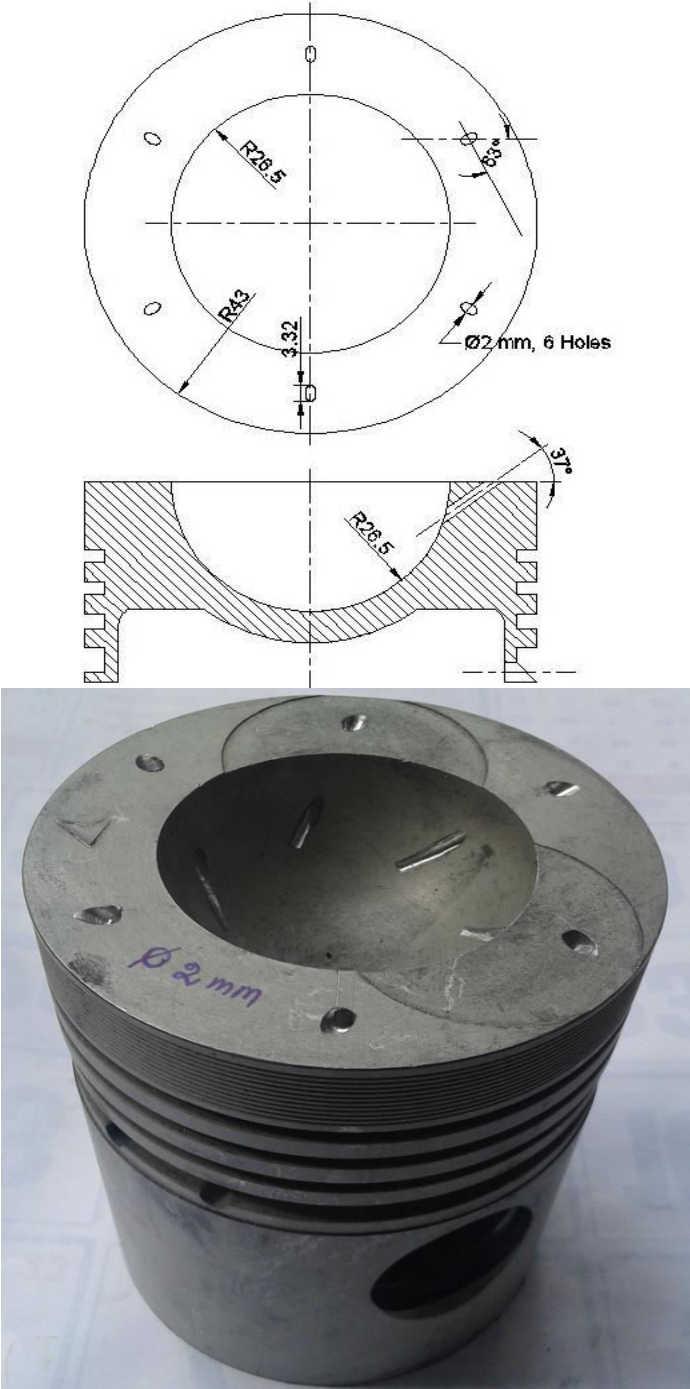


Fig 4.2 Piston 1- ϕ 2mm , 6 Elliptical Holes

Modified Piston –

1

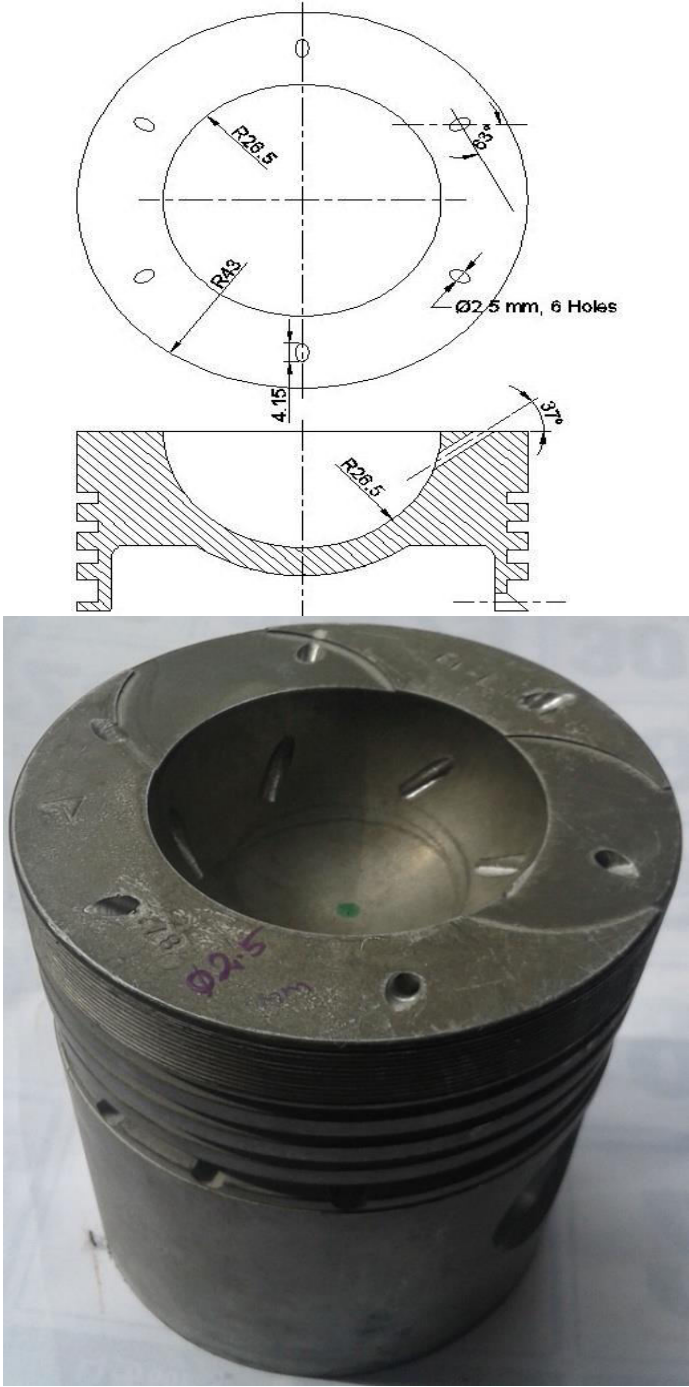


Fig 4.2 Piston 2- ϕ 2.5mm , 6 Elliptical Holes

Modified Piston – 2

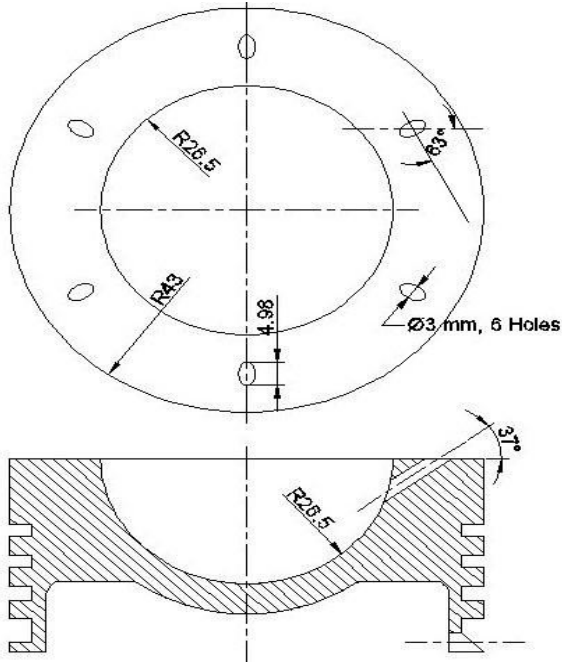


Fig 4.3 Piston 3 - $\varnothing 3 \text{ mm}$, 6 Elliptical Holes



Fig 4.4 Piston 3 - ϕ 3mm , 6 Elliptical Holes

4.3 Brake Thermal Efficiency

The variation of BTE with brake power for diesel fuel with standard piston and modified piston bowls. The piston-2 shows increase in BTE when compared to that of standard piston. The reason is that the modified piston increases the swirl motion as well as increases the squish and tumble thereby increasing the BTE. It shows an increase of 5.71% when compared to that of diesel fuel at full load.

4.4 Brake thermal efficiency

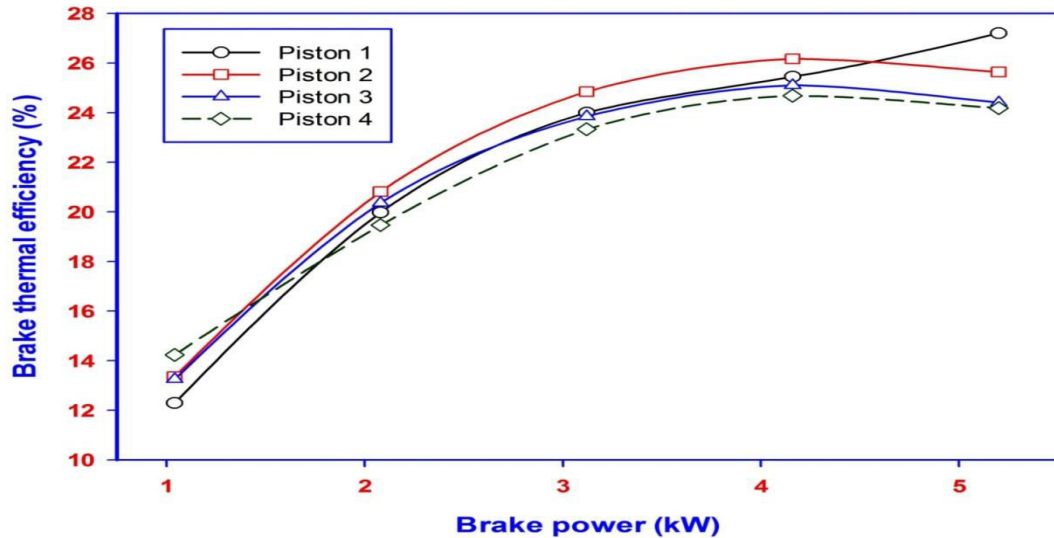


Fig4.5 Brake thermal efficiency

4.5 Specific Fuel Consumption

The variations of specific fuel consumption with brake power for diesel fuel with standard piston and modified piston bowls. Brake power increases SFC decreases. Among the piston-2 geometry shows lower specific fuel consumption when compared to other piston geometry and standard piston geometry. The reason is complete combustion of the fuel achieved by swirl motion of the modified piston.

Results and Discussion

Specific fuel consumption

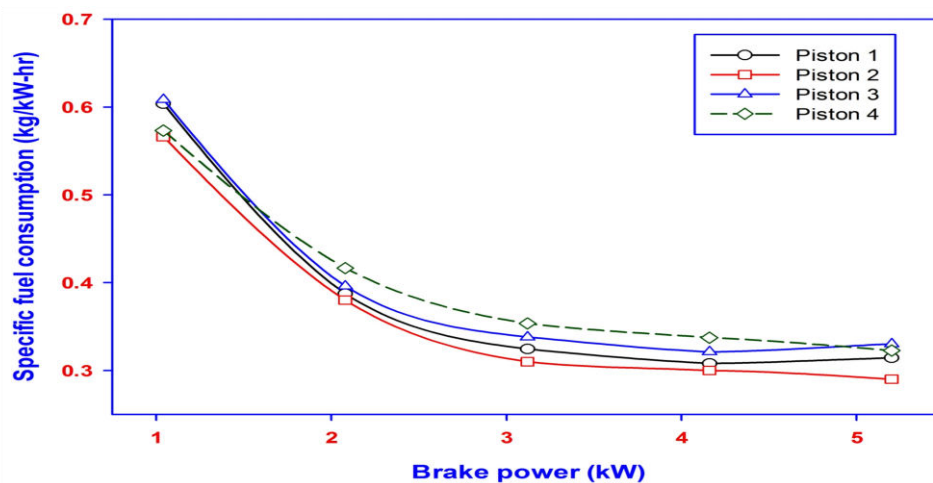


Fig 4.6 Specific Fuel Consumption

4.6 Smoke Density

The variation of smoke density with brake power for various piston with diesel fuel. The piston-2 shows increase in smoke density when compared to that of other piston

configurations. It has shown increase of 23.7% when compared to that of diesel fuel at full load. The reason is increasing smoke density due to flame quenching.

Results and Discussion

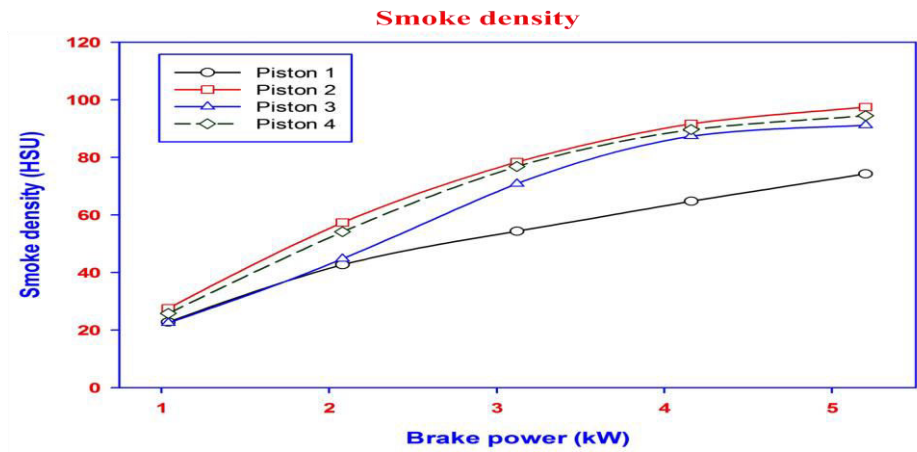


Fig4.7 Smoke Density

4.7 Oxides of Nitrogen

The variations of oxides of nitrogen with brake power for various piston bowl geometry using conventional diesel fuel. The piston-2 configuration shows decrease in NOx concentration when compared to that of diesel and all other blends. An increase of 23.9% was observed when compared to that of standard piston. The increased air motion inside the combustion chamber which reduced combustion temperature as a result of reduced NOx emission.

Results and Discussion

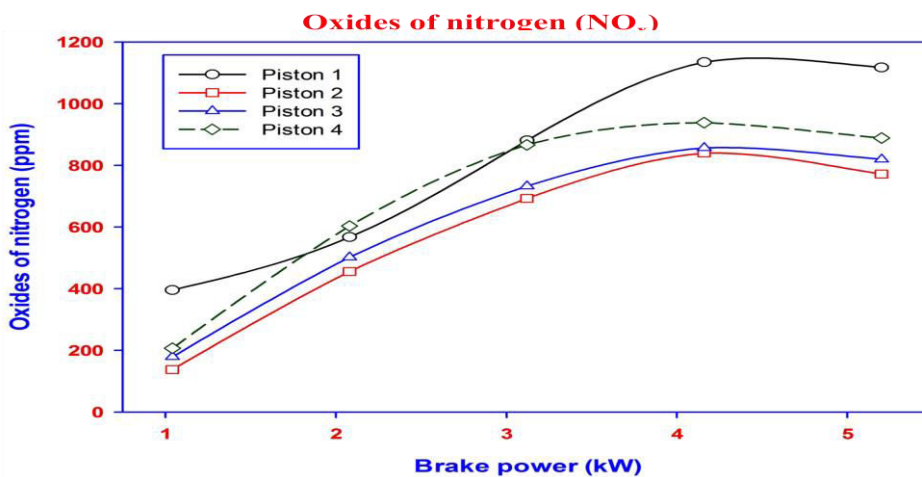


Fig 4.8 Oxides of Nitrogen

4.8 Carbon Monoxide

The variations of carbon monoxide with brake power for various piston bowl geometry. The piston-2 shows reduced CO emission since the design of the piston facilitates the air motion inside the combustion chamber and increasing complete combustion. A decrease of 16.32% was observed when compared to that of diesel fuel.

Results and Discussion

Carbon monoxide (CO)

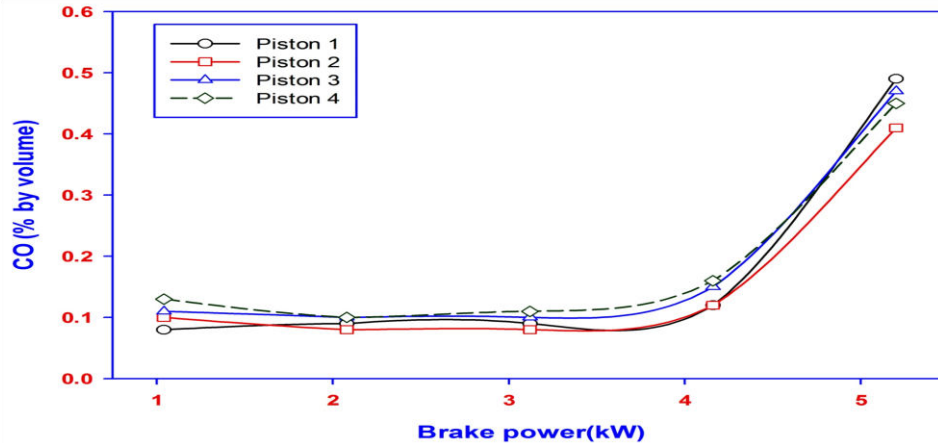


Fig 4.9 Carbon Monoxide

4.8 Hydrocarbon

Variations of hydrocarbon with brake power for various piston bowl geometry. Piston-2 shows decrease in HC emission when compared to that of standard piston. It is due to complete combustion and the piston design facilitates the air fuel mixture to have proper mixing to provide complete combustion.

Results and Discussion

Hydrocarbon (HC)

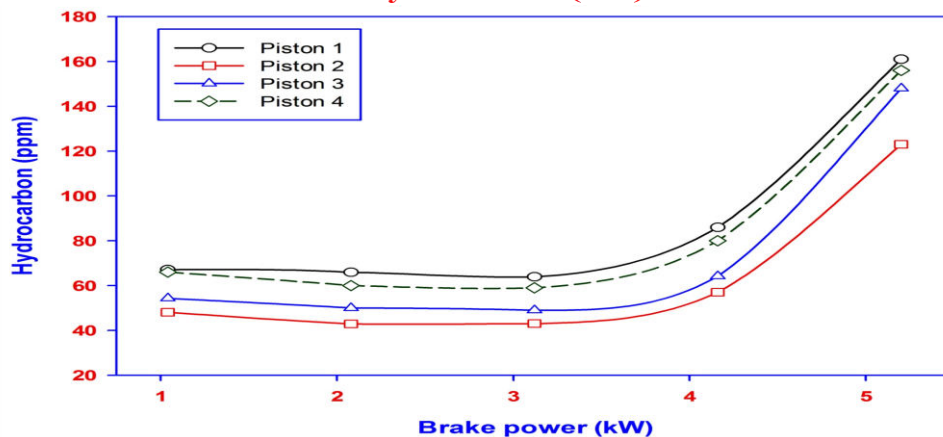


Fig 4.8 Hydrocarbon

V. CONCLUSION

The main conclusion of this studies are

1. The experimental investigations with modified piston bowl geometry using conventional diesel fuel have been carried out to determine the best configuration.
2. In order to enhance the engine performance and emission characteristics modified piston bowl geometry was designed and implemented.
3. Piston-2 geometry increased brake thermal efficiency than that of other configurations and standard piston geometry.
4. Piston-2 with diesel fuel show significant reduction in CO, HC and NO_x emission when compared to that of standard piston.

REFERENCE

- [1] Seung Man Nam, Kye Bock Lee and Seok HO Rhi, "Effect of piston bowl shape on the in cylinder flow characteristics of IC engines."
- [2] J.Li, W.M.Yang, H.An, A.Maghbouli and S.K.Chou (2014), "Effects of piston bowl geometry on combustion and emission characteristics of biodiesel fuelled diesel engine"
- [3] Bhanu Pratap Patel, I.J.Patel, T.M.Patel, G.P.Rathod (2014), "Effect of spiral grooves in piston bowl on exhaust emission of direct injection diesel engine."
- [4] R.Bertodo, T.W.E. Downes, I.D. middlemiss,"Evolution of a new combustion system for diesel emission control."
- [5] M.Horvatin and A.W.Hussmann, "Measurement of air movement in internal combustion engine cylinder."

Communication Skills for Engineering Students

L. M. Sowmiya

Asst.Prof, Dept of English, St.Anne's College of Engineering and Technology, Panruti.

sowmisanjumani@gmail.com

Abstract- Communication is essential for all the organizations. Getting the work done in effective manner has become more significant than having the most knowledge. Employers give considerable value to graduates acquiring a diverse set of skills in different work environment. Besides analytical and problem solving skills, subject specific knowledge, research and improved decision making ability, management skills, understanding of other culture, confidence and competence to work in international environment are considered the most essential qualities for engineers. However, at the bottom of these lies an effective communication skill. If students fail to see the broader scenario of the corporate world and ignore the communication skills, it can endanger a shallow level of understanding. The growing importance placed on oral communication skills by employers has been echoed internationally in these two three decades. Knowledge and technical knowhow are clearly important, but these require to be presented with excellence. Effective communication re-enforce positive impression of the engineer. Lack of serviceable communication skills contributes to the low profile of engineering in general public. A more proactive and accessible style of communication can be more engaging for the people. Indeed oral skills, presentation skills are considered one of the best career enhancers and to the single biggest factor in determining a student's career success or failure.

I. INTRODUCTION

The globalization of business and IT revolution has brought technical communication to the forefront of academia and industry. With the whole world becoming the global market and businesses becoming diverse and result-oriented, professionals and technocrats are facing new challenges in communications every day. A success in this competitive environment depends not just on acquiring knowledge and hard skills, but also on developing effective technical communication skills. This paper aims at making aware the engineering students of rural area and encourages them to improve their communication skills.

II. SIGNIFICANCE OF ENGLISH

English is the most important language in the world. Now it is the official language of international business, air traffic control, shipping, United Nations Diplomacy, world banking, science and technology, academic research, space travel and global computing. It is the major medium of education, publishing and international negotiation. It is perhaps the most flexible of all languages. Therefore, people belonging different parts of the world widely use English. Education has multiplied the role of English language, because universities worldwide often use English as the common mode of learning and communication. English is an international language of the Constitute, the Supreme Court, the High Court, and official departments. English is firmly rooted in the soil of India. A person in Tamil does not speak

Hindi, however he can understand English. Thus, English is a link language. Different people can communicate with one another with the help of English. English is a confidence builder. It will get you anywhere. If you are a good speaker in English means good in all. Therefore, engineers have to communicate in English. Engineering graduates require an ever-increasing range of skills to maintain relevance with the global environment of the new millennium. Communication skills are a vital component.

III. THE INTERNET AND MULTILINGUALISM

The Internet has become increasingly a crucible for world languages. This has direct implications on engineering education, as the Internet is central to various elements of engineering education. It also increases the global access to engineering education information, as under-served languages come online.

The prime language of Internet sites is becoming increasingly regionalized, with the local dominant language being the first choice in language options. English is still strong. The Internet, as an instrument of globalization, contributes to this process of recognizing diversity. This has clear implications for engineering education. This expanded access to the Internet builds a new dimension in the education process in this era of globalization: by combining language education with technology education.

IV. ENGLISH FOR SPECIFIC PURPOSES

The word communication in English is making a charm in these days. It has the power to make the whole world revolve around it. It is central to all activities. Everybody has realized the importance of communication and therefore, they want to be a better communicator. It has left no field untouched: be it a medical, or engineering, Arts or Law, or even Sports or Music. In commerce or Business it has become a must. In academics if you ignore communication you will literally ruin. It won't be an exaggeration if I say you won't survive without communication. If you want to earn bread and butter, you will have to learn communication. If you want to give voice to your requirements, you will have to learn communication. If you want to get a good job, learn to tell that you are fit and capable for it. If you want to get promotion, impress your boss with your effective communication. If you want your work get done learn to persuade and please others by talk. Gone are the days when work was got done under the force of power and pressure of authority. People were helpless and lacking self respect. The fast growing technology and spread of knowledge has made people aware of their rights and status. The relationships between subordinates and superiors are growing tensed. Personal opinions, attitudes and beliefs often act as strong barriers to effective communication. It is obviously difficult to communicate with the people effectively if they have quite rigid views, fixed opinions and strong prejudices. It disrupts the interrelationship and poses a challenge to management. Therefore, the organizations have changed master- servant relationship into partnership relationship. The changing scenario has given birth to a concept of team work. It shows us the necessity of developing team spirit, proceeding with joining hands. You have to respect other's perspectives. We have to stay in tune with our own emotions, as well as emotions of others. You have to offer your personal view points clearly and honestly to avoid confusion. You have to encourage others, praise others, make people valued and appreciated in you communication. If you let others know that they are valued they are likely to give their best. Getting the work done in effective manner has become more important than having the most knowledge. Employers give considerable value to graduates acquiring a diverse set of skills in different work environment. Besides analytical and problem solving skills, subject specific knowledge, research and improved decision making ability, management skills, understanding of other culture, confidence and competence to work in international environment are considered the

most essential qualities for engineers. However, at the bottom of these lies an effective communication skill.

If students fail to see the broader scenario of the corporate world and ignore the communication skills, it can endanger a shallow level of understanding. The growing importance placed on oral communication skills by employers has been echoed internationally in these two three decades. Knowledge and technical know how are clearly important, but these requires to be presented with excellence. Effective communication reinforces positive impression of the engineer. Lack of serviceable communication skills contributes to the low profile of engineering in general public. A more proactive and accessible style of communication can be more engaging for the people. Indeed oral skills, presentation skills are considered one of the best career enhancers and to the single biggest factor in determining a student's career success or failure.

V. NATURE OF TECHNICAL COMMUNICATION

We may define technical communication as a transmission of scientific and technical information from one individual or group to another. This exchange of professional information may include simple definitions of tools, complex descriptions of machines and process, or sophisticated explanation and interpretation of scientific principles. Effective technical communication is a dynamic interchange that may involve a systematic understanding of scientific and technical subjects.

The three important requirements of effective technical communication are:

- A.** Subject competence,
- B.** Linguistic competence, and
- C.** Organizational competence.

A. Subject Competence

Subject competence is the first requirement of technical communication. It is the possession of appropriate knowledge of a particular technical subject matter as well as the possession of highly sophisticated technical or professional skills. An inadequate background in the subject or lack of information might lead to incomplete and ineffective communication.

B. Linguistic Competence

Linguistic competence, on the other hand, is the possession of appropriate language skills and the ability to present scientific facts or information clearly and objectively. As technical communication involves technical presentation of data in reports, proposals, research papers, technical bulletins, manuals, and handbooks, linguistic competence includes several functional skills. Lack of these skills may lead to ineffective or incomplete communication. These skills include the ability to

- B. a. Analyze facts or information for clear presentation,
- B. b. Use appropriate rhetorical devices to present scientific data,
- B. c. Use graphs, charts, and diagrams systematically.

C. Organizational Competence

Since technical communication is a systematic and structured presentation of information, it involves a process of logical and thematic organization. Organizational

competence is the ability to organize technical information in a logical and structured way. It includes several skills such as the ability to sequence thoughts in a sentence, organize a

paragraph according to the needs of the reader and the topic, use appropriate logical ordering, and provide thematic coherence to expression.

The fast growth of technical knowledge coupled with the development of information technology has changed the way we communicate in professional situations. We prefer fast, interactive, and result oriented forms of communication such as voice mail, email, video transmission, teleconferencing, videoconferencing, intranet transmission, and so on to the traditional and slow forms of communication such as letter, memos, newsletter, and so forth.

VI. IMPORTANCE AND NEED FOR TECHNICAL COMMUNICATION

The functional importance of technical communication for an individual of an organization cannot be overemphasized. Whether you are an executive working in a multinational company, an engineer working at the shop floor level, a scientist working in a premier scientific lab, or a technical student of a professional institution, you need effective technical communication skills in order to be successful.

With the information revolution and socio-economic changes in the new millennium, the importance of effective technical communication skills has increased, the whole world has become a global market and the transfer of technical information is playing a key role in economic growth and transformation. As the professional world becomes more diverse, competitive, and result-oriented, the importance of technical communication skills continues to increase.

Revolution in information technology is having a profound impact on technical communication task, and new kinds of communications task or skills will be required in the changed technological environment. These skills include ability to understand and explain complex technical information in a simple and familiar style, ability to understand and explain quantitative data, cultural awareness, capability, and ability to analyze and priorities information.

The changes that have taken place in the field of science and technology reflect several developments in the way technical communication skills are viewed. In fact, there has been a shift in perspective, so that communication skills take priority over technical and professional skills. There is no doubt that good writing and speaking skills are essential to job success. It is also true that some technical skills are as important as communication skills but knowledge of technical or professional skills will be useless if one does not know how to communicate the information and elicit that result from the use and application of these technical and professional skills.

VII. REMEDIES

A. Development of Inner Urge

It is the general observation that the engineering students value technical subjects and underestimate the subject Communication skills. Students neglect it. Considering the scenario of corporate world if they feel that they should develop their communication skills they will make progress.

B. Need to Enrich Vocabulary and Sentence Construction

Language consists of words and sentence structures. Each day they must learn at least five new words and try to use them in their own sentences. The old method of displaying charts of difficult words, phrases and their applications on the walls and daily observance of them will help a lot.

C. Listening

Students must develop a habit of careful listening of English news, lectures, and explanations during tutorials, practical sessions, seminars, technical presentations, academic discussions, and academic interactions and so on. The modern Language Labs cater all their needs. They must make most of it. One cannot be an effective communicator unless one becomes an effective listener.

D. Speaking

Speaking skills are very important for a person's professional survival and growth. It gives practice of articulating words and boosts confidence in speaking. The students of rural area must be encouraged to ask questions in order to remove their fear, as they hesitate to ask questions considering that they may commit error or go wrong. Opportunities must be given to them to voice their opinions, agreements, disagreements, and suggestions, the credits should be given for participating discussions, making presentations of project, product, graphs, tables, charts plans, maps. They must be ensured that speaking skills are the single most important criteria in hiring professionals.

E. Reading

Like listening and speaking, reading is crucial to effective communication. Students need to read technical and business documents: reports, proposals, magazine articles, letters, and instruction manuals. It is hard to imagine any academic professional or business work that does not require efficient reading skills.

F. Writing

It is said that "Reading maketh a complete man, speaking maketh a ready man and writing maketh a perfect man". Writing is very important for students and professionals in all fields. They should practice writing projects reports lab reports, summary, synopsis, abstracts, and subject notes. As they go higher on the ladder of their career they will have to handle the correspondence independently. They will require writing business letters memos, email messages, proposals, minutes, notes reports, professional summaries and so on. Both professional and students need excellent writing skills to survive and excel in their pursuits as there is hardly any academic or professional activity that does not require writing skills.

VIII. CONCLUSION

Language and communication skills are recognized as important elements in the education of the modern engineers. The incorporation of language and communication improvement courses is an important element of continuous learning, and will ultimately contribute to the process of life-long learning.

REFERENCES

- [1] M Ashraf Rizvi, *Effective Technical Communication* (Tata McGraw-Hill, 2007).
- [2] K.K. Sinha, *Business Communication* (Galgotia Publishing Company, 2002).
- [3] Andrea J. Rutherford, *Basic Communication Skills for Technology* (Addison Wesley Longman, 2001).
- [4] R.K. Chadha, *Communication Techniques and Skills* (Dhanpatrai Publications, 2001).
- [5] Dr. Madhumati R. Patil, *Importance Of English Communication For Engineering Students From Rural Areas And Its Remedies*
- [6] Marc J. Riemer, *English and Communication Skills for the Global Engineer.*

Light-Fidelity (Li-Fi) Technology: A Review

M. Bala Murali¹, K.Nithyanandham¹, A. John Peter²

¹*I-Year Mechanical Engineering, St.Anne's College of Engineering and Technology, Panruti*

²*Asst.Prof, Dept of Physics, St.Anne's College of Engineering and Technology, Panruti.*

Abstract- Li-Fi stands for Light-Fidelity, for the fast increasing gadgets and to improve more effective use of lights a new technology is developed which is called- LIFI. Li-Fi is a modern technology which is used in progression with WIFI technology. LIFI uses LED lights which helps in faster and flexible data transfer transmitted through Wi-Fi. As light is everywhere, using light as the transmission medium Li-Fi can provide wireless indoor communication. The data transfer through LIFI is in bits and is much faster than Wi-Fi. Dr. Herald Haas, the professor of mobile communications at the University of Edinburgh, UK, first time publically displayed the proof of Light Fidelity (Li-Fi), a method of Visible Light communication (VLC). Li-Fi is the transfer of data through light by taking fiber out of fiber optics and sending data through LED light.

Keywords— Li-Fi, Wi-Fi, LED Lights, Wireless, VLC, Bits and Fiber optics.

I. INTRODUCTION

The most important day-to-day activities in this fast world are the transfer of data and information. As the world is becoming faster the need of fast data transmission is also increasing. As the numbers of devices that access to the internet are increasing, the limited bandwidth leads to decrease in the speed of the data transfer.



Fig 1: Li-Fi Bulb.

To give a solution to this problem Li-Fi technology is introduced. Li-Fi stands for Light Fidelity. Li-Fi provides better bandwidth, efficiency, availability and security than Wi-Fi and thus increases the data transfer speed. Li-Fi technology provides transmission of data through illumination by taking the fibre out of fibre optics by sending data through an LED light bulb.

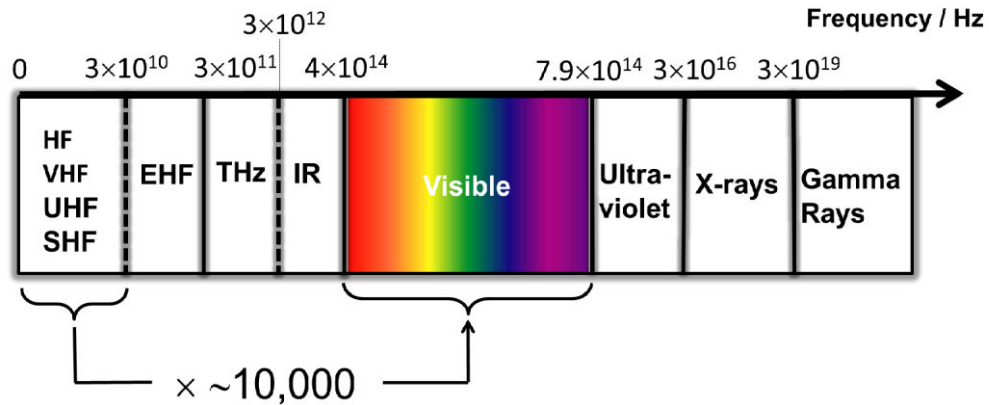


Fig 2: Electromagnetic Spectrum

Lifi uses visible light instead of Gigahertz radio waves for data transfer which makes it fast and cheap mode of wireless communication. The idea of Li-Fi was introduced by a German physicist, Harald Hass, which he also referred to as data through illumination. The term Li-Fi was first used by Haas in his TED Global talk on Visible Light Communication. According to Hass, the light, which he referred to as D-Light, can be used to produce data rates higher than 10 megabits per second which is much faster than our average broadband connection.

II. CONSTRUCTIONS OF LI-FI SYSTEM

The LIFI product consists of 4 primary sub-assemblies:

- Bulb
- RF power amplifier circuit (PA)
- Printed circuit board (PCB)
- Enclosure

The PCB controls the electrical inputs and outputs of the lamp and houses the microcontroller used to manage different lamp functions. An RF (radio-frequency) signal is generated by the solid-state PA and is guided into an electric field about the bulb. The high concentration of energy in the electric field vaporizes the contents of the bulb to a plasma state at the bulb's centre; this controlled plasma generates an intense source of light. All of these subassemblies are contained in an aluminum enclosure.

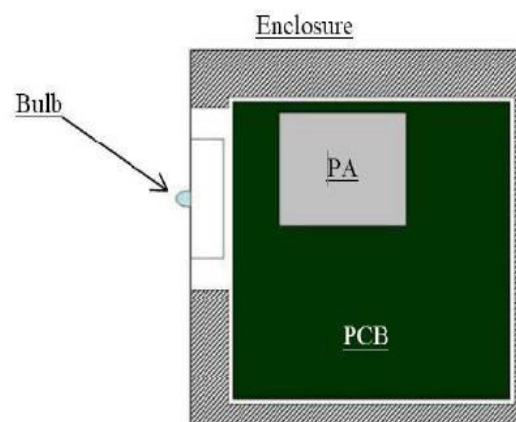


Fig 3: Block Diagram of Li-Fi sub-assemblies.

III. FUNCTIONS OF THE BULB SUB-ASSEMBLY

At the heart of LIFTM is the bulb sub-assembly where a sealed bulb is embedded in a dielectric material. This design is more reliable than conventional light sources that insert degradable electrodes into the bulb. The dielectric material serves two purposes; first as a waveguide for the RF energy transmitted by the PA and second as an electric field concentrator that focuses energy in the bulb. The energy from the electric field rapidly heats the material in the bulb to a plasma state that emits light of high intensity and full spectrum.

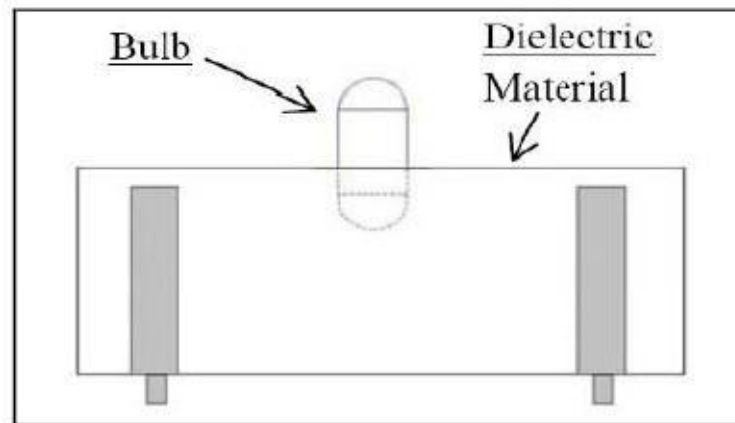


Fig 3: Bulb sub-assembly.

IV. WORKING OF LI-FI

A new era of large brightness light-emitting diodes forms the core part of lifi technology. The

logic is so simple as follows-If the LED light is on, a digital 1 is transmitted. If the LED light is off, a digital 0 is transmitted. These large brightness LEDs lights can be switched on and off very quickly which gives us a very nice chance for transmitting data through light. The working of Li-Fi is very easy as Wi-Fi . There is a light emitter on one corner, for example, an LED, and a photo detector (light sensor) on the other corner. The photo detector registers a binary one when the LED is on; and a binary zero if the LED is off same as microprocessor. To generate any message, flash the LED numerous times or use an array of LEDs of perhaps a few different colours, to obtain data rates in the range of hundreds of megabits per second.

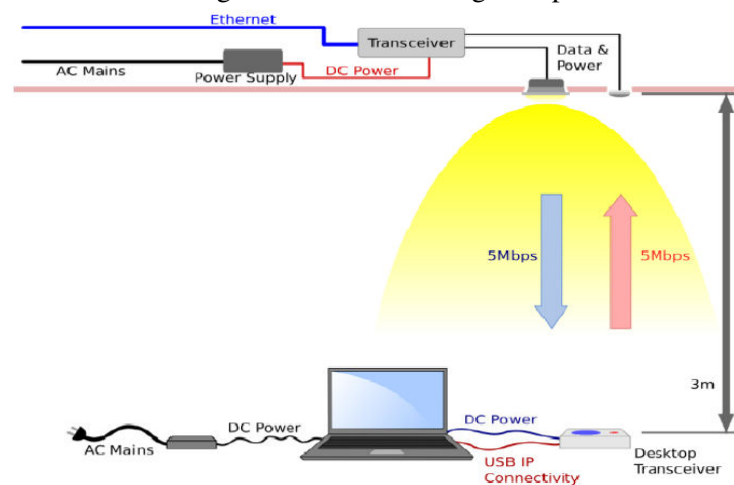


Fig 4: Working Principle of Li-Fi Technology

The data can be encoded in the light by varying the flickering rate at which the LEDs flicker on and off to generate different strings of 1s and 0s. The LED intensity is modulated so rapidly that human eye cannot notice, so the light of the LED appears constant to humans.

Light-emitting diodes can be switched on and off faster than the human eye can detect, causing the light source to appear to be on continuously, even though it is in fact 'flickering'. The on-off activity of the bulb which seems to be invisible enables data transmission using binary codes: switching on an LED is a logical '1', switching it off is a logical '0'. By varying the rate at which the LEDs flicker on and off, information can be encoded in the light to different combinations of 1s and 0s. This method of using rapid pulses of light to transmit information wirelessly is technically referred to as Visible Light Communication (VLC), though it is popularly called as Li-Fi because it can compete with its radio-based rival Wi-Fi.

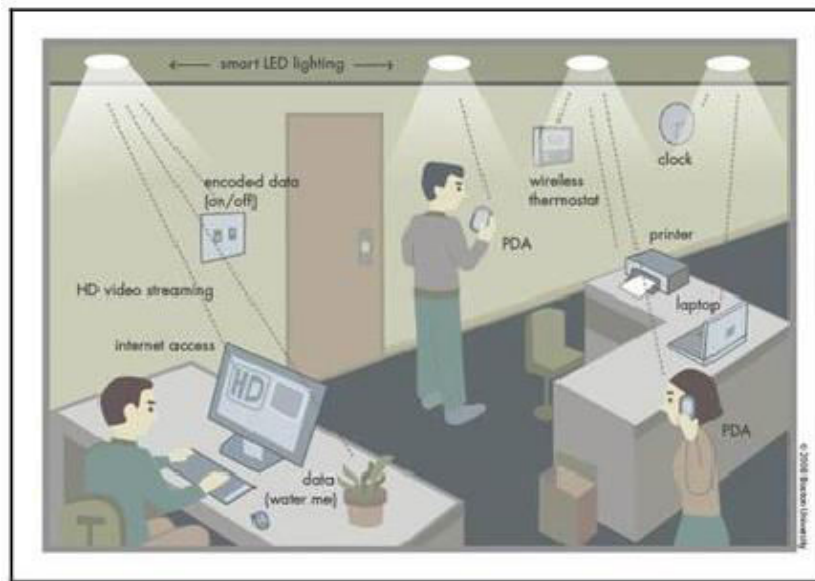


Fig 5: Li-Fi system connecting devices in a room.

V. RECENT ADVANCEMENT ON LI-FI TECHNOLOGY

Researchers at the Heinrich Hertz Institute in Berlin, Germany: have reached data rates of over 500 megabytes per second. A consortium called Li-Fi Consortium 'was formed in October 2011 by a group of companies and industry groups to promote high-speed optical wireless systems and overcome the limited amount of radio based wireless spectrum. According to the Li-Fi Consortium, it is possible to achieve more than 10 Gbps of speed, theoretically which would allow a high-definition film to be downloaded in just 30 seconds. Researchers at University of Strathclyde in Scotland: began the task of bringing high-speed, ubiquitous.

VI. ADVANTAGES OF LI-FI

Li-Fi technology is based upon lights might be any sort of lights. The transfer of data takes place in presence of any kinds of light whatever may be the band width. Due to which the depend of transmitting the data or information will be great and also sufficient information, music, movies, games anything can be downloaded using very less time.

1. **Capacity:** Light itself has 10000 times wider bandwidth than radio waves. Due to which the transfer of data is more effectively possible. So Li-Fi has better capacity.
2. **Efficiency:** LED lights consume less energy and very efficient. As it uses less energy it is cheap and easy to use.

3. **Availability:** As light is present everywhere, Lifi is available everywhere. But for more efficient use of lifi technology LED bulbs must be placed for proper transmission on data for proper transmission on data.
4. **Security:** Light waves cannot penetrate through walls. So they cannot be misused.
5. **Bandwidth:** The visible light is unlicensed and free to use and gives a very large bandwidth.
6. **Data Density:** Li-Fi can achieve about 1000 times the data density of Wifi because visible light can be well contained in the tight illumination area.
7. **Low Cost:** As it requires very few components the cost of it is comparatively low.

VII. LIMITATION OF LI-FI

1. As lifi technology uses light as transmission medium, so if the receiver is somehow blocked in away then the signal will immediately will be cut out.
2. While data transfer interference from external light sources such as sunlight, normal bulbs, and opaque materials can cause loss of reliability and network.
3. As Lifi works in direct line of sight. Slight disturbance can cause to interruption.

VIII. APPLICATIONS OF LI-FI

Some of the future applications of lifi are as follows:

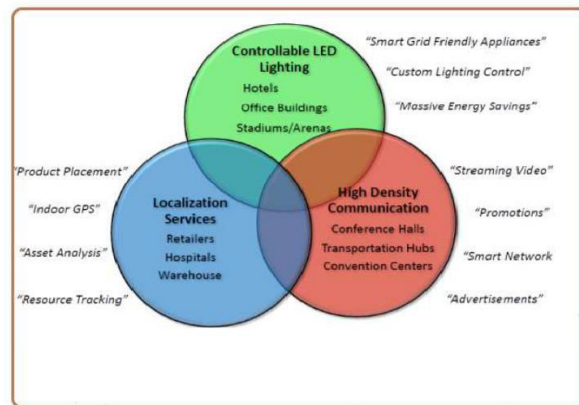


Fig 6: Applications of Li-Fi Technology

1. **Education System:** Lifi is the latest technology that can provide fastest speed internet access. So it can replace the Wifi at Educational Institution and at companies so that they can use the same internet with more fast speed.
2. **Medical applications:** As wifi uses radiations waves which can cause hazardous to the patients in OT(Operation Theatres) while radioactive operations. So Wifi is not allowed there as it can block the signals.
3. **Internet in Aircrafts:** In Aircrafts wifi cannot be used as it can interfere with the navigational systems of the pilots. Thus Lifi Can be used for data transmission. Lifi can Provide high speed internet using the every light source such as overhead reading bulbs.
4. **Underwater Applications:** Lifi can work underwater where Wifi fails completely, thereby providing open endless opportunities for military operations.
5. **Disaster Management:** Lifi can be powerful means of communication in times of earthquakes or hurricanes. Lifi bulbs could provide cheap high speed Web access to every street corner.
6. **Applications in Sensitive Areas:** wifi are bad for sensitive areas such as power plants. Lifi can provide much safer connectivity in such sensitive areas. Also Lifi can be used in petroleum or chemical plants where other transmission medium can be hazardous.
7. **Traffic management:** In traffic signals Lifi can be used which will communicate with the Led lights of the car which can help in traffic management. Also LED car lights can alert drivers when other vehicles are too close thus reducing the chances of accidents.

8. **Replacement for other Technologies:** Lifi can be used in the areas where radio waves technologies such as Wifi are banned.

X. DESIGN OF LI-FI

Important factors we should consider while designing Li-Fi as following:

1. Presence of Light must be line-of-sight.
2. Lamp driver where internet connection, switch and LED lamp connected.
3. For better performance use LED bulbs.
4. A photo detector received data.

X. FUTURE SCOPE

As light is everywhere and free to use possibilities increases to a great extent of the use of Li-Fi technology. If this technology comes to practice each lifi bulb will be used as Wi-Fi hotspot to transmit wireless data. As the lifi technology will be used which will lead to a cleaner, greener, safer and bright future and environment. The concept of lifi is attracting many people as it is free to use without any license and faster means of data transfer. If it develops faster people will more and more use this technology instead of wifi.

XII. CONCLUSION

With the growing technology and increasing use of the internet services, possibilities are very high that use of Lifi technology will be soon in practice. Every bulb will be replaced by Lifi bulbs and might be used like a wifi hotspot for the transmission of data. Using Lifi technology will grant a cleaner, greener and brighter future and environment. The concept of lifi is spreading so fast as it is easy to use, it is attracting interest of people. The use of lifi technology gives a very golden opportunity to replace or to give alternative to the radio based wireless technologies. As the number of people and the access of internet is increasing on such a large scale, accessing internet through wifi will soon be insufficient as the usage is increasing but the bandwidth remains the same. As network traffic will increase it will result in lowering the speed of accessing the internet thus more increasing prices. The airways become clogged making it more difficult to use. Thus the use of Lifi will increase the speed of data transfer and also it is accessible in many banned places thus it will be available for all.

REFERENCES

- [1] Jyoti Rani, Purna Chauhan, Ritika Tripathi, —Li-Fi (Light Fidelity)-The future technology In Wireless communication, International Journal of Applied Engineering Research, ISSN 0973-4562 Vol.7 No.11 (2012).
- [2] Richard Gilliard, Luxim Corporation, —The lifi@ lamp high efficiency high brightness light emitting plasma with long life and excellent color quality.
- [3] Richard P. Gilliard, Marc DeVincentis, Abdeslam Hafidi, Daniel O'Hare, and Gregg Hollingsworth, —Operation of the LiFi Light Emitting Plasma in Resonant Cavity.

Enrich Your English

Mrs.S.Bharathi AP/S&H

Ms.D.Datchayani I year/ EEE

*Science & Humanities, St. Anne's college of Engineering and Technology ,
bharathiabi20@yahoo.com*

Abstract

This article is written on the factors of how to enrich our English language and discuss how to achieve a standard status. With the development of technology, media, science, education etc. English help the students to broaden their knowledge, change the way of thinking and brighten their career prospect. We all know English but how can we enrich it? This paper discusses the various strategies adopted to enrich our English.

Keywords- Pronunciation , vocabulary , grammar , practice , fluency.

INTRODUCTION

We all know learning English is very important today. As an English learner, you surely want to use English fluently. The first step towards that goal is to have a rich vocabulary. Though many find it difficult to gain a large vocabulary, how to enrich your English vocabulary is really simple. The first thing you have to do is to determine what field of words to learn. This means that not all words are worth learning. Good English skills are vital to succeeding in life, in terms of education, career, and personal relationships. This means that many people want to improve their English, but it can be hard to know how to go about it. There are three main areas that have to be worked on: pronunciation, vocabulary, and grammar. Getting the pronunciation right is something that many international students worry about, but that people born in English-speaking countries often forget about, but it is equally important for all. After all, pronouncing the words you use correctly makes you look far more intelligent. The first step to improving pronunciation is often to slow down your speech a little and think a bit more carefully. Pay attention to consonants, particularly at the end of words (as these are often missed off in speech), and make sure sounds like “sh” and “th” come out properly. A good way to improve pronunciation is often to watch English movies in which people are speaking properly. The second way to improve your English is to widen your vocabulary. One good way to do this is to learn a new word (or a few) every day, and make an effort to use them. Reading is also important in learning new words, as is looking up words you don't know in a dictionary so that you will be able to use them yourself. Making sure that you fully understand the meaning is really important, though, because it is no good using new words if you don't use them in the correct place. Because of this, just knowing a dictionary definition may not be enough; you will need to know in what contexts the new word can be used or you could say something that makes no sense. The same applies to colloquial phrases, which many people use incorrectly after hearing them one time (perhaps used by a friend in the wrong context). Understanding the register is very important too, as you don't want to use slang in a formal context, or alienate people in social situations with overly complex words that only serve to make you look arrogant.

The final thing to really work on is grammar, and spelling and punctuation with it. Reading will help a great deal in this respect, as you can learn from seeing it used properly. There are also plenty of websites and books available to help with grammar and

punctuation if you're unsure of how to use something. Improving your grammar is so important because spellcheckers still aren't advanced enough to pick up most errors, or even incorrectly tell us to change something. Pronunciation and vocabulary must be improved though too, as all are equally important and all affect your grasp of the English language. As study has shown, for each individual only 2% of 500,000 English words are enough to use in both social contacts and working alone with professional materials. Therefore, your rich vocabulary should only include about 10,000 words relating to your regular uses. After deciding the field of words you mainly use, you make a plan of learning. First, how many words will you learn a week: five, ten, fifteen or more? Secondly, when will you learn them: at a fixed time every other morning or anytime you feel like to learn some? Thirdly, how often will you review what you have learnt: once a week, once a month or before a test at school? Finally, what subjects will you focus on: sports, music, games or sciences? The answers may vary a great deal from one person to another depending on their memory, schedule and interest. When you have already had a complete plan, you need to think about choosing your own learning methods, or the way to help you remember new words. Basically, there are two methods, which are repetition-based method, you learn words by writing them several times or saying them repeatedly until you remember them all.

1. Some people may not find it necessary to write down what their teacher says, but a lack of attention can result in lack of improvement. It can be quite demanding to study a new language whilst juggling all other day-to-day activities in life, and as such requires a lot of effort. So, to make it easier on yourself, be organised with your learning. Take notes to help you remember things after a busy day, do your homework and get closer to your English fluency goal.

2. Write in your own words! Read something that interests you (about a topic that you are already familiar with) and try to write it again in your own words. This is also known as 'paraphrasing' and can help you to solidify your understanding of what you read, by expressing it in your own way. You will undoubtedly use synonyms, so it may be worth investing in a thesaurus.

3. Exchange correspondence with your friends in English. Reading and writing in English has and always will be an effective way of improving these skills. The more you do, the more you learn, and therefore, the better you get!

4. Search interactive websites that provide online practice and correction! Here are some examples to get you started: [Quizlet](#), [UsingEnglish](#), [CardKiwi](#) or [Grammar Check](#).

5. Utilize social media! There are a great number of online platforms where you can share, chat and comment – all in English! [How to Learn English in a new way!](#)

6. Improve your English writing skills by blogging. Share your learning experiences with others and tell people how you're improving and what you're doing to get there. Don't see this as boasting; it should be used purely to record your progress, give tips that worked well for you to other learners, and most of all, practice your writing skills! That which comes in importance first is reading which helps you greatly in vocabulary building. The more you read, the stronger will be your vocabulary. The reading material may be any kind of reading that gives you benefits you desire. You can read literary works, novels, newspapers, journals, articles and magazines. In this modern day and age, the information is just a click away. You can read lots of stuffs at internet. The reason for this is that, while reading you can not only enrich your vocabulary, but can also understand the meaning of sentences or paragraphs as a whole. In this way, being able to get to the gist allows you to read more speedily and efficiently.

1-Learning a word a day can be a great way. If considered, at the minimum, it will help you learn many words providing you do it constantly. At your convenience or to make this habit little better, you may also do this thing that you can learn other forms of that particular word you have just learned. This way will have given you more benefits by letting you learn a word as well as its different forms. This practice will not only enable you to use that particular word properly, but will also help you make use of a word in different contexts.

2-Engaging in conversation is yet another great way to help you in enriching your vocabulary. You can gain lots of new words by listening to or hearing from your relatives, friends, colleagues and acquaintances. In addition, watching English news bulletin regularly can be of much help and assistance in expanding your vocabulary. Thus, the more words you know, the more you will be able to understand what you hear and read.

3-Maintaining a vocabulary journal is one of the best strategies. It is unlikely that teachers can cover in class the huge number of vocabulary items that students will need to use or understand, so it is equally important to help students with *how* to learn vocabulary as well as with *what* to learn. In this blog post I would like to answer some questions my students usually ask about learning vocabulary, and also to offer some tips and links which I hope can help them to improve their vocabulary.

What is meant by ‘our vocabulary’?

Our own individual vocabulary refers to all the words we know. It includes both our:

- **active vocabulary** – the words we understand and use regularly when speaking or writing, and our
- **passive vocabulary** – the words we understand when we hear them, but do not or cannot use them.

We often recognize a word before we can use it. It takes a long time before we fully know a word.

Why is it important to improve our vocabulary?

A wide vocabulary helps you to understand what you read or listen, and to write and speak well. It is far more difficult to communicate with no vocabulary than with no grammar. *You will improve your English very much if you learn more words and expressions instead of spending most time studying grammar.*

What is meant by really knowing a word?

Really knowing a word means knowing all its different kinds of meanings. Knowing a word also involves understanding its form, i.e. what part of speech it is, how it works grammatically, and how it is pronounced and spelt. In order to pronounce new words correctly you can use the phonetic alphabet for help with pronunciation. You can also use an online, talking dictionary that tells us how to say a word (i.e. includes a sound clip of the pronunciation). You need to say new words a number of times; listen to what you are saying. You need also to use your new words in conversation, in emails and other writing many times before you can be said to have learned them. Make sure you check with your teacher if there is anything you are not sure about. *It takes a lot of practice before you really acquire / learn / know a new word. You should be systematic about studying and review new words at least once every couple of weeks.*

Useful tips to help students improve their vocabulary

1. Record your vocabulary systematically

As far as vocabulary learning is concerned, one of the main problems is recording your vocabulary in a way that will help you remember it. It is a very good idea to have *avocabulary notebook* and to organize it into themes or topics (e.g. appearance, food, clothes, health, holidays, relationships, travel, traffic, etc.). Have one theme per piece of paper and create headings to sort out your words and phrases into really useful ‘word maps’.

Try not to note down single words. Try and find out what other verbs, adjectives, prepositions etc. go together with each word.

2. Learn vocabulary in chunks

The best way of learning new words is to gather together words and phrases in clusters that make sense, that connect with each other – because, simply, it helps the brain remember them.

Apart from helping you to expand your English vocabulary, you need to learn collocations because they will help you to speak and write English in a more natural and accurate way.

3. Use a dictionary

You need to have access to a couple of good dictionaries. If you read or hear a word you don't understand, look up the meaning of the word and write it down in your 'vocabulary notebook'. Good learner dictionaries give students so much help with getting a grasp on vocabulary. Most dictionaries have a key at the beginning to explain the codes. Example sentences are useful for showing you how a word is used in practice. Phrases and collocations show you the different uses of a word and help to further increase your vocabulary. If students are taught how to use them properly they will increase their depth of understanding. With correct usage of a good dictionary, such as the *Oxford Advanced Learner's Dictionary* or the *Cambridge Advanced Learner's Dictionary* students will know how vocabulary is pronounced. They'll also be able to identify which words are from the academic word list, learn synonyms and antonyms etc.

Remember that English is changing every day. The more recently a dictionary was published, the more up-to-date the language will be.

4. Range of contexts

Students need to use new vocabulary in various contexts outside the classroom. They can listen to the news, read some novels or listen to their favourite music in English. The more that language is seen in different contexts, the more students will be extrinsically motivated as they will want to know more. This is much more interesting for students (and teachers) if the focus is on the topic not the language.

CONCLUSION

In this writing, I have discussed how to "enrich your English" and the ways to make English language affluent in official status and education priority. I have also given examples, cite ideas and explanations to the way how a language achieve this status. This paper will give a detailed idea of how to improve the quality of your English.

REFERENCE

- Crystal, David. *The Cambridge Encyclopedia of the English Language*. Cambridge: U of Cambridge, 1997.
English Department, University of Texas at Austen.
<<http://www.utexas.edu/cola/depts/english/>>. Accessed 10 Sept. 2008.

Room Temperature Synthesis of $\text{NaY}(\text{MoO}_4)_2:\text{Pr}^{3+}$ Nanophosphor With Blue Excitation For WLED Applications

Ezekiel.A¹, Padmanathan.D¹, A. John Peter²

¹*I-Year Mechanical Engineering, St. Anne's College of Engineering and Technology, Panruti*
²*Asst.Prof, Dept of Physics, St. Anne's College of Engineering and Technology, Panruti.*

Abstract—The nanostructured $\text{NaY}(\text{MoO}_4)_2:\text{Pr}^{3+}$ phosphor was rapidly synthesized at room temperature by mechanochemically assisted solid state meta-thesis reaction method. The as-synthesized nanophosphor possess scheelite tetragonal crystal structure with space group $I41/a$. Photoluminescent studies revealed that under the excitation of blue light (448 nm), a strong emission in the red region was observed at 647 nm due to the transition from populated $^3\text{P}_0$ level to the $^3\text{F}_3$ lower level of Pr^{3+} ions. The nanostructured $\text{NaY}(\text{MoO}_4)_2:\text{Pr}^{3+}$ material could serve as excellent red phosphor candidate for solid state lighting applications.

Keywords- Phosphor, Solid meta-thesis reaction, Scheelite structure, WLED.

I. INTRODUCTION

Currently, researchers are engaged toward the synthesis of new class of micro/nano structured luminescent phosphors to improve its lumen efficacy for white light emitting diodes (WLEDs) applications. Because, WLEDs are considered as promising next generation solid state lighting devices and play a major role by virtue of its high permanence, high efficiency, low-cost, energy saving, prolongation, environmental friendly, etc. WLEDs have number of prospective applications and used in fluorescent lamps, indicators, back lights, automobile light, traffic signals, etc. The ultimate and hopeful method to attain high quality phosphor-converted WLEDs is by pumping tricolor phosphors with UV InGaN chip or blue GaN chip. However, the commercially available white LED have lack of red emission component results in high correlated color temperature, low lumen efficiency of radiation, and low color-rendering index limits their applications to some extent. Hence, special attention is needed to find out an alternative novel red phosphor material must possess thermally and chemically more stable and show better luminous efficiency with low-cost. Many reports were reported on scheelite type molybdates or tungstates with tetragonal structure due to their feasible luminescence applications in various fields such as laser host materials, fiber optics, WLEDs, scintillation detector, etc. The conventional method of preparation of tricolor phosphor typically requires high temperature and eats a lot of power and time. Whereas, the solid state meta-thesis reaction method (SSM) is an outstanding method does not requires high temperature and external high electrical energy. Using SSM one can synthesize the phosphor with homogeneous, pure and well crystallized powders at room temperature rapidly. The objective of this work is to prepare Pr^{3+} doped $\text{NaY}(\text{MoO}_4)_2$ red phosphor by mechanochemically assisted solid state meta-thesis reaction method and to study their photoluminescence properties. To check the colour purity of the samples

Commission Internationale del'Eclairage (CIE) color chromaticity coordinates were calculated.

II. SYNTHESIS PROCEDURE

Pr^{3+} activated $\text{NaY}(\text{MoO}_4)_2$ phosphor was synthesized by mechanochemically assisted solid state meta-thesis method at room temperature. All the starting materials were of analytical grade and used without any purification. The appropriate amount of $\text{Na}_2\text{MoO}_4 \cdot 2\text{H}_2\text{O}$, $\text{YCl}_3 \cdot 7\text{H}_2\text{O}$, $\text{PrCl}_3 \cdot 7\text{H}_2\text{O}$ were mixed together and pulverized for a period of three hours in a planetary ball mill pulverisette 7 (FRITSCH). Two grinding vials of 15 cm volume with balls with diameter of 12 mm made of tungsten carbide materials were used to pulverize the mixer. The number of grinding balls and the speed of rotation of milling device were kept constant. The final product were washed and centrifuged with double distilled water several times for purification then it was dried at 60-80°C for 2 h in a muffle furnace in air.

III. RESULTS AND DISCUSSION

3.1. Structural and Morphological Analysis

Figure 1 shows the XRD pattern of $\text{NaY}(\text{MoO}_4)_2$ doped with Pr^{3+} . From the XRD pattern, it is observed that the samples are pure and possess scheelite tetragonal crystal phase. All the peaks are indexed and matches well with the JCPDS card no. 25-0828 of $(\text{Na}_{0.5}\text{Y}_{0.5})\text{MoO}_4$ structure. No other extra peaks of impurity were detected. Moreover, it can be noticed an enhanced intensity of peak at (112) about 28.52°. Fig. 2 shows the FESEM image of the sample which clearly depicts that the average particle size was found to be approximately 100 nm.

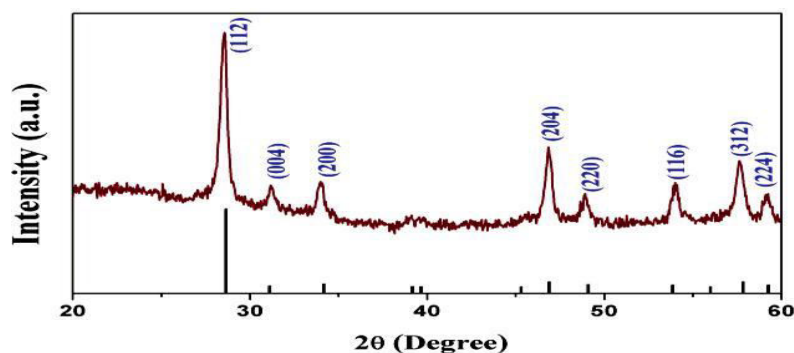


FIGURE 1. XRD pattern of Pr^{3+} activated $\text{NaY}(\text{MoO}_4)_2$ nanophosphor.

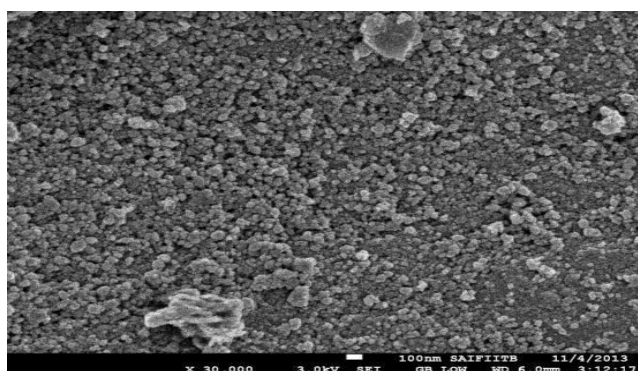


FIGURE 2. FESEM image of the nanophosphor synthesized by solid state meta-thesis reaction method.

3.2. Photoluminescence Properties of $\text{NaY}(\text{MoO}_4)_2:\text{Pr}^{3+}$

Fig. 3 shows the photoluminescence excitation spectra of $\text{NaY}(\text{MoO}_4)_2$ doped with Pr^{3+} sample which consist of three intense and sharp absorption bands observed at 448 nm, 474 nm, 488 nm corresponding to the transitions from unexcited $^3\text{H}_4$ level to excited $^3\text{P}_2$, $^3\text{P}_1$, and $^3\text{P}_0$, levels respectively.

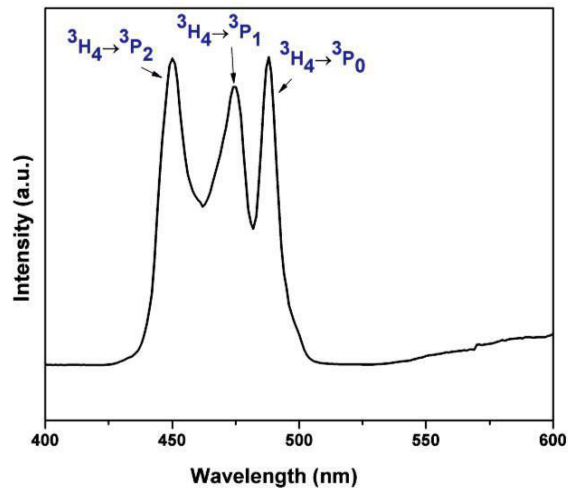


FIGURE 3. PL excitation spectrum of Pr^{3+} activated $\text{NaY}(\text{MoO}_4)_2$ nanophosphor monitored at 647 nm.

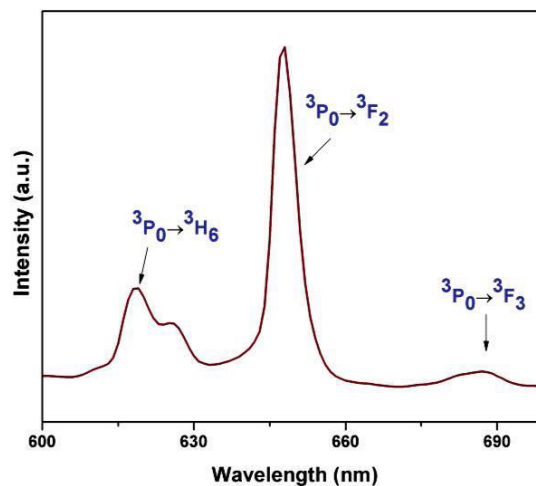


FIGURE 4. PL emission spectrum of $\text{NaY}(\text{MoO}_4)_2:\text{Pr}^{3+}$ excited at $\lambda_{\text{ex}} = 448$ nm.

Fig. 4 shows the room temperature PL emission spectra of $\text{NaY}(\text{MoO}_4)_2$ doped with Pr^{3+} phosphor. Under the excitation of 448 nm blue light, the emission spectra were governed by the characteristic red luminescence primarily originated due to the transition from excited $^3\text{P}_0$ level to the $^3\text{F}_2$ lower level noticed at 647 nm. Also, the transitions observed at $^3\text{P}_0 \rightarrow ^3\text{H}_6$, $^3\text{P}_0 \rightarrow ^3\text{F}_3$ at 619 nm and 687 nm are relatively weak. Fig. 5 shows the corresponding Commission Internationale de l'Éclairage (CIE) diagram and color chromaticity co-ordinates was found to be $x = 0.6989$ and $y = 0.3010$ and occupy red part of the CIE diagram which are very close to the NTSC standard value. Thus, the obtain results suggesting that the material $\text{NaY}(\text{MoO}_4)_2:\text{Pr}^{3+}$ synthesized by solid state meta-thesis route might be useful for promising red phosphor candidate for WLEDs.

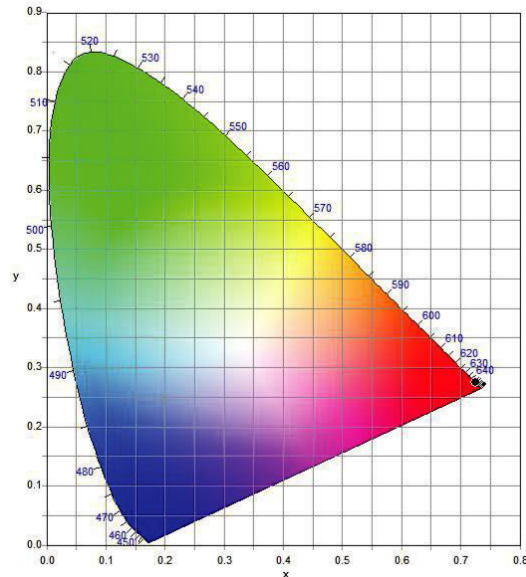


FIGURE 5. CIE (x,y) chromaticity diagram of $\text{NaY}(\text{MoO}_4)_2:\text{Pr}^{3+}$

IV. CONCLUSION

The nano phosphor $\text{NaY}(\text{MoO}_4)_2$ doped with Pr^{3+} has been rapidly synthesized by solid state meta-thesis reaction technique at room temperature. The phase purity of the crystal structure was identified by XRD pattern. FESEM image of the sample clearly depicts the mean particle size was found to be approximately 100 nm. The photoluminescence investigation suggesting that under blue light excitation, Pr^{3+} doped $\text{NaY}(\text{MoO}_4)_2$ nanophosphor shows the strong emission in the red region observed at 647 nm due to the $^3\text{P}_0 \rightarrow ^3\text{F}_2$. In summary, the as-obtained nanophosphor could find the potential applications in solid state lighting applications and red phosphor for W-LED Applications

REFERENCES

- [1] Xu Q, Xu D, and Sun J, "Preparation and luminescence properties of Orange-red $\text{Ba}_3\text{Y}(\text{PO}_4)_3:\text{Sm}^{3+}$ phosphors", *Optical Materials*, Vol.42, pp 210-214, 2015.
- [2] Pawade V. B, and Dhoble S. J, "Blue emission in Eu^{2+} and Ce^{3+} activated novel aluminates based phosphors", *Journal of Luminescence*, Vol. 135, pp. 318-322, 2013.
- [3] Matsunaga T, Takeshita S, and Isobe T, "Synthesis, photoluminescence, and photostability of $\text{Y}_2\text{O}_3:\text{Bi}^{3+}$, Eu^{3+} nanosheets", *Journal of Luminescence*, Vol.165, pp.62-67, 2015.
- [4] Wei S, Yu L, Li F, Sun J, and Li S, "Photoluminescent properties of Eu^{3+} -doped alkaline earth metal molybdates red phosphors with high quenching concentration", *Ceramics International*, Vol. 41, pp.1093- 1100, 2015.
- [5] Yuan S, Yang Y, Fang B, Chen G, "Effects of Doping Ions on Afterglow Properties of $\text{Y}_2\text{O}_2\text{S}:\text{Eu}$ Phosphors", *Opt. Mater.*, Vol. 30, pp. 535- 538, 2007.

Transient Analysis of an M/M/1 Queue with Single Working Vacation and Variant Impatient Behavior

R.Sudhesh¹, A.Azhagappan²

¹*Department of Mathematics, BIT Campus, Anna University,
Tiruchirappalli, Tamilnadu, India.
Email id:sudheshanna@gmail.com*

²*Department of Mathematics, St. Anne's College of Engineering and Technology,
Panruti, Tamilnadu, India.
Email id:azhagappanmaths@gmail.com*

Abstract— This paper studies the transient analysis of an M/M/1 queue with single working vacation and customer's variant impatient behavior. In this model, we consider the system in which the customer under service never becomes impatient during working vacation. But only the customers waiting in queue, during working vacation, abandon the system due to impatience. We derive the time-dependent system size probabilities of the model under consideration explicitly using generating functions and continued fractions. Also the time-dependent mean and variance are deduced. Finally, some numerical illustrations are presented to visualize the analytical results.

Keywords- M/M/1 queue, single working vacations, Impatience, Continued fractions, modified Bessel function, Confluent hypergeometric functions.

I. INTRODUCTION

There are many practical situations like manufacturing industries, communication systems, etc. having wide applications related to queuing models with working vacation and impatient behavior of customers. During working vacation periods, the only arriving customers who find the server busy and wait for their service, become impatient due to the slow service of the server. But the arriving customers during working vacation periods who find the server free and get their service immediately, do not become impatient. This type of situation can be seen in reality as a customer receiving service never wants to abandon the system.

Servi and Finn [2] introduced the M/M/1 queuing model with working vacations where a customer is served at a lower rate instead of stopping the service completely. Later M/M/1 queue with single working vacation was studied by Tian et al. [5] in which the server finds no customer in the system, after the completion of working vacation, does not take another one but remains idle until the arrival of next customer. Sudhesh [3] derived the explicit expression for the time-dependent system size probabilities of an M/M/1 queuing model with system disasters and customer impatience using generating functions and continued fractions. Stationary solution of M/M/1 queuing model with working vacation and impatient customers was obtained by Yue et al. [6]. Sudhesh and Raj [4] investigated the stationary and transient solution for the M/M/1 queuing model with working vacation and also obtained the time-dependent solution of M/M/1 queuing model with exponential vacation.

Selvaraju and Cosmika Goswami [1] derived the steady-state solution for an M/M/1 queuing model with working vacation and customers impatient with an additional condition that the customer under service, during working vacation, never becomes impatient. But only the customers waiting in the queue during working vacation, abandon the system due to impatience. In the literature, so far no research work is carried out to derive the time-

dependent system size probabilities of an M/M/1 queuing model with single working vacation and variant impatient behavior of customers. This gives us the motivation to extend the research work of [1] from steady-state case into transient-state case in finding the system size probabilities.

The rest of the paper is partitioned as follows: In section 2, the time-dependent solution of M/M/1 queuing model with single working vacation and variant impatient customers are analyzed and derived. In section 3, the time-dependent mean and variance are deduced. In section 4, some numerical illustrations are presented to visualize the effect of the parameters. In section 5, this research work is concluded.

II. MODEL DESCRIPTION

Consider an M/M/1 queuing model with single working vacation and impatient customers. Arrival of customers follows Poisson process with rate λ and the service times follow exponential distribution with rate μ_1 . Whenever the system becomes empty, the server starts a working vacation. The service rate during working vacation period is μ_0 which is less than μ_1 . During working vacation, the arrivals become impatient due to the long wait when the server is busy. Upon arrival, an individual finds the system free, immediately starts getting service and does not become impatient. The server vacation time is exponential random variable with parameter γ .

Assume that inter-arrival times, service times during vacation, service times during busy period and vacation times are all independent. The service discipline is first come first served (FCFS). Customers become impatient during working vacation period. That is, each individual customer activates an independent impatience timer, exponentially distributed with parameter ξ such that the customer's service has not been completed before his timer expires; he abandons the system never to return.

Let $\{X(t), t \geq 0\}$ be the number of customers in the system at time t and $R(t)$ be the status of the server at time t , which is defined as follows:

$$R(t) = \begin{cases} 0, & \text{if the server is in single working vacation with service rate } \mu_0 \text{ at time } t, \\ 1, & \text{if the server is busy with service rate } \mu_1 \text{ at time } t. \end{cases}$$

Then $\{X(t), R(t); t \geq 0\}$ is a continuous time Markov process on the state space $S = \{0,0\} \cup \{0,1\} \cup \{n, r : n=1, 2, 3, \dots ; r = 0 \text{ or } 1\}$.

Let
$$P_{0,n}(t) = P\{X(t) = n, R(t) = 0\}; n = 0, 1, 2, \dots \text{ and}$$

$$P_{1,n}(t) = P\{X(t) = n, R(t) = 1\}; n = 0, 1, 2, \dots$$

The various transition rates of the process are

$$q_{(0,n),(0,n+1)} = q_{(1,n),(1,n+1)} = \lambda; q_{(0,n),(1,n)} = \gamma; n = 0, 1, 2, \dots$$

$$q_{(1,n+1),(1,n)} = \mu_1; q_{(0,n),(0,n-1)} = \mu_0 + (n-1)\xi; n = 1, 2, 3, \dots; q_{(1,1),(0,0)} = \mu_1.$$

Then $P_{j,k}(t), j = 0, 1; k = 0, 1, 2, \dots$ satisfy the forward Kolmogorov equations as follows:

$$P'_{0,0}(t) = -(\lambda + \gamma)P_{0,0}(t) + \mu_1 P_{1,1}(t) + \mu_0 P_{0,1}(t) \tag{2.1}$$

$$P'_{0,n}(t) = -(\lambda + \mu_0 + (n-1)\xi + \gamma)P_{0,n}(t) + \lambda P_{0,n-1}(t) + (\mu_0 + n\xi)P_{0,n+1}(t), n \geq 1 \tag{2.2}$$

$$P'_{1,0}(t) = -\lambda P_{1,0}(t) + \gamma P_{0,0}(t) \tag{2.3}$$

$$P'_{1,n}(t) = -(\lambda + \mu_1)P_{1,n}(t) + \lambda P_{1,n-1}(t) + \mu_1 P_{1,n+1}(t) + \gamma P_{0,n}(t), n \geq 1 \tag{2.4}$$

with $P_{0,0}(0) = 1$.

2.1 Transient solution

In this section, we derive the time-dependent system size probabilities of the model considered in terms of modified Bessel function and confluent hypergeometric functions using generating function and continued fractions. The following theorem express $P_{1,n}(t)$ in terms of $P_{0,n}(t)$ and $P_{1,0}(t)$, for $n = 1, 2, 3, \dots$

2.1.1. Theorem. The probabilities $P_{1,n}(t)$ are obtained, for $n = 1, 2, 3, \dots$ from (2.4) in terms of modified Bessel functions as

$$P_{1,n}(t) = \gamma \int_0^t e^{-(\lambda+\mu_1)(t-u)} \sum_{m=1}^{\infty} P_{0,m}(u) \beta^{n-m} [I_{n-m}(\alpha(t-u)) - I_{n+m}(\alpha(t-u))] du + \mu_1 \int_0^t e^{-(\lambda+\mu_1)(t-u)} P_{1,0}(u) \beta^{n+1} [I_{n-1}(\alpha(t-u)) - I_{n+1}(\alpha(t-u))] du \quad (2.5)$$

where $P_{1,0}(t)$ is obtained from (2.3) as

$$P_{1,0}(t) = \gamma \int_0^t P_{0,0}(u) e^{-\lambda(t-u)} du \quad (2.6)$$

where $I_n(t)$ is the modified Bessel function of the first kind of order n , $\alpha = 2\sqrt{\lambda\mu_1}$ and $\beta = \sqrt{\lambda/\mu_1}$.

Proof:

Define $Q(t, z) = \sum_{n=1}^{\infty} P_{1,n}(t) z^n$, $Q(0, z) = 0$.

From (2.4), we can obtain

$$\frac{\partial Q(t, z)}{\partial t} = \left[-(\lambda + \mu_1) + \lambda z + \frac{\mu_1}{z} \right] Q(t, z) + \mu_1 \left(1 - \frac{1}{z} \right) P_{1,0}(t) + \gamma \sum_{n=0}^{\infty} P_{0,n}(t) z^n. \quad (2.7)$$

Solving the above partial differential equation, we can get

$$Q(t, z) = \gamma \int_0^t \left[\sum_{m=0}^{\infty} P_{0,m}(u) z^m \right] e^{-(\lambda+\mu_1)(t-u)} e^{\left(\lambda z + \frac{\mu_1}{z}\right)(t-u)} du + \mu_1 \left(1 - \frac{1}{z} \right) \int_0^t P_{1,0}(u) e^{-(\lambda+\mu_1)(t-u)} e^{\left(\lambda z + \frac{\mu_1}{z}\right)(t-u)} du. \quad (2.8)$$

It is well known that, if $\alpha = 2\sqrt{\lambda\mu_1}$ and $\beta = \sqrt{\lambda/\mu_1}$, then

$$e^{\left(\lambda z + \frac{\mu_1}{z}\right)t} = \sum_{n=-\infty}^{\infty} (\beta z)^n I_n(\alpha t). \quad (2.9)$$

Using (2.9) in (2.8) and then comparing the coefficients of z^n on both sides, for $n = 1, 2, 3, \dots$, we obtain

$$P_{1,n}(t) = \gamma \int_0^t \sum_{m=0}^{\infty} P_{0,m}(u) \beta^{n-m} I_{n-m}(\alpha(t-u)) e^{-(\lambda+\mu_1)(t-u)} du$$

$$+ \mu_1 \int_0^t P_{1,0}(u) \beta^n [I_n(\alpha(t-u)) - \beta I_{n+1}(\alpha(t-u))] e^{-(\lambda+\mu_1)(t-u)} du. \quad (2.10)$$

The above holds for $n = -1, -2, -3, \dots$, with the left hand side replaced by zero. Using $I_{-n}(x) = I_n(x)$, for $n = 1, 2, 3, \dots$,

$$0 = \gamma \int_0^t \sum_{m=0}^{\infty} P_{0,m}(u) \beta^{-n-m} I_{n+m}(\alpha(t-u)) e^{-(\lambda+\mu_1)(t-u)} du + \mu_1 \int_0^t P_{1,0}(u) \beta^{-n} [I_n(\alpha(t-u)) - \beta I_{n-1}(\alpha(t-u))] e^{-(\lambda+\mu_1)(t-u)} du. \quad (2.11)$$

From (2.10) and (2.11), we obtain (2.5) for $n = 1, 2, 3, \dots$.

Evaluation of $P_{1,0}(t)$

Let $\hat{P}(s)$ denotes the Laplace transform of $P(t)$. Taking Laplace transforms of (2.3), we get

$$\hat{P}_{1,0}(s) = \frac{\gamma}{s + \lambda} \hat{P}_{0,0}(s).$$

On Laplace inversion, we get (2.6). Thus we have expressed $P_{1,n}(t)$ in terms of $P_{0,n}(t)$ and $P_{1,0}(t)$, for $n = 1, 2, 3, \dots$ and expressed $P_{1,0}(t)$ in terms of $P_{0,0}(t)$.

The following theorem express $P_{0,n}(t)$ in terms of $P_{0,0}(t)$, for $n = 1, 2, 3, \dots$ and express $P_{0,0}(t)$ explicitly.

2.1.2. Theorem. The probabilities $P_{0,n}(t)$, for $n = 1, 2, 3, \dots$ are obtained from (2.1) and (2.2) using continued fraction in terms of confluent hypergeometric function as

$$P_{0,n}(t) = V_n(t) * P_{0,0}(t) \quad (2.12)$$

where

$$P_{0,0}(t) = \sum_{k=0}^{\infty} \sum_{j=0}^k \sum_{i=0}^j \binom{k}{j} \binom{j}{i} \mu_0^i \lambda^{j-i} \gamma^{k-i} e^{-(\lambda+\gamma)t} \frac{t^k}{k!} * e^{-\lambda t} \frac{t^{j-i-1}}{(j-i-1)!} * V_1^i(t) * \frac{\lambda}{\beta^{j-i+1}} e^{-(\lambda+\mu_1)t} [I_{j-i-1}(\alpha t) - I_{j-i+1}(\alpha t)]^{*(j-i)} * \left[\sum_{m=0}^{\infty} \frac{\lambda}{\beta^{m+1}} e^{-(\lambda+\mu_1)t} [I_{m-1}(\alpha t) - I_{m+1}(\alpha t)] * V_m(t) \right]^{*(k-j)} \quad (2.13)$$

$$V_n(t) = \lambda^n \sum_{k=0}^{\infty} (-\lambda)^k \frac{\prod_{j=1}^k (\mu_0 + (n+j)\xi)}{\xi^k k!} a_{n+k}(t) * \sum_{i=1}^{\infty} \lambda^i b_i(t) \quad (2.14)$$

$$a_k(t) = \frac{1}{\xi^{2k-1} k!} \sum_{r=1}^k \prod_{j=1}^k (\mu_0 + j\xi) \frac{(-1)^{r-1}}{(r-1)!(k-r)!} e^{-(\gamma+\mu_0+r\xi)t}, \quad k = 1, 2, 3, \dots \quad (2.15)$$

$$b_k(t) = \sum_{i=1}^k (-1)^{i-1} a_i(t) * b_{k-i}(t), \quad k = 2, 3, 4, \dots; \quad b_1(t) = a_1(t) \quad (2.16)$$

where $*$ denotes the convolution and $*(k-r)$ denotes the $(k-r)$ -fold convolution.

Proof:

Taking Laplace transform on (2.1) and (2.2), we get, for $n = 1, 2, 3, \dots$

$$\hat{P}_{0,0}(s) = \frac{1}{(s + \lambda + \gamma) - \mu_1 \frac{\hat{P}_{1,1}(s)}{\hat{P}_{0,0}(s)} - \mu_0 \frac{\hat{P}_{0,1}(s)}{\hat{P}_{0,0}(s)}}. \tag{2.17}$$

$$\frac{\hat{P}_{0,n}(s)}{\hat{P}_{0,n-1}(s)} = \frac{\lambda}{(s + \lambda + \mu_0 + (n-1)\xi + \gamma) - (\mu_0 + n\xi) \frac{\hat{P}_{0,n+1}(s)}{\hat{P}_{0,n}(s)}}. \tag{2.18}$$

Solving (2.18) using the methodology given in [3], we obtain, for $n = 1, 2, 3, \dots$,

$$\hat{P}_{0,n}(s) = \left(\frac{\lambda}{\xi}\right)^n \frac{1}{\prod_{i=0}^{n-1} \left(\frac{s + \gamma + \mu_0}{\xi} + i\right)} \frac{{}_1F_1\left(\frac{\mu_0}{\xi} + n; \frac{s + \gamma + \mu_0}{\xi} + n; -\frac{\lambda}{\xi}\right)}{{}_1F_1\left(\frac{\mu_0}{\xi}; \frac{s + \gamma + \mu_0}{\xi}; -\frac{\lambda}{\xi}\right)} \hat{P}_{0,0}(s).$$

$$\hat{P}_{0,n}(s) = \hat{V}_n(s) \hat{P}_{0,0}(s). \tag{2.19}$$

On Laplace inversion, we get (2.12). Using (2.5) and (2.19), for $n = 1$, in (2.17) and after some mathematical manipulations, we obtain

$$\hat{P}_{0,0}(s) = \sum_{k=0}^{\infty} \sum_{i=0}^k \gamma^k \binom{k}{i} \left(\frac{\mu_0}{\gamma}\right)^i \frac{\hat{V}_1^i(s)}{(s + \lambda)^{k+1}} \left[\sum_{m=1}^{\infty} \left(\frac{p_1 - \sqrt{p_1^2 - \alpha^2}}{\alpha\beta}\right)^m \hat{V}_m(s) \right]^{k-i} \tag{2.20}$$

where $p_1 = s + \lambda + \mu_1$. On Laplace inversion, we get (2.13). From (2.19), we can obtain

$$\hat{V}_n(s) = \left(\frac{\lambda}{\xi}\right)^n \frac{1}{\prod_{i=0}^{n-1} \left(\frac{s + \gamma + \mu_0}{\xi} + i\right)} \frac{{}_1F_1\left(\frac{\mu_0}{\xi} + n; \frac{s + \gamma + \mu_0}{\xi} + n; -\frac{\lambda}{\xi}\right)}{{}_1F_1\left(\frac{\mu_0}{\xi}; \frac{s + \gamma + \mu_0}{\xi}; -\frac{\lambda}{\xi}\right)}. \tag{2.21}$$

Using the methodology given in [3], for $n = 1, 2, 3, \dots$, we obtain

$$\hat{V}_n(s) = \frac{\lambda^n}{\xi} \sum_{k=0}^{\infty} (-\lambda)^k \hat{a}_{n+k}(s) \sum_{r=0}^{\infty} \lambda^r \hat{b}_r(s). \tag{2.22}$$

On taking inverse Laplace transforms, we get (2.14), where

$$\hat{a}_k(s) = \frac{\xi^{-k}}{k!} \prod_{j=0}^{k-1} (\mu_0 + j\xi) \sum_{i=1}^k \frac{(-1)^{i-1}}{\xi^{k-1} (i-1)! (k-i)!} \frac{1}{s + \gamma + \mu_0 + (i-1)\xi}, \hat{a}_0(s) = 1, \tag{2.23}$$

for $k = 1, 2, 3, \dots$ $\hat{b}_0(s) = 1$,

$$\hat{b}_k(s) = \begin{vmatrix} \hat{a}_1(s) & 1 & 0 & \dots & 0 & 0 \\ \hat{a}_2(s) & \hat{a}_1(s) & 1 & \dots & 0 & 0 \\ \hat{a}_3(s) & \hat{a}_2(s) & \hat{a}_1(s) & \dots & 0 & 0 \\ \dots & \dots & \dots & \dots & \dots & \dots \\ \hat{a}_{k-1}(s) & \hat{a}_{k-2}(s) & \hat{a}_{k-3}(s) & \dots & \hat{a}_1(s) & 1 \\ \hat{a}_k(s) & \hat{a}_{k-1}(s) & \hat{a}_{k-2}(s) & \dots & \hat{a}_2(s) & \hat{a}_1(s) \end{vmatrix}$$

$$\hat{b}_k(s) = \sum_{i=1}^k (-1)^{i-1} \hat{a}_i(s) \hat{b}_{k-i}(s). \tag{2.24}$$

On Laplace inversion of (2.23) and (2.24), we get (2.15) and (2.16) respectively.

III. MOMENTS

In this section, we derive the time-dependent mean and variance of the number of customers in the system at time t.

3.1 Mean

Let $E(X(t))$ be the average number of customers in the system at time t.

$$E(X(t)) = \sum_{n=1}^{\infty} n(P_{0,n}(t) + P_{1,n}(t)), \quad E(X(0)) = 0.$$

From (2.2), (2.3) and (2.4), we obtain

$$\frac{d}{dt} E(X(t)) = \lambda - \mu_0 \sum_{n=1}^{\infty} P_{0,n}(t) - \xi \sum_{n=1}^{\infty} (n-1)P_{0,n}(t) - \mu_1 \sum_{n=1}^{\infty} P_{1,n}(t).$$

Integrating the above equation, we get

$$E(X(t)) = \lambda t - \mu_0 \sum_{n=1}^{\infty} \int_0^t P_{0,n}(u) du - \xi \sum_{n=1}^{\infty} (n-1) \int_0^t P_{0,n}(u) du - \mu_1 \sum_{n=1}^{\infty} \int_0^t P_{1,n}(u) du. \tag{3.1}$$

3.2 Variance

Let $Var(X(t))$ be the variance number of customers in the system at time t.

$$Var(X(t)) = E(X^2(t)) - (E(X(t)))^2$$

where

$$E(X^2(t)) = \sum_{n=1}^{\infty} n^2 (P_{0,n}(t) + P_{1,n}(t)).$$

From (2.2), (2.3) and (2.4), we obtain

$$\begin{aligned} \frac{d}{dt} E(X^2(t)) &= \lambda + 2\lambda E(X(t)) - \mu_0 \sum_{n=1}^{\infty} (2n-1)P_{0,n}(t) \\ &\quad - \xi \sum_{n=1}^{\infty} (2n^2 - 3n + 1)P_{0,n}(t) - \mu_1 \sum_{n=1}^{\infty} (2n-1)P_{1,n}(t). \end{aligned}$$

On Integration, we get

$$\begin{aligned} E(X^2(t)) &= \lambda t + 2\lambda \int_0^t E(X(u)) du - \mu_0 \sum_{n=1}^{\infty} (2n-1) \int_0^t P_{0,n}(u) du \\ &\quad - \xi \sum_{n=1}^{\infty} (2n^2 - 3n + 1) \int_0^t P_{0,n}(u) du - \mu_1 \sum_{n=1}^{\infty} (2n-1) \int_0^t P_{1,n}(u) du. \end{aligned} \tag{3.2}$$

where $P_{0,n}(t)$ and $P_{1,n}(t)$ are respectively given by (2.12) and (2.5).

IV. NUMERICAL ILLUSTRATIONS

In Fig. 2, the time-dependent system size probabilities are plotted for $\lambda = 1$; $\mu_0 = 1.25$; $\mu_1 = 1.5$ $\xi = 1.7$; $\gamma = 0.1$ and it is assumed that initially there is no customer in the system when the server is in vacation. The transient state system size probabilities are plotted for $\lambda = 1$; $\mu_0 = 1.25$; $\mu_1 = 1.5$ $\xi = 1.7$; $\gamma = 0.1$ in Fig. 3. It is observed that the probability curves except $P_{0,0}(t)$ in Fig. 2, increase initially and attain steady-state when the time t takes

larger values. In Fig. 3, the probability curves increase initially with the increment of time t and they reach a steady-state for large values of t . From Fig. 4 and Fig. 5, we can understand that whenever impatient rate ξ increases, the mean and variance number of customers in the system decreases.

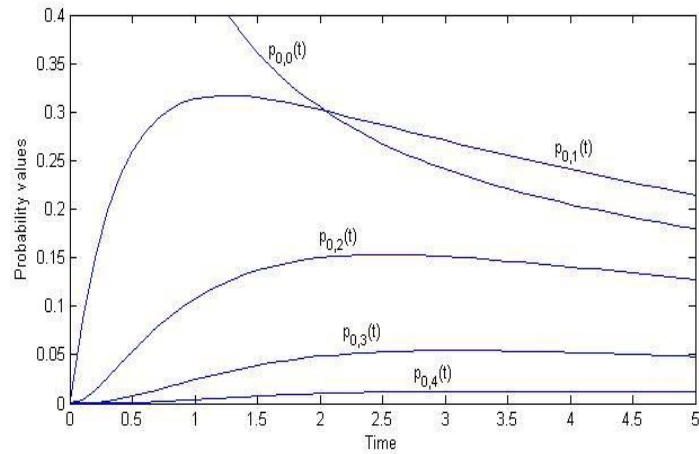


Fig.1 Transient system size probabilities

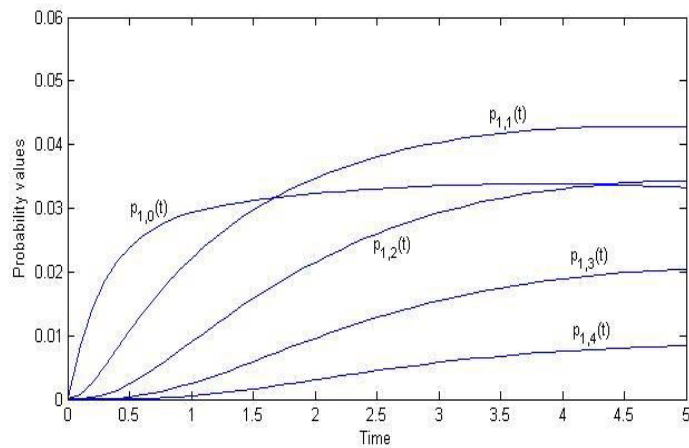


Fig.2 Transient system size probabilities

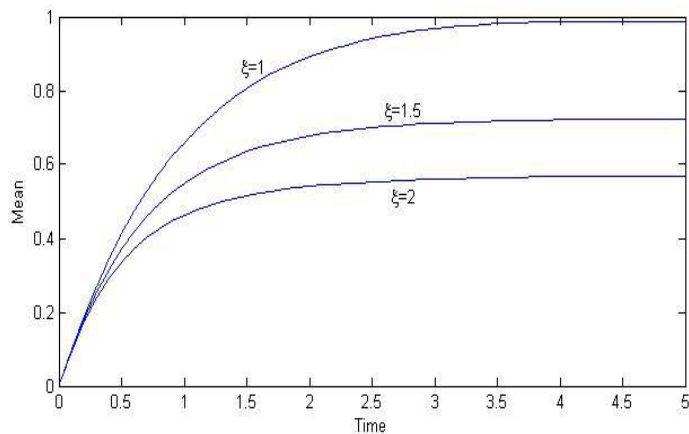


Fig.3 Mean number of customers for different values of ξ

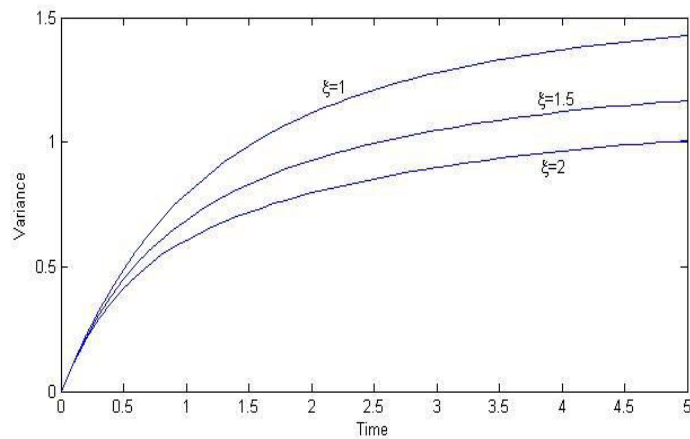


Fig.4 Variance number of customers for different values of ξ

V. CONCLUSION

In this paper, we have derived the time-dependent system size probabilities of an M/M/1 queuing model with single working vacation and customer's variant impatient behavior in terms of modified Bessel functions and confluent hypergeometric functions. Generating function and continued fractions are adapted to derive such solution. Time-dependent mean and variance are obtained and also the results are evaluated numerically.

REFERENCES

- [1] N. Selvaraju and Cosmika Goswami, "Impatient customers in an M/M/1 queue with single and multiple working vacations," *Computers and Industrial Engineering*, vol. 65, pp. 207-215, 2013.
- [2] L. D. Servi and S. G. Finn, "M/M/1 queue with working vacations (M/M/1/WV)," *Performance Evaluation*, vol. 50, pp. 41-52, 2002.
- [3] R. Sudhesh, "Transient analysis of a queue with system disasters and customer impatience," *Queueing Systems*, vol. 66, pp. 95-105, 2010.
- [4] R. Sudhesh and L. F. Raj, "Computational analysis of stationary and transient distribution of single server queue with working vacation," *Global Trends in Computing Communication Systems Communications in Computer and Information Sciences*, vol. 269, pp. 480-489, 2012.
- [5] Tian, Zhao and Wang, "The M/M/1 queue with single working vacation," *International Journal of Information and Management Science*, vol. 19, pp. 621-634, 2008.
- [6] D. Yue, W. Yue and G. Xu, "Analysis of a queuing system with impatient customers and working vacations," In *Proceedings of the 6th international conference on queuing theory and network applications*, 2011, pp. 208-211.

Various Display Technologies

V.Bala Murugan¹, A. John Peter²

¹*I-Year Mechanical Engineering, St.Anne's College of Engineering and Technology, Panruti*

²*Asst.Prof, Dept of Physics, St.Anne's College of Engineering and Technology, Panruti.*

Abstract—A lot has been invented from the past till now in regards with the display technologies. It gives an immense life to electronic device when good display technology are being used. Now a days displays are coming in various sizes for different portable devices like smart phones, tablets, smart watch, televisions, laptops etc. People are expecting better display no matter what device they use. In this paper I have given an overview of some of the past technologies to the technologies till now. Flat-panel displays use Liquid-crystal display (LCD) technology to make them much lighter and thinner when compared with a traditional monitor. A liquid crystal display consists of an array of tiny segments (called pixels) that can be manipulated to present information. Plasma panels, also called gas discharge displays, are constructed by filling the region between two glass plates with a mixture of gases that usually include neon. In LED, A matrix of diodes is arranged to form the pixel positions in the display, and picture definition is stored in refresh buffer. OLED (Organic Light Emitting Diode) technology relies on the organic materials.

Keywords— Display Technology; LCD; LED; Flexible display; Curved display;

I. INTRODUCTION

In today's smart world, people are carrying smart devices all over the places they visit. Wherever people are they are surrounded or accompanied by display devices, such as smart phones, tablets, notebooks and advertising screens. Different devices uses different display technologies to enrich devices facilities. Here in this paper, various popular display technologies has been explain in brief.

II. FLAT PANEL DISPLAY

Sometimes abbreviated as FPD, a flat-panel display is a thin screen display found on all portable computers and it was the new standard for desktop computers few year back. Instead of utilizing the cathode-ray tube technology, flat-panel displays use Liquid-crystal display (LCD) technology to make them much lighter and thinner when compared with a traditional monitor. The picture shows an example of flat-panel display. We can separate flat-panel displays into two categories: **emissive displays** and **nonemissive displays**. The emissive displays (or **emitters**) are devices that displays, and light-emitting diodes (LED) are examples of emissive displays. Nonemissive displays(or **nonemitters**) use optical effects to convert sunlight or light from some other source into graphics patterns. The most important example of a nonemissive flat-panel display is a liquid- crystal device (LCD).



III. LCD DISPLAY

LCDs are commonly used in systems, such as calculators and laptop computers. These non-emissive devices produce a picture by passing polarized light from the surrounding or from an internal light source through a liquid-crystal material that can be aligned to either block or transmit the light. A liquid crystal display consists of an array of tiny segments (called pixels) that can be manipulated to present information. The main advantage of LCD is size. There is no huge picture tube. The drawbacks with LCDs are viewing angle, contrast ratio, and response time.

IV. PLASMA DISPLAY

Plasma panels, also called **gas discharge displays**, are constructed by filling the region between two glass plates with a mixture of gases that usually include neon. A series of vertical conducting ribbons is placed on one glass panel, and a set of horizontal ribbons is built into the other glass panel. Firing voltages applied to a pair of horizontal and vertical conductors cause the gas at the intersection of the two conductors to break down into a glowing plasma of electrons and ions. Picture definition is stored in a refresh buffer, and the firing voltages are applied to refresh the pixel positions (at the intersections of the conductors) 60 times per second.

V. LED DISPLAY

In LED, A matrix of diodes is arranged to form the pixel positions in the display, and picture definition is stored in refresh buffer. As in scan-line refreshing of a CRT, information is read from the refresh buffer and converted to voltage levels that are applied to the diodes to produce the light patterns in the display.

5.1 ADVANTAGES:

- [1] Long Service Life
- [2] Good environmental performance
- [3] Low heat generation
- [4] Low Power
- [5] Many Color Choices

5.2 DISADVANTAGES:

- Sensitive to Voltage Spike
- Heat dissipation in some applications
- Not true full spectrum White LED (unless tri-color)

VI. OLED DISPLAY

OLED means Organic Light Emitting Diode. As the name indicates that it relies on organic materials. Organic Light Emitting Devices (OLED) emit light from active luminescent material in each display pixel. There are various type of OLED like PHOLED (phosphorescent OLED), TOLED (Transparent OLED), FOLED (Flexible OLED), WOLED (White OLED), AMOLED (Active matrix OLED). OLED's basic structure consists of organic materials positioned between the cathode and the anode, which is composed of electric conductive transparent Indium Tin Oxide (ITO). The organic materials compose a multi-layered thin film, which includes the Hole Transporting Layer (HTL), Emission Layer (EML) and the Electron Transporting Layer (ETL). By applying the appropriate electric voltage, holes and electrons are injected into the EML from the anode and the cathode, respectively. The holes and electrons combine inside the EML to form excitons, after which electroluminescence occurs. The transfer material, emission layer material and choice of electrode are the key factors that determine the quality of OLED components.

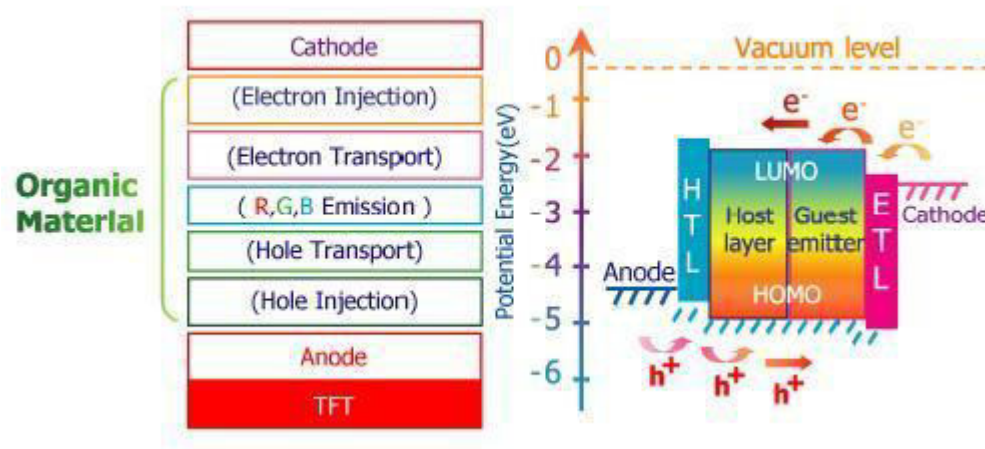


Fig.2 OLED Display Structure

6.1 ADVANTAGES

- Vibrant color
- High Contrast
- High Viewing angle
- Rapid Response Time
- Full motion videos
- Low Cost

VII. AMOLED DISPLAY

The full form of AMOLED is Active Matrix OLED. It has better display quality, thin form factor, and lower power consumption. In this display technology a very thin film has been used which was coated with several organic electroluminescent compounds. The whole technology is too dealt with the pixel quality of the displays. As of now this display technology has been implanted very successfully in small screens like in smart phones. This technology is not only very affordable, but also available with improved quality picture. In very near future AMOLED will be used for bigger screens. The active matrix OLED in AMOLED technology produces a light after it is properly electrically activated. It requires a continuous flow of electricity and that is controlled by two TFTs. The benefit of this technology over others is immense. AMOLED technology consumes lesser power and also the refresh rate is very high than other counterparts. The response time of touch displays developed using this technology is far better compared to others. In future it is going to be used notonly in portable electronics devices, but also in large screens such as more than 50 inches. Already several big names in the electronics world have started using an AMOLED including Samsung.

7.1 ADVANTAGE

- Wide Temperature operation
- Fast Response
- High and constant Gamut color

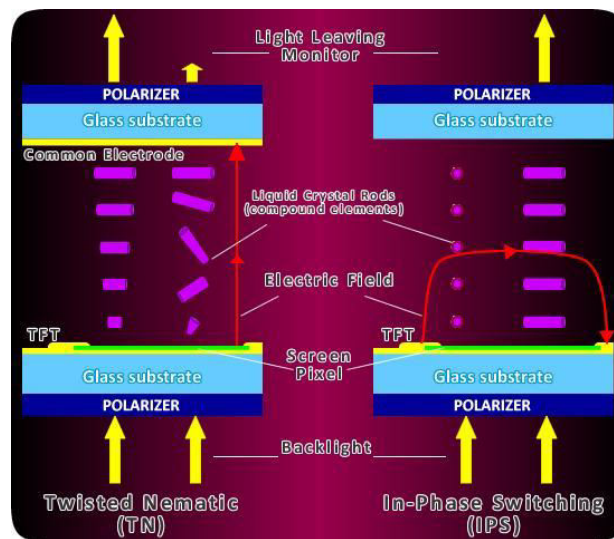
- Wide viewing angle
- Peak brightness
- Low power consumption
- Very slim design

VIII. FLEXIBLE DISPLAY

OLED is an emerging display technology that enables beautiful and efficient displays and lighting panels. Thin OLEDs are already being used in many mobile devices and TVs, and the next generation of these panels will be flexible and bendable. When we talk about flexible OLEDs, it's important to understand what that means exactly. A flexible OLED is based on a flexible substrate which can be either plastic, metal or flexible glass. The plastic and metal panels will be light, thin and very durable - in fact they will be virtually shatter-proof.

IX. IPS DISPLAY

The full form IPS is In-Plane Switching. It is a technology that addresses the two main issues of a standard twisted nematic (TN) TFT display: color and viewing angle. With IPS, the crystals are aligned horizontally to the screen rather than vertically, and the electrical field is applied between each end of the crystal molecules –termed a lateral electric field. In this way, the crystals are kept parallel to the electrode pair, and thus the glass substrate of the screen. The liquid crystal molecules are not anchored to the lower glass substrate, so move more freely into the desired alignment.



XI. CONCLUSIONS

In this paper various display technologies has been discussed from the past to till now. Each technology has some disadvantage and advantage which are discussed briefly. One can use the technology based on the necessity.

REFERENCES

- [1] <http://nptel.ac.in>
- [2] <http://www.udcoled.com>
- [3] <http://www.samsung.com>
- [4] J. Zmija, M.J. Malachowski, "Organic Light Emitting Diodes operation and application in displays", International Scientific Journal, 2009, Vol. 40.
- [5] Ramesh Raskar, Jeroen van Baar, Thomas Willwacher, Srinivas Rao, "Quadric Transfer for Immersive Curved Screen Displays", Eurographics, 2004, Vol. 2004

Photocatalytic disinfection of bacteria by nanocomposite ZnO-TiO₂ and detoxification of cyanide under visible light.

G. Abiramasundari^{*1}, S.Ramya¹, T.Natramiz raja venthan¹.
Department of Chemistry, St.Anne's college of engineering & technology
Mail ID.abiramasundarimphil@gmail.com

Abstract

ZnO-TiO₂ nanocomposite was prepared by modified ammonia evaporation-induced synthetic method. It was characterized by powder X-ray diffraction, transmission electron microscopy, selected area electron diffraction, and energy dispersive X-ray, UV-visible diffuse reflectance, photoluminescence and electrochemical impedance spectroscopies. Incorporation of ZnO leads to visible light absorption, larger charge transfer resistance and lower capacitance. The nanocomposite effectively catalyzes the inactivation of *E. coli* under visible light. Further, the prepared nanocomposite displays selective photocatalysis. While its photocatalytic efficiency to detoxify cyanide with visible light is higher than that of TiO₂ P25.

I. INTRODUCTION

TiO₂ is a photocatalytic material. TiO₂ rutile is activated by visible light itself but its photocatalytic activity is less than that of anatase TiO₂ which is excited by UV-A light [1,2]. Anatase blended with rutile exhibits larger photocatalytic activity. TiO₂ P25 Degussa is a blend of anatase (80%) and rutile (20%). It displays large photocatalytic activity due to synergistic effect between anatase and rutile phases. The charges produced in rutile phase under visible light are stabilized by rapid transfer of electron to anatase phase. Microbial contamination of surface water is a potential health hazard and inexpensive as well as easily adoptable method to disinfect bacteria is of interest. Solar water disinfection is a solution and the WHO' SODIS process requires about 6 h of bright sunlight. A possible alternative for point-of-use water disinfection is TiO₂-photocatalysis. But TiO₂ needs UV light to photocatalytically disinfect bacteria [3-5]. Here we report effective visible light-photocatalytic disinfection of bacteria by ZnO- TiO₂ nanocomposite. About 80% of *E. coli* at a population of 8×10^{14} CFU mL⁻¹ is killed in 30 min under natural sunlight. The precursor of the prepared nanocomposite is commercially available TiO₂ P25. Cyanide ion is highly toxic and is discharged as effluent by electroplating and metal finishing shops. Semiconductor-photo-catalysis is a promising method of cyanide detoxification and TiO₂ and ZnO are the photocatalysts reported under UV light [10-12]. There is no report on cyanide detoxification with visible light and interestingly the prepared ZnO-TiO₂ nanocomposite also catalyzes the cyanide oxidation under visible light. That is, ZnO-TiO₂ serves as a two-in-one material for cyanide detoxification and bacterial disinfection.

II. EXPERIMENTAL

A. ZnO-TiO₂ Nanocomposite

7.5%-ZnO-TiO₂ nanocomposite was obtained by modified ammonia-evaporation-induced synthetic method [13]. TiO₂ P25 gifted by Degussa was used as the precursor. Zn(NH₃)₄²⁺ complex cation was prepared in situ by the addition of ammonia to TiO₂ P25 under vigorous stirring to reach a pH of 10.4; the TiO₂ was suspended in required volume of millimolar Zn²⁺ solution. Formation of white coating over the TiO₂ nanocrystals indicated the

zinc(II) amine complex formation. Continuous stirring for 24 h ensured uniform coating. Evaporation to dryness resulted in the conversion of the complex to hydroxide as shown in Scheme 1. The composite nanoparticles were obtained by calcination for 4 h at 450 8C in a muffle furnace equipped with a PID temperature controller. The heating rate was 10 8C min⁻¹.

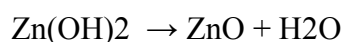
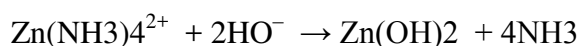
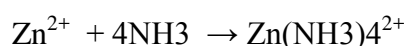
B. Characterization methods

The powder X-ray diffractogram (XRD) of the composite was obtained using a Bruker D8 system employing Cu K_α radiation of wavelength 1.5406 Å at a scan speed of 0.0508 s⁻¹ in a 2θ range of 5–75°. The energy dispersive X-ray (EDX) spectrum of the composite was recorded with a JEOL JSM-5610 scanning electron microscope (SEM) equipped with back electron (BE) detector and EDX. The sample was placed on an adhesive carbon slice supported on copper stubs and coated with 10 nm thick gold using JEOL JFC-1600 auto fine coater prior to measurement.

The transmission electron microscopic (TEM) images and the selected area electron diffraction (SAED) pattern were obtained with a Philips CM 20 TEM equipped with ORIUS CCD camera controller at an acceleration voltage of 200 kV. For the TEM image, the sample was prepared by depositing a methanol suspension of the composite on a carbon coated copper grid. The UV–visible diffuse reflectance spectrum (DRS) of the composite was recorded with a Cary 500 spectrophotometer. A PerkinElmer LS 55 fluorescence spectrometer was used to obtain the photoluminescence (PL) spectrum at room temperature. The nanocomposite was dispersed in carbon tetrachloride and the wavelength of excitation was 250 nm. A HP 4284A Precision LCR meter was used to obtain the electrochemical impedance spectra in air at room temperature over the frequency range of 1 MHz to 20 Hz. The disk area was 0.5024 cm² and the thicknesses of ZnO–TiO₂ and TiO₂ pellets were 2.78 and 2.94 mm, respectively.

C. Bacterial culture

MacConkey agar (Himedia) and nutrient broth (SRL) were used as received. 13.0 g of nutrient broth (5.0 g peptone, 5.0 g NaCl, 2.0 g yeast extract and 1.0 g beef extract) was dissolved in 1 L distilled water and sterilized in an autoclave at 121 8C to get a nutrient broth culture medium of pH 7.4. 55 g of MacConkey agar (20 g peptic digest of animal tissue, 10 g lactose, 5 g sodium taurocholate, 0.04 g neutral red and 20 g agar) was dissolved in 1 L boiling distilled water and also sterilized in an autoclave at 121 8C. This was poured into Petri dish to prepare MacConkey agar plates.



E. coli bacteria were inoculated in nutrient broth (10 mL) and incubated for 24 h at 37 8C. The grown culture (10 mL) was diluted to 100 mL with nutrient broth and used for the photocatalytic study. To count the colonies of E. coli in CFU mL⁻¹, the bacterial solution was successively diluted to 10⁸–10¹⁰ times with the nutrient broth. 10 mL of the diluted E. coli was streaked on the MacConkey agar plate using a loop and incubated at 37 8C for 24 h. The CFU was counted by a viable count method.

For visible light-photocatalysis, an immersion type photo-reactor with a 150 W tungsten halogen lamp fitted into a double walled borosilicate immersion well of 40 mm

outer diameter with inlet and outlet for water circulation was used. A 100 mL borosilicate immersion well of 50 mm outer diameter was employed as the reaction vessel. A photoreactor fitted with 8 W mercury lamps of wavelength 365 nm (Sankyo Denki, Japan) and a highly polished anodized aluminum reflector was used for the UV photocatalytic study. A borosilicate glass tube of 15 mm inner diameter was used as the reaction vessel and was placed at the centre of the reactor. The reactor was illuminated by four lamps fixed mutually at right angle. The heat generated was dissipated by the cooling fans fixed at the bottom of the reactor. The photon flux of the UV light (I) was determined by ferrioxalate actinometry.

Fresh solutions of *E. coli* or cyanide or the dyes of desired concentrations were prepared and used. Deionized distilled water was used throughout the experiments. The pK_a of HCN is 9.3 and to avoid its liberation into the atmosphere cyanide was dissolved in NaOH solution of pH 12.5. The volume of *E. coli* solution illuminated with tungsten lamp or sunlight was 50 mL, that of cyanide with tungsten lamp was 75 mL and those of the dyes with mercury lamps were 25 mL. After the addition of the catalyst to the *E. coli* or cyanide or dye solution, air was bubbled through the solution which kept the catalyst particles under suspension and at constant motion. An Elico dissolved oxygen analyzer PE 135 was employed to measure the dissolved oxygen. The catalyst was separated after the illumination. The leftover *E. coli* was determined by a viable count method, after proper dilution. The cyanide ion was estimated spectrophotometrically (590 nm) after complexing it with ninhydrin in alkaline medium [14].

III. RESULTS AND DISCUSSION

C. Characterization

Fig. 1 is the XRD of the prepared composite oxide. It displays the presence of both anatase and rutile phases of TiO_2 in the composite. The standard JCPDS patterns of anatase (00-021-1272 (*), body centered tetragonal, $a = b = 3.7852 \text{ \AA}$, $c = 9.5139 \text{ \AA}$, $a = b = c = 90.08$) and rutile (01-075-1750 (D), primitive tetragonal, $a = b = 4.5937 \text{ \AA}$, $c = 2.9587 \text{ \AA}$, $a = b = c = 90.08$) match with the observed XRD. Also, the XRD of the composite exhibits the presence of ZnO. The standard JCPDS pattern of zinc oxide (03-065-3411 (D), primitive hexagonal, $a = b = 3.2495 \text{ \AA}$, $c = 5.2069 \text{ \AA}$, $a = b = 90.08$, $g = 120.08$) agrees with the XRD. Further, the XRD shows the absence of zinc titanates, viz., hexagonal $ZnTiO_3$ (JCPDS 85-0547), cubic Zn_2TiO_4 (JCPDS 86-0155), and cubic $Zn_2Ti_3O_8$

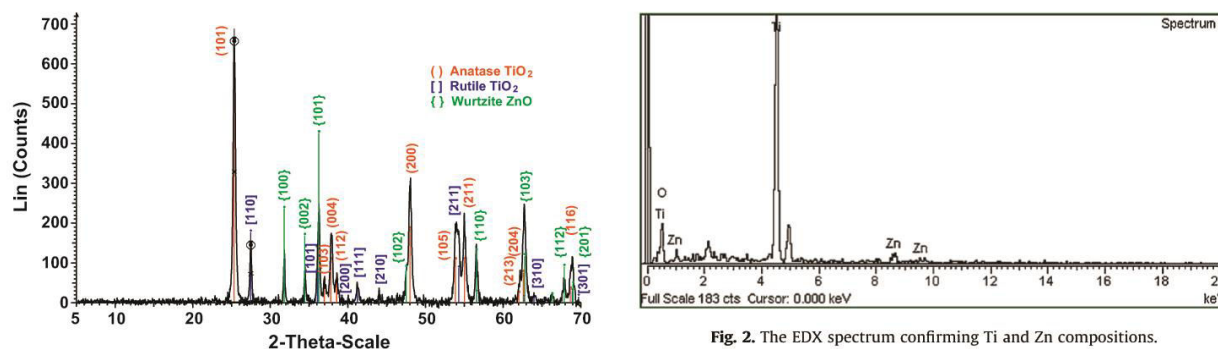


Fig. 2. The EDX spectrum confirming Ti and Zn compositions.

(JCPDS 73-0579), in the prepared composite oxide [15]. The phase percentages of anatase and rutile have been obtained from the integrated intensity of the peaks at 2θ value of 25.38 for anatase and 27.48 for rutile.

The percentage of anatase is given by $A (\%) = 100 / \{1 + 1.265(I_R/I_A)\}$, where I_A is the intensity of the anatase 101-peak at 2θ value of 25.38 and I_R is that of the rutile 110-peak at 2θ value of 27.48

(2u). The obtained phase composition of 78% anatase and 22% rutile is very close to that of the precursor TiO₂ P25. The phase composition of TiO₂ P25 deduced from its recorded powder XRD pattern (not shown) is 81% anatase and 19% rutile. The average crystallite sizes of the nanoparticles have been obtained from the half-width of the full maximum (HWM) of the most intense peaks of the composite oxide and TiO₂ P25 using the Scherrer equation, $D = 0.9\lambda/b \cos u$, where D is the average crystal size, λ is the X-ray wavelength, u is the Bragg angle and b is the HWM in 2u scale.

The specific surface areas of the nanocrystals have been deduced employing the relationship $S = 6/rD$, where S is the specific surface area and r is the material density. Table 1 displays the results. The mean crystallite size of ZnO–TiO₂ is slightly larger than its precursor and this may be due to the nanodeposition of ZnO on TiO₂ crystals. The slight increase in crystal size results in a small decrease of surface area. The EDX spectrum of the sample confirms the presence of Zn in the prepared composite. The counted percentage of Zn is 7.5 and is in agreement with the stoichiometry. Fig. 2 is the EDX spectrum of the composite. The TEM images at different magnifications of the composite are shown in Fig. 3. They confirm the nanoparticulate nature of the composite .

Average crystal size (D), surface area (S), ohmic (R_V) and charge-transfer resistances (R_{CT}), specific conductance (s), and capacitance (C).

The SAED pattern revealing anatase and rutile phases of TiO₂. Measured crystallite size agrees with that obtained by XRD. Further, the TEM images show hexagonal shape of the nanocrystals. At high magnification the lattice fringes are also observed. The SAED pattern of the composite is displayed in Fig. 4. It clearly reveals the presences of anatase and rutile phases of TiO₂.

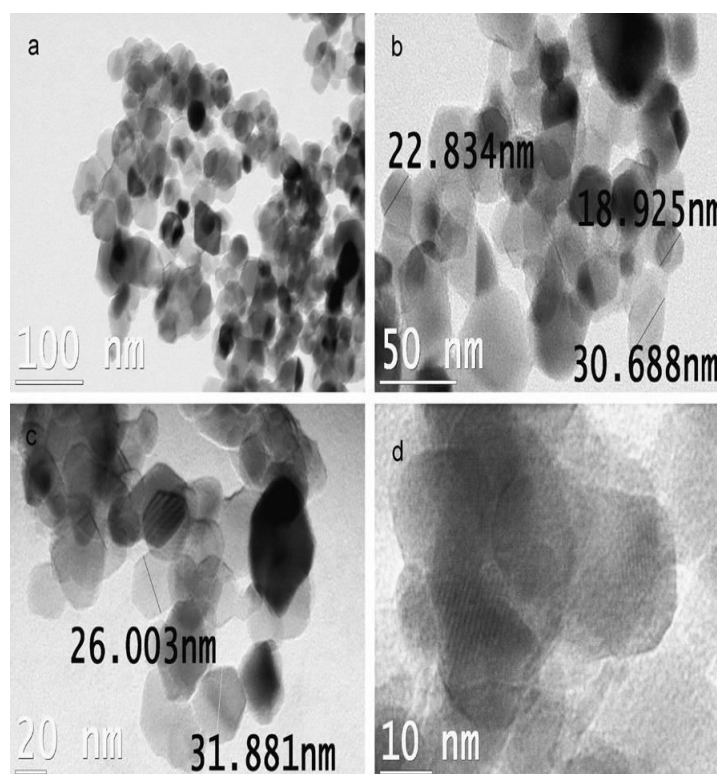


Fig. 3. TEM images at different magnifications showing the size and hexagonal shape of the nanocrystals

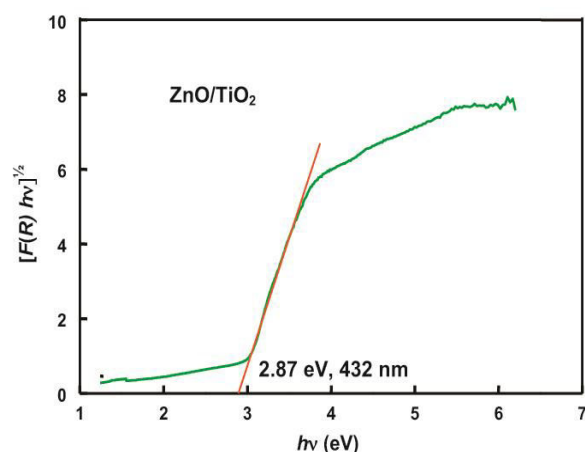
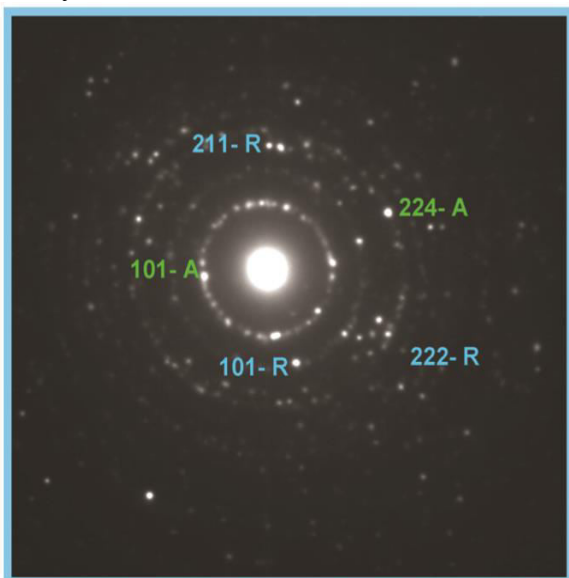


Fig. 6. The Tauc plot displaying indirect band gap.

Fig. 5 displays the DRS of the composite. The reflectance results are presented as $F(R)$. The $F(R)$ values have been obtained by the application of Kubelka–Munk algorithm. The band gap of the composite has been deduced from the Tauc plot. The plot of $[F(R)hv]^{1/2}$ versus photon energy is shown in Fig. 6. The extrapolation of $[F(R)hv]^{1/2}$ to the abscissa at zero $F(R)$ affords the band gap energy as 2.87 eV. This corresponds to an absorption edge of 432 nm. The results fit more satisfactorily the $[F(R)hv]^{1/2}$ versus photon energy plot than the $[F(R)hv]^2$ versus photon energy plot indicating a strong indirect band gap transition.

The electrical properties of a semiconductor could be inferred by fitting the EIS data to a model or an equivalent circuit. The EIS of ZnO–TiO₂ and TiO₂ P25 show decrease of impedance with increase of frequency indicating the capacitance of the oxides studied. Nyquist plot is a popular format of evaluating the impedance data and Fig. 7 displays the same. The semicircular Nyquist plot is the expected response of the simple circuit [16]. The ohmic or uncompensated resistance (R_V) refers to the grain boundary or intergranular resistance and the polarization or electron-transfer (charge-transfer) resistance (R_P or R_{CT}) corresponds to the intragranular or bulk crystal resistance. The R_{CT} is related to the resistance to mass transfer which is known as Warburg resistance. It is controlled by the specific conductance, s . The constant phase element (CPE) is associated with a non-uniform distribution of current due to material heterogeneity and is equivalent to a double layer capacitance (C). Although ZnO–TiO₂ is a composite, its Nyquist plot is a single semicircle indicating the electrical non-heterogeneity of the composite. This determined specific conductance, capacitance, and ohmic and charge-transfer resistances of ZnO–TiO₂ and TiO₂ P25 are displayed in Table 1. The specific conductance has been deduced from the measured charge-transfer resistance and the capacitance has been deduced using the equations $v_{max} = 1/CR_{CT}$ and $= 2\pi f$, where f is the frequency corresponding to the maximum of the semicircular Nyquist plot. Table 1 shows that nanodeposition of ZnO on TiO₂ decreases the specific conductance and capacitance.

D. Disinfection of *E. coli* under visible light.

The temporal profiles of photocatalytic disinfection of *E. coli* by ZnO–TiO₂ under tungsten lamp illumination and also under natural AM1 sunlight are shown in Fig. 8. The corresponding profiles of TiO₂ P25 are also displayed for comparison. Inactivation of *E. coli* by ZnO–TiO₂ in dark is negligible compared to the photocatalytic inactivation. The temporal profiles of *E. coli* inactivation by photolysis (without catalyst) are also shown in Fig. 10. The disinfection with natural sunlight was done under identical solar irradiance by performing the experiments simultaneously, side by side, in summer. The solar irradiance was monitored using a Daystar solar meter (USA).

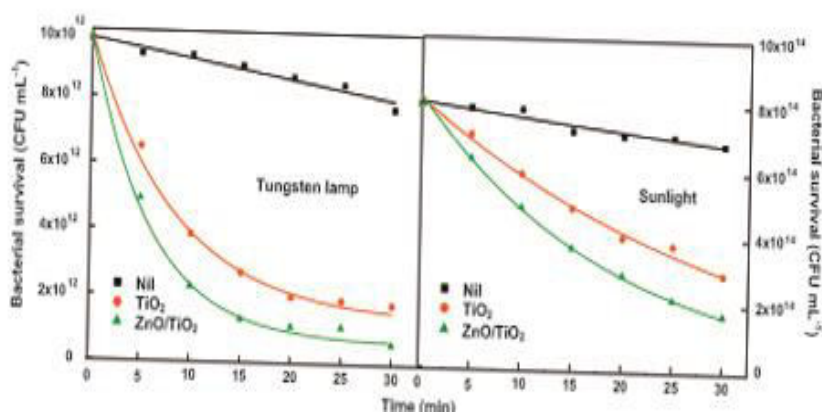
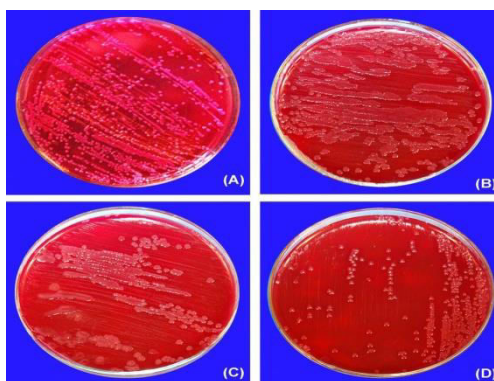


Fig. 8 Temporal profile of *E. coli* disinfection. Catalyst loading = 0.020 g, pH = 7.1, *E. coli* solution = 50 mL, airflow rate = 7.8 mL s⁻¹, [O₂]_{dissolved} = 2.6 mg L⁻¹. Tungsten lamp illumination: light intensity = 1650 W m⁻²; natural sunlight: solar irradiance = 1000 W m⁻²; illumination cross-section = 11.43 cm Fig. 9 Photographs of disinfection of *E. coli* (under 10⁸-times dilution). (A) Prior to illumination (B) Photolysis (no catalyst) (C) TiO₂ (D) ZnO–TiO₂.



E. coli grown in a nutrient broth culture medium were used for the evaluation of the bactericidal activity. The cell population was determined by a viable count method on MacConkey agar plates, after proper dilution of the culture. The displayed temporal profiles clearly demonstrate the effective photocatalytic disinfection of *E. coli* by ZnO–TiO₂ under visible light. The photographs of disinfection of *E. coli* are presented in Fig. 9 A possible explanation for the observed high photocatalytic bactericidal efficiency of ZnO–TiO₂, compared to the N- or N, S-doped TiO₂ [6-9], is the effective binding of ZnO–TiO₂ with *E. coli*. Zinc(II) is more susceptible to coordination with proteins than Fig. 10. Temporal profile of cyanide detoxification under visible light. Catalyst loading = 0.025 g, pH = 12.5, cyanide solution = 75 mL, airflow rate = 7.8 mL s⁻¹, [O₂]_{dissolved} = 28.6 mg L⁻¹, light intensity = 1650

W m².nitrogen or sulfur. Effective attachment of the nanocrystals on E. coli will lead to efficient flow of HO radicals from the illuminated semiconductor to E. coli. The detailed mechanism of photocatalytic inactivation of E. coli has been discussed elsewhere [17]. The EIS results reveal that the photocatalytic efficiency of ZnO–TiO₂ to inactivate E. coli is not determined by charge-transfer resistance, specific conductance and capacitance of the composite.

E. Cyanide detoxification under visible light

Fig. 11 is the time-profile of cyanide detoxification with ZnO– TiO₂ and TiO₂ P25 under illumination by tungsten lamp. The temporal profiles show the larger photocatalytic efficiency of the composite to oxidize cyanide under visible light. The adsorption of cyanide on the composite in dark under the experimental conditions is insignificant. Hence the prepared ZnO–TiO₂ composite is a two-in-one material, efficiently disinfects bacteria and also detoxifies cyanide under visible light. The mechanism of photo-catalytic oxidation of cyanide has been discussed elsewhere [12]

IV. CONCLUSIONS

ZnO–TiO₂ nanocomposite was obtained by modified ammonia-evaporation-induced synthetic method and calcined at 450 8C. It catalyzes effectively the inactivation of E. coli and detoxification of cyanide under visible light. The composite has been characterized by XRD, EDS, TEM, SAED, UV-visible DRS, PL, and EIS. Nanodeposition of ZnO on TiO₂ shifts the optical absorption edge to the visible region but increases the intragranular resistance and decreases the capacitance. The composite is selective in photocatalysis.

V. REFERENCES

- [1] D.C.Hurum, A.G. Agrios, K.A.Gray, T.Rajh, M.C.Thurnauer, J.Phys.Chem.B107(2003)4545–4548.
- [2] A.Sclafani, J.M.Herrmann, J.Phys.Chem.100 (1996) 13655–13661
- [4] R.van Grieken, J.Marugan, C.Sordo, C.Pablos, Catal. Today 144 (2009) 48–54.
- [5] D.M.A.Alrousan, P.S.M.Dunlop, T.A.McMurray, J.A.Byrne, Water Res. 43 (2009) 47–54.
- [6] K.L.Yeung, W.K. Leung, N.Yao, S.Cao, Catal.Today 143 (2009) 218–224.
- [7] A.Rengifo-Herrera, K.Pierzchala, A.Sienkiewicz, L.Forro, J.Kiwi, C.Pulgarin, J.Phys.Chem.C114 (2010) 2717–2723.
- [8] J.A.Rengifo-Herrera, K.Pierzchala, A.Sienkiewicz, L.Forro, J.Kiwi, C.Pulgarin, Appl.Catal.B88(2009) 398–406.
- [9] J.A.Rengifo-Herrera, E.Mielczarski, J.Mielczarski, N.C.Castillo, C.Pulgarin, Appl.Catal.B84(2008) 448–456.
- [10] Y.Liu, J.Li, X.Qiu, C.Burda, J.Photochem.Photobiol.A190(2007)94–100.
- [11] J.Marugan, R.vanGrieken, A.E.Cassano, O.M.Alfano, Catal.Today144(2009)87–93.
- [12] J.Marugan, R.vanGrieken, A.E.Cassano, O.M.Alfano, Appl.Catal.B 85(2008)48–60.
- [13] C.Karunakaran, in: S.Kaneco (Ed.), Photo/Electrochemistry & Photobiology in the Environment, Energy and Fuel, Research Signpost, Trivandrum, 2006, pp. 259– 294.
- [14] Y.Li, B.Tan, Y.Wu, Chem.Mater.20 (2008)567–576.
- [15] P.Nagaraja, M.S.Hemanthakumar, H.S.Yathirajan, J.S.Prakash, Anal.Sci. 18 (2002) 1027–1030.
- [16] Z.Liu, D.Zhou, S.Gong, H.Li, J.Alloys Compd. 475(2009)840–845.
- [17] C.C.Lin, Y.Y.Li, Mater.Chem.Phys.113(2009)334–337.

Transient Analysis of M/M/1 Queue with Server Vacation, Impatient Customers and a Waiting Server Timer

R.Sudhesh¹, A.Azhagappan²

¹*Department of Mathematics, BIT Campus, Anna University,
Tiruchirappalli, Tamilnadu, India.
Email id:sudheshanna@gmail.com*

²*Department of Mathematics, St. Anne's College of Engineering and Technology,
Panruti, Tamilnadu, India.
Email id:azhagappanmaths@gmail.com*

Abstract— In this paper, an M/M/1 queuing model with server vacation and impatient customers is considered in which the server activates a timer T whenever he returns from his vacation to an empty system and waits idle. This type of situation occurs most commonly in many real life situations as a human behavior. The time-dependent system size probabilities are derived explicitly in terms of modified Bessel functions and confluent hypergeometric functions. Also the time-dependent mean and variance are obtained analytically. Finally, some numerical illustrations are presented.

Keywords- M/M/1 queue, server vacation, impatient customers, waiting server timer, Continued fraction, modified Bessel function, Confluent hypergeometric functions.

I. INTRODUCTION

During the last two decades, many researchers carried out works related to queuing systems with server vacations and related to customers' impatience. Customers arrive according to a Poisson process and are served according to an exponential distribution. Whenever the system becomes empty, the server takes vacation. After returning from vacation to an empty system, the server waits dormant and activates a timer T . If an arrival occurs before T expires, the server starts an exhaustive busy period and then takes another vacation. On the other hand, if T expires before an arrival to the empty system, the server starts another vacation immediately after T expires. If T is assumed as zero, then it is reduced to multiple vacation model. If it is assumed that T is infinite, then this is reduced to single vacation model. This is the cause that this policy is called the more general vacation policy.

Customers become impatient due to the long wait in the queue when the server is unavailable. The vacation queuing models are introduced by Doshi [4] in which he discussed many practical problems related to different vacation policies such as multiple vacation, single vacation, system breakdown, etc. He also analyzed the stochastic decomposition property of some single server models. The concept of server vacation with a waiting server timer was first introduced by Boxma et al. [3] in which they discussed a more general vacation policy that generalized the two different vacation policies such as multiple vacation policy and single vacation policy.

Altman and Yechiali [1] analyzed the impatience behavior of some single server queuing models such as M/M/1, M/G/1 queues and the multi-server M/M/c queue, for both multiple and single vacation policies. They also derived that the proportion of customer abandonments in single vacation model is smaller than that of multiple vacation model. Sudhesh [6] derived time-dependent system size probabilities for the M/M/1 queue with system disasters and customer impatience using generating functions and continued fractions. Kalidass and Ramanath [5] derived explicit expressions for the time-dependent as well as its

corresponding steady-state probabilities of the M/M/1 queue with multiple vacations. Ammar [2] obtained the time-dependent probabilities for the impatient behavior of M/M/1 queuing model with multiple vacation where the impatience of customers is due to the absence of the server upon arrival and also obtained the time-dependent mean and variance of the system.

In the literature, so far no research work is carried out to obtain the time-dependent solution of M/M/1 queue with server vacation, impatient customers and a waiting server timer. This gives us the motivation to carry out this research work. In the next section, the transient behavior of an M/M/1 queuing model with server vacation, customers impatient and a waiting server timer is analyzed and the time-dependent solution is expressed in terms of the modified Bessel functions and confluent hypergeometric functions. In section 3, the time-dependent mean and variance of this model is obtained. In section 4, some numerical illustrations are presented to visualize the analytical results. In section 5, this research work is concluded with future directions.

II. MODEL DESCRIPTION

Consider an M/M/1 queuing model with server vacation, customers impatient and a waiting server timer. Customers arrive according to the Poisson process with rate λ and the service times are exponentially distributed with rate μ . The server starts a vacation whenever the system leads to empty state. The server vacation time follows exponential distribution with parameter γ . In our vacation scheme, upon returning from vacation finding the system empty, the server waits idle and activates a timer T which follows exponential distribution with parameter η . If the inter arrival time is shorter than the timer T, the server starts an exhaustive busy period and then takes another vacation. If the timer T is shorter than the inter arrival time, the server takes another vacation immediately after T expires.

During the vacation period, customers become impatient. That is, each individual customer activates an independent impatient timer which follows exponential distribution, with a parameter ξ . If the customer's service has not been completed before his timer expires, he abandons the system and never returns. Assume that inter-arrival times, service times, server waiting times, customers' impatient times and vacation times are all independent. The service discipline is first come first served (FCFS).

Let $\{X(t), t \geq 0\}$ be the number of customers in the system and $J(t)$ be the status of the server at time t, which is defined as follows:

$$J(t) = \begin{cases} 0, & \text{if the server is in vacation at time } t, \\ 1, & \text{if the server is busy at time } t. \end{cases}$$

Then $\{X(t), J(t); t \geq 0\}$ is a continuous time Markov process on the state space $S = \{n, j : n = 0, 1, 2, \dots; j = 0 \text{ or } 1\}$.

Let $P_{0,n}(t) = P\{X(t) = n, J(t) = 0; n = 0, 1, 2, \dots\}$ and

$$P_{1,n}(t) = P\{X(t) = n, J(t) = 1; n = 0, 1, 2, \dots\}.$$

The various transition rates of the process are

$$\begin{aligned} q_{(0,n),(0,n+1)} = q_{(1,n),(1,n+1)} &= \lambda; q_{(0,n),(1,n)} = \gamma; n = 0, 1, 2, \dots \\ q_{(1,n),(1,n-1)} &= \mu; q_{(0,n),(0,n-1)} = n\xi; n = 1, 2, 3, \dots; q_{(1,0),(0,0)} = \eta. \end{aligned}$$

Then $P_{i,j}(t), i = 0, 1; j = 0, 1, 2, \dots$ satisfy the Kolmogorov equations as follows:

$$P'_{1,0}(t) = -(\lambda + \eta)P_{1,0}(t) + \mu P_{1,1}(t) + \gamma P_{0,0}(t) \tag{2.1}$$

$$P'_{1,n}(t) = -(\lambda + \eta)P_{1,n}(t) + \lambda P_{1,n-1}(t) + \mu P_{1,n+1}(t) + \gamma P_{0,n}(t), n \geq 1 \tag{2.2}$$

$$P'_{0,0}(t) = -(\lambda + \gamma)P_{0,0}(t) + \eta P_{1,0}(t) + \xi P_{0,1}(t) \tag{2.3}$$

$$P'_{0,n}(t) = -(\lambda + \gamma + n\xi)P_{0,n}(t) + \lambda P_{0,n-1}(t) + (n+1)\xi P_{0,n+1}(t), \quad n \geq 1 \tag{2.4}$$

with $P_{0,0}(0) = 1$.

2.1. Transient solution

In this section, we derive the time-dependent system size probabilities of the model considered in terms of modified Bessel function and confluent hypergeometric function using generating functions and continued fractions. The following theorem express $P_{1,n}(t)$ in terms of $P_{0,n}(t)$, for $n = 1, 2, 3, \dots$

2.1.1. Theorem. The expression $P_{1,n}(t)$, for $n = 1, 2, 3, \dots$ is obtained from (2.1) and (2.2) in terms of modified Bessel functions as

$$P_{1,n}(t) = \gamma \int_0^t \sum_{m=1}^{\infty} P_{0,m}(u) \beta^{n-m} [I_{n-m}(\alpha(t-u)) - I_{n+m}(\alpha(t-u))] e^{-(\lambda+\mu)(t-u)} du \tag{2.5}$$

where $I_n(t)$ is the modified Bessel function of the first kind of order n, $\alpha = 2\sqrt{\lambda\mu}$ and $\beta = \sqrt{\lambda/\mu}$.

Proof:

Define $P(z, t) = \sum_{n=1}^{\infty} P_{1,n}(t) z^n$, $P(z, 0) = 0$.

From (2.1) and (2.2),

$$\frac{\partial P(z, t)}{\partial t} = \left[-(\lambda + \mu) + \lambda z + \frac{\mu}{z} \right] P(z, t) + \gamma \sum_{n=1}^{\infty} P_{0,n}(t) z^n - \mu P_{1,1}(t). \tag{2.6}$$

Solving the above partial differential equation, we can get

$$P(z, t) = \gamma \int_0^t \left[\sum_{m=1}^{\infty} P_{0,m}(u) z^m \right] e^{-(\lambda+\mu)(t-u)} e^{\left(\lambda z + \frac{\mu}{z}\right)(t-u)} du - \mu \int_0^t P_{1,1}(u) e^{-(\lambda+\mu)(t-u)} e^{\left(\lambda z + \frac{\mu}{z}\right)(t-u)} du. \tag{2.7}$$

It is well known that, if $\alpha = 2\sqrt{\lambda\mu}$ and $\beta = \sqrt{\lambda/\mu}$, then

$$e^{\left(\lambda z + \frac{\mu}{z}\right)t} = \sum_{n=-\infty}^{\infty} (\beta z)^n I_n(\alpha t),$$

where $I_n(t)$ is the modified Bessel function of the first kind of order n.

Comparing the coefficients of z^n on both sides of (2.7) for $n \geq 1$, we get

$$P_{1,n}(t) = \gamma \int_0^t \sum_{m=1}^{\infty} P_{0,m}(u) \beta^{n-m} I_{n-m}(\alpha(t-u)) e^{-(\lambda+\mu)(t-u)} du - \mu \int_0^t P_{1,1}(u) \beta^n I_n(\alpha(t-u)) e^{-(\lambda+\mu)(t-u)} du. \tag{2.8}$$

The above holds for $n = -1, -2, -3, \dots$, with the left hand side replaced by zero. Using $I_{-n}(x) = I_n(x)$, for $n = 1, 2, 3, \dots$,

$$0 = \gamma \int_0^t \sum_{m=1}^{\infty} P_{0,m}(u) \beta^{-n-m} I_{n+m}(\alpha(t-u)) e^{-(\lambda+\mu)(t-u)} du - \mu \int_0^t P_{1,1}(u) \beta^{-n} I_n(\alpha(t-u)) e^{-(\lambda+\mu)(t-u)} du. \tag{2.9}$$

Subtracting (2.9) from (2.8), we obtain (2.5) for $n = 1, 2, 3, \dots$

Thus we have expressed $P_{1,n}(t)$ in terms of $P_{0,n}(t)$, for $n = 1, 2, 3, \dots$

The following theorem expresses $P_{0,n}(t)$ as well as $P_{1,0}(t)$ in terms of $P_{0,0}(t)$ and $P_{0,0}(t)$ is obtained explicitly.

2.1.2. Theorem. The expression $P_{0,n}(t)$ is obtained from (2.3) and (2.4) using continued fraction in terms of confluent hypergeometric function as

$$P_{0,n}(t) = R_n(t) * P_{0,0}(t) \tag{2.10}$$

where

$$P_{0,0}(t) = \sum_{k=0}^{\infty} \sum_{r=0}^k \binom{k}{r} (\eta\gamma)^k \left(\frac{\xi}{\eta\gamma}\right)^r e^{-(\lambda+\gamma)t} \frac{t^k}{k!} * e^{-(\lambda+\eta)t} \frac{t^{k-r-1}}{(k-r-1)!} * R_1^r(t) * \left[\delta(t) + \sum_{m=1}^{\infty} \frac{\lambda}{\beta^{1+m}} [I_{m-1}(\alpha t) - I_{m+1}(\alpha t)] e^{-(\lambda+\mu)t} * R_m(t) \right]^{*(k-r)} \tag{2.11}$$

$$R_n(t) = \lambda^n \sum_{k=0}^{\infty} (-\lambda)^k \binom{n+k}{k} a_{n+k}(t) * \sum_{i=1}^{\infty} \lambda^i b_i(t) \tag{2.12}$$

$$a_k(t) = \frac{1}{\xi^{k-1}} \sum_{r=1}^k \frac{(-1)^{r-1}}{(r-1)!(k-r)!} e^{-(\gamma+r\xi)t}, \quad k = 1, 2, 3, \dots \tag{2.13}$$

$$b_k(t) = \sum_{i=1}^k (-1)^{i-1} a_i(t) * b_{k-i}(t), \quad k = 2, 3, 4, \dots; \quad b_1(t) = a_1(t) \tag{2.14}$$

where $*$ denotes the convolution and $*(k-r)$ denotes the $(k-r)$ -fold convolution.

Proof:

Let $\hat{P}_{0,n}(s)$ be the Laplace transform of $P_{0,n}(t)$.

Taking Laplace transform on (2.4), we get for $n = 1, 2, 3, \dots$

$$\frac{\hat{P}_{0,n}(s)}{\hat{P}_{0,n-1}(s)} = \frac{\lambda}{(s + \lambda + \gamma + n\xi) - (n+1)\xi \frac{\hat{P}_{0,n+1}(s)}{\hat{P}_{0,n}(s)}}. \tag{2.15}$$

Using an identity of confluent hypergeometric function, for $n = 1, 2, 3, \dots$, the above equation can be written as

$$\frac{\hat{P}_{0,n}(s)}{\hat{P}_{0,n-1}(s)} = \frac{\lambda}{\xi} \frac{1}{\left(\frac{s+\gamma}{\xi} + n\right)} \frac{{}_1F_1\left(n+1; \frac{s+\gamma}{\xi} + n+1; -\frac{\lambda}{\xi}\right)}{{}_1F_1\left(n; \frac{s+\gamma}{\xi} + n; -\frac{\lambda}{\xi}\right)}. \tag{2.16}$$

Iterating the above equation for $n = 1, 2, 3, \dots$,

$$\hat{P}_{0,n}(s) = \left(\frac{\lambda}{\xi}\right)^n \frac{1}{\prod_{i=1}^n \left(\frac{s+\gamma}{\xi} + i\right)} \frac{{}_1F_1\left(n+1; \frac{s+\gamma}{\xi} + n+1; -\frac{\lambda}{\xi}\right)}{{}_1F_1\left(1; \frac{s+\gamma}{\xi} + 1; -\frac{\lambda}{\xi}\right)} \hat{P}_{0,0}(s). \quad (2.17)$$

$$\hat{P}_{0,n}(s) = \hat{R}_n(s) \hat{P}_{0,0}(s). \quad (2.18)$$

On Laplace inversion, we get (2.10).

The expression for $R_n(t)$ given in (2.12) is obtained using the methodology applied in [6] and it is the same as that of (A.4) in [6].

Evaluation of $P_{1,0}(t)$

Taking Laplace transform on (2.1), we get

$$\hat{P}_{1,0}(s) = \frac{\mu}{(s+\lambda+\eta)} \hat{P}_{1,1}(s) + \frac{\gamma}{(s+\lambda+\eta)} \hat{P}_{0,0}(s). \quad (2.19)$$

Using (2.5), for $n=1$, in (2.19), we get

$$\hat{P}_{1,0}(s) = \frac{\gamma \hat{P}_{0,0}(s)}{(s+\lambda+\eta)} \left[1 + \sum_{m=1}^{\infty} \hat{R}_m(s) \left(\frac{p - \sqrt{p^2 - \alpha^2}}{\alpha\beta} \right)^m \right]. \quad (2.20)$$

On Laplace inversion, we get

$$P_{1,0}(t) = \gamma e^{-(\lambda+\eta)t} * P_{0,0}(t) * \left[\delta(t) + \sum_{m=1}^{\infty} \frac{\lambda}{\beta^{1+m}} [I_{m-1}(\alpha t) - I_{m+1}(\alpha t)] e^{-(\lambda+\mu)t} * R_m(t) \right]^{*(k-r)}. \quad (2.21)$$

Evaluation of $P_{0,0}(t)$

Laplace transform on (2.3) yields

$$\hat{P}_{0,0}(s) = \frac{1}{(s+\lambda+\gamma) - \eta \frac{\hat{P}_{1,0}(s)}{\hat{P}_{0,0}(s)} - \xi \frac{\hat{P}_{0,1}(s)}{\hat{P}_{0,0}(s)}}. \quad (2.22)$$

Using (2.18) for $n=1$ and (2.20) in (2.22), we get

$$\hat{P}_{0,0}(s) = \sum_{k=0}^{\infty} \binom{k}{r} \frac{\xi^r \hat{R}_1^r(s) (\eta\gamma)^{k-r}}{(s+\lambda+\gamma)^{k+1} (s+\lambda+\eta)^{k-r}} \left[1 + \sum_{m=1}^{\infty} \hat{R}_m(s) \left(\frac{p - \sqrt{p^2 - \alpha^2}}{\alpha\beta} \right)^m \right]^{k-r}. \quad (2.23)$$

On Laplace inversion, we get (2.11). Thus we have expressed $P_{0,n}(t)$ and $P_{1,0}(t)$ in terms of $P_{0,0}(t)$. Also $P_{0,0}(t)$ is expressed explicitly.

2.2. Special cases:

Case (1): When $\eta = \infty$, equation (2.11) reduces to

$$P_{0,0}(t) = \sum_{k=0}^{\infty} \sum_{r=0}^k \binom{k}{r} (\gamma)^{k-r} \xi^r (-1)^k e^{-\lambda t} \frac{t^k}{k!} * R_1^r(t) * \left[\sum_{m=1}^{\infty} \beta^{1-m} [I_{m-1}(\alpha t) - I_{m+1}(\alpha t)] e^{-(\lambda+\mu)t} * R_m(t) \right]^{*(k-r)}$$

which coincides with (4.13) in [2].

Case (2): When $\eta = \infty$, and $\xi = 0$, then $P_{0,n}(t)$ becomes

$$P_{0,n}(t) = \lambda^n e^{-(\lambda+\gamma)t} \frac{t^n}{(n-1)!} * P_{0,0}(t)$$

which coincides with (13) of [5].

III. MOMENTS

In this section, we derive the time-dependent mean and variance of the number of customers in the system at time t .

3.1 Mean

Let $E(X(t))$ be the average number of customers in the system at time t .

$$E(X(t)) = \sum_{n=1}^{\infty} n(P_{0,n}(t) + P_{1,n}(t)), \quad E(X(0)) = 0.$$

From (2.2) and (2.4), we obtain

$$\frac{d}{dt} E(X(t)) = \lambda - \xi \sum_{n=1}^{\infty} n P_{0,n}(t) - \mu \sum_{n=1}^{\infty} P_{1,n}(t).$$

Integrating the above equation, we get

$$E(X(t)) = \lambda t - \xi \sum_{n=1}^{\infty} n \int_0^t P_{0,n}(u) du - \mu \sum_{n=1}^{\infty} \int_0^t P_{1,n}(u) du. \tag{3.1}$$

3.2 Variance

Let $Var(X(t))$ be the variance number of customers in the system at time t .

$$Var(X(t)) = E(X^2(t)) - (E(X(t)))^2$$

where

$$E(X^2(t)) = \sum_{n=1}^{\infty} n^2 (P_{0,n}(t) + P_{1,n}(t)).$$

From (2.2) and (2.4), we obtain

$$\frac{d}{dt} E(X^2(t)) = \lambda + 2\lambda E(X(t)) - \xi \sum_{n=1}^{\infty} (2n^2 - n) P_{0,n}(t) - \mu \sum_{n=1}^{\infty} (2n - 1) P_{1,n}(t).$$

On Integration, we get

$$E(X^2(t)) = \lambda t + 2\lambda \int_0^t E(X(u)) du - \xi \sum_{n=1}^{\infty} (2n^2 - n) \int_0^t P_{0,n}(u) du - \mu \sum_{n=1}^{\infty} (2n - 1) \int_0^t P_{1,n}(u) du. \tag{3.2}$$

where $P_{0,n}(t)$ and $P_{1,n}(t)$ are given by (2.10) and (2.5).

IV. NUMERICAL ILLUSTRATIONS

In Fig. 1, the time-dependent system size probabilities are plotted for $\lambda = 1$; $\mu = 1.5$; $\xi = 0.8$; $\eta = 0.1$; $\gamma = 0.1$ and it is assumed that initially there is no customer in the system in the vacation state. The transient state system size probabilities are plotted for $\lambda = 1$; $\mu = 1.5$; $\xi = 0.8$; $\eta = 0.1$; $\gamma = 0.1$ in Fig. 2 when the system is in busy state. It is observed that the

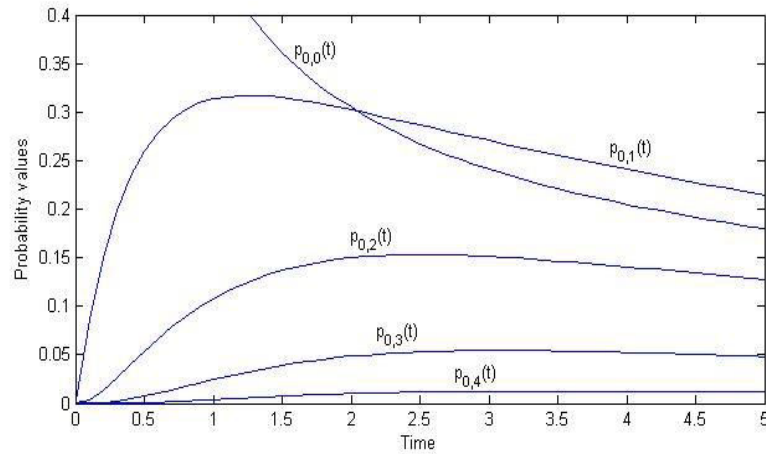


Fig.1 Transient system size probabilities

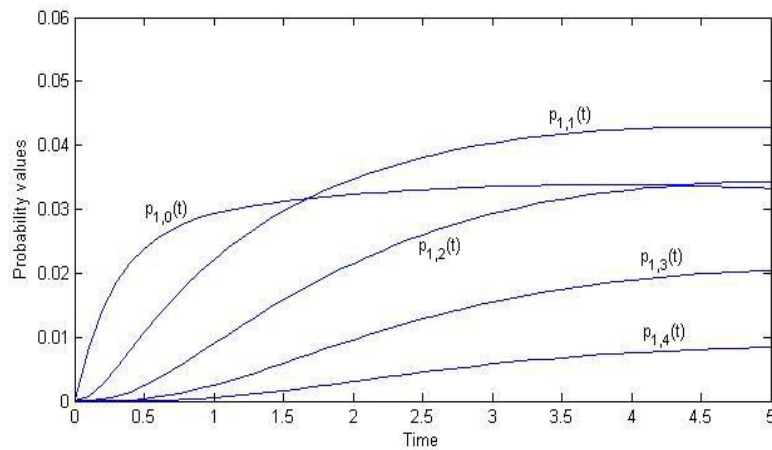


Fig.2 Transient system size probabilities

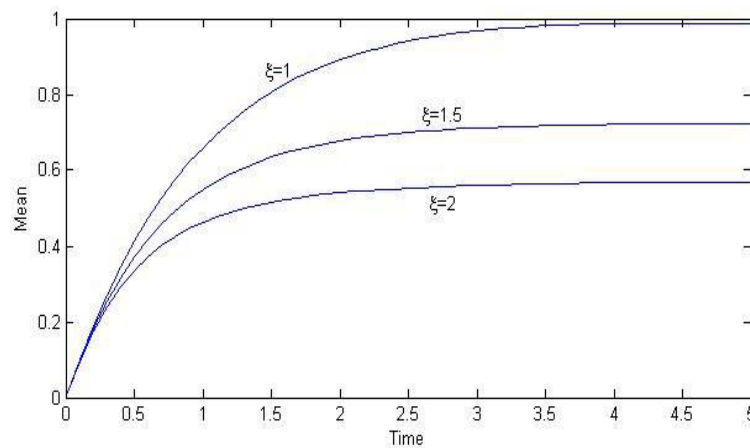


Fig.3 Mean number of customers for different values of ξ

probability curves except $P_{0,0}(t)$ in Fig. 1, increase initially and attain steady-state with the increment of time t . In Fig. 2, the probability curves increase initially with the increment of time t and for large values of t , they reach a steady-state. Fig. 3 and Fig. 4 show that the increase in impatient rate ξ leads to decrease in the mean and variance number of customers in the system.

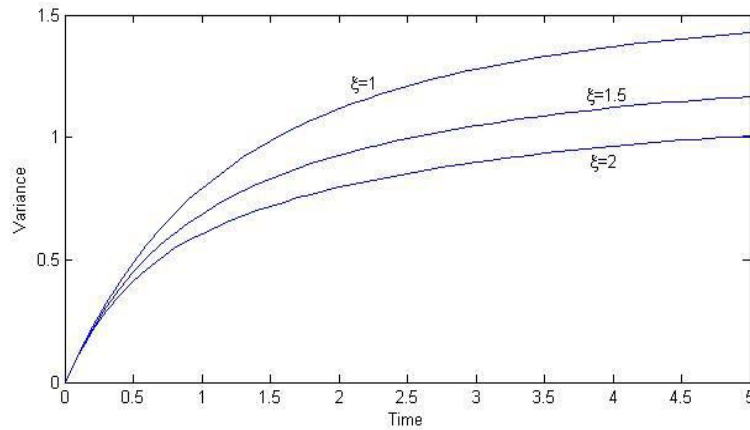


Fig.4 Variance number of customers for different values of ξ

V. CONCLUSION

In this work, we have derived the time-dependent system size probabilities of M/M/1 queuing model with server vacation, customers impatient and a waiting server timer in terms of modified Bessel functions and confluent hypergeometric functions. Generating function and continued fraction techniques are employed to derive such solution. Also we obtained time-dependent mean and variance. Then the results are valuated numerically.

REFERENCES

- [1] E. Altman and U. Yechiali, "Analysis of customers' impatience in queues with server vacation", *Queueing Systems*, vol. 52, pp. 261-279, 2006.
- [2] S. I. Ammar, "Transient analysis of an M/M/1 queue with impatient behavior and multiple vacations", *Applied Mathematics and Computation*, vol. 260, pp. 97-105, 2015.
- [3] O. J. Boxma, S. Schlegel and U. Yechiali, "A note on an M/G/1 queue with a waiting server timer and vacations", *American Mathematical Society Translations*, series 2, vol. 207, pp. 25-35, 2002.
- [4] B. Doshi, "Queueing systems with vacations-a survey", *Queueing Systems*, vol. 1, pp. 29-66, 1986.
- [5] K. Kalidass and K. Ramanath, "Transient analysis of an M/M/1 queue with multiple vacations", *Pakistan Journal of Statistics and Operations Research*, vol. 10, pp. 121-130, 2014.
- [6] R. Sudhesh, "Transient analysis of a queue with system disasters and customer impatience", *Queueing Systems*, vol. 66, pp. 95-105, 2010.

Power Your Entire Home Without Wires

T. Alan Arputha Raj¹, A. John Peter²

¹*1-Year Mechanical Engineering, St. Anne's College of Engineering and Technology, Panruti*

²*Asst. Prof, Dept of Physics, St. Anne's College of Engineering and Technology, Panruti.*

Abstract— Generally the power is transmitted through wires. We cannot imagine the world without electric power. Imagine a future in which wireless power transfer is feasible. As the demand increases day by day, the power generation increases and the power losses is also increased. In our present electricity generation system we waste more than half of our resources. Much of this power is wasted during transmission from power plant generators to the consumer. Now-a-days global scenario has been changed a lot and there is tremendous development in every field. If we don't keep pace with the development of new power technology we have to face a decreasing trend in the development of power sector. The transmission of power without wires may be one noble alternative for electricity transmission. This paper presents a comprehensive review and detailed analysis of various techniques used for wireless power transmission.

Keywords— wireless power transmission, WiTricity

I. INTRODUCTION

The First attempts to transmit energy wirelessly with the purpose of doing so are attributed to Serbian inventor N. Tesla at his laboratory in Long Island; New York .Tesla based his wireless electricity idea on a concept known as electromagnetic induction which was discovered by Michael Faraday in 1831 and holds that electric current flowing through one wire can induce current to flow in another wire, nearby. To illustrate that principle, Tesla built two huge world power towers that would broadcast current into the American air, to be received remotely by electrical devices around the globe. Few believed it could work. And to be fair to the doubters, it didn't exactly. When Tesla first switched on his 200 foot-tall 1000000 volt Colorado Springs tower 130 foot-long bolts of electricity shot out of it, sparks leaped up at the toes of passerby and the grass around the lab glowed blue. it was too much, too soon. Tesla had always tried to introduce worldwide wireless power distribution system. But due to lack of funding and technology of that time, he was not able to complete the task. Then onwards this technology has not been developed up to the level which would be completely applicable for practical purpose. Research has always been going on and recent developments have been observed in this field. But now Tesla dreams have come true. After more than 100 years of dashed hopes, several companies are coming to market with technologies that can safely transmit power through the air. Despite advances wireless power transmission has not been adopted for commercial use. Until this development after all phrases —mobile electronics|| has been a lie: how portable is your laptop if it has to feed every four hour, like an embryo, through a cord? How mobile is your phone if it shuts down after too long away from a plug? And how flexible is your business if your production area can't move the ceiling lights? [2]

II. WIRELESS ELECTRICITY TRANSMISSION

Magnetic induction is a technology that you will probably remember from your physics classes at high school. You need two coils, a transmitter coil and a receiver coil. An alternating current in the transmitter coil generates a magnetic field which induces a voltage in the receiver coil. This voltage can be used to power a mobile device or charge a battery.

Inductive Coupling

The first wireless powering system to market is an inductive device, much like the one Tesla saw in his dreams, but a lot smaller. It looks like a mouse pad and can send power through the air, over a distance of up to a few inches. A powered coil inside that pad creates a magnetic field, which as Faraday predicted, induces current to flow through a small secondary coil that's built into any portable device, such as a flashlight, a phone. The electrical current that then flows in that secondary coil charges the device's onboard rechargeable battery.

Radio-frequency harvesting

The induction systems are only the beginning. Some of the most visually arresting examples of wireless electricity are based on what's known as radio frequency, or RF. While less efficient, they work across distances of up to 85 feet. In these systems, electricity is transformed into radio waves, which are transmitted across a room, then received by so-called power harvesters and translated back into low-voltage direct current.

Magnetically Coupled Resonance

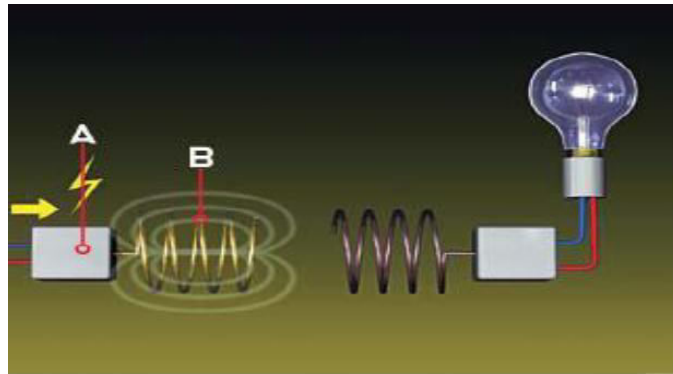
INVENTED BY MIT'S SOLJACIC (who has dubbed it WiTricity), the technique can power an entire room, assuming the room is filled with enabled devices. Though WiTricity uses two coils one powered, one not, just like eCoupled's system it differs radically in the following way: Soljacic's coils don't have to be close to each other to transfer energy. Instead, they depend on so-called magnetic resonance. Like acoustical resonance, which allows an opera singer to break a glass across the room by vibrating it with the correct frequency of her voice's sound waves, magnetic resonance can launch an energetic response in something far away. In this case, the response is the flow of electricity out of the receiving coil and into the device to which it's connected. The only caveat is that receiving coil must be properly "tuned" to match the powered coil.



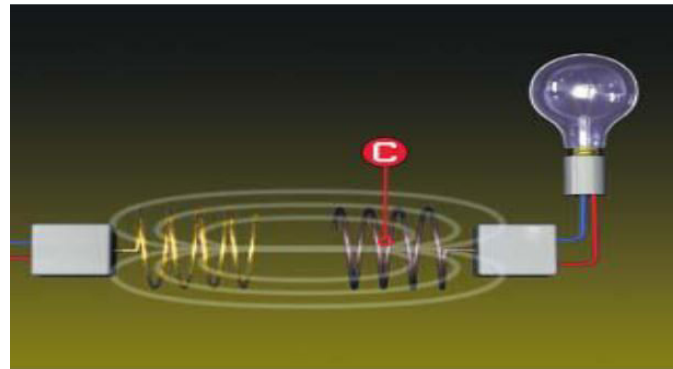
How it works

The concept of wireless electricity works on the principle of using coupled resonant objects for the transfer of electricity to objects without the use of any wires. This concept of WiTricity was made possible using resonance where an object vibrates with the application of a certain frequency of energy. So two objects having similar resonance tend to exchange energy without causing any effects on the surrounding objects. [11]

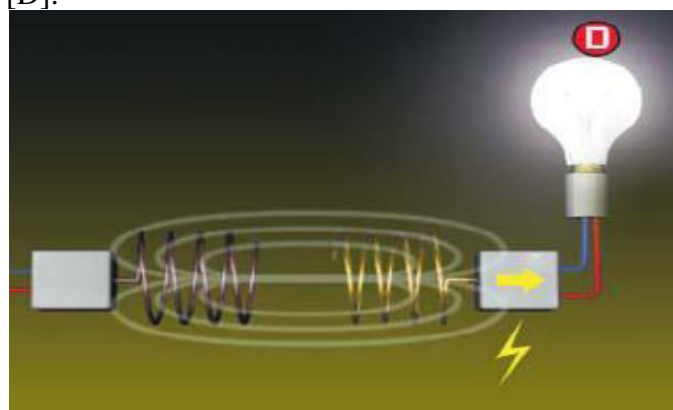
A circuit [A] attached to the wall socket converts the standard 60-hertz current to 10 megahertz and feeds it to the transmitting coil [B]. The oscillating current inside the transmitting coil causes the coil to emit a 10 -megahertz magnetic field



The receiving coil [C] has the exact same dimensions as the sending coil and thus resonates at the same frequency and, in a process called magnetic induction, picks up the energy of the first coil's magnetic field.



The energy of the oscillating magnetic field induces an electrical current in the receiving coil, lighting the bulb [D].



III. RECENT RESEARCH

Japan space scientists make wireless energy breakthrough

Japanese scientists have succeeded in transmitting energy wirelessly, in a key step that could one day make solar power generation in space a possibility,[3] Researchers used microwaves

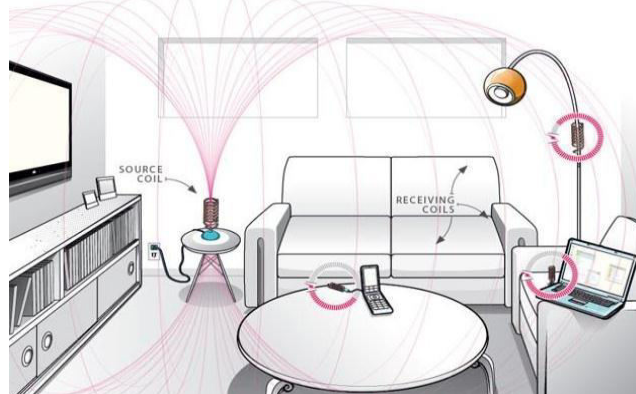
to deliver 1.8 kilowatts of power enough to run an electric kettle through the air with pinpoint accuracy to a receiver 55 meters (170 feet) away. While the distance was not huge,

the technology could pave the way for mankind to eventually tap the vast amount of solar energy available in space and use it here on Earth, a spokesman for The Japan Aerospace Exploration Agency (JAXA) said. "This was the first time anyone has managed to send a high output of nearly two kilowatts of electric power via microwaves to a small target, using a delicate directivity control device," he said. JAXA has been working on devising Space Solar Power Systems for years, the spokesman said. Solar power generation in space has many advantages over its Earth-based cousin, notably the permanent availability of energy, regardless of weather or time of day. While man-made satellites, such as the International Space Station, have long since been able to use the solar energy that washes over them from the sun, getting that power down to Earth where people can use it has been the thing of science fiction. "But it could take decades before we see practical application of the technology—maybe in the 2040s or later," he said. "There are a number of challenges to overcome, such as how to send huge structures into space, how to construct them and how to maintain them.

Need for wireless power transmission

Wireless electricity is one of the most emerging solutions to the global power crisis. It is defined as the transfer of wireless electricity or power from a source to a load without the use of any artificial interconnecting conductors such as wires [13]. Wireless electricity is being used primarily on the basis that at times, wires can be inefficient (power is lost as wires transmit electricity over long distances), inconvenient (in terms of cost and labor) and sometimes hazardous (many people may be electrocuted or put in some sort of danger).

Wireless transmission is employed in cases where instantaneous or continuous energy transfer is needed, but interconnecting wires are inconvenient, hazardous, or impossible.



Number of household points receives electricity at the same frequency using single transmitting coil as long as they all are at resonance. So this setup could Recharge all the devices in a room at once.

IV. APPLICATIONS

Direct Wireless Power—when all the power a device needs is provided wirelessly, and no batteries are required. This mode is for a device that is always used within range of its *WiTricity* power source. **Automatic Wireless Charging**—when a device with rechargeable batteries charges itself while still in use or at rest, without requiring a power cord or battery replacement. This mode is for a mobile device that may be used both in and out of range of its *WiTricity* power source. in the macroscopic world, this scheme could potentially be used to deliver power to robots and computers in a factory room, or electric buses on a highway

(source-cavity would in this case be a “pipe” running above the highway).some other applications where wireless power transmission can be used are Consumer electronics, Transportation, Industry applications, Medical devices, Military applications and Robots.

V. CONCLUSION

In conclusion, it is clear that resonant inductive coupling power transmission would be extremely beneficial to society if it were implemented in homes and homes electronics. From an environmental stand point, this technology could replace disposable batteries and cords, reducing dangerous chemicals and potential for poisoning communities. The transition would be somewhat slow and take many years to show up in a majority of places. However switching to wireless power would increase the efficiency and convenience of these electronics, while lowering the environmental impact in the long run. Wireless power transmission would have many interesting applications. Some of the applications involve simply powering devices or vehicles from a remote power source. However, the energy grid could be affected as well. If long distance, high efficiency wireless power transmission is possible, we could reduce our reliance on transmission lines to transfer energy over long distances. Moreover, wireless power transfer could allow an alternative source of clean energy by transmitting solar power from space back down to places where it is needed on earth. Further research into wireless transmission will show whether some of these plans are feasible.

REFERENCES

- [1] S. Sheik Mohammed, —Wireless Power Transmission – A Next Generation Power Transmission System,
International Journal of Computer Applications, Vol .1,No.13,2012.
- [2] Fastcompany.com
- [3] <http://physorg/nes/2015-03-japan-spacescientists-wireless-energy>
- [4] —WiTricity Corp. — Applications of WiTricity Technolog, www.witricity.com/pages/application.htm
- [5] Nikola Tesla, —The Transmission of Electrical Energy Without Wires as a Means for Furthering Peace,
Electrical
World and Engineer. Jan. 7, p. 21, 1905
- [6] Nikola Tesla, — My Inventions, Ben Johnston, Ed Austin, Hart Brothers, p. 91,1982 Travel, P. 2007
Modeling and
Simulation Design. AK Peters Ltd.
- [7] "Goodbye wires" MIT News, 2007-06-07, <http://web.mit.edu/newsoffice/2007/wireless-0607.html>.
- [8] Vinothkumar, Wireless Energy Transfer Possibility, <http://thinkquestprojects.blogspot.in/2012/01/wireless-energy-transfer-possibility.html>
- [9] Michael Shu, —Wireless Power Transmission, Submitted as coursework for PH240, Stanford University,
Fall 2011,
Dec 9,2011 <http://large.stanford.edu/courses/2011/ph240/shu2/>
- [10] Tesla, N., —The transmission of electric energy without wires, *Electrical World*, March 5, 1904
- [11] Patil C.B. Burali Y. N, —Wireless Electricity Transmission Based On Electromagnetic and Resonance
Magnetic Coupling,*Vol. 2 Issue. 7,2012*
- [12] <http://www.instructables.com/id/Wi-Tricity-Wireless-Electricity-1/>
- [13] B. Renil Randy, M.Hariharan, R. Arasa Kumar, —SECURED WIRELESS POWER
TRANSMISSION USING
RADIO FREQUENCY SIGNAL,IJIST Vol.4, No.3, May 2014
- [14] <http://www.ripublication.com/ijepa.htm>

Design and Implementation of Ultra Low Power, Ultra Wide Band Low Noise Amplifier

Chenna Reddy Peddasomappagari¹, Dr. P. Aruna Priya²

¹*Dept. of Electronics and Communication Engineering, SRM University,
Chennareddy.pulivendula@gmail.com*

²*Dept. of Electronics and Communication Engineering, SRM University,
Arunapriya.p@ktr.srmuniv.ac.in*

Abstract— We presents a design methodology and implementation of an 11-14GHz ultra-wideband (UWB) and ultra-low-power (ULP) reliable Low-Noise Amplifier (LNA).Exploiting Negative feedback advantage of providing stability, feedback series inductance technique is followed to exaggerate bandwidth, noise performance and stability of the LNA. The main variation here employed is the source degeneration inductance to resonance the intrinsic frequencies to increase the frequency. The ULV circuit design challenges are discussed and a new biasing metric for ULV and ULP designs in deep sub-micrometer CMOS technologies is introduced. A new biasing metric, has been implemented that provides substantial ease in the design analysis and implementation. Series inductive peaking in the feedback loop, a 0.4 V, 3.6-mAmp current budget, reuse scheme broadband LNA is implemented in a 45-nm submicron CMOS technology. Simulation results show 5.2-dB voltage gain, 11–14GHz bandwidth, 6-dB NF, 5U associated power gain, $S_{11} < -12$ dB of absolute impedance matching, are simulated using Agilent Advanced Design Systems.

Keywords- Current reuse technique,45-nm, series inductance peaking, low- noise amplifier (LNA), Source and Load rolett stability factor(K), resistive shunt feedback, ultra-low power (ULP), ultra-low voltage(ULV),ultra-wide band (UWB).

I. INTRODUCTION

Following the concepts of ultra-scaling technology, also popularly known as submicron technology to attain high frequency of operational bands has become the only distinguished option for Wireless Sensor Networks. The shrinking of the size of CMOS however reduces the power consumption with tradeoff of operating speed and conversion losses. Health care, environmental monitoring, industrial settings, and agriculture are some field of applications. The nature of these applications imposes severe restrictions on the power consumption of a WSN node. As a result, ultra-low-power (ULP) RF front-end circuits are required to maximize battery lifetime and to allow operation from energy harvested from the environment.

While operation from a low supply voltage is desirable in systems powered by energy harvesting minimize conversion losses, due to second order effects. Consequently, circuits operating from very low supply voltages have become very notable and are under active research [1]–[5]. Along with the above design challenges and the limitations of nanoscale CMOS technologies like, higher output conductance, velocity saturation, and mobility degradation, the high transit frequency, f_T , of short channel effect in CMOS and BiCMOS technologies is a major trade off factor with power consumption to design and employ CMOS RF low power circuits.

A broadband low noise amplifier is vital component in the family of RF circuits front end design. The wide band LNA should meet the draconian constraints and requirements. Any fault in holding these requirements lead to premature failure of LNA device. This compromise was first highlighted in [6] in which a biasing metric is introduced for low-power RF design. While useful, this biasing metric does not include the effects of the output conductance, g_{ds} and the drain–source voltage V_{DS} on the intrinsic gain, both of which are becoming very important in ultra-low voltage (ULV) and ULP designs. To overcome these issues, this paper suggests a copious biasing metric that is feasible for ULV and ULP low noises designs and manifests its applicability by designing an ULP, ULV ultra-wideband low noise amplifier (LNA).

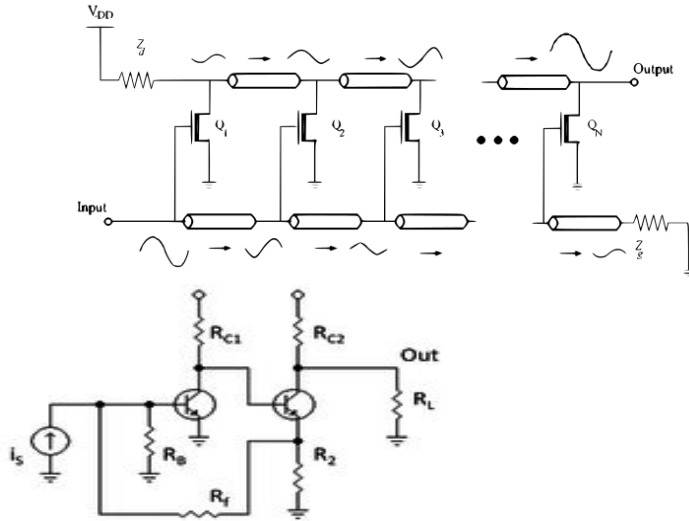


Fig. 1. Distributed n-stage Amplifier LNA

Fig. 2. Cascoded Shunt Feedback LNA

The LNA is the first Volant component in the front-end of the receiver, and is generally considered as one of the most power famish blocks. The high power consumption all is because LNA must provide simultaneous wideband impedance matching, high gain, low noise, high both end stability and high linearity, all of which require exemplary high power and high supply voltages. These mixed specifications have made the design of low-power and low voltage UWB LNAs a challenging research topic.

There are many distinctive techniques to design wide- band LNAs. All show their own pros and cons but usual familiar approach is to employ distributed amplifiers [7]–[9] as shown in Fig. 1, while providing high bandwidths that can span into the multi-gigahertz range amidst results in very high power consumption and large area intake with N-cascoding stages still with lower efficiency.

The resistive shunt feedback architecture is another workable solution for wideband LNA design. This involves placing a feedback resistor around a common source amplifier to realize a wideband 50-K input terminal match impedance as shown in Fig. 2 [16]–[19]. Despite, there is a tradeoff between input matching and the NF of the LNA, and satisfying both the parameters results in high power consumption [17]–[21].

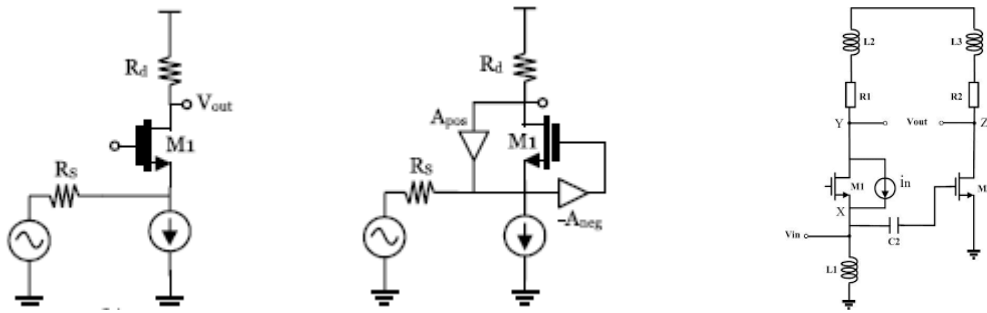


Fig. 3. (a) Common Gate LNA. (b) Mixed design of feedback and forward path. (c) Noise Cancellation Scheme

Another design approach is to use a common gate (CG) transistor as the input stage as illustrated in Fig. 1(a). The desired input impedance of a CG input stage is achieved by adjusting the bias current, aspect ratio, and overdrive voltage such that $1/g_m$ is close to the termination impedance Z_0 . Typically, single-ended Z_0 is 50ohm, and hence a g_m of approximately 20mS is required. In spite of wideband matching, this scheme faces two major problems. The input matching requirement of $g_m R_s = 1$ for CGLNA bounds its noise factor at $F = 1 + \gamma/\alpha$, where $\alpha = g_m/g_{d0}$. Clearly, α should be increased to decrease F . This seems unfeasible because α is constrained at the device level. Two schemes that have been used to improve CG stage circuit performance in reference with noise figure are noise cancellation and source degeneration. A conventional noise cancellation technique in LNAs is demonstrated in Fig. 1(c). Noise cancellation schemes have been shown to enhance the NF, but this comes at the cost of higher power consumption due to extra stages and high supply voltages [11]–[13]. A mixed design of feedback and feedforward techniques, shown in Fig. 1(b), has been used to break the tradeoff between NF, gain, and input matching [14], [15], however, the extra stages add parasitic capacitances and limit the bandwidth of operation. These examples show that reaching a low-power and wideband solution with a CG input stage is a challenging task.

As a result, neoteric circuit design techniques are necessary to mitigate the power consumption. This paper illustrate and depicts the challenges encountered while designing ULPLV circuits, and introduces an extended ultra low power and low voltage (ULPLV) biasing metric to optimize transistor performance. A combination of circuit techniques that are suitable for ULPLV designs are presented, and a broadband resistive-feedback inductance peaking LNA in a 45-nm CMOS technology is designed using these techniques and its measured performance is compared with state-of-the-art works. The principles in the proposed low voltage and low-power design methodology presented here can be readily adapted and applied to other RF circuits.

The following paper is organized as follows. First, ULP model challenges are discussed in Section II. The Proposed ULV, UWB LNA design schematic is presented in Section III. Section IV depicts the circuit stability, Noise Figure (NF) and current budget simulation analysis of the proposed ULP, UWB LNA. Finally, Section V summarizes this paper.

The following paper is organized as follows. First, ULP model challenges are discussed in Section II. The Proposed ULV, UWB LNA design schematic is presented in Section III. Section IV depicts the circuit stability, Noise Figure (NF) and current budget simulation analysis of the proposed ULP, UWB LNA. Finally, Section V summarizes this paper.

II. ULTRA LOW POWER MODEL CHALLENGES

Modern technology needs the requirement high speed and high frequency applications. But both of them come with trade off to each of their own. If not, to satisfy both leads to increase

in enormous power consumption. So the only feasible approach is to scale down the aspect ratio of MOS device. Thus scaling substantially decreases the required supply voltage.

But with rapid scaling in integration of devices and reduction of supply voltage is possible to a level of threshold voltage level. Any variation in setting down has great impact on inversion coefficient, linearity, flicker noise, intrinsic gain.

A. Inversion coefficient

Trans-conductance is the change in the drain current divided by the small change in the gate/source voltage with a constant drain/source voltage. Typical values of gm for a small-signal field effect transistor are 1 to 30 milli-siemens.

The ratio of trans-conductance to the supply drain voltage is known as Trans-conductance Efficiency. The trans-conductance efficiency shows various steady and exponential characteristics depending on a coefficient called as inversion coefficient which represents the level of MOS inversion [22]. The trans-conductance efficiency shows exponential behavior in sub-threshold region also called as weak inversion region (WI). MOS device operates with low voltage supply in WI. Weak inversion corresponds to $IC < 0.1$. But it affects the unity current gain cut off frequency. As there is need to operate at high frequency, therefore this region is not well suited.

In Medium inversion (MI) region gate voltage reaches the threshold voltage. Medium inversion region corresponds to $0.1 < IC < 10$.

Greater change than threshold results in strong inversion region (SI) which provides steady variations due to gate to drain supply voltages and provides better matching. Strong inversion region corresponds to $IC > 10$.

$$IC = I_D/I_0.S = \exp((V_{gs} - V_{T0}) / nU_T) \quad (1)$$

and

$$I_D = 2n\mu_0C_{OX}(W/L)(U_T)^2 \exp((V_{gs} - V_{T0}) / nU_T), \quad (2)$$

$$I_0 = 2n\mu_0C_{OX}(U_T)^2 \quad (3)$$

Where IC is Inversion Coefficient

I_D is drain source current [A]

I_0 is technology current [A]

S is transistor size aspect ratio

n_0 is substrate factor

μ_0 is field mobility factor [$\mu A/V^2$]

C_{OX} is gate-oxide capacitance [$Ff/\mu m^2$]

U_T is thermal voltage [mV]

From 1 and 2, Transconductance efficiency

$$g_m/I_D = 1/(n.U_T.(\sqrt{IC + 0.5} \sqrt{IC} + 1)) \quad (4)$$

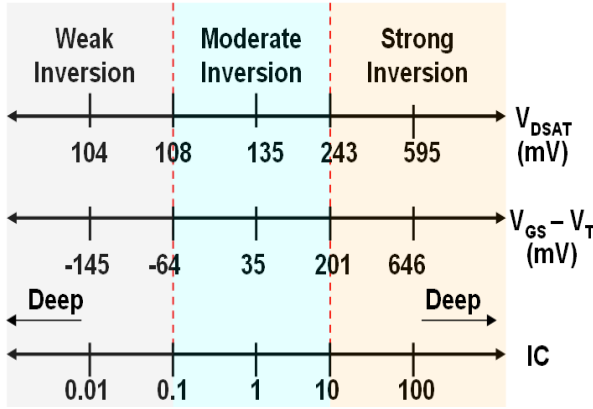


Fig. 4. IC versus (V_{DSAT} , V_{eff})

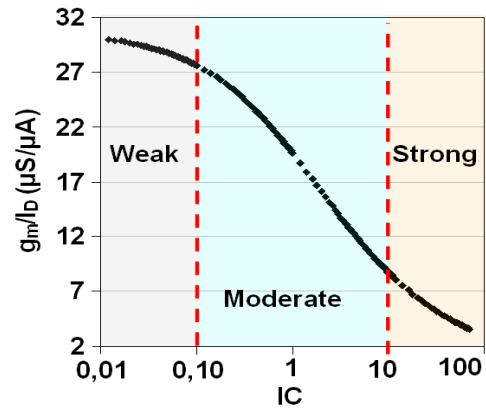


Fig. 5. Trans-conductance Efficiency versus IC

B.

C. Linearity

The linearity of LNA is also gets reduced with usage of ultra low drain supply voltages. The nonlinear behaviour of a MOS device can be expressed in terms of V_{gs} and V_{ds} by a Taylor series.

$$I_{ds}(V_{gs}, V_{ds}) = g_m V_{gs} + g_{ds} V_{ds} + \frac{1}{2} g_m (V_{gs})^2 + \frac{1}{2} g_{ds} (V_{ds})^2 + \frac{1}{6} g_m (V_{gs})^3 + \frac{1}{6} g_{ds} (V_{ds})^3 \quad (5)$$

In the above expression of terms, it can be known that g_m is the strongest contributor the third order harmonic distortions. g_{ds} also varies with V_{ds} and decreases rapidly with decrease in supply voltage resulting non linearity of LNA[24].

D. Dynamic range

Dynamic range is limited by low power supply in analog/RF circuits and offers reduced voltage headroom for cascode structures. So new techniques are required to obtain the same performance while using low power supply voltages.

Transit Frequency

A very common and other important characteristic parameter that affects the gain and NF_{min} proportionally is the transit frequency. This is the frequency at which the extrapolated gain h_{21} of small signal for short channel devices, the carriers enter into velocity saturation. After the velocity of carriers is saturated the device no longer depends on the channel length.

III. PROPOSED ULV, UWB LNA DESIGN SCHEMATIC

The proposed ultra low power, ultra wide band LNA is a combination model that exploits the features of current reuse scheme, series gate inductive peaking and resistive feedback shunt for low power consumption, input matching and to provide high wide-band frequency generation.

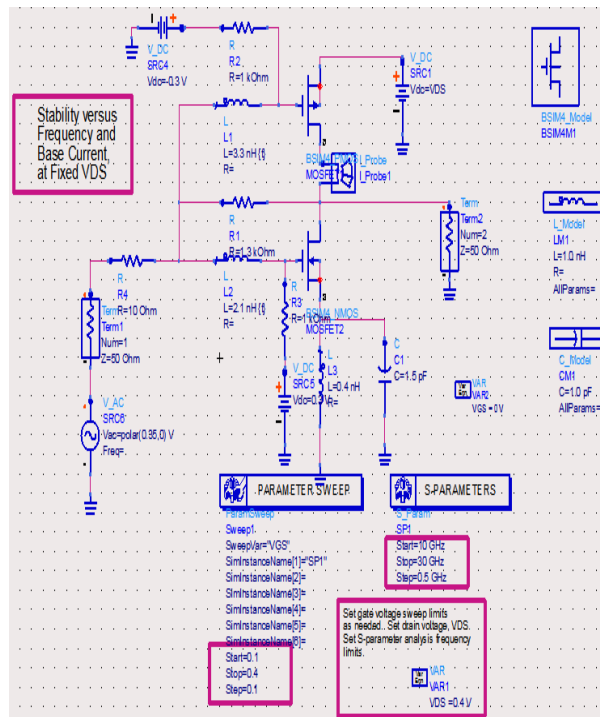
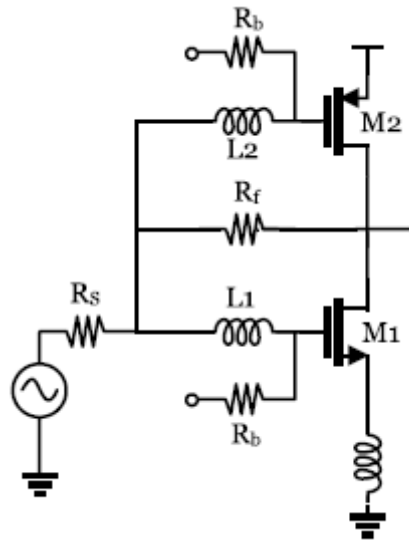


Fig.6. Proposed Current reuse source degeneration, resistive shunt feedback LNA with inductive series peaking in the feedback loop. 7. Proposed Model Schematic of LNA in ADS.

Resistive shunt feedback (R_f) is a viable option for UWB LNA design. It provides wideband input matching with the aid of a feedback network. In this protoplast design, the bias voltages V_{b1} and V_{b2} were used to tune the gate voltages of $M1$ and $M2$ such that to give flexible control over LNA, providing dc feedback to make ensure that the drain voltages are midrail.

A. Low-Power, Low Voltage RF Design Biasing Metric

As earlier said reference[6] had not included the intrinsic gain and output trans-conductance effects, this mitigation of advantage overcome by including the remaining by exploiting the following biasing metric for BSIM model,

$$\text{Biasing Metric}_{(ULP,ULV)} = (gm/ID) \cdot (gm/gds) \cdot fT. \quad (6)$$

In Weak Inversion (WI) region, $g_m = I_D/nU_T$

$$\text{Hence, Biasing Metric}_{(ULP,ULV)} = 1/((nU_T)^2 \cdot g_{ds}) \cdot f_T \quad (7)$$

The above biasing metric is very novel in giving an optimistic value of current budget for the proposed design. The biasing metric by view can be familiarly defined as the product of trans-conductance frequency, intrinsic gain, and transit frequency.

B. Overdrive Gate–Source and Drain–Source Saturation Voltage

The required overdrive gate-source and drain-source voltage saturation voltages for different inversion regions are given below.

In general, Overdrive voltage (V_{od}) = $V_{gs} - V_{th}$, using (1)

$$V_{od} = nU_T \cdot \ln(\sqrt{IC}) \quad (8)$$

The drain–source saturation voltage which is paramount to ascertain that the contrivance is partial in saturation is defined by [23]

$$V_{ds,sat} = 2U_T(\sqrt{IC+0.25})+3U_T \quad (9)$$

IV. PROPOSED CIRCUIT DESIGN ANALYSIS AND SIMULATION

The proposed ultra low power, ultra wide-band Low Noise Amplifier(LNA) schematic using ADS is shown in fig.7. The MOS devices employed are BSIM model in 45nm CMOS technology. Both terminals of the schematic are terminated with a matching impedance of 50 ohms as it represents the resistivity of the cable wire used for communication of signals.

1. Scattering(s) Parameters Simulation

Scattering(s) parameters describe the electrical comportment of linear electrical networks when undergoing sundry steady state stimuli by electrical signals.

The following information must be defined when specifying a set of S-parameters:

1. The frequency
2. The characteristic impedance (often 50 Ω)
3. The allocation of port numbers
4. Conditions which may affect the network, such as temperature, control voltage, and bias current, where applicable.

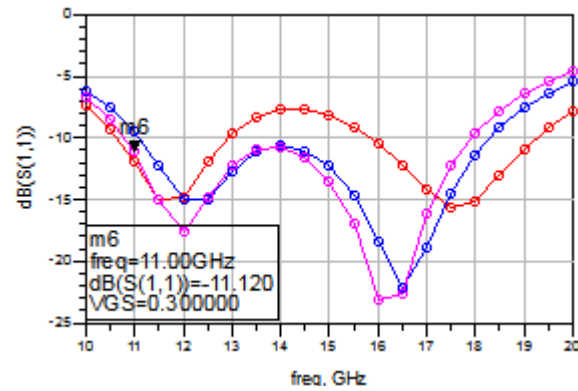


Fig. 8. Input Reflection Coefficient (S_{11}) versus Frequency

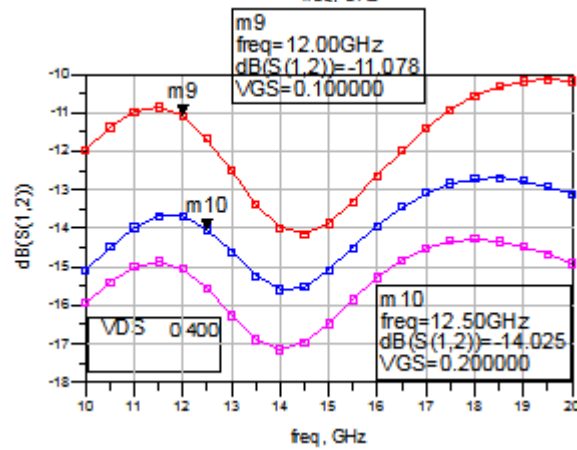


Fig. 9. Reverse Voltage Gain (S_{12}) versus Frequency

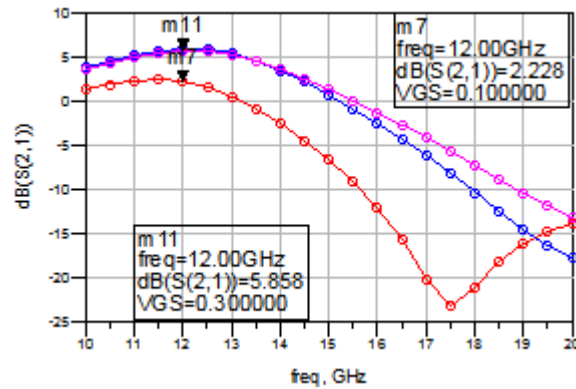


Fig. 10. Forward Gain (S_{21}) versus Frequency.

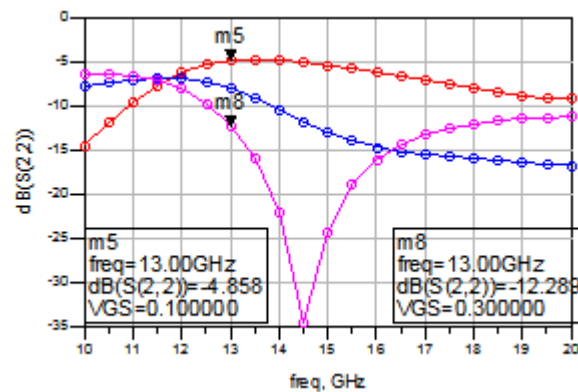


Fig. 11. Output Reflection Coefficient (S_{22}) versus Frequency.

The above all scattering parameter, have justified their minimum value to make an LNA to be operated in the respected wideband thought for.

V. CIRCUIT STABILITY & NOISE FIGURE SIMULATION ANALYSIS OF THE PROPOSED ULP, UWB LNA

In the proposed design, we had used shunt feedback resistance to provide a wide-band operation. A current reuse scheme is also employed for low power consumption. Mainly the series inductive peaking and source degeneration inductors have been added in order to cancel the parasitic intrinsic capacitances and if more required that to resonate them. Thus the source degeneration inductor resonate the capacitance to enhance the bandwidth and forward gain. The only drawback of source degeneration is as it adds little noise on beyond the operating inversion region frequencies [20].

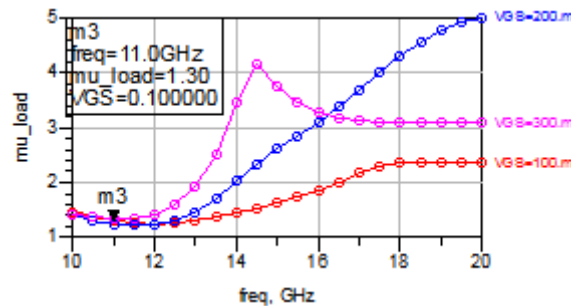
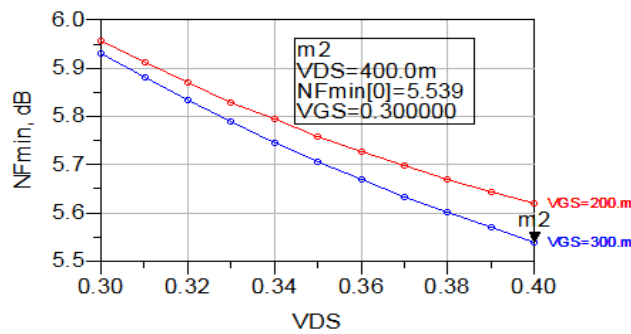


Fig. 12. Minimum Noise Figure versus VGS and VDS Factor

Fig. 14. Geometrically-Derived Load Stability

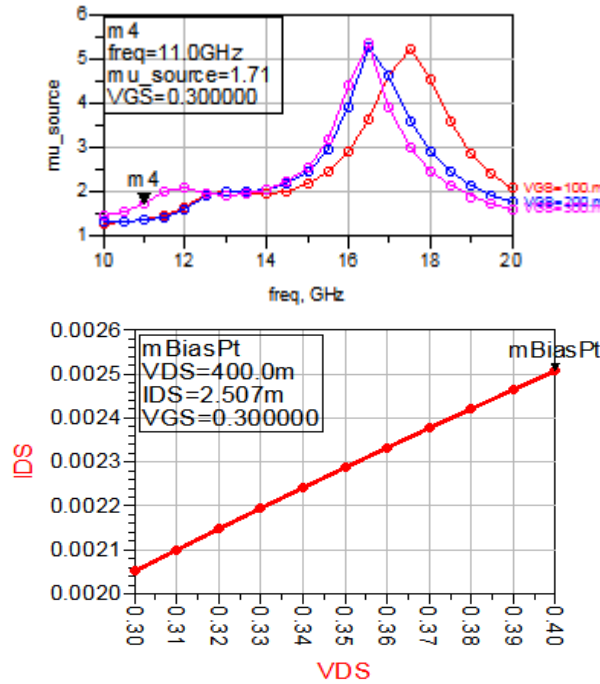


Fig. 13. Geometrically-Derived Source Stability Factor Voltage(V_{DS})

Fig. 16. Current drawn (I_{DS}) versus Supply Voltage(V_{DS})

A. Noise Figure (NF)

The main noise sources in this LNA are the channel noises of $M1$ and $M2$ and the thermal noise of the feedback resistor, R_f . The noise factor of the LNA by neglecting the little noise produced by source degeneration inductance can be expanded as below,

$$NF \sim 1 + (R_f/R_s)(1 + g_{mt}R_s/1 - g_{mt}R_f)^2 + (\gamma g_{mt}/\alpha R_s)[(R_s + R_f)/1 - g_{mt}R_f]^2 \quad (10)$$

In the above expression of NF, the second term is due to the feedback resistor, R_f , and the third term is the noise contribution of the transistors. The minimum noise figure of the proposed LNA is shown in fig. 12.

B. Stability Factor (K)

The LNA should provide stability both at source and load with maximum impedance matching unconditionally, generally known as Rollett's stability factor (K). The stability factor (K) of the LNA with respect to two terminal source and load should be > 1 unconditionally, as shown in fig. 13, 14.

Finally the combined source and load, Rollet stability factor (K) is given as

$$K = (1 - |S_{11}|^2 - |S_{22}|^2 + |\Delta|^2) / (2|S_{12}S_{21}|)$$

$$\text{Where } \Delta = S_{11}S_{22} - S_{12}S_{21}.$$

C. Current Budget

The independent drain-source current that is needed for a biasing voltage at a constant supply voltage for operating at a band of frequency is shown in fig. 15. TABLE II

PERFORMANCE SUMMARY AND COMPARISON WITH STATE-OF-THE-ART LNAs

Parameter	This Work	[14]2009 ISSCC	[33]2011 E. Lett.
3-dB BW(GHz)	11-14	0.3-0.92	2.6-10.5
Power(mW)	1	3.6	0.99
Supply(V)	0.4	1.8	1.1
S_{11} (dB)	<-11	<-9**	<-10
NF_{min} (dB)	5.5	3.6	5.5-6.5
Stability(K)*	>1.38	-	-
Technology	45nm	0.18 μ m	0.18 μ m

*Indicate both combinational source and load stability factor.

**Estimated from the curves.

VI. CONCLUSION

An ULP, ULV wideband CMOS LNA is proposed and designed based on an extended biasing metric for low power and low voltage circuit design. The LNA presented here achieves the lowest power consumption and employs the lowest supply voltage with minimum current budget, when compared with other works. The main highlight of this LNA is it possesses both the source and stability factor(K) of >1.38 in operating band of 11-14GHz. A current-reuse scheme to lower the power consumption, source degeneration to enhance frequency resonance along with inductive series peaking in the feedback path to increase the bandwidth, are analyzed and employed in the LNA. The LNA operates over the bandwidth of 11–14GHz and achieves a voltage gain of 5.8 dB, a minimum NF of 5.5 dB, and a standard stability factor >1, while consuming only 1 mW from a 0.4-V supply voltage.

ACKNOWLEDGMENT

The author expresses his gratitude to SRM University's research lab for supporting this work.

REFERENCES

- [1] N. Stanic, P. Kinget, and Y. Tsividis, "A 0.5 V 900 MHz CMOS receiver front end," in *Symp. Very Large Scale Integr. (VLSI) Circuits, Dig. Tech. Paper*, Jun. 2006, pp. 228–229.
- [2] M. Brandolini, M. Sosio, and F. Svelto, "A 750 mV fully integrated direct conversion receiver front-end for GSM in 90-nm CMOS," *IEEE J. Solid-State Circuits*, vol. 42, no. 6, pp. 1310–1317, Jun. 2007.
- [3] H. C. Chen, T. Wang, T.-H. Kao, and S.-S. Lu, "0.5-V/5.6-GHz CMOS receiver subsystem," *IEEE Trans. Microw. Theory Techn.*, vol. 57, no. 2, pp. 329–335, Feb. 2009.
- [4] A. Balankutty, S.-A. Yu, Y. Feng, and P. Kinget, "A 0.6-V zero-IF/low-IF receiver with integrated fractional-N synthesizer for 2.4-GHz ISM-band applications," *IEEE J. Solid-State Circuits*, vol. 45, no. 3, pp. 538–553, Mar. 2010.
- [5] A. Balankutty and P. R. Kinget, "An ultra-low voltage, low-noise, high linearity 900-MHz receiver with digitally calibrated in-band feed-forward interferer cancellation in 65-nm CMOS," *IEEE J. Solid-State Circuits*, vol. 46, no. 10, pp. 2268–2283, Oct. 2011.
- [6] A. Shameli and P. Heydari, "A novel power optimization technique for ultra-low power RFICs," in *Proc. Int. Symp. Low Power Electron. Design*, Oct. 2006, pp. 274–279.
- [7] F. Zhang and P. Kinget, "Low-power programmable gain CMOS distributed LNA," *IEEE J. Solid-State Circuits*, vol. 41, no. 6, pp. 1333–1343, Jun. 2006.
- [8] P. Heydari, "Design and analysis of a performance-optimized CMOS UWB distributed LNA," *IEEE J. Solid-State Circuits*, vol. 42, no. 9, pp. 1892–1905, Sep. 2007.
- [9] Y.-H. Yu, Y.-J. Chen, and D. Heo, "A 0.6-V low power UWBCMOS LNA," *IEEE Microw. Wireless Compon. Lett.*, vol. 17, no. 3, pp. 229–231, Mar. 2007.
- [10] C.-T. Fu, C.-N. Kuo, and S. Taylor, "Low-noise amplifier design with dual reactive feedback for broadband simultaneous noise and impedance matching," *IEEE Trans. Microw. Theory Techn.*, vol. 58, no. 4, pp. 795–806, Apr. 2010.
- [11] S. Blaakmeer, E. Klumperink, D. Leenaerts, and B. Nauta, "Wideband balun-LNA with simultaneous output balancing, noise-canceling and distortion-canceling," *IEEE J. Solid-State Circuits*, vol. 43, no. 6, pp. 1341–1350, Jun. 2008.
- [12] J. Jussila and P. Sivonen, "A 1.2-V highly linear balanced noise cancelling LNA in 0.13- μ m CMOS," *IEEE J. Solid-State Circuits*, vol. 43, no. 3, pp. 579–587, Mar. 2008.
- [13] K.-H. Chen and S.-I. Liu, "Inductorless wideband CMOS low-noise amplifiers using noise-canceling technique," *IEEE Trans. Circuits Syst. I, Reg. Papers*, vol. 59, no. 2, pp. 305–314, Feb. 2012.
- [14] W. Sanghyun, K. Woonyun, and J. Laskar, "A 3.6 mW differential common-gate CMOS LNA with positive-negative feedback," in *IEEE Int. Solid-State Circuits Conf. Dig. Tech. Paper (ISSCC)*, Feb. 2009, pp. 218–219.
- [15] J. Kim, S. Hoyos, and J. Silva-Martinez, "Wideband common-gate CMOS LNA employing dual negative feedback with simultaneous noise, gain, and bandwidth optimization," *IEEE Trans. Microw. Theory Techn.*, vol. 58, no. 9, pp. 2340–2351, Sep. 2010.
- [16] A. Meamar, C. C. Boon, K. S. Yeo, and A. V. Do, "A wideband low power low-noise amplifier in CMOS technology," *IEEE Trans. Circuits Syst. I, Reg. Papers*, vol. 57, no. 4, pp. 773–782, Apr. 2010.
- [17] C.-W. Kim, M.-S. Kang, P. T. Anh, H.-T. Kim, and S.-G. Lee, "An ultra-wideband CMOS low noise amplifier for 3–5-GHz UWB system," *IEEE J. Solid-State Circuits*, vol. 40, no. 2, pp. 544–547, Feb. 2005.
- [18] J.-H. Zhan and S. Taylor, "A 5 GHz resistive-feedback CMOS LNA for low-cost multi-standard applications," in *IEEE Int. Solid-State Circuits Conf. Dig. Tech. Paper (ISSCC)*, Feb. 2006, pp. 721–730.
- [19] B. Perumana, J.-H. Zhan, S. Taylor, B. Carlton, and J. Laskar, "Resistive feedback CMOS low-noise amplifiers for multiband applications," *IEEE Trans. Microw. Theory Techn.*, vol. 56, no. 5, pp. 1218–1225, May 2008.
- [20] T. Chang, J. Chen, L. Rigge, and J. Lin, "ESD-protected wideband CMOS LNAs using modified resistive feedback techniques with chip-on-board packaging," *IEEE Trans. Microw. Theory Techn.*, vol. 56, no. 8, pp. 1817–1826, Aug. 2008.
- [21] M. Chen and J. Lin, "A 0.1–20 GHz low-power self-biased resistive feedback LNA in 90 nm digital CMOS," *IEEE Microw. Wireless Compon. Lett.*, vol. 19, no. 5, pp. 323–325, May 2009.

- [22] F. Silveira, D. Flandre, and P. Jespers, "A gm/ID based methodology for the design of CMOS analog circuits and its application to the synthesis of a silicon-on-insulator micropower OTA," *IEEE J. Solid-State Circuits*, vol. 31, no. 9, pp. 1314–1319, Sep. 1996.
- [23] C. C. Enz and E. A. Vittoz, *Charge-Based MOS Transistor Modeling: The EKV Model for Low-Power and RF IC Design*. New York, NY, USA: Wiley, 2006. V. Aparin, G. Brown, and L. Larson, "Linearization of CMOS LNA's gate biasing," in *Proc. IEEE Int. Symp. Circuits Syst. (ISCAS)*, May 2004, pp. 748–751.

Chunking and Indexing mechanisms for Data Deduplication in Cloud Storage

Z.Asmathunnisa¹, Dr. P.Yogesh²,

¹Department of CSE, St.Anne's College of Engineering & Tech, zasmath@yahoo.co.in.

²Department Of IST, Anna University, yogesh@annauniv.edu

Abstract— Cloud Computing plays a major role in the business domain today as computing resources are delivered as a utility on demand to customers over the Internet. Cloud storage is one of the services provided by cloud computing which is becoming popular among the Internet users. The cloud storage is to be effectively utilized since the cloud service provider has to accommodate more consumers. At present, there is a vast amount of duplicated data or redundant data in storage systems. Hence, a specialized technique known as data deduplication is used to reduce the redundant data in the storage. Deduplication is a specialized data compression technique for eliminating duplicate copies of repeating data. Many mechanisms such as chunking, indexing, hashing have been proposed for efficient data deduplication in order to save storage space. A special type of chunking algorithm namely Two Thresholds Two Divisors (TTTD) separates a file into variable sized chunks has been proposed in this paper. In this scheme ChunkIDs are obtained by applying hash function to the chunks. The resultant ChunkIDs are used to build indexing keys in B+ tree like index structure. This helps to reduce redundant data volumes so that it could help cloud user to achieve faster retrieval rate.

Keywords-Cloud computing, Data deduplication, Chunking, Indexing, Hashing, B+ tree

I. INTRODUCTION

Cloud computing has emerged as a popular business model for utility computing system. The concept of cloud is to provide computing resources as a utility or a service on demand to customers over the Internet. The concept of cloud computing is to achieve resource virtualization [1]. Cloud computing plays a major role in the business domain [2]. Many definitions of cloud computing exist based on the individual point of view or technology used for system development. In general, we can define cloud computing as a business model that provides computing resources as a service on demand to customers over the Internet [3].

Cloud provides *pool computing resources* together to serve customers via a multi-tenant model. Computing resources are delivered over the Internet where customers can access them through *various client platforms*. Customers can access the resources *on-demand* at any time without human interaction with the cloud provider. From a customers' point of view, computing resources are infinite, and customer demands can rapidly change to meet business objectives. This is facilitated by the ability for cloud services to *scale resources up and down* on demand leveraging the power of virtualization. Moreover, cloud providers are able to *monitor and control* the usage of resources for each customer for billing purposes, optimization resources, capacity planning and other tasks.

Cloud storage is one of the services in cloud computing which provides virtualized storage on demand to customers. Cloud storage can be used in many different ways [4].

Since storage space is limited within an organization, it has to be utilized in an efficient manner. When different users share the storage, there may be lot of duplicate data across the files that belong to those users. Storing the identical content or same file in different locations or devices happen either intentionally for the sake of reliability or due to negligence. Irrespective of the reason if the amount of duplicate data exceeds a threshold then the resource utilization of the cloud reduces drastically.

To solve these problems, data de-duplication [5] technique is applied to eliminate the redundant data and utilize the storage space in an optimized manner. Data deduplication is a

specialized technique for eliminating duplicate copies of repeating data. This technique is used to improve storage utilization and can also be applied to network data transfer to reduce the number of bytes to be sent. It splits the file into several chunks and computes the hash value for those chunks. The hash value of a chunk is termed as its chunkID. A chunk index is maintained with the chunkID and the location of the corresponding chunk. Whenever a chunk of a file enters the storage, its chunkID is compared against the chunk index to detect whether it is a duplicate chunk. Since only chunks of the file are maintained in the storage, it is necessary to maintain the chunkIDs that constitute the file. This is termed as File Recipe.

In this paper, we try to use the properties of B+ tree. B+ tree (BPlusTree) is a type of balanced tree which represents sorted data in a way that allows for efficient insertion, retrieval and removal of records. B+ trees are effectively used in Relational Data Base Management System (RDBMS) [6]. The strength of B+ tree is that all paths from the root to leaf are the same length. It is suitable for indexing large amount of data so that the system can quickly search duplication data and store instance data if it doesn't find any duplication.

The objective of this paper is to propose an efficient structure for the maintenance of the chunk indices that improve the performance of duplicate detection and file retrieval. Rest of the paper is organized as follows: Section 2 discusses the works related to this paper, Section 3 describes the proposed system architecture and modules, Section 4 discusses the experimental results and Section 5 concludes the work.

II. RELATED WORKS

Many research articles have been published regarding the data deduplication. The idea proposed by Jaehong Min, Daeyoung Yoon, and Youjip Won [7] uses an LRU-based index partitioning and context aware chunking mechanism to improve the efficiency of the deduplication process. The proposed LRU indexing mechanism results in extra search time for least recently used chunk index.

Tin Thein Thwel and Ni LarThein [8] have used hash algorithm for creating ChunkID to check duplicate data and an indexing mechanism to speed up the searching facility to identify redundant chunks. The proposed framework uses the minimum and maximum thresholds to eliminate very large-sized and very small-sized chunks which increase the number of chunks which in turn increases the size of look-up table and searching time.

Waraporn Leesakul, Paul Townend and Jie Xu [9] have proposed a dynamic data deduplication scheme for cloud storage, in order to fulfill balance between changing storage efficiency and fault tolerance requirements. In dynamic data deduplication mechanism there is a single metadata server and this could cause scalability problems and also result in a single point of failure.

Prabavathy B, Subha Devi M, Chitra Babu [10] have proposed distributed multi-index for efficient storage when different types of files are handled. Though this idea is well suited for easy computation for the different types of files this suffers from additional overhead in maintaining distributed multi-index for the files.

III. PROPOSED WORK

The objective of the proposed system is to reduce data volumes so that it could help cluster administrators to reduce the cost of running large storage system. This objective is achieved by implementing an efficient data structure that reduces the storage space for chunk_ID and thus it helps to achieve faster retrieval rate of the file. The system architecture and various functional modules of the proposed system are shown as below.

3.1. System Architecture

System Architecture for the proposed data deduplication is as shown in the Figure 1. The functions of various modules are described in this section.

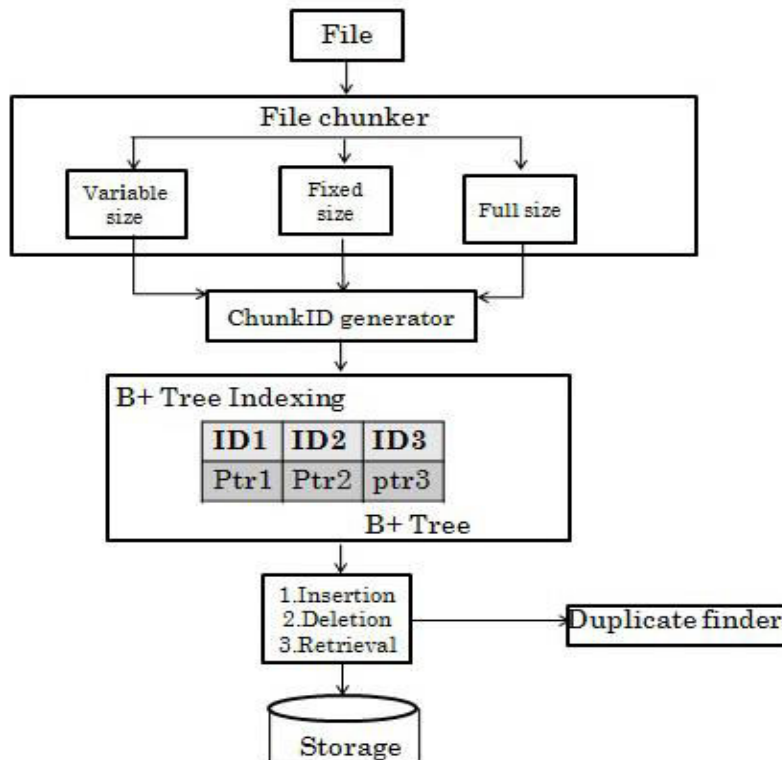


Figure 1. System Architecture

The system includes the following major components: File Chunker, Chunk_ID Generator, Duplicate Finder, Metadata and Storage. The system is able to deal with different file formats such as .PDF, .html, .txt, .doc, etc. Input files are separated into variable length chunks by File Chunker. The Chunk-ID Generator uses the resulted chunks from the File Chunker to generate Chunk_ID by applying Secure Hash Algorithm 1(SHA1).SHA1 produces 160 bits signature for each chunk. Duplicate Finder checks whether that Chunk_ID already exists or not in the Metadata. The resulted Chunk_IDs generated from the Chunk ID Generator are used to construct B+ tree index structure and maintains as metadata. The content of the chunk data are stored in the storage space.

3.2 Functional Modules

A) **File Chunker:** In order to segment the input files as the chunk, Two Threshold Two Divisor [TTTD] algorithm [12], is used which applies a minimum and maximum size threshold when setting the boundaries for every chunk. It uses four parameters- maximum threshold, minimum threshold, main divisor, and the secondary divisor. The maximum and minimum thresholds are used to eliminate very large sized and very small sized chunks in order to control the variations of chunk-size. The main divisor is used to make the chunk size close to our chunk size. The TTTD algorithm is shown below.

Algorithm(T_{min} , T_{max} , D , $Dbkp$)

T_{min} - Minimum chunk size threshold, T_{max} - Maximum chunk size threshold

D - Main Divisor, Dbkp - Backup Divisor
Begin Initialize : currentPosition \leftarrow 0, lastBreakPosition \leftarrow 0, backupBreak \leftarrow 0
Loop L1 : while !endOfFile(inputStream)
 c \leftarrow getNextByte(inputStream)
 Hash \leftarrow updateHash(c)
 if currentPosition - lastBreakPosition < Tmin
 then Goto L1
 If Hash mod Dbkp = Dbkp - I
 then backupBreak \leftarrow currentPosition
 If Hash mod D = D - 1 then
 addBreakpoint(currentPosition)
 backupBreak \leftarrow 0
 lastBreakPosition \leftarrow currentPosition
 Goto L1
 If currentPosition - lastBreakPosition < Tmax
 then Goto L1
 If backupBreak \neq 0 then
 addBreakPoint(backupBreak)
 lastBreakPosition \leftarrow backupBreak
 backupBreak \leftarrow 0
 else addBreakpoint(currentPosition)
 lastBreakPosition \leftarrow currentPosition
 backupBreak \leftarrow 0
 Goto L1
End

B) Chunk_Indexing: Chunk Indexing is achieved through two functional modules namely B+ tree indexing and Duplicate finder.

- *B+ Tree Indexing* – B+ Tree indexing organizes the chunkIDs generated using ChunkID generator in a B+ Tree.
- *Duplicate Finder:* The Duplicate Finder finds the duplicate ChunkID in the existing B+ Tree indexing structure with the incoming ChunkID. Algorithm for Duplicate Finder is as follows:

DuplicateFinder(chunkID, chunkIDMetadata, Chunk)
Begin
 found ~ searchInBPlusTree(chunkID)
 if found in BPlusTree
 then appendBPlusTree(chunkIDMetadata)
 else updateBPlusTree(chunkID, chunkIDMetadata)
 store(chunk)
 endif

End

C) Operations on Chunks(Storage) : The Storage module is responsible for insertion, deletion and retrieval of files.

- **Insertion of file** - Inserts chunks of the file if chunkID is not already found in the index data structure. This is the crucial module in the implementation of the system as this reduces the search time for a file and reduces the database storage. The system inserts chunkID if the ID is unique. If the chunk already exists the reference code is incremented instead of storing it again. This reduced storage space and also brings down the search time during retrieval

Algorithm Insert(ChunkID)

Begin

```

if chunkID found then
    increment reference count
else insert chunkID in B+ tree
end if

```

End

- **Deletion of file**-The chunk deletion algorithm deletes the chunkID from the tree or just decrements the reference count depending on the number of files using that chunk currently. The reference count maintains the number of files that uses that particular chunkID at that particular time.Reducing the count implies that the chunk will no longer be used by any file and thus the chunk gets removed from the database. The ChunkID is removed from the B+ Tree.

Algorithm Deletion(ChunkID)

Begin

```

if reference count equals 0
then delete the chunkID from B+tree
    reconstruct B+ tree
else decrement the reference count
endif

```

End

IV. PERFORMANCE EVALUATION

We have evaluated the proposed scheme in terms of retrieval time. We have compared the performance of the B+ tree based TTTD system against the conventional linear search. When a request arrives to retrieve a file, the corresponding file recipe is obtained. It is forwarded to the storage node where the indices for files is maintained. The locations of the actual chunks are identified from the chunk index and the corresponding storage nodes are contacted. All the chunks that are retrieved from different storage nodes are combined to constitute the file. The constituted file is then provided to the user for his perusal. The hierarchical index with on-disk B+ tree and sequential index are implemented to hold reasonably large number of chunkID entries. File size varies from 10 KB and 1 MB in our experimentation. We have compared the retrieval through B+ tree against the conventional sequential search. We have tabulated our findings in Table 1.

TABLE 1
Performance analysis of retrieval time of files

S.No.	File Size	No.of Chunks	Retrieval Time(in sec)	
			B+ Tree with Hashtable	Sequential
1	10 KB	5	0.124	1
2	50KB	10	0.313	4
3	100KB	26	0.501	10
4	500KB	112	11	14
5	1 MB	257	42	52

V. CONCLUSION

Cloud storage services provided in cloud computing has been increasing in popularity.In order to efficiently utilize the storage space, an efficient deduplication mechanism based on TTTD algorithm has been defined and implemented. Consequently, the storage which was enabled with deduplication contains only the unique chunks of files in storage. In order to facilitate the identification of duplicate chunks while storing and also to retrieve and reconstruct the file from the chunks, chunk index and file recipe are maintained. Chunk index entries of the entire storage cluster are split into several indices. These indices are distributed across different storage nodes. Experiments were conducted to choose a suitable index structure to organize the

chunk entries for their quick retrieval. Workload consisting of different types of files with various sizes are deduplicated and stored in the B+ tree data structure.. The retrieval time for different types of files are computed with the distributed multi-index and is compared against the time taken with the sequential index. Results show that the distributed multi-index performs considerably better compared to the sequential index especially in small sized files.

REFERENCES

- [1] I. Foster, Z. Yong, I. Raicu, and S. Lu, "Cloud Computing and Grid Computing 360-Degree Compared," in Grid Computing Environments Workshop, 2008. GCE '08, 2008, pp. 1-10.
- [2] T. Dillon, W. Chen, and E. Chang, "Cloud Computing: Issues and Challenges," in Advanced Information Networking and Applications (AINA), 2010 24th IEEE International Conference on, 2010, pp. 27-33.
- [3] T. G. Peter Mell, "The NIST Definition of Cloud Computing," National Institute of Standards and Technology NIST Special Publication 800- 145, september 2011.
- [4] SNIA Cloud Storage Initiative, "Implementing, Serving, and Using Cloud Storage,"Whitepaper 2011
- [5] W. Zeng, Y. Zhao, K. Ou and W. Song. "Research on cloud storage architecture and key technologies." In Proceedings of the 2nd International
- [6] ayer.R and Me. Creight, "Organization and Maintenance of Large Ordered Indices", Acta Informatica, Volume I, Springer Berlin/Heidelberg, New York, 1972, pp. 173-189. Conference on Interaction Sciences: Information technology, Culture and Human, pp. 1044-1048. ACM, 2009.
- [7] Jaehong Min, Daeyoung Yoon, and Youjip Won, "Efficient Deduplication Techniques for Modern Backup Operation", IEEE Transactions on computers, Vol. 60, No. 6, June 2011
- [8] Tin Thein Thwel and Ni LarThein, "An Efficient Indexing Mechanism for Data Deduplication", International Conference on Current Trends in Information Technology(CTIT),2009.
- [9] Waraporn Leesakul, Paul Townend, Jie Xu, "Dynamic Data Deduplication in Cloud Storage" , IEEE 8th International Symposium on Service Oriented System Engineering, 2014
- [10] Prabavathy B, Subha Devi M, Chitra Babu, "Multi- Index Technique for Metadata Management in Private Cloud Storage", International Conference on Recent Trends in Information Technology (ICRTIT), 2013
- [11] D. Bhagwat, K. Eshghi, D. D. E. Long and M.Lillibridge. "Extreme Binning:Scalable, parallel deduplication for chunk-based file backup", IEEE International Symposium on Modeling, Analysis and Simulation of Computer and Telecommunication Systems, pp. 1 - 9, 2009 [11]. Extreme Binning exploits file similarity instead of locality, and makes only one disk access for chunk lookup per file. It allows some redundant chunks, which leads to the decrease of the compression ratio of deduplication.
- [12] Eshghi, K., "A Framework for Analyzing and Improving Content-based Chunking Algorithms", Technical Report HPL-2005-30(R. I), HewlettPackard Laboratories, Palo Alto, CA, 2005.

SECURE ROLE BASED ACCESS CONTROL ON ENCRYPTED DATA IN CLOUD STORAGE

Sarah S ¹, Kalaimagal N ², Abila G ³

[1] Associate Professor, Department of IT

[2] [3] B. Tech Final Year IT

Kingston Engineering College

Vellore, India

sarah@kingston.ac.in, kalaichellam22@gmail.com, abila1894@gmail.com

Abstract: With the rapid developments occurring in cloud computing and services, there has been a growing trend to use the cloud for large-scale data storage. This has raised the important security issue of how to control and prevent unauthorized access to data stored in the cloud. One well-known access control model is the role-based access control (RBAC), which provides flexible controls and management by having two mappings, users to roles and roles to privileges on data objects. We propose a secure role-based encryption (SRBE) scheme which integrates the cryptographic techniques with RBAC. Our SRBE scheme allows RBAC policies to be enforced for the encrypted data stored in public clouds. Based on the proposed scheme, we present a secure RBE based hybrid cloud storage architecture which allows an organization to store data securely in a public cloud, while maintaining the sensitive information related to the organization's structure in a private cloud.

Keywords: Cloud computing, RBAC, SRB

I. INTRODUCTION

Hybrid cloud environment is used to provide secured sharing of data in an enterprise. RBE scheme is used to encrypt the data stored in the cloud. RBAC policy is used to assign roles for accessing the data in the cloud. RBAC Policy is used for role based access to the data in public cloud. Mapping Users to roles and Roles to access/Privileges on data in the cloud environment. Third party key distribution is used to share keys for encryption and decryption. Third party Authentication mechanism is used to authenticate the system via trust centre.

II. RBAC SYSTEM

Secured Secret key distribution is not done in cloud computing. User authentication for providing secret key and role is also not done. Re-Encryption of data is done, after user is being revoked. In Role Based Access Control, the users are revoked by not affecting other roles/users. Third party secret key distribution is done for encryption and decryption. Secure Role Based Encryption is used for encryption and decryption of data. RBAC Policies enforces to access the data by getting roles for the user. User's management is done by the system administrator. The secret key is encrypted by the use of Third party Key Distribution. Three party Authentication mechanisms are used to authenticate users. Decryption of data is done by using ISAAC algorithm.

The Architecture of the Secure Role Based Access Control is depicted below:

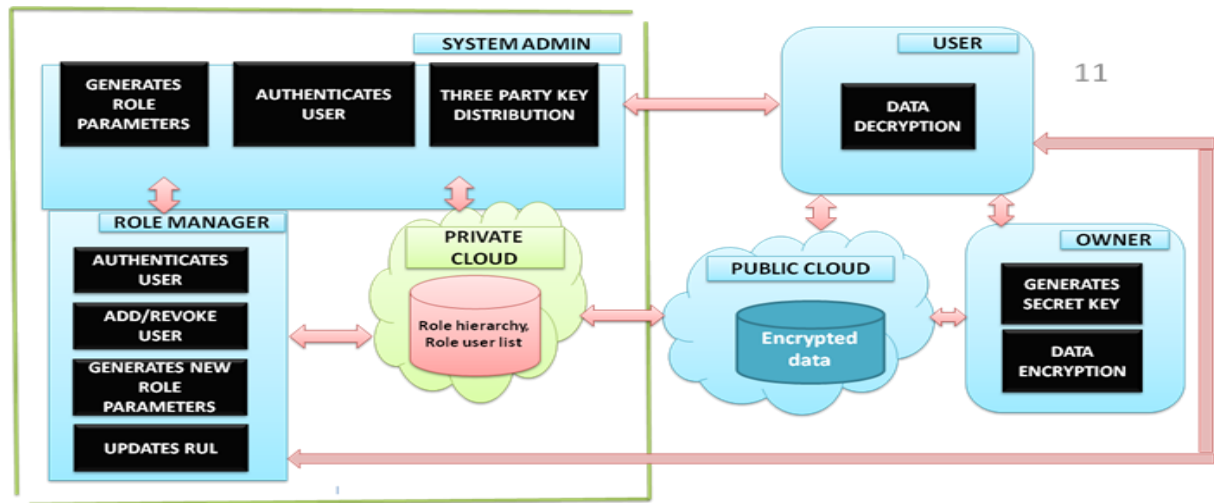


Fig.1.1 Role Based Access Control Architecture

III. DESCRIPTION

1. SYSTEM ADMINISTRATOR (SA):

System Administrator is the certificate authority of the organisation (i.e) trusted third party. SA computes the role parameters to put that role into the organisation's hierarchy. Role parameters represents the position of the role and stored in the private cloud. SA updates the parameters for the role in private cloud when any changes occur in role hierarchy. Administrator provides User with the Secret Decryption Key by verifying the user with identity signed by owner. SA provides Role Manager with Role Secret Key for the Role Manager to add or revoke user.

2. ROLE MANAGER (RM):

Role Manager manages the relationship between users and roles. Each role has its own role parameters defining the user membership and stored in private cloud. The Role Manager computes new role parameters when updating them in the private cloud. It provides user with a position by assigning a role to user.

3. OWNER:

Owner requests for Role public parameters to public cloud which is forwarded to private cloud. Owner computes ISAAC algorithm and generates key for encryption. Encrypted data is stored in public cloud. Secret key with the list of IDs signed by Owner is sent to System Admin through Third party Key Distribution. When the user approaches Owner for permission, Owner provides user with ID with his signature.

4. USER:

User requests for Role public parameters from private cloud through public cloud. User downloads Encrypted data from public cloud. User requests permission from Owner, where owner grants user with ID and signature. User gets authenticated by Role Manager and gets

assigned with a role. User requests for Decryption Key from System Administrator. Data Decryption is done by User.

IV. ALGORITHM USED:

1. Elliptical Curve Cryptography

ECC is an approach to public key cryptography based on the algebraic structure of elliptic curves over finite fields. It is used to generate key pair for encrypting data in public cloud. Using the key pair, Data in public cloud will be encrypted by using ISAAC Algorithm. Then, it is again stored in public cloud.

2. ISAAC Algorithm

The ISAAC key stream generator is a fast software-oriented encryption algorithm. It is one of the Stream cipher algorithm. It encrypts individual characters of a plaintext message one at a time, using an encryption transformation, which varies with time. With the generated key pair data with particular role(plaintext) will be encrypted using this algorithm.

3. IBS Algorithm

ID based Signature algorithm is a type of public key cryptography which is used to sign the User ID. To securely transfer the decryption key to user, third party authentication is required. System Admin acted as third party who has the signed User ID with decryption. It is then verified by user who has signed user ID. So , decryption key is provided to user to decrypt the data in Public cloud.

4. Three Party Key Distribution

Three party Key Distribution Protocol to safeguard the security in larger networks, which uses the merits of classical cryptography. User requests for Public Role parameters from private cloud through public cloud. User requests for permission to the owner to get the decryption key. Role Manager authenticates User with the signed ID and assigns Role to the User. User requests System Administrator, where SA verifies the signed ID using IBS algorithm .SA grants the decryption key to the user after verifying.

V. IMPLEMENTATION

1. Microsoft One drive – Public cloud

Microsoft One drive is a file hosting service allowing users to upload and synchronize files to a cloud storage and then access them from a web browser or a local device. It is used as Public cloud here. It is used to store the encrypted data by owner. Owner using the role public parameters from private cloud(PUBR) to encrypt the data in the public cloud.

2. Dropbox – Private cloud

Drop Box is a cloud storage which can be used as a private cloud. Drop box is used in this concept to store roles to be assigned to the users.

After getting the role parameters database from Hyper SQL, that is uploaded in private cloud.

3. Hyper SQL

Hyper SQL is a relational database management system written in java. It has a JDBC driver and offers both in-memory and disk based tables. It is used to create the database to store role

public parameters for encrypting the data which is stored in public cloud. Using command prompt java files are compiled and database is created to run the query statements. Using Elliptical cryptography, Key pair is generated. Key pair is stored in private folder for safety purpose.

4. Expand drive – Cloud connector

Expand drive is used to connect the two clouds as cloud connector. Two drives are created to copy the required files in another drive

In our paper *data.txt* in Dropbox drive is copied and pasted in One drive to encrypt the data with the role parameters.

5. ISAAC Encryption

The secret message is first entered by owner of the data. The role to which the data can be accessed is assigned by owner. A new text document *encdata.txt* is created to store the encrypted data. The public key generated is used to encrypt the data using Vernam cipher.

6. ISAAC Decryption

The text document *encdata.txt* contains the secret message in encrypted form. The file is stored in one drive which is a public cloud. Later the file is downloaded by the authorized user for decryption. The secret key is shared by Third party key distribution. The secret message is downloaded from Microsoft one drive. With the secret key decryption of the message is done.

VI. PERFORMANCE EVALUATION

1. Determination of Metrics Involved

By using ISAAC and RSA algorithms the performance of encryption and decryption process of text files is calculated through the throughput parameter. Encryption time is calculated as the total plaintext in bytes encrypted divided by the encryption time. Decryption time is calculated as the total plaintext in bytes decrypted divided by the decryption time.

Throughput of encryption = Tp/Et

Tp: total plain text (bytes)

Et: encryption time (second)

2. Performance Evaluation of RBAC System

ISAAC and RSA algorithms can be implemented to different size of text files. Comparison of encryption and decryption time for text files has been done for different text files. This analysis helps to better the performance of the system by showing that it is judicious to use ISAAC algorithm for encrypting different sizes of text files with high throughput. Increase in throughput will speed up the encryption and decryption process.

VII. CONCLUSION

This Paper proposed a new SRBE scheme that achieves efficient user revocation. This Proposed work presented a RBAC based cloud storage architecture which allows an organization to store data securely in a public cloud. Identity based signature algorithm is used to authenticate the user by signing the identity. Therefore, with the third party key distribution, the secret key is distributed to the administrator of the organization with user identity information. Further security against attacks is achieved. Size of the encrypted and decrypted data can be made constant which will reduce security attack. Authorization can be

improvised by other techniques rather than using ID so that many attacks can be avoided. ISAAC algorithm is executed lesser processing time and more throughput level as compared to RSA algorithms. In future, we can evaluate the performance of audio and video files for other parameters such as, memory usage and output byte.

REFERENCES:

- [1] Lan Zhou, Vijay Varadharajan, and Michael Hitchens “Achieving Secure Role-Based Access Control on Encrypted Data in Cloud Storage” IEEE Transactions On Information Forensics and Security, vol. 8, no. 12, pp. 1947-1960, December 2013.
- [2] Zhu Tianyi, Liu Weidong, Song Jiaying “An efficient Role Based Access Control System for Cloud Computing” Computer and Information Technology (CIT), 2011 IEEE 11th International Conference, pp. 97-102,2011.
- [3] Marina Pudovkina “A known plaintext attack on the ISAAC keystream generator” Journal of "Security of information technologies", Moscow, pp. 23-40,2011.
- [4] Wenhui Wang , Jing Han ,Meina Song, Xiaohui Wang “The Design of a Trust and Role Based Access Control Model in Cloud Computing” Pervasive Computing and Applications (ICPCA), 2011 6th International Conference , pp. 330-334,2011
- [5] Ramgovind S, Eloff MM, Smith E ‘The Management of Security in Cloud Computing’ School of Computing, University of South Africa.
- [6] R. Bhadauria, R. Chaki, N. Chaki and S. Sanyal, "A Survey on Security Issues in Cloud Computing, " arxiv.org, arXiv: 1204.0764, 2012.
- [7] S. Sanyal, R. Bhadauria and C. Ghosh, "Secure Communication in Cognitive Radio" International Conference on Computers and Devices for Communications, CODEC-2009, 2009.
- [8] D. P. Agrawal1, H. Deng, R. Poosarla and S Sanyal, "Secure Mobile Computing, " Distributed Computing – IWDC 2003, Springer Berlin/ Heidelberg, 2003, pp. 265-278.
- [9] Dinesha H A1, Prof.V.K Agrawal2, “Framework Design of Secure Cloud Transmission Protocol “, IJCSI International Journal of Computer Science Issues, Vol. 10, Issue 1, No 1, January 2013
- [10] S. Sanyal, R. Bhadauria and C. Ghosh, "Secure Communication in Cognitive Radio," International Conference on Computers and Devices for Communications, CODEC-2009, 2009.

Junction less TFET for Performance Driven Mobile System

KondaVenkata Ashok¹, Dr. P. Aruna Priya²

¹Dept.of Electronics and Communication Engineering, SRM University, ashoksai436@gmail.com

²Dept.of Electronics and Communication Engineering, SRM University, Arunapriya.p@ktr.srmuniv.ac.in

Abstract—Tunnel Field Effect Transistor (TFET) are gaining attention because of good scalability and they have very good leakage current. However, they suffer from low ON-current and high-threshold voltage. In this paper; we have proposed an optimal design for Hetero-Junctionless Tunnel Field Effect Transistor (TFET) using HfO₂ as a dielectric. The device performance and principle are investigated using Sentaurus TCAD Simulator. During this we investigated the Energy Band Diagram Characteristics, Id vs V_{gs} Characteristics and Id vs V_{ds} Characteristics of our proposed device. Numerical Simulations Resulted in outstanding performance of the H-JLTFET resulting in I_{on} ~ 0.02A at room temperature and V_{dd} of 0.5V. This indicates that the H-JLTFET can play an important role in the further development in the low power switching applications.

Keywords—Hetero Junctionless Tunnel Field Effect Transistor (H-JTFET), Low Power Switching Applications, Tunnel Field Effect Transistor (TFET).

I. INTRODUCTION

Metal Oxide Semiconductor Field Effect Transistors (MOSFETS) present several challenges for sub 20-nm Technology because of their steep doping profiles at source and drain junctions. Junctionless FETs provide a solution to this problem as they do not have doping junctions [1]-[3]. They are also suited for high speed applications but their high sub threshold swing, as in complementary metal oxide semiconductors (CMOS), makes them power consuming devices. TFETs have received attention for low power applications because of their low sub threshold swing [4]-[7]. However the low ON current hinders them from many other high speed applications.

Now, Junctionless Tunnel FETS are the subject of intensive studies in device research as they have a low sub threshold swing along with a high ON Current, giving a better speed [8][9]. This device structure utilizes the quantum tunneling using a charge plasma concept. Additionally, it does not have any doping junctions. It has established itself as one of the most promising candidates for future logic circuits, which operate at supply voltages smaller than 0.5V. Moreover, the process budget is reduced because of the junctionless channel. Also, JLTFETs show better electrical performance and less variability than MOSFETs [10]. Because there are no p-n junctions. In this paper we proposed and investigated a new material channels causing higher tunneling in ON state and reduced tunneling in an OFF state. As a result there is improvement in the performance. We have optimized our device Structure using Sentaurus TCAD.

II.DEVICE STRUCTURE AND SIMULATION CONDITIONS

A.Device Structure:

H-JLTFET is made up of dual n+ control gate and dual p+ auxiliary gate at source side. However, channel which is highly doped with uniform n-type region, has work function of $\sim 4.1\text{eV}$ causing creation of p+:i:n+ region due to differences in work function. H-JLTFET has junction between two semiconductors instead of doping junctions in MOSFET.

Heterojunction increases tunneling in device and hence results in higher I_{on} and I_{on}/I_{off} with lower subthreshold swing(ss). Fig1 shows different materials for H-JLTFET channel with Junction Positioning at 45nm.

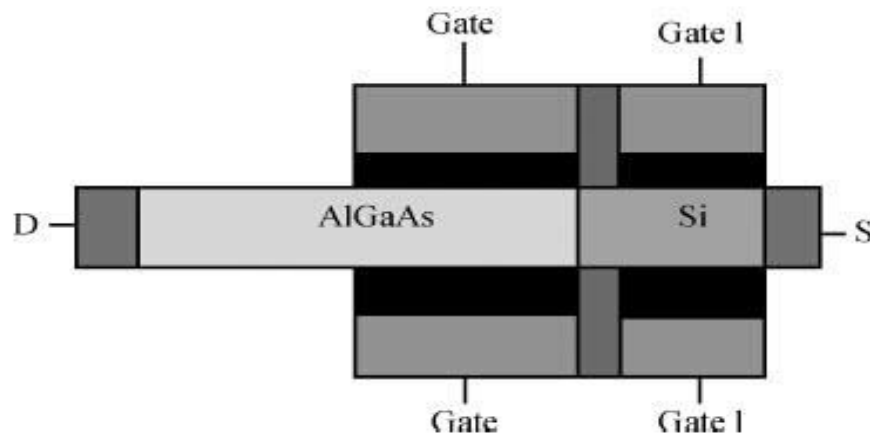


Fig1: Structure of H-JLTFET with junction position at 45nm

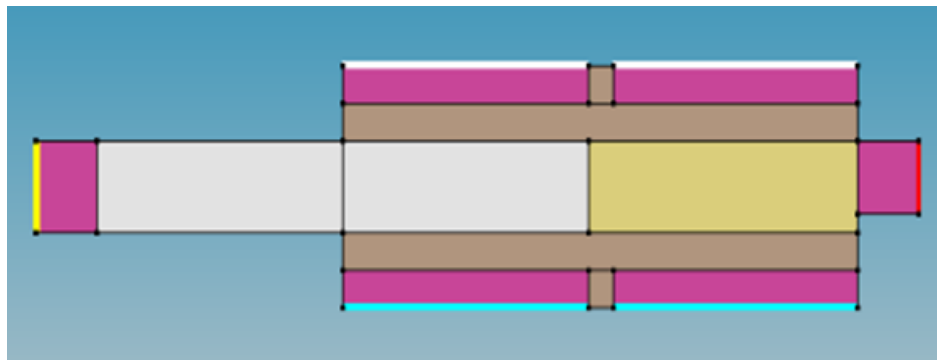


Fig:2 Structure of JL-TFET using Sentaurus TCAD

The materials are chosen on the basis of their electrical properties, especially the band gap. Accordingly, GaAs:Ge and InAs:Si were chosen, which have shown good characteristics. Fig

3 and 4 shows the Energy Band Diagrams for Junctionless TFET and Hetero Junctionless TFET.

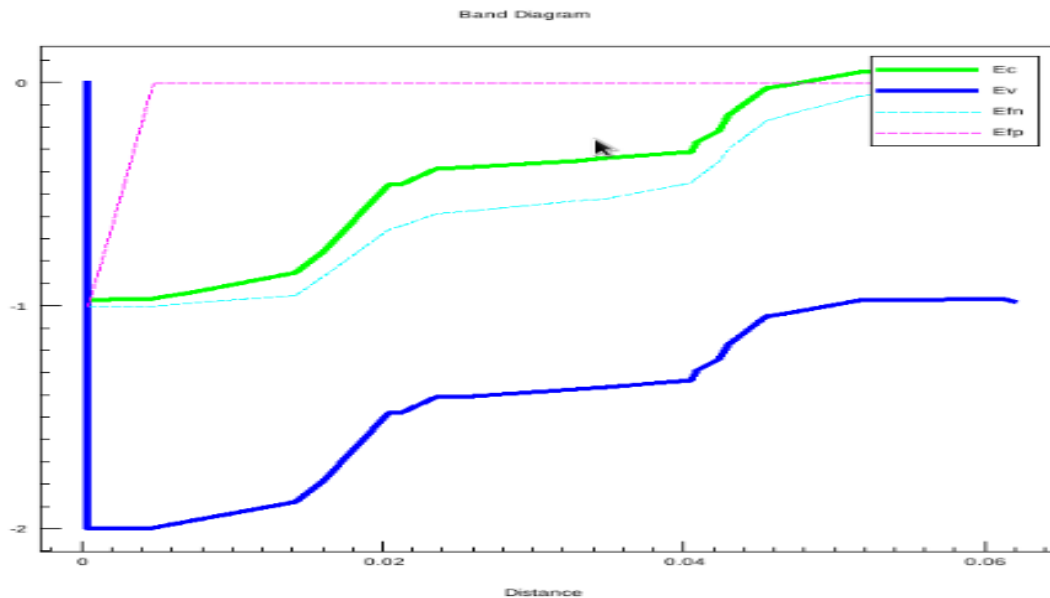


Fig3: Energy Band Diagram for Junctionless TFET (JLTFET)

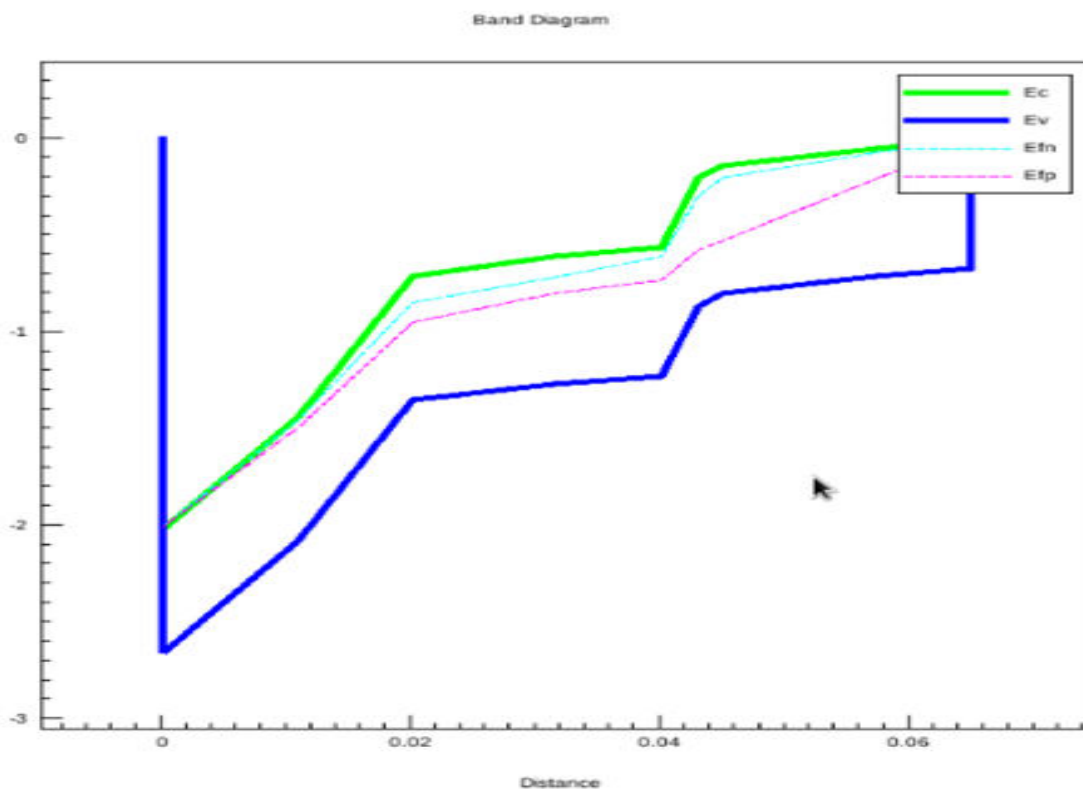


Fig4: Energy Band Diagram for Hetero Junctionless TFET (H-JLTFET)

B. Simulation Setup:

Simulations are done in Sentaurus TCAD using Band-to-Band Tunneling model for including the effect of tunneling [21]. Nonlocal models are used that are independent of electric field at

individual mesh points as tunneling current depends on the band structure along the cross section taken through the device. Apart from that, band gap narrowing model is used because of highly doped channel. Shockley-Read-Hall model is included for transitions that occur in the presence of traps and defects [22], Schenk's trap assisted model is used to account for electrons tunneling through the band gap via trap states [23] and quantum confinement (QC) model [22], [24] for interface trap effect and QC effect due to heavy doping and thin oxide. The parameters used for device simulation of III-V are tabulated in Table 1.

III. OPTIMIZATION OF H-JLTFET

ON-state tunneling occurs at source side and hence the presence of heterojunction near source causes better I_{on} as it creates steeper bands and increase the overlap energy levels. Maximum value of I_{on} depends on source side material as it contributes to ON-state tunneling. GaAs:Ge gives best performance as germanium at source side has low band gap of 1.43 eV causing lower tunneling and resulting in good I_{on}/I_{off} . After varying GaAs:Ge interface position throughout the channel, we observed highest ON-current when interface was at 45nm. Lowest OFF-current was observed when interface was at 67 nm. i.e., only GaAs was present in the channel. Similarly, the simulation resulted highest drain current for heterostructures of GaAs:Si and Si:SiGe when junctions were at 50 and 45 nm, respectively. ON-state tunneling occurs from valance band of source to conduction band of channel. In addition to tunneling at drain side in OFF state i.e., from valance band of channel to conduction band of drain as in JLTFET, H-JLTFET has contribution from source side also, i.e., from valance band of source to conduction band of channel.

IV. RESULTS AND DISCUSSIONS

Fig.5, 6 and 7 shows a comparison of the $I_d - V_g$ Characteristics of our proposed device with the Si-JLTFET and H-JTFET With the same dimensional parameters. It can be observed that the proposed device has much better device characteristic than other. Further, I_{on} of 0.02 A/ μ m and 0.02 μ A/ μ m are observed for the H-JTFET and JTFET respectively. The TFET has lower OFF state current than the JLTFET, as the JTFET has no physical junction but rather junctions created by charge plasma concept. However, the ON state current of the JLTFET is much higher than the TFET because of the inheritance of a junctionless FET. TFET and junctionless FET blended junctionless TFETS have significantly higher I_{on}/I_{off} than the TFET. The Si:InAs heterostructure tremendously improves performance in comparison to the JLTFET, due to increased band to band tunneling on the source side in the ON state. Drain induced barrier lowering (DIBL) is calculated from the following formula

$$DIBL = \frac{V_{th_{V_{DS}=1V}} - V_{th_{V_{DS}=0.05V}}}{V_{DS=1V} - V_{DS=0.05V}}$$

The H-JLTFET has a DIBL of 13.5mV/V. also, a subthreshold slope of 12mV per decade id calculated for $V_{ds}=0.7V$ and $V_{gs}=0.7V$ using the following formula

$$\text{Average subthreshold slope (SS)} = \frac{V_{th} - V_{ref}}{\log \frac{I_{th}}{I_{ref}}}$$

TABLE 1

PARAMETERS FOR DEVICE SIMULATION OF JLTFET

Parameter	Value
Source/channel/drain doping (N_D)	$1 \times 10^{19} \text{ cm}^{-3}$
Effective Oxide Thickness(T_{OX})	2 nm
Gate material workfunction	5.1 eV
Gate Length (L_g)	20 nm
Channel thickness(T_{ch})	5 nm
Supply voltage (V_{DD})	1V
Dielectric Material	HfO ₂ (29)
Interface Position in channel	45nm

The output characteristics of the H-JLTFET for V_{gs} ranging from 0.1V to 0.7V are shown in Fig. We observed an exponential increase in the drain current with increasing gate voltage, demonstrating better gate control. Also, the saturation region is flatter, indicating negligible channel length modulation. Besides, other short channel effects reported previously, especially the kink effect, are highly suppressed.

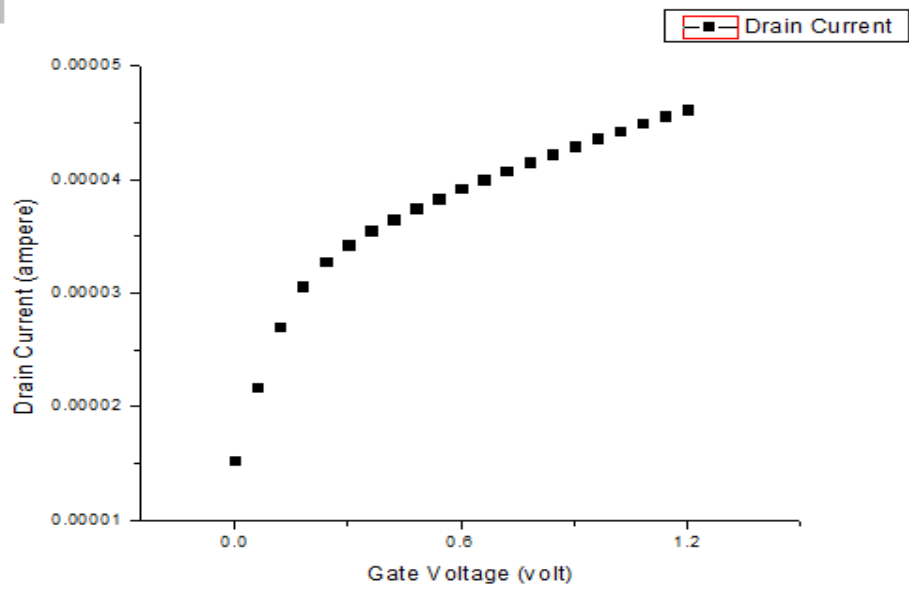


Fig5: Drain Current(I_d) vs V_{gs} for JLTFET using HfO2 as dielectric

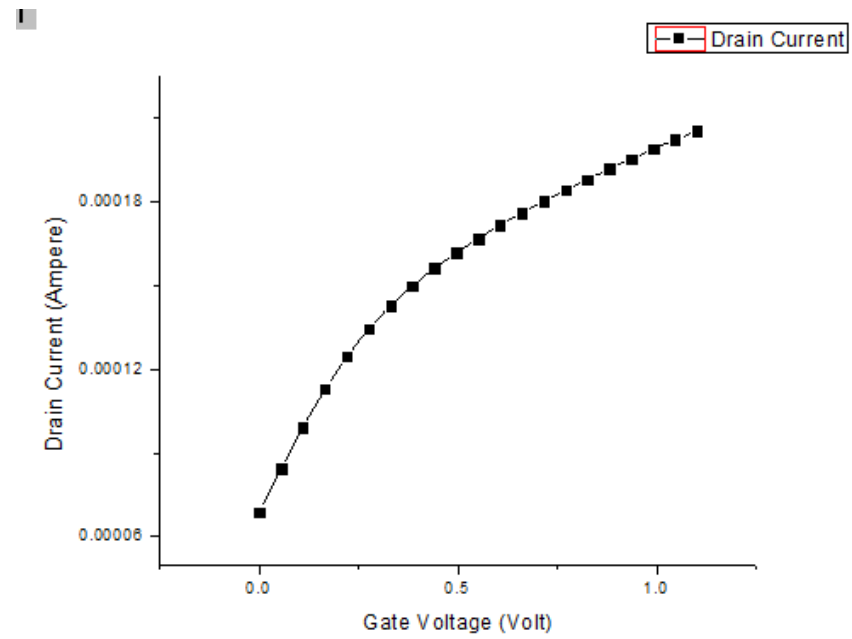


Fig6: Drain Current (I_d) Vs V_{gs} for JLTFET using Si3N4 as Dielectric

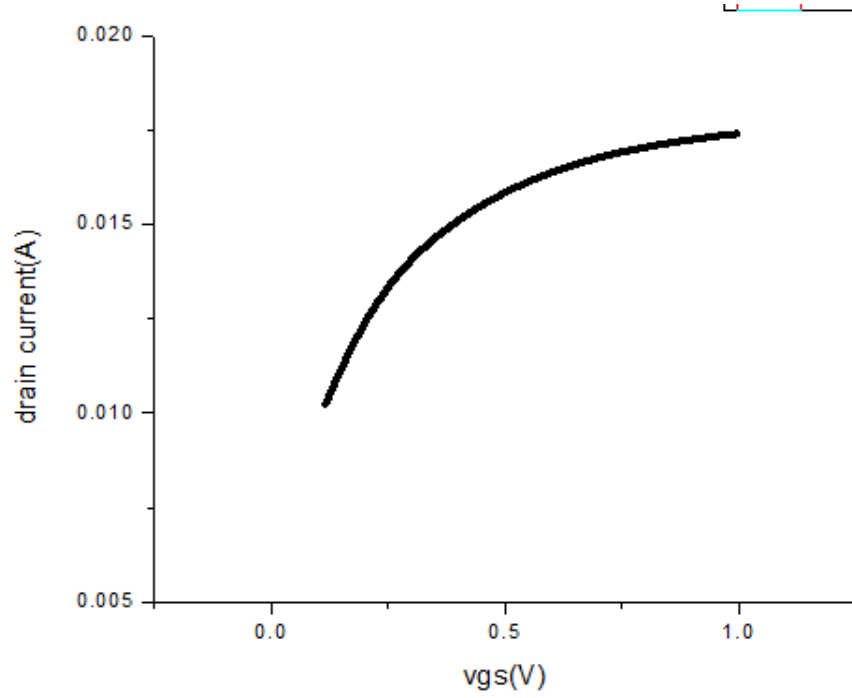


Fig7: Drain Current (I_d) vs V_{gs} for H-JLTFET using material GaAs:Ge

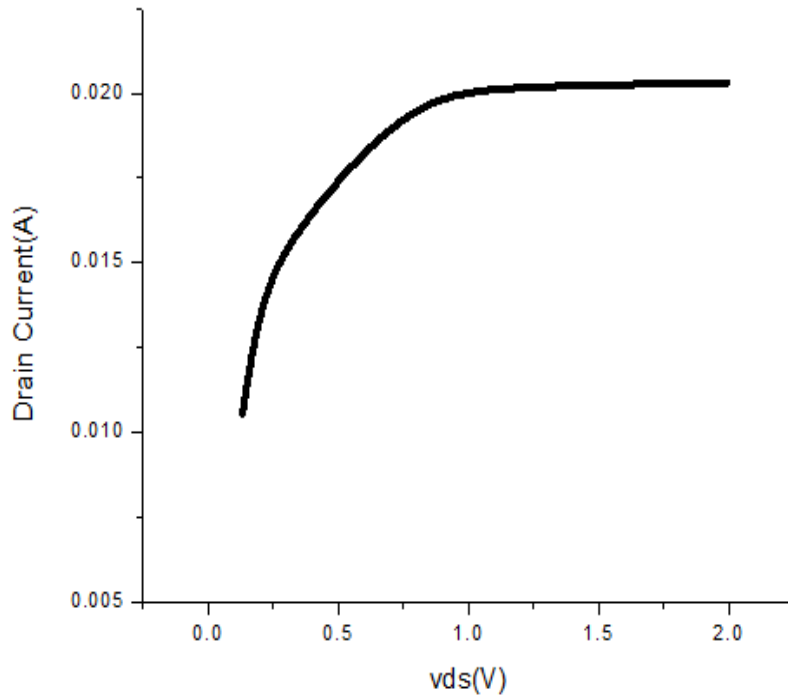


Fig8: Drain Current(I_d)vs V_{ds} For GaAs:Ge H-JTFET

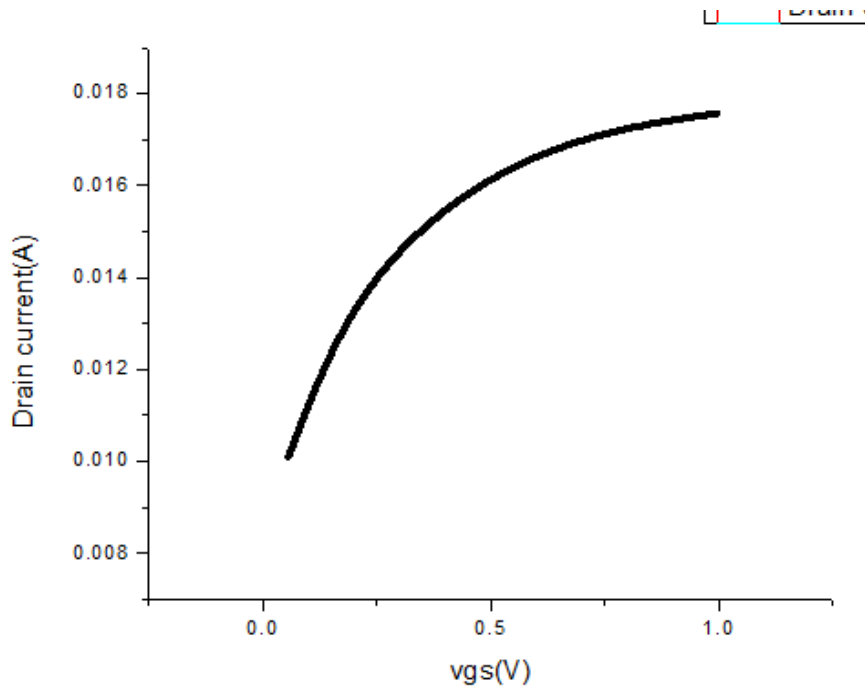


Fig 9: Drain Current(I_d) vs V_{gs} for H-JLTFET using material Si:InAs

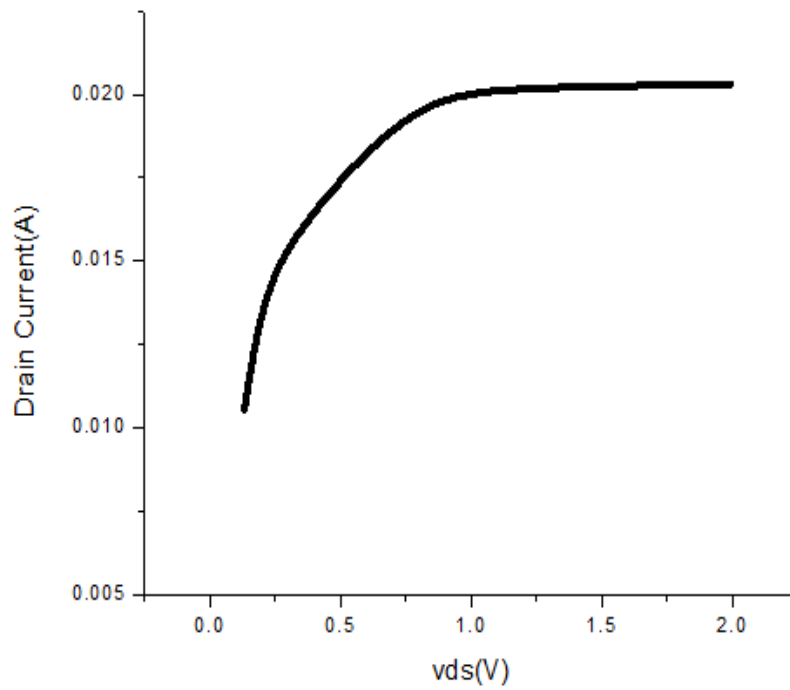


Fig 10: Drain Current (I_d) vs V_{ds} for H-JLTFET using material Si:InAs

V. CONCLUSION

In this work, we proposed an optimal design of a Hetero-Junctionless Tunnel Field Effect Transistor (H-JLTFET) using different materials like GaAs:Ge, Si:InAs etc., and HfO₂ as dielectric and discussed its static operation. Through simulation, we also studied the characteristics of H-JLTFET, especially for switching applications. The device provides high speed operation even at very low supply voltages, with low leakage and a reduced number of steps in the fabrication process, which indicates that the H-JLTFET is a promising candidate for switching performance. In addition, it has the potential for further scalability.

VI. ACKNOWLEDGEMENT

The Author expressing its gratitude to SRM Universities Research Lab for supporting this work.

VII. REFERENCES

1. J.-P. Colinge, C.-W. Lee, A. Afzalian, N. D. Akhavan, R. Yan, I. Ferain, P. Razavi, B. O'Neill, A. Blake, M. White, A.-M. Kelleher, B. McCarthy and R. Murphy, "Nanowire transistors without junctions", *Nat. Nanotechnol.*, 2010, 5(3), 225–229.
2. C.-W. Lee, A. Afzalian, N. D. Akhavan, R. Yan, I. Ferain and J.-P. Colinge, "Junctionless multigate field-effect transistor", *Appl. Phys. Lett.*, 2009, 94(5), 053511–053512.
3. C.-W. Lee, I. Ferain, A. Afzalian, R. Yan, N. Dehdashti Akhavan, P. Razavi, J. Pierre and L. Maltings, "Performance estimation of junctionless multigate transistors", *Solid-State Electron.*, 2010, 54(2), 97–103.
4. K. Boucart and A.M. Ionescu, "Double gate tunnel FET high K gate dielectric", *IEEE Trans. Electron Devices*, 2007, 54, 7.
5. A. M. Ionescu and H. Riel, "Tunnel Field-effect transistors as energy-efficient electronic switches", *Nature*, 2011, 479, 329.
6. K. Boucart, "Length scaling of the Double Gate Tunnel FET with a high-K gate dielectric", *Solid-State Electron.*, 2007, 51, 1500.
7. K. Boucart, "A new definition of threshold voltage in Tunnel FETs", *Solid-State Electron.*, 2008, 52, 1318.
8. B. Ghosh and M. W. Akram, "Junctionless Tunnel Field Effect Transistor", *IEEE Electron Device Lett.*, 2013, 34(5), 584–586.
9. B. Ghosh, P. Bal and P. Mondal, "A junctionless tunnel field effect transistor with low subthreshold slope", *J. Comput. Electron.*, 2013, 12, 428.
10. J. Xiang, "Ge/Si nanowire heterostructures as high performance field-effect transistors", *Nature*, 2006, 441, 489.
11. W. Lu, J. Xiang, B. P. Timko, Y. Wu and C. M. Lieber, "One-dimensional hole gas in germanium/silicon nanowire heterostructures", *Proc. Natl. Acad. Sci. U.S.A.*, 2005, 102, 10046.
12. ATLAS Device Simulation Software, Silvaco Int., Santa Clara, CA, USA, 2012.
13. A. Schenk, A model for the field and temperature dependence of SRH lifetimes in Silicon, *Solid-State Electron.*, 1992, 35, 1585.
14. A. Schenk, Finite-temperature full random-phase approximation model of band gap narrowing for silicon device simulation, *J. Appl. Phys.*, 1998, 84, 7.

15. W. Hansch, Th. Vogelsang, R. Kirchner and M. Orłowski, Carrier Transport Near the Si/SiO₂ Interface of a MOSFET, *Solid-State Electron.*, 1989, 32, 839.
16. C. L. Hinkle, A. M. Sonnet, E. M. Vogel, S. McDonnell, G. J. Hughes, M. Milojevic, et al., "GaAs interfacial self-cleaning by atomic layer deposition," *App. Phys. Lett.*, vol. 92, pp. 071901-1–071901-3, Feb. 2008.
17. Y. Xuan, H. C. Lin, P. D. Ye, and G. D. Wilk, "Capacitance-voltage studies on enhancement-mode InGaAs metal-oxide-semiconductor field-effect transistor using atomic-layer-deposited Al₂O₃ gate dielectric," *Appl. Phys. Lett.*, vol. 88, pp. 263518-1–263518-3, Jun. 2006.
18. P. Palestri, L. De Michielis, M. Iellina, and Selmi. (2013, Jun. 19). Challenges in the Introduction of Band to Band Tunneling in Semiclassical Models for Tunnel-FETs [Online]. Available: http://www.steeper-project.org/resources/Dissemination/Workshops/Sispad2010_Workshop/talk8_Palestri.pdf
19. (2013, Jul. 27). ATLAS User's Manual [Online]. Available: <http://www.silvaco.com>
20. A. Schenk, "A model for the field and temperature dependence of SRH lifetimes in silicon," *Solid-State Electron.*, vol. 35, no. 11, pp. 1585–1596, Nov. 1992.
21. W. Hansch, T. Vogelsang, R. Kirchner, and M. Orłowski, "Carrier transport near the Si/SiO₂ interface of a MOSFET," *Solid-State Electron.*, vol. 32, no. 10, pp. 839–849, Oct. 1989.
22. (2013, Jun. 21). ITRS Roadmap [Online]. Available: <http://www.itrs.net>
23. M. J. Kumar and M. Siva, "The ground plane in buried oxide for controlling short-channel effects in nanoscale SOI MOSFETs," *IEEE Trans. Electron Devices*, vol. 55, no. 6, pp. 1554–1557, Jun. 2008.
24. C.-H. Park, M.-D. Ko, K.-H. Kim, R.-H. Baek, C.-W. Sohn, C. K. Baek, et al., "Electrical characteristics of 20-nm junctionless Si nanowire transistors," *Solid-State Electron.*, vol. 73, pp. 7–10, Jul. 2012.
25. D. Kim, Y. Lee, J. Cai, I. Lauer, L. Chang, S. J. Koester, et al., "Low power circuit design based on heterojunction tunneling transistors (HETTs)," in *Proc. 14th ACM/IEEE ISLPED*, 2009, pp. 219–224

Security for Privacy Preserving Cloud Storage Using Key Based Method

¹R.Gnanakumari,

¹Assistant Professor, Dept. of ECE,

¹Nehru Institute of Engineering and Technology, Coimbatore-105

¹mailtokumari81@gmail.com

Abstract: The flexible distributed storage integrity auditing mechanism is utilize the homomorphism token and distributed erasure-coded data. It moves the application software and databases to the centralized large data centers, where the management of the data and services may not be fully trustworthy. Cloud Service Provider (CSP), address domain will identifies these threats; it can come from two different sources internal and external attacks. In internal attacks, a CSP can be self-interested, untrusted and possibly malicious. In external attacks, data integrity threats may come from outsiders who are beyond the control domain of CSP, for the economically motivated attackers. It allows users to audit the cloud storage with very lightweight communication and computation cost. The proposed scheme is highly efficient and resilient against Byzantine failure, malicious data modification attack, and even server colluding attacks. The cloud data are dynamic in nature, the proposed design further supports secure and efficient dynamic operations on outsourced data, including block modification, deletion, and append.

Index Terms: Data Integrity, Dependable Distributed Storage, Error Localization, Data Dynamics, CSP

1. INTRODUCTION

The Cloud service provider owns and administers the physical infrastructure on which the cloud services are provided. Site owners provide the service to their respective users via sites that are hosted by the cloud service provider. Cloud tenant running a collection of the virtual appliances that are hosted on the cloud infrastructure, the services are provided to the end users through the public internet. Moving data into the cloud offers great convenience to users since they don't have to care about the complexity of direct hardware management. One of the key issues is to effectively detect any unauthorized data modification and corruption, possibly due to server compromise or random Byzantine failures.

The main scheme for ensuring cloud data storage is presented in this section. The first part of the section is devoted to a review of basic tools from coding theory that is needed in the scheme for file distribution across cloud servers. Then, the homomorphic token is introduced. The token computation functions are considering belongs to a family of universal hash function, chosen to preserve the homomorphic properties, which can be perfectly integrated with the verification of erasure coded data. Simple storage service, Elastic Compute cloud both are internet based online services do provide huge amounts of storage space and customizable computing resources, this computing platform shift, however is eliminating the responsibility of local machines for data maintenance at the same time. Cloud infrastructures are much more powerful and reliable than personal computing devices, broad range of both internal and external threats for data integrity still exist.

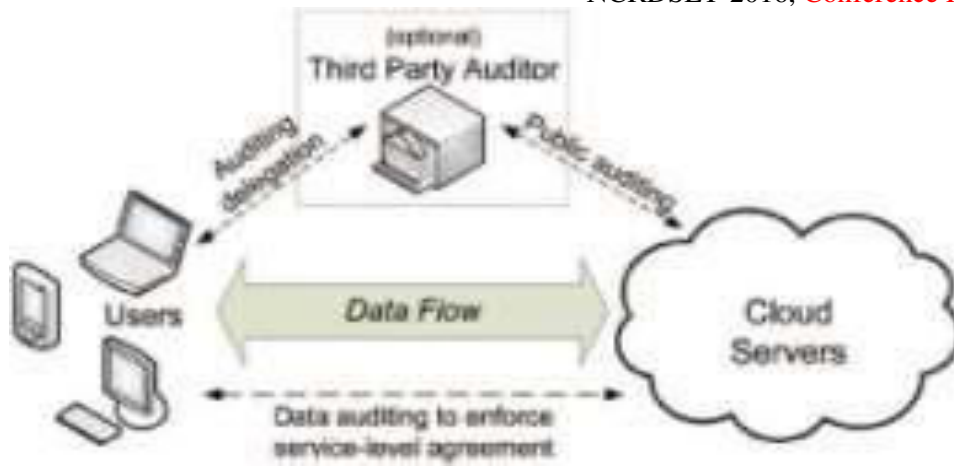


Fig. 1. Cloud storage service architecture

To propose an effective and flexible distributed storage verification scheme with explicit dynamic data support to ensure the correctness and availability of users' data in the cloud. To rely on erasure correcting code in the file distribution preparation to provide redundancies and guarantee the data dependability against Byzantine servers, where a storage server may fail in arbitrary ways.

2. LITERATURE REVIEW

A model for provable data possession (PDP) [1] that allows a client that has stored data at an untrusted server to verify that the server possesses the original data without retrieving it. The model generates probabilistic proofs of possession by sampling random sets of blocks from the server, which drastically reduces I/O costs. In a proof-of-irretrievability system, [2] The first one is privately verifiable and builds elegantly on pseudorandom functions (PRFs); the second allows for publicly verifiable proofs and is built from the signature scheme of Boneh, Lynn, and Shacham in bilinear groups. The multiple-replica provable data possession (MR-PDP)[3] a provably-secure scheme that allows a client that stores a file in a storage system to verify through a challenge-response protocol that each unique replica can be produced at the time of the challenge and that the storage system uses times the storage required to store a single replica.

Protocols are privacy-preserving [4], in that they never reveal the data contents to the auditor. The solution removes the burden of verification from the customer, alleviates both the customer's and storage service's fear of data leakage, and provides a method for independent arbitration of data retention contracts. In a proof-of-irretrievability system, a data storage center must prove to a verifier that he is actually storing all of a client's data. The central challenge is to build systems that are both efficient and provably secure that is, it should be possible to extract the client's data from any prover that passes a verification check. They create the first compact and provably secure proof of irretrievability systems.

It allows for compact proofs with just one authenticator value in practice this can lead to proofs with as little as 40 bytes of communication. To present two solutions with similar structure, the first one is privately verifiable and builds mitigation. To describe approaches and system hooks that support both internal and external auditing of online storage services,

describe motivations for service providers and auditors to adopt these approaches, and list challenges that need to be resolved for such auditing to become a reality. Cloud Computing has been envisioned as the next generation architecture of IT Enterprise. In contrast to traditional solutions, where the IT services are under proper physical, logical and personnel controls, Cloud Computing moves the application software and databases to the large data centers, where the management of the data and services may not be fully trustworthy.

This unique attribute it poses many new security challenges which have not been well understood. It focuses on cloud data storage security, which has always been an important aspect of quality of service. To ensure the correctness of users' data in the cloud, to propose an effective and flexible distributed scheme with two salient features, opposing to its predecessors. By utilizing the Homomorphic token with distributed verification of erasure-coded data, the scheme achieves the integration of storage correctness insurance and data error localization, the identification of misbehaving server(s). Unlike most prior works, the new scheme further supports secure and efficient dynamic operations on data blocks, including: data update, delete and append. Extensive security and performance analysis shows that the proposed scheme is highly efficient and resilient against it, malicious data modification attack, and even server colluding attacks. Cloud Computing has been envisioned as the next- generation architecture of IT Enterprise. It moves the application software and databases to the centralized large data centers, where the management of the data and services may not be fully trustworthy.

Elegantly on pseudorandom functions (PRFs); the second allows for publicly verifiable proofs and is built from the signature scheme of Boneh, Lynn, and Shacham in bilinear groups. Both solutions rely on Homomorphic properties to aggregate a proof into one small authenticator value. A growing number of online service provider's offer to store customers' photos, email, system backups, and other digital assets. Currently, customers cannot make informed decisions about the risk of losing data stored with any particular service provider, reducing their incentive to rely on these services. Because it allows customers to evaluate risks, and it increases the efficiency of insurance based risk

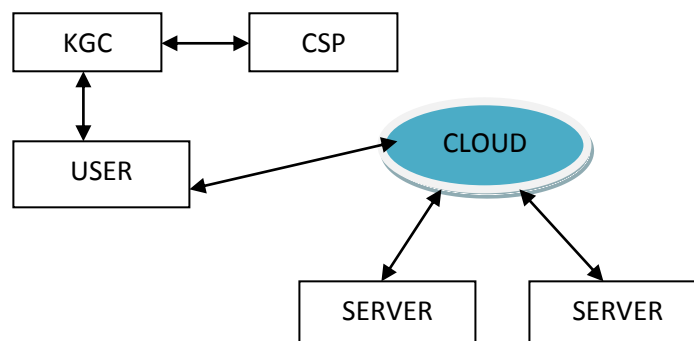


Fig.2. The proposed framework schema of Byzantine Failures.

3. PROPOSED METHODOLOGY

To propose an effective and flexible distributed scheme with explicit dynamic data support, including block update, delete, and append.

a) KGC (Key Generation Center)

- To generate attribute based public key and private key.

b) Pseudo Random Permutation

- It's a technique to pick up the attribute. To rely on erasure-correcting code in the file distribution preparation to provide redundancy parity vectors and guarantee the data dependability. To achieves the key updation process in server side.

3.1. Adversary Model

The adversary model has to capture all kinds of threats towards the cloud data integrity. Due to cloud data do not reside at user's local site but at cloud service providers address domain. It desire to move data that has not been or is rarely accessed to a lower tier of storage than agreed for monetary reasons, but it may also attempt to hide a data loss incident due to management errors, Byzantine failures and so on. For external attacks, data integrity threats may come from outsiders. And also the data while store on the storage center it can check for the previous data similarly to that stored one and make a replace for it. This function made for some software version updations.

3.2. Token Precomputation

Data storage correctness and data error localization simultaneously, this scheme entirely relies on the pre-computed verification tokens. The main idea is before file distribution the user pre- computes a certain number of short verification tokens on individual vector, each token covering a random subset of data blocks. Upon receiving challenge, each cloud server computes a short "signature" over the specified blocks and returns them to the user. The values of these signatures should match the corresponding tokens precomputed by the user.

3.3. File Retrieval and Error Recovery

User can reconstruct the original file by downloading the data vectors from the servers, assuming that they return the correct response values. Verification scheme is based on random spot-checking, so the storage correctness assurance is a probabilistic one. By choosing system parameters appropriately and conducting enough times of verification, can guarantee the successful file retrieval with high probability. The newly recovered blocks can then be redistributed to the misbehaving servers to maintain the correctness of storage.

3.4. Key Generation Center (KGC)

A Key generation center can be consumed by the user does not have the time, feasibility or resources to perform the storage correctness verification. Cloud consumer can optionally delegate this task to an independent third party auditor, it makes the cloud storage securable. KGC should accept consumers data and it generates a key to store in the cloud. It has expertise and capabilities that cloud users do not have and is trusted to assess the cloud

storage service security on behalf of the user upon request. Users rely on the Cloud Server for cloud data storage and maintenance. And also dynamically interact with the Cloud Server to access and update the stored data for various application purposes. The users may resort to KGC for ensuring the storage security of the outsourced data, while hoping to keep the data private.

In most of time it behaves properly and does not deviate from the prescribed protocol execution. During providing the cloud data storage based services, for their own benefits the Cloud Server might neglect to keep or deliberately delete rarely accessed data files which belong to ordinary cloud users. The Cloud Server may decide to hide the data corruptions caused by server hacks or Byzantine failures to maintain reputation. It is in the business of auditing, is reliable and independent, and thus has no incentive to collude with either the Cloud Server or the users during the auditing process. It should be able to efficiently audit the cloud data storage without local copy of data and without bringing in additional on-line burden to cloud users.

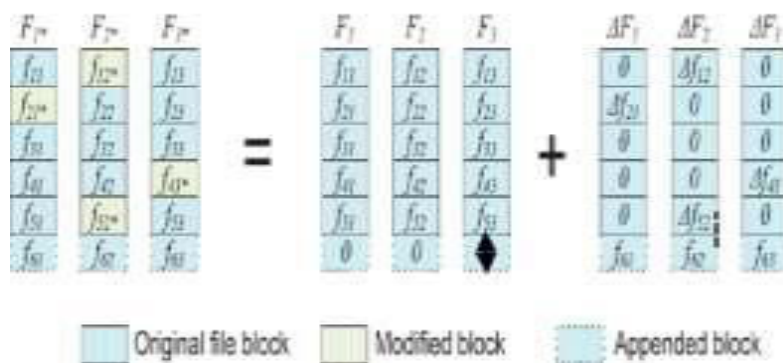


Fig. 3. Logical representation of data dynamics, including block update, append and delete

4. RESULTS AND DISCUSSIONS

The experimental results and performance evaluation on the three combination of partition and grouping on the data storing blocks are illustrated in Fig. 3 where blocks denote results of 1) Blue block represents original block of data storage with a nodal one of 2) White block represents modified block stacking through data storage. Appended block represents nodal form of data.

An effective and flexible distributed scheme with explicit dynamic data support eventually and also it performs reduce the storage space in cloud for better performing. Through detailed security and extensive experiment results

5. CONCLUSION AND FUTURE WORK

To achieve the assurances of cloud data integrity and availability and enforce the quality of dependable cloud storage service for users, To propose an effective and flexible distributed scheme with explicit dynamic data support, including block update, delete, and append. Through detailed security and extensive experiment results, this scheme is highly efficient and resilient to Byzantine failure, malicious data modification attack, and even server colluding attacks. In future this scheme achieves the integration of storage correctness insurance and data error localization. Whenever data corruption has been detected during the storage correctness verification across the distributed servers, can almost guarantee the simultaneous identification of the misbehaving servers.

REFERENCES

- [1] M. Arrington, "Gmail Disaster: Reports of mass Email Deletions," <http://www.tech-crunch.com/2006/12/28/gmail-disaster-reports-of-mass-email-deletions>, Dec. 2006.
- [2] G. Ateniese, R. Burns, R. Curtmola, J. Herring, L. Kissner, Z. Peterson, and D. Song, "Provable Data Possession at Untrusted Stores," Proc. 14th ACM Conf. Computer and Comm. Security (CCS'07), pp. 98-609, Oct. 2007.
- [3] G. Ateniese, R.D. Pietro, L.V. Mancini, and G. Tsudik, "Scalable and Efficient Provable Data Possession," Proc. Fourth Int'l Conf. Security and Privacy in Comm. Networks (SecureComm '08), pp. 1-10, 2008.
- [4] Amazon.com, "Amazon Web Services (AWS)" <http://aws.amazon.com>, 2009.
- [5] Amazon.com, "Amazon S3 Availability Event: July 20, 2008," <http://status.aws.amazon.com/s3-20080720.html>, July 2008.
- [6] A. Juels and B.S. Kaliski Jr., "PORs: Proofs of Retrievability for Large Files," Proc. 14th ACM Conf. Computer and Comm. Security (CCS '07), pp. 584-597, Oct. 2007.
- [7] J. Kincaid, "MediaMax/TheLinkup Closes Its Doors," <http://www.techcrunch.com/2008/07/10/mediamaxthelinkup-closes-its-doors>, July 2008.
- [8] B. Krebs, "Payment Processor Breach May Be Largest Ever," <http://voices.washingtonpost.com/securityfix/2009/01/payment-processor-breach-may-be-largest-ever.html>, Jan. 2009.
- [9] K. Ren, C. Wang, and Q. Wang, "Security Challenges for the Public Cloud," IEEE Internet Computing, vol. 16, no. 1, pp. 69-73, 2012.
- [10] Sun Microsystems, Inc., "Building Customer Trust in Cloud Computing with Transparent Security," <https://www.sun.com/offers/details/-sun-transparency.xml>, Nov. 2009.
- [11] M.A. Shah, M. Baker, J.C. Mogul, and R. Swaminathan, "Auditing to Keep Online Storage Services Honest," Proc. 11th USENIX Workshop Hot Topics in Operating Systems (HotOS '07), pp. 1-6, 2007.
- [12] M.A. Shah, R. Swaminathan, and M. Baker, "Privacy-Preserving Audit and Extraction of Digital Contents," Cryptology ePrint Archive, Report 2008/186, <http://eprint.iacr.org>, 2008.
- [13] C. Wang, Q. Wang, K. Ren, and W. Lou, "Ensuring Data Storage Security in Cloud Computing," Proc. 17th Int'l Workshop Quality of Service (IWQoS '09), pp. 1-9, July 2009.
- [14] S. Wilson, "Appengine Outage," <http://www.cio-weblog.com/50226711/appengine-outage.php>, June 2008.
- [15] Q. Wang, C. Wang, J. Li, K. Ren, and W. Lou, "Enabling Public Verifiability and Data Dynamics for Storage Security in Cloud Computing," Proc. 14th European Conf. Research in Computer Security (ESORICS'09), pp. 355-370, 2009.

AUTHOR PROFILE

Mrs.R.Gnanakumari Graduated in B.E [CSE] from Sri Ramakrishna Engineering College, Bharathiyar University, and Coimbatore. She received Masters Degree in M.E [CSE] from Anna University, Coimbatore. At Present she is working as Assistant Professor in ECE in Nehru Institute of Engineering and Technology, Coimbatore, India. Her research interests include Image Processing and Data Mining. She has published research papers in various National, International conferences and Journals.

Reducing the Energy Consumption in DVFS by using Performance Optimizing Scheme

K.G. HARISHKUMAR¹, K.PUSHPA KUMAR², S.KISHORE³

¹CSE, St. Anne's College of Engineering and Technology, harishkumarkg205@gmail.com

²CSE, St. Anne's College of Engineering and Technology, pushpakumark1994@gmail.com

³CSE, St. Anne's College of Engineering and Technology, aadihotsun@gmail.com

Abstract -Recent mobile devices adopt high-performance processors to support various functions. As a side effect, higher performance inevitably leads to power density increase, eventually resulting in thermal problems. In order to alleviate the thermal problems, off-the-shelf mobile devices rely on dynamic voltage-frequency scaling (DVFS)-based dynamic thermal management (DTM) schemes. Unfortunately, in the DVFS-based DTM schemes, an excessive number of DTM operations worsen not only performance but also power efficiency. In this paper, we propose a temperature-aware DVFS scheme for Android-based mobile devices to optimize power or performance depending on the option. We evaluate our scheme in the off-the-shelf mobile device. Our evaluation results show that our scheme saves energy consumption by 12.7%, on average, when we use the power optimizing option. Our scheme also enhances the performance by 6.3%, on average, by using the performance optimizing scheme, still reducing the energy consumption by 6.7%.

Index Terms -Dynamic thermal management, power management, dynamic volt-age and frequency scaling, Smartphone.

I. INTRODUCTION

EARLIER mobile devices were equipped with relatively lower performance microprocessors, due to the limitation of size and power. However, with the advance of process technology, mobile processor vendors provide multi-core processors of small size running at more than 1 GHz frequency, which still consumes extremely low power compared to desktop processors. Nevertheless, as the processor size scales down, the power density of the processors increases despite the reduction in total power consumption. The increased power density eventually increases on-chip temperature, which causes the reliability problem including permanent damage on the system in the worst case.

Though the thermal problems have been seriously addressed for the past decade, they are still crucial especially in mobile devices. While desktop and server computers have powerful cooling solutions to cool down their processors, most mobile devices do not have them due to the limited space and power consumption. For instance, some of the high-end computer systems utilize liquid cooling to alleviate the thermal problems. However, it is not feasible to apply liquid cooling to mobile devices - even a fan or heat sink is not applied to current mobile devices. Thus, it is necessary to resolve the thermal problems with software thermal management methods at the OS level.

II. RELATED WORK

Thermal problems have been studied in the various levels [10]. From the mechanical side, many efficient cooling solutions have been proposed, such as air cooling with a faster fan or larger heat sink [5], [14] and liquid cooling [4], [9]. These cooling solutions reduce the on-chip temperature without performance degradation. However, mechanical cooling system is limitedly adopted, since it has large size or nonnegligible power consumption. Thus, there also have been many researches on the software thermal management techniques.

For the software thermal management, DVFS is most widely used. Hanson et al. investigated and characterized the thermal response of the processor to DVFS [6] on a real system. They investigated that DVFS has an immediate influence on the on-chip temperature. Thus, DVFS can be a viable solution for thermal management. Liu et al. proposed a design time modeling of DVFS [13] to provide thermal optimization, which prevents run-time thermal emergencies while optimizing the cooling cost and performance. Hanumaiah and Vrudhula proposed the temperature-aware DVFS scheme considering the hard real-time applications [7]. Their scheme makes use of accurate power and thermal models to meet the deadlines of the real-time applications while satisfying the temperature constraints.

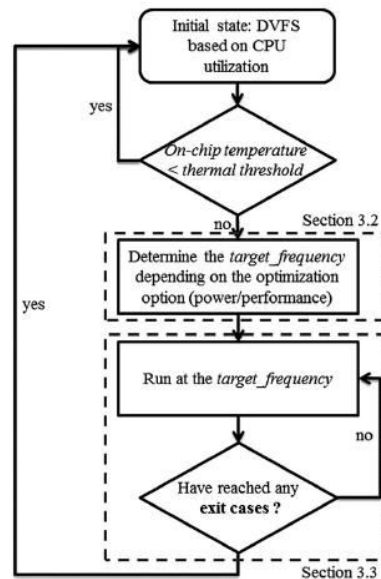


Fig. 1. An overview of the proposed temperature-aware DVFS scheme to co-optimize the power and performance.

III. TEMPERATURE-AWARE DVFS SCHEME

In Section 3.1, we briefly introduce the overview of our proposed DVFS scheme. Then we explain how to determine the CPU frequency that co-optimizes the power and performance, in Section 3.2. Finally, we describe the frequency scaling method and the exit cases in Section 3.3.

3.1 Scheme Overview

Fig. 1 depicts our proposed DVFS scheme. At the initial state, our scheme monitors the on-chip temperature and CPU utilization. While the on-chip temperature remains under the predefined thermal threshold, our scheme determines the CPU frequency based on the CPU utilization. Same as the conventional DVFS scheme, our scheme scales the frequency up to the maximum frequency when the utilization exceeds utilization threshold (80% is used as default). On the other hand, when there is any lower frequency that keeps the utilization under the utilization threshold, it scales down to the lower frequency.

When the on-chip temperature increases up to the thermal threshold, our scheme applies the novel DVFS scheme to co-optimize the power and performance. Our scheme determines an optimal frequency depending on the optimizing option. We refer to this optimal frequency as *target frequency*. The *target frequency* is determined as a relatively higher value when the performance optimizing option is used, compared to when the power optimizing option is used. Once the *target frequency* is determined, our scheme scales the CPU frequency to the *target frequency* until it encounters any of the exit cases.

3.2 Frequency Determination Routine

3.2.1 Power Optimizing Option

When the power optimizing option is used, our scheme minimizes the power consumption, without performance degradation compared to the conventional DTM scheme. Fig. 2 shows an example of the frequency variation with the conventional DTM scheme, when the on-chip temperature increases up to the thermal threshold during the execution of a program that heavily utilizes the CPU. Since the CPU is heavily utilized, the conventional DVFS tries to scale the frequency to the maximum frequency (1400 MHz). However, due to the frequent DTM operation, the frequency is repeatedly scaled down to 800 MHz. Thus, the frequency is repeatedly changed between 800 MHz and 1400 MHz, as shown in Fig. 2. However, as we have briefly mentioned in Section 1, the unstabilized frequency, which implies unstabilized voltage as well, causes power inefficiency [3], [8]. We formulate why frequency and voltage must be stabilized to achieve optimal power efficiency as follows.

- $Power \propto Frequency \times Voltage^2$. (1)

Power consumption is proportional to voltage squared and frequency.

- $Voltage \propto Frequency$. (2)

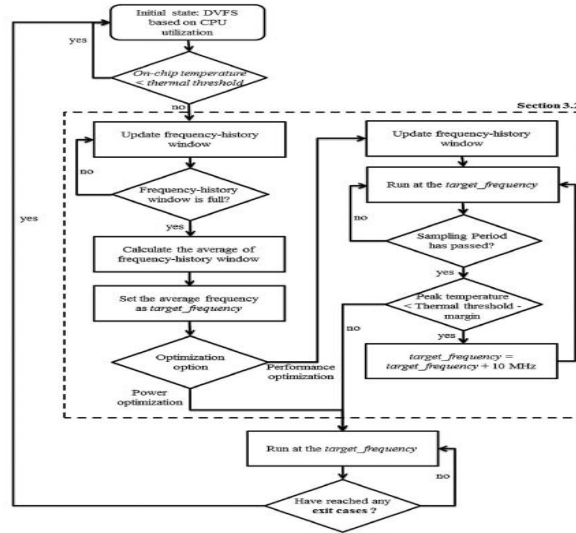
Voltage is proportional to frequency.

- $Power \propto Frequency^3$. (3)

By Equations (1) and (2), power consumption is proportional to cubic frequency.

- $Average[F_1^3, F_2^3, F_3^3, \dots, F_n^3]$
 $\geq Average[F_1, F_2, F_3, \dots, F_n]^3$. (4)

($F_1, F_2, F_3, \dots, F_n$ are the frequencies used at different time slices) Based on the Jensen's inequality [20], average of frequency cubes is larger than cube of average frequency, when the variance of the frequencies is not zero. Furthermore, the difference becomes larger as the variance increases. When there is no variation in the frequencies, both side of the equation has the same value.



The procedure to determine the $target_frequency$, depending on the optimizing option.

By Equations (3) and (4), average of power consumptions in different frequencies is larger than power consumption in average frequency. When the variance of the frequencies is zero, both side of the equation has the same value.

- $Performance \propto Frequency$. (6)

Performance is proportional to frequency.

∴ From Equations (5) and (6), we confirm that running at the average frequency consumes less power compared to running at different frequencies, while achieving same performance.

Therefore, we set the $target_frequency$ as the average frequency of the conventional DTM scheme, to save power. The detailed procedure is described in the left side of the dotted box in Fig. 3. When the temperature increases up to the thermal threshold, our scheme keeps track of the CPU frequency in the frequency-history window; 10 Hz and 6 seconds is used for the sampling rate and window size, respectively in our experiment.² Then our scheme waits until the frequency-history window is filled. In the meantime, the conventional DTM scheme is used. After the frequency-history window is filled, $target_frequency$ is set as the average of the frequency-history window. The $target_frequency$ set by this procedure is used for the power optimizing option.

3.2.2 Performance Optimizing Option

When the performance optimizing option is activated, there are some additional steps to configure the $target_frequency$. The right side of the dotted box in Fig. 3 shows these steps. Our scheme starts by running at the $target_frequency$, which is obtained from the power optimizing option.³ While running at the $target_frequency$, our scheme monitors the on-chip temperature during a pre-defined sampling period to check the peak temperature. In case the peak temperature is less than (thermal threshold-temperature margin), our scheme increases the $target_frequency$ by 10 MHz; sampling period and temperature margin is set as 6 seconds and 2 degrees for our evaluation, by considering on-chip thermal response to the frequency/voltage scaling. (We conducted thermal response test to confirm that the on-chip temperature does not increase by more than 2 degrees within the sampling period, when increasing the frequency by 10 MHz) On the other hand, when the temperature is same or larger than (thermal threshold-temperature margin), our scheme ends the frequency determination routine.

3.3 Actual Frequency Scaling and Exit Cases

After our scheme determines the $target_frequency$, it sets the CPU frequency as the $target_frequency$ until it encounters any exit case. The dotted box in Fig. 4 describes the execution of our algorithm after determining the $target_frequency$. Though it would be best to scale the CPU frequency to exact $target_frequency$, it may not be possible since mobile devices only support discrete frequency levels (in the device used for our evaluation, frequency can be scaled as a granularity of 100 MHz). Therefore, our scheme utilizes the actual frequency scaling routine, described in the upper-part of the dotted box, in Fig. 4. At first, the frequency-history window is updated every 100 ms, which is same as in case of the conventional DVFS scheme. Then, the frequency scaling routine compares the average of recently selected frequencies in the frequency-history window to the $target_frequency$.

When the average frequency is lower than the $target_frequency$, the routine scales the frequency to the lowest selectable frequency (provided by the hardware) that is higher than the $target_frequency$. Otherwise, frequency selection routine scales the frequency to the highest select-able frequency that is same or lower than the $target_frequency$. Consequently, our frequency selection routine alternately scales to two nearest frequencies provided by the hardware, in case the $target_frequency$ itself is not provided by the hardware; for instance, 1100 MHz and 1200 MHz when the $target_frequency$ is 1150 MHz. On the other hand, our scheme scales to the exact $target_frequency$ when the $target_frequency$ is provided by the hardware. In our paper, we refer to running with the frequency scaling routine as running at the $target_frequency$.

While the processor runs at the $target_frequency$, there are two cases where the processor should not run at the $target_frequency$, any more. We define the two exit cases as follows.

- Performance demand decreases: When the frequency which is lower than the $target_frequency$ keeps CPU utilization under the utilization threshold, it is determined that the performance demand has decreased. In this case, the frequency should be scaled down to save power.
- On-chip temperature increases⁴ up to the thermal threshold: In this case, the frequency should be scaled down for reliability. When our scheme encounters an exit case, it exits from the frequency scaling routine, consequently going back to the initial state. After returning to the initial state, frequency is reconfigured by the algorithm introduced in the Sections 3.1 and 3.2. In case that the performance demand has decreased, the frequency scales down to the lowest frequency that keeps the CPU utilization under the utilization threshold. On the other hand, when the temperature has increased to the thermal threshold, our scheme re-enters the frequency determination routine (which is described in Section 3.2) to set new $target_frequency$.

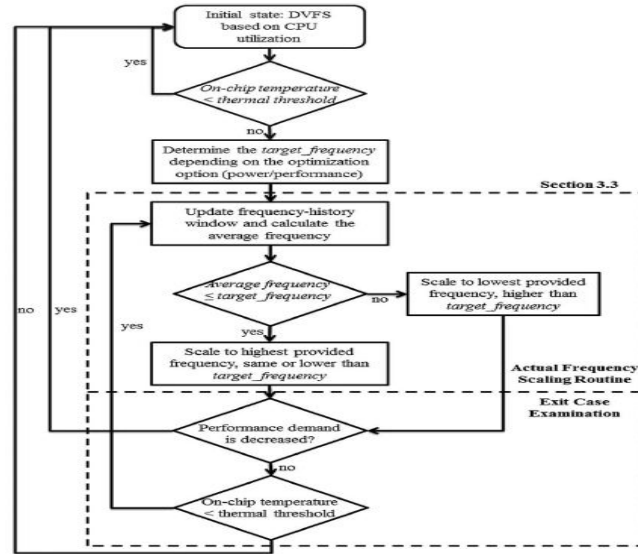


Fig. 4. The frequency scaling method and the exit cases at the $t_{a} \tau_{g} \epsilon_{t} - f_{r} \eta_{b} \epsilon_{D} \epsilon_{Y}$.

IV. EVALUATION

4.1 Evaluation Methodology

4.1.1 Experimental Environments

For our evaluation, we use one of the high-end mobile devices, Odroid-Q [21]. Odroid-Q adopts a high-performance quad-core processor, Exynos 4412 [19], which provides the maximum frequency of 1.4 GHz and discrete frequency steps in granularity of 100 MHz. The device operates with Android ICS (Ice Cream Sandwich) and Linux 3.0.15 kernel. The system utilizes ondemand scaling governor [15] as the base power management policy (DVFS). When the on-chip temperature increases up to the thermal threshold, the conventional DTM scheme overrides power management policy (ondemand), scaling down the frequency to 800 MHz. When the temperature decreases under the thermal threshold, on demand is applied again.

4.1.2 Benchmark

For the evaluation of our scheme, we use 13 embedded benchmark programs from the EEMBC [18]. The programs are classified into four different types. The detailed description of each benchmark program is shown in Table 1. As each benchmark program is designed to run on a single core, we evaluate eight groups of benchmark programs, each composed of four different benchmark programs. Note that our target device has a quad-core processor. The combination of each group is determined arbitrarily to show the evaluation of mixed usage of benchmark programs. The detailed information of each group is shown in Table 2. With the default configuration of each benchmark programs, the execution time varies greatly, which makes it hard to evaluate the performance. To resolve this problem, we first execute each benchmark program on a single core, at the maximum frequency to measure the execution time. Note that DTM is not invoked in our evaluation environment, when utilizing just one core. Then, we adjust the number of iterations for each benchmark program so that all the execution times for benchmark programs are set as 10 minutes at the maximum frequency, when there is no DTM operation.

4.2 Experimental Results

4.2.1 Performance of the Conventional DTM

In this subsection, we describe the DTM rate and execution time of the benchmark groups with the conventional DTM. Fig. 5 shows the DTM operation rate during the execution of each group. DTM operation accounts for 21.6% (Group1) to 44.8% (Group8) of the total execution time. In general, the groups with more network benchmark programs (right side of the figure) have relatively higher DTM rate. On the other hand, groups only composed of the office and consumer benchmark programs have lower DTM rate. With the varying DTM rate, the average CPU frequency for each group also varies from 1270 MHz to 1130 MHz. The average frequency deservedly becomes lower as the DTM rate increases.

The increased DTM rate leads to the increased execution time of each group. Fig. 6 shows the execution time of the groups—note that we have configured the number of iterations so that each benchmark program can be completely executed in 10 minutes, when DTM operation is not invoked. Since the execution time of the 4 benchmark programs in each group may differ, we investigated two different execution times as follows: (1) the average execution time of all the benchmark programs in the group and (2) the longest execution time among the benchmark programs in the group. However, difference between the average and longest execution time is at most 10 seconds for all the groups. Therefore, we refer to the longest execution time as the execution time of the group for the rest of this paper. As the execution time is inversely proportional to the average frequency, the groups that invoke more DTM operations have longer execution time. In case of Group8 where DTM rate is as high as 44.8%, the execution time is also increased by 156 seconds compared to the execution without DTM operation (600 seconds). In case of Group1, the execution time is increased by only 78 seconds due to the lowest DTM rate (21.6%).

4.2.2 Power Optimizing Option

In this subsection, we evaluate our proposed scheme with the power optimizing option, explained in Section 3.2.1. Fig. 7 shows the execution time and system-wide energy consumption of our scheme, each normalized to that of the conventional DTM. As expected, the execution time is nearly the same as in the conventional DTM, since the power optimizing option sets the target frequency as the average frequency of the conventional DTM. While achieving the similar performance, energy consumption is reduced by 12.7%, on average, and 16% in the best case (Group8). In general, the energy saving is larger for the groups with higher DTM rate. The results can be explained by the equations in Section 3.2.1 which describes that larger variance of frequencies worsens the power efficiency more significantly—note that the variance of frequencies becomes larger when the DTM rate becomes larger in the conventional DTM since the benchmark programs are executed at two different frequencies (normal frequency and much lower frequency caused by DTM invocation) for the most of the time. Therefore, our scheme saves more energy by stabilizing the frequency, for the groups with higher DTM rate.

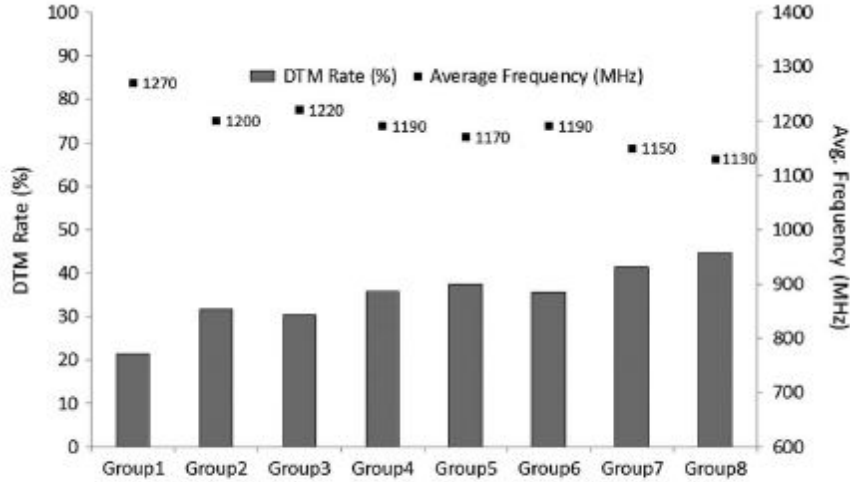


Fig. 5. DTM operation rate and average frequency of the conventional DTM.

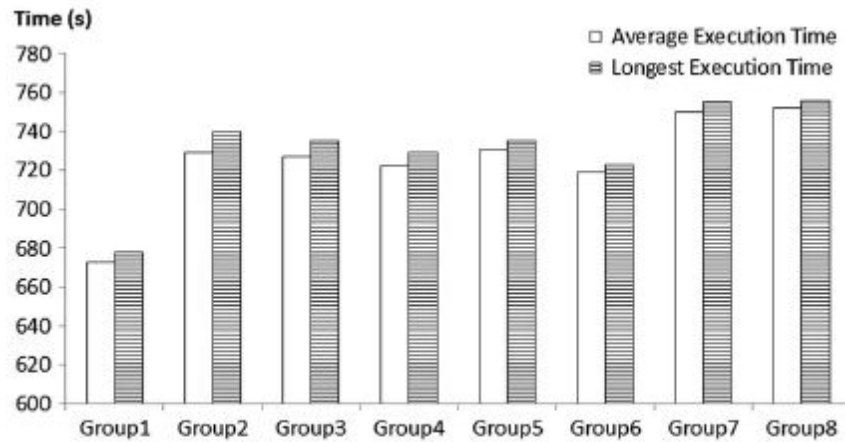


Fig. 6. Execution time of the conventional DTM.

4.2.3 Performance Optimizing Option

In this subsection, we evaluate our proposed scheme with the performance optimizing option. Fig. 9 compares the average frequency of our scheme and the conventional DTM. When our scheme is applied with the performance optimizing option, the average frequency is increased by 30 ~ 130 MHz, depending on the group. The average frequency varies due to the unique thermal characteristics of each group. Nevertheless, the frequency is increased for all the groups, resulting in performance enhancement.

Fig. 10 shows the execution time and system-wide energy consumption of our scheme with the performance optimizing option, each normalized to that of the conventional DTM. As the execution time is inversely proportional to the average frequency, our scheme reduces the execution time by average of 6.3% and maximum of 10% (Group8).

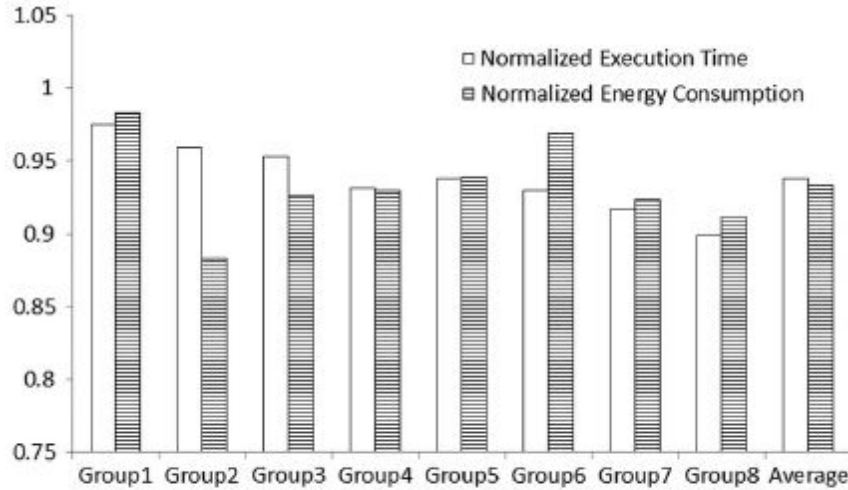


Fig. 10. Normalized execution time and normalized energy consumption of our proposed scheme with performance optimizing option.

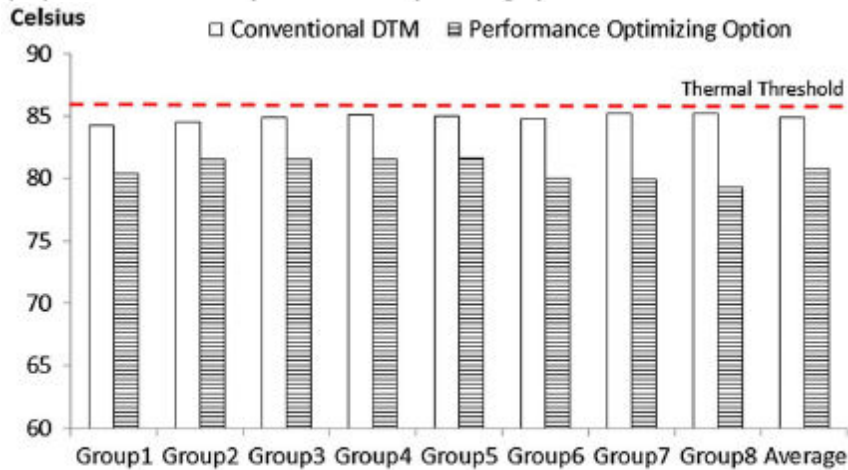


Fig. 11. Average on-chip temperature of conventional DTM scheme and our proposed scheme with performance optimizing option.

V. CONCLUSION

The conventional DTM schemes used in off-the-shelf mobile devices monitor the temperature from the on-chip sensors to maintain thermal reliability. When the temperature is increased up to the thermal threshold, the schemes invoke DTM operation, which scales down the CPU frequency and voltage. Our scheme provides two different options: (1) the power optimizing option that saves energy, and (2) performance optimizing option that enhances the performance. We implement our scheme on an off-the-shelf mobile device to evaluate the scheme based on real measurement. While we evaluate the system power instead of the processor power, the energy saving is as much as 12.7% on average without any performance loss, by using our scheme with the power optimizing option. By using our proposed scheme with the performance optimizing option, performance is enhanced by 6.3% while the energy saving is still as much as 6.7% on average. In addition, our scheme also lowers the on-chip temperature compared to the conventional DTM, regardless of the optimizing option.

REFERENCES:

- [1] D. Brooks and M. Martonosi, "Dynamic thermal management for high-performance microprocessors," Proc. 7th Int. Symp. High-Perform. Comput. Architecture (HPCA), 2001, pp. 171–182.
- [2] A. P. Chandrakasan and R. W. Brodersen, "Minimizing power consumption in digital CMOS circuits," Proc. IEEE, vol. 83, no. 4, pp. 498–523, Apr. 1995.
- [3] J. Chang and M. Pedram, "Energy minimization using multiple supply voltages," IEEE Trans. Very Large Scale Integr. Syst., vol. 5, no. 4, pp. 436–443, Dec. 1997.
- [4] X. Y. Chen, K. C. Toh, and J. C. Chai, "Direct liquid cooling of a stacked multichip module," Proc. 4th Electron. Packag. Technol. Conf., 2002, pp. 380–384.
- [5] A. R. Cho, H. B. Jang, J. H. Lee, and S. W. Chung, "Reducing leakage power by controlling cooling fan speed," Proc. COOLChips XIII, p. 188, 2010, poster.
- [6] H. Hanson, S. W. Keckler, S. Ghiasi, K. Rajamani, F. Rawson, and J. Rubio, "Thermal response to DVFS: Analysis with an Intel Pentium M," Proc. Int. Symp. Low Power Electron. Des. (ISLPED'07), pp. 219–224, 2007.
- [7] V. Hanumaiah and S. Vrudhula, "Temperature-Aware DVFS for hard real-time applications on multicore processors," IEEE Trans. Comput., vol. 61, no. 10, pp. 1484–1494, Oct. 2012.
- [8] T. Ishihara and H. Yasuura, "Voltage scheduling problem for dynamically variable voltage processors," Proc. Int. Symp. Low Power Electron. Des., Aug. 1998, pp. 197–202.
- [9] H. B. Jang, I. Yoon, C. H. Kim, S. Shin, and S. W. Chung, "The impact of liquid cooling on 3D multi-core processors," Proc. IEEE Int. Conf. Comput. Des., 2009, pp. 472–478.
- [10] J. Kong, S. W. Chung, and K. Skadron, "Recent thermal management techniques for microprocessors," ACM Comput. Sur., vol. 44, no. 3, June 2012, pp. 1–42, article 13.
- [11] J. S. Lee, K. Skadron, and S. W. Chung, "Predictive temperature-aware DVFS," IEEE Trans. Comput., vol. 59, no. 1, pp. 127–133, Jan. 2010.
- [12] G. Liu, M. Fan, G. Quan, and M. Qiu, "On-Line predictive thermal management under peak temperature constraints for practical multi-core platforms," J. Low Power Electron., vol. 8, no. 5, pp. 5.

PI Controller Based Bidirectional Soft Switched Converter for Motor Drive Applications

V. C Eugin Martin Raj¹, R. Giritha², V. Rekha³, A. Sowmiya⁴, S. Chandraleka⁵

¹ Assistant Professor, Department of EEE, St Anne's college of Engineering and Technology

^{2, 3, 4, 5} Student, Department of EEE, St Anne's college of Engineering and Technology

Abstract – In recent years bidirectional dc to dc converters are widely used in electric vehicles. In electric vehicles the energy is transferred between battery and motor drive and also the battery acts as a catalyst to provide energy boost. But due to its short driving range and high cost has limited its use. Hence a bidirectional converter is required to control Power flow in both motoring and regenerative braking operation so that the overall drive system efficiency increases significantly. This paper presents a closed loop bidirectional converter with a PI controller for a motor drive system. In order to reduce the losses and to increase the conversion efficiency of the proposed converter all the switches are turned OFF and turned ON at zero current and zero voltage crossing, so the proposed converter act as Zero Current Transient buck to charge the battery and Zero Voltage Transient boost to discharge the battery. The output voltage is maintained constant even with varied input voltage using a PI controller. The proposed topology is verified through simulations using MATLAB/Simulink and the output performances are analyzed.

Key words: Closed loop control, PI controller, Zero Voltage Transient (ZVT), Zero Current Transient (ZCT), Bidirectional Converter, Battery, Separately excited DC motor.

1. Introduction

In soft switching based storage system, the efficiency of system is depends on the size and cost; it can be increased by a combination of batteries or ultra capacitors. Also, the leakage current of ultra capacitor is high so the voltage imbalance problem has to be occurred. The development of high power bi-directional DC-DC converters has become an important topic because of the requirement in energy storage systems. Battery fed electric vehicles are commonly being used for EV applications due to zero emission, guaranteed load leveling, good transient operation and energy recovery during braking operation. Hence converter with bidirectional power flow capabilities is required to connect the battery to the DC motor drive system [2]. The output voltage should not be maintained constant with variation in input voltage in open loop system hence a closed loop system is required [1]. A PI controller based closed loop system is used for controlling the switching pulses so that the output voltage is maintain constant with variation in input voltage [3]. A fractional order PID controller is used to control auxiliary switch so that the efficiency of the converter with soft switching has been increased. An Artificial Intelligence technique is used to tune PI controller (Improved Particle Swarm Optimization algorithms) [4]. In DC distributed power systems PI controllers are not only dampers the bus transients but also keeps the storage voltage level [5]. The energy management system in Hybrid Electric Vehicle is maintained and controlled by using PI controller during charging and discharging of the battery [6]. There are many construction types of power system of multi energy Electric Vehicles such as Fuel Cells + Auxiliary Power Battery+ Ultra Capacitor, Fuel Cells + Ultra Capacitor, Fuel Cells + Power Battery, Power Battery + Ultra Capacitor. Measure and control circuit detects the voltage of

power battery and ultra capacitor to determine the work status of the Ultra Capacitor [8]. A hybrid power source with batteries and super Capacitors gives the power in steady state during transient state [9]. An Ultra Capacitor system for an electric vehicle is used to allow higher acceleration and decelerations of the vehicle with minimal loss of energy and minimal degradation of the main battery [10]. The features of Zero Voltage Switching ensures the high operating frequency, high step-up ratio, low voltage stress across the switches and increase the conversion efficiency of the converter[7]. A resonant network in parallel with the switches achieves Zero Voltage Switching for both active and passive switches without increasing their voltage and current stresses [11]. A Zero Current Transient (ZCT) implement ZCS turn OFF for the transistors without substantially increases in voltage or current stresses in the switches [12]. ZCT PWM FB dc/dc converter not only achieves zero current switching for all switches in the entire load ranges but it also realizes soft commutation for the output rectifier diode. Further the auxiliary circuit also helps to turn on the main switches softly [13]. ZCZVT PWM boost converter differ from a hard switching PWM boost converter by the presence of an additional shunt resonant network formed by two resonant capacitors $CR1$ and $CR2$, a resonant inductor LR a bidirectional auxiliary switch and two auxiliary diodes to provide ZCS and ZVS at both turn ON and turn OFF for the main switch [14]. The ZVT principle is based on the auxiliary circuit carrying higher current than the steady state boost current for a fraction of the switching cycle to achieve soft switching for the switches and diodes used in the converter. So ZVT converters have more conduction losses than the hard switched boost converters but still have higher efficiencies due to reduced switching losses [15].

Generally DC motor drives are categorized in to non- regenerative and regenerative in industry. Non regenerative is normal conventional type, used to control speed and torque in one direction whereas regenerative DC drives are four quadrant drives, not only controlling speed and direction of rotation but also direction of motor torque. This paper is based on regenerative DC drive type with a closed loop system implementing a PI controller to maintain constant output voltage with variation in input voltage. The proposed topology is preferred for maintaining the conversion efficiency and its operating modes are analyzed by the equivalent circuit models during both buck and boost mode of conversion.

2. Proposed Circuit and Operation

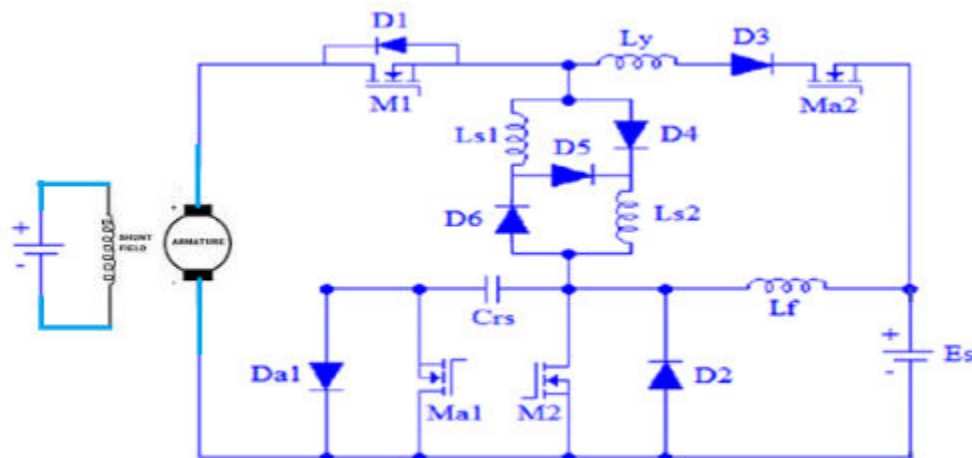


Fig.1. Structure of the proposed circuit

The proposed circuit is shown in Figure. 1, which consists of an auxiliary switch between the battery and separately excited DC motor, which improves the conversion ratio and reduces the leakage current of inductor while charging and discharging. The proposed circuit is operated in two modes such as buck mode and the boost mode. During the buck mode of operation the switch M₁ and the diode D₂ is ON and the circuit act as ZCT buck to charge the battery. Similarly for the boost mode of operation the switch M₂ and the diode D₁ is ON and the circuit act as ZVT boost to discharge the battery. The auxiliary switches M_{a1} and M_{a2}, along with the switched inductors (L_{s1} and L_{s2}) and diodes (D₄, D₅ and D₆) will improve the voltage gain of the system. The auxiliary inductor L_y and resonant capacitors C_{rs} are utilized to achieve soft switching.

2.1 Buck Mode of Operation

During this mode diode D₂ and the switch M₁ is turned ON, the circuit act as a ZCT buck to charge the battery. In this mode input voltage and inductor L_f current are assumed as constant. Similarly all the components present in the circuit considered to be ideal. The one switching cycle consists of six modes of operation.

Mode 1:(t₀ –t₁)

At the starting time of the mode 1 operation is t₀ to t₁, during this time the diode D₂ and the switch M₁ is turned ON. The output current I_{out} is flowing through the diode D₂, the switch is turned ON with the ZCS to charge an ultra capacitor. At the end of the mode the time is t₁, in this period the switched inductor current is reaches to the output current I_{out}. The voltage equation of the mode 1 is given in the following equation (1)

$$E_{low} = \sum_{j=1}^n L_{sj} \frac{dI_j}{dt} + \sum_{j=1}^n \frac{kT_j}{q} + L_f \frac{dI_f}{dt} + nV_T \ln \left[\frac{I_{out}}{I_s} \right]_{D2} + \sum_{j=1}^n I_{out} R_a$$

The output current across the diode D₂ is given in the following equation (2)

$$I_{out} = \frac{E_s}{SL} \quad (2)$$

The current of the switched inductor is defined by the following equation (3)

$$I_{SL} = E_s \left(\frac{1}{(L_{s1} + L_{s2})} \right) + I_{s5} (e^{V_d/(nV_T)} - 1)$$

Where K is the Boltzmann constant, T absolute temperature, q magnitude of the charge, is the ideality factor, I_{s5} is the saturation current of the diode 5, V_d is the voltage across the diode, L_{s1} and L_{s2} are the switched inductors, V_T is the thermal voltage of the diode, E_s is the supply voltage, I_{out} is the output current and SL is the switched inductor.

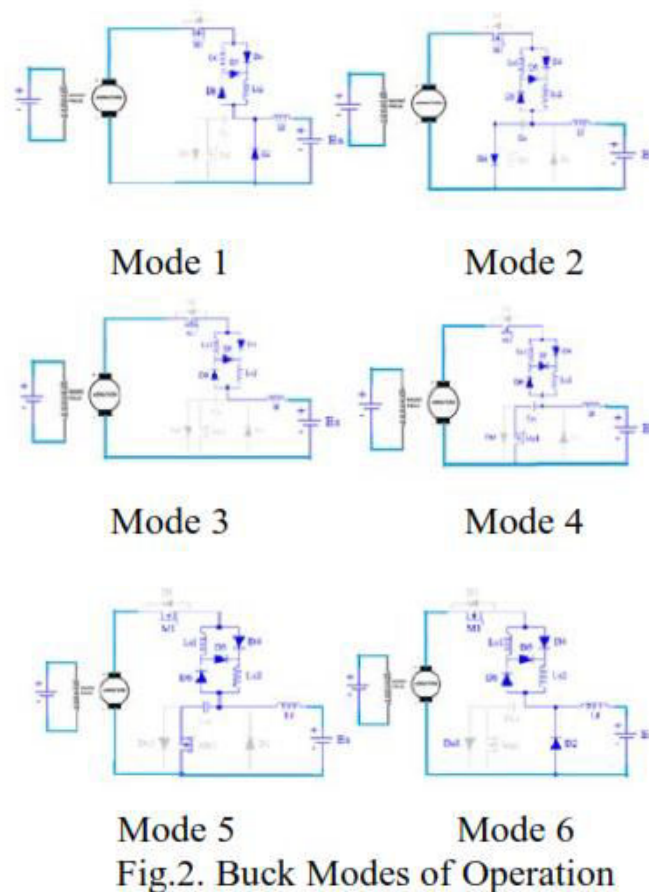
Mode 2: (t₁ – t₂)

During this mode of operation current of the main switch reaches to zero at t = t₁ and the

diode D_2 is turned OFF, i.e., soft switching turn OFF ZCZVS. The resonance of the switched inductors (L_{S1} and L_{S2}) and capacitors C_{RS} start flows through the diode D_{a1} . The resonant condition components current and the voltage of the mode 2 are given in the following equations

Mode 3: ($t_2 - t_3$)

During this mode of operation resonant capacitor current reaches to zero at $t = t_2$. The auxiliary switch M_{a1} is turned off, so the resonance of the inductor and capacitor is stopped. This mode of operation the resonant capacitor C_{RS} voltage reaches $2E_S$ and the switched inductor current reaches to the output current I_{out} . The power flows from the source input to the output enhanced ultra capacitor.



3. PI Controller for DC to DC Converter

PI controllers are mostly implemented in bidirectional converters due its simplicity and ability to tune a few parameters automatically and less overshoot and small settling time can be obtained. PI controllers can be used to solve even a very complex control problem, especially when combined with different blocks.

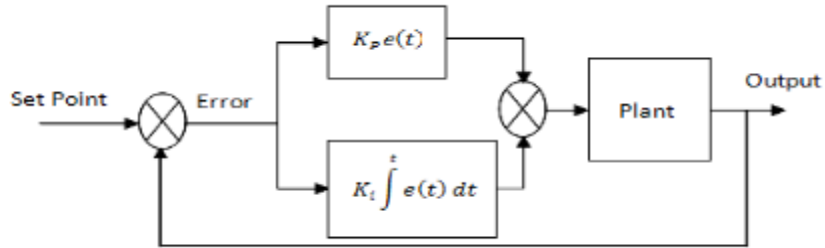


Fig. 6. Structure of PI Controller

The structure of PI controller is shown in fig.6. It is a combination of proportional (P) and Integral (I) parameters, the proportional (P) part are used to set a desired set-point, while the integral part (I) is used to account the accumulation of past errors and rate of change of error in the process respectively

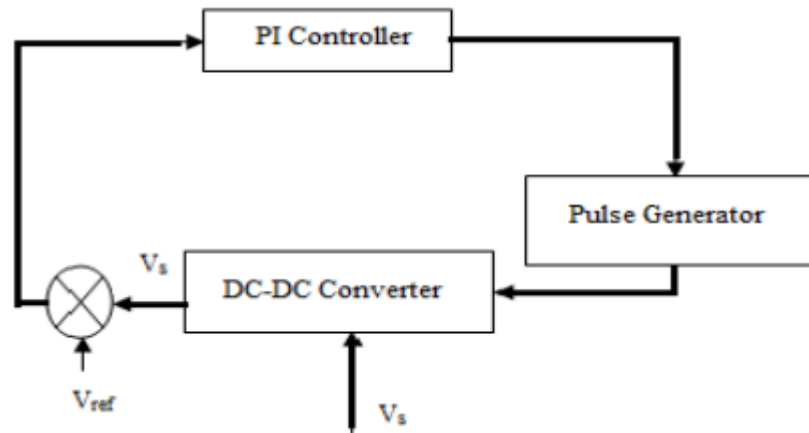


Fig.7. Block diagram of PI Controller for DC to DC Converter

Speed increase and the steady state error decreases but is not eliminated, as K_i increases, the steady state error goes to zero and the system tends towards instability. So Proportional and Integral controllers are never used alone.

4. Results and Discussions

The proposed circuit is simulated in MATLAB/Simulink platform. The simulation model for buck and boost operation with PI compensator and the simulated result waveforms for both buck and boost operation. The proposed circuit with PI controller is validated by injecting a disturbance in the input voltage and the impact of this disturbance in the output is corrected by tuning the PI controller which is shown in the Fig. 10 and 11 for both the modes of operation

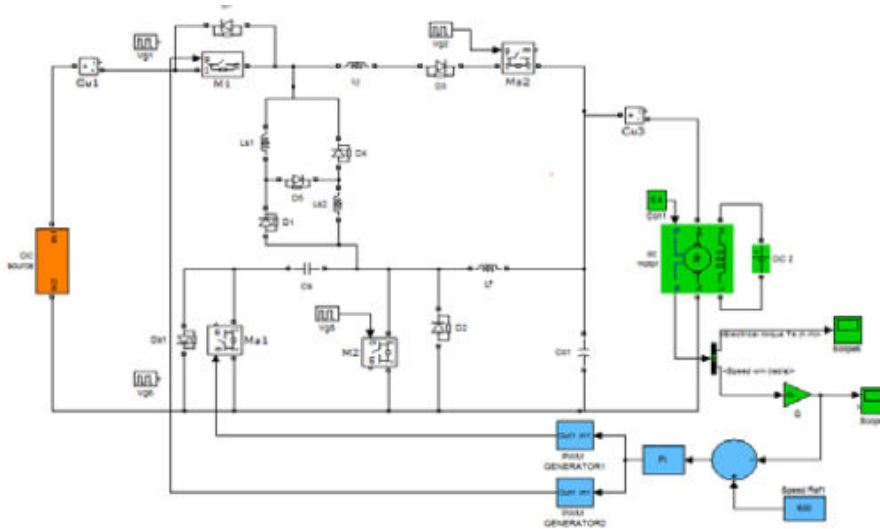


Fig.8. Buck operation of the proposed circuit

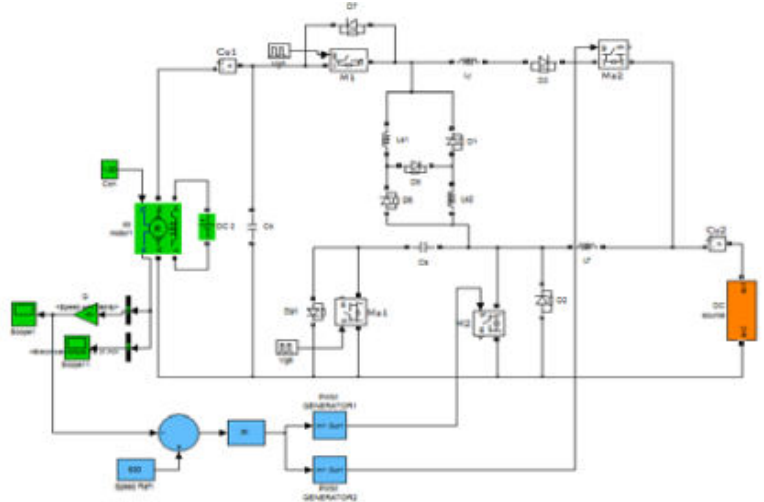
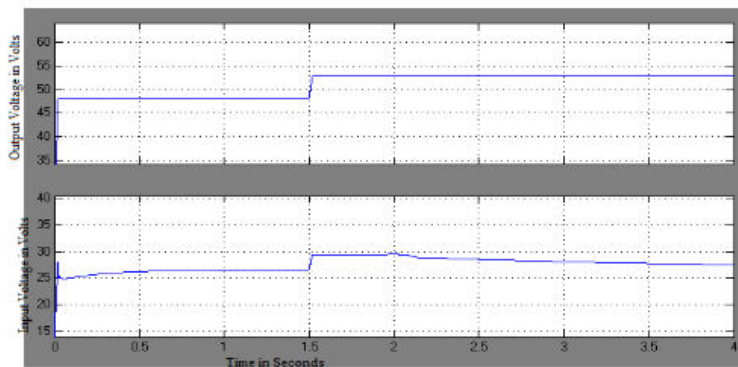
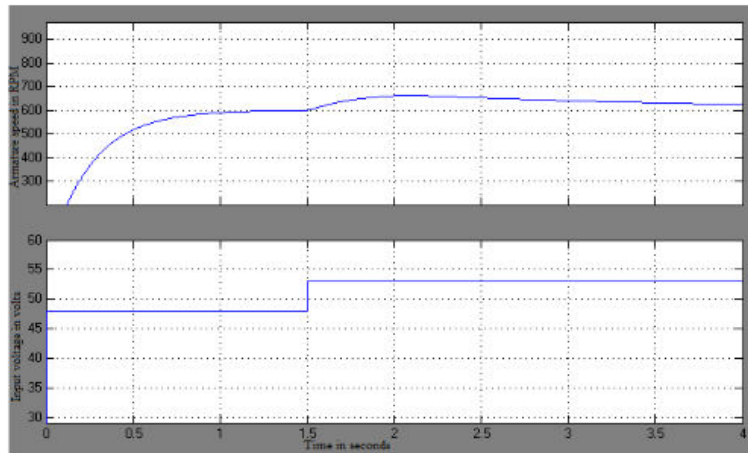


Fig.9. Boost operation of the proposed circuit

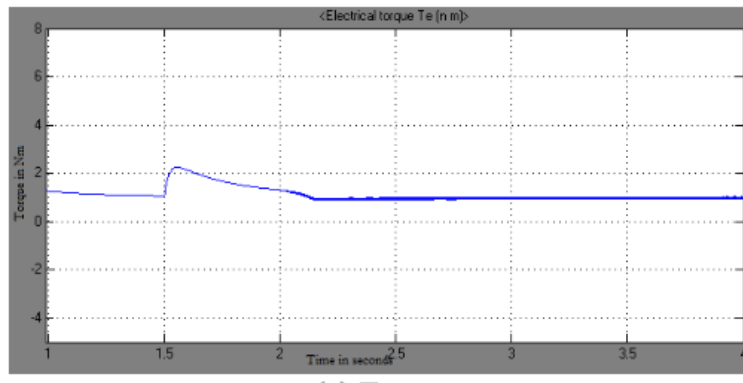
4.1 Results for Buck Operation



(a) Input Voltage and Output Voltage



Armature speed in rpm and Input voltage



Waveforms for buck operation of the proposed circuit

4.3 Results Discussion

The response of the proposed closed loop circuit with PI controller for buck and boost operation are shown in Fig. 10 & 11 respectively. The output voltage during both buck and boost operation is sensed and compare with reference voltage, the error is applied to a PI controller and corrected which is shown in Fig. 10 (a) and Fig 11. (a) respectively. From the waveforms it can be seen that the output voltage gets disturbs, oscillates and settles to the reference value. Similarly the armature speed and torque of the motor corresponding to the input voltage for both the operating modes The main and auxiliary switches M1, M2, Ma1 and Ma2 are turned ON and OFF at zero crossing for both the modes of operation from the corresponding waveforms it can be seen that soft switching is achieved for all the switches of the proposed circuit.

5. Conclusion

In this paper closed loop PI controlled bidirectional soft switching converter is proposed and its responses were analyzed and described with corresponding waveforms. ZCT and ZVT techniques are applied to achieve soft switching for main and auxiliary switches, in order to increase the converter voltage conversion efficiency, but the settling time of the waveforms after error correction is little more and this can be reduced by fine tuning of PI

controller.

References

- [1] S. Preethi, Mahendiravarman, A. Ragavendiran and M. Arunprakash, "Matlab /Simlink based closed Loop Control of Bi-Directional DC – DC Converter" International Journal of Engineering Science and Innovative Technology (IJESIT), Vol. 3, Issue 5, September 2014.
- [2] Premananda Pany, R.K. Singh and R.K. Tripathi, "Bidirectional DC-DC Converter fed drive for electric vehicle system", International Journal of Engineering, Science and Technology, Vol. 3, No. 3, 2011, pp.101-110.
- [3] Atul Kumar and Purna Gaur, "Operation of DC/DC Converter for Hybrid Electric Vehicle", International journal of Electronic and Electrical Engineering, Vol.7, No.4, 2014.
- [4] K. Giridharan and A. Karthikeyan, "Fractional Order PID Controller Based Bidirectional DC/DC Converter", International Journal Of Innovative Research in Science, Engineering and Technology, Vol.3, Issue 3, 2014.
- [5] Soonmin Lee, Bong Jun Seok, Jae Du La and Young Seok Kim, "A Design of a PI Compensator for a Bidirectional DC-DC Converter in a DC Distributed Power System", Journal of International Conference on Electrical Machines and Systems, Vol. 1, No. 3, pp.391-396, 2012.
- [6] S. Saravanan and G. Sugumaran, "Energy Management System in HEV Using PI Controller", International Journal of Electrical, Computer, Electronics and Communication Engineering, Vol. 8, No. 2, 2014.
- [7] R. Sudha and P.M. Dhanasekaran, "DC-DC Converters Using PID Controller and Pulse Width Modulation Technique", International Journal of Engineering Trends and Technology(IJETT), Vol. 7, No.4, 2014.
- [8] Lianbing Li, Lining Sun, Zuojun and Hexu Sun, " Ultracapacitor Control Strategy of EV with Energy Hybridization", IEE Vehicle Power and Propulsion Conference (VPPC), September 3-5, 2008, Harbin, China.
- [9] Sebastien Wasterlain, Alcicek Guven, Hamid Gualous, Jean Francois Fauvarque and Roland Gallay, "Hybrid power source with batteries and supercapacitor for vehicle applications".

Android Based Children Tracking System Using Voice Recognition

¹manju, II/CSE, St. Anne's CET, anishchristy@gmail.com

Abstract- Recently, all over the world, crime against children is increasing at higher rates and it is high time to offer safety support system for the children going to schools. This paper focuses on implementing children tracking system for every child attending school. However the existing systems are not powerful enough to prevent the crime against children since these systems give information about the children group and not about each child resulting in low assurance about their child safety to parents and also does not concentrate on sensing the cry of the child and intimating the same to its parents. The proposed system includes a child module and two receiver modules for getting the information about the missed child on periodical basis. The child module includes ARM7 microcontroller (lpc 2378), Global positioning system (GPS), Global system for mobile communication (GSM), Voice playback circuit and the receiver module includes Android mobile device in parent's hand and the other as monitoring database in control room of the school. Finally, implementation results for the proposed system are provided in this paper.

Keywords—Android, ARM7, GPS, GSM,

I. INTRODUCTION

Recently, all over the world crime against children is increasing at higher rates and it is high time to offer safety support system for the children going to schools. This paper focuses on implementing children tracking system for every child attending school. However the existing systems are not powerful enough to prevent the crime against children since these systems give information about the children group and not about each child resulting in low assurance about their child safety to school authorities and also does not concentrate on sensing the cry of the child and intimating the same.

Children Tracking system is widely used all over the world to assure parents that their wards are safe from suspicious actions and their kid is happy in school atmosphere without crying. The proposed system includes tracking the child's movement to and from school. The information pertaining to missed child is sent to the control room of the school as well as to their respective parents, if they move beyond the coverage area. Not only the information about the child's whereabouts but also whether the child is crying is sent to parents through text message to their Android mobile device. The proposed system includes a child module and receiver module for getting the information about the missed child. The child module includes Cortex M3 (Lpc1768), Global positioning system (GPS), Global system for mobile communication (GSM), Voice recognition module, RFID tag and the receiver modules includes android phone and school module contains Global system for mobile communication (GSM), RFID.

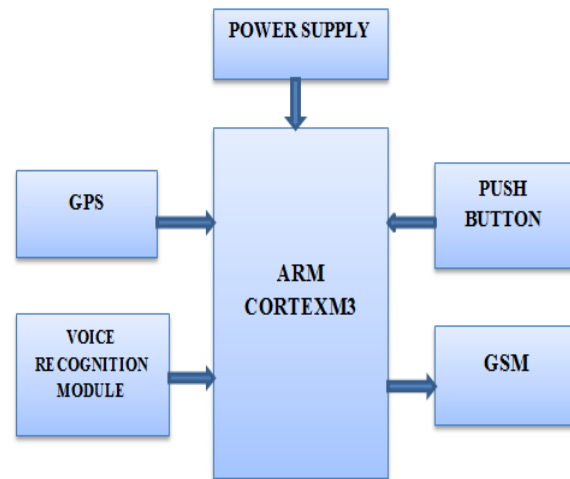


Fig.1.1 Block Diagram of Child module.

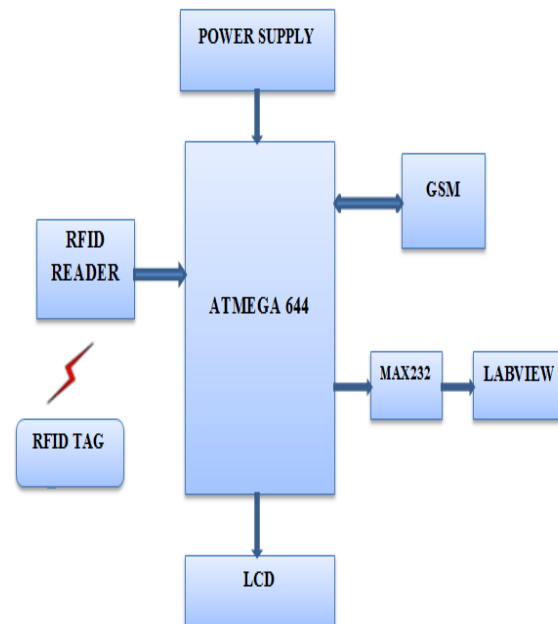


Fig.1.2 Block Diagram of School module.

School module (Figure1.2) includes RFID reader module, ATMEGA644 controller, GSM module, LCD and lab view for monitoring in the school. LCD is used to know whenever tag is to be placed and to know whether it is a valid card or not. RFID tag unique number is read by reader and is sent to ATMEGA 644P controller. If it is a valid card then a msg will be sent to the parent android phone that the child is present in the school and whenever the card is swiped second time then a msg will be sent that your child has left the school through GSM module and the same information will be shown in school mode in excel sheet by using Lab view software. Also whenever child cries or switch is pressed, GPS data also be displayed in school database.

II. DESIGN TECHNOLOGY

GPSTechnology

The Global Positioning System, usually called GPS, and originally named NAVSTAR, is a satellite navigation system used for determining one's precise location almost anywhere on Earth. A GPS unit receives time signal transmissions from multiple satellites, and calculates its position by triangulating this data. The GPS was designed by and is controlled by the United States Department of Defence and can be used by anybody for free. The cost of maintaining the system is approximately \$400 million per year.

GPS Principle

The GPS satellites act as reference points from which receivers on the ground detect their position. The fundamental navigation principle is based on the measurement of pseudo ranges between the user and four satellites. Ground stations precisely monitor the orbit of every satellite and by measuring the travel time of the signals transmitted from the satellite four distances between receiver and satellites will yield accurate position, direction and speed. Though three – range measurements are sufficient, the fourth observation is essential for solving clock synchronization error between receiver and satellite. Thus, the term —pseudo ranges is derived. The secret of GPS measurement is due to the ability of measuring carrier phases to about 1/100 of a cycle equalling to 2 to 3 mm in linear distance. Moreover the high frequency L1 and L2 carrier signal can easily penetrate the ionosphere to reduce its effect. Dual frequency observations are important for large station separation and for eliminating most of the error parameters.

GSMTechnology

The Global System for Mobile communication, usually called GSM, Telecommunications Standards Institute (ETSI) to describe protocols for second generation (2G) digital cellular networks used by mobile phones. The GSM standard was developed as a replacement for first generation (1G) analog cellular networks, and originally described a digital, circuit switched network optimized for full duplex voice telephony. This was expanded over time to include data communications, first by circuit switched transport, then packet data transport via GPRS (General Packet Radio Services) and EDGE (Enhanced Data rates for GSM Evolution or EGPRS).. GSM digitizes and compresses data, then sends it down a channel with two other streams of user data, each in its own time slot. It operates at either the 900 MHz or 1800 MHz frequency band. GSM is the de facto wireless telephone standard in Europe. GSM has over 120 million users worldwide and is available in 120 countries, according to the GSM MOU Association. Since many GSM network operators have roaming agreements with foreign operators, users can often continue to use their mobile phones when they travel to other countries.

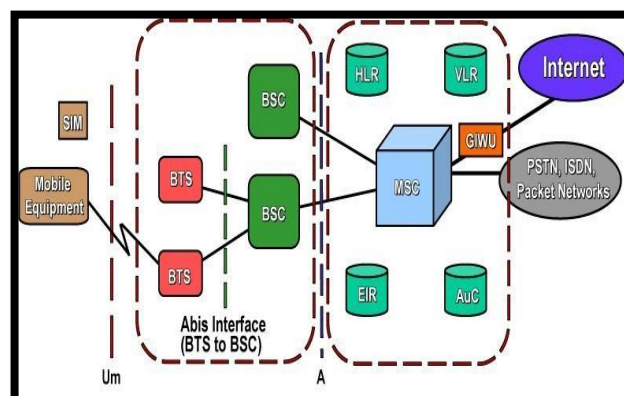


Fig.2.1 GSM Architecture

RFID (Radio Frequency Identification)

Radio-frequency identification (RFID) is the wireless non-contact use of radio-frequency electromagnetic fields to transfer data, for the purposes of automatically identifying and tracking tags attached to objects. The tags contain electronically stored information.



Fig.2.2 RFID Reader Board

Basic RFID consists of an antenna, transceiver and transponder. Antenna emits the radio signals to activate tag and to read as well as write information to it. Reader emits the radio waves, ranging from one to 100 inches, on the basis of used radio frequency and power output. While passing through electronic magnetic zone, RFID tag detects activation signals of reader. Powered by its internal battery or by the reader signals, the tag sends radio waves back to the reader.

III. HARDWARE SYSTEM DESIGN

A. ARM7 (LPC2378)

LPC 2378 belongs to ARM7 (Advance Risc Machine) family. It has high clocking speed and provides enhanced interfacing features with external devices. It needs low power for its functioning thus suiting for this paper. The embedded microcontroller has the knowledge to give AT commands to initiate and send the child information message to Mobile phone through GSM module.

B. GPS

GPS is a multiple – satellite based radio positioning system in which each GPS satellite transmits data that allows user to precisely measure the distance from the selected satellite to his antenna and to compute position, velocity and time parameters to high degree of accuracy [4].

IV. RESULT AND EXPERIMENTAL TOOLS

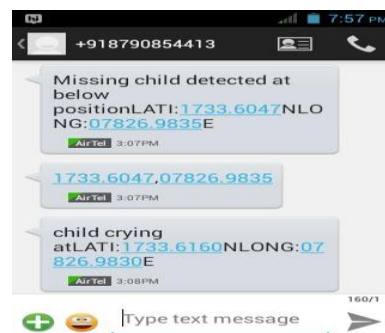
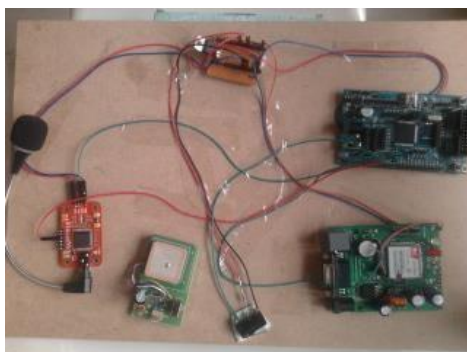


Fig 4.1 Kit Arrangement of ChildModule.

Fig 4.2 Message Displayed In Parent's Mobile.

The above fig shows the output displayed in parent's mobile whenever switch is pressed and also when ever child cry matches with cry in voice Recognition module.

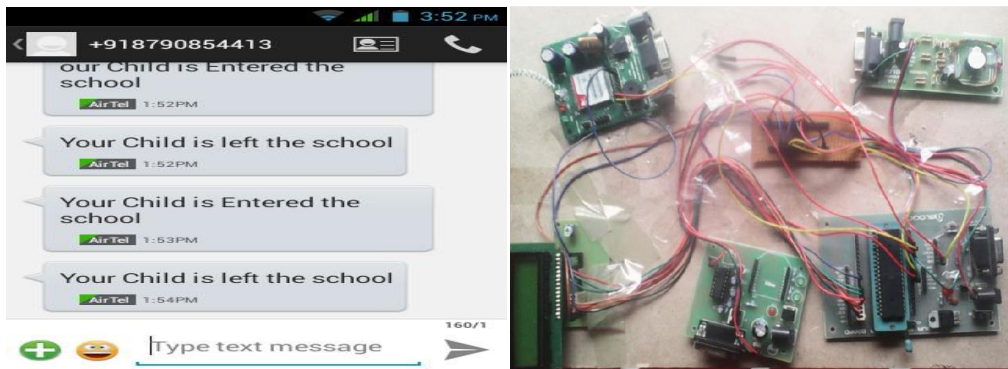


Fig.4.3Arrangement atSchoolmodulFig.4.4MsgDisplayedwhenRFIDTagisread

V. CONCLUSION

In this paper implementation primarily focuses on tracking a child's position and its location is sent to its school control room and parent's mobile. It also focuses on whether the child is present or not in the school and intimating the same to the school and the parent. This paper also focuses on recording a child's cry and when it matches with crying of the child in school the text message containing the location of a child will be sent to the parent and by using longitude and latitude values the location of a child can be traced by using app in the parent's mobile. In future It can be extended to perform the same for all children in the school by reducing the size of the child module. It can be also extended by interfacing a camera to the child module and intimating the missing child or child cry information both to the parents mobile and to the police control room.

REFERENCES

- [1] Yuichiro MORI, Hideharu KOJIMA, Eitaro KOHNO, Shinji INOUE, Tomoyuki OHTA, and Yoshiaki KAKUDA, "A Self-Configurable New Generation Children Tracking System based on Mobile Ad Hoc Networks Consisting of Android Mobile Terminals" proposed in 2011 tenth International symposium on Autonomous decentralized systems. W.-K. Chen, Linear Networks and Systems (Book style). Belmont, CA: Wadsworth, 1993, pp. 123-135.
- [2] Eitaro Kohno, Tomoyuki Ohta, Yoshiaki KAKUDA, Shinji Inoue and Yusuke Akiyama, "Performance Improvement of Hiroshima City Children Tracking System by Correction of Wrong Registrations on School Routes" Proc. 9th IEEE International Symposium on Autonomous Decentralized Systems (ISADS 2009), Athens, Greece, pp.261-265, 2009.
- [3] Lijun Jiang, Lim Nam Hoe, Lay Leong Loon, "Integrated UWB and GPS Location Sensing System in Hospital Environment", proposed in 2010 5th IEEE conference on Industrial Electronics and Applications
- [4] Peng Wang, Zhiwen Zhao, Chongbin Xu, Zushun Wu, Yi Luo, "Design and Implementation of the Low-Power tracking System Based on GPS/GPRS Module" proposed in 2010 5th IEEE conference on Industrial Electronics and Applications.
- [5] Tomoyuki Ohta, Shinji Inoue, Yoshiaki Kakuda, and Kenji Ishida, "An adaptive multihop clustering scheme for ad hoc networks with high mobility," IEICE Transactions on Fundamentals of Electronics, Communications and Computer Sciences (Special Issue on Multidimensional Mobile Information Networks), vol.E86-A, no.7, pp.1689-1697, 2003.

E-Voting System Using Android Smartphone

Y.Jenifer¹, B.Prithivi Bala².

^{1,2} *Students of science and humanities .*

St. Anne's college of engineering and technology (panruti).

Abstract: The objective of this project is to propose a real time capturing system for consumer supplies using Quick Response (QR) code in an Android smart phone. Using Multiplexing and De - multiplexing process encode and decode the information from single QR code with special symbols and split the data back to their QR Code pattern where these QR Code pattern can be read by Android smart phones. Standard image codes like one-dimensional barcodes and two- dimensional codes with black and white patterns identifies a product for its value and basic features but does not authenticate it, moreover not every product that is identified, is used for authenticating manufacturer's warranty.

In particular, we concentrate on the cases where the memory entries and their associations form a binary hamming space or an infinite square grid. Particularly, we focus on minimizing the number of input clues needed to retrieve information with small uncertainty and present good constructions some of which are optimal. In the proposed method the concept of e-voting application is created using android. The authentication is done through the scanning of QR-Code through the mobile scanner application. In this method the voter has to register using the application and the QR-Code will be provided once the registration is successful. On scanning the QR-Code the voter will be asked for the password. Once the authentication is done the voter is made to proceed with the voting process. The main purpose of implementing this concept is to increase the voting percentage. So that the voter is not required to visit the voting centre to cast their vote and also to avoid fake voting.

Key words Quick Response Code, Barcode, etc.

1. INTRODUCTION

The proper execution of democratic rights has become linked to the availability and reliable functioning of advanced information and communication technology (ICT). While modern societies fully rely on ICT for business, work and leisure time activities, the use of ICT for democratic decision making is still in its infancy. In fact, the out date technological concepts for voting have been blamed in part for lost and uncounted votes and could therefore be responsible for biased political decisions making. Countries all over the world are examining e-voting, for it has some striking advantages over traditional paper voting, including security for casting votes, accuracy of counting and analyzing votes, options to conduct voting in a centralized and decentralized manner, etc. The reasons why the e-voting technology has not matured to equivalent levels as known for business and leisure time activities lies mostly in an inherent lack of trust and fear of electronic threats. While most countries are still conceptualizing or testing e- voting systems, three cantons in Switzerland have pioneered the development of e-voting to its full technological maturity. The world is always in improvement and growth in technology, that's why we should go parallel with it, to be able as much as we can get benefit from these improvements.

1.1 VOTING VIA SMS

Each voter can vote by sending an SMS using any kind of mobile connection line or any kind of mobile hand set to the system through the "Mobile Switch Center". For this such type system, an android application is created in Android phone, then the system will start implementing some processes on that SMS which is sent by the voters into the server through a network. A database is installed on the server side to send a result back to the voter by the android system application. The voter can use internet connection through a website which is developed throughout this work.

Backend is created for the two ways connection. Both Android system and the Website are linked to the same (MySQL) database in order to the voter can vote through one of the two ways only one time and if he/she tries to vote again the system will deny him/her.

1.2 VIA INTERNET - VOTING

An electronic voting system (on-line voting, internet voting) is an election system which uses electronic ballot that would allow voters to transmit their secure and secret voted ballot to election officials over the internet. With the prosperity of internet over the years, inventers start to make the use of electronic voting in order to make the voting process more convenient and raise the participation of the civic. From now on, engineers have repeatedly created new technology to improve the feasibility of electronic voting system.

2. LITERATURE REVIEW

2.1 Existing System:

Existing System is the one in which the biometric concept is used where the scanning of finger print is done. For some people it is very intrusive, because is still related to criminal identification. In existing system Encryption and cryptography algorithms are not used. Barcodes are often intended for consumer use where using a barcode device, a consumer can take an image of a barcode on a voter_id card. The barcode must be read using computer vision techniques and barcode can hold information, it makes this vision task in consumer scenarios unusually challenging. Barcode decoder can give the vision algorithm feedback, and develop a progressive strategy of the voter.

2.2 proposed System:

System resides in the new concept of QR-Code and Scanner Application. Candidate details made to hide in the QR-Code. Through scanner application the QR-Code is scanned and details are retrieved. Then the voting is performed. In the proposed system, we are using QR code for recognizes image codes using smart phones to provide various services that can recognize the authenticity of any voter details. So QR code verifies voter_id no by capturing it through the smart phone, then decodes and sends it to the server for authentication. The customer forwards the selected voter_id number list to the server and the response received from the server enables the consumer to decide based on the voter authenticity.

3. DESIGN AND IMPLEMENTATION

The E-Voting is a process that can perform in two ways that are SMS voting and via internet voting. The voter should register first and if a voter is already registered means for that voter QR-Code can be generated if the voter is new to the process he/she had should register and the database will generate the QR-Code for the voter. Then the voter should download the scanning application to his/her mobile to scan the generated QR-Code for the voter. After the scanning

process the database ask the password for an authentication. Then the voter should perform the operation for process to vote.

After the authentication the voter is proceed to vote by selecting candidate post standing. After the selecting candidate then select the district and then select the ward then voter should select the candidate and proceed to vote. Then vote is added on the database. The database sends the conformation message to voter your vote has been successfully registered.

3.1 Generating qr-code image:

In this module we are creating QR Code for encoding the information about the voter. The voter details contains voter_id no, voter_name, DoB, Address. Each pattern is encoded and represented each module in QR Code with black and white special symbols. QR-Code can hold information more than other bar codes. The format of QR Code includes unique Finder Pattern (Position Detection Patterns) located at three corners of the symbol and can be used to locate the positioning of the symbol, size and inclination.

3.2 Mobile authentication module:

This module represents the authentication, which is used for the voter to login their details for the voting processes. Logged voter is redirected to the scanner module. Authentication is used as the basis or authorization determining whether a privilege will be granted to a particular user or process. The validation processes are done on the web server.

Blurring Algorithm In image terms blurring means that each pixel in the source image gets spread over and mixed into surrounding pixels. Another way to look at this is that each pixel in the destination image is made up out of a mixture of surrounding pixels from the source image.

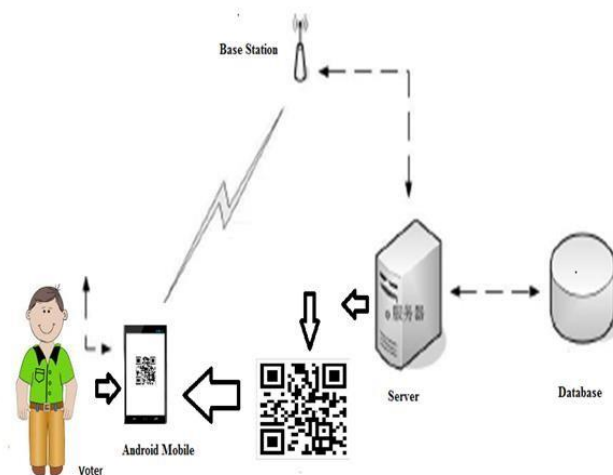


Figure – 1: Overview of Architecture Diagram

3.3 Qr - Code Scanner Module

This module is used to scan the QR-Code and read the value of the QR-Code inside the mobile. QR- Code is a matrix bar code designed to be read by Smartphone. The code contains of black modules arranged in a square pattern on a white background. The information encoded may be text, a URL, or other data. If the voter selects the candidates, the details will directly forward to the server.

3.3.1 Scaling Algorithm:

Scaling Algorithm Image scaling is the process of resizing a digital image. Scaling is a non-trivial process that involves a trade-off between efficiency, smoothness and sharpness. Image is scaled into some standard size by using different scaling methods.

3.4 Web Service Client Module:

This module has the process of storing the selected candidate information from the client, which are send through the web service. All these information's will be stored in the database. We are maintaining a centralized server to receive the selected voter list from the database through internet. In this module the candidate see they data retrieved from the database. The Voter will use this list to perform the voting.

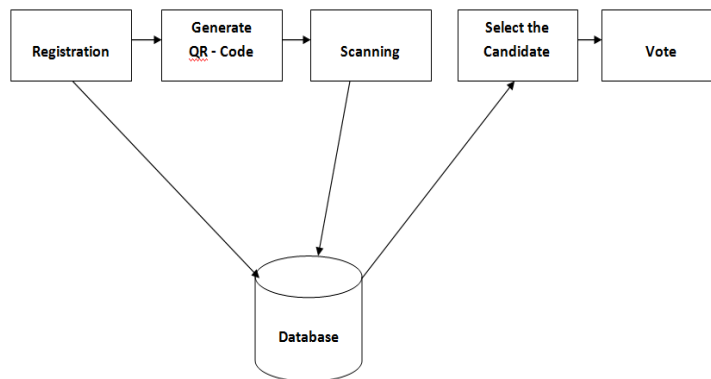


Figure – 2: Data Flow Diagram for E-Voting System

4. CONCLUSION

Context QR codes can provide great value when used in situations that dynamically change depending on the context. Augmented reality is an interesting field for the application of this concept, as it enables user interaction with different technologies. Depending on the context, the characteristics of contextual QR codes assist users to bring them closer into augmented reality and enable content access from different experiences immediately and transparently by taking advantage of the features provided by contextual QR codes. This paper has presented a system that uses contextual QR Codes to activate different actions to deal with different devices and user situations. Our system will demonstrate that it is possible to implement different augmented reality technologies under different contexts.

REFERENCES

- [1] "QR Images: Optimized Image Embedding in QR Codes" Gonzalo J.Garateguy, Member, IEEE, Gonzalo R. Arce, Fellow, IEEE, Daniel L. Lau, Senior Member, IEEE, Ofelia P. Villarreal, Member, IEEE.
- [2] Azuma R. T, "A Survey of Augmented Reality", vol. 4, no. August, pp.355–385, 1997.
- [3] Choi Jang .B, and Kim.G.J, "Organizing and presenting geospatial tags in location based augmented reality", Personal and Ubiquitous Computing, vol.15, no.6, pp.641-647, Nov.2010.
- [4] Kan T.C. Teng, and W. Chou, "Applying QR code in augmented Reality applications," Reality Continuum and its Applications, vol. 1, no.212, pp. 253–258, 2009.
- [5] Madden.L, Professional Augmented Reality Browsers for Smart phones John Wiley & Sons2011, p. 360.
- [6] Reitmayr .G and Schmalstieg .D, "Location based applications for Mobile augmented reality", Proceeding of the Fourth Australasian user, 2003.

NANOSCALE STIFFNESS DISTRIBUTION IN BONE METASTASIS

B.Prithivi bala¹ Y.Jenifer²

^{1,2} *Students of science and humanities .*

St.Anne's college of engineering technology (panruti)

Abstract: Nanomechanical heterogeneity is expected to have an effect on elasticity, injury and bone remodeling. In normal bone, we have two types of cells (osteoclasts and osteoblasts) working together to maintain existing bone. Bone cancers can produce factors that make the osteoclasts work harder. This means that more bone is destroyed than rebuilt, and leads to weakening of the affected bone. We report here the first demonstration of the nanoscale stiffness distribution in bone metastases before and after treatment of animals with the bisphosphonate Risedronate, a drug which is currently used for the treatment of bone metastases in patients with advanced cancers. The strategy used here is applicable to a wide class of biological tissues and may serve as a new reflection for biologically inspired scaffolds technologies.

Keywords: Bone Metastasis, Stiffness, Risedronate.

1.INTRODUCTION

As cancer becomes more advanced, it tends to spread throughout the body, with the bones being a common site of spread for many cancers [1]. Spread of cancer to the bone from its original site is referred to as bone metastases. Treatment may consist of radiation therapy, bisphosphonates, hormone therapy and/or chemotherapy, depending upon the type of cancer from which the metastasis originated [2] [3]. Researchers are evaluating ways to avoid or decrease the ache or break caused by bone metastasis, not just provide treatment once they occur. Myeloma and some secondary bone cancers can produce factors that make the osteoclasts work harder [1]-[4]. This means that more bone is destroyed than rebuilt, and leads to weakening of the affected bone. This can cause pain and means that the bone can fracture or break more easily; in this case, ablation of metastasis bone and implantation of biomaterials are needed. As many natural materials, bone is heterogeneous. Mechanical heterogeneity is expected to exist at different length scales. It has become evident that the nanoscale properties of bone participate in its macroscopic biomechanical function [4]-[7]. At the macroscopic level, considerable variations in mechanical properties have been detected for different tissues locations [8], as well as for regions within a specific location [9]. Microscopically, indentation has further identified differences in modulus and hardness for specific features such as lamellae (thin and thick) in osteons of bone which have been recognized as collagen fibril orientation, as well as variations in mineral composition [10] [11]. The cellular remodeling process resulting in a combination of new and old bone is a result of this heterogeneity at this length scale [12]. Atomic force microscopy (AFM)-based nanoindentation has been used to distinguish mechanically heterogeneous microscale regions in bone tissue from genetically modified mice [13]-[16]. These studies also raise important issues as to whether heterogeneity is advantageous or disadvantageous to the mechanical function of bone [17]. Recently, the detailed study of the consequences of heterogeneity, in particular at the nanoscale, was reported [18].

An inherent feature of bones is their heterogeneity in the collagen fibril orientation and the mineral content. This particular spatial structure has a direct incidence on their elasticity even on the nanometer scale [18]. The elasticity, or equivalently the stiffness, of a material can be quantified using nano-indentation. It consists in fixing a probe (most often a sphere, a cone or a pyramid) at the end of the cantilever of an atomic force microscope (AFM) and to measure the deflection of the cantilever when the material to be characterized is pushed into contact with the probe. The applied force is derived from the deflection, and the indentation is derived from the deflection and

the material displacement. In this way, we obtain a so-called force curve. If the material behaves as an elastic solid, a force curve can be interpreted using Hertzian mechanics [19]. This characterization method was used to compare healthy bone, bone with metastases, and bone after treatment with bisphosphonates. Bisphosphonates drugs are used for the treatment of cancer-related hypercalcemia and treatment of bone metastases in patients with advanced cancers [2]. Bisphosphonates decrease the rate of bone destruction in patients with bone metastases and clinical studies have demonstrated that bisphosphonates can significantly decrease the pain and number of fractures induced by bone metastases. Bisphosphonates are established in the treatment of skeletal metastases [12]. They have a common P-C-P structural feature consisting in a central carbon atom correlated to two phosphonate moieties, and two substituents (R1, R2) (**Figure 1**). Phosphonate and R1 (preferably hydroxyl) groups allow bisphosphonates to bind

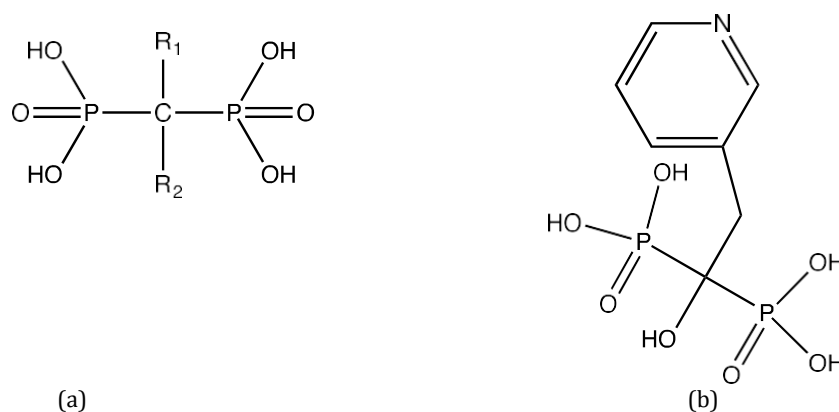


Figure 1. (a) Chemical structure of bisphosphonate drugs. P-C-P common structural feature of bisphosphonates and location of the specific R1 and R2; (b) Chemical structure of the Risedronate (RIS) antitumor drug (2-(3-pyridinyl)-1-hydroxyethylidene-bisphosphonic acid).

avidly to bone hydroxyapatite, while R2 determines their effectiveness to inhibit osteoclast-mediated bone resorption [3]. Clinically, bisphosphonates significantly diminish bone destruction rate, pain and fractures associated with bone metastases [2]. Moreover, there is extensive *in vivo* preclinical evidence that bisphosphonates reduce skeletal tumor burden and inhibit bone metastasis formation in animals [12]. Among proposed mechanisms of actions, bisphosphonates may render bone a less favorable microenvironment for metastasis development by reducing osteoclast-mediated bone resorption, which, in turn, deprives tumor cells of bone-derived growth factors required for their proliferation. Additionally, bisphosphonates were shown to exert direct antitumor action, as they inhibited tumor cell adhesion, invasion, and proliferation, and induced apoptosis of various human tumor cell lines *in vitro* [3]. However, to date this clear direct antitumor potential was not verified *in vivo* [10], due to the high affinity of bisphosphonates for bone mineral which must obstruct their availability for tumor cells. We undeniably observed a significantly higher potency of soluble compared to mineral-bound bisphosphonates at inhibiting tumor cell adhesion to bone *in vitro* [1]. Therefore strategies are needed to optimize bisphosphonates bioavailability and direct antitumor activity *in vivo*. As well, cells are constantly changing their mechanical environment [20] and nanomechanical heterogeneity detection could facilitate damage detection in the extracellular matrix and improved remodelling responses. The heterogeneous nanomechanical prototypes measured experimentally could in turn induce local heterogeneous strains when loaded macroscopically. Such strains are expected to be increased by the softer surrounding cellular matrix of osteocytes [21] and also expected to influence interstitial fluid flow. The objective of this work was to analyze the nanomechanical distribution of breast cancer bone metastasis before and

after treatment of metastatic animals with Risedronate, the usually administrated drug in clinic. In this study, we have first analyzed by radiography, histology and histomorphometry the legs from metastatic mice and compared them with those from animals that had not been injected with breast cancer cells (naïve mice). By radiography, we have analyzed and compared the healthy bone without metastasis (**Figure 2(a)**), bone with metastasis induced after inoculation (**Figure 2(b)**) and the treated bone after treatment by Risedronate (**Figure 2(c)**). After radiography on day 32 after tumor cell injection, we have shown that metastatic animals had large osteolytic lesions in hind limbs when compared to the bones of naïve mice (**Figure 2**, panels b vs a). Metastatic animals were then treated either with the bisphosphonate Risedronate (administered by subcutaneous injection intermined the size of bone metastasis (**Table 1**). Our results indicate clearly the antitumor efficacy of the treatment by Risedronate (0.6 mm^2 for treated bone, compared to 5 mm^2 for bone without treatment). We also performed histology and compared tumor burden and soft tissue volume ratio before and after treatment by Risedronate (**Figure 3** and **Table 2**). The images shown in **Figure 3** are examples that best illustrate the effects of the treatments with Risedronate (**Figure 3(c)**) compared to no treated bone with tumor cells (asterisk in **Figure 3(b)**). To get more information PBS, used here as the vehicle) or the vehicle only. After radiographic analysis, we examined the effect of Risedronate on the extent of bone destruction and de-

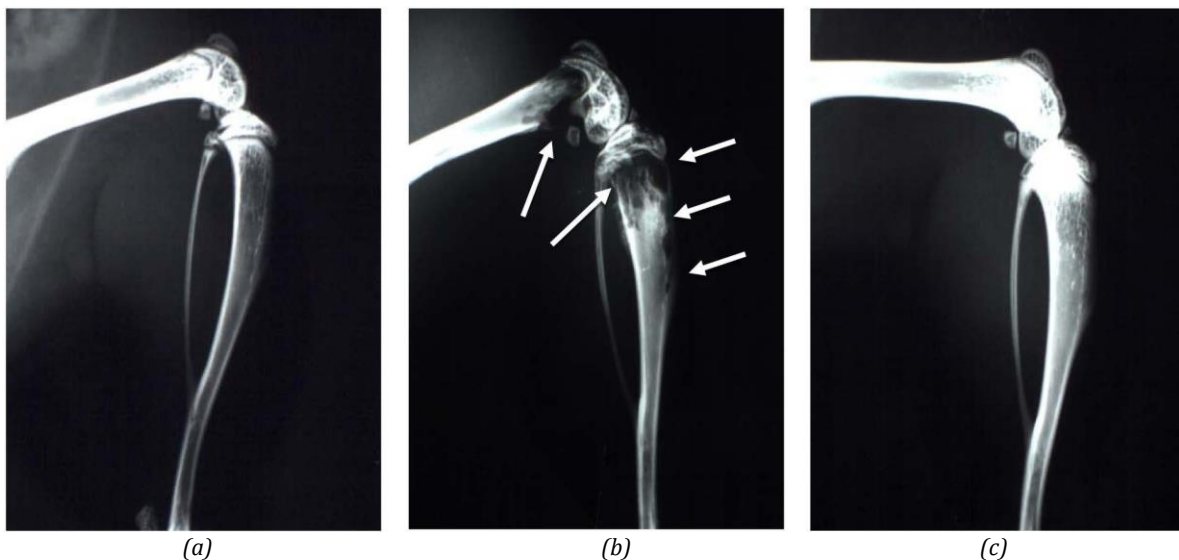


Figure 2. Identification of bone metastasis on radiographs of hind limbs from mice not injected with tumor cells with healthy bone, Naïve (a); b and c radiographs were obtained from different mice at day 32 after CHO- β 3 tumor cells inoculation. PBS was used as vehicle and corresponds to bone with metastasis (b); Risedronate was used to treat mice and the radiographs represent the treated bone (c). The radiographs displayed are examples that best illustrate the effects of treatments. Arrows indicate osteolytic lesions.

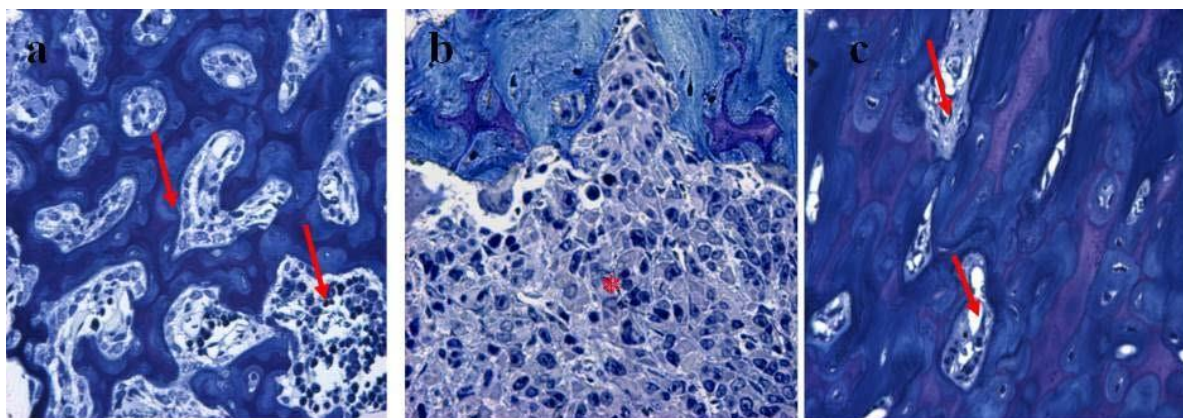


Figure 3. Optical microscopy visualization after semi-thin section ($7\ \mu\text{m}$) Histologic analysis of hind limbs from mice naïve with healthy bone (a); b and c were obtained from different mice at day 32 after CHO- β 3 tumor cells inoculation. PBS was used as vehicle and corresponds to bone with metastasis (b); Risedronate was used to treat mice and represent the treated bone (c). After toluidine blue stain, bone is stained blue and tumor cells zone were represented by asterisk. The arrows indicate the bone marrow.

Table 1. Tumor size determination after radiography.

Treatment*	Radiography (Tumor size)
Naive “healthy bone”	0
Vehicle “bone metastasis”	5 ± 0.6
Risedronate “treated bone”	$0.6 \pm 0.08^{\S}$

*Drug administration was initiated from the time of tumor cell inoculation (day 0) to the end of the protocol (day 32). All measurements were made 32 days after tumor cell injection. Naive animals had not been injected with tumor cells and correspond to the healthy bone. PBS was used as vehicle for animals injected with tumor cells and correspond to bone metastasis. Risedronate animals treated by daily dose of 150 mg/kg, s.c. (clinical dose for patient with bone metastasis). Results are expressed as the mean \pm SD (2 Naive mice, 3 Vehicle mice and 3 Risedronate mice). $^{\S}P < 0.01$, compared to the vehicle-treated group. Statistical pairwise comparisons were made using Mann-Whitney U test.

Table 2. Histomorphometry from histology analysis.

Treatment*	Histomorphometry BV/TV (%)	TB/STV (%)
Naive “healthy bone”	$22.7 \pm 1.8^{\S}$	0
Vehicle “bone metastasis”	9.5 ± 2.6	42.4 ± 3.6
Risedronate “treated bone”	$33.2 \pm 2.4^{\S}$	$6.4 \pm 3.4^{\S}$

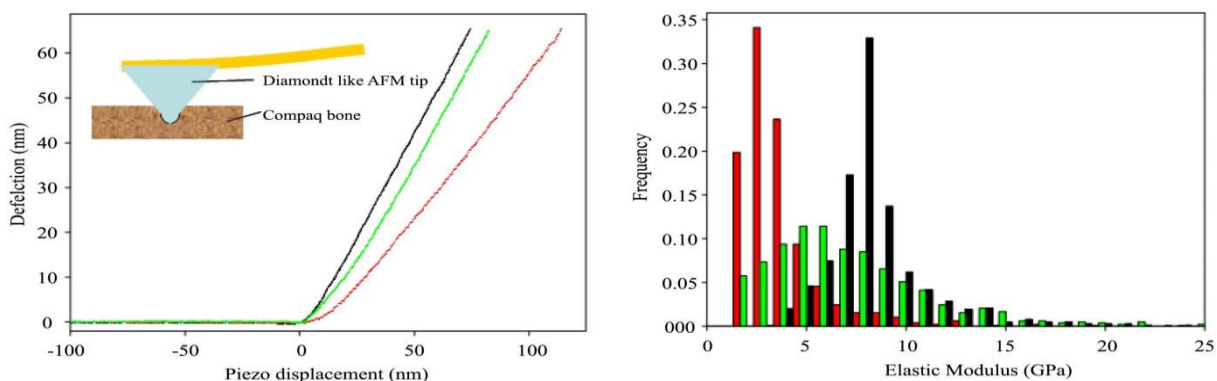
Naive animals are mice that had not been injected with tumor cells. Risedronate (150 $\mu\text{g}/\text{kg}$, daily)

was administered to metastatic animals by subcutaneous injection in 0.1 mL PBS (vehicle). Control mice bearing metastatic lesions received a daily treatment with the vehicle only. *Drug administration was initiated from the time of tumor cell inoculation (day 0) to the end of the protocol (day 32). \checkmark Histomorphometry was performed on legs from naïve and metastatic animals. BV/TV: bone volume/tissue volume ratio (a measurement of the bone volume). TB/STV: tumor burden/soft tissue volume ratio (a measurement of the tumor volume). Results are expressed as the mean \pm SD (2 Naïve mice, 3 Vehicle mice and 3 Risedronate mice). $\S P < 0.01$, compared to the vehicle-treated group. Statistical pairwise comparisons were made using Mann-Whitney U test.

concerning the quantification of bone, we analyzed finely by histomorphometry the histologic data and determined the ratio bone volume/tissue volume and tumor burden/soft tissues volume (**Table 2**). The beneficial effect of the treatment is demonstrated by the increase of the ratio BV/TV from 9.5% for bone without treatment to 33.2% for the treated bone. We have also shown that after treatment the ratio TB/STV was 6.4% in comparison to 42.4% without treatment. Metastatic animals treated with Risedronate had osteolytic lesions that were 95% smaller than those of tumor-bearing animals treated with the vehicle only (**Table 1** and **Figure 2(c)**). Histologic analysis of hind limbs with metastases from vehicle-treated mice showed that tumor cells completely filled the bone marrow cavity and bone trabeculae were almost completely destroyed when compared to the bone histology of legs from naïve mice (**Figure 2**, panels b vs a). By contrast, the extent of bone trabeculae in legs from Risedronate-treated mice was markedly increased, indicating a complete prevention of bone loss by the bisphosphonate (**Figure 2(c)**). In this respect, histomorphometric analysis of metastatic hind limbs from mice treated with Risedronate showed that the bone volume (BV) to tissue volume (TV) ratio was statistically significantly higher than that corresponding to vehicle-treated animals and naïve mice (**Table 2** and **Figure 2**). Risedronate also decreased the tumor burden (TB) to soft tissue volume (STV) ratio by 85% compared with vehicle (**Table 2** and **Figure 2**). In order to get more information about the structure of bone after Risedronate treatment, we analyzed and compared by electron microscopy the bones from naïve animals with those obtained from metastatic animals treated with the bisphosphonate. By optical microscopy, we visualized different cells (**Figure 3**) after semi-thin sections (7 μm) of the different bone and toluidine blue stain. **Figure 3(b)** shows the invasion of bone by tumor cells working harder to destroy bone. In **Figure 3(a)** and **Figure 3(c)**, we have a normal bone with bone marrow section and mineralized bone with osteoblasts and osteoclasts. In **Figure 3(c)**, we can also see more mineralization than in **Figure 3(a)**. This result could be explained by the capacity of Risedronate to induce mineralization.

Bones from naïve animals and metastatic animals treated or not with Risedronate were next analyzed by Atomic Force Microscopy (AFM) in order to examine the ultrastructure and nanomechanical spatial heterogeneity of the bone tissue (**Figure 4**).

The raw indentation curves were obtained by atomic force microscopy with diamond-like tip (**Figure 4(a)**). We report here the first demonstration of the ultrastructure and nanomechanical spatial heterogeneity of bone



(a)

(b)

Figure 4. Representative raw indentation curves (a) and comparison of bone stiffness distribution (b). (a) Raw indentation curves obtained by atomic force microscopy with diamond like tip (100 nm of radius) for naïve healthy bone (black bar), vehicle bone with metastasis (red bar) and Risedronate treated bone (green bar) selected in the highest value of distribution.

(b) Bone stiffness distributions for naïve healthy bone (black bars) with a median of 8.14 GPa (first quartile = 6.39 GPa, third quartile = 10.33 GPa), for bone with metastasis and Risedronate treated bone (green bars) with a median of 5.45 GPa (first quartile = 3.49 GPa, third quartile = 8.08 GPa), and vehicle bone with metastasis (red bars) with a median of 2.38 GPa (first quartile = 1.60 GPa, third quartile = 3.39 GPa), obtained after computation of the elastic modulus from nanoindentation data.

stiffness with metastasis and the effect of the treatment on this nanomechanical distribution. The distribution of elastic modulus highlights the major decrease of elastic modulus in bone with metastasis (see histograms above). The median value is divided by a factor larger than 3 (8.14 GPa for healthy bone, 2.38 GPa for bone with metastasis). The Risedronate treatment reduces this decrease with an intermediate median value of 5.45 GPa. The differences in median and quartile interval underscore in particular the strong softening of malignant bone with respect to the healthy bone. Furthermore, it should be emphasized that the Risedronate treatment leads to a significant recovering of the nanomechanical stiffness. To observe more finely these differences, spatial distribution of elastic modulus has been recorded (**Figure 5**). In **Figure 5**, for each nanoindentation data spaced of 300 nm, the elastic modulus is represented by a colour value. The three types of bone present heterogeneity in the spatial elastic modulus repartition (**Figure 5(b)**),

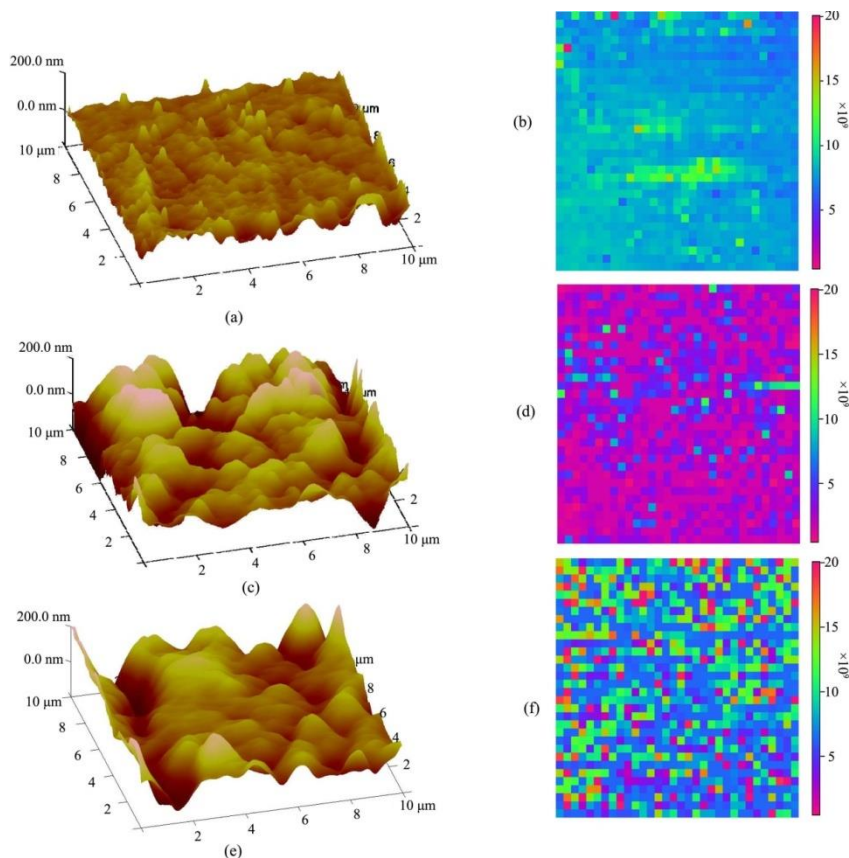


Figure 5. Ultrastructure and nanomechanical spatial heterogeneity of bone stiffness. (a) An a.c. intermittent contact-mode AFM height image ($10 \times 10 \mu\text{m}^2$) viewed perpendicular to the naive healthy bone axis with a RMS of 21.0 nm; (b) 2D contour map ($10 \times 10 \mu\text{m}^2$) of elastic modulus calculated from nanoindentation data (c) An a.c. intermittent contact-mode AFM height image ($10 \times 10 \mu\text{m}^2$) viewed perpendicular to the vehicle bone with metastasis axis with a RMS of 55.3 nm. (d) 2D contour map ($10 \times 10 \mu\text{m}^2$) of elastic modulus calculated from nanoindentation data; (e) An a.c. intermittent contact-mode AFM height image ($10 \times 10 \mu\text{m}^2$) viewed perpendicular to the Risedronate treated bone axis with a RMS of 50.1 nm; (f) 2D contour map ($10 \times 10 \mu\text{m}^2$) of elastic modulus calculated from nanoindentation data.

Figure 5(d), Figure 5(f)), but the bone with metastasis and Risedronate treatment is particular heterogeneous as revealed by the wide range of values of E present in the $10 \times 10 \mu\text{m}^2$ sample (Figure 5(f)). In summary, bone is constantly being broken down and renewed. It is living tissue that needs exercise to gain strength. Bone metastasis occurs when cancer cells from the primary tumor relocate to the bone. Metastatic bone disease develops as a result of the many interactions between tumor cells and bone cells. This leads to disturbance of normal bone metabolism, with the increased osteoclast activity seen in most, if not all, tumor types providing a rational target for treatment. Like many natural materials, bone is mechanically heterogeneous with spatial distributions in the shape, size and composition of its constituent. It is expected that nanomechanical heterogeneity influence elasticity, damage, fracture and remodelling of bone. We report here the first demonstration of the nanoscale stiffness distribution in bone metastasis before and after treatment of animals with Risedronate, a drug which is currently used for the treatment of bone metastases in patients with advanced cancers. This concept is generally applicable to a broad class of natural materials because nanomechanical heterogeneity expected to be ubiquitously presented.

Methods

Specific Drug for Treatment

Bisphosphonate Risedronate [2-(3-pyridinyl)1-hydroxyethylidene-bisphosphonic acid] was obtained from Procter and Gamble Pharmaceuticals (Mason, OH, USA). The drug was dissolved in water and stored at 4°C.

Mouse Model of Breast Cancer Bone Metastasis

All procedures involving mice including their housing and care, the method by which they were killed, and all experimental protocols were conducted in accordance with a code of practice established by the ethical committee in Lyon (France). This study was monitored on a routine basis by the attending veterinarian according to ensure continued compliance with the proposed protocols. Four-week-old female Balb/c athymic (nu/nu) mice were purchased from Charles River (St. Germain sur l'Arbresle, France). The bone metastasis experiments in mice were conducted as previously described, using B02 cells, a subpopulation of the human MDA-MB-231 breast cancer cell line that was selected for the high efficiency with which it metastasizes to bone after intravenous inoculation [22]. B02 cells (5×10^5 cells in 100 μL phosphate-buffered saline) were injected into the tail vein of anesthetized (130 mg/kg ketamin and 8.8 mg/kg xylazin) mice on day 0. Based on an average body weight of 20 g for 4-wk-old mice, risedronate (150 $\mu\text{g}/\text{kg}$ body weight) was given daily to animals by subcutaneous injection in 100 μL PBS (vehicle). Control mice received a daily treatment with the vehicle only. On day 32 after tumor cell inoculation, radiographs of anesthetized animals were taken with the use of MIN-R2000 film (Kodak) in an MX-20 cabinet X-ray system (Faxitron X-ray Corporation). Osteolytic lesions are recognized on radiographs as demarcated radiolucent lesions in the bone. The area of the osteolytic lesions was measured using a Visiolab 2000 computerized image analysis system (Explora Nova, La Rochelle, France) and the extent of bone destruction per animal was expressed in mm^2 , as described previously [22].

Anesthetized animals were killed by cervical dislocation following radiography at day 32.

Bone Histology and Histomorphometry

Bone histology and histomorphometric analysis of bone tissue sections were performed as previously described [22]. Vehicle- and bisphosphonate-treated tumor-bearing animals were killed at day 32, and both hind limbs from each animal were dissected, fixed in 80% (vol/vol) alcohol, dehydrated, and embedded in methyl-methacrylate. A microtome (Polycut E, Reichert-Jung, Heidelberg, Germany) was used to cut 7 μm thick sections of undecalcified long bones, and the sections were stained with Goldner's trichrome. Histologic and histomorphometric analyses were performed on Goldner-stained longitudinal medial sections of tibial metaphysis with the use of a computerized image analysis system (Visiolab 2000). Histomorphometric measurements [bone volume (BV)/tissue volume (TV) and tumor volume (TV)/soft tissue volume (STV) ratios] were performed in a standard zone of the tibial metaphysis, situated at 0.5 mm from the growth plate, including cortical and trabecular bone. The BV/TV ratio represents the percentage of bone tissue. The TV/STV ratio represents the percentage of tumor tissue.

REFERENCES

- [1] Boissier, S., Magnetto, S., Frappart, L., Cuzin, B., Ebetino, F.H., Delmas, P.D. and Clezardin, P. (1997) Bisphosphonates Inhibit Prostate and Breast Carcinoma Cell Adhesion to Unmineralized and Mineralized Bone Extracellular Matrices. *Cancer Research*, 57, 3890-3894.
- [2] Coleman, R.E. (2008) Risks and Benefits of Bisphosphonates. *British Journal of Cancer*, 98, 1736-1740. <http://dx.doi.org/10.1038/sj.bjc.6604382>
- [3] Stresing, V., Daubine, F., Benzaid, I., Monkkonen, H. and Clezardin, P. (2007) Bisphosphonates in Cancer Therapy. *Cancer Letters*, 257, 16-35. <http://dx.doi.org/10.1016/j.canlet.2007.07.007>
- [4] Fantner, G.E., Hassenkam, T., Kindt, J.H., Weaver, J.C., Birkedal, H., Pechenik, L., Cutroni, J.A., Cidade, G.A., Stucky, G.D., Morse, D.E. and Hansma, P.K. (2005) Sacrificial Bonds and Hidden Length Dissipate Energy as Mineralized Fibrils Separate during Bone Fracture. *Nature Materials*, 4, 612-616. <http://dx.doi.org/10.1038/nmat1428>
- [5] Gao, H., Ji, B., Jager, I.L., Arzt, E. and Fratzl, P. (2003) Materials Become Insensitive to Flaws at Nanoscale: Lessons from Nature. *Proceedings of the National Academy of Sciences of the United States of America*, 100, 5597-5600. <http://dx.doi.org/10.1073/pnas.0631609100>
- [6] Gupta, H.S., Wagermaier, W., Zickler, G.A., Raz-Ben Aroush, D., Funari, S.S., Roschger, P., Wagner, H.D. and Fratzl, P. (2005) Nanoscale Deformation Mechanisms in Bone. *Nano Letters*, 5, 2108-2111. <http://dx.doi.org/10.1021/nl051584b>
- [7] Tai, K., Ulm, F.J. and Ortiz, C. (2006) Nanogranular Origins of the Strength of Bone. *Nano Letters*, 6, 2520-2525. <http://dx.doi.org/10.1021/nl061877k>
- [8] Morgan, E.F., Bayraktar, H.H. and Keaveny, T.M. (2003) Trabecular Bone Modulus-Density Relationships Depend on Anatomic Site. *Journal of Biomechanics*, 36, 897-904. [http://dx.doi.org/10.1016/S0021-9290\(03\)00071-X](http://dx.doi.org/10.1016/S0021-9290(03)00071-X)
- [9] Pope, M.H. and Outwater, J.O. (1974) Mechanical Properties of Bone as a Function of Position and Orientation. *Journal of Biomechanics*, 7, 61-66. [http://dx.doi.org/10.1016/0021-9290\(74\)90070-0](http://dx.doi.org/10.1016/0021-9290(74)90070-0)
- [10] Gupta, H.S., Stachewicz, U., Wagermaier, W., Roschger, P., Wagner, H.D. and Fratzl, P. (2006) Mechanical Modulation at the Lamellar Level in Osteonal Bone. *Journal of Materials Research*, 21, 1913-1921. <http://dx.doi.org/10.1557/jmr.2006.0234>
- [11] Rho, J.Y., Roy, M.E., 2nd, Tsui, T.Y. and Pharr, G.M. (1999) Elastic Properties of Microstructural Components of Human Bone Tissue as Measured by Nanoindentation. *Journal of Biomedical Materials Research*, 45, 48-54. [http://dx.doi.org/10.1002/\(SICI\)1097-4636\(199904\)45:1<48::AID-JBM7>3.0.CO;2-5](http://dx.doi.org/10.1002/(SICI)1097-4636(199904)45:1<48::AID-JBM7>3.0.CO;2-5)
- [12] Martin, R.B. and Burr, D.B. (1989) *Structure, Function and Adaptation of Compact Bone*. Raven Press, New York.
- [13] Balooch, G., Balooch, M., Nalla, R.K., Schilling, S., Filvaroff, E.H., Marshall, G.W., Marshall, S.J., Ritchie, R.O., Derynck, R. and Alliston, T. (2005) TGF-Beta Regulates the Mechanical Properties and Composition of Bone Matrix. *Proceedings of the National Academy of Sciences of the United States of America*, 102, 18813-18818. <http://dx.doi.org/10.1073/pnas.0507417102>

Integration disease diagnosis using machine learning & evidence medicine drug identification

N.Gobinathan¹ M. Kosalai devi², M.Abinaya³, K. Kalaiyarasi⁴
CSE, vrs college of Engineering and Technology, gobiruban.net@gmail.com

Abstract-In the Existing System, normal Data Mining based Disease Learning Analysis are very much available from a Structured Data. There is no Evidence Based Medicine Analysis. Big Data Analysis is not Available yet. In the Proposed System, Evidence Based Medicine Analysis is achieved using Big Data Technique. This Process is achieved by 1. Analysis of Patient Health Condition, 2. Formulating Questions, 3. Evidence Gathering & Analysis, 4. Resultant Output. In the Modification, an Automatic Machine Technique is used for Disease Discovery and it's Appropriate Evidence based Medicine Analysis is achieved. Until Disease is not yet Diagnosis Evidence based Medicine Analysis is of no use.

I. INTRODUCTION

A long time the development of big data technologies was inspired by business intelligence and by big science (such as the Large Hadron Collider at CERN). But when in 2009 Google Flu, simply by analyzing Google queries, predicted flu-like illness rates as accurately as the CDC's enormously complex and expensive monitoring network, some analysts started to claim that all problems of modern healthcare could be solved by big data. In 2005, the term Virtual Physiological Human (VPH) was introduced to indicate "a framework of methods and technologies that, once established, will make possible the collaborative investigation of the human body as a single complex system". The idea was quite simple: - To reduce the complexity of living organisms, we decompose them into parts (cells, tissues, organs, organ systems) and investigate one part in isolation from the others. This approach has produced, for example, the medical specialties, where the nephrologists looks only at your kidneys, and the dermatologist only at your skin; this makes it very difficult to cope with multi-organ or systemic diseases, to treat multiple diseases (so common in the ageing population), and in general to unravel systemic emergence due to genotype-phenotype interactions. - But if we can recompose with computer models all the data and all the knowledge we have obtained about each part, we can use simulations to investigate how these parts interact with one another, across space and time and across organ systems.

Though this may be conceptually simple, the VPH vision contains a tremendous challenge, namely the development of mathematical models capable of accurately predicting what will happen to a biological system. To tackle this huge challenge, multifaceted research is necessary: around medical imaging and sensing technologies (to produce quantitative data about the patient's anatomy and physiology), data processing to extract from such data information that in some cases is not immediately available, biomedical modelling to capture the available knowledge into predictive simulations, and computational science and engineering to run huge hyper models (orchestrations of multiple models) under the operational conditions imposed by clinical usage; see also the special issue entirely dedicated to multi scale modelling. But the real challenge is the production of that mechanistic knowledge, quantitative, and defined over space,

time and across multiple space-time scales, capable of being predictive with sufficient accuracy. After ten years of research this has produced a complex impact scenario in which a number of target applications, where such knowledge was already available, are now being tested clinically; some examples of VPH applications that reached the clinical assessment stage

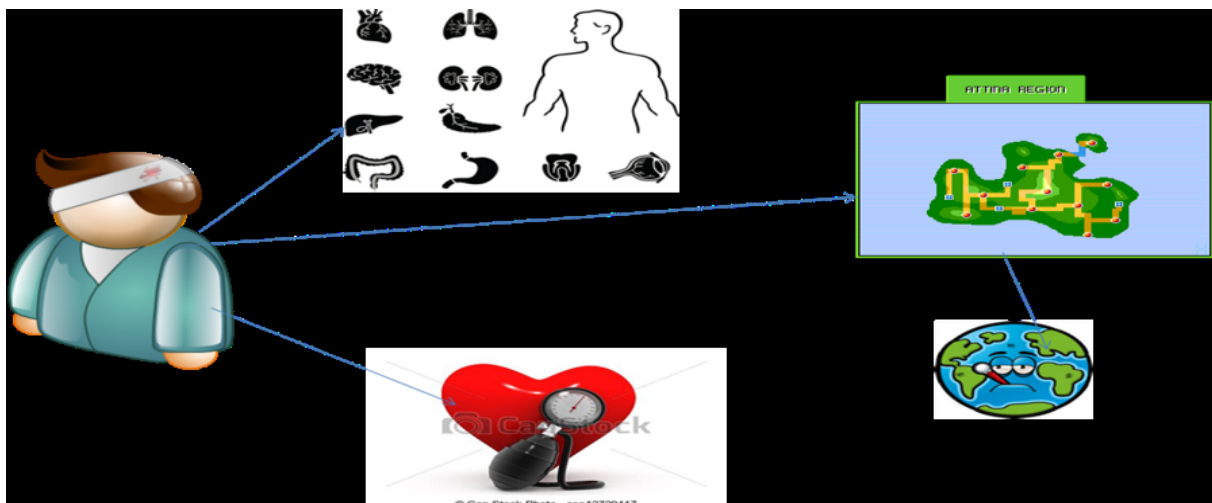
II. SYSTEM ANALYSIS

In the System analysis, normal Data Mining based Disease Learning Analysis are very much available from a Structured Data. There is no Evidence Based Medicine Analysis. Big Data Analysis is not Available yet. Demerits: Waiting time is increased, Unreliable, Less data transmission rate, Less effective In the Contribution work , Evidence Based Medicine Analysis is achieved using Big Data Technique. This Process is achieved by 1. Analysis of Patient Health Condition, 2. Formulating Questions, 3. Evidence Gathering & Analysis, 4. Resultant Output.

2.1 Contribution work

An Automatic Machine Technique is used for Disease Discovery and it's Appropriate Evidence based Medicine Analysis is achieved. Until Disease is not yet Diagnosis Evidence based Medicine Analysis is of no use.

Architecture:



III. DESCRIPTION OF PROPOSED WORK:

3.1 Patient Data Gathering

In this paper user has to register and these data are collected during the first visit at the outpatient clinics and includes information such as birth date, date of last negative and first positive tests, route of infection, and alcohol and drug usage. Data, including clinical data, are collected on a continuous basis every time the patient is seen by the treating physician. This includes such information as the treatment, symptoms of disease, and laboratory results.

3.2 Multi Access Control

we design to implement the three different type of account .because we designed retrieve three different type information form the user side and they are in the below list. Once the User creates an account, they are to login into their account and request the Job from the Service Provider. Based on the User's request, the Service Provider will process the User requested Job and respond to them.

3.3 Patient Account

In this patient account we designed this module we make use of the patient because the patient doesn't known about the prescription validation that is whether prescribed detailed medicine is correct or not. User will be giving their Symptoms & Diagnostic reports to the system for the diagnosis of the disease.

3.4 Research Account

In this research module we designed to deploy the big data analysis. Big data is nothing but vast amount of data with unstructured format in this unstructured format data we can valid information .so we used this concept of get vast of information from the insurance domain to get useful information in the domain of health care.

3.5 Disease based Data Grouping

The big data analyst is going to collect the information about the disease form the insurance server. This can be done once the insurance company accept to allow their customer information to the big data analyst so big data analyst will categories the data based on the disease. By doing this we can easily the get the disease information and list customer applied for the which disease can be indentified and they can be analyzed for the future use.

3.6 Machine Learning Algorithm

In this module user machine is used for auto diagnosis of the disease with reference to the user input of symptoms and reports. System will automatically identify the disease using machine learning algorithm. Server will store a set of trained dataset and its relevant diagnosis pattern. Using this algorithm disease are identified

3.7 Mapping of disease data set & Medicines

In this paper disease data is mapped using user's input of symptoms and related reports. Once the system identifies the buser gives the input of The system is designed to represent data that accurately captures the state of the patient at all times. It allows for an entire patient history to be viewed without the need to track down the patient's previous medical record volume and assists in ensuring data is accurate, appropriate and legible. It reduces the chances of data replication as there is only one modifiable file, which means the file is constantly up to date when viewed at a later date and eliminates the issue of lost forms or paperwork. Due to all the information being in a single file, it makes it much more effective when extracting medical data for the examination of possible trends and long term changes in the patient.

3.8 Big Data Extraction of Useful Information

we implement big data, in this big data we will have lot or vast amount of data that may wanted or unwanted information in simple the information in the big data are unstructured. So in this module the insurance server is going allow permission to access the server by the big data analyst .The big data analyst get the all the information which mention above and extract the information by the technique of map reducing formation to get useful information .which is useful for both insurance and patient.

IV. CONCLUSION

Although sometimes overhyped, big data technologies do have great potential in the domain of computational biomedicine, but their development should take place in combination with other modeling strategies, and not in competition. This will minimise the risk of research investments, and will ensure a constant improvement of in silico medicine, favoring its clinical adoption. We have described five major problems that we believe need to be tackled in order to have an effective integration of big data analytics and VPH modeling in healthcare. For some of these problems there is already an intense on-going research activity, which is comforting. For many years the high-performance computing world was afflicted by a one-size-fits-all mentality that prevented many research domains from fully exploiting the potential of these technologies; more recently the promotion of centers of excellence, etc., targeting specific application domains, demonstrates that the original strategy was a mistake, and that technological research must be conducted at least in part in the context of each application domain. It is very important that the big data research community does not repeat the same mistake. While there is clearly an important research space examining the fundamental methods and technologies for big data analytics, it is vital to acknowledge that it is also necessary to fund domain-targeted research that allows specialised solutions to be developed for specific applications.

REFERENCES

- [1] D. Laney, 3D Data Management: Controlling Data Volume, Velocity, and Variety, META Group, 2001.
- [2] O. Terzo, P. Ruiu, E. Bucci, and F. Xhafa, "Data as a Service (DaaS) for Sharing and Processing of Large Data Collections in the Cloud." pp. 475-480.
- [3] B. Wixom, T. Ariyachandra, D. Douglas, M. Goul, B. Gupta, L. Iyer, U. Kulkarni, J. G. Mooney, G. Phillips-Wren, and O. Turetken, "The Current State of Business Intelligence in Academia: The Arrival of Big Data," Communications of the Association for Information Systems, vol. 34, no. 1, pp. 1, 2014.
- [4] A. Wright, "Big data meets big science," Communications of the ACM, vol. 57, no. 7, pp. 13-15, 2014.
- [5] J. Ginsberg, M. H. Mohebbi, R. S. Patel, L. Brammer, M. S. Smolinski, and L. Brilliant, "Detecting influenza epidemics using search engine query data," Nature, vol. 457, no. 7232, pp. 1012-1014, 02/19/print, 2009.
- [6] J. Manyika, M. Chui, B. Brown, J. Bughin, R. Dobbs, C. Roxburgh, and A. H. Byers, "Big data: The next frontier for innovation, competition, and productivity," 2011.
- [7] J. W. Fenner, B. Brook, G. Clapworthy, P. V. Coveney, V. Feipel, H. Gregersen, D. R. Hose, P. Kohl, P. Lawford, K. M. McCormack, D. Pinney, S. R. Thomas, S. Van Sint Jan, S. Waters, and M. Viceconti, "The EuroPhysiome, STEP and a roadmap for the virtual physiological human," Philos Trans A Math Phys Eng Sci, vol. 366, no. 1878, pp. 2979-99, Sep 13, 2008.

A Review on Air Powered Vehicles

S.Pradeep Devaneyan¹, C.Subramanian², Thamizh Arasan.R³, Ravi Prasath.R⁴

¹*Professor Department of Mechanical Engineering, Christ College of Engineering and Technology,*

²*Senior Asst. Professor Department of Mechanical Engineering, Christ College of Engineering and Technology,*

^{3,4}*Student Department of Mechanical Engineering, Christ College of Engineering and Technology,*

Abstract: Light utility vehicles are becoming very popular means of independent transportation for short distances. Cost and pollution with petrol and diesel are leading vehicle manufacturers to develop vehicles fueled by alternative energies. Engineers are directing their efforts to make use of air as an energy source to run the light utility vehicles. The use of compressed air for storing energy is a method that is not only efficient and clean, but also economical. The major problem with compressed air cars was the lack of torque produced by the "engines" and the cost of compressing the air. Recently several companies have started to develop compressed air vehicles with many advantages and still many serious bottlenecks to tackle. This paper briefly summarize the principle of technology, latest developments, advantages and problems in using compressed air as a source of energy to run vehicles.

Keywords: Environmental pollution, alternative energies, compressed air, air powered vehicles.

I. INTRODUCTION

We are living in a very mobile society so light utility vehicles (LUV) like bikes and cars are becoming very popular means of independent transportation for short distances. Petrol and diesel which have been the main sources of fuel in the history of transportation, are becoming more expensive and impractical (especially from an environmental standpoint). Such factors are leading vehicle manufacturers to develop vehicles fueled by alternative energies. When at present level of technological development fuel-less flying (like birds) i.e., flying based on the use of bio-energy and air power in the atmosphere seems to be almost impossible for human beings then engineers are fascinated at least with the enormous power associated with the human friendly as well as tested source of energy (i.e., air) to make **air-powered vehicles** as one possible alternative. Engineers are directing their sincere efforts to make use of air as an energy source to run the LUVs which will make future bikes and light/small cars running with air power for daily routine distances and the travel will be free from pollution and cost effective.

II. TECHNOLOGY

Mankind has been making use of uncompressed air-power from centuries in different application viz., windmills, sailing, balloon car, hot air balloon flying and hang gliding etc. The use of compressed air for storing energy is a method that is not only efficient and clean, but also economical and has been used since the 19th century to power mine locomotives, and was previously the basis of naval torpedo propulsion. In 1903, the Liquid Air Company located in London manufactured a number of compressed air and liquified air cars. The major problem with compressed air cars was the lack of torque produced by the "engines" and the cost of compressing the air. Recently several companies have started to develop compressed air vehicles,

Although none has been released to the public so far. Compressed air tanks store power really well but are lacking on power density. They tie or beat batteries in the charge / re-charge efficiency and totally kill them on lifespan. Higher pressures are their big problem of compressed

air vehicles while efficiency, cost, toxic chemicals, and lifespan are the big problems associated with chemical batteries.

The principle of compressed-air propulsion is to pres-surize the storage tank and then connect it to something very like a reciprocating steam engine of the vehicle. Instead of mixing fuel with air and burning it in the engine to drive pistons with hot expanding gases, *compressed air vehicles* (CAV) use the expansion of compressed air to drive their pistons. Thus, making the technology free from difficulties, both technical and medical, of using ammonia, petrol, or carbon disulphide as the working fluid. Manufacturers claim to have designed engine that is 90 percent efficient. The air is compressed at pressure about 150 times the rate the air is pressurized into car tyres or bicycle. The tanks must be designed to safety standards appropriate for a pressure vessel. The storage tank may be made of steel, aluminium, carbon fiber, kevlar or other materials, or combinations of the above. The fiber materials are considerably lighter than metals but generally more expensive. Metal tanks can withstand a large number of pressure cycles, but must be checked for corrosion periodically. A company has stated to store air in tanks at 4,500 pounds per square inch (about 30 MPa) and hold nearly 3,200 cubic feet (around 90 cubic metres) of air. The tanks may be refilled at a service station equipped with heat exchangers, or in a few hours at home or in parking lots, plugging the vehicle into an on-board compressor. The cost of driving such a car is typically projected to be around Rs. 60 per 100 km, with a complete refill at the "tank-station" at about Rs. 120 only.

III. DEVELOPMENTS

3.1 Air powered moped.

This has been done by equipping the scooter with a compressed air engine and air tank. Jem Stansfield created the bike by strapping two high-pressure tanks onto the side of his Puch moped. The tanks are basically scuba tanks. He uses the electricity from his house to fill the tanks. The power is then "stored" there, much like a battery, ready for use. The tanks used are carbon-fiber tanks of the sort used by firefighters for oxygen. But still, they're far cheaper than even the lead acid battery used in car now. Of course, the compressor works on electricity, so that's not always a clean power source but recharging options at night or off peak will enhance the chances to use the power that would be wasted otherwise. The top speed is about 18 mph, and it can only go 7 miles before the air pressure runs out and a lot more power could probably be pulled by tweaking his configuration. A small gear on the end of the air drill, connected to the chain of the bike would make a much more elegant solution.

Several companies are investigating and producing prototypes, and others plan to offer air powered cars, buses and trucks. The compressed air is stored in carbon-fiber tanks that are built into the chassis. As the air is released, the pressure drives pistons that power the engine and move the car, and the pistons compress the air into a reservoir so that the process continues. After making a revolution by producing the world's cheapest car-Tata nano, India's largest automaker (Tata Motors) is set to start producing the world's first commercial air-powered vehicle. The "Air Car" will make use of compressed air, as opposed to the gas-and-oxygen explosions of internal-combustion models, to push its engine's pistons. Zero Pollution Motors (ZPM) (USA) also expects to produce the world's first air-powered car for the United States by 2010. An earlier version of the car is noisy and slow, and a tiny bit cumbersome but then this vehicle will not be competing with a Ferrari or Rolls Royce and the manufacturers are also not seeking to develop a Formula One version of the vehicle. The aim of air powered vehicles is the urban motorist: delivery vehicles, taxi drivers, and people who just use their vehicles to nip out to the shops. The latest air car is said to have come on leaps and bounds from the early model. It

is said to be much quieter, a top speed of 110 km/h (65 mph), and a range of around 200 km before you need to fill the tanks up with air.

IV. ADVANTAGES

- In comparison to petrol or diesel powered vehicles “air powered vehicles” have following advantages:
- Air, on its own, is non-flammable, abundant, economical, transportable, storable and, most importantly, nonpolluting.
- Compressed air technology reduces the cost of vehicle production by about 20%, because there is no need to build a cooling system, fuel tank, spark plugs or silencers.
- High torque for minimum volume.
- The mechanical design of the engine is simple and robust.
- Low manufacture and maintenance costs as well as easy maintenance.
- Lighter vehicles would mean less abuse on roads, thus, resulting in longer lasting roads.
- The price of fueling air powered vehicles will be significantly cheaper than current fuels.
- When the air is being compressed at reasonable speeds, it heats up. The heat given off during compression could be reclaimed for space heating or water heating, or used in a stirling engine.
- Transportation of the fuel would not be required due to drawing power off the electrical grid. This presents significant cost benefits. Pollution created during fuel transportation would be eliminated.
- Compressed-air vehicles are comparable in many ways even to electric vehicles and their potential advantages over electric vehicles include:
- Compressed-air vehicles are unconstrained by the degradation problems associated with current battery systems.
- Much like electrical vehicles, air powered vehicles would ultimately be powered through the electrical grid which makes it easier to focus on reducing pollution from one source, as opposed to the millions of vehicles on the road.
- Compressed-air tanks can be disposed of or recycled with less pollution than batteries.
- The tank may be able to be refilled more often and in less time than batteries can be recharged, with re-fueling rates comparable to liquid fuels.
- The tanks used in a compressed air motor have a longer lifespan in comparison with batteries, which, after a while suffer from a reduction in performance.

V. BOTTLE NECKS

Disadvantages of compressed-air vehicles are less well known, since the vehicles are currently at the pre-production stage and have not been extensively tested by independent observers. Some bottlenecks of technology may be summarized as:

- Very little is known about air powered vehicles thus far.
- Compressed air vehicles likely will be less robust than typical vehicles of today. Which poses a danger to users of compressed air vehicles sharing the road with larger, heavier and more rigid vehicles.
- Compressed air has a low energy density comparable to the values of electrochemical lead-acid batteries. While batteries can somewhat maintain their voltage throughout their discharge and chemical fuel tanks provide the same power densities from the first to the last litre, the pressure of compressed air tanks falls as air is drawn off.

- When the air is expanded in the engine, it will cool down *via* adiabatic cooling and lose pressure thus its ability to do work at colder temperatures. It is difficult to maintain or restore the air temperature by simply using a heat exchanger with ambient heat at the high flow rates used in a vehicle, thus the ideal isothermic energy capacity of the tank will not be realised. Cold temperatures will also encourage the engine to ice up.

VI. CONCLUSION

Compressed air for vehicle propulsion is already being explored and now air powered vehicles are being developed as a more fuel-efficient means of transportation. Some auto-mobile companies are further exploring compressed air hy-brids and compressed fluids to store energy for vehicles which might point the way for the development of a cost effective air powered vehicles design. Unfortunately there are still serious problems to be sorted out before air powered vehicles become a reality for common use but there is a hope that with the development in science & technology well supported by the environmental conscious attitude and need to replace costly transportation methods, air-powered vehicles will definitely see the light of the day.

REFERENCE

- [1] Sullivan, M. World's First Air-Powered Car: Zero Emissions By Next Summer, Popular Mechanics [Http://Www.Popularmechanics.Com/Automotive/New_Cars/4217016.Html](http://www.popularmechanics.com/automotive/new_cars/4217016.html) (June 2008 Issue),
- [2] Harley, M.; Ford, G.M. Considering Joint Engine Development, [Http://Www.Autoblog.Com/2008/08/04/Ford-Gm-Considering-Joint-Engine-Development](http://www.autoblog.com/2008/08/04/ford-gm-considering-joint-engine-development), (Accessed Aug 2008).
- [3] From Wikipedia, The Free Encyclopedia. Compressed-Air Car, [Http://En.Wikipedia.Org/Wiki/Air_Car](http://en.wikipedia.org/wiki/Air_Car) (Accessed June 2008).
- [4] Russell, C. The Air Car Becomes A Reality, [Http://Cambrown.Wordpress.Com/2007/03/27/The-Air-Car-Becomes-A-Reality/](http://cambrown.wordpress.com/2007/03/27/the-air-car-becomes-a-reality/) (Accessed May 2007).
- [5] Hamilton, T. Technology Review, The Air Car Preps For Market, [Http://Www.Technologyreview.Com/Energy/20071](http://www.technologyreview.com/energy/20071) (Accessed Janu-Ary 2008).
- [6] Bonser, K., Howstuffworks, How Air-Powered Cars Will Work, [Http://Auto.Howstuffworks.Com/Air-Car.Htm](http://auto.howstuffworks.com/air-car.htm) (Accessed June, 2008).
- [7] Haliburton, M.-S. Pure Energy Systems News, Engineair's Ultra-Efficient Rotary Compressed-Air Motor, [Http://Pesn.Com/2006/05/11/9500269_Engineair_Compressed-Air_Motor/](http://pesn.com/2006/05/11/9500269_engineair_compressed-air_motor/) (Accessed June, 2008).
- [8] Richard, M.G. The Air-Powered Motorcycle By Jem Stansfield, [Http://Www.Instructables.Com/Id/Air-Powered-Bicycle](http://www.instructables.com/Id/Air-Powered-Bicycle) (Accessed April 2008).
- [9] Chen, P.X. Researchers Develop Air-Powered Motorcycle, [Http://Blog.Wired.Com/Gadgets/2008/08/Air-Powered-Mot.Html](http://blog.wired.com/gadgets/2008/08/air-powered-mot.html) (Accessed August 2008).

A Study On Aero Hybrid Concept

S.Pradeep Devaneyan¹, R.Saravanan², D.Mugilan³, K.Gokul Raj⁴

¹Professor Department of Mechanical Engineering, Christ College of Engineering and Technology,

²Senior Asst. Professor Department of Mechanical Engineering, Christ College of Engineering and Technology,

^{3,4}Student Department of Mechanical Engineering, Christ College of Engineering and Technology,

ABSTRACT According to sports history the car should be very efficient and damn fast, but the key enemy for sports car is aerodynamic drag and weight. This aero dynamic drag as friction in surface of the body and it offers resistance to the body. so we designed an concept called aero hybrid technology to reduce the drag .

I. INTRODUCTION

The Aero hybrid technology is an upgradable version of existing hybrid cars in the world .The word aero is used to reduce the drag and makes the sports car more efficient and can gain more speed with an normal mileage of the car. This technology adds as an extra 500 kg to the car as an assumption as we did, but this extra weight can be compensated by the thrust produced by the concept and this weight added cannot affect the efficiency of the sports car.

II. WORKING PRINCIPLE

It is basically a two spool jet engine concept. Where the atmospheric air is sucked inside the car and compressed and exit out at the greater thrust. By doing this method we can reduce the drag over the body and can gain more speed.



Fig2.1:(Without Aero Hybrid technology)

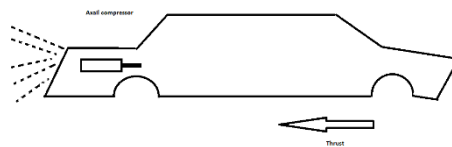


Fig2.2:(With Aero hybrid technology)

2.1 Constructional Details

As we mentioned earlier this technology requires the following components to complete this model

- Axial compressor
- 400 Kw dc motor
- Dc generator
- 610 bhp v10 engine with FSI technology

2.3 Axial Compressor

An axial flow compressor is where the air flow parallel to the stator is the basic principle. It has two parts Rotating part called rotor Stationary part called stator This two components uses three geometry property called COD,CMD,CHD Rotor vanes are arranged closely so that it compresses more air. The compression ratio can be increased by increasing the number of stages in the rotor or the stator vanes and rotor vanes should be tightly constructed

Eg: 14 stage axial compressor produces 44KN of thrust at 29 pressure ratio. The stator vanes and rotor vanes are described at the below pictures

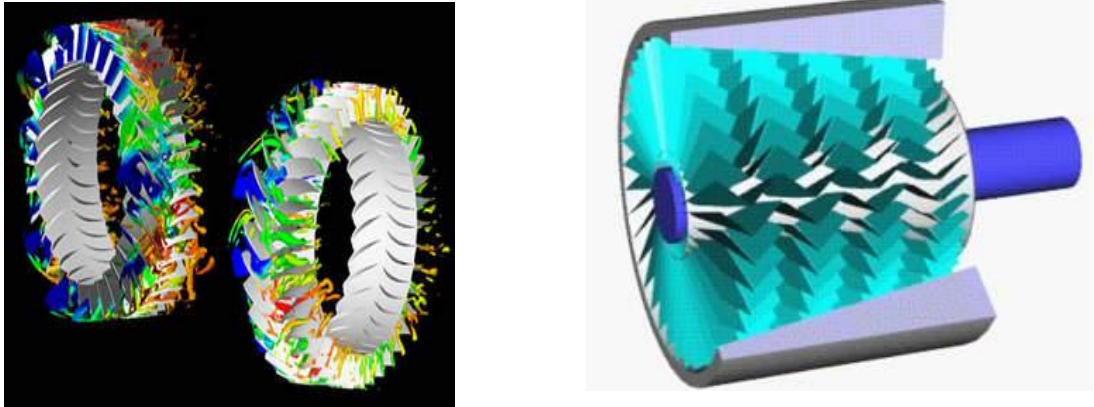


Fig2.3 :rotor and stator

By the side principle concept 1000pounds of thrusts =1000 horse powers.
 $1\text{ pound force} = 0.00445\text{KN}$

Another method of calculating the horse power is produced by the axial compressor = thrust* 6.66

by this method we can produce extra 700-1200horse power .Depending upon the pressure ratio using the compressor and amount of air flow inside the compressor.

2.4 Advantages of axial compressor

It can sucks more air under a narrow opening.

It can produce more ratio

It has high ability to produce more thrust when compared to centrifugal compressor.

2.5 Disadvantages

It has high efficiency under narrow RPM

2.6 Dc Generator

- This works under Flemings Right Hand rule.
- Hence we use 4*4 system, drive shaft is coupled to the generator
- Over the drive shaft,the commutator and a armature is placed. Over that the field winding and the yoke is placed.
- We use the 3phase generator for the maximum power production



Fig2.5 (dc generator)

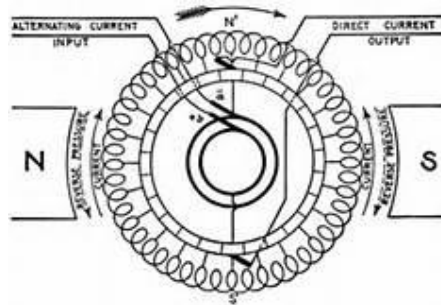


Fig2.6 (armature winding)

Formulae

$$Emf = \text{flux} * 2n/60 \text{ volt}$$

The general Emf formulae is $=\text{flux}*(2n/60)*p/a$ volt

As the generator is placed over the drive shaft without any coupling there is no load. The engine efficiency cannot be reduced under any circumstance

2.5 Engine

Using V10 engine 5.2liter produces 610 horse power or 440Kw of power

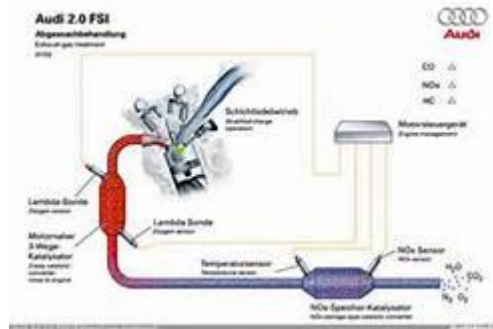


Fig2.7:fsi

FSI- Stratified Fuel Injection System

By using this method we can load the engine to variable condition but no loss in power output.

Engine→Generator→DCmotor→Compressor

2.7 Dc motor

It works on Flemings Left Hand rule .Here the current is given to the armature in anti-clockwise direction. According to our assumption it should produce at least 320 horse power at 4500 RPM to drive the compressor and in turn it can reduce the aerodynamic drag. The condition for the maximum power is

$$PM=VIa -Ia^2Ra$$

To measure the torque $P=(2\pi n/60) *t$

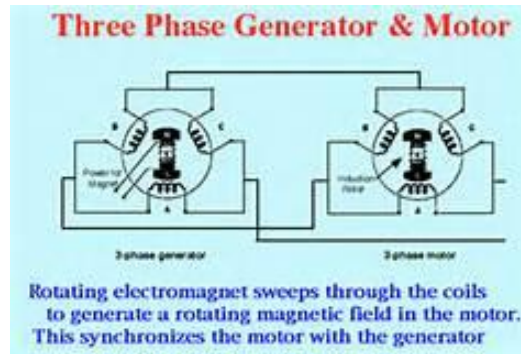


Fig2.8:(generator and motor)

III. WORKING

By compressing all this parts together we can make ready of this concept Initially the engine will be working and it transfer the power to its wheel by 4*4 system. It attain maximum speed the aerodynamic drag is increased, but the aerodynamic drag can be reduced by using the vortex generator.



Fig3.1 :(vortex generator)

But it can't reduce the aerodynamic drag. But it creates more down force this may act as the load to the engine. In our concept there is no friction and down force and so we can attain more speed. **“When the car approaches 200Km the aero hybrid concept starts to work and reduces the drag”**. The axial compressor engages and sucks the air inside the car and send to the diffusers to create the thrust ,which gives extra 700-1000 horse power.

The power to the front wheel is from the transfer case to the drive shaft. The shaft is made up of the carbon fibre which has high tensile strength. Consider carbon fibre of 1m and divided by three we get 0.5m the centre 0.5 m is made up of soft iron and it should have the characteristics of low retentivity and hysteresis loss and so it could produce upto 400 kw of power. After considering all the losses 260kw of power is given to the Dc motor which produces 350 horse power at 4500RPM, and so it can rotate the compressor and a various velocities of load.

It is sufficient to drive the axial compressor and so it could sucks more air and compresses and passes to the diffuser and so we could produce more thrust. This thrust makes the car move forward in addition with the engine power. This car can make top speed of 650 km per hour due to the maximum amount of the thrust produced.

3.1 Advantages

- High cruising speed
- Higher experience of driving
- Save the fuel and money
- Higher efficiency to the existing sports car

3.2 Disadvantages

Difficult in construction and requires high man work time to build the car.

REFERENCE

1. Mistry Manish K., Dr.Pravin P.Rathod, Prof. Sorathiya Arvind S., "Study And Development Of Compressed Air Enginesingle Cylinder: A Review Study", Ijaet/Vol.Iii/ Issue I/January-March, 2012/271-274
2. Gorla, R., And Reddy, S., 2005, Probabilistic Heat Transfer And Structural Analysis Of Turbine Blade, Ijtje, Vol. 22, Pp 1- 11.
3. S.S.Verma, "Air Powered Vehicles", The Open Fuels & Energy Science Journal, 2008, Volume 1, Pp.54-56.
4. Rose Robert, William J. Vincent, 2004, Fuel Cell Vehicle World Survey 2003 - Breakthrough Technologies Institute, February' 2004, Washington, D.C.
5. Gizmag Team, Tata Motors Enters Second Phase Of Air- Car Development [Http://Www.Gizmag.Com/Tatamotors-Air-Car- Mdi/22447/](http://www.gizmag.com/tatamotors-air-car-mdi/22447/)
6. Peter Fairley, "Deflating The Air Car", Ieee Spectrum, 30 Oct 2009.

Combined Air Conditioner Water Heater

A.Sivakumar¹, P.Chandru Deva Kannan², D.Balamurali³, Anto Sam⁴

¹Professor Department of Mechanical Engineering, Christ College of Engineering and Technology,

²Senior Asst. Professor Department of Mechanical Engineering, Christ College of Engineering and Technology,

^{3,4}Student Department of Mechanical Engineering, Christ College of Engineering and Technology,

ABSTRACT: Combined air conditioner water heater which is a working model consists of an outdoor unit of AC, Condenser and an insulated tank. Using this simple setup water can be heated efficiently without any source.

I. INTRODUCTION:

The aptly named Air Conditioner Water Heater has a condenser unit that sits outside of the building, collecting heat that the air conditioner compresses and expels from inside. The heat passes through a copper heat exchanger that connects to a home or building's hot water tank. This unit can cool a 1000-square-foot room and heat about 100 gallons of water per day. At its peak, the ACWH can provide 18,000 BTU, or 1.5 tons of cooling using 1333 watts per hour.

1.1 Need For Combined Air Conditioner Water Heater:

As for capturing waste heat from air conditioning;

- Each ton hour of air conditioning generates around 15,000 Btu of waste heat
- It is not generally appreciated that this 15,000 Btu is produced by approx. 5,000 Btu of electricity
- So the heat rejected by one ton hr of air conditioning consists of the 5,000 Btu.
- 10-12 thousand Btu of heat pumped out of your house
- This amount of heat will heat 24 gal of water 75 deg F

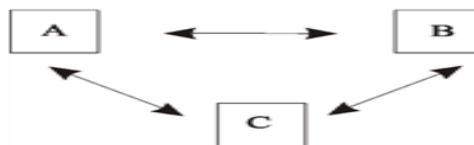
Hence water is heated while cooling a building in order to heat water while cooling a building can help save energy, since the heat recovery process eases the load of the air conditioner. The unit has to be installed relatively close (ideally within 150 feet of) the water heater, however, and only heats water when the air conditioner is running and there is enough hot air to warm the water. Using the unit on a mild summer day won't make a significant dent in water heating costs, but it could have an impact for homes with multiple residents who use hot water throughout the day to shower or wash dishes.

II. PRINCIPLE

Combined air conditioner water heater works under the principle of ZEROTH LAW.

WHAT IS ZEROTH LAW...?

The **Zeroth law of thermodynamics** states that if two thermodynamic systems are each in thermal equilibrium with a third, then they are in thermal equilibrium with each other.



III. CONSTRUCTION:

The combined air conditioner water heater consist of three main units:

1. outdoor air conditioning unit
2. Heating unit(Condenser)
3. Insulated tank

3.1 What does your outside air conditioner unit do?

The outside portion of your air conditioner is most often referred to as the “condenser unit.” Whereas the inside part of your air conditioner is responsible for absorbing heat from your home’s air, your outside unit’s job is to release that heat to the air outside. Without your air conditioners outside unit, the heat that’s removed from your home would have nowhere go!

3.2 What parts are located in your air conditioner is outside unit?

There are a few different parts located in the outside portion of your air conditioner. The most important of those include:

3.3 The compressor ;Your air conditioners compressor adds pressure to the refrigerant that it receives from inside your home in order to increase the refrigerant’s temperature and make it easier to transfer heat in the next step of the cooling process.

3.4 Condenser coils and fan; After leaving the compressor, refrigerant flows through your condenser coils. As this happens, a fan blows air over the coils in order to cool them off and release heat to the air outside.

3.5 Refrigerant lines; Refrigerant lines are what connect your indoor and outdoor units in order to cycle refrigerant and continue the cooling process

IV. HEATING UNIT (CONDENSER):

4.1 Definition of Boiler

Steam boiler or simply a **boiler** is basically a closed vessel into which water is heated until the water is converted into steam at required pressure. This is most basic **definition of boiler**

4.2 Types of Boiler

There are mainly two **types of boiler** – water tube boiler and fire tube boiler. In fire tube boiler, there are numbers of tubes through which hot gases are passed and water surrounds these tubes. Water tube boiler is reverse of the fire tube boiler. In water tube boiler the water is heated inside tubes and hot gasses surround these tubes. These are the main two **types of boiler**

The type of boiler which we are going to use in our CACWH is water tube boiler.

4.3 Water Tube Boiler

A water tube boiler is such kind of boiler where the water is heated inside tubes and the hot gasses surround them.

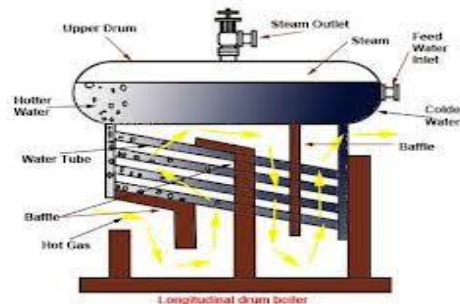


Fig 4.1 Water Tube Boiler

By using this water tube boiler mechanism we construct a Condenser which is made of copper which is a very good conductor of heat. The copper metal is further coated with black paint or black wrapper or black coil to absorb heat from sunlight and further increase the temperature of the tube. The top opening of the Condenser is connected at the top of the insulated tank and the bottom opening of the chamber is connected at the bottom of the tank. This simple set up constitute the Condenser and this Condenser is connected to outdoor unit by welding the Condenser at the four corners of the outdoor unit or by various other convenient methods.

V. INSULATED TANK

Insulated tank is the final unit of the CACWH. insulated means that it is prevented form loss of temperature or gain of temperature. A tank is insulated by various means.

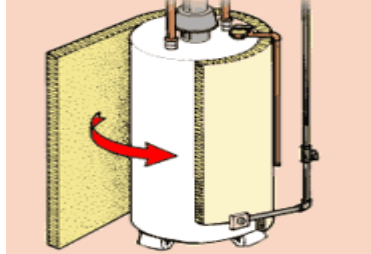


Fig 5.1 Insulated Tank

The most commonly available type of insulated tanks uses blankets or jackets for insulations and those blanket is fiberglass insulation with a vinyl film on the outside, the insulating blanket being wrapped around the tank fixed in place with tape or straps.

It is important that the blanket be the right size for the tank, not block air flow or cover safety and drainage valves, the controls, or block airflow through an exhaust vent, if present. In extremely humid locations, adding insulation to an already well-insulated tank may cause condensation leading to rust, mold, or other operational problems so some air flow must be maintained, usually by convection caused by waste heat, but in particularly humid conditions such ventilation may be fan-assisted. A small tank with a capacity of 200L is enough for this process. The top opening of the Condenser should be connected at the top of the insulating chamber and must be extended to the half height of the tank inside and the bottom of the Condenser should be connected to the bottom of the tank. Only if this set up is achieved their will water available always at the Condenser.

VI. WORKING

As we know the outdoor unit of the air conditioner gives out hot air through the exhaust fan. This hot air is +10deg Celsius greater than that of the ambient temperature(say ambient temp is 34deg Celsius).Now the Condenser made of copper metal coated with black paint is now attached to the outdoor unit so that the hot air from exhaust directly falls on the Condenser.

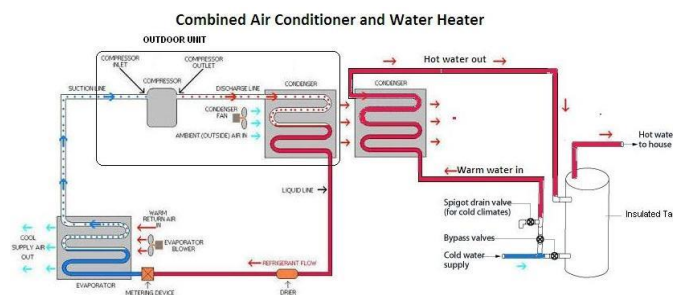


Fig.6.1 Construction of Air Conditioner

The Condenser is designed such that the copper tubes are in zig-zag manner hence more the number of turns of the copper tube the more will be the heating surface and more water can be heated at the same time.

The two point of the Condenser is now connected to the insulated tank, one opening at the top and another at the bottom. It is connected such that the tube connected at the top extended till half the height of the tank inside only because to make available the water

All the time inside the chamber. An insulated tank of small capacity say 200L is enough.

Now as the hot air is passed through the Condenser the water inside the chamber gets heated and moves forward through the top opening and gets collected in the tank. The cold water at the bottom of the tank moves to the Condenser through the bottom opening and gets heated and then moves upward. This takes place as a continuous cyclic process as long as the outdoor unit gives out hot air.

Hence for a particular portion of water in the tank it gains heat of 2deg Celsius for every cycle in the Condenser and if the outdoor unit works throughout the day or night(say it works continuously for eight hours) the water will now be at a suitable heat to be used for bathing and various purposes(say 88deg Celsius).

Thus water is efficiently used without any new input by using combined air conditioner water heater.

REFERENCE

- [1] Sullivan, M. World's First Air-Powered Car: Zero Emissions By Next Summer, Popular Mechanics [Http://Www. Popularmechanics. Com/Automotive/New_Cars/4217016.Html](http://www.popularmechanics.com/automotive/new_cars/4217016.html) (June 2008 Issue),
- [2] Harley, M.; Ford, G.M. Considering Joint Engine Development, [Http://Www.Autoblog.Com/2008/08/04/Ford-Gm-Considering-Joint-Engine-Development](http://www.autoblog.com/2008/08/04/ford-gm-considering-joint-engine-development), (Accessed Aug 2008).
- [3] From Wikipedia, The Free Encyclopedia. Compressed-Air Car, [Http://En.Wikipedia.Org/Wiki/Air_Car](http://en.wikipedia.org/wiki/Air_Car) (Accesed June 2008).
- [4] Russell, C. The Air Car Becomes A Reality, [Http://Cambrown. Wordpress.Com/2007/03/27/The-Air-Car-Becomes-A-Reality/](http://cambrown.wordpress.com/2007/03/27/the-air-car-becomes-a-reality/) (Accessed May 2007).
- [5] Hamilton, T. Technology Review, The Air Car Preps For Market, [Http://Www.Technologyreview.Com/Energy/20071](http://www.technologyreview.com/energy/20071) (Accessed Janu-Ary 2008).
- [6] Bonser, K., Howstuffworks, How Air-Powered Cars Will Work, [Http://Auto.Howstuffworks.Com/Air-Car.Htm](http://auto.howstuffworks.com/air-car.htm) (Accessed June, 2008).
- [7] Haliburton, M.-S. Pure Energy Systems News, Engineair's Ultra-Efficient Rotary Compressed-Air Motor, [Http://Pesn.Com/20 06/05/11/9500269_Engineair_Compressed-Air_Motor/](http://pesn.com/2006/05/11/9500269_engineair_compressed-air_motor/) (Accessed June, 2008).

Compressed-Air Powered Vehicle

S.Pradeep Devaneyan¹, C.Subramanian², D.Balamurali³, Anto Sam⁴

¹*Professor Department of Mechanical Engineering, Christ College of Engineering and Technology,*

²*Senior Asst. Professor Department of Mechanical Engineering, Christ College of Engineering and Technology,*

^{3,4}*Student Department of Mechanical Engineering, Christ College of Engineering and Technology,*

ABSTRACT A compressed-air vehicle is powered by an air engine using compressed air, which is stored in a tank. Instead of mixing fuel with air and burning it in the engine to drive pistons with hot expanding gases, compressed air vehicles (CAV) use the expansion of compressed air to drive their pistons. One manufacturer claims to have designed an engine that is 90 percent efficient. Climate change and energy security require a reduction in travel demand, a model shift and Technological innovation in the transport sector. Through a series of press releases and demonstrations, a car using energy stored in compressed air produced by a compressor has been suggested as an environmental Friendly vehicle of the future. Even under highly optimistic assumptions, the compressed-air car is significantly less efficient than a battery electric vehicle and it produces more greenhouse gas emissions than a conventional gas-powered car with a coal intensive power mix.

I. INTRODUCTION

The first compressed air vehicle was established in France by a Polish engineer Louis Mekarski in 1870. It was patented in 1872 and 1873 and was tested in Paris in 1876. The working principle of Mekarski's engine was the use of energy stored in compressed air to increase gas enthalpy of hot water when it is passed through hot water. Another application of the compressed air to drive vehicles comes from Uruguay in 1984, where Armando Regusci has been involved in constructing these machines. He constructed a four-wheeler with pneumatic engine which travelled 100 km on a single tank in 1992. The Air Car was developed by Luxembourg-based MDI Group founder and former Formula One engineer Guy Negre is which works on compressed air engine (CAE). He developed compressed air-4- cylinders engine run on air and gasoline in 1998 which he claims to be zero pollution cars. It uses compressed air to push its pistons when running at speeds under 35 mph and at higher speeds of 96 mph, the compressed air was heated by a fuel (bio fuel, gasoline, or diesel), due to which the air expanded before entering the engine. A fuel efficiency of about 100 mpg was observed. Light weight vehicles are the next advancement in the development of automobiles. Reducing the weight of the vehicle has many advantages as it increases the overall efficiency of the vehicle, helps in improving maneuverability, requires less energy to stop and run the vehicle. The latest researches are going on around the world in order to come up with innovative ideas. But global warming is also one of the problems which is affecting the man. The temperature of the earth is increasing drastically and this in turn is causing climatic changes. The fossil fuels are widely used as a source of energy in various different fields like power plants, internal & external combustion engines, as heat source in manufacturing industries, etc. But its stock is very limited and due to this tremendous use, fossil fuels are diminishing at faster rate. So, in this world of energy crisis, it is necessary to develop alternative technologies to use renewable energy sources, so that fossil fuels can be conserved. One of the major source of the pollution is the smoke coming out from the automobiles. So an alternative way of producing the running the vehicle must be made so that we can prevent further damage to the earth. The alternative sources of energy available are solar, electric, atmospheric air etc. Air acts like a blanket for the earth. It is the mixture of gasses, which makes it neutral and non-polluting. It has the property to get compressed to a

very high pressure and retain it for a long period of time. It is cheap and can be found abundantly in the atmosphere. So it can be used as an alternative fuel for the automobiles. Much research is going on in this field and scientists are trying to improve the effectiveness of this technology. It is experimentally found that the efficiency of the vehicle ranges from 72-95%. So this can be considered as one of the preferable choices to run the vehicle.

II. MOTIVE OF THE PROJECT

As mentioned above, the recent problem created by the explosion of fossil fuels can be avoided by automobiles which have become slaves of the fossil fuel. They use air as an alternative fuel. The idea of using is many problems like environment disasters (due to compressed air as fuel is not new. There have been exhaust), price rise and scarcity of fossil fuels tends us to use prototypes cars since the 1920s, but the engine we used go towards an alternative fuel. Many of the alternatives here are more efficient than the air power engines which use fuel by products hazardous and the production and in the already existing prototypes. Preparation of many alternate fields is complicated for several decades. The IC engines work in the cycle of engine. Thus, we go for an easily obtainable alternate fuel. This helps to obtain mechanical work at beneficial to us compressed air. The main motive of the output of the Project is to design and implement a car which is eco-friendly, with zero exhaust and emission, economically cost effective using easily obtainable fuel.

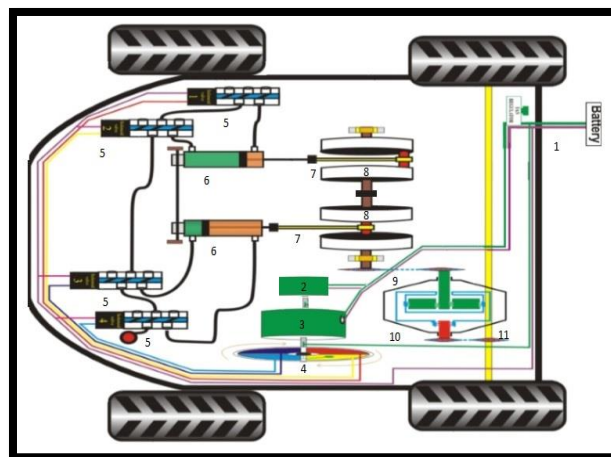


Fig 2.1 lay out

2.1 Parts

1. Battery.
2. Motor.
3. Compressor.
4. Solenoid switch.
5. Solenoid valve (4).
6. Pneumatic piston (2).
7. Connecting rod (2).
8. Crank shaft (2).
9. Chain.
10. Gear box.
11. Back wheel driven shaft.

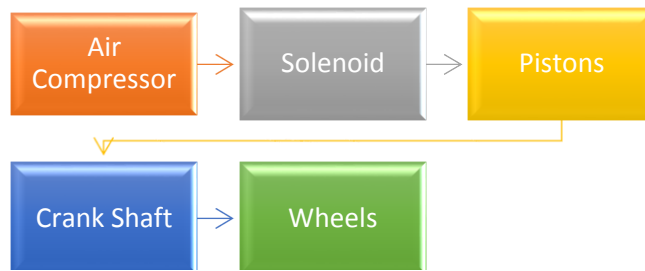


Fig: 2.2 component

III. WORKING

Our project is working in 24V dc current, we divide this current into two parts. In the Solenoid coil, one wire of the 4-coil (negative) is attached with disk and positive current is transmitted by motor with its connecting shaft. Dc motor regulating supply in the secondary 24V dc supply is going to step down transformer through fan regulator for regulate supply. This transformer step-up to 12V dc to 120V dc supply. Now, we fix one bridge rectifier (230V) to convert ac to dc 12V supply for motor. When we operate Auto transformer the motor rotates slowly and fast to transmit ac current to solenoid coil. We used Solenoid valve to transmit compressed air to the cylinder for 4 stroke rotation. In ON condition, Solenoid valve air inlet hole are B and D and outlet hole are E and A. Due to this cylinder expands normally in off condition. Solenoid valve air inlet hole are B and E and outlet hole are D and C. Due to this cylinder squeezes. We weld two crankshafts and connect pneumatic cylinder with them and fix them on body frame with the help of bearing. We weld one sprocket on the right side of crank shaft to transfer its rotation to gear box. Now, we connect 4 solenoid coil with pneumatic cylinder to provide 4 stroke (every coil provide 90 degree rotation when current passes through them). We connect 1:4 gear box with crankshaft to convert crank speed in to wheel torque motion. Due to this, our project is easily move on surface. Now, we take one special dc gear motor (motor shaft is not directly connected with motor so, we transmit ac current to the coil from that shaft) and fix it with circular dick and this motor transmits ac supply to coil.

IV. MATERIALS & METHOD

One can buy the vehicle with the engine or buy an engine to be installed in the vehicle. Typical air engines use one or more expander pistons. In some applications, it is advantageous to heat the air, or the engine, to increase the range or power.

- Tanks
- The tanks must be designed to safety standards appropriate for a pressure vessel.

4.1 The Storage Tank May Be Made Of

- Steel
- Carbon fiber
- Aluminum
- Kevlar
- Other materials or combinations of the above.
- The fiber materials are considerably lighter than metals but generally more expensive. Metal tanks can withstand a large number of pressure cycles, but must be checked for corrosion periodically.
- One compressor stores air in tanks at 4,500 pounds per square inch (about 30 MPa) and holds nearly 3,200 cubic feet (around 90 cubic meters) of air.

- The tanks may be refilled at a service station equipped with heat exchangers, or in a few hours at home or in parking lots, plugging the car into the electric grid via an on-board compressor.

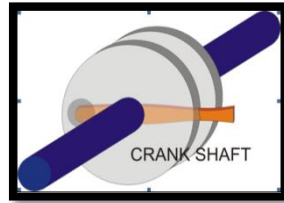


Fig: 4.1 Crank shaft

We arrange one crank shaft with two wheeler scooter.

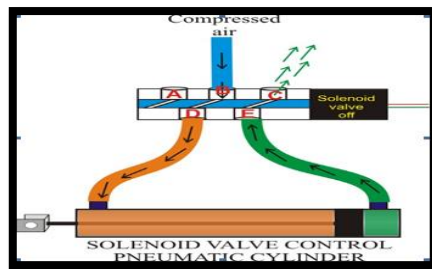


Fig: 4.2 Solenoid valve

Normally, in Off condition Solenoid valve air inlet hole are B and E and outlet hole are D and C and due to this cylinder squeezes.

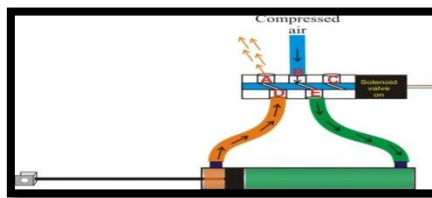


Fig: 4.3 Compressed air

In ON condition, Solenoid valve air inlet hole are B and D and outlet hole are E and A. Due to this cylinder expands.

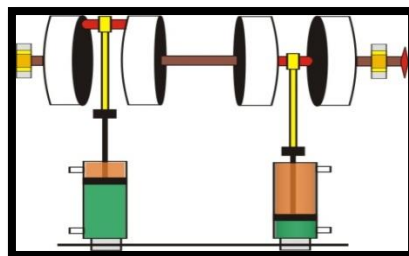


Fig: 4.4 Crankshafts & cylinder

We weld two crankshafts and connect pneumatic cylinder with them and fix them on body frame with the help of bearing. We weld one sprocket on the right side of crank shaft to transfer its rotation to gear box.

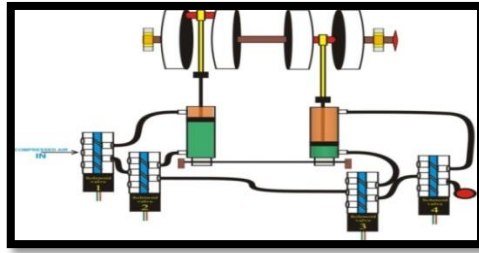


Fig: 4.5 Connect 4 solenoid coil

Now, we connect 4 solenoid coil with pneumatic cylinder to provide 4 stroke (Every coil provides 90 degree rotation when current passes through them).

4.2 Power Transmission

The most important part of the project is power transmission system. As per above information, we are using 4 solenoid coil in our project and these coils act as 4 stock transmission, we are using a simple technique to transmit the same power. We take one circular wooden piece and divide that circle in to four parts as shown below in the fig: 1.1.9, these pieces are metallic cutouts.

- Air Compressor
- Solenoid
- Pistons
- Crank Shaft
- Wheels

Now we take one special dc gear motor (motor shaft is not directly connected with motor, so we are transmit ac current to the coil from that shaft) and fix it with circular dick and this motor transmits ac supply to coil.



Fig: 4.6 Single acting cylider

Single acting cylinders (SAC) use the force imparted by air to move in one direction (usually out), and a spring to return to the "home" position.

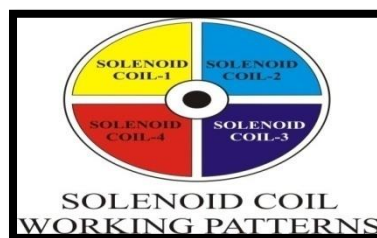


Fig: 4.7 Solenoid coil working pattern

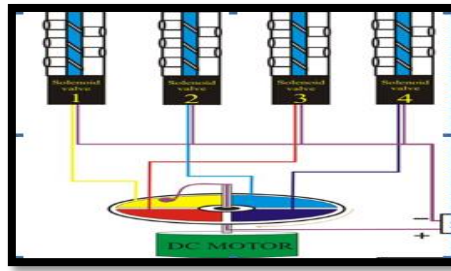


Fig:4.8 Dc motor

4.3 Advantages

- The advantages are well publicized since the developers need to make their machines attractive to investors. Compressed-air vehicles are comparable in many ways to electric vehicles, but use compressed air to store the energy instead of batteries. Their potential advantages over other vehicles include.
- Compressed-air vehicles are unconstrained by the degradation problems associated with current battery systems.
- Lighter vehicles would mean less abuse on roads resulting in longer lasting roads.
- The price of fueling air-powered vehicles will be significantly cheaper than current fuels.

4.4 Disadvantages

- It has relatively less speed.
- Compressor requires external source to run.
-

V. CONCLUSION

There are many applications of mechatronics in the mass produced products used at home. They are to be found in cars in the active solenoid valve, air compressor, piston, engine control, speed control through volume regulator etc. Pollution is one of the major problems faced by the peoples in a routine life. The use of different types of automobile plate has been increased and it plays an important role to create this big problem. Several affords are made by the automobile sector to solve this big problem. Our project deals with the effective electric system to reduce this problem in (a cost efficient way). Air is alternative to other fuels, so during our study we appreciated the importance of electric conversion and found that it is really helpful in controlling the pollution and also it is less expensive than petrol.

REFERENCE

1. Mistry Manish K., Dr.Pravin P.Rathod, Prof. Sorathiya Arvind S., "Study And Development Of Compressed Air Enginesingle Cylinder: A Review Study", Ijaet/Vol.Iii/ Issue I/January-March, 2012/271-274
2. Gorla, R., And Reddy, S., 2005, Probabilistic Heat Transfer And Structural Analysis Of Turbine Blade, Ijtje, Vol. 22, Pp 1- 11.
3. S.S.Verma, "Air Powered Vehicles", The Open Fuels & Energy Science Journal, 2008, Volume 1, Pp.54-56.
4. Rose Robert, William J. Vincent, 2004, Fuel Cell Vehicle World Survey 2003 - Breakthrough Technologies Institute, February' 2004, Washington, D.C.
5. Gizmag Team, Tata Motors Enters Second Phase Of Air- Car Development [Http://Www.Gizmag.Com/Tatamotors-Air-Car- Mdi/22447/](http://www.gizmag.com/tatamotors-air-car-mdi/22447/)
6. Peter Fairley, "Deflating The Air Car", Ieee Spectrum, 30 Oct 2009.

A Study On Green Engine (Piston Less Engine)

S.Pradeep Devaneyan¹, C.Subramanian², Selvamuthukumar.K³, Balaji.R⁴

¹*Professor Department of Mechanical Engineering, Christ College of Engineering and Technology,*

²*Senior Asst. Professor Department of Mechanical Engineering, Christ College of Engineering and Technology,*

^{3,4}*Student Department of Mechanical Engineering, Christ College of Engineering and Technology,*

ABSTRACT The Green Engine is an fascinating engine which has some unique features that were used for the first time in making of engines. It is a PISTONLESS ENGINE with unique features .The efficiency of this engine is high when compared to the contemporary engines and also the exhaust emissions are comparatively minimum .It is used in ships, submarines, mines and military purposes. Electrical generators are produced by this engine. Its significances is because of its small size , light weight, multi – fuels , smooth operations and high thermal efficiency.

I. INTRODUCTION

Coal, petroleum, natural gas, water and nuclear energy are the five main source of energy. The consumption of petroleum constitutes 60 % of energy from all sources. Green engine is an six phase engine which has very low exhaust emission, high efficiency, low vibrations. It is an Internal Combustion Engine. It uniqueness is to adapt to any fuel which is also well burn. It is one of the most interesting discoveries of new millennium. The efficiency of this engine is high when compared to the contemporary engines and also the exhaust emissions are comparatively near to zero

II. NEED TO INVENT

Today our world is facing the major problems regarding energy crises. Along with this we are facing major environmental trouble due to increase in harmful gases which are evolved from nowhere but the combustion of these conventional energy sources. Major portion of fuels is burnt in the engines used for various purposes like automobiles, generators, power plants etc.

2.1 Technical Feature

2.1.1 Direct air intake

It means that there is no inlet pipe, throttle and inlet valves on the air intake system . Air filter is directly connected to the intake part of the engine. The pump loss which consumes the part of engine power is eliminated.

2.1.2 Strong Swirling

As a tangential duct in between combustion chamber and compression chamber , a very swirling which could lost until gas port is opened , can be formed while air is pumped into the mixing and the combustion process can have a satisfying working condition.

2.1.3 Sequential Variable

This greatly revolutionary innovation can provide the most suitable compression ratio for the engine whatever operation made it works on with burning variety of fuels. Therefore, an excellent combustion performance is attained.

2.1.4 Direct Fuel Injection

Direct fuel injection can provide higher output and torque , while at the same time it also enhances the response for acceleration.

2.1.5 Super Air – Fuel Mixing

Since the independent air fuel mixing phase is having enough time for mixing air and fuel under strong swirling and hot situation , the engine is capable to burn any liquid or gas fuels without modifications . An ideal air –fuel mixture could delete CO emission .

Also centrifugal effect coming from both strong swirling and rotation of the burner makes the air fuel mixture denser near the spark plug . It benefits to cold starting and managing lean-burning .

2.1.6 Controllable Combustion Time

Due to the independent combustion phase , compared to the conventional engine whose performance lack of efficient combustion time , resulting in heavy CO emission and low fuel usage rate , the green engine has a sufficient controllable combustion time to match any fuels.

2.1.7 Constant Volume Combustion

The fuels can generate more energy while the combustion occurs on the constant volume also the constant volume technology can allow the engine to have a stable combustion when the lean burning is managed . NO_x emission are decreased .

2.1.8 Vibration Free

As major moving parts , vanes which are counted in little mass and operated symmetrically , the performance of the engine is very smooth . Hence , vibrations are eliminated .

2.1. Self Adapting Sealingsystem

This is another revolutionary innovation applied in green engine. It can eliminate a number of seal plates or strips to achieve gap less seal and to provide most efficient and reliable sealing system with less friction .

III. CONSTRUCTIONAL DETAILS

The green engine is a six phase internal combustion engine with much higher compression ratio . the term PHASE is used instead of stroke because stroke is actually associated to the movement of friction . It is an PISTONLESS ENGINE with features such as sequential variable compression ratio, direct air intake, direct fuel injection ,multi fuel usage etc.It has six process namely INTAKE process, COMPRESSION process , MIXING process , COMBUSTION process , POWER process , EXHAUST process , resulting in high air charge rate.

The engine comprises a set of vanes a pair of rotors which houses a number of small part like containers . In this containers compression , mixing combustion are carried out . It also contain two air in take ports, a pair of fuel injectors and spark plugs. The spark plug are connected to deactivate them when a fuel which does not sparks for ignition is used .

The rotor is made of high heat resistance and low expansion rate material such as ceramic. Whereas, the metal used is an alloy of steel,aluminium,chromium. Eventhough the engine is of symmetric shape, the vanes traverse an unsymmetrical or uneven boundary.The vanes are made in such a way that it comprises of two parts. One going inside a hollow one. At the bottom of the hollow vane is a compressive spring

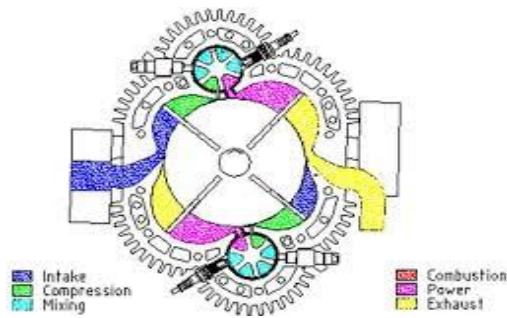


Fig.3.1 Constructional View Of Green Engine

IV. WORKING:

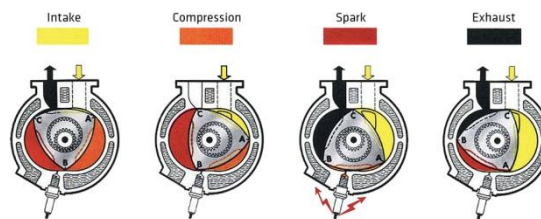


Fig.4.1 Working Phase of Green Engine

4.1 INTAKE

The air arrives to the engine through the direct air intake port. A duct is provided on the sides of the vane and rotor. The duct is so shaped that when the air moves through, strong swirls generate when it gets compressed in the chamber. The air pushes the vane blades which in turn impart a proportionate rotation in the small rotor which houses the chambers. The inlet air duct ends with a very narrow opening to the chamber.

4.2 COMPRESSION

The rushing air from the duct is pushed by the blades into the small chambers in the rotor. The volume of these chambers is comparatively very small naturally the compression obtained by such a procedure is very satisfactory. As earlier known, the compressed air is in a swirling state, ready to be mixed with the fuel which will be injected into the chamber when it will be placed before the injector by the already rotating rotor.

4.3 MIXING

As soon as the chamber comes in front of the fuel injector, the injector sprays fuel into the compressed air the fuel mixes well with the compressed air. The importance of ideal mixing leads to deletion of CO emission. And also because of the strong swirling, a centrifugal effect is exerted in the air fuel mixture. Mixing phase has enough time to produce an ideal air fuel mixture as the spark plug is positioned towards the other end of the rotor or burner.

4.4 COMBUSTION

As the chamber rotates towards the end of its path. It is positioned before the spark plug. A spark flies from the plug into the air fuel mixture. Enabling lean burning of the charge and also a uniform flame front. As soon as the whole charge is ignited, the burner rotates to position itself in front of narrow exit.

4.5 POWER

The expanded gas rushes out of the chamber through the narrow opening. The sudden increase in volume ensures that more power is released (i.e.) the thermal energy is fully utilised.

4.6 EXHAUST

As the thermal energy is fully utilized, the exhaust gases bring along comparatively less heat energy. Because of the complete burning of the charge, poisonous gases like CO are absent in exhaust emission

V. CONCLUSIONS

The green engine prototypes have been recently developed and also because of the unique design, limitations have not been determined to any extent. But even in the faces of the limitations the green engine is sure to serve the purpose to a great extent.

REFERENCE

- [1] Sullivan, M. World's First Air-Powered Car: Zero Emissions By Next Summer, Popular Mechanics [Http://Www.Popularmechanics.Com/Automotive/New_Cars/4217016.Html](http://www.popularmechanics.com/automotive/new_cars/4217016.html) (June **2008** Issue),
- [2] Harley, M.; Ford, G.M. Considering Joint Engine Development, [Http://Www.Autoblog.Com/2008/08/04/Ford-Gm-Considering-Joint-Engine-Development](http://www.autoblog.com/2008/08/04/ford-gm-considering-joint-engine-development), (Accessed Aug **2008**).
- [3] From Wikipedia, The Free Encyclopedia. Compressed-Air Car, [Http://En.Wikipedia.Org/Wiki/Air_Car](http://en.wikipedia.org/wiki/Air_car) (Accessed June **2008**).
- [4] Russell, C. The Air Car Becomes A Reality, [Http://Cambrown.Wordpress.Com/2007/03/27/The-Air-Car-Becomes-A-Reality/](http://cambrown.wordpress.com/2007/03/27/the-air-car-becomes-a-reality/) (Accessed May **2007**).
- [5] Hamilton, T. Technology Review, The Air Car Preps For Market, [Http://Www.Technologyreview.Com/Energy/20071](http://www.technologyreview.com/energy/20071) (Accessed Janu-Ary **2008**).
- [6] Bonser, K., Howstuffworks, How Air-Powered Cars Will Work, [Http://Auto.Howstuffworks.Com/Air-Car.Htm](http://auto.howstuffworks.com/air-car.htm) (Accessed June, **2008**).
- [7] Haliburton, M.-S. Pure Energy Systems News, Engineer's Ultra-Efficient Rotary Compressed-Air Motor, [Http://Pesn.Com/20 06/05/11/9500269_Engineair_Compressed-Air_Motor/](http://pesn.com/2006/05/11/9500269_engineer_compressed-air_motor/) (Accessed June, **2008**).
- [8] Richard, M.G. The Air-Powered Motorcycle By Jem Stansfield, [Http://Www.Instructables.Com/Id/Air-Powered-Bicycle](http://www.instructables.com/id/Air-Powered-Bicycle/) (Accessed April **2008**).
- [9] Chen, P.X. Researchers Develop Air-Powered Motorcycle, [Http://Blog.Wired.Com/Gadgets/2008/08/Air-Powered-Mot.Html](http://blog.wired.com/gadgets/2008/08/air-powered-mot.html) (Ac-Cessed August **2008**).

Magnetic Piston Under Maglev System

S.Pradeep Devaneyan¹, S.Madhanraj², M.Mugilan³,R. Calvin⁴

¹Professor Department of Mechanical Engineering, Christ College of Engineering and Technology,

²Senior Asst. Professor Department of Mechanical Engineering, Christ College of Engineering and Technology,

^{3,4}Student Department of Mechanical Engineering, Christ College of Engineering and Technology,

ABSTRACT- Each and every automobile engine which produce power requires some input, the engines used in our daily life requires input such as petrol, diesel and even electric current which are very costly and produce more heat and cause air pollution. Here we have an idea about a construction of an engine which works in the principle of magnetic propulsion.

I. INTRODUCTION

Internal-combustion engine, one in which combustion of the fuel takes place in a confined space, producing expanding gases that are used directly to provide mechanical power. Such engines are classified as reciprocating or rotary, spark ignition or compression ignition, and two-stroke or four-stroke; the most familiar combination, used from automobiles to lawn mowers, is the reciprocating, spark-ignited, four-stroke gasoline engine. Other types of internal-combustion engines include the reaction engine (see jet propulsion, rocket), and the gas turbine. Engines are rated by their maximum horsepower, which is usually reached a little below the speed at which undue mechanical stresses are developed.

1.1 Disadvantages

- Accuracy of size of piston and
- cylinder is important
- Enormous amount of heat is produced
- Cost of fuel is high
- Availability of fuel is less

1.2 Remedy

To avoid such drawback the magnetic pistons are made, this also produce heat not very less when compared to other engine.

Here this idea is based on the principle of **Van De Graaff** generator and repulsion of magnet

1.3 Techniques Used

- Van De Graaff generator
- Magnetic repulsion
- Maglev System

1.4 Van De Graff

A **Van de Graaff generator** is an electrostatic generator which uses a moving belt to accumulate electric charge on a hollow metal globe on the top of an insulated column, creating very high electric potentials. It produces very high voltage direct current (DC) electricity at low current levels. It was invented by American physicist Robert J. Van de Graaff in 1929. The potential difference achieved in modern Van de Graaff generators can reach 5 megavolts. A tabletop version can produce on the order of 100,000 volts and can store enough energy to produce a visible spark. Small Van de Graaff machines are produced for entertainment, and in physics education to teach electrostatics; larger ones are displayed in science museums.

The Van de Graaff generator was developed as a particle accelerator in physics research, its high potential is used to acceleratesubatomic particles to high speeds in an evacuated tube. It was the most powerful type of accelerator in the 1930s until the cyclotronwas developed. Today it is still used as an accelerator to generate energetic particle and x-ray beams in fields such as nuclear medicine. In order to double the voltage, two generators are often used together, one generating positive and the other negative potential; this is called a **tandem Van de Graaff accelerator**. For example, the Brookhaven National Laboratory TandemVan de Graaff achieves about 30 million volts of potential difference.

The voltage produced by an open-air Van de Graaff machine is limited by arcing and corona discharge to about 5 megavolts. Most modern industrial machines are enclosed in a pressurized tank of insulating gas; these can achieve potentials up to about 25 megavolts.

Van de Graaff Generator

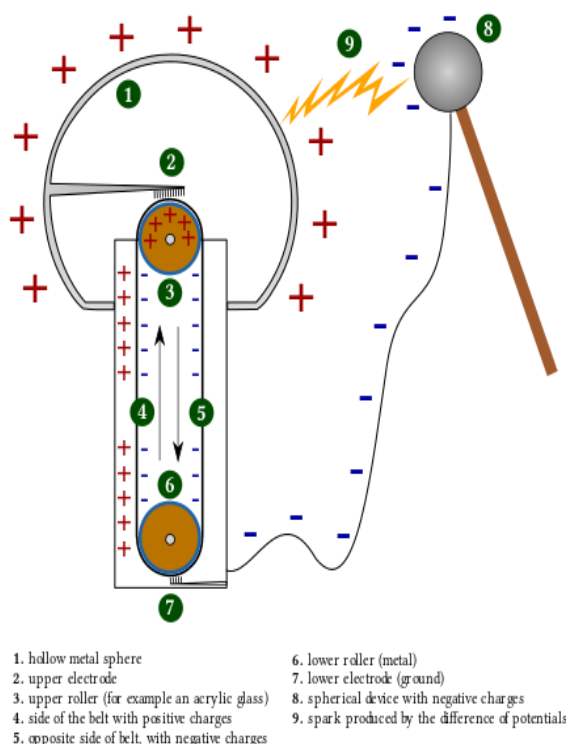


Fig 1.1 Van de Graaf generator construction

II. ELECTRO MAGNET

An electromagnet is a magnet that is created using an electric current -- created by electricity. Since electricity can be turned on and off, so can an electromagnet. It can even be weakened or strengthened by decreasing or increasing the current. Well, the two forces seem very different from each other. The equations that represent them are totally different. But it turns out that they're part of the same electromagnetic force.

When charges, like electrons or protons, are stationary, they produce **electric forces**. But when they're moving, they produce **magnetic forces**. Inside a magnet are lots of tiny moving charges, which gives the magnet its magnetic field.

This knowledge of how magnetism works is important, because it gives us the ability to create electromagnets. Electricity is just a flow of electrons around a circuit, so an electrical wire will produce a magnetic field just like a magnet.

Electromagnets are usually made out of a coil of wire -- a wire curled into a series of 'turns'.

This strengthens and concentrates the magnetic field more than a single stretch of wire. The wire turns are often coiled around a regular magnet, made of a ferromagnetic material like iron. This makes the electromagnet more powerful.

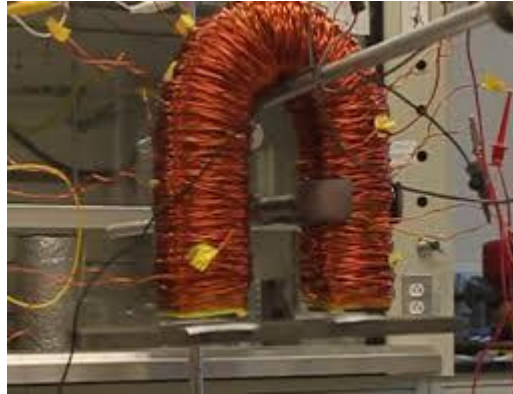


Fig2.1 Electro magnet

III. MAGNETIC REPULSION

The repulsion force will depend only on the distance between the two magnets. The vertical repulsion force will be exactly the same as the horizontal repulsion force at the same distance. Of course, in a vertical situation, where the two magnets are not being supported by table, you will also have gravitational force- but that's completely separate from repulsion force of the magnets.

3.1 Force between two magnetic poles:

If both poles are small enough to be represented as single points then they can be considered to be point magnetic charges. the force between two magnetic poles is given by:

$$F = \frac{\mu q_{m1} q_{m2}}{4\pi r^2}$$

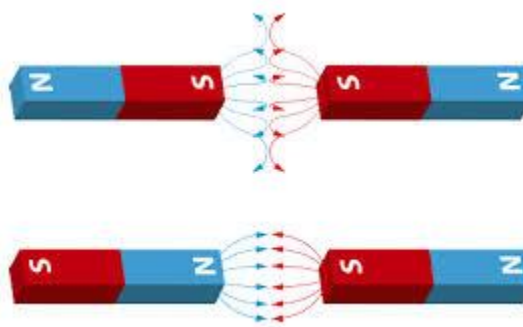


Fig 3.1 Force between two magnetic poles

IV. MAGLEV

Maglev (derived from **magnetic levitation**) is a transport method that uses magnetic levitation to move vehicles without touching the ground. With maglev, a vehicle travels along a guide way using magnets to create both lift and propulsion, there by reducing friction by a great extent and allowing very high speeds.

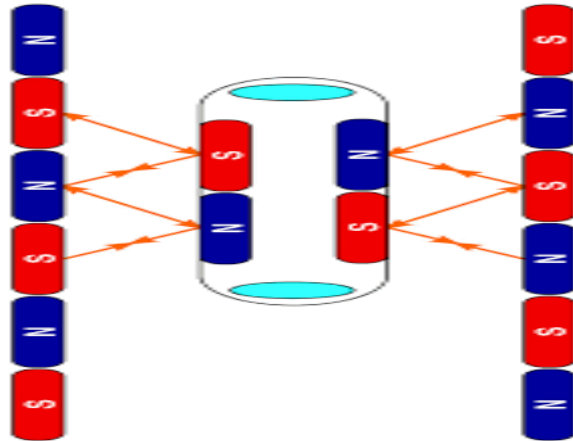


Fig4.1 Maglev

4.1 Cooling cable

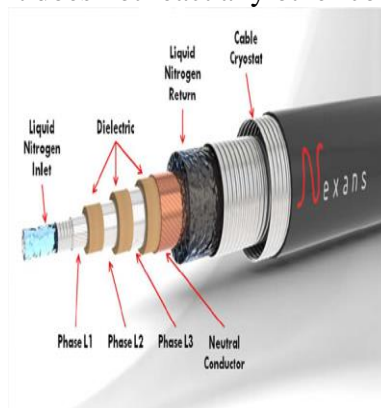
Cooling cable is surrounded by the piston to make it as super conductor

In physics, cryogenics is the study of the production and behaviour of materials at very low temperatures.

It is not well-defined at what point on the temperature scale refrigeration ends and cryogenics begins, but scientists^[1] assume it starts at or below -150°C (123 K ; -238°F). The National Institute of Standards and Technology has chosen to consider the field of cryogenics as that involving temperatures below -180°C or -292.00°F or 93.15 K . This is a logical dividing line, since the normal boiling points of the so-called permanent gases (such as helium, hydrogen, neon, nitrogen, oxygen, and normal air) lie below -180°C while the Freonrefrigerants, hydrogen sulfide, and other common refrigerants have boiling points above -180°C . (above -150°C , -238°F or 123 K). Some of the cryogenics are:

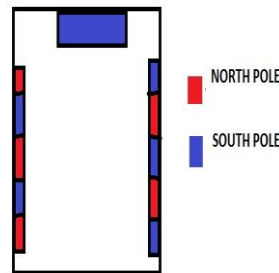
- **Inert Gases:** Inert gases do not react chemically to any great extent. They do not burn or support combustion. Examples of this group are nitrogen, helium, neon, argon and krypton.
- **Flammable Gases:** Some cryogenic liquids produce a gas that can burn in air. The most common examples are hydrogen, methane and liquefied natural gas.

But inert gas is preferable since it does not react any other compound.



*Fig 4.2 Cooling cable***4.2 Design of Cylinder**

The cylinder are arranged in such a way that the inner surface of the combustion cylinder is slightly altered. The cylinder is made up of carbon fibre since it has high tensile strength. In this process of mechanism the series of alternative poles are fixed on the either side of the cylinder in a curved manner this arrangement is to achieve maglev. The negative charge is placed at the top of the cylinder.

*Fig 4.3 Design of Cylinder***4.3 Design of piston:**

The piston is made up of super conducting magnet. The south pole or negative charge of the piston is face upward. Also depression is made on the piston to immerse two magnets by means of insulator. The magnets in the either sides are placed in opposite in direction as shown in figure. The piston is surrounded by the cable of super cooled liquid.

*Fig 4.4 Design of piston***4.4 Working**

Initially the van de graaff generator is started to the battery provided. The charge produced by the generator makes the top surface of the cylinder negative, which is electro-magnet since the process goes on continuously the magnet may demagnetise. So electromagnet is used here. By using ic 555 the current can be supplied in a regular interval.

This system has only two strokes, both are power stroke.

Initially the piston is at the BDC, when the crank move up the piston gets upward thrust which levitate the magnetic piston and moves it upward faster. Now the piston is in TDC now the south pole of the piston deflect when it comes to contact with south-pole of the cylinder top surface. This cyclic process goes on continuously thus working of piston is achieved .the crank position diagram is achieved below.

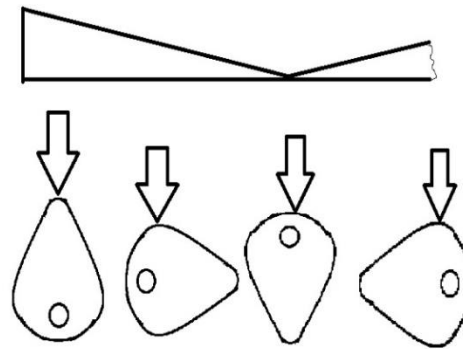


Fig 4.5 Working

4.5 Advantages

- No pollution
- No fuel requirement
- Faster than the combustion engine
- Accuracy is not maintained in designing the piston and cylinder
- No lubricant is needed since no friction is arised

4.6 Disadvantages

- The size of the piston must be large, than the piston used in combustion engine.
- The initial cost of construction is high

REFERENCES

- [1] Sullivan, M. World's First Air-Powered Car: Zero Emissions By Next Summer, Popular Mechanics [Http://Www. Popularmechanics. Com/Automotive/New_Cars/4217016.Html](http://www.popularmechanics.com/automotive/new_cars/4217016.html) (June 2008 Issue),
- [2] Harley, M.; Ford, G.M. Considering Joint Engine Development, [Http://Www.Autoblog.Com/2008/08/04/Ford-Gm-Considering-Joint-Engine-Development](http://www.autoblog.com/2008/08/04/ford-gm-considering-joint-engine-development), (Accessed Aug 2008).
- [3] From Wikipedia, The Free Encyclopedia. Compressed-Air Car, [Http://En.Wikipedia.Org/Wiki/Air_Car](http://en.wikipedia.org/wiki/Air_Car) (Accessed June 2008).
- [4] Russell, C. The Air Car Becomes A Reality, [Http://Cambrown. Wordpress.Com/2007/03/27/The-Air-Car-Becomes-A-Reality/](http://cambrown.wordpress.com/2007/03/27/the-air-car-becomes-a-reality/) (Accessed May 2007).
- [5] Hamilton, T. Technology Review, The Air Car Preps For Market, [Http://Www.Technologyreview.Com/Energy/20071](http://www.technologyreview.com/energy/20071) (Accessed Janu-Ary 2008).
- [6] Bonser, K., Howstuffworks, How Air-Powered Cars Will Work, [Http://Auto.Howstuffworks.Com/Air-Car.Htm](http://auto.howstuffworks.com/air-car.htm) (Accessed June, 2008).
- [7] Haliburton, M.-S. Pure Energy Systems News, Engineer's Ultra-Efficient Rotary Compressed-Air Motor, [Http://Pesn.Com/20 06/05/11/9500269_Engineair_Compressed-Air_Motor/](http://pesn.com/2006/05/11/9500269_engineair_compressed-air_motor/) (Accessed June, 2008).
- [8] Richard, M.G. The Air-Powered Motorcycle By Jem Stansfield, [Http://Www.Instructables.Com/Id/Air-Powered-Bicycle](http://www.instructables.com/Id/Air-Powered-Bicycle) (Accessed April 2008).
- [9] Chen, P.X. Researchers Develop Air-Powered Motorcycle, [Http://Blog.Wired.Com/Gadgets/2008/08/Air-Powered-Mot.Html](http://blog.wired.com/gadgets/2008/08/air-powered-mot.html) (Ac-Cessed August 2008).

Tidal Power Plant Using Oscillating Motion

A.Sivakumar,¹P.Chandru Deva Kannan², M.Srinivasan³, D.Dhinesh Kumar⁴

¹Professor Department of Mechanical Engineering, Christ College of Engineering and Technology,

²Senior Asst. Professor Department of Mechanical Engineering, Christ College of Engineering and Technology.

^{3,4}Student Department of Mechanical Engineering, Christ College of Engineering and Technology.

ABSTRACT Tidal power along tidal shores has been used for centuries to run small tidal mills. Generating electricity by tapping tidal power proved to be very successful only in the last century through the tidal power plant constructed in 1967 in La Rance, France. This used a large barrier to generate the sea level head necessary for driving turbines. Construction of such plants evolved very slowly because of prohibitive costs and concerns about the environmental impact. Developments in the construction of small, efficient and inexpensive underwater turbines admit the possibility of small scale operations that will use local tidal currents to bring electricity to remote locations. To produce an electric current in sea tides this tidal power is used to produce an oscillating motion to producing the Electric power.

I. INTRODUCTION

In this power plant can be easy to producing an electric power in this current can be produce in the sea tids. The tidal is the Renewable resource . It is working among the oscillating motion. The power plant can be mainly working into the sea areas . This power plant can be used for sea near industries and factories.

1.1 Construction

The working of an pendulum power plant in the design of the pendulum in the power plant where there the tidal Power in the sea. In the cylindrical closed steel drum or barrel it can be filled in the 25% of water in the barrel . In the 75% of barrel can be floating into the water and the 25% of barrel can be inside the sea Under the steel rod can be placed into the horizontal place in the center of the barrel the rod can be placed in the barrel.

In the two columns can be placed in the some distance into the sea when this barrel connecting rod can be placed into the center

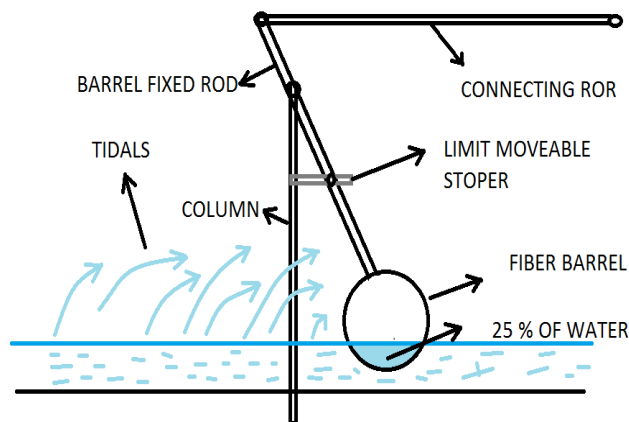


Fig 1.2 lay out of pendulum powerplant

The barrel is connecting into the rod can be placed into the center of the two columns then the rod can be starts oscillation the power of the tidal power the other end of the connecting rod is connected to the another side of the rod in the shaft in the working opposite direction of the rod working among the mechanical work this process the same 6 set of columns where be placed into the sea shore sea area the rod can be connected into the crank case these 6 rod can be connected into the crank shaft these crank shaft can be producing rotating motion the crank is connected to the power generator

where be placed into the sea sore in the sea area in thr rod can be connected into the crank case these 6 rod can be connected into the crank shaft these rod can be connected into rod in the shaft in the working the opposite direction this case if the crank shaft to producing direction the rod working among mechanical an rotating motion. In this crank shaft can be connected into the generator .The generator will produce an electric power.

In this process the ecy way to producing an electric power in the oscillation using tidal ;power plant.a

1.2 Side view of the power plant

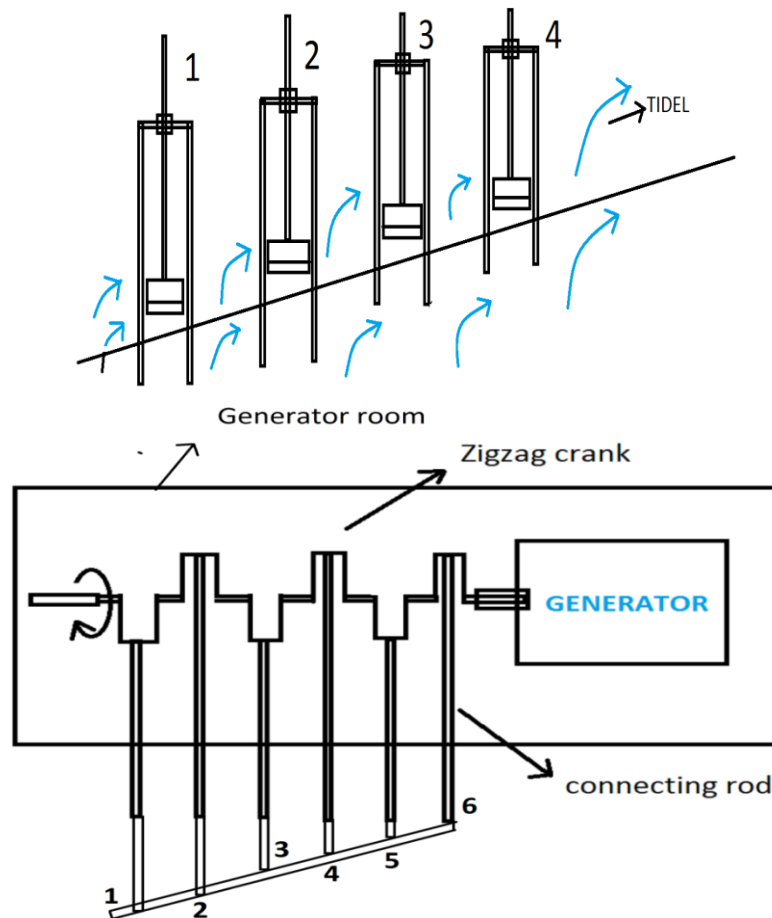


Fig1.3 Side view of the power plant

II. WORKING

The tidal waves strikes the barrel it starts to oscillate the barrel connecting rod is connected to the connecting rod. The connecting rod pulls the crank then the crank starts to move, likewise other 5 barrels starts to oscillate alternately to make a complete the oscillation. Similarly, it continues to oscillate and produce the rotation to the crank. The crank starts to rotate to produce the rotating motion. The generator is coupled to crank and produces electrical energy.

2.1 ADVANTAGES

- *Producing power at any time
- *Construction cost is low
- *power can be producing easily
- * It can be construct at any near seashore area.

2.2 DISADVANTAGES

- *Little noise will be produce
- *the power produced by the tidal waves may be vary

REFERENCES

1. Bernshtein L. B., 1961, Tidal Energy For Electric Power Plants, Israel Program For Scientific Translations, Jerusalem, 378 Pp.
2. Bernshtein L. B. (Ed.), 1996, Tidal Power Plants, Korea Ocean Res. & Development Institute, Seoul, 444 Pp.
3. Cartwright D.E., 1969, Extraordinary Tidal Currents Near St. Kilda, Nature, 223, 928–932. Defant A., 1960, Physical Oceanography, Vol. 2, Pergamon Press, New York, 598 Pp.
4. Egbert G. D., Ray R. D., 2000, Significant Dissipation Of Tidal Energy In The Deep Ocean Inferred From Satellite Altimeter Data, Nature, 405, 775–778.
5. Flather R. A., 1976, A Tidal Model Of The North-West European Continental Shelf, Mem. Soc. Roy. Sci. Liege, 6 (10), 141–164.
6. Garrett C., 1984, Tides And Tidal Power In The Bay Of Fundy, Endeavour, New Ser., 8 (2), 160–167.
7. Garrett C., Cummins P., 2004, Generating Tidal Power From Currents, J. Waterw. Port C-ASCE, 130 (3), 114–118.

Increasing Efficiency of Two Stroke Petrol Engine By Using Pre-Heating Method

A.Sivakumar¹, P.Chandru Deva Kannan², A.Gokulnath³, A.Nithin⁴

¹*Professor Department of Mechanical Engineering, Christ College of Engineering and Technology,*

²*Senior Asst. Professor Department of Mechanical Engineering, Christ College of Engineering and Technology,*

^{3,4}*Student Department of Mechanical Engineering, Christ College of Engineering and Technology,*

ABSTRACT The pre heating was invented by swiss engineer Alfred Buchi in 1905. So I refer this for our project with the primary objective of increasing the thermal efficiency of the process this may be used along or to replace the exhaust pipe. The purpose of the air pre heater is to recover the heat from the exhaust which increases the thermal efficiency of the two stroke petrol engine by reducing the useful heat lost in the exhaust pipe.

I. INTRODUCTION

The concept of increasing the fuel efficiency of petrol engine in this project, is to preheat the intake air which is flowing through the carburetor. The humidity in the atmospheric air affects the petrol vaporization in the carburetor.

1.1 Air-Preheater

An air-preheater is nothing but a heat exchanger in which heat is transferred from a hot fluid to air for useful utilization of energy.

1.2 Air Filter

A particulate air filter is a device composed of fibrous materials which removes solid particulates such as dust, pollen, mould, and bacteria from the air. A chemical air filter consists of an absorbent or catalyst for the removal of airborne molecular contaminants such as volatile organic compounds or ozone.

II. OPERATION OF TWO STROKE ENGINE

A two-stroke, or two-cycle, engine is a type of internal combustion engine which completes a power cycle with two strokes (up and down movements) of the piston during only one crankshaft revolution. This is in contrast to a "four-stroke engine", which requires four strokes of the piston to complete a power cycle. In a two-stroke engine, the end of the combustion stroke and the beginning of the compression stroke happen simultaneously, with the intake and exhaust or (scavenging) functions occurring at the same time.

Two-stroke engines often have a high power-to-weight ratio, usually in a narrow range of rotational speeds called the "power band". Compared to four-stroke engines, two-stroke engines have a greatly reduced number of moving parts, and so can be more compact and significantly lighter.

The first commercial two-stroke engine involving in-cylinder compression is attributed to Scottish engineer Dugald Clerk, who patented his design in 1881. However, unlike most later two-stroke engines, his had a separate charging cylinder. The crankcase-scavenged engine, employing the area below the piston as a charging pump, is generally credited to Englishman Joseph Day. The first truly practical two-stroke engine is attributed to Yorkshireman Alfred Angas Scott, who started producing twin-cylinder water-cooled motorcycles in 1908.

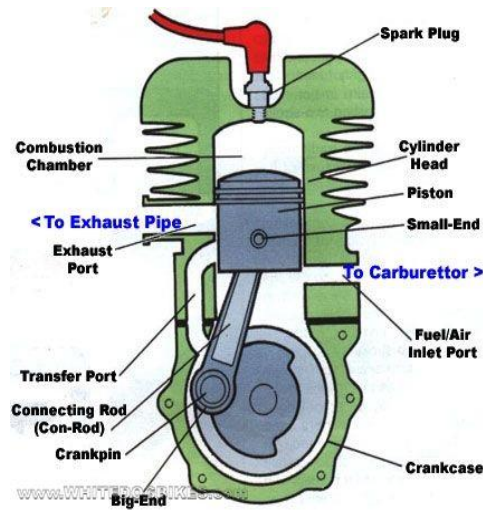


Fig 2.1 Layout Of Two Stroke Petrol Engine

III. WORKING PRINCIPLE

The heat exchanger is located in the engine exhaust pipe. The exhaust pipe consist of a muffler and stay plates, etc. The heat exchanger is made up of 18 gauge EN8.Plate.The inner tube is inserted tightly on the muffler tube. A baffle plate pipe arrangement is made in between the two conic tubes so as to make a spiral path to the incoming air.so that the heat transfer to the air can be increased. Moreover the air is flowing in the counter direction to the exhaust gas there by effective heat transfer can be achieved.

The heat exchanger inlet is fitted with the pre-filter. The outlet is connected to a bypass mechanism through a hose pipe the by-pass mechanism is connected to the carburetor intake. The temperature of the air entering to the carburetor can be maintained constant for a particular degree centigrade. Allow the atmospheric air to mix with the heater air from the heat exchanger. So that the hot air is diluted with atmospheric air and reducing the temperature. So increasing fuel efficiency of the petrol engine system.

Metal-mesh optical filters are optical filters made from stacks of metal meshes and dielectric. They are used as part of an optical path to filter the incoming light to allow frequencies of interest to pass while reflecting other frequencies of light.

Metal-mesh filters have many applications for use in the far infrared (FIR)[1] and submillimeter regions of the electromagnetic spectrum. These filters have been used in FIR and submillimeter astronomical instruments for over 4 decades, in which they serve two main purposes: bandpass or low-pass filters are cooled and used to lower the noise equivalent power of cryogenic bolometers (detectors) by blocking excess thermal radiation outside of the frequency band of observation,[3] and bandpass filters can be used to, define the observation band of the detectors. Metal-mesh filters can also be designed for use at 45° to split an incoming optical signal into several observation paths, or for use as a polarizing half wave plate.

IV. REDUCER

A **reducer** is the component in a pipeline that reduces the pipe size from a larger to a smaller bore (inner diameter).The length of the reduction is usually equal to the average of the larger and smaller pipe diameters. There are two main types of reducer: concentric andeccentric reducers.A

reducer can be used either as nozzle or as diffuser depending on the mach number of the flow. A reducer allows for a change in pipe size to meet hydraulic flow requirements of the system, or to adapt to existing piping of a different size. Reducers are usually concentric but eccentric reducers are used when required to maintain the same top-or bottom-of-pipe level. These fittings are manufactured in inch and metric size.

4.1 Non Return Value

It is a mechanical device a valve, which normally allows liquid or gas to flow through it in only one direction from flow is known as non return value.

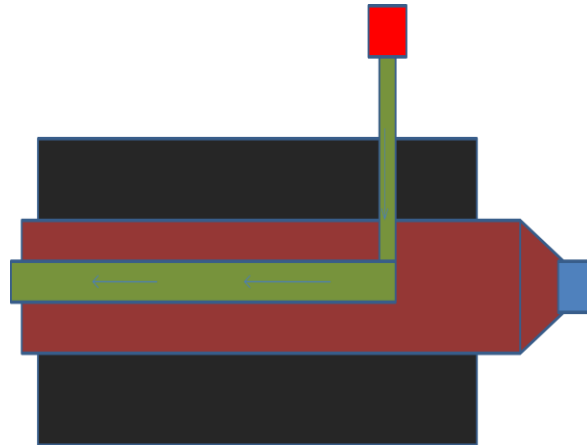


Fig 4.1 Non Return Value

4.1 Non Return Value

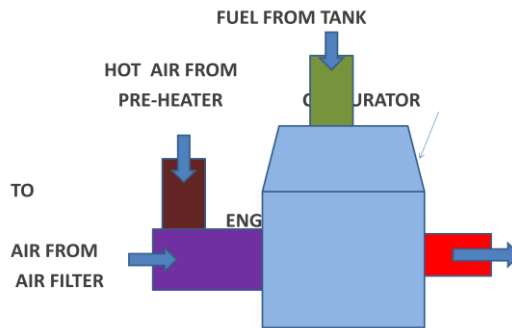


Fig 4.2 layout

4.2 Design

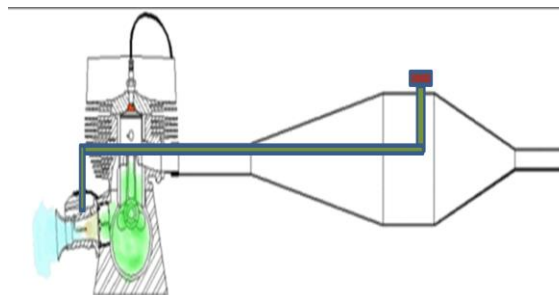


Fig 4.3 Design

4.3 Advantages

- Getting more efficiency to the vehicle
- Low cost
- Less space required
- Control air pollution
- Control noise pollution

4.4 Disadvantage

- Fitting and removing will take more time

4.5 Application

- It applicable in all two stroke automobiles

V. CONCLUSION

This project is made with pre planning, that it provides flexibility in operation. This innovation has made the more desirable and economical. This project “Increasing Efficiency of Two Stroke Petrol Engine Using Pre Heating Method” is designed with the hope that it is very much economical and helpful to automobile vehicle. This project helped us to know the periodic steps in completing a project work. Thus, we have completed the project successfully.

REFERENCES

- [1] Sullivan, M. World's First Air-Powered Car: Zero Emissions By Next Summer, Popular Mechanics [Http://Www. Popularmechanics. Com/Automotive/New_Cars/4217016.Html](http://www.popularmechanics.com/automotive/new_cars/4217016.html) (June 2008 Issue),
- [2] Harley, M.; Ford, G.M. Considering Joint Engine Development, [Http://Www.Autoblog.Com/2008/08/04/Ford-Gm-Considering-Joint-Engine-Development](http://www.autoblog.com/2008/08/04/ford-gm-considering-joint-engine-development), (Accessed Aug 2008).
- [3] From Wikipedia, The Free Encyclopedia. Compressed-Air Car, [Http://En.Wikipedia.Org/Wiki/Air_Car](http://en.wikipedia.org/wiki/Air_Car) (Accessed June 2008).
- [4] Russell, C. The Air Car Becomes A Reality, [Http://Cambrown. Wordpress.Com/2007/03/27/The-Air-Car-Becomes-A-Reality/](http://cambrown.wordpress.com/2007/03/27/the-air-car-becomes-a-reality/) (Accessed May 2007).
- [5] Hamilton, T. Technology Review, The Air Car Preps For Market, [Http://Www.Technologyreview.Com/Energy/20071](http://www.technologyreview.com/energy/20071) (Accessed Janu-Ary 2008).
- [6] Bonser, K., Howstuffworks, How Air-Powered Cars Will Work, [Http://Auto.Howstuffworks.Com/Air-Car.Htm](http://auto.howstuffworks.com/air-car.htm) (Accessed June, 2008).

RANK HOLDERS OF St. ANNE'S CET



K. Bhagyalakshmi
ECE



K. Divya
CSE



A. Micheal Arokia Raj
MECH



M. Ramalakshmi
CSE

PLACEMENTS @ St. ANNE'S CET



28 STUDENTS PLACED @ KARMA IT SOLUTIONS ON 25TH DECEMBER 2015



15 STUDENTS PLACED @ MYOUNG SHIN AUTOMOTIVE PVT LTD ON 04TH JANUARY 2016



28 STUDENTS PLACED @ KARMA IT SOLUTIONS ON 27TH JANUARY 2016

ACHIEVEMENTS @ St. ANNE'S CET



Our College has grabbed ISTE Best Chapter Award in 18th ISTE TN&P Section Convention



Our Football Team Grabbed First Place in Anna University Zonal Sports Meet 2015

St. Anne's College of Engineering and Technology,
Anguchettypalayam, Panruti-607 110,
Cuddalore dt.

www.stannescet.ac.in
stannescet@gmail.com
04142 - 241661,242661

